VOLUME 27 / NUMBER 13
JULY 8, 1989
ACC. NOS. N89-20086 TO N89-20919

STAR
AN ABSTRACT JOURNAL

Scientific and Technical Aerospace Reports

PRODUCED BY THE
SCIENTIFIC AND TECHNICAL
INFORMATION
DIVISION

NASA

NATIONAL AERONAUTICS AND SPACE ADMINISTRATION

WHAT YOU CAN DO FOR *STAR*

All users of this abstract service are urged to forward reports to be considered for announcement in *STAR*. This will aid NASA in its efforts to provide the fullest possible coverage of all scientific and technical publications that might support aeronautics and space research and development. If you have prepared relevant reports (other than those that you will transmit to NASA, DoD, or DOE through the usual contract- or grant-reporting channels), please send them for consideration to the NASA Scientific and Technical Information Facility, P.O. Box 8757, BWI Airport, Maryland 21240.

Reprints of journal articles, book chapters, and conference papers are also welcome. These will be considered for announcement in *STAR's* companion journal, *International Aerospace Abstracts*.

You may specify a particular source to be included in a report announcement if you wish; otherwise the report will be placed on public sale at the National Technical Information Service. Copyrighted publications will be announced but not distributed or sold.

PURCHASE OF *STAR*

The semimonthly issues are available to registered users on annual subscription for $99.00 from the NASA Scientific and Technical Information Facility, ATTN: Registration Services, P.O. Box 8757, BWI Airport, MD 21240. *STAR* is publically available on annual subscription for $99.00 from the Superintendent of Documents, U.S. Government Printing Office, Washington, DC 20402.

PUBLISHED BY:

UNITED STATES GOVERNMENT
NATIONAL AERONAUTICS AND SPACE ADMINISTRATION
SCIENTIFIC AND TECHNICAL INFORMATION DIVISION
Scientific and Technical Aerospace Reports, Volume 27, is prepared by the NASA Scientific and Technical Information Facility operated for the National Aeronautics and Space Administration by RMS Associates.

The Administrator of the National Aeronautics and Space Administration has determined that the publication of this periodical is necessary in the transaction of the public business required by law of this Agency. Use of funds for printing this periodical has been approved by the Director of the Office of Management and Budget through March 22, 1989.

US ISSN 0036-8741

INTRODUCTION

Scientific and Technical Aerospace Reports (STAR) is a major component of a comprehensive National Aeronautics and Space Administration information system covering aeronautics, space, and supporting disciplines. *STAR* is issued on the 8th and 23rd of each month and announces current publications of the following types:

- NASA, NASA contractor, and NASA grantee reports
- Reports issued by other U.S. Government Agencies, domestic and foreign institutions, universities, and private firms
- Translations in report form
- NASA-owned patents and patent applications
- Other U.S. Government Agency and foreign patents and patent applications
- Domestic and foreign dissertations and theses

Journal, book, and conference literature, cover-to-cover journal translations, and certain foreign dissertations are announced in a companion journal, *International Aerospace Abstracts (IAA),* available on subscription from the American Institute of Aeronautics and Astronautics, Technical Information Service, 555 West 57th Street, 12th Floor, New York, New York 10019.

SUBJECT SCOPE

Subject scope of *STAR,* and *IAA* includes all aspects of aeronautics and space research and development, supporting basic and applied research, and applications. Aerospace aspects of earth resources, energy development, conservation, oceanography, environmental protection, urban transportation, and other topics of high national priority are also covered.

OTHER NASA PUBLICATIONS

Other NASA publications and information services are described in the publication, *The NASA Scientific and Technical Information System ... and How to Use It,* available without charge from the NASA Scientific and Technical Information Facility, P.O. Box 8757, BWI Airport, Maryland 21240.

HOW TO USE *STAR* SUBJECT CATEGORIES

STAR is categorized by 10 major subject divisions divided into 76 specific subject categories and one general category/division. The major subject divisions are listed in the Table of Contents, together with a note for each that defines its scope and provides any cross-references. For example:

AERONAUTICS

Includes aeronautics (general); aerodynamics; air transportation and safety; aircraft communications and navigation; aircraft design, testing and performance; aircraft instrumentation; aircraft propulsion and power; aircraft stability and control; and research and support facililties (air).

For related information see also *Astronautics.*

Each major division is further divided into as many as nine specific categories, which are identified by category numbers.

Abstracts in *STAR* are grouped by specific category, the categories appearing in sequential order. Category breaks in the abstract section are identified by the category number and title, and a scope note. Cross-references to other categories are provided as appropriate. For example:

02 AERODYNAMICS

Includes aerodynamics of bodies, combinations, wings, rotors, and control surfaces; and internal flow in ducts and turbomachinery.

For related information see also *34 Fluid Mechanics and Heat Transfer.*

CROSS-REFERENCES

Individual *STAR* abstracts are not ordinarily cross-referenced, except for certain conference reports or book translations that have had separate abstracts written for their component papers or chapters. Citations and abstracts of the components follow immediately after those of the parent document. When the subject content of a component differs sufficiently from the general content of the parent, a cross-reference citation also is printed at the end of the category to which it normally would have been assigned if it were independent.

DOCUMENTS ON MICROFICHE

Documents on microfiche[1] are designated by a pound sign (#) following the accession number. The pound sign is used without regard to the source or quality of the microfiche.

AVAILABILITIES

One or more sources from which a document announced in *STAR* is available to the public is given in each citation. The most commonly indicated sources and their acronyms or abbreviations are listed below. If the publication is available from a source other than those listed, the publisher and his address will be displayed on the availability line or in combination with the corporate source line.

Avail: NTIS. Sold by the National Technical Information Service. Prices for hard copy (HC) and microfiche (MF) are indicated by a price code following the letters HC or MF in the *STAR* citation. Current values for the price codes are given in the tables on page vii.

Initially distributed microfiche under the NTIS SRIM (Selected Research in Microfiche) is available at greatly reduced unit prices. For this service and for information concerning subscription to NASA printed reports, consult the NTIS Subscription Section, Springfield, Va. 22161.

NOTE ON ORDERING DOCUMENTS: When ordering NASA publications (those followed by the * symbol), use the N accession number. NASA patent applications (only the specifications are offered) should be ordered by the US-Patent-Appl-SN number. Non-NASA publications (no asterisk) should be ordered by the AD, PB, or other *report number* shown on the last line of the citation, not by the N accession number. It is also advisable to cite the title and other bibliographic identification.

Avail: SOD (or GPO). Sold by the Superintendent of Documents, U.S. Government Printing Office, in hard copy. The current price and order number are given following the availability line. (NTIS will fill microfiche requests, as indicated above, for those documents identified by a # symbol.)

(1) A microfiche is a transparent sheet of film, 105 by 148 mm in size, containing as many as 60 to 98 pages of information reduced to micro images (not to exceed 26:1 reduction).

Avail: BLL (formerly NLL): British Library Lending Division, Boston Spa, Wetherby, Yorkshire, England. Photocopies available from this organization at the price shown. (If none is given, inquiry should be addressed to the BLL.)

Avail: DOE Depository Libraries. Organizations in U.S. cities and abroad that maintain collections of Department of Energy reports, usually in microfiche form, are listed in *Energy Research Abstracts*. Services available from the DOE and its depositories are described in a booklet, *DOE Technical Information Center - Its Functions and Services* (TID-4660), which may be obtained without charge from the DOE Technical Information Center.

Avail: ESDU. Pricing information on specific data, computer programs, and details on ESDU topic categories can be obtained from ESDU International Ltd. Requesters in North America should use the Virginia address while all other requesters should use the London address, both of which are on page vi.

Avail: Fachinformationszentrum, Karlsruhe. Sold by the Fachinformationszentrum Energie, Physik, Mathematik GMBH, Eggenstein Leopoldshafen, Federal Republic of Germany, at the price shown in deutschmarks (DM).

Avail: HMSO. Publications of Her Majesty's Stationery Office are sold in the U.S. by Pendragon House, Inc. (PHI), Redwood City, California. The U.S. price (including a service and mailing charge) is given, or a conversion table may be obtained from PHI.

Avail: NASA Public Document Rooms. Documents so indicated may be examined at or purchased from the National Aeronautics and Space Administration, Public Documents Room (Room 126), 600 Independence Ave., S.W., Washington, D.C. 20546, or public document rooms located at each of the NASA research centers, the NASA Space Technology Laboratories, and the NASA Pasadena Office at the Jet Propulsion Laboratory.

Avail: Univ. Microfilms. Documents so indicated are dissertations selected from *Dissertation Abstracts* and are sold by University Microfilms as xerographic copy (HC) and microfilm. All requests should cite the author and the Order Number as they appear in the citation.

Avail: US Patent and Trademark Office. Sold by Commissioner of Patents and Trademarks, U.S. Patent and Trademark Office, at the standard price of $1.50 each, postage free. (See discussion of NASA patents and patent applications below.)

Avail: (US Sales Only). These foreign documents are available to users within the United States from the National Technical Information Service (NTIS). They are available to users outside the United States through the International Nuclear Information Service (INIS) representative in their country, or by applying directly to the issuing organization.

Avail: USGS. Originals of many reports from the U.S. Geological Survey, which may contain color illustrations, or otherwise may not have the quality of illustrations preserved in the microfiche or facsimile reproduction, may be examined by the public at the libraries of the USGS field offices whose addresses are listed in this Introduction. The libraries may be queried concerning the availability of specific documents and the possible utilization of local copying services, such as color reproduction.

Avail: Issuing Activity, or Corporate Author, or no indication of availability. Inquiries as to the availability of these documents should be addressed to the organization shown in the citation as the corporate author of the document.

NASA PATENTS AND PATENT APPLICATIONS

Patents and patent applications owned by NASA are announced in *STAR* under appropriate subject categories and are referenced in the *STAR* indexes. In the Report/Accession Number Index, patents are indexed by the NASA Case Number (which appears in lieu of the report number in other indexes), the U.S. Patent Number, the U.S. Patent Application Serial Number, and the U.S. Patent Class. Patent applications for which patents have not yet been issued are indexed by the NASA Case Number and the U.S. Patent Application Serial Number.

NASA *patent application specifications* are sold in paper copy by the National Technical Information Service at price code A02. Microfiche are sold at price code A01. The US-Patent-Appl-SN- number should be used in ordering either paper copy or microfiche from NTIS. Printed copies of *patents* (which are not microfiched) are available for purchase at $1.50 per copy from:

Commissioner of Patents and Trademarks
U.S. Patent and Trademark Office
Washington, D.C. 20231

When ordering patents, the U.S. Patent Number should be used, and payment must be remitted in advance, preferably by money order or check payable to the Commissioner of Patents and Trademarks. Prepaid purchase coupons for ordering are also available from the Patent and Trademark Office. The patents and patent applications announced in *STAR* are owned by NASA and are available for royalty-free licensing. Requests for licensing terms and further information should be addressed to:

Associate General Counsel for Intellectual Property/Code GP
National Aeronautics and Space Administration
Washington, D.C. 20546

ELIGIBILITY AND REGISTRATION FOR NASA INFORMATION PRODUCTS AND SERVICES

A variety of services is available to organizations of the following types that have registered with NASA to receive specific services or products:

1. NASA offices, research centers, contractors, subcontractors, grantees, and consultants;
2. Other U.S. Government agencies and their contractors;
3. Libraries in the United States that have arrangements with NASA to maintain collections of NASA documents for public reference;
4. Other organizations in the United States having a need for NASA documents in work related to aeronautics and space research;
5. Organizations abroad that have established reciprocal document exchange arrangements with NASA.

Only the central service points or central points of document acquisition and control within qualified organizations are eligible to register for NASA products and services. Domestic organizations that may be eligible to receive various classes of NASA publications and services should address their requests for registration or for further information to:

NASA Scientific and Technical Information Facility
ATTN: Registration Services
Post Office Box 8757
BWI Airport, Maryland 21240

Organizations abroad should direct requests to Manager, International STI Activities, NTT, NASA Headquarters, Washington, D.C. 20546.

AVAILABILITY OF *STAR* ABSTRACTS ON MICROFICHE

Microfiche of the abstract sections of this issue and other issues of *STAR* are available on annual subscription from NTIS as PB89-911300, Attn: Subscriptions, 5285 Port Royal Road, Springfield, Virginia 22161. Annual subscription rates are $70.00 North America; $140.00 foreign. Abstract sections for previous years retroactive to 1964 are available at the current rates. Microfiche for individual *STAR* issue abstract sections are not available.

PUBLIC COLLECTIONS OF NASA DOCUMENTS

DOMESTIC: NASA and NASA-sponsored documents and a large number of aerospace publications are available to the public for reference purposes at the library maintained by the American Institute of Aeronautics and Astronautics, Technical Information Service, 555 West 57th Street, 12th Floor, New York, New York 10019

EUROPEAN: An extensive collection of NASA and NASA-sponsored publications is maintained by the British Library Lending Division, Boston Spa, Wetherby, Yorkshire, England for public access. The British Library Lending Division also has available many of the non-NASA publications cited in *STAR*. European requesters may purchase facsimile copy or microfiche of NASA and NASA-sponsored documents, those identified by both the symbols # and * from ESA - Information Retrieval Service European Space Agency, 8-10 rue Mario-Nikis, 75738 Paris CEDEX 15, France.

FEDERAL DEPOSITORY LIBRARY PROGRAM

In order to provide the general public with greater access to U.S. Government publications, Congress established the Federal Depository Library Program under the Government Printing Office (GPO), with 50 regional depositories responsible for permanent retention of material, inter-library loan, and reference services. At least one copy of nearly every NASA and NASA-sponsored publication, either in printed or microfiche format, is received and retained by the 50 regional depositories. A list of the regional GPO libraries, arranged alphabetically by state, appears on the inside back cover. These libraries are *not* sales outlets. A local library can contact a Regional Depository to help locate specific reports, or direct contact may be made by an individual.

ADDRESSES OF ORGANIZATIONS

American Institute of Aeronautics and Astronautics
Technical Information Service
555 West 57th Street, 12th Floor
New York, New York 10019

British Library Lending Division,
Boston Spa, Wetherby, Yorkshire,
England

Commissioner of Patents and Trademarks
U.S. Patent and Trademark Office
Washington, D.C. 20231

Department of Energy
Technical Information Center
P.O. Box 62
Oak Ridge, Tennessee 37830

ESA-Information Retrieval Service
ESRIN
Via Galileo Galilei
00044 Frascati (Rome) Italy

ESDU International
P.O. Box 1633
Manassas, Virginia 22110

ESDU International, Ltd.
251-259 Regent Street
London, W1R 7AD, England

Fachinformationszentrum Energie, Physik, Mathematik GMBH
7514 Eggenstein Leopoldshafen
Federal Republic of Germany

Her Majesty's Stationery Office
P.O. Box 569, S.E. 1
London, England

NASA Scientific and Technical Information Facility
P.O. Box 8757
B.W.I. Airport, Maryland 21240

National Aeronautics and Space Administration
Scientific and Technical Information Division (NTT)
Washington, D.C. 20546

National Technical Information Service
5285 Port Royal Road
Springfield, Virginia 22161

Pendragon House, Inc.
899 Broadway Avenue
Redwood City, California 94063

Superintendent of Documents
U.S. Government Printing Office
Washington, D.C. 20402

University Microfilms
A Xerox Company
300 North Zeeb Road
Ann Arbor, Michigan 48106

University Microfilms, Ltd.
Tylers Green
London, England

U.S. Geological Survey Library
National Center - MS 950
12201 Sunrise Valley Drive
Reston, Virginia 22092

U.S. Geological Survey Library
2255 North Gemini Drive
Flagstaff, Arizona 86001

U.S. Geological Survey
345 Middlefield Road
Menlo Park, California 94025

U.S. Geological Survey Library
Box 25046
Denver Federal Center, MS914
Denver, Colorado 80225

NTIS PRICE SCHEDULES

(Effective January 1, 1989)

Schedule A
STANDARD PRICE DOCUMENTS AND MICROFICHE

PRICE CODE	NORTH AMERICAN PRICE	FOREIGN PRICE
A01	$ 6.95	$13.90
A02	10.95	21.90
A03	13.95	27.90
A04-A05	15.95	31.90
A06-A09	21.95	43.90
A10-A13	28.95	57.90
A14-A17	36.95	73.90
A18-A21	42.95	85.90
A22-A25	49.95	99.90
A99	*	*
NO1	55.00	70.00
NO2	55.00	80.00

Schedule E
EXCEPTION PRICE DOCUMENTS AND MICROFICHE

PRICE CODE	NORTH AMERICAN PRICE	FOREIGN PRICE
E01	$ 9.00	18.00
E02	11.50	23.00
E03	13.00	26.00
E04	15.50	31.00
E05	17.50	35.00
E06	20.50	41.00
E07	23.00	46.00
E08	25.50	51.00
E09	28.00	56.00
E10	31.00	62.00
E11	33.50	67.00
E12	36.50	73.00
E13	39.00	78.00
E14	42.50	85.00
E15	46.00	92.00
E16	50.50	101.00
E17	54.50	109.00
E18	59.00	118.00
E19	65.50	131.00
E20	76.00	152.00
E99	*	*

*Contact NTIS for price quote.

IMPORTANT NOTICE

NTIS Shipping and Handling Charges

U.S., Canada, Mexico — ADD $3.00 per TOTAL ORDER

All Other Countries — ADD $4.00 per TOTAL ORDER

Exceptions — Does NOT apply to:

ORDERS REQUESTING NTIS RUSH HANDLING
ORDERS FOR SUBSCRIPTION OR STANDING ORDER PRODUCTS *ONLY*

NOTE: Each additional delivery address on an order requires a separate shipping and handling charge.

VOLUME 27 NUMBER 13 / JULY 8, 1989

TABLE OF CONTENTS

AERONAUTICS

Includes aeronautics (general); aerodynamics; air transportation and safety; aircraft communications and navigation; aircraft design, testing and performance; aircraft instrumentation; aircraft propulsion and power; aircraft stability and control; and research and support facilities (air).

For related information see also *Astronautics.*

01 AERONAUTICS (GENERAL) 1767

02 AERODYNAMICS 1769

Includes aerodynamics of bodies, combinations, wings, rotors, and control surfaces; and internal flow in ducts and turbomachinery.

For related information see also *34 Fluid Mechanics and Heat Transfer*

03 AIR TRANSPORTATION AND SAFETY 1770

Includes passenger and cargo air transport operations; and aircraft accidents.

For related information see also *16 Space Transportation* and *85 Urban Technology and Transportation.*

04 AIRCRAFT COMMUNICATIONS AND NAVIGATION 1771

Includes digital and voice communication with aircraft; air navigation systems (satellite and ground based); and air traffic control.

For related information see also *17 Space Communications, Spacecraft Communications, Command and Tracking* and *32 Communications and Radar.*

05 AIRCRAFT DESIGN, TESTING AND PERFORMANCE 1772

Includes aircraft simulation technology.

For related information see also *18 Spacecraft Design, Testing and Performance* and *39 Structural Mechanics.* For land transportation vehicles see *85 Urban Technology and Transportation.*

06 AIRCRAFT INSTRUMENTATION 1774

Includes cockpit and cabin display devices; and flight instruments.

For related information see also *19 Spacecraft Instrumentation* and *35 Instrumentation and Photography.*

07 AIRCRAFT PROPULSION AND POWER 1774

Includes prime propulsion systems and systems components, e.g., gas turbine engines and compressors; and onboard auxiliary power plants for aircraft.

For related information see also *20 Spacecraft Propulsion and Power, 28 Propellants and Fuels,* and *44 Energy Production and Conversion.*

08 AIRCRAFT STABILITY AND CONTROL 1777

Includes aircraft handling qualities; piloting; flight controls; and autopilots.

For related information see also *05 Aircraft Design, Testing and Performance.*

09 RESEARCH AND SUPPORT FACILITIES (AIR) 1778

Includes airports, hangars and runways; aircraft repair and overhaul facilities; wind tunnels; shock tubes; and aircraft engine test stands.

For related information see also *14 Ground Support Systems and Facilities (Space).*

ASTRONAUTICS

Includes astronautics (general); astrodynamics; ground support systems and facilities (space); launch vehicles and space vehicles; space transportation; space communications, spacecraft communications, command and tracking; spacecraft design, testing and performance; spacecraft instrumentation; and spacecraft propulsion and power.

For related information see also *Aeronautics*

12 ASTRONAUTICS (GENERAL) 1779

For extraterrestrial exploration see *91 Lunar and Planetary Exploration.*

13 ASTRODYNAMICS 1780

Includes powered and free-flight trajectories; and orbital and launching dynamics.

14 GROUND SUPPORT SYSTEMS AND FACILITIES (SPACE) N.A.

Includes launch complexes, research and production facilities; ground support equipment, e.g., mobile transporters; and simulators.

For related information see also *09 Research and Support Facilities (Air).*

15 LAUNCH VEHICLES AND SPACE VEHICLES 1781

Includes boosters; operating problems of launch/space vehicle systems; and reusable vehicles.

For related information see also *20 Spacecraft Propulsion and Power.*

16 SPACE TRANSPORTATION 1781

Includes passenger and cargo space transportation, e.g., shuttle operations; and space rescue techniques.

For related information see also *03 Air Transportation and Safety* and *18 Spacecraft Design, Testing and Performance.* For space suits see *54 Man/System Technology and Life Support.*

17 SPACE COMMUNICATIONS, SPACECRAFT COMMUNICATIONS, COMMAND AND TRACKING N.A.

Includes telemetry; space communications networks; astronavigation and guidance; and radio blackout.

For related information see also *04 Aircraft Communications and Navigation* and *32 Communications and Radar.*

18 SPACECRAFT DESIGN, TESTING AND PERFORMANCE 1782

Includes satellites; space platforms; space stations; spacecraft systems and components such as thermal and environmental controls; and attitude controls.

For life support systems see *54 Man/System Technology and Life Support.* For related information see also *05 Aircraft Design, Testing and Performance, 39 Structural Mechanics,* and *16 Space Transportation.*

19 SPACECRAFT INSTRUMENTATION N.A.

For related information see also *06 Aircraft Instrumentation* and *35 Instrumentation and Photography.*

20 SPACECRAFT PROPULSION AND POWER 1785

Includes main propulsion systems and components, e.g. rocket engines; and spacecraft auxiliary power sources.

For related information see also *07 Aircraft Propulsion and Power, 28 Propellants and Fuels, 44 Energy Production and Conversion,* and *15 Launch Vehicles and Space Vehicles.*

CHEMISTRY AND MATERIALS

Includes chemistry and materials (general); composite materials; inorganic and physical chemistry; metallic materials; nonmetallic materials; propellants and fuels; and materials processing.

23 CHEMISTRY AND MATERIALS (GENERAL) N.A.

24 COMPOSITE MATERIALS 1786

Includes physical, chemical, and mechanical properties of laminates and other composite materials.

For ceramic materials see *27 Nonmetallic Materials.*

25 INORGANIC AND PHYSICAL CHEMISTRY 1788

Includes chemical analysis, e.g., chromatography; combustion theory; electrochemistry; and photochemistry.

For related information see also *77 Thermodynamics and Statistical Physics.*

26 METALLIC MATERIALS 1790

Includes physical, chemical, and mechanical properties of metals, e.g., corrosion; and metallurgy.

27 NONMETALLIC MATERIALS 1793

Includes physical, chemical, and mechanical properties of plastics, elastomers, lubricants, polymers, textiles, adhesives, and ceramic materials.

For composite materials see *24 Composite Materials.*

28 PROPELLANTS AND FUELS 1797

Includes rocket propellants, igniters and oxidizers; their storage and handling procedures; and aircraft fuels.

For related information see also *07 Aircraft Propulsion and Power, 20 Spacecraft Propulsion and Power,* and *44 Energy Production and Conversion.*

29 MATERIALS PROCESSING 1798

Includes space-based development of products and processes for commercial application.

For biological materials see *55 Space Biology.*

ENGINEERING

Includes engineering (general); communications and radar; electronics and electrical engineering; fluid mechanics and heat transfer; instrumentation and photography; lasers and masers; mechanical engineering; quality assurance and reliability; and structural mechanics.

For related information see also *Physics.*

31 ENGINEERING (GENERAL) 1806

Includes vacuum technology; control engineering; display engineering; cryogenics; and fire prevention.

32 COMMUNICATIONS AND RADAR 1807

Includes radar; land and global communications; communications theory; and optical communications.

For related information see also *04 Aircraft Communications and Navigation* and *17 Space Communications, Spacecraft Communications, Command and Tracking.* For search and rescue see *03 Air Transportation and Safety,* and *16 Space Transportation.*

33 ELECTRONICS AND ELECTRICAL ENGINEERING 1816

Includes test equipment and maintainability; components, e.g., tunnel diodes and transistors; microminiaturization; and integrated circuitry.

For related information see also *60 Computer Operations and Hardware* and *76 Solid-State Physics.*

34 FLUID MECHANICS AND HEAT TRANSFER 1820

Includes boundary layers; hydrodynamics; fluidics; mass transfer and ablation cooling.

For related information see also *02 Aerodynamics* and *77 Thermodynamics and Statistical Physics.*

35 INSTRUMENTATION AND PHOTOGRAPHY 1823

Includes remote sensors; measuring instruments and gages; detectors; cameras and photographic supplies; and holography.

For aerial photography see *43 Earth Resources and Remote Sensing.* For related information see also *06 Aircraft Instrumentation* and *19 Spacecraft Instrumentation.*

36 LASERS AND MASERS 1825

Includes parametric amplifiers.

For related information see also *76 Solid-State Physics.*

37 MECHANICAL ENGINEERING 1829

Includes auxiliary systems (nonpower); machine elements and processes; and mechanical equipment.

38 QUALITY ASSURANCE AND RELIABILITY 1833

Includes product sampling procedures and techniques; and quality control.

39 STRUCTURAL MECHANICS 1835

Includes structural element design and weight analysis; fatigue; and thermal stress.

For applications see *05 Aircraft Design, Testing and Performance* and *18 Spacecraft Design, Testing and Performance.*

GEOSCIENCES

Includes geosciences (general); earth resources and remote sensing; energy production and conversion; environment pollution; geophysics; meteorology and climatology; and oceanography.

For related information see also *Space Sciences.*

42 GEOSCIENCES (GENERAL) **N.A.**

43 EARTH RESOURCES AND REMOTE SENSING **1841**

Includes remote sensing of earth resources by aircraft and spacecraft; photogrammetry; and aerial photography.

For instrumentation see *35 Instrumentation and Photography.*

44 ENERGY PRODUCTION AND CONVERSION **1843**

Includes specific energy conversion systems, e.g., fuel cells; global sources of energy; geophysical conversion; and windpower.

For related information see also *07 Aircraft Propulsion and Power, 20 Spacecraft Propulsion and Power,* and *28 Propellants and Fuels.*

45 ENVIRONMENT POLLUTION **1845**

Includes atmospheric, noise, thermal, and water pollution.

46 GEOPHYSICS **1847**

Includes aeronomy; upper and lower atmosphere studies; ionospheric and magnetospheric physics; and geomagnetism.

For space radiation see *93 Space Radiation.*

47 METEOROLOGY AND CLIMATOLOGY **1848**

Includes weather forecasting and modification.

48 OCEANOGRAPHY **1851**

Includes biological, dynamic, and physical oceanography; and marine resources.

For related information see also *43 Earth Resources and Remote Sensing.*

LIFE SCIENCES

Includes life sciences (general); aerospace medicine; behavioral sciences; man/system technology and life support; and space biology.

51 LIFE SCIENCES (GENERAL) **1852**

52 AEROSPACE MEDICINE **1853**

Includes physiological factors; biological effects of radiation; and effects of weightlessness on man and animals.

53 BEHAVIORAL SCIENCES **1854**

Includes psychological factors; individual and group behavior; crew training and evaluation; and psychiatric research.

54 MAN/SYSTEM TECHNOLOGY AND LIFE SUPPORT **1854**

Includes human engineering; biotechnology; and space suits and protective clothing.

For related information see also *16 Space Transportation.*

55 SPACE BIOLOGY **N.A.**

Includes exobiology; planetary biology; and extraterrestrial life.

MATHEMATICAL AND COMPUTER SCIENCES

Includes mathematical and computer sciences (general); computer operations and hardware; computer programming and software; computer systems; cybernetics; numerical analysis; statistics and probability; systems analysis; and theoretical mathematics.

59 MATHEMATICAL AND COMPUTER SCIENCES (GENERAL) **1855**

60 COMPUTER OPERATIONS AND HARDWARE **1856**

Includes hardware for computer graphics, firmware, and data processing.

For components see *33 Electronics and Electrical Engineering.*

61 COMPUTER PROGRAMMING AND SOFTWARE **1857**

Includes computer programs, routines, algorithms, and specific applications, e.g., CAD/CAM.

62 COMPUTER SYSTEMS **1865**

Includes computer networks and special application computer systems.

63 CYBERNETICS **1868**

Includes feedback and control theory, artificial intelligence, robotics and expert systems.

For related information see also *54 Man/System Technology and Life Support.*

64 NUMERICAL ANALYSIS **1870**

Includes iteration, difference equations, and numerical approximation.

65 STATISTICS AND PROBABILITY **1878**

Includes data sampling and smoothing; Monte Carlo method; and stochastic processes.

66 SYSTEMS ANALYSIS **1878**

Includes mathematical modeling; network analysis; and operations research.

67 THEORETICAL MATHEMATICS **1879**

Includes topology and number theory.

PHYSICS

Includes physics (general); acoustics; atomic and molecular physics; nuclear and high-energy physics; optics; plasma physics; solid-state physics; and thermodynamics and statistical physics.

For related information see also *Engineering.*

70 PHYSICS (GENERAL) **1879**

For precision time and time interval (PTTI) see *35 Instrumentation and Photography;* for geophysics, astrophysics or solar physics see *46 Geophysics, 90 Astrophysics,* or *92 Solar Physics.*

71 ACOUSTICS 1880
Includes sound generation, transmission, and attenuation.
For noise pollution see *45 Environment Pollution.*

72 ATOMIC AND MOLECULAR PHYSICS 1881
Includes atomic structure, electron properties, and molecular spectra.

73 NUCLEAR AND HIGH-ENERGY PHYSICS 1882
Includes elementary and nuclear particles; and reactor theory.
For space radiation see *93 Space Radiation.*

74 OPTICS 1883
Includes light phenomena and optical devices.
For lasers see *36 Lasers and Masers.*

75 PLASMA PHYSICS 1884
Includes magnetohydrodynamics and plasma fusion.
For ionospheric plasmas see *46 Geophysics.* For space plasmas see *90 Astrophysics.*

76 SOLID-STATE PHYSICS 1886
Includes superconductivity.
For related information see also *33 Electronics and Electrical Engineering* and *36 Lasers and Masers.*

77 THERMODYNAMICS AND STATISTICAL PHYSICS 1892
Includes quantum mechanics; theoretical physics; and Bose and Fermi statistics.
For related information see also *25 Inorganic and Physical Chemistry* and *34 Fluid Mechanics and Heat Transfer.*

SOCIAL SCIENCES

Includes social sciences (general); administration and management; documentation and information science; economics and cost analysis; law, political science, and space policy; and urban technology and transportation.

80 SOCIAL SCIENCES (GENERAL) N.A.
Includes educational matters.

81 ADMINISTRATION AND MANAGEMENT 1893
Includes management planning and research.

82 DOCUMENTATION AND INFORMATION SCIENCE 1894
Includes information management; information storage and retrieval technology; technical writing; graphic arts; and micrography.
For computer documentation see *61 Computer Programming and Software.*

83 ECONOMICS AND COST ANALYSIS 1895
Includes cost effectiveness studies.

84 LAW, POLITICAL SCIENCE AND SPACE POLICY 1895
Includes NASA appropriation hearings; aviation law; space law and policy; international law; international cooperation; and patent policy.

85 URBAN TECHNOLOGY AND TRANSPORTATION 1896
Includes applications of space technology to urban problems; technology transfer; technology assessment; and surface and mass transportation.
For related information see *03 Air Transportation and Safety, 16 Space Transportation,* and *44 Energy Production and Conversion.*

SPACE SCIENCES

Includes space sciences (general); astronomy; astrophysics; lunar and planetary exploration; solar physics; and space radiation.
For related information see also *Geosciences.*

88 SPACE SCIENCES (GENERAL) N.A.

89 ASTRONOMY 1896
Includes radio, gamma-ray, and infrared astronomy; and astrometry.

90 ASTROPHYSICS 1897
Includes cosmology; celestial mechanics; space plasmas; and interstellar and interplanetary gases and dust.
For related information see also *75 Plasma Physics.*

91 LUNAR AND PLANETARY EXPLORATION 1900
Includes planetology; and manned and unmanned flights.
For spacecraft design or space stations see *18 Spacecraft Design, Testing and Performance.*

92 SOLAR PHYSICS 1900
Includes solar activity, solar flares, solar radiation and sunspots.
For related information see *93 Space Radiation.*

93 SPACE RADIATION 1901
Includes cosmic radiation; and inner and outer earth's radiation belts.
For biological effects of radiation see *52 Aerospace Medicine.* For theory see *73 Nuclear and High-Energy Physics.*

GENERAL

Includes aeronautical, astronautical, and space science related histories, biographies, and pertinent reports too broad for categorization; histories or broad overviews of NASA programs.

99 GENERAL 1903

Note: N.A. means that no abstracts were assigned to this category for this issue.

SUBJECT INDEX I-1
PERSONAL AUTHOR INDEX I-51
CORPORATE SOURCE INDEX I-59
CONTRACT NUMBER INDEX I-71
REPORT/ACCESSION NUMBER INDEX I-73

TYPICAL CITATION AND ABSTRACT

NASA SPONSORED
ON MICROFICHE
ACCESSION NUMBER
N89-11793*# Draper (Charles Stark) Lab., Inc., Cambridge, Mass.
CORPORATE SOURCE
TITLE
CONTROL OF FLEXIBLE STRUCTURES-2 (COFS-2) FLIGHT CONTROL, STRUCTURE AND GIMBAL SYSTEM INTERACTION STUDY Final Report
AUTHORS
Stanley Fay, Stephen Gates, Timothy Henderson, Lester Sackett, Kim Kirchwey, Isaac Stoddard, and Joel Storch Sep. 1988
PUBLICATION DATE
205 p
CONTRACT OR GRANT
(Contract NAS9-17560)
REPORT NUMBERS
(NASA-CR-172095; R-2088; NAS 1.26:172095) Avail: NTIS HC
AVAILABILITY SOURCE
PRICE CODE
A10/MF A01 CSCL 22B
COSATI CODE
The second Control Of Flexible Structures Flight Experiment (COFS-2) includes a long mast as in the first flight experiment, but with the Langley 15-m hoop column antenna attached via a gimbal system to the top of the mast. The mast is to be mounted in the Space Shuttle cargo bay. The servo-driven gimbal system could be used to point the antenna relative to the mast. The dynamic interaction of the Shuttle Orbiter/COFS-2 system with the Orbiter on-orbit Flight Control System (FCS) and the gimbal pointing control system has been studied using analysis and simulation. The Orbiter pointing requirements have been assessed for their impact on allowable free drift time for COFS experiments. Three fixed antenna configurations were investigated. Also simulated was Orbiter attitude control behavior with active vernier jets during antenna slewing. The effect of experiment mast dampers was included. Control system stability and performance and loads on various portions of the COFS-2 structure were investigated. The study indicates possible undesirable interaction between the Orbiter FCS and the flexible, articulated COFS-2 mast/antenna system, even when restricted to vernier reaction jets. Author

VOLUME 27 NUMBER 13 / JULY 8, 1989

Scientific and Technical Aerospace Reports

A Semimonthly Publication of the National Aeronautics and Space Administration

01 AERONAUTICS (GENERAL)

N89-20086*# National Aeronautics and Space Administration, Washington, DC.
PERFORMANCE AND TEST SECTION FLOW CHARACTERISTICS OF THE NATIONAL FULL-SCALE AERODYNAMICS COMPLEX 40- BY 80-FOOT WIND TUNNEL
Peter T. Zell and Karen Flack Feb. 1989 81 p
(NASA-TM-101065; A-89028; NAS 1.15:101065) Avail: NTIS HC A05/MF A01 CSCL 01A

Results from the performance and test section flow calibration of the 40-by 80-Foot Wind Tunnel are presented. A flow calibration test was conducted in May and June 1987. The goal of the flow calibration test was to determine detailed spatial variations in the 40-by 80-ft test section flow quality throughout the tunnel operational envelope. Data were collected for test section speeds up to 300 knots and for air exchange rates of 0, 5, and 10 percent. The tunnel performance was also calibrated during the detailed mapping of the test section flow field. Experimental results presented indicate that the flow quality in the test section, with the exception of temperature, is relatively insensitive to the level of dynamic pressure and the air exchange rate. The dynamic pressure variation in the test section is within + or - 0.5 deg at all test section velocities. Cross-stream temperature gradients in the test section caused by the air exchange system were documented, and a correction method was established. Streamwise static pressure variation on the centerline is about 1 percent of test section dynamic pressure over 30 ft of the test section length. Author

N89-20087# National Aerospace Lab., Amsterdam (Netherlands). Structures and Materials Div.
ENVIRONMENT-ASSISTED AEROSPACE FATIGUE PROBLEMS IN THE NETHERLANDS
R. J. H. Wanhill 2 Feb. 1988 24 p Presented at the Environmentally Assisted Fatigue Symposium, Sheffield, England, Apr. 1988
(NLR-MP-88004-U; ETN-89-94053) Avail: NTIS HC A03/MF A01

Corrosion and environment-assisted fatigue problems in aircraft, and the measures taken to alleviate them are reviewed. Landing gear, airframes, flying controls, propellers and rotor blades, and engines are discussed. ESA

N89-20088* National Aeronautics and Space Administration, Washington, DC.
AERONAUTICAL ENGINEERING: A CUMULATIVE INDEX TO A CONTINUING BIBLIOGRAPHY (SUPPLEMENT 235)
Feb. 1989 502 p
(NASA-SP-7037(235); NAS 1.21:7037(235)) Avail: NTIS HC A22; NTIS standing order as PB89-914100, $10.50 domestic, $21.00 foreign CSCL 01B

This publication is a cummulative index to the abstracts contained in Supplements 223 through 234 of Aeronautical Engineering: A Continuing Bibliography. The bibliographic series is compiled through the cooperative efforts of the American Institute of Aeronautics and Astronautics (AIAA) and the National Aeronautics and Space Administration (NASA). Seven indexes are included -- subject, personal author, corporate source, foreign technology, contract number, report number and accession number. Author

N89-20089* National Aeronautics and Space Administration, Washington, DC.
AERONAUTICAL ENGINEERING: A CONTINUING BIBLIOGRAPHY WITH INDEXES (SUPPLEMENT 237)
Mar. 1989 150 p
(NASA-SP-7037(237); NAS 1.21:7037(237)) Avail: NTIS HC A08; NTIS standing order as PB89-914100, $10.50 domestic, $21.00 foreign CSCL 01B

This bibliography lists 572 reports, articles, and other documents introduced into the NASA scientific and technical information system in February, 1989. Subject coverage includes: design, construction and testing of aircraft and aircraft engines; aircraft components, equipment and systems; ground support systems; and theoretical and applied aspects of aerodynamics and general fluid dynamics. Author

N89-20090* National Aeronautics and Space Administration, Washington, DC.
AERONAUTICAL ENGINEERING: A CONTINUING BIBLIOGRAPHY WITH INDEXES (SUPPLEMENT 238)
Dec. 1988 126 p
(NASA-SP-7037(238); NAS 1.21:7037(238)) Avail: NTIS HC A08; NTIS standing order as PB89-914100, $10.50 domestic, $21.00 foreign CSCL 01B

This bibliography lists 458 reports, articles, and other documents introduced into the NASA scientific and technical information system in March, 1989. Subject coverage includes: design, construction and testing of aircraft and aircraft engines; aircraft components, equipment and systems; ground support systems; and theoretical and applied aspects of aerodynamics and general fluid dynamics. Author

N89-20091* National Aeronautics and Space Administration, Washington, DC.
AERONAUTICAL ENGINEERING: A CONTINUING BIBLIOGRAPHY WITH INDEXES (SUPPLEMENT 236)
Feb. 1989 119 p
(NASA-SP-7037(236); NAS 1.21:7037(236)) Avail: NTIS HC A06; NTIS standing order as PB89-914100, $10.50 domestic, $21.00 foreign CSCL 01B

This bibliography lists 430 reports, articles, and other documents introduced into the NASA scientific and technical information system in January, 1989. Subject coverage includes: design, construction and testing of aircraft and aircraft engines; aircraft components, equipment and systems; ground support systems; and theoretical and applied aspects of aerodynamics and general fluid dynamics. Author

02 AERODYNAMICS

Includes aerodynamics of bodies, combinations, wings, rotors, and control surfaces; and internal flow in ducts and turbomachinery.

For related information see also *34 Fluid Mechanics and Heat Transfer.*

N89-20092# National Center for Atmospheric Research, Boulder, CO. Atmospheric Technology Div.
POSITION ERROR CALIBRATION OF A PRESSURE SURVEY AIRCRAFT USING A TRAILING CONE
Edward N. Brown Jul. 1988 37 p
(Grant NSF ATM-87-09659)
(PB88-250733; NCAR/TN-313-STR) Avail: NTIS HC A03/MF A01 CSCL 01A

A review is presented of the trailing cone development and testing, application procedures and the results of position error evaluation over a wide speed and altitude range. The position error of the NCAR Sabreliner determined by the trailing cone method is different from the error determined from earlier tower flights. Independent comparisons with pacer aircraft confirm the static pressure differences between the two position error functions. D-values during deceleration maneuvers at the pressure survey altitudes indicate the coefficients of the dynamic pressure terms of either correction function are valid and the versatility of the trailing cone method provides sufficient data to indicate the position error has no significant Mach number sensitivity in the medium to high subsonic range. The uncertainty or the largest expected error in the Sabreliner static pressure measurement after correction for position error is + or - 0.39mb. Author

N89-20093*# Boeing Commercial Airplane Co., Seattle, WA.
DEVELOPMENT AND APPLICATION OF A PROGRAM TO CALCULATE TRANSONIC FLOW AROUND AN OSCILLATING THREE-DIMENSIONAL WING USING FINITE DIFFERENCE PROCEDURES Final Report
Warren H. Weatherill and F. Edward Ehlers Feb. 1989 91 p
(Contract NAS1-17977)
(NASA-CR-181744; NAS 1.26:181744; D6-54693) Avail: NTIS HC A05/MF A01 CSCL 01A

A finite difference method for solving the unsteady transonic flow about harmonically oscillating wings is investigated. The procedure is based on separating the velocity potential into steady and unsteady parts and linearizing the resulting unsteady differential equation for small disturbances. The differential equation for the unsteady potential is linear with spatially varying coefficients and with the time variable eliminated by assuming harmonic motion. Difference equations are derived for harmonic transonic flow to include a coordinate transformation for swept and tapered planforms. A pilot program is developed for three-dimensional planar lifting surface configurations (including thickness) for the CRAY-XMP at Boeing Commercial Airplanes and for the CYBER VPS-32 at the NASA Langley Research Center. An investigation is made of the effect of the location of the outer boundaries on accuracy for very small reduced frequencies. Finally, the pilot program is applied to the flutter analysis of a rectangular wing.
Author

N89-20094*# National Aeronautics and Space Administration. Langley Research Center, Hampton, VA.
SOME LOW-SPEED FLUTTER CHARACTERISTICS OF SIMPLE LOW-ASPECT-RATIO DELTA WING MODELS
Robert V. Doggett, Jr. and David L. Soistmann (Planning Research Corp., Hampton, VA.) Jan. 1989 11 p Presented at the 30th AIAA/ASME/AHS/ASC Structures, Structural Dynamics and Materials Conference, Mobile, AL, 3-4 Apr. 1989
(NASA-TM-101547; NAS 1.15:101547; AIAA-89-1325) Avail: NTIS HC A03/MF A01 CSCL 01A

Some results from a combined experimental and analytical study of the low-speed flutter characteristics of low-aspect-ratio delta wings are presented. Data are presented which show the effects of sweep angle on the flutter characteristics of some simple plate models of constant planform area. The range of sweep angles studied was from 30 to 72 degrees. In addition, flutter results are presented for two 30 deg-sweep clipped-delta wing models. Further, results are presented that show the effects of root clamping (percentage length of the root chord that is cantilevered) for a 45 deg-sweep delta wing. The experimental data are compared with analytical results obtained by using kernel function and doublet lattice subsonic unsteady lifting surface theories. Author

N89-20095*# Institute for Computer Applications in Science and Engineering, Hampton, VA.
MULTIGRID SOLUTION OF THE NAVIER-STOKES EQUATIONS ON TRIANGULAR MESHES Final Report
Dimitri J. Mavriplis, Antony Jameson, and Luigi Martinelli (Princeton Univ., NJ.) Feb. 1989 37 p Submitted for publication
Prepared for NASA, Langley Research Center, Hampton, VA
(Contracts NAS1-18107; NAS1-18605)
(NASA-CR-181786; ICASE-89-11; NAS 1.26:181786) Avail: NTIS HC A03/MF A01 CSCL 01A

A Navier-Stokes algorithm for use on unstructured triangular meshes is presented. Spatial discretization of the governing equations is achieved using a finite element Galerkin approximation, which can be shown to be equivalent to a finite volume approximation for regular equilateral triangular meshes. Integration steady-state is performed using a multistage time-stepping scheme, and convergence is accelerated by means of implicit residual smoothing and an unstructured multigrid algorithm. Directional scaling of the artificial dissipation and the implicit residual smoothing operator is achieved for unstructured meshes by considering local mesh stretching vectors at each point. The accuracy of the scheme for highly stretched trianguiar meshes is validated by comparing computed flat-plate laminar boundary layer results with the well known similarity solution, and by comparing laminar airfoil results with those obtained from various well-established structured quadrilateral-mesh codes. The convergence efficiency of the present method is also shown to be competitive with those demonstrated by structured quadrilateral-mesh algorithms.
Author

N89-20096 Leicester Univ. (England).
HIGH REYNOLDS NUMBER INCOMPRESSIBLE FLOW SIMULATION ABOUT PARACHUTE CANOPIES AND SIMILAR BLUFF BODIES Ph.D. Thesis
Yaacov I. Frucht 1987 219 p
Avail: Univ. Microfilms Order No. BRD-82605

A model for the flow around bluff bodies was developed. It is applied to an investigation of parachute canopy aerodynamic characteristics. The model assumes an axisymmetric incompressible high Reynolds number flow, applicable to the calculation of aerodynamic characteristics at zero angle of attack. The flow is assumed to separate from the canopy at its hemline. The vorticity is carried downstream, forming a free shear layer. In the flow field vorticity is confined to the shear layer, outside it the flow is irrotational. A velocity potential can be defined in the fluid field. The canopy surface is replaced by a vortex ring panel lattice. Each panel contains a circular bound vortex ring which is located at one quarter panel length. For each panel the flow boundary conditions on the canopy surface are fulfilled along a control circle at three quarters of the panel length. In the vortex modelling of the separated wake a number of elements were introduced: improvement of the near wake simulation by accounting for the standing eddy on the canopy under surface; a simple method of calculating the newly created vortex ring strength and location; and reduction of the free parameters from two, the time step and the number of panels representing the canopy surface to one, i.e., the number of panels. Further model validation and implementation were suggested. Methods of model development for asymmetric canopy representation were discussed.
Dissert. Abstr.

N89-20097 Old Dominion Univ., Norfolk, VA.
VISCOUS SHOCK LAYER ANALYSIS OF HYPERSONIC FLOWS OVER LONG SLENDER VEHICLES Ph.D. Thesis

Kam-Pui Lee 1988 222 p
Avail: Univ. Microfilms Order No. DA8823955

A method for solving the viscous shock layer equations for hypersonic flows over long slender bodies is presented. The governing equations are solved by employing a spatial marching implicit finite difference technique. The two first order equations, continuity and normal momentum, are solved simultaneously as a coupled set. This method yields a simple and computationally efficient technique. Flows past hyperboloids and sphere cones with body half angles of 5 to 35 deg are considered. The flow conditions included are from high Reynolds numbers at low altitudes to low Reynolds numbers at high altitudes. Detailed comparisons were made with other predictions and experimental data for slender body flows. The results show that the coupling between the continuity and normal momentum equations is essential and adequate to obtain stable and accurate solutions past long slender bodies. Both the Cebeci-Smith and Baldwin-Lomax turbulence models are found to be adequate for application to long slender bodies. Using the corrected slip models, the viscous shock layer predictions compare favorably with experimental data. Under chemical nonequilibrium conditions, the surface catalytic effects can influence the heat transfer. Dissert. Abstr.

N89-20098*# National Aeronautics and Space Administration. Ames Research Center, Moffett Field, CA.
EVALUATION OF VSAERO IN PREDICTION OF AERODYNAMIC CHARACTERISTICS OF HELICOPTER HUB FAIRINGS
Alexander Louie Feb. 1989 36 p
(NASA-TM-101048; A-88320; NAS 1.15:101048) Avail: NTIS HC A03/MF A01 CSCL 01A

A low-order panel code, VSAERO, was used to predict the aerodynamic characteristics of helicopter hub fairings. Since the simulation of this kind of bluff body by VSAERO was not documented before, the VSAERO solutions were correlated with experimental data to establish their validity. The validation process revealed that simulation of the aerodynamic environment around a hub fairing was sensitive to several modeling parameters. Some of these parameters are body and wake panels arrangement, streamwise and spanwise separation location, and the most prominent one-the wake modeling. Three wake models were used: regular wake, separated wake, and jet model. The regular wake is a wake with negligible thickness (thin wake). It is represented by a single vortex sheet. The separated wake and the jet model in the present application are wakes with finite thickness (thick wake). They consist of a vortex sheet enclosing a region of low-energy flow. The results obtained with the requlr wake were marginally acceptable for sharp-edged hub fairings. For all other cases under consideration, the jet model results correlated slightly better. The separated wake, which seemed to be the most appropriate model, caused the solution to diverge. While the regular wake was straight-forward to apply in simulations, the jet model was not. It requires the user to provide information about the doublet strength gradient on wake panels by guessing the efflux velocities at the wake shedding location. In summary, VSAERO neither predicts accurately the aerodynamic characteristics of helicopter hub fairings nor was cost effective. Author

N89-20099*# National Aeronautics and Space Administration. Langley Research Center, Hampton, VA.
GEOMETRICAL AND STRUCTURAL PROPERTIES OF AN AEROELASTIC RESEARCH WING (ARW-2)
Maynard C. Sandford, David A. Seidel, Clinton V. Eckstrom, and Charles V. Spain (PRC Kentron, Inc., Hampton, VA.) Washington Apr. 1989 40 p
(NASA-TM-4110; L-16545; NAS 1.15:4110) Avail: NTIS HC A03/MF A01 CSCL 01A

Transonic steady and unsteady pressure tests were conducted on a large elastic wing known as the DAST ARW-2 wing. The wing has a supercritical airfoil, an aspect ratio of 10.3, a leading edge sweepback angle of 28.8 deg and is equipped with two inboard and one outboard trailing edge control surfaces. The geometrical and structural characteristics are presented of this elastic wing, using a combination of measured and calculated data, to permit future analyst to compare the experimental surface pressure data with theoretical predictions. Author

N89-20100*# National Aeronautics and Space Administration. Ames Research Center, Moffett Field, CA.
DOCUMENTATION OF TWO- AND THREE-DIMENSIONAL HYPERSONIC SHOCK WAVE/TURBULENT BOUNDARY LAYER INTERACTION FLOWS
Marvin I. Kussoy (Eloret Corp., Sunnyvale, CA.) and Clifford C. Horstman Jan. 1989 26 p
(Contract NCC2-452)
(NASA-TM-101075; A-89048; NAS 1.15:101075) Avail: NTIS HC A03/MF A01 CSCL 01A

Experimental data for a series of two- and three-dimensional shock wave/turbulent boundary layer interaction flows at Mach 7 are presented. Test bodies, composed of simple geometric shapes, were designed to generate flows with varying degrees of pressure gradient, boundary-layer separation, and turning angle. The data include surface-pressure and heat-transfer distributions as well as limited mean-flow-field surveys in both the undisturbed and the interaction regimes. The data are presented in a convenient form for use in validating existing or future computational models of these generic hypersonic flows. Author

N89-20101*# National Aeronautics and Space Administration. Langley Research Center, Hampton, VA.
A CELL-VERTEX MULTIGRID METHOD FOR THE NAVIER-STOKES EQUATIONS
R. Radespiel Jan. 1989 41 p
(NASA-TM-101557; NAS 1.15:101557) Avail: NTIS HC A03/MF A01 CSCL 01A

A cell-vertex scheme for the Navier-Stokes equations, which is based on central difference approximations and Runge-Kutta time stepping, is described. Using local time stepping, implicit residual smoothing, a multigrid method, and carefully controlled artificial dissipative terms, very good convergence rates are obtained for a wide range of two- and three-dimensional flows over airfoils and wings. The accuracy of the code is examined by grid refinement studies and comparison with experimental data. For an accurate prediction of turbulent flows with strong separations, a modified version of the nonequilibrium turbulence model of Johnson and King is introduced, which is well suited for an implementation into three-dimensional Navier-Stokes codes. It is shown that the solutions for three-dimensional flows with strong separations can be dramatically improved, when a nonequilibrium model of turbulence is used. Author

N89-20102# National Aerospace Lab., Amsterdam (Netherlands). Flight Dynamics Div.
OBSERVED REYNOLDS NUMBER EFFECTS ON AIRFOILS AND HIGH ASPECT RATIO WINGS AT TRANSONIC FLOW CONDITIONS
A. Elsenaar 1 Feb. 1988 49 p Presented at the AGARD Special Course on Boundary Layer Simulation Methodology in Transonic Wind Tunnel Testing, Brussels, Belgium and Tullahoma, 1988
(NLR-MP-88006-U; ETN-89-94055) Avail: NTIS HC A03/MF A01

Variation of airfoil and high aspect ratio wing aerodynamic characteristics (lift, pitching moment, drag, drag divergence, and buffet boundaries) as a function of Reynolds number is discussed. Examples related to drag, maximum lift, and pitching moment show that tests with free transition behave qualitatively different from flows with mostly turbulent boundary layer development (whether caused by natural transition close to the leading edge or by artificial means such as fixation). Free transition results can even be very misleading for flight conditions. For Reynolds number effects observed on configurations with fully turbulent boundary layer flow, a distinction between direct Reynolds number effects (resulting from changes in boundary layer development) and indirect Reynolds number effects (that appear as changes in pressure distribution) is made. The question of how relevant two-dimensional flows are

to high aspect ratio wings is addressed. It is argued that certain conditions must be met before one can speak of a good correspondence between two- and three-dimensional flows. The utility of wind tunnel tests for flight prediction is reviewed. ESA

N89-20103# Institut Franco-Allemand de Recherches, Saint-Louis (France).
BASE FLOW INVESTIGATION BEHIND AXI-AND NON-AXISYMMETRIC BLUNT BODIES
C. Berner 10 Dec. 1987 13 p Presented at ICALEO '87 - 6th International Congress on Application of Lasers and Electro-Optics, San Diego, CA, 8-12 Nov., 1987
(ISL-CO-246/87; ETN-89-94112) Avail: NTIS HC A03/MF A01

Experimental investigations of the flow field in the near-wake of blunt afterbodies are presented. Measurements were performed by a two- or three-dimensional frequency shifted laser Doppler velocimeter. Experiments were conducted in a blowdown type annular nozzle whose Mach number variation ranged between 0.2 and 0.9. Models consist of a cylindrical afterbody, and a conical and a triangular boattail. Results include mean velocities and the corresponding mean square velocity fluctuations. They show interesting features of the mean flow field and give accurate information about afterbody flows like local flow direction, size and shape of the recirculating regions, rear stagnation point location, and the differences in flow structure. ESA

N89-20104# Midwest Research Inst., Golden, CO. Solar Energy Research Inst.
AERODYNAMIC PRESSURE AND FLOW-VISUALIZATION MEASUREMENT FROM A ROTATING WIND TURBINE BLADE
C. P. Butterfield Nov. 1988 13 p Presented at the ASME Energy-Sources Technology Conference and Exhibition and 7th Intersociety Cryogenic Symposium, Houston, TX, 22 Jan. 1989
(Contract DE-AC02-83CH-10093)
(DE89-000854; SERI/TP-217-3433; CONF-890102-14) Avail: NTIS HC A03

Aerodynamic, load, flow-visualization, and inflow measurements have been made on a 10-m, three-bladed, downwind, horizontal-axis wind turbine (HAWT). A video camera mounted on the rotor was used to record nighttime and daytime video images of tufts attached to the low-pressure side of a constant-chord, zero-twist blade. Load measurements were made using strain gages mounted at every 10 percent of the blade's span. Pressure measurements were made at 80 percent of the blade's span. Pressure taps were located at 32 chordwise positions, revealing pressure distributions comparable with wind tunnel data. Inflow was measured using a vertical-plane array of eight propvane and five triaxial (U-V-W) prop-type anemometers located 10 m upwind in the predominant wind direction. One objective of this comprehensive research program was to study the effects of blade rotation on aerodynamic behavior below, near, and beyond stall. To this end, flow patterns are presented here that reveal the dynamic and steady behavior of flow conditions on the blade. Pressure distributions are compared to flow patterns and two-dimensional wind tunnel data. Separation boundary locations are shown that change as a function of spanwise location, pitch angle, and wind speed. DOE

N89-20105# Minnesota Univ., Minneapolis. Dept. of Aerospace Engineering and Mechanics.
AERODYNAMICS OF TWO-DIMENSIONAL SLOTTED BLUFF BODIES
F. Takahashi and H. Higuchi 30 Apr. 1988 131 p Prepared for Sandia National Labs., Albuquerque, NM
(Contract DE-AC04-76DP-00789)
(DE89-007288; SAND-88-7151) Avail: NTIS HC A07/MF A01

Aerodynamic characteristics of two-dimensional, slotted bluff bodies were experimentally investigated. Flow visualizations, base pressure measurements, mean velocity vector measurements, and drag force measurements were conducted to analyze effects of spacing ratio (i.e., porosity), curvature, and vent. Low porosity model configurations produced stable near-wake patterns with enhanced vortex sheddings of overall wake formations. Model curvature reduced drag forces and weakened the vortex sheddings. Stabilizing effect of curvature on the near-wake patterns was also found. A vent combined with large model curvature was found to control drag force effectively, as well as suppressing vortex sheddings. DOE

N89-20106# Air Force Academy, CO.
THRUST GENERATION BY AN AIRFOIL IN HOVERING MODE
Peter Freymuth Jan. 1989 31 p
(AD-A203785; FJSRL-TR-89-0002) Avail: NTIS HC A03/MF A01 CSCL 20D

An airfoil is operated in combined plunging and pitching motion to generate a thrusting jet in a still air environment. The device serves as a simple, generic and two-dimensional model for hovering flight of small birds and insects. When properly tuned the device produces very large average thrust coefficients. The vortical signature of the tuned jet is a vortex street with reverse sense of rotation as the vortices of a Karman street. GRA

N89-20107# Naval Civil Engineering Lab., Port Hueneme, CA.
PRESSURE COEFFICIENTS FOR BASIC TENSIONED-MEMBRANE STRUCTURE FORMS
M. Jacoby Nov. 1988 89 p
(Contract C0078E-4-101)
(AD-A203866; NCEL-TN-1789) Avail: NTIS HC A05/MF A01 CSCL 01A

This report details FY85 wind tunnel tests on basic tensioned-membrane structure forms, data reduction and analysis, and results. Models of parallel and diagonally-arched structures were tested. Testing was performed at the James A. Forestal Laboratory wind tunnel, Princeton University, and the environment wind tunnel located at the Naval Civil Engineering Laboratory (NCEL). All data and results have been converted to pressure coefficient form to facilitate their use in wind load calculations. This section details the basic equations and principles used for building aerodynamics and wind tunnel testing. The pressure distribution around a body immersed in a moving fluid is primarily a function of the local variation in fluid velocity produced by the body. GRA

03 AIR TRANSPORTATION AND SAFETY

Includes passenger and cargo air transport operations; and aircraft accidents.

For related information see also *16 Space Transportation* and *85 Urban Technology and Transportation.*

N89-20108# National Transportation Safety Board, Washington, DC. Bureau of Safety Programs.
AIRCRAFT ACCIDENT DATA, US GENERAL AVIATION, CALENDAR YEAR 1986 Annual Review Report
25 Oct. 1988 166 p
(PB89-121453; NTSB/ARG-88/01) Avail: NTIS HC A08/MF A01 CSCL 01C

The report presents a statistical compilation and review of general aviation accidents which occurred in 1986 in the United States, its territories and possessions, and in international waters. The accidents reported are all those involving U.S. registered aircraft not conducting operations under 14 CFR 121, 14 CFR 125, 14 CFR 127, or 14 CFR 135. The report is divided into five sections: All Accidents; Fatal Accidents; Serious Injury Accidents; Property Damage Accidents and Midair Collision Accidents. Several tables present accident parameters for 1986 accidents only, and each section includes tabulations which present comparative statistics for 1986 and for the five-year period 1981 to 1985. GRA

N89-20109# National Transportation Safety Board, Washington, DC. Bureau of Field Operations.
AIRCRAFT ACCIDENT REPORTS: BRIEF FORMAT, US CIVIL AND FOREIGN AVIATION, ISSUE NUMBER 12 OF 1986 ACCIDENTS
30 Mar. 1988 427 p
(PB88-916902; NTSB/AAB-88/02) Avail: NTIS HC A19/MF A01; also available on subscription, North American Continent HC $185.00/year; all others write for quote CSCL 01C

The publication contains selected aircraft accident reports in Brief Format occurring in U.S. civil and foreign aviation operations during Calendar Year 1986. Approximately 200 General Aviation and Air Carrier accidents contained in the publication represent a random selection. The publication is issued irregularly, normally eighteen times each year. The Brief Format represents the facts, conditions, circumstances, and probable cause(s) for each accident. GRA

N89-20110# National Transportation Safety Board, Washington, DC. Bureau of Field Operations.
AIRCRAFT ACCIDENT REPORTS, BRIEF FORMAT, US CIVIL AND FOREIGN AVIATION, ISSUE NUMBER 14 OF 1986 ACCIDENTS
11 Aug. 1988 347 p
(PB88-916904; NTSB/AAB-88/04) Avail: NTIS HC A15/MF A01; also available on subscription, North American Continent HC $185.00/year; all others write for quote CSCL 01C

The publication contains selected aircraft accident reports in Brief Format occurring in U.S. civil and foreign aviation operations during Calendar Year 1986. Approximately 200 General Aviation and Air Carrier accidents contained in the publication represent a random selection. The publication is issued irregularly, normally eighteen times each year. The Brief Format represents the facts, conditions, circumstances and probable cause(s) for each accident. GRA

N89-20111*# Sierra Nevada Corp., Reno.
ANALYSIS OF DOPPLER RADAR WINDSHEAR DATA Final Report
F. Williams, P. McKinney, and F. Ozmen Jan. 1989 189 p
(Contract NAS1-18598)
(NASA-CR-181762; NAS 1.26:181762; DOT/FAA/PS-88/19)
Avail: NTIS HC A09/MF A01 CSCL 01C

The objective of this analysis is to process Lincoln Laboratory Doppler radar data obtained during FLOWS testing at Huntsville, Alabama, in the summer of 1986, to characterize windshear events. The processing includes plotting velocity and F-factor profiles, histogram analysis to summarize statistics, and correlation analysis to demonstrate any correlation between different data fields. Author

N89-20112# National Transportation Safety Board, Washington, DC. Bureau of Accident Investigation.
AIRCRAFT ACCIDENT REPORT: CONTINENTAL AIRLINES, INC., FLIGHT 1713, MCDONNELL DOUGLAS DC-9-14, N626TX, STAPLETON INTERNATIONAL AIRPORT, DENVER, COLORADO, NOVEMBER 15, 1987
27 Sep. 1988 97 p
(PB88-910411; NTSB/AAR-88/09) Avail: NTIS HC A05/MF A01; also available on subscription, North American Continent HC $70.00/year; all others write for quote CSCL 01C

The National Transportation Safety Board decided that the probable cause of the accident was the captain's failure to have the aircraft deiced a second time after a delay before takeoff that led to upper wing surface contamination and a loss of control during rapid takeoff rotation by the first officer. Contributing to the accident were the absence of regulatory or management controls governing operations by newly qualified flight crew members and the confusion that existed between the flight crew and the air traffic controllers that led to the delay in departure. Author

04 AIRCRAFT COMMUNICATIONS AND NAVIGATION

Includes digital and voice communication with aircraft; air navigation systems (satellite and ground based); and air traffic control.

For related information see also *17 Space Communications, Spacecraft Communications, Command and Tracking* and *Communications and Radar.*

N89-20113*# Jet Propulsion Lab., California Inst. of Tech., Pasadena.
HIGH-DYNAMIC GPS TRACKING Final Report
S. Hinedi and J. I. Statman 15 Dec. 1988 95 p
(Contract NAS7-918)
(NASA-CR-184868; JPL-Publ-88-35; NAS 1.26:184868) Avail: NTIS HC A05/MF A01 CSCL 17G

The results of comparing four different frequency estimation schemes in the presence of high dynamics and low carrier-to-noise ratios are given. The comparison is based on measured data from a hardware demonstration. The tested algorithms include a digital phase-locked loop, a cross-product automatic frequency tracking loop, and extended Kalman filter, and finally, a fast Fourier transformation-aided cross-product frequency tracking loop. The tracking algorithms are compared on their frequency error performance and their ability to maintain lock during severe maneuvers at various carrier-to-noise ratios. The measured results are shown to agree with simulation results carried out and reported previously. Author

N89-20114# Royal Signals and Radar Establishment, Malvern (England).
THE APPLICATION OF SOFTWARE FAULT TOLERANCE TO AIR TRAFFIC CONTROL: STUDY CONTRACT OVERVIEW
L. N. Simcox Jun. 1988 21 p
(BR108567; RSRE-Memo-4114) Avail: NTIS HC A03/MF A01

An overview of research done on the application of software fault tolerance to air traffic control (ATC) systems is provided. A requirements analysis of the London Air Traffic Control Centre (LATCC) was developed using the CORE method with automated support. This was then taken as the basis for a MASCOT design of the LATCC Radar Data Processing subsystem. This design was converted into one with the software fault tolerant features of Recovery Blocks in a MASCOT-like environment. Author

N89-20115# National Aerospace Lab., Amsterdam (Netherlands). Flight Div.
THE APPLICATION OF TRAJECTORY PREDICTION ALGORITHMS FOR PLANNING PURPOSES IN THE NETHERLANDS AIR TRAFFIC CONTROL (ATC) SYSTEM
J. N. P. Beers, T. B. Dalm, J. M. tenHave, and H. Visscher 29 Oct. 1986 15 p Submitted for publication
(NLR-MP-87031-U; ETN-89-94034) Avail: NTIS HC A03/MF A01

The Netherlands ATC-environment, the basic set-up of the trajectory prediction module, improvements realized, and the performance figures are presented. Applications of the trajectory prediction results in the system are listed, including data distribution rules, presentation of estimated times of arrival, boundary estimates, and, in particular, long-term detection of conflicts for overflying aircraft, planning in inbound traffic for Schiphol airport, and planning of departure times for an efficient engine start-up procedure. ESA

N89-20116# National Aerospace Lab., Amsterdam (Netherlands). Informatics Div.
FUTURE SATELLITE NAVIGATION SYSTEMS, WITH EMPHASIS ON NAVSTAR GPS
O. B. M. Pietersen 31 May 1987 26 p Presented at the Post Academic Course on Radionavigation Systems, Delft, The Netherlands, 17-19 Jun. 1987
(NLR-MP-87034-U; ETN-89-94035) Avail: NTIS HC A03/MF A01

The principles of NAVSTAR GPS, GLONASS, NAVSAT, and GRANAS are described. Similarities between NAVSTAR and GLONASS are noted. The harmonized NAVSAT/GRANAS concept is outlined. ESA

N89-20117# National Aerospace Lab., Amsterdam (Netherlands). Flight Div.
CONTINUOUS-DISCRETE FILTERING FOR SYSTEMS WITH MARKOVIAN SWITCHING COEFFICIENTS
H. A. P. Blom 30 Oct. 1987 20 p Presented at the 21st Asilomar Conference on Signals, Systems and Computers, Pacific Grove, CA, 2-4 Nov. 1987
(NLR-MP-87076-U; ETN-89-94046) Avail: NTIS HC A03/MF A01

The classical continuous-time linear system with Markovian switching coefficients is extended, to incorporate jumps in R sup n which occur simultaneously with coefficient switching. This system is defined by a stochastic differential equation in a hybrid space, which is driven by a Brownian motion and a Poisson random measure with a randomly time-changed mean measure. The exact continuous-discrete filter for such a system is approximated by a numerical algorithm, which is in its most simple form the interacting multiple model algorithm. For application to the problem of tracking a maneuvering aircraft, given measurements of uncertain origin, the obtained methods can easily be combined with probabilistic data association. ESA

N89-20118# National Aerospace Lab., Amsterdam (Netherlands). Informatics Div.
SYSTEM SIMULATION USING THE PROMISE SIMULATION PACKAGE
G. J. Dekker and H. deJong 7 Jan. 1987 18 p In DUTCH; ENGLISH summary
(NLR-MP-87081-U; ETN-89-94050) Avail: NTIS HC A03/MF A01

The PROMISE computer-based, general simulation tool for studying systems consisting of concurrent processes exchanging discrete signals that influence these processes is described. Because of its general set-up, it can be applied to simulation of a variety of discrete systems. Through the modular approach of its set-up, models and submodels of the simulated system can be easily substituted for other (sub) models (if necessary more detailed) without affecting the general structure of the simulator. This enables not only fast and effective parameter studies, but also versatile detailed studies of various relevant aspects. ESA

N89-20119# Sandia National Labs., Albuquerque, NM. Exploratory Systems Development Div.
TRAJECTORY SCORING IN RECTANGULAR COORDINATES USING TRANSPONDER-INTERROGATOR RANGE AND RANGE RATE DATA
Jeff Hollowell Jan. 1989 247 p
(Contract DE-AC04-76DP-00789)
(DE89-007005; SAND-87-1850) Avail: NTIS HC A11/MF A01

Range and range rate measurements taken from a transponder-interrogator ranging system are processed via an extended Kalman filter and an extended Kalman smoother to provide an accurate time-position history of a vehicle's trajectory by estimating the errors in the vehicle's inertial navigation system. The necessary equations are derived in rectangular coordinates. As such, they are only valid for low altitude flights over a small geographic area. The equations are implemented in a FORTRAN program which is used to process flight data gathered at Edgewood, NM. DOE

N89-20120# Maryland Univ., College Park. Center for Automation Research.
VISION-BASED NAVIGATION FOR AUTONOMOUS GROUND VEHICLES Annual Report No. 1, Jul. 1984 - Jul. 1985
Larry S. Davis Jul. 1988 24 p
(Contract DACA76-84-C-0004)
(AD-A203712; ETL-0509) Avail: NTIS HC A03/MF A01 CSCL 12I

An experimental facility for performaning research in vision was built for autonomous navigation of ground vehicles. A computational framework was developed for constructing visual navigation systems. Some topical areas of discussion are: The Maryland Visual Navigation System; System Architecture; System Modules; Image Processing; Visual Knowledge Base; Geometry; Vision Executive; 3-D Representation; Predictor; Sensor Control; Navigator; Pilot; and Planner. E.R.

N89-20330*# Jet Propulsion Lab., California Inst. of Tech., Pasadena.
DERIVING A GEOCENTRIC REFERENCE FRAME FOR SATELLITE POSITIONING AND NAVIGATION
R. P. Malla (Sterling Software, Pasadena, CA.) and S.-C. Wu *In its* The Telecommunications and Data Acquisition Report 15 Nov. 1988 p 1-13 (For primary document see N89-20329 13-32)
Avail: NTIS HC A12/MF A01 CSCL 17G

N89-20331*# Jet Propulsion Lab., California Inst. of Tech., Pasadena.
DETERMINATION OF GPS ORBITS TO SUBMETER ACCURACY
W. I. Bertiger, S. M. Lichten, and E. C. Katsigris *In its* The Telecommunications and Data Acquisition Report 15 Nov. 1988 p 14-27 (For primary document see N89-20329 13-32)
Avail: NTIS HC A12/MF A01 CSCL 17G

05 AIRCRAFT DESIGN, TESTING AND PERFORMANCE

Includes aircraft simulation technology.

For related information see also *18 Spacecraft Design, Testing and Performance* and *39 Structural Mechanics*.For land transportation vehicles see *85 Urban Technology and Transportation.*

N89-20121*# Illinois Univ., Urbana-Champaign. Dept. of Aeronautical and Astronautical Engineering.
AEROSPACE VEHICLE DESIGN, SPACECRAFT SECTION FINAL PROJECT REPORTS
May 1988 344 p
(Grant NGT-21-002-080)
(NASA-CR-184741; NAS 1.26:184741; AAE-241-Vol-1) Avail: NTIS HC A15/MF A01 CSCL 01C

The objective was to create a manned Martian aircraft which can perform: scientific surveys of particular sites distant from the base; a deployment of scientific instrument packages by air drop that land rovers cannot accomplish; and rescue operations. Designing the airfoil requires a wing which can operate within the low Reynolds numbers apparent on Mars. The airfoil, NASA NLF(1)-1015 was chosen. The design of the aircraft is comparable to a P-38 military aircraft. The aircraft uses fuel cells to power the two propellers. A rocket-assisted takeoff is necessary to enable Romulus to liftoff. Although the design and creation of Romulus would be an expensive adventure, such a vehicle could be most useful in evaluating the Mars surface and in creating a habitat for mankind. B.G.

N89-20122*# Illinois Univ., Urbana-Champaign. Dept. of Aeronautical and Astronautical Engineering.
AEROSPACE VEHICLE DESIGN, SPACECRAFT SECTION FINAL PROJECT REPORTS
May 1988 354 p
(Grant NGT-21-002-080)
(NASA-CR-184742; NAS 1.26:184742; AAE-241-Vol-2) Avail: NTIS HC A16/MF A01 CSCL 01C

The next major step in the evolution of the space program is the exploration of the planet Mars. In preparation for this, much research is needed on the problem of surveying the planet surface. An aircraft appears to be a viable solution because it can carry men and equipment large distances in a short period of time as

compared with ground transportation. The problems and design of an aircraft which would be able to survey the planet Mars are examined. Author

N89-20123*# Illinois Univ., Urbana-Champaign. Dept. of Aeronautical and Astronautical Engineering.
AEROSPACE VEHICLE DESIGN, SPACECRAFT SECTION
May 1988 703 p
(Grant NGT-21-002-080)
(NASA-CR-184743; NAS 1.26:184743; AAE-241-Vol-3) Avail: NTIS HC A99/MF E03 CSCL 01C

Research results are presented for the following groups: Project Mars Airplane Vehicle and Reconnaissance Instrument Carrier (MAVRIC), ACME, ARES, Project ACRONYM, Mars Aircraft Recepticle with Technical Instruments, Aerobraking, and Navigation (MARTIAN), and NOMADS. Each project is described by the following areas of focus: mission planning and costs; aerobraking systems; structures and thermal control systems; attitude and articulation control systems; comman and data control systems; science instrumentation; and power and propulsion systems. B.G.

N89-20124*# National Aeronautics and Space Administration. Ames Research Center, Moffett Field, CA.
HUB AND BLADE STRUCTURAL LOADS MEASUREMENTS OF AN SA349/2 HELICOPTER
Gloria K. Yamauchi, Ruth M. Heffernan, and Michel Gaubert (Societe Nationale Industrielle Aerospatiale, Marignane, France) Dec. 1988 136 p
(NASA-TM-101040; A-88300; NAS 1.15:101040) Avail: NTIS HC A07/MF A01 CSCL 01C

Data from 23 flight conditions, including level flights ranging from advance ratio mu = 0.14 to 0.37 and steady turning flights from advance ratio mu = 0.26 to 0.35, are presented for an Aerospatiale SA349/2 Gazelle helicopter. The data include hub loads data (for 6 of the 23 conditions), blade structural data at eleven different blade radial stations, and fuselage structural data. All dynamic data are presented as harmonic analysis coefficients (ten harmonics per rotor revolution). The data acquisition and reduction procedures are also documented. Blade structural and inertial properties are provided in addition to control system geometry and properties. Author

N89-20125*# Planning Research Corp., Hampton, VA. Aerospace Technologies Div.
ON THE RELATIONSHIP BETWEEN MATCHED FILTER THEORY AS APPLIED TO GUST LOADS AND PHASED DESIGN LOADS ANALYSIS
Thomas A. Zeiler and Anthony S. Pototzky Apr. 1989 27 p Presented at the Gust Specialists Meeting, Mobile, AL, 6 Apr. 1989
(Contract NAS1-18000)
(NASA-CR-181802; NAS 1.26:181802) Avail: NTIS HC A03/MF A01 CSCL 01C

A theoretical basis and example calculations are given that demonstrate the relationship between the Matched Filter Theory approach to the calculation of time-correlated gust loads and Phased Design Load Analysis in common use in the aerospace industry. The relationship depends upon the duality between Matched Filter Theory and Random Process Theory and upon the fact that Random Process Theory is used in Phased Design Loads Analysis in determining an equiprobable loads design ellipse. Extensive background information describing the relevant points of Phased Design Loads Analysis, calculating time-correlated gust loads with Matched Filter Theory, and the duality between Matched Filter Theory and Random Process Theory is given. It is then shown that the time histories of two time-correlated gust load responses, determined using the Matched Filter Theory approach, can be plotted as parametric functions of time and that the resulting plot, when superposed upon the design ellipse corresponding to the two loads, is tangent to the ellipse. The question is raised of whether or not it is possible for a parametric load plot to extend outside the associated design ellipse. If it is possible, then the use of the equiprobable loads design ellipse will not be a conservative design practice in some circumstances. Author

N89-20126# National Aerospace Lab., Amsterdam (Netherlands). Structures and Material Dept.
MATCHING POWER SPECTRA DENSITY (PSD)-DESIGN LOAD
R. Noback 18 Aug. 1987 16 p Presented at the 65th AGARD Structures and Materials Panel and Flight of Flexible Aircraft in Turbulence Workshop, Cesme, Turkey, 4-9 Oct. 1987 Sponsored by The Netherlands Agency for Aerospace Programs, Delft, The Netherlands
(NLR-MP-87059-U; ETN-89-94040) Avail: NTIS HC A03/MF A01

It is shown that it is possible to generate equal probability design load conditions using power spectral density-design loads obtained with the design envelope criterion, and the correlation coefficients between these loads. The correlation coefficients can be calculated easily together with the A-values. The matrix of correlation coefficients can be used to define an N-dimensional surface. For the two-dimensional case this surface reduces to an ellipse. Each point on the surface defines an equal probability design load condition. It can be shown that such a condition is in equilibrium. Each design load condition can be used to calculate an estimate for the stress in a point of the structure. The method also can be used to generate design load conditions for the complete structure, for example the wing. A problem arises if stresses have to be calculated for a section of the structure for which the design vaiues of the loads and the correlation coefficients were not calculated. It then seems logical to interpolate within a design load condition. This however leads to inconsistent Values of both loads and stresses in that section. The same problem arises in a discrete gust analysis if the design load conditions are defined as the loads occurring at the same time. A possible solution is to interpolate between the corresponding design loads and correlation coefficients of the adjoining sections. ESA

N89-20127# Rockwell International Corp., Columbus, OH. North American Aircraft Operations.
POWER EFFICIENT HYDRAULIC SYSTEMS. VOLUME 1: STUDY PHASE Final Report, Oct. 1985 - Jul. 1988
Richard V. Hupp and Robert K. Haning Jul. 1988 239 p
(Contract N62269-85-C-0259)
(AD-A203899; NA-88-0001-Vol-1; NADC-88066-60-Vol-1) Avail: NTIS HC A11/MF A01 CSCL 13G

Energy saving concepts for aircraft hydraulic systems were studied in a two-phase program. Task 1 was an investigation of methods and techniques to reduce overall hydraulic system power requirements by lowering system demands and increasing component efficiencies. Task 2 involved hardware demonstration test on selected concepts. Task 1: Study Phase. A baseline hydraulic system for an advanced aircraft design was established. Twenty energy saving techniques were studied as candidates for application to the baseline vehicle. A global systems analysis approach was employed. The candidates were compared on the basis of total fuel consumption and six qualitative factors. Nine of the most promising techniques were applied to a Target System . The target system had a 28 percent reduction in energy consumption and an 868 lb weight reduction over the baseline aircraft. GRA

N89-20128# Rockwell International Corp., Columbus, OH. North American Aircraft Operations.
POWER EFFICIENT HYDRAULIC SYSTEMS. VOLUME 2: HARDWARE DEMONSTRATION PHASE Final Report, Oct. 1985 - Jul. 1988
Richard V. Hupp and Robert K. Haning Jul. 1988 204 p
(Contract N62269-85-C-0259)
(AD-A203900; NA-88-0001-Vol-2; NADC-88066-60-Vol-2) Avail: NTIS HC A10/MF A01 CSCL 13G

Energy saving concepts for aircraft hydraulic systems were studied in a two-phase program. Task 1 was an investigation of methods and techniques to reduce overall hydraulic system power

requirements by lowering system demands and increasing component efficiencies. Task 2 involved hardware demonstration tests on selected concepts. Hardware demonstration phase. Two techniques demonstrated for energy savings were control valves with overlap and dual pressure level systems. Tests were conducted on control valves, a servo actuator, dual pressure pumps, and a lightweight hydraulic system simulator. Valves with 0.002 in. overlap reduced system energy consumption 18 percent compared to using valves with zero lap. Operation at 4000 psi reduced system energy consumption 53 percent compared to operation at 8000 psi. Pressure level switching was accomplished with good results.
GRA

06 AIRCRAFT INSTRUMENTATION

Includes cockpit and cabin display devices; and flight instruments.

For related information see also *19 Spacecraft Instrumentation* and *35 Instrumentation and Photography.*

N89-20129# National Aerospace Lab., Amsterdam (Netherlands). Hoofdafdeling: Vliegtuigen.
ELECTRONICS IN CIVIL AVIATION
F. J. Abbink 5 Nov. 1987 20 p In DUTCH; ENGLISH summary Presented at the KIVI-NIRIA Symposium on Electronics in Aerospace, Utrecht, The Netherlands, 5 Nov. 1987
(NLR-MP-87009-U; ETN-89-94031) Avail: NTIS HC A03/MF A01

The development of the electronic systems which are used in airliners for communication, navigation, identification, flight control, engine control, for the acquisition and presentation of flight and system data, as well as for air traffic control is reviewed. The development of these systems was made possible by developments in microelectronics, computer technology, and display technology. Developments in electronics systems in civil aviation, as fly-by-wire, full authority digital engine control, satellite navigation, satellite communication, and the microwave landing system, and their implications on future air traffic control are considered. ESA

N89-20130# National Aerospace Lab., Amsterdam (Netherlands). Flight Div.
THE DATA ACQUISITION SYSTEM FOR THE FOKKER 100 TEST AIRCRAFT
S. Storm vanLeeuwen and A. Voskes (Fokker B.V., Amsterdam, Netherlands) 28 Jul. 1987 15 p Presented at the 18th Annual Flight Test Engineers Symposium, Amsterdam, The Netherlands, 2 Oct. 1987 Previously announced in IAA as A88-51465
(NLR-MP-87047-U; ETN-89-94036) Avail: NTIS HC A03/MF A01

The data acquisition system for the Fokker 100 test aircraft (capability, electrical lay-out, real time presentation facilities, and performance parameters) is described. The take-off and landing performance measuring system and the automatic noise measuring system are highlighted. It was decided to keep the data acquisition systems for both test aircraft identical. The savings on the design costs and the possibility of using each aircraft for most of the flight tests counterbalance the extra cost in instrumentation. The data acquisition systems perform to specification. ESA

07 AIRCRAFT PROPULSION AND POWER

Includes prime propulsion systems and systems components, e.g., gas turbine engines and compressors; and onboard auxilliary power plants for aircraft.

For related information see also *20 Spacecraft Propulsion and Power, 28 Propellants and Fuels,* and *44 Energy Production and Conversion.*

N89-20131 Cornell Univ., Ithaca, NY.
AN ANALYTICAL AND NUMERICAL STUDY OF AXIAL FLOW COMPRESSOR INSTABILITY Ph.D. Thesis
Frances Elizabeth McCaughan 1988 192 p
Avail: Univ. Microfilms Order No. DA8821176

An axial-flow compressor is an important component of the turbo-jet engine. It is of great interest to characterize the possible modes of response of this system with respect to variations in the values of the governing parameters. A mathematical model of an idealized axial-flow compression system was developed by Moore and Greitzer. The properties of this model, which consists of a set of partial differential equations, were investigated by both analytical and numerical means. A single-harmonic truncation of the full model was investigated by means of modern dynamical systems theory. A thorough investigation is made of the stability of the equilibria and periodic solutions, revealing period-doubling bifurcations which lead to apparently chaotic behavior. Using Cornell's supercomputing facilities, an extensive study of the full set of partial differential equations using a pseudo-spectral numerical scheme was also performed. The effects of the parameters on the rotating stall performance are investigated. The effects of inlet guide vane loss on rotating stall performance were also discussed. An evaluation is made of the h prime = -g approximation, and a spectral analysis of the rotating stall cell determined from the full model suggests why this breaks down.
Dissert. Abstr.

N89-20132*# Pratt and Whitney Aircraft, East Hartford, CT. Commercial Engineering Dept.
STRUCTURAL TAILORING OF ADVANCED TURBOPROPS (STAT) PROGRAMMER'S MANUAL
K. W. Brown and P. R. Harvey Mar. 1989 53 p
(Contract NAS3-23941)
(NASA-CR-182164; NAS 1.26:182164; PWA-5967-51) Avail: NTIS HC A04/MF A01 CSCL 21E

The Structural Tailoring of Advanced Turboprops (STAT) computer program was developed to perform numerical optimizations on highly swept propfan blades. This manual describes the functionality of the STAT system from a programmer's viewpoint. It provides a top-down description of module intent and interaction. The purpose of this manual is to familiarize the programmer with the STAT system should he/she wish to enhance or verify the program's function. Author

N89-20133*# National Aeronautics and Space Administration. Lewis Research Center, Cleveland, OH.
EXPERIMENTAL INVESTIGATION OF TRANSONIC OSCILLATING CASCADE AERODYNAMICS
Daniel H. Buffum and Sanford Fleeter (Purdue Univ., West Lafayette, IN.) Jan. 1989 15 p Presented at the 27th Aerospace Sciences Meeting, Reno, NV, 9-12 Jan. 1989; sponsored in part by AIAA Previously announced in IAA as A89-26369
(Grant NAG3-656)
(NASA-TM-101993; E-4697; NAS 1.15:101993) Avail: NTIS HC A03/MF A01 CSCL 21E

Fundamental experiments are performed in the NASA Lewis Transonic Oscillating Cascade Facility to investigate the subsonic and transonic aerodynamics of cascaded airfoils executing torsion mode oscillations at realistic values of reduced frequency. In particular, an unsteady aerodynamic influence coefficient technique is developed and utilized. In this technique, only one airfoil in the cascade is oscillated at a time, with the resulting airfoil surface unsteady pressure distribution measured on one dynamically

instrumented reference airfoil. The unsteady aerodynamics of an equivalent cascade with all airfoils oscillating at any specified interblade phase angle are then determined through a vector summation of these data. These influence coefficient determined oscillating cascade data were correlated with: (1) data obtained in this cascade with all airfoils oscillating at several interblade phase angle values; and (2) predictions from a classical linearized unsteady cascade model. Author

N89-20134*# Cornell Univ., Ithaca, NY.
PROPULSION OVER A WIDE MACH NUMBER RANGE Final Report M.S. Thesis
Edwin L. Resler, Jr. and Barry M. Greenberg Mar. 1989 71 p (Grant NAG3-803)
(NASA-CR-182267; NAS 1.26:182267) Avail: NTIS HC A04/MF A01 CSCL 21E

Criteria is presented to assess the relative merits of different propulsion systems. Previous references focus mainly on subsonic or low supersonic flight speeds. The main focus here is on a higher range, from low supersonic to orbital velocities. Air breathing propulsion systems for hypersonic flight persent the engine designer with circumstances that differ in important fundamental ways from those encountered in engines designed for operation at subsonic or low supersonic speeds. This analysis highlights the importance of various features of hypersonic engine design. Since the performance of hypersonic engines are energy limited, unlike low speed engines which are stagnation pressure limited, the efficient use of the energy of the fuel used is critical to minimize the take-off fuel mass fraction of the vehicle. Furthermore, since the required energy increase of a vehicle per incremental speed change increases with speed, the engine must be designed to operate efficiently at high speed. An analysis of engine performance in terms of entropy changes of the flow passing through the engine allows comparison of various engine designs as well as a convenient method to determine the effect of individual engine component efficiencies on overall engine performance. Author

N89-20135*# National Aeronautics and Space Administration. Lewis Research Center, Cleveland, OH.
TOWARD IMPROVED DURABILITY IN ADVANCED AIRCRAFT ENGINE HOT SECTIONS
Daniel E. Sokolowski, ed. Washington Apr. 1989 121 p Proceedings of the 33rd ASME International Gas Turbine and Aeroengine Congress and Exposition, Amsterdam, Netherlands, 5-9 Jun. 1988 Previously announced in IAA as A88-54137
(NASA-TM-4087; E-4468; NAS 1.15:4087) Avail: NTIS HC A06/MF A01 CSCL 21E

The conference on durability improvement methods for advanced aircraft gas turbine hot-section components discussed NASA's Hot Section Technology (HOST) project, advanced high-temperature instrumentation for hot-section research, the development and application of combustor aerothermal models, and the evaluation of a data base and numerical model for turbine heat transfer. Also discussed are structural analysis methods for gas turbine hot section components, fatigue life-prediction modeling for turbine hot section materials, and the service life modeling of thermal barrier coatings for aircraft gas turbine engines. For individual titles, see N89-20136 through N89-20144.

N89-20136*# National Aeronautics and Space Administration. Lewis Research Center, Cleveland, OH.
NASA HOST PROJECT OVERVIEW
Daniel E. Sokolowski *In its* Toward Improved Durability in Advanced Aircraft Engine Hot Sections Apr. 1989 p 1-4 Previously announced in IAA as A88-54138 (For primary document see N89-20135 13-07)
Avail: NTIS HC A06/MF A01 CSCL 21E

NASA's Hot Section Technology (HOST) program has developed improved analytical models for the aerothermal environment, thermomechanical loading, material behavior, structural response, and service life of aircraft gas turbine engines' hot section components. These models, in conjunction with sophisticated computer codes, can be used in design analyses of critical combustor and turbine elements. Toward these ends, efforts were undertaken in instrumentation, combustion, turbine heat transfer, structural analysis, fatigue-fracture, and surface protection. Attention is presently given to the organization of HOST activities and their specific subject matter. Author

N89-20137*# National Aeronautics and Space Administration. Lewis Research Center, Cleveland, OH.
ADVANCED HIGH TEMPERATURE INSTRUMENT FOR HOT SECTION RESEARCH APPLICATIONS
D. R. Englund and R. G. Seasholtz *In its* Toward Improved Durability in Advanced Aircraft Engine Hot Sections Apr. 1989 p 5-21 Previously announced in IAA as A88-54139 (For primary document see N89-20135 13-07)
Avail: NTIS HC A06/MF A01 CSCL 21E

Programs to develop research instrumentation for use in turbine engine hot sections are described. These programs were initiated to provide improved measurements capability as support for a multidisciplinary effort to establish technology leading to improved hot section durability. Specific measurement systems described here include heat flux sensors, a dynamic gas temperature measuring system, laser anemometry for hot section applications, an optical system for viewing the interior of a combustor during operation, thin film sensors for surface temperature and strain measurements, and high temperature strain measuring systems. The state of development of these sensors and measuring systems is described, and, in some cases, examples of measurements made with these instruments are shown. Work done at the NASA Lewis Research Center and at various contract and grant facilities is covered. Author

N89-20138*# National Aeronautics and Space Administration. Lewis Research Center, Cleveland, OH.
ASSESSMENT, DEVELOPMENT, AND APPLICATION OF COMBUSTOR AEROTHERMAL MODELS
J. D. Holdeman, H. C. Mongia, and E. J. Mularz (Army Aviation Systems Command, Cleveland, OH.) *In its* Toward Improved Durability in Advanced Aircraft Engine Hot Sections Apr. 1989 p 23-37 Previously announced in IAA as A88-54140 (For primary document see N89-20135 13-07)
Avail: NTIS HC A06/MF A01 CSCL 21E

The gas turbine combustion system design and development effort is an engineering exercise to obtain an acceptable solution to the conflicting design trade-offs between combustion efficiency, gaseous emissions, smoke, ignition, restart, lean blowout, burner exit temperature quality, structural durability, and life cycle cost. For many years, these combustor design trade-offs have been carried out with the help of fundamental reasoning and extensive component and bench testing, backed by empirical and experience correlations. Recent advances in the capability of computational fluid dynamics codes have led to their application to complex 3-D flows such as those in the gas turbine combustor. A number of U.S. Government and industry sponsored programs have made significant contributions to the formulation, development, and verification of an analytical combustor design methodology which will better define the aerothermal loads in a combustor, and be a valuable tool for design of future combustion systems. The contributions made by NASA Hot Section Technology (HOST) sponsored Aerothermal Modeling and supporting programs are described. Author

N89-20139*# National Aeronautics and Space Administration. Lewis Research Center, Cleveland, OH.
REVIEW AND ASSESSMENT OF THE DATABASE AND NUMERICAL MODELING FOR TURBINE HEAT TRANSFER
H. J. Gladden and R. J. Simoneau *In its* Toward Improved Durability in Advanced Aircraft Engine Hot Sections Apr. 1989 p 39-55 Previously announced in IAA as A88-54141 (For primary document see N89-20135 13-07)
Avail: NTIS HC A06/MF A01 CSCL 21E

The objectives of the NASA Hot Section Technology (HOST) Turbine Heat Transfer subproject were to obtain a better understanding of the physics of the aerothermodynamic

phenomena and to assess and improve the analytical methods used to predict the flow and heat transfer in high-temperature gas turbines. At the time the HOST project was initiated, an across-the-board improvement in turbine design technology was needed. A building-block approach was utilized and the research ranged from the study of fundamental phenomena and modeling to experiments in simulated real engine environments. Experimental research accounted for approximately 75 percent of the funding while the analytical efforts were approximately 25 percent. A healthy government/industry/university partnership, with industry providing almost half of the research, was created to advance the turbine heat transfer design technology base. Author

N89-20140*# National Aeronautics and Space Administration. Lewis Research Center, Cleveland, OH.
STRUCTURAL ANALYSIS METHODS DEVELOPMENT FOR TURBINE HOT SECTION COMPONENTS
R. L. Thompson *In its* Toward Improved Durability in Advanced Aircraft Engine Hot Sections Apr. 1989 p 57-82 Previously announced in IAA as A88-54142 (For primary document see N89-20135 13-07)
Avail: NTIS HC A06/MF A01 CSCL 21E

The structural analysis technologies and activities of the NASA Lewis Research Center's gas turbine engine HOT Section Technoloogy (HOST) Program are summarized. The technologies synergistically developed and validated include: time-varying thermal/mechanical load models; component-specific automated geometric modeling and solution strategy capabilities; advanced inelastic analysis methods; inelastic constitutive models; high-temperature experimental techniques and experiments; and nonlinear structural analysis codes. Features of the program that incorporate the new technologies and their application to hot section component analysis and design are described. Improved and, in some cases, first-time 3-D nonlinear structural analyses of hot section components of isotropic and anisotropic nickel-base superalloys are presented. Author

N89-20141*# General Electric Co., Cincinnati, OH.
STRUCTURAL ANALYSIS APPLICATIONS
R. L. McKnight *In* NASA, Lewis Research Center, Toward Improved Durability in Advanced Aircraft Engine Hot Sections Apr. 1989 p 83-95 Previously announced in IAA as A88-54143 (For primary document see N89-20135 13-07)
Avail: NTIS HC A06/MF A01 CSCL 21E

An account is given of the application of computer codes for the efficient conduct of three-dimensional inelastic analyses to aircraft gas turbine combustor, turbine blade, and turbine stator vane components. The synergetic consequences of the program's activities are illustrated by an evaluation of the computer analyses of thermal barrier coatings and of the Space Shuttle Main Engine's High Pressure Fuel Turbopump turbine blading. This software, in conjunction with state-of-the-art supercomputers, can significantly reduce design-task burdens. Author

N89-20142*# National Aeronautics and Space Administration. Lewis Research Center, Cleveland, OH.
FATIGUE LIFE PREDICTION MODELING FOR TURBINE HOT SECTION MATERIALS
G. R. Halford, T. G. Meyer, R. S. Nelson, D. M. Nissley, and G. A. Swanson *In its* Toward Improved Durability in Advanced Aircraft Engine Hot Sections Apr. 1989 p 97-107 Previously announced in IAA as A88-54144 Prepared in cooperation with Pratt and Whitney Aircraft, East Hartford, CT (For primary document see N89-20135 13-07)
Avail: NTIS HC A06/MF A01 CSCL 21E

A major objective of the fatigue and fracture efforts under the NASA Hot Section Technology (HOST) program was to significantly improve the analytic life prediction tools used by the aeronautical gas turbine engine industry. This was achieved in the areas of high-temperature thermal and mechanical fatigue of bare and coated high-temperature superalloys. The cyclic crack initiation and propagation resistance of nominally isotropic polycrystalline and highly anisotropic single crystal alloys were addressed. Life prediction modeling efforts were devoted to creep-fatigue interaction, oxidation, coatings interactions, multiaxiality of stress-strain states, mean stress effects, cumulative damage, and thermomechanical fatigue. The fatigue crack initiation life models developed to date include the Cyclic Damage Accumulation (CDA) and the Total Strain Version of Strainrange Partitioning (TS-SRP) for nominally isotropic materials, and the Tensile Hysteretic Energy Model for anisotropic superalloys. A fatigue model is being developed based upon the concepts of Path-Independent Integrals (PII) for describing cyclic crack growth under complex nonlinear response at the crack tip due to thermomechanical loading conditions. A micromechanistic oxidation crack extension model was derived. The models are described and discussed. Author

N89-20143*# National Aeronautics and Space Administration. Lewis Research Center, Cleveland, OH.
LIFE MODELING OF THERMAL BARRIER COATINGS FOR AIRCRAFT GAS TURBINE ENGINES
R. A. Miller *In its* Toward Improved Durability in Advanced Aircraft Engine Hot Sections Apr. 1989 p 109-115 Previously announced in IAA as A88-54145 (For primary document see N89-20135 13-07)
Avail: NTIS HC A06/MF A01 CSCL 21E

Thermal barrier coating life models developed under the NASA Lewis Research Center's Hot Section Technology (HOST) Program are summarized. An initial laboratory model and three design-capable models are discussed. Current understanding of coating failure mechanisms are also summarized. The materials and structural aspects of thermal barrier coatings have been successfully integrated under the HOST program to produce models which may now or in the near future be used in design. Efforts on this program continue at Pratt and Whitney Aircraft where their model is being extended to the life prediction of physical vapor deposited thermal barrier coatings. Author

N89-20144*# National Aeronautics and Space Administration. Lewis Research Center, Cleveland, OH.
VIEWS ON THE IMPACT OF HOST
J. B. Esgar (Sverdrup Technology, Inc., Cleveland, OH.) and Daniel E. Sokolowski *In its* Toward Improved Durability in Advanced Aircraft Engine Hot Sections Apr. 1989 p 117-123 Previously announced in IAA as A88-54146 (For primary document see N89-20135 13-07)
Avail: NTIS HC A06/MF A01 CSCL 21E

The Hot Section Technology (HOST) Project, which was initiated by NASA Lewis Research Center in 1980 and concluded in 1987, was aimed at improving advanced aircraft engine hot section durability through better technical understanding and more accurate design analysis capability. The project was a multidisciplinary, multiorganizational, focused research effort that involved 21 organizations and 70 research and technology activities and generated approximately 250 research reports. No major hardware was developed. To evaluate whether HOST had a significant impact on the overall aircraft engine industry in the development of new engines, interviews were conducted with 41 participants in the project to obtain their views. The summarized results of these interviews are presented. Emphasis is placed on results relative to three-dimensional inelastic structural analysis, thermomechanical fatigue testing, constitutive modeling, combustor aerothermal modeling, turbine heat transfer, protective coatings, computer codes, improved engine design capability, reduced engine development costs, and the impacts on technology transfer and the industry-government partnership. Author

N89-20145# Army Aviation Engineering Flight Activity, Edwards AFB, CA.
AIRWORTHINESS AND FLIGHT CHARACTERISTICS EVALUATION OF AN IMPROVED ENGINE AIR FILTRATION SYSTEM ON THE UH-1H HELICOPTER Final Report, 16 Sep. 1987 - 29 Mar. 1988
James D. Brown, John S. Lawrence, Paul W. Losier, Charles E. Cassil, and Matthew S. Graham May 1988 160 p

(AD-A203446; USAAEFA-86-16) Avail: NTIS HC A08/MF A01 CSCL 21E

The U.S. Army Aviation Engineering Flight Activity conducted an Airworthiness and Flight Characteristics evaluation of the UH-1H aircraft with an Improved Engine Air Filtration System (IEAFS) installed and with the standard filter installed between 16 September 1987 and 29 February 1988. Aircraft performance and handling qualities, engine-air induction system compatibility, and engine performance with the IEAFS installed were evaluated. This evaluation was conducted at Edwards AFB, California. Twenty-five flights were conducted for a total of 20.1 productive flight hours. The aircraft performance and handling qualities, engine vibrations, and inlet temperature characteristics with the IEAFS installed are not significantly different from those of the standard UH-1H. The inlet pressure distortion and engine installation losses with the IEAFS installed are less than those of the standard UH-1H. One deficiency, the poor reliability of the IEAFS latch rivets, was identified. One shortcoming, the poor reliability of the latch lever locking device, was identified. Both the deficiency and the shortcoming should be corrected before production. GRA

N89-20146*# Oklahoma Univ., Norman. School of Aerospace and Mechanical Engineering.
A FIRST SCRAMJET STUDY
George Emanuel Apr. 1989 55 p
(Grant NAG1-886)
(NASA-CR-184965; NAS 1.26:184965) Avail: NTIS HC A04/MF A01 CSCL 21E

A variety of related scramjet engine topics are examined. The flow is assumed to be 1-D, the gas is thermally and calorically perfect, and focus is on low hypersonic Mach numbers. The thrust and lift of an exposed half nozzle, which is used on the aerospace plane, is evaluated as well as a fully confined nozzle. A rough estimate of the drag of an aerospace plane is provided. Thermal effects and shock waves are next discussed. A parametric scramjet model is then presented based on the influence coefficient method, which evaluates the dominant scramjet processes. The independent parameters are the ratio of specific heats, a nondimensional heat addition parameter, and four Mach numbers. The total thrust generated by the combustor and nozzle is shown to be independent of the heat release distribution and the combustor exit Mach number, providing thermal choking is avoided. An operating condition for the combustor is found that maximizes the thrust. An alternative condition is explored when this optimum is no longer realistic. This condition provides a favorable pressure gradient and a reasonable area ratio for the combustor. Parametric results based on the model is provided. Author

08 AIRCRAFT STABILITY AND CONTROL

Includes aircraft handling qualities; piloting; flight controls; and autopilots.

For related information see also *05 Aircraft Design, Testing and Performance.*

N89-20147 Virginia Polytechnic Inst. and State Univ., Blacksburg.
ROBUST STABILIZATION OF LINEAR TIME-INVARIANT UNCERTAIN SYSTEMS VIA LYAPUNOV THEORY Ph.D. Thesis
Chien-Hsiang Chao 1988 114 p
Avail: Univ. Microfilms Order No. DA8817401

The problem of synthesizing a robust stabilizing feedback controller for linear time-invariant systems with constant uncertainties that are not required to satisfy matching conditions is considered. Only the bounds on the uncertainties are required and no statistical property of the uncertainties is assumed. The systems under consideration are described by linear state equations with uncertainties. Lyapunov theory is exploited to establish the conditions for stabilizability of the closed loop system. Linear controller design is also investigated. Under the same assumptions for the existence of a stabilizing discontinuous controller, it is shown that a linear robust stabilizing controller always exists. Three examples are included to illustrate the design procedures for robust controllers. Dissert. Abstr.

N89-20148 Purdue Univ., West Lafayette, IN.
MODAL COST ANALYSIS OF FLEXIBLE STRUCTURES: MODELING FLEXIBLE STRUCTURES FOR CONTROL DESIGN Ph.D. Thesis
Anren Hu 1987 200 p
Avail: Univ. Microfilms Order No. DA8814487

The integration issues of structural modeling and control design for large flexible structures are very important for developing sound models in a closed loop environment. Consideration of these issues leads one to conclude that the modeling problem and control problem are not independent. The connection between these two problems must be understood to develop reliable control algorithms and reduce the cost of extensive laboratory and flight testing. It is this input-output type phenomenon which must be reflected in structural modeling. The modal costs represent the contribution of a vibration mode in the system response for given input and output locations. A complete modal cost analysis is provided for certain distributed parameter systems and shows that structural modeling and model reduction methods should be influenced by the specific control objectives. The analysis proceeds via the following steps: Convergence properties of modal costs are discussed for vibration of various simple continua. Open loop model cost analysis is applied to finite element models of beam-like structures. Finite element models are used to develop Linear Quadratic Gaussian control laws while exact models are used to evaluate performance of the resulting closed loop systems. A comprehensive modal cost analysis is presented for simple continua and discusses its implications in subsequent control system design. Dissert. Abstr.

N89-20149 California Univ., Los Angeles.
ACTIVE CONTROL HELICOPTER AEROMECHANICAL AND AEROELASTIC INSTABILITIES Ph.D. Thesis
Marc D. Takahashi 1988 367 p
Avail: Univ. Microfilms Order No. DA8822168

The active control of three helicopter rotor instabilities is investigated using a coupled rotor/fuselage helicopter analysis. The mathematical model is derived to capture air resonance and includes important features such as blade torsional flexibility, unsteady aerodynamics, and forward flight, which are effects that were ignored in the few previous studies on air resonance control. Because of these modeling features, two other aeroelastic instabilities can also be simulated with the model and a brief investigation into the active control of these instabilities is made. The first of these is a flap-lag-torsion instability inforward flight and the second is a flap-lag instability that is induced by the presence of the fuselage degrees of freedom. A realistic helicopter configuration experiencing an air resonance instability is then selected and it is used in two active control studies. In the first study, open loop damping data is presented and the effect of blade torsional flexibility, unsteady aero-dynamics, forward flight, periodic terms, and trim solution is shown. The model is then used with linear optimal control theory to investigate the influence of these effects on the closed loop damping. In the second study, the feasibility of designing simple implemetable controllers to suppress air resonance throughout a wide range of operating conditions is demonstrated. The control design method is also applied to a different configuration experiencing a fuselage induced flap-lag instability. Dissert. Abstr.

N89-20150 Massachusetts Inst. of Tech., Cambridge.
ON-BOARD AUTOMATIC AID AND ADVISORY FOR PILOTS OF CONTROL-IMPAIRED AIRCRAFT Ph.D. Thesis
Elaine Ann Wagner 1988 261 p
Avail: Univ. Microfilms Order No. DA8821885

The consideration of the problem of aircraft control failures from a broader, more meaningful viewpoint than with control loop reconfiguration or redesign is presented. The additional considerations involved in making full recoveries from control failures are first categorized. Performance and operating constraints

that are best taken into account explicitly are presented, and there is a discussion of the sometimes very important role of explicit post-failure retrim of the aircraft. Because it can be expected that pilots, if unaided, may continue often to be unable to recover aircraft after control failure, these considerations were cast in the form of knowledge and capabilities that an automatic aid and pilot advisory system should have. Because automatic emergency control is seen to be a very significant part of the proposed system, a rule-based expert-type system to find a successful control strategy was developed for elevator failures on the C-130. This system directs pre-simulation of the control strategy, changing it on the basis of empirical guidelines concerning simple, objective features of the aircraft response to the strategy. The advisory function of the recovery-aiding system is also described. The issues of pilot interface are discussed, as well as what to calculate to support the advisory during various flight phases. Dissert. Abstr.

N89-20151*# Jet Propulsion Lab., California Inst. of Tech., Pasadena.

FLEXIBLE STRUCTURE CONTROL LABORATORY DEVELOPMENT AND TECHNOLOGY DEMONSTRATION Final Report

H. C. Vivian, P. E. Blaire, D. B. Eldred, G. E. Fleischer, C.-H. C. Ih, N. M. Nerheim, R. E. Scheid, and J. T. Wen 1 Oct. 1987 213 p

(Contract NAS7-918)

(NASA-CR-184867; JPL-Publ-88-29; NAS 1.26:184867) Avail: NTIS HC A10/MF A01 CSCL 22B

An experimental structure is described which was constructed to demonstrate and validate recent emerging technologies in the active control and identification of large flexible space structures. The configuration consists of a large, 20 foot diameter antenna-like flexible structure in the horizontal plane with a gimballed central hub, a flexible feed-boom assembly hanging from the hub, and 12 flexible ribs radiating outward. Fourteen electrodynamic force actuators mounted to the hub and to the individual ribs provide the means to excite the structure and exert control forces. Thirty permanently mounted sensors, including optical encoders and analog induction devices provide measurements of structural response at widely distributed points. An experimental remote optical sensor provides sixteen additional sensing channels. A computer samples the sensors, computes the control updates and sends commands to the actuators in real time, while simultaneously displaying selected outputs on a graphics terminal and saving them in memory. Several control experiments were conducted thus far and are documented. These include implementation of distributed parameter system control, model reference adaptive control, and static shape control. These experiments have demonstrated the successful implementation of state-of-the-art control approaches using actual hardware. Author

N89-20152*# Jet Propulsion Lab., California Inst. of Tech., Pasadena.

MODELING AND CONTROL OF FLEXIBLE STRUCTURES

J. S. Gibson and D. L. Mingori (California Univ., Los Angeles.) 15 Dec. 1988 140 p

(Contract NAS7-918)

(NASA-CR-184862; JPL-Publ-88-40; NAS 1.26:184862) Avail: NTIS HC A07/MF A01 CSCL 22A

This monograph presents integrated modeling and controller design methods for flexible structures. The controllers, or compensators, developed are optimal in the linear-quadratic-Gaussian sense. The performance objectives, sensor and actuator locations and external disturbances influence both the construction of the model and the design of the finite dimensional compensator. The modeling and controller design procedures are carried out in parallel to ensure compatibility of these two aspects of the design problem. Model reduction techniques are introduced to keep both the model order and the controller order as small as possible. A linear distributed, or infinite dimensional, model is the theoretical basis for most of the text, but finite dimensional models arising from both lumped-mass and finite element approximations also play an important role. A central purpose of the approach here is to approximate an optimal infinite dimensional controller with an implementable finite dimensional compensator. Both convergence theory and numerical approximation methods are given. Simple examples are used to illustrate the theory. Author

09 RESEARCH AND SUPPORT FACILITIES (AIR)

Includes airports, hangars and runways; aircraft repair and overhaul facilities; wind tunnels; shock tubes; and aircraft engine test stands.

For related information see also *14 Ground Support Systems and Facilities (Space).*

N89-20153# Helsinki Univ. of Technology, Espoo (Finland). Radio Lab.

ANECHOIC CHAMBER EVALUATION AT 85 GHz

A. Lehto, J. Tuovinen, H. Valmu, and A. Raeisaenen 1988 22 p

(PB89-125199; ISBN-951-754-571-1; S-174) Avail: NTIS HC A03/MF A01 CSCL 14B

The anechoic chamber of the Telecommunications Laboratory of the Technical Research Center of Finland (12 x 12 x 17 cu m) was evaluated at the frequency of 85 GHz. The reflectivity level was measured by using the free space voltage standing wave ratio method and by directly comparing the reflected power with the direct power. The reflectivity level into the direction of the main beam of a corrugated horn receiving antenna (G = 25 dB) was -53 dB to -65dB when a waveguide end was used as the transmitting antenna and about -80 dB when a diagonal horn (G = 28 dB) was used as the transmitting antenna. The backwall reflection was about -40 dB. The measurements were performed at the height of the center line of the room and also at the height of about 2 meters above the floor pyramids. There was no significant differences in the results. Neither was any polarization dependence observed. Author

N89-20154# Army Research Inst. of Environmental Medicine, Natick, MA.

QUANTIFICATION OF ENVIRONMENTAL CHAMBERS BY AIR VELOCITY MAPPING

Stephen K. Chang and Richard R. Gonzalez Sep. 1988 35 p

(AD-A200923; USARIEM-T-20-88) Avail: NTIS HC A03/MF A01 CSCL 04B

The air velocity profile of a U.S. Army Research Institute of Environment Medicine (USARIEM) test chamber was mapped using an anemometer free system. This particular chamber houses an articulated copper manikin. It was found that the air velocity within the chamber is a disparate property. Airflow patterns are significantly different chamber fan speed settings, and the practice of employing a single thermal or cup anemometer to monitor chamber air velocity, in general, is inadequate. It is recommended that the air velocity profile of a given test chamber should be mapped by techniques described in this report, for all protocol studies in which air velocity data are important, such as clothing insulation evaluation and convective heat transfer studies. GRA

N89-20155# JAYCOR, Vienna, VA.

ENGINEERING AND TECHNICAL EFFORTS TO DESIGN AND CONSTRUCT A 10 MW GYROTRON LABORATORY Final Report, Jul. 1986 - 14 Jul. 1988

George L. Bergeron, III, Robert C. Lee, Mar L. Barsanti, Terry D. Hahn, and Mark A. Czarnaski 18 Jan. 1989 114 p

(Contract N00014-86-C-2322)

(AD-A203851; JAYCOR-J206-89-001/6261) Avail: NTIS HC A06/MF A01 CSCL 09A

The scope of this effort was diverse with emphasis placed on five major tasks: experiment design and construction of 10 GHz 10 MW long pulse gyrotron; numerical and computational analysis for the gyrotron laboratory; technical efforts for pulsed power microwave experiments; operation of the Gyrotron Test Facility;

and the quasi-optical gyrotron. Also included is a section identified as additional efforts. These efforts include the tunable oscillator and low power phase-locked oscillator experiments and are an extension of work done under the pulsed power experiments.
GRA

12 ASTRONAUTICS (GENERAL)

For extraterrestrial exploration see *91 Lunar and Planetary Exploration.*

N89-20156# European Space Agency, Paris (France).
THE CLUSTER MISSION: SCIENTIFIC AND TECHNICAL ASPECTS OF THE INSTRUMENTS
T. D. Guyenne, comp. Oct. 1988 103 p
(ESA-SP-1103; ISSN-0379-6566; ETN-89-94132) Avail: NTIS HC A06/MF A01; ESA Publications Div., ESTEC, Noordwijk, Netherlands, $10 US or 25 Dutch guilders

The Cluster mission, magnetic field measuring, wave experiments, electric field measurement, ionospheric sounding, particle spectrometry, particle imaging detectors, and spacecraft potential control are discussed. For individual titles, see N89-20157 through N89-20169.

N89-20157*# National Aeronautics and Space Administration. Goddard Space Flight Center, Greenbelt, MD.
CLUSTER: A FLEET OF FOUR SPACECRAFT TO STUDY PLASMA STRUCTURES IN THREE DIMENSIONS **c18**
R. Schmidt (European Space Agency. European Space Research and Technology Center, ESTEC, Noordwijk, Netherlands) and M. L. Goldstein *In* ESA, The Cluster Mission: Scientific and Technical Aspects of the Instruments Oct. 1988 p 7-13 (For primary document see N89-20156 13-12)
Avail: NTIS HC A06/MF A01; ESA Publications Div., ESTEC, Noordwijk, Netherlands, $10 US or 25 Dutch guilders CSCL 22B

The four Cluster spacecraft are spin stabilized spacecraft which are designed and built under stringent requirements as far as electromagnetic cleanliness is concerned. Conductive surfaces and low electromagnetic background noise are mandatory for accurate electric field and cold plasma measurements. The mission is implemented in collaboration between ESA and NASA. A Russian mission will be closely coordinated with Cluster. ESA

N89-20158*# National Aeronautics and Space Administration. Goddard Space Flight Center, Greenbelt, MD.
THE MAGNETIC FIELD INVESTIGATION ON CLUSTER **c46**
A. Balogh, S. W. H. Cowley, D. J. Southwood, G. Musmann, H. Luhr, F. M. Neubauer, K.-H. Glassmeier, W. Riedler, M. F. Heyn (Oesterreichische Akademie der Wissenschaften, Vienna.), and M. H. Acuna et al *In* ESA, The Cluster Mission: Scientific and Technical Aspects of the Instruments Oct. 1988 p 15-20 Prepared in cooperation with California Univ., Lo s Angeles, Danish Space Research Inst., Lyngby, Centre National d'Etudes des Telecommunications, Issy-les-Moulineaux, France, and JPL, Pasadena, CA (For primary document see N89-20156 13-12)
Avail: NTIS HC A06/MF A01; ESA Publications Div., ESTEC, Noordwijk, Netherlands, $10 US or 25 Dutch guilders CSCL 04A

The magnetic field investigation of the Cluster four-spacecraft mission is designed to provide intercalibrated measurements of the B magnetic field vector. The instrumentation and data processing of the mission are discussed. The instrumentation is identical on the four spacecraft. It consists of two triaxial fluxgate sensors and of a failure tolerant data processing unit. The combined analysis of the four spacecraft data will yield such parameters as the current density vector, wave vectors, and the geometry and structure of discontinuities. ESA

N89-20159# Centre de Recherches en Physique de l'Environnement, Issy-les-Moulineaux (France).
WAVE EXPERIMENT CONSORTIUM **c46**
A. Roux and B. delaPorte *In* ESA, The Cluster Mission: Scientific and Technical Aspects of the Instruments Oct. 1988 p 21-23 (For primary document see N89-20156 13-12)
Avail: NTIS HC A06/MF A01; ESA Publications Div., ESTEC, Noordwijk, Netherlands, $10 US or 25 Dutch guilders

The scientific objectives of the consortium are explained, together with its capability to achieve them in the course of the Cluster mission. The five experiments and the interfaces between them are shown. The need for a technical coordination led to the formation of a technical coordination office (WECTCO). The tasks of the WECTCO are indicated. ESA

N89-20160# Centre de Recherches en Physique de l'Environnement, Issy-les-Moulineaux (France).
STAFF: THE SPATIO-TEMPORAL ANALYSIS OF FIELD FLUCTUATIONS EXPERIMENT **c46**
N. Cornilleau-Wehrlin, A. Bahnsen, P. Gough, D. A. Gurnett, G. Gustafsson, C. C. Harvey, D. Hubert, W. Kofman, F. Lefeuvre, and R. Manning (Observatoire de Paris-Meudon, France) et al *In* ESA, The Cluster Mission: Scientific and Technical Aspects of the Instruments Oct. 1988 p 25-30 (For primary document see N89-20156 13-12)
Avail: NTIS HC A06/MF A01; ESA Publications Div., ESTEC, Noordwijk, Netherlands, $10 US or 25 Dutch guilders

The experiment to be implemented in the four Cluster spacecraft consists of a three axial search coil magnetometer to measure the magnetic components of electromagnetic fluctuations (up to 4 kHz) and a spectrum analyzer to perform on board each satellite the auto and cross correlations between electric and magnetic components. The technical description of the experiment is given, including the time resolution and the number of spectral matrix coefficients transmitted for the different operational modes foreseen. ESA

N89-20161*# National Aeronautics and Space Administration. Goddard Space Flight Center, Greenbelt, MD.
THE SPHERICAL PROBE ELECTRIC FIELD AND WAVE EXPERIMENT **c32**
G. Gustafsson, T. Aggson, R. Bostrom, L. P. Block, C. Cattell, P. M. E. Decreau, A. Egeland, C.-G. Falthammar, R. J. L. Grard, and D. A. Gurnett (Iowa Univ., Iowa City.) et al *In* ESA, The Cluster Mission: Scientific and Technical Aspects of the Instruments Oct. 1988 p 31-36 (For primary document see N89-20156 13-12)
Avail: NTIS HC A06/MF A01; ESA Publications Div., ESTEC, Noordwijk, Netherlands, $10 US or 25 Dutch guilders CSCL 20N

The experiment is designed to measure the electric field and density fluctuations with sampling rates up to 40,000 samples/sec. The description includes Langmuir sweeps that can be made to determine the electron density and temperature, the study of nonlinear processes that result in acceleration of plasma, and the analysis of large scale phenomena where all four spacecraft are needed. ESA

N89-20162# Centre National de la Recherche Scientifique, Orleans (France). Lab. de Physique et Chimie de l'Environnement.
WHISPER: A SOUNDER AND HIGH FREQUENCY WAVE ANALYZER EXPERIMENT **c75**
P. M. E. Decreau, J. G. Trotignon, P. Canu, H. DeFeraudy, G. Gustafsson, A. Bahnsen, I. B. Iversen, M. Jespersen, D. A. Gurnett, and L. J. C. Woolliscroft (Sheffield Univ., England) *In* ESA, The Cluster Mission: Scientific and Technical Aspects of the Instruments Oct. 1988 p 37-43 (For primary document see N89-20156 13-12)
Avail: NTIS HC A06/MF A01; ESA Publications Div., ESTEC, Noordwijk, Netherlands, $10 US or 25 Dutch guilders

The experiment described aims to measure accurately the total plasma density within the range from 0.2 to 80/cc. It is based on a resonance sounding technique which was proved to be successful in ionospheric dense plasma as well as on dilute space plasmas. Whisper also provides a continuous survey of one electric component of plasma waves in the frequency range from 4 to 80 kHz with an accuracy of 160 Hz at best. ESA

N89-20163# Iowa Univ., Iowa City. Dept. of Physics and Astronomy.
THE WIDEBAND PLASMA WAVE INTERACTION **c75**
D. A. Gurnett, R. R. Shaw, R. L. Huff, and D. L. Krichner *In* ESA, The Cluster Mission: Scientific and Technical Aspects of the Instruments Oct. 1988 p 45-48 (For primary document see N89-20156 13-12)
Avail: NTIS HC A06/MF A01; ESA Publications Div., ESTEC, Noordwijk, Netherlands, $10 US or 25 Dutch guilders

The wideband plasma wave investigation for the Cluster experiment is designed to provide the high resolution spectral analysis required to clearly identify many types of plasma waves detected in the Earth's magnetosphere. The system provides measurements of electric and magnetic fields in selected frequency ranges from 10 Hz to 600 kHz. Continuous waveforms are digitized, formatted, and transferred to the spacecraft telemetry system using either a real time mode or a burst data mode. ESA

N89-20164# Sheffield Univ. (England).
THE DIGITAL WAVE PROCESSING EXPERIMENT **c75**
L. J. C. Woolliscroft, J. A. Thompson, P. M. E. Decreau, M. Parrot, A. Egeland, I. B. Iversen, H. C. Koons, P. J. Christiansen, M. P. Gough, and G. Gustafsson (Swedish Inst. of Space Physics, Uppsala.) et al *In* ESA, The Cluster Mission: Scientific and Technical Aspects of the Instruments Oct. 1988 p 49-54 (For primary document see N89-20156 13-12)
Avail: NTIS HC A06/MF A01; ESA Publications Div., ESTEC, Noordwijk, Netherlands, $10 US or 25 Dutch guilders

A wide variety of geophysical plasmas will be investigated by the Cluster mission. The digital wave processing (DWP) experiment implements the four ESA/NASA Cluster satellites as a component of the wave experiment consortium. The processing system within the DWP will also perform particle and wave particle correlations so as to study directly wave-particle interactions. The DWP instrument employs an architecture with parallel processing and re-allocatable tasks to provide a high reliability system. ESA

N89-20165# Max-Planck-Inst. fuer Physik und Astrophysik, Garching (Germany, F.R.).
THE ELECTRON DRIFT INSTRUMENT **c75**
G. Paschmann, F. Melzner, G. Haerendel, O. H. Bauer, W. Baumjohann, M. Boehm, M. Nakamura, N. Sckopke, R. Treumann, and C. E. McIlwain (California Univ., San Diego, La Jolla.) et al *In* ESA, The Cluster Mission: Scientific and Technical Aspects of the Instruments Oct. 1988 p 55-63 (For primary document see N89-20156 13-12)
Avail: NTIS HC A06/MF A01; ESA Publications Div., ESTEC, Noordwijk, Netherlands, $10 US or 25 Dutch guilders

The instrument, implementing the ESA/NASA Cluster mission, measures the drift of a weak beam of test electrons which for certain emission directions return to the spacecraft after one gyration. This is related to the electrical field and the gradient in the magnetic field, which by use of different electron energies can be separately determined. The magnetic field strength is also measured. ESA

N89-20166# Centre d'Etude Spatiale des Rayonnements, Toulouse (France).
THE ION SPECTROMETRY EXPERIMENT TO MEASURE THE PROPERTIES OF THE IONIC PLASMA COMPOSITION AND DISTRIBUTION FUNCTIONS AT ENERGIES BETWEEN 0 AND 40keV/e **c75**
H. Reme, J. M. Bosqued, J. A. Sauvaud, A. Cros, J. Dandouras, C. dUston, E. Moebius, D. Hovestadt, B. Klecker, and G. Paschmann (Max-Planck-Inst. fuer Physik und Astrophysik, Garching, Germany, F.R.) et al *In* ESA, The Cluster Mission: Scientific and Technical Aspects of the Instruments Oct. 1988 p 65-76 (For primary document see N89-20156 13-12)
Avail: NTIS HC A06/MF A01; ESA Publications Div., ESTEC, Noordwijk, Netherlands, $10 US or 25 Dutch guilders

The ionic plasma spectrometry package described is capable of obtaining full three-dimensional ion distributions with high time resolution with mass per charge composition determination onboard the four Cluster spacecraft. It consists of a hot ion analyzer and a time of flight ion composition and distribution function analyzer, plus a sophisticated multiprocessor based instrument control and data processing system. ESA

N89-20167# Mullard Space Science Lab., Dorking (England).
PEACE: A PLASMA ELECTRON AND CURRENT EXPERIMENT **c75**
A. D. Johnstone, A. J. Coates, D. S. Hall, B. N. Maehlum, S. J. Schwartz, M. Thomsen, and J. D. Winningham (Southwest Research Inst., Houston, TX.) *In* ESA, The Cluster Mission: Scientific and Technical Aspects of the Instruments Oct. 1988 p 77-84 (For primary document see N89-20156 13-12)
Avail: NTIS HC A06/MF A01; ESA Publications Div., ESTEC, Noordwijk, Netherlands, $10 US or 25 Dutch guilders

An electron analyzer to measure the three-dimensional velocity distribution of electrons on the multispacecraft Cluster mission is described, with emphasis on the steps taken to meet the special requirements imposed by the novel character of the mission. The technical description includes electron optics, readout systems, onboard data processing equipment, calibration, and flight operations. ESA

N89-20168# Max-Planck-Inst. fuer Aeronomie, Katlenburg-Lindau (Germany, F.R.).
RAPID: RESEARCH WITH ADAPTIVE PARTICLE IMAGING DETECTORS **c75**
B. Wilken, W. I. Axford, P. Daly, A. Korth, G. Kremser, W. H. Ip, V. M. Vasyliunas, J. B. Blake, J. F. Fennell, and L. R. Lyons (Aerospace Corp., Los Angeles, CA.) et al *In* ESA, The Cluster Mission: Scientific and Technical Aspects of the Instruments Oct. 1988 p 85-93 (For primary document see N89-20156 13-12)
Avail: NTIS HC A06/MF A01; ESA Publications Div., ESTEC, Noordwijk, Netherlands, $10 US or 25 Dutch guilders

The spectrometer for the Cluster mission is an advanced particle detector for the analysis of suprathermal plasma distributions in the energy range from 20 to 400 keV for electrons and ions. The detection principle for the ionic component is based on a two-dimensional analysis of particle velocity and energy. Electrons are identified by the energy range relationship. ESA

N89-20169*# Jet Propulsion Lab., California Inst. of Tech., Pasadena.
ACTIVE SPACECRAFT POTENTIAL CONTROL: AN ION EMITTER EXPERIMENT **c18**
W. Riedler, R. Goldstein, M. Hamelin, B. N. Maehlum, J. Troim, R. C. Olsen, A. Pedersen, R. J. L. Grard, R. Schmidt, and F. Rudenauer (Oesterreichisches Forschungszentrum Seibersdorf G.m.b.H., Vienna.) et al *In* ESA, The Cluster Mission: Scientific and Technical Aspects of the Instruments Oct. 1988 p 95-102 (For primary document see N89-20156 13-12)
Avail: NTIS HC A06/MF A01; ESA Publications Div., ESTEC, Noordwijk, Netherlands, $10 US or 25 Dutch guilders

The cluster spacecraft are instrumented with ion emitters for charge neutralization. The emitters produce indium ions at 6 keV. The ion current is adjusted in a feedback loop with instruments measuring the spacecraft potential. The system is based on the evaporation of indium in the apex field of a needle. The design of the active spacecraft potential control instruments, and the ion emitters is presented. ESA

13 ASTRODYNAMICS

Includes powered and free-flight trajectories; and orbital and launching dynamics.

N89-20170# Defense Mapping Agency, Washington, DC.
DMA (DEFENSE MAPPING AGENCY) ORBIT DETERMINATION OF THE NAVY NAVIGATION SATELLITE SYSTEM FOR 1987 Final Report, Jan. - Dec. 1987
J. K. Murphy and Robert J. Jones 3 Oct. 1988 44 p
(AD-A203496) Avail: NTIS HC A03/MF A01 CSCL 22B

The Defense Mapping Agency Hydrographic/Topographic Center (DMAHTC) performs precise orbit computations for Navy Navigation Satellite System (NNSS) satellites, also called TRANSIT, using Doppler observations collected by a worldwide network of stations. Equipment at these sites is configured around either a Tranet 2 or a Magnavox 1502 DS receiver. Table 1 lists the current stations while Figure 1 shows the tracking network configuration. Recorded Doppler counts, surface weather measurements, and other appropriate data are transmitted daily via satellite communications or over other telecommunication links to DMAHTC for processing, time corrections and orbit determination. There are two classes of NNSS satellites - the Oscar and the Nova. The Nova satellites represent the latest generation of TRANSIT satellites. For Nova satellite 30480 and Oscar satellites 30110, 30130, 30200, 30240 and 30300, data were processed in one-day fits. Table 2 and Figure 2 provide additional information on these satellites. GRA

14 GROUND SUPPORT SYSTEMS AND FACILITIES (SPACE)

Includes launch complexes, research and production facilities; ground support equipment, e.g., mobile transporters; and simulators.

For related information see also *09 Research and Support Facilities (Air).*

No abstracts in this category.

15 LAUNCH VEHICLES AND SPACE VEHICLES

Includes boosters; operating problems of launch/space vehicle systems; and reusable vehicles.

For related information see also *20 Spacecraft Propulsion and Power.*

N89-20171*# National Aeronautics and Space Administration. Lewis Research Center, Cleveland, OH.

A DEFINITION STUDY OF THE ON-ORBIT ASSEMBLY OPERATIONS FOR THE OUTBOARD PHOTOVOLTAIC POWER MODULES FOR SPACE STATION FREEDOM M.S. Thesis - Toledo Univ.

Thomas J. Sours Mar. 1989 89 p

(NASA-TM-102006; E-4712; NAS 1.15:102006) Avail: NTIS HC A05/MF A01 CSCL 22B

A concept is described for the assembly of the outboard PV modules for Space Station Freedom. Analysis of the on-orbit assembly operations was performed using CADAM design graphics software. A scenario for assembly using the various assembly equipment, as currently defined, is described in words, tables and illustrations. This work is part of ongoing studies in the area of space station assembly. The outboard PV module and the assembly equipment programs are all in definition and preliminary design phases. An input is provided to the design process of assembly equipment programs. It is established that the outboard PV module assembly operations can be performed using the assembly equipment currently planned in the Space Station Freedom Program. Author

N89-20172# Sandia National Labs., Albuquerque, NM. Plasma Theory Div.

RECONNECTION LAUNCHER PROJECTILE HEATING USING THE MODIFIED REGGIE CODE

J. R. Freemen Jan. 1989 17 p

(Contract DE-AC04-76DP-00789)

(DE89-007294; SAND-88-2679) Avail: NTIS HC A03/MF A01

Modified REGGIE is a variant of the REGGIE reconnection launcher code. It was written to provide a more economical tool for studying multi-stage projectile heating. The validity of the approximations made in modified REGGIE was determined by comparisons with both full REGGIE and WARP-10 computations. Modified REGGIE runs about seven times faster than full REGGIE. Modified REGGIE was used to study projectile heating for a specific force profile proposed by M. Cowan. The total energy dissipated after seven stages was reduced by a factor of about eight compared to the present day conventional discrete coil system. This reduction would allow higher peak velocities to be achieved prior to ablation. DOE

16 SPACE TRANSPORTATION

Includes passenger and cargo space transportation, e.g., shuttle operations; and space rescue techniques.

For related information see also *03 Air Transportation and Safety* and *18 Spacecraft Design, Testing and Performance.* For space suits see *54 Man/System Technology and Life Support.*

N89-20173*# Auburn Univ., AL. Dept. of Aerospace Engineering.

UNMANNED, SPACE-BASED, REUSABLE ORBITAL TRANSFER VEHICLE, DARVES. VOLUME 1: TRADE ANALYSIS AND DESIGN Final Report

Jun. 1988 54 p

(Grant NGT-21-002-080)

(NASA-CR-184711; NAS 1.26:184711) Avail: NTIS HC A04/MF A01 CSCL 22B

The design of an unmanned, space-based, reusable Orbital Transfer Vehicle (OTV) is presented. This OTV will be utilized for the delivery and retrieval of satellites from geosynchronous Earth orbit (GEO) in conjunction with a space station assumed to be in existence in low Earth orbit (LEO). The trade analysis used to determine the vehicle design is presented, and from this study a vehicle definition is given. Author

N89-20174*# Auburn Univ., AL. Dept. of Aerospace Engineering.

UNMANNED, SPACE-BASED, REUSABLE ORBITAL TRANSFER VEHICLE, DARVES. VOLUME 2: DATA AND CALCULATIONS Final Report

Jun. 1988 37 p

(Grant NGT-21-002-080)

(NASA-CR-184712; NAS 1.26:184712) Avail: NTIS HC A03/MF A01 CSCL 22B

Results for trajectory analysis, fuel analysis, and analysis of aerobraking maneuvers are presented. Calculations are included for thickness and mass of the propellant tanks; determination of weight (avionics module); numerical integration program; hydrostatic pressure due to acceleration; and propellant tank pressurization. B.G.

N89-20175*# Virginia Univ., Charlottesville. WWSR, Inc.

TWO DESIGNS FOR AN ORBITAL TRANSFER VEHICLE: A COMPARISON OF TWO OTVs Summary Report

1988 19 p Presented at the NASA/USRA Advanced Design Program Summer Conference, Jun. 1988

(Grant NGT-21-002-080)

(NASA-CR-184696; NAS 1.26:184696; Rept-1) Avail: NTIS HC A03/MF A01 CSCL 22B

The basic components of the design for the orbital transfer vehicle (OTV) are outlined. The Project Orion and the MOVERS OTV design are compared. The nature of the work and the specifics will be reviewed. The propellant systems are summarized along with the dollar savings. The strengths and weaknesses are highlighted for each OTV. B.G.

N89-20176*# Virginia Univ., Charlottesville. WWSR, Inc.
TWO DESIGNS FOR AN ORBITAL TRANSFER VEHICLE. PROJECT ORION: A PROPOSAL FOR A MANNED ORBITAL TRANSFER VEHICLE FOR THE 21ST CENTURY
1988 129 p Presented at the NASA/USRA Advanced Design Program Summer Conference, Jun. 1988
(Grant NGT-21-002-080)
(NASA-CR-184697; NAS 1.26:184697; Rept-2) Avail: NTIS HC A07/MF A01 CSCL 22B

The most optimal design for a chemical propellant, manned OTV that fulfills the described constraints is presented. The design of the Project Orion OTV and its subsystems are examined. B.G.

N89-20177*# Virginia Univ., Charlottesville. Modular Orbital Vehicle Engineering Research Society.
TWO DESIGNS FOR AN ORBITAL TRANSFER VEHICLE Final Report
Richard Davis, Miles Duquette, Rebecca Fredrick, Daniel Schumacher, Schaeffer Somers, Stanley Stafira, James Williams, and Mark Zelinka May 1988 193 p
(Grant NGT-21-002-080)
(NASA-CR-184698; NAS 1.26:184698; Rept-3) Avail: NTIS HC A09/MF A01 CSCL 22B

The Orbital Transfer Vehicle (OTV) and systems were researched in the following areas: avionics, crew systems, electrical power systems, environmental control/life support systems, navigation and orbital maneuvers, propulsion systems, reaction control systems (RCS), servicing systems, and structures. B.G.

N89-20178*# National Aeronautics and Space Administration. Marshall Space Flight Center, Huntsville, AL.
STS-27R OV-104 ORBITER TPS DAMAGE REVIEW TEAM, VOLUME 1 Summary Report
John W. Thomas, comp. Feb. 1989 77 p
(NASA-TM-100355-Vol-1; NAS 1.15:100355-Vol-1) Avail: NTIS HC A05/MF A01 CSCL 22B

Following the return to earth on December 2, 1988, of Orbiter OV-104, Atlantis, it was observed that there was substantial Thermal Protection System (TPS) tile damage present on the lower right fuselage and wing. Damage sites were more numerous than on previous flights and conversely, there was almost no damage present on Atlantis' left side. A review team investigated the cause beginning with a detailed inspection of the Atlantis TPS damage, and a review of related inspection reports to establish an indepth anomaly definition. An exhaustive data review followed. A fault tree and several failure scenarios were developed. Finally, the failure scenarios were categorized as either not possible, possible but not probable, or probable. This and other information gained during the review formed the basis for the team's findings and recommendations. The team concluded that the most probable cause of the severe STS-27R Orbiter tile damage is that the ablative insulating material covering the RH SRB Nose Cap dislodged and struck the Orbiter tile near 85 seconds into flight and possibly that debris from other sources, including repaired insulation and missing joint cork, caused minor tile damage. Findings are presented, and recommendations that are believed pertinent to minimizing the potential for inflight debris are described. Author

N89-20179*# National Aeronautics and Space Administration. Lewis Research Center, Cleveland, OH.
EXPENDABLE LAUNCH VEHICLE TRANSPORTATION FOR THE SPACE STATION
Robert R. Corban Oct. 1988 13 p Presented at the 39th Congress of the International Astronautical Federation, Bangalore, India, 8-15 Oct. 1988 Previously announced in IAA as A89-17720
(NASA-TM-101947; E-4636; NAS 1.15:101947) Avail: NTIS HC A03/MF A01 CSCL 22B

Logistics transportation will be a critical element in determining the Space Station Freedom's level of productivity and possible evolutionary options. The current program utilizes the Space Shuttle as the only logistics support vehicle. Augmentation of the total transportation capability by expendable launch vehicles (ELVs) may be required to meet demanding requirements and provide for enhanced manifest flexibility. The total operational concept from ground operations to final return of support hardware or its disposal is required to determine the ELV's benefits and impacts to the Space Station Freedom program. The characteristics of potential medium and large class ELVs planned to be available in the mid-1990's (both U.S. and international partners' vehicles) indicate a significant range of possible transportation systems with varying degrees of operational support capabilities. The options available for development of a support infrastructure in terms of launch vehicles, logistics carriers, transfer vehicles, and return systems is discussed. Author

17 SPACE COMM., SPACECRAFT COMM., COMMAND & TRACKING

Includes telemetry; space communications networks; astronavigation and guidance; and radio blackout.

For related information see also *04 Aircraft Communications and Navigation* and *32 Communications and Radar.*

N89-20340*# Jet Propulsion Lab., California Inst. of Tech., Pasadena.
VLA TELEMETRY PERFORMANCE WITH CONCATENATED CODING FOR VOYAGER AT NEPTUNE
S. J. Dolinar, Jr. *In its* The Telecommunications and Data Acquisition Report 15 Nov. 1988 p 112-133 (For primary document see N89-20329 13-32)
Avail: NTIS HC A12/MF A01 CSCL 09F

N89-20344*# California Inst. of Tech., Pasadena. Dept. of Electrical Engineering.
THE DECODING OF REED-SOLOMON CODES
R. J. McEliece *In* JPL, The Telecommunications and Data Acquisition Report 15 Nov. 1988 p 153-167 (For primary document see N89-20329 13-32)
Avail: NTIS HC A12/MF A01 CSCL 09F

18 SPACECRAFT DESIGN, TESTING AND PERFORMANCE

Includes satellites; space platforms; space stations; spacecraft systems and components such as thermal and environmental controls; and attitude controls.

For life support systems see *54 Man/System Technology and Life Support.* For related information see also *05 Aircraft Design, Testing and Performance, 39 Structural Mechanics,* and *16 Space Transportation.*

N89-20180*# Colorado Univ., Boulder. Dept. of Aerospace Engineering.
L1 LIBRATION POINT MANNED SPACE HABITAT Final Report
Marvin Luttges, Steve Johnson, Gary Banks, Richard Johnson, Christian Meyer, Scott Pepin, and Robert MacElroy [1989] 83 p
(Grant NGT-21-002-080)
(NASA-CR-184732; NAS 1.26:184732) Avail: NTIS HC A05/MF A01 CSCL 22B

Second generation stations or Manned Space Habitats (MSHs) are discussed for an Earth-Moon libration point and in lunar orbit. The conceptual design of such a station is outlined. Systems and subsystems described reflect anticipation of moderate technology growth. The evolution of the L1 environments is discussed, several selected subsystems are outlined, and how the L1 MSH will complete some of its activities is described. B.G.

N89-20181*# Essex Corp., Huntsville, AL.
EXTRAVEHICULAR ACTIVITY AT GEOSYNCHRONOUS EARTH ORBIT Final Technical Report

Nicholas Shields, Jr., Arthur E. Schulze, Gerald P. Carr, and William Pogue (CAMUS, Inc., Huntsville, AL.) 22 Jan. 1988 238 p
(Contract NAS9-17779)
(NASA-CR-172112; NAS 1.26:172112) Avail: NTIS HC A11/MF A01 CSCL 22B

The basic contract to define the system requirements to support the Advanced Extravehicular Activity (EVA) has three phases: EVA in geosynchronous Earth orbit; EVA in lunar base operations; and EVA in manned Mars surface exploration. The three key areas to be addressed in each phase are: environmental/biomedical requirements; crew and mission requirements; and hardware requirements. The structure of the technical tasks closely follows the structure of the Advanced EVA studies for the Space Station completed in 1986. Author

N89-20182*# Martin Marietta Aerospace, Denver, CO. Astronautics Group.
SUPERFLUID HELIUM TANKER (SFHT) STUDY Final Report
Ralph N. Eberhardt, Sam M. Dominick, John E. Anderson, John P. Gille, Tim A. Martin, John S. Marino, Howard L. Paynter, R. Eric Traill, Alfred Herzl, and Sam Gotlib et al Sep. 1988 187 p
(Contract NAS9-17854)
(NASA-CR-172110; NAS 1.26:172110; MCR-88-1402) Avail: NTIS HC A09/MF A01 CSCL 22B

Replenishment of superfluid helium (SFHe) offers the potential of extending the on-orbit life of observatories, satellite instruments, sensors and laboratories which operate in the 2 K temperature regime. A reference set of resupply customers was identified as representing realistic helium servicing requirements and interfaces for the first 10 years of superfluid helium tanker (SFHT) operations. These included the Space Infrared Telescope Facility (SIRTF), the Advanced X-ray Astrophysics Facility (AXAF), the Particle Astrophysics Magnet Facility (Astromag), and the Microgravity and Materials Processing Sciences Facility (MMPS)/Critical Point Phenomena Facility (CPPF). A mixed-fleet approach to SFHT utilization was considered. The tanker permits servicing from the Shuttle cargo bay, in-situ when attached to the OMV and carried to the user spacecraft, and as a depot at the Space Station. A SFHT Dewar ground servicing concept was developed which uses a dedicated ground cooling heat exchanger to convert all the liquid, after initial fill as normal fluid, to superfluid for launch. This concept permits the tanker to be filled to a near full condition, and then cooled without any loss of fluid. The final load condition can be saturated superfluid with any desired ullage volume, or the tank can be totally filed and pressurized. The SFHT Dewar and helium plumbing system design has sufficient component redundancy to meet fail-operational, fail-safe requirements, and is designed structurally to meet a 50 mission life usage requirement. Technology development recommendations were made for the selected SFHT concept, and a Program Plan and cost estimate prepared for a phase C/D program spanning 72 months from initiation through first launch in 1997. Author

N89-20183*# Auburn Univ., AL.
VEHICLE FOR SPACE TRANSFER AND RECOVERY (VSTAR), VOLUME 1 Final Report
Jun. 1988 101 p
(Grant NGT-21-002-080)
(NASA-CR-184827; NAS 1.26:184827) Avail: NTIS HC A06/MF A01 CSCL 22B

The Vehicle Space Transfer and Recovery (VSTAR) system is designed as a manned orbital transfer vehicle (MOTV) with the primary mission of Satellite Launch and Repair (SLR). VSTAR will provide for economic use of high altitude spaceflight for both the public and private sector. VSTAR components will be built and tested using earth based facilities. These components will then be launched using the space shuttle, into low earth orbit (LEO) where it will be constructed on a U.S. built space station. Once in LEO the vehicle components will be assembled in modules which can then be arranged in various configurations to perform the required missions. Author

N89-20184*# Auburn Univ., AL.
VEHICLE FOR SPACE TRANSFER AND RECOVERY (VSTAR), VOLUME 2: SUBSTANTIATING ANALYSES AND DATA Final Report
Jun. 1988 63 p
(Grant NGT-21-002-080)
(NASA-CR-184828; NAS 1.26:184828) Avail: NTIS HC A04/MF A01 CSCL 22B

The Vehicle Space Transfer and Recovery (VSTAR) system is designed as a manned orbital transfer vehicle (MOTV) with the primary mission of Satellite Launch and Repair (SLR). Reference materials, calculations and trade studies used in the analysis and selection of VSTAR components. Each major VSTAR system is examined separately. Simple graphs and tables are used to make qualitative comparisons of various VSTAR component candidates. Equations and/or calculations used for a particular analysis are also included where applicable. Author

N89-20185# Alcatel Standard Electrica S.A., Madrid (Spain).
REVIEW OF NETWORK PLANNING METHODS APPLICABLE TO INTEGRATED SATELLITE TERRESTRIAL NETWORKS (ISTN) Final Report
O. GonzalezSoto and C. Mayoral Paris, France ESA Jul. 1988 13 p
(Contract ESTEC-7170/87-NL-PR)
(ESA-CR(P)-2691; ETN-89-93919) Avail: NTIS HC A03/MF A01

Traffic forecast, network planning, modeling and management, signaling and interfacing techniques were reviewed in relation to their application to the ISTN, in a so-called ESCO study. The data, procedures and methodology used in the ECO study are validated through the analysis of the documentation generated during that study, giving the conformance with the reports or suggesting modifications or improvements to increase the quality of the results of the study. The adequacy of the methodology used in each particular work package of the ESCO study; the correctness and reliability of the procedures; the compatibility of assumptions; and the accuracy the data representing demand and cost values are emphasized. ESA

N89-20186# Dynamic Engineering, Inc., Heverlee (Belgium).
ERROR LOCALIZATION AND UPDATING OF SPACECRAFT STRUCTURES MATHEMATICAL MODELS Final Report
E. Dascotte Paris, France ESA Jun. 1988 173 p
(Contract ESTEC-7512/87-NL-PH)
(ESA-CR(P)-2697; ETN-89-93938) Avail: NTIS HC A08/MF A01

A procedure for updating finite element models for structural analysis was evaluated by means of a clamped porch, a tuning fork, an elastic clamped beam, and a spacecraft structure. Bayesian parameter estimation yields better error localization than the pseudo-inverse technique, although in general, this results in a slower iteration speed. Updated models can be used with more confidence when coupled with other structures or when a static analysis is performed. A higher number of eigenmodes included in the updating procedure yields better results for error localization. If the number of equations equals or is larger than the number of parameters, errors can be exactly identified. Measurement errors on the eigenfrequency can have an important influence on the parameter estimations. Amplification and reduction factors, as well as weighting coefficients prove to be valuable for optimizing convergence characteristics. ESA

N89-20187 Utah State Univ., Logan.
ABLATION OF MATERIALS IN THE LOW EARTH ORBITAL ENVIRONMENT Ph.D. Thesis
Russel Roger Laher 1987 176 p
Avail: Univ. Microfilms Order No. DA8823639

The ablation of external surfaces of a spacecraft in orbit by gas molecules in the atmosphere is investigated. A near-earth orbiting spacecraft moves through the atmosphere at about 8 km/sec. This relative speed allows gas molecules to impinge upon spacecraft surfaces with energies in the range of 5 to 10 eV, a

sufficient amount, in many cases, to ablate molecules of surface material at an appreciable rate, as demonstrated from analyses of materials flown on Space Shuttle missions STS-1 through STS-5, STS-8 and STS-41G, and the results of the analyses on materials retrieved from the Solar Maximum Mission satellite is given. The physical parameters of both the atmosphere and the surface materials that control this process, and possible mechanisms for surface ablation are examined. Based upon these considerations, two different ablation models, one for polycrystalline materials and one for amorphous materials are formulated for use in computing ablation rates of materials exposed to the low earth orbital environment. Using a standard atmosphere with altitude profiles of temperatures and concentrations for both neutral and ionic species, maximum ablation rates as a function of satellite altitude in the 100 to 1000 km range are estimated for elementary polycrystalline solids from sputtering data obtained from laboratory measurements. Dissert. Abstr.

N89-20188# General Accounting Office, Washington, DC.
SPACE STATION: NASA EFFORTS TO ESTABLISH A DESIGN-TO-LIFE-CYCLE COST PROCESS
May 1988 46 p
(GAO/NSIAD-88-147) Avail: NTIS HC A03/MF A01

NASA's implementation of actions regarding space station operations cost management is reviewed. Although the definition phase has been completed, NASA is still developing major portions of the operations cost management system described in its Dec. 1985 report, including a cost management policy and cost benchmarks. NASA is currently considering a draft directive to help establish a management system that would systematically consider and assess life cycle cost impacts of design proposals. E.R.

N89-20189# Royal Inst. of Tech., Stockholm (Sweden). Dept. of Plasma Physics.
MEASUREMENT OF QUASI-STATIC AND LOW FREQUENCY ELECTRIC FIELDS ON THE VIKING SATELLITE
L. P. Block, Carl-Gunne Faelthammar, P.-A. Lindqvist, G. T. Marklund, F. S. Mozer, and A. Pedersen (European Space Agency. European Space Research and Technology Center, ESTEC, Noordwijk, Netherlands) Mar. 1987 19 p Sponsored by the Swedish Board for Space Activities, Stockholm, Sweden
(TRITA-EPP-87-02; ISSN-0348-7539; ETN-89-93725) Avail: NTIS HC A03/MF A01

The instrument for measurement of quasi-static and low frequency (dc and slowly varying) electric fields on the Swedish Viking satellite is described. The instrument uses 3 spherical probe pairs to measure the full three-dimensional electric field vector with 18.75 ms time resolution. The probes are kept near plasma potential by means of a controllable bias current. A guard covering part of the booms is biased to a negative voltage to prevent photoelectrons escaping from the probes from reaching the satellite body. Current-voltage sweeps are performed to determine the plasma density and temperature and to select the optimal bias current. The bias currents to the probes and the voltage offset on the guards as well as the current-voltage sweeps are controlled by an on-board microprocessor which can be programmed from the ground and allows great flexibility. ESA

N89-20190# Air Force Inst. of Tech., Wright-Patterson AFB, OH. School of Engineering.
ASSESSING POTENTIAL BENEFITS FOR SERVICE/REPAIR AND RETRIEVAL OF SATELLITES: A PILOT DECISION ANALYSIS M.S. Thesis
Michael A. DelPinto Dec. 1988 124 p
(AD-A203830; AFIT/GSO/MA/88D-1) Avail: NTIS HC A06/MF A01 CSCL 22A

The Air Force is considering adopting an on-orbit service/repair strategy for some of its satellites. The decision must be made on a program-by-program basis. A pilot decision analysis was conducted to demonstrate the application of the decision analysis methodology to the decision. A pilot model, using influence diagrams, was developed for a general satellite program. Several spreadsheet programs were constructed for use with the pilot model. A scenario was presented involving a hypothetical communications satellite program. The pilot model was applied to the program and an initial decision analysis was performed. The salient aspects of the analysis were presented to exhibit the advantages of decision analysis as a methodology for structuring and analyzing the decision. The example analysis revealed the strongpoints of the methodology when applied to the case of a decision maker faced with a decision involving uncertainty, complexity, and value preferences. The pilot model and analysis serve as a foundation upon which further application of the decision analysis technique to the on-orbit service/repair decision can build. GRA

N89-20191# Naval Postgraduate School, Monterey, CA.
DESIGN OF A THREE-AXIS STABILIZED ORION SATELLITE USING AN ALL-THRUSTER ATTITUDE CONTROL SYSTEM M.S. Thesis
Suzanne M. Dee Dec. 1988 116 p
(AD-A203953) Avail: NTIS HC A06/MF A01 CSCL 22B

An all-thruster three-axis stabilized attitude control system has been designed for the Naval Postgraduate School (NPS) satellite bus, ORION. The satellite is a cylinder, 19 inches in diameter, 35 inches in length, 250 pounds maximum mass with 32 pounds for payloads. ORION will be ejected from an extended Get-Away-Special (GAS) canister. Launch from any GAS can configure expendable booster or the space shuttle is assumed. The minimization techniques of Pontryagin have been used to derive control laws that support fuel efficient operation. A minimum time cost function is applied in the acquisition phase to reduce rates to acceptable levels. A weighted minimum fuel-time cost function is used during the on-station phase. Bang-Off-Bang control with two switching curves is employed outside of a boundary region. Inside the boundary region, four pulse limit cycle control with time constants on the order of 100 seconds is applied. GRA

N89-20157*# National Aeronautics and Space Administration. Goddard Space Flight Center, Greenbelt, MD.
CLUSTER: A FLEET OF FOUR SPACECRAFT TO STUDY PLASMA STRUCTURES IN THREE DIMENSIONS
R. Schmidt (European Space Agency. European Space Research and Technology Center, ESTEC, Noordwijk, Netherlands) and M. L. Goldstein *In* ESA, The Cluster Mission: Scientific and Technical Aspects of the Instruments Oct. 1988 p 7-13 (For primary document see N89-20156 13-12)
Avail: NTIS HC A06/MF A01; ESA Publications Div., ESTEC, Noordwijk, Netherlands, $10 US or 25 Dutch guilders CSCL 22B

N89-20169*# Jet Propulsion Lab., California Inst. of Tech., Pasadena.
ACTIVE SPACECRAFT POTENTIAL CONTROL: AN ION EMITTER EXPERIMENT
W. Riedler, R. Goldstein, M. Hamelin, B. N. Maehlum, J. Troim, R. C. Olsen, A. Pedersen, R. J. L. Grard, R. Schmidt, and F. Rudenauer (Oesterreichisches Forschungszentrum Seibersdorf G.m.b.H., Vienna.) et al *In* ESA, The Cluster Mission: Scientific and Technical Aspects of the Instruments Oct. 1988 p 95-102 (For primary document see N89-20156 13-12)
Avail: NTIS HC A06/MF A01; ESA Publications Div., ESTEC, Noordwijk, Netherlands, $10 US or 25 Dutch guilders

19 SPACECRAFT INSTRUMENTATION

For related information see also *06 Aircraft Instrumentation* and *35 Instrumentation and Photography.*

No abstracts in this category.

20 SPACECRAFT PROPULSION AND POWER

Includes main propulsion systems and components, e.g., rocket engines; and spacecraft auxilliary power sources.

For related information see also *07 Aircraft Propulsion and Power, 28 Propellants and Fuels, 44 Energy Production and Conversion,* and *15 Launch Vehicles and Space Vehicles.*

N89-20192*# National Aeronautics and Space Administration. Lewis Research Center, Cleveland, OH.

ADVANCED TECHNOLOGY FOR FUTURE SPACE PROPULSION SYSTEMS

Larry A. Diehl Mar. 1989 24 p Presented at a Symposium on Space Commercialization: Roles of Developing Countries, Nashville, TN, 5-10 Mar. 1989; sponsored in part by Tennessee Univ. Space Inst.; AIAA and IAA

(NASA-TM-101951; E-4646; NAS 1.15:101951) Avail: NTIS HC A03/MF A01 CSCL 21H

The NASA Project Pathfinder contains programs to provide technologies for future transfer vehicles including those powered by both advanced chemical and electric propulsion rockets. This paper discusses the Chemical Transfer Propulsion and Cargo Vehicle Propulsion elements of Pathfinder. The program requirements and goals for both elements are discussed, and technical activities which are planned or underway are summarized. Recent progress in programs which support or proceed the Pathfinder activities is detailed. In particular, the NASA Program for Advanced Orbital Transfer Vehicle Propulsion, which acted as the precursor for the Chemical Transfer Propulsion element of Pathfinder is summarized. Author

N89-20193*# National Aeronautics and Space Administration. Lewis Research Center, Cleveland, OH.

THE EMITTANCE OF SPACE RADIATOR MATERIALS MEASURED AT ELEVATED TEMPERATURES

Michael J. Mirtich, Frank DiFilippo, Jennifer Barry, and Michael Kussmaul (Cleveland State Univ., OH.) Apr. 1988 15 p Presented at the 15th International Conference on Metallurgical Coatings, San Diego, CA, 11-15 Apr. 1988; sponsored in part by the American Vacuum Society

(NASA-TM-101948; E-4641; NAS 1.15:101948) Avail: NTIS HC A03/MF A01 CSCL 10B

The spectral emittances of textured space radiator materials between 1.7 and 14.7 micrometers have been evaluated at room temperature and elevated temperature (630 C) in air. Heating in air caused a permanent increase in spectral emittance for all materials tested: HCl/ion beam textured 304 stainless steel, untextured Ti (6 percent Al, 4 percent V), and sandblasted Ti (6 percent Al, 4 percent V). Changes in the surface chemistry and/or surface morphology of these materials were also observed. Elevated temperature spectral emittance was measured in an argon atmosphere and compared to the measurements in air. Similarity between the room temperature and elevated temperature spectral emittance measurements was also investigated, and limited agreement was found. Author

N89-20194*# National Aeronautics and Space Administration. Lewis Research Center, Cleveland, OH.

FREE-PISTON STIRLING TECHNOLOGY FOR SPACE POWER

Jack G. Slaby 1989 21 p Prepared for presentation at the International Conference on Space Power, Cleveland, OH, 5-7 Jun. 1989; sponsored in part by the International Astronautical Federation

(NASA-TM-101956; E-4653; NAS 1.15:101956) Avail: NTIS HC A03/MF A01 CSCL 10B

An overview is presented of the NASA Lewis Research Center free-piston Stirling engine activities directed toward space power. This work is being carried out under NASA's new Civil Space Technology Initiative (CSTI). The overall goal of CSTI's High Capacity Power element is to develop the technology base needed to meet the long duration, high capacity power requirements for future NASA space missions. The Stirling cycle offers an attractive power conversion concept for space power needs. Discussed here is the completion of the Space Power Demonstrator Engine (SPDE) testing-culminating in the generation of 25 kW of engine power from a dynamically-balanced opposed-piston Stirling engine at a temperature ratio of 2.0. Engine efficiency was approximately 22 percent. The SPDE recently has been divided into two separate single-cylinder engines, called Space Power Research Engine (SPRE), that now serve as test beds for the evaluation of key technology disciplines. These disciplines include hydrodynamic gas bearings, high-efficiency linear alternators, space qualified heat pipe heat exchangers, oscillating flow code validation, and engine loss understanding. Author

N89-20195*# Rogers and Associates Engineering Corp., Gainesville, FL.

SPACE SHUTTLE PROPULSION ESTIMATION DEVELOPMENT VERIFICATION Final Report

Robert M. Rogers 28 Feb. 1989 198 p

(Contract NAS8-36152)

(NASA-CR-183582; NAS 1.26:183582; TR-89-1-Vol-2) Avail: NTIS HC A09/MF A01 CSCL 21H

The application of extended Kalman filtering to estimating the Space Shuttle Propulsion performance, i.e., specific impulse, from flight data in a post-flight processing computer program is detailed. The flight data used include inertial platform acceleration, SRB head pressure, SSME chamber pressure and flow rates, and ground based radar tracking data. The key feature in this application is the model used for the SRB's, which is a nominal or reference quasi-static internal ballistics model normalized to the propellant burn depth. Dynamic states of mass overboard and propellant burn depth are included in the filter model to account for real-time deviations from the reference model used. Aerodynamic, plume, wind and main engine uncertainties are also included for an integrated system model. Assuming uncertainty within the propulsion system model and attempts to estimate its deviations represent a new application of parameter estimation for rocket powered vehicles. Illustrations from the results of applying this estimation approach to several missions show good quality propulsion estimates. Author

N89-20196*# Morton Thiokol, Brigham City, UT. Aerospace Group.

FLIGHT MOTOR SET 360L001 (STS-26R), VOLUME 1 Final Report

Glen A. Ricks Dec. 1988 330 p

(Contract NAS8-30490)

(NASA-CR-183576; NAS 1.26:183576; TWR-17272-Vol-1; Publ-89435) Avail: NTIS HC A15/MF A01 CSCL 21H

The NASA space shuttle flight STS-26R, launched at 11:37.00.009 a.m. EDT on 29 Sep. 1988, used the redesigned solid rocket motors (RSRM) 360LOO1A and 360LOO1B. Evaluation of the ground environment instrumentation (GEI) data recorded prior to flight showed: (1) no launch commit criteria violations, (2) that the field joint heater and aft skirt thermal conditioning systems performed adequately, and (3) that the GEI data showed good agreement with thermal model predictions. Evaluation of the developmental flight instrumentation (DFI) revealed excellent agreement with both the predicted and required ballistic specifications. All parameters were well within the CEI specification requirements including propellant burn rates, specific impulse values, and thrust imbalance. Recorded strain values also indicated satisfactory radial growth and stress levels, as well as verification of adequate safety factors. Postflight inspection of the insulation, seals, case, and nozzles showed overall excellent performance. Some thermal DFI protective cork was missing, and inoperative field joint vent valves on the thermal protection cork allowed water entry into the field joints upon splashdown. Evaluation of these anomalies, as well as complete evaluation of all RSRM components, is presented. Author

N89-20197*# Rogers and Associates Engineering Corp., Gainesville, FL.
SPACE SHUTTLE PROPULSION ESTIMATION DEVELOPMENT VERIFICATION, VOLUME 1 Final Report
Robert M. Rogers 28 Feb. 1989 179 p
(Contract NAS8-36152)
(NASA-CR-183581; NAS 1.26:183581; TR-89-1-Vol-1) Avail: NTIS HC A09/MF A01 CSCL 21H

The results of the Propulsion Estimation Development Verification are summarized. A computer program developed under a previous contract (NAS8-35324) was modified to include improved models for the Solid Rocket Booster (SRB) internal ballistics, the Space Shuttle Main Engine (SSME) power coefficient model, the vehicle dynamics using quaternions, and an improved Kalman filter algorithm based on the U-D factorized algorithm. As additional output, the estimated propulsion performances, for each device are computed with the associated 1-sigma bounds. The outputs of the estimation program are provided in graphical plots. An additional effort was expended to examine the use of the estimation approach to evaluate single engine test data. In addition to the propulsion estimation program PFILTER, a program was developed to produce a best estimate of trajectory (BET). The program LFILTER, also uses the U-D factorized algorithm form of the Kalman filter as in the propulsion estimation program PFILTER. The necessary definitions and equations explaining the Kalman filtering approach for the PFILTER program, the models used for this application for dynamics and measurements, program description, and program operation are presented. Author

N89-20198*# Battelle Columbus Labs., OH.
STUDIES AND ANALYSES OF THE SPACE SHUTTLE MAIN ENGINE. FAILURE INFORMATION PROPAGATION MODEL DATA BASE AND SOFTWARE
A. E. Tischer 15 Dec. 1987 571 p
(Contract NASw-3737)
(NASA-CR-183586; NAS 1.26:183586; BCD-SSME-TR-87-2)
Avail: NTIS HC A24/MF A01 CSCL 21H

The failure information propagation model (FIPM) data base was developed to store and manipulate the large amount of information anticipated for the various Space Shuttle Main Engine (SSME) FIPMs. The organization and structure of the FIPM data base is described, including a summary of the data fields and key attributes associated with each FIPM data file. The menu-driven software developed to facilitate and control the entry, modification, and listing of data base records is also discussed. The transfer of the FIPM data base and software to the NASA Marshall Space Flight Center is described. Complete listings of all of the data base definition commands and software procedures are included in the appendixes. Author

N89-20199*# National Aeronautics and Space Administration. Lewis Research Center, Cleveland, OH.
IDENTIFICATION OF SPACE SHUTTLE MAIN ENGINE DYNAMICS
Ahmet Duyar, Ten-Huei Guo (Sverdrup Technology, Inc., Cleveland, OH.), and Walter C. Merrill 1989 15 p Proposed for presentation at the American Control Conference, Pittsburgh, PA, 21-23 Jun. 1989; sponsored by AIAA, ASME, AIChE, AISE, ISA and SCS
(NASA-TM-101982; E-4680; NAS 1.15:101982) Avail: NTIS HC A03/MF A01 CSCL 21H

System identification techniques are used to represent the dynamic behavior of the Space Shuttle Main Engine. The transfer function matrices of the linearized models of both the closed loop and the open loop system are obtained by using the recursive maximum likelihood method. Author

23 CHEMISTRY AND MATERIALS (GENERAL)

No abstracts in this category.

24 COMPOSITE MATERIALS

Includes physical, chemical, and mechanical properties of laminates and other composite materials.
For ceramic materials see *27 Nonmetallic Materials.*

N89-20200*# Wyoming Univ., Laramie. Composite Materials Research Group.
STATIC TENSILE AND TENSILE CREEP TESTING OF FIVE CERAMIC FIBERS AT ELEVATED TEMPERATURES Final Report
Richard S. Zimmerman and Donald F. Adams Dec. 1988 129 p
(NASA Order A-39603-C)
(NASA-CR-184690; NAS 1.26:184690; UW-CMRG-R-88-115)
Avail: NTIS HC A07/MF A01 CSCL 11D

Static tensile and tensile creep testing of five ceramic fibers at elevated temperature was performed. J.P. Stevens, Co., Astroquartz 9288 glass fiber, Nippon Carbon, Ltd., (Dow Corning) Nicalon NLM-102 silicon carbide fiber, and 3M Company Nextel 312, 380, and 480 alumina/silica/boria fibers were supplied in unsized tows. Single fibers were separated from the tows and tested in static tension and tensile creep. Elevated test temperatures ranged from 400 to 1300 C and varied for each fiber. Room temperature static tension was also performed. Computer software was written to reduce all single fiber test data into engineering constants using ASTM Standard Test Method D3379-75 as a reference. A high temperature furnace was designed and built to perform the single fiber elevated temperature testing up to 1300 C. A computerized single fiber creep apparatus was designed and constructed to perform four fiber creep tests simultaneously at temperatures up to 1300 C. Computer software was written to acquire and reduce all creep data. Author

N89-20201 Connecticut Univ., Storrs.
AN ANALYSIS OF AN INCOMPRESSIBLE, FIBER-REINFORCED MATERIAL SUBJECTED TO FINITE STRAINS IN THE DIRECTION OF REINFORCEMENT Ph.D. Thesis
Donald Lynn Cox 1988 150 p
Avail: Univ. Microfilms Order No. DA8822916

A general stress analysis method for application to problems involving fiber-reinforced polymeric materials subjected to finite deformations in the direction of reinforcement is developed. The idea for this grew out of a need to analyze certain Navy structures used to isolate acoustic sensors from unwanted acoustic or vibratory excitation. These structures, manufactured from reinforced polymeric materials are expected to withstand finite stretching in the direction of reinforcement and remain elastic. Early attempts at modelling the behavior of such a material assumed it to be inextensible in the direction of reinforcement. More recently, a numerical approach was taken wherein the reinforcing material or cords were assumed to behave in a linearly elastic way. In the approach taken here, a constitutive relationship is developed following the guiding principles of modern continuum mechanics for an incompressible, fiber-reinforced continuum with no constraint placed on the degree of extensibility; that is, the material is allowed to experience finite strain in the direction of reinforcement. This constitutive relation is investigated numerically using a nonlinear finite element program developed for this work. The numerical results are then compared with actual finite strain data obtained using sheets of nylon reinforced neoprene. In brief, it was found

that the method does a good job of matching experimental data, at least within the bounds of the experiments performed.
Dissert. Abstr.

N89-20202 Virginia Polytechnic Inst. and State Univ., Blacksburg.
PREDICTION MODEL FOR THE ONSET OF EDGE-EFFECT DELAMINATION AT HOLES IN COMPOSITE LAMINATES Ph.D. Thesis
Doron Shalev 1988 133 p
Avail: Univ. Microfilms Order No. DA8825339

Composite laminates are prone to delamination at free edges, straight edges or at holes, due to the mismatch at interfaces where two adjacent plies have different fiber orientations and/or different material properties. The linear analysis of the mismatch at the edge results in a mathematical singularity. That phenomenon occurs in a boundary layer and has to be treated mathematically and physically as such. In the literature it is called the Boundary Layer Effect or simply the Edge Effect. It is of great importance to recognize and be able to predict delamination locations at edges prone to such events. The goal was to create a model capable of providing such a prediction. In an effort to generalize the model, the more complicated case of a free edge at holes in the composite laminate was chosen rather than the case of a straight free edge. A sequel of three major efforts was completed: Development of the analysis of the free-edge effect at a hole in a composite laminate; performance of an extensive experimental program to provide data for the creation of the prediction model; and on the basis of the analysis, establishment of the model, and comparison with the experimental results. Dissert. Abstr.

N89-20203 Ohio State Univ., Columbus.
THERMAL-MECHANICAL BEHAVIOR OF THIN FILMS AND LAMINATES Ph.D. Thesis
Chih-Ping Wu 1988 308 p
Avail: Univ. Microfilms Order No. DA8820374

Thermal-mechanical behavior of thin films and laminates is investigated. The first theme involves an analysis which develops analytical expressions for determining the intrinsic stress in a film/substrate material from measured curvatures of thin beam or plate specimens. This approach differs from that of previous investigators in that nonlinear geometric effects are included. The second topic studied entails the effects of physical damage upon the thermal-mechanical response of layered media. Kachanov's theory of damage is employed for deriving the moment-curvature relation for a simple beam comprised of two dissimilar layers that are perfectly bonded together. Twenty one possible failure paths for such a bi-material beam which depend on the Young's modulus ratio, damage modulus ratio and thickness ratio between the two different layers, are analyzed and discussed. Finally, Kachanov's theory is applied to the problem of matrix cracking in cross-ply composite laminates subjected to uniaxial loading. Comparisons with experimental data reveal that this theoretical analysis may be employed to predict the threshold stress required to initiate transverse matrix cracking, provided that the effects of other damage modes is negligible. Dissert. Abstr.

N89-20204 Delaware Univ., Newark.
THEORETICAL MODELLING AND EXPERIMENTAL CHARACTERIZATION OF FLEXIBLE COMPOSITES UNDER FINITE DEFORMATION Ph.D. Thesis
Shen-Yi Luo 1988 235 p
Avail: Univ. Microfilms Order No. DA8824220

A theoretical and experimental study is presented of the constitutive relations of flexible composites. The major focuses are: (1) the conceptual development of flexible composites with wavy fibers; (2) the theoretical modeling development for predicting and optimizing the nonlinear elastic finite deformation behavior of flexible composites; and (3) process and test method development for making and characterizing such composites. The fabrication techniques for flexible composites based on unidirectional straight fibers and wavy fibers were developed. Experiments were conducted to study the elastic behavior of flexible composites under finite deformation. Dissert. Abstr.

N89-20205*# Norfolk State Coll., VA. Dept. of Chemistry and Physics.
A (13)C NMR ANALYSIS OF THE EFFECTS OF ELECTRON RADIATION ON GRAPHITE/POLYETHERIMIDE COMPOSITES Final Report
Milton W. Ferguson 29 Mar. 1989 9 p
(Contract NCC1-115)
(NASA-CR-182818; NAS 1.26:182818) Avail: NTIS HC A02/MF A01 CSCL 11D

Initial investigations have been made into the use of high resolution nuclear magnetic resonance (NMR) for the characterization of radiation effects in graphite and Kevlar fibers, polymers, and the fiber/matrix interface in graphite/polyetherimide composites. Sample preparation techniques were refined. Essential equipment has been procured. A new NMR probe was constructed to increase the proton signal-to-noise ratio. Problem areas have been identified and plans developed to resolve them. Author

N89-20206*# National Aeronautics and Space Administration. Lewis Research Center, Cleveland, OH.
FINITE ELEMENT APPLICATIONS TO EXPLORE THE EFFECTS OF PARTIAL BONDING ON METAL MATRIX COMPOSITE PROPERTIES
J. J. Caruso, D. Trowbridge, and C. C. Chamis Apr. 1989 25 p Presented at the 30th Structures, Structural Dynamics and Materials Conference, Mobile, AL, 3-5 Apr. 1989; sponsored in part by AIAA, ASME, ASCE, AHS, and ACS
(NASA-TM-101482; E-4610; NAS 1.15:101482) Avail: NTIS HC A03/MF A01 CSCL 11D

The mechanics of materials approach (definition of E, G, Nu, and Alpha) and the finite element method are used to explore the effects of partial bonding and fiber fracture on the behavior of high temperature metal matrix composites. Composite ply properties are calculated for various degrees of disbonding to evaluate the sensitivity of these properties to the presence of fiber/matrix disbonding and fiber fracture. The mechanics of materials approach allows for the determination of the basic ply material properties needed for design/analysis of composites. The finite element method provides the necessary structural response (forces and displacements) for the mechanics of materials equations. Results show that disbonding of fractured fibers affect only E sub (111) and alpha sub (111) significantly. Author

N89-20207 British Petroleum Co. Ltd., London (England).
PREPARATION OF COMPOSITES Patent Application
Alan Robert Begg, inventor (to British Petrole and Andrew David Tarrant, inventor (to British Petrole 7 Mar. 1987 4 p Filed 26 Mar. 1987 Priority 2 Apr. 1986 GB 8608030
(EP-0-240-251-A2; EP-PATENT-APPL-SN-87302635.5; INT.CLASS-C22C-1/05; INT.CLASS-B22F-7/00; ETN-89-94067)
Avail: UK Patent Office, 25 Southampton Buildings, London WC2A 1AY, England

A method of making metal matrix composites containing at least 40 pct v/v of a hard material such as SiC and a matrix of aluminum, magnesium, or alloys of either is presented. The method involves ball milling powders of the respective components. Other mixing techniques do not enable such a high proportion of hard material to be incorporated into the composite. The composites are useful to produce components resistant to wear. ESA

N89-20208# Construcciones Aeronauticas S.A., Madrid (Spain). Div. de Proyectos.
PAINT TESTS ON LAMINATED MATERIAL FORMED BY CARBON FIBER COMPOSITES AND TEDLAR LAYERS [ENSAYO DE PINTADO EN LAMINADOS DE FIBRA DE CARBONO CON TEDLAR]
J. Bravo and A. Camacho 25 Jul. 1988 11 p In SPANISH
(I-279/88; ETN-89-94130) Avail: NTIS HC A03/MF A01

The use of bonded Tedlar layers to protect both sides of carbon fiber composite components forming a wing edge is investigated.

Painting tests were carried out using specimens covered with Tedlar bonded layers. The steps of polyurethane painting are described. Results show that the paint procedure used on Tedlar is acceptable. The specifications regarding adherence, moisture resistance, and Skydral resistance are satisfied. ESA

N89-20209# Army Lab. Command, Watertown, MA. Material Technology Lab.
ANION CONTROLLED MICROSTRUCTURES IN THE AL2O3-AIN SYSTEM
James W. McCauley, K. M. Krishnan, R. S. Rai, G. Thomas, and A. Zangvill Nov. 1988 22 p
(AD-A203671; MTL-TR-88-30) Avail: NTIS HC A03/MF A01 CSCL 11B

The phase equilibria of the pseudo-binary Al2O3-AIN composition join has been extensively investigated, especially with respect to the processing of ALON--a nitrogen stabilized aluminum oxide spinel phase that can be sintered into transparent polycyrstalline ceramics. The system exhibits a wide variety of features and resulting microstructures: two spinel phases, vapor-solid and liquid-solid eutectics, AIN polytype-like structures, and alpha-Al2O3/spinel modulated structures. This system provides a unique perspective to a series of quite different materials based on a constant cation chemistry, with a continuous variation in the O/N anion ratio. GRA

N89-20210# Naval Ship Research and Development Center, Bethesda, MD. Ship Materials Engineering Dept.
INSTRUMENTED IMPACT TESTING OF COMPOSITE MATERIALS
Roger M. Crane and Thomas D. Juska Jan. 1989 36 p
(AD-A203842; DTRC/SME-88/73) Avail: NTIS HC A03/MF A01 CSCL 11D

One material characteristic that is gaining increased importance in composite materials is their impact resistance. The test method has been widely accepted in the aerospace industry for determining a degree of toughness is the instrumented impact test followed by post-impact compression testing. This combination of tests is called Compression After Impact (CAI) testing. Two aspects that are important to the results are the energy absorbed during the impact test and the resultant compression strength after impact. This paper discusses the instrumentation developed to record the impact event. The hardware and software are presented with a detailed description of the algorithms used for the determination of the energy absorbed by the composite from the impact testing. Sample results from the impact testing are presented, along with a discussion of their results. GRA

25 INORGANIC AND PHYSICAL CHEMISTRY

Includes chemical analysis, e.g., chromatography; combustion theory; electrochemistry; and photochemistry.

For related information see also *77 Thermodynamics and Statistical Physics.*.

N89-20211# Texas Univ., Austin. Dept. of Chemistry.
VECTORIAL ELECTRON TRANSFER ON DESIGNED SURFACES Annual Report, Feb. 1987 - Jan. 1988
Allen J. Bard, Alan Campion, Marye Anne Fox, Thomas E. Mallouk, Stephen E. Webber, and J. Michael White 1988 80 p
(Contract GRI-5082-260-0756)
(PB88-240031; GRI-88/0166) Avail: NTIS HC A05/MF A01 CSCL 07D

Silica supported WS2 and Ni-doped WS2 were found to be good catalysts for the reduction of water to hydrogen. In systems employing CdS/SiO2 sensitizer particles, WS2/SiO2 was more active and stable for hydrogen generation than Pt/SiO2. The compounds n-TiO2 and n-SiTiO3 were sensitized by absorbed dyes ruthenium(II) tris (2,2'-bipyridine 4,4'-dicarboxylic acid and zinc tetrakis (4-carboxyphenyl) porphyrin; quantum efficiencies for sensitization were 10 to 60 percent and were maximized at monolayer dye coverage. The II-VI semiconductor particles (ZnS, ZnSe, CdS, CdSe) were produced in Nafion membranes and in Langmuir-Blodgett multilayer films by exposure of the M(2+)-containing matrix to gaseous H2S or H2Se. Quantum size effects are manifested in the optical spectra of these particles, the absorbance onset being blueshifted by approximately 0.4 eV. A method was developed for polymerization of polypyrrole on TiO2 and CdS particles. The polypyrrole layer binds fluorescein anions which sensitize the semiconductor for photocatalytic hydrogen evolution, and the polymer inhibits photocorrosion of CdS. The Cu electrodes used in the electrochemical reduction of CO2 to SH4 were examined by XPS and Auger spectroscopy; no evidence is seen for Cu(I) and Cu(II) carbidic species as intermediates in the reduction. Alkoxyl groups are identified as possible intermediates. GRA

N89-20212 Wayne State Univ., Detroit, MI.
EFFECTS OF TURBULENCE ON RATE OF COMBUSTION OF FUEL SPRAYS Ph.D. Thesis
Bachir Meftah 1987 274 p
Avail: Univ. Microfilms Order No. DA8809116

More understanding of the effects of the upstream turbulence characteristics on the combustion rate of premixed fuel sprays is needed to improve the performance of furnaces, combustors and certain internal combustion engines. The objective is to demonstrate the existence of a propagating wave in heterogeneous flame mixtures as in gaseous flames and to establish the feasibility of measuring the average combustion rate in turbulent flames by combining separate measurements of the flame characteristics (velocity and thickness) at the flame front. A combustor is designed and built. A 1-D flame front (a conical V-flame) is set up in a cylindrical combustion chamber in a dilute premixes spray of fuel number 2. A model solving the transport equations for the two-phase flow is implemented. It produces a full solution including profiles for the temperature, mass fractions and droplets velocities. This model accounts for droplet size distribution, droplet velocity distribution and a submodel for the turbulence characteristics RMS velocity and length scale. Dissert. Abstr.

N89-20213# Instituto de Pesquisas Energeticas e Nucleares, Sao Paulo (Brazil).
STUDY OF VIBRATIONAL AND RAPID LOCAL MOTIONS OF HYDROGEN IN THE STORAGE COMPOUND TI0.8ZR0.2 CRMNH3 BY SLOW NEUTRON SCATTERING Ph.D. Thesis
J. MestnikFilho 1987 188 p In PORTUGESE
(DE88-704797; INIS-BR-1338) Avail: NTIS (US Sales Only) HC A09/MF A01

The vibrational and the rapid local motions of hydrogen in the storage compound Ti(0.8)Zr(0.2)CrMnH3 were studied by slow neutron scattering with the beryllium filter time-of-flight spectrometer. The form of the density of states of the normal modes of vibrations in host metal does no appear to change on hydrogenation, but a shift of 25 percent towards lower frequencies has been observed. Debye temperatures for the metal and corresponding hydride have been estimated to be respectively (522 + or - 15) K and (311 + or - 10) K. An energy distribution consisting of three peeks approximately 50 MeV (FWHM) wide corresponding to the energy transfer of 85, 115 and 141 MeV was observed and were attributed to hydrogen local vibrations in three types of interstices which differs in composition of Ti and Zr atoms. In the quasielastic scattering, a broadening of 15 micro eV was detected for the momentum transfer Q = 1/2.1 A and for temperature T = 125 C. The broadening was attributed to rapid local motions of hydrogen in a dumb-bell of length equal to the jump length for diffusion of approximately 3 A. DOE

N89-20214# Argonne National Lab., IL. Chemical Technology Div.
FLUORINE AS AN OXIDANT IN COMBUSTION CALORIMETRY
P. A. G. OHare 1988 18 p Presented at the 4th Polish Conference on Calorimetry and Thermal Analysis, Warsaw, Poland, 5-9 Sep. 1988

(Contract W-31-109-eng-38)
(DE89-003626; CONF-8809198-1) Avail: NTIS HC A03/MF A01

Oxygen-bomb calorimetry has been used with some success over the years for the determination of enthalpies of formation delta sub f H deg sub m of inorganic compounds. This method, however, has a number of drawbacks, the most significant of which is the formation of complicated and ill-defined oxides as reaction products. Substitution of fluorine for oxygen, as the oxidizing gas, eliminates many of those problems. Because of the aggressive nature of fluorine, it can be used to study even the most refractory of materials, but its disadvantages are that it requires very careful handling and special apparatus. A portion of the present paper will discuss the precautions that must be taken, and the special calorimetric equipment that has been constructed. The main scope of the paper, however, is concerned with our recent results obtained for some high-purity chalcogenides. We have performed measurements on both the crystalline and vitreous forms of As Se. The enthalpies of formation have been deduced from the calorimetric enthalpies of fluorination. The following preliminary results at 298.15 K have been obtained and are compared in the paper with published values: delta sub f H deg sub m (As2Se3, cr) = -(83.7+-4.5) kJ- mol-1 and delta sub f H deg m (As2Se3, vit) = -(59.4+-4.3)kJ-mol-1. The enthalpy of transition is -(24.3+-3.9)kJ-mol-1, only about 60 per cent of the previous literature value. DOE

N89-20215*# Jet Propulsion Lab., California Inst. of Tech., Pasadena.
INVESTIGATION OF SPRAY DISPERSION AND PARTICULATE FORMATION IN DIESEL FUEL FLAMES Final Report, 2 Dec. 1983 - 30 Jun. 1988
L. H. Back, C. P. Bankston, E. Y. Kwack, J. Bellan, and K. Harstad 15 Aug. 1988 85 p Sponsored in part by NASA and DOE
(Contract MIPR-109-86)
(NASA-CR-184820; NAS 1.26:184820; JPL-D-5704; AD-A201079; ARO-21092.6-EG) Avail: NTIS HC A05/MF A01 CSCL 21B

An experimental study of electrostatical atomized and dispersed diesel fuel jets was conducted at various back pressures to 40 atm. A new electrostatic injection technique was utilized to generate continuous, stable fuel sprays at charge densities of 1.5 - 2.0 C/m3 of fluid at one atm, and about 1.0 C/m3 at 40 atm. Flowrates were varied from 0.5 to 2.5 ml/s and electric potentials to -18 kV. Visual observations showed that significant enhanced dispersion of charged fuel jets occurred at high back pressures compared to aerodynamic breakup and dispersion. The average drop size was about the same as the spray triode orifice diameter, and was between the Kelly theory and the Rayleigh limit. The ignition tests, done only at one atm, indicated stable combustion of the electrostatically dispersed fuel jets. GRA

N89-20216 Michigan Univ., Ann Arbor.
DIFFUSIVE BURNING OF PLANE LIQUID AND SPRAY JETS IN A COFLOWING OXIDIZER STREAM Ph.D. Thesis
Joon Bae Kim 1988 116 p
Avail: Univ. Microfilms Order No. DA8821599

The combustion of unconfined plane liquid fuel and spray jets moving at the same speed as the surrounding oxidizing gas is investigated. This problem is the heterogeneous analog of the Burke-Schumann problem with the gaseous fuel jet replaced by a liquid or spray jet. The Burke-Schumann limit is assumed to be applicable so that combustion occurs at a thin flame sheet where the diffusive flux of fuel and oxidizer are in stoichiometric proportion. Use of the Shvab-Zeldovich formulation then results in homogeneous equations for energy and species conservation, and application of the Howarth Transformation then reduces these equations to incompressible form. A characteristic equation, which incorporates the effects of vaporization, combustion, and the flow is obtained from the overall energy and species balance at the jet surface, and the corresponding eigenvalue is identified as the rate of vaporization at the jet surface. The effects of liquid jet and spray parameters and fuel and oxidizer properties on the jet and flame lengths, the flame shape, and on the species and temperature distributions were determined and are presented in dimensionless form. The advantage of the present analysis is that it permits the investigation of the effects of a wide variety of parameters on the behavior of heterogeneous jet flames with minimal computational effort. Dissert. Abstr.

N89-20217# Illinois Univ. at Urbana-Champaign, Savoy. Dept. of Mechanical and Industrial Engineering.
RADIATIVE HEAT TRANSFER AUGMENTATION IN HIGH TEMPERATURE COMBUSTION SYSTEMS WITH APPLICATION TO RADIANT TUBE BURNERS Annual Report, Apr. 1987 - Mar. 1988
J. E. Peters, M. Q. Brewster, and R. O. Buckius Apr. 1988 54 p
(Contract GRI-5086-232-1368)
(PB89-133805; GRI-88/0186) Avail: NTIS HC A04/MF A01 CSCL 21B

Gas fired radiant tube heaters provide an indirect heating source for applications in which direct contact cannot be permitted between combustion gases and the workpiece. The program is a fundamental study designed to help improve the performance of such burners through enhancement of both the magnitude and the uniformity of the flame radiation, increased flame stability and reduced energy loss out the exhaust. In particular, the use of porous/fibrous ceramic materials that could be inserted into the flame to increase flame radiation and to provide a stabilization region for the flame is under investigation. A radiant tube burner facility designed for radiation heat transfer measurement studies on radiant tubes was constructed. Preliminary observations of porous material behavior in flames indicated that partially stabilized zirconia and silicon carbide reticulated ceramics warrant further consideration. Author

N89-20218*# Missouri Univ., Rolla. Dept. of Mechanical and Aerospace Engineering and Engineering Mechanics.
MODELING OF HYDROGEN-AIR DIFFUSION FLAME Interim Report
K. M. Isaac Mar. 1989 16 p
(Grant NAG1-861)
(NASA-CR-184844; NAS 1.26:184844) Avail: NTIS HC A03/MF A01 CSCL 21B

An analytical and computational study of opposed jet diffusion flame for the purpose of understanding the effects of contaminants in the reactants and thermal diffusion of light species on extinction and reignition of diffusion flames is in progress. The methodologies that have been attempted so far are described. Results using a simple, one-step reaction for the hydrogen-air counterflow diffusion flame are presented. These results show the correct trends in the profiles of chemical species and temperature. The extinction limit can be clearly seen in the plot of temperature vs. Damkohler number. Author

N89-20219# Illinois Univ., Urbana-Champaign. Dept. of Chemistry.
TRANSPORT AND RELAXATION PROCESSES IN SUPERCRITICAL FLUIDS Technical Progress Report, 20 Oct. 1988 - 19 Jan. 1989
Jiri Jonas 1989 9 p
(Contract DE-FG22-85PC-80503)
(DE89-005910; DOE/PC-80503/T13) Avail: NTIS HC A02/MF A01

In this period our efforts concentrated on two main projects. First, we finished the theoretical interpretation of the experimental data on transport and relaxation properties of naphthalene in supercritical fluids. Second, we investigated the intermolecular interactions in the CH(sub 3) OH-CO(sub 2) system. DOE

N89-20220# Chemical Research and Development Center, Aberdeen Proving Ground, MD.
WATER ADSORPTION EQUILIBRIA ON MICROPOROUS CARBONS Technical Report, Feb. 1987 - Jul. 1988
John J. Mahle and David K. Friday Nov. 1988 39 p

(Contract DAAA15-87-D-0004; DA Proj. 1C1-61102-A-71-A)
(AD-A203536; CRDEC-TR-018) Avail: NTIS HC A03/MF A01 CSCL 07D

Water vapor adsorption and desorption equilibria was measured for BPL, ASC, ASC-TEDA, and CWS carbons, a polymeric beaded carbon and a foreign military filter carbon. The effect of temperature was considered over the range of 15 to 35 C. An isotherm expression was developed to describe capillary condensation on a particle with a disperse pore size distribution. This expression was fit to the measured data in order to compare the pore size distributions of the sample studies. A second isotherm expression was proposed based on a modification of the Antoine equation. This equation proved useful in obtaining a best fit correlation to the adsorption data. GRA

N89-20221# Iowa Univ., Iowa City. Dept. of Chemistry.
NEW APPROACHES TO FLUOROCARBON SYNTHESIS Final Report, 15 Nov. 1984 - 14 Nov. 1988
Donald J. Burton 14 Nov. 1988 45 p
(Grant AF-AFOSR-0009-85; AF Proj. 2303)
(AD-A203641; AFOSR-89-0065TR) Avail: NTIS HC A03/MF A01 CSCL 07C

The objectives of this project were: (1) to develop new, novel, stereospecific general methods for the preparation of polyfluorinated organometallic intermediates - particularly routes that could be applicable to the synthesis of polyfunctionalized fluorocarbons; (2) to use commercially available precursors (where applicable) as the source of fluorine in reactive intermediates - to enable easy utilization of the methodology by other workers and to facilitate scale up of the synthetic procedures; (3) to understand (mechanistically) the sequence of reactions and the type of transient reactive intermediates involved - order to establish the synthetic methodology on firm mechanistic principles and to permit rational extrapolation for future development of additional new synthetic reagents: and (4) to utilize the unique compounds obtained to probe general mechanistic principles of physical-organic chemistry. GRA

N89-20222# Flow Research, Inc., Kent, WA. Applied Mechanics Div.
VORTEX-TRANSPORT ELEMENT SIMULATION OF A CONFINED MIXING LAYER Final Report, Sep. 1987 - Mar. 1988
Peyman Givi Nov. 1988 43 p
(Contract F33615-87-C-2790)
(AD-A203791; TR-442; AFWAL-TR-88-2136) Avail: NTIS HC A03/MF A01 CSCL 21B

An improved vortex-transport element numerical scheme has been employed to simulate the spatial evolution of a two-dimensional planar, constant density mixing layer formed behind a splitter plate configuration. This scheme uses vortex elements to discretize the region of high vorticity, and transport elements to discretize the region of high scalar gradients. This improved vortex method offers a method of accurately resolving the areas of high strain by redistributing the neighboring elements within those regions. The resulting scheme has been used to simulate the convective transport of a conserved scalar variable in the shear layer, and the results show favorable agreement with experimental data for the mean and the rms values of the scalar quantity. The effects of harmonic forcing are shown to accelerate the mechanism of the rollup and pairing within the domain, which results in an increase in the convolution of the surfaces. This would be of crucial interest to the problem of active combustion control in a reacting mixing layer simulation. GRA

N89-20223# Dayton Univ., OH.
CONDENSATION AND STORAGE OF HYDROGEN CLUSTER IONS Final Report, Nov. 1985 - Feb. 1988
John T. Bahns Nov. 1988 114 p
(Contract F04611-83-C-0046)
(AD-A203801; UDR-TR-88-28; AFAL-TR-88-056) Avail: NTIS HC A06/MF A01 CSCL 07B

This report reviews the cluster ion approach to containerless condensation and introduces the concept of pseudo wall. An experimental pseudo wall device, designed for the study of containerless condensation techniques, is described. Calculations indicate that the proposed device will be capable of confining cluster ions in the mass range 2 to 107 for time exceeding 104 seconds. A next generation device is projected to be capable of containing a total mass of 0.3 milligrams. GRA

26 METALLIC MATERIALS

Includes physical, chemical, and mechanical properties of metals, e.g., corrosion; and metallurgy.

N89-20224# Academia Sinica, Beijing (China). Inst. of Mechanics.
EXPERIMENTAL STUDY OF SPALL DAMAGE IN AN ALUMINIUM ALLOY
Letian Shen, Yileng Bai, and Shidu Zhao 1987 9 p Sponsored by Institute of Scientific and Technical Information of China, Beijing
(PB89-112619; ISTIC-TR-C-000138) Avail: NTIS HC A02/MF A01 CSCL 11F

A study is reported of spallation with the concept of damage function defined by the residual strength of spalled specimen. Based on this, it is hopeful to develop a simple approach continuously characterizing spall damage of materials. The relevant stress wave profiles are also presented. Author

N89-20225# Oak Ridge Y-12 Plant, TN.
SOLUBILITY OF HYDROGEN, DEUTERIUM AND TRITIUM IN PALLADIUM METAL
G. L. Powell and R. Laesser (Institut fuer Festkoerperforschung Kernforschungsanlage, Juelich, Germany, F.R.) 20 Dec. 1988 41 p
(Contract DE-AC05-84OS-21400)
(DE89-005304; Y-2395) Avail: NTIS HC A03/MF A01

The solubility of hydrogen, deuterium, and tritium in palladium has been measured, described analytically over a wide temperature range (296 to 1460 K), and used to calculate enthalpies of reaction, isotope separation factors, and phase boundaries. DOE

N89-20226# Rolls-Royce Ltd., Derby (England).
MICROSTRUCTURAL INFLUENCE ON LOW CYCLE FATIGUE STRENGTH OF IMI550
N. D. R. Goddard, H. M. Flower (Imperial Coll. of Science and Technology, London, England), and M. T. Cope 6 Jun. 1988 7 p Presented at the 6th World Conference on Titanium: Titanium '88, Cannes, France, 6-9 Jun. 1988
(PNR90500; ETN-89-93692) Copyright Avail: NTIS HC A02/MF A01

The microstructural influence on the low cycle fatigue performance of the alpha+beta alloy Ti-4Al-4Mo-2Sn-0.5Si is investigated. The experimental results are assessed in terms of the separate factors which contribute to total fatigue life and their implications for deliverable fatigue strength. It is shown that the tested microstructures result in similar performances, which may allow choices of structures based on other factors. ESA

N89-20227*# National Aeronautics and Space Administration. Lewis Research Center, Cleveland, OH.
FAILURE ANALYSIS OF A STIRLING ENGINE HEAT PIPE
Thomas J. Moore, James E. Cairelli, and Kaveh Khalili (Stirling Thermal Motors, Inc., Ann Arbor, MI.) Mar. 1989 13 p
(NASA-TM-101418; E-4516; NAS 1.15:101418) Avail: NTIS HC A03/MF A01 CSCL 11F

Failure analysis was conducted on a heat pipe from a Stirling Engine test rig which was designed to operate at 1073 K. Premature failure had occurred due to localized overheating at the leading edge of the evaporator fin. It was found that a crack had allowed air to enter the fin and react with the sodium coolant. The origin of the crack was found to be located at the inner surface of the

Inconel 600 fin where severe intergranular corrosion had taken place. Author

N89-20228*# National Aeronautics and Space Administration. Lewis Research Center, Cleveland, OH.
MECHANICAL PROPERTIES OF MODIFIED LOW COBALT POWDER METALLURGY UDIMET 700 TYPE ALLOYS
Fredric H. Harf Mar. 1989 29 p
(NASA-TM-101481; E-4609; NAS 1.15:101481) Avail: NTIS HC A03/MF A01 CSCL 11F

Eight superalloys derived from Udimet 700 were prepared by powder metallurgy, hot isostatically pressed, heat treated and their tensile and creep rupture properties determined. Several of these alloys displayed properties superior to those of Udimet 700 similarly prepared, in one case exceeding the creep rupture life tenfold. Filter clogging by extracted gamma prime, its measurement and significance are discussed in an appendix. Author

N89-20229# Oak Ridge National Lab., TN.
COMPOSITIONAL EFFECTS ON PROCESSING AND PROPERTIES OF NICKEL ALUMINIDES
V. K. Sikka 1988 27 p Presented at the Fall Meeting of the Materials Research Society, Boston, MA, 28 Nov. 1988
(Contract DE-AC05-84OR-21400)
(DE89-005133; CONF-881155-28) Avail: NTIS HC A03/MF A01

Compositional effects on hot and cold workability of ductile-ordered nickel aluminides are described. Compositional affects studied variation of chromium, aluminium, iron, and zirconium. The hot and cold workability of various nickel-aluminide alloys was ranked with respect to workability of stainless steel. The nickel-aluminide alloy containing chromium and low zirconium (IC-218LZr) had the best combination of hot and cold workability. This alloy also offered a good combination of strength and ductility values over a range of test temperatures. DOE

N89-20230# Argonne National Lab., IL. Materials Science Div.
IN-SITU HVEM STUDIES OF THE EARLY STAGES OF OXIDATION OF NICKEL AND NICKEL-CHROMIUM ALLOYS
P. Marikar (Rutgers - The State Univ., New Brunswick, NJ.), M. B. Brodsky, C. H. Sowers, and Nestor J. Zaluzec Nov. 1988 24 p Presented at the Electron Microscopy of Surfaces and Interfaces, Oak Brook, IL, 16-19 May 1988
(Contract W-31-109-eng-38)
(DE89-005833; CONF-8805152-2) Avail: NTIS HC A03

In-site oxidation of nickel, nickel-5, and nickel-25 atomic percent chromium single crystals of (100) orientation was studied by electron diffraction and contrast experiments both in a high voltage electron microscopy environmental cell, and conventional 100 KeV transmission electron microscopes. Environmental cell studies were conducted at temperatures between 500 and 700 C, and at oxygen partial pressures of 2.7 Pa and 2.4 kPa Torr for periods up to 90 minutes. The oxidation process was characterized using bright-field, dark-field imaging and selected area diffraction techniques, as well as X-ray energy dispersive and electron energy loss spectroscopy. Oxidation was observed to begin in within 40 seconds. Simultaneous nucleation of small NiO crystallites of 5 to 10 nm diameter, and growth of bright rectangular facets were observed, eventually resulting in non-uniform sample thickness. The epitaxial relationships were determined for Ni (100) and Ni-5 Cr (100). These results and the conditions for the formation of Cr2O3 are discussed and compared with those for oxidation processes in bulk alloys. DOE

N89-20231# National Aerospace Lab., Amsterdam (Netherlands). Structures and Materials Div.
QUENCH SENSITIVITY OF AIRFRAME ALUMINUM ALLOYS
H. J. Kolkman, W. G. J. tHart, and L. Schra 29 Jan. 1988 10 p Presented at the 8th International Conference on the Strength of Metals and Alloys, Tampere, Finland, 22-26 Aug. 1988
(NLR-MP-88003-U; ETN-89-94052) Avail: NTIS HC A02/MF A01

The quench sensitivity of six precipitation hardened aluminum alloys for aerospace applications was investigated and explained by means of transmission electron microscopy. The quench sensitivity is mainly caused by the solute depletion associated with heterogeneous precipitation at dispersoids for low quench rates. ESA

N89-20232# Los Alamos National Lab., NM. Materials Science and Technology Div.
ELECTRODEPOSITION OF ALUMINIUM, ALUMINIUM/MAGNESIUM ALLOYS AND MAGNESIUM FROM ORGANOMETALLIC ELECTROLYTES
Anton Mayer 1988 11 p Presented at the 1st International Congress on High-Tech-Materials and Finishing, Berlin, Fed. Republic of Germany, 12 Mar. 1989
(Contract W-7405-eng-36)
(DE89-003483; LA-UR-88-3723; CONF-890343-1) Avail: NTIS HC A03/MF A01

The electrodeposition of aluminum, magnesium, and the combination of these metals from nonaqueous media is discussed. Plating baths for depositing Al/Mg alloys or for plating essentially pure Mg were developed. These solutions contain alkali meal fluoride or quaternary ammonium halide/aluminium alkyl complexes and dialkyl magnesium dissolved in aromatic hydrocarbons. Alloy deposits over the whole composition range can be plated from these solutions by varying the relative quantities of the aluminium and magnesium alkyls and by changing the bath-operating parameters. DOE

N89-20233# Los Alamos National Lab., NM.
ANALYSIS OF THE STRAIN-RATE SENSITIVITY AT HIGH STRAIN RATES IN fcc AND bcc METALS
Paul S. Follansbee 1988 15 p Presented at the 4th International Conference on Mechanical Properties of Materials at High Rates of Strain, Oxford, England, 19-22 Mar. 1989
(Contract W-7405-eng-36)
(DE89-005471; LA-UR-88-4213; CONF-890324-1) Avail: NTIS HC A03/MF A01

The development of a constitutive model based on the use of internal state variables and phenomenological models describing glide kinetics is reviewed. Application of the model to the deformation of fcc metals and alloys is illustrated, with an emphasis on the behavior at high strain rates. Preliminary results in pure iron and 4340 steel are also presented. Deformation twinning is observed in iron samples deformed in the Hopkinson pressure bar. The influence of twinning on the proposed constitutive is discussed. DOE

N89-20234# Colorado School of Mines, Golden. Dept. of Physics.
OPTICAL SECOND HARMONIC GENERATION IN METAL MONOLAYERS AND METAL SURFACES
T. E. Furtak and J. Miragliotta (Exxon Research and Engineering Co., Annandale, NJ.) 1988 3 p Presented at the 35th National Vacuum Symposium and 4th International Laser Science Conference, Atlanta, GA, 2 Oct. 1988
(Contract DE-FG02-86ER-45253)
(DE89-006123; DOE/ER-45253/4; CONF-881002-45) Avail: NTIS HC A02/MF A01

Information about the structure of foreign metal monolayers can be obtained through measurements of the polarization dependence of optical second harmonic generation. We have used this phenomenon to monitor electrochemically controlled deposition of hexagonal metals on the (111) face of Ag. In the process, we have learned more about resonant second harmonic effects involving intrinsic excitations of the monolayer as well as surface influences within the Ag substrate. DOE

N89-20235# Colorado School of Mines, Golden. Center for Welding and Joining Research.
THE ROLE OF COMPOSITION AND MICROSTRUCTURE GRADIENTS ON WELD METAL PROPERTIES AND BEHAVIOR
Progress Report, 1 Jan. - 31 Dec. 1988

D. K. Matlock and D. L. Olson Jan. 1989 64 p
(Contract DE-FG02-87ER-45308)
(DE89-006789; DOE/ER-45308/2; MT-CWR-089-029) Avail: NTIS HC A04/MF A01

The effects of weld metal compositional and microstructural gradients on phase transformation, microstructural stability, and mechanical properties are considered from a fundamental basis in weld metal alloys which are primarily austenitic (e.g., stainless steels). Models which incorporate compositional gradients are developed to predict the resulting weld metal properties and behavior. The mechanical properties of weld metal are modeled based on composite theory in which individual weld metal zones are considered as discrete elements within a composite structure. DOE

N89-20236# Lehigh Univ., Bethlehem, PA. Dept. of Mechanical Engineering and Mechanics.
CORROSION FATIGUE OF IRON-CHRONIUM NICKEL ALLOYS: FRACTURE MECHANICS AND CHEMISTRY Progress Report, 1 Jun. - 31 Dec. 1988
Robert P. Wei 27 Jan. 1989 5 p
(Contract DE-FG02-88ER-45354)
(DE89-006985; DOE/ER-45354/T1) Avail: NTIS HC A02/MF A01

Principal efforts during 1 June to 31 December 1988 are as follows: (1) preparation and characterization of a high-purity heat of FeCrNi alloy; (2) critical assessment and further development of electrochemical techniques for measuring the kinetics of electrochemical reactions with bare steel surfaces; and (3) characterizations of the crystallographic nature of fracture surfaces produced by aqueous corrosion fatigue in a 304 stainless steel (Fe18Cr9Ni alloy) to provide background information on embrittlement mechanisms and to explore various analytical techniques. Progress in each of the areas is briefly summarized in this report. DOE

N89-20237# California Univ., Berkeley. Lawrence Berkeley Lab. Dept. of Materials Science and Mineral Engineering.
EXPLORATORY ALLOY DEVELOPMENT IN THE SYSTEM Al-Sc-X Ph.D. Thesis
Ralph Raymond Sawtell Nov. 1988 88 p
(Contract DE-AC03-76SF-00098)
(DE89-007088; LBL-26283) Avail: NTIS HC A05/MF A01

The goal of this work has been to improve the cost/performance balance in Al-Sc-X alloys by optimizing the precipitation hardening component of strengthening in these alloys. The approach involved selecting ternary additions that would interact with Sc in the L1(sub 2) phase precipitates known to form in Al-Sc alloys, modifying the precipitates and increasing overall precipitate volume fraction. The rare earth (RE) elements were chosen as candidates because of their chemical similarity to Sc. Stabilities of various phases in the Al-RE and Al-Sc-RE systems were considered with emphasis on conditions favorable to formation of the L1(sub 2) Al(sub 3)(Sc,RE) phase. The thermodynamics of precipitation of this phase in an Al matrix was then considered. Having established the likelihood of interaction of various RE in L1(sub 2) precipitates attention was turned to effects of these variations in precipitate character on relative strengthening efficiency. The precipitates become more effective obstacles as size of the RE addition increases. An experimental program was developed to investigate effects of RE size at a constant level of alloying on the trade-off between effects of greater precipitate strengthening efficiency provided by larger RE and the accompanying reduction in degree of substitution and, thus, volume fraction. DOE

N89-20238# Michigan State Univ., East Lansing.
SOFTENING MECHANISMS AND MICROSTRUCTURAL INSTABILITIES DURING HIGH TEMPERATURE LOW CYCLE FATIGUE OF Ni, Ni3Al AND THEIR METAL MATRIX COMPOSITES Progress Report, 1 Jun. 1988 - 31 May 1989
G. Gottstein Jan. 1989 7 p
(Contract DE-FG02-85ER-45205)
(DE89-007117; DOE/ER-45205/4) Avail: NTIS HC A02/MF A01

The microstructural development and mechanical behavior associated with high temperature low cycle fatigue were investigated and modeled. Fatigue crack growth during high temperature low cycle fatigue was accompanied by dynamic recrystallization, but dynamic recrystallization did not interfere with the propagation of cracks along cavitated boundaries. The occurrence of dynamic recrystallization in Ni3Al was evidenced by high temperature compression tests. Preliminary results of computer simulation of high temperature cyclic deformation indicate that the extensive microstructural changes during high temperature low cycle fatigue can be successfully modeled by SIBM and orientation dependent grain boundary sliding. The recrystallization texture development in Ni3Al is governed by fast growing orientations with 25 (100) orientation relationship between growing and consumed grains. MMCs with Ni3Al(B) matrix and Al2O3 continuous fiber reinforcement have been successfully produced by vacuum hot pressing. Together with Siemens/Nicolet a fully automatic orientation mapping system with synchrotron radiation has been assembled and will be tested in April 1989. DOE

N89-20239# California Univ., Berkeley. Lawrence Berkeley Lab. Dept. of Materials Science and Mineral Engineering.
MICROSTRUCTURAL AND MAGNETIC CHARACTERIZATION IN SOFT MAGNETIC Fe-Si-Al (SENDUST) ALLOY Ph.D. Thesis
June Dong Kim Dec. 1988 112 p
(Contract DE-AC03-76SF-00098)
(DE89-007130; LBL-26334) Avail: NTIS HC A06/MF A01

Microstructure and its effect on magnetic domain structure and domain wall motion has been studied to understand the role of microstructure in determining the magnetic properties of a soft magnetic Sendust alloy. Electron microscopy of dark field imaging utilizing superlattice reflections has been mainly used to investigate the ordering behavior and corresponding microstructural changes, and Lorentz electron microscopy allowed the effect of microstructure on magnetic domain structure and wall motion to be observed. Antiphase boundaries (APBs) and other imperfections have been shown clearly and simultaneously with the observation of magnetic domain walls, even with the objective lens off. DOE

N89-20240# International Centre for Theoretical Physics, Trieste (Italy).
SURFACE AND INTERFACE LOCAL DENSITY OF STATES FOR Nb, V AND Ta
R. Baquero, A. Camacho, and L. Quiroga Sep. 1988 18 p
Submitted for publication
(DE88-705365; IC-88/290) Avail: NTIS (US Sales Only) HC A03/MF A01

We have calculated the local density of states at the surface and in the interface for the transition metals Nb, V and Ta using empirical tight-binding Hamiltonians and the formulae of the Surface Green Function Matching (SFGM) method. We get the local density of states at the surface and at the inner atomic layers. The effect of the surface is strong and very localized. We notice that certain characteristics of the Surface Local Density of States (SLDOS) correlate well with the known magnetic and superconducting properties of each metal. We do not take into account strain and assume an ideal interface but we do take into account charge neutrality in the interface and at the surface using the Friedel sum rule in a standard way. DOE

N89-20241# Westinghouse Electric Corp., Philadelphia, PA. Advanced Energy Systems.
DEVELOPMENT OF TOOLING AND TECHNIQUES FOR REMOTE FIELD METALLOGRAPHY
C. Bagnall 1988 16 p Presented at the 5th Brazilian Symposium on Piping and Pressure Vessels, Salvador, Brazil, 25 Oct. 1988
(Contract DE-AC09-76SR-00001)
(DE89-005400; DP-MS-88-206; CONF-8810288-1) Avail: NTIS HC A03/MF A01

Recent experience with tooling designed for remote field

metallography (RFM) and field surveillance metallography is presented. Results of examinations conducted on ferrous and non-ferrous vessels are described. The potential synergistic benefits to be gained by combining RFM or field surveillance metallography (FSM) techniques with other NDE analytical devices are discussed. DOE

N89-20242# Lawrence Livermore National Lab., CA.
CONSTITUTIVE PROPERTIES OF COPPER AND TANTALUM AT HIGH RATES OF TENSILE STRAIN: EXPANDING RING RESULTS
W. H. Gourdin 16 Dec. 1988 8 p Presented at the 4th International Conference on Mechanical Properties of Materials at High Rates of Strain, Oxford, United Kingdom, 20 Mar. 1989
(Contract W-7405-eng-48)
(DE89-006197; UCRL-98812; CONF-890324-4) Avail: NTIS HC A02/MF A01

The electromagnetic launch technique has been used to study the properties of Oxygen-Free Electronic (OFE) grade copper, processed to yield uniform grain sizes between 10 and 150 to 200 micrometers with minimal texture, and 99.9 percent tantalum rings with grain sizes of 25 and 65 micrometers expanded at peak strain rates of nearly 10,000/s. The results for OFE copper indicate an increasing flow stress as grain size decreases and are in good accord with data available in the literature. Tantalum specimens likewise show an increase in the flow stress as grain size decreases, but display virtually no apparent work hardening. The data are briefly compared to constitutive models in the literature. DOE

N89-20243# Allied-Signal Aerospace Co., Kansas City, MO.
ANALYSIS OF BRASS ALLOYS BY WAVELENGTH DISPERSIVE X-RAY SPECTROMETRY Final Report
W. G. Frede Feb. 1989 22 p
(Contract DE-AC04-76DP-00613)
(DE89-007595; KCP-613-4058) Avail: NTIS HC A03/MF A01

A method was developed to determine the concentration of copper, zinc, iron, lead, and tin in brass alloys using wavelength dispersive X-ray spectrometry. This metnod incorporates the use of a 24-position sample carrousel for unattended operation and a minicomputer for data collection and analysis. The concentration of the five elements of interest is calculated using a fundamental parameters computer program for X-ray fluorescence analyses. Using this method, the standard deviation for each element is Cu, 0.016 percent; Zn, 0.015 percent; Fe, 0.0002 percent; Pb, 0.0019 percent; and Sn, 0.009 percent. DOE

N89-20244# Army Lab. Command, Watertown, MA. Material Technology Lab.
WELDABILITY OF 2519-T87 ALUMINUM ALLOY Final Report
Jack H. Devletian, Sandra M. DeVincent, and Steven A. Gedeon Dec. 1988 33 p
(AD-A203519; MTL-TR-88-47) Avail: NTIS HC A03/MF A01 CSCL 11F

Test results show that 2519-T87 is weldable to itself and to 5083-H131. A wide variety of filler metals, weld parameters, and post-weld heat treatments were studied to determine the effect on weld mechanical properties, hot crack susceptibility, microstructure, and ballistic integrity. Previously reported 2519-T87 weldment ballistic failures have been discovered to be invalid. New ballistic weldments of 2519-T87 welded to itself were successfully qualified to the shock test in MIL-STD-1946. GRA

N89-20245# Army Lab. Command, Watertown, MA. Material Technology Lab.
X-RAY DIFFRACTION STUDY OF PHASE FORMATION AND GROWTH IN NITROGEN IMPLANTED IRON: TEMPERATURE EFFECTS
Ronald J. Arnott, Forrest C. Burns, Louis G. Carreiro, David R. Chipman, and William J. Croft Nov. 1988 15 p
(AD-A203625; MTL-TR-88-38) Avail: NTIS HC A03/MF A01 CSCL 11F

We report preliminary results from an ongoing study of iron nitride grains formed in high purity iron under nitrogen ion bombardment. Under various implantation conditions, different iron nitride phases grow large enough to produce sharp X-ray diffraction lines. We have used these lines to examine the influence of target temperature during implantation. Between 200 C and 400 C increasing target temperature, which enhances dopant mobility, reduces the retained dose of nitrogen and restricts the formation of nitride phases. Over this temperature range, however, increasing vacancy mobility favors the growth of nitride grains and X-ray line breadth data suggests an optimum temperature for growth of Fe4N grains. GRA

N89-20246# Naval Research Lab., Washington, DC. Mechanics of Materials Branch.
WELDED JOINT INTEGRITY ANALYSIS: RELATIVE CRITICALITY OF WELD DEFECT AND REMOTE DEFORMATION
V. Gensheimer DeGiorgi, P. Matic, and M. I. Jolles 9 Dec. 1988 23 p
(AD-A203756; AD-E900863; NRL-MR-6022) Avail: NTIS HC A03/MF A01 CSCL 11F

Structural integrity problems which deal with welded sections are common in the pressure vessel and piping industry. The current work uses continuum fracture toughness concepts to determine the structural integrity of a butt welded plate with a lack of penetration defect in the weld material. The difference in weld and base metal properties are explicitly included in the computational simulation. The analysis technique presented does not require the analyst to assume a failure location. The critical strain energy density associated with fracture of a material at the continuum scale is used as the failure criterion. GRA

N89-20247# Lehigh Univ., Bethlehem, PA. Inst. of Fracture and Solid Mechanics.
ELECTROCHEMICAL CONSIDERATIONS OF CRACK GROWTH IN THE FERROUS ALLOYS Technical Report, No. 21, 1 Jan. - 31 Dec. 1988
R. P. Wei Nov. 1988 25 p
(Contract N00014-83-K-0107)
(AD-A203811; IFSM-88-153) Avail: NTIS HC A03/MF A01 CSCL 20K

Environmentally assisted crack growth in ferrous alloys in aqueous environments is multifaceted problem of technological importance. Recent studies of electrochemical reactions with bare metal surfaces and of crack growth response have provided a clear demonstration of electrochemical reaction control of crack growth in steels. These studies also showed the importance of localized transient reactions with bare metal surfaces at the crack tip and the need for a new approach to the measurement of electrochemical reaction kinetics. In this paper, a framework is outlined for the identification and modeling of crack growth response in aqueous environments in terms of the underlying chemical processes. This framework serves as a basis for fundamental understanding, and for the rotational interpretation and utilization of crack growth data. GRA

27 NONMETALLIC MATERIALS

Includes physical, chemical, and mechanical properties of plastics, elastomers, lubricants, polymers, textiles, adhesives, and ceramic materials.

For composite materials see *24 Composite Materials*.

N89-20248*# California Univ., Los Angeles. Dept. of Chemical Engineering.
EXPERIMENTS WITH METALLIC AND CERAMIC POROUS MEDIA Report, 30 Dec. 1988
T. H. K. Frederking, P. Abbassi, P. K. Khandhar, and Jack Luna Dec. 1988 62 p
(Grant NAG2-516)
(NASA-CR-184819; NAS 1.26:184819; UCLA-ENG-8838) Avail: NTIS HC A04/MF A01 CSCL 11B

Work in the area of mechano-caloric phenomena was initiated during 1988 with startup in the Summer 1988 period. The ideal system utilizing He-II super-phenomena is modeled readily, within the frame of thermodynamics energetics, using the concept of an ideal superleak. The real system however uses porous media of non-ideal pore-grain ingredients. The early phase of experimental and related modeling studies is outlined for the time period from Summer 1988 to the end of 1988. Author

N89-20249 Colorado State Univ., Fort Collins.
LONG TERM LUBRICATION OF CERAMICS AT HIGH TEMPERATURES Ph.D. Thesis
Kyu Yong Lee 1988 178 p
Avail: Univ. Microfilms Order No. DA8821303

The use of high performance ceramics as sliding components in engines can vastly increase fuel efficiency. However, a major problem that needs to be solved is the lubrication of ceramics at high temperatures. To study high temperature ceramic lubrication, an instrumented high temperature wear testing machine was designed and constructed. Unlubricated room temperature and high temperature wear tests of aluminum oxide sliding against aluminum oxide showed very high wear rates, unsuitable for any long term sliding applications. Based on wear tests conducted at room temperature with aluminum oxide using oil and sputter deposited films of graphite, the following conclusions were drawn: (1) the friction mechanism in alumina with good surface finish at room temperature is adhesion; (2) good reduction in wear and friction can be obtained without extraction of wear debris; and (3) the dominant mechanism of wear in alumina at room temperature must be a combination of adhesion and brittle fracture. Dissert. Abstr.

N89-20250# Pennsylvania Univ., Philadelphia. Dept. of Materials Science and Engineering.
ENVIRONMENTAL EFFECTS ON THE TIME DEPENDENT FAILURE OF NON-OXIDE CERAMICS Final Report, 15 Aug. 1984 - 14 Jul. 1988
Richard E. Tressler 3 Nov. 1988 197 p
(Contract DAAG29-84-K-0170)
(AD-A202391; ARO-21690.16-MS) Avail: NTIS HC A09/MF A01 CSCL 11B

The mechanical and chemical factors that contribute to time dependent strength changes have been investigated for a variety of non-oxide materials including silicon nitride, silicon carbide and siliconized silicon carbide. The flaw behavior in an as-machined and oxidized HIP'ed silicon nitride under static load was investigated at various stress intensities, times, and temperatures. Flaw origins were of the pore/cavity and iron-based inclusion type. There was no strength increase or degradation in as-machined and oxidized samples static loaded for ten hours at 1100 C in air below the threshold stress intensity. The threshold stress intensity for crack growth at 1100 C were determined to be 1.75 and 2.00 MPa.m1/2 for the as-machined and oxidized HIPSN, respectively. A strength decrease with increased applied stress was observed in as-machined specimens static loaded at 1200 C and 1300 C in air. This effect is due to the creation of a new flaw population with more severe flaws. GRA

N89-20251*# Howard Univ., Washington, DC. Dept. of Physics and Astronomy.
GLASS CORROSION IN NATURAL ENVIRONMENT Semiannual Progress Report No. 1
Arthur N. Thorpe Feb. 1989 44 p
(Grant NAG5-1057)
(NASA-CR-184843; NAS 1.26:184843) Avail: NTIS HC A03/MF A01 CSCL 11C

A series of studies of the effects of solutes which appear in natural aqueous environments, specifically Mg and Al, under controlled conditions, permit characterization of the retardation of silicate glass leaching in water containing such solutes. In the case of Mg the interaction with the glass appears to consist of exchange with alkali ions present in the glass to a depth of several microns. The effect of Al can be observed at much lower levels, indicating that the mechanism in the case of Al involves irreversible formation of aluminosilicate species at the glass surface. Author

N89-20252*# National Aeronautics and Space Administration. Lewis Research Center, Cleveland, OH.
CRYSTALLIZATION KINETICS OF BaO-Al2O3-SiO2 GLASSES
Narottam P. Bansal (Case Western Reserve Univ., Cleveland, OH.) and Mark J. Hyatt May 1988 22 p Presented at the 90th Annual Meeting of the American Ceramic Society, Cincinnati, OH, 1-5 May 1988
(NASA-TM-101964; E-4662; NAS 1.15:101964) Avail: NTIS HC A03/MF A01 CSCL 11C

Barium aluminosilicate glasses are being investigated as matrix materials in high-temperature ceramic composites for structural applications. Kinetics of crystallization of two refractory glass compositions in the barium aluminosilicate system were studied by differential thermal analysis (DTA), X-ray diffraction (XRD), and scanning electron microscopy (SEM). From variable heating rate DTA, the crystallization activation energies for glass compositions (wt percent) 10BaO-38Al2O3-51SiO2-1MoO3 (glass A) and 39BaO-25Al2O3-35SiO2-1MoO3 (glass B) were determined to be 553 and 558 kJ/mol, respectively. On thermal treatment, the crystalline phases in glasses A and B were identified as mullite (3Al2O3-2SiO2) and hexacelsian (BaO-Al2O3-2SiO2), respectively. Hexacelsian is a high-temperature polymorph which is metastable below 1590 C. It undergoes structural transformation into the orthorhombic form at approximately 300 C accompanied by a large volume change which is undesirable for structural applications. A process needs to be developed where stable monoclinic celsian, rather than hexacelsian, precipitates out as the crystal phase in glass B. Author

N89-20253*# National Aeronautics and Space Administration. Lewis Research Center, Cleveland, OH.
DESIGN, DEVELOPMENT AND APPLICATIONS OF NOVEL TECHNIQUES FOR STUDYING SURFACE MECHANICAL PROPERTIES
Kazuhisa Miyoshi 1989 12 p Presented at the Spring Meeting of the Materials Research Society, San Diego, CA, 24-28 Apr. 1989
(NASA-TM-101959; E-4654; NAS 1.15:101959) Avail: NTIS HC A03/MF A01 CSCL 11C

Research is reviewed for the adhesion, friction, and micromechanical properties of materials and examples of the results presented. The ceramic and metallic materials studied include silicon carbide, aluminum oxide, and iron-base amorphous alloys. The design and operation of a torsion balance adapted for study of adhesion from the Cavendish balance are discussed first. The pull-off force (adhesion) and shear force (friction) required to break the interfacial junctions between contacting surfaces of the materials were examined at various temperatures in a vacuum. The surface chemistry of the materials was analyzed by X-ray photoelectron spectroscopy. Properties and environmental conditions of the surface regions which affect adhesion and friction-such as surface segregation, composition, crystal structure, surface chemistry, and temperature were also studied. Author

N89-20254# Boston Univ., MA. Dept. of Chemistry.
PHOTOINDUCED ELECTRON TRANSFER IN ORDERED POLYMERS Progress Report, 1 May - 31 Dec. 1988
Guilford Jones, II 31 Dec. 1988 5 p
(Contract DE-FG02-88ER-13905)
(DE89-006986; DOE/ER-13905/1) Avail: NTIS HC A02/MF A01

Long-range photoinduced electron transfer between potential electron donors and acceptors is of considerable current interest in terms of strategies for artificial photosynthesis and studies regarding the redox properties of proteins. Electron transfer over organized arrays of significant dimension (e.g., 10 nm) may also be important for molecule-based bistable switches or rectifiers. As part of a program of study of long range electron transfer involving biopolymers, we report early investigations of the interaction of the xanthene dye, eosin (EY), with synthetic peptides constructed

of the amino acid residues, lysine (Lys), tryptophan (Trp), and tyrosine (Tyr). The principal interest in these systems has to do with the well ordered secondary structures (e.g., alpha-helices) adopted by peptide polymers and the capabilities for synthetic modification of peptide side chains and end groups with chromophores or electroactive substituents. Work which is completed or well underway includes synthesis of Trp homopolymer (20 to 25 Trp amino acid residues) with EY attached specifically at the N-terminus. Model compounds in which the xanthene dye is attached to one or two Trp residues have been prepared along with copolymers of Trp or Tyr and Lys with randomally labeled EY at Lys side chains. Photoinduced electron transfer between variously attached eosin pendants and co-bound Trp units has been studied using fluorescence quenching and laser flash photolysis methods. Also, as a model for events occurring for the synthetic peptides, electron transfer quenching of eosin singlet and triplet excited states by substituted phenols, representative of the pendant groups of Tyr residues has been investigated. The observation of ultra-long-lived contact radical ion pairs which result from the quenching of an excited quinone molecule and the photolysis of quinone charge-transfer complexes constitute another theme of continuing research. DOE

N89-20255 British Petroleum Co. Ltd., London (England).
RAPID CURE ACRYLIC ADHESIVE COMPOSITIONS Patent Application
Stephen Alan Taylor, inventor (to British Petrole 2 Dec. 1987 5 p Filed 23 Apr. 1987 Priority 30 Apr. 1986 GB 8610526; Priority 1 May 1986 GB 8610659
(EP-0-247-726-A2; EP-PATENT-APPL-SN-87303603.2; INT.CLASS-C09J-3/14; INT.CLASS-C08F-220/00; ETN-89-94068)
Avail: UK Patent Office, 25 Southampton Buildings, London WC2A 1AY, England

An adhesive composition comprising an acrylic functional urethane elastomer, an acrylic monomer, an organic sulfimide, an organic sulfinate or a salt thereof, a peroxide initiator, and a tertiary amine curing accelerator is proposed. The curing accelerator preferably has at least two tertiary nitrogen atoms in its structure and is a reactive organic dye. The adhesive composition is curable aerobically, has faster curing rates than achieved hitherto, and shows improved bond-strengths when compared with conventional tertiary amine curing accelerators. ESA

N89-20256# International Centre for Theoretical Physics, Trieste (Italy).
ON THE DIMERIZATION OF LINEAR POLYMERS
C. deAragaoCarvalho Aug. 1988 12 p
(DE88-705341; IC-88/191) Avail: NTIS (US Sales Only) HC A03/MF A01

We use the continuum limit of the Su-Schrieffer-Heeger model for linear polymers to construct its effective potential (Gibbs free energy) both at zero and finite temperature. We study both trans and cis-polymers. Our results show that, depending on a renormalization condition to be extracted from experiment, there are several possibilities for the minima of the dimerized ground state of cis-polymers. All calculations are done in the one-loop approximation. DOE

N89-20257# Los Alamos National Lab., NM. Materials Science and Technology Div.
STRUCTURE-PROPERTY CHARACTERIZATION OF A SHOCK-LOADED BORON CARBIDE-ALUMINUM CERMET
W. R. Blumenthal and G. T. Gray, III 1989 9 p Presented at the 4th International Conference on Mechanical Properties of Materials at High Rates of Strain, Oxford, England, 19-22 Mar. 1989
(Contract W-7405-eng-36)
(DE89-005455; LA-UR-88-4059; CONF-890324-2) Avail: NTIS HC A02/MF A01

Shock-recovery experiments were performed on a 65 vol percent B4C-Al cermet as a function of shock pressure. Samples were recovered largely intact due to the use of confinement and soft-recovery techniques. Post-shock examination by optical and transmission electron microscopy (TEM) showed the B4C structure to be unchanged up to 5 GPa, while the Al phase exhibited a high density of randomly distributed dislocations. After a shock of 10.6 GPa some of the B4C grains displayed dislocation debris, but the majority showed no evidence of plastic deformation. Uniaxial compression testing of the unshocked cermet showed a 24 percent increase in strength from 1.94 GPa to 2.4 GPa with an increase in strain rate from 0.001/s to 100.0/s. DOE

N89-20258# Oak Ridge National Lab., TN. Metals and Ceramics Div.
THE INFLUENCE OF THICKNESS AND WAVELENGTH ON THE MECHANICAL PROPERTIES OF A COMPOSITIONALLY MODULATED CERAMIC THIN FILM
W. C. Oliver, F. A. List, and R. A. McKee 1988 6 p Presented at the Fall Meeting of the Materials Research Society, Boston, MA, 28 Nov. 1988
(Contract DE-AC05-84OR-21400)
(DE89-006033; CONF-881155-39) Avail: NTIS HC A02/MF A01

The hardness and modulus of thin (less than 1 micrometer) ceramic films have been investigated using the differential mechanical properties microprobe (DMPM). The DMPM consists of a computer controlled ultra-low load indentation system with a special system that allows the elastic stiffness of the contact to be determined continuously during the indentation process. The films were deposited in a molecular beam epitaxy (MBE) system utilizing unique high temperature effusion cells. Two specimens have been studied. The first is a wedge shaped layer of amorphous Al(sub 2)O(sub 3) on a silicon substrate. The thickness of the layer varies from 0 to 990 nm at the two extreme sides of a 3 in. silicon wafer. The effect of layer thickness on the hardness and modulus as measured with the DMPM has been quantified for this system. The second specimen is made up of 38 repetitions of alternating layers of crystalline TiO(sub 2) and amorphous Al(sub 2)O(sub 3). The wavelength of the composition modulation and the thickness of the film varies uniformly from 0 to 38 nm and from 0 to 1460 nm respectively across the 3 in. diameter of the silicon substrate. DOE

N89-20259# Oak Ridge National Lab., TN. Metals and Ceramics Div.
HARDNESS OF AMORPHOUS HARD CARBON FILMS DETERMINED BY THE ULTRA-LOW LOAD MICROINDENTATION TECHNIQUE
D. L. Joslin (Tennessee Univ., Knoxville.), M. E. OHern, C. J. McHargue, R. E. Clausing, and W. C. Oliver 1989 9 p Presented at the Symposium on Lasers and Optics, Los Angeles, CA, 15 Jan. 1989
(Contract DE-AC05-84OR-21400)
(DE89-006129; CONF-890142-2) Avail: NTIS HC A02/MF A01

Amorphous carbon films variously designated as i-C, alpha-C:H, diamond-like or hard carbon films, have interesting optical and mechanical properties and are candidates for wear and corrosion protection in a wide range of applications. Because the depth of penetration by the indenter in normal hardness tests often approaches or exceeds the thickness of the diamond-like coating film, hardness data may reflect large substrate effects. This paper gives the results of ultra-low load microindentation hardness measurements which allow data to be obtained for indentation depths as small as 20 nm. The data also yield information on the elastic modulus of the coatings. Films were obtained from a number of sources and had been prepared by several techniques. The hardness values are in the range of 7 to 15 GPa and depend on the exact preparation parameters. The hardness data will be compared to those obtained by the Knoop technique. DOE

N89-20260# Oak Ridge Gaseous Diffusion Plant, TN. Materials and Chemistry Technology.
A DYNAMIC FLOW-WEIGHTED PORE SIZE DISTRIBUTION TEST
Douglas E. Fain 1988 18 p Presented at the Fine Particle Society Meeting, Santa Clara, CA, 19 Jul. 1988

(Contract DE-AC05-84OT-21400)
(DE89-006191; K/QT-188; CONF-8807110-2) Avail: NTIS HC A03/MF A01

An accurately measured pore size distribution can be important in evaluating the characteristics and functional performance of a porous material. Pore size distributions are usually measured by evaluating the change in volume of a material deposited in the porous material under varying conditions that can be related to a pore size. The distribution of volume may or may not be easily related to other properties that are functions of other moments of the pore size distribution. A method has been developed for measuring the fraction of the flow of an inert gas through various pore size channels in a porous material. The measurement is accomplished by using a mixture of an inert gas such as nitrogen and a condensable gas such as carbon tetrachloride. The test begins with the partial pressure of the condensable gas near unity. The condensable gas will fill all of the pores of the material and there is no flow of nitrogen through the material. As the pressure of the mixture is incrementally decreased, a range of pore sizes is opened and the flow of nitrogen increases. These data provide the accumulated total flow of nitrogen as a function of pore size. This paper gives the theory associated with the test, describes the apparatus for making the measurements, and shows some results. DOE

N89-20261# Lawrence Livermore National Lab., CA.
THE APPLICATION OF STATISTICAL EXPERIMENTAL DESIGN TO THE DEVELOPMENT OF LOW-DENSITY POLYMER FOAMS
Blanca L. Haendler, Lucy M. Hair, and Fung-Ming Kong Dec. 1988 14 p Presented at the Symposium on Computer Applications in Applied Polymer Science, Toronto, Ontario, 5 Jun. 1988
(Contract W-7405-eng-48)
(DE89-006774; UCRL-97490; CONF-8806139-2) Avail: NTIS HC A03/MF A01

Statistical experimental designs have been used to improve the development of low-density polymer foams for use as direct-drive targets for Laser Inertial Confinement Fusion (ICF). For polystyrene foams, which are made by polymerization of a high-internal-phase emulsion, a three-variable Box-Behnken response surface methodology experiment led to quick identification of a reproducibility problem, which was resolved by moving to a different density regime. This experiment also confirmed the crucial role the surfactant (Span 80) plays in this system. For resorcinol-formaldehyde foams, which are made by a condensation polymerization in dilute solution, a fractional-factorial screening study identified key variables which were then investigated further. The striking result here was that testing ranges of variables outside what had previously been considered led to better quality samples with much lower densities. DOE

N89-20262# Brookhaven National Lab., Upton, NY.
THERMOGRAVIMETRIC ANALYSIS OF POLYMERIC MATERIALS FOR AN INTERMEDIATE TEMPERATURE SOLID ELECTROLYTE. 2: POLYMER MIXTURES
Tien Le and Clovis A. Linkous Oct. 1988 46 p
(Contract DE-AC02-76CH-00016)
(DE89-006980; BNL-42170-Pt-2) Avail: NTIS HC A04/MF A01

The thermal stability of 17 candidate polymeric materials were tested for weight-loss under a steam atmosphere. A number of polymers which were stable under steam treatment were also tested under N sub 2 atmosphere. The following 13 polymers were stable in steam atmosphere for 4 hours or more showed promise for use as a solid polymer electrolyte: polybenzimidazole (PBI), phosphate PBI, polyimide, Teflon, polyamide resin, poly(phenylene sulfide), Nafion, poly(ethylene oxide), poly(acrylonitrile), poly(vinylpyrrolidone), poly(ethylene glycol), and poly(2-vinylpyridine). Four stable polymers at 300 to 400 C and six stable polymers at 200 C in steam atmosphere were crossed with each other by blending or compressing methods. Mixtures involving poly(vinylpyrrolidone) gave a protective effect, i.e., the onset temperature of decomposition of the vinylpyrrolidone was increased by incorporation into a high temperature polymer matrix. DOE

N89-20263# International Centre for Theoretical Physics, Trieste (Italy).
NUCLEATION OF SUPERCONDUCTIVITY IN CERAMIC OXIDES
A. G. Saif and J. Chela-Flores Aug. 1988 10 p Submitted for publication
(DE88-705364; IC-88/286) Avail: NTIS (US Sales Only) HC A02/MF A01

We discuss the nucleation of superconductivity in the interior of a bulk specimen, as well as at the surface of ceramic superconductors. We base our work on phenomenological equations, in which superconductivity coexists with antiferromagnetism. The prediction of the evolution of H sub c sub 2 with small variations on the coupling constant may serve to test the underlying phenomenological theory. DOE

N89-20264# Dayton Univ., OH. Research Inst.
A COMPREHENSIVE REVIEW OF MODELING OF IMPACT DAMAGE IN CERAMICS Final Technical Report, Mar. - Oct. 1988
A. M. Rajendran and W. H. Cook Dec. 1988 99 p
(Contract F33615-86-C-5064)
(AD-A203477; AD-E801843; AFATL-TR-88-143) Avail: NTIS HC A05/MF A01 CSCL 19D

This report reviews high strain rate experimental and analytical methods available for characterizing ceramic material behavior. Also, a discussion on the ceramic failure mechanisms upon impact loading conditions is provided. Theoretical basis for constitutive and failure modeling of ceramic type brittle material is discussed. Models that are reported in open literature are reviewed and categorized based on their theoretical approaches. The salient features of a few recently reported constitutive/damage theories, which combine either the micromechanics or the continuum damage mechanics for the stress-strain relationship with fracture mechanics for damage accumulation description, are described and tabulated. Recent attempts to employ such models in the calculation of armor penetration problems are briefly discussed. GRA

N89-20265# Aerojet Solid Propulsion Co., Sacramento, CA.
ENERGETIC THERMOPLASTIC ELASTOMER SYNTHESIS Quarterly Report No. 5, 1 Sep. - 30 Nov. 1988
R. W. Fletcher and H. W. Cheung 30 Nov. 1988 2 p
(Contract N00014-87-C-0098)
(AD-A203594) Avail: NTIS HC A02/MF A01 CSCL 11J

Work has continued during reporting period on the synthesis of triblock polymers comprising of the BAMO-AMMO-BAMO structure. We have synthesized polymers for NWC's effort to elucidate structure and resolve the structure/property relationship. As required structures have been requested, we have supplied the appropriate sample. This has included homo polymers as will as di- and tri-blocks. We have also supplied the University of Massachusetts with multiple half pound quantities of each homo polymer to support their blocklinking efforts. Each of these investigators will report the results of their work separately. GRA

N89-20266# Connecticut Univ., Storrs. Liquid Crystalline Polymer Research Center.
SYNTHESIS AND PHYSICAL PROPERTIES OF LIQUID CRYSTALLINE ALKYLISOCYANATE COPOLYMERS Interim Report, 11 Jan. 1988
B. Durairaj (Koppers Co., Inc., Monroeville, PA.), E. T. Samulski, and M. T. Shaw 11 Jan. 1989 26 p
(Contract N00014-86-K-0772)
(AD-A203631; TR-32) Avail: NTIS HC A03/MF A01 CSCL 07F

Liquid crystalline copolymer containing 50:50 mole ratios of undecylisocyanate with propyl, butyl, hexyl, and octylisocyanate were synthesized and characterized. By making copolymers, the

temperature range of isotropic state (i.e. range between the clearing and decomposition temperatures) was increased over that for poly (undecylisocyanate). The results from various analyses showed that all the copolymers undergo decomposition at 180 C. The dependence of Tg on alkyl side chain length and copolymer composition was consistent with that for other alkyl-side-chain polymers. GRA

N89-20267# Connecticut Univ., Storrs. Dept. of Chemical Engineering.
THE EFFECT OF DEFORMATION HISTORY ON THE MORPHOLOGY AND PROPERTIES OF BLENDS OF POLYCARBONATE AND A THERMOTROPIC LIQUID CRYSTALLINE POLYMERS Interim Technical Report, 11 Jan. 1989
A. Kohli, N. Chung, and R. A. Weiss 11 Jan. 1989 30 p
(Contract N00014-86-K-0772)
(AD-A203632; TR-33) Avail: NTIS HC A03/MF A01 CSCL 07F

The addition of an immiscible LCP phase improves the melt processability of a host thermoplastic polymer. In addition, by employing a suitable deformation history, the LCP phase may be elongated and oriented such that a microfibrillar morphology can be retained in the solid state. This has important ramifications for the development of self-reinforcing polymer blends to compete with conventional inorganic fiber-reinforced polymers. Shear flows are generally ineffective at developing these morphologies, but flows that incorporate an extensional region, such as the converging flow found at the entrance to a capillary or die can produce an elongated LCP phase. Simple extensional flows, such as melt drawing, are most effective at producing LCP microfibrils, and their efficiency increases with increasing draw ratio. The moduli of highly drawn blends were well approximated by a composite's analogy of long uniaxially oriented LCP fibers in a PC matrix. GRA

N89-20268# Illinois Univ., Chicago. Circle Dept. of Chemistry.
EVALUATION OF SOLID LUBRICANTS: TEMPERATURE PROGRAMMED DESORPTION OF MoS2 ON MOLYBDENUM AND OF ION-IMPLANTED MoS2 ON MOLYBDENUM Final Report
Richard P. Burns, Daniel E. Piece, Helen M. Dauplaise, Kenneth A. Gabriel, and Lawrence J. Mizerka Nov. 1988 30 p
(Contract DAAL04-86-K-0003; DA Proj. 1L1-61101-A-91-A)
(AD-A203741; MTL-TR-88-36) Avail: NTIS HC A03/MF A01 CSCL 11H

Thermal Programmed Desorption (TPD) is utilized in order to assess the lubricating properties of metal dichalcogenide films applied to a number of metal substrates. TPD spectra documenting desorption and decomposition products were analyzed for MoS2 burnished on molybdenum metal with and without subsequent 86 kV nitrogen ion implantation. Desorption order, rate, energy, and the pre-exponential of evolved lubricant and nitrogen species from the molybdenum substrates were determined. The surface chemistry of heated lubricant-substrate system was investigated by means of X-ray Photoelectron Spectroscopy (XPS). GRA

N89-20269# Battelle Memorial Inst., Columbus, OH.
SULFIDE AND PHOSPHIDE ANALOGS OF OXYNITRIDE CERAMICS Final Report, 19 Mar. 1986 - 18 Nov. 1988
Peter J. Melling 17 Jan. 1989 75 p
(Contract N00014-86-C-0313)
(AD-A203805) Avail: NTIS HC A04/MF A01 CSCL 11B

A survey of compositions in the GeGaPS system, initially based on the Beta-Sialon system (Si4A12O2N6) was carried out. Most of the samples were prepared by sealed tube melting (using a fused quartz tube) of mixtures of the elements in a rocking furnace. When it was found that these materials are sensitive to oxygen contamination a pressure melting system was constructed in which melts were prepared in vitreous carbon crucibles under an inert gas overpressure. There is a requirement for new materials which are transparent in the 8 to 14 micro meter wavelength range and have superior thermal shock resistance, toughness, mechanical strength, and abrasion resistance compared to existing materials. The purpose of this work was to evaluate the possibility of preparing sulfide-phosphide analogs of oxynitride glasses and glass ceramics in the GeGaPS system. If the silicon nitride structure could be prepared in this system, large improvements in mechanical properties are expected. GRA

N89-20270# Texas Univ., Arlington. Dept. of Chemistry.
NEW VINYLIDENE FLUORIDE COPOLYMERS: POLY(VINYL ACETATE-CO-VINYLIDENE FLUORIDE)
V. Panchalingam and John R. Reynolds 9 Jan. 1989 16 p
(Contract N00014-86-K-0769)
(AD-A203939; TR-13) Avail: NTIS HC A03/MF A01 CSCL 07F

Copolymers of vinylidene fluoride and vinyl acetate have been prepared at varied compositions and characterized by 1H-NMR, 13C-NMR, FTIR, DSC and TGA. Copolymers were obtained as both THF soluble and insoluble fractions with the former having a relatively random distribution of monomers along the chain and the latter being somewhat blocky in nature. GRA

28 PROPELLANTS AND FUELS

Includes rocket propellants, igniters, and oxidizers; their storage and handling procedures; and aircraft fuels.

For related information see also *07 Aircraft Propulsion and Power, 20 Spacecraft Propulsion and Power,* and *44 Energy Production and Conversion.*

N89-20271*# Astronautics Corp. of America, Madison, WI. Astronautics Technology Center.
LUNAR SURFACE BASE PROPULSION SYSTEM STUDY, VOLUME 1 Final Report
Feb. 1987 418 p
(Contract NAS9-17468)
(NASA-CR-171982-Vol-1; NAS 1.26:171982-Vol-1) Avail: NTIS HC A18/MF A01 CSCL 21I

The efficiency, capability, and evolution of a lunar base will be largely dependent on the transportation system that supports it. Beyond Space Station in low Earth orbit (LEO), a Lunar-derived propellant supply could provide the most important resource for the transportation infrastructure. The key to an efficient Lunar base propulsion system is the degree of Lunar self-sufficiency (from Earth supply) and reasonable propulsion system performance. Lunar surface propellant production requirements must be accounted in the measurement of efficiency of the entire space transportation system. Of all chemical propellant/propulsion systems considered, hydrogen/oxygen (H/O) OTVs appear most desirable, while both H/O and aluminum/oxygen propulsion systems may be considered for the lander. Aluminized-hydrogen/oxygen and Silane/oxygen propulsion systems are also promising candidates. Lunar propellant availability and processing techniques, chemical propulsion/vehicle design characteristics, and the associated performance of the total transportation infrastructure are reviewed, conceptual propulsion system designs and vehicle/basing concepts, and technology requirements are assessed in context of a Lunar Base mission scenario. Author

N89-20272# EG and G Mound Applied Technologies, Miamisburg, OH.
THE DYNAMIC RESPONSE AT HIGH-EXPLOSIVE INERT-SOLID INTERFACE AS PREDICTED BY FINITE DIFFERENCE/ELEMENT COMPUTER PROGRAMS
Tien S. Chou 20 Jan. 1989 19 p
(Contract DE-AC04-88DP-43495)
(DE89-007303; MLM-3562) Avail: NTIS HC A03/MF A01

A one-dimensional model of high explosive charge was designed to test the computational results of shock wave propagation predicted by three two-dimensional solid dynamics computer programs. The test showed excellent agreement of the wave patterns and the pressure-velocity history profiles at the material interface as the stress waves resulting from the high explosive

detonation interacted with inert solid materials. The peak pressure and the particle velocity at the interface were estimated with a simple one-dimensional analysis. The corresponding values from all three program calculations agreed well with the estimates.
DOE

N89-20273# Pennsylvania State Univ., University Park. Coll. of Earth and Mineral Sciences.
THERMAL STABILITY OF JET FUEL Quarterly Report No. 1, Oct. - Dec. 1988
Semih Eser, Harold H. Schobert, Janice Perison, and Ronald M. Copenhaver 1988 21 p
(Contract DE-AC22-88PC-88827)
(DE89-006754; DOE/PC-88827/T1) Avail: NTIS HC A03/MF A01

The overall objective of this program is to investigate the effect of chemical components on the thermal stability of jet fuel. Specific objectives include the determination of the high temperature thermal stability of a suite of model compounds typical of those present as trace contaminants in the fuel, investigation of the thermal ability of various fractions of a coal-derived and a petroleum-derived JP-8 jet fuel, the determination of the thermal stability of the unfractionated fuels, and the development of the relationship between the stability of the whole material and the behavior of model compounds of fuel fractions. Six model compounds (phenols) and 1-naphthol have been heat treated at temperatures ranging from 250 to 400 C for 1 to 4 hours. Experiments were carried out using the microautoclave reactors. An initial cold nitrogen pressure of 100 psig instead of 500 psig was employed for high-temperature reactions. Some of the thermal treatments at 300, 350 and 400 C have led to distinct changes in the appearance of the starting materials, forming homogeneous liquids from solid compounds in certain cases. Observations are summarized.
DOE

N89-20274# EG and G Mound Applied Technologies, Miamisburg, OH.
APPLICATION OF RIGOROUS NONLINEAR REGRESSION TO THE DECOMPOSITION KINETICS OF EXPLOSIVES
James M. Pickard 15 Feb. 1989 23 p
(Contract DE-AC04-88DP-43495)
(DE89-007598; MLM-3570) Avail: NTIS HC A03/MF A01

A method based on rigorous nonlinear regression is used to determine global rate parameters for the condensed-phase decomposition of an explosive monitored by isothermal differential scanning calorimetry (DSC). Nonlinear regression provides relative errors for global rate parameters, quantitative assessments for the quality of the regression fit, and absolute errors for the resultant Arrhenius parameters. Application of this method is demonstrated for evaluation of global rate parameters for the decomposition of 2,2',4,4',6,6'-hexanitroazobenzene (HNAB) at constant volume and constant pressure.
DOE

N89-20275# Air Force Astronautics Lab., Edwards AFB, CA.
RHEOMETRICS STRESS RHEOMETER APPLICATIONS Final Report, Jun. - Aug. 1988
William Geisler 1 Aug. 1988 23 p
(AD-A203667; AFAL-TR-88-115) Avail: NTIS HC A03/MF A01 CSCL 19A

A method of training AFAL/RKPL personnel in the use of the Rheometrics Stress Rheometer (RSR) was needed to reduce the large amount of time required to train an individual to operate the RSR. This paper serves as a guide to the RSR for the newcomer. By working with the laboratory's technicians, I was able to determine what information needed to be provided to the newcomer immediately, and which information could easily be obtained from the RSR's operations guide.
GRA

29 MATERIALS PROCESSING

Includes space-based development of products and processes for commercial applications.
For biological materials see *55 Space Biology*.

N89-20276*# National Aeronautics and Space Administration, Washington, DC.
MICROGRAVITY SCIENCE AND APPLICATIONS FLIGHT PROGRAMS, JANUARY - MARCH 1987, SELECTED PAPERS, VOLUME 1
Oct. 1988 487 p
(NASA-TM-4069-Vol-1; NAS 1.15:4069-Vol-1) Avail: NTIS HC A21/MF A01 CSCL 22A

A compilation of papers presented at this conference is given. The science dealing with materials and fluids and with fundamental studies in physics and chemistry in a low gravity environment is examined. Program assessments are made along with directions for progress in the future use of the space shuttle program. For individual titles, see N89-20277 through N89-20304.

N89-20277*# National Aeronautics and Space Administration. Marshall Space Flight Center, Huntsville, AL.
CONTINUOUS FLOW ELECTROPHORESIS SYSTEM EXPERIMENTS ON SHUTTLE FLIGHTS STS-6 AND STS-7
Robert S. Snyder, Percy H. Rhodes, and Teresa Y. Miller *In* NASA, Washington, Microgravity Science and Applications Flight Programs, January - March 1987, Selected Papers, Volume 1 Oct. 1988 p 5-26 (For primary document see N89-20276 13-29)
Avail: NTIS HC A21/MF A01 CSCL 22A

The development of a space continuous flow electrophoresis system (CFES) is discussed. The objectives of the experiment were: (1) to use a model sample material at a high concentration to evaluate the continuous flow electrophoresis process in the McDonnell Douglass CFES instrument and compare its separation resolution and sample throughput with related devices on Earth, and (2) to expand the basic knowledge of the limitations imposed by fluid flows and particle concentration effects on the electrophoresis process by careful design and evaluation of the space experiment. Hemoglobin and polysaccharide were selected as samples of concentration effects. The results from space show a large band spread of the high concentration of the single species of hemoglobin that was principally due to the mismatch of electrical conductivity between the sample and buffer.
Author

N89-20278*# National Aeronautics and Space Administration. Marshall Space Flight Center, Huntsville, AL.
PREPARATIVE ELECTROPHORESIS FOR SPACE
Percy H. Rhodes and Robert S. Snyder *In* NASA, Washington, Microgravity Science and Applications Flight Programs, January - March 1987, Selected Papers, Volume 1 Oct. 1988 p 27-46 Previously announced as N88-10977 (For primary document see N89-20276 13-29)
Avail: NTIS HC A21/MF A01 CSCL 22A

A premise of continuous flow electrophoresis is that removal of buoyance-induced thermal convection caused by axial and lateral temperature gradients results in ideal performance of these instruments in space. Although these gravity dependent phenomena disturb the rectilinear flow in the separation chamber when high voltage gradients or thick chamber are used, distortion of the injected sample stream due to electrodynamic effects cause major broadening of the separated bands. The electrophoresis separation process is simple, however flow local to the sample filament produced by the applied electric field were not considered. These electrohydrodynamic flows distort the sample stream and limit the separation. Also, electroosmosis and viscous flow combine to further distort the process. A moving wall concept is being proposed for space which will eliminate and control the disturbances. The moving wall entrains the fluid to move as a rigid body and produces a constant residence time for all samples distributed across the chamber thickness. The moving wall electrophoresis chamber can only be operated in space because there is no viscous flow in the chamber to stabilize against thermal convection.
Author

N89-20279*# National Aeronautics and Space Administration. Ames Research Center, Moffett Field, CA.

HETEROGENEITY IN THE GROWTH HORMONE PITUITARY GLAND SYSTEM OF RATS AND HUMANS: IMPLICATIONS TO MICROGRAVITY BASED RESEARCH

W. C. Hymer, R. Grindeland, C. Hayes, J. W. Lanham, C. Cleveland, P. Todd, and Dennis R. Morrison (National Aeronautics and Space Administration. Lyndon B. Johnson Space Center, Houston, TX.) *In* NASA, Washington, Microgravity Science and Applications Flight Programs, January - March 1987, Selected Papers, Volume 1 Oct. 1988 p 47-88 (For primary document see N89-20276 13-29)
Avail: NTIS HC A21/MF A01 CSCL 22A

The cell separation techniques of velocity sedimentation, flow cytometry and continuous flow electrophoresis were used to obtain enriched populations of growth hormone (GH) cells. The goal was to isolate a GH cell subpopulation which releases GH molecules which are very high in biological activity, it was important to use a method which was effective in processing large numbers of cells over a short time span. The techniques based on sedimentation are limited by cell density overlaps and streaming. While flow cytometry is useful in the analytical mode for objectively establishing cell purity, the numbers of cells which can be processed in the sort mode are so small as to make this approach ineffective in terms of the long term goals. It was shown that continuous flow electrophoresis systems (CFES) can separate GH cells from other cell types on the basis of differences in surface charge. The bioreactive producers appear to be more electrophoretically mobile than the low producers. Current ground based CFES efforts are hampered by cell clumping in low ionic strength buffers and poor cell recoveries from the CFES device. Author

N89-20280*# National Aeronautics and Space Administration. Lyndon B. Johnson Space Center, Houston, TX.

KIDNEY CELL ELECTROPHORESIS IN SPACE FLIGHT: RATIONALE, METHODS, RESULTS AND FLOW CYTOMETRY APPLICATIONS

P. Todd, Dennis R. Morrison, Grant H. Barlow, Marian L. Lewis, J. W. Lanham, C. Cleveland, K. Williams, M. E. Kunze, and C. L. Goolsby (Pennsylvania State Univ., University Park.) *In* NASA, Washington, Microgravity Science and Applications Flight Programs, January - March 1987, Selected Papers, Volume 1 Oct. 1988 p 89-118 (For primary document see N89-20276 13-29)
(Contracts NAS9-15583; NAS9-16550; NAS9-17440; NAS9-16389)
Avail: NTIS HC A21/MF A01 CSCL 22A

Cultures of human embryonic kidney cells consistently contain an electrophoretically separable subpopulation of cells that produce high levels of urokinase and have an electrophoretic mobility about 85 percent as high as that of the most mobile human embryonic kidney cells. This subpopulation is rich in large epithelioid cells that have relatively little internal structure. When resolution and throughput are adequate, free fluid electrophoresis can be used to isolate a broad band of low mobility cells which also produces high levels of plasminogen activators (PAs). In the course of performing this, it was discovered that all electrophoretic subpopulations of cultured human embryonic kidney cells produce some PAs and that separate subpopulations produce high quantities of different types of PA's. This information and the development of sensitive assays for this project have provided new insights into cell secretion mechanisms related to fibrinolysis. These advances would probably not have been made without the NASA program to explore fundamental questions of free fluid electrophoresis in space. Author

N89-20281*# National Aeronautics and Space Administration. Marshall Space Flight Center, Huntsville, AL.

DEMIXING KINETICS OF PHASE SEPARATED POLYMER SOLUTIONS IN MICROGRAVITY

D. E. Brooks, S. B. Bamberger, J. M. Harris (Alabama Univ., Huntsville.), J. VanAlstine, and R. S. Snyder *In* NASA, Washington, Microgravity Science and Applications Flight Programs, January - March 1987, Selected Papers, Volume 1 Oct. 1988 p 119-131 (For primary document see N89-20276 13-29)
Avail: NTIS HC A21/MF A01 CSCL 22A

Phase separated solutions of two neutral polymers in buffer provide a useful and versatile medium for the partition separation of biological cells. However, the efficiency of such separations is orders of magnitude lower than the thermodynamic limit. To test the hypothesis that this inefficiency is at least partially due to the convection and sedimentation that occur during the gravity driven demixing that follows introduction of cells to the systems, a series of experiments were begun aimed at performing cell partition in a low g environment. Demixing of isopycnic three polymer solvent systems was studied, experiments were performed on KC-135 aircraft and one shuttle middeck experiment was completed. Analysis of the results of these experiments and comparisons with the predictions of scaling relations for the dependence of phase domain size on time, derived for a number of possible demixing mechanisms, are presented. Author

N89-20282*# Arizona Univ., Tucson. Center for Separation Science.

HORMONE PURIFICATION BY ISOELECTRIC FOCUSING IN SPACE

M. Bier *In* NASA, Washington, Microgravity Science and Applications Flight Programs, January - March 1987, Selected Papers, Volume 1 Oct. 1988 p 133-146 (For primary document see N89-20276 13-29)
(Contract NAS8-32950)
Avail: NTIS HC A21/MF A01 CSCL 22A

The objective of the program was the definition and development of optimal methods for electrophoretic separations in microgravity. The approach is based on a triad consisting of ground based experiments, mathematical modeling and experiments in microgravity. Zone electrophoresis is a rate process, where separation is achieved in uniform buffers on the basis of differences in electrophoretic mobilities. Optimization and modeling of continuous flow electrophoresis mainly concern the hydrodynamics of the flow process, including gravity dependent fluid convection due to density gradients and gravity independent electroosmosis. Optimization of focusing requires a more complex model describing the molecular transport processes involved in electrophoresis of interacting systems. Three different focusing instruments were designed, embodying novel principles of fluid stabilization. Fluid stability was achieved by: (1) flow streamlining by means of membrane elements in combination with rapid fluid recycling; (2) apparatus rotation in combination with said membrane elements; and (3) shear stress induced by rapid recycling through a narrow gap channel. Author

N89-20283*# Baylor Coll. of Medicine, Houston, TX. Dept. of Biochemistry.

DEVELOPMENT OF IMMUNOASSAYS FOR HUMAN UROKINASE

M. Zouhair Atassi *In* NASA, Washington, Microgravity Science and Applications Flight Programs, January - March 1987, Selected Papers, Volume 1 Oct. 1988 p 147-153 (For primary document see N89-20276 13-29)
(Contract NAS9-17403)
Avail: NTIS HC A21/MF A01 CSCL 22A

Radioimmune assays (RIA) and enzyme linked immune assays for measurement of pro-urokinase and the two active forms of the enzyme were developed. Polyclonal and monoclonal antibodies, with desired specificities against preselected synthetic regions of urokinase (UK), were obtained by immunization with the respective synthetic peptides and used to develop RIA for zymogen and the two activated forms of UK. Author

N89-20284*# Rice Univ., Houston, TX. Dept. of Chemical Engineering.

HYDRODYNAMIC EFFECTS ON CELL GROWTH IN AGITATED MICROCARRIER BIOREACTORS

Robert S. Cherry and E. Terry Papoutsakis *In* NASA, Washington, Microgravity Science and Applications Flight Programs, January - March 1987, Selected Papers, Volume 1 Oct. 1988 p 155-157

(For primary document see N89-20276 13-29)
(Contract NAS9-17403)
Avail: NTIS HC A21/MF A01 CSCL 22A

The net growth rate of bovine embryonic kidney cells in microcarrier bioreactor is the result of a variable death rate imposed on a cell culture trying to grow at a constant intrinsic growth rate. The death rate is a function of the agitation conditions in the system, and increases at higher agitation because of increasingly energetic interactions of the cell covered microcarriers with turbulent eddies in the fluid. At very low agitation rates bead-bead bridging becomes important; the large clumps formed by bridging can interact with larger eddies than single beads, leading to a higher death rate at low agitation. The growth and death rate were correlated with a dimensionless eddy number which compares eddy forces to the buoyant force on the bead. Author

N89-20285*# Rice Univ., Houston, TX. Dept. of Chemical Engineering.
AN EXPERT SYSTEM BASED INTELLIGENT CONTROL SCHEME FOR SPACE BIOREACTORS
Ka-Yiu San *In* NASA, Washington, Microgravity Science and Applications Flight Programs, January - March 1987, Selected Papers, Volume 1 Oct. 1988 p 159-162 (For primary document see N89-20276 13-29)
Avail: NTIS HC A21/MF A01 CSCL 22A

An expert system based intelligent control scheme is being developed for the effective control and full automation of bioreactor systems in space. The scheme developed will have the capability to capture information from various resources including heuristic information from process researchers and operators. The knowledge base of the expert system should contain enough expertise to perform on-line system identification and thus be able to adapt the controllers accordingly with minimal human supervision. Author

N89-20286*# Rice Univ., Houston, TX. Biomedical Engineering Lab.
SHEAR STRESS INDUCED STIMULATION OF MAMMALIAN CELL METABOLISM
L. V. McIntire, J. A. Frangos, and S. G. Eskin (Baylor Coll. of Medicine, Houston, TX.) *In* NASA, Washington, Microgravity Science and Applications Flight Programs, January - March 1987, Selected Papers, Volume 1 Oct. 1988 p 163-173 (For primary document see N89-20276 13-29)
(Contract NAS9-17403; NAG9-207; NIH-HL-18672; NIH-HL-17437)
Avail: NTIS HC A21/MF A01 CSCL 22A

A flow apparatus was developed for the study of the metabolic response of anchorage dependent cells to a wide range of steady and pulsatile shear stresses under well controlled conditions. Human umbilical vein endothelial cell monolayers were subjected to steady shear stresses of up to 24 dynes/sq cm, and the production of prostacyclin was determined. The onset of flow led to a burst in prostacyclin production which decayed to a long term steady state rate (SSR). The SSR of cells exposed to flow was greater than the basal release level, and increased linearly with increasing shear stress. It is demonstrated that shear stresses in certain ranges may not be detrimental to mammalian cell metabolism. In fact, throughout the range of shear stresses studied, metabolite production is maximized by maximizing shear stress. Author

N89-20287*# National Aeronautics and Space Administration. Lyndon B. Johnson Space Center, Houston, TX.
BIOCHEMICAL ASSAYS ON PLASMINOGEN ACTIVATORS AND HORMONES FROM KIDNEY SOURCES
Grant H. Barlow, Marian L. Lewis (Krug International, Houston, TX.), and Dennis R. Morrison *In* NASA, Washington, Microgravity Science and Applications Flight Programs, January - March 1987, Selected Papers, Volume 1 Oct. 1988 p 175-193 (For primary document see N89-20276 13-29)
Avail: NTIS HC A21/MF A01 CSCL 22A

Investigations were established for the purpose of analyzing the conditioned media from human embryonic kidney cell subpopulations separated in space by electrophoresis. This data is based on the experiments performed on STS-8 on the continuous flow electrophoresis system. The primary biological activity that was analyzed was plasminogen activator activity, but some assays for erythropoeitin and human granulocyte colony stimulating activity were also performed. It is concluded that a battery of assays are required to completely define the plasminogen activator profile of a conditioned media from cell culture. Each type of assay measures different parts of the mixture and are influenced by different parameters. The functional role of each assay is given along with an indication of which combination of assays are required to answer specific questions. With this type of information it is possible by combinations of assays with mathematical analysis to pinpoint a specific component of the system. Author

N89-20288*# National Aeronautics and Space Administration. Lyndon B. Johnson Space Center, Houston, TX.
HUMAN CELL CULTURE IN A SPACE BIOREACTOR
Dennis R. Morrison *In* NASA, Washington, Microgravity Science and Applications Flight Programs, January - March 1987, Selected Papers, Volume 1 Oct. 1988 p 195-215 (For primary document see N89-20276 13-29)
Avail: NTIS HC A21/MF A01 CSCL 22A

Microgravity offers new ways of handling fluids, gases, and growing mammalian cells in efficient suspension cultures. In 1976 bioreactor engineers designed a system using a cylindrical reactor vessel in which the cells and medium are slowly mixed. The reaction chamber is interchangeable and can be used for several types of cell cultures. NASA has methodically developed unique suspension type cell and recovery apparatus culture systems for bioprocess technology experiments and production of biological products in microgravity. The first Space Bioreactor was designed for microprocessor control, no gaseous headspace, circulation and resupply of culture medium, and slow mixing in very low shear regimes. Various ground based bioreactors are being used to test reactor vessel design, on-line sensors, effects of shear, nutrient supply, and waste removal from continuous culture of human cells attached to microcarriers. The small Bioreactor is being constructed for flight experiments in the Shuttle Middeck to verify systems operation under microgravity conditions and to measure the efficiencies of mass transport, gas transfer, oxygen consumption and control of low shear stress on cells. Author

N89-20289*# National Aeronautics and Space Administration. Lyndon B. Johnson Space Center, Houston, TX.
CELLULAR EFFECTS OF MICROGRAVITY
Dennis R. Morrison *In* NASA, Washington, Microgravity Science and Applications Flight Programs, January - March 1987, Selected Papers, Volume 1 Oct. 1988 p 217-226 (For primary document see N89-20276 13-29)
Avail: NTIS HC A21/MF A01 CSCL 22A

Experiments are recounted that test the effects of microgravity on cells, from the 60's up to the present. Results of these experiments are briefly discussed. Author

N89-20290*# National Aeronautics and Space Administration. Lyndon B. Johnson Space Center, Houston, TX.
ANTIBODY ENHANCEMENT OF FREE-FLOW ELECTROPHORESIS
H. H. P. Cohly, Dennis R. Morrison, and M. Zouhair Atassi *In* NASA, Washington, Microgravity Science and Applications Flight Programs, January - March 1987, Selected Papers, Volume 1 Oct. 1988 p 227-234 Prepared in cooperation with Baylor Coll. of Medicine, Houston, TX (For primary document see N89-20276 13-29)
Avail: NTIS HC A21/MF A01 CSCL 22A

Specific T cell clones and antibodies (ABs) were developed to study the efficiency of purifying closely associated T cells using Continuous Flow Electrophoresis System. Enhanced separation is accomplished by tagging cells first with ABs directed against the antigenic determinants on the cell surface and then with ABs against the Fc portion of the first AB. This second AB protrudes sufficiently beyond the cell membrane and glycocalyx to become

the major overall cell surface potential determinant and thus causes a reduction of electrophoretic mobility. This project was divided into three phases. Phase one included development of specific T cell clones and separation of these specific clones. Phase two extends these principles to the separation of T cells from spleen cells and immunized lymph node cells. Phase three applies this double antibody technique to the separation of T cytotoxic cells from bone marrow. Author

N89-20291*# Houston Univ., TX. Dept. of Chemical Engineering.
THE STRESS RESPONSE SYSTEM OF PROTEINS: IMPLICATIONS FOR BIOREACTOR SCALEUP
Charles F. Goochee *In* NASA, Washington, Microgravity Science and Applications Flight Programs, January - March 1987, Selected Papers, Volume 1 Oct. 1988 p 235-248 (For primary document see N89-20276 13-29)
Avail: NTIS HC A21/MF A01 CSCL 22A

Animal cells face a variety of environmental stresses in large scale bioreactors, including periodic variations in shear stress and dissolved oxygen concentration. Diagnostic techniques were developed for identifying the particular sources of environmental stresses for animal cells in a given bioreactor configuration. The mechanisms by which cells cope with such stresses was examined. The individual concentrations and synthesis rates of hundreds of intracellular proteins are affected by the extracellular environment (medium composition, dissolved oxygen concentration, ph, and level of surface shear stress). Techniques are currently being developed for quantifying the synthesis rates and concentrations of the intracellular proteins which are most sensitive to environmental stress. Previous research has demonstrated that a particular set of stress response proteins are synthesized by mammalian cells in response to temperature fluctuations, dissolved oxygen deprivation, and glucose deprivation. Recently, it was demonstrated that exposure of human kidney cells to high shear stress results in expression of a completely distinct set of intracellular proteins. Author

N89-20292*# Alabama Univ., Birmingham.
PROTEIN CRYSTAL GROWTH IN A MICROGRAVITY ENVIRONMENT
Charles E. Bugg *In* NASA, Washington, Microgravity Science and Applications Flight Programs, January - March 1987, Selected Papers, Volume 1 Oct. 1988 p 249-265 (For primary document see N89-20276 13-29)
(Contract NAS8-36611)
Avail: NTIS HC A21/MF A01 CSCL 22A

Protein crystal growth is a major experimental problem and is the bottleneck in widespread applications of protein crystallography. Research efforts now being pursued and sponsored by NASA are making fundamental contributions to the understanding of the science of protein crystal growth. Microgravity environments offer the possibility of performing new types of experiments that may produce a better understanding of protein crystal growth processes and may permit growth environments that are more favorable for obtaining high quality protein crystals. A series of protein crystal growth experiments using the space shuttle was initiated. The first phase of these experiments was focused on the development of micro-methods for protein crystal growth by vapor diffusion techniques, using a space version of the hanging drop method. The preliminary space experiments were used to evolve prototype hardware that will form the basis for a more advanced system that can be used to evaluate effects of gravity on protein crystal growth. Author

N89-20293*# EG and G Energy Measurements, Inc., Goleta, CA.
GROWTH OF MERCURIC IODIDE (HgI2) FOR NUCLEAR RADIATION DETECTORS
L. vandenBerg and W. F. Schnepple *In* NASA, Washington, Microgravity Science and Applications Flight Programs, January - March 1987, Selected Papers, Volume 1 Oct. 1988 p 269-286 (For primary document see N89-20276 13-29)
Avail: NTIS HC A21/MF A01 CSCL 22A

Mercuric iodide is a material used for the fabrication of the sensing element in solid state X-ray and gamma ray detecting instruments. The operation of the devices is determined to a large degree by the density of structural defects in the single crystalline material used in the sensing element. Since there were strong indications that the quality of the material was degraded by the effects of gravity during the growth process, a research and engineering program was initiated to grow one or more crystals of mercuric iodide in the reduced gravity environment of space. A special furnace assembly was designed which could be accommodated in a Spacelab rack, and at the same time made it possible to use the same growth procedures and controls used when growing a crystal on the ground. The space crystal, after the flight, was subjected to the same evaluation methods used for earth-grown crystals, so that comparisons could be made. Author

N89-20294*# Clarkson Univ., Potsdam, NY. Dept. of Chemical Engineering.
MODELLING THE GROWTH OF TRIGLYCINE SULPHATE CRYSTALS IN SPACELAB 3
Hak-Do Yoo, William R. Wilcox, Ravindra Lal, and James D. Trolinger (Spectron Development Labs., Inc., Costa Mesa, CA.) *In* NASA, Washington, Microgravity Science and Applications Flight Programs, January - March 1987, Selected Papers, Volume 1 Oct. 1988 p 289-335 (For primary document see N89-20276 13-29)
(Contract NAS8-32945)
Avail: NTIS HC A21/MF A01 CSCL 22A

Two triglycine sulphate crystals were grown from an aqueous solution in Spacelab 3 aboard a Space Shuttle. Using a diffusion coefficient of 0.00002 sq cm/s, a computerized simulation gave reasonable agreement between experimental and theoretical crystal sizes and interferometric lines in the solution near the growing crystal. This diffusion coefficient is larger than most measured values, possibly due to fluctuating accelerations on the order of .001 g (Earth's gravity). The average acceleration was estimated to be less than .000001 g. At this level, buoyancy driven convection is predicted to add approx. 20 percent to the steady state growth rate. Only very slight distortion of the interferometric lines was observed at the end of a 33 hr run. It is suggested that the time to reach steady state convective transport may be inversely proportional to g at low g, so that the full effect of convection was not realized in these experiments. Author

N89-20295*# GTE Labs., Inc., Waltham, MA.
A COMPARATIVE STUDY OF THE INFLUENCE OF BUOYANCY DRIVEN FLUID FLOW ON GaAs CRYSTAL GROWTH
J. A. Kafalas and A. H. Bellows *In* NASA, Washington, Microgravity Science and Applications Flight Programs, January - March 1987, Selected Papers, Volume 1 Oct. 1988 p 337-347 (For primary document see N89-20276 13-29)
(Contract NAS3-24644)
Avail: NTIS HC A21/MF A01 CSCL 22A

A systematic investigation of the effect of gravity driven fluid flow on GaAs crystal growth was performed. It includes GaAs crystal growth in the microgravity environment aboard the Space Shuttle. The program involves a controlled comparative study of crystal growth under a variety of earth based conditions with variable orientation and applied magnetic field in addition to the microgravity growth. Earth based growth will be performed under stabilizing as well as destabilizing temperature gradients. The boules grown in space and on earth will be fully characterized to correlate the degree of convection with the distribution of impurities. Both macro- and micro-segregation will be determined. The space growth experiment will be flown in a self-contained payload container through NASA's Get Away Special program. Author

N89-20296*# Massachusetts Inst. of Tech., Cambridge. Dept. of Materials Science and Engineering.
GROWTH OF GaAs CRYSTALS FROM THE MELT IN A PARTIALLY CONFINED CONFIGURATION
Harry C. Gatos and Jacek Lagowski *In* NASA, Washington, Microgravity Science and Applications Flight Programs, January - March 1987, Selected Papers, Volume 1 Oct. 1988 p 349-375 (For primary document see N89-20276 13-29)
(Contract NAS8-36604)
Avail: NTIS HC A21/MF A01 CSCL 22A

The experimental approach was directed along two main goals: (1) the implementation of an approach to melt growth in a partially confined configuration; and (2) the investigation of point defect interaction and electronic characteristics as related to thermal treatment following solidification and stoichiometry. Significant progress was made along both fronts. Crystal growth of GaAs in triangular ampuls was already carried out successfully and consistent with the model. In fact, pronounced surface tension phenomena which cannot be observed in ordinary confinement system were identified and should premit the assessment of Maragoni effects prior to space processing. Regarding thermal treatment, it was discovered that the rate of cooling from elevated temperatures is primarily responsible for a whole class of defect interactions affecting the electronic characteristics of GaAs and that stoichiometry plays a critical role in the quality of GaAs. Author

N89-20297*# National Aeronautics and Space Administration. Marshall Space Flight Center, Huntsville, AL.
GROWTH OF SOLID SOLUTION SINGLE CRYSTALS
S. L. Lehoczky and F. R. Szofran *In* NASA, Washington, Microgravity Science and Applications Flight Programs, January - March 1987, Selected Papers, Volume 1 Oct. 1988 p 377-390 Previously announced as N88-14212 (For primary document see N89-20276 13-29)
Avail: NTIS HC A21/MF A01 CSCL 22A

Based on the thermophysical properties of Hg sub 1-x Cd sub x Te alloys, the reasons are discussed for the failure of conventional Bridgman-Stockbarger growth methods to produce high quality homogeneous crystals in the prescence of Earth's gravity. The deleterious effects are considered which arise from the dependence of the thermophysical properties on temperature and composition and from the large amount of heat carried by the fused silica ampules. An improved growth method, developed to optimize heat flow conditions, is described and experimental results are presented. The problems associated with growth in a gravitational environment are discussed. The anticipated advantages of growth in microgravity are given and the implications of the requirements for spaceflight experiments are summarized. Author

N89-20298*# National Aeronautics and Space Administration. Langley Research Center, Hampton, VA.
MICROGRAVITY SCIENCE AT LANGLEY RESEARCH CENTER
Archibald L. Fripp, William J. Debnam, Jr., Glenn A. Woodell, Ivan O. Clark, Roger K. Crouch, Frederick M. Carlson, and Richard T. Simchick (PRC Kentron, Inc., Hampton, VA.) *In* NASA, Washington, Microgravity Science and Applications Flight Programs, January - March 1987, Selected Papers, Volume 1 Oct. 1988 p 391-407 (For primary document see N89-20276 13-29)
Avail: NTIS HC A21/MF A01 CSCL 22A

Although space research is still in an embryonic state, a combination of Earth based and space flight experiments are being coupled to yield a better understanding of the complex interaction of heat and fluid flow on the dynamics of crystal growth. Continued efforts on the ground as well as additional flight opportunities are needed to continue the drive to fully understand the advantages, both scientifically and economically, of microgravity crystal growth. Author

N89-20299*# National Aeronautics and Space Administration. Lewis Research Center, Cleveland, OH.
ISOTHERMAL DENDRITIC GROWTH: A LOW GRAVITY EXPERIMENT
M. E. Glicksman, R. C. Hahn, T. A. Lograsso, E. R. Rubinstein, M. E. Selleck (Rensselaer Polytechnic Inst., Troy, NY.), and E. Winsa *In* NASA, Washington, Microgravity Science and Applications Flight Programs, January - March 1987, Selected Papers, Volume 1 Oct. 1988 p 411-425 (For primary document see N89-20276 13-29)
Avail: NTIS HC A21/MF A01 CSCL 22A

The Isothermal Dendritic Growth Experiment is an active crystal growth experiment designed to test dendritic growth theory at low undercoolings where convection prohibits such studies at 1 g. The experiment will be essentially autonomous, though limited in-flight interaction through a computer interface is planned. One of the key components of the apparatus will be a crystal growth chamber capable of achieving oriented single crystal dendritic growth. Recent work indicates that seeding the chamber with a crystal of the proper orientation will not, in and of itself, be sufficient to meet this requirement. Additional flight hardware and software required for the STS flight experiment are currently being developed at NASA Lewis Research Center and at Rensselaer Polytechnic Institute. Author

N89-20300*# National Aeronautics and Space Administration. Lewis Research Center, Cleveland, OH.
ISOTHERMAL SOLIDIFICATION IN A BINARY ALLOY MELT
V. Laxmanan (Case Western Reserve Univ., Cleveland, OH.) *In* NASA, Washington, Microgravity Science and Applications Flight Programs, January - March 1987, Selected Papers, Volume 1 Oct. 1988 p 427-457 (For primary document see N89-20276 13-29)
Avail: NTIS HC A21/MF A01 CSCL 22A

A space shuttle experiment employing the General Purpose (Rocket) Furnace (GPF) in its isothermal mode of operation is manifested on MSL-3, circa 1989. The central aim of this experiment is to investigate the effect of reduced gravity levels on the segregation behavior in a slowly, and isothermally, cooled sample of a binary Pb-15 wt percent Sn alloy. This experiment would thus be able to simulate, in a small laboratory sample, about 20 mm dia 60 mm high and weighing about 150 grams, some aspects of the segregation phenomena occurring in large industrial ingots. Ground-based experiments conducted in the single-cavity simulator of the GPF, located at Marshall Space Flight Center (MSFC), in support of the microgravity experiment are described in detail. The results of the MSFC experiments are compared with other related experiments conducted at Case Western Reserve University (CWRU), wherein the isothermal constraints were relaxed. Author

N89-20301*# Tennessee Univ. Space Inst., Tullahoma.
CASTING AND SOLIDIFICATION TECHNOLOGY (CAST): DIRECTIONAL SOLIDIFICATION PHENOMENA IN A METAL MODEL AT REDUCED GRAVITY
M. H. McCay *In* NASA, Washington, Microgravity Science and Applications Flight Programs, January - March 1987, Selected Papers, Volume 1 Oct. 1988 p 459-467 (For primary document see N89-20276 13-29)
Avail: NTIS HC A21/MF A01 CSCL 22A

The Casting and Solidification Technology (CAST) experiment will study the phenomena that occur during directional solidification of an alloy, e.g., constitutional supercooling, freckling, and dendrite coarsening. The reduced gravity environment of space will permit the individual phenomena to be examined with minimum complication from buoyancy driven flows. Author

N89-20302*# Massachusetts Inst. of Tech., Cambridge.
DENDRITIC GROWTH AND STRUCTURE OF UNDERCOOLED NICKEL BASE ALLOYS
M. C. Flemings and Y. Shiohara *In* NASA, Washington, Microgravity Science and Applications Flight Programs, January -

March 1987, Selected Papers, Volume 1 Oct. 1988 p 469-483 (For primary document see N89-20276 13-29)
Avail: NTIS HC A21/MF A01 CSCL 22A

The principal objectives of this overall investigation are to: study means for obtaining high undercooling in levitation melted droplets, and study structures produced upon the solidification of these undercooled specimens. Thermal measurements are made of the undercooling, and of the rapid recalescence, to develop an understanding of the solidification mechanism. Comparison of results is made with the modeling studies. Characterization and metallographic work is done to gain an understanding of the relationship between rapid solidification variables and the structures so produced. In ground based work to date, solidification of undercooled Ni-25 wt percent Sn alloy was observed by high-speed cinematography and the results compared with optical temperature measurements. Also in ground based work, high-speed optical temperature measurements were made of the solidification behavior of levitated metal samples within a transparent glass medium. Two undercooled Ni-Sn alloys were examined. Measurements were carried out on samples at undercoolings up to 330 K. Microstructures of samples produced in ground based work were determined by optical metallography and by SEM, and microsegregation by electron microprobe measurements. A series of flight tests were planned to conduct experiments similar to the ground based experiments. The Space Shuttle Columbia carried an alloy undercooled experiment in the STS 61-C mission in January 1986. A sample of Ni-32.5 wt percent Sn eutectic was melted and solidified under microgravity conditions. Author

N89-20303*# Grumman Aerospace Corp., Bethpage, NY. Research Center.

THE INFLUENCES OF CONVECTION ON DIRECTIONAL SOLIDIFICATION OF EUTECTIC Bi/MnBi

David J. Larson, Jr. *In* NASA, Washington, Microgravity Science and Applications Flight Programs, January - March 1987, Selected Papers, Volume 1 Oct. 1988 p 485-510 (For primary document see N89-20276 13-29)
Avail: NTIS HC A21/MF A01 CSCL 22A

Eutectic alloys of Bi-Mn were directionally solidified using the Bridgman-Stockbarger technique to determine the influences of gravitationally-driven thermo-solutal convection on the Bi-MnBi rod eutectic. Experiments were conducted that varied the level of convection by varying the growth parameters and growth orientation, by microgravity damping, by applied magnetic field damping, and by imposing forced convection. Peltier interface demarcation and in-situ thermocouple measurements were used to monitor interface velocity and thermal gradient and to evaluate interface planarity. Author

N89-20304*# Johns Hopkins Univ., Baltimore, MD. Dept. of Metallurgy.

Pb-Zn LIQUID METAL DIFFUSION

R. B. Pond, Sr. and J. M. Winter, Jr. (Marvalaud, Inc., Westminster, MD.) *In* NASA, Washington, Microgravity Science and Applications Flight Programs, January - March 1987, Selected Papers, Volume 1 Oct. 1988 p 511-521 (For primary document see N89-20276 13-29)
Avail: NTIS HC A21/MF A01 CSCL 22A

The Lead-Zinc binary equilibrium system is currently being investigated. Ground based studies of this system were performed to examine the possibility of obtaining a couple which, after diffusion, could be examined continuously along the diffusion axis by quantitative metallography to determine the extent of diffusion. The specimens were analyzed by X-ray fluorescence in the scanning electron microscope to provide exact information on the chemical composition gradient. Two diffusion experiments were run simultaneously in the multipurpose furnace, each in its own isothermal cavity. Two flight samples, two flight backup samples, and two flight space samples were generated. B.G.

N89-20305*# National Aeronautics and Space Administration, Washington, DC.

MICROGRAVITY SCIENCE AND APPLICATIONS FLIGHT PROGRAMS, JANUARY - MARCH 1987, SELECTED PAPERS, VOLUME 2

Oct. 1988 297 p
(NASA-TM-4069-Vol-2; NAS 1.15:4069-Vol-2) Avail: NTIS HC A13/MF A01 CSCL 22A

Topics addressed include: glasses and ceramics; combustion science; fluids and transport phenomena; and critical phenomena. For individual titles, see N89-20306 through N89-20320.

N89-20306*# Rensselaer Polytechnic Inst., Troy, NY. Dept. of Materials Engineering.

FLUORIDE GLASS: CRYSTALLIZATION, SURFACE TENSION

R. H. Doremus *In* NASA, Washington, Microgravity Science and Applications Flight Programs, January - March 1987, Selected Papers, Volume 2 Oct. 1988 p 525-535 (For primary document see N89-20305 13-29)
Avail: NTIS HC A13/MF A01 CSCL 22A

Fluoride glass was levitated acoustically in the ACES apparatus on STS-11, and the recovered sample had a different microstructure from samples cooled in a container. Further experiments on levitated samples of fluoride glass are proposed. These include nucleation, crystallization, melting observations, measurement of surface tension of molten glass, and observation of bubbles in the glass. Ground experiments are required on sample preparation, outgassing, and surface reactions. The results should help in the development and evaluation of containerless processing, especially of glass, in the development of a contaminent-free method of measuring surface tensions of melts, in extending knowledge of gas and bubble behavior in fluoride glasses, and in increasing insight into the processing and properties of fluoride glasses. Author

N89-20307*# Missouri Univ., Rolla. Graduate Center for Materials Research.

CONTAINERLESS PROCESSING OF GLASS FORMING MELTS IN SPACE

D. E. Day and C. S. Ray *In* NASA, Washington, Microgravity Science and Applications Flight Programs, January - March 1987, Selected Papers, Volume 2 Oct. 1988 p 537-556 (For primary document see N89-20305 13-29)
Avail: NTIS HC A13/MF A01 CSCL 22A

The near weightlessness of a material in the reduced gravity environment of space offers the opportunity of melting and cooling glass forming compositions without a container. This reduces the heterogeneous nucleation/crystallization which usually occurs at the walls of the container, thereby, extending the range of glass forming compositions. Based primarily on this idea, containerless glass forming experiments, which used a single axis acoustic levitator/furnace (SAAL), were conducted on SPAR rocket flights, 6 and 8, and on Space Shuttle mission, STS-7 and STS-61A. The experiments on the Space Shuttle were designed to include other studies related to melt homogenization and mixing, development of techniques for preparing uncontaminated preflight samples, and simple shaping experiments. Author

N89-20308*# Jet Propulsion Lab., California Inst. of Tech., Pasadena.

ACOUSTIC CONTAINERLESS EXPERIMENT SYSTEM: A NON-CONTACT SURFACE TENSION MEASUREMENT

D. D. Elleman, T. G. Wang, and M. Barmatz *In* NASA, Washington, Microgravity Science and Applications Flight Programs, January - March 1987, Selected Papers, Volume 2 Oct. 1988 p 557-567 (For primary document see N89-20305 13-29)
Avail: NTIS HC A13/MF A01 CSCL 22A

The Acoustic Containerless Experiment System (ACES) was flown on STS 41-B in February 1984 and was scheduled to be reflown in 1986. The primary experiment that was to be conducted with the ACES module was the containerless melting and processing of a fluoride glass sample. A second experiment that was to be conducted was the verification of a non-contact surface

tension measurement technique using the molten glass sample. The ACES module consisted of a three-axis acoustic positioning module that was inside an electric furnace capable of heating the system above the melting temperature of the sample. The acoustic module is able to hold the sample with acoustic forces in the center of the chamber and, in addition, has the capability of applying a modulating force on the sample along one axis of the chamber so that the molten sample or liquid drop could be driven into one of its normal oscillation modes. The acoustic module could also be adjusted so that it could place a torque on the molten drop and cause the drop to rotate. In the ACES, a modulating frequency was applied to the drop and swept through a range of frequencies that would include the n = 2 mode. A maximum amplitude of the drop oscillation would indicate when resonance was reached and from that data the surface tension could be calculated. For large viscosity samples, a second technique for measuring surface tension was developed. The results of the ACES experiment and some of the problems encountered during the actual flight of the experiment will be discussed. Author

N89-20309*# Jet Propulsion Lab., California Inst. of Tech., Pasadena. Microgravity Science and Materials Group.
CRYSTAL NUCLEATION IN LITHIUM BORATE GLASS
Gary L. Smith, George F. Neilson, and Michael C. Weinberg *In* NASA, Washington, Microgravity Science and Applications Flight Programs, January - March 1987, Selected Papers, Volume 2 Oct. 1988 p 569-591 Sponsored by NASA, Washington (For primary document see N89-20305 13-29)
Avail: NTIS HC A13/MF A01 CSCL 22A

Crystal nucleation measurements were made on three lithium borate compositions in the vicinity of Li2O-2Br2O3. All nucleation measurements were performed at 500 C. Certain aspects of the nucleation behavior indicated (tentatively) that it proceeded by a homogeneous mechanism. The steady state nucleation rate was observed to have the largest value when the Li2O concentration was slightly in excess of the diborate composition. The change in nucleation rate with composition is controlled by the variation of viscosity as well as the change in free energy with composition. The variation of nucleation rate is explained qualitatively in these terms. Author

N89-20310*# Clarkson Univ., Potsdam, NY. Dept. of Chemical Engineering.
PHYSICAL PHENOMENA IN CONTAINERLESS GLASS PROCESSING
R. Shankar Subramanian and Robert Cole *In* NASA, Washington, Microgravity Science and Applications Flight Programs, January - March 1987, Selected Papers, Volume 2 Oct. 1988 p 593-603 (For primary document see N89-20305 13-29)
Avail: NTIS HC A13/MF A01 CSCL 22A

Flight experiments are planned on drops containing bubbles. The experiments involve stimulating the drop via non-uniform heating and rotation. The resulting trajectories of the bubbles as well as the shapes of the drops and bubble will be videotaped and analyzed later frame-by-frame on the ground. Supporting ground based experiments are planned in the area of surface tension driven motion of bubbles, the behavior of compound drops settling in an immiscible liquid and the shapes and trajectories of large bubbles and drops in a rotating liquid. Theoretical efforts will be directed at thermocapillary migration of drops and bubbles, surfactant effects on such migration, and the behavior of compound drops. Author

N89-20311*# California Univ., San Diego, La Jolla. Dept. of Applied Mechanics and Engineering Science.
PARTICLE CLOUD COMBUSTION IN REDUCED GRAVITY
A. L. Berlad *In* NASA, Washington, Microgravity Science and Applications Flight Programs, January - March 1987, Selected Papers, Volume 2 Oct. 1988 p 605-641 (For primary document see N89-20305 13-29)
Avail: NTIS HC A13/MF A01 CSCL 22A

The prinicipal objectives of this microgravity experiment program are to obtain flame propagation rate and flame extinction limit data for several important premixed, quiescent particle cloud combustion systems under near zero-gravity conditions. The data resulting from these experiments are needed for utilization with currently available and tractable flame propagation and extinction theory. These data are also expected to provide standards for the evaluation of fire hazards in particle suspensions in both Earth-based and space-based applications. Both terrestrial and space-based fire safety criteria require the identification of the critical concentrations of particulate fuels and inerts at the flame extinction conditions. Author

N89-20312*# Kentucky Univ., Lexington. Dept. of Mechanical Engineering.
SCIENTIFIC SUPPORT FOR AN ORBITER MIDDECK EXPERIMENT ON SOLID SURFACE COMBUSTION
Robert A. Altenkirch, M. Vedha-Nayagam, and Nataraj Srikantaiah *In* NASA, Washington, Microgravity Science and Applications Flight Programs, January - March 1987, Selected Papers, Volume 2 Oct. 1988 p 643-674 (For primary document see N89-20305 13-29)
Avail: NTIS HC A13/MF A01 CSCL 22A

The objective is to determine the mechanism of gas-phase flame spread over solid fuel surfaces in the absence of any buoyancy or externally imposed gas-phase flow. Such understanding can be used to improve the fire safety aspects of space travel by providing information that will allow judicious selections of spacecraft materials and environments to be made. The planned experiment consists of measuring the flame spread rate over thermally thin and thermally thick fuels in a closed container in the low-gravity environment of the Space Shuttle. Measurements consist of flame spread rate and shape obtained from two views of the process as recorded on movie film and surface and gas-phase temperatures obtained from fine-wire thermocouples. The temperature measurements along with appropriate modeling provide information about the gas-to-solid heat flux. Environmental parameters to be varied are the oxygen concentration and pressure. Author

N89-20313*# Princeton Univ., NJ.
DROPLET COMBUSTION AT REDUCED GRAVITY
F. L. Dryer and F. A. Williams *In* NASA, Washington, Microgravity Science and Applications Flight Programs, January - March 1987, Selected Papers, Volume 2 Oct. 1988 p 675-691 (For primary document see N89-20305 13-29)
Avail: NTIS HC A13/MF A01 CSCL 22A

The current work involves theoretical analyses of the effects identified, experiments in the NASA Lewis drop towers performed in the middeck areas of the Space Shuttle. In addition, there is laboratory work associated with the design of the flight apparatus. Calculations have shown that some of the test-matrix data can be obtained in drop towers, and some are achievable only in the space experiments. The apparatus consists of a droplet dispensing device (syringes), a droplet positioning device (opposing, retractable, hollow needles), a droplet ignition device (two matched pairs of retractable spark electrodes), gas and liquid handling systems, a data acquisition system (mainly giving motion-picture records of the combustion in two orthogonal views, one with backlighting for droplet resolution), and associated electronics. Author

N89-20314*# Case Western Reserve Univ., Cleveland, OH. Dept. of Mechanical and Aerospace Engineering.
SURFACE TENSION DRIVEN CONVECTION EXPERIMENT
Simon Ostrach and Yasuhiro Kamotani *In* NASA, Washington, Microgravity Science and Applications Flight Programs, January - March 1987, Selected Papers, Volume 2 Oct. 1988 p 695-713 (For primary document see N89-20305 13-29)
Avail: NTIS HC A13/MF A01 CSCL 22A

Thermocapillary flow is driven by a thermally induced surface tension variation along a liquid free surface. In the Earth-gravity environment such flows are usually overshadowed by buoyancy driven flows, but at reduced gravity conditions their influence could be significant. A comprehensive theoretical and experimental

research program was stated 12 years ago and is still being continued. Past work done at Case Western Reserve University as well as work done by others is reviewed. The justification for low-gravity experiments is presented. Author

N89-20315*# Massachusetts Inst. of Tech., Cambridge.
ELECTROMAGNETIC, HEAT AND FLUID FLOW PHENOMENA IN LEVITATED METAL DROPLETS BOTH UNDER EARTHBOUND AND MICROGRAVITY CONDITIONS
Julian Szekely *In* NASA, Washington, Microgravity Science and Applications Flight Programs, January - March 1987, Selected Papers, Volume 2 Oct. 1988 p 715-735 (For primary document see N89-20305 13-29)
Avail: NTIS HC A13/MF A01 CSCL 22A

The purpose is to develop an improved understanding of the electromagnetic, heat, and fluid flow phenomena in electromagnetically levitated metal droplets, both under earthbound and microgravity conditions. The main motivation for doing this work, together with the past accomplishments, and the plans for future research are discussed. Author

N89-20316*# Jet Propulsion Lab., California Inst. of Tech., Pasadena.
THE DYNAMICS OF FREE LIQUID DROPS
T. G. Wang, E. H. Trinh, A. P. Croonquist, and D. D. Elleman *In* NASA, Washington, Microgravity Science and Applications Flight Programs, January - March 1987, Selected Papers, Volume 2 Oct. 1988 p 739-761 Sponsored by NASA, Washington (For primary document see N89-20305 13-29)
Avail: NTIS HC A13/MF A01 CSCL 22A

The behavior of rotating and oscillating free liquid drops was studied by many investigators theoretically for many years. More recent numerical treatments have yielded predictions which are yet to be verified experimentally. The purpose is to report the results of laboratory work as well as that of the experiments carried out in space during the flight of Spacelab 3, and to compare it with the existing theoretical studies. Ground-based experiments were attempted as a first approximation to the ideal boundary conditions used by the theoretical treatments by neutralizing the overwhelming effects of the Earth's gravitational field with an outside supporting liquid and with the use of levitation technology. The viscous and inertial loading of such a suspending fluid was found to profoundly effect the results, but the information thus gathered has emphasized the uniqueness of the experimental data obtained in the low-gravity environment of space. Author

N89-20317*# National Bureau of Standards, Gaithersburg, MD. Thermophysics Div.
DYNAMIC THERMOPHYSICAL MEASUREMENTS IN SPACE
Ared Cezairliyan and Archie P. Miller *In* NASA, Washington, Microgravity Science and Applications Flight Programs, January - March 1987, Selected Papers, Volume 2 Oct. 1988 p 763-771 (For primary document see N89-20305 13-29)
Avail: NTIS HC A13/MF A01 CSCL 22A

The objective is to develop an accurate dynamic technique which, in a microgravity environment, would enable performance of thermophysical measurements on high-melting-point electrically conducting substances in their liquid state. In spite of the critical need in high temperature technologies related to spacecraft, nuclear reactors, effects of power laser radiation, and in validating theoretical models in related areas, no accurate data on thermophysical properties exist. This is primarily due to the limitation of the reliable steady-state techniques to temperatures below about 2000 K, and the accurate millisecond-resolution pulse heating techniques to the solid state of the specimen. The limitation of the millisecond-resolution techniques to temperatures below the melting point stems from the fact that the specimen collapses due to the gravitational force once it starts to melt. The rationale for the use of the microgravity is that by performing the dynamic experiments in a microgravity environment the specimen will retain its geometry, and thus it will be possible to extend the accurate thermophysical measurements to temperatures above the melting point of high-melting-point substances. Author

N89-20318*# National Aeronautics and Space Administration. Marshall Space Flight Center, Huntsville, AL.
THE FIRST PRODUCTS MADE IN SPACE: MONODISPERSE LATEX PARTICLES
J. W. Vanderhoff, M. S. El-Aasser, F. J. Micale, E. D. Sudol, C.-M. Tseng, H.-R. Sheu (Lehigh Univ., Bethlehem, PA.), and D. M. Kornfeld *In* NASA, Washington, Microgravity Science and Applications Flight Programs, January - March 1987, Selected Papers, Volume 2 Oct. 1988 p 773-789 (For primary document see N89-20305 13-29)
(Contract NAS8-32951)
Avail: NTIS HC A13/MF A01 CSCL 22A

The preparation of large particle size 3 to 30 micrometers monodisperse latexes in space confirmed that original rationale unequivocally. The flight polymerizations formed negligible amounts of coagulum as compared to increasing amounts for the ground-based polymerizations. The number of offsize large particles in the flight latexes was smaller than in the ground-based latexes. The particle size distribution broadened and more larger offsize particles were formed when the polymerizations of the partially converted STS-4 latexes were completed on Earth. Polymerization in space also showed other unanticipated advantages. The flight latexes had narrower particle size distributions than the ground-based latexes. The particles of the flight latexes were more perfect spheres than those of the ground-based latexes. The superior uniformity of the flight latexes was confirmed by the National Bureau of Standards acceptance of the 10 micrometer STS-6 latex and the 30 micrometer STS-11 latexes as Standard Reference Materials, the first products made in space for sale on Earth. The polymerization rates in space were the same as those on Earth within experimental error. Further development of the ground-based polymerization recipes gave monodisperse particles as large as 100 micrometers with tolerable levels of coagulum, but their uniformity was significantly poorer than the flight latexes. Careful control of the polymerization parameters gave uniform nonspherical particles: symmetrical and asymmetrical doublets, ellipsoids, egg-shaped, ice cream cone-shaped, and popcorn-shaped particles. Author

N89-20319*# Stanford Univ., CA. Dept. of Physics.
THE LAMBDA POINT EXPERIMENT IN MICROGRAVITY
J. A. Lipa *In* NASA, Washington, Microgravity Science and Applications Flight Programs, January - March 1987, Selected Papers, Volume 2 Oct. 1988 p 791-803 (For primary document see N89-20305 13-29)
Avail: NTIS HC A13/MF A01 CSCL 22A

The motivation and potential for performing very high resolution measurements of the heat capacity singularity at the lambda point of helium in microgravity conditions was briefly discussed. It is clear that tests extending deep into the asymptotic region can be performed, where the theoretical predictions take on their simplest form. This advantageous situation should lead to a major improvement in the understanding of the range of applicability of current theoretical ideas in this field. The lambda transition holds out the prospect of giving the maximum advance of any system, and with the application of cryogenic techniques, the potential of this system can be realized. The technology for the initial experiments is already developed, and results could be obtained in 1990. Author

N89-20320*# Maryland Univ., College Park. Inst. for Physical Science and Technology.
CRITICAL FLUID LIGHT SCATTERING
Robert W. Gammon *In* NASA, Washington, Microgravity Science and Applications Flight Programs, January - March 1987, Selected Papers, Volume 2 Oct. 1988 p 805-830 (For primary document see N89-20305 13-29)
(Grant NAG3-727)
Avail: NTIS HC A13/MF A01 CSCL 22A

The objective is to measure the decay rates of critical density fluctuations in a simple fluid (xenon) very near its liquid-vapor critical point using laser light scattering and photon correlation spectroscopy. Such experiments were severely limited on Earth

by the presence of gravity which causes large density gradients in the sample when the compressibility diverges approaching the critical point. The goal is to measure fluctuation decay rates at least two decades closer to the critical point than is possible on earth, with a resolution of 3 microK. This will require loading the sample to 0.1 percent of the critical density and taking data as close as 100 microK to the critical temperature. The minimum mission time of 100 hours will allow a complete range of temperature points to be covered, limited by the thermal response of the sample. Other technical problems have to be addressed such as multiple scattering and the effect of wetting layers. The experiment entails measurement of the scattering intensity fluctuation decay rate at two angles for each temperature and simultaneously recording the scattering intensities and sample turbidity (from the transmission). The analyzed intensity and turbidity data gives the correlation length at each temperature and locates the critical temperature. The fluctuation decay rate data from these measurements will provide a severe test of the generalized hydrodynamic theories of transport coefficients in the critical regions. When compared to equivalent data from binary liquid critical mixtures they will test the universality of critical dynamics. Author

N89-20321*# National Aeronautics and Space Administration. Lewis Research Center, Cleveland, OH.
PARTICLE CLOUD MIXING IN MICROGRAVITY
H. Ross, L. Facca, V. Tangirala, and A. L. Berlad (California Univ., San Diego, La Jolla.) Jan. 1989 14 p Presented at the 26th Aerospace Sciences Meeting, Reno, NV, 11-14 Jan. 1988; sponsored in part by AIAA
(NASA-TM-101484; E-4618; NAS 1.15:101484; AIAA-88-0453) Avail: NTIS HC A03/MF A01 CSCL 22A

Quasi-steady flame propagation through clouds of combustible particles requires quasi-steady transport properties and quasi-steady particle number density. Microgravity conditions may be employed to help achieve the conditions of quiescent, uniform clouds needed for such combustion studies. Joint experimental and theoretical NASA-UCSD studies were concerned with the use of acoustic, electrostatic, and other methods of dispersion of fuel particulates. Results of these studies are presented for particle clouds in long cylindrical tubes. Author

31 ENGINEERING (GENERAL)

Includes vacuum technology; control engineering; display engineering; cryogenics; and fire prevention.

N89-20322*# National Aeronautics and Space Administration. Goddard Space Flight Center, Greenbelt, MD.
DUCTILE-REGIME TURNING OF GERMANIUM AND SILICON
Peter N. Blake and Ronald O. Scattergood (North Carolina State Univ., Raleigh.) 1989 22 p
(NASA-TM-101231; NAS 1.15:101231) Avail: NTIS HC A03/MF A01 CSCL 13H

Single-point diamond turning of silicon and germanium was investigated in order to clarify the role of cutting depth in coaxing a ductile chip formation in normally brittle substances. Experiments based on the rapid withdrawal of the tool from the workpiece have shown that microfracture damage is a function of the effective depth of cut (as opposed to the nominal cutting depth). In essence, damage created by the leading edge of the tool is removed several revolutions later by lower sections of the tool edge, where the effective cutting depth is less. It appears that a truly ductile cutting response can be achieved only when the effective cutting depth, or critical chip thickness, is less than about 20 nm. Factors such as tool rake angle are significant in that they will affect the actual value of the critical chip thickness for transition from brittle to ductile response. It is concluded that the critical chip thickness is an excellent parameter for measuring the effects of machining conditions on the ductility of the cut and for designing tool-workpiece geometry in both turning and grinding. Author

N89-20323# A/G Technology Corp., Needham, MA.
MEMBRANE VAPOR ENRICHER FOR WATER FOR INJECTION (WFI) PRODUCTION, PHASE 1 Final Report, 15 Dec. 1986 - 15 Dec. 1987
Arye Gollan and Myles H. Kleper 15 Dec. 1987 56 p
(Contract DAMD17-87-C-7012; DA Proj. 3M2-63002-D-840)
(AD-A201354) Avail: NTIS HC A04/MF A01 CSCL 13I

The U.S. Armed Forces have a logistical requirement for a continuous demand, high purity, Water For Injection (WFI) system to alleviate the logistical burden of transport and maintenance of large supplies of parenteral solutions. In this program, the feasibility of incorporating permeable membrane gas separation technology as the key element in the WFI production process has been evaluated. These high productivity, imperfection-free gas permeable membranes are highly selective to water vapor and are packaged in compact and lightweight hollow fiber module elements. GRA

N89-20324*# National Aeronautics and Space Administration. Lewis Research Center, Cleveland, OH.
LOW FREQUENCY VIBRATION ISOLATION TECHNOLOGY FOR MICROGRAVITY SPACE EXPERIMENTS
Carlos M. Grodsinsky and Gerald V. Brown 1989 10 p Proposed for presentation at the 12th Biennial Conference on Mechanical Vibration and Noise, Montreal, Quebec, 17-20 Sep. 1989; sponsored by ASME
(NASA-TM-101448; E-4557; NAS 1.15:101448) Avail: NTIS HC A02/MF A01 CSCL 13B

The dynamic acceleration environment observed on Space Shuttle flights to date and predicted for the Space Station has complicated the analysis of prior microgravity experiments and prompted concern for the viability of proposed space experiments requiring long-term, low-g environments. Isolation systems capable of providing significant improvements in this environment exist, but have not been demonstrated in flight configurations. This paper presents a summary of the theoretical evaluation for two one degree-of-freedom (DOF) active magnetic isolators and their predicted response to both direct and base excitations, that can be used to isolate acceleration sensitive microgravity space experiments. Author

N89-20325# Sheffield Univ. (England). Dept. of Control Engineering.
ESTIMATING NONLINEAR MODELS
S. A. Billings Mar. 1988 26 p Presented at the SERC Vacation School on Signal Processing for Control, Coventry, England, 17-22 Apr. 1986 Sponsored by the United Kingdom Science Engineering and Research Council
(RR-328; ETN-89-94071) Avail: NTIS HC A03/MF A01

Time and frequency domain identification methods for nonlinear systems are reviewed. Parametric methods, prediction error methods, structure detection, model validation, and experiment design are discussed. Identification of a liquid level system, a heat exchanger, and a turbocharge automotive diesel engine are illustrated. Rational models are introduced. Spectral analysis for nonlinear systems is treated. Recursive estimation is mentioned. ESA

N89-20326# Lawrence Livermore National Lab., CA.
FINITE ELEMENT MODELING OF A HYDROFORMED SHEET METAL COVER
Bradley N. Maker Dec. 1988 23 p Prepared in cooperation with Allied-Signal Aerospace Co., Kansas City, MO
(Contract W-7405-eng-48)
(DE89-006798; UCID-21614) Avail: NTIS HC A03/MF A01

This report summarizes an effort to model numerically the hydroform production of a sheet metal cover. After reviewing the initial drawings specifying the part, process engineers at Allied-Signal Kansas City assigned it a low feasibility index, indicating the part would be difficult to manufacture. At their request, this work was performed. Potential benefits included expediting production by minimizing the trial and error effort to determine forming parameters, i.e., blank size, pressure, and lubricant condition. These parameters could be in theory, determined from

the computer model. It was noted at the start of the study that little lead time was available, and the computer results may not be available soon enough to assist process development. In this case, the benefit of increasing in-house analysis capability for use on future projects was seen as sufficient justification of this work. As this indeed became the case, this report is intended to include detailed notes on the construction and execution of the finite element model, in the hope that it may serve as a guide for future analysis. DOE

N89-20327*# Georgia Inst. of Tech., Atlanta. School of Mechanical Engineering.
HIGH SPEED, PRECISION MOTION STRATEGIES FOR LIGHTWEIGHT STRUCTURES Semiannual Progress Report, 15 May - 14 Nov. 1988
Wayne J. Book 25 Jan. 1989 29 p
(Grant NAG1-623)
(NASA-CR-184651; NAS 1.26:184651) Avail: NTIS HC A03/MF A01 CSCL 13B

Research on space telerobotics is summarized. Adaptive control experiments on the Robotic Arm, Large and Flexible (RALF) were preformed and are documented, along with a joint controller design for the Small Articulated Manipulator (SAM), which is mounted on the RALF. A control algorithm is described as a robust decentralized adaptive control based on a bounded uncertainty approach. Dynamic interactions between SAM and RALF are examined. Unstability of the manipulator is studied from the perspective that the inertial forces generated could actually be used to more rapidly damp out the flexible manipulator's vibration. Currently being studied is the modeling of the constrained dynamics of flexible arms. E.R.

32 COMMUNICATIONS AND RADAR

Includes radar; land and global communications; communications theory; and optical communications.

For related information see also *04 Aircraft Communications and Navigation* and *17 Space Communications, Spacecraft Communications, Command and Tracking.* For search and rescue see *03 Air Transportation and Safety,* and *16 Space Transportation.*

N89-20328# National Telecommunications and Information Administration, Washington, DC.
SUM (SPECTRUM USE MEASURE) DATA BASE: A NEW MEASURE OF SPECTRUM USE
Robert J. Mayher, Robin H. Haines, Steven E. Litts, Leslie A. Berry, Gerald F. Hurt, and Carl A. Winkler Aug. 1988 113 p
(PB89-108674; NTIA-88-236) Avail: NTIS HC A06/MF A01 CSCL 17B

A new technique is described for calculating the spectrum space used by existing frequency assignments. The Spectrum Use Measure (SUM) model determines the amount of spectrum used at a given location or the probability that a given location is unavailable for a new assignment. These quantities, stored in a SUM data base, can be used to produce maps, histograms and indices of spectrum use. The SUM technique was effectively applied to the 1710 to 1850 MHz and the 7750 to 7900 MHz bands. It is concluded that the SUM technique is an effective indicator of spectrum use and it is recommended that it should be used when evaluating service bands. Author

N89-20329*# Jet Propulsion Lab., California Inst. of Tech., Pasadena.
THE TELECOMMUNICATIONS AND DATA ACQUISITION REPORT Progress Report, Jul. - Sep. 1988
E. C. Posner, ed. 15 Nov. 1988 267 p
(NASA-CR-184672; JPL-TDA-PR-42-95; NAS 1.26:184672) Avail: NTIS HC A12/MF A01 CSCL 17B

Deep Space Network and Systems topics addressed include: tracking and ground-base navigation; communications, spacecraft-ground; station control and system technology; capabilities for existing projects; and network upgrading and sustaining. For individual titles, see N89-20330 through N89-20354.

N89-20330*# Jet Propulsion Lab., California Inst. of Tech., Pasadena.
DERIVING A GEOCENTRIC REFERENCE FRAME FOR SATELLITE POSITIONING AND NAVIGATION **c04**
R. P. Malla (Sterling Software, Pasadena, CA.) and S.-C. Wu *In its* The Telecommunications and Data Acquisition Report 15 Nov. 1988 p 1-13 (For primary document see N89-20329 13-32)
Avail: NTIS HC A12/MF A01 CSCL 17G

With the advent of Earth-orbiting geodetic satellites, nongeocentric datums or reference frames have become things of the past. Accurate geocentric three-dimensional positioning is now possible and is of great importance for various geodetic and oceanographic applications. While relative positioning accuracy of a few centimeters has become a reality using very long baseline interferometry (VLBI), the uncertainty in the offset of the adopted coordinate system origin from the geocenter is still believed to be on the order of 1 meter. Satellite laser ranging (SLR), however, is capable of determining this offset to better than 10 cm, but this is possible only after years of measurements. Global Positioning System (GPS) measurements provide a powerful tool for an accurate determination of this origin offset. Two strategies are discussed. The first strategy utilizes the precise relative positions that were predetermined by VLBI to fix the frame orientation and the absolute scaling, while the offset from the geocenter is determined from GPS measurements. Three different cases are presented under this strategy. The reference frame thus adopted will be consistent with the VLBI coordinate system. The second strategy establishes a reference frame by holding only the longitude of one of the tracking sites fixed. The absolute scaling is determined by the adopted gravitational constant (GM) of the Earth; and the latitude is inferred from the time signature of the Earth rotation in the GPS measurements. The coordinate system thus defined will be a geocentric Earth-fixed coordinate system. Author

N89-20331*# Jet Propulsion Lab., California Inst. of Tech., Pasadena.
DETERMINATION OF GPS ORBITS TO SUBMETER ACCURACY **c04**
W. I. Bertiger, S. M. Lichten, and E. C. Katsigris *In its* The Telecommunications and Data Acquisition Report 15 Nov. 1988 p 14-27 (For primary document see N89-20329 13-32)
Avail: NTIS HC A12/MF A01 CSCL 17G

Orbits for satellites of the Global Positioning System (GPS) were determined with submeter accuracy. Tests used to assess orbital accuracy include orbit comparisons from independent data sets, orbit prediction, ground baseline determination, and formal errors. One satellite tracked 8 hours each day shows rms error below 1 m even when predicted more than 3 days outside of a 1-week data arc. Differential tracking of the GPS satellites in high Earth orbit provides a powerful relative positioning capability, even when a relatively small continental U.S. fiducial tracking network is used with less than one-third of the full GPS constellation. To demonstrate this capability, baselines of up to 2000 km in North America were also determined with the GPS orbits. The 2000 km baselines show rms daily repeatability of 0.3 to 2 parts in 10 to the 8th power and agree with very long base interferometry (VLBI) solutions at the level of 1.5 parts in 10 to the 8th power. This GPS demonstration provides an opportunity to test different techniques for high-accuracy orbit determination for high Earth orbiters. The best GPS orbit strategies included data arcs of at least 1 week, process noise models for tropospheric fluctuations, estimation of GPS solar pressure coefficients, and combine processing of GPS carrier phase and pseudorange data. For data arc of 2 weeks, constrained process noise models for GPS dynamic parameters significantly improved the situation. Author

N89-20332*# Jet Propulsion Lab., California Inst. of Tech., Pasadena.
TWO-WAY COHERENT DOPPLER ERROR DUE TO SOLAR CORONA
P. W. Kinman and S. W. Asmar *In its* The Telecommunications and Data Acquisition Report 15 Nov. 1988 p 28-31 (For primary document see N89-20329 13-32)
Avail: NTIS HC A12/MF A01 CSCL 17B

Two-way coherent Doppler errors resulting from phase scintillations induced on the uplink by the solar corona are considered. It is shown that this error can be estimated by taking statistics on the differential Doppler measurements. Typical estimates for the error are given for four Sun-Earth-probe angles and for integration times ranging from 1 second to 1 minute. These results are based on data collected during the 1985 Voyager 2 conjunction. Author

N89-20333*# Jet Propulsion Lab., California Inst. of Tech., Pasadena.
DYNAMIC MODELS FOR SIMULATION OF THE 70-M ANTENNA AXIS SERVOS **c37**
R. E. Hill *In its* The Telecommunications and Data Acquisition Report 15 Nov. 1988 p 32-50 (For primary document see N89-20329 13-32)
Avail: NTIS HC A12/MF A01 CSCL 13I

Dynamic models for the various functional elements of the 70 m antenna axis servos are described. The model representing the digital position controller, the linear and nonlinear properties of the physical hardware, and the dynamics of the flexible antenna structure are encoded in six major function blocks. The general modular structure of the function blocks facilitates their adaptation to a variety of dynamic simulation studies. Model parameter values were calculated from component specifications and design data. A simulation using the models to predict limit cycle behavior produced results in excellent agreement with field test data from the DSS 14 70-m antenna. Author

N89-20334*# Jet Propulsion Lab., California Inst. of Tech., Pasadena.
A NEW ALGORITHM FOR MODELING FRICTION IN DYNAMIC MECHANICAL SYSTEMS **c37**
R. E. Hill *In its* The Telecommunications and Data Acquisition Report 15 Nov. 1988 p 51-57 (For primary document see N89-20329 13-32)
Avail: NTIS HC A12/MF A01 CSCL 13I

A method of modeling friction forces that impede the motion of parts of dynamic mechanical systems is described. Conventional methods in which the friction effect is assumed a constant force, or torque, in a direction opposite to the relative motion, are applicable only to those cases where applied forces are large in comparison to the friction, and where there is little interest in system behavior close to the times of transitions through zero velocity. An algorithm is described that provides accurate determination of friction forces over a wide range of applied force and velocity conditions. The method avoids the simulation errors resulting from a finite integration interval used in connection with a conventional friction model, as is the case in many digital computer-based simulations. The algorithm incorporates a predictive calculation based on initial conditions of motion, externally applied forces, inertia, and integration step size. The predictive calculation in connection with an external integration process provides an accurate determination of both static and Coulomb friction forces and resulting motions in dynamic simulations. Accuracy of the results is improved over that obtained with conventional methods and a relatively large integration step size is permitted. A function block for incorporation in a specific simulation program is described. The general form of the algorithm facilitates implementation with various programming languages such as FORTRAN or C, as well as with other simulation programs. Author

N89-20335*# Jet Propulsion Lab., California Inst. of Tech., Pasadena.
THEORETICAL COMPARISON OF MASER MATERIALS FOR A 32-GHz MASER AMPLIFIER **c36**
James R. Lyons *In its* The Telecommunications and Data Acquisition Report 15 Nov. 1988 p 58-70 (For primary document see N89-20329 13-32)
Avail: NTIS HC A12/MF A01 CSCL 20E

The computational results of a comparison of maser materials for a 32 GHz maser amplifier are presented. The search for a better maser material is prompted by the relatively large amount of pump power required to sustain a population inversion in ruby at frequencies on the order of 30 GHz and above. The general requirements of a maser material and the specific problems with ruby are outlined. The spin Hamiltonian is used to calculate energy levels and transition probabilities for ruby and twelve other materials. A table is compiled of several attractive operating points for each of the materials analyzed. All the materials analyzed possess operating points that could be superior to ruby. To complete the evaluation of the materials, measurements of inversion ratio and pump power requirements must be made in the future. Author

N89-20336*# Jet Propulsion Lab., California Inst. of Tech., Pasadena.
ON 32-GHz CRYOGENICALLY COOLED HEMT LOW-NOISE AMPLIFIERS **c33**
J. J. Bautista, G. G. Ortiz, K. H. G. Duh, W. F. Kopp, P. Ho, P. C. Chao, M. Y. Kao, P. M. Smith, and J. M. Ballingall (General Electric Co., Syracuse, NY.) *In its* The Telecommunications and Data Acquisition Report 15 Nov. 1988 p 71-81 (For primary document see N89-20329 13-32)
(Contract JPL-957352)
Avail: NTIS HC A12/MF A01 CSCL 09C

The cryogenic noise temperature performance of a two-stage and a three-stage 32 GHz High Electron Mobility Transistor (HEMT) amplifier was evaluated. The amplifiers employ 0.25 micrometer conventional AlGaAs/GaAs HEMT devices, hybrid matching input and output microstrip circuits, and a cryogenically stable dc biasing network. The noise temperature measurements were performed in the frequency range of 31 to 33 GHz over a physical temperature range of 300 K down to 12 K. Across the measurement band, the amplifiers displayed a broadband response, and the noise temperature was observed to decrease by a factor of 10 in cooling from 300 K to 15 K. The lowest noise temperature measured for the two-stage amplifier at 32 GHz was 35 K with an associated gain of 16.5 dB, while the three-stage amplifier measured 39 K with an associated gain of 26 dB. It was further observed that both amplifiers were insensitive to light. Author

N89-20337*# Jet Propulsion Lab., California Inst. of Tech., Pasadena.
CROSS-GUIDE COUPLER MODELING AND DESIGN **c33**
J. Chen *In its* The Telecommunications and Data Acquisition Report 15 Nov. 1988 p 82-88 (For primary document see N89-20329 13-32)
Avail: NTIS HC A12/MF A01 CSCL 09C

Modeling of cross-guide couplers based on the theory of equivalent electric and magnetic dipoles of an aperture is described. Additional correction factors due to nonzero wall thickness and large aperture are also included in this analysis. Comparisons of the measured and calculated results are presented for cross-guide couplers with circular or cross-shaped coupling apertures. A cross-guide coupler was designed as a component of the C-band feed to support the Phobos mission. Author

N89-20338*# Jet Propulsion Lab., California Inst. of Tech., Pasadena.
MODAL ANALYSIS APPLIED TO CIRCULAR, RECTANGULAR, AND COAXIAL WAVEGUIDES **c33**
D. J. Hoppe *In its* The Telecommunications and Data Acquisition Report 15 Nov. 1988 p 89-96 (For primary document see

N89-20329 13-32)
Avail: NTIS HC A12/MF A01 CSCL 09C

Recent developments in the analysis of various waveguide components and feedhorns using Modal Analysis (Mode Matching Method) are summarized. A brief description of the theory is presented, and the important features of the method are pointed out. Specific examples in circular, rectangular, and coaxial waveguides are included, with comparisons between the theory and experimental measurements. Extensions to the methods are described. Author

N89-20339*# Jet Propulsion Lab., California Inst. of Tech., Pasadena.
CONCEPTUAL DESIGN OF A 1-MW CW X-BAND TRANSMITTER FOR PLANETARY RADAR
A. M. Bhanji, D. J. Hoppe, B. L. Conroy, and A. J. Freiley *In its* The Telecommunications and Data Acquisition Report 15 Nov. 1988 p 97-111 (For primary document see N89-20329 13-32)
Avail: NTIS HC A12/MF A01 CSCL 17B

A proposed conceptual design to increase the output power of an existing X-band radar transmitter used for planetary radar exploration from 365 kW to 1 MW CW is presented. The basic transmitter system requirements as dictated by the specifications for the radar are covered. The characteristics and expected performance of the high-power klystrons are considered, and the transmitter power amplifier system is described. Also included is the design of all of the associated high-power microwave components, the feed system, and the phase-stable exciter. The expected performance of the beam supply, heat exchanger, and monitor and control devices is also presented. Finally, an assessment of the state-of-the-art technology needed to meet system requirements is given and possible areas of difficulty are summarized. Author

N89-20340*# Jet Propulsion Lab., California Inst. of Tech., Pasadena.
VLA TELEMETRY PERFORMANCE WITH CONCATENATED CODING FOR VOYAGER AT NEPTUNE c17
S. J. Dolinar, Jr. *In its* The Telecommunications and Data Acquisition Report 15 Nov. 1988 p 112-133 (For primary document see N89-20329 13-32)
Avail: NTIS HC A12/MF A01 CSCL 09F

Current plans for supporting the Voyager encounter at Neptune include the arraying of the Deep Space Network (DSN) antennas at Goldstone, California, with the National Radio Astronomy Observatory's Very Large Array (VLA) in New Mexico. Not designed as a communications antenna, the VLA signal transmission facility suffers a disadvantage in that the received signal is subjected to a gap or blackout period of approximately 1.6 msec once every 5/96 sec control cycle. Previous analyses showed that the VLA data gaps could cause disastrous performance degradation in a VLA stand-alone system and modest degradation when the VLA is arrayed equally with Goldstone. New analysis indicates that the earlier predictions for concatenated code performance were overly pessimistic for most combinations of system parameters, including those of Voyager-VLA. The periodicity of the VLA gap cycle tends to guarantee that all Reed-Solomon codewords will receive an average share of erroneous symbols from the gaps. However, large deterministic fluctuations in the number of gapped symbols from codeword to codeword may occur for certain combinations of code parameters, gap cycle parameters, and data rates. Several mechanisms for causing these fluctuations are identified and analyzed. Even though graceful degradation is predicted for the Voyager-VLA parameters, catastrophic degradation greater than 2 dB can occur for a VLA stand-alone system at certain non-Voyager data rates inside the range of the actual Voyager rates. Thus, it is imperative that all of the Voyager-VLA parameters be very accurately known and precisely controlled. Author

N89-20341*# Jet Propulsion Lab., California Inst. of Tech., Pasadena.
A LONG CONSTRAINT LENGTH VLSI VITERBI DECODER FOR THE DSN c61
J. I. Statman, G. Zimmerman, F. Pollara, and O. Collins *In its* The Telecommunications and Data Acquisition Report 15 Nov. 1988 p 134-142 (For primary document see N89-20329 13-32)
Avail: NTIS HC A12/MF A01 CSCL 09B

A Viterbi decoder, capable of decoding convolutional codes with constraint lengths up to 15, is under development for the Deep Space Network (DSN). The objective is to complete a prototype of this decoder by late 1990, and demonstrate its performance using the (15, 1/4) encoder in Galileo. The decoder is expected to provide 1 to 2 dB improvement in bit SNR, compared to the present (7, 1/2) code and existing Maximum Likelihood Convolutional Decoder (MCD). The decoder will be fully programmable for any code up to constraint length 15, and code rate 1/2 to 1/6. The decoder architecture and top-level design are described. Author

N89-20342*# Jet Propulsion Lab., California Inst. of Tech., Pasadena.
LONG DECODING RUNS FOR GALILEO'S CONVOLUTIONAL CODES c61
C. R. Lahmeyer and K.-M. Cheung *In its* The Telecommunications and Data Acquisition Report 15 Nov. 1988 p 143-147 (For primary document see N89-20329 13-32)
Avail: NTIS HC A12/MF A01 CSCL 09B

Decoding results are described for long decoding runs of Galileo's convolutional codes. A 1 k-bit/sec hardware Viterbi decoder is used for the (15, 1/4) convolutional code, and a software Viterbi decoder is used for the (7, 1/2) convolutional code. The output data of these long runs are stored in data files using a data compression format which can reduce file size by a factor of 100 to 1 typically. These data files can be used to replicate the long, time-consuming runs exactly and are useful to anyone who wants to analyze the burst statistics of the Viterbi decoders. The 1 k-bit/sec hardware Viterbi decoder was developed in order to demonstrate the correctness of certain algorithmic concepts for decoding Galileo's experimental (15, 1/4) code, and for the long-constraint-length codes in general. The hardware decoder can be used both to search for good codes and to measure accurately the performance of known codes. Author

N89-20343*# Jet Propulsion Lab., California Inst. of Tech., Pasadena.
PERFORMANCE OF GALILEO'S CONCATENATED CODES WITH NONIDEAL INTERLEAVING
K.-M. Cheung and S. J. Dolinar, Jr. *In its* The Telecommunications and Data Acquisition Report 15 Nov. 1988 p 148-152 (For primary document see N89-20329 13-32)
Avail: NTIS HC A12/MF A01 CSCL 17B

The Galileo spacecraft employs concatenated coding schemes with Reed-Solomon interleaving depth 2. The bit error rate (BER) performance of Galileo's concatenated codes, assuming different interleaving depths (including infinite interleaving depth) are compared. It is observed that Galileo's depth 2 interleaving, when used with the experimental (15, 1/4) code, requires about 0.4 to 0.5 dB additional signal-to-noise ratio to achieve the same BER performance as the concatenated code with ideal interleaving. When used with the standard (7, 1/2) code, depth 2 interleaving requires about 0.2 dB more signal-to-noise ratio than ideal interleaving. Author

N89-20344*# California Inst. of Tech., Pasadena. Dept. of Electrical Engineering.
THE DECODING OF REED-SOLOMON CODES c17
R. J. McEliece *In* JPL, The Telecommunications and Data Acquisition Report 15 Nov. 1988 p 153-167 (For primary document see N89-20329 13-32)
Avail: NTIS HC A12/MF A01 CSCL 09F

Reed-Solomon (RS) codes form an important part of the high-rate downlink telemetry system for the Magellan mission, and the RS decoding function for this project will be done by DSN. Although the basic idea behind all Reed-Solomon decoding algorithms was developed by Berlekamp in 1968, there are dozens

of variants of Berlekamp's algorithm in current use. An attempt to restore order is made by presenting a mathematical theory which explains the working of almost all known RS decoding algorithms. The key innovation that makes this possible is the unified approach to the solution of the key equation, which simultaneously describes the Berlekamp, Berlekamp-Massey, Euclid, and continued fractions approaches. Additionally, a detailed analysis is made of what can happen to a generic RS decoding algorithm when the number of errors and erasures exceeds the code's designed correction capability, and it is shown that while most published algorithms do not detect as many of these error-erasure patterns as possible, by making a small change in the algorithms, this problem can be overcome. Author

N89-20345*# Jet Propulsion Lab., California Inst. of Tech., Pasadena.

PERFORMANCE OF EFFICIENT Q-SWITCHED DIODE-LASER-PUMPED Nd:YAG AND Ho:YLF LASERS FOR SPACE APPLICATIONS **c36**

W. K. Marshall, K. Cowles, and H. Hemmati *In its* The Telecommunications and Data Acquisition Report 15 Nov. 1988 p 168-173 (For primary document see N89-20329 13-32)

Avail: NTIS HC A12/MF A01 CSCL 20E

Solid-state lasers pumped by continuous-wave diode lasers can be Q-switched to obtain high peak power output pulses. The dependence of laser-pulse energy, average output power, peak power, and pulse width on pulse-repetition frequency in Q-switched Nd:YAG and Ho:YLF lasers is determined and compared. At low pulse repetition rates, the much longer upper-stage lifetime in Ho:YLF gives a distinct advantage. At higher pulse rates, the overall laser efficiency and the stimulated emission cross section are more important parameters, leading to an advantage for Nd:YAG. The results are of significance for designing lasers for use in space optical communications and remote sensing systems. Author

N89-20346*# Jet Propulsion Lab., California Inst. of Tech., Pasadena.

CALCULATIONS OF LASER CAVITY DUMPING FOR OPTICAL COMMUNICATIONS

D. L. Robinson and M. D. Rayman *In its* The Telecommunications and Data Acquisition Report 15 Nov. 1988 p 174-179 (For primary document see N89-20329 13-32)

Avail: NTIS HC A12/MF A01 CSCL 17B

For deep-space pulse-position modulation (PPM) optical communication links using Nd:YAG lasers, two types of laser transmitter modulation techniques are available for efficiently producing laser pulses over a broad range of repetition rates: Q-switching and cavity dumping. The desired modulation scheme is dependent on the required pulse repetition frequency and link parameters. These two techniques are discussed, theoretical and numerical calculations of the internal energy of the laser cavity in cavity dumping are described, and an example of cavity dumping is applied to a link for a proposed experiment package on Cassini. Author

N89-20347*# Jet Propulsion Lab., California Inst. of Tech., Pasadena.

AN INTEGRAL SUNSHADE FOR OPTICAL RECEPTION ANTENNAS

E. L. Kerr *In its* The Telecommunications and Data Acquisition Report 15 Nov. 1988 p 180-195 (For primary document see N89-20329 13-32)

Avail: NTIS HC A12/MF A01 CSCL 17B

Optical reception antennas (telescopes) must be capable of receiving communications even when the deep-space laser source is located within a small angle of the Sun. Direst sunlight must not be allowed to shine on the primary reflector of an optical reception antenna, because too much light would be scattered into the signal detectors. A conventional sunshade that does not obstruct the antenna aperture would have to be about five times longer than its diameter in order to receive optical communications at a solar elongation of 12 degrees without interference. Such a long sunshade could not be accommodated within the dome of any existing large-aperture astronomical facility, and providing a new dome large enough would be prohibitively expensive. It is also desirable to reduce the amount of energy a space-based large-aperture optical reception facility would expend orienting a structure with such a sizable moment of inertia. Since a large aperture optical reception antenna will probably have a hexagonally segmented primary reflector, a sunshade consisting of hexagonal tubes can be mounted in alignment with the segmentation without producing any additional geometric obstruction. An analysis of the duration and recurrence of solar-conjunction communications outages (caused when a deep-space probe near an outer planet appears to be closer to the Sun than a given minimum solar elongation), and the design equations for the integral sunshade are appended. Author

N89-20348*# Jet Propulsion Lab., California Inst. of Tech., Pasadena.

SHUTTERS AND SLATS FOR THE INTEGRAL SUNSHADE OF AN OPTICAL RECEPTION ANTENNA

E. L. Kerr and C. W. DeVore *In its* The Telecommunications and Data Acquisition Report 15 Nov. 1988 p 196-201 (For primary document see N89-20329 13-32)

Avail: NTIS HC A12/MF A01 CSCL 17B

Optical reception antennas used at a small Sun-Earth-probe angle (small solar elongation E) require sunshading to prevent intolerable scattering of light from the surface of the primary mirror. An integral sunshade consisting of hexagonal tubes aligned with the segmentation of a large mirror was proposed for use down to E = 12 degrees. For smaller angles, asterisk-shaped vanes inserted into the length of the hexagonal tubes would allow operation down to about 6 degrees with a fixed obscuration of 3.6 percent. Two alternative methods are investigated to extend the usefulness of the integral sunshade to smaller angles by adding either variable-area shutters to block the tube corners that admit off-axis sunlight or by inserting slats (partial vanes) down the full length of some tubes. Slats are effective for most operations down to 6 degrees, and obscure only 1.2 percent. For E between 10.75 and 12 degrees, shutters cause even less obscuration. Author

N89-20349*# Jet Propulsion Lab., California Inst. of Tech., Pasadena.

EFFECT OF EARTH ALBEDO VARIATION ON THE PERFORMANCE OF A SPATIAL ACQUISITION SUBSYSTEM ABOARD A PLANETARY SPACECRAFT

C.-C. Chen *In its* The Telecommunications and Data Acquisition Report 15 Nov. 1988 p 202-211 (For primary document see N89-20329 13-32)

Avail: NTIS HC A12/MF A01 CSCL 17B

The effect of Earth albedo variation on the pointing and tracking subsystem of a planetary optical communication package is analyzed. By studying the Cramer-Rao bound of the tracking error variance, it is shown that, when the Earth albedo is precisely known, the variance in spatial tracking error is inversely proportional to the total signal count. In contrast, a small uncertainty in the Earth albedo can result in an irreducible error in the tracking subsystem. Author

N89-20350*# Jet Propulsion Lab., California Inst. of Tech., Pasadena.

A PRELIMINARY WEATHER MODEL FOR OPTICAL COMMUNICATIONS THROUGH THE ATMOSPHERE

K. S. Shaik *In its* The Telecommunications and Data Acquisition Report 15 Nov. 1988 p 212-218 (For primary document see N89-20329 13-32)

Avail: NTIS HC A12/MF A01 CSCL 17B

A preliminary weather model is presented for optical propagation through the atmosphere. It can be used to compute the attenuation loss due to the atmosphere for desired link availability statistics. The quantitative results that can be obtained from this model provide good estimates for the atmospheric link budget necessary for the design of an optical communication system. The result is extended to provide for the computation of joint attenuation probability for n sites with uncorrelated weather patterns. Author

N89-20351*# Jet Propulsion Lab., California Inst. of Tech., Pasadena.
AN EXTENDED KALMAN FILTER BASED AUTOMATIC FREQUENCY CONTROL LOOP **c33**
S. Hinedi *In its* The Telecommunications and Data Acquisition Report 15 Nov. 1988 p 219-228 (For primary document see N89-20329 13-32)
Avail: NTIS HC A12/MF A01 CSCL 09C

An Automatic Frequency Control (AFC) loop based on an Extended Kalman Filter (EKF) is introduced and analyzed in detail. The scheme involves an EKF which operates on a modified set of data in order to track the frequency of the incoming signal. The algorithm can also be viewed as a modification to the well known cross-product AFC loop. A low carrier-to-noise ratio (CNR), high-dynamic environment is used to test the algorithm and the probability of loss-of-lock is assessed via computer simulations. The scheme is best suited for scenarios in which the frequency error variance can be compromised to achieve a very low operating CNR threshold. This technique can easily be incorporated in the Advanced Receiver (ARX), requiring minimum software modifications. Author

N89-20352*# Jet Propulsion Lab., California Inst. of Tech., Pasadena.
TRANSMITTER DATA COLLECTION USING Ada **c33**
B. L. Conroy *In its* The Telecommunications and Data Acquisition Report 15 Nov. 1988 p 229-236 (For primary document see N89-20329 13-32)
Avail: NTIS HC A12/MF A01 CSCL 09C

A data collection system installed on the 400 kilowatt X-band transmitter of the Goldstone Solar System Radar is described. The data collection system is built around the off-the-shelf IEEE 488 instrumentation, linked with fiber optics, controlled by an inexpensive computer, and uses software written in the Ada language. The speed and accuracy of the system is discussed, along with programming techniques used for both data collection and reduction. Author

N89-20353*# Jet Propulsion Lab., California Inst. of Tech., Pasadena.
DSN 70-METER ANTENNA X-BAND GAIN, PHASE, AND POINTING PERFORMANCE, WITH PARTICULAR APPLICATION FOR VOYAGER 2 NEPTUNE ENCOUNTER
S. D. Slobin and D. A. Bathker *In its* The Telecommunications and Data Acquisition Report 15 Nov. 1988 p 237-245 (For primary document see N89-20329 13-32)
Avail: NTIS HC A12/MF A01 CSCL 17B

The gain, phase, and pointing performance of the Deep Space Network (DSN) 70 m antennas are investigated using theoretical antenna analysis computer programs that consider the gravity induced deformation of the antenna surface and quadripod structure. The microwave effects are calculated for normal subreflector focusing motion and for special fixed-subreflector conditions that may be used during the Voyager 2 Neptune encounter. The frequency stability effects of stepwise lateral and axial subreflector motions are also described. Comparisons with recently measured antenna efficiency and subreflector motion tests are presented. A modification to the existing 70 m antenna pointing squint correction constant is proposed. Author

N89-20354*# Jet Propulsion Lab., California Inst. of Tech., Pasadena.
POINTING A GROUND ANTENNA AT A SPINNING SPACECRAFT USING CONSCAN-SIMULATION RESULTS
A. Mileant and T. Peng *In its* The Telecommunications and Data Acquisition Report 15 Nov. 1988 p 246-260 (For primary document see N89-20329 13-32)
Avail: NTIS HC A12/MF A01 CSCL 17B

The results are presented for an investigation of ground antenna pointing errors which are caused by fluctuations of the receiver AGC signal due to thermal noise and a spinning spacecraft. Transient responses and steady-state errors and losses are estimated using models of the digital Conscan (conical scan) loop, the FFT, and antenna characteristics. Simulation results are given for the on-going Voyager mission and for the upcoming Galileo mission, which includes a spinning spacecraft. The simulation predicts a 1 sigma pointing error of 0.5 to 2.0 mdeg for Voyager, assuming an AGC loop SNR of 35 to 30 dB with a scan period varying from 128 to 32 sec, respectively. This prediction is in agreement with the DSS 14 antenna Conscan performance of 1.7 mdeg for 32 sec scans as reported in earlier studies. The simulation of Galileo predicts 1 mdeg error with a 128 sec scan and 4 mdeg with a 32 sec scan under similar AGC conditions. Author

N89-20355*# Ohio State Univ., Columbus. ElectroScience Lab.
ELECTROMAGNETIC PROPERTIES OF ICE COATED SURFACES Semiannual Report
A. Dominick, E. Walton, N. Wang, and L. Beard Feb. 1989 19 p
(Grant NsG-3913)
(NASA-CR-184780; NAS 1.26:184780; ESL-720964-2) Avail: NTIS HC A03/MF A01 CSCL 20N

The electromagnetic scattering from ice coated structures is examined. The influence of ice is shown from a measurement standpoint and related to a simple analytical model. A hardware system for the realistic measurement of ice coated structures is also being developed to use in an existing NASA Lewis icing tunnel. Presently, initial measurements have been performed with a simulated tunnel to aid in the development. Author

N89-20356*# National Telecommunications and Information Administration, Boulder, CO. Inst. for Telecommunication Sciences.
SUITABILITY OF ANSI STANDARDS FOR QUANTIFYING COMMUNICATION SATELLITE SYSTEM PERFORMANCE
Robert D. Cass Aug. 1988 99 p Sponsored by NASA, Lewis Research Center, Cleveland, OH
(NASA-CR-182884; NAS 1.26:182884; PB89-113526; NTIA-88-234) Avail: NTIS HC A05/MF A01 CSCL 17B

A study on the application of American National Standards X3.102 and X3.141 to various classes of communication satellite systems from the simple analog bent-pipe to NASA's Advanced Communications Technology Satellite (ACTS) is discussed. These standards are proposed as means for quantifying the end-to-end communication system performance of communication satellite systems. An introductory overview of the two standards are given followed by a review of the characteristics, applications, and advantages of using X3.102 and X3.141 to quantify with a description of the application of these standards to ACTS. Author

N89-20357*# Notre Dame Univ., IN. Dept. of Electrical and Computer Engineering.
ERROR CONTROL TECHNIQUES FOR SATELLITE AND SPACE COMMUNICATIONS Semiannual Status Report
Daniel J. Costello, Jr. Mar. 1989 92 p
(Grant NAG5-557)
(NASA-CR-184825; NAS 1.26:184825) Avail: NTIS HC A05/MF A01 CSCL 17B

The performance of bandwidth efficient trellis codes on channels with phase jitter, or those disturbed by jamming and impulse noise is analyzed. An heuristic algorithm for construction of bandwidth efficient trellis codes with any constraint length up to about 30, any signal constellation, and any code rate was developed. Construction of good distance profile trellis codes for sequential decoding and comparison of random coding bounds of trellis coded modulation schemes are also discussed. M.G.

N89-20358*# Ohio State Univ., Columbus. ElectroScience Lab.
THE OGIVE AS A RCS COMPACT RANGE STANDARD
A. Dominek and T. Nguyen Jan. 1989 26 p
(Grant NsG-1613)
(NASA-CR-184832; NAS 1.26:184832; OSU-719493-3) Avail: NTIS HC A03/MF A01 CSCL 17B

E- and H-plane radar cross section (RCS) patterns at 4 and 10 GHz are provided (based upon moment method calculations)

for a perfectly conducting ogive to be used as a compact range verification standard. The dimensions of the ogive are 36 in. and 9.546 in. long with half tip angles of 15 deg and 20 deg, respectively. Comparison between the calculations and measurements are also provided. Author

N89-20359# ISEL, Madrid (Spain).
ELECTRONICALLY STEERABLE TERMINAL ANTENNA (ESTA) PROJECT, PHASE 2 Final Report
Jordi Gil, Ignacio Aguilar, Albert Fergile, C. Martin, J. Barbero, J. E. Caballero, P. delCastillo, A. Gonzalez, M. L. Hernanz, and J. Vasallo Paris, France ESA Feb. 1988 173 p Prepared in cooperation with Instituto de Electronica de Communicaciones, Madrid (Spain)
(Contract ESTEC-6101/84-NL-GM)
(ESA-CR(P)-2599; ETN-89-93644) Avail: NTIS HC A08/MF A01

The feasibility of a full adaptative antenna terminal was considered, but such a terminal is too expensive for breadboarding and an electronically steerable antenna filling the gap between low gain and complex high gain terminals is proposed. The beam is steered towards the satellite following the inputs provided by the position and navigation instruments of the mobile. No moving parts are used. The manufacturing and testing of a maritime antenna prototype as well as the design of a lower complexity antenna for land mobile application were completed. Simple and advanced terminals were studied. Both include protection against multipath; the advanced terminals also include protection against interferences. Results for the maritime prototype are good enough and agree with expectations. The expected performances of the land antenna should be checked in a manufacturing project. The much lower level of complexity of this antenna compared to the maritime one, will result in a low price product with high performances, probably allowing voice communications without vocoders. ESA

N89-20360# SPARNEX, Antwerp (Belgium).
CONCEPTUAL STUDY OF THE SIGNALLING POINT OF THE MASTER STATION FOR A TST/SS-TDMA SYSTEM. PHASE 1: OVERVIEW AND SELECTION OF SIGNALLING POINTS Final Report
P. deBoer and J. Wuyts Paris, France ESA 1 Mar. 1988 124 p
(Contract ESTEC-7027/87-NL-JG(SC))
(SX/SP-01; ESA-CR(P)-2662; ETN-89-93924) Avail: NTIS HC A06/MF A01

Enhancement of the master control terminal of the advanced satellite communication network, called TST/SS-TDMA system, by the integration of a CCITT-7 signalling point, extracted from an ISDN oriented digital telephone exchange, was studied. The number 7 signalling points of the following switching systems were investigated: GID-SC; MS-7; system X; EWSD; System 12; AFDT1; E10-B; and AXE. Criteria used for selection of the candidate signalling points are the main characteristics of the studied signalling modules, such as: capacity, modularity and control structure, technology, and interest of the manufacturer in collaborating with ESA. It is concluded that the proposed integration is technically feasible and further activity should concentrate on System 12 and system AXE as representative workable solutions. ESA

N89-20361# Helsinki Univ. of Technology, Espoo (Finland). Electromagnetics Lab.
COMPLEX-VALUED FUNCTIONALS IN VARIATIONAL ANALYSIS OF WAVEGUIDES WITH IMPEDANCE BOUNDARIES
Markku I. Oksanen and Ismo V. Lindell Jun. 1988 25 p
(PB89-128896; ISBN-951-754-557-6; Rept-30) Avail: NTIS HC A03/MF A01 CSCL 20N

Stationary complex-valued functionals are discussed and seen to have unique stationary points if they are analytic, which corresponds to analyticity of functions in complex-valued function theory. As an application, the problem of wave propagation in a circular waveguide with an impedance boundary, along with the corresponding two-dimensional resonator problem is considered. It is seen that the variational method for non-standard eigenvalue problems, introduced a few years ago, can be generalized to complex-valued functionals if the functional is analytic. The method can be applied to result in simple analytic formulae for the waveguide with impedance boundaries. Author

N89-20362*# Jet Propulsion Lab., California Inst. of Tech., Pasadena.
EFFICIENT DETECTION AND SIGNAL PARAMETER ESTIMATION WITH APPLICATIONS TO HIGH DYNAMIC GPS RECEIVERS
R. Kumar 15 Dec. 1988 40 p
(Contract NAS7-918)
(NASA-CR-184861; JPL-Publ-88-42; NAS 1.26:184861) Avail: NTIS HC A03/MF A01 CSCL 17B

A novel technique for simultaneously detecting data and estimating the parameters of a received carrier signal phase modulated by unknown data and experiencing very high Doppler, Doppler rate, etc. is discussed. Such a situation arises, for example, in the case of Global Positioning Systems (DPS) where the signal parameters are directly related to the position, velocity and acceleration of the GPS receiver. The proposed scheme is based upon first estimating the received signal local (data dependent) parameters over two consecutive bit periods, followed by the detection of a possible jump in these parameters. The presence of a detected jump signifies a data transition which is then removed from the received signal. This effectively demodulated signal is then processed to provide the estimates of global (data independent) parameters of the signal related to the position, velocity, etc. of the receiver. One of the key features of the proposed algorithm is the introduction of two different schemes which can provide an improvement of up to 3 dB over the conventional implementation of Kalman filter as applied to phase and frequency estimation, under low to medium signal-to-noise ratio conditions. Author

N89-20363*# Ohio State Univ., Columbus. ElectroScience Lab.
IMPROVED COMPUTER SIMULATION OF THE TCAS 3 CIRCULAR ARRAY MOUNTED ON AN AIRCRAFT
R. G. Rojas, Y. C. Chen, and Walter D. Burnside Mar. 1989 191 p
(Grant NsG-1498)
(NASA-CR-184907; NAS 1.26:184907; ELS-TR-716199-12)
Avail: NTIS HC A09/MF A01 CSCL 20N

The Traffic advisory and Collision Avoidance System (TCAS) is being developed by the Federal Aviation Administration (FAA) to assist aircraft pilots in mid-air collision avoidance. This report concentrates on the computer simulation of the enchanced TCAS 2 systems mounted on a Boeing 727. First, the moment method is used to obtain an accurate model for the enhanced TCAS 2 antenna array. Then, the OSU Aircraft Code is used to generate theoretical radiation patterns of this model mounted on a simulated Boeing 727 model. Scattering error curves obtained from these patterns can be used to evaluate the performance of this system in determining the angular position of another aircraft with respect to the TCAS-equipped aircraft. Finally, the tracking of another aircraft is simulated when the TCAS-equipped aircraft follows a prescribed escape curve. In short, the computer models developed in this report have generality, completeness and yield reasonable results. Author

N89-20364*# Ohio State Univ., Columbus. ElectroScience Lab.
ANALYSIS OF MODIFIED SMI METHOD FOR ADAPTIVE ARRAY WEIGHT CONTROL
R. L. Dilsavor and R. L. Moses Feb. 1989 88 p
(Grant NAG3-536)
(NASA-CR-184904; NAS 1.26:184904; ELS-TR-716111-6) Avail: NTIS HC A05/MF A01 CSCL 09C

An adaptive array is applied to the problem of receiving a desired signal in the presence of weak interference signals which need to be suppressed. A modification, suggested by Gupta, of

the sample matrix inversion (SMI) algorithm controls the array weights. In the modified SMI algorithm, interference suppression is increased by subtracting a fraction F of the noise power from the diagonal elements of the estimated covariance matrix. Given the true covariance matrix and the desired signal direction, the modified algorithm is shown to maximize a well-defined, intuitive output power ratio criterion. Expressions are derived for the expected value and variance of the array weights and output powers as a function of the fraction F and the number of snapshots used in the covariance matrix estimate. These expressions are compared with computer simulation and good agreement is found. A trade-off is found to exist between the desired level of interference suppression and the number of snapshots required in order to achieve that level with some certainty. The removal of noise eigenvectors from the covariance matrix inverse is also discussed with respect to this application. Finally, the type and severity of errors which occur in the covariance matrix estimate are characterized through simulation. Author

N89-20365# Research Inst. of National Defence, Linkoeping (Sweden).

DIGITAL RADIO LINK: MULTIPATH FADING ON A 7 GHz LINE-OF-SIGHT LINK

Stefan Mattsson Nov. 1987 29 p

(FOA-C-30428-3.3; ISSN-0347-3708; ETN-89-93738) Avail: NTIS HC A03/MF A01; Swedish Defense Research Establishment, Box 1165, S-581 11 Linkoping, Sweden, 50 Swedish crowns

Propagation measurements on a 7 GHz, 34 Mb/sec 53 km link were made to characterize the radio channel with suitable models during multipath propagation causing frequency selective or flat fading within the actual bandwidth. From the narrow band sweep measurements, the propagation parameters, corresponding to frequency selective events, are extracted by a minimum square fit of a modeled 3-way transfer function to observed transfer functions. The statistical distributions of measured wide band fade depth are estimated for an unprotected and a space diversity channel using antenna separation of 8 m. The statistical distribution of the durations of deep fades are estimated. The optimal choice of vertical antenna separation is discussed, concerning the ability to combat severe frequency selective fading. A three ray model is shown to be appropriate. Measurements of fade duration show that 70 percent of all fading events with fade depths of 34 dB or more have durations below 3 sec. A fit of the CCIR-proposed prediction of mean fade duration to measured mean fade duration shows that the CCIR-model with C=52 is useful for studied conditions. Based on the CCIR-model, the mean fade duration decreases with increasing fade depth. On the actual 53 km path, fading events with fade depths exceeding the flat fade margin 40 dB have a mean duration below 2 sec. ESA

N89-20366# Research Inst. of National Defence, Linkoeping (Sweden).

DIGITAL RADIO LINK: MULTIPATH PROPAGATION ON A MICROWAVE LINE-OF-SIGHT PATH

Stefan Mattsson Nov. 1987 134 p Sponsored by the Swedish Administration of Defence Material/Telecommunication Network Div., Stockholm, Sweden

(FOA-C-30430-3.3; ISSN-0347-3708; ETN-89-93739) Avail: NTIS HC A07/MF A01; Swedish Defense Research Establishment, Box 1165, S-581 11 Linkoping, Sweden, 50 Swedish crowns

Wave propagation investigations by narrowband sweep measurements were performed on a 7 GHz high-capacity 53 km link to model the radio channel during periods of multipath fading, especially frequency selective fading. The multipath mechanism is analyzed, including calculations of path length differences. The measuring system, based on event controlled spectral registration, is described together with the algorithm for extraction of propagation parameters from experimental data. The parameters are estimated by a minimum square fit on a modeled 3-way transfer function to observed transfer functions. Statistical distributions of fade depth and durations of deep fades are presented for a single and a space diversity channel. The calculated improvement achieved by space diversity and adaptive equalization is presented in terms of reduced outage-time. The optimal design of space diversity is discussed, concerning the ability to combat severe frequency selective fading on digital line of sight links. ESA

N89-20367# Research Inst. of National Defence, Linkoeping (Sweden). Dept. of Information Technology.

SAR PROCESSING ON THE ARRAY PROCESSOR NMX-432

Bertil Brusmark, Anders I. Gustavsson, and Anders Nelander Sep. 1988 66 p Sponsored by the Swedish Board for Space Activities

(FOA-C-30503-3.3; ISSN-0347-3708; ETN-89-93743) Avail: NTIS HC A04/MF A01; Swedish Defense Research Establishment, Box 1165, S-581 11 Linkoping, Sweden, 50 Swedish crowns

The SAR processing on the array processor NMX-432 is described. The SAR processing system consists of the array processor and the host computer MicroVAX II with two 300 Mbyte disks and one 6250 bpi tape unit. The SAR programs are written in FORTRAN-77 with subroutine calls to the array processor vector library. Execution time is 50 min for a quarter of a complete Seasat SAR scene. Listings are enclosed. ESA

N89-20368# Helsinki Univ. of Technology, Espoo (Finland).

A STUDY OF EMI-ENDURANCE OF TWO POLLING-TYPE LOCAL AREA NETWORKS USED IN REAL-TIME AUTOMATION APPLICATIONS IN A SIMULATED ELECTRICAL ENVIRONMENT Ph.D. Thesis - Tampere Univ. of Technol.

Josu Takala (Stroemberg Industry/Automation, Vaasa, Finland) 1988 113 p

(EI-62; ISBN-951-666-254-4; ISSN-0001-6845; ETN-89-93750) Avail: NTIS HC A06/MF A01

Three modelling ideas: disturbance generator, applying risk, and availability area to be used in the planning, testing and use of real-time automation applications installed in EMI-environments (electromagnetic interference), for the evaluation of EMI-endurance of a local area network (LAN) used on the process data bus level are presented. The effect of electrical disturbances is taken into consideration by the disturbance generator. It takes into consideration parameters affecting the EMI-endurance of a LAN: the physical installation, and parameters of the data communications, and of the electrical transient disturbances. Generation of messages, disturbances, and the network were simulated and tested. The time stationary probability distributions of the performance and unreliability are evaluated as a function of the disturbance voltage. By using the time stationary probability distributions of EMI-levels measured from field conditions, and the probability distributions, the risks and availability areas of a LAN-based system can be evaluated in different EMI-conditions. ESA

N89-20369# National Aerospace Lab., Amsterdam (Netherlands). Space/Informatics Div.

DATA COMPRESSION AS A MEANS TO DISSEMINATE MORE METEOSAT DATA OVER THE EXISTING CHANNEL

W. C. Huisman and J. B. Boerger 1988 16 p Presented at the 6th Meteosat Scientific Users Meeting, Amsterdam, The Netherlands, 25-27 Nov. 1986

(Contract ESA-6141/84-D)

(NLR-MP-86063-U; ETN-89-94030) Avail: NTIS HC A03/MF A01

Data compression methods for operational remote sensing (meteorology) were studied to determine the feasibility of data compression in the Meteosat imagery-data dissemination mission. User requirements indicate that decompressed Meteosat imagery should contain no errors. This implies that the data compression methods must be reversible and the compressed data must be protected against transmission errors using error-correcting coding methods. The compression ratio (about 2) that must be achievable is easily attainable with practical data compression methods which can be implemented in real-time operating hardware. ESA

N89-20370# National Aerospace Lab., Amsterdam (Netherlands). Informatics Div.
ELECTROMAGNETIC COMPATIBILITY (EMC) TEST FACILITIES
C. Wagemaker 12 Feb. 1988 10 p In DUTCH; ENGLISH summary Presented at the NERG Working Meeting on Electronic Interference, Eindhoven, The Netherlands, 5 Nov. 1987
(NLR-MP-88010-U; ETN-89-94058) Avail: NTIS HC A02/MF A01

Installation and the use of EMC facilities are reviewed. It is concluded that a great deal of effort is needed to maintain such a facility, to guarantee the reliability of the test results. ESA

N89-20371# Sheffield Univ. (England). Dept. of Control Engineering.
TESTING FOR NONLINEARITY USING A PREDICTION ERROR FILTER
J. C. PeytonJones and S. A. Billings Sep. 1988 25 p
(RR-332; ETN-89-94074) Avail: NTIS HC A03/MF A01

A nonlinearity test based on changes in the noise and system frequency response functions caused by filtering the prediction error sequence during linear identification is introduced. The technique avoids the complicated computations involved in determining bispectral densities or dispersion functions, is not dependent on special properties of the input, and is robust against noise. The filter may also be chosen to make the test insensitive to misspecification of the linear model, so that the test may be applied at any stage of the identification process, thereby allowing early detection of nonlinear dynamics in the data. The basis of the test for the noise free, unbiased case, is outlined, showing that filtering changes the nonlinear structure of any system which can be represented by a Volterra series. The behavior of noise and linear bias under filtering is examined, since these effects could be confused with nonlinearity unless appropriate choices of filter and filtering technique are made. The test is applied to simulations of a nonlinear (Duffings equation) system. Results are good, although the efficacy of the test remains to be established through further simulation and tests on real data. ESA

N89-20372# Sandia National Labs., Albuquerque, NM.
SYMBOLS FOR COMMUNICATION CIRCUIT DESIGN AND DOCUMENTATION
Michael George, Lyndon G. Pierson, and Edward L. Witzke (BDM Corp., Albuquerque, NM.) 1988 11 p Presented at the Phoenix Conference on Computers and Communications, Scottsdale, AZ, 22 Mar. 1989
(Contract DE-AC04-76DP-00789)
(DE88-013002; SAND-88-1967C; CONF-890314-1) Avail: NTIS HC A03/MF A01

A set of communication symbols has been developed at Sandia National Laboratories for designing and documenting communication circuits. The symbols can depict devices in a circuit, show proper interfacing of devices, and show the propagation of clocks, data, and control signals through the circuit. This paper defines the communication symbols and illustrates their usage. DOE

N89-20373# Los Alamos National Lab., NM.
A PORTABLE CW/FM-CW DOPPLER RADAR FOR LOCAL INVESTIGATION OF SEVERE STORMS
Wesley P. Unruh, Michael A. Wolf, and Howard B. Bluestein (Oklahoma Univ., Norman.) 1988 4 p Presented at the 24th Conference on Radar Meteorology, Tallahassee, FL, 27-31 Mar. 1989
(Contract W-7405-eng-36)
(DE89-005445; LA-UR-88-3868; CONF-890355-1) Avail: NTIS HC A02/MF A01

During the 1987 spring storm season we used a portable 1-W X-band CW Doppler radar to probe a tornado, a funnel cloud, and a wall cloud in Oklahoma and Texas. This same device was used during the spring storm season in 1988 to probe a wall cloud in Texas. The radar was battery powered and highly portable, and thus convenient to deploy from our chase vehicle. The device separated the receding and approaching Doppler velocities in real time and, while the radar was being used, it allowed convenient stereo data recording for later spectral analysis and operator monitoring of the Doppler signals in stereo headphones. This aural monitoring, coupled with the ease with which an operator can be trained to recognize the nature of the signals heard, made the radar very easy to operate reliably and significantly enhanced the quality of the data being recorded. At the end of the 1988 spring season, the radar was modified to include FM-CW ranging and processing. These modifications were based on a unique combination of video recording and FM chirp generation, which incorporated a video camera and recorder as an integral part of the radar. After modification, the radar retains its convenient portability and the operational advantage of being able to listen to the Doppler signals directly. The original mechanical design was unaffected by these additions. During the summer of 1988, this modified device was used at the Langmuir Laboratory at Socorro, New Mexico in an attempt to measure vertical convective flow in a thunderstorm. DOE

N89-20374# Lawrence Livermore National Lab., CA.
MODELING THE BEHAVIOR OF PULSED, HIGH POWER MICROWAVE ANTENNA SYSTEMS
Richard W. Ziolkowski, Marvin J. Barth, and J. Brian Grant Aug. 1988 11 p Presented at the 4th National High Power Microwave Conference, Monterey, CA, 9 May 1988
(Contract W-7405-eng-48)
(DE89-006280; UCRL-99364; CONF-8805132-13) Avail: NTIS HC A03

In an attempt to quantify the performance of pulsed antenna systems, we have combined TSAR, a three-dimensional finite difference time domain electromagnetics modeling code, and MAXWELL3, the finite element counterpart of TSAR, with a general purpose near-to-far field transform post-processor FAR. TSAR and MAXWELL3 predict for a particular geometry the fields over a generally specified surface and the post-processor FAR then generates from these near-fields, the far-field time histories and/or the field patterns at particular frequencies via a Fourier transform. The application of these algorithms to modeling the overall antenna system performance when breakdown regions occur near the antenna is being studied and will be discussed. DOE

N89-20375# EG and G Energy Measurements, Inc., Los Alamos, NM. Los Alamos Operations.
A RELATIVISTIC FLUID CODE FOR HIGH-POWER MICROWAVE PROPAGATION
Gerald Graham and Robert Roussel-Dupre (Los Alamos National Lab., NM.) 1988 14 p Presented at the IEEE International Conference on Plasma Science, Seattle, WA, 6 Jun. 1988
(Contract DE-AC08-88NV-10617)
(DE89-006598; CONF-880651-1) Avail: NTIS HC A03/MF A01

The propagation of a high-power microwave pulse through the atmosphere is treated with a relativistic fluid code. In this treatment, the first three moments of the Boltzmann equation are used to obtain fluid equations for electron density, mean momentum, and thermal energy. Particle, momentum, and energy exchange rates for elastic, inelastic and ionization collisions are included in the calculation. The effects of electron spatial diffusion and the ponderomotive force are contained in the relativistic form of the Boltzmann equation. For an incident plane parallel microwave pulse, the fluid equations and Maxwell's equations are solved to obtain the temporal behavior of the fields as the microwave propagates through the atmosphere. Theory and applications of the relativistic fluid code are presented. DOE

N89-20376# Air Force Geophysics Lab., Hanscom AFB, MA.
DENSITY MEASUREMENTS WITH COMBINED RAMAN-RAYLEIGH LIDAR (LIGHT DETECTION AND RANGING)
Phan Dao, Wayne Klemetti, Dwight Sipler, W. P. Moskowitz, and G. Davidson (Photometrics, Inc., Woburn, MA.) 3 Jan. 1989 7 p Presented at the SPIE Symposium, Innovative Science and Technology for Government and Civilian Applications, Los Angeles,

CA, 15-20 Jan. 1989
(AD-A203561; AFGL-TR-89-0001) Avail: NTIS HC A02/MF A01 CSCL 17I

A combined Raman-Rayleigh Lidar (Light Detection And Ranging) has recently been implemented at the Air Force Geophysics Laboratory's ground-based lidar station to measure neutral density from the lower stratosphere to the upper mesosphere. Rayleigh Lidar reliability measures relative densities in the region above 30 km. In this region, atmospheric extinction can be neglected and backscattering is primarily due to Rayleigh scattering. However, when density measurements are needed for the lower stratosphere two complications arise: the contribution of aerosol (Mie and Rayleigh) signal and the effect of aerosol attenuation. Vibrational Raman scattering, being an elastic process for molecules only, can be used to resolve the first ambiguity. The second difficulty requires an inversion technique to help determine the attenuation profile from the Lidar signal and provide a transmission correction of this signal. For the lower stratosphere, the technique adopted in this laboratory is a three-step treatment of data. In step 1 Klett inversion is applied on the elastic scattering signal (Mie and Rayleigh) to obtain a transmission altitude profile. In step 2 the molecular signal from the Raman Lidar is corrected for atmospheric attenuation. In step 3 Raman data for below 25 km is spliced to Rayleigh data for above 25 km to give the entire profile of neutral density. GRA

N89-20377# Advanced Decision Systems, Mountain View, CA.
LINEAR FEATURE EXTRACTION FROM RADAR IMAGERY: SBIR (SMALL BUSINESS INNOVATIVE RESEARCH) PHASE 2, OPTION 1 Technical Report, 16 Oct. 1986 - 15 Jun. 1987
Gary D. Conner, David L. Milgram, Daryl T. Lawton, and Christopher C. McConnell Apr. 1988 46 p
(Contract DACA72-86-C-0004)
(AD-A203688; AI/DS-TR-3139-02; ETL-0497) Avail: NTIS HC A03/MF A01 CSCL 17I

The goal of this effort is to develop and demonstrate prototype processing capabilities for a knowledge-based system to automatically extract and analyze linear features from synthetic aperture radar (SAR) imagery. This effort constitutes Phase 2 funding through the Defense Small Business Innovative Research (SBIR) Program. Previous work examined the feasibility of the technology issues involved in the development of an automatedlinear feature extraction system. This Option 1 Final Report documents this examination and the technologies involved in automating this image understanding task. In particular, it reports on a major software delivery containing an image processing algorithmic base, a perceptual structures manipulation package, a preliminary hypothesis management framework and an enhanced user interface. GRA

N89-20378# Aerojet Electrosystems Co., Azusa, CA.
INVESTIGATION OF EXTENSIONS TO THE DISTORTED BORN APPROXIMATION IN STRONG FLUCTUATION THEORY Final Report
A. Stogryn Oct. 1988 58 p
(Contract N00014-87-C-0784)
(AD-A203698; AESC-9316) Avail: NTIS HC A04/MF A01 CSCL 17I

This study, considers some scattering problems relevant to the analysis of brightness temperatures and scattering cross sections of sea ice and its snow cover. The work reported here to examines how the heretofore neglected contribution of the incoherent field to the emissivity and scattering cross sections of a random medium may be taken into account. Two main technical problems which are solved. Strong fluctuation theory equations are derived for the second moments of the electric field in an anisotropic medium. A derived equation is the basis for a detailed reduction of the second moment equation to a form which is practical for numerical computation. The problem of a layered medium with a spherically symmetric correlation function is considered. The spherical symmetry of the correlation function implies that a scalar description of the dielectric properties of the medium is valid and results in the elimination of several technical problems which would arise had an anisotropic correlation function been assumed. Thus, the theory is applicable to snow cover on sea ice as well as old sea ice (provided that the correlation functions describing brine pockets in the ice is spherically symmetric as is suggested by some studies) but will not be directly applicable to young and first year ice which are anisotropic. GRA

N89-20379# Federal Aviation Agency, Atlantic City, NJ.
TEST REPORT FOR THE DIRECT ACCESS RADAR/NATIONAL AIRSPACE SYSTEM (DARC/NAS) BI-DIRECTIONAL INTERFACE TEST
Robert V. DiMeo, T. C. Mullany, A. Tedford, and L. Grossman Jan. 1989 67 p
(AD-A203748; DOT/FAA/CT-TN89/11) Avail: NTIS HC A04/MF A01 CSCL 17I

The results of the DARC/NAS (HOST) bi-directional interface testing are described in this report. The DARC and NAS systems were physically connected by the General Purpose Output (GPO)/General Purpose Input (GPI) lines. Controller and supervisory messages were entered automatically by time from both the DARC and NAS systems. Both systems used common simulated radar data. Results were examined by analyzing recorded data to determine the transparency of the system. GRA

N89-20380# Naval Weapons Center, China Lake, CA. Attack Weapons Dept.
ANALOG AUTOMATIC CONTROL LOOPS IN RADAR AND EW (ELECTRONIC WARFARE) Final Report, 1968 - 1988
Richard Smith Hughes Nov. 1988 252 p
(AD-A203758; AD-E900863; NWC-TP-6967) Avail: NTIS HC A12/MF A01 CSCL 09A

This report discusses the design and analysis of the basic building blocks of many radar and Electronic Warfare (EW) systems, active and semiactive missiles, and antiradiation missiles (ARMs), namely automatic gain control, signal thresholding, and range tracking. GRA

N89-20381# Naval Research Lab., Washington, DC. Concept Development Branch.
IMPLEMENTING RECURRENT BACK-PROPAGATION ON THE CONNECTION MACHINE Final Report
E. M. Deprit 2 Dec. 1988 111 p
(AD-A203796; NRL-9167) Avail: NTIS HC A06/MF A01 CSCL 12F

Pineda's Recurrent back-Propagation algorithm for neural networks has been implemented on the Connection Machine, a massively parallel processor. Two fundamentally different graph architectures underlying the nets were tested-one based on arcs, the other on nodes. Confirming the predominance of communication over computation, performance measurements underscore the necessity to make connections the basic unit of representation. Comparisons between these graphs algorithms lead to important conclusions concerning the parallel implementation of neural nets in both software and hardware. GRA

N89-20382# Illinois Univ., Urbana. Dept. of Electrical and Computer Engineering.
RECONFIGURABLE ANTENNAS Interim Report, Sep. 1985 - Sep. 1986
Y. T. Lo, S. L. Chuang, P. Aoyagi, J. Brenneman, and M. Davidovitz Jul. 1988 76 p
(Contract F19628-85-K-0052)
(AD-A203847; UIEM-86-10; UILV-ENG-86-2558; RADC-TR-88-96) Avail: NTIS HC A05/MF A01 CSCL 09A

Engineering investigations were conducted in several areas related to the analysis and design of an integrated phased array utilizing microstrip antenna elements. Two types of electromagnetically coupled feed structures for microstrip antenna elements were examined in greater detail. An amplifier design, compatible with the electromagnetic feed, was synthesized. An integrated active array element with a coplanar waveguide feed was constructed and tested. Preliminary testing of the active element has shown that it has very good performance

characteristics. The active amplifier adds 13 dB of gain to the antenna element. A two-element passive array utilizing electromagnetically coupled feeds was also designed, constructed tested. Finally, a rigorous full-wave analysis was made for a circular patch antenna electromagnetically fed with a microstrip line directly underneath the patch. The results show that a properly designed system can have efficient coupling and excitation for the antenna. GRA

N89-20161*# National Aeronautics and Space Administration. Goddard Space Flight Center, Greenbelt, MD.
THE SPHERICAL PROBE ELECTRIC FIELD AND WAVE EXPERIMENT
G. Gustafsson, T. Aggson, R. Bostrom, L. P. Block, C. Cattell, P. M. E. Decreau, A. Egeland, C.-G. Falthammar, R. J. L. Grard, and D. A. Gurnett (Iowa Univ., Iowa City.) et al *In* ESA, The Cluster Mission: Scientific and Technical Aspects of the Instruments Oct. 1988 p 31-36 (For primary document see N89-20156 13-12) Avail: NTIS HC A06/MF A01; ESA Publications Div., ESTEC, Noordwijk, Netherlands, $10 US or 25 Dutch guilders CSCL 20N

33 ELECTRONICS AND ELECTRICAL ENGINEERING

Includes test equipment and maintainability; components, e.g., tunnel diodes and transistors; microminiaturization; and integrated circuitry.

For related information see also *60 Computer Operations and Hardware* and *76 Solid-State Physics.*

N89-20383# National Inst. of Standards and Technology, Gaithersburg, MD. Electrosystems Div.
RESEARCH FOR ELECTRIC ENERGY SYSTEMS Annual Report, 1987
Richard J. VanBrunt, ed. Nov. 1988 86 p
(PB89-132310; NISTIR-88/3886) Avail: NTIS HC A05/MF A01 CSCL 09C

The report summarizes the technical accomplishments during fiscal year 1987 from a U.S. Department of Energy sponsored program at the National Bureau of Standards to provide technical support for DOE's research on electrical energy systems. Major activities associated with each of the four subtasks that constitute the program are highlighted. These include research on: (1) electric field and ion measurements; (2) fundamental physical and chemical processes in commonly used gaseous dielectrics like SF6; (3) development of advanced methods for observing and catagorizing prebreakdown interfacial phenomena in liquid dielectrics; and (4) evaluation of advanced methods for characterizing transient measurements by use of step response and convolution integrals as they apply to free standing dividers. Author

N89-20384# Helsinki Univ. of Technology, Espoo (Finland). Electronic Circuit Design Lab.
TESTING OF TIME DOMAIN SIMULATORS FOR NONLINEAR ELECTRONIC CIRCUITS
O. Vityaz (Kiev Polytechnic, USSR) and V. Porra Jul. 1988 70 p
(PB89-125132; ISBN-951-754-551-7; Rept-4) Avail: NTIS HC A04/MF A01 CSCL 09C

Three new performance parameters for nonlinear time domain simulation programs running in different computers are proposed. These parameters can be used as a measure of simulation efficiency when comparing different programs. A set of 37 problems is presented to test the time domain simulators and to demonstrate the use of the performance parameters. Author

N89-20385*# National Aeronautics and Space Administration. Lewis Research Center, Cleveland, OH.
THE MARS CLIMATE FOR A PHOTOVOLTAIC SYSTEM OPERATION
Joseph Appelbaum and Dennis J. Flood 1989 21 p Prepared for presentation at the International Conference on Space Power, Cleveland, OH, 5-7 Jun. 1989; sponsored in part by International Astronautical Federation Prepared in cooperation with Tel-Aviv Univ. (Israel).
(NASA-TM-101994; E-4645; NAS 1.15:101994) Avail: NTIS HC A03/MF A01 CSCL 10B

Detailed information on the climatic conditions on Mars are very desirable for the design of photovoltaic systems for establishing outposts on the Martian surface. The distribution of solar insolation (global, direct and diffuse) and ambient temperature is addressed. This data are given at the Viking lander's locations and can also be used, to a first approximation, for other latitudes. The insolation data is based on measured optical depth of the Martian atmosphere derived from images taken of the sun with a special diode on the Viking cameras; and computation based on multiple wavelength and multiple scattering of the solar radiation. The ambient temperature (diurnal and yearly distribution) is based on direct measurements with a thermocouple at 1.6 m above the ground at the Viking lander locations. The insolation and ambient temperature information are short term data. New information about Mars may be forthcoming in the future from new analysis of previously collected data or from future flight missions. The Mars climate data for photovoltaic system operation will thus be updated accordingly. Author

N89-20386*# National Aeronautics and Space Administration. Ames Research Center, Moffett Field, CA.
AN AIRFOIL PITCH APPARATUS-MODELING AND CONTROL DESIGN
Daniel R. Andrews Mar. 1989 13 p Prepared for presentation at the 35th Instrument Society of America Instrumentation Symposium, Orlando, FL, 1-4 May 1989 Submitted for publication
(NASA-TM-101076; A-89051; NAS 1.15:101076) Avail: NTIS HC A03/MF A01 CSCL 09C

The study of dynamic stall of rapidly pitching airfoils is being conducted at NASA Ames Research Center. Understanding this physical phenomenon will aid in improving the maneuverability of fighter aircraft as well as civilian aircraft. A wind tunnel device which can linearly pitch and control an airfoil with rapid dynamic response is needed for such tests. To develop a mechanism capable of high accelerations, an accurate model and control system is created. The model contains mathematical representations of the mechanical system, including mass, spring, and damping characteristics for each structural element, as well as coulomb friction and servovalve saturation. Electrical components, both digital and analog, linear and nonlinear, are simulated. The implementation of such a high-performance system requires detailed control design as well as state-of-the-art components. This paper describes the system model, states the system requirements, and presents results of its theoretical performance which maximizes the structural and hydraulic aspects of this system. Author

N89-20387*# Jet Propulsion Lab., California Inst. of Tech., Pasadena.
A COMPARISON OF FREQUENCY ESTIMATION TECHNIQUES FOR HIGH-DYNAMIC TRAJECTORIES
V. A. Vilnrotter, S. Hinedi, and R. Kumar 15 Sep. 1988 71 p Prepared in cooperation with Air Force Armament Lab., Elgin AFB, FL
(Contract NAS7-918)
(NASA-CR-184865; JPL-Publ-88-21; NAS 1.26:184865) Avail: NTIS HC A04/MF A01 CSCL 09C

A comparison is presented for four different estimation techniques applied to the problem of continuously estimating the parameters of a sinusoidal Global Positioning System (GPS) signal, observed in the presence of additive noise, under extremely high-dynamic conditions. Frequency estimates are emphasized, although phase and/or frequency rate are also estimated by some of the algorithms. These parameters are related to the velocity, position, and acceleration of the maneuvering transmitter. Estimated performance at low carrier-to-noise ratios and high dynamics is investigated for the purpose of determining the useful

operating range of an approximate Maximum Likelihood (ML) estimator, an Extended Kalman Filter (EKF), a Cross-Product Automatic Frequency Control (CPAFC) loop, and a digital phase-locked loop (PPL). Numerical simulations are used to evaluate performance while tracking a common trajectory exhibiting high dynamics. Author

N89-20388# Institut Franco-Allemand de Recherches, Saint-Louis (France).
PRODUCTION OF PULSED ELECTRON BEAMS BY TRIGGERED PSEUDO-SPARK DISCHARGES
K. Stockwald and M. Schwertl 8 Dec. 1987 24 p
(ISL-CO-245/87; ETN-89-94111) Avail: NTIS HC A03/MF A01

Multielectrode pseudo-spark chambers driven by a high-voltage pulser were used to produce triggerable intense electron-beam pulses, with I max = 500 A, t pulse = 15 ns, j max = 100,000 A/sq cm Ee max = 70 to 80 keV. A triggerable operation mode with low jitter (5 to 10 ns) in trigger delay is obtained by preionizing the discharge path with the help of a dc auxiliary discharge driven inside the discharge geometry prior to applying the high-voltage pulse. The developing mechanisms of the discharge can be shortened by increasing the current intensity of the dc discharge and thereby the build-up time of the discharge can be adapted to the build-up time of the high-voltage pulse (150 ns). Characteristics of the produced electron-beam pulses are obtained by Faraday-cup measurements and beam-target interaction effects. ESA

N89-20389# Edgerton, Germeshausen and Grier, Inc., Idaho Falls, ID.
GROUP TESTING OF LEAD-ACID BATTERIES FOR ELECTRIC VEHICLES
A. F. Burke and J. E. Hardin 1989 11 p Presented at the Battery Conference on Application and Advances, Long Beach, CA, 17 Jan. 1989
(Contract DE-AC07-76ID-01570)
(DE89-005415; EGG-M-88466; CONF-890160-1) Avail: NTIS HC A03

This study was concerned with the module variability of three lead-acid battery packs--namely, 120 V ALCO 2200, 108 V EV-2300, and 96 V Gel/Cell batteries. Each battery pack was discharged for a range of constant powers and over The Simplified FUDS. A microcomputer-based (IBM XT) data acquisition system was used to obtain module and pack voltage data at selected times during the discharges. For each time Lotus 1-2-3 software was used to determine the average, maximum and minimum module voltages and the standard deviation (STD) of the module voltages. It was found that the STD varied from a minimum of about 0.015 V to a maximum of 0.5 V for the batteries tested. The module variability of the ALCO 2200 batteries was much smaller than that of the EV-2300 batteries at all states-of-charge and currents up to 400 A. The Phase 3 Gel/Cells had module variability comparable to that of the ALCO 2200 for SOC greater than 40 percent, but the variability of the Gel/Cells increased rapidly at lower states-of-charge. The module variabilities resulted in differences in module capacities of up to 12 percent for discharge schedules requiring high power (400 A). DOE

N89-20390# Sandia National Labs., Albuquerque, NM.
IMAGE-PROJECTION ION-BEAM LITHOGRAPHY
Paul A. Miller 1989 12 p Presented at the SPIE Symposium on Microlithography, San Jose, CA, 26 Feb. 1989
(Contract DE-AC04-76DP-00789)
(DE89-005773; SAND-88-2090C; CONF-890255-1) Avail: NTIS HC A03/MF A01

Image-projection ion-beam lithography promises high-throughput patterning with wide process latitude, excellent resolution, and minimal damage to underlying circuit layers. The process involves extracting helium ions from a plasma source, transmitting the ions at low voltage through a stencil reticle, and then accelerating and focusing the ions electrostatically onto the wafer. A key feature is the use of image demagnification which simplifies reticle fabrication and inspection, and leads to low power loading on the reticle and long reticle life. In this paper we report computational studies aimed at improving field size, linearity, and telecentricity over that demonstrated experimentally in the pioneering work by Ion Microfabrication Systems, GmbH (Vienna) during the past decade. We study a mechanically simple arrangement of equal-radii coaxial tubular lenses. We employ ion column optimization by simulated annealing and uncover a new optimization strategy which may be applicable in other optimization work. The resulting column design is much improved over our initial attempts based on an iterative optimization procedure. However, we still are unable to eliminate image distortion, and we would need either to rely on reticle predistortion or on use of a more complex electrode system for a production application. DOE

N89-20391# Brookhaven National Lab., Upton, NY. Dept. of Applied Science.
THE INFLUENCE OF SURFACE CAPACITANCE ON THE MEASUREMENTS OF LOCALIZED CORROSION TRANSIENTS
H. S. Isaacs and A. J. Davenport 1988 6 p Presented at the Electrochemical Society Fall Meeting, Chicago, IL, 9 Oct. 1988
(Contract DE-AC02-76CH-00016)
(DE89-006172; BNL-42092; CONF-881061-13) Avail: NTIS HC A02/MF A01

Difficulty is encountered in measuring the early stages of localized corrosion transients because of the charging of the capacitance of the passive surface surrounding the actively corroding area. Measurements of the transmission of potential pulses have been carried out on wire electrodes and show that the propagation rate of the signal was that expected from the product of the surface capacity and solution resistance. DOE

N89-20392# Los Alamos National Lab., NM.
TEST OF RADIATION HARDNESS OF CMOS TRANSISTORS UNDER NEUTRON IRRADIATION
H. F. W. Sadrozinski, W. A. Rowe, A. Seiden, E. Spencer (California Univ., Santa Cruz.), C. M. Hoffman, D. Holtkamp, W. W. Kinnison, W. F. Sommer, Jr., and H. J. Ziock 1989 7 p Presented at the 5th European Symposium on Semiconductor Detectors: New Developments on Radiation Detectors, Munich, Fed. Republic of Germany, 21 Feb. 1989
(Contract W-7405-eng-36)
(DE89-006511; LA-UR-89-295; CONF-890247-2) Avail: NTIS HC A02/MF A01

We have tested 2 micrometer CMOS test structures from various foundries in the LAMPF Beam stop for radiation damage under prolongued neutron irradiation. The fluxes employed covered the region expected to be encountered at the SSC and led to fluences of up to 10 to the 14th power neutrons/sq cm in about 500 hrs of running. We show that test structures which have been measured to survive ionizing radiation of the order MRad also survive these high neutron fluences. DOE

N89-20393# Sandia National Labs., Albuquerque, NM. Battery Development Div.
SCREENING STUDY OF LITHIATED CATHOLYTE MIXES FOR A LONG-LIFE Li(Si)/FeS2 THERMAL BATTERY
Ronald A. Giuidotti, Frederick W. Reinhardt, and William F. Hammetter Dec. 1988 84 p
(Contract DE-AC04-76DP-00789)
(DE89-006857; SAND-85-1737) Avail: NTIS HC A05/MF A01

The inability of the standard catholyte used by Sandia National Laboratories to meet all of the discharge requirements of a 60-min Li(Si)/FeS2 thermal battery necessitated the evaluation of lithiated catholytes as a replacement. Over 100 experimental mixes were examined as part of a screening study using a 5-cell battery as a test vehicle. Parameters studied included: catholyte composition (extent of lithiation), lithiation agents (Li2S, Li alloys, Li2O), processing technique (single step vs. multiple step, heating conditions), type of electrolyte-binder mix used in the catholyte (SiO2-based vs. MgO-based), and the effect of Fe2O3 impurity in the mix. The deformation behavior at 530 C of pellets of the more promising lithiated catholytes was measured, to evaluate

their behavior under simulated battery-discharge conditions. A thermoanalytical study was also conducted to help identify deleterious chemical reactions which occur during heating of the precursor mixes, and to define the chemistry associated with the lithiation processes. The better lithiated catholytes were subjected to performance-verification tests and were then tested in the 10-cell 60-min thermal battery. The best overall results were obtained with Li2O-lithiated catholytes, with optimum performance occurring at a Li/FeS2 mole ratio of approximately 0.16. The initial voltage transient which normally occurs upon activation of Li(Si)/FeS2 thermal batteries was totally eliminated and the pulse performance of the battery near the end of life was significantly improved. DOE

N89-20394# Sandia National Labs., Albuquerque, NM.
MECHANISMS FOR THE OPERATION OF A LASER-TRIGGERED VACUUM SWITCH
Paul J. Brannon and Merle E. Riley Nov. 1988 21 p
(Contract DE-AC04-76DP-00789)
(DE89-007059; SAND-88-2162) Avail: NTIS HC A03/MF A01

A new model for the operation of a laser-triggered vacuum switch utilizing a composite target pellet in the cathode is given along with supporting experimental results. It is shown that two separate mechanisms are responsible for the operation of the switch, namely, one mechanism for the initial current and a separate mechanism for the current buildup. DOE

N89-20395# Sandia National Labs., Albuquerque, NM. Storage Batteries Div.
GLOSSARY OF TESTING TERMINOLOGY FOR RECHARGEABLE BATTERIES
Paul C. Butler Oct. 1988 28 p
(Contract DE-AC04-76DP-00789)
(DE89-007061; SAND-88-2852) Avail: NTIS HC A03/MF A01

The Battery Test Working Task Force was formed in 1983 for the purpose of coordinating the evaluation of development rechargeable batteries by DOE-funded labs. The Task Force developed this glossary of testing terminology to improve the accuracy of communication and to permit meaningful comparisons of test results. It consists of a section of technical terms and a separate section of programmatic phrases and acronyms. The glossary emphasizes terms related to electric vehicle batteries due to the significant development and testing activities in this area. DOE

N89-20396# International Centre for Theoretical Physics, Trieste (Italy).
EVALUATION OF THE KUBO FORMULA FOR THE CONDUCTIVITY USING THE RECURSION METHOD
Alfredo Levy Yeyati, Mariana Weissmann (Comision Nacional de Energia Atomica, Buenos Aires, Argentina), and Enrique Anda Sep. 1988 24 p Submitted for publication
(DE88-705359; IC-88/255) Avail: NTIS (US Sales Only) HC A03/MF A01

We propose a numerical algorithm based on the recursion method to calculate the conductivity of a disordered system described by a tight-binding Hamiltonian. It has the advantage that the density of states and the conductivity can be obtained in a single recursion calculation. The method is applied to simple one and two-dimensional incommensurate systems in order to check the validity of the assumptions made and the numerical efficiency. The calculated conductivity shows a clear drop when the Fermi energy crosses a mobility edge. Potential applications of this work to other systems are discussed. DOE

N89-20397# Los Alamos National Lab., NM.
BUNCH BEAM PRODUCTION AND MICROWAVE GENERATION IN REDITRONS
Thomas J. T. Kwan, Harold A. Davis, Robert D. Fulton, and Eugene G. Sherwood 1989 12 p Presented at the SPIE Conference on Optics, Electro-optics and Laser Applications in Science and Engineering: OE/LASE '89, Los Angeles, CA, 15 Jan. 1989
(Contract W-7405-eng-36)
(DE89-006530; LA-UR-89-167; CONF-890145-14) Avail: NTIS HC A03/MF A01

We have discovered in our two-dimensional particle-in-cell simulations that the oscillation of virtual cathodes in reditrons can produce a highly modulated electron beam. Full (100 percent) current modulation of the leakage electron beam was observed in our simulations. The modulation is at the frequency of the oscillating virtual cathode and the transverse magnetic mode generated by the reditron. We had further incorporated an inverse diode in the reditron and showed that the kinetic energy of the modulated electron beam was efficiently converted into transverse electromagnetic waves. Our simulations showed an efficiency of 26 percent and the time averaged microwave power was about 6 GW. DOE

N89-20398# Lawrence Livermore National Lab., CA. Microwave and Pulsed Power Thrust Area.
WORKSHOP ON TRANSIENT INDUCED INSULATOR FLASHOVER IN VACUUM
1988 262 p Workshop held at Livermore, CA, 24 Aug. 1988
(Contract W-7405-eng-48)
(DE89-006727; CONF-8808171) Avail: NTIS HC A12

A workshop to discuss the state-of-the-art in transient induced insulator flashover in vacuum was convened at the Pleasanton Hilton at the Club Hotel on August 24-25, 1988. The workshop was attended by 39 participants. Flashover of vacuum-insulator surfaces is the limiting factor in virtually all well designed high voltage, pulsed systems where such interfaces are needed. They are critical to many LLNL present and future applications. The workshop participants attempted via presentations and lively discussions to summarize the state-of-the-art in the field and to outline the critical research topics which could lead to advances in understanding and applications. Several new results were presented at the workshop and an intense discussion session resulted in the formulation of a set of research recommendations and priorities. DOE

N89-20399# Pacific Northwest Labs., Richland, WA.
ASSESSMENT OF HIGH-TEMPERATURE BATTERY SYSTEMS
R. K. Sen Feb. 1989 103 p Presented at the High-Temperature Battery Systems Workshop, Washington, DC, 16 Aug. 1988
(Contract DE-AC06-76RL-01830)
(DE89-007554; PNL-SA-16675; CONF-8808137-Summ) Avail: NTIS HC A06/MF A01

Three classes of high-temperature batteries are being developed internationally with transportation and stationary energy storage applications in mind: sodium/sulfur, lithium/metal sulfide, and sodium/metal chloride. Most attention is being given to the sodium/sulfur system. The Office of Energy Storage and Distribution (OESD) and the Office of Transportation Systems (OTS) of the U.S. Department of Energy (DOE) are actively supporting the development of this battery system. It is anticipated that pilot-scale production facilities for sodium/sulfur batteries will be in operation in the next couple of years. The lithium/metal sulfide and the sodium/metal chloride systems are not receiving the same level of attention as the sodium/sulfur battery. Both of these systems are in an earlier stage of development than sodium/sulfur. OTS and OESD are supporting work on the lithium/iron sulfide battery in collaboration with the Electric Power Research Institute (EPRI); the work is being carried out at Argonne National Laboratory (ANL). The sodium/metal chloride battery, the newest member of the group, is being developed by a Consortium of South African and British companies. The assessment includes recommendations to DOE for a proposed high-temperature battery research and development program. DOE

N89-20400# California Univ., Los Angeles. Dept. of Computer Science.
ON-LINE ARITHMETIC ALGORITHMS AND STRUCTURES FOR VLSI Final Report, 15 Dec. 1984 - 14 Dec. 1987
Miloes D. Ercegovac and Tomas Lang Nov. 1988 93 p

(Contract N00014-85-K-0159)
(AD-A203421) Avail: NTIS HC A05/MF A01 CSCL 09A

The research and development problem we have investigated in this project is the VLSI implementation of fast and highly parallel algorithms based on one-line arithmetic. The on-line approach is characterized by simple interconnection requirements and digit-level pipelining suitable for highly concurrent special-purpose VLSI designs. The objective of the project was to evaluate the feasibility and efficiency of on-line approach in NMOS and CMOS VLSI implementations. GRA

N89-20401# International Business Machines Corp., Manassas, VA. Systems Integration Div.
VERY HIGH SPEED INTEGRATED CIRCUITS (VHSIC). PHASE 2: SUBMICROMETER TECHNOLOGY DEVELOPMENT, INTEROPERABILITY STANDARDS Report, 1 Oct. 1985 - 31 Oct. 1988
Dale Rickard, George Anderson, and George McIver 30 Nov. 1988 257 p
(Contract DAAK20-85-C-0376; AF Proj. 2700)
(AD-A203629; SLCET-TR-85-0376-8) Avail: NTIS HC A12/MF A01 CSCL 09A

This report covers the Interoperability Standards developed under the VHSIC Phase 2 Submicrometer Technology Development Program. The Interoperability Standards are the result of joint effort by the three VHSIC Phase 2 contractors and representatives of the Army, Air Force and Navy to develop standards for the interconnection and operation of integrated circuits fabricated with 0.5 micrometer technology. An introductory description and a copy of each standard is provided. The standards developed are: (1) The Pi-bus standard interconnect system bus, (2) The TM-bus standard system maintenance bus, (3) The ETM-bus standard chip level maintenance bus, and (4) Electrical and Clocking Interface to VHSIC Chips. GRA

N89-20402# Axiomatix, Los Angeles, CA.
DEDICATED VERSUS HALF-DUPLEX RECEIVER TOPOLOGY IN JAMMED, FULLY CONNECTED CDMA NETWORKS: THEORY AND NUMERICAL COMPARISONS Interim Technical Report
Andreas Polydoros and Unjeng Cheng 23 Dec. 1988 20 p
(Contract DAAL03-87-C-0007)
(AD-A203635) Avail: NTIS HC A03/MF A01 CSCL 09A

In our previous report we introduced the notion of topology-selective jamming in conjunction with a fully-connected network topology, equipped with Code Division Multiple Access (CDMA) capability. Spread-spectrum modulation was employed, both as a multiple-access tool as well as an antijam aid. In particular, we assumed an arbitrary topology of dedicated transmitters (TR) and receivers (RVCR) in a statistically symmetrical model, where every TR can be heard by every RCVR; in this sense, the network is fully-connected. The number of TRs (NT) was fixed and, in general, different from the number of RCVRs, NR. A special case is when NT=NR, which is essentially equivalent to a network of full duplex modems. Since full-duplex is but a special case, we prefer the nomenclature dedicated, which is applicable to more general scenarios such as multi-receiver satellites, two-level hierarchical networks with dedicated receivers/repeaters, etc. In such environments, the present theory would provide performance estimates (throughput-delay) within a local subnet of connected radios. The goal of the present report is to extend that theory to the case where the modems are nondedicated, i.e., half-duplex. This means that a unit will alternate between the receiving mode and the transmitting mode; it is not dedicated solely to either of the two functions and it cannot do both at the same time, as in the full-duplex case. GRA

N89-20403# Princeton Univ., NJ. Dept. of Electrical Engineering and Computer Science.
DIGITAL SIGNAL PROCESSING Final Report, 15 Jul. 1985 - 31 Aug. 1988
John B. Thomas and Kenneth Steiglitz Dec. 1988 8 p
(Contract DAAG29-85-K-0191)
(AD-A203744; ARO-22711.3-EL) Avail: NTIS HC A02/MF A01 CSCL 09A

Topics addressed include: Regularity in VLSI Design, Architecture for Signal Processing and Regular Computation, Cellular Automata and Regular Computation, Data Communications, Communication Networks, Signal Detection and Estimation, Matched Filtering, and Density Function Representation. GRA

N89-20404# Army Tank-Automotive Command, Warren, MI.
DESIGN AND IMPLEMENTATION OF THE HAZARD CONTROL BOX FOR THE RIDE MOTION SIMULATOR Final Technical Report, Oct. 1987 - May 1988
Gregory R. Hudas Dec. 1988 27 p
(AD-A203752; TACOM-TR-13414) Avail: NTIS HC A03/MF A01 CSCL 09A

This report describes the design and implementation of the Computer Automated Measurement and Control (CAMAC) Hazard Control Box for use as an electronic safety device for the Ride Motion Simulator. This device uses comparitor circuitry to detect any exceeded position limit of the simulator, alert the operator, and halt the simulation immediately. The box is uniquely interfaced to a MicroVAX/CAMAC computer system through a change-of-state module. Other options to the box include a ramp down toggle switch, and an emergency stop electronic switch. GRA

N89-20336*# Jet Propulsion Lab., California Inst. of Tech., Pasadena.
ON 32-GHz CRYOGENICALLY COOLED HEMT LOW-NOISE AMPLIFIERS
J. J. Bautista, G. G. Ortiz, K. H. G. Duh, W. F. Kopp, P. Ho, P. C. Chao, M. Y. Kao, P. M. Smith, and J. M. Ballingall (General Electric Co., Syracuse, NY.) *In its* The Telecommunications and Data Acquisition Report 15 Nov. 1988 p 71-81 (For primary document see N89-20329 13-32)
(Contract JPL-957352)
Avail: NTIS HC A12/MF A01 CSCL 09C

N89-20337*# Jet Propulsion Lab., California Inst. of Tech., Pasadena.
CROSS-GUIDE COUPLER MODELING AND DESIGN
J. Chen *In its* The Telecommunications and Data Acquisition Report 15 Nov. 1988 p 82-88 (For primary document see N89-20329 13-32)
Avail: NTIS HC A12/MF A01 CSCL 09C

N89-20338*# Jet Propulsion Lab., California Inst. of Tech., Pasadena.
MODAL ANALYSIS APPLIED TO CIRCULAR, RECTANGULAR, AND COAXIAL WAVEGUIDES
D. J. Hoppe *In its* The Telecommunications and Data Acquisition Report 15 Nov. 1988 p 89-96 (For primary document see N89-20329 13-32)
Avail: NTIS HC A12/MF A01 CSCL 09C

N89-20351*# Jet Propulsion Lab., California Inst. of Tech., Pasadena.
AN EXTENDED KALMAN FILTER BASED AUTOMATIC FREQUENCY CONTROL LOOP
S. Hinedi *In its* The Telecommunications and Data Acquisition Report 15 Nov. 1988 p 219-228 (For primary document see N89-20329 13-32)
Avail: NTIS HC A12/MF A01 CSCL 09C

N89-20352*# Jet Propulsion Lab., California Inst. of Tech., Pasadena.
TRANSMITTER DATA COLLECTION USING Ada
B. L. Conroy *In its* The Telecommunications and Data Acquisition Report 15 Nov. 1988 p 229-236 (For primary document see N89-20329 13-32)
Avail: NTIS HC A12/MF A01 CSCL 09C

34 FLUID MECHANICS AND HEAT TRANSFER

Includes boundary layers; hydrodynamics; fluidics; mass transfer; and ablation cooling.

For related information see also *02 Aerodynamics* and *77 Thermodynamics and Statistical Physics.*

N89-20405# Rocky Research Corp., Boulder City, NV.
FEASIBILITY OF A COMPLEX COMPOUND HEAT PUMP Annual Report, Jul. 1987 - Jun. 1988
Uwe Rockenfeller and James Langeliers Jul. 1988 75 p
(Contract GRI-5086-260-1251)
(PB89-115273; GRI-88/0202) Avail: NTIS HC A04/MF A01 CSCL 20D

The feasibility of a double effect gas fired heat pump using ammoniated solid vapor complex compounds as the working media is examined. The cycle takes advantage of the coordinative characteristic of complex compound ligand bonds resulting in large coordination spheres with only one degree of freedom. The cycle has high efficiency, no moving parts, and minimum electrical parasitic requirements. Media properties of the candidate materials were experimentally verified with respect to stability, equilibrium pressure and reactivities in adsorption and desorption processes. A bench scale proof of concept system was constructed and operated. The computer model was complemented with media heat capacity properties and coefficients of performance indicating COPc of about 1.0 and COPH of about 2.1 should be achievable. Author

N89-20406# Virginia Polytechnic Inst. and State Univ., Blacksburg. Dept. of Mechanical Engineering.
STANDARD TEST CASE FOR A LOW SPEED, TURBULENT JUNCTION VORTEX FLOW Final Report
F. J. Pierce, M. D. Harsh, C. M. Kim, S. K. Nath, and J. Shin Sep. 1988 17 p
(Contract N00014-86-K-0036)
(PB89-110779; VIP-E-88-86) Avail: NTIS HC A03/MF A01 CSCL 20D

The mean flow structure upstream, around, within and in the near wake of a turbulent junction or horseshoe vortex is reported for an incompressible, subsonic flow. Measurements of the primitive variables of velocity and pressure are reported on all surfaces bounding the region of the vortex flow, and on two transverse and one streamwise plane within the flow field itself for comparisons between the measured and any calculated flow variables. The data is a highly detailed, coherent, self-consistent set offered to the computational fluid mechanics community as a standard test case for the evaluation of the capability of numerical solvers intended for predicting the flow field in such a complex, separated, three-dimensional turbulent flow. Author

N89-20407*# National Aeronautics and Space Administration. Lewis Research Center, Cleveland, OH.
CONTROL-VOLUME BASED NAVIER-STOKES EQUATION SOLVER VALID AT ALL FLOW VELOCITIES
S.-W. Kim Feb. 1989 40 p
(NASA-TM-101488; E-4629; ICOMP-89-5; NAS 1.15:101488)
Avail: NTIS HC A03/MF A01 CSCL 20D

A control-volume based finite difference method to solve the Reynolds averaged Navier-Stokes equations is presented. A pressure correction equation valid at all flow velocities and a pressure staggered grid layout are used in the method. Example problems presented herein include: a developing laminar channel flow, developing laminar pipe flow, a lid-driven square cavity flow, a laminar flow through a 90-degree bent channel, a laminar polar cavity flow, and a turbulent supersonic flow over a compression ramp. A k-epsilon turbulence model supplemented with a near-wall turbulence model was used to solve the turbulent flow. It is shown that the method yields accurate computational results even when highly skewed, unequally spaced, curved grids are used. It is also shown that the method is strongly convergent for high Reynolds number flows. Author

N89-20408 Virginia Polytechnic Inst. and State Univ., Blacksburg.
NAVIER-STOKES PREDICTION OF THE THREE DIMENSIONAL FLOW-FIELD OF JETS IN A CROSSFLOW USING THE FINITE ELEMENT METHOD Ph.D. Thesis
Tae Shik Oh 1988 183 p
Avail: Univ. Microfilms Order No. DA8813618

A Prandtl-type eddy viscosity model including the first-order effect of turbulence structure deals with curved free-shear flows. The model is generalized to account for the effect of arbitrary cross-section of the jets injected from a various nozzle configurations into a uniform cross-flow. The finite-element procedures follow a Galerkin type variational formulation with the penalty approximation for pressure in a consistent manner. Significant savings in computational time and storage are achieved. A slip condition is employed to model the wall flow and stress-free conditions are used for the farfield and outflow boundaries. Numerical predictions are performed for three problems: a single circular jet in a crossflow, a single streamwise aligned rectangular (aspect ratio 4) jet in a crossflow, and dual side-by-side rectangular jets in a crossflow, all at a jet-to-crossflow velocity ratio 4, which is important for V/STOL and applications. Dissert. Abstr.

N89-20409*# National Aeronautics and Space Administration. Langley Research Center, Hampton, VA.
UPDATED USERS' GUIDE FOR TAWFIVE WITH MULTIGRID
N. Duane Melson and Craig L. Streett Washington May 1989 68 p
(NASA-TM-4109; L-16543; NAS 1.15:4109) Avail: NTIS HC A04/MF A01 CSCL 20D

A program for the Transonic Analysis of a Wing and Fuselage with Interacted Viscous Effects (TAWFIVE) was improved by the incorporation of multigrid and a method to specify lift coefficient rather than angle-of-attack. A finite volume full potential multigrid method is used to model the outer inviscid flow field. First order viscous effects are modeled by a 3-D integral boundary layer method. Both turbulent and laminar boundary layers are treated. Wake thickness effects are modeled using a 2-D strip method. A brief discussion of the engineering aspects of the program is given. The input, output, and use of the program are covered in detail. Sample results are given showing the effects of boundary layer corrections and the capability of the lift specification method. Author

N89-20410# Helsinki Univ. Technology, Otaniemi (Finland). Lab. of Aerodynamics.
FLUX VECTOR SPLITTING IN GENERAL CURVILINEAR COORDINATES
Timo Siikonen 1988 32 p
(PB89-127393; ISBN-951-754-589-4; B-14) Avail: NTIS HC A03/MF A01 CSCL 20D

Two dimensional Euler equations were solved using the flux vector splitting method. The discretization is made in a finite volume form. The resulting equations are solved with an approximately factored implicit scheme. Two different boundary procedures were utilized. In the first approach, the characteristic variables are used to determine the state at the boundary. In the second approach, the boundary fluxes are calculated in the same way as the interior fluxes. Results are presented for subsonic, transonic, and supersonic flows. Comparisons are made with the results obtained with other methods. GRA

N89-20411*# Institute for Computer Applications in Science and Engineering, Hampton, VA.
RESOLUTION REQUIREMENTS FOR NUMERICAL SIMULATIONS OF TRANSITION Final Report
Thomas A. Zang, Steven E. Krist, and M. Yousuff Hussaini Jan. 1989 32 p Prepared in cooperation with NASA, Langley Research Center, Hampton, VA Submitted for publication

(Contract NAS1-18107)
(NASA-CR-181799; ICASE-89-9; NAS 1.26:181799) Avail: NTIS HC A03/MF A01 CSCL 20D

The resolution requirements for direct numerical simulations of transition to turbulence are investigated. A reliable resolution criterion is determined from the results of several detailed simulations of channel and boundary-layer transition. Author

N89-20412*# Institute for Computer Applications in Science and Engineering, Hampton, VA.
A SIMPLE NONLINEAR MODEL FOR THE RETURN TO ISOTROPY IN TURBULENCE Final Report
Sutanu Sarkar and Charles G. Speziale Feb. 1989 30 p Submitted for publication
(Contract NAS1-18605)
(NASA-CR-181797; ICASE-89-10; NAS 1.26:181797) Avail: NTIS HC A03/MF A01 CSCL 20D

A quadratic nonlinear generalization of the linear Rotta model for the slow pressure-strain correlation of turbulence is developed. The model is shown to satisfy realizability and to give rise to no stable non-trivial equilibrium solutions for the anisotropy tensor in the case of vanishing mean velocity gradients. The absence of stable non-trivial equilibrium solutions is a necessary condition to ensure that the model predicts a return to isotropy for all relaxational turbulent flows. Both the phase space dynamics and the temporal behavior of the model are examined and compared against experimental data for the return to isotropy problem. It is demonstrated that the quadratic model successfully captures the experimental trends which clearly exhibit nonlinear behavior. Direct comparisons are also made with the predictions of the Rotta model and the Lumley model. Author

N89-20413# Tampere Univ. of Technology (Finland). Dept. of Mechanical Engineering.
ZEOLITE/METHANOL: THE ADSORPTION HEAT PUMP
Martti Haerkoenen Feb. 1988 142 p In FINNISH; ENGLISH summary
(DE88-756310; TTKK-LT-58) Avail: NTIS (US Sales Only) HC A07/MF A01

This work deals with adsorption heat pump processes. The adsorption process was studied both theoretically and experimentally. Experiments were carried out using different types of synthetic zeolites as an adsorbent and methanol vapor as an adsorbate. Adsorption equilibrium curves were determined, heat of adsorption was measured calorimetrically and sorption kinetics was studied. The pump process was tested experimentally using the pairs 5A/CH(sub 3)OH, 13X/CH(sub 3)OH and 5A/H(sub 2)O. In order to study the effect of various parameters on the process, a simple numerical simulation model was developed and tested. DOE

N89-20414# Lawrence Livermore National Lab., CA.
TIME RESOLVED STUDY OF LIGHT EMITTED BY DETONATION ARRIVAL AT THE SURFACE OF HIGH EXPLOSIVES IN VARIOUS ENVIRONMENTS
Kerry L. Bahl and William G. VonHolle 24 Mar. 1988 7 p Presented at the 19th International ICT Conference on Combustion and Detonation, Karlsruhe, Federal Republic of Germany, 29 Jun. 1988
(Contract W-7405-eng-48)
(DE89-005657; UCRL-97701; CONF-880693-5) Avail: NTIS HC A02/MF A01

In search of a way to accurately measure time of arrival of detonation fronts, we have been using an electronic streak camera equipped with a light intensifier to record intensity-time histories of the light that is emitted when a detonation front emerges through the surface of high explosives in contact with various environments. Streak records at writing speeds up to 100 mm/microsec were obtained of detonations in air, argon, water and vacuum when the high explosive (HE) was either bare or covered with materials such as: aluminum silicofluoride (Al2(SiF6)3), PETN powder, polymethyl methacrylate (PMM), glass, aluminum foils, transparent tape, black ink, potassium chloride crystals, sodium chloride crystals and lithium fluoride crystals. The result of this study is that we believe that we can measure the time of arrival of a detonation front at a bare HE surface in air to within a few nanoseconds. DOE

N89-20415*# Texas A&M Univ., College Station. Dept. of Aerospace Engineering.
COMPUTATIONAL FLUID DYNAMICS AND AEROTHERMODYNAMICS Final Report, Jan. 1987 - Dec. 1988
Leland A. Carlson Mar. 1989 652 p
(Grant NAG9-192)
(NASA-CR-180079; NAS 1.26:180079; TAMRF-5671-89-01)
Avail: NTIS HC A99/MF A01 CSCL 20D

The primary objective was the development of nonequilibrium radiation and chemistry models suitable for engineering applications associated with the flow fields about aeroassisted orbital transfer vehicles (AOTVs), the aero-assisted flight experiment vehicle (AFE), and other vehicles operating at superorbital velocities and very high attitudes. Author

N89-20416# Aeronautical Research Inst. of Sweden, Stockholm. Aerodynamics Dept.
SOLUTIONS TO THE NAVIER-STOKES EQUATIONS USING A k-EPSILON TURBULENCE MODEL
Peter Eliasson 19 Apr. 1988 40 p Sponsored by the Swedish Board for Technical Development
(FFA-TN-1988-19; ETN-89-93730) Avail: NTIS HC A03/MF A01

The two-dimensional incompressible Navier-Stokes equations were solved numerically with the k-epsilon turbulence model for a flow over a backward facing step and in a rotating channel. The standard high Reynolds number model of the k-epsilon turbulence model was adopted. For the solution of the equations, an explicit Runge-Kutta, finite-volume solver was used. A stability analysis was performed for the condition of the local time step for the Runge-Kutta scheme. Results are presented in two dimensions for a flow over a backward facing step and in a rotating channel. The results are in very good agreement with experimental results for cases without rotation where the flow is not separated. Satisfactory results are also obtained over the backward facing step where the flow is separated, but the overall flow field seems to depend on the size of the mesh. It is shown that the standard k-epsilon turbulence model should not be used for rotating flow. ESA

N89-20417# Office National d'Etudes et de Recherches Aerospatiales, Paris (France).
LA RECHERCHE AEROSPATIALE, BIMONTHLY BULLETIN, NUMBER 1988-2, 243/JANUARY-FEBRUARY
ESA Nov. 1988 67 p Transl. into ENGLISH of La Recherche Aerospatiale (France), no. 1988-2, Jan. - Feb. 1988
(ESA-TT-1134; ETN-89-93910) Avail: NTIS HC A04/MF A01

Millimetric wave resonant cavities for contactless humidity measurements; detection of laminar-turbulent transition by infrared thermography; numerical solution of the Navier-Stokes equations by a multigrid method; an upwind scheme for computing supersonic flows around a tactical missile; and computation of the pressure in an incompressible rotational flow of inviscid fluid are discussed. ESA

N89-20418# Technische Univ., Delft (Netherlands). Faculty of Technical Mathematics and Informatics.
NUMERICAL STUDY OF NONLINEAR WAVE INTERACTIONS IN BUBBLY TWO-PHASE FLOW
A. J. N. Vreenegoor, P. Wilders, and J. A. Geurst 1988 21 p
(Rept-88-50; ISSN-0920-8577; ETN-89-94017) Copyright Avail: NTIS HC A03/MF A01

Variational methods were applied for the derivation of two-phase flow equations governing the inviscid dynamic behavior of bubbly liquid/gas mixtures. The corresponding equations, which possess real characteristics at marginal stability, are investigated with respect to their suitability for producing stable and reliable numerical results. The applied numerical method is based on a scheme

introduced by Lerat (1985). The interaction of acoustic waves and nonlinear concentration waves is used as a test case. Lerat's method works well. Although there is a large spreading in the order of magnitude of the physical variables, the computations proceed without any problems. Acoustic waves may be reflected by nonlinear concentration waves exhibiting a high gradient in the gas fraction. Bubble deformation has a reducing effect on acoustic waves. On the time scale investigated, nonlinear void-fraction waves reassume their initial shape after interaction with an acoustic disturbance. ESA

N89-20419# Technische Univ., Delft (Netherlands). Faculty of Technical Mathematics and Informatics.
DIFFERENTIAL EQUATIONS OF VISCOUS FLUID FLOW IN GENERAL CONDITIONS
C. Cuvelier 1988 47 p
(Rept-88-57; ISSN-0920-8577; ETN-89-94024) Copyright Avail: NTIS HC A03/MF A01

Numerical simulation of irregular flow shapes is considered. The governing transport equations, and boundary conditions written in terms of both Cartesian and contravariant vector and tensor components and arbitrary nonorthogonal coordinates are derived. The derivations are carried out for the three-dimensional situation. Simplifications for the two-dimensional case are discussed. The governing differential equations are presented one by one in an expanded form which is suitable for discretization in a finite volume fashion. ESA

N89-20420# National Aerospace Lab., Amsterdam (Netherlands). Informatics Div.
A NUMERICAL METHOD FOR THE SIMULATION OF LIQUID-SOLID BODY DYNAMICS
M. E. S. Vogels 1 Jan. 1988 13 p Presented at the 12th IMACS World Congress on Scientific Computation, Paris, France, 18-22 Jul. 1988
(Contract NIVR-02306N)
(NLR-MP-87030-U; ETN-89-94033) Avail: NTIS HC A03/MF A01

A numerical method for the simulation of the motion of a solid body with a cavity partially filled with liquid is presented. The coupled problem is partitioned into two subproblems, the motion of the solid body and the motion of the liquid in the cavity. The two subprocesses can be integrated using different time steps. The method is applied to the free, unconstrained, motion of a narrow annular tank partially filled with an inviscid liquid. In the test cases the liquid mass constitutes 10 pct, 50 pct, and 90 pct, of the total mass respectively. Results suggest that the fundamental frequency increases with increasing liquid mass fraction. ESA

N89-20421# Helsinki Univ. of Technology, Espoo (Finland). Dept. of Technical Physics.
QUASI-CLASSICAL CALCULATIONS FOR SUPERFLUIDS Ph.D. Thesis
Weiyi Zhang 1988 25 p Sponsored by the Chinese Ministry of Education and the Helsinki University of Technology, Espoo, Finland
(ETN-89-94118) Avail: NTIS HC A03/MF A01

The order parameter of superfluid He3-B near surfaces was calculated using the quasiclassical theory and a thin-dirty-layer surface scattering model. The calculation shows that there are macroscopic spin currents flowing along the surface even without the mass current, a phenomenon which is consistent with the rotation symmetry and may favor the nucleation of spin-current vortices. The order parameter is used to study the effects of a rough surface on the tunneling density of states of He3-B. Quasiclassical methods are used to study the reflection of quasiparticle wave packets at diffusely scattering surfaces of He3. In addition to conversion into the nonmagnetic and magnetic holes, and partial reflection into the nonmagnetic and magnetic particle wave packets in the principal direction, diffuse background scattering of nonmagnetic and magnetic particles and holes into all directions is found. The effective viscosity of Poiseuille flow of He3-B between parallel plates is calculated as a function of temperature and pressure for arbitrarily rough surfaces using the Andreev scattering coefficient. Effects of rough interfaces on current-phase relations in planar junctions were calculated. ESA

N89-20422# Von Karman Inst. for Fluid Dynamics, Rhode-Saint-Genese (Belgium).
A CALCULATION METHOD FOR COMPRESSIBLE THREE DIMENSIONAL TURBULENT BOUNDARY LAYER FLOWS
L. J. Johnston Jul. 1988 82 p
(VKI-TN-167; ETN-89-94121) Avail: NTIS HC A05/MF A01

A calculation method for compressible 3D boundary layers is described. The method involves a finite difference discretization of the governing mean flow equations. The differencing scheme used to discretize spanwise derivatives adapts automatically to the sign of the local crossflow within the boundary layer. A plane-by-plane solution procedure in the spanwise direction enables second-order accuracy to be maintained throughout the whole flow field. A normal coordinate scaling with the local total momentum thickness removes most of the boundary layer growth in computational space. The method is applied to a range of experimental flows, including compressible subsonic and supersonic free stream conditions. The Cebeci-Smith algebraic turbulence model is used for the initial validation of the calculation method. A simple modification to this model is tested, involving an explicit dependence of the outer eddy viscosity on the crossflow within the boundary layer. A significantly improved prediction of an infinite swept wing flow experiment is obtained. ESA

N89-20423# Von Karman Inst. for Fluid Dynamics, Rhode-Saint-Genese (Belgium).
AN EXPLICIT FINITE DIFFERENCES SOLVER FOR THE INCOMPRESSIBLE REYNOLDS AVERAGED NAVIER-STOKES EQUATIONS, OPTIMIZED FOR THE ALLIANT DSP 9000 COMPUTER
C. Benocci Jul. 1988 38 p
(VKI-TM-45; ETN-89-94122) Avail: NTIS HC A03/MF A01

A solver for the incompressible, Reynolds averaged Navier-Stokes equations, based upon the projection method, was optimized for the Alliant DSP 9000 computer. It is shown that the straightforward explicit form with local time stepping is preferable for the predictor step, and that use of an explicit pressure correction technique is fundamental to exploit fully the advantages of vectorial-concurrent execution. It is also shown that hybrid differencing of the advection term yields results superior to the use of an explicit artificial diffusivity. The limits of the linear k-epsilon turbulence model for the prediction of flow round a backward facing step are confirmed. ESA

N89-20424# Center for Mathematics and Computer Science, Amsterdam (Netherlands). Dept. of Numerical Mathematics.
MULTIGRID AND DEFECT CORRECTION FOR THE STEADY NAVIER-STOKES EQUATION
Barry Koren Mar. 1988 16 p Presented at the 4th GAMM-Seminar on Robust Multi-Grid Methods, Kiel, Fed. Republic of Germany, 22-24 Jan. 1988 Sponsored by ESA, France and Avions Marcel Dassault-Breguet Aviation, Saint-Cloud, France
(CWI-NM-R8803; B8821060; ETN-89-94180) Copyright Avail: NTIS HC A03/MF A01

Theoretical and experimental convergence results are presented for multigrid and iterative defect correction applied to finite volume discretizations of the steady, 2D, compressible Navier-Stokes equations. Iterative defect correction is introduced for circumventing the difficulty in finding a solution of discretized equations with a second- or higher-order accurate convective part. As a smoothing technique, use is made of point Gauss-Seidel relaxation with, inside the latter, Newton iteration as a basic solution method. The multigrid technique appears to be very efficient for smooth as well as non-smooth problems. Iterative defect correction appears to be very efficient for smooth problems only, though still reasonably efficient for non-smooth problems. ESA

N89-20425# Lawrence Livermore National Lab., CA.
NUMERICAL SIMULATION OF TURBULENT MIXING IN SHOCK-TUBE EXPERIMENTS
Karnig O. Mikaelian 28 Nov. 1988 11 p Presented at the Workshop on the Physics of Compressible Turbulent Mixing, Princeton, NJ, 24-27 Oct. 1988
(Contract W-7405-eng-48)
(DE89-005101; UCRL-100098; CONF-8810234-5) Avail: NTIS HC A03/MF A01

We have carried out a number of 2D numerical simulations on an ALE code for shock-tube experiments in which a shock crosses one or more contact discontinuities and, after traveling through a homogeneous medium, reflects off a rigid wall at the end of the shock-tube and re-crosses the contact discontinuity. We have considered two-fluid and three-fluid experiments: the first fluid, which carries the original shock, is air; the other fluids are helium, freon, SF, or air again. Helium is lighter than air, while freon and SF are heavier than air. The interface(s) between the fluids serve as contact discontinuities and are subjected to the original shock, the re-shock, and subsequent rarefactions/compressions. DOE

N89-20426# Calspan Corp., Buffalo, NY.
TRANSMISSION AND REFLECTION ON PRESSURE WAVES BY COMPRESSOR AND TURBINE STAGES, BASED ON AN ACTUATOR-DISK MODEL Technical Report, 1 Jun. 1986 - 1 Sep. 1987
W. J. Rae, P. F. Batcho, and M. G. Dunn 1 Feb. 1988 49 p
(Contract DNA001-83-C-0182; DNA Proj. N99-QMXA)
(AD-A203513; CALSPAN-7170-7; DNA-TR-88-58) Avail: NTIS HC A03/MF A01 CSCL 20D

The amplitudes of the pressure waves transmitted and reflected by an actuator disk due to the impingement of an incident pressure wave calculated. Analytic expressions for the wave amplitudes are derived for the limit where the incident pressure rise is small and these formulas, as well as direct calculations, are used to estimate the effect of multiple wave reflections from a pair of actuator disks. These predictions help to explain a number of phenomena that have been observed in measurements made when shock-tube generated overpressure waves were sent into an operating engine. GRA

N89-20427# Massachusetts Inst. of Tech., Cambridge. Acoustics and Vibration Lab.
DYNAMIC WALL PRESSURE MEASUREMENTS
Patrick Leehey Aug. 1988 31 p
(Contract N00014-86-K-0183)
(AD-A203551; A/V-97457-2) Avail: NTIS HC A03/MF A01 CSCL 20D

The state of the art in measurement and interpretation of dynamic wall pressure beneath a turbulent boundary layer is reviewed. The mean pressure increase for shear flow over an orifice in a wall is explained, using triple deck theory, to stem from streamline contraction resulting from removal of the no-slip boundary condition. The effect in viscous hole diameters is too small to suggest that the dynamic pressure increase reported by Bull and Thomas (1976) for flow over a pinhole microphone stems from this mechanism. It appears that any failure of high frequency spectra to collapse when made non-dimensional on inner wall variables is more likely due to transducer proudness or to error in the measurement of mean wall shear stress. The Corcos model is shown to be inadequate to describe cross-spectrum measurements. Both amplitude and phase depend also on the ratio of transducer separation to displacement boundary layer thickness. GRA

N89-20428# California Univ., Berkeley. Dept. of Mechanical Engineering.
VORTICITY DISTRIBUTIONS IN UNSTEADY FLOW SEPARATION Final Technical Report, 1 Aug. 1986 - 1 Nov. 1988
Frederick M. Sherman 8 Nov. 1988 21 p
(Grant AF-AFOSR-0168-86; AF Proj. 2307)
(AD-A203733; AFOSR-89-0057TR) Avail: NTIS HC A03/MF A01 CSCL 20D

Computational analysis and results are reported for three problems. (1) Development of a laminar boundary layer on both the windward and leeward sides of a plate which is moved impulsively normal to its plane. The model of inviscid flow outside the boundary layer includes a moving and intensifying line vortex, which approximates the vortex spiral cast off from the edge of the plate. (2) Mutually-induced movement and interdiffusion of counter-rotating viscous line vortices, simulated by the random-vortex method. (3) Development of flow separation on a slender elliptical cylinder, which is impulsively set into rotation around its central axis, also simulated by the random-vortex method. GRA

N89-20429# Naval Postgraduate School, Monterey, CA.
FLOW VISUALIZATION OF TIME-VARYING STRUCTURAL CHARACTERISTICS OF DEAN VORTICES IN A CURVED CHANNEL M.S. Thesis
David Wayne Bella Dec. 1988 109 p
(AD-A203875) Avail: NTIS HC A06/MF A01 CSCL 20D

The time varying development and structure of Dean vortices were studied using flow visualization. Observations were made over a range of Dean numbers from 40 to 200 using a transparent channel with mild curvature, 40:1 aspect ratio, and an inner to outer radius ratio of 0.979. Seven flow visualization techniques were tried but only one, a wood burning smoke generator, produced usable results. Different vortex characteristics were observed and documented in sequences of photographs spaced one quarter of a second apart at locations ranging from 85 to 135 degrees from the start of curvature. Evidence is presented that supports the twisting/rocking nature of the flow. GRA

35 INSTRUMENTATION AND PHOTOGRAPHY

Includes remote sensors; measuring instruments and gages; detectors; cameras and photographic supplies; and holography.

For aerial photography see *43 Earth Resources and Remote Sensing.* For related information see also *06 Aircraft Instrumentation,* and *19 Spacecraft Instrumentation.*

N89-20430*# National Aeronautics and Space Administration. Marshall Space Flight Center, Huntsville, AL.
IMPROVED CAPABILITIES OF THE MULTISPECTRAL ATMOSPHERIC MAPPING SENSOR (MAMS)
Gary J. Jedlovec, K. Bryan Batson, Robert J. Atkinson, Chris C. Moeller, W. Paul Menzel (National Oceanic and Atmospheric Administration, Madison, WI.), and Mark W. James Jan. 1989 80 p
(NASA-TM-100352; NAS 1.15:100352) Avail: NTIS HC A05/MF A01 CSCL 14B

The Multispectral Atmospheric Mapping Sensor (MAMS) is an airborne instrument being investigated as part of NASA's high altitude research program. Findings from work on this and other instruments have been important as the scientific justification of new instrumentation for the Earth Observing System (EOS). This report discusses changes to the instrument which have led to new capabilities, improved data quality, and more accurate calibration methods. In order to provide a summary of the data collected with MAMS, a complete list of flight dates and locations is provided. For many applications, registration of MAMS imagery with landmarks is required. The navigation of this data on the Man-computer Interactive Data Access System (McIDAS) is discussed. Finally, research applications of the data are discussed and specific examples are presented to show the applicability of these measurements to NASA's Earth System Science (ESS) objectives. Author

N89-20431# Academia Sinica, Beijing (China). Cryogenic Lab.
NEW TYPE OF CAPACITIVE TEMPERATURE SENSOR FOR USE AT LOW TEMPERATURE AND IN STRONG MAGNETIC FIELD
Pu-fen Chen and Jin-wan Li 1987 8 p Sponsored by Institute of Scientific and Technical Information of China, Beijing
(PB89-111108; ISTIC-TR-C-000183) Avail: NTIS HC A02/MF A01 CSCL 14B

Preliminary measurements are reported on the characteristics of the miniature PMN ceramic condensers as a temperature sensor. The condenser has dimensions of 6x4x2.5 cu mm. The capacitance decreases monotonously from 1400 nF at 250 K to 18 nF at 2 K. The relative temperature sensitivity (Delta C/Delta T)(1/C) is 3 percent to 0.5 percent in the temperature range from 250 K to 2 K. The capacitance was uneffected by the magnetic field up to 5 T at 4.2 K. Author

N89-20432*# Texas Univ. at Dallas, Richardson. Center for Space Sciences.
AFE ION MASS SPECTROMETER DESIGN STUDY Final Technical Report, 1 Jun. 1987 - 31 Mar. 1989
Willie Wright 14 Mar. 1989 51 p
(Contract NCC1-119)
(NASA-CR-184838; NAS 1.26:184838) Avail: NTIS HC A04/MF A01 CSCL 14B

This final technical report covers the activities engaged in by the University of Texas at Dallas, Center for Space Sciences in conjunction with the NASA Langley Research Center, Systems Engineering Division in design studies directed towards defining a suitable ion mass spectrometer to determine the plasma parameter around the Aeroassisted Flight Experiment vehicle during passage through the earth's upper atmosphere. Additional studies relate to the use of a Langmuir probe to measure windward ion/electron concentrations and temperatures. Selected instrument inlet subsystems were tested in the NASA Ames Arc-Jet Facility. Author

N89-20433# National Ocean Service, Rockville, MD. Office of Charting and Geodetic Services.
POTENTIAL OF LARGE FORMAT CAMERA PHOTOGRAPHY
Roop C. Malhotra Aug. 1988 33 p
(PB89-122485; NOAA-TR-NOS-128; CGS-13) Avail: NTIS HC A03/MF A01 CSCL 14E

The simulated system study explores the potential of large format camera (LFC) photography for conducting photogrammetric control extension. The study is based on a series of error propagation analyses in photogrammetric triangulation of a block of 22 LFC photographs. The photographs, which have an approx. scale of 1:755,000, were taken during the Oct. 1984 NASA shuttle mission STS-41G. Several present and future systems of data acquisition and reduction were simulated. Author

N89-20434# Helsinki Univ. of Technology, Espoo (Finland). Dept. of Technical Physics.
ON THE PERFORMANCE OF THE DELPHI HADRON CALORIMETER Ph.D. Thesis
Markku Ellila 1988 53 p Sponsored by the Academy of Finland
(Ph-159; ISBN-951-666-259-5; ISSN-0355-2721; ETN-89-94119) Avail: NTIS HC A04/MF A01

High energy physics studied at electron-positron colliders is reviewed. The principles of hadronic energy measurement in experimental high energy physics are introduced. The large electron-positron storage ring (LEP) under construction at CERN is presented together with its experimental program, including the DELPHI experiment. The design and operation of the DELPHI hadron calorimeter are outlined. The expected performance of the calorimeter was studied by exposing a small prototype, of 1 cu m, to hadron and muon beams. The energy resolution is 80 pct per sq rt E. A combination of a lead-glass electromagnetic calorimeter and the hadron calorimeter prototype gives a resolution of 45 pct for 9 GeV/c pions, whereas the hadron calorimeter alone measures the energy with a 35 pct resolution. Dead-space effects were also studied, to assess resolution degradation in the center of the barrel where inactive detector ends are staggered. The FWHM of the measured signal increases from 50 pct to 60 pct for a 37.5 GeV pion beam at the center of the staggered dead-space. The performance of the calorimeter in fast muon triggering was studied. The results indicate that a trigger efficiency higher than 90 pct can be reached in the region theta less than 30 deg, except for a small slot (delta theta = 2.96 deg) between the barrel and the end-cap, without the second-level trigger being disturbed by an unacceptable number of false triggers. The efficiency in the very forward region of the end-cap can reach 80 pct or more in the same conditions. ESA

N89-20435# Argonne National Lab., IL. Materials Science Div.
NEW DIRECTIONS IN SPECTROSCOPY FOR THE ANALYTICAL ELECTRON MICROSCOPE
Nestor J. Zaluzec Aug. 1988 5 p Presented at the 4th Annual Analytical Electron Microscopy Conference, Tokyo, Japan, 30 Aug. 1988
(Contract W-31-109-eng-38)
(DE89-005824; CONF-8808186-1) Avail: NTIS HC A02/MF A01

The concept of using the transmission electron microscope as a high spatial resolution microcharacterization laboratory is now well established, and AEM has been extremely successful over the last decade in solving problems in materials science. Rather than review past accomplishments we shall instead address the topic of the new spectroscopies in the AEM suggesting directions which may develop into fruitful methodologies in the near future. DOE

N89-20436# Lawrence Livermore National Lab., CA.
THE EFFECTS OF VARIATIONS IN THE PHOTOCATHODE VOLTAGES OF ELECTRONIC STREAK CAMERAS
M. W. Bowers, G. L. Biggs, J. J. Ronchetto, and A. T. Teruya Aug. 1988 10 p Presented at the 32nd International Technical Symposium on Optical and Opto-Electronic Applied Sciences and Engineering, San Diego, CA, 14 Aug. 1988
(Contract W-7405-eng-48)
(DE89-006776; UCRL-99282; CONF-880887-30) Avail: NTIS HC A02/MF A01

Electronic streak cameras are used to record subnanosecond data at the Nevada Test Site. It has been found that externally induced variations in the photocathode voltage of the streak tube can produce both temporal and spatial errors on the output image. An electron beam tracing code was used to model the magnification as a function of photocathode voltage and signal input position for streak tubes manufactured by RCA, ITT, and Kentech. Laboratory tests were also performed where pulsed and radio frequency signals were induced upon the photocathode and the errors on the resultant image were compared with the error predicted by the electron beam code. Also, methods for processing the distortion in digitized images were investigated. This paper will discuss the results of these investigations. DOE

N89-20437*# Oak Ridge National Lab., TN.
OPTICAL JOHNSON NOISE THERMOMETRY
R. L. Shepard, T. V. Blalock, L. C. Maxey, M. J. Roberts, and M. L. Simpson 1989 20 p Presented at the NASA Workshop on Non-Contact Temperature Measurement, Pasadena, CA, 17 Jan. 1989 Sponsored by NASA, Marshall Space Flight Center, Huntsville, AL
(Contract DE-AC05-84OR-21400)
(NASA-CR-184964; NAS 1.26:184964; DE89-006036; CONF-890168-1) Avail: NTIS HC A03/MF A01 CSCL 14B

A concept is being explored that an optical analog of the electrical Johnson noise may be used to measure temperature independently of emissivity. The concept is that a laser beam may be modulated on reflection from a hot surface by interaction of the laser photons with the thermally agitated conduction electrons or the lattice phonons, thereby adding noise to the reflected laser beam. If the reflectance noise can be detected and quantified in a background of other noise in the optical and

signal processing systems, the reflectance noise may provide a noncontact measurement of the absolute surface temperature and may be independent of the surface's emissivity. DOE

N89-20438# Lawrence Livermore National Lab., CA. Environmental Sciences Div.
CURRENT STATUS OF THE NAVSEA BACKSCATTER ABSORPTION GAS IMAGING (BAGI) DEVELOPMENT PROJECT
Thomas J. Kulp, Randall Kennedy, Darrel Garvis, Thomas G. McRae, and Joe Stahovec (Naval Sea Systems Command, Washington, DC.) Jan. 1989 14 p Presented at the SPIE Conference on Optics, Electro-Optics and Laser Applications in Science and Engineering: OE/LASE '89, Los Angeles, CA, 15 Jan. 1989
(Contract W-7405-eng-48)
(DE89-006728; UCRL-99287; CONF-890145-13) Avail: NTIS HC A03/MF A01

The Backscatter Absorption Gas Imaging (BAGI) technique allows the real-time visualization of visibly undetectable gas clouds. A BAGI instrument has been built that consists of a laser active-imager and allows gas imaging to be performed on at least 60 gas species at ranges of up to 30 m. The tunability of the CO2 laser used in the instrument also allows some gas discrimination. A longer-range (300 m) instrument is currently being constructed. The use of image-processing techniques, in addition to hardware modifications (such as rapid wavelength switching) will allow more information to be extracted from BAGI images. Data such as approximate cloud size, approximate gas concentration range, and visible gas flow patterns, will be useful for experimental verification of gas-transport models as well as for other practical applications. DOE

N89-20439# Massachusetts Inst. of Tech., Cambridge. Artificial Intelligence Lab.
REAL-TIME PART POSITION SENSING
Steven J. Gordon and Warren P. Seering May 1988 34 p
(Contracts N00014-85-K-0124; N00014-86-K-0685)
(AD-A203580; AI-M-1032) Avail: NTIS HC A03/MF A01
CSCL 14D

A light stripe vision system is used to measure the location of polyhedral features of parts from a single frame of video camera output. The geometric conditions which assure location of the feature when the light plane intersects three of the feature's faces are given. Issues such as accuracy in locating the line segments of intersection in the image and combining redundant information from multiple measurements and multiple sources are addressed. In 2.5 seconds, a prototype sensor was capable of locating a two inch cube to an accuracy (one standard deviation) of .002 inches (.055 mm) in translation and .1 degrees (.0015 radians) in rotation. When integrated with a manipulator, the system was capable of performing high precision assembly tasks. GRA

36 LASERS AND MASERS

Includes parametric amplifiers.
For related information see also *76 Solid-State Physics.*

N89-20440# Naval Research Lab., Washington, DC. Geophysical and Plasma Dynamics Branch.
STIMULATED RAMAN SCATTERING OF INTENSE LASER RADIATION IN A NUCLEAR-DISTURBED SPACE PLASMA Interim Report
M. J. Keskinen and Y. C. Lee 8 Nov. 1988 18 p Prepared in cooperation with Science Applications International Corp., McLean, VA; and Maryland Univ., College Park
(AD-A200951; NRL-MR-6369) Avail: NTIS HC A03/MF A01
CSCL 20F

Stimulated Raman scattering of intense laser radiation propagating in a nuclear-disturbed space plasma environment has been investigated. For parameters typical of a single high altitude nuclear explosion (HANE), we use propagation due to Raman scattering, particularly for 10 micrometer radiation, 10 micrometer, respectively, and for beam power densities on the order of 100000 W/sq cm. Here gamma is the growth rate for simulated Raman scattering. For the multiple HANE case, approximate growth times 1/gamma about .001 to .01 sec can be achieved for laser wavelengths 1 micrometer 10 micrometer with beam power densities of 100000 W/sq cm. As a result, a single burst HANE is not likely, due to stimulated Raman scattering, to effect the propagation of laser radiation with wavelengths of 10 micrometer and 1 micrometer and power densities on the order of 100000 W/sq cm. However, the multiburst HANE environment may degrade laser propagation due to Raman scattering, particularly for 10 micrometer radiation. GRA

N89-20441# Lawrence Livermore National Lab., CA.
Q-SWITCHED, INTRACAVITY DOUBLED Nd:YAG LASER SIDE-PUMPED BY A LASER DIODE ARRAY
I. L. Bass and R. W. Presta 1989 9 p Presented at the Symposium on Lasers and Optics, Los Angeles, CA, 15-20 Jan. 1989
(Contract W-7405-eng-48)
(DE89-005349; UCRL-99702; CONF-890142-3) Avail: NTIS HC A02/MF A01

An intracavity-doubled, Q-switched, Nd:YAG laser side pumped by a pulsed, 3-bar, laser-diode array, produced a second harmonic output of 1.75 mJ/pulse at an optical conversion efficiency of 11.5 percent. We demonstrated the use of this laser to pump a pulsed dye laser via an optical fiber. DOE

N89-20442# Los Alamos National Lab., NM.
PULSED LASER EFFECTS PHENOMENOLOGY
Ronald S. Dingus, S. Robert Goldman, Ronald C. Kirkpatrick, Lee M. Montierth, and E. K. Stover 1988 11 p Presented at the SPIE Conference on Optics, Electro-optics and Laser Applications in Science and Engineering: OE/LASE '89, Los Angeles, CA, 15 Jan. 1989
(Contract W-7405-eng-36)
(DE89-005466; LA-UR-88-4278; CONF-890145-1) Avail: NTIS HC A03/MF A01

A comprehensive overview of the phenomenology associated with the interaction of intense laser beams with matter is presented. The beam is assumed to be incident on a solid or liquid target located within a transport medium. The discussion is first categorized by the type of this medium; namely, vacuum, gas, liquid, solid or particulate. Then the dependence of the interaction is further classified by the laser flux, pulselength, wavelength and the target properties. The various classes of behavior are discussed along with the conditions for their occurrence. Classes discussed include: slow bulk heating, transparent vapor from the target surface, secondary energy transport to the ablation surface, laser absorption at the critical surface, shock induced blowoff, photoelectric cross section dependence on temperature and density, laser supported combustion and detonation, contained vaporization and Mie scattering. DOE

N89-20443# Los Alamos National Lab., NM.
DEVELOPMENT KrF LASERS FOR INERTIAL CONFINEMENT FUSION
J. F. Figueira, L. A. Rosocha, M. S. Sorem, and D. B. Harris 1989 8 p Presented at the SPIE Conference on Optics, Electro-optics and Laser Applications in Science and Engineering: OE/LASE '89, Los Angeles, CA, 15 Jan. 1989
(Contract W-7405-eng-36)
(DE89-005469; LA-UR-88-4206; CONF-890145-5) Avail: NTIS HC A02/MF A01

High peak power rare gas halide lasers for applications in Inertial Confinement Fusion are being developed at laboratories across the world. The United States Department of Energy sponsors a program conducted at the Los Alamos National Laboratory and the Naval Research Laboratory. The Los Alamos laser development program is composed of three major elements; the Aurora Laser Facility is a 1 terawatt KrF laser designed as an integrated performance demonstration of a target qualified excimer laser

system; an advanced design effort evaluates concepts that offer the improved performance and lower cost that will be essential for the construction of future lasers in the 0.5 to 10 MJ class; and a laser technology program that addresses both performance and cost issues that will be important in advanced laser system designs. DOE

N89-20444# Lawrence Livermore National Lab., CA.
HIGH POWER INDUCTION FREE ELECTRON LASER
John L. Miller Dec. 1988 7 p Presented at the Modeling and Simulation of Laser Systems, Los Angeles, CA, 15-20 Jan. 1989
(Contract W-7405-eng-48)
(DE89-006208; UCRL-99062; CONF-890154-2) Avail: NTIS HC A02/MF A01

Free electron laser (FEL) amplifiers driven by linear induction accelerators have considerable potential for scaling to high average powers. The high electron beam current produces large single pass gain and extraction efficiency, resulting in high peak power. The pulse repetition frequency scaling is limited primarily by accelerator and pulsed power technology. Two FEL experiments have been performed by the Beam Research Program at the Lawrence Livermore National Laboratory (LLNL): The ELF experiment used the 3.5-MeV beam from the Experimental Test Accelerator (ETA) and operated at a wavelength of 8.6 mm. This device achieved an overall single-pass gain of 45 dB, an output power of 1.5 GW, and an extraction efficiency of 35 percent. The microwave beam was confined in a waveguide in the 4-m-long wiggler. The PALADIN experiment uses the 45-MeV beam from the Advanced Test Accelerator and operates at a wavelength of 10.6 micrometers. Using a 15-m long wiggler a single pass gain of 27 dB was produced. Gain guiding was observed to confine the amplified beam within a beam tube that had a Fresnel number less than 1. The results of these experiments have been successfully modeled using a three dimensional particle simulation code. The Program also has ongoing efforts to develop wiggler, pulsed power and induction linac technology. A focus of much of this work is the ETA-II accelerator, which incorporates magnetic pulse compression drivers. One application of ETA-II will be to drive a 1 mm wavelength FEL. The microwave output will be used for a plasma heating experiment. DOE

N89-20445# Los Alamos National Lab., NM.
ILS (INTRACAVITY LASER SPECTROSCOPY) FOR BEAM SENSING (EXPERIMENT) Final Report
Hiroshi W. Hoida and Frank C. Jahoda Jan. 1989 48 p
(Contract W-7405-eng-36)
(DE89-006376; LA-11369-MS) Avail: NTIS HC A03/MF A01

Intracavity laser spectroscopy (ILS) was studied with lithium as the absorber within a dye laser. Also studied was lithium within a chromium-perovskite solid-state laser. The dye laser was turned on quickly for one mode of operation as well as scanned in wavelength for the other two modes of operation. The wavelength scanning was accomplished with a birefringent electro-optic tuner, which was varied in scanning frequency and wavelength amplitude. For broadband ILS with the laser turned on quickly, the absorption was observed to grow exponentially until it saturated. Two different modes of operation were observed when the laser was scanned. At low frequencies (less than 30kHz) the results were similar to the broadband ILS in that the depth of the growth was dependent on the spectral dwell time (the time the laser lases at one wavelength). For fast scanning at the cavity resonance period, the absorption feature broadened in wavelength as the resonance frequency was approached although the total absorption remained about the same. The chromium-perovskite solid-state laser was also used with broadband ILS. The absorption feature was observed. DOE

N89-20446# Consultec Scientific, Inc., Knoxville, TN.
ASSESSMENT OF RESEARCH NEEDS FOR LASER TECHNOLOGIES APPLIED TO ADVANCED SPECTROGRAPHIC METHODS Project Status Report
31 Jan. 1989 6 p
(Contract DE-AC01-88ER-30131)
(DE89-006455; DOE/ER-30131/T1) Avail: NTIS HC A02/MF A01

Our project to assess the DOE/OHER research needs for laser technologies applied to advanced spectrographic methods is progressing well and on schedule. The main panel met in Knoxville in November 1988 to discuss the impact that laser spectroscopy and technology could make on future directions of the OHER. It was a very enthusiastic meeting which resulted in a number of quite valuable suggestions. Following this meeting, nearly every panel member has completed his first assignment, and, as anticipated, the work has been extremely good. My only objection is that of length; we have now amassed about 150 double-spaced pages. Generally speaking, we now need to look for gaps, decide on deletions, and then proceed with the project. DOE

N89-20447*# Hampton Inst., VA. Dept. of Physics.
DIRECT SOLAR-PUMPED IODINE LASER AMPLIFIER Semiannual Progress Report, 1 Sep. 1988 - 28 Feb. 1989
Kwang S. Han, In Heon Hwang, and Larry V. Stock Feb. 1989 30 p
(Grant NAG1-441)
(NASA-CR-184813; NAS 1.26:184813) Avail: NTIS HC A03/MF A01 CSCL 20E

This semiannual progress report covers the period from September 1, 1988 to February 28, 1989 under NASA grant NAG-1-441 entitled, Direct Solar-Pumped Iodine Laser Amplifier. During this period, the research effort was concentrated on the solar pumped master oscillator power amplifier (MOPA) system using n-C3F7I. In the experimental work, the amplification measurement was conducted to identify the optimum conditions for amplification of the center's Vortek solar simulator pumped iodine laser amplifier. A modeling effort was also pursued to explain the experimental results in the theoretical work. The amplification measurement of the solar simulator pumped iodine laser amplifier is the first amplification experiment on the continuously pumped amplifier. The small signal amplification of 5 was achieved for the triple pass geometry of the 15 cm long solar simulator pumped amplifier at the n-C3F7I pressure of 20 torr, at the flow velocity of 6 m/sec and at the pumping intensity of 1500 solar constants. The XeCl laser pumped iodine laser oscillator, which was developed in the previous research, was employed as the master oscillator for the amplification measurement. In the theoretical work, the rate equations of the amplifier was established and the small signal amplification was calculated for the solar simulator pumped iodine laser amplifier. The amplification calculated from the kinetic equations with the previously measured rate coefficients reveals very large disagreement with experimental measurement. Moreover, the optimum condition predicted by the kinetic equation is quite discrepant with that measured by experiment. This fact indicates the necessity of study in the measurement of rate coefficients of the continuously pumped iodine laser system. Author

N89-20448# Los Alamos National Lab., NM. Chemical and Laser Sciences Div.
DAMAGE TO SILVER COATINGS FROM HIGH AVERAGE POWER 1-MICRON LASER
Virgil R. Sanders, L. John Jolin, and S. Salazar 1988 6 p Presented at the Laser Induced Damage in Optical Materials, Boulder, CO, 26 Oct. 1988
(Contract W-7405-eng-36)
(DE89-005476; LA-UR-88-4236; CONF-8810284-1) Avail: NTIS HC A02/MF A01

Optical coatings are being developed for use in high average power, pseudo continuous wave, 1-micron lasers. In particular, the subject of this study is a silver coating to be applied to a cooled substrate for use in a radio frequency-free electron laser (RF-FEL). Damage threshold measurements and finite element calculations were made that demonstrate the pure thermal nature of heating, and eventual damage, RF-FEL pulse format. DOE

N89-20449# Lawrence Livermore National Lab., CA.
GROUND STATE DEPLETED LASER EXPERIMENTS

R. Beach, R. Solarz, S. Mitchell, L. Brewer, and S. Weinzapfel 1989 18 p Presented at the SPIE Conference on Optics, Electro-Optics and Laser Applications in Science and Engineering: Los Angeles, CA, 15 Jan. 1989
(Contract W-7405-eng-48)
(DE89-006146; UCRL-99458; CONF-890145-2) Avail: NTIS HC A03/MF A01

Spectroscopic measurements have been performed at Livermore in various Nd doped glass and crystalline materials to extract parameters (stark resolved emission spectra, branching ratios, fluorescence lifetimes, and stimulated emission cross sections) important to the design of a GSD laser. This study has allowed us to identify several systems amenable to experimental demonstration. The results of a demonstration in one of these systems consisting of a sample of Nd doped Y(sub 2)SiO(sub 5) which is pumped by a flash lamp pumped dye laser will be presented. Measurements are made to document the degree to which the ground state of the laser has been depleted. An important problem present in GSD lasers, illustrated by the results of our demonstration, is holding off the gain of the (4) F(sub 3/2) - (4) I(sub 11/2) transition which typically has an emission cross section 5 to 10 times larger than the desired (4) F(sub 3/2) - (4) I(sub 9/2) transition cross section. Several possible techniques for holding off the (4) F(sub 3/2) - (4) I(sub 11/2) transition are discussed. These techniques include segmented laser designs, and the co-doping of laser samples with elements having a large absorption cross section in the 1.06 micron region while being relatively free of absorption in the 0.92 micrometer region of the spectrum. DOE

N89-20450# Lawrence Livermore National Lab., CA.
GROUND STATE DEPLETED (GSD) SOLID STATE LASERS: PRINCIPLES, CHARACTERISTICS, AND SCALING
William F. Krupke and Lloyd L. Chase Jan. 1989 18 p Presented at the SPIE Conference on Optics, Electro-Optics and Laser Applications in Science and Engineering: Los Angeles, CA, 15 Jan. 1989
(Contract W-7405-eng-48)
(DE89-006149; UCRL-99430; CONF-890145-12) Avail: NTIS HC A03/MF A01

A novel class of rare earth doped solid state lasers is described. The Ground State Depleted (GSD) laser is pumped by an intense narrowband laser source and is characterized by: an unusually low laser ion doping density, an unusually large fractional excited population inversion density, a gain element that is optically thick at the pump wavelength, and a gain element that has a substantially uniform gain distribution. These features enable efficient room temperature operation of rare earth ion laser transitions terminating on the ground manifold. The relationships between laser parameters (cross sections, saturation fluences and fluxes, bleaching wave velocities, etc) are given and laser performance scaling relationships are presented and discussed. DOE

N89-20451# Lawrence Livermore National Lab., CA.
SIMULATION OF SUPERRADIANT FREE-ELECTRON LASERS
W. M. Sharp, W. M. Fawley, S. S. Yu, A. M. Sessler, R. Bonifacio, and L. deSalvoSouza (Milan Univ., Italy) Jan. 1989 16 p Presented at the 10th International Free-Electron Laser Conference, Jerusalem, Israel, 29 Aug. 1988 Prepared in cooperation with Istituto Nazionale di Fisica Nucleare, Milan, Italy
(Contract W-7405-eng-48)
(DE89-006156; UCRL-98676; CONF-8808146-12) Avail: NTIS HC A03/MF A01

It has been suggested that slippage effects in a single-pass free-electron laser can generate an output signal near the electron beam tail with a peak amplitude many times greater than the expected saturated value. The growth of such superradiant pulses in a helical-wiggler FEL is characterized here using 1-D and 2-D numerical simulations. The 1-D calculations show the effects of detuning, energy spread, and the axial current distribution on superradiant pulses, while preliminary 2-D simulations illustrate the effects of betatron motion and the radial structure of the electron beam. DOE

N89-20452# Lawrence Livermore National Lab., CA.
VALIDITY OF 1D FREE-ELECTRON LASER SIDEBAND MODELS
W. M. Sharp and S. S. Yu Jan. 1989 25 p Presented at the 9th International Free-Electron Laser Conference, Williamsburg, VA, 14 Sep. 1987
(Contract W-7405-eng-48)
(DE89-006284; UCRL-96880; CONF-8709110-25) Avail: NTIS HC A03/MF A01

Analytical 1-D models have been used to estimate sideband growth in a free-electron laser (FEL) with a constant-amplitude primary wave. A simple 2-D sideband model is used here to show that the 1-D approximation is valid only when the beam radius r sub b is large compared with (2 k sub s min(omega sub 0, d phi sub 0/dz)) sup -1/2, where k sub s and phi sub 0 are the wavenumber and phase of the primary wave and omega sub 0 is the maximum synchrotron wavenumber of trapped electrons. For smaller r sub b values, sideband growth rates are reduced below 1D predictions, and both the growth rate scaling with beam density and the primary-wave amplitude, are altered. DOE

N89-20453# California Univ., Berkeley. Lawrence Berkeley Lab. Accelerator and Fusion Research Div.
STATUS OF LBL/LLNL FEL (FREE ELECTRON LASER) RESEARCH FOR TWO BEAM ACCELERATOR APPLICATIONS
D. B. Hopkins and A. M. Sessler Nov. 1988 20 p Presented at the Workshop on Physics of Linear Colliders, Capri, Italy, 13 Jun. 1988
(Contract DE-AC03-76SF-00098)
(DE89-006656; LBL-26253; CONF-8806258-5) Avail: NTIS HC A03/MF A01

For this workshop, we review the status of free electron laser (FEL) research being conducted at LBL and LLNL as part of a broader program of research on two beam accelerators (TBAs). We discuss measurements made on high power 35 and 138 GHz FELs and their problem areas. Experience with 35 GHz accelerator section fabrication is summarized. Induction accelerator-driven FELs for use as power sources for high-gradient accelerators are discussed, along with preliminary cost estimates for this type of power source. Finally, a promising new version of an FEL/TBA is discussed. DOE

N89-20454# Lawrence Livermore National Lab., CA.
LASER DIODE COOLING FOR HIGH AVERAGE POWER APPLICATIONS
D. Mundinger, R. Beach, W. Benett, R. Solarz, and V. Sperry 1989 10 p Presented at the SPIE Conference on Optics, Electro-Optics and Laser Applications in Science and Engineering, Los Angeles, CA, 15 Jan. 1989
(Contract W-7405-eng-48)
(DE89-006777; UCRL-100245; CONF-890145-11) Avail: NTIS HC A02/MF A01

Many applications for semiconductor lasers that require high average power are limited by the instability to remove the waste heat generated by the diode lasers. In order to reduce the cost and complexity of these applications a heat sink package has been developed which is based on water cooled silicon microstructures. Thermal resistivities of less than 0.025 C (W/sq cm) have been measured which should be adequate for up to CW operation of diode laser arrays. This concept can easily be scaled to large areas and is ideal for high average power solid state laser pumping. Several packages which illustrate the essential features of this design have been fabricated and tested. The theory of operation will be briefly covered, and several conceptual designs will be described. Also, the fabrication and assembly procedures and measured levels of performance will be discussed. DOE

N89-20455# Mound Lab., Miamisburg, OH.
LASER IGNITION OF ENERGETIC MATERIALS WITH A PULSED Nd:YAG LASER
L. R. Dosser, S. A. Siwecki, T. M. Beckman, and T. C. Girmann 1988 5 p Presented at the LASERS '88, Lake Tahoe, NV, 5 Dec. 1988

(Contract DE-AC04-88DP-43495)
(DE89-006861; MLM-3566(OP); CONF-881244-5) Avail: NTIS HC A02

The laser is an ideal ignition source for energetic materials. It permits precise control of the ignition energy, and parameters such as the ignition threshold and the time to ignition can be determined. Optical fibers are used to deliver the ignition pulse and to monitor the time required to complete the burn of the energetic material. The light emission from the interaction of the Q-switched pulse from the Nd:YAG laser with two secondary explosives, pentaerythritol tetranitrate (PETN) and 1,3,5-triamino trinitrobenzene (TATB), has been spectrally resolved using a 0.25 m monochromator with an optical multichannel analyzer detector. These spectra show definite band structure, which indicates that these experiments may lead to an understanding of the ignition chemistry. DOE

N89-20456# Brookhaven National Lab., Upton, NY. Center for Accelerator Physics.
THREE DIMENSIONAL NUMERICAL ANALYSIS OF A HIGH-GAIN FREE-ELECTRON LASER
Juan C. Gallardo 19 Oct. 1988 30 p
(Contract DE-AC02-76CH-00016)
(DE89-006981; BNL-41996) Avail: NTIS HC A03/MF A01

We present a novel approach to the 3-dimensional high-gain free electron laser amplifier problem. The method allows us to write the laser field as an integral equation which can be efficiently and accurately evaluated on a small computer. The model is general enough to allow the inclusion of various initial electron beam distributions to study the gain reduction mechanism and its dependence on the physical parameters. DOE

N89-20457# Brookhaven National Lab., Upton, NY. Center for Accelerator Physics.
PRELIMINARY STUDIES OF AN INFRARED FREE-ELECTRON LASER OSCILLATOR AT THE ATF(BNL)
Juan C. Gallardo 19 Oct. 1988 21 p
(Contract DE-AC02-76CH-00016)
(DE89-006982; BNL-41997) Avail: NTIS HC A03/MF A01

In this report, I present results of a theoretical 1-D model discussed by G. Dattoli, A. Reniere and myself. The validity of a steady-state analysis is discussed and some estimates are given of the effects introduced by the lethargy of the laser pulse due to the finite length of the e sup minus pulse. Also, I present analytical expressions for the laser pulse in terms of supermodes (wave-packets of cavity modes), their evolution, physical width as well as the associated frequency spectrum. Next, I present results obtained with a 3-D code for the single pass, small-signal gain. In the appendix, I summarize the symbols used in this report. DOE

N89-20458# EG and G Mound Applied Technologies, Miamisburg, OH.
LASER ILLUMINATED HIGH SPEED PHOTOGRAPHY OF ENERGETIC MATERIALS AND COMPONENTS WITH A COPPER VAPOR LASER
Larry R. Dosser, John W. Reed, and Margaret A. Stark 1988 3 p Presented at LASERS '88, Lake Tahoe, NV, 5 Dec. 1988
(Contract DE-AC04-88DP-43495)
(DE89-006379; MLM-3565(OP); CONF-881244-6) Avail: NTIS HC A02/MF A01

Because components containing energetic materials function in a rapid and often violent manner, specialized diagnostics are required to study these events. Laser illuminated high speed photography has recently been used to record the functioning of these devices. A copper vapor laser capable of producing pulse rates of up to 10,000 pulses per second has been synchronized with a high speed film camera to record multiple laser illuminated images of the functioning component. This type of photography allows us to distinguish between hot particles and cold particles, measure burn rates, detect the effect of composition changes on performance, and observe the effect of design changes. Recent examples of the application of this technique are discussed. DOE

N89-20459# Los Alamos National Lab., NM.
REVIEW OF LONG-PULSE LASER DEVELOPMENT
Robert C. Sze 1989 10 p Presented at the Conference on Deep Blue and Ultraviolet Lasers Technology and Applications, Los Angeles, CA, 15 Jan. 1989
(Contract W-7405-eng-36)
(DE89-006514; LA-UR-89-284; CONF-890166-1) Avail: NTIS HC A03/MF A01

A brief review of some present techniques to obtain long-pulse laser action in excimer discharge devices will be presented. An attempt will be made to point out the strengths and weaknesses of these techniques. DOE

N89-20460# New Mexico Univ., Albuquerque. Center for Advanced Studies.
THE CHIRPED-PULSE FREE-ELECTRON LASER Final Technical Report, Sep. 1987 - Oct. 1988
Gerald T. Moore Jan. 1989 6 p
(Contract DE-FG04-87ER-13788)
(DE89-006792; DOE/ER-13788/2) Avail: NTIS HC A02/MF A01

This is the final report of a theoretical and numerical investigation into the operation of pulsed free-electron lasers in which the electron energy depends on the time of injection into the wiggler. Such energy chirping over each of a train of electron micropulses injected into an FEL oscillator is expected to give rise to a laser pulse inside the optical resonator with a chirped carrier frequency. DOE

N89-20461# Brookhaven National Lab., Upton, NY. National Synchrotron Light Source.
AMPLIFIED SPONTANEOUS EMISSION IN A SINGLE PASS FREE ELECTRON LASER
Li Hua Yu and S. Krinsky 1988 10 p Presented at the 10th International Free-Electron Laser Conference, Jerusalem, Israel, 29 Aug. 1988
(Contract DE-AC02-76CH-00016)
(DE89-007048; BNL-42192; CONF-8808146-14) Avail: NTIS HC A02/MF A01

We discuss the relationship of the effective start-up noise in a single pass free electron laser to the spontaneous radiation emitted in the initial gain length of the wiggler magnet. Also, it is noted that the number of modes in the output is related to the phase space volume occupied by the spontaneous radiation emitted in the first gain length. DOE

N89-20462# Naval Research Lab., Washington, DC. Plasma Physics Div.
ACHIEVING ADEQUATE BEAM QUALITY FOR COMMERCIAL LASER FUSION REACTORS
S. P. Obenchain, R. H. Lehmberg, A. J. Schmitt, and S. E. Bodner Feb. 1989 27 p
(Contract DE-AI03-79DP-40092)
(DE89-007474; NRL-MR-6222) Avail: NTIS HC A03/MF A01

In this paper we discuss the laser-beam-smoothing techniques for obtaining the highly symmetric illumination required for high gain laser fusion. We review the various beam smoothing techniques and discuss the constraints placed on these techniques if they are to be implemented on commercial fusion reactors. DOE

N89-20463# Ames Lab., IA.
FUNDAMENTAL AND APPLIED STUDIES OF NEW IONIZATION TECHNIQUES FOR INORGANIC MASS SPECTROMETRY Ph.D. Thesis
Jonathan Kevin Schoer Feb. 1989 89 p
(Contract W-7405-eng-82)
(DE89-007567; IS-T-1355) Avail: NTIS HC A05/MF A01

In the current work, pulsed laser energy was delivered to a substrate on which a solid sample was deposited. The laser power density was kept near the threshold of ion production so that a low number of ions were generated. Each pulse of the laser resulted in a scan by a Time-of-Flight Mass Spectrometer. Ions produced

were detected using a multichannel plate detector. The arrival times of the first eight ions were recorded by an 8-channel Time-to-Digital converter. Each conventional mass spectrum was obtained from 1000 individual scans of the mass spectrum. Individual scans of the mass range were tested statistically to determine if the detection of two ions in a given scan was a random occurrence or a predictable event. In the latter case, the ions are said to be associated. The present work provides a critical evaluation of ion association as a structural tool for studying complex solid materials. Vanadium-phosphorous-oxygen (VPO) catalysts were used as samples. DOE

N89-20464# Dartmouth Coll., Hanover, NH. Dept. of Physics.
THE CERENKOV FREE-ELECTRON LASER Final Report, Aug. 1985 - Jul. 1988
John E. Walsh 22 Nov. 1988 51 p
(Contract DAAG29-85-K-0176)
(AD-A203531; ARO-22668.15-PH) Avail: NTIS HC A04/MF A01 CSCL 09C

In the Cerenkov free-electron laser experiments, dielectric-loaded quasi-optic resonators were used to couple the electron beam to the electromagnetic field. Three types of electron beam generators were employed: a pulse-transformer-based modulator (which operates in the 50 to 250 KV range), a Marx generator (which operated in the 500 kv to 1.1 MV range), and a circular RF accelerator (microtron) operating at 5 Mev. The pulse-transformer-based system was used primarily for mm-wavelength experiments. On the fundamental branch (TM01) of a cylindrical shell-loaded guide, operation between 30 and 150 GHz was obtained. A single resonator will typically tune over a 20 to 30 percent range and the electronic efficiency peaked near the lower end of the tuning curve for a fixed resonator geometry. The magnitude of the efficiency at wavelengths near 3 mm was typically 4 to 6 percent. Operation on TM02 at lower efficiency (0.1 to 1 percent) was used to extend the operating range above 300 Ghz (350 Ghz typical). However, efficiencies were obtained on occasion. Overall, the moderate-beam-voltage driven C-FEL is a simple, robust source of mm- and near-mm-wavelength radiation. Its principle disadvantage is the requirement for very careful beam focussing since any substantial charging of the dielectric liner will disrupt the beam flow. GRA

N89-20335*# Jet Propulsion Lab., California Inst. of Tech., Pasadena.
THEORETICAL COMPARISON OF MASER MATERIALS FOR A 32-GHz MASER AMPLIFIER
James R. Lyons *In its* The Telecommunications and Data Acquisition Report 15 Nov. 1988 p 58-70 (For primary document see N89-20329 13-32)
Avail: NTIS HC A12/MF A01 CSCL 20E

N89-20345*# Jet Propulsion Lab., California Inst. of Tech., Pasadena.
PERFORMANCE OF EFFICIENT Q-SWITCHED DIODE-LASER-PUMPED Nd:YAG AND Ho:YLF LASERS FOR SPACE APPLICATIONS
W. K. Marshall, K. Cowles, and H. Hemmati *In its* The Telecommunications and Data Acquisition Report 15 Nov. 1988 p 168-173 (For primary document see N89-20329 13-32)
Avail: NTIS HC A12/MF A01 CSCL 20E

37 MECHANICAL ENGINEERING

Includes auxiliary systems (nonpower); machine elements and processes; and mechanical equipment.

N89-20465 California Univ., Berkeley.
ELEMENTS OF DESIGN, UNIFYING PRINCIPLES AND APPLICATIONS Ph.D. Thesis
Jerry Stephen Marks 1987 96 p
Avail: Univ. Microfilms Order No. DA8813988

Matters of relevance to engineering design in general are discussed as well as the conceptual background for a particular design example. The design methodology developed and described illustrates the potential utility of mathematical techniques. However, it is important to realize that mathematical and/or computer analysis does not drive the design process; analysis assumes a subservient role with respect to creativity and judgment. With an ever increasing emphasis on analytical technique in the training of engineers, the role of analysis with respect to design is often ambiguous and the limitations are generally not appreciated. This issue is discussed. Fundamental limitations of mathematics, and formal languages in general, with respect to design are described. The set concept serves as the basis for virtually all of mathematics. A general design concept is described which utilizes boundary nonuniformities that act in concert to complement and offset essential design nonuniformities. The success of this concept is exemplified by magnet designs which are presented as illustration. Dissert. Abstr.

N89-20466 California Univ., Berkeley.
ANALYSIS OF THE DYNAMICS OF GUIDED ROTATING FREE CENTER PLATES Ph.D. Thesis
Kirk Barrows Price 1987 66 p
Avail: Univ. Microfilms Order No. DA8814024

Annular plates that are free to translate along the axis of symmetry, with the inside edge constrained to be perpendicular to that axis, were not studied extensively. Such plates are termed free center or floating plates. The vibration and response of a rotating, flexible, annular plate that is free to translate while its central clamping collar remains perpendicular to the axis of rotation are examined. The plate surfaces are acted on by arbitrarily positioned linear bearings, called guides, and by external forces distributed around the rim. The motivation for the problem is the analysis and design of guided floating circular saws, which are widely used in the sawmill industry. The plate and clamping collar are modeled as an annular plate with two concentric regions of different thicknesses and material properties. An exact solution, following Kirchhoff plate theory, yields the eigenvalues and modes for the floating plate. This is done for a wide range of plate geometries. The eigenmodes of the freely vibrating floating plate are used in a Galerkin expansion to solve the vibration and response problems of the guided plate. The exact solution of a guided rotating beam verifies the insensitivity of the first critical speed to guide parameters for systems with one or two guides. Dissert. Abstr.

N89-20467# Helsinki Univ. of Technology, Espoo (Finland). Lab. of Machine Design.
INFLUENCE OF LUBRICATION ON CERAMIC AND STEEL SLIDING CONTACTS
Peter Andersson and Olli Yiostalo 1988 22 p
(PB89-125090; ISBN-951-754-527-4; C-215) Avail: NTIS HC A03/MF A01 CSCL 13I

The paper compares dry and lubricated wear test results for alumina, silicon carbide and steel, all sliding on steel. Dry tests were performed with a pin-on-disk machine and the lubricated tests with a journal bearing test machine under conditions of boundary lubrication. In dry wear tests, materials transfer from one of the surfaces to the other was found to occur, while in lubricated test this was either reduced or inhibited. Wear rates during lubricated tests were about three orders of magnitude smaller than during unlubricated tests. The coefficient of friction at the end of a test was found to lie in the range of 0.37 to 0.68 for different sliding pairs in the dry tests, while in lubricated tests it remained at 0.02 to 0.03, showing the benefits of lubrication when applicable. Author

N89-20468# Battelle Columbus Labs., OH.
DEVELOPMENT OF A ROTARY VALUE FOR PULSE COMBUSTION APPLICATIONS Final Report, Jun. 1986 - Mar. 1988
Paul E. George and John M. Corliss 31 Oct. 1988 63 p
(Contract GRI-5086-234-1280)

(PB89-131114; GRI-88/0185) Avail: NTIS HC A04/MF A01 CSCL 13I

Research demonstrated the technical feasibility of a computer-controlled inlet-air rotary valve for pulse combustion applications. The results show that a Schimdt pulse combustor operated with a rotary valve provides similar performance in terms of heat transfer, pressure boost and turndown ratio to that of aero-valved and flapper-valved pulse combustors. The benefits of scale-up ease, design flexibility and tolerance of adverse conditions do not justify the added cost of the valve, motor and control systems for most industrial applications. GRA

N89-20469 Illinois Univ., Chicago.
DYNAMIC MODELING AND LINEARIZATION FOR REAL-TIME CONTROL OF A PANTOGRAPH MANIPULATOR Ph.D. Thesis
Yueh-Jaw Lin 1988 223 p
Avail: Univ. Microfilms Order No. DA8821018

The computational complexity of inverse dynamics has been the main problem for manipulator real time control. The dynamic modeling, control algorithm design, and computer motion simulation of an electromechanically actuacted, three d.o.f. pantograph type manipulator is examined. The pantograph manipulator had decoupled kinematic relationships, and its inverse dynamics is potentially to be computational efficient. Both Extended D'Alembert and Lagrange method are used to derive the equations of motion of the manipulator. The Extended D'Alembert method uses the special geometry of the manipulator, and only the forces/torques in one particular plane need to be consided. The computational efficiencies of both methods are evaluated. Due to the need for structured equations of motion for a linear control algorithm, the equations derived by using Lagrange's method are selected for linearization. The coefficients of the dynamic equations are linearized using the piecewise surface fitting scheme coded in a computer software. In order to evaluate the performance of the linearized model, both the exact and linearized dynamic models are simulated by using a closed loop feedback control algorithm. Dissert. Abstr.

N89-20470*# Georgia Inst. of Tech., Atlanta. School of Mechanical Engineering.
ACTIVE VIBRATION CONTROL OF A LARGE FLEXIBLE MANIPULATOR BY INERTIAL FORCE AND JOINT TORQUE Ph.D. Thesis
Soo Han Lee Jun. 1988 18 p
(Grant NAG1-623)
(NASA-CR-184786; NAS 1.26:184786) Avail: NTIS HC A03/MF A01 CSCL 13I

The efficiency and positional accuracy of a lightweight flexible manipulator are limited by its flexural vibrations, which last after a gross motion is completed. The vibration delays subsequent operations. In the proposed work, the vibration is suppressed by inertial force of a small arm in addition to the joint actuators and passive damping treatment. The proposed approach is: (1) Dynamic modeling of a combined system, a large flexible manipulator and a small arm, (2) Determination of optimal sensor location and controller algorithm, and (3) Verification of the fitness of model and the performance of controller. Author

N89-20471# Kentucky Univ., Lexington.
LONG-TERM EVALUATION OF THE ACOUSTIC EMISSION WELD MONITOR Final Report, Sep. 1986 - Feb. 1988
Theodore Hopwood, II Feb. 1988 65 p
(Contract DTFH61-86-C-00118)
(PB88-122642; UKTRP-88-6; FHWA/TS-88/021) Avail: NTIS HC A04/MF A01 CSCL 13H

The Kentucky Transportation Research Program conducted an extended 10-month evaluation of the Acoustic Emission Weld Monitor (AEWM) in a bridge fabrication shop. That device was used to detect welding flaws during typical production of butt-welds on flanges and webs used in steel bridges. A total of 153 welds were monitored. AEWM test results were compared with visual inspection and double-blind results of conventional nondestructive tesing routinely conducted on the welds. The AEWM did not miss any flaws detected visually or by nondestructive testing. Three AEWM flaw indications were confirmed by conventional nondestructive testing (radiography). The AEWM has shown the sensitivity to detect AWS code-rejectable defects. Due to the success of the unit in detecting flaws, further development is warranted. Author

N89-20472*# Mechanical Technology, Inc., Latham, NY.
HIGH SPEED BALANCING APPLIED TO THE T700 ENGINE Final Report
J. Walton, C. Lee, and M. Martin Mar. 1989 110 p Prepared in cooperation with Army Aviation Systems Command, Cleveland, OH
(Contracts NAS3-23929; NAS3-24633; DA Proj. 1L1-62209-AH-76)
(NASA-CR-180899; NAS 1.26:180899; MTI-87TR56; AVSCOM-TR-88-C-007) Avail: NTIS HC A06/MF A01 CSCL 13I

The work performed under Contracts NAS3-23929 and NAS3-24633 is presented. MTI evaluated the feasibility of high-speed balancing for both the T700 power turbine rotor and the compressor rotor. Modifications were designed for the existing Corpus Christi Army Depot (CCAD) T53/T55 high-speed balancing system for balancing T700 power turbine rotors. Tests conducted under these contracts included a high-speed balancing evaluation for T700 power turbines in the Army/NASA drivetrain facility at MTI. The high-speed balancing tests demonstrated the reduction of vibration amplitudes at operating speed for both low-speed balanced and non-low-speed balanced T700 power turbines. In addition, vibration data from acceptance tests of T53, T55, and T700 engines were analyzed and a vibration diagnostic procedure developed. Author

N89-20473# Helsinki Univ. of Technology, Espoo (Finland).
APPLICATION OF PARAMETER ADAPTIVE APPROACH TO SERVO CONTROL OF A HYDRAULIC MANIPULATOR Ph.D. Thesis - Oulu Univ.
Pentti Vaha 1988 90 p Sponsored by the Technical Research Centre of Finland, Oulu, Finland; the Finnish Technology Foundation, Finland; and the Tauno Tonning Foundation, Finland
(Ma-51; ISBN-951-666-269-2; ISSN-0355-2713; ETN-89-93751)
Avail: NTIS HC A05/MF A01

A method for compensating changes in manipulator dynamics to cope with the increased requirements for better servo control of manipulator motion is introduced. The dynamic model of the manipulator arm is linearized and presented in a state space form. The parameters of the linearized model are estimated on line and used for tuning of the servo controller. The control of the manipulator is experimentally examined in computed path control, for a regular and irregular path. The test runs are carried out with a loaded and unloaded manipulator. A simulation study with simple process models is utilized to examine the adaptive properties of the method. The ability of the estimator to track changing parameters during path servoing are examined and the significance of the velocity in adaptive servocontrol applications is outlined. The derived control law is verified and the effects of feedforward and feedback parts both together and separately are examined with constant multivariable processes in servo applications. The results indicate the applicability of the method for servocontrol of manipulators. ESA

N89-20474# National Aerospace Lab., Amsterdam (Netherlands). Space Div.
TRANSLATIONAL AND ROTATIONAL DYNAMICS OF RIGID SPACECRAFT-BASED MANIPULATORS
P. Th. L. M. vanWoerkom 5 Jan. 1987 175 p
(Contract NIVR-02506N)
(NLR-TR-87014-U; ETN-89-94062) Avail: NTIS HC A08/MF A01

The case of a spacecraft-based manipulator with rigid links is studied. Approaches to mathematical modeling are reviewed, and arguments for using the so-called Newton-Euler approach are presented. The equations obtained are manipulated to obtain a

compact vector equation, suitable for analysis of inverse dynamics as well as forward dynamics. Results are compared with literature. Applications and extensions are described, and recommendations for further research on the subject are presented. ESA

N89-20475# Technische Univ., Eindhoven (Netherlands). Dept. of Electrical Engineering.
BREADBOARD TEST-SOFTWARE AND WRIST JOINT MODELING FOR HERMES ROBOT ARM Thesis
A. C. M. vanMulken Oct. 1988 154 p
(ETN-89-94155) Avail: NTIS HC A08/MF A01

Software for the electronic unit checkout equipment of the Hermes robot arm breadboard was developed for model tests. Nonlinear modelling of the breadboard and simulations for velocity and position feedback are summarized. The simulations show that stiction causes the most difficulties for control at setpoint-changes. ESA

N89-20476# Oak Ridge National Lab., TN. Instruments and Controls Div.
A CAMERA STABILIZATION TECHNIQUE FOR A TELEOPERATED VEHICLE
H. M. Costello, William R. Hamel, Stephen M. Killough, and J. C. Rowe 1988 9 p Presented at the 3rd Topical Meeting on Robotics and Remote Systems, Charleston, SC, 13 Mar. 1989
(Contract DE-AC05-84OR-21400)
(DE89-003923; CONF-890304-15) Avail: NTIS HC A02/MF A01

The Instrumentation and Controls Division Telerobotic Systems Section, in participation with the U.S. Marine Corps Ground-Air TeleRobotic System Program, has completed a study in camera stabilization for a teleoperated combat vehicle (TOV). The technique developed uses accelerometer feedback from the camera to attenuate disturbances viewed on the remote display. A model of the high mobility multipurpose wheeled vehicle (HMMWV) was developed to study the dynamics of the camera disturbances. A stabilization control algorithm was developed, and a test stand implementation to reduce camera jitter performed admirably. The camera control system can be implemented on the TOV to track motion of less than 1 Hz while attenuating disturbances in the 1- to 10-Hz range. Disturbances greater than 20 Hz can be effectively reduced with passive damping types of suspension. Less expensive than currently used gyro-based units, the system requires minimal additions to the TOV and is easily maintained. DOE

N89-20477# Du Pont de Nemours (E. I.) and Co., Aiken, SC. Robotics Technology.
APPLICATION-BASED CONTROL OF AN AUTONOMOUS MOBILE ROBOT
John J. Fisher 1988 9 p Presented at the 3rd Topical Meeting on Robotics and Remote Systems, Charleston, SC, 13 Mar. 1989
(Contract DE-AC09-76SR-00001)
(DE89-004380; DP-MS-88-99; CONF-890304-19) Avail: NTIS HC A02/MF A01

Industry response to new technology is governed, almost without exception, by the systems available to meet real world needs, not tools which prove the feasibility of the technology. To this end, SRL is developing robust control strategies and tools for potential autonomous vehicle applications on site. This document describes the work packages developed to perform remote tasks and a integrated control environment which allows rapid vehicle applications development and diagnostic capabilities. DOE

N89-20478# Du Pont de Nemours (E. I.) and Co., Aiken, SC.
DEVELOPMENT OF A REMOTE INSPECTION ROBOT AND CAMERA POSITIONERS FOR REACTOR TANK INSPECTION
B. R. Birmingham, M. A. Killian, D. J. Pak, and J. K. Parmer 1988 7 p Presented at the 3rd Topical Meeting on Robotics and Remote Systems, Charleston, SC, 13 Mar. 1989
(Contract DE-AC09-76SR-00001)
(DE89-004381; DP-MS-88-114; CONF-890304-18) Avail: NTIS HC A02/MF A01

The Equipment Engineering Division of the Savannah River Laboratory has developed an integrated system of special purpose robots, camera positioners, nondestructive evaluation (NDE) data acquisition and analysis instrumentation, electronic controls, and auxiliary hardware to perform remote ultrasonic and eddy current inspections inside the Savannah River Plant's nuclear reactor tanks. This paper presents the mechanical development of the remote inspection robot and camera positioner. The robot utilizes six degrees-of-freedom to precisely position various NDE sensors while scanning the inside wall of the reactor tank. The 3-axis camera positioners provide high-resolution views of the inspection activities. DOE

N89-20479# Oak Ridge National Lab., TN. Center for Engineering Systems Advanced Research.
DEVELOPMENT OF THE HERMIES 3 MOBILE ROBOT RESEARCH TESTBED AT OAK RIDGE NATIONAL LABORATORY
Wayne W. Manges, William R. Hamel, Charles R. Weisbin, Ralph Einstein, Barry L. Burks, David H. Thompson, Rascy R. Feezell, and Stephen M. Killough 1988 9 p Presented at the 3rd Topical Meeting on Robotics and Remote Systems, Charleston, SC, 13 Mar. 1989
(Contract DE-AC05-84OR-21400)
(DE89-004797; CONF-890304-22) Avail: NTIS HC A02/MF A01

The latest robot in the Hostile Environment Robotic Machine Intelligence Experiment Series (HERMIES) is now under development at the Center for Engineering Systems Advanced Research (CESAR) in the Oak Ridge National Laboratory. The HERMIES 3 robot incorporates a larger than human size 7-degree-of-freedom manipulator mounted on a 2-degree-of-freedom mobile platform including a variety of sensors and computers. The deployment of this robot represents a significant increase in research capabilities for the CESAR laboratory. The initial on-board computer capacity of the robot exceeds that of 20 Vax 11/780s. The navigation and vision algorithms under development make extensive use of the on-board NCUBE hypercube computer while the sensors are interfaced through five VME computers running the OS-9 real-time, multitasking operating system. This paper describes the motivation, key issues, and detailed design trade-offs of implementing the first phase (basic functionality) of the HERMIES 3 robot. DOE

N89-20480# Oak Ridge National Lab., TN. Instrumentation and Controls Div.
FORCE-REFLECTING MASTER-SLAVE CONTROL AND ROBOTIC CONTROL OF A TRACTION-DRIVE DIFFERENTIAL PITCH-YAW JOINT
Reid L. Kress and Hugh M. Costello 1988 9 p Presented at the 3rd Topical Meeting on Robotics and Remote Systems, Charleston, SC, 12-13 Mar. 1989
(Contract DE-AC05-84OR-21400)
(DE89-005107; CONF-890304-32) Avail: NTIS HC A02/MF A01

A master-slave control algorithm and a Proportional-Integral (PI) robotic control algorithm were developed and implemented for a traction-drive differential, pitch-yaw joint using torque, velocity, and position feedback. To make the drive trains' performance less sensitive to load variations, a basic proportional control loop using a torque sensor with an inner velocity loop was developed. Next, output position loops were constructed by feeding back drive-train angles determined from kinematically decoupled pitch and yaw position measurements. A robotic-mode, PI control action was implemented on the position error and experimental results were compared with simulated results for step and ramp inputs. Master-slave operation was demonstrated using proportional position control loops for each of two test stands. Experimental results showed that the control loops exhibited satisfactory robotic and master-slave performance. DOE

N89-20481*# Oak Ridge National Lab., TN.
TELEROBOTIC MANIPULATOR DEVELOPMENTS FOR GROUND-BASED SPACE RESEARCH
J. N. Herndon, S. M. Babcock, P. L. Butler, H. M. Costello, R. L. Glassell, Reid L. Kress, D. P. Kuban, J. C. Rowe, D. M. Williams, and A. J. Meintel (National Aeronautics and Space Administration. Langley Research Center, Hampton, VA.) 1988 21 p Presented at the 3rd Topical Meeting on Robotics and Remote Systems, Charleston, SC, 13-16 Mar. 1989 Sponsored by NASA
(Contract DE-AC05-84OR-21400)
(NASA-CR-184736; NAS 1.26:184736; DE89-005109; CONF-890304-31) Avail: NTIS HC A03/MF A01 CSCL 13I

New opportunities for the application of telerobotic systems to enhance human intelligence and dexterity in the hazardous environment of space are presented by the National Aeronautics and Space Administration (NASA) Space Station Program. Because of the need for significant increases in extravehicular activity and the potential increase in hazards associated with space programs, emphasis is being heightened on telerobotic systems research and development. The Automation Technology Branch at NASA Langley Research Center currently is sponsoring the Laboratory Telerobotic Manipulator (LTM) program at Oak Ridge National Laboratory to develop and demonstrate ground-based telerobotic manipulator system hardware for research and demonstrations aimed at future NASA applications. The LTM incorporates traction drives, modularity, redundant kinematics, and state-of-the-art hierarchical control techniques to form a basis for merging the diverse technological domains of robust, high-dexterity teleoperations and autonomous robotic operation into common hardware to further NASA's research. DOE

N89-20482# Oak Ridge National Lab., TN. Engineering, Physics and Mathematics Div.
WORLD MODELLING AND MULTI-SENSOR INTEGRATION FOR A MOBILE ROBOT
M. Beckerman, L. A. Farkas (Cornell Univ., Ithaca, NY.), J. P. Jones, R. C. Mann, and C. W. Glover 1988 9 p Presented at the 3rd Topical Meeting on Robotics and Remote Systems, Charleston, SC, 13-16 Mar. 1989
(Contract DE-AC05-84OR-21400)
(DE89-005124; CONF-890304-2) Avail: NTIS HC A02/MF A01

In this paper we present a strategy for the reduction of systematic errors through the fusion of ultrasonic range and visual intensity information. This is done within a framework consisting of several world models, integration procedures, and sensor models which include appropriate sensor-specific signal and information processing algorithms. Among the world models are linked lists of geometric features extracted from the intensity images, and 2D Cartesian maps built from the sonar range data. Spatial reasoning was used in the fusion of ultrasonic data from multiple scans, and in the analysis of visual edge information following exchange of range and angular information across the sensor domains. DOE

N89-20483# Midwest Research Inst., Golden, CO. Solar Energy Research Inst.
DESIGN AND TESTING OF A DISSOCIATED METHANOL VEHICLE
Michael E. Karpuk Feb. 1989 107 p
(Contract DE-AC02-83CH-10093)
(DE89-007051; DOE/CH-10093/H5) Avail: NTIS HC A06/MF A01

The concept of dissociating methanol with exhaust gas heat to improve the efficiency of methanol-burning engines has often been described in the literature. The concept has been controversial with conflicting results from analysis and experimentation. In this report, we describe the design and testing of a dissociated methanol vehicle based on a Ford Escort. This work draws heavily on the experience gained by Finegold et al. (1984) when they built a dissociated methanol Chevrolet Citation at the Solar Energy Research Institute (SERI). The improvements that we incorporated into the dissociated methanol Ford Escort include a very active, custom palladium on gamma-alumina dissociation catalyst, a liquid methanol injection system for starting and high power operation, and a custom microprocessor-based engine controller provided by Ford Motor Company. The goal of the work described in this report was to design, build, and test a dissociated methanol vehicle to measure the fuel economy and emissions benefits compared to lean burning liquid methanol. The original test plan called for transient testing using the EPA city and highway driving cycle tests. However, technical and funding problems prevented that testing. Steady-state vehicle testing was performed that revealed many of the benefits and problems of the dissociated methanol concept. DOE

N89-20484# Oak Ridge National Lab., TN. Engineering Div.
DESIGN OF REMOTE MAINTENANCE TOOLING AND FIXTURES FOR THE ADVANCED SERVOMANIPULATOR REMOTE MAINTENANCE DEMONSTRATION
P. E. Arakawa, D. M. Williams, and E. C. Bradley 1989 17 p Presented at the 3rd Topical Meeting on Robotics and Remote Systems, Charleston, SC, 13 Mar. 1989
(Contract DE-AC05-84OR-21400)
(DE89-003114; CONF-890304-9) Avail: NTIS HC A03

The basic approach for design of remotely maintainable equipment is to incorporate individually replaceable modules. These modules typically possess features that will enhance remote handling, such as captive cone-head fasteners, tapered guides, remotely operated disconnects, and lift points that allow the modules to be oriented in the proper position. The use of special fixtures or tooling to accomplish remote maintainability is usually discouraged due to the added storage and handling requirements for these items. However, due to the complex nature of some equipment and the associated maintenance requirements, special tooling/fixtures may be required for some maintenance tasks. A number of fixtures were fabricated and used on the advanced servomanipulator (ASM) maintenance demonstration. Details of the actual experimental task are given in a companion paper in this meeting entitled, Demonstration of Remote Maintenance of the Advanced Servomanipulator. This paper describes the various fixtures used and the special functional requirements that influenced their design. The remote maintenance demonstration was successfully performed using these fixtures. DOE

N89-20485# Los Alamos National Lab., NM.
AXIALLY ACCELERATED SABOTED RODS SUBJECTED TO LATERAL FORCES
Donald Allen Rabern Mar. 1989 103 p
(Contract W-7405-eng-36)
(DE89-007466; LA-11494-MS) Avail: NTIS HC A06/MF A01

The methodology and analysis used to characterize the performance of a sabot/rod as it is subjected to lateral and axial loading during launch is presented. The methodology described incorporates the experimental and numerical portions of the evaluation. Three separate sabot/rod designs are evaluated for their performance in the launch tube and are compared with one another. The experimental portion of the research involved full-scale testing of two separate sabot/rod designs in a 120-mm launch tube that was slightly bent. When launched through the bent tube, the sabot/rod system was forced to negotiate lateral displacements at axial velocities of approximately 5400 fps. This combination of axial velocity and lateral displacement produced significant lateral loading on the sabot/rod system. A 2.3-MeV X-ray unit was used to determine the lateral displacement that occurred as the sabot/rod was forced through the bent tube. After the sabot/rod exited the launch tube, the sabot separation and rod straightness were recorded by four 150-keV X-ray units. The numerical portion of the research involved three-dimensional modeling of the sabot/rod systems in three launch tube environments: a perfectly straight launch tube, an existing accuracy tube, and the slightly bent tube used in the experimental program. Because of the good agreement between the experimental and numerical models, stress, strain, and displacement time histories were obtained from the numerical work and used to evaluate each of the three sabot/rod systems in three launch environments. A dynamic analysis was performed for each of the nine separate

models. Sliding surfaces, nonlinear constitutive relations, and multiple materials were used for each analysis. Results from both the experimental and numerical analyses are presented. DOE

N89-20486# Army Military Personnel Center, Alexandria, VA.
CROSS-COORDINATED CONTROL: AN EXPERIMENTALLY VERIFIED TECHNIQUE FOR THE HYBRID TWIST AND WRENCH CONTROL OF A VOLTAGE-CONTROLLED INDUSTRIAL ROBOT Final Report, Aug. 1985 - Dec. 1988
Mark L. Swinson 30 Dec. 1988 236 p
(AD-A203406) Avail: NTIS HC A11/MF A01 CSCL 12I

Applications for modern industrial robots have generally been limited to low-precision, non-contact tasks, because in practice, it is generally not possible to adequately engineer even a manufacturing environment to a sufficiently high degree of precision such that position control, alone, is adequate. Cross-coordinated control serves to extend that range by providing a practical, experimentally verified solution to the problem of simultaneously controlling both the motion of and the constraint forces acting upon a robot end-effector, which is in contact with a rigid environment. This work provides a semi-empirical method for the hybrid control of a voltage-controlled industrial robot, such that the geometric constraints are explicitly accounted for. The kinestatic analysis was based on a model of the environment using Ball's reciprocal screws to characterize the nature of the constraints. The resulting theoretical development, combined with a laboratory implementation which employed an instrumented, anisotropic, mechanically complaint wrench sensor, resulted in a system that is kinematically, dynamically and kinestatically stable. Consequently, this approach constitutes a general solution to the problem of performing the commonly encountered industrial tasks which, if automated, would require contact between the robot's end-effector and a rigid environment. This method is well suited for implementation as an augmentation, thus permitting the continued use of most existing motion control hardware and software.
GRA

N89-20487# Carnegie-Mellon Univ., Pittsburgh, PA. Robotics Inst.
DEVELOPMENT OF AN INTEGRATED MOBILE ROBOT SYSTEM AT CMU (CARNEGIE MELLON UNIVERSITY), JUNE 1987 Annual Technical Report, Jul. 1986 - Jun. 1987
Steve Shafer and William Whittaker Jul. 1988 109 p
(Contract DACA76-86-C-0019; DARPA Order 5682)
(AD-A203689; CMU-RI-TR-88-10; ETL-0508) Avail: NTIS HC A06/MF A01 CSCL 17G

This report describes progress in development of an integrated mobile robot system at the Carnegie Mellon Robotics Institute from July 1986 to June 1987. This research was sponsored by DARPA as part of the Strategic Computing Vision Program. Our program includes a broad agenda of research in the development of mobile robot vehicles. In the year covered by this report, we addressed two major areas in vehicle development (NAVLAB vehicle and Robot control system) and two major areas in robot architecture development (CODGER blackboard and Navigation architecture). We built the NAVLAB mobile robot vehicle by outfitting a commercial truck chassis with computer-controlled drive and steering controls and a set of on-board computer workstations. The NAVLAB serves as a mobile navigation laboratory that allows researchers to interact intensively with the system during testing and execution. We also developed a real-time controller system for the NAVLAB using a collection of coordinated processors and software. The CODGER blackboard system incorporate substantial features for geometric reasoning and task synchronization that have been incorporated in blackboards before. We also developed the Driving Pipeline architecture for coordinating road following, obstacle avoidance, and vehicle motion control. This hardware and software combination is the basis for the New Generation System (NGS) for robot vision and navigation, which will tie together existing and emerging technologies. GRA

N89-20488# Carnegie-Mellon Univ., Pittsburgh, PA. Robotics Inst.
THE 1987 YEAR END REPORT FOR ROAD FOLLOWING AT CANEGIE MELLON Annual Report, 15 Jan. 1987 - 14 Jan. 1988
Charles E. Thorpe and Takeo Kanade Aug. 1988 126 p
(Contract DACA76-85-C-0003; NSF DCR-86-04199; ARPA Order 5351)
(AD-A203946; ETL-0514; CMU-RI-TR-88-4) Avail: NTIS HC A07/MF A01 CSCL 17G

This report describes progress in vision and navigation for outdoor mobile robots at the Carnegie Mellon Robotics Institute during 1987. This research centers on guiding outdoor autonomous vehicles. In 1987 we concentrated on five areas: (1) Road following. We expanded our road tracking system to better handle shadows and bright sunlight. (2) Range data interpretation. Our range interpretation work has expanded from processing a single frame, to combining several frames of data into a terrain map. (3) Expert systems for image interpretation. We explored finding roads in very difficult scenes, without relying on strong a priori road color or shape models. (4) Car recognition. We recognize cars in color images by a hierarchy of grouping image features, and predicting where to look for other image features. (5) Geometric camera calibration. Our new method for calibration avoids complex non-linear optimizations found in other calibration schemes.
GRA

N89-20333*# Jet Propulsion Lab., California Inst. of Tech., Pasadena.
DYNAMIC MODELS FOR SIMULATION OF THE 70-M ANTENNA AXIS SERVOS
R. E. Hill *In its* The Telecommunications and Data Acquisition Report 15 Nov. 1988 p 32-50 (For primary document see N89-20329 13-32)
Avail: NTIS HC A12/MF A01 CSCL 13I

N89-20334*# Jet Propulsion Lab., California Inst. of Tech., Pasadena.
A NEW ALGORITHM FOR MODELING FRICTION IN DYNAMIC MECHANICAL SYSTEMS
R. E. Hill *In its* The Telecommunications and Data Acquisition Report 15 Nov. 1988 p 51-57 (For primary document see N89-20329 13-32)
Avail: NTIS HC A12/MF A01 CSCL 13I

38 QUALITY ASSURANCE AND RELIABILITY

Includes product sampling procedures and techniques; and quality control.

N89-20489*# Cleveland State Univ., OH.
RELIABILITY-BASED FAILURE ANALYSIS OF BRITTLE MATERIALS
Lynn M. Powers and Louis J. Ghosn Feb. 1989 128 p
(Contract NCC3-46)
(NASA-CR-184799; NAS 1.26:184799) Avail: NTIS HC A07/MF A01 CSCL 09D

The reliability of brittle materials under a generalized state of stress is analyzed using the Batdorf model. The model is modified to include the reduction in shear due to the effect of the compressive stress on the microscopic crack faces. The combined effect of both surface and volume flaws is included. Due to the nature of fracture of brittle materials under compressive loading, the component is modeled as a series system in order to establish bounds on the probability of failure. A computer program was written to determine the probability of failure employing data from a finite element analysis. The analysis showed that for tensile loading a single crack will be the cause of total failure but under compressive loading a series of microscopic cracks must joint together to form a dominant crack. Author

N89-20490*# National Aeronautics and Space Administration. Lewis Research Center, Cleveland, OH.
NONDESTRUCTIVE EVALUATION OF ADVANCED CERAMICS
Stanley J. Klima and Harold E. Kautz 1988 11 p Presented at the 26th Automotive Technology Development Contractor's Coordination Meeting, Dearborn, MI, 24-27 Oct. 1988; sponsored by DOE
(NASA-TM-101489; E-4632; NAS 1.15:101489) Avail: NTIS HC A03/MF A01 CSCL 14D

A review is presented of Lewis Research Center efforts to develop nondestructive evaluation techniques for characterizing advanced ceramic materials. Various approaches involved the use of analytical ultrasonics to characterize monolythic ceramic microstructures, acousto-ultrasonics for characterizing ceramic matrix composites, damage monitoring in impact specimens by microfocus X-ray radiography and scanning ultrasonics, and high resolution computed X-ray tomography to identify structural features in fiber reinforced ceramics. Author

N89-20491# Construcciones Aeronauticas S.A., Madrid (Spain). Div. de Proyectos.
FATIGUE TEARDOWN TESTS OF THE AGED REAR SUPPORT OF THE A320 AIRCRAFT [TEARDOWN DEL REAR SUPPORT ENVEJECIDO DEL A-320 ENSAYADO A FATIGA]
J. M. Martin and J. M. Bernardo 27 Jun. 1988 13 p In SPANISH
(I-271/88; ETN-89-94129) Avail: NTIS HC A03/MF A01

The progressive damage of the A320 rear support observed after manufacturing and test steps are reported. The evolution of each defect and the generation of additional defects is studied using ultrasound, macrofractographic and penetrating liquid methods. Defects numbered 3 and 4 appeared during the teardown tests. The third was detected by manual pulsed ultrasound echo methods. The fourth was detected during macrographic inspection of defect 2. The ultrasonic detection method used to analyze the evolution of defects during testing is adequate, since the micrographic measurements are of the same order. ESA

N89-20492# Construcciones Aeronauticas S.A., Madrid (Spain). Div. de Proyectos.
NONDESTRUCTIVE TESTS OF ELEMENTS MAMUFACTURED USING DIFFUSION BONDING AND SUPERPLASTIC FORMING [INSPECCION NO DESTRUCTIVA DE ELEMENTOS FABRICADOS MEDIANTE SOLDADURA POR DIFUSION Y CONFORMADO SUPERPLASTICO]
V. Cortes, C. Valdecantos, B. Sainz, and J. M. Bernardo 1988 12 p In SPANISH Presented at the 7th Jornadas Tecnicas de Soldadura
(ETN-89-94131) Avail: NTIS HC A03/MF A01

A nondestructive inspection method was investigated on a structural aircraft component made of Ti-6Al-4V alloy. Typical expected defects and detectability are discussed. It is shown that the immersion method with reflector is less conditioned by the specimen geometry and does not require a large resolution. Results obtained on a welded piece of 2 mm width are included. It is shown that the method can detect 100 percent of the macrodefects above a surface of 3 x 3 mm. ESA

N89-20493# Oak Ridge National Lab., TN.
EDDY CURRENT INSPECTION OF FERROMAGNETIC MATERIALS USING PULSED MAGNETIC SATURATION
C. V. Dodd, W. E. Deeds, and L. D. Chitwood 1988 10 p Presented at the International Conference on Fossil Power Plant Rehabilitation: Trends in Life Management and Reliability Technology, Cincinnati, OH, 27 Feb. 1989
(Contract DE-AC05-84OR-21400)
(DE89-005339; CONF-890219-1) Avail: NTIS HC A02/MF A01

A pulsed eddy-current system has been designed and developed for nondestructive evaluation of ferromagnetic steam generator tubing from the bore side. A large current pulse is sent through a driver coil to produce magnetic saturation all the way through the wall of a tube. A pickup coil monitors the field produced by the driver coil and produces a pulse whose shape is dependent on the electromagnetic properties of the tube as well as the driving pulse. The output pulse heights at selected times are used as data that are computer-correlated with calibration data taken from machined standards. The magnitude and length of the pulse can be increased to saturate thicker tubes, or shortened for very thin sections of ferromagnetic materials. Tube walls 5 mm thick have been tested with pulses of 500 kW peak power and tubes 0.2 mm thick have been tested with 400 watt pulses. Advanced pulsed instruments are set up entirely with signals from a controlling computer sent over the IEEE-488 bus, which then transmits the data back to the computer. The controlling computer, which may be either a PC-AT or a IBM System 9000, can analyze, display and store the data in real time. The system has demonstrated the capability to detect small flaws located near the outside of thick ferromagnetic tubing in the presence of other artifacts on the tube outside diameter. DOE

N89-20494# California Univ., Berkeley. Lawrence Berkeley Lab. Research Medicine and Radiation Biophysics Div.
DISCRETE ANALYSIS OF STOCHASTIC NMR Ph.D. Thesis
Sam Tak-Sum Wong Dec. 1988 120 p
(Contract DE-AC03-76SF-00098)
(DE89-007016; LBL-26440) Avail: NTIS HC A07/MF A01

Stochastic NMR is an efficient technique for high field in-vivo imaging and spectroscopic studies in cases where the peak RF power required may be prohibitively high for conventional pulsed NMR techniques. This dissertation presents a theoretical analysis of a stochastic NMR method of acquiring spectroscopy data. The spin system is excited with RF pulses where the flip angles or the phases of the pulses are samples of a discrete stochastic process. The method is formulated as a stochastic difference equation which is then converted to ordinary deterministic difference equations describing the input-output cross-correlation, average signal power and signal power spectrum. The solutions of these equations are used to evaluate the stochastic, technique in terms of peak RF power requirement, spectral distortions and signal-to-noise ratio. Experimental results are also presented which verify the results of the discrete analysis. The analysis shows that the maximum signal-to-noise ratio is achieved when the RMS flip angle is approximately the Ernst angle. When the RMS flip angle is below the Ernst angle, the input-output cross-correlation is a good estimate of the FID. Increase of excitation power causes line broadening. In addition, the use of random flip angle, fixed phase excitation causes a notch artifact and non-uniform response across the spectrum both of which are not found in two new types of excitation, the random phase excitation and the random quadrature excitation. The signal power spectrum is also a good estimate of the real spectrum. The approximation of the cross-correlation by a time average causes systematic noise. The amount of systematic noise is found to be significantly reduced when an entire maximum length sequence (MLS) is used for excitation. Noise-like distortion at high power MLS excitation is discovered to be related to the number of feedback paths in the MLS generator. DOE

N89-20495# Flow Research, Inc., Kent, WA.
LASER-BASED INSPECTION TECHNOLOGY FOR FOSSIL HEAT EXCHANGER TUBING Final Report, Apr. 1987 - Oct. 1988
J. L. Doyle 1988 25 p
(Contract DE-FG01-87CE-15328)
(DE89-005811; DOE/CE-15328/T1) Avail: NTIS HC A03

In April of 1987, the U.S. Department of Energy, under the auspices of the Energy Related Inventions Program, awarded Flow Research, Inc. a grant to assist in the development of a laser-based inspection technology for fossil heat exchanger tubing. The primary goals of the program were to assemble a field prototype laser inspection system that could be demonstrated in the commercial utility industry, and to test the system in the field. As stated in FLOW's proposal TD227054, there were three principle tasks outlined for this program. First, a set of specifications would be generated, based on interviews with individuals involved with plant operations and NDE service-related activities. A key aspect of

this effort would be the identification of a single probe design that could be used in a common size of heat exchanger tubing. The second task of this project would be the assembling of a prototype system that would be capable of being proof-tested in the field. To accomplish this, a probe would be designed and fabricated. In addition, improvements would be required in the pre-existing electronic support system, to make the system more field worthy. And finally, a field-worthy computer would be acquired and software modifications would be required to make the output usable for utility applications. DOE

39 STRUCTURAL MECHANICS

Includes structural element design and weight analysis; fatigue; and thermal stress.

For applications see *05 Aircraft Design, Testing and Performance* and *18 Spacecraft Design, Testing and Performance.*

N89-20496# Sydney Univ. (Australia). School of Civil and Mining Engineering.
COMPRESSION TESTS OF WELDED CHANNEL SECTION COLUMNS
K. J. R. Rasmussen and G. J. Hancock Mar. 1988 81 p
(PB88-246020; R-566) Avail: NTIS HC A05/MF A01 CSCL 20K

A test program is described investigating the compressive strength of channel section columns of slender cross section. The program consisted of different geometries of cross section, each fabricated by welding from high strength steel. Specimens were tested both concentrically and eccentrically between pinned ends, and for each section geometry fixed ended stub column tests were also performed. Additional tests were performed to determine the local buckling load of the sections under uniform compression. The local buckling loads obtained from testing are compared with theoretically determined local buckling loads. The test strengths are compared with strength predictions of the AISC Load and Resistance Factor Design Specification, the draft Limit State Australian Standard, the British Standard BS5950, Part 1 and the Eurocode3 Specification for the design of steel buildings. Author

N89-20497# Sydney Univ. (Australia). School of Civil and Mining Engineering.
ELASTIC STABILITY OF LAP-JOINTED CYLINDRICAL SHELLS UNDER AXIAL COMPRESSION
J. M. Rotter and Jian-Guang Teng Feb. 1988 41 p
(PB88-245980; R-562) Avail: NTIS HC A03/MF A01 CSCL 20K

Light gauge circular silos and tanks are often built from rolled steel plate with lap joints running around the circumference. A parametric study is undertaken to explore the problem of the buckling of lap jointed cylindrical shells under axial compression and internal pressure using a nonlinear stability analysis for shells of revolution. The results are compared with the predictions of earlier limited analytical studies, and with existing experimental results. Bolted and welded lap joints of different lengths and thicknesses are studied comprehensively. Lap joints are shown to be a source of special concern only if fabrication errors lead to a significant imperfection adjacent to the lap joint. The increase in the buckling strength caused by internal pressure is found to be less than that predicted by the ECCS code for shell buckling. Author

N89-20498# Air Force Systems Command, Wright-Patterson AFB, OH.
STRUCTURAL MECHANICS: CONTEMPORARY STATE AND PROSPECTS FOR DEVELOPMENT (SELECTED PORTIONS)
V. V. Bolotin, I. I. Goldenblat, and A. F. Smirnov 19 Aug. 1988 83 p Transl. into ENGLISH from Stroitelnaya Mekhanika (Moscow, USSR), 1972 p 3, 65-98, 190-191
(AD-A198766; FTD-ID(RS)-T-0438-88) Avail: NTIS HC A05/MF A01 CSCL 20K

In recent years, many works have been published on structural mechanics and its application to calculation of structures, aircraft, ships and machines. However, among these investigations are still insufficient works of survey character, which give respresentation about the level of the interesting U.S. field of science as a whole. Survey/coverage in no way pretends to completeness; authors paid attention to those works which were close to their scientific interests. Examined in detail are sections dealing the theory of the elastoplastic calculation of constructions, statistical dynamics and the theory of the reliability of constructions, and mechanics of construction with the composite materials. A special chapter is dedicated to the application of electronic computers to structural mechanics. GRA

N89-20499# Florida Univ., Gainesville. Dept. of Engineering Science Mechanics and Aerospace Engineering.
A DISPLACEMENT PATTERN MATCHING APPLICATION IN ELASTIC-PLASTIC HYBRID STRESS ANALYSIS Final Technical Report, 1 Jun. 1987 - 31 May 1988
Jim Sirkus Aug. 1988 125 p
(Contract F49620-85-C-0013)
(AD-A199028; AD-E801748; AFATL-TR-88-101) Avail: NTIS HC A06/MF A01 CSCL 20K

A two-dimensional hybrid experimental-numerical technique for elastic-plastic stress analysis is presented. This technique results from merging two relatively new technologies in engineering mechanics: boundary element methods and image processing. A syntactic pattern recognition scheme termed Displacement Pattern Matching determines displacement boundary conditions to be used in an elastic-plastic boundary element (EPBEM) code. The result is an automated stress analysis tool. Displacement pattern matching is a process where displacements measured by tracking an arbitrary array of black spots on a white specimen are compared in a double exposure format to determine displacements. Displacement pattern matching is a full-field technique, with spatial resolution on the order .0001 inch. GRA

N89-20500# Sydney Univ. (Australia). School of Civil and Mining Engineering.
NON-SYMMETRIC BIFURCATION OF GEOMETRICALLY NON-LINEAR ELASTIC-PLASTIC AXISYMMETRIC SHELLS UNDER COMBINED LOADS INCLUDING TORSION
Jian-Guang Teng and J. M. Rotter Apr. 1988 65 p
(PB89-102149; R-561) Avail: NTIS HC A04/MF A01 CSCL 20K

A finite element formulation is presented for the nonsymmetric bifurcation analysis of geometrically nonlinear elastic-plastic shells of revolution. The shell may be branched and segmented. The loads are axisymmetric but may include in-plane shears. A new nonlinear shell theory is adopted which includes nonlinear strains arising from in-plane displacements. For the determination of the nonlinear prebuckling load deflection path, the J sub 2 flow theory of plasticity is used. For the nonsymmetric bifurcation analysis, three alternatives are provided. A new efficient and automatic solution procedure is described to determine the critical buckling mode, and hence the critical buckling stress. Several example problems are analyzed and the predictions of the present analysis are compared with available theoretical and experimental results. The effect of using different plasticity theories in the stability analysis is also briefly discussed. Author

N89-20501 North Carolina State Univ., Raleigh.
DETERMINATION OF THE IMPULSE RESPONSE OF A VISCOELASTIC BEAM USING A FRACTIONAL DERIVATIVE CONSTITUTIVE MODEL Ph.D. Thesis
James Andrew Cooke 1988 110 p
Avail: Univ. Microfilms Order No. DA8815492

The mechanical behavior of most viscoelastic materials is characterized by loading rate-dependent properties, even under loads of small magnitude. Several classical means exist for modeling viscoelastic constitutive behavior. These techniques can

be used with basic equations of mechanics for the solution of structural viscoelastic problems. One viable addition to these classical forms is the fractional derivative representation for viscoelastic behavior. A fractional derivative technique is used to model the dynamic viscoelastic behavior of a polypropylene rod. A three-parameter fractional derivative is used to represent the storage and loss moduli of the polypropylene material. For the dynamic analytical evaluation, the Bernoulli-Euler and the Timoshenko simply-supported beam models for flexural vibrations are used with the inclusion of the fractional derivative for the viscoelastic properties. Laplace transformation methods are used to facilitate solution. The beam model is excited transversely at the center of the span by a Dirac delta function. The calculated time domain displacement from the fractional derivative viscoelastic beam is compared with beam equations formulated using the standard Kelvin-Voigt and the classical hysteretic damping constitutive models under identical conditions. The results are also compared to experimental deflection data from a simply-supported polypropylene beam impacted at center span. Dissert. Abstr.

N89-20502# Sydney Univ. (Australia). School of Civil and Mining Engineering.
ELASTIC STABILITY OF CYLINDRICAL SHELLS WITH CIRCUMFERENTIAL WELDED JOINTS UNDER AXIAL COMPRESSION
J. M. Rotter and Jian-Guang Teng Mar. 1988 39 p
(PB89-125082; R-564) Avail: NTIS HC A03/MF A01 CSCL 20K

Metal silos and tanks are subject to axial compressive stresses in their cylindrical shell walls. The buckling strength is very sensitive to geometric imperfections in the wall. The most regular and well defined imperfection is the local depression adjacent to a circumferential weld, caused by the plate rolling process and shrinkage of the weld. The elastic buckling strengths of cylindrical shells under axial compression, with imperfections arising at circumferential welded joints, were examined. The effects of the welded joint depression amplitude, the shell radius to thickness ratio, a change of shell plate thickness at the weld, and internal pressurization are all examined. It is shown that a welded joint depression is one of the most deleterious practical imperfection forms currently known. Author

N89-20503# Sydney Univ. (Australia). School of Civil and Mining Engineering.
EXPERIMENTS ON THE BUCKLING OF THIN-WALLED MODEL SILO STRUCTURES
J. M. Rotter, P. T. Jumikis, S. P. Fleming, and S. J. Porter May 1988 43 p
(PB89-125124; R-570) Avail: NTIS HC A03/MF A01 CSCL 20K

Many failures of silos in service have occured by buckling under axial compression and eccentric discharge of the stored solids has been implicated in a number of them. Little is known about buckling failures in which the wall stresses are directly induced by stored solids, or about the increases in buckling strength which derive from the stiffness of a stored granular solid in contact with the silo walls. Experiments are described in which these effects were studied. Model silos were loaded to failure, and the wall stresses and the consequent buckling failures were caused solely by a stored granular solid. These experiments were designed to explore the buckling strength and behavior of thin walled flat bottomed silos on initial filing and during discharge. Both concentric and eccentric discharge conditions in funnel flow silos are described. Buckling failures with both stable and unstable characteristics are noted. GRA

N89-20504# Lehigh Univ., Bethlehem, PA. Engineering Lab.
TRIPPING OF ASYMMETRICAL STIFFENERS UNDER COMBINED LOADING Final Report
Alexis Ostapenko and Dongho Yoo Aug. 1988 64 p
(Contract DTMA91-86-C-60117)
(PB89-126171; FRITZ ENGINEERING LAB-513.3; MA-RD-840-88035) Avail: NTIS HC A04/MF A01 CSCL 20K

Presented is a study of the tripping strength of asymmetrical longitudinal plate stiffeners subjected to a combination of axial and lateral loads. The loaded edges were taken to be simply supported. The method of analysis is based on the principle of minimum total potential, and ten displacement functions were used to describe the deformations of the plate and stiffeners. First yielding was used as the criterion of ultimate strength. Instability under axial loading was investigated for the symmetrical (Tee) and asymmetrical (Angle) stiffeners. Angle stiffeners showed greater capabity than Tee stiffeners for lower values of the slenderness ratio (L/r), but lower capacity for higher values of the slenderness ratio, especially, after consideration of the deformations of the stiffener web. A modified effective width concept was introduced into the analysis to consider the effect of postbuckling plate deformations under combined loading condition. A relationship for the interaction between the axial and lateral loads when the lateral loading is applied in the direction from plate to stiffener. When the lateral loading is applied in the other direction, the interaction is almost linear. The computer program developed during the study was the main tool to provide the needed numerical results. Author

N89-20505# Minnesota Dept. of Transportation, Saint Paul. Physical Research Section.
METHODS AND MATERIALS FOR REDUCING CRACK REFLECTANCE Final Report No. 1, 1987
Tom Ravn, Ron Cassellius, and Roger Olson Dec. 1987 38 p Sponsored by Federal Highway Administration, St. Paul, MN
(PB89-114532; FHWA/MN/RD-05; MN/DOT-INVESTIGATION-202-1) Avail: NTIS HC A03/MF A01 CSCL 20K

The study was initiated to study methods, procedures and/or materials that may reduce premature pavement failures of an asphaltic concrete overlay on an existing bituminous road. The methods included in the study were asphalt additives in the wearing course, full coverage fabric, asphalt rubber interlayer (SAML) and asphalt rubber seal coat (SAM). No material or method was found to totally eliminate reflective cracking. The test sections using softer asphalt (200 to 300 PEN) in the wearing course provided the best results, with the carbon black and sulfur additives minimizing the flushing that was prevalent in the 200 to 300 PEN. control section. Author

N89-20506# Jiaotong Univ., Shanghai (China). Dept. of Mechanical Engineering.
LARGE DEFLECTION ANALYSIS OF THIN ELASTIC SHELLS BY HYBRID STRESS METHOD
Zhengxing Liu and Rong Ye 1987 9 p Sponsored by Institute of Scientific and Technical Information of China, Beijing
(PB89-111504; ISTIC-TR-C-000199) Avail: NTIS HC A02/MF A01 CSCL 20K

Based on the incremental complementary energy principle, a stress hybrid model is developed for the geometrically nonlinear analysis of plates and shells. According to the compatibility of both interior and boundary displacements for an element and the equilibrium of stresses at the interior of the element, an inconsistent model which satisfies partially the stress equilibrium equation, and establishes a three node, fifteen degree of freedom, triangular shallow shell element is utilized. Formulas are derived in the Updated Lagrangian coordinate system. Numerical examples demonstrate that the assumed stress hybrid model is very efficient. Author

N89-20507 Brown Univ., Providence, RI.
ANALYSIS OF DYNAMIC ELASTIC-PLASTIC FRACTURE PHENOMENA: STEADY CRACK GROWTH AND TRANSIENT LOADING OF A STATIONARY CRACK Ph.D. Thesis
Jonathan Tuttle Leighton 1988 122 p
Avail: Univ. Microfilms Order No. DA8822550

Attention is focused on the asymptotic stress and deformation fields near the edge of a mode 1 crack propagating steadily in an elastic-perfectly plastic incompressible material under plane strain conditions. Features of previously reported results on this problem

are reviewed, with a view toward establishing discriminating characteristics. An asymptotic solution is constructed which has the properties that the angular variation of stress and particle velocity around the crack tip are continuous and the plastic strains are bounded at the crack tip. The influence of inertia and rate-sensitivity on the competition between cleavage and ductile fracture is examined. Finite element computations are performed on the plane strain transient loading of a semi-infinite crack in an infinite rate-sensitive body. It is found that, as the elastodynamic K-field established itself around the crack tip, features of the Riedel-Rice field emerge within the K-field but do not establish themselves completely. Local brittle and ductile fracture criteria are adopted, and the time required to meet these criteria is found from the numerical results. A comparison of the two fracture criteria shows the qualitative features of the effect of rate sensitivity on the cleavage-ductility fracture competition. Dissert. Abstr.

N89-20508 Brown Univ., Providence, RI.
COMPUTATIONAL STUDIES IN NONLINEAR FRACTURE MECHANICS Ph.D. Thesis
Fong Zhong Li 1988 163 p
Avail: Univ. Microfilms Order No. DA8822551

This thesis is composed of three chapters. In the first chapter, a concise derivation of the volume integral expression for calculating the energy release rate is given. Finite element implementations of the volume integral formulations are outlined for both two dimensional and three dimensional problems. For illustrative purposes, numerical examples are presented for a fully plastic, plane strain, edge-cracked panel subject to combined tension and bending to prove the effectiveness of the volume integral methods. In chapter 2, finite element solutions for near tip stress and deformation fields in elastic-power law creeping solids are used to investigate the dominance of the asymptotic crack tip fields. With geometry changes neglected, the full range from small scale to extensive creep is analyzed. Finite deformation effects on the crack tip fields are considered. Chapter 3 gives the finite element solution for growing cracks under transient creep conditions for a power law creep material with a given density of cavitating grain boundary facets. Attentions are focused on the crack growth rates and the stress and deformation characterization for growing cracks. The effects of various material parameters on the crack growth rate are also analyzed. Dissert. Abstr.

N89-20509 Michigan Univ., Ann Arbor.
GREEN'S FUNCTION FORMULATION OF PLANE CRACK PROBLEMS FOR GENERAL ANISOTROPIC MATERIALS Ph.D. Thesis
Francisco Antonio Sturla 1988 119 p
Avail: Univ. Microfilms Order No. DA8821658

The widespread use of composites in structural applications has led to increased interest in the elastic and thermoelastic behavior of anisotropic materials. Problems involving the presence of a slit-like crack in an infinite general anisotropic material arise in the study of fracture mechanics. The isothermal problem of a plane crack in a general anisotropic infinite body subjected to a uniform stress field at infinity is reviewed, using two methods: Fourier transforms and continuously distributed dislocations. The method of Fourier transforms was used to formulate thermoelastic problems in anisotropic materials. In particular, a solution is given in the literature for the plane crack obstructing a uniform heat flux in a homogeneous anisotropic medium, but it is valid only when the material has certain symmetries, i.e., where the K (sub 12) component of the conductivity tensor is zero. The thermoelastic Green's functions for plane problems in general anisotropy was developed. The Green's functions and the solution due to a dislocation are used to solve the plane crack problem in a homogeneous general anisotropic body perturbing an otherwise uniform heat flow. Dissert. Abstr.

N89-20510 Cincinnati Univ., OH.
A REFINED THEORY FOR PLATE BENDING WITH OPTIMIZED STRESS FIELD Ph.D. Thesis
Diaa M. Hosny 1988 221 p
Avail: Univ. Microfilms Order No. DA8822826

The bending behavior of plates can be analyzed by classical plate theory or by refined theories or higher-order plate theories which account for transverse shear deformation. These theories are able to satisfy the differential equations of either equilibrium or compatibility, but not both simultaneously. A plate bending theory is proposed which assumes components of stress in a form which satisfies Cauchy's local equilibrium and stress boundary conditions and yet leaves enough freedom in the quantities involved better to satisfy the conditions of local compatibility. A finite difference Levenberg-Marquardt algorithm is used to minimize the error in these local compatibility equations. The theory is applied to a variety of problems using a single optimization parameter. The solutions are compared to solutions based upon Reissner's formulation, elasticity solutions and those of other refined and higher-order theories. One problem is also analyzed by three-dimensional finite element techniques utilizing NASTRAN. Those results are compared to the solutions obtained by elasticity and by the proposed theory. Dissert. Abstr.

N89-20511 Brown Univ., Providence, RI.
THEORETICAL AND COMPUTATIONAL STUDIES IN PLASTICITY AND FRACTURE Ph.D. Thesis
Brian Moran 1988 136 p
Avail: Univ. Microfilms Order No. DA8822568

A framework for the derivation of crack tip contour integrals is presented. The conditions under which the integrals are physically meaningful are outlined. The domain integral method is discussed as a means of representing crack tip integrals and as an efficient method for their numerical evaluation. A finite element formulation for transient analysis of viscoplastic solids is presented. The formulation is based on explicit integration of the equations of motion and the plastic rate equations. A number of simple numerical examples are presented to illustrate the method. Constitutive and computational aspects of finite deformation plasticity are considered. The focus is on formulations which reduce the classical treatment of hyperelasticity for vanishing plastic strain rates and are amenable to implicit and explicit computation. An implicit scheme, involving equilibrium iteration, and an explicit scheme without iteration are considered. A numerical example is presented to illustrate the features of the two schemes. The crack tip stress and deformation fields in an axisymmetric fracture specimen are examined. The effects of material rate sensitivity and void nucleation and growth on fracture initiation using a rate-dependent version of Gurson's model for porous plastic solids are investigated. The plane strain HRR fields are shown to hold within several blunted openings of the crack tip. The influence of rate sensitivity is to promote cleavage fracture under higher loading stress. Dissert. Abstr.

N89-20512*# Textron Bell Helicopter, Fort Worth, TX.
COUPLED ROTOR/FUSELAGE DYNAMIC ANALYSIS OF THE AH-1G HELICOPTER AND CORRELATION WITH FLIGHT VIBRATIONS DATA Final Report
J. C. Corrigan, J. D. Cronkhite, R. V. Dompka, K. S. Perry, J. P. Rogers, and S. G. Sadler Jan. 1989 144 p
(Contract NAS1-17496)
(NASA-CR-181723; NAS 1.26:181723) Avail: NTIS HC A07/MF A01 CSCL 20K

Under a research program designated Design Analysis Methods for VIBrationS (DAMVIBS), existing analytical methods are used for calculating coupled rotor-fuselage vibrations of the AH-1G helicopter for correlation with flight test data from an AH-1G Operational Load Survey (OLS) test program. The analytical representation of the fuselage structure is based on a NASTRAN finite element model (FEM), which has been developed, extensively documented, and correlated with ground vibration test. One procedure that was used for predicting coupled rotor-fuselage vibrations using the advanced Rotorcraft Flight Simulation Program C81 and NASTRAN is summarized. Detailed descriptions of the analytical formulation of rotor dynamics equations, fuselage dynamic equations, coupling between the rotor and fuselage, and

solutions to the total system of equations in C81 are included. Analytical predictions of hub shears for main rotor harmonics 2p, 4p, and 6p generated by C81 are used in conjunction with 2p OLS measured control loads and a 2p lateral tail rotor gearbox force, representing downwash impingement on the vertical fin, to excite the NASTRAN model. NASTRAN is then used to correlate with measured OLS flight test vibrations. Blade load comparisons predicted by C81 showed good agreement. In general, the fuselage vibration correlations show good agreement between anslysis and test in vibration response through 15 to 20 Hz. Author

N89-20513# Rice Univ., Houston, TX. Dept. of Civil Engineering.
NONNORMAL ACCELERATIONS DUE TO YIELDING IN A PRIMARY STRUCTURE
David C. K. Chen and L. D. Lutes (Texas A&M Univ., College Station.) 19 Sep. 1988 53 p Sponsored in part by National Center for Earthquake Engineering Research, Buffalo, NY prepared in cooperation with Texas A and M Univ., College Station
(Grant NSF ECE-86-07591)
(PB89-131437; NCEER-88-0030) Avail: NTIS HC A04/MF A01 CSCL 20K

Response nonnormality is investigated for a yielding primary structure subjected to a normally distributed ground acceleration. This is a preliminary step in the nonlinear investigation of primary-secondary systems, since this primary acceleration is the base excitation of a light secondary system. The nonlinearity considered is bilinear hysteretic yielding in the primary structure. Results are presented from simulation, and from analysis of a simplified nonhysteretic substitute structure. The study of the nonnormality of acceleration is an extension of previous investigations which focused on displacement nonnormality. The nonlinear but nonhysteretic substitute structural model used here is a substantially improved version of an earlier model. The substitute structure is one for which the stationary Fokker-Planck equation can be solved to obtain values for probability distribution and moments of response. Analytical and numerical results for the substitute structure are compared with those from simulation of the bilinear hysteretic system. Author

N89-20514*# National Aeronautics and Space Administration. Lewis Research Center, Cleveland, OH.
RESULTS OF INPHASE AXIAL-TORSIONAL FATIGUE EXPERIMENTS ON 304 STAINLESS STEEL
Peter J. Bonacuse and Sreeramesh Kalluri (Sverdrup Technology, Inc., Cleveland, OH.) Mar. 1989 22 p Prepared in cooperation with Army Aviation Research and Development Command, Cleveland, OH
(NASA-TM-101464; E-4576; NAS 1.15:101464; AVSCOM-TR-88-C-022) Avail: NTIS HC A03/MF A01 CSCL 20K

A series of axial-torsional, inphase, strain-controlled, low-cycle fatigue tests were performed at room temperature on tubular specimens of 304 stainless steel. The program was conducted in cooperation with the task group on multiaxial fatigue research of ASTM committee E-09. The objective was to quantify the variability in multiaxial test results among several laboratories. Only included is data which was generated at the NASA Lewis Research Center's High Temperature Fatigue and Structures Laboratory. The experimental equipment and procedures used are described. The tubular specimens were polished on the outer surface to aid in the use of a cellulose film surface replication technique for crack detection. However, cracking initiated predominantly on the internal surface for all specimens. Honing of the bore of the tubular specimens lessened but did not entirely eliminate this problem. The observed fatigue lives are compared with lives calculated from three multiaxial life models. Constants for the life prediction models were obtained from uniaxial and torsional tests performed on the same heat of material. The observed fatigue lives agreed with calculated lives to within a factor of two for all but one of the life prediction models. Author

N89-20515# Technische Univ., Eindhoven (Netherlands).
A NUMERICAL IMPLEMENTATION OF THE SCHAPERY MODEL FOR NONLINEAR VISCOELASTICITY Ph.D. Thesis
Henricus Franciscus Rooijackers 1988 115 p
(ETN-89-93895) Avail: NTIS HC A06/MF A01

A constitutive equation for nonlinear viscoelasticity is derived, starting from irreversible thermodynamics. The three-dimensional formulation of the Schapery model is obtained: a single integral model using internal variables to take history effects into account. This model can describe anisotropic material behavior. A large number of other material models can be seen as simplifications of the derived model. For the numerical implementation in a finite element package, the formulation is simplified to describe isotropic material behavior. An axisymmetric element is developed and applied in the simulation of complex problems where the nonlinear viscoelastic behavior of the material as well as the large deformations of the structure itself, play a significant role. Due to its generality, the three-dimensional Schapery model is very well suited for efficient simulation of the mechanical behavior of a large class of viscoelastic materials. ESA

N89-20516# Aeronautical Research Inst. of Sweden, Stockholm. Structures Dept.
POSTBUCKLING FINITE ELEMENT (FE) ANALYSIS OF A STIFFENED CURVED PANEL LOADED IN SHEAR
Rolf Jarlas May 1988 48 p
(Contract FMV-FFL-82250-85-273-25-001)
(FFA-TN-1988-23; ETN-89-93731) Avail: NTIS HC A03/MF A01

Results from nonlinear finite element postbuckling analyses are compared with experimental results from tests with a complex stiffened curved panel loaded in shear. Different methods are used to pass through areas exhibiting convergence problems. It is shown that for this type of analyses it is better to use displacement control than to use the arc-length method. The convergence problems when new buckles appear are easier to handle when eigenmodes are added as imperfections because the initialization starts earlier and the transition into a postbuckled state becomes more smooth. It is also shown that the sign of the added eigenmodes is important. In spite of the relatively large effort spent, it was not possible to obtain a satisfactory agreement between computed data and the experimental data. Possible explanations for this are discussed. ESA

N89-20517# Aeronautical Research Inst. of Sweden, Stockholm. Structures Dept.
IMPLEMENTATION OF A HIERARCHICAL WEDGE ELEMENT IN THE SELF-ADAPTIVE FINITE ELEMENT (FE) PROGRAM STRIPE
Urban Falk and Anders I. Gustavsson Sep. 1988 31 p Sponsored by the Defence Material Administration, Stockholm, Sweden
(FFA-TN-1988-36; ETN-89-93732) Avail: NTIS HC A03/MF A01

A three-dimensional self-adaptive finite element (FE) method in linear elastomechanics is considered. A wedge-shaped finite element with hierarchical interpolation functions based on the p-version of the finite element method is derived. This element is implemented in the self-adaptive FE-program STRIPE and is fully compatible with the previously implemented brick-shaped finite element. The characteristics of the element are demonstrated by solving examples. ESA

N89-20518# European Space Agency, Paris (France).
MODELING FLEXIBILITY OF MECHANISMS WITH ADAMS
F. Panin (European Space Agency. European Space Research and Technology Center, ESTEC, Noordwijk, Netherlands) Aug. 1988 51 p
(ESA-STM-242; ISSN-0379-4075; ETN-89-93904) Copyright Avail: NTIS HC A04/MF A01; ESA Publications Div., Noordwijk, Netherlands, 20 Dutch guilders

The Automatic Dynamic Analysis of Mechanical Systems (ADAMS) general purpose computer program was developed for

the kinematic, static, and dynamic analysis of two and three-dimensional mechanical systems. All the nonlinearities present in the mechanism to be modelled can be considered and included in the simulation, such as large displacements, blacklash, friction, contact forces, and characteristics of bushings and driving units. The ADAMS permits the user to build up the system model as a set of rigid bodies connected by joints. The forces acting between/on these bodies may be defined as functions of the system variables. If a required element of the mechanism or mechanical phenomenon has not yet been implemented in ADAMS, the user may define it either externally to the ADAMS package through FORTRAN subroutines or internally to the input data set which defines the model, the choice depending on the complexity of the problem to be described. While the FIELD statement may be used to model a general force-displacement relationship, the BEAM statement is designed to model such a relationship for a uniform cross section beam in particular. This means that it is possible to develop two techniques to include the flexibility of parts in the model. A separate technique to model complex flexible parts uses standard SFORCE statements to represent flexible constraints. While this leaves a great freedom to the analyst when modeling parts and constraints, the results should be examined critically as they are particularly sensitive to the assumptions and intermediate steps required. ESA

N89-20519# National Aerospace Lab., Amsterdam (Netherlands). Structures and Materials Div.

BULGING CRACKS IN PRESSURIZED FUSELAGES: A NUMERICAL STUDY

E. Riks 17 Nov. 1987 33 p

(Contract NIVR-06404N)

(NLR-MP-87058-U; ETN-89-94039) Avail: NTIS HC A03/MF A01

The possibility to obtain useful results by means of commercially available nonlinear finite element techniques in analyses of pressurized, stiffened, thin walled shells cylindrical shells was studied. Unstiffened as well as stiffened configurations based on actual fuselage designs were considered. It is shown that the nonlinear effect is large for large aspect ratios of the cracks and that stiffeners have, in general, a considerable effect on the stress intensity factors. ESA

N89-20520# National Aerospace Lab., Amsterdam (Netherlands). Structures and Materials Div.

ANALYSIS OF CRACK OPENING BEHAVIOR BY APPLICATION OF A DISCRETIZED STRIP YIELD MODEL

A. U. deKoning and G. Liefting (Technische Hogeschool Twente, Enschede, Netherlands) 1 Mar. 1986 41 p Presented at the International Symposium on Fatigue Crack Closure, Charleston, WV, May 1986

(Contract NIVR-1823/01702-N)

(NLR-MP-87065-U; ETN-89-94043) Avail: NTIS HC A03/MF A01

The crack opening behavior of a fatigue crack in a centrally cracked panel was studied using a discretized version of the Dugdale and Barenblatt model. The effect of crack growth was also included. Results obtained for constant amplitude loading agree with data in the literature. The effect of application of single overload-underload combinations and of simple block loading programs on the crack opening behavior were analyzed. The results were compared with predictions based on an empirical model (CORPUS). The criteria used in the CORPUS model to select significant load excursions in the applied load sequence were checked. Both models were used to predict crack growth under a simplified landing gear load sequence. The predicted crack opening loads and the crack growth agree with experimental data. ESA

N89-20521# National Aerospace Lab., Amsterdam (Netherlands).

CURRENT STATUS OF FLIGHT SIMULATION FATIGUE CRACK GROWTH CONCEPTS

R. J. H. Wanhill and J. Schijve 15 Jan. 1988 19 p Presented at the 3rd French Metallurgical Society International Spring Meeting, Paris, France, Jun. 1988

(NLR-MP-88001-U; ETN-89-94051) Avail: NTIS HC A03/MF A01

Crack growth models and methods of crack growth prediction are compared with respect to applicability and limitations. Research areas for improvement of crack growth prediction are specified. Fatigue crack growth predictions should be considered acceptable if within a factor of 2 of test results, and if they show the correct trends for variations of spectrum and test parameters. Although the choice of crack growth model depends on particular circumstances, it is preferable, certainly in the long term, to concentrate on improving and using crack opening models. Improvement of crack opening models, in particular their ability to deal with plane strain/plane stress conditions and more complicated crack geometries, requires developments in analytical and experimental determinations of near-tip crack opening and the compilation of flight simulation fatigue test data banks. Usable models and methods for predicting short crack growth are years away. Their applicability will probably be restricted to damage tolerance of engine disks and blades and durability analysis of airframes. A better description of constant amplitude fatigue crack growth is needed, especially at low and high stress intensity levels and high stress ratios. More understanding is required of the interrelations between microstructure, fracture mechanisms, fracture topography, threshold, crack growth curve transition points, and crack opening behavior. ESA

N89-20522# National Aerospace Lab., Amsterdam (Netherlands). Structures and Materials Div.

FRACTURE CONTROL GUIDELINES FOR STRESS CORROSION

R. J. H. Wanhill 12 Feb. 1988 29 p Submitted for publication

(NLR-MP-88007-U; ETN-89-94056) Avail: NTIS HC A03/MF A01

The actual and potential uses of fracture mechanics to characterize stress corrosion cracking and to provide stress corrosion fracture control in engineering structures are discussed. Four levels of increasing refinement are identified: preliminary screening; data comparisons; design concepts and trade studies; and final design and materials, including recommendations for safety and reliability. For corrosion fatigue plus cyclic stress corrosion the more or less regular cracking process that is characteristic of fatigue means that in principle the prediction of crack growth lives and the establishment of inspection schedules should be less difficult than for stress corrosion alone. This seems to be the case for constant amplitude fatigue loading, but there is a dearth of information for variable amplitude fatigue. The compilation of variable amplitude fatigue crack growth data banks, using representative load histories, environments, cycle frequencies and waveforms, would be useful, both for directly enabling crack growth predictions by empirical interpolation, and for improvements in crack growth modeling. ESA

N89-20523# National Aerospace Lab., Amsterdam (Netherlands). Structures and Materials Div.

PREDICTION OF LOW AND HIGH CRACK GROWTH RATES UNDER CONSTANT AND VARIABLE AMPLITUDE LOADING

A. U. deKoning and D. J. Dougherty (Purdue Univ., Indianapolis, IN.) 22 Feb. 1988 14 p Presented at the 3rd Int. Spring Meeting on Fatigue Crack Growth under Variable Amplitude Loading, Paris, France, 15-17 Jun. 1988

(NLR-MP-88012-U; ETN-89-94059) Avail: NTIS HC A03/MF A01

Applicability of rainflow counting to crack growth analysis of complex loading is discussed. The rainflow counting method can account for the effects of small and high loading cycles under spectrum loading conditions. Mathematical formulation of an incremental crack growth law is presented. The model includes effects of threshold and closure. The model discriminates between crack growth associated with secondary plastic flow and that of primary flow under stationary crack opening conditions. The sum of each contribution is equated to the total crack growth. The crack growth model can be used to improve the counting method

by predicting the effect of different treatment of the load cycles collected in the residue. The model was applied to constant amplitude crack growth data found in the literature. The agreement between the curve fit growth rate and the experimental results is excellent. The effects of threshold and high stress intensity levels are shown to be properly described by the model. ESA

N89-20524# Southampton Univ. (England). Inst. of Sound and Vibration Research.
COMPARISON BETWEEN PREDICTED AND MEASURED ROTATIONAL FREQUENCY RESPONSE FUNCTIONS
H. G. Lee Aug. 1988 31 p
(ISVR-TR-164; ETN-89-94086) Avail: NTIS HC A03/MF A01

A lightly damped free-free beam was used to measure the rotational frequency response functions. A small exciting block was used to apply the rotational excitation. Because the beam was very lightly damped, a damping tape can be attached to provide better resolution around the resonances. It is shown that it is possible to measure the parameters of frequency response functions accurately and also possible to deduce parameters using modal identification. ESA

N89-20525# Aeronautical Research Inst. of Sweden, Stockholm. Structures Dept.
ESTIMATION OF THE EQUIVALENT INITIAL FLOW SIZE (EIFS) DISTRIBUTION AND PREDICTION OF FAILURE PROBABILITIES FOR DIFFERENT PARAMETER VARIATIONS
Lars Moraeus Oct. 1987 30 p Sponsored by the Swedish Board for Technical Development
(FFA-TN-1987-35; ETN-89-94123) Avail: NTIS HC A03/MF A01

The prediction of the probability of failure due to excessive cracking in aircraft structures was studied. Equivalent initial flaw size (EIFS) distribution for an aluminum alloy (2024-T3) was determined using experimental crack growth data for small cracks. The results show that the statistical basis for the EIFS determination must be considerably larger in order to draw any conclusions regarding the generic properties of the EIFS-distribution. Parameter influences on the probability of failure are investigated by using a hypothetical aircraft structure. Results show that the effect of varying the standard deviation of the extreme loads and the crack growth rate correlation time is almost negligible. ESA

N89-20526# Aeronautical Research Inst. of Sweden, Stockholm. Structures Dept.
A THEORETICAL, NUMERICAL AND EXPERIMENTAL EXAMINATION OF IN SITU PROPERTIES OF ADHESIVES
Ronald Bredemo Mar. 1988 52 p
(FFA-TN-1988-05; ETN-89-94124) Avail: NTIS HC A04/MF A01

A method for determining the elastic properties of thin adhesive layers was studied. Analytical methods as well as a finite element method were utilized. Experiments in order to establish the stiffness characteristics of a particular adhesive joint were carried out. In what respect a limited change in geometry influences on the stiffness and on the ultimate load of the adhesive joint was also studied. ESA

N89-20527# Oak Ridge National Lab., TN. Engineering Technology Div.
NEAR THRESHOLD FATIGUE CURVE BASED ON THE DISLOCATION SHIELDING MODEL OF FRACTURE
S. J. Chang and T. Mura (Northwestern Univ., Evanston, IL.) 1988 7 p Presented at the 7th International Conference on Fracture, Houston, TX, 20 Mar. 1989
(Contract DE-AC05-84OR-21400)
(DE88-011854; CONF-890310-1) Avail: NTIS HC A02/MF A01

Dislocation pileup along an inclined direction from a crack tip has been observed in metals during tensile deformation in an electron microscope. Dislocations are emitted from the crack tip, move through a dislocation-free zone and pile up in the plastic zone. The problem of inclined pileup of screw dislocations at a crack tip with a dislocation-free zone has been solved by applying the Wiener-Hopf method. Result can be used to calculate the crack tip blunting and the local stress intensity K for the applied stress intensity K (sub 3). According to the fatigue theory of Laird, the crack propagation per cycle has the order of magnitude of the blunting. The blunting versus K (sub 3) is then plotted. It has the shape of the near threshold fatigue curve. To plot this curve, the local stress intensity K has been assumed to be the critical value K (sub g) for the dislocation emission at the crack tip. DOE

N89-20528# Los Alamos National Lab., NM.
A STEREOLOGICAL ANALYSIS OF DUCTILE FRACTURE BY MICROVOID COALESCENCE
James H. Steele, Jr. 1988 24 p Presented at the 7th International Conference on Fracture, Houston, TX, 20 Mar. 1989
(Contract W-7405-eng-36)
(DE89-000355; LA-UR-88-3167; CONF-890310-2) Avail: NTIS HC A03/MF A01

A stereological analysis for ductile fracture by microvoid coalescence is presented based upon the model of Widgery and Knott which postulates that microvoids link with a propagating crack if they lie within a certain interaction distance of its plane. A 3-dimensional analytical expression for dimple density and shape is developed from this model using projected image relationships for a thin slab. Void nucleation and growth are incorporated into the analysis using numerical integration of the Rice-Tracey growth equation over the appropriate strain range. An evaluation of the stereological approach is given using tensile data from a spheroidized 1045 steel to predict the effect of hydrostatic pressure upon the dimple density. The analysis, which is consistent with observed correlations between dimple density and second phase particle density, is shown to provide an estimate of dimple size and microroughness parameter used in local stain models for microvoid coalescence. DOE

N89-20529# Sandia National Labs., Albuquerque, NM.
EFFECT OF SURFACE STRESS ON STRESS CORROSION OF SILICATE GLASS
Terry A. Michalske and Bruce C. Bunker 1988 13 p Presented at the 7th International Conference on Fracture, Houston, TX, 20 Mar. 1989
(Contract DE-AC04-76DP-00789)
(DE89-004584; SAND-88-3183C; CONF-890310-4) Avail: NTIS HC A03/MF A01

Slow crack growth data, solution analysis and surface stress measurements are used to develop a model to explain the low crack velocity behavior of multicomponent silicate glasses. We show that the low crack velocity plateau previously observed for binary alkali silicate glasses also occurs in sodium borosilicate glasses. Our model for this behavior involves the generation of surface stress on the crack walls behind the crack tip and the effect of the stress to increase the crack tip stress intensity. We find that glasses that show preferential removal of alkali from the surface layer during aqueous corrosion can develop surface tensile stress. Surface stresses on the order of 30 MPa were measured in acidic conditions. Using a simple fracture mechanics formulation, we were able to use our data for leached layer formation rate and development of surface tensile stress to quantitatively predict the onset of a low velocity plateau in sodium borosilicate glasses. DOE

N89-20530# Purdue Univ., West Lafayette, IN. School of Mechanical Engineering.
DIAGNOSTICS FOR INTELLIGENT CONTROL OF MPD ENGINES Final Report, 1985 - 1988
R. Shoureshi 15 Nov. 1988 141 p
(Grant AF-AFOSR-0278-86; AF Proj. 2308)
(AD-A203640; AFOSR-89-0060TR) Avail: NTIS HC A07/MF A01 CSCL 20K

Magnetoplasmadynamic (MPD) thrusters are examples of distributed parameter systems that have temporal and spatial variations. In order to establish an intelligent diagnostic system for MPD thrusters, fundamental theorems had to be derived for

the general case of diagnostics of distributed systems. Advanced mathematical techniques of semigroups and groups, equivalent norms, invariant principle, Lyapunov functional, etc., have been integrated with control schemes in order to develop criterion for stability, controllability and observability of distributed parameter systems. A simple model of the MPD thruster was developed and used in evaluation of the resulted theorems. Instability conditions for MPD thrusters are derived and stabilizability inputs are presented. This research has led to new understanding for the general problem of distributed parameter systems. GRA

42 GEOSCIENCES (GENERAL)

No abstracts in this category.

43 EARTH RESOURCES AND REMOTE SENSING

Includes remote sensing of earth resources by aircraft and spacecraft; photogrammetry; and aerial photography.

For instrumentation see *35 Instrumentation and Photography.*

N89-20531*# Science and Technology Corp., Hampton, VA.
THE INVESTIGATION OF ADVANCED REMOTE SENSING, RADIATIVE TRANSFER AND INVERSION TECHNIQUES FOR THE MEASUREMENT OF ATMOSPHERIC CONSTITUENTS Final Report, 15 Dec. 1977 - 15 Mar. 1985
Adarsh Deepak and Pi-Huan Wang Mar. 1985 320 p
(Contract NAS1-15198)
(NASA-CR-172599; NAS 1.26:172599) Avail: NTIS HC A14/MF A01 CSCL 04A

The research program is documented for developing space and ground-based remote sensing techniques performed during the period from December 15, 1977 to March 15, 1985. The program involved the application of sophisticated radiative transfer codes and inversion methods to various advanced remote sensing concepts for determining atmospheric constituents, particularly aerosols. It covers detailed discussions of the solar aureole technique for monitoring columnar aerosol size distribution, and the multispectral limb scattered radiance and limb attenuated radiance (solar occultation) techniques, as well as the upwelling scattered solar radiance method for determining the aerosol and gaseous characteristics. In addition, analytical models of aerosol size distribution and simulation studies of the limb solar aureole radiance technique and the variability of ozone at high altitudes during satellite sunrise/sunset events are also described in detail. Author

N89-20532 Hull Univ. (England).
REMOTE SENSING IN REFRACTIVE TURBULENCE Ph.D. Thesis
Joao De Lemos Pinto 1986 175 p
Avail: Univ. Microfilms Order No. BRDX83208

Atmospheric laser based remote sensing was investigated and developed, using visible and infrared lasers, by various research groups. On the whole, remote sensing is favored when based on infrared lasers. The design of a highly sensitive system has to involve an end-to-end beam control design, i.e., the system designer has to consider carefully the laser system, the propagation path effects and the target characteristics. Of prime import, is the assessment of the limitations imposed by atmospheric turbulence. Depending on its strength, refractive turbulence can cause a wandering in all directions and an eventual breakup of the transmitted beam and a scintillation effect. The sensitivity and accuracy of a remote sensing measurement is also affected by the stability of the laser and the detection system. In a remote sensing system, the laser beam is usually transmitted and received through a telescope in order to reduce the average power density along the propagation path and the beam divergence, thereby achieving longer ranges or smaller spot sizes in the far field. Dissert. Abstr.

N89-20533*# Louisiana State Univ., Baton Rouge. Coastal Ecology Inst.
UTILIZING REMOTE SENSING OF THEMATIC MAPPER DATA TO IMPROVE OUR UNDERSTANDING OF ESTUARINE PROCESSES AND THEIR INFLUENCE ON THE PRODUCTIVITY OF ESTUARINE-DEPENDENT FISHERIES Final Report
Joan A. Browder, L. Nelson May, Alan Rosenthal (National Marine Fisheries Service, Miami, FL), Robert H. Baumann, and James G. Gosselink 20 Dec. 1988 188 p
(Contract NAS5-28756)
(NASA-CR-183417; NAS 1.26:183417) Avail: NTIS HC A09/MF A01 CSCL 08C

The land-water interface of coastal marshes may influence the production of estuarine-dependent fisheries more than the area of these marshes. To test this hypothesis, a spatial model was created to explore the dynamic relationship between marshland-water interface and level of disintegration in the decaying coastal marshes of Louisiana's Barataria, Terrebonne, and Timbalier basins. Calibrating the model with Landsat Thematic Mapper satellite imagery, a parabolic relationship was found between land-water interface and marsh disintegration. Aggregated simulation data suggest that interface in the study area will soon reach its maximum and then decline. A statistically significant positive linear relationship was found between brown shrimp catch and total interface length over the past 28 years. This relationship suggests that shrimp yields will decline when interface declines, possibly beginning about 1995. Author

N89-20534# Begeleidingscommissie Remote Sensing, Delft (Netherlands). Research Inst. for Forestry and Landscape Planning.
THE SUITABILITY OF REMOTE SENSING FOR SURVEYING AND MONITORING LANDSCAPE PATTERNS. VOLUME A: PILOT STUDY - LANDSAT IMAGERY. VOLUME B: PEPS PROJECT NO. 73 - SPOT IMAGERY
J. M. J. Farjon Feb. 1988 79 p Original contains color illustrations
(BCRS-87-12-Vol-A/B; ETN-89-93871) Avail: NTIS HC A05/MF A01

The possibility of using LANDSAT Thematic Mapper and SPOT satellite imagery for land use mapping was studied. Image analysis and processing requirements, and the utilization of geographic information systems were investigated. For individual titles, see N89-20535 through N89-20536.

N89-20535# Begeleidingscommissie Remote Sensing, Delft (Netherlands). Research Inst. for Forestry and Landscape Planning.
THE SUITABILITY OF REMOTE SENSING FOR SURVEYING AND MONITORING LANDSCAPE PATTERNS. VOLUME A: PILOT STUDY - LANDSAT IMAGERY
J. M. J. Farjon, S. I. Kamstra, P. G. Lentjes, and W. J. C. Hoeffnagel *In its* The Suitability of Remote Sensing for Surveying and Monitoring Landscape Patterns. Volume A: Pilot Study - LANDSAT Imagery. Volume B: PEPS Project No. 73 - SPOT Imagery Feb. 1988 p 7-47 Original contains color illustrations (For primary document see N89-20534 13-43)
Avail: NTIS HC A05/MF A01

The utility of satellite imagery and image processing methods, in particular those of RESEDA (REmote SEnsing DAta processing) system, was assessed. Ways in which patterns of tree vegetation, watercourses, and land use can be inferred from comparing remote sensing imagery with field inventories were studied. Results show that LANDSAT-TM images are reasonably suitable for area inventories. Problems are due to small units that are heterogeneous

in terms of spectral signature, giving rise to many mixed pixels, which are difficult to distinguish as such. The suitability of TM images for the inventory of linear vegetations of trees seems to be limited because there are too many unsuitable classifications (35 pct) and missed lines (50 pct). Using various filters to extract line elements from the image gives less good results than visual interpretation because the computer gives undesired lines that would be discarded immediately in a visual interpretation. The MAP2 raster-based geographical information system is shown to be useful. ESA

N89-20536# Begeleidingscommissie Remote Sensing, Delft (Netherlands). Research Inst. for Forestry and Landscape Planning.

THE SUITABILITY OF REMOTE SENSING FOR SURVEYING AND MONITORING LANDSCAPE PATTERNS. VOLUME B: PEPS PROJECT NO. 73 - SPOT IMAGERY

J. M. J. Farjon, P. G. Lentjes, F. B. vanderLaan (National Aerospace Lab., Amsterdam, Netherlands), and W. J. C. Hoeffnagel *In its* The Suitability of Remote Sensing for Surveying and Monitoring Landscape Patterns. Volume A: Pilot Study - LANDSAT Imagery. Volume B: PEPS Project No. 73 - SPOT Imagery Feb. 1988 p 49-84 Original contains color illustrations (For primary document see N89-20534 13-43)

Avail: NTIS HC A05/MF A01

The SPOT spatial, spectral, and temporal resolution for line plantings, watercourses, and major land use classes (grassland, arable land, coniferous forest of different ages, deciduous forest of different ages, orchards and built-up areas) was assessed. The results show that the limit of the spatial resolution is 5 m. Orientation and context influence the spatial resolution only slightly. The reliable distinction of landuse classes is limited to major categories: agricultural land, forests and man-made objects. A further subdivision of landuse categories can presumably be achieved by application of more advanced image-processing software and/or imagery from another period of the year. The most promising applications of SPOT imagery are small-scale mapping and monitoring over large areas of broadly defined classes that correspond with distinct spectral classes: agricultural land, forests and man-made objects. The improvement of the available techniques, i.e., contextual image-processing and the elimination of mixed pixel influence with the aid of geographic information systems improves the accuracy of small-scale mapping of landscape patterns over large areas. Using SPOT for the large-scale mapping of landscape patterns in small areas is not be competitive with aerial photographs because of the higher costs involved and the poorer degree of detection. ESA

N89-20537# Begeleidingscommissie Remote Sensing, Delft (Netherlands).

LAND USE INVENTORIES USING SATELLITE IMAGES IN THE REGION HAAREN-HELVOIRT-UDENHOUT, NORTH BRABANT (THE NETHERLANDS) [GRONDGEBRUIK SINVENTARISATIES MET SATELLIETOPNAMEN IN HET GEBIED HAAREN-HELVOIRT-UDENHOUT, N-BRABANT]

Apr. 1988 37 p In DUTCH Prepared in cooperation with DHV raadgevend Ingenieursbureau B.V.. Amersfoot, The Netherlands and Dienst Ruimtelijkeordening, Natuurbeheer, landschap en Volkshuisvesting, The Netherlands Original contains color illustrations

(BCRS-88-07; ETN-89-93876) Avail: NTIS HC A03/MF A01

Satellite imagery was investigated as an alternative to aerial photographs for mapping of vegetation and aspects of land use and water management. A methodology for the execution of a vegetation growth type mapping was developed. Land use and water management for a region were mapped, using digital images from LANDSAT Thematic Mapper and SPOT. The results demonstrate the feasibility of satellite pictures for inventories. ESA

N89-20538# Begeleidingscommissie Remote Sensing, Delft (Netherlands).

PROCESSING AND APPLICATION OF DIGITAL AVHRR-IMAGERY FOR LAND AND SEA SURFACES Final Report

J. N. Roozekrans and G. J. Prangsma Aug. 1988 106 p Prepared in cooperation with Royal Netherlands Meteorological Inst., The Hague Original contains color illustrations

(BCRS-Proj. TO-3.1)

(BCRS-88-08; ETN-89-93877) Avail: NTIS HC A06/MF A01

A software-package for reading NOAA AVHRR-data tapes, calibration of the raw data, cloud detection, calculation of Earth surface parameters, and geometric correction of images was adjusted to perform automatically. Applications of AVHRR data, including observation (and perhaps warning) of damage in the agriculture caused by drought, night-frost etc; monitoring of meteorology related, troublesome situations for traffic like fog, snow and frost; locating fronts in the sea surface temperature, which might be areas with increased occurrence of certain fish-species, and input of sea surface temperature data for meteorological, oceanographic, and climate models were assessed. Results show that the AVHRR is a powerful tool for the monitoring of processes in the Earth-atmosphere system, especially for the monitoring of sea (lake) surface parameters. The coarse spatial resolution renders Advanced Very High Resolution Radiometer (AVHRR) data less suitable for land surfaces. ESA

N89-20539# Begeleidingscommissie Remote Sensing, Delft (Netherlands).

PHASE A STUDY FOR THE EXTENSION OF THE CAESAR SCANNER WITH A SENSOR MODULE FOR THE FAR INFRARED [FASE A STUDIE VOOR DE UITBREIDING VAN DE CAESAR SCANNER MET EEN SENSOR MODULE VOOR HET VERDERE INFRAROOD]

P. Binnenkade, H. Pouwels, H. Bokhoven, and C. Smorenburg (Technische Physische Dienst TNO-TH, Delft, Netherlands) Aug. 1988 91 p In DUTCH

(BCRS-Proj. TE-1.7)

(BCRS-88-09; TPD-733.002; ETN-89-93878) Avail: NTIS HC A05/MF A01

The extension of the CAESAR airborne scanner with a module for measurements in the thermal IR range, using the pushbroom scanning principle, was studied in the project CATS (CAESAR Airborne Thermal Scanner). An inventory of available detector arrays and a first dimensioning of the scanner were made. An optical concept and a preliminary design of electronics for data processing were made. Software aspects and the PARES programming systems are presented. The built-in possibilities of CATS in the METRO aircraft are discussed. The results of the study open the way to a successful development of CATS and demonstrate the feasibility of this scanner. ESA

N89-20540# National Aerospace Lab., Amsterdam (Netherlands). Space Div.

A SYSTEMATIC WORLDWIDE LANDCOVER OF SATELLITE MOSAICS

F. B. vanderLaan 31 Aug. 1987 7 p Presented at the Willie Nordberg Symposium on Remote Sensing towards Operational Cartographic Application, Graz, Austria, Sep. 1987

(NLR-MP-87062-U; ETN-89-94041) Avail: NTIS HC A02/MF A01

The increasing gap between the number of detailed satellite images (of, e.g., LANDSAT) recorded and the number actually used is discussed. A major cause for limited use of potentially available imagery is the cost. A complete range of national, continental, and worldwide applications has not developed for that reason. Possibilities for a wide use of imagery at affordable cost, particularly in developing regions are outlined. A central role in making satellite imagery available at a large scale is given to printed mosaics, in view of the high printing quality possible. ESA

N89-20541# National Aerospace Lab., Amsterdam (Netherlands). Space Div.
LAND USE INVENTORY USING LANDSAT THEMATIC MAPPER IMAGERY TO STUDY ENVIRONMENTAL POLLUTION
F. B. vanderLaan, O. F. Schoumans, and H. A. M. Thunnissen (Netherlands Soil Survey Inst., Wageningen.) 31 Aug. 1987 14 p Presented at the Willi Nordberg Symposium on Remote Sensing towards Operational Cartographic Application, Graz, Austria, Sep. 1987
(NLR-MP-87063-U; ETN-89-94042) Avail: NTIS HC A03/MF A01

The ability to obtain up-to-date information on agricultural land use from LANDSAT TM imagery by means of classification was investigated in a pilot study on a 50,000 ha area. The study was meant to supply information on agricultural land use that could not be obtained in other ways. Land use information was particularly required on the cultivation of maize and other crops, grasslands, coniferous and deciduous forest, and heather and grass-invaded heather. This information was to be used to investigate and to predict the effects of manure on soils, surface water, and ground water and the effects of national policies to solve the manure problems, caused by the rearing of large concentrations of animals in the part of the Netherlands studied. The accuracy of the results for the most important classes varies between 80 percent and over 95 percent. The result is due to the excellent quality and timing of the image, the ecological homogeneity of the area, and the spectral differentiation between the classes. ESA

N89-20542# National Aerospace Lab., Amsterdam (Netherlands). Space Div.
TWELVE YEAR OVERVIEW OF CLOUDFREE LANDSAT IMAGERY OF THE NETHERLANDS
F. B. vanderLaan 12 Nov. 1987 31 p In DUTCH; ENGLISH summary Submitted for publication
(NLR-MP-87072-U; ETN-89-94045) Avail: NTIS HC A03/MF A01

Twelve years of LANDSAT quick-look images were used to assess the chances of obtaining cloud free imagery from the Netherlands. In 12yr 27 complete cloud free coverages were recorded for which less than 4 recording dates need to be purchased; 18 of these fall in the autumn, winter, spring period in which the image quality is low. Nine cloud free coverages are recorded in summertime. Counting per quarter scene, a cloud free image becomes available on average five times per year. Once every 2yr complete cloud free coverage from a usefull and high quality image can be expected from the whole of the Netherlands. ESA

N89-20543# Massachusetts Inst. of Tech., Cambridge. Lab. of Electronics.
ACTIVE AND PASSIVE REMOTE SENSING OF ICE Final Report, 16 Feb. 1983 - 30 Sep. 1988
Jin An Kong 2 Feb. 1989 23 p
(Contract N00014-83-K-0258)
(AD-A203943) Avail: NTIS HC A03/MF A01 CSCL 17I

Fully polarimetric scattering properties of earth terrain media are studied with three-layer random medium model. The top scattering layer is modeled as an isotropic random medium which is characterized by a scalar permittivity. The middle scattering layer is modeled as an anisotropic radom medium with a symmetric permittivity tensor whose optic axis can be tilted depending on the preferred alignment of the embedded scatterers. The bottom layer is considered as a homogeneous half-space. Volume scattering effects of both random media are descreibed by three dimensional correlation functions with variances and correlation lengths corresponding to the strengths of the permittivity fluctuations and the physical sizes of the inhomogeneities, respectively. The strong fluctuation theory is used to derive the mean fields in the random media under the bilocal approximation with singularities of the dyadic Greens's functions properly taken into consideration. With the dicrete scatterer concept, effecive permittivities of the random media are calculated by two-phase mixing formulas. Then, the Born approximation is used to calculate the covariance matrix which described the fully polarimetric scattering properties of the remotely sensed media. The polarimetric informtion is useful in the identification, classification, and radar image simulation of earth terrain media. Author

44 ENERGY PRODUCTION AND CONVERSION

Includes specific energy conversion systems, e.g., fuel cells; global sources of energy; geophysical conversion; and windpower.

For related information see also *07 Aircraft Propulsion and Power, 20 Spacecraft Propulsion and Power,* and *28 Propellants and Fuels.*

N89-20544# International Fuel Cells Corp., South Windsor, CT.
PHOSPHORIC ACID FUEL CELL SUBSYSTEM TECHNOLOGY Final Report, Feb. 1987 - Feb. 1988
J. M. King and G. W. Scheffler Sep. 1988 64 p
(Contract GRI-5086-294-1430)
(PB88-100515; FCR-9594A; GRI-88/0215) Avail: NTIS HC A04/MF A01 CSCL 10B

Subsystem improvements beyond those achieved in prior GRI and DOE approved activities were investigated. Concepts with reduced material and processing cost were investigated for the repeating elements of the cell stack. Initial evaluations of these concepts through fabrication trials, functional performance and material properties investigations were successful. Several improvements to the fuel processor were investigated. An improved approach for operation on fuel gas containing oxygen was defined. A concept for improving efficiency was shown to be feasible in a rig test. Improved catalyst candidates for several fuel processor functions were identified and a material was identified which would lead to reduced cost for a fuel processing filter. An advanced power conditioner was identified which provides both improved operating capability and a 25 percent reduction in size compared to that used previously. Experimental hardware for evaluation of this concept was fabricated. An integrated controller was defined and an approach to providing both on-site and remote diagnosis of power plant problems was incorporated. Author

N89-20545*# National Aeronautics and Space Administration. Lewis Research Center, Cleveland, OH.
MARS MANNED TRANSPORTATION VEHICLE
Marla E. Perez-Davis and Karl A. Faymon Jul. 1987 12 p Presented at the Case for Mars III, Boulder, CO, 18-22 Jul. 1987; sponsored in part by American Astronautical Society; Jet Propulsion Lab.; NASA, Ames Res. Ctr.; NASA, Johnson Space Ctr; NASA, Marshall Space Flight Ctr.; and The Planetary Society
(NASA-TM-101487; E-4627; NAS 1.15:101487) Avail: NTIS HC A03/MF A01 CSCL 13F

A viable power system technology for a surface transportation vehicle to explore the planet Mars is presented. A number of power traction systems were investigated, and it was found that a regenerative hydrogen-oxygen fuel cell appears to be attractive for a manned Mars rover application. Mission requirements were obtained from the Manned Mars Mission Working Group. Power systems weights, power, and reactants requirements were determined as a function of vehicle weights for vehicles weighing from 6,000 to 16,000 lb (2,722 to 7,257 kg), (Earth weight). The vehicle performance requirements were: velocity, 10 km/hr; range, 100 km; slope climbing capability, 30 deg uphill for 50 km; mission duration, 5 days; and crew, 5. Power requirements for the operation of scientific equipment and support system capabilities were also specified and included in this study. The concept developed here would also be applicable to a Lunar based vehicle for Lunar exploration. The reduced gravity on the Lunar surface, (over that on the Martian surface), would result in an increased range or capability over that of the Mars vehicle since many of the power and energy requirements for the vehicle are gravity dependent. Author

N89-20546# National Inst. of Standards and Technology, Gaithersburg, MD.
ENERGY RELATED INVENTIONS PROGRAM: A JOINT PROGRAM OF THE DEPARTMENT OF ENERGY AND THE NATIONAL INSTITUTE OF STANDARDS AND TECHNOLOGY Status Report
F. L. Hart Oct. 1988 308 p Sponsored in part by DOE, Washington, DC
(PB89-141154; NISTIR-88/4005) Avail: NTIS HC A14/MF A01 CSCL 10A

A brief description of the Energy Related Inventions Program and of all inventions recommended by the National Institute of Standards and Technology (formerly the National Bureau of Standards) to the Department of Energy since the inception of the program, including a brief summary of the current status of each are discussed. Author

N89-20547# Sater (Bernard L.), Olmsted Falls, OH.
EDGE ILLUMINATED VENTICAL MULTIJUNCTION Quarterly Progress Report No. 5, 1 Sep. - 31 Dec. 1988
B. L. Sater 1989 2 p
(Contract DE-FG01-87CE-15337)
(DE89-006246; DOE/CE-15337/T5) Avail: NTIS HC A02/MF A01

Two-dimensional computer analysis establishing optimum wafer and diffusion parameters for the wafers of the VMJ solar cell is essentially finished. The analysis of various parameters such as each diffusion depth, doping profiles and the recombinations losses at ohmic contacts and exposed surface were studied for their sensitivity effects on overall performance. During this quarter, two other sources for diffusions were investigated. Using ion implantation processing on sample wafers, we achieved a factor of two improvement in this lifetime parameter. (However, we also learned that the measurement method used may not in fact tell us what the true bulk minority-carrier lifetime really is. There are three separate regions in the pulsed conductivity lifetime measurement transient and with careful observation of the third region it appears that the bulk lifetime may be 300 microseconds). A minority-carrier lifetime of 300 microseconds minimum should give good starting point for good cell performance. DOE

N89-20548# Massachusetts Inst. of Tech., Los Alamos, NM. School of Chemical Engineering Practice-Los Alamos Station.
HEAT AND MASS TRANSPORT IN FUEL CELL ELECTRODES
S. Sung and C. Krueger Jan. 1989 59 p
(Contract W-7405-eng-36)
(DE89-006378; LA-11484-MS; MIT-LANL-2) Avail: NTIS HC A04/MF A01

The operation of a hydrogen/oxygen fuel cell is dependent on the rate at which product water can be removed from the cathode. The carbon-Teflon paper boundary between the cathode and air supply has been studied regarding the transport phenomena occurring within it. Heat and water removal and the transport of oxygen to the cathode have been considered. Experiments run on a simulated fuel cell revealed that gravity is important in water drainage through a carbon-Teflon felt. Preliminary experiments conducted have indicated several modifications to the existing apparatus. A theoretical model has been developed in which the carbon-Teflon paper is treated as a porous continuum. Transport rates and temperature and pressure profiles can be estimated by numerically solving the equations governing heat, mass, and momentum transfer. Experimental results will be used to verify the model. DOE

N89-20549*# Jet Propulsion Lab., California Inst. of Tech., Pasadena.
CHARACTERIZATION OF PRODUCTION GaAs SOLAR CELLS FOR SPACE
B. E. Anspaugh 15 Dec. 1988 37 p
(Contract NAS7-918)
(NASA-CR-184863; JPL-Publ-88-39; NAS 1.26:184863) Avail: NTIS HC A03/MF A01 CSCL 10A

The electrical performance of GaAs solar cells was characterized as a function of irradiation with protons and electrons with the underlying goal of producing solar cells suitable for use in space. Proton energies used varied between 50 keV and 10 MeV, and damage coefficients were derived for liquid phase epitaxy GaAs solar cells. Electron energies varied between 0.7 and 2.4 MeV. Cells from recent production runs were characterized as a function of electron and proton irradiation. These same cells were also characterized as a function of solar intensity and operating temperature, both before and after the electron irradiations. The long term stability of GaAs cells during photon exposure was examined. Some cells were found to degrade with photon exposure and some did not. Calibration standards were made for GaAs/Ge solar cells by flight on a high altitude balloon. Author

N89-20550# Arizona Univ., Tucson. Dept. of Biochemistry.
MECHANISMS OF PHOTOCHEMICAL ENERGY CONVERSION BY CHLOROPHYLL Progress Report, 1 Jul. 1986 - 28 Feb. 1989
Gordon Tollin 28 Feb. 1989 13 p
(Contract DE-FG02-86ER-13631)
(DE89-006820; DOE/ER-13631/12) Avail: NTIS HC A03/MF A01

Large and small unilamellar vesicles have been compared with respect to chlorophyll triplet quenching and electron transfer occurring at the inner and outer bilayer surfaces. Unexpectedly, large vesicles display inside-outside asymmetry, which is reversed in direction from that of small vesicles, indicating that factors in addition to lipid packing density asymmetry are responsible for the asymmetric behavior. Varying the ionic strength of the medium and the surface charge suggests that a transmembrane potential, in which the exterior surface is more negative than the interior, is also involved in causing asymmetry. Experiments using valinomycin indicate that ionophores, by generating electrostatic effects within the bilayer, exert more selective effects on membrane photochemical processes than do charges on the membrane surface. DOE

N89-20551# National Aerospace Lab., Amsterdam (Netherlands). Structures and Materials Div.
NEN 6096, DESIGN RESOLUTION FOR SMALL WIND TURBINES
H. H. Ottens and L. A. H Machielse 20 Jan. 1988 11 p In DUTCH; ENGLISH summary Presented at the National Wind Energy Conference 1988, Noordwijkerhout, The Netherlands, 22-24 Feb. 1988
(NLR-MP-88005-U; ETN-89-94054) Avail: NTIS HC A03/MF A01

A draft regulation for safety for windturbine (NEN 6096) was published in the Netherlands. Special attention was paid to structural safety. In the final version, the results of the project Design criteria for small wind turbines were incorporated. The methodology and terminology of the draft design standards for buildings (NEN 6700 series) were adapted. ESA

N89-20552# National Aerospace Lab., Amsterdam (Netherlands). Structures and Materials Div.
WISPER: INTRODUCING VARIABLE-AMPLITUDE LOADING IN WIND TURBINE DESIGN
A. A. tenHave 10 Mar. 1988 10 p Presented at the BWEA Wind Energy Association 10th Annual Conference, London, England, 23-25 Mar. 1988
(NLR-MP-88017-U; ETN-89-94061) Avail: NTIS HC A02/MF A01

A variable-amplitude test loading sequence was established for use in the fatigue evaluation of horizontal-axis wind turbine blades. This standard, baptized WISPER, is thought to be a better design tool in the fatigue laboratory as compared to procedures employing constant-amplitude data. The conflicting effects of constant-amplitude versus variable-amplitude loading are highlighted and the approach using loading standards is discussed. These views are translated into the field of wind turbine design. ESA

N89-20553# Midwest Research Inst., Golden, CO. Solar Energy Research Inst.
PHOTOVOLTAIC ENERGY PROGRAM SUMMARY. VOLUME 1: OVERVIEW, FISCAL YEAR 1988
Jan. 1989 15 p
(Contract DE-AC02-83CH-10093)
(DE89-000855; DOE/CH-10093/40-Vol-1) Avail: NTIS HC A03/MF A01

1988 has been a year for major advances in photovoltaic (PV) technology. There has been unprecedented progress, both in the laboratory and in the industry along with more technical advances and worldwide market acceptance in new applications. If this year has been any barometer, photovoltaic energy products are rapidly moving toward the goal of supplying a part of U.S. utility power in the 1990s. This report reviews some of the technology achievements in photovoltaics this year. DOE

N89-20554# Westinghouse Research and Development Center, Pittsburgh, PA.
DENDRITIC WEB SILICON PHOTOVOLTAIC CELL RESEARCH
R. G. Seidensticker, J. P. McHugh, R. H. Hopkins, D. L. Meier, J. A. Spitznagel, and S. Y. Lein Jan. 1989 104 p Prepared for Sandia National Labs., Albuquerque, NM
(Contract DE-AC04-76DP-00789)
(DE89-007289; SAND-88-7040) Avail: NTIS HC A06/MF A01

This report summarizes a program for which the overall goal was improving the understanding of the material and device factors that limit the performance of solar cells fabricated from dendritic web silicon. An analytical model for crystal defect generation was developed, starting with the temperature distribution in the growing crystal and continuing through the effect of thermal stress on defect structures observed in dendritic web crystals grown in carefully characterized thermal conditions. Good agreement exists between the model and experiment. The origin of dislocations in the silicon web was discrete sources, probably freezing silicon droplets, in the bounding dendrites; these sources can be eliminated by localized heating with a laser during the growth process. Thermal stresses farther from the growth front can be controlled by a thermal modifier designed to reduce buckling of the web crystal and the concommitant dislocation generation. These crystal defects were correlated with solar cell performance by fabricating devices on well-characterized web material and correlating performance with residual stress. Low-stress, high-perfection material was conducive to high-quality cells; high-stress material led to poorer cells with a yield characteristic depending on the sign of the stress. The mechanism by which dislocations degrade cell quality was not completely identified but appears due to dislocation-impurity interactions. For example, antimony-doped material yields better cells than phosphorus-doped material. DOE

N89-20555# North Carolina Univ., Chapel Hill.
ENERGY CONVERSION PROCESSES BASED ON MOLECULAR EXCITED STATES Progress Report, 1 Aug. 1988 - 31 Jul. 1989
Thomas J. Meyer Feb. 1989 9 p
(Contract DE-FG05-86ER-13633)
(DE89-007322; DOE/ER-13633/3) Avail: NTIS HC A02/MF A01

In the past year significant progress has been made in three related areas. We have continued to develop new MLCT excited state systems. This work involves a combination of synthetic chemistry and photophysical measurements to elucidate excited state properties. In a second area, the synthetic chemistry has been developed for the attachment of metal-to-ligand charge transfer (MLCT) chromophores to a soluble 1:1 copolymer of styrene and p-chloromethylstyrene. The extent of loading of the chromophore or of electron or energy transfer quenchers can be varied systematically by controlling the preparative conditions. In a third area, our work has continued on the preparation of thin film molecular level assemblies which contain chromophore/quencher combinations, and the investigation of their properties. We have extended our earlier results on chemical binding in chlorosulfonated polystyrene films to a variety of organic or inorganic chromophores. DOE

N89-20556# Foster Wheeler Corp., Livingston, NJ.
COMMERCIAL DIRECT ABSORPTION RECEIVER DESIGN STUDIES
S. F. Wu and T. V. Narayanan Dec. 1988 93 p
(Contract DE-AC04-76DP-00789)
(DE89-007290; SAND-88-7038) Avail: NTIS HC A05

As part of a joint Sandia/SERI study, we designed a commercial-sized molten salt direct absorption receiver for a solar central receiver plant. Thermal and structural analyses of several possible configurations showed the most severe conditions for the absorber arise from operational thermal stresses. For this reason, we selected a thin, cylindrical, pretensioned shell to eliminate potentially damaging compressive stresses. The shell is also compressively loaded from inside through a rigid subpanel and a layer of dense fiber insulation to provide vibration dampening and horizontal pretensioning of the shell. This receiver will be 40 percent lighter and 30 percent less expensive than a salt-in-tube receiver of comparable size, and its annual performance benefits are substantial. The newly designed direct absorption receiver has the potential to reduce levelized energy costs from solar central receiver plants by about 15 percent. DOE

45 ENVIRONMENT POLLUTION

Includes atmospheric, noise, thermal, and water pollution.

N89-20557# Federal Aviation Administration, Washington, DC. Office of Environment and Energy.
A MICROCOMPUTER POLLUTION MODEL FOR CIVILIAN AIRPORTS AND AIR FORCE BASES. MODEL APPLICATION AND BACKGROUND
H. M. Segal Aug. 1988 94 p Sponsored in part by AFESC, Tyndall AFB, FL
(AD-A199794; FAA-EE-88-5; AFESC/ESL-TR-88-55) Avail: NTIS HC A05/MF A01 CSCL 24A

This is the last of three reports describing the Emissions and Dispersion Modeling System (EDMS). It consists of an accumulation of five key documents describing the development and use of the EDMS model. This report is prepared in accordance with discussions with the EPA and requirements outlined in the March 27, 1980 Federal Register for submitting air quality models to the EPA. Model development and use, the influence of aircraft operations on air quality at airports, the Simplex A (a simplified atmospheric dispersion Model for airport use), microcomputer graphics in atmospheric dispersion modeling, and pollution from motor vehicles and aircraft at Stapleton International Airport are discussed. Atmospheric Dispersion Modeling; Pollution from Motor Vehicles and Aircraft at Stapleton International Airport (Abbreviated Report). (FR) GRA

N89-20558# Radian Corp., Research Triangle Park, NC. Progress Center.
NATIONAL AIR TOXICS INFORMATION CLEARINGHOUSE: ONGOING RESEARCH AND REGULATORY DEVELOPMENT PROJECTS, JULY 1988 Interim Report
Susan Kay M. Buchanan and Theresa K. Moody Jul. 1988 194 p
(Contract EPA-68-02-4330)
(PB89-103428; DCN-88-239-001-44-07; EPA/450/5-88/004)
Avail: NTIS HC A09/MF A01 CSCL 13B

The document is divided into 2 parts and an appendix. The first part lists 365 air toxic projects currently in progress at EPA, NIOSH, and state and local agencies. A brief description of each project and a contact name, office, and telephone number are given. The second part contains the index that allows readers to locate projects of interest. Projects are indexed by agency, project type, chemical name, Chemical Abstract Service number, and

source category Standard Industrial Classification Code. The appendix lists regulatory development projects on toxic chemicals underway at the EPA's Office of Drinking Water. Author

N89-20559# National Oceanic and Atmospheric Administration, Silver Spring, MD. Air Resources Lab.
HYBRID SINGLE-PARTICLE LAGRANGIAN INTEGRATED TRAJECTORIES (HY-SPLIT): MODEL DESCRIPTION
Roland R. Draxler Sep. 1988 29 p
(PB89-127591; NOAA-TM-ERL-ARL-166) Avail: NTIS HC A03/MF A01 CSCL 13B

The algorithms and equations used in the development of a long-range transport and dispersion model are presented. The model calculation methods are a hybrid between Eulerian and Lagrangian approaches. A single pollutant particle represents the initial source. Advection and diffusion calculations are made in a Lagrangian framework. However, meteorological input data can either be gridded from rawinsonde observations or archived from the output of an Eulerian primitive equation forecast model. As the dimensions of the initial particle diffuse into regions of different wind direction or speed, the single particle is divided into multiple particles to provide a better representation of the more complex flow field. Air concentrations are calculated on a fixed three-dimensional grid by integrating all particle masses over the sampling time. Author

N89-20560# Energy and Environmental Research Corp., Irvine, CA.
KINETIC MODELING OF NOx FORMATION AND DESTRUCTION AND COMBUSTIBLES BURNOUT
J. A. Cole, J. C. Kramlich, and W. S. Lanier Oct. 1988 453 p
(Contract EPA-68-02-4247)
(PB89-124358; EPA/600/7-88/021) Avail: NTIS HC A20/MF A01 CSCL 13B

A model of the gas-phase chemistry involved in the combustion of simple hydrocarbon fuels and the interconversion of fixed nitrogen species are described. One focus was on modeling the chemistry involved in reburning and other advanced NOx control strategies. A second focus was on the decay rate of various hydrocarbon species under high-temperature conditions. This provided an initial step toward the chemistry needed to model fuel burnout in small combustors; e.g., wood stoves. The approach was to compare rates for elementary reactions as represented in the different compilations available in the literature. Where inconsistencies appeared, the original literature on the rates was consulted. The mechanism was tested against benchmark data so that the key reactions that controlled any inconsistencies could be identified. Adjustments to the rates were allowed if they fell within the error bounds of the original determination. GRA

N89-20561# Environmental Protection Agency, Research Triangle Park, NC. Atmospheric Sciences Research Lab.
DISPERSION OF DENSE GAS RELEASES IN A WIND TUNNEL
William B. Petersen, William H. Snyder, J. Y. Ku, and S. T. Rao (New York State Dept. of Environmental Conservation, Albany.) Oct. 1988 13 p
(PB89-118509; EPA/600/D-88/207) Avail: NTIS HC A03/MF A01 CSCL 13B

Two dense gas projects undertaken at the US EPA Fluid Modeling Facility are documented. The basic nature of the transport and dispersion of a dense gas plume was investigated in a simulated neutral atmospheric boundary layer. The two dense gas releases were CO2 and SF6. The configuration of the wind tunnel was the same for both gases, except that the wind speed had to be increased 20 percent in the SF6 study to avoid laminarization of the plume. The plumes were tracked by mixing a small fraction of ethane with the dense gases and using flame ionization detectors to measure downwind lateral and vertical concentration profiles. The increased density clearly has very significant effects. The vertical spread of the SF6 plume was about two-thirds that of the CO2 plume. Perhaps the most unusual finding was that the shapes of the vertical distributions remained similar far downstream and high non-Gaussian in the outer reaches of the plume. GRA

N89-20562# National Oceanic and Atmospheric Administration, Boulder, CO. Wave Propagation Lab.
NOAA (NATIONAL OCEANIC AND ATMOSPHERIC ADMINISTRATION) X-BAND RADAR MEASUREMENTS IN 3CPO (CLOUD CHEMISTRY CLOUD PHYSICS ORGANIZATION)
Brooks E. Martner, A. Shelby Frisch, and Robert A. Kropfli Oct. 1988 65 p
(PB89-127823; NOAA-TM-ERL-WPL-153) Avail: NTIS HC A04/MF A01 CSCL 13B

The NOAA Wave Propagation Lab participated in the Cloud Chemistry Cloud Physics Org. field project in east central Illinois in the summer of 1988. The lab planned to use its circular polarization diversity Doppler X-band radar to study venting of polluted boundary layer air by convective clouds using a new technique known as TRACIR. The technique and the experimental plan are described and a summary of the radar operations is given. Numerous measurements were made with the radar in clear air conditions using vertical scans and the Velocity Azimuth Display (VAD) method to obtain data on turbulence characteristics of the planetary boundary layer. The VAD measurements and analysis procedures are described as well as a test of the efficiency of the NOAA airborne chaff cutters. GRA

N89-20563# Argonne National Lab., IL. Energy and Environmental Systems Div.
IMPLICATIONS OF THE GREENHOUSE EFFECT FOR THE MIDWEST ECONOMY
David G. Streets and Cary N. Bloyd 1988 21 p Presented at the 16th Annual Illinois Energy Conference, Chicago, IL, 17 Nov. 1988
(Contract W-31-109-eng-38)
(DE89-004195; CONF-8811140-1) Avail: NTIS HC A03/MF A01

Although a great deal of research effort has been devoted to determining potential future changes in carbon dioxide concentrations, global temperature changes and ecosystem effects, relatively little attention has thus far been paid to potential regional impacts and the formulation of coherent policies to combat the problems. This paper will discuss how the Midwest might fare under conditions of higher mean temperatures or a major Federal control program; it also discusses some of the research and development activities underway at Argonne National Laboratory that could help develop a balanced portfolio of technologies for combating the greenhouse effect. For the purposes of this paper we have defined a six-state region--consisting of the states of Illinois, Indiana, Michigan, Minnesota, Ohio, and Wisconsin--to typify the Midwest. These are the same states that comprise Federal Region 5. Temperatures were averaged for the thirty-year period 1950 through 1980 and do not include some of the higher summer temperatures we have been experiencing in the 1980s. DOE

N89-20564# Pacific Northwest Labs., Richland, WA.
THE CAUSES AND CONSEQUENCES OF GLOBAL CLIMATE CHANGE
W. T. Hinds Nov. 1988 24 p Presented at the United States Department of Agriculture (USDA) National Agriculture Research and Extension User's Advisory Board Meeting, Lafayette, IN, 9 Nov. 1988
(Contract DE-AC06-76RL-01830)
(DE89-004355; PNL-SA-16339; CONF-8811143-1) Avail: NTIS HC A03/MF A01

The intent of this paper is to outline the science underlying our understanding of the causes and consequences of global warming research, including: how a global warming might be induced; how sure we can be about both causes and consequences; and what research is currently underway. DOE

N89-20565# Lawrence Livermore National Lab., CA. Atmospheric and Geophysical Sciences Div.
SCENARIOS FOR FUTURE CLIMATE CHANGE: RESULTS OF GCM (GENERAL CIRCULATION MODEL) SIMULATIONS
Michael C. MacCracken 27 Sep. 1988 10 p Presented at the

First United States-Canada Symposium on the Impact of Climate Change on the Great Lakes Basin, Chicago, IL, 27-29 Sep. 1988
(Contract W-7405-eng-48)
(DE89-006151; UCRL-100144; CONF-8809282-1) Avail: NTIS HC A02/MF A01

The continuing emissions of gases that are able to increase the efficiency with which the atmosphere traps infrared radiation are beginning to alter the global climate. During the next century, theoretical simulations project that global average temperatures will rise by several degrees Celsius above their pre-industrial baseline and that precipitation patterns may shift seasonally and spatially. Although research is being intensified so that detailed regional estimates can be provided, projected increases in summer temperatures and the accompanying increased evaporation, especially during natural warm excursions such as the summer of 1988, appear to pose troubling conditions for water supplies, agriculture, transport, and other activities dependent on water resources. DOE

N89-20566# Pacific Northwest Labs., Richland, WA.
AIRCRAFT OPERATIONS AND AIRBORNE MEASUREMENT OF PERFLUOROTRIMETHYLCYCLOHEXANE (PTCH) DURING ANATEX
Richard N Lee, Kenneth M. Busness, and Barbara Stunder (National Oceanic and Atmospheric Administration, Silver Spring, MD.) Sep. 1988 5 p Presented at the 6th Joint Conference on Applications of Air Pollution Meteorology, Anaheim, CA, 29 Jan. 1989
(Contract DE-AC06-76RL-01830)
(DE89-006934; PNL-SA-16316; CONF-890133-5) Avail: NTIS HC A02

This paper describes PNL aircraft operations during the ANATEX field program and presents tracer concentration data obtained with the on-board analyzer for missions conducted on March 4, 1987. Also presented are preliminary sequential sampler data. Since final reduction of these data have not been completed, sequential sampler data have been normalized with respect to peak tracer loading to yield relative rather than absolute tracer concentrations in these sample. DOE

46 GEOPHYSICS

Includes aeronomy; upper and lower atmosphere studies; ionospheric and magnetospheric physics; and geomagnetism.

For space radiation see *93 Space Radiation.*

N89-20567*# Alabama Univ., Huntsville. Dept. of Computer Science.
THE BEHAVIOR OF THE ELECTRON DENSITY AND TEMPERATUE AT MILLSTONE HILL DURING THE EQUINOX TRANSITION STUDY SEPTEMBER 1984
P. G. Richards, D. G. Torr, M. J. Buonsanto, and K. L. Miller (Utah State Univ., Logan.) [1989] 21 p
(Grant NAGw-996)
(NASA-CR-184737; NAS 1.26:184737) Avail: NTIS HC A03/MF A01 CSCL 04A

The ionospheric electron density and temperature variations is simulated during the equinox transition study in September 1984 and the results are compared with measurements made at Millstone Hill. The agreement between the modeled and measured electron density and temperature for the quiet day (18 September) is very good but there are large differences on the day of the storm (19 September). On the storm day, the measured electron density decreases by a factor of 1.7 over the previous day, while the model density actually increases slightly. The model failure is attributed to an inadequate increase in the ratio of atomic oxygen to molecular neutral densities in the MSIS neutral atmosphere model, for this particular storm. A factor of 3 to 5 increase in the molecular to atomic oxygen density ratio at 300 km is needed to explain the observed decrease in electron density. The effect of vibrationally excited N sub 2 on the electron density were studied and found to be small. Author

N89-20568# National Center for Atmospheric Research, Boulder, CO. Climate and Global Dynamics Div.
GENERATION OF CCM FORMAT HISTORY TAPES FROM ANALYZED DATA FOR SELECTED PERIODS (RD2CFM VERSION 01)
Thomas A. Mayer Oct. 1988 77 p
(Grant NSF ATM-87-09659)
(PB89-124507; NCAR/TN-322-IA) Avail: NTIS HC A05/MF A01 CSCL 04A

The Community Climate Model (CCM) and the modular processor require that input data be in CCM history tape form. The purpose of the software described herein is to generate such history tapes from various analyses of observed data, add climatological lower boundary data where necessary, and output the data in a Type 1 or Type 2 CCM history tape format at an arbitrary resolution on either pressure or sigma surfaces. History tapes with data on sigma surfaces may be used by either the model or the processor while history tapes with data on pressure surfaces may be used by the processor only. There are three common uses for these history tapes. They may be used to start the model. They may be used as a data source against which model forecasts may be verified in the processor. Finally, in conjunction with the processor, they may be used to perform data analysis of one of the analyzed data sources without using the model at all. Author

N89-20569# National Center for Atmospheric Research, Boulder, CO.
REPORT OF THE DOCUMENTATION ADVISORY COMMITTEE
Linda Bath, Christopher Burghart, David Chapman, Martin Corrigan, Mary Downton, Kelvin Droegemeier, Kevin Ingels, John Merrill, Victor Tisone, and Robin Vaughan et al Oct. 1988 76 p
(Grant NSF ATM-87-09659)
(PB89-124556; NCAR/TN-323-STR) Avail: NTIS HC A05/MF A01 CSCL 04A

The Documentation Advisory Committee was formed to provide user input and advice concerning documentation for the Scientific Computing Division (SCD) of the National Center for Atmospheric Research computing systems. Sub-committees were formed within the Committee to survey the users concerning their documentation needs, to evaluate the current status of SCD documentation, and to investigate the feasibility of implementing an online documentation system at NCAR. Author

N89-20570 Iowa State Univ. of Science and Technology, Ames.
NUMERICAL STUDIES OF BAROTROPIC STABILITY OF STRATOSPHERIC STATES Ph.D. Thesis
Gloria Lisa Manney 1988 118 p
Avail: Univ. Microfilms Order No. DA8825940

The linear stability properties of basic states relevant to the stratosphere are studied in a barotropic nondivergent spectral model on a sphere. The stability of realistic zonally symmetric jets and zonally asymmetric basic states are examined. Dissert. Abstr.

N89-20571# Royal Inst. of Tech., Stockholm (Sweden). Dept. of Plasma Physics.
A NUMERICAL MODEL OF IONOSPHERIC CONVECTION DERIVED FROM FIELD-ALIGNED CURRENTS AND THE CORRESPONDING CONDUCTIVITY
L. G. Blomberg and G. T. Marklund Mar. 1988 22 p
(TRITA-EPP-88-03; ISSN-0348-7539; ETN-89-93726) Avail: NTIS HC A03/MF A01

A numerical model for the calculation of ionospheric convection patterns from given distributions of field-aligned current and ionospheric conductivity is described. The model includes a coupling between the conductivity and the field-aligned current, so that the conductivity peaks in regions of upward current, as usually observed by measurements. The model is very flexible in that the input distributions, the field-aligned current, and the conductivity are parameterized in a convenient way. From the primary model output, namely the ionospheric electrostatic potential (or convection) in the corotating frame, a number of other quantities

can be computed. These include: the potential in a Sun-fixed frame (the transformation takes into account the nonalignment of the Earth's magnetic and geographic axes); the potential in the magnetospheric equatorial plane (projected using either a dipole magnetic field model or the Tsyganenko-Usmanov model, and the assumption of vanishing parallel electric field); the distribution of ionospheric (horizontal) current; and Joule heating in the ionosphere. The model was used with input data inferred from satellite measurements to calculate the high-latitude potential distribution prevailing during a particular event. The model potential variation along the satellite orbit is found to be in excellent agreement with the measured electric field. ESA

N89-20572# Swedish Inst. of Space Physics, Kiruna.
SCIENTIFIC RESULTS FROM THE SWEDISH VIKING SATELLITE Status Report, 1988
Bengt Hultqvist 1988 36 p Original contains color illustrations
(IRF-SR-196; ISSN-0284-1703; ETN-89-93735) Avail: NTIS HC A03/MF A01

Results from the Swedish Viking satellite on global distribution of magnetosphere-ionosphere interaction; auroral morphology and substorm dynamics; heating and expulsion of ionospheric plasma into the magnetosphere; field aligned acceleration into the ionosphere; and electron and ion wave generation are discussed. ESA

N89-20573# International Centre for Theoretical Physics, Trieste (Italy).
SOLITON GEOMETRY AND THE VACUUM GRAVITATIONAL FIELD EQUATIONS
Metin Gurses Aug. 1988 17 p
(DE88-705340; IC-88/190) Avail: NTIS (US Sales Only) HC A03/MF A01

A soliton geometry is introduced on manifolds with arbitrary dimensions. The usual soliton connection 1-form defined by Crampin et al. is recovered when the soldering form is a 0-form. It is shown that the vacuum Einstein field equations admit a soliton connection and a soldering 1-form. An associated linear equation with a spectral parameter of Einstein's vacuum field equations are found and some properties of this equation are explored. An example of a Baecklund transformation is also given. DOE

N89-20574# Los Alamos National Lab., NM. Computing and Communications Div.
APPLYING EXPERTISE TO DATA IN THE GEOLOGIST'S ASSISTANT EXPERT SYSTEM
K. P. Berkbigler, G. J. Papcun, N. L. Marusak, and J. E. Hutson 1988 9 p Presented at the 3rd Topical Meeting on Robotics and Remote Systems, Charleston, SC, 13 Mar. 1989
(Contract W-7405-eng-36)
(DE89-003463; LA-UR-88-3750; CONF-890304-12) Avail: NTIS HC A02/MF A01

The Geologist's Assistant combines expert system technology with numerical pattern-matching and online communication to a large database. This paper discusses the types of rules used for the expert system, the pattern-matching technique applied, and the implementation of the system using a commercial expert system development environment. DOE

N89-20575# Ensco, Inc., Melbourne, FL.
WAVEFORM DATA COLLECTION FOR SOURCE INVERSION STUDIES Annual Report, 15 Jun. 1987 - 14 Jun. 1988
William N. Alexander, Raymond H. Kimmel, and Lauren Malaspina 2 Aug. 1988 18 p
(Contract F08606-87-C-0017)
(AD-A203419; DCS-SYR-88-80) Avail: NTIS HC A03/MF A01 CSCL 08K

The primary purpose of this contract on seismic waveform collection activities is to provide a data base of digital long period seismograms from selected large underground explosions, to be used in source inversion research. An added task requires the collection of digital Lg phases to be used in magnitude studies. Digital seismograms in this data base are collected by hand-digitizing analog seismograms from stations in the World Wide Standard Seismograph Network and by collecting existing digital data from stations in the Atomic Energy Detection System (AEDS). A number of waveforms have also been hand-digitized from AEDS analog recordings. GRA

N89-20158*# National Aeronautics and Space Administration. Goddard Space Flight Center, Greenbelt, MD.
THE MAGNETIC FIELD INVESTIGATION ON CLUSTER
A. Balogh, S. W. H. Cowley, D. J. Southwood, G. Musmann, H. Luhr, F. M. Neubauer, K.-H. Glassmeier, W. Riedler, M. F. Heyn (Oesterreichische Akademie der Wissenschaften, Vienna.), and M. H. Acuna et al *In* ESA, The Cluster Mission: Scientific and Technical Aspects of the Instruments Oct. 1988 p 15-20 Prepared in cooperation with California Univ., Lo s Angeles, Danish Space Research Inst., Lyngby, Centre National d'Etudes des Telecommunications, Issy-les-Moulineaux, France, and JPL, Pasadena, CA (For primary document see N89-20156 13-12)
Avail: NTIS HC A06/MF A01; ESA Publications Div., ESTEC, Noordwijk, Netherlands, $10 US or 25 Dutch guilders CSCL 04A

N89-20159# Centre de Recherches en Physique de l'Environnement, Issy-les-Moulineaux (France).
WAVE EXPERIMENT CONSORTIUM
A. Roux and B. delaPorte *In* ESA, The Cluster Mission: Scientific and Technical Aspects of the Instruments Oct. 1988 p 21-23 (For primary document see N89-20156 13-12)
Avail: NTIS HC A06/MF A01; ESA Publications Div., ESTEC, Noordwijk, Netherlands, $10 US or 25 Dutch guilders

N89-20160# Centre de Recherches en Physique de l'Environnement, Issy-les-Moulineaux (France).
STAFF: THE SPATIO-TEMPORAL ANALYSIS OF FIELD FLUCTUATIONS EXPERIMENT
N. Cornilleau-Wehrlin, A. Bahnsen, P. Gough, D. A. Gurnett, G. Gustafsson, C. C. Harvey, D. Hubert, W. Kofman, F. Lefeuvre, and R. Manning (Observatoire de Paris-Meudon, France) et al *In* ESA, The Cluster Mission: Scientific and Technical Aspects of the Instruments Oct. 1988 p 25-30 (For primary document see N89-20156 13-12)
Avail: NTIS HC A06/MF A01; ESA Publications Div., ESTEC, Noordwijk, Netherlands, $10 US or 25 Dutch guilders

47 METEOROLOGY AND CLIMATOLOGY

Includes weather forecasting and modification.

N89-20576# National Center for Atmospheric Research, Boulder, CO. Climate and Global Dynamics Div.
REPORT OF THE 2ND WORKSHOP ON THE COMMUNITY CLIMATE MODEL
David L. Williamson, ed. May 1988 58 p Workshop held in Boulder, CO, 27 Jul. - 7 Aug. 1987
(Grant NSF ATM-87-09659)
(PB88-250741; NCAR/TN-310-PROC) Avail: NTIS HC A04/MF A01 CSCL 04B

The Climate and Global Dynamics (CGD) Division of the National Center for Atmospheric Research (NCAR) sponsored a workshop for present and future users of the NCAR Community Climate Model (CCM) from 27 July to 7 August 1987. The workshop was timed to coincide with the general release of a new model version denoted CCM1. The first week of the workshop was devoted to scientific lectures by university and NCAR scientists on work involving the model. The second week of the workshop was devoted to tutorials on the newly released version. These covered the numerical algorithms, physical parameterization and the code structure itself. Author

N89-20577# National Weather Service, Silver Spring, MD. Techniques Development Lab.
OBJECTIVE ASSESSMENT OF 1984-85 VAS PRODUCTS AS INDICES OF THUNDERSTORM AND SEVERE LOCAL STORM POTENTIAL
D. H. Kitzmiller and W. E. McGovern Mar. 1988 45 p
(PB89-107668; NOAA-TM-NWS-TDL-78) Avail: NTIS HC
A03/MF A01 CSCL 04B

Objective experiments were carried out to decide which VAS derived moisture and stability indices contain the greatest amount of predictive information with respect to thunderstorm and severe local storm events. In these experiments, stability and moisture parameters derived from 1700 GMT VAS retrievals were compared and correlated to storm observations during the subsequent 2000-0000 GMT period. The amount of predictive information in these indices was also compared to that possessed by indices derived from VAS retrievals taken earlier in the day, and from concurrently available radiosondes and numerical weather forecasts. The correlation in the form of the computed information ratio was used as a measure of predictive power in these experiments. It was found that precipitable water and modified versions of the classic K index which included the latest surface data have the highest values of information ratio for general thunderstorm events. It was also found that updating of stability measurements leads to modest increases in predictive information. Author

N89-20578# National Weather Service, Kansas City, MO.
UTILITY OF A GEOGRAPHIC INFORMATION SYSTEM IN MODELLING CLIMATIC SUITABILITY
Bartlett C. Hagemeyer Sep. 1988 23 p
(PB89-109516; NOAA-TM-NWS-CR-92) Avail: NTIS HC
A03/MF A01 CSCL 04B

A long term climatological data base for the eastern U.S. was developed as input into a Geographical Information System to test its ability to determine the most suitable climate for human existence using a simple, generic, cartographic model which considered physiological and psychological factors as well as climate hazards and costs. Results indicate the model is objective and sensitive to variations in climatic variables. Portions of South Carolina and Texas were found to be most suitable, but the model was not biased toward southern states in general. Mountain areas and large bodies of water showed a distinct influence on the climate ratings. Author

N89-20579# National Weather Service, Garden City, NY.
CLIMATOLOGICAL WORKSHEET PROGRAM
John Taylor Nov. 1988 11 p
(PB89-122527; NOAA-NWS-ERCP-5MC) Avail: NTIS HC
A03/MF A01 CSCL 04B

The Climatological Worksheet Program is written in BASIC for use on the IBM PC and EPSON printer. It consists of two programs, B:WKS and B:WKS2, both designed to run daily to produce a table of local climatological values. B:WKS is designed to run on its own, whereas B:WKS2 is designed to run with the B:CL1 program. These programs are described. GRA

N89-20580# National Weather Service, Garden City, NY. Scientific Services Div.
EXAMINATION OF NGM (NESTED GRID MODEL) LOW LEVEL TEMPERATURE
Joseph A. Ronco, Jr. Nov. 1988 28 p
(PB89-122543; NOAA-TM-NWS-ER-79) Avail: NTIS HC
A03/MF A01 CSCL 04B

Nested Grid Model (NGM) low level temperatures, initial and forecast, are available to forecasters in a FOUS message for selected locations. The NGM low level temperature forecasts are examined for any bias, and any changes in bias since NGM low level temperatures became available. GRA

N89-20581# National Weather Service, Garden City, NY. Scientific Services Div.
RELATIONSHIP OF WIND SHEAR, BUOYANCY AND RADAR TOPS TO SEVERE WEATHER, 1988
Hugh M. Stone Nov. 1988 21 p
(PB89-122519; NOAA-TM-NWS-ER-80) Avail: NTIS HC
A03/MF A01 CSCL 04B

Shear and stability data for the eastern United States were correlated with severe weather occurrences during the spring and summer seasons. Also included is a sample from 14 stations in the Midwest. Statistically significant correlations were found for various measures of both shear and stability. GRA

N89-20582# National Weather Service, Garden City, NY. Scientific Services Div.
NATIONAL WEATHER SERVICE PHILADELPHIA FORECAST OFFICE, 1987 NOAA (NATIONAL OCEANIC AND ATMOSPHERIC ADMINISTRATION) WEATHER RADIO SURVEY AND QUESTIONNAIRE
Robert P Wanton Oct. 1988 28 p
(PB89-111785; NOAA-TM-NWS-ER-78) Avail: NTIS HC
A03/MF A01 CSCL 04B

The questionnaire pertains to weather terminology, weather and weather-related events, and NOAA Weather Radio. The messages aired are given and the total number of responses are tabulated. The survey was informative but a monumental project. The NOAA Radio has a large listening audience in Philadelphia, some 26,000 listeners. GRA

N89-20583 Florida State Univ., Tallahassee.
BOUNDARY LAYER STRUCTURE AND DYNAMICS IN OUTER HURRICANE RAINBANDS Ph.D. Thesis
Mark Dillon Powell 1988 247 p
Avail: Univ. Microfilms Order No. DA8822464

Results of hurricane boundary layer experiments are presented. Comparisons of precipitation, kinematic, and thermodynamic structures in Hurricanes Josephine (1984), Earl (1986), and Floyd (1981) indicate that principal rainbands have common characteristic mesoscale and convective scale features in the boundary layer. The two-dimensional mesoscale structure suggests that rainbands are made up of a linear aggregate of cellular reflectivity elements (on the inner, upshear side of the band) and stratiform rain (on the outer downshear side). The band is oriented perpendicular to the shear above the boundary layer and cells move downband at about 80 percent of the maximum wind. Alongband and crossband wind maxima, and maximum equivalent potential temperatures are located on the outer side of the band axis, with minima 4 to 8 km to the inner side. Updrafts and downdrafts are preferentially located on the inner side of the band axis, along with maximum crossband convergence, cyclonic shear vorticity, and minimum equivalent potential temperatures. Downdraft transport of cool and dry air from middle levels on the inner side of the rainband was responsible for modifying mixed layer structure adjacent to the band on alongband scales of 100 km. An undisturbed mixed layer of 500 m was present on the outer side of the band while a variety of structures were observed on the inner side indicative of both disturbed and recovering mixed layers. A mixed layer model, applied to low level flow trajectories from the outer rainband to the eyewall, suggests reasons for transitional changes in hurricane intensity. Dissert. Abstr.

N89-20584# National Weather Service, Salt Lake City, UT.
PRELIMINARY ANALYSIS OF CLOUD-TO-GROUND LIGHTNING IN THE VICINITY OF THE NEVADA TEST SITE
Carven Scott Nov. 1988 23 p
(PB89-128649; NOAA-TM-NWS-WR-204) Avail: NTIS HC
A03/MF A01 CSCL 04B

Cloud to ground lightning (CG) constitutes a severe hazard to both personnel and sensitive equipment. The Weather Service Nuclear Support Office operates an Automatic Lightning Detection Network to ensure maximum protection on the Nevada Test Site. The lightning network is described in detail. The accuracy and detection efficiency of the system is also investigated. Lightning

data were collected and analyzed for the period Jul. 1986 to Aug. 1987. Of particular interest in the data set was the temporal variation of both positive and negative CG flashes. In addition, factors that may influence the character and distribution of lightning flashes were studied. Author

N89-20585 Washington Univ., Seattle.
RADIATION, TURBULENCE AND MICROPHYSICS IN THE STRATIFORM REGIONS OF TROPICAL CLOUD CLUSTERS Ph.D. Thesis
Dean Daniel Churchill 1988 134 p
Avail: Univ. Microfilms Order No. DA8826375

A 2-D, kinematic, hydrostatic model, incorporating ice and water cloud microphysics, short and long wave radiation, and convective adjustment, is used to diagnose the thermodynamic, water vapor and hydrometeor fields of mesoscale tropical cloud clusters. The goal is to describe the role of radiation in the stratiform portions of tropical cloud clusters, and to describe the behavior of cloud clusters in the upper troposphere and lower stratosphere. At the top of the stratiform area of a tropical squall-line during the night, energy loss due to infrared flux divergence was balanced by horizontal temperature advection and vertical eddy flux convergence of moist static energy. No change in the hydrometeor was produced by addition of radiation. Cooling due to melting and evaporation of precipitation in the low troposphere caused convective and overturning beneath stratiform cloud base, and scud formed. Radiatively driven convective overturning maintained saturation in cirrostratus cumulonimbogenitus. Tropical cirrus of this type remained for a long period of time. Infrared radiation was responsible for its duration, but no precipitation was formed. Dissert. Abstr.

N89-20586 Washington Univ., Seattle.
THREE-DIMENSIONAL KINEMATICS OF RAINBANDS IN MIDLATITUDE CYCLONES Ph.D. Thesis
Owen Hertzman 1988 278 p
Avail: Univ. Microfilms Order No. DA8826387

The 3-D kinematics of 4 precipitation features in a warm occlusion and a warm front are investigated using data from scanning dual Doppler radars. The high density of measurements resolves the structure of the weak vertical motions associated with the precipitation. Kinematic fields are described with respect to the small scale precipitation cores that made up two rainbands. The 3-D motions in the core relative frame provide insights into relationships between the kinematic and precipitation fields. Two rainbands were situated near the centers of cyclonic vorticity and upward motion in the young warm occlusion. They were oriented perpendicular to the wind shear in the vertical and they appeared to be maintained through the interaction of small scale updrafts and band scale, nondivergent cyclonic circulations. Updrafts, forced by convergence in the boundary layer ahead of the surface occlusion and ahead of the cold air aloft, enhanced the growth of precipitation at and above the level of the bandscale cyclonic circulations. These circulations played an important role in determining the widths of the rainbands. Kinematic factors that played a role in the formation of the precipitation associated with the warm front are discussed. Dissert. Abstr.

N89-20587*# National Aeronautics and Space Administration. Langley Research Center, Hampton, VA.
ANGULAR RADIATION MODELS FOR EARTH-ATMOSPHERE SYSTEM. VOLUME 2: LONGWAVE RADIATION
J. T. Suttles, R. N. Green, G. L. Smith, B. A. Wielicki, I. J. Walker, V. R. Taylor, and L. L. Stowe (National Oceanic and Atmospheric Administration, Washington, DC.) Apr. 1989 88 p
(NASA-RP-1184-Vol-2; L-16503; NAS 1.61:1184-Vol-2) Avail: NTIS HC A05/MF A01 CSCL 04B

The longwave angular radiation models that are required for analysis of satellite measurements of Earth radiation, such as those from the Earth Radiation Budget Experiment (ERBE) are presented. The models contain limb-darkening characteristics and mean fluxes. Limb-darkening characteristics are the longwave anisotropic factor and the standard deviation of the longwave radiance. Derivation of these models from the Nimbus 7 ERB (Earth Radiation Budget) data set is described. Tabulated values and computer-generated plots are included for the limb-darkening and mean-flux models. Author

N89-20588*# National Aeronautics and Space Administration. Goddard Space Flight Center, Greenbelt, MD.
AN ASSESSMENT MODEL FOR ATMOSPHERIC COMPOSITION
Michael J. Prather, ed. Jan. 1988 56 p Proceedings of a workshop held at NASA Goddard Inst. for Space Studies, New York, NY, 10-13 Jan. 1988
(NASA-CP-3023; Rept-89-31; NAS 1.55:3023) Avail: NTIS HC A04/MF A01 CSCL 04B

Predicting future perturbations to global air quality and climate requires, as a prerequisite, prognostic models for the composition of the Earth's atmosphere. Such assessment models are needed to evaluate the impact on our environment of different social choices that affect emissions of the photochemically and radiatively important trace gases. Our presentation here of a prototype assessment model is intended to encourage public scientific discussions of the necessary components of the model and their interactions, with the recognition that models similar to this will likely be used by the Environmental Protection Agency and other regulatory agencies in order to assess the effect of changes in atmospheric composition on climate over the next century. Author

N89-20589*# National Aeronautics and Space Administration. Goddard Space Flight Center, Greenbelt, MD.
VERIFICATION OF REGIONAL CLIMATES OF GISS GCM. PART 2: SUMMER
Leonard M. Druyan and David Rind Jan. 1989 54 p
(NASA-TM-100722; NAS 1.15:100722) Avail: NTIS HC A04/MF A01 CSCL 04B

Verification is made of the synoptic fields, sea-level pressure, precipitation rate, 200mb zonal wind and the surface resultant wind generated by two versions of the Goddard Institute for Space Studies (GISS) climate model. The models differ regarding the horizontal resolution of the computation grids and the specification of the sea-surface temperatures. Maps of the regional distributions of seasonal means of the model fields are shown alongside maps that show the observed distributions. Comparisons of the model results with observations are discussed and also summarized in tables according to geographic region. Author

N89-20590# Pacific Northwest Labs., Richland, WA.
OBSERVED AND MODELED TERRAIN-INDUCED SHEAR IN TRACER TRAJECTORIES
J. C. Doran and E. D. Skyllingstad Sep. 1988 16 p Presented at the 6th Joint Conference on Applications of Air Pollution Meteorology, Anaheim, CA, 29 Jan. 1989
(Contract DE-AC06-76RL-01830)
(DE89-006938; PNL-SA-16318; CONF-890133-4) Avail: NTIS HC A03/MF A01

In this paper we discuss two cases in which surface observations provided generally similar wind field patterns but in which the winds aloft differed significantly. The differences, which are simulated well by a primitive equation model, are attributed to the effects of terrain blocking, which is difficult to incorporate into objective interpolation schemes. Implications for plume trajectory predictions are also discussed. Our area of interest lies in a semi-arid region in southeastern Washington; for the numerical simulations we concentrated on a domain 100 by 100 km in size. The central, eastern, and northeastern portions of the region are relatively flat with only a gentle rise toward the northeast corner of the domain. The northwestern and southern regions have considerably more terrain relief, with ridge lines extending up to 1000 m above the lowest points in the central basin. The Columbia River enters near the northwest corner of the domain and is joined by the Yakima River near the southeast corner. A contour map of the central part of the region is included. In the summer of 1982, limited tracer measurements were made with an aircraft to study

some of the circulation patterns that develop in this area. On several days, starting about an hour after sunrise, SF was released for approximately 90 min at an elevation of 10 m AGL near the center of the basin. DOE

N89-20591# Brookhaven National Lab., Upton, NY. Atmospheric Sciences Div.
3CPO, CLOUD CHEMISTRY AND CLOUD PHYSICS ORGANIZATION: DATA INDEX, JUNE 1988
Joyce Tichler, Kathy Norden, and Darla Sharp (Pacific Northwest Labs., Richland, WA.) Dec. 1988 95 p
(Contract DE-AC02-76CH-00016)
(DE89-007011; BNL-42203) Avail: NTIS HC A06/MF A01

This document is an index of the data that was collected as part of the Cloud Chemistry and Cloud Physics Organization (3CPO) cooperative convective storms program which took place in June 1988 in east central Illinois. The objective of 3CPO was to assemble at a common time and location, the necessary measurement facilities to provide a previously unattained description of convective storm characteristics in polluted environments. DOE

N89-20592# Conservation and Renewable Energy Inquiry and Referral Service, Silver Spring, MD.
CLIMATE FUNDAMENTALS FOR SOLAR ENERGY SYSTEMS
Apr. 1988 6 p
(DE89-007319; DOE/CE-0219) Avail: NTIS HC A02/MF A01

Climate greatly influences the performance of any solar energy system. How many daylight hours are there in January. How much cloud cover is there in March. These are some of the first questions that must be asked when considering a solar heating or photovoltaic system for your home or community. The more direct sunlight a solar energy system receives, the better it will perform. In this fact sheet, sunlight is referred to as solar radiation. (It is also called solar irradiance and insolation.) Microclimate also has an important effect on solar heating and photovoltaic systems. Microclimate refers to the weather patterns (e.g., winds, fog, frost) that are unique to the building site. DOE

N89-20593# Battelle Pacific Northwest Labs., Richland, WA.
THE DEVELOPMENT AND STRUCTURE OF NOCTURNAL SLOPE WINDS IN A SIMPLE VALLEY Final Report, Sep. 1985 - Dec. 1988
J. C. Doran, T. W. Horst, and C. D. Whiteman Dec. 1988 93 p
(Contract DAAG29-85-K-0231)
(AD-A203427; ARO-22773.2-GS) Avail: NTIS HC A05/MF A01 CSCL 04B

This report describes the results of a project to study the evolution and structure of nocturnal slope flows that form on the sidewalls of a simple valley. The valley chosen for the project was located in southeastern Washington. The measurement sites were located in a straight 1.5-km-long section of the valley, with the ridgetops approximately 225 m above the valley floor. The east sidewall was quite smooth, had little vegetation other than grasses, and had a nearly constant 23-degree slope angle. The west sidewall was more irregular, steeper, and had more vegetation. Towers were erected on both sidewalls, and wind and temperature data were collected there on six nights in October of 1986. A Doppler sodar measured winds throughout the depth of the valley and above, and a tethered balloon was used to obtain temperature measurements and additional wind data in the valley during the first few hours after sunset. GRA

N89-20594# Naval Oceanography Command Detachment, Asheville, NC.
SUMMARY OF METEOROLOGICAL OBSERVATIONS, SURFACE (SMOS) FOR NORFOLK, VIRGINIA Reference Report, 1955 - 1986
Dec. 1988 687 p
(AD-A203644) Avail: NTIS HC A99/MF A02 CSCL 04B

This data report consists of a six part statistical summary of surface weather observations. The six parts are: Part 1 - Weather Conditions/Atmospheric Phenomena, Part 2 - Precipitation/Snowfall/Snow Depth, Part 3 - Surface Winds, Part 4 - Ceiling versus Visibility/Sky Cover, Part 5 - Psychrometric Summaries, Part 6 - Station Pressure/Sea Level Pressure. GRA

N89-20595# Colorado State Univ., Fort Collins. Dept. of Civil Engineering.
LONG-RANGE FORECASTING OF STORMINESS OVER THE NORTHERN HEMISPHERE OCEANS Final Report, 1 Jun. 1986 - 31 Dec. 1988
Elmar R. Reiter and Bruce C. Macdonald Jan. 1989 12 p
(Contract N00014-86-K-0544)
(AD-A203949) Avail: NTIS HC A03/MF A01 CSCL 04A

The focus of this research was directed toward heavy weather at sea specifically to marine bombs and their predictability. The approach involved analyses of bombs which occur overland, in order to determine the key signatures of bomb development. The two were: (1) A comprehensive diagnostic effort aimed at examining the nature of explosive cyclogenesis, including a comparison of bombs and nonexplosive, or regular, cyclones. The generation of vorticity, divergence, and latent heating patterns at the incipient, explosive, and mature phases of bombs were analyzed and compared to similar phases of regular cyclones, and (2) A numerical modeling of the bombs and regular cyclones using the same cases studied as in the diagnostic effort. A feature component was developed and incorporated into an existing numerical model to improve prediction of central sea level pressure in a bomb. The model was also used to examine the sensitivity of cyclogenesis to slight adjustments in the input data fields, and to examine the trajectories of air parcels which were deemed to be important to explosive cyclogenesis. GRA

48 OCEANOGRAPHY

Includes biological, dynamic, and physical oceanography; and marine resources.

For related information see also *43 Earth Resources and Remote Sensing.*

N89-20596# National Oceanic and Atmospheric Administration, Seattle, WA. Marine Environmental Lab.
CTD/O2 MEASUREMENTS DURING 1986 AS PART OF THE EQUATORIAL PACIFIC OCEAN CLIMATE STUDIES (EPOCS)
J. M. Lynch, L. J. Mangum, and S. P. Hayes Aug. 1988 262 p
(PB89-102859; NOAA-DR-ERL-PMEL-24; CONTRIB-1063) Avail: NTIS HC A12/MF A01 CSCL 08C

During 1986, CTD data were collected in the eastern equatorial Pacific as part of the Equatorial Pacific Ocean Climate Studies (EPOCS) program, which began its field program in 1979. Summaries of CTD data from three cruises in 1986 are presented. Station locations, meteorological conditions and profiles of temperature, salinity, sigma-T, and oxygen are shown for each cast. Additionally, T-S diagrams and section plots along 110 deg W, 140 deg W, 15 deg S and the equator are presented. GRA

N89-20597# National Oceanic and Atmospheric Administration, Seattle, WA. Marine Environmental Lab.
BEAUFORT SEA MESOSCALE CIRCULATION STUDY: PRELIMINARY RESULTS
A. Aagaard, C. H. Pease, and S. A. Salo Jul. 1988 179 p
(PB89-121693; NOAA-TM-ERL-PMEL-82; CONTRIB-1040) Avail: NTIS HC A09/MF A01 CSCL 08C

The Beaufort Sea Mesoscale Circulation Study was initiated in the autumn of 1986 and included measurements of currents, winds, and ice velocities, as well as observations of state variables and nutrient distributions in the ocean and state variables in the polar atmosphere, principally between Barrow and Demarcation Point along the American Beaufort Sea shelf. The preliminary results from observations made during the first year of the project, including current velocity results from meters recovered through the ice in April 1987, hydrographic and nutrient sections completed in October 1986 and April 1987, wind velocity, air pressure and temperature records recovered continuously through the end of

1987, ARGOS buoy tracks through 1987, and a representative sample of analyzed weather maps during the first year are given. Data collection continued through April 1988. The total data set is extraordinary in the temporal and spatial extent of its synoptic coverage, and in the variety of its constituent measurements. The data set is also extremely large, and its full reduction and analysis will provide an exceptional opportunity for improving the understanding of the shelf circulation and its forcing, as well as conditions important to the marine ecology of the area. Author

N89-20598# National Oceanic and Atmospheric Administration, Miami, FL. Oceanographic and Meteorological Labs.
CURRENT VELOCITY AND HYDROGRAPHIC OBSERVATIONS IN THE SOUTHWESTERN NORTH ATLANTIC OCEAN: SUBTROPICAL ATLANTIC CLIMATE STUDIES (SACS), 1987
Anne Marie Wilburn, Elizabeth Johns, and Mark Bushnell Aug. 1988 92 p
(PB89-114011; NOAA-DR-ERL-AOML-12) Avail: NTIS HC A05/MF A01 CSCL 08C

The main objectives of the Subtropical Atlantic Climate Studies (STACS) program are to increase understanding of the dynamics of the North Atlantic circulation in global climate, to develop the capability to monitor the climatically important processes, and to develop coupled ocean atmospheric general circulation models. Data is provided on the observational studies of western boundary currents, extending the study area southward to Brazil (4 deg N) in order to examine the contribution of cross equatorial boundary currents to the North Atlantic mass and heat fluxes. Pegasus and CTD data are given for various sections. GRA

N89-20599# Colorado School of Mines, Golden.
SIMULTANEOUS INVERSION OF VECTOR AND TOTAL FIELD AEROMAGNETIC DATA USING BAYESIAN INFERENCE: A CASE STUDY FROM THE COBB OFFSET OF THE JUAN DE FUCA RIDGE Ph.D. Thesis
Warren T. Dewhurst Sep. 1988 267 p
(PB89-114193; T-3365) Avail: NTIS HC A12/MF A01 CSCL 08C

The application of the measurement of all three components (north, east, and downward) of the Earth's magnetic field is introduced. In addition, numerical inversion techniques are presented which facilitate the interpretation of the data over an active oceanic ridge, the Cobb Offset of the Juan de Fuca Spreading Center. High resolution bathymetry, obtained using a state-of-the-art mapping system, SEABEAM, and single channel seismic data, numerically provide geologic constraints in the inversion process. The research represents the first application of vector magnetic observations for a geophysical investigation. The Juan de Fuca Spreading Ridge, located off the coast of the states of Washington and Oregon, demonstrates tectonic motion not fully explained by rigid plate theory. In particular, the Cobb Offset, a horizontal displacement between two opposing ridge segments, is shown to be the product of opposing along-strike ridge propagation rather than transform faulting. Estimates of the apparent magnetization and the geometry of the magnetic source material (i.e., basalt) are also presented. GRA

N89-20600# Skidaway Inst. of Oceanography, Savannah, GA.
BIOLOGICAL PROCESSES IN THE WATER COLUMN OF THE SOUTH ATLANTIC BIGHT: ZOOPLANKTON RESPONSES Progress Report, Jun. 1988 - Jun. 1989
Gustav-Adolpho Paffenhoefer Feb. 1989 11 p
(Contract DE-FG09-85ER-60354)
(DE89-006828; DOE/ER-60354/T4) Avail: NTIS HC A03/MF A01

It is our objective to determine the major processes governing the abundance, composition and disruption of zooplankton as part of the interdisciplinary southeastern U.S. continental shelf program of the Department of Energy. We will study the effects of physical processes such as along- and cross shelf advection and frontogenesis, on the development and fate of zooplankton populations during winter. Our proposed research consists of shipboard sampling, laboratory experiments and in situ determination of zooplankton abundance over time. The last objective represents a novel approach because the observations are: (1) non-destructive with great spatial resolution, and (2) occur on current meter arrays at similar scales as measurements of current velocity and direction. Results to date show prolonged residence times of upwelled water masses on the middle and inner shelf during summer which results in the development of massive copepod and tunicate populations. During spring, the extent of displacement of nearshore zooplankton was a function of wind stress. Our results can be used to predict the impact of energy-related technology on the ecosystem of the southeastern continental shelf. DOE

51 LIFE SCIENCES (GENERAL)

N89-20601# Pittsburgh Univ., PA. Graduate School of Public Health.
NEW MODELS TO ASSESS BEHAVIORAL AND PHYSIOLOGICAL PERFORMANCE OF ANIMALS DURING INHALATION EXPOSURES Ph.D. Thesis
Dolores Elizabeth Malek Oct. 1988 164 p
(Grant NIST-NANB-4001)
(PB89-128946; NIST/GCR-88/551) Avail: NTIS HC A08/MF A01 CSCL 06C

Previously the toxicity of fire smoke has been examined primarily in sedentary animals and lethality was noted. The evaluation of escape potential from a toxic environment, however, requires the measurement of sublethal responses in active animals that are escape predictive. To address this need, the mouse track model and the guinea pig ergometer model have been developed. The mouse track model was a ventilated S shaped exposure system. Performance was evaluated by two sublethal responses, distance traveled/time and incapacitation. A novel feature of the mouse track model was its ability to detect an early deterioration in performance before incapacitation and death. The guinea pig ergometer model was designed where a 4.9L exposure chamber enclosed a motor driven rubberized wheel. Extrapolation of exercising guinea pig data to human was similar to theoretical models that predict human response to CO. Humans were estimated to progress five times the distance of the guinea pig at a similar level of toxicity for CO. Author

N89-20602*# Lockheed Engineering and Sciences Co., Washington, DC.
USSR SPACE LIFE SCIENCES DIGEST, ISSUE 21
Lydia Razran Hooke, P. Lynn Donaldson, Victoria Garshnek, and Joseph Rowe Washington NASA Mar. 1989 108 p
(Contract NASw-4292)
(NASA-CR-3922(24); NAS 1.26:3922(24)) Avail: NTIS HC A06/MF A01 CSCL 06C

This is the twenty-first issue of NASA's USSR Space Life Sciences Digest. It contains abstracts of 37 papers published in Russian language periodicals or books or presented at conferences and of a Soviet monograph on animal ontogeny in weightlessness. Selected abstracts are illustrated with figures and tables from the original. A book review of a work on adaptation to stress is also included. The abstracts in this issue have been identified as relevant to 25 areas of space biology and medicine. These areas are: adaptation, biological rhythms, body fluids, botany, cardiovascular and respiratory systems, cytology, developmental biology, endocrinology, enzymology, equipment and instrumentation, exobiology, gravitational biology, habitability and environmental effects, hematology, human performance, life support systems, mathematical modeling, metabolism, microbiology, musculoskeletal system, neurophysiology, operational medicine, perception, psychology, and reproductive system. Author

N89-20603# California Univ., Berkeley. Lawrence Berkeley Lab. Engineering Div.
THE DEVELOPMENT OF A COMPTON LUNG DENSITOMETER

Billy W. Loo, Fred S. Goulding, Norm W. Madden, and Daniel S. Simon (California Univ., San Francisco.) Nov. 1988 18 p Presented at the IEEE Nuclear Science Symposium, Orlando, FL, 9 Nov. 1988
(Contract DE-AC03-76SF-00098)
(DE89-006654; LBL-25170; CONF-881103-36) Avail: NTIS HC A03/MF A01

A field instrument is being developed for the non-invasive determination of absolute lung density using unique Compton backscattering techniques. A system consisting of a mono-energetic gamma-ray beam and a shielded high resolution high-purity-germanium (HPGe) detector in a close-coupled geometry is designed to minimize errors due to multiple scattering and uncontrollable attenuation in the chestwall. Results of studies on system performance with phantoms, the optimization of detectors, and the fabrication of a practical gamma-ray source are presented. DOE

N89-20604# California Univ., Berkeley. Lawrence Berkeley Lab. Accelerator and Fusion Research Div.
X-RAY MICROSCOPY FOR THE LIFE AND PHYSICAL SCIENCES
D. Attwood, Y. Vladimirsky, D. Kern, W. Meyer-Ilse, J. Kirz, S. Rothman, H. Rarback, N. Iskander, K. McQuaid, and H. Ade (State Univ. of New York, Stony Brook.) et al Jun. 1988 6 p Presented at the Topical Meeting on Short Wavelength Coherent Radiation Generation and Applications, North Falmouth, MA, 26 Sep. 1988 Prepared in cooperation with International Business Machines Corp., Hopewell Junction, NY
(Contracts DE-AC03-76SF-00098; DE-AC02-76CH-00016)
(DE89-006707; LBL-26232; CONF-8809281-1) Avail: NTIS HC A02/MF A01

In this brief report we describe two recent X-ray microscopy experiments which demonstrate achievements of significant milestones in the development of high spatial resolution X-ray microscopy for the life and physical sciences. In one series of experiments it was clearly demonstrated that X-ray optical systems are capable of forming images of nanostructure patterns associated with future microelectronic devices, to a spatial resolution better than 0.1 microns. In the second set of experiments, unaltered biological material was imaged in its natural state without recourse to sectioning, staining, fixing or drying, at a spatial resolution well beyond that of the optical microscope, and with a delivered energy dose well below that of an electron microscope. DOE

52 AEROSPACE MEDICINE

Includes physiological factors; biological effects of radiation; and effects of weightlessness on man and animals.

N89-20605# National Library of Medicine, Bethesda, MD.
MEDICAL SUBJECT HEADINGS, TREE STRUCTURES, 1989
Jul. 1988 521 p
(PB89-100028; NLM/MED-89/02) Avail: NTIS HC A22/MF A01 CSCL 06P

All Medical Subject Headings currently in use by the National Library of Medicine's indexers, catalogers, and searchers are arranged in a hierarchical manner showing relationships between broader and narrower terms. Included are minor and geographical descriptors. GRA

N89-20606# ICON Consultants, Birmingham, AL.
USING DEPTH RECOVERY IN HUMANS Final Report, Aug. 1987 - Jun. 1988
Thomas K. Kuyk 7 Jul. 1988 61 p
(Contract F33615-87-C-0541)
(AD-A201278; AAMRL-TR-88-035) Avail: NTIS HC A04/MF A01 CSCL 23C

This program investigated the relevant information content contained in a physiologically based model of the human visual system with regard to the efficient extraction of depth through stereopsis. A computational system was developed using the Gabor representational scheme to model the spatial weighting functions of simple and complex cells known to exist in primate visual cortex. The algorithm was implemented in a foveated representation produced by a complex-logarithmic, conformal mapping of each image yielding the advantage of both high resolution and a wide field-of-view. The algorithm was tested by extracting depth arrays from random-dot stereograms. The results demonstrated that the depth mapping was accurate and in excellent agreement with the percept produced when human observers fused the same stereo images. The significance of this approach is that it models not a visual system but rather an experimentally verified model of the primate visual system. This is critical to the effective application of human information processing techniques to specialized or intelligent image processing systems. GRA

N89-20607# Iowa Univ., Iowa City. Dept. of Physical Therapy Education.
INFLUENCES OF MUSCLE FIBER COMPOSITION AND STRENGTH ON EMG (ELECTROMYOGRAPHIC ACTIVITY), SPINAL MOTION AND LOAD ACCELERATION DURING A REPETITIVE LIFTING TASK
Thomas Michael Cook and Gary L. Soderberg May 1988 81 p
(Grant PHS-OH-01929)
(PB89-131221) Avail: NTIS HC A05/MF A01 CSCL 06P

The changes which occur over time in the erector spinae muscles of the lower back in the instantaneous fatigue state were studied in relation to the selected kinematic and kinetic features of lifting. The influences of muscle fiber composition and lifting strength on changes in electromyographic activity (EMG), spinal motion, and load acceleration during this time period were investigated. A total of 24 male volunteers participated in the study. A great deal of variability was noted in regard to EMG amplitude and EMG center frequency from the L3 erector spinae musculature in regard to the range of motion of the lumbar segment, and in regard to the maximum vertical acceleration applied to the load being lifted. A significant relationship was noted between the EMG amplitude and EMG center frequency trends during repetitive lifting but not among these EMG measures and trunk range of motion, maximum load acceleration, height, or weight. A significant relationship was noted between lifting strength of the subject and the amount of trunk range of motion at the beginning of the lifting session and to the height and weight of the subject. Finally, significant relations were noted between muscle fiber composition and the maximum vertical acceleration applied to the load at the beginning of the lifting session. Author

N89-20608# International Centre for Theoretical Physics, Trieste (Italy).
PROPAGATION OF THE NERVE IMPULSE UNDER THE EFFECT OF A MAGNETIC FIELD
J. Chela-Flores, E. M. El-Sayed, and X. Y. Wang Sep. 1988 18 p Submitted for publication
(DE88-705371; IC-88/323) Avail: NTIS (US Sales Only) HC A03/MF A01

The recent significant advance in superconductivity at high temperatures has raised an important problem in biophysics, in view of the underlying interest that has arisen in experiments in which very high magnetic fields are needed (in the multi-tesla range). This is occurring against a theoretical background in which there is no reliable way of estimating the effect of magnetic fields on the central nervous system. This has led us to discuss the problem of the coupling of magnetic fields with the coherent propagation of the polarization of the plasma membrane along the axon. Our work lies within the context of the phenomenological model of nerve impulse propagation due to Hodgkin and Huxley. Using the concept of gauge invariance we find that the magnetic field has a non negligible effect on the velocity of propagation of the action potential in the limit of the Fitzhugh-Nagumo equation without recovery, but more realistic cases do not change the main conclusions of this work. DOE

N89-20609# Defence Research Establishment Ottawa, (Ontario).
WHY COLD-WET MAKES ONE FEEL CHILLED: A LITERATURE REVIEW
Rita M. Crow Jun. 1988 16 p
(AD-A203452; DREO-TN-88-22) Avail: NTIS HC A03/MF A01 CSCL 06J

This paper reviews physiological experiments which have been carried out to determine if heat loss from the body is greater in cold-wet temperatures and humidities. It also reviews the effect of solar radiation the interaction of skin and humidity and skin and temperature and other postulations for the cold-wet sensation. It concludes that the best explanation for the chilling effect of cold-wet is the penetration of fine experiments would be needed to confirm this. GRA

53 BEHAVIORAL SCIENCES

Includes psychological factors; individual and group behavior; crew training and evaluation; and psychiatric research.

N89-20610*# National Aeronautics and Space Administration. Ames Research Center, Moffett Field, CA.
PRECISION IN THE PERCEPTION OF DIRECTION OF A MOVING PATTERN
Leland S. Stone Dec. 1988 21 p
(NASA-TM-101080; A-89062; NAS 1.15:101080) Avail: NTIS HC A03/MF A01 CSCL 05I

The precision of the model of pattern motion analysis put forth by Adelson and Movshon (1982) who proposed that humans determine the direction of a moving plaid (the sum of two sinusoidal gratings of different orientations) in two steps is qualitatively examined. The volocities of the grating components are first estimated, then combined using the intersection of constraints to determine the velocity of the plaid as a whole. Under the additional assumption that the noise sources for the component velocities are independent, an approximate expression can be derived for the precision in plaid direction as a function of the precision in the speed and direction of the components. Monte Carlo simulations verify that the expression is valid to within 5 percent over the natural range of the parameters. The expression is then used to predict human performance based on available estimates of human precision in the judgment of single component speed. Human performance is predicted to deteriorate by a factor of 3 as half the angle between the wavefronts (theta) decreases from 60 to 30 deg, but actual performance does not. The mean direction discrimination for three human observers was 4.3 plus or minus 0.9 deg (SD) for theta = 60 deg and 5.9 plus or minus 1.2 for theta = 30 deg. This discrepancy can be resolved in two ways. If the noises in the internal representations of the component speeds are smaller than the available estimates or if these noises are not independent, then the psychophysical results are consistent with the Adelson-Movshon hypothesis. Author

N89-20611# Institute for Perception RVO-TNO, Soesterberg (Netherlands). Afdeling Cognitive Psychologie.
COGNITIVE PSYCHOLOGY AT THE INSTITUTE FOR PERCEPTION
A. F. Sanders Dec. 1987 44 p In DUTCH; ENGLISH summary
(IZF-1987-41; TDCK-88-0288; ETN-89-94065) Avail: NTIS HC A03/MF A01

Cognitive psychology research since the 1960's is reviewed. Research on generating random sequences and internal models is recalled. Imagery, associational knowledge networks, learning functional rules, and subjective probabilities involved in decision making are discussed. This last theme can be further classified as research on gambling, decision heuristics, risk taking in traffic, and decision making in complex command and control systems. Research on internal models in ship maneuvering is mentioned. ESA

N89-20612# Center for Mathematics and Computer Science, Amsterdam (Netherlands). Dept. of Interactive Systems.
THE POWER OF PHYSICAL REPRESENTATIONS
Varol Akman and Paul J. W. tenHagen May 1988 26 p Presented at the 2nd Eurographics Workshop on Intelligent CAD Systems: Implementational Issues, Veldhoven, Netherlands, 11-15 Apr. 1988
(CWI-CS-R8819; B8827443; ETN-89-94176) Copyright Avail: NTIS HC A03/MF A01

It is argued that common sense reasoning about the physical world as exemplified by, Iron sinks in water, or If a ball is dropped it gains speed, will be indispensable in future programs. To make such predictions (envisioning), programs should use abstract entities (such as the gravitational field), principles (such as the principle of superposition), and laws (such as the conservation of energy) of physics for representation and reasoning. ESA

N89-20613# Illinois Univ., Savoy. Aviation Research Lab.
COMPONENTIAL ANALYSIS OF PILOT DECISION MAKING Final Report, Jun. 1986 - Sep. 1987
Christopher D. Wickens, Alan Stokes, Barbara Barnett, and Tom Davis, Jr. Aug. 1988 94 p
(Contract F33615-85-D-0514)
(AD-A203711; AAMRL-TR-88-017) Avail: NTIS HC A05/MF A01 CSCL 05H

This report describes the development of a computerized pilot decision-making simulator/trainer known as MIDIS, and its utilization as a research tool in the validation of an information-processing model of pilot decision making. Efforts in this project followed two parallel but interacting tracks: development of decision scenarios for the MIDIS program, following the sequence of a realistic IFR flight, and compilation of a cognitive test battery, based on an information processing model of decision making, and designed to assess individual differences in those cognitive attributes determined to be important in effective decision making. Subjects consisted of thirty eight instrument rated pilots subdivided into two groups on the basis of reported hours of flight experience. The experiment consisted of four parts: administration - of the cognitive test battery, pre-flight planning, a practice flight, and the actual MIDIS run. Subjects were scored as to the optimality and latency of their choices, and their rated confidence. The results indicated that low and high experienced pilots did not differ from each other in terms of their judgement performance, but that high experience pilots expressed slightly greater confidence in their decisions. The two groups however did differ in terms of what problem variables degraded decision performance, and what individual abilities affected that performance. In particular, novice decision performance was partially predicted by information processing tests related to spatial abilities, working memory capacity, mathematical ability and by tests of declarative knowledge. GRA

54 MAN/SYSTEM TECHNOLOGY AND LIFE SUPPORT

Includes human engineering; biotechnology; and space suits and protective clothing.

For related information see also *16 Space Transportation.*

N89-20614# Army Aeromedical Research Lab., Fort Rucker, AL.
SPH-4 HELMET RETENTION ASSEMBLY REINFORCEMENT Final Report
Ronald W. Palmer and J. L. Haley, Jr. Jul. 1988 23 p
(AD-A200432; USAARL-88-10) Avail: NTIS HC A02/MF A01 CSCL 05H

The purpose of a helmet's retention assembly is to keep the helmet firmly and securely in place on the wearer's head, thus preventing the exposure of the cranium to direct impact. The standard SPH-4 retention assembly is prone to excessive elongation under stress, and allows excessive helmet displacement

and cranium exposure. A modified SPH-4 retention assembly, reinforced with 0.75-inch tubular nylon webbing; was manufactured in this laboratory and tested quasi-statically on a testing machine which exerted a force at a constant speed. A standard SPH-4 retention assembly was also tested as a control. The reinforced retention assembly withstood a 450-lb load without failure. Elongation of the reinforced retention assembly, measured at 300-lb load, was almost 50 percent less than that of the standard retention assembly measured at the same load. GRA

N89-20615*# George Washington Univ., Washington, DC. Science Communication Studies.
NUTRITIONAL MODELS FOR A CONTROLLED ECOLOGICAL LIFE SUPPORT SYSTEM (CELSS): LINEAR MATHEMATICAL MODELING
Rose C. Wade NASA Mar. 1989 135 p
(Contracts NASw-3165; NASw-4324)
(NASA-CR-4229; NAS 1.26:4229) Avail: NTIS HC A07/MF A01 CSCL 06K

The NASA Controlled Ecological Life Support System (CELSS) Program is involved in developing a biogenerative life support system that will supply food, air, and water to space crews on long-duration missions. An important part of this effort is in development of the knowledge and technological capability of producing and processing foods to provide optimal diets for space crews. This involves such interrelated factors as determination of the diet, based on knowledge of nutrient needs of humans and adjustments in those needs that may be required as a result of the conditions of long-duration space flight; determination of the optimal mixture of crops required to provide nutrients at levels that are sufficient but not excessive or toxic; and consideration of the critical issues of spacecraft space and power limitations, which impose a phytomass minimization requirement. The complex interactions among these factors are examined with the goal of supplying a diet that will satisfy human needs while minimizing the total phytomass requirement. The approach taken was to collect plant nutritional composition and phytomass production data, identify human nutritional needs and estimate the adjustments to the nutrient requirements likely to result from space flight, and then to generate mathematical models from these data. Author

N89-20616# Technische Univ., Delft (Netherlands). Faculty of Technical Mathematics and Informatics.
DIRECT MANIPULATION AND OTHER STYLES OF MAN-MACHINE INTERACTION
J. M. Versendaal 1988 18 p
(Rept-88-53; ISSN-0920-8577; ETN-89-94020) Copyright Avail: NTIS HC A03/MF A01

The direct manipulation (DM) approach to user-computer iteraction, where the user directly manipulates the object presented on the screen is discussed. It is shown that DM is quite complex with respect to conventional dialog styles. Direct manipulation is actually a highly interwoven question/answer dialog style. Feedback in DM is often more complex than feedback in conventional dialog styles; syntactic feedback and semantic feedback in DM systems are often mixed. As a consequence it is more difficult to describe DM systems than to describe systems based on other dialog styles. Modeling a DM system by separating the syntactic and semantic aspects of the system is not possible. Modeling the design process of DM systems is possible using an object-oriented approach which can be used in information system modeling as well. Once an object-oriented conceptual model is specified for a certain DM system, this model can be part of the run time of the DM system. ESA

N89-20617# Technische Univ., Delft (Netherlands). Faculty of Technical Mathematics and Informatics.
USER INTERFACES AND HIGHLY INTERACTIVE SYSTEMS: SURVEY OF CURRENT RESEARCH
J. M. Versendaal 1988 33 p
(Rept-88-60; ISSN-0920-8577; ETN-89-94026) Copyright Avail: NTIS HC A03/MF A01

The state of the art in highly interactive system design, particularly in design of user-computer dialogs, is reviewed. Methodologies for interactive system design are described. Management systems for user interfaces and interactive applications are discussed. The object oriented approach for user interface and interactive system design is outlined. ESA

N89-20618# Institute for Perception RVO-TNO, Soesterberg (Netherlands). Afdeling Thermofysiologie.
SAFE WORKING TIME LIMITS IN IMPERMEABLE PROTECTIVE CLOTHING: RECOMMENDATIONS BASED UPON EXPERIMENTAL MEASUREMENTS
F. J. G. vandeLinde Oct. 1987 35 p In DUTCH; ENGLISH summary
(Contract A81/K/041)
(IZF-1987-28; TDCK-87-4844; ETN-89-94064) Avail: NTIS HC A03/MF A01

Safe working time limits in water vapor impermeable protective clothing are calculated for young, well-trained men. The approach is largely empirical. The equations used are simple, and can easily be incorporated in a hand held computer. They offer the possibility for implementation of auxiliary cooling, and alterations of the thermal state of the body prior to work. Literature data is applied to extend the predictions to different ages, gender, and fitness. Decontamination work, previously determined to be moderately heavy, can generally be carried out for over 2 hr at ambient temperatures of 15 C and lower. At higher environmental or metabolic load, individual factors play an important role in the individual's capacity to work in impermeable clothing, and may limit the individual tolerance to less than 30 min. ESA

55 SPACE BIOLOGY

Includes exobiology; planetary biology; and extraterrestrial life.

No abstracts in this category.

59 MATHEMATICAL AND COMPUTER SCIENCES (GENERAL)

N89-20619*# Institute for Computer Applications in Science and Engineering, Hampton, VA.
CUMULATIVE REPORTS AND PUBLICATIONS THROUGH DECEMBER 31, 1988 Final Report
Feb. 1989 64 p Prepared in cooperation with NASA, Langley Research Center, Hampton, VA
(Contracts NAS1-18107; NAS1-18605)
(NASA-CR-181784; NAS 1.26:181784) Avail: NTIS HC A04/MF A01 CSCL 12A

This document contains a complete list of ICASE Reports. Since ICASE Reports are intended to be preprints of articles that will appear in journals or conference proceedings, the published reference is included when it is available. Author

60 COMPUTER OPERATIONS AND HARDWARE

Includes hardware for computer graphics, firmware, and data processing.

For components see *33 Electronics and Electrical Engineering.*

N89-20620# National Center for Atmospheric Research, Boulder, CO.
EXPERIENCES ON A CRAY-2 (TRADE NAME) RUNNING UNICOS
M. Pernice Aug. 1988 40 p
(Grant NSF ATM-87-09659)
(PB88-250725; NCAR/TN-316-STR) Avail: NTIS HC A03/MF A01 CSCL 09B

The CRAY X-MP/48 at the National Center for Atmospheric Research (NCAR) was installed and became operational in the fourth quarter of 1986. By the end of the second quarter of 1988, the X-MP was saturated. It is expected that NCAR will replace the X-MP with the next generation supercomputer sometime in 1990-1992. The users of NCAR's computing facilities have been using the batch-oriented Cray Operating System (COS) since the installation of NCAR's first CRAY-1 in 1977. Concerns have been expressed about the impact of UNIX on supercomputer performance, particularly on the performance of applications that require substantial amounts of Input and Output (I/O) operations. Author

N89-20621# National Inst. of Standards and Technology, Gaithersburg, MD. Advanced Systems Div.
PERFORMANCE EVALUATION AND ANALYTIC MODELING OF SHARED-MEMORY COMPUTERS
James R. Nechvatal Sep. 1988 30 p Sponsored by Office of Export Administration, Washington, DC
(PB89-113542; NISTIR-88/3857) Avail: NTIS HC A03/MF A01 CSCL 09B

Analytic performance models for shared-memory computers are surveyed and discussed. The purpose is to assess these models to determine if they are relevant to the task of assisting the Office of Export Administration in establishing guidelines for exports of computers. The focus of the study is on the assumptions made by modelers regarding interconnection networks and memory access patterns exhibited by applications. The great majority of models concentrate on analyzing a small collection of networks. Furthermore, most modelers make strong assumptions regarding the independence and uniform distribution of memory accesses. The consequences of these assumptions in the resulting models are noted. Author

N89-20622 British Petroleum Co. Ltd., London (England).
MEMORY ARCHITECTURE FOR MULTIPROCESSOR COMPUTERS Patent Application
Christopher John Mottershead, Inventor 7 Oct. 1987 22 p Filed 2 Apr. 1987 Priority 4 Apr. 1986 GB 8608312
(EP-PATENT-0-240-354-A1; EP-PATENT-APPL-SN-87302898.9; INT.CLASS-G06F-15/16; ETN-89-94066) Avail: UK Patent Office, 25 Southampton Buildings, London WC2A 1AY, England

A multiprocessor computer comprising a plurality of identical processing elements, each of which comprises a processor, local memory addressable by the processor, and an arbitration unit for controlling access to the local memory from other processing elements is presented. At least one processing element is connected to X neighbors (where X is an integer which is at least 1) for the sharing of data. The memory space addressable by the processor in the processing elements is divided into a least X + 1 regions. Addressing different regions of memory space causes data to be accessed in either the local memory or in the memories of neighboring processing elements. ESA

N89-20623 British Petroleum Co. Ltd., London (England).
DATA STORAGE AND TRANSFER APPARATUS Patent Application
John Norman Harrison, inventor and Christopher John Mottershead, inventor 28 Oct. 1987 12 p Filed 23 Apr. 1987 Priority 23 Apr. 1986 GB 8609848
(EP-0-243-189-A1; EP-PATENT-APPL-SN-87303599.2; INT.CLASS-G06F-13/28; ETN-89-94069) Avail: UK Patent Office, 25 Southampton Buildings, London WC2A 1AY, England

A data storage and transfer apparatus comprising at least two addressable memories each having an address bus is presented. A data bus links the memories. The data moving means comprises two address generating means for generating source and destination addresses on the respective address buses to cause data to be transferred from one memory to the other. ESA

N89-20624 British Petroleum Co. Ltd., London (England).
IMPROVEMENTS RELATING TO CONTROL FLOW IN COMPUTERS Patent Application
John Norman Harrison, inventor, Derek Owen Morris, inventor, and Christopher John Mottershead, inventor 2 Sep. 1987 19 p Filed 6 Feb. 1987 Priority 6 Feb. 1986 GB 8603013; Priority 15 Mar. 1986 GB 8606452
(EP-0-234-785-A1; EP-PATENT-APPL-SN-87301083.9; INT.CLASS-G06F-15/06; ETN-89-94070) Avail: UK Patent Office, 25 Southampton Buildings, London WC2A 1AY Engalnd

A computer with a computation processor and an instruction memory where instructions relating to computation are stored, and also a control flow processor and a control flow memory where instructions relating to the control flow of the program are stored is proposed. The computation instructions processed by the computation processor are determined in accordance with control flow instructions processed in the control flow processor. The invention is particularly applicable to SIMD computers. ESA

N89-20625 Technische Univ., Delft (Netherlands). Dept. of Physics.
THE DELFT ISING SYSTEM PROCESSOR Ph.D. Thesis
Arne Hoogland 1987 112 p
(ISBN-9-09-001753-4; ETN-89-94137) Copyright Avail: A. Hoogland, Technische Universiteit Delft, Dept. of Applied Physics, P.O. Box 5046, 2600 GA Delft, The Netherlands

A computer was built for Monte Carlo calculations of Ising spin systems with short-range interactions. The hardware structure of the machine is described, including the extension of the machine to Monte Carlo renormalization group calculations. The hardware random-number generator employed is described and its quality is discussed. As a demonstration of the performance of the processor, results are given. The machine is an order of magnitude faster than general purpose computers. Design of a next-generation special-purpose machine for discrete spin systems is considered. ESA

N89-20626# Lawrence Livermore National Lab., CA.
SOFTWARE RELIABILITY ENGINEERING
J. Dennis Lawrence 1988 16 p Presented at the Structured Development Forum X, San Francisco, CA, 8-11 Aug. 1988
(Contract W-7405-eng-48)
(DE89-006781; UCRL-98827; CONF-880894-3) Avail: NTIS HC A03/MF A01

There are cases in which a computer system failure can have a serious impact on human life and health, property, and finances. This paper argues that structured development, for such systems, must give serious consideration to reliability and safety of both the computer system and the more general system which the computer is controlling. Activities can be carried out during the system life cycle which can improve reliability and safety. After a general discussion of software reliability engineering, the paper gives specific suggestions for activities during the requirements analysis and design phases of the life cycle. DOE

N89-20627# Sandia National Labs., Albuquerque, NM.
EPS'88: COMBINING THE BEST FEATURES OF VON NEUMANN AND DATAFLOW COMPUTING
V. G. Grafe, J. E. Hoch, and G. S. Davidson Jan. 1989 18 p
(Contract DE-AC04-76DP-00789)
(DE89-007291; SAND-88-3128) Avail: NTIS HC A03/MF A01

A new parallel architecture is presented which combines the beneficial features of both dataflow and von Neumann computers. Dynamic exploitation of parallelism is supported by a direct match dataflow scheduling mechanism. The dataflow scheduling mechanism can be applied to individual instructions or to groups of instructions. These groups of instructions are executed in a predetermined order, as in von Neumann machines. This deterministic scheduling allows the reuse of data through common memory locations and the use of local state (registers) to minimize resource requirements and latency. The foundation of this architecture includes single clock, direct matching of operands, dynamically allocated frame-based data storage, and a general repeat function that can dispatch instructions in a predetermined order. The ability to execute fully and partially ordered instruction streams makes the architecture amenable to both imperative and functional languages. The operation of the processor architecture, the associated structured memory system, proposed interconnections, and programming considerations are described. The entire architecture has been captured in a functional simulator, and hardware implementations of several of the vital parts are underway. DOE

N89-20628# Lawrence Livermore National Lab., CA. Seismic Monitoring Research Program
DATMS: A FRAMEWORK FOR DISTRIBUTED ASSUMPTION BASED REASONING
Cindy L. Mason (California Univ., Davis.) and Rowland R. Johnson 1988 16 p Presented at the Distributed Artificial Intelligence Workshop, Lake Arrowhead, CA, 20 May 1988
(Contract W-7405-eng-48)
(DE89-006282; UCRL-98743; CONF-8805252-1) Avail: NTIS HC A03/MF A01

The Distributed ATMS, DATMS, is a problem solving framework for multi-agent assumption based reasoning using Assumption-based Truth Maintenance Systems. It is based on the problem solving paradigm of result sharing rule-based expert systems using assumption based reasoning. We are implementing and experimenting with the DATMS under MATE, a Multi-Agent Test Environment, using C and COMMON-LISP on a network of SUN family workstations. This framework was motivated by the problem of seismic interpretation for Comprehensive or Low-Yield Test Ban Treaty verification, where a wide spread network of seismic sensor stations are required to monitor treaty compliance, and seismologists use assumption based reasoning in a collaborative fashion to interpret the seismic data. The DATMS framework differs from other previously designed problem solving organizations in its method of reasoning the ability to support an explanation facility and in addressing the problem of culpability. DOE

N89-20629# Bolt, Beranek, and Newman, Inc., Cambridge, MA.
RESEARCH IN DISTRIBUTED PERSONAL COMPUTER-BASED INFORMATION SYSTEMS, VOLUME 1 Final Report, Apr. - Oct. 1984
Harry C. Forsdick and Robert H. Thomas Aug. 1988 99 p
(Contract F30601-81-C-0256)
(AD-A203780; BBN-5901-Vol-1; RADC-TR-88-159-Vol-1) Avail: NTIS HC A05/MF A01 CSCL 12G

The primary focus of the personal computer task area is the development of an electronic message system called Diamond, which will run in a distributed personal computer environment. The message system will: Support a user interface that exploits the capabilities of advanced single-user computers, handle message that contain data other than text, have a distributed architecture, operate in a secure fashion, permit use from a variety of user access points and have a transportable implementation. GRA

61 COMPUTER PROGRAMMING AND SOFTWARE

Includes computer programs, routines, alogorithms, and specific applications, e.g., CAD/CAM.

N89-20630# Purdue Univ., West Lafayette, IN. Dept. of Computer Sciences.
PARALLEL ALGORITHMS FOR PDE SOLVERS Final Report, Oct. 1984 - Feb. 1988
John R. Rice 15 Jul. 1988 5 p
(Grant AF-AFOSR-0385-84; AF Proj. 2304)
(AD-A199625; AFOSR-88-1136TR) Avail: NTIS HC A02/MF A01 CSCL 12F

This report lists all of the 39 scientific publications, these, technical reports and conference presentations supported by the grant AFOSR-84-0385. The principal focus of the results are in: (1) The Collocation Method: New versions developed for parallel machines, new results on the convergence and new software were developed, and (2) Mapping Algorithms on to Parallel Machines. Fast heuristic algorithms were found, analyzed and tested, a prototype system for automatically mapping PDE algorithms on to parallel architectures were developed. GRA

N89-20631*# Wake Forest Univ., Winston-Salem, NC.
SYMBOLIC INVERSION OF CONTROL RELATIONSHIPS IN MODEL-BASED EXPERT SYSTEMS Final Report, Jun. - Dec. 1988
Stan Thomas 1988 22 p
(Grant NAG10-0045)
(NASA-CR-182857; NAS 1.26:182857) Avail: NTIS HC A03/MF A01 CSCL 09B

Symbolic inversion is examined from several perspectives. First, a number of symbolic algebra and mathematical tool packages were studied in order to evaluate their capabilities and methods, specifically with respect to symbolic inversion. Second, the KATE system (without hardware interface) was ported to a Zenith Z-248 microcomputer running Golden Common Lisp. The interesting thing about the port is that it allows the user to have measurements vary and components fail in a non-deterministic manner based upon random value from probability distributions. Third, INVERT was studied as currently implemented in KATE, its operation documented, some of its weaknesses identified, and corrections made to it. The corrections and enhancements are primarily in the way that logical conditions involving AND's and OR's and inequalities are processed. In addition, the capability to handle equalities was also added. Suggestions were also made regarding the handling of ranges in INVERT. Last, other approaches to the inversion process were studied and recommendations were made as to how future versions of KATE should perform symbolic inversion. B.G.

N89-20632*# Institute for Computer Applications in Science and Engineering, Hampton, VA.
A HYBRID-PERTURBATION-GALERKIN TECHNIQUE WHICH COMBINES MULTIPLE EXPANSIONS Final Report
James F. Geer and Carl M. Andersen (College of William and Mary, Williamsburg, VA.) Jan. 1989 38 p Submitted for publication
(Contract NAS1-18107)
(NASA-CR-181781; ICASE-89-8; NAS 1.26:181781) Avail: NTIS HC A03/MF A01 CSCL 09B

A two-step hybrid perturbation-Galerkin method for the solution of a variety of differential equations type problems is found to give better results when multiple perturbation expansions are employed. The method assumes that there is parameter in the problem formulation and that a perturbation method can be sued to construct one or more expansions in this perturbation coefficient functions multiplied by computed amplitudes. In step one, regular and/or singular perturbation methods are used to determine the perturbation coefficient functions. The results of step one are in the form of one or more expansions each expressed as a sum of

perturbation coefficient functions multiplied by a priori known gauge functions. In step two the classical Bubnov-Galerkin method uses the perturbation coefficient functions computed in step one to determine a set of amplitudes which replace and improve upon the gauge functions. The hybrid method has the potential of overcoming some of the drawbacks of the perturbation and Galerkin methods as applied separately, while combining some of their better features. The proposed method is applied, with two perturbation expansions in each case, to a variety of model ordinary differential equations problems including: a family of linear two-boundary-value problems, a nonlinear two-point boundary-value problem, a quantum mechanical eigenvalue problem and a nonlinear free oscillation problem. The results obtained from the hybrid methods are compared with approximate solutions obtained by other methods, and the applicability of the hybrid method to broader problem areas is discussed. Author

N89-20633# National Weather Service, Salt Lake City, UT. Forecast Office.
WATCHDOG PROGRAM
William R. Schneider and Craig C. Peterson Oct. 1988 21 p (PB89-122535; NOAA-NWS-WRCP-57) Avail: NTIS HC A03/MF A01 CSCL 09B

The Watchdog program was designed as a highly efficient multi-tasking assembly language background scheduler. It performs four tasks: time schedules, event schedules, monitors the ADMs for RUN commands, and emulates the CLI at the dashes. The methodology and software structure are explained. GRA

N89-20634# Academia Sinica, Beijing (China). The Computing Center.
ADAPTIVE FE ALGORITHM FOR VARIATIONAL INEQUALITY PROBLEMS
Jun-zhi Cui and Bing Xu 1987 9 p Sponsored by Institute of Scientific and Technical Information of China, Beijing (PB89-111512; ISTIC-TR-C-000200) Avail: NTIS HC A02/MF A01 CSCL 09B

The adaptive finite element algorithm for obstacle problems is described along with its main results and numerical examples. Author

N89-20635*# Institute for Computer Applications in Science and Engineering, Hampton, VA.
DOMAIN DECOMPOSITION METHODS FOR SYSTEMS OF CONSERVATION LAWS: SPECTRAL COLLOCATION APPROXIMATIONS Final Report
Alfio Quarteroni (Cattolica Univ., Brescia, Italy) Jan. 1989 37 p Prepared in cooperation with Consiglio Nazionale delle Ricerche, Pavia (Italy). Prepared for NASA, Langley Research Center, Hampton, VA
(Contract NAS1-18605)
(NASA-CR-181773; ICASE-89-5; NAS 1.26:181773) Avail: NTIS HC A03/MF A01 CSCL 09B

Hyperbolic systems of conversation laws are considered which are discretized in space by spectral collocation methods and advanced in time by finite difference schemes. At any time-level a domain deposition method based on an iteration by subdomain procedure was introduced yielding at each step a sequence of independent subproblems (one for each subdomain) that can be solved simultaneously. The method is set for a general nonlinear problem in several space variables. The convergence analysis, however, is carried out only for a linear one-dimensional system with continuous solutions. A precise form of the error reduction factor at each iteration is derived. Although the method is applied here to the case of spectral collocation approximation only, the idea is fairly general and can be used in a different context as well. For instance, its application to space discretization by finite differences is straight forward. Author

N89-20636*# Institute for Computer Applications in Science and Engineering, Hampton, VA.
NUMERICAL STUDIES OF IDENTIFICATION IN NONLINEAR DISTRIBUTED PARAMETER SYSTEMS Final Report
H. T. Banks, C. K. Lo, Simeon Reich, and I. G. Rosen (University of Southern California, Los Angeles.) Jan. 1989 21 p Prepared in cooperation with NASA, Langley Research Center, and Brown Univ., Providence, RI
(Contracts NAS1-18107; NAS1-18605; NAG1-517; F49620-86-C-0111; NSF MCS-85-04316; AF-AFOSR-0356-87)
(NASA-CR-181771; ICASE-89-3; NAS 1.26:181771) Avail: NTIS HC A03/MF A01 CSCL 09B

An abstract approximation framework and convergence theory for the identification of first and second order nonlinear distributed parameter systems developed previously by the authors and reported on in detail elsewhere are summarized and discussed. The theory is based upon results for systems whose dynamics can be described by monotone operators in Hilbert space and an abstract approximation theorem for the resulting nonlinear evolution system. The application of the theory together with numerical evidence demonstrating the feasibility of the general approach are discussed in the context of the identification of a first order quasi-linear parabolic model for one dimensional heat conduction/mass transport and the identification of a nonlinear dissipation mechanism (i.e., damping) in a second order one dimensional wave equation. Computational and implementational considerations, in particular, with regard to supercomputing, are addressed. Author

N89-20637*# Institute for Computer Applications in Science and Engineering, Hampton, VA.
OPTIMAL FEEDBACK CONTROL INFINITE DIMENSIONAL PARABOLIC EVOLUTION SYSTEMS: APPROXIMATION TECHNIQUES Final Report
H. T. Banks and C. Wang Jan. 1989 60 p Prepared in cooperation with NASA, Langley Research Center
(Contracts NAS1-18107; NAS1-18605; NAG1-517; F49620-86-C-0111; NSF MCS-85-04316; AF-AFOSR-0398-84)
(NASA-CR-181772; ICASE-89-4; NAS 1.26:181772) Avail: NTIS HC A04/MF A01 CSCL 09B

A general approximation framework is discussed for computation of optimal feedback controls in linear quadratic regular problems for nonautonomous parabolic distributed parameter systems. This is done in the context of a theoretical framework using general evolution systems in infinite dimensional Hilbert spaces. Conditions are discussed for preservation under approximation of stabilizability and detectability hypotheses on the infinite dimensional system. The special case of periodic systems is also treated. Author

N89-20638*# Institute for Computer Applications in Science and Engineering, Hampton, VA.
RUN-TIME SCHEDULING AND EXECUTION OF LOOPS ON MESSAGE PASSING MACHINES Final Report
Kay Crowley, Joel Saltz, Ravi Mirchandaney, and Harry Berryman (Yale Univ., New Haven, CT.) Jan. 1989 27 p Prepared for NASA, Langley Research Center, Hampton, VA
(Contracts NAS1-18605; N00014-86-K-0310)
(NASA-CR-181785; ICASE-89-7; NAS 1.26:181785) Avail: NTIS HC A03/MF A01 CSCL 09B

Sparse system solvers and general purpose codes for solving partial differential equations are examples of the many types of problems whose irregularity can result in poor performance on distributed memory machines. Often, the data structures used in these problems are very flexible. Crucial details concerning loop dependences are encoded in these structures rather than being explicitly represented in the program. Good methods for parallelizing and partitioning these types of problems require assignment of computations in rather arbitrary ways. Naive implementations of programs on distributed memory machines requiring general loop partitions can be extremely inefficient. Instead, the scheduling mechanism needs to capture the data reference patterns of the loops in order to partition the problem. First, the indices assigned to each processor must be locally numbered. Next, it is necessary to precompute what information is needed by each processor at various points in the computation. The precomputed information is then used to generate an execution template designed to carry out the computation, communication,

and partitioning of data, in an optimized manner. The design is presented for a general preprocessor and schedule executer, the structures of which do not vary, even though the details of the computation and of the type of information are problem dependent. Author

N89-20639# Satellites International Ltd., Newbury (England).
ADAPTIVE DATA COMPRESSION SYSTEM STUDY Final Report
N. S. Bray, C. K. Chan, A. K. Ward, B. E. Patchett, M. A. Birdseye, E. R. Breeveld, A. J. Coates, R. A. Gowen, H. E. Huckle, and A. D. Johnstone (Mullard Space Science Lab., Dorking, England) et al Paris, France ESA Jul. 1988 85 p Prepared in cooperation with Science Research Council, Chilton (England); and Mullard Space Science Lab., Dorking (England)
(Contract ESA-7087/87-NL-PP(SC))
(SIL/CR/7129/6; ESA-CR(P)-2678-Vol-1; ETN-89-93914)
Copyright Avail: NTIS HC A05/MF A01

The effectiveness and the feasibility of implementing data compression algorithms in the spacecraft environment, particularly the CLUSTER and SOHO missions, were assessed. Each CLUSTER and SOHO experiment was examined and its data characteristics were defined for different magnetospheric regions or different degrees of solar activity as appropriate. Suitable instruments from previous missions were identified as possible data sources to be used in a payload simulator. The simulated data were used to evaluate candidate data compression algorithms, in order to identify which algorithm was best suited to which experiment, under which conditions. The selected algorithms were then implemented on breadboard development systems using processors which might be used in an on-board system, in order to assess the feasibility of the data compression techniques when constrained by the spacecraft environment. A system architecture and design specification for the adaptive data compression system is proposed, and could lead to an elegant breadboard or engineering model. ESA

N89-20640*# New Mexico State Univ., Las Cruces. Knowledge Systems Group.
CONSEQUENCES OF NONCLASSICAL MEASUREMENT FOR THE ALGORITHMIC DESCRIPTION OF CONTINUOUS DYNAMICAL SYSTEMS
Chris Fields 1989 14 p
(Grant NAGw-1592)
(NASA-CR-184851; NAS 1.26:184851) Avail: NTIS HC A03/MF A01 CSCL 09B

Continuous dynamical systems intuitively seem capable of more complex behavior than discrete systems. If analyzed in the framework of the traditional theory of computation, a continuous dynamical system with countably many quasistable states has at least the computational power of a universal Turing machine. Such an analysis assumes, however, the classical notion of measurement. If measurement is viewed nonclassically, a continuous dynamical system cannot, even in principle, exhibit behavior that cannot be simulated by a universal Turing machine. Author

N89-20641*# National Aeronautics and Space Administration. Lewis Research Center, Cleveland, OH.
AUTOMATING THE MULTIPROCESSING ENVIRONMENT
Dale J. Arpasi Mar. 1989 10 p
(NASA-TM-4103; E-4426; NAS 1.15:4103) Avail: NTIS HC A02/MF A01 CSCL 09B

An approach to automate the programming and operation of tree-structured networks of multiprocessor systems is discussed. A conceptual, knowledge-based operating environment is presented, and requirements for two major technology elements are identified as follows: (1) An intelligent information translator is proposed for implementating information transfer between dissimilar hardware and software, thereby enabling independent and modular development of future systems and promoting a language-independence of codes and information; (2) A resident system activity manager, which recognizes the systems capabilities and monitors the status of all systems within the environment, is proposed for integrating dissimilar systems into effective parallel processing resources to optimally meet user needs. Finally, key computational capabilities which must be provided before the environment can be realized are identified. Author

N89-20642*# Jet Propulsion Lab., California Inst. of Tech., Pasadena.
HYPERCUBE MATRIX COMPUTATION TASK Report, 1986-1988
Ruel H. Calalo, William A. Imbriale, Nathan Jacobi, Paulett C. Liewer, Thomas G. Lockhart, Gregory A. Lyzenga, James R. Lyons, Farzin Manshadi, and Jean E. Patterson 1 Aug. 1988 189 p
(Contract NAS7-918)
(NASA-CR-184869; JPL-Publ-88-31; NAS 1.26:184869) Avail: NTIS HC A09/MF A01 CSCL 09B

A major objective of the Hypercube Matrix Computation effort at the Jet Propulsion Laboratory (JPL) is to investigate the applicability of a parallel computing architecture to the solution of large-scale electromagnetic scattering problems. Three scattering analysis codes are being implemented and assessed on a JPL/California Institute of Technology (Caltech) Mark 3 Hypercube. The codes, which utilize different underlying algorithms, give a means of evaluating the general applicability of this parallel architecture. The three analysis codes being implemented are a frequency domain method of moments code, a time domain finite difference code, and a frequency domain finite elements code. These analysis capabilities are being integrated into an electromagnetics interactive analysis workstation which can serve as a design tool for the construction of antennas and other radiating or scattering structures. The first two years of work on the Hypercube Matrix Computation effort is summarized. It includes both new developments and results as well as work previously reported in the Hypercube Matrix Computation Task: Final Report for 1986 to 1987 (JPL Publication 87-18). Author

N89-20643*# Jet Propulsion Lab., California Inst. of Tech., Pasadena.
A COMMUNICATION CHANNEL MODEL OF THE SOFTWARE PROCESS
R. C. Tausworthe 15 Oct. 1988 25 p
(Contract NAS7-918)
(NASA-CR-184866; JPL-Publ-88-25; NAS 1.26:184866) Avail: NTIS HC A03/MF A01 CSCL 09B

Reported here is beginning research into a noisy communication channel analogy of software development process productivity, in order to establish quantifiable behavior and theoretical bounds. The analogy leads to a fundamental mathematical relationship between human productivity and the amount of information supplied by the developers, the capacity of the human channel for processing and transmitting information, the software product yield (object size), the work effort, requirements efficiency, tool and process efficiency, and programming environment advantage. Also derived is an upper bound to productivity that shows that software reuse is the only means than can lead to unbounded productivity growth; practical considerations of size and cost of reusable components may reduce this to a finite bound. Author

N89-20644*# Jet Propulsion Lab., California Inst. of Tech., Pasadena.
INCREMENTAL DEVELOPMENT AND PROTOTYPING IN CURRENT LABORATORY SOFTWARE DEVELOPMENT PROJECTS: PRELIMINARY ANALYSIS
Martha Ann Griesel 15 Dec. 1988 41 p
(Contract NAS7-918)
(NASA-CR-184860; JPL-Publ-88-41; NAS 1.26:184860) Avail: NTIS HC A03/MF A01 CSCL 09B

Several Laboratory software development projects that followed nonstandard development processes, which were hybrids of incremental development and prototyping, are being studied. Factors in the project environment leading to the decision to use a nonstandard development process and affecting its success are analyzed. A simple characterization of project environment based

on this analysis is proposed, together with software development approaches which have been found effective for each category. These approaches include both documentation and review requirements. Author

N89-20645# Department of Energy, Washington, DC. Office of High Energy and Nuclear Physics.
FASTBUS STANDARD ROUTINES
May 1988 155 p
(DOE/ER-0367) Avail: NTIS HC A08/MF A01

Standard routines for use with the FASTBUS standard modular high speed data acquisition and control system of ANSI/IEEE Std 960-1986 and IEC Publication 935 are defined. Some basic concepts that are common to all routines are described, as well as routines involved in the management and use of the FASTBUS environment, descriptions of the operational parameters which form part of the FASTBUS environment, and descriptions of the buffer modes which are used to control access to user data buffers by action routines. Also described are routines for carrying out simple and compound transactions on FASTBUS and primitive FASTBUS actions, routines for handling asynchronous events on FASTBUS - responding to service requests and to interrupt messages, routines that are either system or port dependent, and the response of the implementation to errors. Routines are described for controlling this and for extracting status information about previous action. The final section contains a list of all the error codes along with their severity. Author

N89-20646*# Illinois Univ., Urbana-Champaign. Dept. of Computer Science.
A CLASS HIERARCHICAL, OBJECT-ORIENTED APPROACH TO VIRTUAL MEMORY MANAGEMENT
Vincent F. Russo, Roy H. Campbell, and Gary M. Johnston 1989 21 p Sponsored in part by AT and T METRONET, and NSF CISE
(Grants NsG-1471; NAG1-163)
(NASA-CR-184876; NAS 1.26:184876) Avail: NTIS HC A03/MF A01 CSCL 09B

The Choices family of operating systems exploits class hierarchies and object-oriented programming to facilitate the construction of customized operating systems for shared memory and networked multiprocessors. The software is being used in the Tapestry laboratory to study the performance of algorithms, mechanisms, and policies for parallel systems. Described here are the architectural design and class hierarchy of the Choices virtual memory management system. The software and hardware mechanisms and policies of a virtual memory system implement a memory hierarchy that exploits the trade-off between response times and storage capacities. In Choices, the notion of a memory hierarchy is captured by abstract classes. Concrete subclasses of those abstractions implement a virtual address space, segmentation, paging, physical memory management, secondary storage, and remote (that is, networked) storage. Captured in the notion of a memory hierarchy are classes that represent memory objects. These classes provide a storage mechanism that contains encapsulated data and have methods to read or write the memory object. Each of these classes provides specializations to represent the memory hierarchy. Author

N89-20647# Lawrence Livermore National Lab., CA. Methods Development Group.
USER'S MANUAL FOR DYNA2D: AN EXPLICIT TWO-DIMENSIONAL HYDRODYNAMIC FINITE ELEMENT CODE WITH INTERACTIVE REZONING AND GRAPHICAL DISPLAY
John O. Hallquist Mar. 1988 147 p
(Contract W-7405-eng-48)
(DE89-006695; UCID-18756-Rev-3) Avail: NTIS HC A07/MF A01

This revised report provides an updated user's manual for DYNA2D, a vectorized, explicit, two-dimensional, axisymmetric and plane strain finite element code for analyzing the large deformation dynamics and hydrodynamic response of inelastic solids. A contact-impact algorithm permits gaps and sliding with friction along material interfaces. By a specialization of this algorithm, such interfaces can be rigidly tied to admit variable zoning without the need of transition regions. Spatial discretization is achieved by the use of 4-node solid element, and the equations-of-motion are integrated by the central difference method. An interactive rezoner eliminated the need to terminate the calculation when the mesh becomes too distorted. Rather, the mesh can be rezoned and the calculation continued. The command structure for the rezoner is described and illustrated by an example. DOE

N89-20648# Stockholm Univ. (Sweden). Inst. of Physics.
A PASCAL CROSS-ASSEMBLER FOR THE 6809 MICROPROCESSOR
G. Erlandsson Apr. 1988 34 p
(USIP-88-05; ETN-89-93733) Avail: NTIS HC A03/MF A01

A cross assembler for the Motorola 6809 microprocessor is given. Concepts illustrated include the identification, listing, and translation of mnemonics and identifiers, the use of hash tables, and the formal construction of a deterministic finite automation. The finished program, although not complete in all details is in extensive practical use, and is found more convenient for interactive work than a commercial assembler for the same processor. ESA

N89-20649# Helsinki Univ. of Technology, Espoo (Finland). Systems Analysis Lab.
BASIS REPRESENTATIONS IN LARGE-SCALE LINEAR PROGRAMMING SOFTWARE Ph.D. Thesis
Leena Aittoniemi 1988 63 p Sponsored by the Academy of Finland, the Finnish Cultural Foundation, Finland, the Wihuri Foundation, Finland and the Ahlstrom Foundation, Finland
(Ma-50; ISBN-951-666-268-4; ISSN-0355-2713; ETN-89-93752)
Avail: NTIS HC A04/MF A01

Kernels of simplex-based linear programming software: computation of an LU-factorization for a given basis matrix and its update in subsequent LP-iterations are discussed. Besides mathematical aspects, the proper implementation of the algorithms is emphasized. On each simplex iteration the basis representation is updated either in product form or as an LU-factorization. Two sets of linear equations are solved on each iteration; these operations are called forward and backward transformations. Total computing time spent in the update and forward and backward transformations is compared in different approaches. A sparse LU-factorization is discussed, and an implementation of an efficient LU-update is presented. Data structures which reduce the time complexity of the factorization and updates as well as forward and backward transformations are developed. Numerical experiments with large real-life test problems demonstrate the superiority of the techniques. ESA

N89-20650# Technische Univ., Delft (Netherlands). Faculty of Technical Mathematics and Informatics.
INCREMENTAL DISPLAY OF CONSTRUCTIVE SOLID GEOMETRY (CSG) MODELS USING LOCAL UPDATING
Willem F. Bronsvoort and Harry Garnaat 1988 26 p
(Rept-88-51; ISSN-0920-8577; ETN-89-94018) Copyright Avail: NTIS HC A03/MF A01

A local updating strategy for making incremental changes to a geometric model and its displayed image is described. Only those parts of a model that are affected by modifications are computed and redisplayed, which considerably increases efficiency compared to updating the complete model and its display. Methods for local updating in a solid modeling system with a constructive solid geometry (CSG) scan-line visible-surface algorithm that can display shaded images directly from a CSG tree using polyhedral primitives are presented. Precise determination of the screen areas that must be updated is performed in three stages: rectangular areas, edges, and parts of scan-lines of interest are successively determined. ESA

N89-20651# Technische Univ., Delft (Netherlands). Faculty of Technical Mathematics and Informatics.
DIRECTIONS IN REUSING SOFTWARE
Frans Ververs, Jan vanKatwijk, and Liesbeth Dusink 1988 30 p
(Rept-88-58; ISSN-0920-8577; ETN-89-94025) Copyright Avail: NTIS HC A03/MF A01

Reusability of software and the use of software components are discussed. Two main strategies are identified, reuse based on transformational approaches and reuse based on the direct application of software components. Projects dealing with support of software reuse are reviewed. ESA

N89-20652# National Aerospace Lab., Amsterdam (Netherlands).
TOOLS FOR THE DEVELOPMENT OF INFORMATION SYSTEMS AT NLR
J. J. Schuurman 7 Dec. 1987 25 p In DUTCH; ENGLISH summary Presented at the SURF Symposium, Delft, The Netherlands, 7 Dec. 1986
(NLR-MP-87079-U; ETN-89-94048) Avail: NTIS HC A03/MF A01

A software infrastructure which serves as a test bed for the development of new information systems and reflects the infrastructure for information processing needed in industry was developed in such a way that the components of the infrastructure can be used for the development of difficult information systems. On the one hand this ensures a uniform approach to the development of information system; on the other hand a uniform interaction of the information system to the outside world is preserved. For practical reasons the elements of the software infrastructure are available as standard tools. The components of the software infrastructure available in the NLR computer network are described. This software infrastructure results in a higher efficiency in research and in support of engineering activities. ESA

N89-20653# National Aerospace Lab., Amsterdam (Netherlands).
NEXT 2.0, AN EXPERT SYSTEM SHELL FOR ENGINEERING APPLICATIONS
P. J. Kat and J. C. Donker 2 Feb. 1988 24 p In DUTCH; ENGLISH summary Presented at the Netherlands AI Conference 1988, Amsterdam, The Netherlands, 12-13 Apr. 1988; sponsored by the Vereniging voor Kunstmatige Intelligentia
(NLR-MP-88015-U; ETN-89-94060) Avail: NTIS HC A03/MF A01

The NEXT 2.0 expert system shell was developed. The NEXT has a hybrid knowledge representation based on frames, rules, and tasks and several inference methods and information sources. The inference and control is coordinated by an agenda-mechanism. The NEXT 2.0 is available on a CYBER under NOS/VE and on a VAX under VMS. Supply of other implementations can be negotiated. ESA

N89-20654 National Physical Lab., Teddington (England). Div. of Information Technology and Computing.
EVALUATION OF THE RTP PASCAL-MALPAS IL TRANSLATOR
G. ONeill Sep. 1988 23 p
(NPL-DITC-128/88; ISSN-0262-5369; ETN-89-94088) Copyright Avail: National Physical Laboratory, Teddington, Middlesex, TW11 OLW, England

Automatic translation of source codes to an intermediate language (IL) for assessment by the Malvern Program Analysis Suite (MALPAS) was tested using Pascal as input language. The evaluation shows that the documentation is clear, informative and well presented. The subset of Pascal covered by the Translator is basically level 0 with minor restrictions and extensions. The Translator does not generate any IL code corresponding to the required Pascal constant maxint. Replacement of maxint by the appropriate literal constant can cause the semantic analyzer to crash. Running the MALPAS package is made simple by the use of command qualifiers which select the type of analysis to be performed. The source text and IL text listings, and particularly the output of the various analyzers, are all clearly laid out. The control flow, data use, and information flow analyzers were used on a variety of translated Pascal programs and produce informative results which are, in many cases, easily related to the Pascal source texts. The semantic analyzer, although of obvious use with assembler source programs, seems to be less useful with some programs written in Pascal. However the experience of other MALPAS users shows that these particular programs are not typical in this respect of most safety-critical software written in Pascal. ESA

N89-20655# Groningen Rijksuniversiteit (Netherlands). Dept. of Mathematics and Computing Sciences.
REDUCING THE PROOF BURDEN WHEN REASONING WITH CONGRUENCE TYPES
Paul Chisholm 1988 22 p
(CS-8807; ETN-89-94156) Avail: NTIS HC A03/MF A01

The addition of the subset type to Martin-Lof's (1979) type theory is considered. This does not effectively increase the power of the theory. Nor can it be used to reduce the proof obligations when proving propositions. The use of the subset type in conjunction with congruence types is investigated. It is shown that the subset type can be used to significantly reduce the burden of proof when justifying properties of congruence types which have no computational significance. As an example, the cardinality operation over a type of finite sets is considered. Two different proofs of its specification are given. In the first, the subset type is not used. In the second (and much simpler) proof, the subset type is used. ESA

N89-20656# Groningen Rijksuniversiteit (Netherlands). Dept. of Mathematics and Computing Sciences.
AN ALGEBRAIC CALCULUS OF COMMANDS
Wim H. Hesselink 1988 25 p
(CS-8808; ETN-89-94157) Avail: NTIS HC A03/MF A01

For the purpose of program transformation, an algebraic calculus of commands that is based on Dijkstra's predicate transformers is developed. The program constructors guards and assertions, composition and choice are treated. As an example, a purely algebraic proof that a certain recursive procedure is equivalent to skip is given. ESA

N89-20657# Groningen Rijksuniversiteit (Netherlands). Dept. of Mathematics and Computing Science.
QUADRATIC BLENDING SURFACES FOR COMPLEX CORNERS, PART 2
Menno Kosters 1988 18 p
(CS-8809-Pt-2; ETN-89-94158) Avail: NTIS HC A03/MF A01

The problem of finding quadratic blending surfaces is solved for a very general class of corners. The method relies on simple properties of quadratic hypersurfaces and can be easily automated. The resulting blendings are easily computed, have simple descriptions and are well suited for subsequent computations which may need to be done, for instance for rendering purposes. The method is applied to an example considered earlier, yielding a previously unknown blending. ESA

N89-20658# Groningen Rijksuniversiteit (Netherlands). Dept. of Mathematics and Computing Science.
AN EXPLORATION OF THE BIRD-MEERTENS FORMALISM
Roland Backhouse 1988 66 p
(CS-8810; ETN-89-94159) Avail: NTIS HC A04/MF A01

Two formalisms for the calculation of programs: the Eindhoven quantifier notation and the formalism developed by Bird and Meertens are considered. Although the former is applied to derive imperative programs and the latter to derive functional programs, there is a remarkable similarity in the formal games that are played. The Bird-Meertens formalism is analyzed by expressing and deriving within it the basic rules applicable in the Eindhoven quantifier notation. It is shown that the basic properties of quantification over finite domains can all be expressed and proved within the

Bird-Meertens formalism. However, to conclude that the expressiveness of the formalisms is equivalent is wrong. The Bird-Meertens formalism is apparently more economical than the quantifier notation and permits a much greater separation of concerns in the statement and proof of the basic properties. However, the statement of the cartesian product and generalized range disjunction rules in the Bird-Meertens formalism are disappointing. ESA

N89-20659# Groningen Rijksuniversiteit (Netherlands). Dept. of Mathematics and Computing Science.
DO-IT-YOURSELF TYPE THEORY
Erik Saaman, Roland Backhouse, Paul Chisholm, and Grant Malcolm 1988 83 p Sponsored in part by the United Kindgom Science and Engineering Research Council
(CS-8811; ETN-89-94160) Avail: NTIS HC A05/MF A01

The notion of propositions as types, fundamental to Martin-Lof's theory of types, is discussed. The elegant structure of the rules which characterizes Martin-Lof's theory is discussed. It is shown how the elimination and computation rules for a given type constructor are derived from its formation and introduction rules, for free type structures, for congruence types, and for types with information loss. The mechanisms for deriving basic properties of type constructors - (closure, individuality, and cancellation properties) are also considered. The way that algorithm development is conducted in a constructive framework is treated, particularly the relationship between the formulation of inductive hypotheses and the construction of invariant properties. Two ways of defining and reasoning about binary numerals are compared. Constructive reasoning on mutually recursive type structures is mentioned. ESA

N89-20660# Center for Mathematics and Computer Science, Amsterdam (Netherlands). Dept. of Interactive Systems.
A VECTOR-LIKE ARCHITECTURE FOR RASTER GRAPHICS
Varol Akman, Paul J. W. tenHagen, and Fons A. A. M. Kuijk Jan. 1988 21 p Presented at the 2nd Eurographics Workshop on Graphics Hardware, Amsterdam, Netherlands, 24-25 Aug. 1987 Submitted for publication
(CWI-CS-R8802; B8821057; ETN-89-94167) Avail: NTIS HC A03/MF A01

A computer graphics object description scheme called pattern representation is outlined. In this scheme, only one type of primitive, a pattern consisting of a domain function and a color function, is permitted. Patterns have an associated set of operations. This is reminiscent of abstract data types (or more properly, the ideas of object-orientation) and provides conceptual simplicity in several interactive graphic tasks. In the image generation model an application as defined by the user contains possibly nongraphical data. It is in continuous coordinates and there is no limit to the variety of primitives that can be present (the high level). At the medium level, only patterns are allowed. In a sense, patterns are preprocessed representations for filled areas and resemble scanline representations. At the medium level patterns still overlap. At the low level are the resulting visible regions. Up to this point everything can still be kept in the object space. The display controller maps them to the image space. ESA

N89-20661# Center for Mathematics and Computer Science, Amsterdam (Netherlands). Dept. of Software Technology.
METRIC SEMANTICS FOR CONCURRENCY
J. W. deBakker (Vrije Univ., Amsterdam, Netherlands) and J.-J. Ch. Meyer Jan. 1988 29 p
(CWI-CS-R8803; B8821058; ETN-89-94168) Copyright Avail: NTIS HC A03/MF A01

The semantics of concurrency and semantic models built on metric structures are reviewed. Uniform or schematic versus nonuniform or interpreted languages; operational versus denotational semantics; and linear time versus branching time models are discussed. The operational models are based on Plotkin's transition systems. Language constructs which receive particular attention are recursion and merge, synchronization and global nondeterminacy, process creation, and communication with value passing. Semantic equivalence results are established. In the definitions and in the derivation of these equivalences, Banach's theorem for contracting functions is used. ESA

N89-20662# Center for Mathematics and Computer Science, Amsterdam (Netherlands). Dept. of Software Technology.
SOME OBSERVATIONS ON REDUNDANCY IN A CONTEXT
F. W. Vaandrager Mar. 1988 23 p Sponsored in part by the Commission of the European Communities
(ESPRIT Proj. 432)
(CWI-CS-R8812; B8821070; ETN-89-94172) Copyright Avail: NTIS HC A03/MF A01

Let x be a process which can perform an action a when it is in state s: the situation where x is placed in a context which blocks a whenever x is in s is considered. The option of doing a in state s is redundant in such a context and x can be replaced by a process x' which is identical to x, except for the fact that x' cannot do a when it is in s (irrespective of the context). A simple, compositional proof technique, which uses information about the traces of processes to detect redundancies in a process specification is presented. As an illustration of the technique, a modular verification of a simple workcell architecture is presented. ESA

N89-20663# Center for Mathematics and Computer Science, Amsterdam (Netherlands). Dept. of Interactive Systems.
AN EXACT INCREMENTAL HIDDEN SURFACE REMOVAL ALGORITHM
A. A. M. Kuijk, Paul J. W. tenHagen, and Varol Akman May 1988 20 p
(CWI-CS-R8818; B8827442; ETN-89-94175) Copyright Avail: NTIS HC A03/MF A01

An incremental hidden surface removal algorithm (HSRA) was developed to be embedded in an architecture for raster graphics. The algorithm can be classified as exact since it operates in object space, rather than image space. It can be classified as incremental because this HSRA is able to support addition, removal, and changes on a single object or a group of objects. Thus a firm basis for powerful interaction and animation is established. Due to specially designed data structures for both geometric objects as well as storage of these objects, the hidden surface removal calculation on a complete scene has the same time complexity as existing algorithms. However, the effort needed for incremental changes is much less than any known algorithm. The data structures and the algorithm are designed to exploit parallelism in computation. ESA

N89-20664# Center for Mathematics and Computer Science, Amsterdam (Netherlands). Dept. of Numerical Mathematics.
FACTORING WITH THE QUADRATIC SIEVE ON LARGE VECTOR COMPUTERS
Herman J. J. teRiele, Walter M. Lioen, and Dirk T. Winter Jun. 1988 14 p Submitted for publication Sponsored in part by Dutch Working Group on the Use of Supercomputers, Netherlands
(CWI-NM-R8805; B8827436; ETN-89-94182) Copyright Avail: NTIS HC A03/MF A01

The multiple polynomial version of the quadratic sieve factorization method was run on a Cyber 205 and on a NEC SX-2 vector computer. Various numbers in the 50 to 92 decimal digits range were factorized, as a contribution to the Cunningham project, Brent's Table of factors of Mersenne numbers, and a proof by Brent and Cohen of the nonexistence of odd perfect numbers below 10 to the 200th power. The NEC program is 5 to 10 times faster than the Cyber one, and 5 to 10 times faster than the Davis and Holdridge Cray X/MP program. ESA

N89-20665# Los Alamos National Lab., NM. Cognitive Systems Engineering Group.
A SOFTWARE MODEL FOR SIMULATION IN COMPUTER-BASED TRAINING
Lois M. Spangenberg, Linda M. Nonno, and John A. DeVries, II 1988 10 p Presented at the Conference on Technology in

Training and Education, Atlanta, GA, 1 Mar. 1989
(Contract W-7405-eng-36)
(DE89-003469; LA-UR-88-3669; CONF-890344-1) Avail: NTIS HC A02/MF A01

This paper explores the requirements for Simulation-Based Training (SBT) and describes the Los Alamos model for an SBT authoring system. Although the use of simulation as an instructional strategy provides realistic training opportunities at high cognitive levels (e.g., evaluation, synthesis, analysis), it is at the expense of complexity beyond the capabilities of available authoring systems to create. Cognitive Systems Engineering (CSE) at Los Alamos is exploring a middle ground between conventional CBT and complex simulations. The CSE model proposes the separation of simulation and courseware as the key to successful SBT development. DOE

N89-20666# Oak Ridge National Lab., TN. Mathematical Sciences Section.
PARALLEL DIRECT SOLUTION OF SPARSE LINEAR SYSTEMS
Esmond Ng 1988 17 p Presented at the Workshop on Parallel and Vector Computing, Austin, TX, 17 Oct. 1988
(Contract DE-AC05-84OR-21400)
(DE89-006030; CONF-8810297-1) Avail: NTIS HC A03/MF A01

In this paper the direct solution of sparse linear systems on multiprocessor systems is considered. Elimination trees are used as a tool for identifying and exploiting parallelism in the parallel numerical factorization of the coefficient matrix. Some open problems are described and results of some numerical experiments are provided. DOE

N89-20667# Stanford Univ., CA. Systems Optimization Lab.
INERTIA-CONTROLLING METHODS FOR QUADRATIC PROGRAMMING
Philip E. Gill, Walter Murray, Micheal A. Saunders, and Margaret H. Wright (Bell Telephone Labs., Inc., Murray Hill, NJ.) Nov. 1988 40 p
(Contract DE-FG03-87ER-25030)
(DE89-006996; SU-SOL-88-3) Avail: NTIS HC A03/MF A01

Active-set quadratic programming (QP) methods use a working set to define the search direction and multiplier estimates. In the method proposed by Fletcher in 1971, and in several subsequent mathematically equivalent methods, the working set is chosen to control the inertia of the reduced Hessian, which is never permitted to have more than one nonpositive eigenvalue. (We call such methods inertia-controlling). This paper presents an overview of a generic inertia-controlling QP method, including the equations satisfied by the search direction when the reduced Hessian is positive definite, singular and indefinite. Recurrence relations are derived that define the search direction and Lagrange multiplier vector through equations related to the Karush-Kuhn-Tucker system. We also discuss connections with inertia-controlling methods that maintain an explicit factorization of the reduced Hessian matrix. DOE

N89-20668# Sandia National Labs., Albuquerque, NM. Exploratory Systems Development Div.
COMBINING SEGMENTATION AND TRACKING FOR THE CLASSIFICATION OF MOVING OBJECTS IN VIDEO SCENES
Gregory W. Donohoe 1988 9 p Presented at the 22nd Asilomar Conference on Signals, Systems and Computers, Pacific Grove, CA, 30 Oct. 1988
(Contract DE-AC04-76DP-00789)
(DE89-007000; SAND-88-2140C; CONF-8810202-6) Avail: NTIS HC A02/MF A01

This paper describes a method of detecting, tracking and identifying moving objects in video scenes. The method is based on an adaptive change detector which detects and tracks moving objects and extracts silhouettes of the objects from the background so they can be classified by shape. The adaptive change detector uses estimates of image noise and contrast to dynamically adjust decision thresholds. A principal feature of this method is the synergistic interaction between the tracker, the segmenter and the classifier to eliminate uninteresting objects, to improve estimates of the background and noise, to guide threshold selection, and to influence feature selection classification. DOE

N89-20669# Stanford Univ., CA. Systems Optimization Lab.
A PARALLEL DECOMPOSITION ALGORITHM FOR STAIRCASE LINEAR PROGRAMS
Robert Entriken Dec. 1988 22 p
(Contracts DE-FG03-87ER-25028; DE-AC05-84OR-21400)
(DE89-007023; SU-SOL-88-21) Avail: NTIS HC A03/MF A01

As part of an extended research project on the parallel decomposition of linear programs, a parallel algorithm for Staircase Linear Programs was designed and implemented. This class of problems encompasses a large range of planning problems and when decomposed has simple subproblem formulations and communication patterns. This makes its solution a manageable step toward our eventual goal of producing a general code that automatically exploits problem structures of various forms. The results presented here were derived from an implementation for a Sequent Balance 8000 shared-memory multiprocessor. The algorithm itself is message-based but can run on either shared- or distributed-memory parallel computers. A simple diet planning problem is used to demonstrate the principles of the algorithm's development and performance. When applied to this problem, the parallel decomposition algorithm shows promise relative to present serial optimization codes. The nonlinear optimization code MINOS 5.1 is used both as a basis for comparison and as a generic subproblem solver. The greatest room for speedup is in exploiting problem structures. The results show that decomposition can improve efficiency even with a single processor. Examples are given where multiple processors lead to still greater efficiency. DOE

N89-20670# Sandia National Labs., Albuquerque, NM.
AUGER ELECTRON AND X-RAY PHOTOELECTRON DATA PROCESSING FOR THE PERSONAL COMPUTER
Paul W. Mott Jan. 1989 12 p
(Contract DE-AC04-76DP-00789)
(DE89-007292; SAND-88-3122) Avail: NTIS HC A03/MF A01

A low cost Auger electron spectroscopy (AES)/X-ray photoelectron spectroscopy (XPS) data processing system for IBM compatible personal computers is described. The system has been designed to interface with most computer controlled electron spectrometers. The data system is based on a large software package named PC ACSES (Personal Computer Analysis Code for Scanning Electron Spectrometers). This software utilizes a mouse driven interface and provides the user with a wide range of easily accessible data processing options. Features of the system include data manipulation, manual and automatic quantification, flexible annotation and high quality plotter output. In addition, the system can incorporate a 512 x 512 image framestore and powerful digital image processing routines. The image processing capabilities of PC-ACSES allow the user to optimize both secondary electron (SEM) and elemental images, add color to images with histogram painting, create customized pseudo-color image overlays, and annotate images with variable size fonts and micron markers. This PC (personal computer) based data processing system provides a low cost alternative to high-end commercial systems by combining inexpensive computer hardware with advanced software. DOE

N89-20671# Sandia National Labs., Albuquerque, NM. Applied Mechanics Div.
AN ALGORITHM FOR AUTOMATED QUADRILATERAL MESH GENERATION FOR PLANAR REGIONS
J. R. Koteras, C. B. Selleck, and R. E. Jones Jan. 1989 25 p
(Contract DE-AC04-76DP-00789)
(DE89-007299; SAND-86-2059) Avail: NTIS HC A03/MF A01

This paper describes an algorithm which will automatically generate an all quadrilateral mesh for planar regions with material interfaces. The algorithm uses an interior quadtree approximation of the region to be meshed as the basis for the mesh generation. Once the interior quadtree is generated, a layer of elements is

generated between the interior quadtree boundary and the boundary of the planar region. Smoothing techniques are then used to produce well shaped elements throughout the object. This procedure has been implemented in a code and examples of meshes produced with this approach are shown. The algorithm described here provides a basis for an automated mesh generator which will produce all hexahedral meshes for three-dimensional solids. DOE

N89-20672# International Centre for Theoretical Physics, Trieste (Italy).
MULTIFRACTALS
R. E. Amritkar and N. Gupte Sep. 1988 185 p Submitted for publication
(DE88-705369; IC-88/307) Avail: NTIS (US Sales Only) HC A09/MF A01

We review the framework set up for the multifractal analysis of self-similar sets. This framework provides a way of extracting the singular structure of the sets analysed and has proven to be useful in a wide variety of physical contexts. We discuss some of the diverse applications of the framework. The framework has also provided the basis for significant advances in the analysis of dynamical systems. We review various developments based on the multifractal framework. These include the thermodynamic formalism, the inverse problem and the framework required for partially self-similar sets. We discuss the consequences of these developments for the analysis of attractors of systems on the border-line of chaos and give an outline of the developing field of the analysis of chaotic attractors. A brief account of other developments like the effect of fluctuations and the renormalization group analysis of multifractals is also provided. DOE

N89-20673# Lawrence Livermore National Lab., CA.
THE USE OF GKS (GRAPHICAL KERNEL SYSTEM) AND CGM (COMPUTER GRAPHICS METAFILE) FOR THE DISPLAY OF GRAPHICS PRODUCTS
Hoyt Walker, Robert P. Freis, Dean N. Williams, and Carolyn D. Wimple Jan. 1989 22 p Presented at the 8th Biennial CUBE Symposium, Albuquerque, NM, 16 Nov. 1988
(Contract W-7405-eng-48)
(DE89-006734; UCRL-99285; CONF-8811110-2) Avail: NTIS HC A03/MF A01

Graphics standards have an important role to play in the development of production graphics systems. The easier porting and reduced maintenance of software that utilizes standards provides a strong incentive for developers to embrace these standards. However, no single standard is likely to meet all the requirements of a complex system. For example, the Graphical Kernal System (GKS) provides a robust standard addressing the creation of two-dimensional vector graphic products, but the GKS standard does not include a sanctioned metafile format. For installation-independent archival and transfer of pictures, the Computer Graphics Metafile (CGM) standard has been developed. While many vendors of GKS packages provide device drivers for the CGM formats, the GKS and the CGM standards do not precisely correspond which leads to some problems when utilizing these two standards together. A mechanism for resolving these difficulties has been developed for use as part of an operational emergency response system residing at Lawrence Livermore National Laboratory. This mechanism requires the insertion of user-defined information into CGM files, and access to a complete set of primitive attribute information maintained in tables that are external to the graphics programs. DOE

N89-20674# Oak Ridge National Lab., TN. Mathematical Sciences Div.
A PARALLEL DECOMPOSITION ALGORITHM FOR STAIRCASE LINEAR PROGRAMS
Robert Entriken (Stanford Univ., CA.) Dec. 1988 28 p
(Contract DE-AC05-84OR-21400)
(DE89-007883; ORNL/TM-11011) Avail: NTIS HC A03/MF A01

As part of an extended research project on the parallel decomposition of linear programs, a parallel algorithm for Staircase Linear Programs was designed and implemented. This class of problems encompasses a large range of planning problems and when decomposed has simple subproblem formulations and communication patterns. This makes its solution a manageable step toward our eventual goal of producing a general code that automatically exploits problem structures of various forms. The results presented here were derived from an implementation for a Sequent Balance 8000 shared-memory multiprocessor. The algorithm itself is message-based but can run on either shared- or distributed-memory parallel computers. A simple diet planning problem is used to demonstrate the principles of the algorithm's development and performance. When applied to this problem, the parallel decomposition algorithm shows promise relative to present serial optimization codes. The nonlinear optimization code MINOS 5.1 is used both as a basis for comparison and as a generic subproblem solver. The greatest room for speedup is in exploiting problem structures. The results show that decomposition can improve efficiency even with a single processor. Examples are given where multiple processors lead to still greater efficiency. DOE

N89-20675# Institute for Defense Analyses, Alexandria, VA.
DEVELOPMENT OF THE UNIVERSITY OF MARYLAND RAMCAD (RELIABILITY AND MAINTAINABILITY COMPUTER-AIDED DESIGN) FOR ELECTRONIC SYSTEMS Final Report, Sep. 1985 - Aug. 1987
Karen J. Richter Oct. 1988 312 p
(Contract MDA903-84-C-0031)
(AD-A203616; AD-E501060; IDA-M-425; IDA/HQ-88-33027)
Avail: NTIS HC A14/MF A01 CSCL 12E

This report covers the system architecture, the human-machine interface, and the engineering analyses routines of the University of Maryland RAMCAD system through Version 3, completed in the summer of 1987. For each of these areas, the background development, including lessons learned in that development, is detailed, the capabilities of Version 3 are outlined, and the future needs, including targeted research tasks, ongoing development and long term goals, are given. Appendices include the major research papers published by the University of Maryland RAMCAD group. GRA

N89-20676# Washington Univ., Seattle. Dept. of Computer Science.
VALIANT'S MAXIMUM ALGORITHM WITH SEQUENTIAL MEMORY ACCESSES
Robert Cypher Apr. 1988 5 p
(Contract N00014-86-K-0264; AF-AFOSR-0023-88)
(AD-A203713; TR-88-03-08) Avail: NTIS HC A02/MF A01 CSCL 12A

This paper examines the performance of Valiant's PRAM algorithm for finding the maximum of a set of numbers, assuming that a modified PRAM model is used. The modified PRAM is like a standard CRCW PRAM, except that multiple read or write requests to a single memory location are handled sequentially. It is shown that using this model, Valiant's algorithm requires O(sqrt(N)) time to find the maximum of N numbers using N processors, and that it does require time proportional to sqrt(N) infinitely often. GRA

N89-20677# Unisys Corp., Paoli, PA.
INTEGRATING SYNTAX, SEMANTICS, AND DISCOURSE DARPA (DEFENSE ADVANCED RESEARCH PROJECTS AGENCY) NATURAL LANGUAGE UNDERSTANDING PROGRAM Status Report, 1 Aug. - 31 Oct. 1988
Lynette Hirschman 21 Nov. 1988 3 p
(Contract N00014-85-C-0012; ARPA Order 5262)
(AD-A203747) Avail: NTIS HC A02/MF A01 CSCL 05B

A merged lexicon for all domains has been created. The merged lexicon contains about 2400 distinct root words. A tool for extracting lexical items from a dictionary, given a word list, was used to obtain items from the merged lexicon for the resource management domain. Approximately 47 percent of the vocabulary (or 448 words)

in this domain is new. However a large number of these words are proper names of ships and locations, which are relatively trivial to enter. There are about 225 other words, including about 50 verbs. Because there are so few verbs, we expect adding the lexical entries to take only a few days. GRA

N89-20678# Naval Research Lab., Washington, DC. Lab. for Computational Physics and Fluid Dynamics.
FORTRAN CODES FOR COMPUTING THE SPACE-TIME CORRELATIONS OF TURBULENT FLOW IN A CHANNEL Interim Report, Jun. - Dec. 1988
R. A. Handler and F. Rosenthal 30 Dec. 1988 48 p
(AD-A203749; NRL-MR-6381) Avail: NTIS HC A03/MF A01 CSCL 20D

Several groups have recently performed direct numerical simulations of turbulent flow in a channel at low Reynolds numbers. These simulations generate enormous quantities of data which have been used to investigate the validity of current theories of turbulence, etc. However, before detailed investigations can be undertaken, it is important to first check some basic statistics of the turbulence such as the mean velocity profile, turbulence intensities, and Reynolds stress profiles, beyond these one-point statistics so that length and time scales of the turbulence can be determined. This report describes FORTRAN codes which enable rapid evaluation of the two point correlations from a given dataset. Computer codes have been developed which compute the space time correlations in turbulent channel flow. The two-point spatial correlation function is computed by Fourier transforming the appropriate wavenumber spectrum. The wavenumber spectrum is computed by averaging over an appropriate number of ensembles and using geometric symmetries to improve the smoothness of the results. Space-time correlations are computed in a similar manner. GRA

N89-20679# Massachusetts Inst. of Tech., Cambridge. Artificial Intelligence Lab.
INTELLIGENCE IN SCIENTIFIC COMPUTING
Harold Abelson, Michael Eisenberg, Mathew Halfant, Jacob Katzenelson, and Elisha Sack Nov. 1988 37 p
(Contract N00014-86-K-0180)
(AD-A203815; AI-M-1094) Avail: NTIS HC A03/MF A01 CSCL 12I

Combining numerical techniques with ideas from symbolic computation and with methods incorporating knowledge of science and mathematics leads to a new category of intelligent computational tools for scientists and engineers. These tools autonomously prepare simulation experiments from high-level specifications of physical models. For computationally intensive experiments, they automatically design special-purpose numerical engines optimized to perform the necessary computations. They actively monitor numerical and physical experiments. They interpret experimental data and formulate numerical results in qualitative terms. They enable their human users to control computational experiments in terms of high-level behavioral descriptions. GRA

N89-20680# Naval Postgraduate School, Monterey, CA.
IMPLEMENTATION OF A LANGUAGE TRANSLATOR FOR THE COMPUTER AIDED PROTOTYPING SYSTEM M.S. Thesis
Charles Edwin Altizer Dec. 1988 162 p
(AD-A203876) Avail: NTIS HC A08/MF A01 CSCL 12E

Rapid prototyping is a method of software system development that is gaining much support presently. Rapid prototyping allows the designer to quickly produce a model of a system or part of a system which the user can see and thus verify if his requirements have been met. The prototype specifications can then be efficiently converted to an accurate set of program specifications that the programmers can implement as a final working system. The Computer Aided Prototyping System (CAPS) is a rapid prototyping system that will automate many of the processes of prototyping such as code generation of prototype modules and searching for reusable components. One of the many components of CAPS is a language translator which translates a prototype specification written in the Prototype System Description Language (PSDL) into a set of Ada procedures and packages. The Ada procedures and packages, when executed in proper order, will effectively execute the prototype. This thesis demonstrates an implementation of the translator component of the CAPS. An attribute grammar tool, Kodiyak, is used to build a translator which implements the major constructs of PDSL and produces Ada code to implement PSDL operators according to their control constraints. GRA

N89-20681# Massachusetts Inst. of Tech., Cambridge. Artificial Intelligence Lab.
PARALLEL ALGORITHMS FOR COMPUTER VISION Annual Report, No. 2, 31 Aug. 1986 - 31 Aug. 1987
Tomaso Poggio and James Little Mar. 1988 25 p
(Contract DACA76-85-C-0010)
(AD-A203947; ETL-0495) Avail: NTIS HC A03/MF A01 CSCL 12I

Much work during the past year has focused on building our Vision Machine system. The Vision Machine is a testbed for the research on parallel vision algorithms and their integration. The system consists of an input device-a movable two camera Eye-Head system with six degrees of freedom--and the 16K Connection Machine (CM-1). We have concentrated on implementing and testing early vision algorithms, and on developing a new sophisticated technique for their integration. The output of the integration stage will be used for navigation and recognition tasks. From August 31, 1986 to August 31, 1987, we have been using the Connection Machine delivered on July 31, 1986 by Thinking Machines corporation. We have developed and tested a substantial body of vision software on the machine. We have also nearly completed, well ahead of schedule, the development of an integrated Vision Machine that includes several early vision algorithms, and integration stage of middle vision. As outlined in our original proposal, we have begun to explore parallel algorithms at the higher level of recognition. We have also studied the performance of alternative, nonconventional architectures for navigation, and worked on the difficult issue of alternative parallel languages for the Connection Machine, in addition to LISP and C. The body of this report gives an overview of the results of our research during the second twelve month of funding. GRA

N89-20341*# Jet Propulsion Lab., California Inst. of Tech., Pasadena.
A LONG CONSTRAINT LENGTH VLSI VITERBI DECODER FOR THE DSN
J. I. Statman, G. Zimmerman, F. Pollara, and O. Collins *In its* The Telecommunications and Data Acquisition Report 15 Nov. 1988 p 134-142 (For primary document see N89-20329 13-32)
Avail: NTIS HC A12/MF A01 CSCL 09B

N89-20342*# Jet Propulsion Lab., California Inst. of Tech., Pasadena.
LONG DECODING RUNS FOR GALILEO'S CONVOLUTIONAL CODES
C. R. Lahmeyer and K.-M. Cheung *In its* The Telecommunications and Data Acquisition Report 15 Nov. 1988 p 143-147 (For primary document see N89-20329 13-32)
Avail: NTIS HC A12/MF A01 CSCL 09B

62 COMPUTER SYSTEMS

Includes computer networks and special application computer systems.

N89-20682# Massachusetts Inst. of Tech., Cambridge. Artificial Intelligence Lab.
AN OPERATING ENVIRONMENT FOR THE JELLYBEAN MACHINE
Brian K. Totty May 1988 157 p
(Contracts N00014-80-C-0622; N00014-85-K-0124)
(AD-A201042; AI-M-1070) Avail: NTIS HC A08/MF A01 CSCL 12I

The Jellybean Machine is a scalable Multiple Instruction/Multiple Data concurrent processor consisting of special purpose Reduced Instruction Set Computer (RISC) processors loosely coupled into a low latency network. The problem with such a machine is to find a way to efficiently coordinate the collective power of the distributed processing elements. A foundation of efficient, powerful services is required to support this system. To provide this supportive operating environment, an operating system kernel that serves many of the initial needs of the machine was developed. This Jellybean Operating System Software provides an object-based storage model, where typed contiguous blocks act as the basic metric of storage. This memory model is complemented by a global virtual naming scheme that can reference objects residing on any node of the network. Migration mechanisms allow object relocation among different nodes, and permit local catching of code. A low cost process control system based on fast-allocated contexts allows parallelism at a significantly fine gain (on the order of 30 instructions per task). The system services are developed in detail, and may be of interest to other designers of fine gain, distributed memory processing networks. The initial performance estimates are satisfactory. Optimizations will require more insight into how the machine will perform under real-world conditions. GRA

N89-20683*# Draper (Charles Stark) Lab., Inc., Cambridge, MA.
RELIABILITY AND PERFORMANCE EVALUATION OF SYSTEMS CONTAINING EMBEDDED RULE-BASED EXPERT SYSTEMS Final Report
Robert M. Beaton, Milton B. Adams, and James V. A. Harrison Feb. 1989 35 p
(Contract NAS9-17560)
(NASA-CR-181769; NAS 1.26:181769) Avail: NTIS HC A03/MF A01 CSCL 09B

A method for evaluating the reliability of real-time systems containing embedded rule-based expert systems is proposed and investigated. It is a three stage technique that addresses the impact of knowledge-base uncertainties on the performance of expert systems. In the first stage, a Markov reliability model of the system is developed which identifies the key performance parameters of the expert system. In the second stage, the evaluation method is used to determine the values of the expert system's key performance parameters. The performance parameters can be evaluated directly by using a probabilistic model of uncertainties in the knowledge-base or by using sensitivity analyses. In the third and final state, the performance parameters of the expert system are combined with performance parameters for other system components and subsystems to evaluate the reliability and performance of the complete system. The evaluation method is demonstrated in the context of a simple expert system used to supervise the performances of an FDI algorithm associated with an aircraft longitudinal flight-control system. Author

N89-20684*# National Aeronautics and Space Administration. Lewis Research Center, Cleveland, OH.
A MESSAGE PASSING KERNEL FOR THE HYPERCLUSTER PARALLEL PROCESSING TEST BED
Richard A. Blech, Angela Quealy (Sverdrup Technology, Inc., Cleveland, OH.), and Gary L. Cole 1989 10 p Presented at the 4th Conference on Hypercubes, Concurrent Computers and Applications, Monterey, CA, 6-8 Mar. 1989; sponsored by DOE, Strategic Defense Initiative Organization, Dept. of the Air Force, AFOSR and NASA, Ames Research Center
(NASA-TM-101952; E-4652; NAS 1.15:101952) Avail: NTIS HC A02/MF A01 CSCL 09B

A Message-Passing Kernel (MPK) for the Hypercluster parallel-processing test bed is described. The Hypercluster is being developed at the NASA Lewis Research Center to support investigations of parallel algorithms and architectures for computational fluid and structural mechanics applications. The Hypercluster resembles the hypercube architecture except that each node consists of multiple processors communicating through shared memory. The MPK efficiently routes information through the Hypercluster, using a message-passing protocol when necessary and faster shared-memory communication whenever possible. The MPK also interfaces all of the processors with the Hypercluster operating system (HYCLOPS), which runs on a Front-End Processor (FEP). This approach distributes many of the I/O tasks to the Hypercluster processors and eliminates the need for a separate I/O support program on the FEP. Author

N89-20685*# National Aeronautics and Space Administration. Lewis Research Center, Cleveland, OH.
INITIAL OPERATING CAPABILITY FOR THE HYPERCLUSTER PARALLEL-PROCESSING TEST BED
Gary L. Cole, Richard A. Blech, and Angela Quealy (Sverdrup Technology, Inc., Cleveland, OH.) Mar. 1989 10 p Presented at the 4th Conference on Hypercubes, Concurrent Computers, and Applications, Monterey, CA, 6-8 Mar. 1989; sponsored in part by DOE, Strategic Defense Initiative Organization, USAF, and NASA, Ames Research Center
(NASA-TM-101953; E-4647; NAS 1.15:101953) Avail: NTIS HC A02/MF A01 CSCL 09B

The NASA Lewis Research Center is investigating the benefits of parallel processing to applications in computational fluid and structural mechanics. To aid this investigation, NASA Lewis is developing the Hypercluster, a multi-architecture, parallel-processing test bed. The initial operating capability (IOC) being developed for the Hypercluster is described. The IOC will provide a user with a programming/operating environment that is interactive, responsive, and easy to use. The IOC effort includes the development of the Hypercluster Operating System (HYCLOPS). HYCLOPS runs in conjunction with a vendor-supplied disk operating system on a Front-End Processor (FEP) to provide interactive, run-time operations such as program loading, execution, memory editing, and data retrieval. Run-time libraries, that augment the FEP FORTRAN libraries, are being developed to support parallel and vector processing on the Hypercluster. Special utilities are being provided to enable passage of information about application programs and their mapping to the operating system. Communications between the FEP and the Hypercluster are being handled by dedicated processors, each running a Message-Passing Kernel, (MPK). A shared-memory interface allows rapid data exchange between HYCLOPS and the communications processors. Input/output handlers are built into the HYCLOPS-MPK interface, eliminating the need for the user to supply separate I/O support programs on the FEP. Author

N89-20686# Sandia National Labs., Albuquerque, NM.
A STRUCTURAL ANALYSIS ALGORITHM FOR MASSIVELY PARALLEL COMPUTERS
Robert E. Benner, Gary R. Montry, and John L. Gustafson Dec. 1988 11 p Presented at the Workshop on Methods and Algorithms for PDE's on Advance Processors, Austin, TX, 17 Oct. 1988
(Contract DE-AC04-76DP-00789)
(DE89-005055; SAND-88-3363C; CONF-8810280-2) Avail: NTIS HC A03/MF A01

We describe a high performance parallel algorithm based on the conjugate gradient method for large structural analysis problems. The algorithm has been tested on a 1024-processor hypercube. Three performance models are measured: 1024-processor speedup is 502 when problem size is fixed, 987 when execution time is fixed, and 1019 when problem size per processor is fixed. The latter two models best show the practical capabilities of large ensembles. Sustained performance is 132 MFLOPS (64-bit), matching or surpassing performance of more conventional processing methods. Measurements show the techniques will extend to even higher levels of parallelism than the 1024-processor level explored here. DOE

N89-20687# Center for Mathematics and Computer Science, Amsterdam (Netherlands). Dept. of Software Technology.
THE ALGEBRA OF SYNCHRONOUS PROCESSES
W. P. Weijland Jan. 1988 38 p
(CWI-CS-R8807; B8821065; ETN-89-94169) Copyright Avail: NTIS HC A03/MF A01

The algebra of synchronous processes (ASP), which describes synchronous cooperation of processes, is presented. One of the main differences between ASP and the algebraical theory SCCS or Milner (1983) is the representation of parallelism, which is done by considering a computation step as a vector, each component of which represents an atomic action on the corresponding channel. An example from computer integrated manufacturing illustrates the theory. ESA

N89-20688# Center for Mathematics and Computer Science, Amsterdam (Netherlands). Dept. of Software Technology.
A COMPOSITIONAL SEMANTICS FOR CONCURRENT PROLOG
Joost N. Kok Feb. 1988 17 p Presented at the Symposium on Theoretical Aspects of Computer Science, Bordeaux, France, Feb. 1988 Submitted for publication
(Grant NWO-125-20-04)
(CWI-CS-R8809; B8821067; ETN-89-94170) Copyright Avail: NTIS HC A03/MF A01

It is shown that a model designed for imperative languages can be used to give a formal description of Concurrent Prolog. This model is compositional: for any two conjunctions C1, C2 the meaning of (C1 and C2) can be obtained by applying a function to the meanings of C1 and C2. A domain where some choices made during the computation are recorded in certain tree-like structures, and which allows for interleaving is used. Tree-like structures are employed because it is not possible to use flat structures (like traces or sequences of substitutions). They do not contain enough information to handle deadlock or infinite computations. Such phenomena require that one knows at a certain moment in time all the alternatives. The domain is obtained as a solution of a domain equation. Metric topological tools are used to find a solution of the domain equation, and to define operations on elements of the domain. The semantic function maps goals, given a program P, to elements of the domain. This function is defined recursively. The model can handle finite and infinite computations. ESA

N89-20689# Los Alamos National Lab., NM. Computing and Communications Div.
A LOCAL AREA NETWORK DIAGNOSTIC ASSISTANT EXPERT SYSTEM
S. M. Mniszewski, E. A. Peter, and S. C. Lloyd 1988 9 p Presented at the 3rd Topical Meeting on Robotics and Remote Systems, Charleston, SC, 13 Mar. 1989
(Contract W-7405-eng-36)
(DE89-003575; LA-UR-88-3827; CONF-890304-14) Avail: NTIS HC A02/MF A01

We are currently developing a stand-alone Local Area Network (LAN) Diagnostic Assistant expert system to assist system managers in diagnosing network-related hardware and software malfunctions. The goal of this system is to aid in identifying malfunctions associated with a single workstation, a group of workstations, communications between workstations, and general statements of the Ethernet not working type of problems. The system consists of a geographical editor for data entry and modification of LAN information and a diagnostic environment for solving problems. Much work has been done in laying the initial framework for the system in the areas of LAN representation, the problem-solving strategy, and the user interface. We used a hierarchical frame-based representation for the LAN. Information for the strategy mechanism was gathered through case studies and background information. Ideas from heuristic classification were incorporated into the strategy mechanism. As in any system development, a majority of the time was spent developing a good user interface. We used graphics renditions wherever natural and minimized keyboard input by using mouse-selectable buttons and menus. Currently, a prototype version of the system is available that assists with some single-workstation problems. DOE

N89-20690# Oak Ridge National Lab., TN. Mathematical Sciences Section.
MULTIPROGRAMMING A DISTRIBUTED-MEMORY MULTIPROCESSOR
Michael R. Leuze, Lawrence W. Dowdy, and Kee Hyun Park (Vanderbilt Univ., Nashville, TN.) Jan. 1989 27 p
(Contract DE-AC05-84OR-21400)
(DE89-007850; ORNL/TM-11064) Avail: NTIS HC A03/MF A01

The development of computing systems with large numbers of processors has been motivated primarily by the need to solve large complex problems more quickly than is possible with uniprocessor systems. Traditionally, multiprocessor systems have been uniprogrammed, i.e., dedicated to the execution of a single set of related processes, since this approach provides the fastest response for an individual program once it begins execution. However, if the goal of a multiprocessor system is to minimize average response time or to maximize throughput, then multiprogramming must be considered. In this paper, a model of a simple multiprocessor system with a two-program workload is reviewed; the model is then applied to an Intel iPSC/2 hypercube multiprocessor with a workload consisting of parallel wavefront algorithms for solving triangular systems of linear equations. Throughputs predicted by the model are compared with throughputs obtained experimentally from an actual system. The results provide validation for the model and indicate that significant performance improvements for multiprocessor systems are possible through multiprogramming. DOE

N89-20691# Oak Ridge National Lab., TN. Mathematical Sciences Section.
THE EFFECT OF TIME CONSTRAINTS ON SCALED SPEED-UP
Patrick H. Worley Jan. 1989 38 p
(Contract DE-AC05-84OR-21400)
(DE89-007877; ORNL/TM-11031) Avail: NTIS HC A03/MF A01

Gustafson, Montry, and Benner introduced the concept of scaled speed-up to characterize the capabilities of distributed-memory MIMD multiprocessors. They argued that, for a fixed-size problem, the behavior of the speed-up of an algorithm as a function of the number of processors, the speed-up curve, can be too pessimistic a measure of a multiprocessor architecture. Instead, they measured the speed-up of algorithms when size of the corresponding problem grew with the number of processors. They referred to the resulting function as the scaled speed-up curve. The scaled speed-up curve is a function of how the size of the problem is allowed to grow. We demonstrate that allowing the size of a problem to grow to fill the available memory can produce dramatically different results from allowing the size of a problem to grow subject to satisfying an upper bound on the execution time. In particular, if a constraint on the execution time is enforced, then the scaled speed-up curve is often very similar to the speed-up curve for a fixed-size problem. We show that no more than 50 processors can be used efficiently for some common problems in scientific computation when using the current generation of distributed-memory multiprocessors. For other problems, we show that the scaled speed-up curve indicates that massively parallel computers will be useful even if the execution time is constrained. In all of the cases examined, a meaningful interpretation of the scaled speed-up curve depends on a constraint on the execution time. DOE

63 CYBERNETICS

Includes feedback and control theory, artificial intelligence, robotics and expert systems.

For related information see also *54 Man/System Technology and Life Support.*

N89-20692*# Georgia Inst. of Tech., Atlanta. Center for Human-Machine Systems Research.
HUMAN-COMPUTER INTERACTION IN DISTRIBUTED SUPERVISORY CONTROL TASKS Semiannual Status Report, 15 Apr. - 14 Oct. 1988
Christine M. Mitchell Jan. 1989 156 p
(Grant NAG5-1044)
(NASA-CR-184671; NAS 1.26:184671) Avail: NTIS HC A08/MF A01 CSCL 09B

An overview of activities concerned with the development and applications of the Operator Function Model (OFM) is presented. The OFM is a mathematical tool to represent operator interaction with predominantly automated space ground control systems. The design and assessment of an intelligent operator aid (OFMspert and Ally) is particularly discussed. The application of OFM to represent the task knowledge in the design of intelligent tutoring systems, designated OFMTutor and ITSSO (Intelligent Tutoring System for Satellite Operators), is also described. Viewgraphs from symposia presentations are compiled along with papers addressing the intent inferencing capabilities of OFMspert, the OFMTutor system, and an overview of intelligent tutoring systems and the implications for complex dynamic systems. For individual titles, see N89-20693 through N89-20697.

N89-20693*# Georgia Inst. of Tech., Atlanta. Center for Human-Machine Systems Research.
VIEW GRAPHS FOR GSFC COLLOQUIUM ON OFMspert
Christine M. Mitchell *In its* Human-Computer Interaction in Distributed Supervisory Control Tasks Jan. 1989 20 p (For primary document see N89-20692 13-63)
Avail: NTIS HC A08/MF A01 CSCL 09B

Viewgraphs providing an overview of activities concerned with the development and testing of the Operator Function Model (OFM) expert system (OFMspert) are presented. The OFM is a mathematical tool for representing operator interaction with predominantly automated space ground control systems. OFM provides cognitive task analysis and served as the basis for the design of an intelligent operator's associate called OMFspert. An experimental implementation of OFMspert, referred to as Ally, was developed. An empirical evaluation of Ally was conducted to determine the effectiveness of a supervisory control team consisting of a human operator and Ally versus a control team consisting of two human operators. The experiment was carried out in the GT-MSOCC (Georgia Tech MultiSatellite Operations Control Center) domain, a research tool consisting of a high fidelity implementation of the operator interface to a GSFC ground control system. The viewgraphs outline the experimental design, operator performance measures, and preliminary results. M.G.

N89-20694*# National Aeronautics and Space Administration. Lyndon B. Johnson Space Center, Houston, TX.
USE OF ARTIFICIAL INTELLIGENCE IN SUPERVISORY CONTROL
Aaron Cohen and Jon D. Erickson *In* Georgia Inst. of Tech., Human-Computer Interaction in Distributed Supervisory Control Tasks Jan. 1989 48 p (For primary document see N89-20692 13-63)
Avail: NTIS HC A08/MF A01 CSCL 09B

Viewgraphs describing the design and testing of an intelligent decision support system called OFMspert are presented. In this expert system, knowledge about the human operator is represented through an operator/system model referred to as the OFM (Operator Function Model). OFMspert uses the blackboard model of problem solving to maintain a dynamic representation of operator goals, plans, tasks, and actions given previous operator actions and current system state. Results of an experiment to assess OFMspert's intent inferencing capability are outlined. Finally, the overall design philosophy for an intelligent tutoring system (OFMTutor) for operators of complex dynamic systems is summarized. M.G.

N89-20695*# Georgia Inst. of Tech., Atlanta. Center for Human-Machine Systems Research.
INTENT INFERENCING WITH A MODEL-BASED OPERATOR'S ASSOCIATE
Patricia M. Jones, Christine M. Mitchell, and Kenneth S. Rubin *In its* Human-Computer Interaction in Distributed Supervisory Control Tasks Jan. 1989 19 p (For primary document see N89-20692 13-63)
(Rept-88-2) Avail: NTIS HC A08/MF A01 CSCL 09B

A portion of the Operator Function Model Expert System (OFMspert) research project is described. OFMspert is an architecture for an intelligent operator's associate or assistant that can aid the human operator of a complex, dynamic system. Intelligent aiding requires both understanding and control. The understanding (i.e., intent inferencing) ability of the operator's associate is discussed. Understanding or intent inferencing requires a model of the human operator; the usefulness of an intelligent aid depends directly on the fidelity and completeness of its underlying model. The model chosen for this research is the operator function model (OFM). The OFM represents operator functions, subfunctions, tasks, and actions as a heterarchic-hierarchic network of finite state automata, where the arcs in the network are system triggering events. The OFM provides the structure for intent inferencing in that operator functions and subfunctions correspond to likely operator goals and plans. A blackboard system similar to that of Human Associative Processor (HASP) is proposed as the implementation of intent inferencing function. This system postulates operator intentions based on current system state and attempts to interpret observed operator actions in light of these hypothesized intentions. Author

N89-20696*# Georgia Inst. of Tech., Atlanta. Center for Human-Machine Systems Research.
OFMTutor: AN OPERATOR FUNCTION MODEL INTELLIGENT TUTORING SYSTEM
Patricia M. Jones *In its* Human-Computer Interaction in Distributed Supervisory Control Tasks Jan. 1989 45 p (For primary document see N89-20692 13-63)
Avail: NTIS HC A08/MF A01 CSCL 09B

The design, implementation, and evaluation of an Operator Function Model intelligent tutoring system (OFMTutor) is presented. OFMTutor is intended to provide intelligent tutoring in the context of complex dynamic systems for which an operator function model (OFM) can be constructed. The human operator's role in such complex, dynamic, and highly automated systems is that of a supervisory controller whose primary responsibilities are routine monitoring and fine-tuning of system parameters and occasional compensation for system abnormalities. The automated systems must support the human operator. One potentially useful form of support is the use of intelligent tutoring systems to teach the operator about the system and how to function within that system. Previous research on intelligent tutoring systems (ITS) is considered. The proposed design for OFMTutor is presented, and an experimental evaluation is described. M.G.

N89-20697*# Georgia Inst. of Tech., Atlanta. Center for Human-Machine Systems Research.
A SURVEY OF INTELLIGENT TUTORING SYSTEMS: IMPLICATIONS FOR COMPLEX DYNAMIC SYSTEMS
Rose W. Chu *In its* Human-Computer Interaction in Distributed Supervisory Control Tasks Jan. 1989 19 p (For primary document see N89-20692 13-63)
Avail: NTIS HC A08/MF A01 CSCL 09B

An overview of the research in the field of intelligent tutorial systems (ITS) is provided. The various approaches in the design and implementation of ITS are examined and discussed in the context of problem solving in an environment of a complex dynamic system (CDS). Issues pertaining to a CDS and the nature of human problem solving especially in light of a CDS are considered. An

overview of the architecture of an ITS is provided as the basis for the in-depth examination of various systems. Finally, the implications for the design and evaluation of an ITS are discussed. Author

N89-20698*# Institute for Computer Applications in Science and Engineering, Hampton, VA.
FAULT-TOLERANCE OF A NEURAL NETWORK SOLVING THE TRAVELING SALESMAN PROBLEM Final Report
P. Protzel, D. Palumbo, and M. Arras (College of William and Mary, Williamsburg, VA.) Feb. 1989 15 p Submitted for publication
(Contract NAS1-18605)
(NASA-CR-181798; ICASE-89-12; NAS 1.26:181798) Avail: NTIS HC A03/MF A01 CSCL 09B

This study presents the results of a fault-injection experiment that stimulates a neural network solving the Traveling Salesman Problem (TSP). The network is based on a modified version of Hopfield's and Tank's original method. We define a performance characteristic for the TSP that allows an overall assessment of the solution quality for different city-distributions and problem sizes. Five different 10-, 20-, and 30- city cases are sued for the injection of up to 13 simultaneous stuck-at-0 and stuck-at-1 faults. The results of more than 4000 simulation-runs show the extreme fault-tolerance of the network, especially with respect to stuck-at-0 faults. One possible explanation for the overall surprising result is the redundancy of the problem representation. Author

N89-20699# National Aerospace Lab., Amsterdam (Netherlands). Structures and Materials Div.
BORDERED EQUATIONS IN CONTINUATION METHODS: AN IMPROVED SOLUTION TECHNIQUE
E. Riks and C. C. Rankin (Lockheed Missiles and Space Co., Palo Alto, CA.) 13 Dec. 1987 26 p Sponsored by The Netherlands Agency for Aerospace Programs, Delft, The Netherlands
(NLR-MP-87057-U; ETN-89-94038) Avail: NTIS HC A03/MF A01

Continuation methods with adaptive path parameters, such as arc-length continuation, based on bordered equations where the governing matrix is nonsymmetric with respect to one column and row are discussed. In the conventional way of solving these systems, the factored submatrix of the total system becomes singular at special solution points such as limit points and bifurcation points. This means that the solution process may suffer from an ill-conditioned systems matrix in the vicinity of such points. A variant of the Gaussian block elimination technique that does not have these disadvantages is presented. The method is closely related to the method of substructuring (as is the former) and it has additional amenities that make it particularly suited for stability analysis. ESA

N89-20700# Sheffield Univ. (England). Dept. of Control Engineering.
ON THE STRUCTURE AND CONTROL OF PIECEWISE-LINEAR SYSTEMS
S. P. Banks and Saadi A. Khathur Jul. 1988 29 p
(RR-334; ETN-89-94076) Avail: NTIS HC A03/MF A01

The behavior of piecewise-linear systems is studied by dissecting the ambient space into a geometric simplicial complex. This allows the application of algebric topology to obtain a numerical procedure for the determination of the global topology of the trajectories of such systems. Piecewise-linear systems (without control) are examined by making a simplicial decomposition of !R sup N and deriving a numerical technique for the recursive evaluation of the homology groups of a simplicial approximation to a trajectory of the system. This is very similar to the standard numerical techniques (Runge-Kutta, etc.) for the numerical evaluation of the phase-plane trajectories. Optimal control of piecewise-linear control systems is considered, extending the linear-quadratic regulator problem to these systems. It is shown how to apply the simplicial approximation theorem to obtain a piecewise-approximation to a continuous nonlinear systems. The evaluation of the optimal control for such a system is mentioned. ESA

N89-20701# Center for Mathematics and Computer Science, Amsterdam (Netherlands). Dept. of Pure Mathematics.
LECTURES ON LINEAR AND NONLINEAR FILTERING
Michiel Hazewinkel Jan. 1988 36 p
(CWI-PM-R8801; B8817045; ETN-89-94194) Copyright Avail: NTIS HC A03/MF A01

The so-called Lie-algebraic approach to the general problems of filtering and identification is introduced. This approach is also known as the reference probability approach and is based on the socalled Duncan-Mortensen-Zakai equation. Wei-Norman theory is an important tool especially when the estimation Lie algebra is (topologically) solvable as is the case in a number of important classes of examples, including identification of linear systems (which is a nonlinear filtering problem). In numerous other cases the estimation Lie algebra is a Heisenberg-Weyl algebra, which implies that finite dimensional exact recursive filters (for nonconstant statistics) can not exist. It appears that a more sensitive invariant than the estimation Lie algebra itself is needed to study systematically the questions of existence and construction approximate finite dimensional recursive filters. Proposals in this direction are described. Some of them lead to asymptotic possibly nonconverging series for the unnormalized conditional density. ESA

N89-20702# Oak Ridge National Lab., TN. Robotics and Intelligent Systems Program.
AUTOMATIC LEARNING BY AN AUTONOMOUS MOBILE ROBOT
G. deSaussure, P. F. Spelt, Stephen M. Killough, F. G. Pin, and Charles R. Weisbin 1989 6 p Presented at the 3rd Topical Meeting on Robotics and Remote Systems, Charleston, SC, 13 Mar. 1989
(Contract DE-AC05-84OR-21400)
(DE89-003120; CONF-890304-10; CESAR-88/62) Avail: NTIS HC A02/MF A01

This paper describes recent research in automatic learning by the autonomous mobile robot HERMIES-IIB at the Center for Engineering Systems Advanced Research (CESAR). By acting on the environment and observing the consequences during a set of training examples, the robot learns a sequence of successful manipulations on a simulated control panel. The robot learns to classify panel configurations in order to deal with new configurations that are not part of the original training set. DOE

N89-20703# Oak Ridge National Lab., TN. Instruments and Controls Div.
SENSOR CAPABILITIES FOR THE HERMIES EXPERIMENTAL ROBOT
Stephen M. Killough and William R. Hamel 1988 8 p Presented at the 3rd Topical Meeting on Robotics and Remote Systems, Charleston, SC, 13 Mar. 1989
(Contract DE-AC05-84OR-21400)
(DE89-003180; CONF-890304-11) Avail: NTIS HC A02/MF A01

The Center for Engineering Systems Advanced Research at the Oak Ridge National Laboratory has developed an experimental robot, the HERMIES, to test artificial intelligence concepts. This paper describes the capabilities provided for navigation and control. The authors conclude that the sensor suite, which enables the robot to recognize, locate, and grasp objects, makes HERMIES-IIB a powerful tool for robotics and artificial intelligence research. DOE

N89-20704# Oak Ridge National Lab., TN.
INCREASING USER-FRIENDLINESS IN AI SYSTEMS
Anurag Agarwal and M. L. Emrich Oct. 1988 31 p Presented at the National Governor's Association Meeting: Finding the Future Conference, Washington, DC, 12 Dec. 1988

(Contract DE-AC05-84OR-21400)
(DE89-005093; CONF-881249-3) Avail: NTIS HC A03/MF A01

Recent trends have shown a rise in the number of non-technical computer users. This has resulted in increased emphasis on User Systems Interfaces (USI). New technology which has been developed includes: laser/optical mice, touch screens, voice synthesizers, and voice analyzers. This paper details hardware and software that have been the focus of recent research. The implementation of SOFTMAN, a software manager aid is also discussed. As part of its USI, SOFTMAN has each of the above interfaces. Future technologies and research paths will also be discussed. DOE

N89-20705# Oak Ridge National Lab., TN. Instrumentation and Controls Div.

GAIN SELECTION FOR AN INDEPENDENT JOINT MRAC (MODEL-REFERENCE ADAPTIVE CONTROLLER) FOR ROBOTIC MANIPULATORS

J. F. Jansen and Reid L. Kress 1988 9 p Presented at the 3rd Topical Meeting on Robotics and Remote Systems, Charleston, SC, 12-13 Mar. 1989
(Contract DE-AC05-84OR-21400)
(DE89-005110; CONF-890304-30) Avail: NTIS HC A02/MF A01

This paper discusses how the gains of an independent Model-Reference Adaptive Controller should be set for robotic/telerobotic applications. Potential vibrational problems and their reduction will be discussed. This type of controller can be easily added to a conventional PD Controller with minimum software changes. DOE

N89-20706# California Univ., Berkeley. Lawrence Berkeley Lab. Dept. of Mechanical Engineering.

DYNAMIC MECHANICAL SYSTEM DESIGN USING QUALITATIVE AND SYMBOLIC REASONING

Young-Jin Kim and Alice M. Agogino Dec. 1988 11 p
(Contract W-7405-eng-48)
(DE89-006771; UCRL-21179) Avail: NTIS HC A03/MF A01

This report describes the results of a three-month project to perform preliminary research for use in preparation of UCB Campus-LLNL collaborative research proposal. The goal of this research is to develop and implement artificial intelligence methods for the design, modeling and analysis of dynamic physical systems. Bond graphs and a library of dynamic system primitives form the basis of the knowledge representation scheme. Bond graphs abstract physical systems into basic elements that represent localized dynamic properties of small parts of the system. This research deals with mechanical systems, in which there are natural hierarchies of subsystems which are in turn comprised of primitive components. The subsystems developed in this research are divided into three classes: resistance fields, inertial fields and capacitance fields. Basic categories from the mechanical systems domain are examined to derive the characteristics of each subsystem. We propose that future research begin with the development of a library of natural modeling primitives for physical subsystems along with rules for creating a network from such primitives. We modify Karnopp and Rosenberg's mechanical translation construction method to generate the automatic bond graph representation of mechanical system in a rule/frame-based format. We outline a knowledge-based methodology to define a bond graph description of complex dynamic physical systems from an integration of simpler primitives and component classes. We conclude with a framework for integrating earlier work in predicting and directing the behavior of dynamic systems using qualitative and symbolic reasoning for providing a mathematical description of the behavior of the system along with recommendations concerning the design parameters. DOE

N89-20707# Sandia National Labs., Albuquerque, NM.

INTEGRATING MULTIPLE VIEWS INTO A SINGLE REPRESENTATION OF A RANGE IMAGED OBJECT

S. A. Stansfield 1988 8 p Presented at the SPIE Conference, Boston, MA, 1 Nov. 1988
(Contract DE-AC04-76DP-00789)
(DE89-005921; SAND-88-3350C; CONF-8811162-1) Avail: NTIS HC A02/MF A01

In this paper we review recent work in representing generic, or basic level, objects. Our representation is frame-based and includes spatial information in the form of a set of aspects. The representation will be used for recognition of range-imaged objects. The paper describes the structured-lighting system and the vision algorithms used to process the data and presents some preliminary results. DOE

N89-20708# Oak Ridge National Lab., TN. Engineering Physics and Mathematics Div.

A CONCURRENT APPROACH TO MODEL BASED MOTION DETECTION

Henrik I. Christensen (Aalborg Univ., Denmark) Jan. 1989 24 p
(Contract DE-AC05-84OR-21400)
(DE89-007853; ORNL/TM-11051; CESAR-89/01) Avail: NTIS HC A03/MF A01

In robot-vision it is important to be able to acquire and describe dynamically changing scenes. A token based method for real-time motion detection is described here. This method uses a prediction-verification scheme to cope with ambiguous motion patterns. To improve performance it is investigated how the application may be implemented on a concurrent architecture like a hypercube. An implementation based on the SPMD approach is presented together with some experimental results. The results demonstrate the system's ability to handle ambiguous situations. Timing results indicate the system has a potential for tracking of less than 10 objects or more than 40 objects, while the advantage of using a concurrent architecture for 10 to 40 objects is very small. DOE

64 NUMERICAL ANALYSIS

Includes iteration, difference equations, and numerical approximation.

N89-20709# Brown Univ., Providence, RI. Lab. for Engineering Man/Machine Systems.

ALGEBRAIC NONPLANAR CURVE AND SURFACE ESTIMATION IN 3-SPACE WITH APPLICATIONS TO POSITION ESTIMATION

Gabriel Taubin Feb. 1988 39 p Sponsored in part by IBM Watson Research Center, Yorktown Heights, NY
(PB88-227616; LEMS-43) Avail: NTIS HC A03/MF A01
CSCL 12A

The problem of minimal parameter representation and estimation for complex planar and nonplanar curves and surfaces in 3-E is discussed. The representation is based on concepts from algebraic geometry; a planar curve is the set of roots of a polynomial of two variables; a surface in 3-space is the set of roots of a polynomial of three variables; and a nonplanar curve is the intersection of two different surfaces. The authors show that the surface of interesting complex objects in 3-space can be represented by single high degree polynomials, and a similar statement applies to the representation of complex two-dimensional (planar) curves singly or jointly. An approximate expression for the mean square distance from a set of points to a curve or surface is developed, not only for quadratic surfaces, but for surfaces and curves defined by smooth functions, particularly for polynomials of higher degree. Author

N89-20710*# National Aeronautics and Space Administration. Lewis Research Center, Cleveland, OH.

ON THE EQUIVALENCE OF GAUSSIAN ELIMINATION AND GAUSS-JORDAN REDUCTION IN SOLVING LINEAR EQUATIONS

Nai-kuan Tsao Feb. 1989 22 p Prepared in cooperation with Wayne State Univ., Detroit, MI

(NASA Order C-99066-G)
(NASA-TM-101466; ICOMP-89-2; E-4577; NAS 1.15:101466)
Avail: NTIS HC A03/MF A01 CSCL 12A

A novel general approach to round-off error analysis using the error complexity concepts is described. This is applied to the analysis of the Gaussian Elimination and Gauss-Jordan scheme for solving linear equations. The results show that the two algorithms are equivalent in terms of our error complexity measures. Thus the inherently parallel Gauss-Jordan scheme can be implemented with confidence if parallel computers are available. Author

N89-20711# Helsinki Univ. of Technology, Espoo (Finland). Inst. of Mathematics.
FORMULA RELATED TO THE CAYLEY-HAMILTON EQUATION
Jerry Segercrantz Oct. 1988 9 p
(PB89-128003; HTKK-MAT-A261; ISBN-951-754-640-8) Avail: NTIS HC A02/MF A01 CSCL 12A

The problem of finding a simple and natural proof of the well-known Cayley-Hamilton equation has been treated in the past in various articles. An interesting improvement was made by Lehti with the observation that the concept of the induced transformation can be employed to give certain formulas a compact and elegant form. The Cayley-Hamilton equation is obtained as a kind of limit case of a more general formula expressing an induced transformation as a linear combination of powers of the linear transformation considered. In the present article the formula in question is used to derive an equation resembling the Cayley-Hamilton equation, but of lower degree than the dimension n of the underlying vector space V, provided that the rank of the linear transformation concerned is smaller than n-1. Author

N89-20712# Massachusetts Inst. of Tech., Cambridge. Sea Grant Coll. Program.
PIECEWISE CONTINUOUS ALGEBRAIC SURFACES IN TERMS OF B-SPLINES
Nicholas M. Patrikalakis and George A. Kriezis Aug. 1988 81 p
(Grant NOAA-NA86AA-D-SG-89)
(PB89-109136; MITSG-88-5; RT-16) Avail: NTIS HC A05/MF A01 CSCL 12A

A method is described for representing shape using portions of algebraic surfaces bounded by rectangular boxes described in terms of triple product Bernstein polynomials and some of their properties are described. The method is extended to handle piecewise continuous algebraic surfaces within rectangular boxes defined in terms of triple products of B-spline basis functions. Next two techniques for sculptured shape creation using primitive data are studied. The first is based on geometric manipulation of existing primitives and the second on approximation/interpolation of lower dimensional entities using least squares techniques. In addition, several interrogation techniques used in the creation and analysis of piecewise continuous algebraic surfaces are presented, such as contouring, ray tracing, volume and moment of inertia and curvature evaluations. Author

N89-20713# Harbin Inst. of Tech. (China).
FINITE ELEMENT TECHNIQUE FOR THE INVERSE PROBLEM OF A PARTIAL DIFFERENTIAL EQUATION AND ITS APPLICATION TO PARAMETER IDENTIFICATION OF STRUCTURE
Deming Wang and Jiaqi Liu 1987 10 p Sponsored by Institute of Scienctific and Technical Information of China, Beijing
(PB89-111439; ISTIC-TR-C-000192) Avail: NTIS HC A02/MF A01 CSCL 12A

A method of Pulse Spectrum-Finite Element Technique is presented for solving the inverse problem of partial differential equation. Numerical simulations for the parameter identification of the vibrational beam structure are given. GRA

N89-20714# Academia Sinica, Beijing (China).
NUMERICAL METHOD OF APPLYING MEAN VALUE THEOREM
Jike Wu and Hui Li (Peking Univ., China) 1987 11 p Sponsored by Institute of Scientific and Technical Information of China, Beijing
(PB89-111447; ISTIC-TR-C-000193) Avail: NTIS HC A03/MF A01 CSCL 12A

A numerical method is presented to solve some elliptic differential equations by using the mean value theorems of their solutions. The method requires less storage and computational work. Author

N89-20715# Colorado State Univ., Fort Collins. Dept. of Computer Science.
AN ANALYSIS OF REDUCED HESSIAN METHODS FOR CONSTRAINED OPTIMIZATION
Richard H. Byrd and Jorge Nocedal 31 Aug. 1988 45 p
(Contracts DAAL03-88-K-0086; DE-FG02-87ER-25047; AF-AFOSR-0251-85; NSF CCR-87-02403; NSF CCR-86-02071)
(AD-A201078; CU-CS-398-88; ARO-24923.1-MA) Avail: NTIS HC A03/MF A01 CSCL 12D

This document studies the convergence properties of reduced Hessian successive quadratic programming for equality constrained optimization. The method uses a backtracking line search, and updates an approximation to the reduced Hessian of the Lagrangian by means of the BFGS formula. Two merit functions are considered for the line search: the l1 function and the Fletcher exact penalty function. We give conditions under which local and superlinear convergence is obtained, and also prove a global convergence result. The analysis allows the initial reduced Hessian approximation to be any positive definite matrix, and does not assume that the iterates converge, or that the matrices are bounded. The effects of a second order correction step, a watchdog procedure and of the choice of null space basis are considered. This work can be seen as an extension of the well known results of Powell (1976) for unconstrained optimization to reduced Hessian methods. GRA

N89-20716*# Institute for Computer Applications in Science and Engineering, Hampton, VA.
ANALYSIS OF REGULARIZED NAVIER-STOKES EQUATIONS, 2 Final Report
Yuh-Roung Ou and S. S. Sritharan (University of Southern California, Los Angeles.) Feb. 1989 68 p Submitted for publication
(Contracts NAS1-18605; N00014-86-K-0679; AF-AFOSR-0079-89)
(NASA-CR-181801; ICASE-89-14; NAS 1.26:181801) Avail: NTIS HC A04/MF A01 CSCL 12A

A practically important regularization of the Navier-Stokes equations was analyzed. As a continuation of the previous work, the structure of the attractors characterizing the solutions was studied. Local as well as global invariant manifolds were found. Regularity properties of these manifolds are analyzed. Author

N89-20717*# Illinois Univ., Urbana. Dept. of Computer Science.
MONOTONICALLY IMPROVING APPROXIMATE ANSWERS TO RELATIONAL ALGEBRA QUERIES
Kenneth P. Smith and J. W. S. Liu 4 Apr. 1989 20 p
(Contract NAG1-613; N00014-87-K-0827)
(NASA-CR-184874; NAS 1.26:184874) Avail: NTIS HC A03/MF A01 CSCL 12A

We present here a query processing method that produces approximate answers to queries posed in standard relational algebra. This method is monotone in the sense that the accuracy of the approximate result improves with the amount of time spent producing the result. This strategy enables us to trade the time to produce the result for the accuracy of the result. An approximate relational model that characterizes approximate relations and a partial order for comparing them is developed. Relational operators which operate on and return approximate relations are defined. Author

N89-20718*# Institute for Computer Applications in Science and Engineering, Hampton, VA.
SPECTRAL METHODS FOR CFD Final Report
Thomas A. Zang, Craig L. Streett, and M. Yousuff Hussaini Feb. 1989 70 p Presented at the von Karman Inst. Lecture Survey on Computation Fluid Dynamics, 6-10 Mar. 1989 Prepared in cooperation with NASA, Langley Research Center, Hampton, VA
(Contract NAS1-18605)
(NASA-CR-181803; ICASE-89-13; NAS 1.26:181803) Avail: NTIS HC A04/MF A01 CSCL 12A

One of the objectives of these notes is to provide a basic introduction to spectral methods with a particular emphasis on applications to computational fluid dynamics. Another objective is to summarize some of the most important developments in spectral methods in the last two years. The fundamentals of spectral methods for simple problems will be covered in depth, and the essential elements of several fluid dynamical applications will be sketched. Author

N89-20719# Centro Brasileiro de Pesquisas Fisicas, Rio de Janeiro.
ANTIPODAL UNIVERSES IN THE TOPOLOGY S(SUP 3)xR AND H(SUP 3)xR
F. Deeke Sasse, I. Damiao Soares, and J. Tiomno 1988 29 p
(DE88-704999; CBPF-NF-004/88) Avail: NTIS (US Sales Only) HC A03/MF A01

We introduce a two-parameter family of left-invariant metrics gL and right-invariant metrics gR on the Lie groups S(sup 3)xR and H(sup 3)xR with the aim of characterizing causality features in such universes. DOE

N89-20720# Instituto de Fisica Teorica, Sao Paulo (Brazil).
VERTEX OPERATORS AND JORDAN FIELDS
L. A. Ferreira, J. F. Gomes, and A. H. Zimerman 1988 13 p
(DE88-705078; IFT-P-22/88) Avail: NTIS (US Sales Only) HC A03/MF A01

The construction of Lie algebras in terms of Jordan algebras generators is discussed. The key to the construction is the triality relation already incorporated into matrix products. A generalization to Kac-Moody algebras in terms of vertex operators is proposed and may provide a clue for the construction of new representations of Kac-Moody algebras in terms of Jordan fields. DOE

N89-20721# Lawrence Livermore National Lab., CA. User Systems Div.
SLAP (SPARSE LINEAR ALGEBRA PACKAGE) FOR THE MASSES
Mark K. Seager 12 Dec. 1988 17 p Presented at the Workshop on Methods and Algorithms for PDE's on Advance Processors, Austin, TX, 17-18 Oct. 1988
(Contract W-7405-eng-48)
(DE89-006209; UCRL-100195; CONF-8810280-1) Avail: NTIS HC A03/MF A01

A Sparse Linear Algebra Package (SLAP), written in FORTRAN77, for the iterative solution of large sparse symmetric and non-symmetric linear systems is presented. SLAP Version 2.0 consists of three levels of routines: high level, core and utility. The core routines implement the following preconditioned iterative methods: iterative refinement, conjugate gradient, conjugate gradient on the normal equations, bi-conjugate gradient, bi-conjugate gradient squared, orthomin and generalized minimum residual. All of these methods do not require the data structure of the matrix being solved nor of the preconditioning matrix, but do require the user to supply a matrix vector product and preconditioning routines. The high level routines assume one of two specific data structures and provide the required user routines. The preconditioners supported are diagonal scaling and incomplete factorization. One of the SLAP data structures allows for the vectorization of the matrix multiply and the backsolve of the incomplete factorization operations on machines with hardware gather/scatter capabilities. We present results for SLAP on the Cray Y/MP and Alliant FX/8 machines. DOE

N89-20722# Technische Univ., Delft (Netherlands). Faculty of Technical Mathematics and Informatics.
SET THEORY, CHAPTER 4
B. Balcar and P. Stepanek 1988 100 p
(Rept-88-47; ISSN-0920-8577; ETN-89-94015) Copyright Avail: NTIS HC A05/MF A01

The method of generic extensions of models of set theory is explained, based on a theory of Boolean algebras. Complete Boolean algebras and those properties of them that are relevant for investigations of generic extensions, for example dense subsets, partitions of unity, saturatedness, and distributivity, are emphasized. Constructions of algebras using free products and factorization, and the Stone theorem about duality are given. The notion of a generic set is introduced. The Generic Extension Theorem is presented and proved. ESA

N89-20723# Technische Univ., Delft (Netherlands). Faculty of Technical Mathematics and Informatics.
WHO'S AFRAID OF NONSYMMETRIC MATRICES: A DISCUSSION OF ELEMENTARY ITERATIVE METHODS
A. E. P. Veldman 1988 51 p
(Rept-88-49; ISSN-0920-8577; ETN-89-94016) Copyright Avail: NTIS HC A04/MF A01

The iterative solution of nonsymmetric matrices is discussed. Elementary iterative methods like JOR, SOR, and explicit time-integration are discussed; it is explained how relaxation factors have to be chosen. The theory is applied to convection-diffusion equations at large mesh-Peclet numbers. It is demonstrated that it is not difficult to obtain the solution by iterative means, even in situations where the coefficient matrix possesses a very large skew-symmetric part. ESA

N89-20724# Technische Univ., Delft (Netherlands). Faculty of Technical Mathematics and Informatics.
ITERATIVE SOLUTION OF LARGE SPARSE SYSTEM OF LINEAR EQUATIONS
J. J. Rusch, ed., A. E. P. Veldman, Henk A. vanderVorst, P. Sonneveld, and M. A. Viergever 1988 60 p Presented at a Special-Topic Lecture Series, Delft, Netherlands, 1988
(Rept-88-52; ISSN-0920-8577; ETN-89-94019) Copyright Avail: NTIS HC A04/MF A01

Model problems, basic ideas behind iterative methods, and simple iterative methods (such as Jacobi, Gauss-Seidel, JOR, SOR, SLOR) are introduced. Convergence behavior and the calculation of relaxation parameters are considered. Hybrid iterative methods: Chebyshev acceleration, conjugate gradients and Lanczos are reviewed. Preconditioning is discussed, and variants, such as bi-CG and CGS as well as their convergence behavior are examined. ESA

N89-20725# Technische Univ., Delft (Netherlands). Faculty of Technical Mathematics and Informatics.
HIGH PERFORMANCE PRECONDITIONING
Henk A. vanderVorst 1988 19 p
(Rept-88-54; ISSN-0920-8577; ETN-89-94021) Copyright Avail: NTIS HC A03/MF A01

Discretization of second order elliptic PDE over 3-D rectangular regions is discussed. Vector and parallel aspects of the so-called incomplete LU decompositions, which are among the most frequently used preconditioners are considered. Since the problems with respect to vector or parallel execution are similar for both the symmetric and the nonsymmetric case, and since the preconditioners do not depend on the basic iteration method, only the most simple case, namely the preconditioned conjugate gradients algorithm for symmetric positive definite systems is studied. However, most of the ideas outlined can be carried over immediately to the other situations (including SSOR and Gauss-Seidel preconditioning or smoothing). It is shown that, especially in the 3-D case, the preconditioned algorithm can be implemented by vectorized code, which takes as much CPU-time per iteration step as the unpreconditioned version. As preconditioning usually reduces significantly the number of iteration

steps, this reduction then immediately translates to a similar reduction in CPU-time. ESA

N89-20726# Technische Univ., Delft (Netherlands). Faculty of Technical Mathematics and Informatics.
RIEMANNIAN GEOMETRY ON FAMILIES OF LINEAR SYSTEMS, THE DETERMINISTIC CASE
Bernard Hanzon 1988 66 p
(Rept-88-62; ISSN-0920-8577; ETN-89-94027) Copyright Avail: NTIS HC A04/MF A01

The geometry of families of linear systems in linear system identification and in parametrization of linear systems is considered. It is argued that besides knowledge of the topology one needs also knowledge of the Riemannian geometry of such families. Natural candidates for such a Riemannian geometry are presented, for families of i/o-stable systems with fixed McMillan degree. It turns out that they can be determined by straightforward matrix calculations, which involve solving for Lyapunov equations. For a special case the Riemannian geometry and the corresponding inner metric is completely determined. For the general case, a group of isometries is presented. It is shown that popular canonical forms like the observability and controllability canonical forms behave badly in the sense that the Riemannian metric tensor degenerates, in the neighborhood of systems with smaller McMillan degree. The state bundle over a family of linear systems of fixed order is emphasized. ESA

N89-20727# Technische Univ., Delft (Netherlands). Faculty of Technical Mathematics and Informatics.
AN EFFICIENT METHOD FOR SOLVING FREE-BOUNDARY PROBLEMS
R. M. S. M. Schulkes and C. Cuvelier 1988 21 p
(Rept-88-63; ISSN-0920-8577; ETN-89-94028) Copyright Avail: NTIS HC A03/MF A01

It is shown how the influence of the unknown position of the free boundary can be reduced to the free boundary itself. This leads to an attractive numerical procedure for solving free-boundary problems, called total linearization (TL). The method is used to solve a capillary free boundary problem and numerical properties of the method are investigated. In certain situations the convergence rate is not quadratic, but the iterative procedure as defined by the TL method converges significantly faster than the linearly converging Trial method. The radius of convergence of the TL method is determined by the boundary conditions of the free boundary problem; it can be prohibitively small for certain boundary conditions. In general the TL method provides an efficient procedure for solving the capillary free boundary problem. ESA

N89-20728# Sheffield Univ. (England). Dept. of Control Engineering.
SPECTRAL ANALYSIS OF BLOCK STRUCTURED NONLINEAR SYSTEMS
S. A. Billings and K. M. Tsang Feb. 1988 19 p
(RR-329; ETN-89-94072) Avail: NTIS HC A03/MF A01

A unified identification theory for nonlinear systems which can be represented by cascade, multiplicative, and feedback connections of linear dynamic and static nonlinear subsystems is presented. It is shown that such systems can be identified in terms of the individual component subsystems often using very simple extensions of the well known correlation and spectral analysis algorithms. However, results show that while classical correlation and spectral analysis are excellent for analyzing linear systems they must be applied with caution to systems with nonlinear characteristics. Averaging can be exploited to make certain nonlinear effects go to zero for certain classes of input. Classical correlation or spectral analysis for cascade systems for example yields estimates which are, apart from a scale factor, quite independent of the nonlinear characteristics. The nonlinearity, no matter how severe, becomes invisible with this type of analysis, it averages out to zero. The danger is that the extension of linear averaging techniques to nonlinear systems can lead to a totally false interpretation of the results, all the more severe if the analyst has only one set of data to study because experimentation on the process is expensive. It is easy in such a situation to come to a totally misleading conclusion because certain terms average out for that particular input. ESA

N89-20729# Sheffield Univ. (England). Dept. of Control Engineering.
THE RELATIONSHIP BETWEEN AN ORTHOGONAL ESTIMATION ALGORITHM AND OTHER LEAST SQUARES ROUTINES
W. Luo and S. A. Billings Mar. 1988 19 p
(RR-331; ETN-89-94073) Avail: NTIS HC A03/MF A01

An orthogonal parameter estimation algorithm based on a recurrence decomposition for stochastic nonlinear system identification is outlined. This method is compared with algorithms which utilize the information matrix X'X and other routines based on the regression matrix X. Procedures which could improve the present algorithm are also discussed. ESA

N89-20730# Sheffield Univ. (England). Dept. of Control Engineering.
IDENTIFICATION OF MIMO NONLINEAR SYSTEMS USING A FORWARD-REGRESSION ORTHOGONAL ESTIMATOR
S. A. Billings, S. Chen, and M. J. Korenberg Jun. 1988 38 p
(Grant SERC-GR/D/30587)
(RR-333; ETN-89-94075) Avail: NTIS HC A03/MF A01

An orthogonal least squares estimator, originally derived for single-input single-output systems, is extended to multi-input multi-output nonlinear systems. The estimator can provide information about the structure, or which terms to include in the model, and final parameter estimates in a very simple and efficient manner. Multivariable nonlinear model validity tests are discussed, and the results of applying the orthogonal estimator to both simulated and real data are included. It is shown that this estimator efficiently combines structure determination with parameter estimation and, when coupled with model validity tests, is particularly powerful in identifying parsimonious models for structure-unknown systems. ESA

N89-20731# Sheffield Univ. (England). Dept. of Control Engineering.
NONLINEAR INPUT-OUTPUT MAPS FOR BILINEAR SYSTEMS AND STABILITY
B. Chanane and S. P. Banks Jun. 1988 15 p
(RR-335; ETN-89-94077) Avail: NTIS HC A03/MF A01

Two nonlinear input-output representations of bilinear systems are presented. Sufficient conditions for L sup inf stability are derived. These representations compare favorably with the standard Volterra series representation. ESA

N89-20732# Sheffield Univ. (England). Dept. of Control Engineering.
REALIZATION AND GENERALIZED FREQUENCY RESPONSE FOR NONLINEAR INPUT-OUTPUT MAPS
B. Chanane and S. P. Banks Jul. 1988 19 p
(RR-336; ETN-89-94078) Avail: NTIS HC A03/MF A01

A realization theory and generalized frequency response for an input-output map are presented. Relations with the realization of finite Volterra series are outlined. A simple example shows that the representations have improved convergence properties. ESA

N89-20733# Sheffield Univ. (England). Dept. of Control Engineering.
SPECTRAL ANALYSIS FOR NONLINEAR SYSTEMS. PART 1: PARAMETRIC NONLINEAR SPECTRAL ANALYSIS
S. A. Billings and K. M. Tsang Jul. 1988 32 p
(Grant SERC-GR/D/75809)
(RR-337; ETN-89-94079) Avail: NTIS HC A03/MF A01

A methodology for identifying the generalized frequency response functions of a wide class of nonlinear system is presented. The method consists of estimating the parameters in a NARMAX model description of the system and then computing the generalized frequency response functions directly from the estimated model. Although the derivation of the algorithms often

involves complex mathematics the final procedures that are implemented are particularly simple, and are both easy to use and interpret. While other more sophisticated algorithms were developed to provide alternative solutions to the problems posed, the combination of the orthogonal estimator and the probing algorithm provides a powerful toolkit for the analysis of nonlinear systems in the frequency domain. The methods are upwardly extendable to multi-input multi-output systems. ESA

N89-20734# Groningen Rijksuniversiteit (Netherlands). Dept. of Mathematics and Computing Science.
COMMAND ALGEBRAS, RECURSION AND PROGRAM TRANSFORMATION
Wim H. Hesselink 1988 63 p
(CS-8812; ETN-89-94161) Avail: NTIS HC A04/MF A01

Dijkstra's language of guarded commands is extended with recursion and transformed into algebra. The semantics is expressed in terms of weakest preconditions and weakest liberal preconditions. Extreme fixed points are used to deal with recursion. Unbounded nondeterminacy is allowed. The algebraic setting enables efficient transformation rules for recursive procedures to be developed. The main result is an algebraic version of the rule of computational induction. In this version, certain parts of the programs are restricted to finite nondeterminacy. It is shown that without this restriction the rule would not be valid. Applications of the rule are presented. ESA

N89-20735# Groningen Rijksuniversiteit (Netherlands). Dept. of Mathematics.
A FINITE ELEMENT STABILITY ANALYSIS FOR THE MARANGONI PROBLEM IN A RECTANGULAR CONTAINER WITH RIGID SIDEWALLS
A. I. vandeVooren and H. A. Dijkstra 1988 38 p Sponsored in part by the Netherlands Technology Foundation
(TW-285; ETN-89-94162) Avail: NTIS HC A03/MF A01

A two-dimensional rectangular box partially filled with a fluid containing a solute which evaporates at the upper surface is analyzed. The system is considered under zero-gravity. For sufficiently large Marangoni number the quiescent state becomes unstable due to surface tension effects. By aid of a Galerkin method using splines the eigenvalues and eigenvectors of the linearized system are determined. Each eigenvalue corresponds to a critical Marangoni number for a certain mode (eigenvector). The eigenvalues were investigated as functions of the aspect ratio of the box. Two different symmetries are possible for the modes and it is shown that only eigenvalues pertaining to modes of different symmetry can coincide. ESA

N89-20736# Groningen Rijksuniversiteit (Netherlands). Dept. of Mathematics and Computing Science.
TOWARD A QUASI-PERIODIC BIFURCATION THEORY
B. L. J. Braaksma, H. W. Broer, and G. B. Huitema 1988 62 p Sponsored in cooperation with the Conselho Nacional de Pesquisas, Sao Jose des Campos, Brazil
(Grant ZWO-10-70-10)
(ZW-8803; ETN-89-94166) Avail: NTIS HC A04/MF A01

A normal form theory is given near a nonhyperbolic invariant torus in a vector field which is not necessarily integrable, but which does have an equivariant normal derivative. This theory is formal in the normal directions and involves an induction process on the successive terms of the Taylor expansion in these directions. At each step of this process a small divisor problem has to be solved: on the level of Fourier series the normal form transformations have to converge. A Lie algebra approach is used. As a consequence of this theory, up to small divisor conditions, formal integrability for the vector field is obtained. The normalized Taylor series may even be equivariant with respect to a torus-group of higher dimension, depending on its normal linear part. Models for a quasi-periodic bifurcation theory are suggested: up to generic conditions, in the normal direction formulas similar to the saddle-node, the period-doubling, and the Hopf bifurcation are found. ESA

N89-20737# Center for Mathematics and Computer Science, Amsterdam (Netherlands). Dept. of Software Technology.
ARITHMETIC CLASSIFICATION OF PERFECT MODELS OF STRATIFIED PROGRAMS
Krzysztof R. Apt and Howard A. Blair (Syracuse Univ., NY.) Mar. 1988 16 p
(CWI-CS-R8810; B8821068; ETN-89-94171) Copyright Avail: NTIS HC A03/MF A01

The recursion theoretic complexity of the perfect (Herbrand) models of stratified logic programs is studied. It is shown that these models lie arbitrarily high in the arithmetic hierarchy. A byproduct is a similar characterization of the recursion theoretic complexity of the set of consequences in a number of formalisms for nonmonotonic reasoning. Under some circumstances this complexity can be brought down to recursive enumerability. ESA

N89-20738# Center for Mathematics and Computer Science, Amsterdam (Netherlands). Dept. of Applied Mathematics.
UNIFORM ASYMPTOTIC EXPANSIONS OF A CLASS OF INTEGRALS IN TERMS OF MODIFIED BESSEL FUNCTIONS, WITH APPLICATION TO CONFLUENT HYPERGEOMETRIC FUNCTIONS
N. M. Temme Mar. 1988 22 p
(CWI-AM-R8806; B8817050; ETN-89-94177) Copyright Avail: NTIS HC A03/MF A01

The integral F lambda (z, alpha) = the integral between 0 and infinity t sup (lambda-1) e sup (-zt -alpha/t) ft (dt) is considered for large values of z; alpha and lambda are uniformity parameters in (0, inf). The asymptotic expansion is given in terms of the modified Bessel function K lambda (2 sqrt alpha z). The asymptotic nature of the expansion is discussed and error bounds are constructed for the remainders in the expansions. An example for confluent hypergeometric or Whittaker functions is given. In this example the integrals are transformed to standard forms and the mappings are investigated. ESA

N89-20739# Center for Mathematics and Computer Science, Amsterdam (Netherlands). Dept. of Numerical Mathematics.
MATRIX DEPENDENT PROLONGATIONS AND RESTRICTIONS IN A BLACK BOX MULTIGRID SOLVER
P. M. deZeeuw Feb. 1988 30 p Submitted for publication
(CWI-NM-R8801; B8821059; ETN-89-94178) Copyright Avail: NTIS HC A03/MF A01

Multigrid methods are studied for the solution of linear systems resulting from the nine point discretization of a general linear second order elliptic partial differential equation in two dimensions. The rate of convergence of standard multigrid methods often deteriorates when the coefficients in the differential equation are discontinuous, or when dominating first order terms are present. These difficulties may be overcome by choosing the prolongation and restriction operators in a special way. A way to do this is proposed. As a result, a black box solver (written in standard FORTRAN 77) was developed. Numerical experiments for hard test problems are described and comparison is made with other algorithms: the standard MG method and a method introduced by Kettler. A significant improvement of robustness and efficiency is found. ESA

N89-20740# Center for Mathematics and Computer Science, Amsterdam (Netherlands). Dept. of Numerical Mathematics.
THE USE OF SMOOTHING TECHNIQUES IN THE METHOD OF LINES
P. J. vanderHouwen and B. P. Sommeijer Mar. 1988 9 p
(CWI-NM-R8802; B8821061; ETN-89-94179) Copyright Avail: NTIS HC A02/MF A01

A space discretization method for parabolic partial differential equations which is based on conventional discretization techniques and smoothing matrices is described. The method leads to systems of ordinary differential equations (ODE) which are considerably less stiff than the ODEs obtained by conventional discretization methods. It turns out that the stiffness is reduced to an extent that ordinary predictor-corrector methods become feasible

integration methods. Experiments illustrate this type of space discretization method. ESA

N89-20741# Center for Mathematics and Computer Science, Amsterdam (Netherlands). Dept. of Numerical Mathematics.
A NUMERICAL STUDY OF THREE MOVING GRID METHODS FOR ONE-DIMENSIONAL PARTIAL DIFFERENTIAL EQUATIONS WHICH ARE BASED ON THE METHOD OF LINES
R. M. Furzeland (Koninklijke/Shell-Lab., Amsterdam, Netherlands), J. G. Verwer, and P. A. Zegeling Jun. 1988 36 p Submitted for publication
(Contract STW-CWI55.092)
(CWI-NM-R8806; B8827437; ETN-89-94183) Copyright Avail: NTIS HC A03/MF A01

Three Lagrangian-based moving grid methods for systems of 1-D time-dependent partial differential equations were compared to assess which method offers the best prospects for reliable, efficient, and robust method of lines (MOL) application, with as little user intervention as possible. Method 1 is the finite difference method of Petzold (1987). Method 2 is a finite difference method based on the semidiscrete Lagrangian form. Method 3 is the finite element method of Miller et al (1981, 1983). Method 2 is preferred. It is easier to work with and to implement than Method 3 and also more efficient. The grid movement of Method 2 is directly attached to equidistribution in space of a chosen monitor function. This approach provides a better and more unique way of automatically adjusting the grid to large spatial gradients. An important feature of the approach of Method 2 is the grid smoothing capability. Although this involves two method parameters, the choice of these parameters is not troublesome. Method 1 is not recommended for general use. ESA

N89-20742# Center for Mathematics and Computer Science, Amsterdam (Netherlands). Dept. of Mathematical Statistics.
ESTIMATING A REGRESSION FUNCTION
Sara A. vandeGeer (Bristol Univ., England) Jun. 1988 22 p
(CWI-MS-R8805; B8827732; ETN-89-94188) Copyright Avail: NTIS HC A03/MF A01

An entropy approach is proposed to establish rates of convergence for estimators of a regression function. General regression problems are considered, with linear regression, splines, and isotonic regression as special cases. The estimation methods studied are least squares, minimum L1-norm, and penalized least squares. Common features of these methods and various regression problems are highlighted. ESA

N89-20743# Center for Mathematics and Computer Science, Amsterdam (Netherlands). Dept. of Operations Research and System Theory.
WAITING-TIME APPROXIMATIONS FOR CYCLIC-SERVICE SYSTEMS WITH MIXED SERVICE STRATEGIES
W. P. Groenendijk Jan. 1988 14 p Submitted for publication
(CWI-OS-R8802; B8813493; ETN-89-94190) Copyright Avail: NTIS HC A03/MF A01

An approximation method for mean waiting times in cyclic-service systems with a mixture of exhaustive/gated/1-limited service strategies is presented. The method provides a unification and generalization of known good approximations for single strategies. The results of an exact analysis of the two-queue case where one queue is served exhaustively and the other queue 1-limited, support the approximation idea. ESA

N89-20744# Center for Mathematics and Computer Science, Amsterdam (Netherlands). Dept. of Operations Research and System Theory.
STATE REPRESENTATIONS OF LINEAR SYSTEMS WITH OUTPUT CONSTRAINTS
J. M. Schumacher Mar. 1988 19 p Submitted for publication
(CWI-OS-R8807; B8813498; ETN-89-94192) Copyright Avail: NTIS HC A03/MF A01

Representations in state space form are derived for linear systems that are described by input/state/output equations, and that are subjected to a number of constant linear constraints on the outputs. In the case of a linear system without further structure, the state representation of the constrained system turns out to be essentially nonunique in general. For linear Hamiltonian systems, however, there is a natural choice of the representation which preserves the Hamiltonian structure, and which leads to a unique solution (under a certain nondegeneracy condition). A by-product is an algebraic proof of the rule: a system with n degrees of freedom under k constraints becomes a system with n-k degrees of freedom. Similar results are obtained for linear systems with a gradient structure. ESA

N89-20745# Center for Mathematics and Computer Science, Amsterdam (Netherlands). Dept. of Pure Mathematics.
A SHORT TUTORIAL ON LIE ALGEBRAS
Michiel Hazewinkel Jan. 1988 13 p
(CWI-PM-R8802; B8817046; ETN-89-94195) Copyright Avail: NTIS HC A03/MF A01

Terms encountered in Lie algebra are defined. Homomorphisms, isomorphisms, subalgebras, and ideals are illustrated. Lie algebras of vector fields are introduced. Simple, nilpotent, and solvable algebras are discussed. Representations, including the adjoint representation, are treated. Lie groups are mentioned. ESA

N89-20746# Center for Mathematics and Computer Science, Amsterdam (Netherlands). Dept. of Pure Mathematics.
A TUTORIAL INTRODUCTION TO DIFFERENTIABLE MANIFOLDS AND CALCULUS ON MANIFOLDS
Michiel Hazewinkel Jan. 1988 28 p
(CWI-PM-R8803; B8817047; ETN-89-94196) Copyright Avail: NTIS HC A03/MF A01

The basic definitions and concepts of differentiable manifolds are illustrated. Differentiable vector bundles are introduced. Vector fields are considered. Riemann manifolds are presented. Calculus on manifolds is outlined. ESA

N89-20747# Center for Mathematics and Computer Science, Amsterdam (Netherlands). Dept. of Mathematical Statistics.
ASYMPTOTIC NORMALITY OF MINIMUM L SUB 1 NORM ESTIMATORS IN LINEAR REGRESSION
Sara A. vandeGeer (Bristol Univ., England) Jun. 1988 8 p
(CWI-MS-R8806; B8827733; ETN-89-94199) Copyright Avail: NTIS HC A02/MF A01

It is shown that the minimum L1-norm estimator in linear regression is asymptotically normal with covariance matrix proportional to the inverse of the covariance matrix of the regressors. The method of proof uses asymptotic equicontinuity of Vapnik-Chervonekis graph classes of functions. ESA

N89-20748# International Centre for Theoretical Physics, Trieste (Italy).
NONLINEAR PARTIAL DIFFERENTIAL EQUATIONS ON HOMOGENEOUS SPACES
Metin Gurses, O. Oguz, and S. Salihoglu (Istanbul Univ., Turkey) Aug. 1988 31 p
(DE88-705342; IC-88/192) Avail: NTIS (US Sales Only) HC A03/MF A01

The work of A.K.N.S. which is based on the s1(2,R) valued soliton connection is extended to obtain new integrable coupled nonlinear partial differential equations. This is achieved by assuming the soliton connection having values in a semisimple Lie, Kac-Moody, Lie super algebras. Extensions of some of the integrable nonlinear p.d.e's are given explicitly. In particular the coupled NLS equations on various homogeneous spaces and the coupled modified KdV equations are obtained on symmetric spaces. DOE

N89-20749# International Centre for Theoretical Physics, Trieste (Italy).
SECOND ORDER DEGENERATE ELLIPTIC EQUATIONS
Duong Minh Duc Aug. 1988 22 p Submitted for publication
(DE88-705347; IC-88/203) Avail: NTIS (US Sales Only) HC A03/MF A01

Using an improved Sobolev inequality we study a class of

elliptic operators which is degenerate inside the domain and strongly degenerate near the boundary of the domain. Our results are applicable to the L(sup 2)-boundary value problem and the mixed boundary problem. DOE

N89-20750# International Centre for Theoretical Physics, Trieste (Italy).
IRREDUCIBLE FINITE-DIMENSIONAL REPRESENTATIONS OF THE LIE SUPERALGEBRA gl(n/1) IN A GELFAND-ZETLIN BASIS
Tchavdar D. Palev Aug. 1988 21 p
(DE88-705350; IC-88/207) Avail: NTIS (US Sales Only) HC A03/MF A01

All finite-dimensional irreducible representations of the general linear Lie superalgebra gl(n/1) are studied. For each representation a concept of a Gelfand-Zetlin basis is defined. Expressions for the transformation of the basis under the action of the generators are written down. DOE

N89-20751# Texas Univ., Austin. Inst. for Fusion Studies.
APPLICATION OF NEWTON'S METHOD TO LAGRANGIAN DYNAMICAL SYSTEMS
Hyung-tae Kook and James D. Meiss 3 Jan. 1989 19 p
(Contract DE-FG05-80ET-53088)
(DE89-007024; DOE/ET-53088/358; IFSR-358) Avail: NTIS HC A03/MF A01

An algorithm for Newton's method is presented to find periodic orbits for N degree-of-freedom Lagrangian mappings. The computation time of the method is proportional to n, the period of the orbit, and the required storage space is reduced to omicron(n). The construction of the algorithm is based upon block-diagonalization of the Hessian matrix of the action function. The index of the action function, which is closely related to orbital stability, is obtained during execution of the algorithm. DOE

N89-20752# Argonne National Lab., IL. Mathematics and Computer Science Div.
ON AUTOMATIC DIFFERENTIATION
Andreas Griewank 1988 27 p Presented at the 13th International Symposium on Mathematical Programming, Tokyo, Japan, 29 Aug. 1988
(Contract W-31-109-eng-38)
(DE89-005779; CONF-8808190-1) Avail: NTIS HC A03/MF A01

In comparison to symbolic differentiation and numerical differencing, the chain rule based technique of automatic differentiation is shown to evaluate partial derivatives accurately and cheaply. In particular it is demonstrated that the reverse mode of automatic differentiation yields any gradient vector at no more than five times the cost of evaluating the underlying scalar function. After developing the basic mathematics we describe several software implementations and briefly discuss the ramifications for optimization. DOE

N89-20753# Joint Inst. for Nuclear Research, Dubna (USSR).
COMBINED ALGORITHMS IN NONLINEAR PROBLEMS OF MAGNETOSTATICS
M. Gregus, B. N. Khoromsky, G. E. Mazurkevich, and E. P. Zhidkov May 1988 14 p Presented at BEM-10: 10th Boundary Element Meeting, Southampton, United Kingdom, 6 Sep. 1988
(DE89-006591; JINR-E-11-88-481; CONF-880974-2) Avail: NTIS (US Sales Only) HC A03

To solve boundary problems of magnetostatics in unbounded two- or three-dimensional regions, we construct combined algorithms based on a combination of the method of boundary integral equations with the grid methods. We study the question of substantiation of the combined method in nonlinear magnetostatic problems without the preliminary discretization of equations and give some results on the convergence of iterative processes that arise in nonlinear cases. We also discuss economical iterative processes and algorithms that solve boundary integral equations on certain surfaces. Finally, examples of numerical solutions of magnetostatic problems that arose when modelling the fields of electrophysical installations are given, too. DOE

N89-20754# Sandia National Labs., Albuquerque, NM. Exploratory Radar Development Div.
QUANTIZATION ANALYSIS OF THE REAL-TIME SAR DIGITAL IMAGE FORMATION PROCESSOR
Neeraj Magotra Dec. 1988 70 p
(Contract DE-AC04-76DP-00789)
(DE89-007533; SAND-88-3204) Avail: NTIS HC A04/MF A01

This report presents a quantization analysis of the digital image formation processor (IFP) of a linear-FM synthetic aperture radar (SAR). The IFP is configured as a patch processor and forms the final image by performing a two dimensional Fast Fourier Transform (FFT). The quantization analysis examines the effects of using fixed precision arithmetic in the image formation process. Theoretical bounds for the worst-case errors introduced by using fixed point arithmetic and experimental results verifying the theoretical bounds are presented. DOE

N89-20755# Cornell Univ., Ithaca, NY. Dept. of Theoretical and Applied Mechanics.
HARTFEM: A FINITE ELEMENT PROGRAM FOR THERMAL AND VISCOPLASTIC DEFORMATION PROBLEMS
Vinod K. Banthia 1989 79 p
(Contract DE-FG02-84ER-45055)
(DE89-007788; DOE/ER-45055/14) Avail: NTIS HC A05/MF A01

The objective of this report is to give a compact summary, and guide for study, of the theoretical basis of the finite element computer program HARTFEM. Here we summarize the capabilities of the program, its structure and the methods and assumptions used in the program. Only highlights of the methods are described here. A reference list, where more detailed descriptions can be obtained, is provided at the end of the report. The main feature of the program is its capability of modelling time-dependent material deformation at high temperatures using the state variable model due to Hart. Apart from deformation modelling, the program is also capable of solving steady state and transient heat conduction problems. A coupled thermoelastic problem can also be solved. Field problems (e.g., seepage, fluid flow, electric conduction, etc.) that are governed by equations similar to that of heat conduction can also be solved with slightly different interpretation of the variables. DOE

N89-20756# Oak Ridge National Lab., TN. Engineering Physics and Mathematics Div.
PARABOLIC SYSTEMS WITH NONLINEAR COMPETITIVE INTERACTIONS
C. Cosner, S. Lenhart (Tennessee Univ., Knoxville.), and V. Protopopescu Jan. 1989 21 p
(Contract DE-AC05-84OR-21400)
(DE89-007814; ORNL/TM-11071) Avail: NTIS HC A03/MF A01

A parabolic system with nonlinear local or nonlocal interactions is considered, with specific applications to the description of competition/combat situations. Global existence and comparison results are proven under suitable assumptions on the interaction terms. Comparisons with solutions of the equivalent ordinary differential (space independent) model, that has been previously used in modelling combat are of special interest. The stationary state of such a system (corresponding to a stalemate) is also considered. Under certain conditions on the interaction, domain size and boundary conditions, a uniqueness result is obtained for the stationary state. A simple example shows that these conditions are sharp and uniqueness may be lost when they are not fulfilled. DOE

N89-20757# Oak Ridge National Lab., TN. Mathematical Sciences Section.
PARALLEL DIRECT SOLUTION OF SPARSE LINEAR SYSTEMS

Esmond Ng Jan. 1989 23 p
(Contract DE-AC05-84OR-21400)
(DE89-007855; ORNL/TM-11045) Avail: NTIS HC A03/MF A01

In this paper the direct solution of sparse linear systems on multiprocessor systems is considered. Elimination trees are used as a tool for identifying and exploiting parallelism in the parallel numerical factorization of the coefficient matrix. Some open problems are described and results of some numerical experiments are provided. DOE

N89-20758# Oak Ridge National Lab., TN. Mathematical Sciences Section.
A FAST ALGORITHM FOR REORDERING SPARSE MATRICES FOR PARALLEL FACTORIZATION
John G. Lewis, Barry W. Peyton, and Alex Pothen (Pennsylvania State Univ., University Park.) Jan. 1989 45 p
(Contract DE-AC05-84OR-21400)
(DE89-007873; ORNL/TM-11040) Avail: NTIS HC A03/MF A01

Jess and Kees introduced a method for ordering a sparse symmetric matrix A for efficient parallel factorization. The parallel ordering is computed in two steps. First, the matrix A is ordered by some fill-reducing ordering. Second, a parallel ordering of A is computed from the filled graph that results from factoring A using the initial fill-reducing ordering. Among all orderings whose fill lies in the filled graph, this parallel ordering achieves the minimum number of parallel steps in the factorization of A. Jess and Kees did not specify the implementation details of an algorithm for either step of this scheme. Liu and Mirzaian (1987) designed an algorithm implementing the second step, but it has time and space requirements higher than the cost of computing common fill-reducing orderings. We present here a new fast algorithm that implements the parallel ordering step by exploiting the clique tree representation of a chordal graph. We succeed in reducing the cost of the parallel ordering step well below that of the fill-reducing step. Our algorithm has time and space complexity linear in the number of compressed subscripts of L, i.e., the sum of the sizes of the maximal cliques of the filled graph. Empirically we demonstrate running times nearly identical to Liu's heuristic Composite Rotations algorithm that approximates the minimum number of parallel steps. DOE

N89-20759# Oak Ridge National Lab., TN. Engineering Physics and Mathematics Div.
TWO DIMENSIONAL MAPS GENERATED BY COMPETITIVE SYSTEMS
Y. Y. Azmy and V. Protopopescu Feb. 1989 35 p
(Contract DE-AC05-84OR-21400)
(DE89-007878; ORNL/TM-11026) Avail: NTIS HC A03/MF A01

By discretizing time and space in a partial differential equation (PDE) model for competitive systems, we derive the corresponding discrete maps. We analyze these maps from an analytical and numerical viewpoint with emphasis on the military interpretation of the system. For the one-species map, we study the effect of convection on the bifurcation behavior and we find periodic solutions. For the two-species map, we limit our analysis to an illustrative example, but we indicate the general procedure. DOE

N89-20760# California Univ., Davis. Dept. of Electrical and Computer Engineering.
DEVELOPMENT OF MATHEMATICAL MODELS FOR APPLICATION IN IMAGE PROCESSING Final Report, 15 Mar. 1982 - 30 Sep. 1987
Anil K. Jain Apr. 1988 29 p
(Contract DAAG29-82-K-0077)
(AD-A203619; ARO-18532.7-EL) Avail: NTIS HC A03/MF A01 CSCL 12E

This is the final report for ARO research grant DAAG29-82-K-0077 for the period of March 1982 to September 1987. Research was conducted on several topics on image processing with special emphasis on mathematical modeling. Research topics include: two-dimensional stochastic models for images, two-dimensional spectral factorization and spectral estimation, Radon transform theory for random fields, image data compression, image analysis and shape inspection based on contour processing using spline functions, pattern inspection based on mathematical morphology, Radon transform based image processing algorithms, and VLSI architectures of image processing and computer vision algorithms. A brief summary of results obtained together with a list of publications and theses is included. GRA

N89-20761# Army Missile Command, Redstone Arsenal, AL. Advanced Sensors Directorate.
USING RANDOM NUMBER GENERATORS ON THE SENSOR SIGNAL PROCESSING SYSTEM Interim Technical Report, 1988
Jonathan A. Mills Jun. 1988 12 p
(AD-A203702; AD-E951251; AMSMI/TR-RD-AS-88-9) Avail: NTIS HC A03/MF A01 CSCL 12F

This report describes the use of three random number generators installed on the SSPS VAX 11/785. There are three random number generators: a uniform (URAND), normal (ANRMRN), and exponential (EXPRN). GRA

N89-20762# Colorado Univ., Boulder. Dept. of Computer Science.
SEQUENTIAL AND PARALLEL METHODS FOR UNCONSTRAINED OPTIMIZATION
Robert B. Schnabel 20 Oct. 1988 40 p
(Contract DAAL03-88-K-0086)
(AD-A203807; CU-CS-414-88; ARO-24923.2-MA) Avail: NTIS HC A03/MF A01 CSCL 12D

This paper reviews some interesting recent developments in the field of unconstrained optimization. First we discuss some recent research regarding secant (quasi-Newton) methods. This includes analysis that has led to an improved understanding of the comparative behavior of the BFGS, DFP, and other updates in the Broyden class, as well as computational and theoretical work that has led to a revival of interest in the symmetric rank one update. Second we discuss recent research in methods that utilize second derivatives. We describe tensor methods for unconstrained optimization, which have achieved considerable gains in efficiency by augmenting the standard quadratic model with low rank third and fourth order terms, in order to allow the model to interpolate some function and gradient information from previous iterations. Finally, we will review some work that has been done in constructing general purpose methods for solving unconstrained optimization problems on parallel computers. This research has led to a renewed interest in various ways of performing the linear algebra computations in secant methods, and to new algorithms that make use of multiple concurrent function evaluations. GRA

N89-20763# Naval Postgraduate School, Monterey, CA.
PSEUDO-BAYESIAN STABILITY OF CSMA (CARRIER SENSE MULTIPLE ACCESS) AND CSMA/CD (COLLISION DETECTION) LOCAL AREA NETWORKS M.S. Thesis
Murat A. Boyana Dec. 1988 66 p
(AD-A203834) Avail: NTIS HC A04/MF A01 CSCL 12G

This thesis investigates the stability of the random multiaccess protocols, slotted Carrier Sense Multiple Access (CSMA) and slotted CSMA/Collision Detection(CD), utilizing one power level and two power levels to create beneficial power capture effect. Use of more than two equally spaced power levels provides no significant improvement in the throughout achievable when realistic capture thresholds are considered. The investigation centers on a technique known as pseudo-Bayesian stability. Another task of this thesis is to stabilize multi-channel slotted CSMA and slotted CSMA/CD with pseudo-Bayesian technique. The multichannel slotted CSMA and slotted CSMA/CD show a large improvement in throughput over a traditional single channel with a combined bit rate. GRA

N89-20764# Air Force Inst. of Tech., Wright-Patterson AFB, OH. School of Engineering.
THE INITIAL VALUE PROBLEM FOR FRACTIONAL ORDER DIFFERENTIAL EQUATIONS WITH CONSTANT COEFFICIENTS Final Report, Jun. 1987 - Jun. 1988
Ronald L. Bagley 30 Sep. 1988 83 p
(AD-A203843; AFIT-TR-EN-88-1) Avail: NTIS HC A05/MF A01 CSCL 13M

Systems of fractional order differential equations are constructed to solve for viscoelastically damped structural motion. To reduce computational effort the equations of motion are cast as an initial value problem where the history dependence is approximated by retaining events only from the recent past. Several strong parallels arise with ordinary, linear differential equations. These parallels plus the well-posed nature of the fractional order differential equations leads one to view the fractional order initial value problem as an extension of the theory of ordinary, linear differential equations with constant coefficients. GRA

65 STATISTICS AND PROBABILITY

Includes data sampling and smoothing; Monte Carlo method; and stochastic processes.

N89-20765# Technische Univ., Delft (Netherlands). Faculty of Technical Mathematics and Informatics.
DETECT: DEPENDENCY TREE EVALUATION AND CONFIDENCE TEST
Roger Cooke, Jan vanNoortwijk, and Rudi Waij 1988 64 p
(Rept-88-55; ISSN-0920-8577; ETN-89-94022) Copyright Avail: NTIS HC A04/MF A01

A user guide for the DETECT program, which performs Monte Carlo simulation and can model dependencies, is presented. The Monte Carlo simulation of dependence between two variables each uniformly distributed over the interval (0,1), and other possible distributions are discussed. The dependency tree and the dependency list, representing the dependencies between more than two variables, are discussed. The input of formula, theta, and the entire simulation process are described. The assessed distribution of theta and its confidence bounds are discussed. The input, output, and distribution files are considered. Two examples from practice are given. ESA

N89-20766# Technische Univ., Delft (Netherlands). Faculty of Technical Mathematics and Informatics.
ASYMPTOTIC BEHAVIOR OF RANDOM DISCRETE EVENT SYSTEMS
J. A. C. Resing, R. E. deVries, G. Hooghiemstra, M. S. Keane, and G. J. Olsder 1988 30 p
(Rept-88-56; ISSN-0920-8577; ETN-89-94023) Copyright Avail: NTIS HC A03/MF A01

The asymptotic behavior of discrete event dynamic systems (DEDS) in which the activity times are random variables is analyzed. It shown that a central limit theorem holds for DEDS and consequently that the cycle time of the system is asymptotically normally distributed. ESA

N89-20767# Center for Mathematics and Computer Science, Amsterdam (Netherlands). Dept. of Algorithmics and Architecture.
TWO DECADES OF APPLIED KOLMOGOROV COMPLEXITY. IN MEMORIAM: ANDREI NIKOLAEVICH KOLMOGOROV, 1903 - 1987
Ming Li (Harvard Univ., Cambridge, MA.) and Paul M. B. Vitanyi Apr. 1988 48 p Presented at the 3rd IEEE Structure in Complexity Theory Conference, Washington, DC, Jun. 1988 Submitted for publication
(CWI-CS-R8813; B8821071; ETN-89-94173) Copyright Avail: NTIS HC A03/MF A01

The main ideas of Kolmogorov complexity are introduced, and applications of this elegant notion are reviewed. Application of the fact that some strings are compressible includes a strong version of Godel's incompleteness theorem. Applications of lower bound arguments that rest on the fact that certain strings cannot be compressed at all range from Turing machines to electronic chips. Probability theory and a priori probability applications range from foundational issues to the theory of learning and inductive inference in artificial intelligence. Resource-bounded Kolmogorov complexity applications range from NP-completeness and the P versus NP question, to cryptography. ESA

N89-20768# Center for Mathematics and Computer Science, Amsterdam (Netherlands). Dept. of Software Technology.
THE CERTAINTY FACTOR MODEL AND ITS BASIS IN PROBABILITY THEORY
L. C. vanderGaag Apr. 1988 43 p
(CWI-CS-R8816; B8827440; ETN-89-94174) Copyright Avail: NTIS HC A03/MF A01

The certainty factor model proposed by Shortliffe and Buchanan (1984) for handling uncertainty in rule-based top-down reasoning expert systems is considered. The basic notions of rule-based top-down reasoning expert systems that are used in the model, such as production rules and derivations, are defined to allow a formal description of the model. In this formalization the functions used in the model are extended with the notion of derivation. In the model two basic measures of uncertainty are defined: the measures of belief and disbelief. These measures are defined in terms of a probability set function, and are approximated. It is shown that in some cases these functions respect the probabilistic basis by making rather strong assumptions. In other cases the approximation functions cannot be shown to be consistent with the foundation in probability theory suggested in by Shortliffe and Buchanan. In actual implementations of the certainty factor model the measures of belief and disbelief are not used. A third function derived from these two basic measures is used: the (redefined) certainty factor function. This function is defined in terms of the measures of belief and disbelief. For the purpose of subsequently computing certainty factors again an approximation function is defined. This approximation function respects the definition of the certainty factor function. ESA

N89-20769# Center for Mathematics and Computer Science, Amsterdam (Netherlands). Dept. of Mathematical Statistics.
CENSORING, TRUNCATION AND FILTERING IN STATISTICAL MODELS BASED ON COUNTING PROCESSES
Per Kragh Anderson, Ornulf Borgan, Richard D. Gill, and Niels Keiding (Copenhagen Univ., Denmark) Mar. 1988 39 p
(CWI-MS-R8803; B8827730; ETN-89-94186) Copyright Avail: NTIS HC A03/MF A01

The formulation of statistical models for life history data based on counting processes is reviewed. Examples include survival data with (possibly time-dependent) covariates and continuous time Markov processes. Complete life history data are discussed and explicit modeling of mechanisms causing incomplete information like (right) censoring, filtering, and left truncation is superimposed onto the model for the complete data. The concepts of independent censoring and noninformative censoring are defined, and inference from such models based on (partial) likelihoods is discussed. ESA

66 SYSTEMS ANALYSIS

Includes mathematical modeling; network analysis; and operations research.

N89-20770*# National Aeronautics and Space Administration. Ames Research Center, Moffett Field, CA.
QUEUING THEORY MODELS FOR COMPUTER NETWORKS
David C. Galant Feb. 1989 34 p
(NASA-TM-101056; A-89013; NAS 1.15:101056) Avail: NTIS HC A03/MF A01 CSCL 12B

A set of simple queuing theory models which can model the average response of a network of computers to a given traffic

load has been implemented using a spreadsheet. The impact of variations in traffic patterns and intensities, channel capacities, and message protocols can be assessed using them because of the lack of fine detail in the network traffic rates, traffic patterns, and the hardware used to implement the networks. A sample use of the models applied to a realistic problem is included in appendix A. Appendix B provides a glossary of terms used in this paper. This Ames Research Center computer communication network is an evolving network of local area networks (LANs) connected via gateways and high-speed backbone communication channels. Intelligent planning of expansion and improvement requires understanding the behavior of the individual LANs as well as the collection of networks as a whole. Author

67 THEORETICAL MATHEMATICS

Includes topology and number theory.

N89-20771# Groningen Rijksuniversiteit (Netherlands). Systems and Control Group.
WELL-POSEDNESS OF INFINITE-DIMENSIONAL LINEAR SYSTEMS IN TIME AND FREQUENCY DOMAIN
R. F. Curtain Aug. 1988 43 p Revised
(TW-287; B8827852; ETN-89-94163) Avail: NTIS HC A03/MF A01

It is shown that for a system (C,A,B) on the Hilbert space H to have a well-defined Hankel operator, it is sufficient that A generates a C0-semigroup on H; (A,B) defines a bounded controllability map from L2 (0,T;U) to H, and (C,A) defines a bounded observability map from H to L2 (0,T;Y), where the input and output spaces U and Y are Hilbert spaces. The system is well-posed in time and frequency domain if in addition its generalized transfer function is in H sup inf. This well-posedness concept is used to prove a general theorem on the equivalence of input-output stability and exponential stability for a very large class of infinite-dimensional system. ESA

N89-20772# Groningen Rijksuniversiteit (Netherlands). Systems and Control Group.
ROBUST STABILITY OF NORMALIZED COPRIME FACTORS: THE INFINITE DIMENSIONAL CASE
R. F. Curtain 1988 32 p
(TW-291; ETN-89-94164) Avail: NTIS HC A03/MF A01

The problem of robustly stabilizing a linear system subject to H inf-bounded perturbations in the numerator and the denominator of its normalized left coprime factorizations is considered for a class of infinite dimensional systems. This class has possibly unbounded, finite-rank input and output operators which includes many delay and distributed systems. The optimal stability margin is expressed in terms of the solutions of the control and filter algebraic Riccati equations. ESA

N89-20773# International Centre for Theoretical Physics, Trieste (Italy).
ON HETEROTIC SUPERMANIFOLDS
S. Randjbar-Daemi, A. Salam, and J. Strathdee Aug. 1988 34 p Prepared in cooperation with Imperial Coll. of Science and Technology, London (England).
(DE88-705339; IC-88/180) Avail: NTIS (US Sales Only) HC A03/MF A01

The geometry of heterotic supermanifolds is discussed with particular reference to patching conditions and gauge fixing. Superfield formalism is used and the associated torsion constraints are solved explicitly in an arbitrary gauge, that is without imposing gauge conditions. Finite gauge transformations are constructed. The structure group associated with Wess-Zumino type gauges is obtained and is reduced by further refinements of the gauge conditions up to the stage at which the standard description of the super Riemann surface is recovered. It is shown that any invariant functional of the super 3-bein can depend only on a finite number of parameters, i.e., the moduli and super moduli. Chiral superfields and the structure of action functionals are discussed and, finally the integration measure in supermoduli space is derived by an application of the Faddeev-Popov prescription. DOE

N89-20774# Florida Atlantic Univ., Boca Raton.
SCHEMA-BASED THEORIES OF PROBLEM SOLVING Final Report, 1 Nov. 1987 - 31 Aug. 1988
Stephen K. Reed 21 Oct. 1988 74 p Prepared in cooperation with San Diego State Univ., CA
(Grant AF-AFOSR-0008-88; AF Proj. 2313)
(AD-A203731; AFOSR-89-0055TR) Avail: NTIS HC A04/MF A01 CSCL 05I

The objective of this research is to develop a schema-based model of problem solving to account for how students attempt to solve algebra word problems. One project, consisting of 3 experiments, investigated how students combine examples and procedures (rules) to solve problems. In Experiments 1, subjects rated how useful the solution for one problem would be for solving another problem. Experiment 2 investigated criteria for selecting a good example and showed how the usefulness of an example is determined by the transformational distance from the test problem. Experiment 3 compared 3 groups of students who received either an example, a set of procedures or both in order to evaluate a quantitative model of how students use examples, procedures, and their general knowledge. A second set of experiments investigated whether a detailed comparison of 2 isomorphic problems would result in a more abstract representation of those problems. The results indicated that schema abstraction did not occur for word problems. GRA

70 PHYSICS (GENERAL)

For precision time and time interval (PTTI) see *35 Instrumentation and Photography;* for geophysics, astrophysics or solar physics see *46 Geophysics, 90 Astrophysics,* or *92 Solar Physics.*

N89-20775# Naval Postgraduate School, Monterey, CA.
BREMSSTRAHLUNG RADIATION EFFECTS IN RARE EARTH PERMANENT MAGNETS
Henry B. Luna, Xavier K. Maruyama, Nicholas J. Colella, John S. Hobbs, Robert S. Hornady, Bernhard Kulke, and James V. Palomar (Lawrence Livermore National Lab., CA.) 15 Dec. 1988 21 p Presented at the 10th International Free-Electron Laser Conference, Jerusalem, Israel, 29 Aug. 1988
(Contract W-7405-eng-48)
(DE89-006207; UCRL-100167; CONF-8808146-13) Avail: NTIS HC A03/MF A01

Advances in rare earth permanent magnet (REPM) technology have made possible new applications. Two such applications are the use of permanent magnetic lenses for accelerator and beam transport systems and the expanding use in undulators and wigglers of synchrotron radiation and free electron laser systems. Both applications involve potential exposure of REPM's to high radiation fields. We have investigated the radiation hardness of several different varieties of REPM's up to 2 gigarads of absorbed dose from a mixed electron-photon (bremsstrahlung) field. Sm2Co17, Nd2Fe14B and an experimental REPM, Pr15Fe79B6, from several different manufacturers have been investigated. Of the samples irradiated, Sm2Co17 proved to be the most resistant to bremsstrahlung radiation. However, details of manufacturing techniques produced significantly different results. We observed that REPM's of nominally identical stoichiometric composition from different manufacturers did not show the same rate of remanence loss. We present details of our experiment and absorbed dose modeling and a summary of radiation effects measurements of which we are aware. Our study of these radiation damage experiments lead us to the empirical observation that the order of radiation hardness is Sm2Co17, SmCo5 and Nd2Fe14B, regardless of the source of radiation, i.e., gammas, electrons, protons or neutrons. DOE

71 ACOUSTICS

Includes sound generation, transmission and attenuation. For noise pollution see *45 Environmental Pollution.*

N89-20776*# Sverdrup Technology, Inc., Cleveland, OH.
NOISE GENERATED BY A FLIGHT WEIGHT, AIR FLOW CONTROL VALVE IN A VERTICAL TAKEOFF AND LANDING AIRCRAFT THRUST VECTORING SYSTEM Final Report
Ronald G. Huff Feb. 1989 55 p Prepared in cooperation with Huff (Ronald G.) and Associates, North Olmsted, OH
(Contract NAS3-25266)
(NASA-CR-182232; E-4556; NAS 1.26:182232) Avail: NTIS HC A04/MF A01 CSCL 20A

Tests were conducted in the NASA Lewis Research Center's Powered Lift Facility to experimentally evaluate the noise generated by a flight weight, 12 in. butterfly valve installed in a proposed vertical takeoff and landing thrust vectoring system. Fluctuating pressure measurements were made in the circular duct upstream and downstream of the valve. This data report presents the results of these tests. The maximum overall sound pressure level is generated in the duct downstream of the valve and reached a value of 180 dB at a valve pressure ratio of 2.8. At the higher valve pressure ratios the spectra downstream of the valve is broad banded with its maximum at 1000 Hz. Author

N89-20777*# National Aeronautics and Space Administration. Langley Research Center, Hampton, VA.
ACOUSTIC TEST OF A MODEL ROTOR AND TAIL ROTOR: RESULTS FOR THE ISOLATED ROTORS AND COMBINED CONFIGURATION
R. M. Martin, C. L. Burley, and J. W. Elliott Feb. 1989 73 p
(NASA-TM-101550; NAS 1.15:101550) Avail: NTIS HC A04/MF A01 CSCL 20A

Acoustic data from a model scale main rotor and tail rotor experiment in the NASA Langley 14 by 22 Foot Subsonic Tunnel are presented for the main rotor and trail rotor in isolation and for the two rotors operating together. Results for the isolated main rotor show the importance of the rotor flapping conditions on mid-frequency noise content. High levels of main rotor retreating side blade-vortex interaction noise are shown to radiate downstream of the model. The isolated tail rotor noise results show the dominance of harmonic noise in the thrusting direction. The occurrence of tail rotor broadband noise is seen by the broadening of the tail rotor harmonics and is attributed to fuselage wake turbulence. The combined main and tail rotor data are presented to show the dominance of each rotor's different noise sources at different directivity locations. Author

N89-20778*# National Aeronautics and Space Administration. Langley Research Center, Hampton, VA.
HIGH INTENSITY ACOUSTIC TESTS OF A THERMALLY STRESSED ALUMINUM PLATE IN TAFA
Chung Fai Ng and Sherman A. Clevenson Feb. 1989 42 p
(NASA-TM-101552; NAS 1.15:101552) Avail: NTIS HC A03/MF A01 CSCL 20A

An investigation was conducted in the Thermal Acoustic Fatigue Apparatus at the Langley Research Center to study the acoustically excited random motion of an aluminum plate which is buckled due to thermal stresses. The thermal buckling displacements were measured and compared with theory. The general trends of the changes in resonances frequencies and random responses of the plate agree with previous theoretical prediction and experimental results for a mechanically buckled plate. Author

N89-20779*# National Aeronautics and Space Administration. Lewis Research Center, Cleveland, OH.
UNSTEADY BLADE PRESSURE MEASUREMENTS ON A MODEL COUNTERROTATION PROPELLER
Laurence J. Heidelberg and Richard P. Woodward Apr. 1989 22 p Presented at the 12th Aeroacoustics Conference, San Antonio, TX, 10-12 Apr. 1989; sponsored inpart by AIAA
(NASA-TM-102002; E-4684; NAS 1.15:102002; AIAA-89-1144)
Avail: NTIS HC A03/MF A01 CSCL 20A

In an exploratory effort an advanced counterrotation propeller instrumented with blade-mounted pressure transducers was tested in the NASA Lewis 9- by 15-Foot Anechoic Wind Tunnel at a simulated takeoff and landing speed of Mach 0.20. The propeller's aft diameter was reduced to investigate possible noise reductions resulting from reduced blade row interaction with the tip vortex. The propeller was tested at three blade row spacings at fixed blade setting angles, at the maximum blade row spacing at higher blade setting angles and at propeller axis angles attack to the flow up to + or - 16 deg. A limited number of unsteady blade surface pressure measurements were made on both rotors of the model counterrotation propeller. Emphasis was placed on determining the effects of rotor-rotor interactions on the blade surface pressures. A unique method of processing the pressure signals was developed that enables even weak interaction waveforms and spectra to be separated from the total signal. The interaction on the aft rotor was many times stronger than that on the forward rotor. The fundamental rotor interaction tone exhibited complicated behavior but generally increased with rotational speed and blade setting angle and decreased with rotor spacing. With the propeller axis at an angle to the flow, the phase response of the aft rotor appeared to be significantly affected by the presence of the forward rotor. Author

N89-20780 National Physical Lab., Teddington (England). Div. of Radiation Science and Acoustics.
THE EVALUATION OF IMPULSIVE NOISE
B. F. Berry Sep. 1987 96 p Original contains color illustrations
(NPL-AC-111; ISSN-0143-7143; ETN-89-94089) Copyright
Avail: National Physical Laboratory Teddington, Middlesex, TW11 OLW, England

Experiments were conducted to investigate the dependence of annoyance on basic physical parameters of impulsive noises. Subjects, in a simulated living-room environment, made numerical category scale judgements on the annoyance of various noise exposures. These included recordings of real impulsive noises, e.g., pile driver noise, digitally-synthesized impulsive noises, and low-variability road traffic noise. Using data from these experiments, the performance of a number of objective descriptors of impulsive noise was compared. The method of classifying noises as impulsive or nonimpulsive used in EEC Directive 79/113 and elsewhere, which uses the impulse time-weighting characteristic of IEC 651, is shown to be unsatisfactory. The method developed in work on helicopter noise and described in NPL Acoustics Report AC 93 is found to give the best fit between objective and subjective data. ESA

N89-20781# Ohio State Univ., Columbus. Dept. of Welding Engineering.
INVESTIGATIONS OF ULTRASONIC WAVE INTERACTIONS AT IMPERFECT BOUNDARIES SEPARATING ANISOTROPIC MATERIALS
L. Adler 1988 7 p
(Contract DE-FG02-84ER-45057)
(DE89-007089; DOE/ER-45057/T3) Avail: NTIS HC A02/MF A01

Our research is an extension of our earlier work to study perfect interfaces between anisotropic materials. The main objective of this work is to obtain a better understanding of ultrasonic wave interaction with imperfect interfaces of polycrystalline materials. The main directions of this research project were: (1) analytical work to calculate the attenuation coefficients of various anisotropy factors considering statistically random distribution of plane interfaces separating anisotropic domains; (2) modeling different boundary imperfections and incorporating them into our analytical solutions for anisotropic interfaces; (3) development of experimental techniques capable of distinguishing between contributions due to inherent elastic discontinuities versus material imperfections at the interface. Part of this effort was concentrated on system development of acoustic microscopy and laser generation and detection of ultrasound. Most experiments utilize stainless steel-copper combinations. DOE

N89-20782# Ames Lab., IA. Dept. of Engineering Science and Mechanics.
PARAXIAL APPROXIMATIONS FOR ULTRASONIC BEAM PROPAGATION IN LIQUID AND SOLID MEDIA WITH APPLICATIONS TO NODESTRUCTIVE EVALUATION Ph.D. Thesis
Byron Peel Newberry Feb. 1989 152 p
(Contract W-7405-eng-82)
(DE89-007569; IS-T-1394) Avail: NTIS HC A08/MF A01

Quantitative models can play an important role in the development and validation of ultrasonic nondestructive evaluation procedures. Successful prediction of inspection results can greatly reduce the time and monetary expense incurred by a completely experimental approach. One type of model, which is necessary in order to make such predictions, is a model for the propagation of the ultrasonic beams which are generated by the transducers used in nondestructive inspections. Two examples of this type of model have been derived in this work. The first predicts the radiation field only on the axis of a focused elliptical piston transducer radiating into an isotropic material and possibly through a bicylindrically curved interface. The solution takes the form of either a simple analytical formula for some cases or a simple numerical integration over a finite interval for other cases. The second example predicts the full off-axis radiation field produced in either an isotopic or anisotropic material and possibly transmitted through a bicylindrically curved interface. The solution takes the form of a series summation over a set of Gauss-Hermite eigenfunctions. Both models are derived from the angular spectrum of plane waves approach and have made use of the paraxial, or Fresnel, approximation. DOE

N89-20783# Ames Lab., IA.
A PRIOR KNOWLEDGE BASED OPTIMAL WIENER FILTERING APPROACH TO ULTRASONIC SCATTERING AMPLITUDE ESTIMATION Ph.D. Thesis
Steven Phelps Neal Feb. 1989 209 p
(Contract W-7405-eng-82)
(DE89-007574; IS-T-1257) Avail: NTIS HC A10/MF A01

Advances in component life prediction techniques have prompted increased interest in quantitative nondestructive characterization of flaws in engineering materials. Flaw characterization techniques utilize a signature from the flaw. In ultrasonics, the signature is estimated from noise-corrupted experimental measurements of the scattered acoustic wave field resulting from insonification of the flaw. Estimating the flaw's signature involves removing the effects of the measurement system in the presence of noise. In the frequency domain, the flaw's signature is called a scattering amplitude. The purpose of this work is to evaluate an optimal Wiener filtering approach to scattering amplitude estimation. DOE

N89-20784# Indiana Univ., Bloomington. Dept. of Chemistry.
NOISE: FRIEND OR FOE
Gary M. Hieftje 28 Oct. 1988 17 p
(Contract N00014-86-K-0366)
(AD-A203491; INDU/DC/GMH-TR-42) Avail: NTIS HC A03/MF A01 CSCL 20A

In this presentation, it is shown that noise can be not only a source of difficulty in measurement situations, but can also be used as an information carrier. In most situations, noise serves to obscure signals whose detection is desired. In such situations, it is important to distinguish between additive and multiplicative noise. Additive noise can be overcome by means of conventional signal-processing techniques such as lock-in amplification, signal averaging, and others. In contrast, multiplicative noise can be overcome only through a division-based process such as internal standardization. From another viewpoint, noise can serve nicely as distinctive information carrier and as a vehicle by which time-dependent phenomena can be measured. This approach has a number of advantages, including signal-to-noise enhancement and the examination of systems which cannot readily be perturbed by pulsed methods. GRA

72 ATOMIC AND MOLECULAR PHYSICS

Includes atomic structure, electron properties, and molecular spectra.

N89-20785 Max-Planck-Inst. fuer Physik und Astrophysik, Munich (Germany, F.R.). Inst. fuer Extraterrestrische Physik.
PRODUCTION OF D, D* AND Ds MESONS IN 200 GeV/c pi(-), K(-) AND p-Si INTERACTIONS
S. Barlag, H. Becker, T. Boehringer, M. Bosman, V. Castillo, V. Chabaud, D. Buchholz, C. Damerell, C. Daum (Nationaal Inst. voor Kernfysica en Hoge Energiefysica, Amsterdam, Netherlands), and H. Dietl et al Jul. 1988 27 p Submitted for publ. Prepared in coop. with Bristol Univ., United Kingdom, Inst. of Nuclear Physics, Krakow, Poland, Consejo Superior de Invest. Cientificas, Valencia, Spain, Valencia Univ., Spain and Technische Univ., Munich, Fed. Rep. of Germany
(MPI-PAE/Exp-El-192; ETN-89-93807) Copyright Avail: Fachinformationszentrum Karlsruhe, 7514
Eggenstein-Leopoldshafen 2, Fed. Republic of Germany

The NA32 experiment at the CERN SPS collected 38 million hadronic interactions with incident 200 GeV/c pi(-), K(-), and p beams. A segmented silicon active target and a telescope of high resolution silicon microstrip counters were used to select fully reconstructed D(0) yields K(-) pi(+), D(o) yields K(-) pi(+) pi(+) pi(-), D(+) yields K(-) pi(+) pi(+), D(+) sub s yields K(-) K(+) pi(+), and charge conjugate decays. The integrated cross-sections for D(0), D(+) D(*+), and D(+) sub s meson production and the dependence of the cross-section on longitudinal and transverse momentum of the D are presented. ESA

N89-20786# Stockholm Univ. (Sweden). Inst. of Physics.
ON PARTICLE ANTIPARTICLE MIRROR SYMMETRY
C. Jarlskog May 1988 18 p Sponsored by the Swedish National Research Council, Stockholm, Sweden
(USIP-88-06; ETN-89-93734) Avail: NTIS HC A03/MF A01

Charge conjugation (C) and parity (P) are introduced, and understanding of P and C violation is reviewed. The origin of CP violation; conditions for CP violation; angle-independent parametrization of the quark mixing matrix; and CP triangles and the CP-violation area are discussed. ESA

N89-20787# California Univ., Berkeley. Lawrence Berkeley Lab. Materials and Chemical Sciences Div.
INFRARED SPECTROSCOPY OF WEAKLY BOUND MOLECULAR IONS Ph.D. Thesis
Lisa I-Ching Yeh Nov. 1988 179 p
(Contract DE-AC03-76SF-00098)
(DE89-006602; LBL-26331) Avail: NTIS HC A09/MF A01

The infrared spectra of a series of hydrated hydronium cluster ions and of protonated ethane ion are presented. A tandem mass spectrometer is ideally suited to obtaining the spectra of such weakly bound molecular ions. Traditional absorption spectroscopy is not feasible in these situations, so the techniques described in this thesis make use of some consequence of photon absorption with higher sensitivity than simply attenuation of laser power. That consequence is dissociation. By first mass selecting the parent ion under study and then mass selecting the fragment ion formed from dissociation, the near unit detection efficiency of ion counting methods has been used to full advantage. DOE

N89-20788# International Centre for Theoretical Physics, Trieste (Italy).
THEORY OF RAMAN SCATTERING BY SURFACE POLARITONS IN A FOUR MEDIA SYSTEM
John S. Nkoma Aug. 1988 27 p Submitted for publication
(DE88-705358; IC-88/247) Avail: NTIS (US Sales Only) HC A03/MF A01

The method of linear response theory is used to determine the response functions for surface polaritons in a four media system (or bounded bilayer). The dispersion relation is found when the pole of the derived response function vanishes. The expressions for the scattered intensity for both back and forward scattering are derived. The scattered intensity depends on a polarization

which is the result of the coupling of the incident light to the vibrational coordinates and electric fields associated with electric-dipole-active lattice vibrations in the bilayer. Expressions for the Raman cross-section by surface polaritons in the four media system are derived for both back and forward scattering. Numerical results are presented by using parameters for a sapphire substrate-(GaP-GaAs) bilayer-vacuum system. DOE

N89-20789# Wisconsin Univ., Madison. Dept. of Chemistry.
COLLISIONAL ENERGY TRANSFER IN HIGHLY VIBRATIONALLY EXCITED POLYATOMIC MOLECULES Final Report, 1 Nov. 1986 - 31 Oct. 1988
F. Fleming Crim 9 Dec. 1988 22 p
(Grant AF-AFOSR-0033-26; AF Proj. 2303)
(AD-A203728; AFOSR-89-0056TR) Avail: NTIS HC A03/MF A01 CSCL 07D

The three objectives of this work are to determine the nature of highly vibrationally excited polyatomic molecules, to determine the rate constants and pathways for the collisional relaxation of these molecules, and to probe the electronic spectroscopy of these molecules. We have created and implemented approaches for accomplishing these objectives and have demonstrated their feasibility by studying the collisional energy transfer in highly vibrational excited acetylene. We have found that the collisional self relaxation rates of single angular momentum states with 10,000/cm of vibrational energy are a substantial fraction of the gas kinetic collision rates. The rate constant is about a factor of two smaller for relaxation by atomic partners. GRA

73 NUCLEAR AND HIGH-ENERGY PHYSICS

Includes elementary and nuclear particles; and reactor theory.

For space radiation see *93 Space Radiation.*

N89-20790# EG and G Mound Applied Technologies, Miamisburg, OH.
LIGHT-WEIGHT RADIOISOTOPE HEATER UNIT FINAL SAFETY ANALYSIS REPORT (LWRHU FSAR). VOLUME 3: NUCLEAR RISK ANALYSIS DOCUMENT
30 Nov. 1988 43 p Prepared in cooperation with NUS Corp., Gaithersburg, MD
(Contracts DE-AC04-88DP-43495; DE-AC01-87NE-32134)
(DE89-005496; MLM-3540-Vol-3; NUS-5153-Vol-3) Avail: NTIS HC A03/MF A01

The Light-Weight Radioisotope Heater Unit (LWRHU) Final Safety Analysis Report (FSAR), Volume 2, Accident Model Document (AMD) describes potential accident scenarios during the Galileo mission and evaluates the response of the LWRHUs to the associated accident environments. Any resulting source terms, consisting of PuO2 (with Pu-238 the dominant radionuclide), are then described in terms of curies released, particle size distribution, release location, and probabilities. This volume (LWRHU-FSAR, Volume 3, Nuclear Risk Analysis Document (NRAD)) contains the radiological analyses which estimate the consequences of the accident scenarios described in the AMD. It also contains the quantification of mission risks resulting from the LWRHUs based on consideration of all accident scenarios and their probabilities. Estimates of source terms and their characteristics derived in the AMD are used as inputs to the analyses in the NRAD. The Failure Abort Sequence Trees (FASTs) presented in the AMD define events for which source terms occur and quantify them. Based on this information, three types of source term cases (most probable, maximum, and expectation) for each mission phase were developed for use in evaluating the radiological consequences and mission risks. DOE

N89-20791# Nationaal Inst. voor Kernfysica en Hoge Energiefysica, Amsterdam (Netherlands).
LITERATURE SEARCH ON KICKERS AND SEPTA FOR THE AMSTERDAM PULSE STRETCHER (APS) [LITERATUUR ONDERZOEK NAAR KICKERS EN SEPTA VOOR DE AMSTERDAM PULSE STRETCHER]
J. Kuijt and A. v.d.Linden 1988 36 p In DUTCH; ENGLISH summary
(LINO-158; ETN-89-93881) Avail: NTIS HC A03/MF A01

A study of the literature was performed with a view to the design of kickers and septa for the injection and extraction line of the Amsterdam Pulse Stretcher Ring (APS) in the UPDATE project. The UPDATE kickers were given the following specifications: deflection angle 2 mrad, pulse width 2 micrometer, fall time 70 ans, available length 2 m. A comparison of the characteristic parameters (kick strength, pulse characteristics, required peak power) with the existing system shows correspondence with two ferrite kicker designs (CERN-CPS and ELSA), the Los Alamos TEM-kicker, and the Saskatoon electrostatic kicker. On account of the relative simplicity of construction and the pulse forming network, the Saskatoon kicker was chosen as the starting point for a design study. Septum magnets and electrostatic wire septa are overviewed. ESA

N89-20792# Maryland Univ., College Park. Dept. of Electrical Engineering.
REVIEW OF INTENSE ELECTRON BEAM TRANSPORT IN GASES
W. W. Destler, J. Rodgers, Z. Segalov, C. D. Striffler, R. L. Yao, X. Zhang, and J. Guillory 1988 12 p Presented at the 7th International Conference on High-Power Particle Beams, Karlsruhe, Federal Republic of Germany, 4 Jul. 1988
(Contract DE-AC05-85ER-40216)
(DE89-005397; CONF-880713-22) Avail: NTIS HC A03/MF A01

In this review, recent results from three different experimental configurations will be discussed. In the first, intense electron beams are injected into gas-filled drift tubes and ionization of the gas at the beamfront results in the creation of a neutralizing plasma channel that allows for effective beam propagation. In the second configuration, a preformed plasma channel is produced by various methods in the drift tube. In this manner beamfront erosion can be significantly reduced and transverse instabilities can be suppressed. In the third configuration, intense electron beams are injected through a localized plasma into vacuum. Beam space charge effects accelerate ions downstream where they provide a channel of neutralization that permits effective electron beam propagation into the vacuum region. In this paper theoretical considerations and recent experimental results pertaining to intense beam propagation in gases and background plasmas are summarized. A more detailed presentation is given of the third configuration. DOE

N89-20793# Stanford Linear Accelerator Center, CA.
LOW EMITTANCE THERMIONIC ELECTRON GUNS
W. B. Herrmannsfeldt Jan. 1989 11 p Presented at the Physics of Particle Accelerators Summer School, Batavia, IL, 20 Jul. - 14 Aug. 1987
(Contract DE-AC03-76SF-00515)
(DE89-005944; SU-SLAC-PUB-4843; CONF-8707208-1) Avail: NTIS HC A03/MF A01

This paper discusses the following topics in electron guns: self fields; external fields; thermal-emittance-limited guns; and guns for electron linacs. DOE

74 OPTICS

Includes light phenomena; and optical devices.
For lasers see *36 Lasers and Masers.*

N89-20794# Gallagher Associates, Inc., West Lafayette, IN.
[QUASI-OPTICAL MICROWAVE COMPONENTS FOR FIVE DIFFERENT OPTICAL PATHS WITHIN THE MFTF-B MACHINE] Final Design Report
Nov. 1988 8 p Prepared for Lawrence Livermore National Lab., CA
(Contract W-7405-eng-48)
(DE89-005543; UCRL-21134) Avail: NTIS HC A02/MF A01

The task is to design the quasi-optical microwave components for each of five different optical paths within the MFTF-B machine. Each path contains two reflectors. The function of the two reflectors in each path is to modify the output field of a waveguide to a desired pattern within the plasma. For all five beam paths, the waveguide output is assumed to be a TE 01 mode as decided at the July 18, design review. Each optical train consists of two reflectors. The first reflector is an off axis paraboloid which focuses the beam. The first reflector also contains the groove pattern of the twist polarizer. The second reflector receives the polarized beam from the first reflector. The function of the second reflector is to modify the phase of the polarized wavefront received from the first reflector. This modification shapes the wavefront profile in the plasma. DOE

N89-20795*# Ohio State Univ., Columbus. ElectroScience Lab.
GEOMETRICAL OPTICS DESIGN OF A COMPACT RANGE GREGORIAN SUBREFLECTOR SYSTEM BY THE PRINCIPLE OF THE CENTRAL RAY
Giancarlo Clerici and Walter D. Burnside Jan. 1989 245 p
(Grant NsG-1613)
(NASA-CR-184810; NAS 1.26:184810; TR-719493-4) Avail: NTIS HC A11/MF A01 CSCL 20F

In recent years, the compact range has become very popular for measuring Radar Cross Section (RCS) and antenna patterns. The compact range, in fact, offers several advantages due to reduced size, a controlled environment, and privacy. On the other hand, it has some problems of its own, which must be solved properly in order to achieve high quality measurement results. For example, diffraction from the edges of the main reflector corrupts the plane wave in the target zone and creates spurious scattering centers in RCS measurements. While diffraction can be minimized by using rolled edges, the field of an offset single reflector compact range is corrupted by three other errors: the taper of the reflected field, the cross polarization introduced by the tilt of the feed and the aperture blockage introduced by the feed itself. These three errors can be eliminated by the use of a subreflector system. A properly designed subreflector system offers very little aperture blockage, no cross-polarization introduced and a minimization of the taper of the reflected field. A Gregorian configuration has been adopted in order to enclose the feed and the ellipsoidal subreflector in a lower chamber, which is isolated by absorbers from the upper chamber, where the main parabolic reflector and the target zone are enclosed. The coupling between the two rooms is performed through a coupling aperture. The first cut design for such a subreflector system is performed through Geometrical Optics ray tracing techniques (GO), and is greatly simplified by the use of the concept of the central ray introduced by Dragone. The purpose of the GO design is to establish the basic dimensions of the main reflector and subreflector, the size of the primary and secondary illuminating surfaces, the tilt angles of the subreflector and feed, and estimate the feed beamwidth. At the same time, the shape of the coupling aperture is initially determined. Author

N89-20796# California Univ., Berkeley. Lawrence Berkeley Lab. Engineering Div.
GERMANIUM BLOCKED IMPURITY BAND INFRARED DETECTORS
C. S. Rossington and E. E. Haller Aug. 1988 7 p Presented at the 4th International Conference on Infrared Physics, Zurich, Switzerland, 22 Aug. 1988
(Contract DE-AC03-76SF-00098)
(DE89-006607; LBL-26386; CONF-880870-2) Avail: NTIS HC A02/MF A01

Germanium blocked impurity band (BIB) photoconductors have been fabricated and characterized for responsivity, dark current, and noise equivalent power. BIB photoconductors theoretically provide an extension of the spectral response, a reduction in sensitivity to cosmic radiation and a reduction in noise characteristics compared with conventional photoconductors. Silicon BIB detectors have been successfully developed by researchers at Rockwell International, which do indeed meet their theoretical potential. In the proper configuration, these same Si BIB detectors are capable of continuous detection of individual photons in the wavelength range from 0.4 to 28 micrometers. Until the BIB concept was developed, detection of individual photons was only possible with photomultiplier tubes which detected visible light. Due to the successes of the Si BIB detectors, it seemed natural to extend this concept to Ge detectors, which would then allow an extension of the spectral response over conventional Ge detectors from approximately 100 to approximately 200 micrometers. DOE

N89-20797# Los Alamos National Lab., NM. Chemical and Laser Sciences Div.
CAVITY RINGDOWN MEASUREMENTS OF HIGH-REFLECTION MIRRORS AT 1.06 MICRONS
L. John Jolin, Virgil R. Sanders, and Thomas P. Turner 1988 10 p Presented at the Boulder Damage Symposium, Boulder, CO, 26 Oct. 1988
(Contract W-7405-eng-36)
(DE89-006512; LA-UR-89-293; CONF-8810296-1) Avail: NTIS HC A02/MF A01

A 1064 nm cavity-ringdown reflectometer was used to study reflectances of a variety of high reflectance dielectric coatings and silver mirrors. Reflectances of the dielectric coatings were measured at near-normal angle of incidence. The multilayer dielectric high reflectors included ZrO2, HfO2, SiN4, TiO2, and Al2O3, which were used in combination with SiO2 in conventional quarter-wave designs. Reflectors from more than a dozen vendors were surveyed in this effort. Metallic reflectors investigated were silver and silver protected with a thin (10 A) alumina overcoat. These reflectors were tested at both normal incidence and at high (grazing) angles. The results of these studies show that, although high reflectances (R is greater than 0.9990) can be achieved for 1064 nm multilayer dielectrics, the majority are not of this caliber. Reflectances for dielectric designs ranged from 0.96 to greater than 0.9990. The silver mirrors exhibited predictable behavior with reflectances of 0.992 at near-normal angle. DOE

N89-20798# Los Alamos National Lab., NM.
PROPOSED EXTENDED TUNING RANGE FOR THE LOS ALAMOS MID-INFRARED ADJUSTABLE, COHERENT LIGHT EXPERIMENT (MIRACLE) FACILITY
A. H. Lumpkin, D. W. Feldman, R. W. Warren, W. E. Stein, J. M. Watson, J. E. Sollid, B. E. Newnam, J. C. Goldstein, and W. J. Johnson 1988 11 p Presented at the 10th International Free Electron Laser Conference, Jerusalem, Israel, 29 Aug. 1988
(Contract W-7405-eng-36)
(DE89-006550; LA-UR-89-17; CONF-8808191-1) Avail: NTIS HC A03/MF A01

The Los Alamos Free-Electron Laser (FEL) Facility has been in operation as an oscillator in the 10 micron wavelength regime since 1983. Operations from 10 to 45 micron have been recently demonstrated which would provide a new applications capability: A Mid-Infrared Adjustable Coherent Light Experiment (MIRACLE) Facility. We propose to extend this tunability from 3 to 160 microns by upgrading the injector, accelerator, and resonator cavity. Potential applications in material science (high-temperature superconductors) and biophysics (DNA spectroscopy) for this wavelength regime are briefly addressed. DOE

N89-20799# Indiana Univ., Bloomington. Dept. of Chemistry.
LUMINESCENCE ORIGINATING IN AN OPTICAL FIBER

Mary K. Carroll, Frank V. Bright, and Gary M. Hieftje 28 Oct. 1988 13 p
(Contract N00014-86-K-0366)
(AD-A203494; INDU/DC/GMH-TR-44) Avail: NTIS HC A03/MF A01 CSCL 20F

Recently, there has been considerable research into the development and applications of fiber optic spectroscopic sensors. The large number of recent reviews attest to the widespread interest in this area (1 to 6). Fiber optics have several advantages over conventional optics; they can easily be miniaturized, and can be used at a remote distance from the laboratory and/or under harsh conditions. Our research group has been active in the area of fiber-optic chemical sensors. In the course of setting up an instrumental system for sensor research, we discovered some unusual luminescence behavior originating in the optical fiber itself. When a pulsed, high-energy, ultraviolet laser beam was coupled into a fused silica fiber, the fiber was seen to glow a bright red color. The color was intense enough to be seen with the naked eye in a well-lit room, and appeared to be uniform along the length of the fiber. We proceeded to study this observed emission. This report summarizes our observations. GRA

N89-20800# Smithsonian Astrophysical Observatory, Cambridge, MA.
SUPPORT OF MARK 3 OPTICAL INTERFEROMETER Final Report, 1 Dec. 1985 - 31 May 1988
Michael Shao Nov. 1988 49 p
(Contract N00014-86-C-2105)
(AD-A203665) Avail: NTIS HC A03/MF A01 CSCL 20F

In the three year period of this contract we have built and installed a long baseline stellar interferometer on Mt. Wilson. A number of papers describing the instrument and results from that instrument have appeared. Th Mark 3 interferometer is the most astronomically productive interferometer to date. The success of the Mark 3 has led the USNO to decide to build a dedicated four element interferometer array for fundamental astrometry and NRL/ONR to build a six element imaging array. In conclusion, we have successfully completed the task of building a long baseline interferometric observatory. GRA

N89-20801# Army Missile Command, Redstone Arsenal, AL. Research Directorate.
DIGITAL PROCESSING OF SPECKLE IMAGES Final Technical Report, period ending Jan. 1988
Charles R. Christensen and Anil K. Jain Apr. 1988 46 p
(AD-A203703; AD-E951202; AMSMI/TR-RD-RE-88-4) Avail: NTIS HC A03/MF A01 CSCL 20F

A digital simulation of an image with speckle noise from coherent illumination was developed and verified by comparison with experimentally obtained imagery. The digital simulation was then used to obtain detection probability statistics and to evaluate the utility of several digital filtering techniques for speckle reduction. Homomorphic Wiener filtering produced the best noise reduction with the least degradation in image resolution. GRA

N89-20802# Rochester Univ., NY. Inst. of Optics.
DIFFRACTION THEORY FOR POLYGONAL APERTURES Ph.D. Thesis
Ronald Edward English, Jr. Jul. 1988 102 p
(Contract DAAL03-86-K-0173)
(AD-A203778; ARO-24626.57-PH-U1R) Avail: NTIS HC A06/MF A01 CSCL 09E

We explain and describe diffraction from polygonal apertures over a wide range of sizes and observation distances. In the first case considered, a small square aperture (2a X 2a, ka much less than 1, where k = 2pi/lambda is the wavenumber) in a perfectly conducting plane screen of vanishing thickness diffracts a normally incident, linear polarized, monochromatic plane wave. Within the vector framework of Maxwell's equations, we hypothesize a solution for the dominant component of the electric field. Subsequently, by means of an integro-differential equation formulation of the diffraction problem applied to small apertures, we substantiate the solution. The solution represents the first three terms in a more general expansion for the aperture field. Physical intuition and the solutions for circular aperture field. Physical intuition and the solutions for circular apertures and slits motivate use to propose this expansion. Numerical calculations validate the solution over most of the aperture except in the close vicinity of the corners of the aperture. This limited expansion does not achieve an accurate description of the field near the corners. In the remainder of the investigation we treat diffraction within the realm of Fourier optics. We develop a Gaussian beam expansion and use it to describe diffraction from a plane-screen corner of arbitrary angle. GRA

75 PLASMA PHYSICS

Includes magnetohydrodynamics and plasma fusion.
For ionospheric plasmas see *46 Geophysics*. For space plasmas see *90 Astrophysics*.

N89-20803# Academia Sinica, Hefei (China). Inst. of Plasma Physics.
LOW FREQUENCY MHD INSTABILITY IN A HOT ELECTRON PLASMA
Chaosong Huang, Zhaoxing Ren, and Lijian Qiu 1987 9 p Sponsored by Institute of Scientific and Technical Information of China, Beijing
(PB89-111546; ISTIC-TR-C-000203) Avail: NTIS HC A02/MF A01 CSCL 20I

Low frequency interchange instability in a hot electron plasma is studied. Line-typing of conducting end plates is considered. A dispersion relation is derived. Stability criteria are found. GRA

N89-20804# Academia Sinica, Beijing (China). Inst. of Mechanics.
IMPEDANCE MATCHING OF RF PLASMA
Yunming Chen 1987 9 p Sponsored by Institute of Scientific and Technical Information of China, Beijing
(PB89-112502; ISTIC-TR-C-000150) Avail: NTIS HC A02/MF A01 CSCL 20I

The characteristics of RF plasma and RF oscillator are derived theoretically, their interception determines the working point. Then follow the discussions of Colpitz circuit with emphasis on the impedance matching, the scaling, the stability and its industrial application. All predictions were confirmed by experiments.
Author

N89-20805# Oak Ridge National Lab., TN. Central Engineering.
DEVELOPMENT OF A REMOTELY MAINTAINABLE RADIO-FREQUENCY MODULE FOR THE COMPACT IGNITION TOKAMAK
J. D. Snider 1988 8 p Presented at the 3rd Topical Meeting on Robotics and Remote Systems, Charleston, SC, 13 Mar. 1989
(Contract DE-AC05-84OR-21400)
(DE89-004913; CONF-890304-26) Avail: NTIS HC A02/MF A01

The Compact Ignition Tokamak (CIT) will require reliable remote handling (RH) systems to overcome failures in diagnostic and operational equipment. Oak Ridge National Laboratory (ORNL) is responsible for the ex-vessel remote maintenance systems for the CIT. Part of this effort is performing remote maintenance demonstrations on replicas of various CIT equipment. To ensure successful RH, the machine must be designed with proven remote maintenance features. In the demonstrations, critical remote maintenance features are tested before actual CIT equipment designs are finalized. Designs and procedures required to remotely remove and install a radio-frequency (RF) module from a modplane port on the tokamak were recently demonstrated at ORNL. This testing identified both successful design features for remote maintenance of the RF module and areas that require further development. DOE

N89-20806# Los Alamos National Lab., NM.
IMPROVED PLASMA CONFINEMENT AND EVIDENCE FOR A PRESSURE-DRIVEN INSTABILITY FROM REDUCED MAGNETIC FIELD ERRORS IN THE CTX SPHEROMAK
J. C. Fernandez, F. J. Wysocki, T. R. Jarboe, C. W. Barnes, I. Henins, S. O. Knox, and G. J. Marklin 1989 4 p Presented at the 16th European Conference on Controlled Fusion and Plasma Physics, Venice, Italy, 13 Mar. 1989
(Contract W-7405-eng-36)
(DE89-005475; LA-UR-88-4232; CONF-890302-1) Avail: NTIS HC A02/MF A01

The 0.67 m radius mesh flux conserver (MFC) in CTX was replaced by a solid flux conserver (SFC), resulting in greatly reduced field errors. Decreased spheromak open flux led to vastly improved decaying discharges, including increased global energy confinement times tau sub E (from 20 to 180 microns) and corresponding magnetic energy decay times tau sub B sup 2 (from 0.7 to 2 ms). Improved confinement allowed the observation of a pressure-driven instability which ejects plasma from the spheromak interior to the wall. DOE

N89-20807# Los Alamos National Lab., NM.
PLASMA FOCUS SOURCES: SUPPLEMENT TO THE NEUTRON RESONANCE RADIOGRAPHY WORKSHOP PROCEEDINGS
Vittorio Nardi and Jan Brzosko Jan. 1989 24 p Workshop held in Los Alamos, NM, 27-29 Jul. 1987
(Contract W-7405-eng-36)
(DE89-006927; LA-11393-C-Suppl; CONF-8707124-Suppl) Avail: NTIS HC A03/MF A01

Since their discovery, plasma focus discharges have been recognized as very intense pulsed sources of deuterium-deuterium (D-D) or deuterium-tritium (D-T) fusion-reaction neutrons, with outstanding capabilities. Specifically, the total neutron emission/shot, Y (sub n), and the rate of neutron emission, Y (sub n), of an optimized plasma focus (PF) are higher than the corresponding quantities observed in any other type of pinched discharge at the same level of powering energy W (sub 0). Recent developments have led to the concept and experimental demonstration of an Advanced Plasma Focus System (APF) that consists of a Mather-geometry plasma focus in which field distortion elements (FDEs) are inserted in the inter-electrode gap for increasing the neutron yield/shot, Y (sub n). The FDE-induced redistribution of the plasma current increases Y (sub n) by a factor approximate to or greater than 5 to 10 above the value obtained without FDEs under otherwise identical conditions of operation of the plasma focus. For example, an APF that is fed by a fast capacitor bank with an energy, W (sub 0) = 6 kJ, and voltage, V (sub 0) = 16.5 kV provides Y (sub n) congruent to 4 x 10 to the 9th D-D neutrons/shot (pure D2 filling) and Y (sub n) = 4 x 10 to the 11th D-T neutrons/shot (filling is 50 pct deuterium and 50 pct tritium). The FDE-induced increase of Y (sub n) for fixed values of (W sub 0, V sub 0), the observed scaling law Y (sub n) proportional to W (sub 0) squared for optimized plasma focus systems, and our experience with neutron scattering in bulk objects lead us to the conclusion that we can use an APF as a source of high-intensity neutron pulses (10 to the 14th n/pulse) in the field off neutron radiography (surface and bulk) with a nanosecond or millisecond time resolution. DOE

N89-20808# Johns Hopkins Univ., Baltimore, MD.
EXTREME ULTRAVIOLET AND SOFT X-RAY DIAGNOSTICS OF HIGH-TEMPERATURE PLASMAS Progress Report
W. Moos 1989 15 p
(Contract DE-FG02-86ER-53214)
(DE89-007070; DOE/ER-53214/11) Avail: NTIS HC A03/MF A01

This paper describes recent progress in experiments performed on the TEXT and DIII-D tokamaks. This paper also discusses our future plans for the on-going work related to the poloidal magnetic field diagnostic and edge and scrape-off plasma physics and the novel diagnostics and their scientific and technical background. The budget is discussed briefly. DOE

N89-20809# Oak Ridge National Lab., TN.
TRANSPORT MODELING OF ECH AND NEUTRAL-BEAM-HEATED PLASMAS IN THE ADVANCED TOROIDAL FACILITY
H. C. Howe, L. D. Horton, E. C. Crume, J. H. Harris, R. C. Isler, J. B. Wilgen, and W. R. Wing 1989 4 p Presented at the 16th European Conference on Controlled Fusion and Plasma Physics, Venice, Italy, 13 Mar. 1989
(Contract DE-AC05-84OR-21400)
(DE89-006131; CONF-890302-4) Avail: NTIS HC A02/MF A01

Results of time-dependent transport modeling of the Advanced Toroidal Facility (ATF) plasmas are compared with a typical ungettered, neutral-beam-heated discharge. A summary of ATF machine parameters is given by Murakami. The model is adjusted to give agreement between measured diagnostics signals and the corresponding values inferred from the model plasma. With this agreement, the main features of the discharge are reproduced including the radiation-induced temperature collapse. DOE

N89-20810# California Univ., Berkeley. Lawrence Berkeley Lab. Accelerator and Fusion Research Div.
HEAVY ION INDUCTION LINAC DRIVERS FOR INERTIAL CONFINEMENT FUSION
E. P. Lee and J. Hovingh (Lawrence Livermore National Lab., CA.) Oct. 1988 8 p Presented at the 8th Topical Meeting on Technology of Fusion Energy, Salt Lake City, UT, 9 Oct. 1988
(Contract DE-AC03-76SF-00098)
(DE89-006603; LBL-25047; CONF-881031-61) Avail: NTIS HC A02/MF A01

Intense beams of high energy heavy ions (e.g., 10 GeV Hg) are an attractive option for an inertial confinement fusion (ICF) driver because of their favorable energy deposition characteristics. The accelerator systems to produce the beams at the required power level are a development from existing technologies of the induction linac, RF linac/storage ring, and synchrotron. The high repetition rate of the accelerator systems, and the high efficiency which can be realized at high current make this approach especially suitable for commercial ICF. The present report gives a summary of the main features of the induction linac driver system, which is the approach now pursued in the USA. The main subsystems, consisting of injector, multiple beam accelerator at low and high energy, transport and pulse compression lines, and final focus are described. Scale relations are given for the current limits and other features of these subsystems. DOE

N89-20811# Michigan Univ., Ann Arbor. Dept. of Nuclear Engineering.
THE MAGNETICALLY INSULATED INERTIAL CONFINEMENT FUSION (MICF): A NOVEL APPROACH Progress Report, 1 Jun. 1988 - 31 Jan. 1989
T. Kammash Jan. 1989 10 p
(Contract DE-FG02-87ER-13723)
(DE89-007473; DOE/ER-13723/2) Avail: NTIS HC A02/MF A01

Significant and encouraging progress has been achieved in our study of the magnetically Insulated Inertial Confinement Fusion (MICF) system since the last progress report that seems to further solidify, in our judgement, its potential as a power producing reactor. Chief among the accomplishments are: derivation of classical transport processes across magnetic fields in plasma that contain multiple species at different temperatures; further examination of the stability question and its impact on the Q (ratio of fusion energy to input energy, i.e., energy multiplication factor) value of the system; a more detailed analysis of the radiation transport in MICF. It is shown that most of the bremsstrahlung absorption takes place in a very thin region of the metal surface adjacent to the cold plasma region we call the halo region; and a more careful investigation of the dynamics of the boundaries between the various regions of the target, and its role in the burn dynamics of the system. DOE

N89-20812# Indiana Univ., Bloomington. Dept. of Chemistry.
A NEW PROCEDURE FOR DETERMINATION OF ELECTRON TEMPERATURES AND ELECTRON CONCENTRATIONS BY THOMSON SCATTERING AND ANALYTICAL PLASMAS
Huang Mao and Gary M. Hieftje 28 Oct. 1988 41 p
(Contract N00014-86-K-0366)
(AD-A203489; INDU/DC/GMH-TR-46) Avail: NTIS HC A03/MF A01 CSCL 20I

A new data-treatment procedure allows for more accurate determination of electron temperatures and electron concentrations in analytical plasmas. A Thomson scattering spectrum, useful for these determinations, is often not purely Gaussian in shape, even when the probed electrons possess a Maxwellian velocity distribution. Nonetheless, an unambiguous relationship exists between electron temperatures and concentrations that truly exist in a plasma and those calculated from a distorted Thompson scattering spectrum. Understanding this relationship permits a look-up table to be constructed, from which observed values can be corrected. Theory concerning this procedure is described and details for using it with both a ruby laser and frequency doubled Nd: YAG laser are discussed. Examples of electron temperature and electron concentration determined with this procedure in an ICP are given. The possibility of using the new procedure to study electron energy distributions is also assessed. GRA

N89-20813# California Univ., San Diego, La Jolla. Inst. for Pure and Applied Physical Sciences.
DEVELOPMENT OF A PLASMA PINCH PHOTOCATHODE Final Report, 1 Sep. 1985 - 31 Dec. 1987
John F. Asmus 1989 16 p
(Contract N00014-85-K-0598)
(AD-A203944) Avail: NTIS HC A03/MF A01 CSCL 20G

The need in advanced Linacs is for a high-performance (emittance, current, and life) cathode that will not poison in the only moderately good vacuums of such systems. Our approach embodies the durability of an unsensitized metal photocathode that is illuminated by a high-Z, high-density plasma pinch formed from a liquid-jet source in vacuum. The principal advantage of this pinch over a laser is both its simplicity and its ability to efficiently produce high-power vacuum ultraviolet radiation. The laser-guided gas-embedded pinch vacuum-ultraviolet source has been converted to a liquid-jet configuration in vacuum. This was undertaken for several reasons. First, the necessity of interposed high-density background gas is avoided. Second, a channel-forming guide laser beam is no longer needed. Finally, a wide variety of high-Z low cost substances are available in liquid form. For these reasons the liquid-jet approach makes sense for a rep-rate version of the pinch illuminator. Background gas absorption of hard UV is lessened. A large gas-transport system is not needed. Radiation output may be optimized through selection of the liquid's vapor pressure, surface tension, density, and composition. GRA

N89-20162# Centre National de la Recherche Scientifique, Orleans (France). Lab. de Physique et Chimie de l'Environnement.
WHISPER: A SOUNDER AND HIGH FREQUENCY WAVE ANALYZER EXPERIMENT
P. M. E. Decreau, J. G. Trotignon, P. Canu, H. DeFeraudy, G. Gustafsson, A. Bahnsen, I. B. Iversen, M. Jespersen, D. A. Gurnett, and L. J. C. Woolliscroft (Sheffield Univ., England) *In* ESA, The Cluster Mission: Scientific and Technical Aspects of the Instruments Oct. 1988 p 37-43 (For primary document see N89-20156 13-12)
Avail: NTIS HC A06/MF A01; ESA Publications Div., ESTEC, Noordwijk, Netherlands, $10 US or 25 Dutch guilders

N89-20163# Iowa Univ., Iowa City. Dept. of Physics and Astronomy.
THE WIDEBAND PLASMA WAVE INTERACTION
D. A. Gurnett, R. R. Shaw, R. L. Huff, and D. L. Krichner *In* ESA, The Cluster Mission: Scientific and Technical Aspects of the Instruments Oct. 1988 p 45-48 (For primary document see N89-20156 13-12)
Avail: NTIS HC A06/MF A01; ESA Publications Div., ESTEC, Noordwijk, Netherlands, $10 US or 25 Dutch guilders

N89-20164# Sheffield Univ. (England).
THE DIGITAL WAVE PROCESSING EXPERIMENT
L. J. C. Woolliscroft, J. A. Thompson, P. M. E. Decreau, M. Parrot, A. Egeland, I. B. Iversen, H. C. Koons, P. J. Christiansen, M. P. Gough, and G. Gustafsson (Swedish Inst. of Space Physics, Uppsala.) et al *In* ESA, The Cluster Mission: Scientific and Technical Aspects of the Instruments Oct. 1988 p 49-54 (For primary document see N89-20156 13-12)
Avail: NTIS HC A06/MF A01; ESA Publications Div., ESTEC, Noordwijk, Netherlands, $10 US or 25 Dutch guilders

N89-20165# Max-Planck-Inst. fuer Physik und Astrophysik, Garching (Germany, F.R.).
THE ELECTRON DRIFT INSTRUMENT
G. Paschmann, F. Melzner, G. Haerendel, O. H. Bauer, W. Baumjohann, M. Boehm, M. Nakamura, N. Sckopke, R. Treumann, and C. E. McIlwain (California Univ., San Diego, La Jolla.) et al *In* ESA, The Cluster Mission: Scientific and Technical Aspects of the Instruments Oct. 1988 p 55-63 (For primary document see N89-20156 13-12)
Avail: NTIS HC A06/MF A01; ESA Publications Div., ESTEC, Noordwijk, Netherlands, $10 US or 25 Dutch guilders

N89-20166# Centre d'Etude Spatiale des Rayonnements, Toulouse (France).
THE ION SPECTROMETRY EXPERIMENT TO MEASURE THE PROPERTIES OF THE IONIC PLASMA COMPOSITION AND DISTRIBUTION FUNCTIONS AT ENERGIES BETWEEN 0 AND 40keV/e
H. Reme, J. M. Bosqued, J. A. Sauvaud, A. Cros, J. Dandouras, C. dUston, E. Moebius, D. Hovestadt, B. Klecker, and G. Paschmann (Max-Planck-Inst. fuer Physik und Astrophysik, Garching, Germany, F.R.) et al *In* ESA, The Cluster Mission: Scientific and Technical Aspects of the Instruments Oct. 1988 p 65-76 (For primary document see N89-20156 13-12)
Avail: NTIS HC A06/MF A01; ESA Publications Div., ESTEC, Noordwijk, Netherlands, $10 US or 25 Dutch guilders

N89-20167# Mullard Space Science Lab., Dorking (England).
PEACE: A PLASMA ELECTRON AND CURRENT EXPERIMENT
A. D. Johnstone, A. J. Coates, D. S. Hall, B. N. Maehlum, S. J. Schwartz, M. Thomsen, and J. D. Winningham (Southwest Research Inst., Houston, TX.) *In* ESA, The Cluster Mission: Scientific and Technical Aspects of the Instruments Oct. 1988 p 77-84 (For primary document see N89-20156 13-12)
Avail: NTIS HC A06/MF A01; ESA Publications Div., ESTEC, Noordwijk, Netherlands, $10 US or 25 Dutch guilders

N89-20168# Max-Planck-Inst. fuer Aeronomie, Katlenburg-Lindau (Germany, F.R.).
RAPID: RESEARCH WITH ADAPTIVE PARTICLE IMAGING DETECTORS
B. Wilken, W. I. Axford, P. Daly, A. Korth, G. Kremser, W. H. Ip, V. M. Vasyliunas, J. B. Blake, J. F. Fennell, and L. R. Lyons (Aerospace Corp., Los Angeles, CA.) et al *In* ESA, The Cluster Mission: Scientific and Technical Aspects of the Instruments Oct. 1988 p 85-93 (For primary document see N89-20156 13-12)
Avail: NTIS HC A06/MF A01; ESA Publications Div., ESTEC, Noordwijk, Netherlands, $10 US or 25 Dutch guilders

76 SOLID-STATE PHYSICS

Includes superconductivity.

For related information, see also *33 Electronics and Electrical Engineering* and *36 Lasers and Masers.*

N89-20814# Helsinki Univ. of Technology, Espoo (Finland). Low Temperature Lab.
EXPERIMENTS WITH NEGATIVE IONS IN (3)He SUPERFLUIDS

K. K. Nummila, J. T. Simola, and J. S. Korhonen Oct. 1988 69 p
(PB89-127682; TKK-F-A634; ISBN-951-754-626-2) Avail: NTIS HC A04/MF A01 CSCL 20L

The interaction between negative ions and (3)He superfluids was studied by using a time-of-flight spectrometer having a 0.001 relative resolution. The ions guided through a sample of rotating (3)He-A were found to be focused into the cores of the vortices present in this rotating superfluid. Two different vortex types, with different core structures and presumably different numbers of the circulation quanta associated with them, were found. The ion mobility along the vortex cores, mu sub c, observed in the absence of external magnetic field, can be explained by the mobility anisotropy of the A-phase, which indicates that the vortices are continuous, i.e., consist of A-phase even in the core. In finite magnetic fields a qualitatively similar continuous vortex structure was found, a result compatible with the earlier NMR experiments, but also a new vortex type with an anomalously high mu sub c was seen when the vortex sample was prepared adiabatically. The observed strong ion focusing indicates broken w-symmetry in the core textures. This is in contradiction with the earlier numerical calcuations on the optimal continuous vortex texture. GRA

N89-20815# Belden Wire and Cable, Geneva, IL.
SHIELDING EFFECTIVENESS OF SUPERCONDUCTIVE PARTICLES IN PLASTICS
T. Pienkowski, J. Kincaid, M. T. Lanagan, R. B. Poeppel, J. T. Dusek, D. Shi, and K. C. Goretta (Argonne National Lab., IL.) Sep. 1988 6 p Presented at the Wire and Cable Symposium, Reno, NV, 15 Nov. 1988
(Contract W-31-109-eng-38)
(DE89-003888; CONF-8811129-1) Avail: NTIS HC A02/MF A01

The ability to cool superconductors with liquid nitrogen instead of liquid helium has opened the door to a wide range of research. The well known Meissner effect, which states superconductors are perfectly diamagnetic, suggests shielding applications. One of the drawbacks to the new ceramic superconductors is the brittleness of the finished material. Because of this drawback, any application which required flexibility (e.g., wire and cable) would be impractical. Therefore, this paper presents the results of a preliminary investigation into the shielding effectiveness of YBa2Cu3O(sub 7-x) both as a composite and as a monolithic material. Shielding effectiveness was measured using two separate test methods. One tested the magnetic (near field) shielding, and the other tested the electromagnetic (far field) shielding. No shielding was seen in the near field measurements on the composite samples, and only one heavily loaded sample showed some shielding in the far field. The monolithic samples showed a large amount of magnetic shielding. DOE

N89-20816# Argonne National Lab., IL.
ELECTRONIC STRUCTURE CALCULATION BY NONLINEAR OPTIMIZATION: APPLICATION TO METALS
R. Benedek, B. I. Min, C. Woodward, and J. Garner (Bradley Univ., Peoria, IL.) Apr. 1988 8 p Presented at the Computer Simulation Studies in Condensed Matter Physics: Recent Developments, Athens, GA, 23 Feb. 1988
(Contract W-31-109-eng-38)
(DE89-005852; CONF-880272-3) Avail: NTIS HC A02/MF A01

There is considerable interest in the development of novel algorithms for the calculation of electronic structure (e.g., at the level of the local-density approximation of density-functional theory). In this paper we consider a first-order equation-of-motion method. Two methods of solution are described, one proposed by Williams and Soler, and the other base on a Born-Dyson series expansion. The extension of the approach to metallic systems is outlined and preliminary numerical calculations for Zintl-phase NaTl are presented. DOE

N89-20817# Oak Ridge National Lab., TN.
MICROSTRUCTURAL CHARACTERIZATION OF ALPHA-AI2O3 IMPLANTED WITH IRON
P. S. Sklad, J. D. McCallum, S. J. Pennycook, C. J. McHargue, C. W. White, and A. Perez (Lyon-1 Univ., Villeurbanne, France) 1988 6 p Presented at the Fall Meeting of the Materials Research Society, Boston, MA, 28 Nov. 1988
(Contract DE-AC05-84OR-21400)
(DE89-006037; CONF-881155-38) Avail: NTIS HC A02/MF A01

The microstructural and compositional changes produced in the near surface region of single crystals of alpha-Al2O3 by ion-implantation with iron have been investigated by a number of complementary techniques, including Rutherford backscattering spectroscopy (RBS), conversion-electron Moessbauer spectroscopy (CEMS), analytical electron microscopy (AEM), and scanning transmission electron microscopy (STEM). Iron precipitates, 1 to 3 nm in diameter, have been identified in as-implanted material at depths corresponding to the peak in the deposited iron concentration profile. The same techniques have been used to monitor the redistribution of iron and the corresponding changes in valence state during post-implantation annealing. Electron microscopy has been to correlate RSB and CEMS results with the microstructural development. DOE

N89-20818 Pennsylvania Univ., Philadelphia.
A QUANTITATIVE STUDY OF PATTERN FORMATION IN DENDRITIC CRYSTAL GROWTH FROM SUPERSATURATED SOLUTION Ph.D. Thesis
Andrew Joseph Dougherty 1988 172 p
Avail: Univ. Microfilms Order No. DA8824728

The patterns formed in dendritic crystal growth can have characteristic length scales considerably larger than any intrinsic scales of the underlying system. These macroscopic scales result from a complex interaction of microscopic and macroscopic dynamics. Recent theoretical work has focused on the relationship between the macroscopic properties of steady state dendritic tips and the underlying microscopic material properties. In particular, the tip speed radius of curvature, and mean initial sidebranch spacing, are predicted to be determined by a solvability condition involving the anisotropy in the surface tension at the solid-liquid interface. These predictions were not tested for any materials prior to this work. The complex structure of the time-dependent sidebranches is also not well understood, and is an important area for research. Experiments on the dendritic growth of NH4Br from supersaturated aqueous solution are reported. Digital image processing is used to perform precise measurements of interfacial contours and to provide a quantitative characterization of the growing patterns. The time-dependence of the sidebranch structure near the tip is characterized. Dissert. Abstr.

N89-20819 Maryland Univ., College Park.
A MOLECULAR DYNAMICS STUDY OF SURFACE KINETICS AND EPITAXIAL CRYSTAL GROWTH Ph.D. Thesis
Sun Mok Paik 1988 188 p
Avail: Univ. Microfilms Order No. DA8827107

A Molecular Dynamics simulation technique was employed to study various dynamical properties of crystal surfaces, and epitaxial crystal growth. Initially, the dependence of atomic kinetics on the thickness of quasi-two dimensional thin films was investigated. Subsequently, static substrate effects and a variety of surface dynamics were included. The phenomenon of surface structural phase transitions which may occur at growth fronts was studied. Lastly, a Molecular Beam Epitaxy (MBE) growth simulation was performed on a model system. Dissert. Abstr.

N89-20820*# Stanford Univ., CA. Electronics Lab.
RESEARCH AND DEVELOPMENT OF HgZnTe AS AN INFRARED MATERIAL Final Technical Report, 2 Aug. 1988 - 2 Feb. 1989
A. K. Wahi, I. Lindau, and W. E. Spicer 28 Mar. 1989 19 p
(Grant NAG1-851)
(NASA-CR-184840; NAS 1.26:184840) Avail: NTIS HC A03/MF A01 CSCL 20L

Interfacial morphology and Fermi level pinning behavior at the interfaces of Al, Ag, and Pt with UHV-cleaved CdTe and ZnTe

have been studied using X-ray and ultraviolet photoemission spectroscopies. Results are compared to metal/HgCdTe interface formation, where the weak HgTe bond and consequent ease of Hg loss strongly influence semiconductor disruption and metal-semiconductor intermising. For Al/CdTe, the strong Al-Te reaction yields a significantly more extensive Al-Te reacted region than has been observed for HgCdTe. The Al/ZnTe interface is observed to be more abrupt than Al/CdTe. The final Fermi level pinning positions, Ef-Evbm for Al, Ag, and Pt on p-type CdTe and p-ZnTe have been determined. Efi is found to be roughly the same for both CdTe and ZnTe, with the value for ZnTe lying approximately 0.2 eV closer to the VBM for all three metals. From these results, one would expect Schottky barriers of about the same height for these metals on p-CdTe and p-ZnTe; and also that, in principle, metal interfaces with the two alloys HgCdTe and HgZnTe would have the same properties. Comparisons and implications for electrical behavior of metal contacts to the alloys are discussed. Author

N89-20821*# Jet Propulsion Lab., California Inst. of Tech., Pasadena.
HEAVY ION INDUCED SINGLE EVENT PHENOMENA (SEP) DATA FOR SEMICONDUCTOR DEVICES FROM ENGINEERING TESTING
Donald K. Nichols, Mark A. Huebner, William E. Price, L. S. Smith, and James R. Coss Jul. 1988 71 p
(Contract NAS7-918)
(NASA-CR-184864; JPL-Publ-88-17; NAS 1.26:184864) Avail: NTIS HC A04/MF A01 CSCL 20L

The accumulation of JPL data on Single Event Phenomena (SEP), from 1979 to August 1986, is presented in full report format. It is expected that every two years a supplement report will be issued for the follow-on period. This data for 135 devices expands on the abbreviated test data presented as part of Refs. (1) and (3) by including figures of Single Event Upset (SEU) cross sections as a function of beam Linear Energy Transfer (LET) when available. It also includes some of the data complied in the JPL computer in RADATA and the SPACERAD data bank. This volume encompasses bipolar and MOS (CMOS and MHNOS) device data as two broad categories for both upsets (bit-flips) and latchup. It also includes comments on less well known phenomena, such as transient upsets and permanent damage modes. Author

N89-20822# Georgia Inst. of Tech., Atlanta. School of Physics.
THE STRUCTURE AND REACTIVITY OF HETEROGENEOUS SURFACES AND STUDY OF THE GEOMETRY OF SURFACE COMPLEXES Progress Report, 1 Jan. - 31 Dec. 1988
Uzi Landman 1988 32 p
(Contract DE-FG05-86ER-45234)
(DE89-005726; DOE/ER-45234/3) Avail: NTIS HC A03/MF A01

This research covers a wide range and scope of material systems and phenomena encompassing a number of systems in various degrees of aggregation (finite clusters and extended systems), thermodynamic states (liquids and solids under equilibrium and non-equilibrium conditions), and characteristic interactions (metals, ionic and polar materials and covalent interactions). Progress during this report is discussed under the following categories: (1) Materials preparation and growth: Liquid-phase and Molecular Beam Epitaxial growth of semiconductors (silicon); amorphous semiconductors. (2) Material surfaces and interfaces: Phase-transformations (surface premelting); surface probes (tip-substrate interactions in Atomic Force Microscopy, AFM); stressed interfaces and interphase (solid-liquid at equilibrium and under shear stress). (3) Finite aggregates: The structure and dynamics of ground state and excited state atomic and molecular clusters and fragmentation dynamics; size dependence of physical phenomena in finite material systems; excess electron attachment, solvation, migration and spectroscopy in polar molecular clusters (water and ammonia); quantum droplets ((He-4) sub n, 50 less than n less than 300) at finite temperature. DOE

N89-20823# Oak Ridge National Lab., TN.
IRRADIATION AS A TOOL FOR STUDYING SOLID STATE AMORPHIZATION PHENOMENA
D. F. Pedraza 1988 26 p Presented at the Metallurgical Society Fall Meeting and American Society for Metals Materials Week, Chicago, IL, 24 Sep. 1988
(Contract DE-AC05-84OR-21400)
(DE89-006034; CONF-880901-16) Avail: NTIS HC A03/MF A01

An overview of selected experimental results on amorphization induced by irradiation and by ion implantation is first presented. This overview and other general observations on the microstructural evolution that precedes the transition to the amorphous state of irradiated crystalline materials expose some of the important data that must be accounted for by theory. A perspective of our present understanding of irradiation-induced amorphization is then presented. As described in previous work, the theory assumes a localized buildup of complexes (coupled interstitial/vacancy pairs) to a critical value as the mechanism of amorphization. The theory of complex formation implies that the production of a defective state characterized by localized anisotropic distortions of the crystalline lattice leads to amorphization. It is proposed that this concept can be generalized to encompass solid state amorphization transitions other than those induced by irradiation. Examples available in the literature to support this idea are presented. It is therefore suggested that irradiation can be used as a valuable tool to study other solid state amorphization transitions. DOE

N89-20824# Los Alamos National Lab., NM.
ELECTRON SPECTROSCOPY STUDIES OF HIGH TEMPERATURE SUPERCONDUCTORS: Y(SUB 1)-xPr(SUB x)Ba2Cu3O(SUB 7)-DELTA
J. S. Kang, J. W. Allen, B. W. Lee, M. B. Maple, Z. X. Shen, J. J. Yeh, W. P. Ellis, W. E. Spicer, and I. Lindau (Stanford Univ., CA.) 1989 13 p Presented at the International Symposium on the Electronic Structure of High-Tc Superconductors, Rome, Italy, 5 Oct. 1988 Prepared in cooperation with Bell Telephone Labs., Inc., Murray Hill, NJ
(Contract W-7405-eng-36)
(DE89-006554; LA-UR-89-258; CONF-8810255-2) Avail: NTIS HC A03/MF A01

We itemize our previous work on high T sub c superconductors, and describe more fully the results of an electron spectroscopy study and impurity Anderson Hamiltonian analysis of the Pr 4f spectrum of Y(sub 1)-xPr(sub x)Ba2Cu3O(sub 7)-delta, a system in which superconductivity is quenched as x increases. It has been speculated that Pr has valence 4+, resulting in extra charge in the Cu-O planes, and causing T sub c suppression. We find that the Pr valence is close to 3+ for all x but that there is extensive Pr 4f hybridization with other valence band states. The Cu valence is essentially unchanged with x. From these findings, we speculate that Pr 4f hybridization with other valence band states has enabled Pr spin fluctuations to cause the T sub c suppression. DOE

N89-20825# Georgia Inst. of Tech., Atlanta. School of Physics.
CRYSTALLINE METAL-SEMICONDUCTOR SUPERLATTICES Progress Report, 1 Jul. 1986 - 31 Oct. 1988
Armet Erbil 1988 11 p
(Contract DE-FG05-86ER-45266)
(DE89-006619; DOE/ER-45266/T1) Avail: NTIS HC A03/MF A01

In this report, we provide a summary of the progress made during the grant period (July 1, 1986 to October 31, 1988). Initially the focus of this program was on the development of underlying science and technology for the fabrication of metal-semiconductor superlattices. The major motivation for this work was to search for excitonic superconductivity in these structures as predicted by theory, in addition to the obvious microelectronic applications. After the discovery of superconductivity with transition temperatures above 77K, naturally we have turned our attention also to this new class of materials. We describe briefly below our work carried

under this program on the development of metal-semiconductor superlattices (artificially layered materials) and on the copper oxide based superconductors (naturally layered materials). DOE

N89-20826# California Univ., Berkeley. Dept. of Materials Science and Mineral Engineering.
SOME STRUCTURAL FEATURES OF HIGH-T(SUB c) SUPERCONDUCTORS Ph.D. Thesis
Chengfong Joseph Jou Nov. 1988 86 p
(Contract DE-AC03-76SF-00098)
(DE89-006667; LBL-26107) Avail: NTIS HC A05/MF A01

Some structural features of high-T sub c oxide superconductors including Ti-Ca-Ba-Cu-O, Bi-Ca-Sr-Cu-O, Y-Ba-Cu-O, La-(Ba,Sr,Ca)-Cu-O, Ba-K-Bi-O and Ba-Pb-Bi-O systems are systematically examined. Based on common features in these systems in addition to CuO2 layers, an imperfect macro-resonance-cell (MRC) description is proposed that provides a basis for qualitatively understanding the superconductivity in these systems. It is proposed that boundary layer coupling plays a major role in determining the different T sub c values of these systems. The YBCO system is particularly interesting for its unusual linear chain structure at the boundary layer. This chain structure originating from oxygen ordering on the basal plane also results in micro-twinned morphology in orthorhombic phase. A nucleation-and-growth mechanism for this twin formation associated with the second order phase transformation is proposed. An oxygen-depleted twin boundary model is also discussed, which explains why stoichiometric, YBa2Cu3O7, is difficult to achieve. DOE

N89-20827# Helsinki Univ. of Technology, Espoo (Finland). Lab. of Physics.
X-RAY DIFFRACTION AND ELLIPSOMETRIC STUDIES OF ZINC SULFIDE THIN FILMS GROWN BY ATOMIC LAYER EPITAXY Ph.D. Thesis
Markku Oikkonen 1988 49 p Sponsored by the Academy of Finland and the Emil Aaltonen Foundation, Finland
(Ph-161; ISBN-951-666-264-1; ISSN-0355-2721; ETN-89-94120)
Avail: NTIS HC A03/MF A01

The microstructure of ZnS thin films grown by atomic layer epitaxy (ALE) is investigated using X-ray diffraction and a single-line technique. Crystal structure, preferred orientation, crystallinity, crystallite size, crystallite size distribution, and microstrain are determined. Complex refractive indexes of the films are determined in the wavelength range 400 to 600 nm using spectroscopic ellipsometry. A two-layer model is employed, where the uppermost layer takes into account the surface roughness. Density of ZnS thin films is determined using ellipsometry and He(+)-ion backscattering spectrometry. In the first tens of nanometers of an ALE ZnS thin film the crystallinity and void content strongly depend on the substrate properties. Most of the films were grown on soda glass. It is found that after the bottom layer, at the distances from 50 to 100 nm to 300 to 400 nm from the substrate the crystallinity is good, crystallites are large, the specific orientation is strong, the void content is low, and the optical properties resemble those of bulk ZnS. At distances larger than 300 to 400 nm the surface roughness and the void content in the upper parts of the film increase because of the more and more randomly packed large crystallites. Substrate temperature and source materials affect the growth of all parts of the films. ESA

N89-20828# International Centre for Theoretical Physics, Trieste (Italy).
THERMODYNAMIC CHARACTERISTICS OF Y-Ba-Cu-O TYPE COMPOUNDS IN THE MODEL OF STRONG ELECTRON-PHONON COUPLING
A. A. Golubov Aug. 1988 15 p Submitted for publication
(DE88-705343; IC-88/195) Avail: NTIS (US Sales Only) HC A03/MF A01

Based on recently measured phonon density of states of Y-Ba-Cu-O an investigation of the strong electron-phonon coupling model is carried out. The numerical solutions of the real axis Eliashberg equations are obtained for a number of phonon spectra parameters. Isotope shifts of T (sub c), spectral behavior of the pairing energy delta (omega) and the ratio 2delta (sub g)/T (sub c) (where delta (sub g) is the gap edge) are calculated. The model gives a small oxygen isotope shift for rather moderate values of the electron-phonon coupling constant lambda of approximately 3. The results strongly suggest the weak coupling with high frequency phonon modes and strong coupling with low frequency modes. DOE

N89-20829# International Centre for Theoretical Physics, Trieste (Italy).
ENERGY GAP IN S- AND D-WAVE PAIRING SUPERCONDUCTORS
O. V. Dolgov (Academy of Sciences, USSR, Moscow.) and A. A. Golubov Aug. 1988 8 p
(DE88-705344; IC-88/197) Avail: NTIS (US Sales Only) HC A02/MF A01

The ratio 2delta (sub g)/T (sub c), where delta (sub g) is the gap edge, T (sub c) is the critical temperature, is calculated in the framework of the model of strong electron-phonon coupling. Both isotropic and anisotropic pairing cases are considered. It is shown that the isotropic Eliashberg model cannot account for the large values of the ratio 2delta (sub g)/T (sub c) for the reasonable values of the electron-phonon coupling parameter lambda, while anisotropic pairing can resolve this problem. DOE

N89-20830# International Centre for Theoretical Physics, Trieste (Italy).
LOCALIZED VERSUS ITINERANT PICTURE OF LIGHT-T(SUB c) SUPERCONDUCTING OXIDES
Andrzej M. Oles and Jan Zaanen Aug. 1988 14 p
(DE88-705345; IC-88/198) Avail: NTIS (US Sales Only) HC A03/MF A01

The physical consequences of the model Hamiltonian which describes the Cu(3d sub x squared - y squared) and 0(2p sub x(y)) orbitals of CuO2 planes in high-T (sub c) superconducting oxides are discussed in the localized and itinerant regime. We show by a direct calculation that the hole correlations at Cu sites are strong and that the antiferromagnetic state of La2CuO4 and YBa2Cu3O6 can be well described in terms of the itinerant model. DOE

N89-20831# International Centre for Theoretical Physics, Trieste (Italy).
RESONANCE TUNNELLING AND BREAKDOWN OF THE QUANTUM HALL EFFECT (QHE) IN STRONG ELECTRIC FIELDS
V. L. Pokrovsky, L. P. Pryadko, and A. L. Talapov (Academy of Sciences, USSR, Moscow) Aug. 1988 21 p Submitted for publication
(DE88-705348; IC-88/204) Avail: NTIS (US Sales Only) HC A03/MF A01

Resonance scattering of electrons on impurities is shown to play a crucial role in nonlinear conductivity under QHE conditions at zero temperature. The dissipative current as a function of an electric field and Landau level filling factor is calculated. DOE

N89-20832# Sandia National Labs., Albuquerque, NM.
CARRIER DENSITY AND EXCITATION ENERGY DEPENDENT GAMMA-X PHOTOLUMINESCENCE OF TYPE-II GaAs/AlAs SUPERLATTICES
G. R. Olbright, A. Owyoung, H. P. Hjalmarson, and T. M. Brennan 1988 5 p Presented at the Quantum Wells for Optics and Optoelectronics, Salt Lake City, UT, 6 Mar. 1989
(Contract DE-AC04-76DP-00789)
(DE89-002988; SAND-88-3019C; CONF-890312-1) Avail: NTIS HC A02/MF A01

Experimental and theoretical photoluminescence studies of Type-II GaAs/AlAs superlattices exhibit unusual behavior of GAMMA- and X-point features that reveal energy dependent relaxation channels and GAMMA- and X-point populations that depend on carrier heating and band filling. DOE

N89-20833# Lawrence Livermore National Lab., CA. Chemistry and Materials Science Dept.
ANION GRAIN BOUNDARY DIFFUSION IN Cr2O3 AND Cr2O3-0.09 WEIGHT PERCENT Y2O3
Wayne E. King and J. H. Park (Argonne National Lab., IL.) Jun. 1988 7 p Presented at the Spring Meeting of the Materials Research Society, Reno, NV, 4 Apr. 1988
(Contracts W-7405-eng-48; W-31-109-eng-38)
(DE89-006281; UCRL-98955; CONF-880408-45) Avail: NTIS HC A02/MF A01

Anion diffusivities in the lattice and along grain boundaries have been measured on sintered polycrystals of Cr2O3 and Cr2O3-0.09 weight percent Y2O3 at 1100 C and at the oxygen partial pressure corresponding to that of the Cr/Cr2O3 equilibrium at that temperature. Results show that under the same conditions, anion diffusion is significantly faster than cation diffusion. The results are discussed in terms of their implications for the reactive element effect on high temperature oxidation of chromia forming alloys. DOE

N89-20834# Sandia National Labs., Albuquerque, NM.
PROGRESS IN LINEAR OPTICS, NON-LINEAR OPTICS AND SURFACE ALIGNMENT OF LIQUID CRYSTALS
H. L. Ong, R. B. Meyer, A. J. Hurd, A. J. Karn, S. M. Arakelian, Y. R. Shen, P. N. Sanda, D. B. Dove, S. A. Jansen, and R. Hoffmann (Cornell-Sydney Univ. Astronomy Center, Sydney, Australia) 1989 10 p Presented at the 2nd International Topical Meeting on Optics of Liquid Crystals, Torino, Italy, 14 Oct. 1988
(Contract DE-AC04-76DP-00789)
(DE89-006507; SAND-89-0231C; CONF-8810295-1) Avail: NTIS HC A02/MF A01

We first discuss the progress in linear optics, in particular, the formulation and application of geometrical-optics approximation and its generalization. We then discuss the progress in non-linear optics, in particular, the enhancement of a first-order Freedericksz transition and intrinsic optical bistability in homeotropic and parallel oriented nematic liquid crystal cells. Finally, we discuss the liquid crystal alignment and surface effects on field-induced Freedericksz transition. DOE

N89-20835# Northwestern Univ., Evanston, IL. Dept. of Materials Science and Engineering.
DEFECT CLUSTERING AND RELATED PROPERTIES OF OXIDES Annual Technical Progress Report
J. B. Cohen, F. C. Engelhart, D. E. Ellis, and T. O. Mason Jan. 1989 9 p
(Contract DE-FG02-84ER-45097)
(DE89-006620; DOE/ER-45097/T4) Avail: NTIS HC A02/MF A01

This report discusses research programs on the crystal structure of different metal oxides. Electrical properties of some oxides are also discussed. DOE

N89-20836# California Univ., Berkeley. Lawrence Berkeley Lab. Research Medicine and Radiation Biophysics Div.
COMPENSATION FOR CRYSTAL PENETRATION IN HIGH RESOLUTION POSITRON TOMOGRAPHY
Ronald H. Huesman, Eva M. Salmeron, and John R. Baker Nov. 1988 10 p Presented at the IEEE Nuclear Science Symposium, Orlando, FL, 9 Nov. 1988
(Contract DE-AC03-76SF-00098)
(DE89-006660; LBL-26308; CONF-881103-34) Avail: NTIS HC A02/MF A01

We have characterized the effects of crystal penetration by annihilation photons in circular ring positron tomographs. They are most serious in high resolution instruments having small detectors. When annihilation photons are not normally incident and penetrate some distance into the scintillator before interacting, the measurement of their transverse position becomes uncertain. This penetration of photons into the detector material before interaction is a statistical process which leads to significant displacement and anisotropy of the point spread function. The subject of this work is mathematical correction of emission datasets by performing a two-dimensional spatially variant deconvolution of the emission data in sinogram format. Examples for the Donner 600-Crystal Positron Tomograph are presented, and the amplification of statistical errors resulting from the correction procedure is also discussed. DOE

N89-20837# California Univ., Berkeley. Lawrence Berkeley Lab.
SURFACE STRUCTURES DETERMINED USING ELECTRON DIFFRACTION Ph.D. Thesis
Louis Joseph Terminello Nov. 1988 153 p
(Contract DE-AC03-76SF-00098)
(DE89-006669; LBL-26300) Avail: NTIS HC A08/MF A01

The surface structures of c(2 x 2)S/Cr(001) and (1 x 1) PH(sub x)/Ge(111) were determined using angle resolved photoemission extended fine structure (ARPEFS). For the chromium study, the S-Cr(1) layer separation was shown to be 1.17 A with a fourfold hollow adsorption site, and an 8 pct contraction of the first-to-second layer Cr separation was measured with 0.02 A precision. Structural information was obtained from multiple-scattering, spherical-wave (MSSW) analysis out to a 15 A path-length difference and demonstrated the near-surface sensitivity of ARPEFS. The study of PH(sub x)/Ge(111) revealed an unanticipated adsorption site of a phosphine molecular fragment. An atop site was observed which had the P atom tilting 16 degree from normal and situated 2.26 A above the surface. Each adsorption system contributed to the refinement of the ARPEFS technique by extending the depth to which ARPEFS can recover structural information, and by uncovering lateral displacements of adsorbates from high symmetry sites. The surface electron-energy-loss fine structure (SEELFS) technique was also investigated using Cu M(sub 2,3) extended fine structure. This work confirmed a 0.2 A error in determining interatomic distances. Inaccurate central atom phase shifts have been blamed for this anomaly, and in this work an attempt was made to calculate better phase shifts based on a more rigorous description of the central atom potential. The results were incomplete, but did indicate that a time-dependent formulation of the central-atom potential would be more appropriate. A new spectrometer capable of measuring multiple, angle-resolved photoemission spectra is described. The paraboloidal mirror analyzer was developed to efficiently measure multiple ARPEFS spectra from the same sample. The performance of this analyzer, which includes its angle- and energy-resolving capabilities, was demonstrated. DOE

N89-20838# Massachusetts Inst. of Tech., Cambridge. Dept. of Materials Science and Engineering.
GRAIN BOUNDARY KINETICS. PART 2: IN-SITU OBSERVATION OF THE ROLE OF GRAIN BOUNDARY DISLOCATIONS IN HIGH-ANGLE BOUNDARY MIGRATION
S. E. Babcock and R. W. Balluffi Jan. 1989 35 p
(Contract DE-FG02-87ER-45310)
(DE89-006791; DOE/ER-45310/16) Avail: NTIS HC A03/MF A01

The capillarity-induced motion of near-sigma 5 grain boundaries in Au was directly observed and video-recorded by means of hot-stage in-situ transmission electron microscopy. The observed boundary motion differed from the boundary displacement caused by the stress-induced passage of secondary grain boundary dislocation (SGBD)-steps along the boundary which was studied in Part 1 of this work in the following respects. It occurred in a jerky fashion, no translation of one abutting crystal with respect to the other was observed, and quantitative evidence proved that SGBDs were not involved. These results ruled out the SGBD-Step Model for the observed motion which was identified as common long-range boundary migration. In-situ observations of the migration of more general high-angle boundaries in polycrystalline Al films revealed similar jerky motion and an apparent lack of any significant contribution to migration by observed SGBDs. DOE

N89-20839# Pacific Northwest Labs., Richland, WA.
HIGH PRESSURE RAMAN SPECTROSCOPY OF TiO2 THIN FILMS

Nancy J. Hess (Washington Univ., Seattle.) and Gregory J. Exarhos Dec. 1988 11 p Presented at the SPIE Conference on Optics, Electro-optics and Laser Applications in Science and Engineering, Los Angeles, CA, 15-20 Jan. 1989
(Contracts DE-AC06-76RL-01830; DE-AM06-70RL-02225)
(DE89-006937; PNL-SA-16168; CONF-890145-9) Avail: NTIS HC A03/MF A01

The pressure dependences of the Raman active modes in submicrometer films of the anatase and rutile crystalline phases of TiO2 have been determined at pressures approaching 90 Kbar. Films investigated have been prepared by reactive sputter deposition and sol-gel techniques. Band frequency shifts as a function of applied pressure for the rutile phase are in agreement with measurements from single crystal samples. However, sol-gel films (anatase) exhibit larger frequency shifts than powder or single crystal samples, and do not undergo the expected pressure-induced phase transformation to the TiO2-II phase. This anomalous pressure response is discussed in terms of the complex film microstructure evaluated from TEM cross-sectional measurements. DOE

N89-20840# Wisconsin Univ., Madison. Dept. of Materials Science and Engineering.
STUDIES OF ALTERNATIVE-CRYSTALLIZATION-PHASE NUCLEATION Annual Report
Thomas F. Kelly and W. Nicholas G. Hitchon Feb. 1989 3 p
(Contract DE-FG02-85ER-45215)
(DE89-007220; DOE/ER-45215/5) Avail: NTIS HC A02/MF A01

Progress is supported of phase studies, with an emphasis on nucleation, in the following systems: nickel-chromium, iron-manganese, iron-cobalt, silicon, germanium, and liquid metals. DOE

N89-20841# EG and G Energy Measurements, Inc., Santa Barbara, CA.
MATERIAL SELECTION FOR ELECTROOPTIC DEFLECTORS
Sep. 1988 76 p
(Contract DE-AC08-88NV-10617)
(DE89-007343; EGG-10617-2010) Avail: NTIS HC A05/MF A01

The selection of a material for a practical device is generally guided by a number of criteria, including cost, size, difficulty of fabrication, durability, driver requirements, and system constraints. A quantitative analysis can usually be made for comparison, or a figure of merit can be computed. In the case of materials for electrooptical (EO) devices the choice is often made based on the availability of materials meeting some minimum system requirement. For fast EO deflectors, where a large number of resolvable spots is required, the choice of materials is quite limited. A model of just such a device is proposed; it is based on the resolution of 400 spots and reasonable boundary conditions. The model predicts that to be successful, an EO material must be chosen that has a linear EO coefficient of at least 336 pm/V. A survey was conducted of the EO materials which are generally available. Based on the model and the survey, Czochralski crystal growth of strontium barium niobate (SBN:60) is recommended. Although SBN:60 does not have the largest EO coefficient, it may be the easiest to grow in the required size and optical quality, thus satisfying the availability criterion. It should be borne in mind that many materials may be grown by this technique and there are many new and potential applications for EO materials. DOE

N89-20842# International Centre for Theoretical Physics, Trieste (Italy).
NONLINEAR DYNAMICAL PHENOMENA IN LIQUID CRYSTALS
X. Y. Wang and Z. M. Sun (Nanjing Univ., China) Sep. 1988 26 p Presented at the International Conference on Singular Behavior and Nonlinear Dynamics, Samos, Greece, 18-26 Aug. 1988 Submitted for publication
(DE88-705367; IC-88/305) Avail: NTIS (US Sales Only) HC A03/MF A01

Because of the existence of the orientational order and anisotropy in liquid crystals, strong nonlinear phenomena and singular behaviors, such as solitary wave, transient periodic structure, chaos, fractal and viscous fingering, can be excited by a very small disturbance. These phenomena and behaviors are in connection with physics, biology and mathematics. DOE

N89-20843# International Centre for Theoretical Physics, Trieste (Italy).
FINITE SIZE EFFECTS IN WIGNER CRYSTALLIZATION OF ELECTRONS ON LIQUID HELIUM LAYERS
M. Sunjic (Zagreb Univ., Yugoslavia) and Z. Lenac Sep. 1988 13 p Submitted for publication
(DE88-705370; IC-88/317) Avail: NTIS (US Sales Only) HC A03/MF A01

Phase diagrams for the formation of a two-dimensional Wigner lattice of electrons on thin liquid helium layers deposited on metallic substrates are calculated, taking into account finite electron size normal to the surface and the substrate screening. Finite size effects soften the direct electron repulsion, but also weaken the screening effects, so that the total interaction is actually stronger than in the point electron approximation. Both the high density and the low density (classical) regimes are affected, and in particular the solid phase is shifted to lower densities, in agreement with the experiment. In this system it also becomes possible to study the gradual transition from classical to quantum regimes. DOE

N89-20844# Southern Methodist Univ., Dallas, TX. Dept. of Physics.
EFFECTS OF ENVIRONMENT ON TUNNELING SPECTROSCOPY OF GOLD FILMS
G. C. Wetsel, Z. M. Liu, T. L. Weng, M. W. Gosney, and R. J. Warmack (Oak Ridge National Lab., TN.) 1988 5 p Presented at the Fall Meeting of the Materials Research Society, Boston, MA, 28 Nov. 1988
(Contract DE-AC05-84OR-21400)
(DE89-006040; CONF-881155-43) Avail: NTIS HC A02/MF A01

A scanning tunneling microscope with a tunneling-current dynamic range of four orders of magnitude has been used in tunneling-spectroscopy studies of Au surfaces in moderate vacuum and in various gases at atmospheric pressure. Rapid scans of z-motion transducer voltage (V sub z) were measured as a function of tunneling current (I sub t) under computer control. Drift-corrected plots of log(I sub t) versus V sub z were essentially linear. The mean barrier potential was determined from the slope of these plots and the measured displacement-versus-V sub z calibration curve. Barrier potentials so determined are compared for different environmental conditions of the Au surface. DOE

N89-20845# Lawrence Livermore National Lab., CA. Chemistry and Materials Science.
A FIRST-PRINCIPLES METHOD FOR THE DETERMINATION OF THE ELECTRONIC STRUCTURE OF GRAIN BOUNDARIES
X.-G. Zhang (Northwestern Univ., Evanston, IL.), Erik C. Sowa, and A. Gonis 1989 7 p Presented at the Acta-Scripta Conference on Metal-ceramic Interfaces, Santa Barbara, CA, 15 Jan. 1989
(Contract W-7405-eng-48)
(DE89-006148; UCRL-100199; CONF-890165-1) Avail: NTIS HC A02/MF A01

This paper describes and illustrates a first-principle approach to the solution of the Schroedinger equation, and hence the determination of the corresponding electronic structure, associated with systems containing surfaces and interface regions such as grain boundaries. The method is based on the formalism of Multiple-Scattering Theory (MST), on the recently formulated concept of Semi-Infinite Periodicity (SIP), and on the property of removal invariance satisfied by systems with SIP. Semi-infinite periodicity is defined as the periodic repetition of a basic unit with well-defined physical properties, e.g., scattering properties, along a given direction. In our method, this concept replaces that of full translational invariance. DOE

N89-20846# California Univ., Berkeley. Lawrence Berkeley Lab. Accelerator and Fusion Research Div.
A STUDY OF THE EFFECTS OF COPPER TO SUPERCONDUCTOR RATIO ON STABILITY
W. V. Hassenzahl Aug. 1988 16 p Presented at the Japan-US Seminar on Basic Mechanisms of Helium Heat Transfer and Related Influence on Stability of Superconducting Magnets, Fukuoka, Japan, 29 Aug. 1988
(Contract DE-AC03-76SF-00098)
(DE89-006604; LBL-25818; CONF-8808143-2) Avail: NTIS HC A03/MF A01

Accelerator dipole magnets operate with very low copper to superconductors ratios (R). This ability to operate with low R is significant in its impact on cost. The optimum value of R has been an issue of considerable debate. This study shows that the minimum propagating zone length is greatest for copper to superconductor ratios well below 1.5, which appears to be in contradiction with some of the data. DOE

N89-20847# California Univ., Berkeley. Lawrence Berkeley Lab. Dept. of Physics.
RESONANCE ELECTRONIC RAMAN SCATTERING IN RARE EARTH CRYSTALS Ph.D. Thesis
Glen Monroe Williams 10 Nov. 1988 248 p
(Contract DE-AC03-76SF-00098)
(DE89-007446; LBL-26344) Avail: NTIS HC A11/MF A01

The intensities of Raman scattering transitions between electronic energy levels of trivalent rare earth ions doped into transparent crystals were measured and compared to theory. A particle emphasis was placed on the examination of the effect of intermediate state resonances on the Raman scattering intensities. Two specific systems were studied: Ce(3+)(4f1) in single crystals of LuPO4 and Er(3+)(4f11) in single crystals of ErPO4. DOE

N89-20848# Connecticut Univ., Storrs. Dept. of Mechanical Engineering.
A MICROMECHANICAL VISCOPLASTIC STRESS-STRAIN MODEL WITH GRAIN BOUNDARY SLIDING Progress Report, 15 Apr. 1988 - 14 Apr. 1989
E. H. Jordan 1989 5 p
(Contract DE-FG02-88ER-13894)
(DE89-007712; DOE/ER-13894/1) Avail: NTIS HC A02/MF A01

The goal of the project is the construction and verification of a visco-plastic stress-strain behavior model of a polycrystalline metal where the polycrystalline behavior is derived from single crystal behavior in a manner that accounts for the interaction of differently oriented grains. During this period, steps have been taken to make specimen and associated grips. In addition, major improvements in the tension-torsion test set up have been implemented to obtain higher data quality. The test plan formulated calls for testing both Hastelloy-X single crystal and Hastelloy-X polycrystalline tension-torsion specimen at an elevated temperature. A polycrystalline specimen has been installed in the grips with the calibrated extensometer and this specimen has been heated to 871 C and the resulting temperature distribution adjusted by modifying the induction coil to achieve a uniform temperature. This specimen will be tested to check out all aspects of the setup. The first single crystal specimen test will be completed by the end of the first year and determination of constants for the single crystal model previously constructed will be the primary task early in the second year of this grant. DOE

N89-20849# Stanford Univ., CA. Center for Materials Research.
A STUDY OF FERROELECTRICITY IN SINGLE CRYSTAL COMPOUNDS OF THE TYPE AFB5 AND A3B2F12 Final Technical Report, 1 Jan. 1987 - 30 Jun. 1988
Robert S. Feigelson Oct. 1988 23 p
(Contract N00014-87-K-0124)
(AD-A203610; SU-CMR-88-12) Avail: NTIS HC A03/MF A01 CSCL 07B

Phase relations in the PbF2/AlF3 binary system were studied in order to facilitate the preparation of single crystals of a reportedly high dielectric constant ternary ferroelectric phase. A phase diagram for the composition range 50 to 100 mole percent lead fluoride was developed and crystals of the incongruently melting Pb3AL2F12 phase were grown using Bridgman growth techniques. A new inverted Bridgman method was developed to help induce melt convection during growth, thereby reducing the build-up of unwanted species at the growth interface. GRA

N89-20850# City Coll. of the City Univ. of New York. Dept. of Physics.
ULTRAFAST PHYSICS IN MICROSTRUCTURE AND ALLOY SYSTEMS Annual Report, 1 Dec. 1987 - 30 Nov. 1988
Robert Alfano 1 Dec. 1988 12 p
(Grant AF-AFOSR-0031-86; AF Proj. 2305)
(AD-A203639; RF-447230; AFOSR-89-0053TR) Avail: NTIS HC A02/MF A01 CSCL 07B

We have continued to employ picosecond and femtosecond techniques to investigate ultrafast physics in semiconductor bulk and microstructures. We have: (1) determined exciton dissociation time by ionized carbon acceptors in Gallium Arsenides Quantum wells; (2) proposed and demonstrated a new optical approach to measure directly momentum relaxation times which are related to electron mobilities in QWs; (3) determined intervalley scattering in GaAs bulk and double-barrier tunneling structures experimentally and theoretically; (4) determined X6T6 scattering time of 0.5 ps in GaAs by picosecond IR absorption spectroscopy; and (5) observed stimulated excitonic emission in spherical (dot) quantum wells under picosecond UV excitation at room temperature. GRA

N89-20851# Auburn Univ., AL. Dept. of Electrical Engineering.
FEASIBILITY STUDY OF HIGH TEMPERATURE SUPERCONDUCTOR OPENING SWITCHES Final Report, 15 Mar. - 30 Sep. 1988
Mike Fernandez and Yonhua T. Tzeng Dec. 1988 21 p
(Contract DNA001-85-C-0183)
(AD-A203699; AFATL-TR-88-145) Avail: NTIS HC A03/MF A01 CSCL 11B

Raw materials and equipment were obtained and new high temperature superconductors (HTSC'S) were fabricated. YBCO material showed promising response to a 1T electromagnetic field. Three methods of quenching superconductivity examined. Four-point measurement technique used. HTSC samples were long bars of bulk material with silver contacts, YBaSaCaO material has 200 times higher normal state resistivity than YBCO, but low current density. Pulsed current quenching experiment caused sample to quench immediately, but took several MSEC to recover. Magnet pulse circuit and microwave experiments set up. Magnetic quenching approach provides a fast operation of the switch but requires circuits for generating fast magnetic pulses. Microwave quenching was mainly a thermal process and thus was slow. Conclusion: Feasibility demonstrated. GRA

77 THERMODYNAMICS AND STATISTICAL PHYSICS

Includes quantum mechanics; theoretical physics; and Bose and Fermi statistics.

For related information see also *25 Inorganic and Physical Chemistry* and *34 Fluid Mechanics and Heat Transfer.*

N89-20852 Sussex Univ., Brighton (England).
GENERAL RELATIVITY, SCALAR FIELDS AND COSMIC STRINGS Ph.D. Thesis
Adrian Benedict Burd 1987 192 p
Avail: Univ. Microfilms Order No. BRDX83013

This thesis is divided into three, essentially self contained, parts. In the first part, the structure of classical 3-D space-times is examined. Here, what is known about the gravitational theories in these models is reviewed and extended. The nonexistence is investigated of a Newtonian limit to the relativistic theories showing that in the prescence of certain matter terms, Newtonian gravity

can be obtained as a suitable weak field limit. A number of new, exact static and nonstatic solutions are presented to the equations of 3-D general relativity with scalar field and perfect fluid sources. The second part contains a study of certain cosmological models which have self-interacting scalar fields obeying an exponential potential. The techniques of phase portrait analysis are used to study the N-dimensional cosmological models as well as some anisotropic models. The last section is a review of the cosmic string picture of galaxy formation. The structure of the string is examined from the viewpoint of the fields. Dissert. Abstr.

N89-20853# Centro Brasileiro de Pesquisas Fisicas, Rio de Janeiro.
INTRODUCTION TO STRINGS AND SUPERSTRINGS
Michel Rausch deTraubenberg 1988 122 p In FRENCH
(DE88-704998; CBPF-MO-001/88) Avail: NTIS (US Sales Only) HC A06/MF A01

We discuss the main features on the formulation of string theory that, in a primitive level, describe the hadronic phenomenon of duality. We also study an extension of the models of closed and strings with spin. Then, by using supersymmetry, the theory of superstrings and heterotic strings is formulated with the aim of unifying the fundamental interactions and matter. DOE

N89-20854# Centro Brasileiro de Pesquisas Fisicas, Rio de Janeiro.
EINSTEINS'S THEORY OF GRAVITY IN FIERZ VARIABLES
M. Novello and N. PintoNeto 1988 77 p
(DE88-705004; CBPF-NF-012/88) Avail: NTIS (US Sales Only) HC A05/MF A01

We present a complete theory of massive and massless spin-two field using Fierz variables A (sub alpha beta mu) its relationship with the standard variable Psi (sub mu upsilon) and the bridge relation which allows the passage from one representation to the other. We develop the Hamiltonian formalism for both the massive and the massless cases. The theory thus presented is nothing but Einstein's General Relativity in the Jordan - Lichnerowicz formulation. We then discuss an unification program in which a new short-range force is postulated. This force becomes the local counterpart of gravity in the same way we can think that weak interaction is the short-range counterpart of electrodynamics. DOE

N89-20855# Instituto de Fisica Teorica, Sao Paulo (Brazil).
REMARK ON THE GRAVITATIONAL FIELD PRODUCED BY AN INFINITE STRAIGHT STRING
G. Francisco and G. E. A. Matsas 1988 18 p
(DE88-705077; IFT-P-20/88) Avail: NTIS (US Sales Only) HC A03/MF A01

We compare the results predicted by Newtonian Gravity and General Relativity regarding the field produced by an infinite string with constant density lambda. A simple gedanken experiment is suggested to stress the remarkable differences between these two theories. The existence of the usual Newtonian limit is discussed in this case. DOE

N89-20856# Brookhaven National Lab., Upton, NY. Physics Dept.
LATTICE GAUGE THEORY AND MONTE CARLO METHODS
Michael Creutz Nov. 1988 26 p Presented at the 32nd Semester in the Stefan Banach International Mathematical Center, Gauge Theories of the Fundamental Interactions, Warsaw (Poland), 19 Sep. - 3 Dec. 1988
(Contract DE-AC02-76CH-00016)
(DE89-005666; BNL-42086) Avail: NTIS HC A03/MF A01

Lattice gauge theory is now the primary non-perturbative technique for quantum field theory. The lattice represents an ultraviolet cutoff, and renormalization group arguments show how the bare coupling must be varied to obtain the continuum limit. Expansions in the inverse of the coupling constant demonstrate quark confinement in the strong coupling limit. Numerical simulation has become the approach to calculating hadronic properties. The basic algorithms for obtaining appropriately weighted gauge field configurations are discussed. Algorithms for treating fermionic fields, which still require considerably more computer time than needed for purely bosonic simulations, are also discussed. Some particularly promising recent approaches are based on global accept-reject steps and should display a rather favorable dependence of computer time on the system volume. DOE

N89-20857# International Centre for Theoretical Physics, Trieste (Italy).
INTEGRABLE TWO DIMENSIONAL SUPERSYSTEMS
K. C. Tripathy and L. K. Tripathy (Delhi Univ., India) Aug. 1988 9 p Submitted for publication
(DE88-705355; IC-88/233) Avail: NTIS (US Sales Only) HC A02/MF A01

The integrability of two dimensional time-dependent classical systems is examined in N=2 superspace using Dirac's second class constraints. The invariants involving quadratic powers in velocities for super harmonic oscillator and super Kepler potentials have been derived. DOE

N89-20858# Chicago Univ., IL.
THERMODYNAMICS OF FINITE-TIME PROCESSES: ACCOMPLISHMENTS AND WORK IN PROGRESS, 1986–1989
R. S. Berry 1989 9 p
(Contract DE-FG02-86ER-13488)
(DE89-006726; DOE/ER-13488/1) Avail: NTIS HC A02/MF A01

Work on thermodynamics in the following processes/ research areas is briefly described: geometric thermodynamics, thermodynamics, dissipative engines, radiations and the slowing of an atomic beam, time-constrained adiabatic engines, a Hamilton's principle for nonequilibrium systems with heat flow, separation processes, paradigmatic models and strategies for optimal process designs. DOE

80 SOCIAL SCIENCES (GENERAL)

Includes educational matters.

No abstracts in this category.

81 ADMINISTRATION AND MANAGEMENT

Includes management planning and research.

N89-20859# General Accounting Office, Washington, DC.
SPACE OPERATIONS: TESTING OF NASA'S TECHNICAL AND MANAGEMENT INFORMATION SYSTEM
Mar. 1988 8 p
(GAO/IMTEC-88-28) Avail: NTIS HC A02/MF A01

The status of the development of the National Aeronautics and Space Administration's Technical and Management Information System (TMIS) is presented. TMIS is intended to support the design, development, and operation of the planned space station. The parameters involved in the development of TMIS are data base management, project management, document management, electronic mail, workstations, hardware, interfaces and networking. It is estimated that initial operating capability (IOC) will be available at all NASA Centers by June 1988. M.G.

N89-20860# Center for Mathematics and Computer Science, Amsterdam (Netherlands). Dept. of Operations Research and System Theory.
MINIMIZING TOTAL COMPLETION TIME IN THE TWO-MACHINE FLOW SHOP BY LAGRANGIAN RELAXATION
S. L. vandeVelde Jun. 1988 11 p Submitted for publication
(CWI-OS-R8808; B8827728; ETN-89-94193) Copyright Avail: NTIS HC A03/MF A01

A branch-and-bound algorithm is presented for the two-machine flow shop problem with the objective of minimizing the sum of the job completion times. Lower bounds and precedence constraints result from a Lagrangian relaxation of this problem. The Lagrangian subproblem turns out to be a linear ordering problem, that is polynomially solvable for appropriate choices of the Lagrangian multipliers. Published lower bounds are shown to coincide with two of these choices. Dominance criteria are given to restrict the search tree. Computational experiments show that the proposed algorithm outperforms the previously best method. ESA

82 DOCUMENTATION AND INFORMATION SCIENCE

Includes information management; information storage and retrieval technology; technical writing; graphic arts; and micrography.

For computer documentation see *61 Computer Programming and Software.*

N89-20861# American Inst. of Aeronautics and Astronautics, Washington, DC.
BARRIERS TO THE INTERNATIONAL TRANSFER OF INFORMATION IN AEROSPACE AND DEFENSE
James J. Harford and Barbara Lawrence [1988] 5 p Presented at the Meeting on Barriers to Information Transfer and Approaches Toward Their Reduction, Washington, DC, 23-24 Sep. 1987; sponsored by AGARD Contained in AGARD-CP-430 accessioned as N88-30458
Avail: NTIS HC A02/MF A01

An overview of the barriers to the international transfer of information, particularly in the aerospace and defense area is discussed. The role of the professional society, motives, and types of barriers are also discussed. B.G.

N89-20862# National Technical Information Service, Springfield, VA.
SUPPLY AND USE OF JAPANESE TECHNICAL LITERATURE IN THE UNITED STATES
David B. Shonyo and Janet H. Geffner Feb. 1988 33 p Presented at the American Association for the Advancement of Science Annual Meeting, Boston, MA, Feb. 1988
(PB88-230842) Avail: NTIS HC A03/MF A01 CSCL 05B

Some of the barriers to easy access to scientific and technical information (STI) that originates in Japan are considered, along with some to the ways that researchers can gain an entry to this body of literature. Examples are quoted from a series of case studies of information centers in the U.S. which have been reasonably successful in providing their clients with Japanese STI. It is shown that, although there has been a great deal of interest in Japanese STI in the West, the actual demand for this kind of information has not been great, especially as measured in commercial terms. Some possible reasons for this are discussed. Finally, the results of a series of interviews with end users of Japanese STI are summarized. Author

N89-20863# Commerce Dept., Washington, DC. Office of Japanese Technical Literature.
CURRENT STATUS OF JAPANESE TO ENGLISH MACHINE TRANSLATION: REPORT TO CONGRESS
Tamami Kusuda Jul. 1988 18 p
(PB89-128276) Avail: NTIS HC A03/MF A01 CSCL 05B

The primary obstacle to access to the Japanese technical literature is the Japanese language. Manual translation of Japanese technical material tends to be very expensive and, especially in specialized technical fields, is often inaccurate. Machine-aided Translation (MT) offers the hope of eventually gaining a much broader access to Japanese scientific and technical literature. The report to the US Congress assesses the present state of Japanese-to-English MT. Consideration is given to the MT process itself, and to current activities in the U.S., Japan, and Europe. Attention is also given to the status of optical Japanese character recognition devices as an input method for MT systems. GRA

N89-20864# Office of Technology Assessment, Washington, DC.
REPORT ON FEDERAL INFORMATION DISSEMINATION: RESPONSES TO DECISION ANALYSIS FRAMEWORK FOR GPO (GOVERNMENT PRINTING OFFICE) STRATEGIC ALTERNATIVES
F. J. Romano 4 Jan. 1988 65 p
(PB89-114649) Avail: NTIS HC A04/MF A01 CSCL 05B

To address the issues, OTA has developed a decision analysis framework to collect data and opinions as a prelude to the establishment of meaningful alternatives that will best serve the American people, the Federal infrastructure and the GPO. The specific task was an evaluation of GPO technology, products and relationships with its customers. To accomplish the task it was necessary to develop alternative sources of data since neither GPO nor any other Government entity maintains the kind of information considered necessary to understand and analyze many relevant aspects. The result is a snapshot of Federal information as viewed from the standpoint of the GPO and sample Executive agencies. GRA

N89-20865# BDM Corp., McLean, VA.
COMPARATIVE LEXICON OF US-SOVIET MILITARY TECHNICAL TERMINOLOGY
1988 541 p Sponsored by Foreign Broadcast Information Service, Washington, DC
(PB89-125553) Avail: NTIS HC A23/MF A01 CSCL 05B

The objective of the Lexicon is to expand a Western reader's understanding of the intended meaning of Soviet military authors writing about their profession. This understanding is vital to the work of U.S. analysts who may not read Russian, but who are charged with the responsibility of analyzing Soviet military capabilities and intentions. It is also a useful reference for professional translators who must accurately render the intended meaning of Soviet military writings into English. The Comparative Lexicon of U.S. - Soviet Military - Technical Terminology is as much an analyst's reference as it is a translator's aid. Author

N89-20866# Massachusetts Inst. of Tech., Cambridge. Artificial Intelligence Lab.
USING ENGLISH FOR INDEXING AND RETRIEVING
Boris Katz Oct. 1988 32 p
(Contract N00014-85-K-0124)
(AD-A202227; AI-M-1096) Avail: NTIS HC A03/MF A01 CSCL 05G

This paper describes a natural language system START. The system analyzes English text and automatically transforms it into an appropriate representation, the knowledge base, which incorporates the information found in the text. The user gains access to information stored in the knowledge base by querying it in English. The system analyzes the query and decides through a matching process what information in the knowledge base is relevant to the question. Then it retrieves this information and formulates its response in English. GRA

N89-20867# Satellites International Ltd., Newbury (England).
ADAPTIVE DATA COMPRESSION SYSTEM STUDY, EXECUTIVE SUMMARY
N. S. Bray, C. K. Chan, A. K. Ward, B. E. Patchett, M. A. Birdseye, E. R. Breeveld, A. J. Coates, R. A. Gowen, H. E. Huckle, and A. D. Johnstone (Mullard Space Science Lab., Dorking, England) et al Paris, France ESA Jul. 1988 21 p Prepared in cooperation with Science Research Council, Chilton (England); and Mullard Space Science Lab., Dorking (England)
(Contract ESA-7087/87-NL-PP(SC))
(SIL/CR/7129/7; ESA-CR(P)-2678-Vol-2; ETN-89-93915)
Copyright Avail: NTIS HC A03/MF A01

The procedures used to examine the data compression algorithms for the CLUSTER and SOHO missions are presented. A number of compression algorithms were evaluated. Some of

these algorithms are well known in the literature, while others have been developed from existing implementations to suit the characteristics of the types of data under consideration in order to obtain improved fully reversible compression performance. Only those compression algorithms or schemes which are likely to be suitable for on-board implementation are discussed. The operation of a general data compression algorithm can be broken down into three distinct phases. The first phase is the decorrelation of the source data in which redundant information is reduced or removed. Then the correlated data stream is separated into small blocks whose sizes may vary from typically 4 to 256 for the algorithms which are described. Finally, the decorrelated data in these blocks are optimally coded for fully or partially reversible reconstruction. M.G.

N89-20868# International Atomic Energy Agency, Vienna (Austria).
GEOLOGICAL DATA INTEGRATION TECHNIQUES: PROCEEDINGS
Sep. 1988 389 p Presented at the Technical Committee Meeting held in Vienna, Austria, 13-17 Oct. 1986
(DE88-705255; IAEA-TECDOC-472; CONF-8610449) Avail: NTIS (US Sales Only) HC A17/MF A01

The objectives of this Technical Committee are to bring together current knowledge on geological data handling and analysis technologies as developed in the mineral and petroleum industries for geological, geophysical, geochemical and remote sensing data that can be applied to uranium exploration and resource appraisal. The recommendation for work on this topic was first made at the meeting of the NEA-IAEA Joint Group of Experts on R and D in Uranium Exploration Techniques (Paris, May 1984). In their report, processing of integrated data sets was considered to be extremely important in view of the very extensive data sets built up over the recent years by large uranium reconnaissance programmes. With the development of large, multidisciplinary data sets which includes geochemical, geophysical, geological and remote sensing data, the ability of the geologist to easily interpret large volumes of information has been largely the result of developments in the field of computer science in the past decade. Advances in data management systems, image processing software, the size and speed of computer systems and significantly reduced processing costs have made large data set integration and analysis practical and affordable. The combined signatures which can be obtained from the different types of data significantly enhance the geologists ability to interpret fundamental geological properties thereby improving the chances of finding a significant ore body. This volume is the product of one of a number of activities related to uranium geology and exploration during the past few years with the intent of bringing new technologies and exploration techniques to the IAEA Member States. DOE

N89-20869# Defense Applied Information Technology Center, Alexandria, VA. Hypermedia Lab.
THE DoD GATEWAY INFORMATION SYSTEM (DGIS): THE DEVELOPMENT TOWARD ARTIFICIAL INTELLIGENCE AND HYPERMEDIA IN COMMON COMMAND LANGUAGE
Allan D. Kuhn Dec. 1988 18 p
(AD-A203674; DAITC/TR-88/009; DTIC-TR-89/4) Avail: NTIS HC A02/MF A01 CSCL 05B

DGIS CCL Development began with C language prototyping to study its feasibility and issues. The study raised the potential of employing Artificial Intelligence, and DGIS CCL is now proceeding on two levels. The first level in incorporating Artificial Intelligence as a means to handle the heterogeneous universe of diverse information systems. This is done with PROLOG, using its logic programming capabilities for structuring knowledge base and blackboard architectures. The knowledge bases contain information about the target system commands and operating characteristics, and about users to establish a more graceful and human response in the human-machine interface. AI-based CCL, still in development, is available to all DGIS users. The second level incorporates the hypermedia capabilities of bit-map systems, to run concurrently with those that are ASCII-dependent. A desktop environment is being developed that includes icon selection, windowing technology, simultaneous query invoking and results display n multiple target systems, and color as an enhancing feature. As a part of the hypermedia application, integration with media peripherals such as CD-ROM databases will also be included. GRA

N89-20870# Bolt, Beranek, and Newman, Inc., Cambridge, MA.
RESEARCH IN DISTRIBUTED PERSONAL COMPUTER-BASED INFORMATION SYSTEMS, VOLUME 2 Final Report No. 5, Oct. 1983 - Mar. 1984
Harry C. Forsdick and Robert H. Thomas Aug. 1988 77 p
(Contract F30602-81-C-0256; ARPA Order 4224)
(AD-A203845; BBN-5723-Vol-2; RADC-TR-88-159-Vol-2) Avail: NTIS HC A05/MF A01 CSCL 12G

The primary focus of the personal computer task area is the development of an electronic message system called Diamond, which will run in a distributed personal computer environment. The message system will: support a user interface that exploits the capabilities of advanced single-user computers, handle messages that contain data other than text, have a distributed architecture, operate in a secure fashion, permit use from a variety of user access points, and have a transportable implementation. Section 2 discusses work on the Diamond multimedia message system and related activities. Work in Jade, the Jericho Pascal operating system, is described in Section 3. Section 4 presents our activities related to the development of the Jade programming environment. Work on the Interlisp system for the Jericho computer is described in Section 5. Section 6 discusses our work of Aleph. Section 7 describes recent Hermes maintenance activity. GRA

83 ECONOMICS AND COST ANALYSIS

Includes cost effectiveness studies.

N89-20871*# Ecosystems International, Inc., Gambrills, MD.
COMMERCIAL POTENTIAL OF EUROPEAN AND JAPANESE SPACE PROGRAMS, TASK 5 Final Report
Sep. 1987 89 p
(Contract NASw-4065)
(NASA-CR-184659; NAS 1.26:184659) Avail: NTIS HC A05/MF A01 CSCL 05C

The current and expected future competitive status in the commercialization of space of the two principal programs competitive with NASA: the European Space Agency (ESA) and the program sponsored by the Ministry of International Trade and Industry (MITI) of Japan are evaluated, quantitatively assessed, and presented in usable format. B.G.

84 LAW, POLITICAL SCIENCE AND SPACE POLICY

Includes NASA appropriation hearings; aviation law; space law and policy; international law; international cooperation; and patent policy.

N89-20872# General Accounting Office, Washington, DC.
NUCLEAR POWER SAFETY: INTERNATIONAL MEASURES IN RESPONSE TO CHERNOBYL ACCIDENT
Apr. 1988 41 p
(GAO/NSIAD-88-131BR) Avail: NTIS HC A03/MF A01

The potential for an expanded nuclear safety role in the International Atomic Energy Agency (IAEA) is examined. Specifically, whether IAEA can undertake greater responsibility for inspecting nuclear power reactors and can it set an international mechanism for rapid response to mitigate the consequence of a nuclear accident is studied. The results are summarized. Author

N89-20873# Committee on Commerce, Science, and Transportation (U.S. Senate).
NASA AUTHORIZATION

1988 103 p Hearing before the Subcommittee on Science, Technology and Space of the Committee on Commerce, Science and Transportation, 100th Congress, 2d session, part 1
(S-Hrg-100-579; GPO-83-952) Avail: Subcommittee on Science, Technology and Space, Senate, Washington, DC 20510 HC free

Hearings before the Science, Technology, and Space Subcommittee of the Senate are presented. The scope and direction, the health and well-being of the nation's Space and Technology Program are discussed. All written testimony and submittals for the record are included. B.G.

85 URBAN TECHNOLOGY AND TRANSPORTATION

Includes applications of space technology to urban problems; technology transfer; technology assessment; and surface and mass transportation.

For related information see also *03 Air Transportation and Safety, 16 Space Transportation,* and *44 Energy Production and Conversion.*

N89-20874# General Accounting Office, Washington, DC.
TECHNOLOGY TRANSFER: CONSTRAINTS PERCEIVED BY FEDERAL LABORATORY AND AGENCY OFFICIALS
Mar. 1988 25 p
(GAO/RCED-88-116BR) Avail: NTIS HC A03/MF A01

Federal laboratory and agency officials were interviewed to identify constraints to transferring technology from Federal labs to U.S. businesses. Following are four major constraints which were identified by several labs: (1) while recent changes in the law allow Federal labs to patent and exclusively license inventions, Federal computer software is publicly disseminated, thus businesses do not have an incentive to fully develop and market it; (2) because Federal labs generally cannot conduct proprietary research and therefore competitors can obtain access to research results, businesses are less inclined to enter into collaborative research efforts; (3) the requirement that several of the DOE's contractor operated labs must request the Department to waive its title rights to inventions that they make causes uncertainty and delay and reduces industry interest in getting involved; and (4) Federal labs, in their efforts to be fair in providing businesses opportunities to collaborate on research, may institute burdensome and time consuming procedures that inhibit industry participation. Author

88 SPACE SCIENCES (GENERAL)

No abstracts in this category.

89 ASTRONOMY

Includes radio, gamma-ray, and infrared astronomy, and astrometry.

N89-20875*# National Aeronautics and Space Administration. Goddard Space Flight Center, Greenbelt, MD.
FORBIDDEN CORONAL IRON LINE EMISSION IN THE PUPPIS A SHOCK FRONT: THE EFFECT OF INHOMOGENEITIES
Richard G. Teske (Michigan Univ., Ann Arbor.) and Robert Petre [1986] 27 p
(NASA-TM-89284; NAS 1.15:89284) Avail: NTIS HC A03/MF A01 CSCL 03A

We have obtained CCD images of the shock front at the eastern rim of Puppis A in (Fe X) lambda 6374 and (Fe XIV) lambda 5303 and have compared the optical data to Einstein HRI soft X-ray data. The observed part of the remnant is complex, containing density irregularities. Optical and X-ray data are consistent in showing a nearly flat gradient of ionization behind the shock. To determine conditions in the shock, scans of surface brightness across it in the optical lines were compared to surface brightnesses predicted by idealized Sedov models. We were unable to match both the red and green line scans by a simple, single-component model, and have ascribed the failure to the presence of the density inhomogeneities. Our result has important implications for the determination of SNR shock front models by means of fitting X-ray data with Sedov models. Author

N89-20876# Case Western Reserve Univ., Cleveland, OH.
PUBLICATIONS OF THE OBSERVATORY OF THE UNIVERSITY OF MICHIGAN. VOLUME 12, NO. 2: WAVELENGTH IDENTIFICATIONS IN THE MAGNETIC CP STAR HR 4816 (HD 110066)
W. P. Bidelman, Charles R. Cowley, and John C. Roemmelt (Michigan Univ., Ann Arbor.) Jun. 1988 54 p
Avail: NTIS HC A04/MF A01

The unusually sharp spectral lines of HR 4816 make it particularly well suited for identification work at high dispersion. The 2A/mm spectrogram (EC 103) was taken at the Lick Observatory. The UT data of mid-exposure was 7.26 June 1960, (2437092.76). The bulk of the identifications were made in 1960, from wavelengths measured with a conventional engine. In the list, the stellar wavelengths are in the first column, followed by an estimate of the intensity and character of the line, the identifications begin in column 4 with decimal fractions of an angstrom. The multiplet number follows the symbol for the atomic spectrum. B.G.

N89-20877 Edinburgh Univ. (Scotland).
SELECTION EFFECTS IN OPTICAL QUASAR SURVEYS Ph.D. Thesis
Crispin Julian Keable 1988 266 p
Avail: Univ. Microfilms Order No. BRD-82983

An investigation into the selection effects of optical quasar surveys is described. This is accomplished via the accumulation and comparison of optical quasar surveys of different types, which are then used to generate a survey free from selection effects. An automatic search of a deep C.F.H.T. grens plate over 1 degree squared in the center of the field was undertaken. Slit spectroscopic observations were made of 26 candidates from this survey. An automatic photometric survey was also undertaken, using direct plates in the five wavebands U, J, V, R, and I from the U.K. Schmidt telescope. CCD frames were obtained in each of the wavebands from various sources, to allow calibration of data from the Schmidt plates. Spectroscopy indicates that the automatic grens survey is complete, except for overlapped spectra. This is in part due to the linear dispersion of the transmission grating. The photometric survey readily identifies objects which have peculiar colors, but a detailed examination of the properties of these objects must await further work. Finally, a synthetic survey was constructed, using all of the information available for each object. Redshift estimates were possible for about 30 percent of the 130 candidates (the higher redshift objects). Examination of the survey indicates that it is largely free from selection effects below a redshift of z = 3.4. Dissert. Abstr.

N89-20878 Maryland Univ., College Park.
MULTICOLOR SURFACE PHOTOMETRY OF POWERFUL RADIO GALAXIES Ph.D. Thesis
Eric Philip Smith 1988 262 p
Avail: Univ. Microfilms Order No. DA8818219

The CCD images of 72 powerful radio galaxies were obtained with the KPNO 2.1 m, 4 m and CTIO 4 m telescopes utilizing B, V, and R filters to study the colors and other photometric properties of these large systems. The GASP software package was used for the data reduction and detailed 2-D surface photometry. In addition, image modeling techniques were employed to investigate the contributions to galaxy properties by point-like nuclear sources seen in some of these galaxies. Dissert. Abstr.

N89-20879 California Inst. of Tech., Pasadena.
ISOPHOTOMETRY OF BRIGHTEST ELLIPTICAL GALAXIES IN RICH CLUSTERS Ph.D. Thesis
Alain C Porter 1988 472 p
Avail: Univ. Microfilms Order No. DA8820983

Ellipse fitting isophotometry of 175 brightest elliptical galaxies in Abell clusters (BCEs) are presented. Galaxy structure is traced to an average major axis of 50 kpc, and sometimes beyond 100 kpc. The data consist not only of major and minor axis surface brightness profiles, but also of isphote ellipticity, major axis position angle, and centroid position profiles. Almost all BCEs have some local structure that does not show in an azimuthally averaged brightness profile. However, local structure shows no correlation with global parameters such as galaxy luminosity or size. These results echo earlier findings for field ellipticals. The average ellipticity of a BCE is a strongly increasing function of physical radius, as are most individual ellipticity profiles. This explains why cD halos are highly flattened. The deficit of large round isophotes is so marked that the isoluminosity surfaces of BCEs at large radii cannot be drawn from a population of randomly oriented oblate spheroids. This the first example of galaxies for which such an exclusion has been possible. Dissert. Abstr.

N89-20880*# Chicago Univ., IL. Dept. of Astronomy and Astrophysics.
ON THE EFFECTS OF COSMIONS UPON THE STRUCTURE AND EVOLUTION OF VERY LOW MASS STARS
E. E. DeLuca, K. Griest, R. Rosner, and J. Wang (Illinois Univ., Urbana-Champaign.) Feb. 1989 8 p
(NASA-CR-182958; NAS 1.26:182958; FERMILAB-Pub-89/49-A)
Avail: NTIS HC A02/MF A01 CSCL 03A

A number of recent studies have suggested that cosmions, or WIMPS, may play an important role in the energetics of the solar interior; in particular, it has been argued that these hypothetical particles may transport sufficient energy within the nuclear-burning solar core so as to depress the solar core temperature to the point of resolving the solar neutrino problem. Solutions to the solar neutrino problem have proven themselves to be quite nonunique, so that it is of some interest whether the cosmion solution can be tested in some independent manner. It is argued that if cosmions solve the solar neutrino problem, then they must also play an important role in the evolution of low mass main sequence stars; and, second, that if they do so, then a simple (long mean free path) model for the interaction of cosmions with baryons leads to changes in the structure of the nuclear-burning core which may be in principal observable. Such changes include suppression of a fully-convective core in very low mass main sequence stars; and a possible thermal runaway in the core of the nuclear burning region. Some of these changes may be directly observable, and hence may provide independent constraints on the properties of the cosmions required to solve the solar neutrino problem, perhaps even ruling them out. Author

N89-20881# General Accounting Office, Washington, DC.
SPACE SCIENCE: STATUS OF THE HUBBLE SPACE TELESCOPE PROGRAM
May 1988 31 p
(GAO/NSIAD-88-118BR) Avail: NTIS HC A03/MF A01

The current status of the NASA's Hubble Space Telescope (HST) program is reviewed. The following questions are addressed: (1) what is the current status of the program with respect to cost, schedule, and performance; (2) what is the role of the Space Telescope Institute; and (3) what are NASA's plans for providing on-orbit maintenance to the space telescope. The objectives, scope, and methodology are discussed and summarized. E.R.

N89-20882# Geneva Observatory (Switzerland).
GRIDS OF EVOLUTIONARY MODELS FROM 0.85 TO 120 SOLAR MASSES: OBSERVATIONAL TESTS AND THE MASS LIMITS
Andre Maeder and Georges Meynet 1988 33 p Submitted for publication
(Ser-C-Prepubl-Fasc-29; ETN-89-93745) Avail: NTIS HC A03/MF A01

Grids of stellar evolutionary models with composition X=0.70, Z=0.02 are computed with mass loss and moderate core overshooting. Comparisons between models and cluster observations are performed for low and intermediate mass stars in order to determine the amount of core overshooting. The comparisons cover: (1) the main sequence width of intermediate and old open star clusters, (2) the blue extension of the loops described in the HR diagram during the He-burning phase, (3) the number ratio of blue to red giants in the He-phase, (4) the luminosity difference between the yellow giants and the MS turnoff, and (5) the upper mass limit for degenerate He-burning. In agreement with the results for high mass stars, the tests clearly suggest moderate overshooting from convective cores with a distance of overshooting =0.25 H sub P, rather than in favor of no or of large overshooting. The consequence of this moderate overshooting on several stellar mass limits is substantial, but not drastic. The models also suggest that the consequences of overshooting in pre-MS evolution could be important for the further evolution of solar mass stars. ESA

N89-20883# Geneva Observatory (Switzerland).
TABLES OF EVOLUTIONARY STAR MODELS FROM 0.85 TO 120 SOLAR MASSES WITH OVERSHOOTING AND MASS LOSS
Andre Maeder and Georges Meynet 1988 16 p Previously announced in IAA as A89-24943 Submitted for publication
(Ser-C-Prepubl-Fasc-30; ETN-89-93746) Avail: NTIS HC A03/MF A01

The tables of evolutionary star models for Pop 1 composition in the 0.85 to 120 solar mass range with overshooting and mass loss are presented. Most of the tracks are described by 40 points, at well chosen corresponding evolutionary stages in order to allow the computation of accurate isochrones. ESA

N89-20884# Geneva Observatory (Switzerland).
THE UPPER MAIN SEQUENCE OF OB ASSOCIATIONS. 1: SPECTRAL TYPES AND LINES OF C AND N OF SOUTHERN SINGLE-LINED O STARS
G. Mathys 1988 20 p Previously announced in IAA as A89-24944 Submitted for publication
(Ser-C-Prepubl-Fasc-32; ETN-89-93748) Avail: NTIS HC A03/MF A01

The properties of the stars on the upper main sequence of OB associations are studied in order to provide constraints on evolutionary models. The single-lined O stars belonging to the southern associations Vel OB1, Car OB1, Cen OB1 and Sco OB1 are considered. Spectral type is derived in Conti's classification scheme for O stars, amended to include the O9.7 subtype and to deal with fairly high S/N CCD spectra (compared with the original photographic material for which the classification methodology was devised). The behavior of the C and N lines of these stars is examined to determine whether CNO-processed material is visible at their surface. Stars in which the observed behavior of the C and N lines indicates that CNO-processed elements may be seen at the surface are presented. ESA

90 ASTROPHYSICS

Includes cosmology; celestial mechanics; space plasmas; and interstellar and interplanetary gases and dust.
For related information see also *75 Plasma Physics*.

N89-20885# Chalmers Univ. of Technology, Goeteborg (Sweden). Space Observatory.
MOLECULAR RADIO LINE OBSERVATIONS OF MASS LOSS FROM RED GIANTS
H. Olofsson 1988 12 p
(PB89-102313; Rept-88-29) Avail: NTIS HC A03/MF A01 CSCL 03B

The number of molecules detected at radio wavelengths in

envelopes around red giants stands presently at 36. Among these, OH and CO have proven to be the most useful for the study of a circumstellar envelope. The mass loss rate of the central star can be relatively accurately estimated, and it appears possible to trace its evolution with time. Also, the fascinating objects in transition from the red giant phase to the planetary nebula phase are becoming observationally accessible. GRA

N89-20886 Texas Univ., Austin.
LITHIUM DEPLETION AND ROTATION IN MAIN SEQUENCE STARS Ph.D. Thesis
Suchitra Cadambi Balachandran 1988 216 p
Avail: Univ. Microfilms Order No. DA8816386

The mechanism which transports surface lithium to warm inner regions of the star where it can be destroyed is not clearly understood. The role of rotation in the depletion of this fragile element in main sequence stars was investigated. Theoretical calculations predict that mixing should occur when a rapidly rotating star is spun down on the main sequence. It is known that lithium depletion increases with age and, at a given age, towards later spectral types. Hence, a sample of F stars which have just evolved off the main sequence was chosen. Rotational velocities in these stars range between 100 km/s for the higher mass stars to less than 10 km/s for the lower mass stars. Using high resolution spectra, lithium abundances and projected rotational velocities were determined in about 200 F stars. Lithium abundances and rotational velocities were also determined in 46 F, G and K stars in the young cluster alpha Per. Rapid rotators are found to have a cosmic lithium abundance. Large Li depletions are found only in the slow rotators. If lithium depletion is not causally connected with rotation, it may be difficult to explain the very rapid depletion of lithium. The sharp Li depletion seen in the Hyades is not seen in alpha Per and, hence, must occur after the stars reach the main sequence. Dissert. Abstr.

N89-20887 Edinburgh Univ. (Scotland).
THE HIGH-REDSHIFT EVOLUTION OF RADIO GALAXIES AND QUASARS Ph.D. Thesis
James Scott Dunlop 1987 393 p
Avail: Univ. Microfilms Order No. BRD-82972

The results of an extensive optical/infrared study of radio galaxies and quasars in the Parkes Selected Regions are presented. The data are then analyzed to place new constraints on the high redshift evolution of the radio source population. Also an investigation is presented into the star formation histories of the galaxies in the sample. A brief investigation was made into the high redshift evolution of optically-selected quasars and a discussion is presented of some of the possible connections between radio source and star formation activity. Dissert. Abstr.

N89-20888 Maryland Univ., College Park.
THE PHYSICS OF WAVE-PARTICLE INTERACTION WITH APPLICATIONS TO ASTROPHYSICS Ph.D. Thesis
Homayoun Karimabadi 1988 280 p
Avail: Univ. Microfilms Order No. DA8818415

The physics of electromagnetic wave particle interactions in the limit of a strong static magnetic field is investigated using Hamiltonian and multiple time scale techniques. For small wave amplitude, the system is integrable and the motion in phase space is regular. For amplitudes exceeding a threshold value, the system become nonintegrable and the particle motion in phase space becomes stochastic. The stochasticity is caused by the overlapping of the adjacent resonances. The particle dynamics in various limits is discussed using a novel graphical technique for analyzing the particle motion. A diffusion equation analogous to the Fokker-Planck equation is derived and used to examine the effect of the wave on an ensemble of particles. The diffusion is in momentum space and is due to the stochastic motion of particles in phase space. Dissert. Abstr.

N89-20889 Minnesota Univ., Minneapolis.
DUST SHELLS AROUND MIRAS AND OH/IR STARS Ph.D. Thesis
Kyung-Won Suh 1988 83 p
Avail: Univ. Microfilms Order No. DA8823572

Models for mass-losing Miras and OH/IR stars were made to explain the properties of the dust shells around them using more accurate information about the material in the shell and the physical processes including pulsations. Dust opacity which was deduced from observations and experimental data were applied to various density distributions, calculated the model emergent spectra, and compared with observations. Contrary to previous suggestions, observations fit fairly well using density distribution rho varies as 1/r squared, which is physically plausible, with proper choice of opacities. The time scales for dust formation, growth, and movement are calculated to be compared with pulsation periods. The change of the emergent spectrum depending on the phase of pulsation can be explained fairly well by changing dust condensation radius (for fixed dust condensation temperature) in step with the change in stellar luminosity. The effects of stellar wind models and pulsation models on dust shells with attention to emergent spectra are discussed. Dissert. Abstr.

N89-20890 Louisiana State Univ., Baton Rouge.
STAR FORMATION, USING 3-D EXPLICIT EULERIAN HYDRODYNAMICS Ph.D. Thesis
Harold Alden Williams 1988 268 p
Avail: Univ. Microfilms Order No. DA8819991

Evolutions of rapidly rotating, self-gravitating objects initially in axisymmetric equilibrium were studied using a 3-D Newtonian hydrodynamic computer code with an eye toward understanding angular momentum transport in dynamically evolving protostars. First, a number of evolutions were modeled using an existing explicit, Eulerian, finite difference code that is accurate to first-order in its spatial differences. The bar-mode dynamic instability was explored by considering several models with different degrees of compressibility. The hydrodynamic code was modified to include second-order-accurate spatial differences and was rewritten so that it now vectorizes well. The results obtained from running a model in the second-order code are qualitatively similar to the results obtained from the first-order code. Quantitatively, however, the answers are somewhat different and are, presumably, more reliable. In the second-order code, growth rates no longer need to be corrected for the effects of numerical viscosity to agree with the predictions of linear theory. Higher order nonaxisymmetric Fourier modes are also no longer damped. Dissert. Abstr.

N89-20891 Sussex Univ., Brighton (England).
COSMOLOGY AND SUPERSTRINGS Ph.D. Thesis
David Tak-Man Wong 1987 164 p
Avail: Univ. Microfilms Order No. BRDX83062

The comological implications of the latest theory of quantum gravity, superstrings (in particular, the heterotic superstring) were examined. After a general introduction into quantum gravity and a review of string theory, with emphasis on the modern interpretation and the derivation of the low energy limit, the study concentrates on the 10-dimensional cosmology predicted by superstrings. The possibility of recovering a cosmology which resembles that of the standard model is considered. An approximate Friedmann solution is found, and its stability against linear perturbations of the scale factors and the dilation field analyzed. Some Lagrangians are unstable, due to singular perturbations. A region of stability, against linear perturbations, is found. The early stages of the universe are studied. The field equations are analyzed numerically. For a wide range of initial values the solutions are unphysical, but two more reasonable solutions exist for some initial data. In the first solution both the ordinary 3-D and the extra 6-D move toward constant values. The second solution resembles that of the Kaluza-Klein higher dimensional cosmology, and so does help to alleviate the Horizon Problem. Dissert. Abstr.

N89-20892 Illinois Univ., Urbana-Champaign.
MIXING AND NUCLEOSYNTHESIS IN LOW- AND INTERMEDIATE-MASS AGB STARS Ph.D. Thesis

David Earl Hollowell 1988 183 p
Avail: Univ. Microfilms Order No. DA8823147

The existence of carbon stars brighter than M (sub bol) = -4 can be understood in terms of dredge up in thermally pulsing asymptotic giant branch (AGB) stars. Models include the effect that carbon recombination has upon opacity, and it is shown that a low-metallicity, low-envelope mass, low-core mass AGB star can transform into a carbon star with a brightness -5.0 is less than M (sub bol) is less than -4.2. Neutron capture occurs on iron-seed nuclei during a shell flash, and the products of this nucleosynthesis may be carried to the stellar surface during the dredge-up phase. The carbon recombination that induces dredge up in these models also induces mixing of H-1 and C-12 in such a way that a layer of C-13 and N-14 is formed in the region between the hydrogen-burning and helium-burning shells. During a subsequent thermal pulse this matter is engulfed into a hot, convective shell and the C-13 is rapidly converted into O-16 and neutrons. This neutron source also produces approximately 20 to 50 neutrons per iron-seed nucleus at the convective shell base, but only 10 to 20 percent of these neutrons are captured by the iron-seed nuclei as over one half of these neutrons are absorbed by Ne-22. Dissert. Abstr.

N89-20893 State Univ. of New York, Buffalo.
SOLUTIONS AND STABILITY OF A CLOSED-GEODESIC BLACK HOLE MODEL Ph.D. Thesis
Zoran Pazameta 1988 58 p
Avail: Univ. Microfilms Order No. DA8824020

A perfect fluid with polytropic equation of state is employed as a source for Einstein's equations, within the context of Sachs' closed-geodesic black hole paradigm. Along with the vanishing covariant divergence of the stress-energy tensor, the equation of state enables determination of the pressure and density functions, uniquely, for a polytrope of general index, n. The metric for this object is then found in closed form, for any value of n. A general expression for the metric of a Klein-Gordon scalar field source is also obtained, and an approximate solution for a particular source of this type is presented. The stability of the perfect-fluid metrical solution is investigated, by coupling the black hole metric to an anisotropic, and then isotropic, cosmological background. Preliminary work on generalizing the closed-geodesic model to the rotating case is appended. Dissert. Abstr.

N89-20894 Stanford Univ., CA.
PRIMORDIAL NUCLEOSYNTHESIS AND LATE DECAYING PARTICLES: A NEW MODEL OF NUCLEOSYNTHESIS Ph.D. Thesis
Glenn David Starkman 1988 81 p
Avail: Univ. Microfilms Order No. DA8826239

The effects of late decaying (10 to the 4th power s is less than or equal to tau less than or equal to 10 to the 5th power s), massive (M approximately greater than 5GeV) particles on the primordial synthesis of the light elements are addressed. The effects of such particles on light element abundances are analyzed first; it is shown that whereas radiative decays can lead to photo-dissociation, hadronic decays can cause significant light element production. It emerges that, for a wide range of particle parameters, production and destruction balance in such a way as to lead to light element abundances in agreement with current observations. The final abundances are independent of the results of any earlier epoch of nucleosynthesis, so long as in some such era sufficient helium-4 was produced. This relaxes the bound on the cosmic baryon number density imposed by Standard Big Bang Nucleosynthesis (SBBN), and in particular allows for the possibility that the universe is closed entirely by baryons. Several observational predictions are indicated which can be used to differentiate between this new model of nucleosynthesis and SBBN. Dissert. Abstr.

N89-20895 Illinois Univ., Urbana-Champaign.
MAGNETOSPHERES OF NEUTRON STARS ACCRETING FROM DISKS Ph.D. Thesis
Gregory Jay Zylstra 1988 220 p
Avail: Univ. Microfilms Order No. DA8823301

Quantitative models are presented of magnetosphere of a magnetic star surrounded by a thin plasma disk. The model is motivated by the currently accepted picture of many accretion powered pulsars as strongly magnetic neutron stars accreting from disks. It may also be relevant to the luminous galactic bulge X-ray sources that display quasi-periodic oscillations in intensity. These QPO sources are thought by some to be weakly magnetic neutron stars accreting from disks. In constructing these models, it was assumed that the magnetic field is static and axisymmetric about the axis of the disk. It was also assumed that the magnetic field is in force free equilibrium. The validity of these simplifying assumptions for astrophysical systems is discussed in detail. The boundary conditions on the magnetic field at the disk were chosen to mimic the expected electrodynamic interactions between a magnetic neutron star and an accretion disk. These boundary conditions cause the second order partial differential equation for the magnetic flux function to be nonlinear. This equation is solved iteratively using finite difference techniques on a grid of points covering the volume of the magnetosphere. Dissert. Abstr.

N89-20896*# Fermi National Accelerator Lab., Batavia, IL. Astrophysics Center.
FRAGMENTATION OF COSMIC-STRING LOOPS
Thomas York Jan. 1989 17 p
(Grant NAGw-1340)
(NASA-CR-184892; NAS 1.26:184892; FERMILAB-Pub-89/32-A)
Avail: NTIS HC A03/MF A01 CSCL 03B

The fragmentation of cosmic string loops is discussed, and the results of a simulation of this process are presented. The simulation can evolve any of a large class of loops essentially exactly, including allowing fragments that collide to join together. Such reconnection enhances the production of small fragments, but not drastically. With or without reconnections, the fragmentation process produces a collection of nonself-intersecting loops whose typical length is on the order of the persistence length of the initial loop. Author

N89-20897# Royal Inst. of Tech., Stockholm (Sweden). Dept. of Plasma Physics.
ASTROPHYSICS IN A NUTSHELL: FROM THE TELESCOPE TO THE SPUTNIK
Hannes Alfven and Carl-Gunne Faelthammar Mar. 1988 19 p
(TRITA-EPP-88-04; ISSN-0348-7539; ETN-89-93727) Avail: NTIS HC A03/MF A01

Progress in astrophysics due to the introduction of new methods of observation is reviewed. The Copernican revolution was more due to the introduction of the telescope than to the heliocentric model invented 2000 yr earlier. The decisive importance of electromagnetic effects in astrophysics originated from Langmuir's invention of the plasma probe and from Birkeland's terrella experiment and his observations of plasma in space (aurora). A similar revolution was introduced by space research which made possible in situ measurements in cosmic plasmas and opened the X-ray and gamma ray regions to observation. The result is a drastic revision of essential parts of astrophysics (including cosmology) leading to the plasma Universe model. ESA

N89-20898# Royal Inst. of Tech., Stockholm (Sweden). Dept. of Plasma Physics.
HAS THE UNIVERSE AN ORIGIN
Hannes Alfven Jul. 1988 14 p
(TRITA-EPP-88-07; ISSN-0348-7539; ETN-89-93728) Avail: NTIS HC A03/MF A01

It is demonstrated that there are no observational facts which unquestionably speak in favor of the Big Bang hypothesis. The Sputnik revolution makes it necessary to revise important parts of astrophysics, and is also fatal to the Big Bang. It seems necessary to turn back to the view of an ungenerated (and indestructable) Universe. ESA

N89-20899# Royal Inst. of Tech., Stockholm (Sweden). Dept. of Plasma Physics.
ASTROPHYSICAL SIGNIFICANCE OF OBSERVATIONS AND EXPERIMENTS IN THE EARTH'S MAGNETOSPHERE
Carl-Gunne Faelthammar Aug. 1988 36 p Presented at the International School and Workshop on Astrophysics, Varenna, Italy, 24 Aug.-3 Sep. 1988
(TRITA-EPP-88-09; ISSN-0348-7539; ETN-89-93729) Avail: NTIS HC A03/MF A01

The Earth magnetosphere as a sample of cosmical plasma, which is accessible to in situ measurements and even active experimentation is discussed. The Universe consists almost entirely of plasmas that will forever be out of reach of such scrutiny, so the empirical knowledge gained in the magnetosphere is essential to the understanding of astrophysical phenomena. The Earth's magnetosphere contains plasmas with wide ranges of density and temperature, and is also the site of a rich variety of plasma physical processes that are of fundamental astrophysical interest. In situ observation of such processes proved some theories of cosmical plasma to be misleading. It provides knowledge on many fundamental aspects of cosmic plasmas, such as conduction of electric current, support of magnetic-field aligned electric fields, filamentary and cellular structure, violation of the law of frozen-in magnetic fields, energization of charged particles, rapid release of magnetic energy, chemical separation, and critical velocity interaction between plasma and neutral gas. ESA

N89-20900# International Centre for Theoretical Physics, Trieste (Italy).
BLACK HOLES AS POSSIBLE SOURCES OF CLOSED AND SEMICLOSED WORLDS
V. P. Frolov, M. A. Markov (Academy of Sciences, USSR, Moscow), and V. F. Mukhanov May 1988 38 p
(DE88-705336; IC-88/91) Avail: NTIS (US Sales Only) HC A03/MF A01

The internal structure of spacetime inside a black hole is investigated on the assumption that some limiting curvature exists. It is shown that the Schwarzschild metric inside a black hole can be attached to the de Sitter one at some spacelike junction hypersurface which represents a short transition layer. After passing the deflation stage the de Sitter space inside the black hole begins to inflate and may become a source of a new macroscopic Universe. The corresponding conformal Penrose diagrams are given. The described model may be considered as an example of a creation of a closed or semiclosed world in laboratory. The fate of an evaporating black hole is also briefly discussed. DOE

N89-20901# International Centre for Theoretical Physics, Trieste (Italy).
NONEXISTENCE THEOREMS FOR YANG-MILLS FIELDS OUTSIDE THE BLACK HOLE OF THE SCHWARZSCHILD SPACETIME
A. K. M. Masood-ul-Alam and Yanglian Pan Aug. 1988 12 p
(DE88-705351; IC-88/211) Avail: NTIS (US Sales Only) HC A03/MF A01

In this paper, the authors prove some nonexistence theorems for regular static Yang-Mills fields outside the black hole of the Schwarzschild spacetime under certain boundary conditions. DOE

91 LUNAR AND PLANETARY EXPLORATION

Includes planetology; and manned and unmanned flights.
For spacecraft design or space stations see *18 Spacecraft Design, Testing and Performance.*

N89-20902*# Jet Propulsion Lab., California Inst. of Tech., Pasadena.
TO URANUS AND BEYOND
Jan. 1987 28 p Original contains color illustrations
(NASA-EP-260; JPL-400-303; NAS 1.19:260) Avail: NTIS; SOD HC $2.00 as 033-000-01004-4 CSCL 03B

Voyager 2, a sophisticated robotic spacecraft that originally was to fly past Jupiter and Saturn and to last four years, was launched in 1977. Since then it has flown by Uranus and is headed towards Neptune, and still is in contact with spacecraft monitors. Features of Voyager 2, Uranus, its moons and rings, and details of the spacecraft's encounter with Uranus are described. Included is a brief history of Uranus' discovery and astronomers' observations. E.R.

N89-20903 State Univ. of New York, Stony Brook.
CARBON MONOXIDE AND DISEQUILIBRIUM DYNAMICS IN SATURN AND JUPITER Ph.D. Thesis
Keith Stephen Noll 1987 161 p
Avail: Univ. Microfilms Order No. DA8815793

High resolution spectra of Jupiter and Saturn were obtained in order to study their composition and dynamics. The shapes of CO absorption lines in Jupiter are broad, giving strong evidence in favor of internal mixing as the source of CO in Jupiter. Further, it was found that the O abundance at 1100 K must be nearly solar. No variations in CO abundance were found between the North Equatorial Belt, the North Tropical Zone, and the Great Red Spot. Because CO is very sensitive to variations in the rate of mixing, it is concluded that there are no gross variations in mixing with location on Jupiter. CO was observed in Saturn for the first time. The source of CO in Saturn is uncertain, although theory favors an external source to an internal one. If Saturn's rings are the source of O that eventually leads to CO in Saturn, the rate of influx required imposes an upper limit to the lifetime of the rings. The first evidence was found of GeH(sub 4) in the atmosphere of Saturn. Absorption lines in the P and R branch of GeH(sub 4) are observed, although no evidence of the stronger Q branch was found. The abundance of GeH(sub 4) is consistent with the expected disequilibrium from internal mixing in Saturn.
Dissert. Abstr.

92 SOLAR PHYSICS

Includes solar activity, solar flares, solar radiation and sunspots.
For related information see *93 Space Radiation.*

N89-20904# National Center for Atmospheric Research, Boulder, CO.
INTEGRATED ANALYSIS PACKAGE FOR Mk-3 K-CORONAMETER OBSERVATIONS: A USER'S MANUAL
S. Archuleta and R. Beutner (Colorado Univ., Boulder.) Jul. 1988 56 p
(Grant NSF ATM-87-09659)
(PB88-250717; NCAR/TN-318-IA) Avail: NTIS HC A04/MF A01 CSCL 03B

The use of the Integrated Analysis Package, (IAP), the primary software tool for visual, graphical, and quantitative numerical analysis of solar coronal data acquired with the Mark 3 Coronameter is described. IAP was written for use on a VAX 11/780 (haovax, HV) running Berkley Unix version 4.2, but it can easily be ported to other Unix machines. As an accompaniment to the Technical Note, there also exists an IAP Maintenance Manual, providing in house programmers a road map to the code. Author

N89-20905*# National Academy of Sciences - National Research Council, Washington, DC. Panel on Long-Term Observations.
LONG-TERM SOLAR-TERRESTRIAL OBSERVATIONS Final Report
26 Aug. 1988 82 p Sponsored in part by National Climate Program Office, Rockville, MD, NSF, Washington, DC, NASA, Washington, DC and Department of Agriculture, Washington, DC
(Grant NA87AA-D-CP041)
(NASA-CR-184695; NAS 1.26:184695; PB89-104657) Avail: NTIS HC A05/MF A01 CSCL 03B

The results of an 18-month study of the requirements for

long-term monitoring and archiving of solar-terrestrial data is presented. The value of long-term solar-terrestrial observations is discussed together with parameters, associated measurements, and observational problem areas in each of the solar-terrestrial links (the sun, the interplanetary medium, the magnetosphere, and the thermosphere-ionosphere). Some recommendations are offered for coordinated planning for long-term solar-terrestrial observations. GRA

N89-20906# National Oceanic and Atmospheric Administration, Boulder, CO. Space Environment Lab.
SELSIS (THE SPACE ENVIRONMENT LABORATORY SOLAR IMAGING SYSTEM): INITIAL REQUIREMENTS
Viola J. Hill and David M. Speich Jul. 1988 91 p
(PB89-113039; NOAA-TM-ERL-SEL-78) Avail: NTIS HC A05/MF A01 CSCL 03B

The Space Environment Laboratory Solar Imaging System (SELSIS) Initial Requirements defines the requirements for: routinely acquiring solar images, the image-processing required to provide operational and research quality data, the needs for the image distribution and archival systems, and the image analysis and display capabilities required for operational and research use. SELSIS will provide near real-time solar images to SEL for use by four different user groups; the Space Environment Services Center (SESC) and the USAF Space Forecast Center (SFC) for use in their operational solar forecast centers, the Space Environment Laboratory (SEL) research group, and the National Geophysical Data Center (NGDC) for archival and distribution to other potential users. GRA

N89-20907 California Inst. of Tech., Pasadena.
MAGNETIC FIELDS AND SUPERGRANULE VELOCITY FIELDS ON THE QUIET SUN Ph.D. Thesis
Haimin Wang 1988 222 p
Avail: Univ. Microfilms Order No. DA8820997

The quiet sun magnetic fields and supergranule velocity fields were examined. Six themes were studied: (1) the statistical properties of quiet sun magnetic fields, including size distribution, evolution, flux budget of magnetic flux elements, and the magnetic diffusion constant; (2) the supergranule velocity fields, finding their average lifetime; (3) the contrast of faculae near the solar limb, showing no obvious contrast increase or decrease; (4) the separation velocities of new bipoles, with values several times smaller than the values estimated by the theory of magnetic buoyancy; (5) the application of local correlation tracking technique to BBSO videomagnetogram data and detecting approximate radial intranetwork flow; and (6) the relationship was studied between magnetic fields and convection velocity fields, and found that ephemeral regions have a light tendency to emerge at or near the boundaries of supergranules. Dissert. Abstr.

N89-20908# National Geophysical Data Center, Boulder, CO.
SOLAR-GEOPHYSICAL DATA NUMBER 530, OCTOBER 1988. PART 2: (COMPREHENSIVE REPORTS). DATA FOR APRIL 1988 AND MISCELLANEOUS
Helen E. Coffey, ed. and John A. McKinnon, ed. Oct. 1988 78 p
(Contract N00014-86-F-0049)
(PB89-130827; SGD-530-Pt-2; ISSN-0038-9011; LC-79-640375)
Avail: NTIS HC A05/MF A01 CSCL 03B

Comprehensive solar geophysical data is presented for Apr. and Oct. 1988. Solar activity data is presented in graph form for solar flares, solar radio bursts, solar X-rays from GOES satellites, mass ejection from the sun, and active prominences and filaments. E.R.

N89-20909# National Geophysical Data Center, Boulder, CO.
SOLAR-GEOPHYSICAL DATA NUMBER 530, OCTOBER 1988. PART 1: (PROMPT REPORTS). DATA FOR SEPTEMBER, AUGUST 1988 AND LATE DATA
Helen E. Coffey, ed. and John A. McKinnon, ed. Oct. 1988 134 p
(Contract N00014-86-F-0049)
(PB89-130835; SGD-530-Pt-1; ISSN-0038-0911; LC-79-640375)
Avail: NTIS HC A07/MF A01 CSCL 03B

A detailed index for Sep. and Oct. 1988 is presented. Data in graph form is presented for solar activities including solar flux and sunspots, solar flares, and solar radio bursts. E.R.

N89-20910# Tufts Univ., Medford, MA. Dept. of Physics and Astronomy.
VERY LARGE ARRAY OBSERVATIONS OF THE SUN WITH RELATED OBSERVATIONS USING THE SMM (SOLAR MAXIMUM MISSION) SATELLITE Final Technical Report, 1 Jan. 1983 - 31 Aug. 1988
Kenneth R. Lang 12 Oct. 1988 63 p
(Grant AF-AFOSR-0019-83; AF Proj. 2311)
(AD-A203873; AFOSR-89-0044TR) Avail: NTIS HC A04/MF A01 CSCL 03B

Observations of solar active regions with the Very Large Array (VLA) have led to new information about the origin and prediction of explosive bursts, or solar flares, that can directly interfere with high-flying aircraft or disrupt communications with them. We have shown that energetic particles and radiation are expelled during explosive bursts from coronal loops. Several new insights into these exploding loops have been provided using the VLA together with supporting observations with the Solar Maximum Mission (SMM) satellite and the Nancay Radioheliograph (NR). The VLA uniquely provides spatial resolution at radio wavelengths, while the SMM gives X-ray data and the NR provides resolution in time and frequency. All three instruments were used to study the quiescent, or non-flaring, emission from coronal loops, radio bursts from coronal loops, and radio bursts from nearby stars. The ubiquitous coronal loops dominate the structure of the solar corona. Multiple wavelength VLA observations specify the three dimensional structure of solar active regions; they uniquely specify the strength, evolution and structure of the magnetic fields in coronal loops, while also providing constraints on the density and temperature of the energetic plasma trapped within them. Thermal cyclotron lines provide a sensitive measurement of the coronal magnetic field, while comparisons with simultaneous SMM X-ray observations delineate the various radiation mechanisms. GRA

93 SPACE RADIATION

Includes cosmic radiation; and inner and outer earth's radiation belts.

For biological effects of radiation see *52 Aerospace Medicine*. For theory see *73 Nuclear and High-Energy Physics*.

N89-20911# Los Alamos National Lab., NM.
STUDY OF ULTRA-HIGH ENERGY EMISSION FROM CYGNUS X-3 AND HERCULES X-1 Ph.D. Thesis
Brenda Lynn Dingus Nov. 1988 160 p
(Contract W-7405-eng-36)
(DE89-004543; LA-11431-T) Avail: NTIS HC A08

The Cygnus experiment, consisting of an extensive air shower detector and a muon detector, was built at Los Alamos, New Mexico (latitude 36 N, longitude 107 W, altitude 2310 meters), to search for point sources of ultra-high energy (greater than 10 to the 14th eV) particles. These particles must be long-lived neutral particles because of the long source distances and the presence of the intragalactic magnetic field. Gamma rays are the most likely candidates because of the short neutron lifetime and the small neutrino cross section. Therefore, the muon content of the source showers is examined to determine if these events are muon poor as is expected for gamma-initiated showers. The data set from April 1986 to July 1987 is searched for continual emission from Cygnus X-3 and Hercules X-1, and an upper bound to flux is determined for both sources. The flux limit for Cygnus X-3, 2.0 x 10 to the 13th/sq cm/sec above 50 TeV, is lower than previous ultra-high energy observations. Hercules X-1 has never been observed continually at ultra-high energies. Cygnus X-3 is observed

for a shorter interval of time, beginning on 17 April 1986 and ending 1 June 1986. There is one chance in 300 that the observation is due to a random fluctuation. The signal is correlated with the 4.8 hour orbital period, and the muon content of the showers in the signal is inconsistent with the conventional prediction of gamma-initiated showers. An episodic signal is also reported for Hercules X-1, and it consists of two bursts of less than one hour duration on 24 July 1986. The probability is one chance in 12,000 that this observation is not associated with Hercules X-1. The signal is pulsed at frequency near, but significantly different from, the X-ray pulsar frequency. The muon content of the signal showers is also anomalous, assuming the showers are initiated by gamma rays. DOE

N89-20912 Colorado Univ., Boulder.
APERTURE SYNTHESIS OBSERVATIONS OF SOLAR AND STELLAR RADIO EMISSION Ph.D. Thesis
Timothy Stephen Bastian 1987 301 p
Avail: Univ. Microfilms Order No. DA8808258

The results of observations using the Very Large Array are presented in three major sections. The first discusses maximum entropy-type image reconstruction techniques that were applied. Both single disk and interferometer data were used to generate full disk images of the sun at a wavelength of approximately 21 cm. Using a set of six such images obtained during the sun's decline from sunspot maximum to minimum, a number of previously unreported phenomena were noted. Among these: (1) a systematic decrease in quiet sun's brightness temperature as it declined to minimum; (2) a systematic decrease in the sun's radius at 21 cm; and (3) evidence for the evolution of polar coronal holes during the course of the solar cycle. The observed variation, though not noted previously at radio wavelengths, is entirely consistent with white light K coronagraph data. The results reported here explain the conflicting nature of a number of past observations. The second section presents the results of a long term survey of magnetic cataclysmic variables (CVs). Cataclysmic variables are close binary systems which contain a white dwarf accreting mass from a late-type secondary, typically a dwarf of spectral type G, K, or M. The third section presents new results on flare stars in the solar neighborhood and in the Pleiades. Of the nearly 170 sources found in the Pleiades' fields, all but two were determined to be extragalactic. Neither of the two stellar radio sources is a known flare star or a Pleiades member. Dissert. Abstr.

N89-20913 Iowa Univ., Iowa City.
NONTHERMAL RADIO EMISSION FROM RS CVN BINARIES AND SIMILAR SYSTEMS Ph.D. Thesis
Dirk H. Morris 1988 116 p
Avail: Univ. Microfilms Order No. DA8815115

Enhanced emission at radio, optical, and X-ray frequencies appears to be a characteristic feature of late-type stars in close binary systems. This emission is thought to originate through an enhanced dynamo mechanism caused by rapid differential rotation in the stellar convective zone. A large scale study of such systems, and a two dimensional magnetospheric model which reproduces many of the observed properties is presented. The radio emission consists of two components: a slowly varying, moderately circularly polarized component and short duration flares. The former is well modeled by gyrosynchrotron emission from mildly relativistic electrons in an inhomogeneous plasma. Correlations of L(sub tau) with various stellar parameters such as rotational period, rossby number and color index were investigated. The implications that these observations have for modeling the physical environment from which the emission arises are discussed and a detailed two dimensional model presented. The model calculations integrate the equation of radiative transfer (employing gyrosynchrotron emissivity and absorption coefficients) along lines of sight with varying impact parameters through a single magnetospheric cut defined by the ray paths and the magnetic field axis. The emergent spectral and polarization characteristics are presented and compared to the observations. Dissert. Abstr.

N89-20914 Maryland Univ., College Park.
THE GALACTIC LARGE-SCALE FAR-INFRARED EMISSION OBSERVED BY IRAS: IMPLICATIONS FOR THE MORPHOLOGY, PHYSICAL CONDITIONS, AND ENERGETICS OF DUST IN THE INTERSTELLAR MEDIUM Ph.D. Thesis
Thomas John Sodroski 1988 204 p
Avail: Univ. Microfilms Order No. DA8818220

The IRAS observations of the 60 and 100 micrometer Galactic plane emission, from which the contribution of the zodiacal light was subtracted, are combined with available CO12, 5 GHz radio-continuum, and H I observations of the Galactic plane to study the energetics of the dust that gives rise to the Galaxy's large-scale far-infrared emission. Two independent modeling approaches for deriving large-scale Galactic properties are presented. Comparisons of the results with current models of the Galactic large-scale FIR emissions are made. Dissert. Abstr.

N89-20915 Maryland Univ., College Park.
MEASUREMENT OF THE COSMIC RAY IRON SPECTRUM ABOVE 60 GeV/n AND DESIGN AND CALIBRATION OF A LARGE ISOTOPIC COMPOSITIONAL EXPERIMENT Ph.D. Thesis
Joseph Andre Esposito 1988 251 p
Avail: Univ. Microfilms Order No. DA8827065

Data from the 1983 balloon flight of the High Energy Gas Cherenkov Spectrometer (HEGCS) are analyzed. The value of the spectral index of the Galactic Cosmic Ray (GCR) spectrum contains information regarding the source, propagation and galactic confinement of these particles. Measurement of high energy iron flux was performed by the High Energy Particle Astrophysics group at Goddard Space Flight Center through the use of the HEGCS experiment. The HEGCS instrument is composed of three diffuse radiation chambers. Two charge determining scintillation hodoscopes measure the nuclear charge and trajectory of incident cosmic ray particles and provide a fast event trigger. A gas Cherenkov chamber, with a threshold Lorentz factor of 51, is used to determine the particle velocity from which the energy per nucleon can be found. The Cherenkov data from the HEGCS flight were analyzed through the use of maximum likelihood techniques. The spectral index of GCR iron, above 60 GeV/n, was determined to be 2.56 + or - 0.11. A Large Isotopic Composition Experiment (ALICE) was designed and calibrated. The constructed instrument was calibrated in the laboratory using cosmic ray muons and then flown from the remote launch facility in Canada during August, 1987. A computer simulation of the experiment was developed to estimate the instrument resolution. Dissert. Abstr.

N89-20916 Heidelberg Univ. (Germany, F.R.). Inst. fuer Physik.
COSMIC RAY TRACKING: A NEW APPROACH TO HIGH ENERGY GAMMA-ASTRONOMY
J. Heintze, P. Lennert, S. Polenz, B. Schmidt, W. Brueckner, B. Povh, and J. Spitzer (Max-Planck-Inst. fuer Kernphysik, Heidelberg, Germany, F.R.) 1988 27 p Presented at the 3rd Topical Seminar on Perspectives for Experimental Apparatus at Future High Energy Machines and Underground Laboratories, San Miniato, Italy, 7-11 Mar. 1988 Submitted for publication
(HD-PY88/05; ETN-89-93783) Avail: Fachinformationszentrum Karlsruhe, 7514 Eggentein-Ledpoldshafen 2, Fed. Republic of Germany

An extensive air shower (EAS) array based on the measurement of individual cosmic ray tracks and muon identification is proposed. Air showers can be detected in the range from 1 trillion eV up to the highest energies. The direction of the primary gamma ray is reconstructed with accuracies typically in the range of 0.1 to 0.3 deg. The sensitivity for the detection of point sources is improved by a factor of 100 in comparison to existing conventional EAS arrays or atmospheric Cerenkov telescopes. ESA

N89-20917# Centro Brasileiro de Pesquisas Fisicas, Rio de Janeiro.
MESON PRODUCTION AND NUCLEAR FRAGMENTATION OF NUCLEUS IN THE ATMOSPHERE
C. E. NaviaOjeda, H. M. Portella, H. V. Pinto, F. A. Pinto, and R.

H. C. Maldonado 1988 24 p Prepared in cooperation with Universidade Federal Fluminense, Niteroi (Brazil)
(DE88-705019; CBPF-NF-032/88) Avail: NTIS (US Sales Only) HC A03/MF A01

Propagation of the primary and secondary cosmic ray in the atmosphere is calculated analytically. Two different cases of primary cosmic ray composition are used; the first case concerns the mixed composition of very heavy, heavy, middle, light nuclei and nucleons; and the second case considers only nucleons in the primary cosmic ray flux. The mechanism of multiple meson production is formulated according to the wounded nucleon model for nucleus-nucleus interaction and the scaling model for nucleon-nucleon interaction. The mechanism of nuclei fragmentation is formulated according to the experimental values of the fragmentation parameters at low energy. The calculated results of the electromagnetic flux are compared with the results of mountain experiments with large scale emulsion chamber and experimental data at airplane altitude. From these comparisons the calculation of electromagnetic flux altitude variation of the first case gives the best fit with experimental data than the second case. DOE

99 GENERAL

N89-20918*# National Aeronautics and Space Administration. Lyndon B. Johnson Space Center, Houston, TX.
RESEARCH AND TECHNOLOGY OF THE LYNDON JOHNSON SPACE CENTER Annual Report, 1988
Mar. 1989 169 p
(NASA-TM-100473; S-590; NAS 1.15:100473) Avail: NTIS HC A08/MF A01 CSCL 05D

Johnson Space Center accomplishments in new and advanced concepts during 1988 are highlighted. This year, reports are grouped in sections Space System Technology, Solar System Sciences, Space Transportation Technology, and Medical Sciences. Summary sections describing the role of Johnson Space Center in each program are followed by descriptions of significant tasks. Descriptions are suitable for external consumption, free of technical jargon, and illustrated to increase ease of comprehension. Author

N89-20919# Research Inst. of National Defence, Linkoeping (Sweden). Div. of Information Systems.
[ACTIVITIES REPORT OF THE DIVISION OF INFORMATION SYSTEMS] Annual Report, Fiscal Year 1987-88
Joergen Fransson, ed. and Gunilla Siverskog, ed. Jul. 1988 80 p
(FOA-C-30499-3.3; ISSN-0347-3708; ETN-89-93740) Avail: NTIS HC A05/MF A01; Swedish Defense Research Establishment, Box 1165, S-581 11 Linkoping, Sweden, 50 Swedish crowns

Research concerning computer vision; knowledge based techniques; data security; antisubmarine warfare; and space technology is summarized. ESA

Typical Subject Index Listing

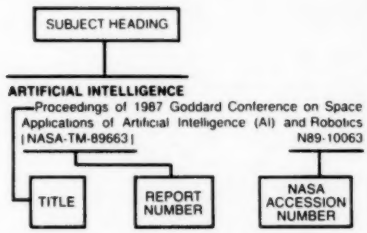

The subject heading is the key to the subject content of the document. Titles, report numbers, and accession numbers of pertinent documents are provided under each subject heading. When the title is insufficiently descriptive of the document content, a title extension has been added, separated from the title by three hyphens. The report number helps to indicate the type of document cited (e.g., NASA report, NASA translation, NASA contractor report). The NASA accession number is the number by which the document abstracts are arranged in this journal and by which the document is sold or requested. The titles, with title extensions if present, are arranged under each subject heading in ascending accession number order. The subject headings have been selected from the latest revision of the *NASA Thesaurus* (NASA SP-7064).

A

A-320 AIRCRAFT
Fatigue teardown tests of the aged rear support of the A320 aircraft
[I-271/88] N89-20491

ABLATION
Ablation of materials in the low earth orbital environment N89-20187

ABSORBENTS
Zeolite/methanol: The adsorption heat pump
[DE88-756310] N89-20413

ABSORPTION SPECTRA
ILS (Intracavity Laser Spectroscopy) for beam sensing (experiment)
[DE89-006376] N89-20445

ABSTRACTS
USSR Space Life Sciences Digest, Issue 21
[NASA-CR-3922(24)] N89-20602

ABUNDANCE
Publications of the Observatory of the University of Michigan. Volume 12, no. 2: Wavelength identifications in the magnetic CP star HR 4816 (HD 110066) N89-20876

ACCELERATION (PHYSICS)
Axially accelerated saboted rods subjected to lateral forces
[DE89-007466] N89-20485
Nonnormal accelerations due to yielding in a primary structure
[PB89-131437] N89-20513

ACCELERATORS
Status of LBL/LLNL FEL (Free Electron Laser) research for two beam accelerator applications
[DE89-006656] N89-20453

ACCESS CONTROL
Waiting-time approximations for cyclic-service systems with mixed service strategies
[CWI-OS-R8802] N89-20743
Using English for indexing and retrieving
[AD-A202227] N89-20866

ACCIDENT PREVENTION
Nuclear power safety: International measures in response to Chernobyl accident
[GAO/NSIAD-88-131BR] N89-20872

ACCIDENTS
Light-Weight Radioisotope Heater Unit Final Safety Analysis Report (LWRHU FSAR). Volume 3: Nuclear risk analysis document
[DE89-005496] N89-20790

ACCRETION DISKS
Magnetospheres of neutron stars accreting from disks N89-20895

ACETATES
New vinylidene fluoride copolymers: Poly(vinyl acetate-co-Vinylidene fluoride)
[AD-A203939] N89-20270

ACETYLENE
On the dimerization of linear polymers
[DE88-705341] N89-20256

ACOUSTIC EMISSION
Long-term evaluation of the acoustic emission weld monitor
[PB88-122642] N89-20471

ACOUSTIC FATIGUE
High intensity acoustic tests of a thermally stressed aluminum plate in TAFA
[NASA-TM-101552] N89-20778

ACOUSTIC LEVITATION
Fluoride glass: Crystallization, surface tension N89-20306
Containerless processing of glass forming melts in space N89-20307
Acoustic containerless experiment system: A non-contact surface tension measurement N89-20308

ACOUSTIC MEASUREMENT
Acoustic test of a model rotor and tail rotor: Results for the isolated rotors and combined configuration
[NASA-TM-101550] N89-20777

ACOUSTIC SIMULATION
The evaluation of impulsive noise
[NPL-AC-111] N89-20780

ACRYLIC RESINS
Rapid cure acrylic adhesive compositions
[EP-0-247-726-A2] N89-20255

ACTIVE CONTROL
Active control helicopter aeromechanical and aeroelastic instabilities N89-20149
Flexible structure control laboratory development and technology demonstration
[NASA-CR-184867] N89-20151
Active vibration control of a large flexible manipulator by inertial force and joint torque
[NASA-CR-184786] N89-20470

ACTUATOR DISKS
Transmission and reflection on pressure waves by compressor and turbine stages, based on an actuator-disk model
[AD-A203513] N89-20426

ADA (PROGRAMMING LANGUAGE)
Transmitter data collection using Ada N89-20352

ADAPTIVE CONTROL
Flexible structure control laboratory development and technology demonstration
[NASA-CR-184867] N89-20151
Low frequency vibration isolation technology for microgravity space experiments
[NASA-TM-101448] N89-20324
Application of parameter adaptive approach to servo control of a hydraulic manipulator
[MA-51] N89-20473
Bordered equations in continuation methods: An improved solution technique — structural analysis
[NLR-MP-87057-U] N89-20699
Gain selection for an independent joing MRAC (Model-Reference Adaptive Controller) for robotic manipulators
[DE89-005110] N89-20705

ADDRESSING
Data storage and transfer apparatus
[EP-0-243-189-A1] N89-20623

ADHESION
Design, development and applications of novel techniques for studying surface mechanical properties
[NASA-TM-101959] N89-20253

ADHESION TESTS
A theoretical, numerical and experimental examination of in situ properties of adhesives
[FFA-TN-1988-05] N89-20526

ADHESIVE BONDING
Paint tests on laminated material formed by carbon fiber composites and Tedlar layers
[I-279/88] N89-20208
Rapid cure acrylic adhesive compositions
[EP-0-247-726-A2] N89-20255

ADHESIVES
Rapid cure acrylic adhesive compositions
[EP-0-247-726-A2] N89-20255
A theoretical, numerical and experimental examination of in situ properties of adhesives
[FFA-TN-1988-05] N89-20526

ADIABATIC CONDITIONS
Thermodynamics of finite-time processes: Accomplishments and work in progress, 1986--1989
[DE89-006726] N89-20858

ADJUSTING
Proposed extended tuning range for the Los Alamos mid-infrared adjustable, coherent light experiment (MIRACLE) facility
[DE89-006550] N89-20798

ADSORPTION
Water adsorption equilibria on microporous carbons
[AD-A203536] N89-20220
Zeolite/methanol: The adsorption heat pump
[DE88-756310] N89-20413

AERIAL PHOTOGRAPHY
Potential of large format camera photography
[PB89-122485] N89-20433

AEROASSIST
Computational fluid dynamics and aerothermodynamics
[NASA-CR-180079] N89-20415

AERODYNAMIC CHARACTERISTICS
High Reynolds number incompressible flow simulation about parachute canopies and similar bluff bodies N89-20096
Evaluation of VSAERO in prediction of aerodynamic characteristics of helicopter hub fairings
[NASA-TM-101048] N89-20098
Aerodynamics of two-dimensional slotted bluff bodies
[DE89-007288] N89-20105

AERODYNAMIC COEFFICIENTS
Thrust generation by an airfoil in hovering mode
[AD-A203785] N89-20106

AERODYNAMIC CONFIGURATIONS
Documentation of two- and three-dimensional hypersonic shock wave/turbulent boundary layer interaction flows
[NASA-TM-101075] N89-20100

AERODYNAMIC HEATING
Reconnection launcher projectile heating using the modified REGGIE code
[DE89-007294] N89-20172

AERODYNAMIC LOADS
Aerodynamic pressure and flow-visualization measurement from a rotating wind turbine blade
[DE89-000854] N89-20104
Hub and blade structural loads measurements of an SA349/2 helicopter
[NASA-TM-101040] N89-20124

AERODYNAMICS
Aeronautical engineering: A cumulative index to a continuing bibliography (supplement 235)
[NASA-SP-7037(235)] N89-20088
Aeronautical engineering: A continuing bibliography with indexes (supplement 237)
[NASA-SP-7037(237)] N89-20089
Aeronautical engineering: A continuing bibliography with indexes (supplement 238)
[NASA-SP-7037(238)] N89-20090
Aeronautical engineering: A continuing bibliography with indexes (supplement 236)
[NASA-SP-7037(236)] N89-20091

Pressure coefficients for basic tensioned-membrane structure forms
[AD-A203866] N89-20107

AEROELASTICITY
Some low-speed flutter characteristics of simple low-aspect-ratio delta wing models
[NASA-TM-101547] N89-20094
Active control helicopter aeromechanical and aeroelastic instabilities N89-20149

AERONAUTICAL ENGINEERING
Aeronautical engineering: A cumulative index to a continuing bibliography (supplement 235)
[NASA-SP-7037(235)] N89-20088
Aeronautical engineering: A continuing bibliography with indexes (supplement 237)
[NASA-SP-7037(237)] N89-20089
Aeronautical engineering: A continuing bibliography with indexes (supplement 238)
[NASA-SP-7037(238)] N89-20090
Aeronautical engineering: A continuing bibliography with indexes (supplement 236)
[NASA-SP-7037(236)] N89-20091

AEROSOLS
Density measurements with combined Raman-Rayleigh LIDAR (Light Detection And Ranging)
[AD-A203561] N89-20376
The investigation of advanced remote sensing, radiative transfer and inversion techniques for the measurement of atmospheric constituents
[NASA-CR-172599] N89-20531
3CPO, Cloud Chemistry and Cloud Physics Organization: Data index, June 1988
[DE89-007011] N89-20591

AEROSPACE ENGINEERING
L1 libration point manned space habitat
[NASA-CR-184732] N89-20180

AEROSPACE ENVIRONMENTS
AFE ion mass spectrometer design study
[NASA-CR-184838] N89-20432

AEROSPACE MEDICINE
USSR Space Life Sciences Digest, Issue 21
[NASA-CR-3922(24)] N89-20602

AEROTHERMODYNAMICS
Toward improved durability in advanced aircraft engine hot sections
[NASA-TM-4087] N89-20135
NASA HOST project overview N89-20136
Assessment, development, and application of combustor aerothermal models N89-20138
Review and assessment of the database and numerical modeling for turbine heat transfer N89-20139
Views on the impact of HOST N89-20144
Computational fluid dynamics and aerothermodynamics
[NASA-CR-180079] N89-20415

AFTERBODIES
Base flow investigation behind axi-and non-axisymmetric blunt bodies
[ISL-CO-246/87] N89-20103

AH-1G HELICOPTER
Coupled rotor/fuselage dynamic analysis of the AH-1G helicopter and correlation with flight vibrations data
[NASA-CR-181723] N89-20512

AIR
Modeling of hydrogen-air diffusion flame
[NASA-CR-184844] N89-20218

AIR FILTERS
Airworthiness and flight characteristics evaluation of an improved engine air filtration system on the UH-1H helicopter
[AD-A203446] N89-20145

AIR FLOW
Quantification of environmental chambers by air velocity mapping
[AD-A200923] N89-20154

AIR INTAKES
Development of a rotary value for pulse combustion applications
[PB89-131114] N89-20468

AIR LAND INTERACTIONS
Current velocity and hydrographic observations in the southwestern North Atlantic Ocean: Subtropical Atlantic Climate Studies (SACS), 1987
[PB89-114011] N89-20598

AIR POLLUTION
A microcomputer pollution model for civilian airports and Air Force bases. Model application and background
[AD-A199794] N89-20557
National Air Toxics Information Clearinghouse: Ongoing research and regulatory development projects, July 1988
[PB89-103428] N89-20558
NOAA (National Oceanic and Atmospheric Administration) X-band radar measurements in 3CPO (Cloud Chemistry Cloud Physics Organization)
[PB89-127823] N89-20562
Implications of the greenhouse effect for the midwest economy
[DE89-004195] N89-20563

AIR QUALITY
A microcomputer pollution model for civilian airports and Air Force bases. Model application and background
[AD-A199794] N89-20557
An assessment model for atmospheric composition
[NASA-CP-3023] N89-20588

AIR TRAFFIC CONTROL
The application of software fault tolerance to air traffic control: Study contract overview
[BR108567] N89-20114
The application of trajectory prediction algorithms for planning purposes in the Netherlands Air Traffic Control (ATC) system
[NLR-MP-87031-U] N89-20115
Improved computer simulation of the TCAS 3 circular array mounted on an aircraft
[NASA-CR-184907] N89-20363

AIR WATER INTERACTIONS
CTD/O2 measurements during 1986 as part of the Equatorial Pacific Ocean Climate Studies (EPOCS)
[PB89-102859] N89-20596

AIRBORNE EQUIPMENT
Electronics in civil aviation
[NLR-MP-87009-U] N89-20129
The data acquisition system for the Fokker 100 test aircraft
[NLR-MP-87047-U] N89-20130
Phase A study for the extension of the CAESAR scanner with a sensor module for the far infrared
[BCRS-88-09] N89-20539

AIRBORNE/SPACEBORNE COMPUTERS
The digital wave processing experiment --- Cluster mission N89-20164

AIRCRAFT
Aerospace vehicle design, Spacecraft Section final project reports
[NASA-CR-184741] N89-20121

AIRCRAFT ACCIDENT INVESTIGATION
Aircraft accident data, US general aviation, calendar year 1986
[PB89-121453] N89-20108
Aircraft accident reports: Brief format, US civil and foreign aviation, issue number 12 of 1986 accidents
[PB88-916902] N89-20109
Aircraft accident reports, brief format, US civil and foreign aviation, issue number 14 of 1986 accidents
[PB88-916904] N89-20110
Aircraft accident report: Continental Airlines, Inc., Flight 1713, McDonnell Douglas DC-9-14, N626TX, Stapleton International Airport, Denver, Colorado, November 15, 1987
[PB88-910411] N89-20112

AIRCRAFT ACCIDENTS
Aircraft accident data, US general aviation, calendar year 1986
[PB89-121453] N89-20108
Aircraft accident reports: Brief format, US civil and foreign aviation, issue number 12 of 1986 accidents
[PB88-916902] N89-20109
Aircraft accident reports, brief format, US civil and foreign aviation, issue number 14 of 1986 accidents
[PB88-916904] N89-20110
Aircraft accident report: Continental Airlines, Inc., Flight 1713, McDonnell Douglas DC-9-14, N626TX, Stapleton International Airport, Denver, Colorado, November 15, 1987
[PB88-910411] N89-20112

AIRCRAFT COMMUNICATION
Improved computer simulation of the TCAS 3 circular array mounted on an aircraft
[NASA-CR-184907] N89-20363

AIRCRAFT CONSTRUCTION MATERIALS
Paint tests on laminated material formed by carbon fiber composites and Tedlar layers
[I-279/88] N89-20208
Structural mechanics: Contemporary state and prospects for development (selected portions)
[AD-A198766] N89-20498

AIRCRAFT CONTROL
Power efficient hydraulic systems. Volume 2: Hardware demonstration phase
[AD-A203900] N89-20128
On-board automatic aid and advisory for pilots of control-impaired aircraft N89-20150

AIRCRAFT DESIGN
Aerospace vehicle design, Spacecraft Section final project reports
[NASA-CR-184742] N89-20122
Aerospace vehicle design, Spacecraft Section
[NASA-CR-184743] N89-20123
Power efficient hydraulic systems. Volume 1: Study phase
[AD-A203899] N89-20127
Power efficient hydraulic systems. Volume 2: Hardware demonstration phase
[AD-A203900] N89-20128

AIRCRAFT ENGINES
Toward improved durability in advanced aircraft engine hot sections
[NASA-TM-4087] N89-20135
NASA HOST project overview N89-20136
Review and assessment of the database and numerical modeling for turbine heat transfer N89-20139
Structural analysis applications N89-20141
Life modeling of thermal barrier coatings for aircraft gas turbine engines N89-20143
Views on the impact of HOST N89-20144

AIRCRAFT HYDRAULIC SYSTEMS
Power efficient hydraulic systems. Volume 1: Study phase
[AD-A203899] N89-20127
Power efficient hydraulic systems. Volume 2: Hardware demonstration phase
[AD-A203900] N89-20128

AIRCRAFT MAINTENANCE
Environment-assisted aerospace fatigue problems in The Netherlands
[NLR-MP-88004-U] N89-20087

AIRCRAFT MANEUVERS
Continuous-discrete filtering for systems with Markovian switching coefficients
[NLR-MP-87076-U] N89-20117

AIRCRAFT NOISE
Noise generated by a flight weight, air flow control valve in a vertical takeoff and landing aircraft thrust vectoring system
[NASA-CR-182232] N89-20776

AIRCRAFT RELIABILITY
Airworthiness and flight characteristics evaluation of an improved engine air filtration system on the UH-1H helicopter
[AD-A203446] N89-20145

AIRCRAFT STRUCTURES
Matching Power Spectra Density (PSD)-design load --- aircraft structures
[NLR-MP-87059-U] N89-20126
A (13)C NMR analysis of the effects of electron radiation on graphite/polyetherimide composites
[NASA-CR-182818] N89-20205
Electromagnetic properties of ice coated surfaces
[NASA-CR-184780] N89-20355
Structural mechanics: Contemporary state and prospects for development (selected portions)
[AD-A198766] N89-20498
Current status of flight simulation fatigue crack growth concepts
[NLR-MP-88001-U] N89-20521
Estimation of the Equivalent Initial Flow Size (EIFS) distribution and prediction of failure probabilities for different parameter variations
[FFA-TN-1987-35] N89-20525

AIRFOIL OSCILLATIONS
Experimental investigation of transonic oscillating cascade aerodynamics
[NASA-TM-101993] N89-20133

AIRFOIL PROFILES
An airfoil pitch apparatus-modeling and control design
[NASA-TM-101076] N89-20386

AIRFOILS
Thrust generation by an airfoil in hovering mode
[AD-A203785] N89-20106

AIRFRAME MATERIALS
Quench sensitivity of airframe aluminum alloys
[NLR-MP-88003-U] N89-20231

AIRPORTS
A microcomputer pollution model for civilian airports and Air Force bases. Model application and background
[AD-A199794] N89-20557

ALGEBRA
An algebraic calculus of commands
[CS-8808] N89-20656
The algebra of synchronous processes
[CWI-CS-R8807] N89-20687
Algebraic nonplanar curve and surface estimation in 3-space with applications to position estimation
[PB88-227616] N89-20709
Piecewise continuous algebraic surfaces in terms of B-splines
[PB89-109136] N89-20712
Monotonically improving approximate answers to relational algebra queries
[NASA-CR-184874] N89-20717
SLAP (Sparse Linear Algebra Package) for the masses
[DE89-006209] N89-20721
Schema-based theories of problem solving
[AD-A203731] N89-20774

ALGORITHMS
Multigrid solution of the Navier-Stokes equations on triangular meshes
[NASA-CR-181786] N89-20095
Space shuttle propulsion estimation development verification, volume 1
[NASA-CR-183581] N89-20197
A new algorithm for modeling friction in dynamic mechanical systems N89-20334
Long decoding runs for Galileo's convolutional codes N89-20342
The decoding of Reed-Solomon codes N89-20344
Effect of earth albedo variation on the performance of a spatial acquisition subsystem aboard a planetary spacecraft N89-20349
An extended Kalman filter based automatic frequency control loop N89-20351
Pointing a ground antenna at a spinning spacecraft using Conscan-simulation results N89-20354
Error control techniques for satellite and space communications
[NASA-CR-184825] N89-20357
Analysis of modified SMI method for adaptive array weight control
[NASA-CR-184904] N89-20364
Linear feature extraction from radar imagery: SBIR (Small Business Innovative Research) phase 2, option 1
[AD-A203688] N89-20377
Evaluation of the Kubo formula for the conductivity using the recursion method
[DE88-705359] N89-20396
On-line arithmetic algorithms and structures for VLSI
[AD-A203421] N89-20400
Dynamic modeling and linearization for real-time control of a pantograph manipulator N89-20469
Using depth recovery in humans
[AD-A201278] N89-20606
Parallel algorithms for PDE solvers
[AD-A199625] N89-20630
Adaptive FE algorithm for variational inequality problems
[PB89-111512] N89-20634
Adaptive data compression system study --- scientific satellite
[SIL/CR/7129/6] N89-20639
User's manual for DYNA2D: An explicit two-dimensional hydrodynamic finite element code with interactive rezoning and graphical display
[DE89-006695] N89-20647
An exact incremental hidden surface removal algorithm
[CWI-CS-R8818] N89-20663
Parallel direct solution of sparse linear systems
[DE89-006030] N89-20666
A parallel decomposition algorithm for Staircase Linear Programs
[DE89-007023] N89-20669
An algorithm for automated quadrilateral mesh generation for planar regions
[DE89-007299] N89-20671
A parallel decomposition algorithm for Staircase Linear Programs
[DE89-007883] N89-20674
Valiant's maximum algorithm with sequential memory accesses
[AD-A203713] N89-20676
Parallel algorithms for computer vision
[AD-A203947] N89-20681
A message passing kernel for the hypercluster parallel processing test bed
[NASA-TM-101952] N89-20684
The effect of time constraints on scaled speed-up
[DE89-007877] N89-20691
Integrating multiple views into a single representation of a range imaged object
[DE89-005921] N89-20707
An analysis of reduced Hessian methods for constrained optimization
[AD-A201078] N89-20715
Monotonically improving approximate answers to relational algebra queries
[NASA-CR-184874] N89-20717
SLAP (Sparse Linear Algebra Package) for the masses
[DE89-006209] N89-20721
The relationship between an orthogonal estimation algorithm and other least squares routines
[RR-331] N89-20729
Application of Newton's method to Lagrangian dynamical systems
[DE89-007024] N89-20751
Combined algorithms in nonlinear problems of magnetostatics
[DE89-006594] N89-20753
A fast algorithm for reordering sparse matrices for parallel factorization
[DE89-007873] N89-20758
Lattice gauge theory and Monte Carlo methods
[DE89-005666] N89-20856
Adaptive data compression system study, executive summary --- scientific satellite
[SIL/CR/7129/7] N89-20867
ALIGNMENT
Progress in linear optics, non-linear optics and surface alignment of liquid crystals
[DE89-006507] N89-20834
ALKYL COMPOUNDS
Synthesis and physical properties of liquid crystalline alkylisocyanate copolymers
[AD-A203631] N89-20266
ALLOYS
Casting And Solidification Technology (CAST): Directional solidification phenomena in a metal model at reduced gravity N89-20301
ALUMINIDES
Compositional effects on processing and properties of nickel aluminides
[DE89-005133] N89-20229
ALUMINUM
Glass corrosion in natural environment
[NASA-CR-184843] N89-20251
High intensity acoustic tests of a thermally stressed aluminum plate in TAFA
[NASA-TM-101552] N89-20778
ALUMINUM ALLOYS
Experimental study of spall damage in an aluminium alloy
[PB89-112619] N89-20224
Quench sensitivity of airframe aluminum alloys
[NLR-MP-88003-U] N89-20231
Electrodeposition of aluminium, aluminium/magnesium alloys and magnesium from organometallic electrolytes
[DE89-003483] N89-20232
Microstructural and magnetic characterization in soft magnetic Fe-Si-Al (Sendust) alloy
[DE89-007130] N89-20239
Weldability of 2519-T87 aluminum alloy
[AD-A203519] N89-20244
ALUMINUM COMPOUNDS
Exploratory alloy development in the system Al-Sc-X
[DE89-007088] N89-20237
Research and development of HgZnTe as an infrared material
[NASA-CR-184840] N89-20820
ALUMINUM NITRIDES
Anion controlled microstructures in the Al2O3-AlN system
[AD-A203671] N89-20209
ALUMINUM OXIDES
Anion controlled microstructures in the Al2O3-AlN system
[AD-A203671] N89-20209
AMBIENT TEMPERATURE
The Mars climate for a photovoltaic system operation
[NASA-TM-101994] N89-20385
AMORPHOUS MATERIALS
Hardness of amorphous hard carbon films determined by the ultra-low load microindentation technique
[DE89-006129] N89-20259
Irradiation as a tool for studying solid state amorphization phenomena
[DE89-006034] N89-20823
AMPLIFIERS
Theoretical comparison of maser materials for a 32-GHz maser amplifier N89-20335
ANALOG CIRCUITS
Analog automatic control loops in radar and EW (Electronic Warfare)
[AD-A203758] N89-20380
ANALOGIES
A communication channel model of the software process
[NASA-CR-184866] N89-20643
ANALOGS
Sulfide and phosphide analogs of oxynitride ceramics
[AD-A203805] N89-20269
ANECHOIC CHAMBERS
Anechoic chamber evaluation at 85 GHz
[PB89-125199] N89-20153
ANIONS
Anion controlled microstructures in the Al2O3-AlN system
[AD-A203671] N89-20209
Anion grain boundary diffusion in Cr2O3 and Cr2O3-0.09 weight percent Y2O3
[DE89-006281] N89-20833
ANISOTROPIC FLUIDS
Solutions and stability of a closed-geodesic black hole model N89-20893
ANISOTROPY
Green's function formulation of plane crack problems for general anisotropic materials N89-20509
Investigations of ultrasonic wave interactions at imperfect boundaries separating anisotropic materials
[DE89-007089] N89-20781
ANNUAL VARIATIONS
Verification of regional climates of GISS GCM. Part 2: Summer
[NASA-TM-100722] N89-20589
ANNULAR PLATES
Analysis of the dynamics of guided rotating free center plates N89-20466
ANOMALIES
Flight motor set 360L001 (STS-26R), volume 1
[NASA-CR-183576] N89-20196
ANTENNA ARRAYS
Analysis of modified SMI method for adaptive array weight control
[NASA-CR-184904] N89-20364
Reconfigurable antennas
[AD-A203847] N89-20382
ANTENNA COMPONENTS
Reconfigurable antennas
[AD-A203847] N89-20382
ANTENNA DESIGN
The Telecommunications and Data Acquisition Report
[NASA-CR-184672] N89-20329
Dynamic models for simulation of the 70-M antenna axis servos N89-20333
A new algorithm for modeling friction in dynamic mechanical systems N89-20334
An integral sunshade for optical reception antennas N89-20347
Shutters and slats for the integral sunshade of an optical reception antenna N89-20348
DSN 70-meter antenna X-band gain, phase, and pointing performance, with particular application for Voyager 2 Neptune encounter N89-20353
Pointing a ground antenna at a spinning spacecraft using Conscan-simulation results N89-20354
Electronically Steerable Terminal Antenna (ESTA) project, phase 2
[ESA-CR(P)-2599] N89-20359
Modeling the behavior of pulsed, high power microwave antenna systems
[DE89-006280] N89-20374
Geometrical optics design of a compact range Gregorian subreflector system by the principle of the central ray
[NASA-CR-184810] N89-20795
ANTENNA FEEDS
Cross-guide coupler modeling and design N89-20337
Modal analysis applied to circular, rectangular, and coaxial waveguides N89-20338
ANTENNA RADIATION PATTERNS
Analysis of modified SMI method for adaptive array weight control
[NASA-CR-184904] N89-20364
Geometrical optics design of a compact range Gregorian subreflector system by the principle of the central ray
[NASA-CR-184810] N89-20795
ANTIBODIES
Development of immunoassays for human urokinase N89-20283
Antibody enhancement of free-flow electrophoresis N89-20290
ANTIFERROMAGNETISM
Localized versus itinerant picture of light-T(sub c) superconducting oxides
[DE88-705345] N89-20830
ANTIPARTICLES
On particle antiparticle mirror symmetry
[USIP-88-06] N89-20786
ANTIREFLECTION COATINGS
Edge illuminated ventical multijunction
[DE89-006246] N89-20547
ANTISUBMARINE WARFARE
Activities report of the Division of Information Systems
[FOA-C-30499-3.3] N89-20919
APERTURES
Cross-guide coupler modeling and design N89-20337
Diffraction theory for polygonal apertures
[AD-A203778] N89-20802
APPLICATIONS PROGRAMS (COMPUTERS)
Studies and analyses of the space shuttle main engine. Failure information propagation model data base and software
[NASA-CR-183586] N89-20198
APPROPRIATIONS
NASA authorization
[S-HRG-100-579] N89-20873
APPROXIMATION
Adaptive FE algorithm for variational inequality problems
[PB89-111512] N89-20634

Domain decomposition methods for systems of conservation laws: Spectral collocation approximations [NASA-CR-181773] N89-20635
On the structure and control of piecewise-linear systems [RR-334] N89-20700
Algebraic nonplanar curve and surface estimation in 3-space with applications to position estimation [PB88-227616] N89-20709
Waiting-time approximations for cyclic-service systems with mixed service strategies [CWI-OS-R8802] N89-20743
Censoring, truncation and filtering in statistical models based on counting processes [CWI-MS-R8803] N89-20769

AQUEOUS SOLUTIONS
Glass corrosion in natural environment [NASA-CR-184843] N89-20251

ARCHITECTURE (COMPUTERS)
Implementing recurrent back-propagation on the connection machine [AD-A203796] N89-20381
Application-based control of an autonomous mobile robot [DE89-004380] N89-20477
Force-reflecting master-slave control and robotic control of a traction-drive differential pitch-yaw joint [DE89-005107] N89-20480
Telerobotic manipulator developments for ground-based space research [NASA-CR-184736] N89-20481
Development of an integrated mobile robot system at CMU (Carnegie Mellon University), June 1987 [AD-A203689] N89-20487
Eddy current inspection of ferromagnetic materials using pulsed magnetic saturation [DE89-005339] N89-20493
Memory architecture for multiprocessor computers [EP-PATENT-0-240-354-A1] N89-20622
Improvements relating to control flow in computers [EP-0-234-785-A1] N89-20624
Software reliability engineering [DE89-006781] N89-20626
Epa'88: Combining the best features of von Neumann and dataflow computing [DE89-007291] N89-20627
DATMS: A framework for distributed assumption based reasoning [DE89-006282] N89-20628
A vector-like architecture for raster graphics [CWI-CS-R8802] N89-20660
A software model for simulation in computer-based training [DE89-003469] N89-20665
An algorithm for automated quadrilateral mesh generation for planar regions [DE89-007299] N89-20671
The use of GKS (Graphical Kernel System) and CGM (Computer Graphics Metafile) for the display of graphics products [DE89-006734] N89-20673
Development of the University of Maryland RAMCAD (Reliability and Maintainability Computer-Aided Design) for electronic systems [AD-A203616] N89-20675
Parallel algorithms for computer vision [AD-A203947] N89-20681
Initial operating capability for the hypercluster parallel-processing test bed [NASA-TM-101953] N89-20685
A local area network diagnostic assistant expert system [DE89-003575] N89-20689
Increasing user-friendliness in AI systems [DE89-005093] N89-20704
On automatic differentiation [DE89-005779] N89-20752

ARCTIC OCEAN
Beaufort Sea mesoscale circulation study: Preliminary results [PB89-121693] N89-20597

ARIANE LAUNCH VEHICLE
Expendable launch vehicle transportation for the space station [NASA-TM-101947] N89-20179

ARITHMETIC
On-line arithmetic algorithms and structures for VLSI [AD-A203421] N89-20400
Arithmetic classification of perfect models of stratified programs [CWI-CS-R8810] N89-20737

ARMOR
Weldability of 2519-T87 aluminum alloy [AD-A203519] N89-20244

ARRAYS
Q-switched, intracavity doubled Nd:YAG laser side-pumped by a laser diode array [DE89-005349] N89-20441
Support of Mark 3 optical interferometer [AD-A203665] N89-20800

ARTIFICIAL INTELLIGENCE
Vision-based navigation for autonomous ground vehicles [AD-A203712] N89-20120
Real-time part position sensing [AD-A203580] N89-20439
Development of the HERMIES 3 mobile robot research testbed at Oak Ridge National Laboratory [DE89-004797] N89-20479
Using depth recovery in humans [AD-A201278] N89-20606
Symbolic inversion of control relationships in model-based expert systems [NASA-CR-182857] N89-20631
Consequences of nonclassical measurement for the algorithmic description of continuous dynamical systems [NASA-CR-184851] N89-20640
Intelligence in scientific computing [AD-A203815] N89-20679
Use of artificial intelligence in supervisory control N89-20694
Automatic learning by an autonomous mobile robot [DE89-003120] N89-20702
Sensor capabilities for the HERMIES experimental robot [DE89-003180] N89-20703
Increasing user-friendliness in AI systems [DE89-005093] N89-20704
Dynamic mechanical system design using qualitative and symbolic reasoning [DE89-006771] N89-20706
Integrating multiple views into a single representation of a range imaged object [DE89-005921] N89-20707
The DoD Gateway Information System (DGIS): The development toward artificial intelligence and hypermedia in common command language [AD-A203674] N89-20869

ASPHALT
Methods and materials for reducing crack reflectance [PB89-114532] N89-20505

ASSEMBLER ROUTINES
Watchdog Program [PB89-122535] N89-20633
A PASCAL cross-assembler for the 6809 microprocessor [USIP-88-05] N89-20648

ASTRODYNAMICS
Modeling and control of flexible structures [NASA-CR-184862] N89-20152

ASTRONOMICAL MODELS
Multicolor surface photometry of powerful radio galaxies N89-20878
Dust shells around Miras and OH/IR stars N89-20889
Star formation, using 3-D explicit Eulerian hydrodynamics N89-20890
Mixing and nucleosynthesis in low- and intermediate-mass AGB stars N89-20892
Magnetospheres of neutron stars accreting from disks N89-20895
Black holes as possible sources of closed and semiclosed worlds [DE88-705336] N89-20900
Nonthermal radio emission from RS CVN binaries and similar systems N89-20913
The galactic large-scale far-infrared emission observed by IRAS: Implications for the morphology, physical conditions, and energetics of dust in the interstellar medium N89-20914

ASTRONOMICAL PHOTOMETRY
Isophotometry of brightest elliptical galaxies in rich clusters N89-20879

ASTRONOMICAL SPECTROSCOPY
Forbidden coronal iron line emission in the Puppis A shock front: The effect of inhomogeneities [NASA-TM-89284] N89-20875

ASTRONOMY
Support of Mark 3 optical interferometer [AD-A203665] N89-20800

ASTROPHYSICS
Dust shells around Miras and OH/IR stars N89-20889
Astrophysics in a nutshell: From the telescope to the Sputnik [TRITA-EPP-88-04] N89-20897

ASYMMETRY
Tripping of asymmetrical stiffeners under combined loading [PB89-126171] N89-20504
Who's afraid of nonsymmetric matrices? A discussion of elementary iterative methods [REPT-88-49] N89-20723

ASYMPTOTIC GIANT BRANCH STARS
Mixing and nucleosynthesis in low- and intermediate-mass AGB stars N89-20892

ASYMPTOTIC PROPERTIES
Asymptotic normality of minimum L sub 1 norm estimators in linear regression [CWI-MS-R8806] N89-20747
Asymptotic behavior of random discrete event systems [REPT-88-56] N89-20766

ASYMPTOTIC SERIES
Uniform asymptotic expansions of a class of integrals in terms of modified Bessel functuons, with application to confluent hypergeometric functions [CWI-AM-R8806] N89-20738

ATLANTIC OCEAN
Current velocity and hydrographic observations in the southwestern North Atlantic Ocean: Subtropical Atlantic Climate Studies (SACS), 1987 [PB89-114011] N89-20598

ATLANTIS (ORBITER)
STS-27R OV-104 Orbiter TPS damage review team, volume 1 [NASA-TM-100355-VOL-1] N89-20178

ATMOSPHERIC ATTENUATION
A preliminary weather model for optical communications through the atmosphere N89-20350
Density measurements with combined Raman-Rayleigh LIDAR (Light Detection And Ranging) [AD-A203561] N89-20376

ATMOSPHERIC CHEMISTRY
NOAA (National Oceanic and Atmospheric Administration) X-band radar measurements in 3CPO (Cloud Chemistry Cloud Physics Organization) [PB89-127823] N89-20562

ATMOSPHERIC CIRCULATION
Scenarios for future climate change: Results of GCM (General Circulation Model) simulations [DE89-006151] N89-20565
Verification of regional climates of GISS GCM. Part 2: Summer [NASA-TM-100722] N89-20589
Beaufort Sea mesoscale circulation study: Preliminary results [PB89-121693] N89-20597

ATMOSPHERIC COMPOSITION
The investigation of advanced remote sensing, radiative transfer and inversion techniques for the measurement of atmospheric constituents [NASA-CR-172599] N89-20531
An assessment model for atmospheric composition [NASA-CP-3023] N89-20588

ATMOSPHERIC ELECTRICITY
Preliminary analysis of cloud-to-ground lightning in the vicinity of the Nevada test site [PB89-128649] N89-20584

ATMOSPHERIC GENERAL CIRCULATION MODELS
Current velocity and hydrographic observations in the southwestern North Atlantic Ocean: Subtropical Atlantic Climate Studies (SACS), 1987 [PB89-114011] N89-20598

ATMOSPHERIC MODELS
A numerical model of ionospheric convection derived from field-aligned currents and the corresponding conductivity --- ionosphere [TRITA-EPP-88-03] N89-20571
Report of the 2nd Workshop on the Community Climate Model [PB88-250741] N89-20576
Examination of NGM (Nested Grid Model) low level temperature [PB89-122543] N89-20580
Radiation, turbulence and microphysics in the stratiform regions of tropical cloud clusters N89-20585
Observed and modeled terrain-induced shear in tracer trajectories [DE89-006938] N89-20590

ATMOSPHERIC MOISTURE
Improved capabilities of the Multispectral Atmospheric Mapping Sensor (MAMS) [NASA-TM-100352] N89-20430

ATMOSPHERIC RADIATION
Characterization of production GaAs solar cells for space [NASA-CR-184863] N89-20549

ATMOSPHERIC REFRACTION
Remote sensing in refractive turbulence N89-20532

ATMOSPHERIC TEMPERATURE
Examination of NGM (Nested Grid Model) low level temperature [PB89-122543] N89-20580

ATMOSPHERIC TURBULENCE
Remote sensing in refractive turbulence N89-20532

Relationship of wind shear, buoyancy and radar tops to severe weather, 1988
[PB89-122519] N89-20581
Radiation, turbulence and microphysics in the stratiform regions of tropical cloud clusters N89-20585

ATOMIC BEAMS
Thermodynamics of finite-time processes: Accomplishments and work in progress, 1986--1989
[DE89-006726] N89-20858

ATOMIC STRUCTURE
Electronic structure calculation by nonlinear optimization: Application to metals
[DE89-005852] N89-20816
A first-principles method for the determination of the electronic structure of grain boundaries
[DE89-006148] N89-20845

ATOMIZING
Investigation of spray dispersion and particulate formation in diesel fuel flames
[NASA-CR-184820] N89-20215

AUGER EFFECT
Auger electron and X-ray photoelectron data processing for the personal computer
[DE89-007292] N89-20670

AUGER SPECTROSCOPY
Auger electron and X-ray photoelectron data processing for the personal computer
[DE89-007292] N89-20670

AUTOMATIC CONTROL
On-board automatic aid and advisory for pilots of control-impaired aircraft N89-20150
Design and implementation of the hazard control box for the ride motion simulator
[AD-A203752] N89-20404
Application-based control of an autonomous mobile robot
[DE89-004380] N89-20477
Automating the multiprocessing environment
[NASA-TM-4103] N89-20641

AUTOMATIC FREQUENCY CONTROL
An extended Kalman filter based automatic frequency control loop N89-20351

AUTOMATIC GAIN CONTROL
Analog automatic control loops in radar and EW (Electronic Warfare)
[AD-A203758] N89-20380

AUTOMATION
A study of EMI-endurance of two polling-type local area networks used in real-time automation applications in a simulated electrical environment
[EL-62] N89-20368

AUTOMOBILE ENGINES
Design and testing of a dissociated methanol vehicle
[DE89-007051] N89-20483

AUTOMOBILE FUELS
Design and testing of a dissociated methanol vehicle
[DE89-007051] N89-20483

AUTONOMOUS NAVIGATION
Vision-based navigation for autonomous ground vehicles
[AD-A203712] N89-20120
The 1987 year end report for road following at Canegie Mellon
[AD-A203946] N89-20488

AVIONICS
Electronics in civil aviation
[NLR-MP-87009-U] N89-20129

AXIAL COMPRESSION LOADS
Elastic stability of cylindrical shells with circumferential welded joints under axial compression
[PB89-125082] N89-20502

AXIAL FLOW
An analytical and numerical study of axial flow compressor instability N89-20131

AXIAL LOADS
Axially accelerated saboted rods subjected to lateral forces
[DE89-007466] N89-20485
Elastic stability of lap-jointed cylindrical shells under axial compression
[PB88-245980] N89-20497
Non-symmetric bifurcation of geometrically non-linear elastic-plastic axisymmetric shells under combined loads including torsion
[PB89-102149] N89-20500
Experiments on the buckling of thin-walled model silo structures
[PB89-125124] N89-20503
Tripping of asymmetrical stiffeners under combined loading
[PB89-126171] N89-20504

AXIAL STRESS
Elastic stability of cylindrical shells with circumferential welded joints under axial compression
[PB89-125082] N89-20502
Results of inphase axial-torsional fatigue experiments on 304 stainless steel
[NASA-TM-101464] N89-20514

B

BACKSCATTERING
Current status of the NAVSEA Backscatter Absorption Gas Imaging (BAGI) development project
[DE89-006726] N89-20438
Active and passive remote sensing of ice
[AD-A203943] N89-20543
The development of a Compton lung densitometer
[DE89-006654] N89-20603

BACKWARD FACING STEPS
Solutions to the Navier-Stokes equations using a k-epsilon turbulence model
[FFA-TN-1988-19] N89-20416
An explicit finite differences solver for the incompressible Reynolds averaged Navier-Stokes equations, optimized for the Alliant DSP 9000 computer
[VKI-TM-45] N89-20423

BALANCING
High speed balancing applied to the T700 engine
[NASA-CR-180899] N89-20472

BALLISTICS
Base flow investigation behind axi-and non-axisymmetric blunt bodies
[ISL-CO-246/87] N89-20103
Space shuttle propulsion estimation development verification
[NASA-CR-183582] N89-20195
Flight motor set 360L001 (STS-26R), volume 1
[NASA-CR-183576] N89-20196

BARIUM COMPOUNDS
Material selection for electrooptic deflectors
[DE89-007343] N89-20841

BARIUM OXIDES
Thermodynamic characteristics of Y-Ba-Cu-O type compounds in the model of strong electron-phonon coupling
[DE88-705343] N89-20828

BAROTROPIC FLOW
Analysis of Doppler radar windshear data
[NASA-CR-181762] N89-20111
Numerical studies of barotropic stability of stratospheric states N89-20570

BARYONS
Primordial nucleosynthesis and late decaying particles: A new model of nucleosynthesis N89-20894

BASE FLOW
Base flow investigation behind axi-and non-axisymmetric blunt bodies
[ISL-CO-246/87] N89-20103

BAYES THEOREM
Simultaneous inversion of vector and total field aeromagnetic data using Bayesian inference: A case study from the Cobb Offset of the Juan de Fuca Ridge
[PB89-114193] N89-20599
Pseudo-Bayesian stability of CSMA (Carrier Sense Multiple Access) and CSMA/CD (Collision Detection) local area networks
[AD-A203834] N89-20763

BAYS (TOPOGRAPHIC FEATURES)
Biological processes in the water column of the South Atlantic Bight: Zooplankton responses
[DE89-006828] N89-20600

BEAM INJECTION
Review of intense electron beam transport in gases
[DE89-005397] N89-20792
Low emittance thermionic electron guns
[DE89-005944] N89-20793
Transport modeling of ECH and neutral-beam-heated plasmas in the advanced toroidal facility
[DE89-006131] N89-20809

BEAM INTERACTIONS
On the performance of the DELPHI hadron calorimeter
[PH-159] N89-20434
Pulsed laser effects phenomenology
[DE89-005466] N89-20442

BEAMS (RADIATION)
Stimulated Raman scattering of intense laser radiation in a nuclear-disturbed space plasma
[AD-A200951] N89-20440
Paraxial approximations for ultrasonic beam propagation in liquid and solid media with applications to nodestructive evaluation
[DE89-007569] N89-20782

BEAMS (SUPPORTS)
Determination of the impulse response of a viscoelastic beam using a fractional derivative constitutive model N89-20501

BEHAVIOR
Luminescence originating in an optical fiber
[AD-A203494] N89-20799

BENDING
A refined theory for plate bending with optimized stress field N89-20510

BESSEL FUNCTIONS
Uniform asymptotic expansions of a class of integrals in terms of modified Bessel functuons, with application to confluent hypergeometric functions
[CWI-AM-R8806] N89-20738

BIBLIOGRAPHIES
Aeronautical engineering: A cumulative index to a continuing bibliography (supplement 235)
[NASA-SP-7037(235)] N89-20088
Aeronautical engineering: A continuing bibliography with indexes (supplement 237)
[NASA-SP-7037(237)] N89-20089
Aeronautical engineering: A continuing bibliography with indexes (supplement 238)
[NASA-SP-7037(238)] N89-20090
Aeronautical engineering: A continuing bibliography with indexes (supplement 236)
[NASA-SP-7037(236)] N89-20091

BIG BANG COSMOLOGY
Has the Universe an origin
[TRITA-EPP-88-07] N89-20898

BINARY ALLOYS
Isothermal solidification in a binary alloy melt N89-20300

BINARY MIXTURES
Feasibility of a complex compound heat pump
[PB89-115273] N89-20405

BINARY STARS
Nonthermal radio emission from RS CVN binaries and similar systems N89-20913

BIOASSAY
Biochemical assays on plasminogen activators and hormones from kidney sources N89-20287

BIOCHEMISTRY
Biochemical assays on plasminogen activators and hormones from kidney sources N89-20287

BIOENGINEERING
Membrane vapor enricher for Water For Injection (WFI) production, phase 1
[AD-A201354] N89-20323

BIONICS
Using depth recovery in humans
[AD-A201278] N89-20606

BIOPROCESSING
Kidney cell electrophoresis in space flight: Rationale, methods, results and flow cytometry applications N89-20280
An expert system based intelligent control scheme for space bioreactors N89-20285

BIOREACTORS
Hydrodynamic effects on cell growth in agitated microcarrier bioreactors N89-20284
An expert system based intelligent control scheme for space bioreactors N89-20285
Human cell culture in a space bioreactor N89-20288
The stress response system of proteins: Implications for bioreactor scaleup N89-20291

BIT ERROR RATE
Performance of Galileo's concatenated codes with nonideal interleaving N89-20343

BLACK HOLES (ASTRONOMY)
Solutions and stability of a closed-geodesic black hole model N89-20893
Black holes as possible sources of closed and semiclosed worlds
[DE88-705336] N89-20900
Nonexistence theorems for Yang-Mills fields outside the black hole of the Schwarzschild spacetime
[DE88-705351] N89-20901

BLUE STARS
The upper main sequence of OB associations. 1: Spectral types and lines of C and N of southern single-lined O stars
[SER-C-PREPUBL-FASC-32] N89-20884

BLUFF BODIES
High Reynolds number incompressible flow simulation about parachute canopies and similar bluff bodies N89-20096
Aerodynamics of two-dimensional slotted bluff bodies
[DE89-007288] N89-20105

BLUNT BODIES
Base flow investigation behind axi-and non-axisymmetric blunt bodies
[ISL-CO-246/87] N89-20103

BODY CENTERED CUBIC LATTICES
Analysis of the strain-rate sensitivity at high strain rates in fcc and bcc metals
[DE89-005471] N89-20233

BODY TEMPERATURE
Why cold-wet makes one feel chilled: A literature review
[AD-A203452] N89-20609
BOMB CALORIMETERS
Fluorine as an oxidant in combustion calorimetry
[DE89-003626] N89-20214
BONDING
Finite element applications to explore the effects of partial bonding on metal matrix composite properties
[NASA-TM-101482] N89-20206
BOOLEAN ALGEBRA
Set theory, chapter 4
[REPT-88-47] N89-20722
BORN APPROXIMATION
Investigation of extensions to the distorted Born approximation in strong fluctuation theory
[AD-A203698] N89-20378
BORON CARBIDES
Structure-property characterization of a shock-loaded boron carbide-aluminum cermet
[DE89-005455] N89-20257
BOUNDARIES
Complex-valued functionals in variational analysis of waveguides with impedance boundaries
[PB89-128896] N89-20361
BOUNDARY LAYER FLOW
A calculation method for compressible three dimensional turbulent boundary layer flows
[VKI-TN-167] N89-20422
Vorticity distributions in unsteady flow separation
[AD-A203733] N89-20428
BOUNDARY LAYER SEPARATION
Dynamic wall pressure measurements
[AD-A203551] N89-20427
Vorticity distributions in unsteady flow separation
[AD-A203733] N89-20428
BOUNDARY LAYERS
Multigrid solution of the Navier-Stokes equations on triangular meshes
[NASA-CR-181786] N89-20095
Vorticity distributions in unsteady flow separation
[AD-A203733] N89-20428
Boundary layer structure and dynamics in outer hurricane rainbands N89-20583
BOUNDARY VALUE PROBLEMS
Numerical method of applying mean value theorem
[PB89-111447] N89-20714
An efficient method for solving free-boundary problems
[REPT-88-63] N89-20727
The use of smoothing techniques in the method of lines
[CWI-NM-R8802] N89-20740
Combined algorithms in nonlinear problems of magnetostatics
[DE89-006591] N89-20753
The initial value problem for fractional order differential equations with constant coefficients
[AD-A203843] N89-20764
BOXES (CONTAINERS)
Design and implementation of the hazard control box for the ride motion simulator
[AD-A203752] N89-20404
BRANCHING (MATHEMATICS)
Toward a quasi-periodic bifurcation theory --- dynamical systems
[ZW-8803] N89-20736
BRASSES
Analysis of brass alloys by wavelength dispersive X-ray spectrometry
[DE89-007595] N89-20243
BREADBOARD MODELS
Breadboard test-software and wrist joint modeling for Hermes robot arm
[ETN-89-94155] N89-20475
BREMSSTRAHLUNG
Bremsstrahlung radiation effects in rare earth permanent magnets
[DE89-006207] N89-20775
BRIDGMAN METHOD
The influences of convection on directional solidification of eutectic Bi/MnBi N89-20303
BRIGHTNESS DISTRIBUTION
Isophotometry of brightest elliptical galaxies in rich clusters N89-20879
BRIGHTNESS TEMPERATURE
Investigation of extensions to the distorted Born approximation in strong fluctuation theory
[AD-A203698] N89-20378
Aperture synthesis observations of solar and stellar radio emission N89-20912
BRITTLE MATERIALS
Reliability-based failure analysis of brittle materials
[NASA-CR-184799] N89-20489
BROADBAND
The wideband plasma wave interaction --- Cluster mission N89-20163
BROKEN SYMMETRY
On particle antiparticle mirror symmetry
[USIP-88-06] N89-20786
BUBBLES
Fluoride glass: Crystallization, surface tension N89-20306
Numerical study of nonlinear wave interactions in bubbly two-phase flow
[REPT-88-50] N89-20418
BUCKLING
Elastic stability of lap-jointed cylindrical shells under axial compression
[PB88-245980] N89-20497
Experiments on the buckling of thin-walled model silo structures
[PB89-125124] N89-20503
Tripping of asymmetrical stiffeners under combined loading
[PB89-126171] N89-20504
Postbuckling Finite Element (FE) analysis of a stiffened curved panel loaded in shear
[FFA-TN-1988-23] N89-20516
BUOYANCY
A comparative study of the influence of buoyancy driven fluid flow on GaAs crystal growth N89-20295
Droplet combustion at reduced gravity N89-20313
Relationship of wind shear, buoyancy and radar tops to severe weather, 1988
[PB89-122519] N89-20581
BURNERS
Radiative heat transfer augmentation in high temperature combustion systems with application to radiant tube burners
[PB89-133805] N89-20217
BUTTERFLY VALVES
Noise generated by a flight weight, air flow control valve in a vertical takeoff and landing aircraft thrust vectoring system
[NASA-CR-182232] N89-20776

C

C (PROGRAMMING LANGUAGE)
The DoD Gateway Information System (DGIS): The development toward artificial intelligence and hypermedia in common command language
[AD-A203674] N89-20869
C BAND
Cross-guide coupler modeling and design N89-20337
CALIBRATING
Position error calibration of a pressure survey aircraft using a trailing cone
[PB88-250733] N89-20092
The magnetic field investigation on Cluster N89-20158
Improved capabilities of the Multispectral Atmospheric Mapping Sensor (MAMS)
[NASA-TM-100352] N89-20430
The 1987 year end report for road following at Canegie Mellon
[AD-A203946] N89-20488
Cavity ringdown measurements of high-reflection mirrors at 1.06 microns
[DE89-006512] N89-20797
CALORIMETERS
On the performance of the DELPHI hadron calorimeter
[PH-159] N89-20434
CAMERAS
Real-time part position sensing
[AD-A203580] N89-20439
Development of a remote inspection robot and camera positioners for reactor tank inspection
[DE89-004381] N89-20478
CANOPIES
High Reynolds number incompressible flow simulation about parachute canopies and similar bluff bodies N89-20096
CAPACITANCE
The influence of surface capacitance on the measurements of localized corrosion transients
[DE89-006172] N89-20391
New type of capacitive temperature sensor for use at low temperature and in strong magnetic field
[PB89-111108] N89-20431
CAPILLARY FLOW
Surface tension driven convection experiment N89-20314
CARBON
Water adsorption equilibria on microporous carbons
[AD-A203536] N89-20220
Hardness of amorphous hard carbon films determined by the ultra-low load microindentation technique
[DE89-006129] N89-20259
CARBON DIOXIDE
Scenarios for future climate change: Results of GCM (General Circulation Model) simulations
[DE89-006151] N89-20565
CARBON DIOXIDE LASERS
Current status of the NAVSEA Backscatter Absorption Gas Imaging (BAGI) development project
[DE89-006728] N89-20438
CARBON FIBER REINFORCED PLASTICS
Paint tests on laminated material formed by carbon fiber composites and Tedlar layers
[I-279/88] N89-20208
CARBON MONOXIDE
3CPO, Cloud Chemistry and Cloud Physics Organization: Data index, June 1988
[DE89-007011] N89-20591
Carbon monoxide and disequilibrium dynamics in Saturn and Jupiter N89-20903
CARBON STARS
Mixing and nucleosynthesis in low- and intermediate-mass AGB stars N89-20892
CARRIER TO NOISE RATIOS
High-dynamic GPS tracking
[NASA-CR-184668] N89-20113
CARTESIAN COORDINATES
Trajectory scoring in rectangular coordinates using transponder-interrogator range and range rate data
[DE89-007005] N89-20119
CASCADE FLOW
Experimental investigation of transonic oscillating cascade aerodynamics
[NASA-TM-101993] N89-20133
CASTING
Casting And Solidification Technology (CAST): Directional solidification phenomena in a metal model at reduced gravity N89-20301
CATACLYSMIC VARIABLES
Aperture synthesis observations of solar and stellar radio emission N89-20912
CATHOLYTES
Screening study of lithiated catholyte mixes for a long-life Li(Si)/FeS2 thermal battery
[DE89-006857] N89-20393
CAUCHY PROBLEM
Analysis of regularized Navier-Stokes equations, 2
[NASA-CR-181801] N89-20716
CAVITATION FLOW
Control-volume based Navier-Stokes equation solver valid at all flow velocities
[NASA-TM-101488] N89-20407
CAVITIES
Cavity ringdown measurements of high-reflection mirrors at 1.06 microns
[DE89-006512] N89-20797
CEILINGS (METEOROLOGY)
Summary of meteorological observations, surface (SMOS) for Norfolk, Virginia
[AD-A203644] N89-20594
CELL DIVISION
Hydrodynamic effects on cell growth in agitated microcarrier bioreactors N89-20284
CELLS (BIOLOGY)
Demixing kinetics of phase separated polymer solutions in microgravity N89-20281
Shear stress induced stimulation of mammalian cell metabolism N89-20286
Human cell culture in a space bioreactor N89-20288
Cellular effects of microgravity N89-20289
Antibody enhancement of free-flow electrophoresis N89-20290
The stress response system of proteins: Implications for bioreactor scaleup N89-20291
Using depth recovery in humans
[AD-A201278] N89-20606
CENSORED DATA (MATHEMATICS)
Censoring, truncation and filtering in statistical models based on counting processes
[CWI-MS-R8803] N89-20769
CENTRIFUGAL FORCE
Flow visualization of time-varying structural characteristics of dean vortices in a curved channel
[AD-A203875] N89-20429
CERAMIC FIBERS
Static tensile and tensile creep testing of five ceramic fibers at elevated temperatures
[NASA-CR-184690] N89-20200
CERAMIC MATRIX COMPOSITES
Nondestructive evaluation of advanced ceramics
[NASA-TM-101489] N89-20490
CERAMICS
Life modeling of thermal barrier coatings for aircraft gas turbine engines N89-20143

Anion controlled microstructures in the Al2O3-AlN system
[AD-A203671] N89-20209
Radiative heat transfer augmentation in high temperature combustion systems with application to radiant tube burners
[PB89-133805] N89-20217
Experiments with metallic and ceramic porous media
[NASA-CR-184819] N89-20248
Long term lubrication of ceramics at high temperatures N89-20249
Environmental effects on the time dependent failure of non-oxide ceramics
[AD-A202391] N89-20250
Design, development and applications of novel techniques for studying surface mechanical properties
[NASA-TM-101959] N89-20253
The influence of thickness and wavelength on the mechanical properties of a compositionally modulated ceramic thin film
[DE89-006033] N89-20258
Nucleation of superconductivity in ceramic oxides
[DE88-705364] N89-20263
A comprehensive review of modeling of impact damage in ceramics
[AD-A203477] N89-20264
Sulfide and phosphide analogs of oxynitride ceramics
[AD-A203805] N89-20269
Microgravity Science and Applications Flight Programs, January - March 1987, selected papers, volume 2
[NASA-TM-4069-VOL-2] N89-20305
New type of capacitive temperature sensor for use at low temperature and in strong magnetic field
[PB89-111108] N89-20431
Influence of lubrication on ceramic and steel sliding contacts
[PB89-125090] N89-20467
Nondestructive evaluation of advanced ceramics
[NASA-TM-101489] N89-20490

CERENKOV RADIATION
The Cerenkov free-electron laser
[AD-A203531] N89-20464

CERMETS
Structure-property characterization of a shock-loaded boron carbide-aluminum cermet
[DE89-005455] N89-20257

CHALCOGENIDES
Fluorine as an oxidant in combustion calorimetry
[DE89-003626] N89-20214

CHANNEL FLOW
Resolution requirements for numerical simulations of transition
[NASA-CR-181799] N89-20411
Fortran codes for computing the space-time correlations of turbulent flow in a channel
[AD-A203749] N89-20678

CHANNELS (DATA TRANSMISSION)
A communication channel model of the software process
[NASA-CR-184866] N89-20643

CHARACTER RECOGNITION
Current status of Japanese to English machine translation: Report to Congress
[PB89-128276] N89-20863

CHARACTERIZATION
Theoretical comparison of maser materials for a 32-GHz maser amplifier N89-20335
On 32-GHz cryogenically cooled HEMT low-noise amplifiers N89-20336
Microstructural characterization of alpha-Al2O3 implanted with iron
[DE89-006037] N89-20817
Publications of the Observatory of the University of Michigan. Volume 12, no. 2: Wavelength identifications in the magnetic CP star HR 4816 (HD 110066) N89-20876

CHARGE CARRIERS
Carrier density and excitation energy dependent GAMMA-X photoluminescence of Type-II GaAs/AlAs superlattices
[DE89-002988] N89-20832

CHARGE COUPLED DEVICES
Forbidden coronal iron line emission in the Puppis A shock front: The effect of inhomogeneities
[NASA-TM-89284] N89-20875

CHARGE EXCHANGE
Energy conversion processes based on molecular excited states
[DE89-007322] N89-20555

CHARM (PARTICLE PHYSICS)
Production of D, D* and Ds mesons in 200 GeV/c pi(-), K(-) and p-Si interactions
[MPI-PAE/EXP-EL-192] N89-20785

CHEMICAL COMPOSITION
Compositional effects on processing and properties of nickel aluminides
[DE89-005133] N89-20229
In-situ HVEM studies of the early stages of oxidation of nickel and nickel-chromium alloys
[DE89-005833] N89-20230
The role of composition and microstructure gradients on weld metal properties and behavior
[DE89-006789] N89-20235
Exploratory alloy development in the system Al-Sc-X
[DE89-007088] N89-20237
Analysis of brass alloys by wavelength dispersive X-ray spectrometry
[DE89-007595] N89-20243
Screening study of lithiated catholyte mixes for a long-life Li(Si)/FeS2 thermal battery
[DE89-006857] N89-20393
Studies of alternative-crystallization-phase nucleation
[DE89-007220] N89-20840

CHEMICAL EXPLOSIONS
Time resolved study of light emitted by detonation arrival at the surface of high explosives in various environments
[DE89-005657] N89-20414

CHEMICAL PROPULSION
Two designs for an orbital transfer vehicle. Project Orion: A proposal for a manned orbital transfer vehicle for the 21st Century
[NASA-CR-184697] N89-20176

CHEMICAL REACTIONS
New approaches to fluorocarbon synthesis
[AD-A203641] N89-20221
Vortex-transport element simulation of a confined mixing layer
[AD-A203791] N89-20222
The application of statistical experimental design to the development of low-density polymer foams
[DE89-006774] N89-20261

CHEMISORPTION
Feasibility of a complex compound heat pump
[PB89-115273] N89-20405

CHIPS (ELECTRONICS)
Very High Speed Integrated Circuits (VHSIC). Phase 2: Submicrometer technology development, interoperability standards
[AD-A203629] N89-20401

CHLOROPHYLLS
Mechanisms of photochemical energy conversion by chlorophyll
[DE89-006820] N89-20550

CHROMIUM ALLOYS
In-situ HVEM studies of the early stages of oxidation of nickel and nickel-chromium alloys
[DE89-005833] N89-20230
Corrosion fatigue of iron-chronium nickel alloys: Fracture mechanics and chemistry
[DE89-006985] N89-20236

CHROMIUM OXIDES
Anion grain boundary diffusion in Cr2O3 and Cr2O3-0.09 weight percent Y2O3
[DE89-006281] N89-20833

CIRCUITS
Testing of time domain simulators for nonlinear electronic circuits
[PB89-125132] N89-20384
Impedance matching of RF plasma
[PB89-112502] N89-20804

CIRCULAR WAVEGUIDES
Modal analysis applied to circular, rectangular, and coaxial waveguides N89-20338
Complex-valued functionals in variational analysis of waveguides with impedance boundaries
[PB89-128896] N89-20361

CIVIL AVIATION
Aircraft accident reports: Brief format, US civil and foreign aviation, issue number 12 of 1986 accidents
[PB88-916902] N89-20109
Aircraft accident reports, brief format, US civil and foreign aviation, issue number 14 of 1986 accidents
[PB88-916904] N89-20110
Electronics in civil aviation
[NLR-MP-87009-U] N89-20129

CLASSIFICATIONS
Active and passive remote sensing of ice
[AD-A203943] N89-20543
Combining segmentation and tracking for the classification of moving objects in video scenes
[DE89-007000] N89-20668
Arithmetic classification of perfect models of stratified programs
[CWI-CS-R8810] N89-20737

CLIMATE
The Mars climate for a photovoltaic system operation
[NASA-TM-101994] N89-20385
Generation of CCM format history tapes from analyzed data for selected periods (RD2CFM version 01)
[PB89-124507] N89-20568
Report of the 2nd Workshop on the Community Climate Model
[PB88-250741] N89-20576
Verification of regional climates of GISS GCM. Part 2: Summer
[NASA-TM-100722] N89-20589
Climate fundamentals for solar energy systems
[DE89-007319] N89-20592

CLIMATE CHANGE
The causes and consequences of global climate change
[DE89-004355] N89-20564

CLIMATOLOGY
The causes and consequences of global climate change
[DE89-004355] N89-20564
Generation of CCM format history tapes from analyzed data for selected periods (RD2CFM version 01)
[PB89-124507] N89-20568
Report of the 2nd Workshop on the Community Climate Model
[PB88-250741] N89-20576
Utility of a geographic information system in modelling climatic suitability
[PB89-109516] N89-20578
Climatological Worksheet Program
[PB89-122527] N89-20579
Examination of NGM (Nested Grid Model) low level temperature
[PB89-122543] N89-20580
National Weather Service Philadelphia Forecast Office, 1987 NOAA (National Oceanic and Atmospheric Administration) weather radio survey and questionnaire
[PB89-111785] N89-20582
Verification of regional climates of GISS GCM. Part 2: Summer
[NASA-TM-100722] N89-20589
Current velocity and hydrographic observations in the southwestern North Atlantic Ocean: Subtropical Atlantic Climate Studies (SACS), 1987
[PB89-114011] N89-20598

CLOSED ECOLOGICAL SYSTEMS
Nutritional models for a Controlled Ecological Life Support System (CELSS): Linear mathematical modeling
[NASA-CR-4229] N89-20615

CLOUD COVER
Twelve year overview of cloudfree LANDSAT imagery of The Netherlands
[NLR-MP-87072-U] N89-20542
Radiation, turbulence and microphysics in the stratiform regions of tropical cloud clusters N89-20585

CLOUD PHYSICS
NOAA (National Oceanic and Atmospheric Administration) X-band radar measurements in 3CPO (Cloud Chemistry Cloud Physics Organization)
[PB89-127823] N89-20562
3CPO, Cloud Chemistry and Cloud Physics Organization: Data index, June 1988
[DE89-007011] N89-20591

CLOUDS
Particle cloud mixing in microgravity
[NASA-TM-101484] N89-20321

CLOUDS (METEOROLOGY)
Twelve year overview of cloudfree LANDSAT imagery of The Netherlands
[NLR-MP-87072-U] N89-20542

CLUMPS
Defect clustering and related properties of oxides
[DE89-006620] N89-20835

CMOS
Test of radiation hardness of CMOS transistors under neutron irradiation
[DE89-006511] N89-20392

COALESCING
A stereological analysis of ductile fracture by microvoid coalescence
[DE89-000355] N89-20528

COASTAL WATER
Utilizing remote sensing of thematic mapper data to improve our understanding of estuarine processes and their influence on the productivity of estuarine-dependent fisheries
[NASA-CR-183417] N89-20533

CODE DIVISION MULTIPLE ACCESS
Dedicated versus half-duplex receiver topology in jammed, fully connected CDMA networks: Theory and numerical comparisons
[AD-A203635] N89-20402

CODING
Long decoding runs for Galileo's convolutional codes N89-20342

Implementation of a language translator for the computer aided prototyping system
[AD-A203876] N89-20680

COGNITION
The power of physical representations
[CWI-CS-R8819] N89-20612

COGNITIVE PSYCHOLOGY
Cognitive psychology at the Institute for Perception
[IZF-1987-41] N89-20611

COHERENT LIGHT
Proposed extended tuning range for the Los Alamos mid-infrared adjustable, coherent light experiment (MIRACLE) facility
[DE89-006550] N89-20798

COLD PLASMAS
Cluster: A fleet of four spacecraft to study plasma structures in three dimensions N89-20157

COLD WEATHER TESTS
Why cold-wet makes one feel chilled: A literature review
[AD-A203452] N89-20609

COLLISION AVOIDANCE
Improved computer simulation of the TCAS 3 circular array mounted on an aircraft
[NASA-CR-184907] N89-20363

COLLISION PARAMETERS
On the performance of the DELPHI hadron calorimeter
[PH-159] N89-20434

COLLISIONS
Pseudo-Bayesian stability of CSMA (Carrier Sense Multiple Access) and CSMA/CD (Collision Detection) local area networks
[AD-A203834] N89-20763

COLLOCATION
Domain decomposition methods for systems of conservation laws: Spectral collocation approximations
[NASA-CR-181773] N89-20635

COLUMNS (SUPPORTS)
Compression tests of welded channel section columns
[PB88-246020] N89-20496

COMBINED STRESS
Non-symmetric bifurcation of geometrically non-linear elastic-plastic axisymmetric shells under combined loads including torsion
[PB89-102149] N89-20500

COMBUSTIBLE FLOW
Particle cloud mixing in microgravity
[NASA-TM-101484] N89-20321

COMBUSTION
Radiative heat transfer augmentation in high temperature combustion systems with application to radiant tube burners
[PB89-133805] N89-20217
Flow visualization of time-varying structural characteristics of dean vortices in a curved channel
[AD-A203875] N89-20429

COMBUSTION CHAMBERS
Assessment, development, and application of combustor aerothermal models N89-20138
Structural analysis applications N89-20141
Development of a rotary valve for pulse combustion applications
[PB89-131114] N89-20468

COMBUSTION CONTROL
Vortex-transport element simulation of a confined mixing layer
[AD-A203791] N89-20222

COMBUSTION EFFICIENCY
Assessment, development, and application of combustor aerothermal models N89-20138
Design and testing of a dissociated methanol vehicle
[DE89-007051] N89-20483

COMBUSTION PHYSICS
Microgravity Science and Applications Flight Programs, January - March 1987, selected papers, volume 2
[NASA-TM-4089-VOL-2] N89-20305

COMFORT
Safe working time limits in impermeable protective clothing: Recommendations based upon experimental measurements
[IZF-1987-28] N89-20618

COMMUNICATION
The Telecommunications and Data Acquisition Report
[NASA-CR-184672] N89-20329
Symbols for communication circuit design and documentation
[DE88-013002] N89-20372
Barriers to the international transfer of information in aerospace and defense N89-20861

COMMUNICATION NETWORKS
Review of network planning methods applicable to Integrated Satellite Terrestrial Networks (ISTN)
[ESA-CR(P)-2691] N89-20185
Conceptual study of the signalling point of the master station for a TST/SS-TDMA system. Phase 1: Overview and selection of signalling points
[SX/SP-01] N89-20360
Digital signal processing
[AD-A203744] N89-20403

COMMUNICATION SATELLITES
Assessing potential benefits for service/repair and retrieval of satellites: A pilot decision analysis
[AD-A203830] N89-20190
Suitability of ANSI standards for quantifying communication satellite system performance
[NASA-CR-182884] N89-20356

COMPARISON
High-dynamic GPS tracking
[NASA-CR-184868] N89-20113

COMPLEX COMPOUNDS
Feasibility of a complex compound heat pump
[PB89-115273] N89-20405

COMPLEXITY
Two decades of applied Kolmogorov complexity. In memoriam: Andrei Nikolaevich Kolmogorov, 1903 - 1987
[CWI-CS-R8813] N89-20767

COMPOSITE MATERIALS
A (13)C NMR analysis of the effects of electron radiation on graphite/polyetherimide composites
[NASA-CR-182818] N89-20205
Instrumented impact testing of composite materials
[AD-A203842] N89-20210
The effect of deformation history on the morphology and properties of blends of polycarbonate and a thermotropic liquid crystalline polymers
[AD-A203632] N89-20267

COMPOSITE STRUCTURES
Prediction model for the onset of edge-effect delamination at holes in composite laminates N89-20202

COMPRESSIBLE BOUNDARY LAYER
A calculation method for compressible three dimensional turbulent boundary layer flows
[VKI-TN-167] N89-20422

COMPRESSION LOADS
Reliability-based failure analysis of brittle materials
[NASA-CR-184799] N89-20489
Compression tests of welded channel section columns
[PB88-246020] N89-20496
Elastic stability of lap-jointed cylindrical shells under axial compression
[PB88-245980] N89-20497

COMPRESSION TESTS
Compression tests of welded channel section columns
[PB88-246020] N89-20496

COMPRESSIVE STRENGTH
Instrumented impact testing of composite materials
[AD-A203842] N89-20210
Reliability-based failure analysis of brittle materials
[NASA-CR-184799] N89-20489
Compression tests of welded channel section columns
[PB88-246020] N89-20496
Elastic stability of cylindrical shells with circumferential welded joints under axial compression
[PB89-125082] N89-20502
Experiments on the buckling of thin-walled model silo structures
[PB89-125124] N89-20503

COMPRESSORS
An analytical and numerical study of axial flow compressor instability N89-20131
Transmission and reflection on pressure waves by compressor and turbine stages, based on an actuator-disk model
[AD-A203513] N89-20426

COMPTON EFFECT
The development of a Compton lung densitometer
[DE89-006654] N89-20603

COMPUTATION
Unmanned, space-based, reusable orbital transfer vehicle, DARVES. Volume 2: Data and calculations
[NASA-CR-184712] N89-20174
Diffusive burning of plane liquid and spray jets in a coflowing oxidizer stream N89-20216
Evaluation of the Kubo formula for the conductivity using the recursion method
[DE88-705359] N89-20396
Intelligence in scientific computing
[AD-A203815] N89-20679

COMPUTATIONAL FLUID DYNAMICS
Development and application of a program to calculate transonic flow around an oscillating three-dimensional wing using finite difference procedures
[NASA-CR-181744] N89-20093
A cell-vertex multigrid method for the Navier-Stokes equations
[NASA-TM-101557] N89-20101
Assessment, development, and application of combustor aerothermal models N89-20138
Standard test case for a low speed, turbulent junction vortex flow
[PB89-110779] N89-20406
Computational fluid dynamics and aerothermodynamics
[NASA-CR-180079] N89-20415
La Recherche Aerospatiale, bimonthly bulletin, number 1988-2, 243/January-February
[ESA-TT-1134] N89-20417
Differential equations of viscous fluid flow in general conditions
[REPT-88-57] N89-20419
Quasi-classical calculations for superfluids
[ETN-89-94118] N89-20421
Cumulative reports and publications through December 31, 1988
[NASA-CR-181784] N89-20619
Spectral methods for CFD
[NASA-CR-181803] N89-20718
Who's afraid of nonsymmetric matrices? A discussion of elementary iterative methods
[REPT-88-49] N89-20723

COMPUTATIONAL GRIDS
Multigrid solution of the Navier-Stokes equations on triangular meshes
[NASA-CR-181786] N89-20095
Differential equations of viscous fluid flow in general conditions
[REPT-88-57] N89-20419
Multigrid and defect correction for the steady Navier-Stokes equation
[CWI-NM-R8803] N89-20424
Examination of NGM (Nested Grid Model) low level temperature
[PB89-122543] N89-20580
A numerical study of three moving grid methods for one-dimensional partial differential equations which are based on the method of lines
[CWI-NM-R8806] N89-20741

COMPUTER AIDED DESIGN
Structural analysis applications N89-20141
Direct manipulation and other styles of man-machine interaction
[REPT-88-53] N89-20616
Tools for the development of information systems at NLR
[NLR-MP-87079-U] N89-20652
Quadratic blending surfaces for complex corners, part 2
[CS-8809-PT-2] N89-20657
Development of the University of Maryland RAMCAD (Reliability and Maintainability Computer-Aided Design) for electronic systems
[AD-A203616] N89-20675
Dynamic mechanical system design using qualitative and symbolic reasoning
[DE89-006771] N89-20706

COMPUTER ASSISTED INSTRUCTION
Human-computer interaction in distributed supervisory control tasks
[NASA-CR-184671] N89-20692
OFMTutor: An operator function model intelligent tutoring system N89-20696
A survey of intelligent tutoring systems: Implications for complex dynamic systems N89-20697

COMPUTER DESIGN
The Delft Ising system processor
[ISBN-9-09-001753-4] N89-20625

COMPUTER GRAPHICS
User's manual for DYNA2D: An explicit two-dimensional hydrodynamic finite element code with interactive rezoning and graphical display
[DE89-006695] N89-20647
Incremental display of Constructive Solid Geometry (CSG) models using local updating
[REPT-88-51] N89-20650
Quadratic blending surfaces for complex corners, part 2
[CS-8809-PT-2] N89-20657
A vector-like architecture for raster graphics
[CWI-CS-R8802] N89-20660
An exact incremental hidden surface removal algorithm
[CWI-CS-R8818] N89-20663
An algorithm for automated quadrilateral mesh generation for planar regions
[DE89-007299] N89-20671
The use of GKS (Graphical Kernel System) and CGM (Computer Graphics Metafile) for the display of graphics products
[DE89-006734] N89-20673

COMPUTER INFORMATION SECURITY
Activities report of the Division of Information Systems
[FOA-C-30499-3.3] N89-20919

COMPUTER NETWORKS
Performance evaluation and analytic modeling of shared-memory computers
[PB89-113542] N89-20621
Automating the multiprocessing environment
[NASA-TM-4103] N89-20641
COMPUTER PROGRAMMING
Transmitter data collection using Ada N89-20352
Cross-coordinated control: An experimentally verified technique for the hybrid twist and wrench control of a voltage-controlled industrial robot
[AD-A203406] N89-20486
Report of the Documentation Advisory Committee
[PB89-124556] N89-20569
Climatological Worksheet Program
[PB89-122527] N89-20579
Direct manipulation and other styles of man-machine interaction
[REPT-88-53] N89-20616
Automating the multiprocessing environment
[NASA-TM-4103] N89-20641
A communication channel model of the software process
[NASA-CR-184866] N89-20643
Fastbus standard routines
[DOE/ER-0367] N89-20645
Incremental display of Constructive Solid Geometry (CSG) models using local updating
[REPT-88-51] N89-20650
Directions in reusing software
[REPT-88-58] N89-20651
Reducing the proof burden when reasoning with congruence types
[CS-8807] N89-20655
Factoring with the quadratic sieve on large vector computers
[CWI-NM-R8805] N89-20664
Implementation of a language translator for the computer aided prototyping system
[AD-A203876] N89-20680
Initial operating capability for the hypercluster parallel-processing test bed
[NASA-TM-101953] N89-20685
HARTFEM: A finite element program for thermal and viscoplastic deformation problems
[DE89-007788] N89-20755
COMPUTER PROGRAMS
Development and application of a program to calculate transonic flow around an oscillating three-dimensional wing using finite difference procedures
[NASA-CR-181744] N89-20093
Evaluation of VSAERO in prediction of aerodynamic characteristics of helicopter hub fairings
[NASA-TM-101048] N89-20098
Space shuttle propulsion estimation development verification
[NASA-CR-183582] N89-20195
Space shuttle propulsion estimation development verification, volume 1
[NASA-CR-183581] N89-20197
The dynamic response at high-explosive inert-solid interface as predicted by finite difference/element computer programs
[DE89-007303] N89-20272
The Telecommunications and Data Acquisition Report
[NASA-CR-184672] N89-20329
Modal analysis applied to circular, rectangular, and coaxial waveguides N89-20338
A long constraint length VLSI Viterbi decoder for the DSN N89-20341
A preliminary weather model for optical communications through the atmosphere N89-20350
SAR processing on the array processor NMX-432
[FOA-C-30503-3.3] N89-20367
Modeling the behavior of pulsed, high power microwave antenna systems
[DE89-006280] N89-20374
A relativistic fluid code for high-power microwave propagation
[DE89-006598] N89-20375
Updated users' guide for TAWFIVE with multigrid
[NASA-TM-4109] N89-20409
Tripping of asymmetrical stiffeners under combined loading
[PB89-126171] N89-20504
The investigation of advanced remote sensing, radiative transfer and inversion techniques for the measurement of atmospheric constituents
[NASA-CR-172599] N89-20531
Generation of CCM format history tapes from analyzed data for selected periods (RD2CFM version 01)
[PB89-124507] N89-20568
Report of the Documentation Advisory Committee
[PB89-124556] N89-20569
Climatological Worksheet Program
[PB89-122527] N89-20579
Long-range forecasting of storminess over the Northern Hemisphere oceans
[AD-A203949] N89-20595
Software reliability engineering
[DE89-006781] N89-20626
Symbolic inversion of control relationships in model-based expert systems
[NASA-CR-182857] N89-20631
Hypercube matrix computation task
[NASA-CR-184869] N89-20642
Incremental development and prototyping in current laboratory software development projects: Preliminary analysis
[NASA-CR-184860] N89-20644
Fortran codes for computing the space-time correlations of turbulent flow in a channel
[AD-A203749] N89-20678
Parallel algorithms for computer vision
[AD-A203947] N89-20681
An operating environment for the jellybean machine
[AD-A201042] N89-20682
A message passing kernel for the hypercluster parallel processing test bed
[NASA-TM-101952] N89-20684
Gain selection for an independent joing MRAC (Model-Reference Adaptive Controller) for robotic manipulators
[DE89-005110] N89-20705
SLAP (Sparse Linear Algebra Package) for the masses
[DE89-006209] N89-20721
Development of mathematical models for application in image processing
[AD-A203619] N89-20760
Star formation, using 3-D explicit Eulerian hydrodynamics N89-20890
COMPUTER STORAGE DEVICES
Performance evaluation and analytic modeling of shared-memory computers
[PB89-113542] N89-20621
A class Hierarchical, object-oriented approach to virtual memory management
[NASA-CR-184876] N89-20646
Valiant's maximum algorithm with sequential memory accesses
[AD-A203713] N89-20676
An operating environment for the jellybean machine
[AD-A201042] N89-20682
COMPUTER SYSTEMS DESIGN
Applying expertise to data in the Geologist's Assistant expert system
[DE89-003463] N89-20574
Adaptive data compression system study --- scientific satellite
[SIL/CR/7129/6] N89-20639
Tools for the development of information systems at NLR
[NLR-MP-87079-U] N89-20652
Adaptive data compression system study, executive summary --- scientific satellite
[SIL/CR/7129/7] N89-20867
Activities report of the Division of Information Systems
[FOA-C-30499-3.3] N89-20919
COMPUTER SYSTEMS PERFORMANCE
Experiences on a CRAY-2 (trade name) running UNICOS
[PB88-250725] N89-20620
Performance evaluation and analytic modeling of shared-memory computers
[PB89-113542] N89-20621
Improvements relating to control flow in computers
[EP-0-234-785-A1] N89-20624
Multiprogramming a distributed-memory multiprocessor
[DE89-007850] N89-20690
Parallel direct solution of sparse linear systems
[DE89-007855] N89-20757
COMPUTER SYSTEMS PROGRAMS
The application of software fault tolerance to air traffic control: Study contract overview
[BR108567] N89-20114
An algebraic calculus of commands
[CS-8808] N89-20656
Monotonically improving approximate answers to relational algebra queries
[NASA-CR-184874] N89-20717
COMPUTER SYSTEMS SIMULATION
Tools for the development of information systems at NLR
[NLR-MP-87079-U] N89-20652
COMPUTER TECHNIQUES
Structural analysis applications N89-20141
Direct manipulation and other styles of man-machine interaction
[REPT-88-53] N89-20616
Cumulative reports and publications through December 31, 1988
[NASA-CR-181784] N89-20619
Incremental display of Constructive Solid Geometry (CSG) models using local updating
[REPT-88-51] N89-20650
Factoring with the quadratic sieve on large vector computers
[CWI-NM-R8805] N89-20664
A software model for simulation in computer-based training
[DE89-003469] N89-20665
Implementation of a language translator for the computer aided prototyping system
[AD-A203876] N89-20680
Queuing theory models for computer networks
[NASA-TM-101056] N89-20770
Research in distributed personal computer-based information systems, volume 2
[AD-A203845] N89-20870
COMPUTER VISION
Vision-based navigation for autonomous ground vehicles
[AD-A203712] N89-20120
Development of an integrated mobile robot system at CMU (Carnegie Mellon University), June 1987
[AD-A203689] N89-20487
Parallel algorithms for computer vision
[AD-A203947] N89-20681
A concurrent approach to model based motion detection
[DE89-007853] N89-20708
Activities report of the Division of Information Systems
[FOA-C-30499-3.3] N89-20919
COMPUTERIZED SIMULATION
System simulation using the PROMISE simulation package
[NLR-MP-87081-U] N89-20118
A definition study of the on-orbit assembly operations for the outboard photovoltaic power modules for Space Station Freedom
[NASA-TM-102006] N89-20171
Welded joint integrity analysis: Relative criticality of weld defect and remote deformation
[AD-A203756] N89-20246
Finite element modeling of a hydroformed sheet metal cover
[DE89-006798] N89-20326
Dynamic models for simulation of the 70-M antenna axis servos N89-20333
A new algorithm for modeling friction in dynamic mechanical systems N89-20334
An extended Kalman filter based automatic frequency control loop N89-20351
A study of EMI-endurance of two polling-type local area networks used in real-time automation applications in a simulated electrical environment
[EL-62] N89-20366
Modeling the behavior of pulsed, high power microwave antenna systems
[DE89-006280] N89-20374
A comparison of frequency estimation techniques for high-dynamic trajectories
[NASA-CR-184865] N89-20387
Bunch beam production and microwave generation in reditrons
[DE89-006530] N89-20397
Zeolite/methanol: The adsorption heat pump
[DE88-756310] N89-20413
Numerical simulation of turbulent mixing in shock-tube experiments
[DE89-005101] N89-20425
Simulation of superradiant free-electron lasers
[DE89-006156] N89-20451
Breadboard test-software and wrist joint modeling for Hermes robot arm
[ETN-89-94155] N89-20475
Edge illuminated ventical multijunction
[DE89-006246] N89-20547
Applying expertise to data in the Geologist's Assistant expert system
[DE89-003463] N89-20574
Verification of regional climates of GISS GCM. Part 2: Summer
[NASA-TM-100722] N89-20589
Componential analysis of pilot decision making
[AD-A203711] N89-20613
A software model for simulation in computer-based training
[DE89-003469] N89-20665
Multifractals
[DE88-705369] N89-20672
The use of GKS (Graphical Kernel System) and CGM (Computer Graphics Metafile) for the display of graphics products
[DE89-006734] N89-20673

Compensation for crystal penetration in high resolution positron tomography
[DE89-006660] N89-20836
Geological data integration techniques: Proceedings
[DE88-705255] N89-20666
Measurement of the cosmic ray iron spectrum above 60 GeV/n and design and calibration of a large isotopic compositional experiment N89-20915

CONCATENATED CODES
VLA telemetry performance with concatenated coding for Voyager at Neptune N89-20340
Performance of Galileo's concatenated codes with nonideal interleaving N89-20343

CONCRETES
Methods and materials for reducing crack reflectance
[PB89-114532] N89-20505

CONCURRENT PROCESSING
System simulation using the PROMISE simulation package
[NLR-MP-87061-U] N89-20118
An explicit finite differences solver for the incompressible Reynolds averaged Navier-Stokes equations, optimized for the Alliant DSP 9000 computer
[VKI-TM-45] N89-20423
Metric semantics for concurrency
[CWI-CS-R8803] N89-20661
The algebra of synchronous processes
[CWI-CS-R8807] N89-20687
A compositional semantics for Concurrent Prolog
[CWI-CS-R8809] N89-20688
A concurrent approach to model based motion detection
[DE89-007853] N89-20708

CONDENSING
Condensation and storage of hydrogen cluster ions
[AD-A203801] N89-20223

CONDUCTIVE HEAT TRANSFER
Numerical studies of identification in nonlinear distributed parameter systems
[NASA-CR-181771] N89-20636

CONES
Position error calibration of a pressure survey aircraft using a trailing cone
[PB88-250733] N89-20092

CONFERENCES
Toward improved durability in advanced aircraft engine hot sections
[NASA-TM-4087] N89-20135
Microgravity Science and Applications Flight Programs, January - March 1987, selected papers, volume 2
[NASA-TM-4069-VOL-2] N89-20305
Workshop on Transient Induced Insulator Flashover in Vacuum
[DE89-006727] N89-20398
Report of the 2nd Workshop on the Community Climate Model
[PB88-250741] N89-20576

CONFIDENCE LIMITS
DETECT: Dependency tree evaluation and confidence test
[REPT-88-55] N89-20765

CONFINEMENT
Vortex-transport element simulation of a confined mixing layer
[AD-A203791] N89-20222

CONFORMAL MAPPING
Realization and generalized frequency response for nonlinear input-output maps
[RR-336] N89-20732

CONGRESSIONAL REPORTS
Current status of Japanese to English machine translation: Report to Congress
[PB89-128276] N89-20863
NASA authorization
[S-HRG-100-579] N89-20873

CONGRUENCES
Reducing the proof burden when reasoning with congruence types
[CS-8807] N89-20655

CONSERVATION LAWS
Domain decomposition methods for systems of conservation laws: Spectral collocation approximations
[NASA-CR-181773] N89-20635

CONSTITUTIVE EQUATIONS
Theoretical modelling and experimental characterization of flexible composites under finite deformation N89-20204
Analysis of the strain-rate sensitivity at high strain rates in fcc and bcc metals
[DE89-005471] N89-20233
A numerical implementation of the Schapery model for nonlinear viscoelasticity
[ETN-89-93895] N89-20515

CONSTRUCTION
Engineering and technical efforts to design and construct a 10 MW gyrotron laboratory
[AD-A203851] N89-20155

CONSUMABLES (SPACECRAFT)
Superfluid Helium Tanker (SFHT) study
[NASA-CR-172110] N89-20182

CONTAINERLESS MELTS
Containerless processing of glass forming melts in space N89-20307
Acoustic containerless experiment system: A non-contact surface tension measurement N89-20308
Physical phenomena in containerless glass processing N89-20310

CONTAMINANTS
Modeling of hydrogen-air diffusion flame
[NASA-CR-184844] N89-20218

CONTINENTAL SHELVES
Biological processes in the water column of the South Atlantic Bight: Zooplankton responses
[DE89-006828] N89-20600

CONTINUUM MODELING
An analysis of an incompressible, fiber-reinforced material subjected to finite strains in the direction of reinforcement N89-20201

CONTRAROTATING PROPELLERS
Unsteady blade pressure measurements on a model counterrotation propeller
[NASA-TM-102002] N89-20779

CONTROL BOARDS
Automatic learning by an autonomous mobile robot
[DE89-003120] N89-20702

CONTROL SIMULATION
Vortex-transport element simulation of a confined mixing layer
[AD-A203791] N89-20222

CONTROL STABILITY
Diagnostics for intelligent control of MPD engines
[AD-A203640] N89-20530

CONTROL SYSTEMS DESIGN
Vision-based navigation for autonomous ground vehicles
[AD-A203712] N89-20120
Modal cost analysis of flexible structures: Modeling flexible structures for control design N89-20148
Modeling and control of flexible structures
[NASA-CR-184862] N89-20152
Design of a three-axis stabilized orion satellite using an all-thruster attitude control system
[AD-A203953] N89-20191
Identification of space shuttle main engine dynamics
[NASA-TM-101982] N89-20199
An expert system based intelligent control scheme for space bioreactors N89-20285
High speed, precision motion strategies for lightweight structures
[NASA-CR-184651] N89-20327
Conceptual study of the signalling point of the master station for a TST/SS-TDMA system. Phase 1: Overview and selection of signalling points
[SX/SP-01] N89-20360
Development of a rotary value for pulse combustion applications
[PB89-131114] N89-20468
Dynamic modeling and linearization for real-time control of a pantograph manipulator N89-20469
Application of parameter adaptive approach to servo control of a hydraulic manipulator
[MA-51] N89-20473
Cross-coordinated control: An experimentally verified technique for the hybrid twist and wrench control of a voltage-controlled industrial robot
[AD-A203406] N89-20486
Development of an integrated mobile robot system at CMU (Carnegie Mellon University), June 1987
[AD-A203689] N89-20487
Optimal feedback control infinite dimensional parabolic evolution systems: Approximation techniques
[NASA-CR-181772] N89-20637
Gain selection for an independent joing MRAC (Model-Reference Adaptive Controller) for robotic manipulators
[DE89-005110] N89-20705

CONTROL THEORY
Active control helicopter aeromechanical and aeroelastic instabilities N89-20149
Design of a three-axis stabilized orion satellite using an all-thruster attitude control system
[AD-A203953] N89-20191
Optimal feedback control infinite dimensional parabolic evolution systems: Approximation techniques
[NASA-CR-181772] N89-20637
Spectral analysis of block structured nonlinear systems
[RR-329] N89-20728

CONTROL VALVES
Power efficient hydraulic systems. Volume 2: Hardware demonstration phase
[AD-A203900] N89-20128

CONTROLLERS
Modeling and control of flexible structures
[NASA-CR-184862] N89-20152

CONVECTION
Vortex-transport element simulation of a confined mixing layer
[AD-A203791] N89-20222
Droplet combustion at reduced gravity N89-20313
Surface tension driven convection experiment N89-20314

CONVECTIVE FLOW
Preparative electrophoresis for space N89-20278
Demixing kinetics of phase separated polymer solutions in microgravity N89-20281
Radiation, turbulence and microphysics in the stratiform regions of tropical cloud clusters N89-20585

CONVERGENCE
Multigrid and defect correction for the steady Navier-Stokes equation
[CWI-NM-R8803] N89-20424
Numerical studies of identification in nonlinear distributed parameter systems
[NASA-CR-181771] N89-20636
Iterative solution of large sparse system of linear equations
[REPT-88-52] N89-20724
Estimating a regression function
[CWI-MS-R8805] N89-20742

COOLING
Dendritic growth and structure of undercooled nickel base alloys N89-20302
Laser diode cooling for high average power applications
[DE89-006777] N89-20454

COPOLYMERS
Photoinduced electron transfer in ordered polymers
[DE89-006986] N89-20254
Energetic thermoplastic elastomer synthesis
[AD-A203594] N89-20265
Synthesis and physical properties of liquid crystalline alkylisocyanate copolymers
[AD-A203631] N89-20266
New vinylidene fluoride copolymers: Poly(vinyl acetate-co-Vinylidene fluoride)
[AD-A203939] N89-20270

COPPER
Constitutive properties of copper and tantalum at high rates of tensile strain: Expanding ring results
[DE89-006197] N89-20242
A first-principles method for the determination of the electronic structure of grain boundaries
[DE89-006148] N89-20845
A study of the effects of copper to superconductor ratio on stability
[DE89-006604] N89-20846

COPPER OXIDES
Some structural features of high-T(sub c) superconductors
[DE89-006667] N89-20826
Thermodynamic characteristics of Y-Ba-Cu-O type compounds in the model of strong electron-phonon coupling
[DE88-705343] N89-20828

CORNERS
Quadratic blending surfaces for complex corners, part 2
[CS-8809-PT-2] N89-20657

CORONAGRAPHS
Integrated analysis package for Mk-3 K-coronameter observations: A user's manual
[PB88-250717] N89-20904

CORONAL HOLES
Aperture synthesis observations of solar and stellar radio emission N89-20912

CORROSION PREVENTION
Environment-assisted aerospace fatigue problems in The Netherlands
[NLR-MP-88004-U] N89-20087

CORROSION RESISTANCE
Glass corrosion in natural environment
[NASA-CR-184843] N89-20251

COSMIC PLASMA
Astrophysical significance of observations and experiments in the Earth's magnetosphere
[TRITA-EPP-88-09] N89-20899

COSMIC RAY SHOWERS
Cosmic ray tracking: A new approach to high energy gamma-astronomy
[HD-PY88/05] N89-20916

COSMIC RAYS
Measurement of the cosmic ray iron spectrum above 60 GeV/n and design and calibration of a large isotopic compositional experiment N89-20915
Meson production and nuclear fragmentation of nucleus in the atmosphere
[DE88-705019] N89-20917
COSMOLOGY
Antipodal universes in the topology S(sup 3)xR and H(sup 3)xR
[DE88-704999] N89-20719
General relativity, scalar fields and cosmic strings N89-20852
Cosmology and superstrings N89-20891
Solutions and stability of a closed-geodesic black hole model N89-20893
Fragmentation of cosmic-string loops
[NASA-CR-184892] N89-20896
Astrophysics in a nutshell: From the telescope to the Sputnik
[TRITA-EPP-88-04] N89-20897
COST ANALYSIS
Modal cost analysis of flexible structures: Modeling flexible structures for control design N89-20148
Space Station: NASA efforts to establish a design-to-life-cycle cost process
[GAO/NSIAD-88-147] N89-20188
Space Science: Status of the Hubble Space Telescope Program
[GAO/NSIAD-88-118BR] N89-20881
COSTS
Commercial potential of European and Japanese space programs, task 5
[NASA-CR-184659] N89-20871
COUNTING
Censoring, truncation and filtering in statistical models based on counting processes
[CWI-MS-R8803] N89-20769
COUPLING
Energy gap in S- and D-wave pairing superconductors
[DE88-705344] N89-20829
COVARIANCE
Analysis of modified SMI method for adaptive array weight control
[NASA-CR-184904] N89-20364
CRACK INITIATION
Fatigue life prediction modeling for turbine hot section materials N89-20142
Analysis of crack opening behavior by application of a discretized strip yield model
[NLR-MP-87065-U] N89-20520
Estimation of the Equivalent Initial Flow Size (EIFS) distribution and prediction of failure probabilities for different parameter variations
[FFA-TN-1987-35] N89-20525
CRACK PROPAGATION
Fatigue life prediction modeling for turbine hot section materials N89-20142
The role of composition and microstructure gradients on weld metal properties and behavior
[DE89-006789] N89-20235
Softening mechanisms and microstructural instabilities during high temperature low cycle fatigue of Ni, Ni3Al and their metal matrix composites
[DE89-007117] N89-20238
Electrochemical considerations of crack growth in the ferrous alloys
[AD-A203811] N89-20247
Environmental effects on the time dependent failure of non-oxide ceramics
[AD-A202391] N89-20250
Analysis of dynamic elastic-plastic fracture phenomena: Steady crack growth and transient loading of a stationary crack N89-20507
Computational studies in nonlinear fracture mechanics N89-20508
Analysis of crack opening behavior by application of a discretized strip yield model
[NLR-MP-87065-U] N89-20520
Current status of flight simulation fatigue crack growth concepts
[NLR-MP-88001-U] N89-20521
Fracture control guidelines for stress corrosion
[NLR-MP-88007-U] N89-20522
Prediction of low and high crack growth rates under constant and variable amplitude loading
[NLR-MP-88012-U] N89-20523
Near threshold fatigue curve based on the dislocation shielding model of fracture
[DE88-011854] N89-20527
Effect of surface stress on stress corrosion of silicate glass
[DE89-004584] N89-20529
CRACKING (FRACTURING)
Reliability-based failure analysis of brittle materials
[NASA-CR-184799] N89-20489
Green's function formulation of plane crack problems for general anisotropic materials N89-20509
Bulging cracks in pressurized fuselages: A numerical study
[NLR-MP-87058-U] N89-20519
Prediction of low and high crack growth rates under constant and variable amplitude loading
[NLR-MP-88012-U] N89-20523
Estimation of the Equivalent Initial Flow Size (EIFS) distribution and prediction of failure probabilities for different parameter variations
[FFA-TN-1987-35] N89-20525
CRACKS
Methods and materials for reducing crack reflectance
[PB89-114532] N89-20505
CRAY COMPUTERS
Experiences on a CRAY-2 (trade name) running UNICOS
[PB88-250725] N89-20620
CREEP ANALYSIS
Computational studies in nonlinear fracture mechanics N89-20508
CREEP PROPERTIES
Compositional effects on processing and properties of nickel aluminides
[DE89-005133] N89-20229
CREEP TESTS
Static tensile and tensile creep testing of five ceramic fibers at elevated temperatures
[NASA-CR-184690] N89-20200
CRITERIA
L1 libration point manned space habitat
[NASA-CR-184732] N89-20180
CRITICAL POINT
Critical fluid light scattering N89-20320
CRITICAL TEMPERATURE
Some structural features of high-T(sub c) superconductors
[DE89-006667] N89-20826
CROP INVENTORIES
Land use inventories using satellite images in the region Haaren-Helvoirt-Udenhout, North Brabant (The Netherlands)
[BCRS-88-07] N89-20537
CROPS
Nutritional models for a Controlled Ecological Life Support System (CELSS): Linear mathematical modeling
[NASA-CR-4229] N89-20615
CROSS FLOW
Navier-Stokes prediction of the three dimensional flow-field of jets in a crossflow using the finite element method N89-20408
CRYOGENIC EQUIPMENT
Superfluid Helium Tanker (SFHT) study
[NASA-CR-172110] N89-20182
CRYOGENIC FLUID STORAGE
Superfluid Helium Tanker (SFHT) study
[NASA-CR-172110] N89-20182
CRYSTAL DEFECTS
Dendritic web silicon photovoltaic cell research
[DE89-007289] N89-20554
Defect clustering and related properties of oxides
[DE89-006620] N89-20835
CRYSTAL GROWTH
X-ray diffraction study of phase formation and growth in nitrogen implanted iron: Temperature effects
[AD-A203625] N89-20245
Growth of mercuric iodide (HgI2) for nuclear radiation detectors N89-20293
Modelling the growth of triglycine sulphate crystals in Spacelab 3 N89-20294
Growth of solid solution single crystals N89-20297
Microgravity science at Langley Research Center N89-20298
Isothermal dendritic growth: A low gravity experiment N89-20299
Surface tension driven convection experiment N89-20314
A quantitative study of pattern formation in dendritic crystal growth from supersaturated solution N89-20818
Crystalline metal-semiconductor superlattices
[DE89-006619] N89-20825
Material selection for electrooptic deflectors
[DE89-007343] N89-20841
Nonlinear dynamical phenomena in liquid crystals
[DE88-705367] N89-20842
A study of ferroelectricity in single crystal compounds of the type AFB5 and A3B2F12
[AD-A203610] N89-20849
CRYSTAL LATTICES
Irradiation as a tool for studying solid state amorphization phenomena
[DE89-006034] N89-20823
CRYSTAL STRUCTURE
In-situ HVEM studies of the early stages of oxidation of nickel and nickel-chromium alloys
[DE89-005833] N89-20230
Design, development and applications of novel techniques for studying surface mechanical properties
[NASA-TM-101959] N89-20253
Protein crystal growth in a microgravity environment N89-20292
Some structural features of high-T(sub c) superconductors
[DE89-006667] N89-20826
X-ray diffraction and ellipsometric studies of zinc sulfide thin films grown by atomic layer epitaxy
[PH-161] N89-20827
Defect clustering and related properties of oxides
[DE89-006620] N89-20835
Surface structures determined using electron diffraction
[DE89-006669] N89-20837
Studies of alternative-crystallization-phase nucleation
[DE89-007220] N89-20840
CRYSTALLINITY
Synthesis and physical properties of liquid crystalline alkylisocyanate copolymers
[AD-A203631] N89-20266
Crystalline metal-semiconductor superlattices
[DE89-006619] N89-20825
CRYSTALLIZATION
Crystallization kinetics of BaO-Al2O3-SiO2 glasses
[NASA-TM-101964] N89-20252
Fluoride glass: Crystallization, surface tension N89-20306
Containerless processing of glass forming melts in space N89-20307
Studies of alternative-crystallization-phase nucleation
[DE89-007220] N89-20840
Finite size effects in Wigner crystallization of electrons on liquid helium layers
[DE88-705370] N89-20843
CRYSTALLOGRAPHY
X-ray diffraction and ellipsometric studies of zinc sulfide thin films grown by atomic layer epitaxy
[PH-161] N89-20827
CRYSTALS
Crystal nucleation in lithium borate glass N89-20309
Compensation for crystal penetration in high resolution positron tomography
[DE89-006660] N89-20836
CULTURE TECHNIQUES
Human cell culture in a space bioreactor N89-20288
CURVE FITTING
Piecewise continuous algebraic surfaces in terms of B-splines
[PB89-109136] N89-20712
CURVED PANELS
Postbuckling Finite Element (FE) analysis of a stiffened curved panel loaded in shear
[FFA-TN-1988-23] N89-20516
CURVES (GEOMETRY)
Algebraic nonplanar curve and surface estimation in 3-space with applications to position estimation
[PB88-227616] N89-20709
CYCLIC LOADS
Prediction of low and high crack growth rates under constant and variable amplitude loading
[NLR-MP-88012-U] N89-20523
WISPER: Introducing variable-amplitude loading in wind turbine design
[NLR-MP-88017-U] N89-20552
CYCLOGENESIS
Three-dimensional kinematics of rainbands in midlatitude cyclones N89-20586
CYCLOHEXANE
Aircraft operations and airborne measurement of perfluorotrimethylcyclohexane (PTCH) during ANATEX
[DE89-006934] N89-20566
CYCLOTRON RESONANCE DEVICES
Engineering and technical efforts to design and construct a 10 MW gyrotron laboratory
[AD-A203851] N89-20155
CYLINDRICAL SHELLS
Elastic stability of lap-jointed cylindrical shells under axial compression
[PB88-245980] N89-20497
Elastic stability of cylindrical shells with circumferential welded joints under axial compression
[PB89-125082] N89-20502
Experiments on the buckling of thin-walled model silo structures
[PB89-125124] N89-20503
Bulging cracks in pressurized fuselages: A numerical study
[NLR-MP-87058-U] N89-20519

CZOCHRALSKI METHOD
A comparative study of the influence of buoyancy driven fluid flow on GaAs crystal growth N89-20295

D

DAMAGE
Nonnormal accelerations due to yielding in a primary structure
[PB89-131437] N89-20513
DAMAGE ASSESSMENT
STS-27R OV-104 Orbiter TPS damage review team, volume 1
[NASA-TM-100355-VOL-1] N89-20178
Experimental study of spall damage in an aluminium alloy
[PB89-112619] N89-20224
Damage to silver coatings from high average power 1-micron laser
[DE89-005476] N89-20448
Fatigue teardown tests of the aged rear support of the A320 aircraft
[I-271/88] N89-20491
DAMPING
The influences of convection on directional solidification of eutectic Bi/MnBi N89-20303
DAST PROGRAM
Geometrical and structural properties of an Aeroelastic Research Wing (ARW-2)
[NASA-TM-4110] N89-20099
DATA ACQUISITION
The data acquisition system for the Fokker 100 test aircraft
[NLR-MP-87047-U] N89-20130
Transmitter data collection using Ada N89-20352
Waveform data collection for source inversion studies
[AD-A203419] N89-20575
Fastbus standard routines
[DOE/ER-0367] N89-20645
Report on federal information dissemination: Responses to decision analysis framework for GPO (Government Printing Office) strategic alternatives
[PB89-114649] N89-20864
Long-term solar-terrestrial observations
[NASA-CR-184695] N89-20905
DATA BASE MANAGEMENT SYSTEMS
Applying expertise to data in the Geologist's Assistant expert system
[DE89-003463] N89-20574
Monotonically improving approximate answers to relational algebra queries
[NASA-CR-184874] N89-20717
Space operations: Testing of NASA's technical and management information system
[GAO/IMTEC-88-28] N89-20859
DATA BASES
Review and assessment of the database and numerical modeling for turbine heat transfer N89-20139
Studies and analyses of the space shuttle main engine. Failure information propagation model data base and software
[NASA-CR-183586] N89-20198
National Air Toxics Information Clearinghouse: Ongoing research and regulatory development projects, July 1988
[PB89-103428] N89-20558
Waveform data collection for source inversion studies
[AD-A203419] N89-20575
Beaufort Sea mesoscale circulation study: Preliminary results
[PB89-121693] N89-20597
DATA COMPRESSION
Data compression as a means to disseminate more Meteosat data over the existing channel
[NLR-MP-86063-U] N89-20369
Adaptive data compression system study — scientific satellite
[SIL/CR/7129/6] N89-20639
Development of mathematical models for application in image processing
[AD-A203619] N89-20760
Adaptive data compression system study, executive summary — scientific satellite
[SIL/CR/7129/7] N89-20867
DATA INTEGRATION
Geological data integration techniques: Proceedings
[DE88-705255] N89-20868
DATA LINKS
Data storage and transfer apparatus
[EP-0-243-189-A1] N89-20623
DATA PROCESSING
Review of network planning methods applicable to Integrated Satellite Terrestrial Networks (ISTN)
[ESA-CR(P)-2691] N89-20185
The 1987 year end report for road following at Canegie Mellon
[AD-A203946] N89-20488
Watchdog Program
[PB89-122535] N89-20633
Auger electron and X-ray photoelectron data processing for the personal computer
[DE89-007292] N89-20670
Surface structures determined using electron diffraction
[DE89-006669] N89-20837
Using English for indexing and retrieving
[AD-A202227] N89-20866
Geological data integration techniques: Proceedings
[DE88-705255] N89-20868
Integrated analysis package for Mk-3 K-coronameter observations: A user's manual
[PB88-250717] N89-20904
Long-term solar-terrestrial observations
[NASA-CR-184695] N89-20905
DATA REDUCTION
Pressure coefficients for basic tensioned-membrane structure forms
[AD-A203866] N89-20107
Review of network planning methods applicable to Integrated Satellite Terrestrial Networks (ISTN)
[ESA-CR(P)-2691] N89-20185
DATA SMOOTHING
The use of smoothing techniques in the method of lines
[CWI-NM-R8802] N89-20740
DATA STORAGE
Data storage and transfer apparatus
[EP-0-243-189-A1] N89-20623
DATA STRUCTURES
Basis representations in large-scale linear programming software
[MA-50] N89-20649
DATA TRANSMISSION
VLA telemetry performance with concatenated coding for Voyager at Neptune N89-20340
Performance of Galileo's concatenated codes with nonideal interleaving N89-20343
Efficient detection and signal parameter estimation with applications to high dynamic GPS receivers
[NASA-CR-184861] N89-20362
Digital signal processing
[AD-A203744] N89-20403
Performance evaluation and analytic modeling of shared-memory computers
[PB89-113542] N89-20621
Data storage and transfer apparatus
[EP-0-243-189-A1] N89-20623
DEBRIS
STS-27R OV-104 Orbiter TPS damage review team, volume 1
[NASA-TM-100355-VOL-1] N89-20178
DECAY RATES
Critical fluid light scattering N89-20320
DECISION MAKING
Assessing potential benefits for service/repair and retrieval of satellites: A pilot decision analysis
[AD-A203830] N89-20190
Componential analysis of pilot decision making
[AD-A203711] N89-20613
DATMS: A framework for distributed assumption based reasoning
[DE89-006282] N89-20628
Incremental development and prototyping in current laboratory software development projects: Preliminary analysis
[NASA-CR-184860] N89-20544
Report on federal information dissemination: Responses to decision analysis framework for GPO (Government Printing Office) strategic alternatives
[PB89-114649] N89-20864
DECISION THEORY
Assessing potential benefits for service/repair and retrieval of satellites: A pilot decision analysis
[AD-A203830] N89-20190
DECODING
The decoding of Reed-Solomon codes N89-20344
DECOMPOSITION
Application of rigorous nonlinear regression to the decomposition kinetics of explosives
[DE89-007598] N89-20274
Domain decomposition methods for systems of conservation laws: Spectral collocation approximations
[NASA-CR-181773] N89-20635
A parallel decomposition algorithm for Staircase Linear Programs
[DE89-007883] N89-20674
DEEP SPACE NETWORK
The Telecommunications and Data Acquisition Report
[NASA-CR-184672] N89-20329
Determination of GPS orbits to submeter accuracy N89-20331
DSN 70-meter antenna X-band gain, phase, and pointing performance, with particular application for Voyager 2 Neptune encounter N89-20353
DEFECTS
Long-term evaluation of the acoustic emission weld monitor
[PB88-122642] N89-20471
Defect clustering and related properties of oxides
[DE89-006620] N89-20835
DEFLECTION
Non-symmetric bifurcation of geometrically non-linear elastic-plastic axisymmetric shells under combined loads including torsion
[PB89-102149] N89-20500
Large deflection analysis of thin elastic shells by hybrid stress method
[PB89-111504] N89-20506
DEFLECTORS
Material selection for electrooptic deflectors
[DE89-007343] N89-20841
DEFORMATION
An analysis of an incompressible, fiber-reinforced material subjected to finite strains in the direction of reinforcement N89-20201
Analysis of the strain-rate sensitivity at high strain rates in fcc and bcc metals
[DE89-005471] N89-20233
Welded joint integrity analysis: Relative criticality of weld defect and remote deformation
[AD-A203756] N89-20246
The effect of deformation history on the morphology and properties of blends of polycarbonate and a thermotropic liquid crystalline polymers
[AD-A203632] N89-20267
HARTFEM: A finite element program for thermal and viscoplastic deformation problems
[DE89-007788] N89-20755
DEGENERATION
Second order degenerate elliptic equations
[DE88-705347] N89-20749
DEICING
Aircraft accident report: Continental Airlines, Inc., Flight 1713, McDonnell Douglas DC-9-14, N626TX, Stapleton International Airport, Denver, Colorado, November 15, 1987
[PB88-910411] N89-20112
DELAMINATING
Prediction model for the onset of edge-effect delamination at holes in composite laminates N89-20202
DELTA WINGS
Some low-speed flutter characteristics of simple low-aspect-ratio delta wing models
[NASA-TM-101547] N89-20094
DENDRITIC CRYSTALS
Isothermal dendritic growth: A low gravity experiment N89-20299
Dendritic growth and structure of undercooled nickel base alloys N89-20302
Dendritic web silicon photovoltaic cell research
[DE89-007289] N89-20554
A quantitative study of pattern formation in dendritic crystal growth from supersaturated solution N89-20618
DENSITOMETERS
The development of a Compton lung densitometer
[DE89-006654] N89-20603
DENSITY MEASUREMENT
Critical fluid light scattering N89-20320
Density measurements with combined Raman-Rayleigh LIDAR (Light Detection And Ranging)
[AD-A203561] N89-20376
DEPLETION
Ground state depleted laser experiments
[DE89-006146] N89-20449
Ground State Depleted (GSD) solid state lasers: Principles, characteristics, and scaling
[DE89-006149] N89-20450
DEPOSITION
Optical second harmonic generation in metal monolayers and metal surfaces
[DE89-006123] N89-20234
DESCRIPTIVE GEOMETRY
Incremental display of Constructive Solid Geometry (CSG) models using local updating
[REPT-88-51] N89-20650
Quadratic blending surfaces for complex corners, part 2
[CS-8809-PT-2] N89-20657
DESIGN
Aerospace vehicle design, Spacecraft Section final project reports
[NASA-CR-184741] N89-20121

DESIGN ANALYSIS
Aerospace vehicle design, Spacecraft Section final project reports
[NASA-CR-184741] N89-20121
Aerospace vehicle design, Spacecraft Section final project reports
[NASA-CR-184742] N89-20122
Aerospace vehicle design, Spacecraft Section
[NASA-CR-184743] N89-20123
Engineering and technical efforts to design and construct a 10 MW gyrotron laboratory
[AD-A203851] N89-20155
Two designs for an orbital transfer vehicle: A comparison of two OTVs
[NASA-CR-184696] N89-20175
Two designs for an orbital transfer vehicle. Project Orion: A proposal for a manned orbital transfer vehicle for the 21st Century
[NASA-CR-184697] N89-20176
Commercial direct absorption receiver design studies
[DE89-007290] N89-20556
DESIGN TO COST
Space Station: NASA efforts to establish a design-to-life-cycle cost process
[GAO/NSIAD-88-147] N89-20188
DESORPTION
Evaluation of solid lubricants: Temperature programmed desorption of MoS2 on molybdenum and of ion-implanted MoS2 on molybdenum
[AD-A203741] N89-20268
DETECTION
Efficient detection and signal parameter estimation with applications to high dynamic GPS receivers
[NASA-CR-184861] N89-20362
Real-time part position sensing
[AD-A203580] N89-20439
ILS (Intracavity Laser Spectroscopy) for beam sensing (experiment)
[DE89-006376] N89-20445
DETONATION
Time resolved study of light emitted by detonation arrival at the surface of high explosives in various environments
[DE89-005657] N89-20414
DETONATION WAVES
The dynamic response at high-explosive inert-solid interface as predicted by finite difference/element computer programs
[DE89-007303] N89-20272
Time resolved study of light emitted by detonation arrival at the surface of high explosives in various environments
[DE89-005657] N89-20414
DEUTERIUM
Solubility of hydrogen, deuterium and tritium in palladium metal
[DE89-005304] N89-20225
DIAMAGNETISM
Shielding effectiveness of superconductive particles in plastics
[DE89-003888] N89-20815
DICTIONARIES
Glossary of testing terminology for rechargeable batteries
[DE89-007061] N89-20395
DIELECTRICS
Research for electric energy systems
[PB89-132310] N89-20383
The Cerenkov free-electron laser
[AD-A203531] N89-20464
DIESEL FUELS
Investigation of spray dispersion and particulate formation in diesel fuel flames
[NASA-CR-184820] N89-20215
DIFFERENTIAL CALCULUS
A tutorial introduction to differentiable manifolds and calculus on manifolds
[CWI-PM-R8803] N89-20746
DIFFERENTIAL EQUATIONS
Second order degenerate elliptic equations
[DE88-705347] N89-20749
The initial value problem for fractional order differential equations with constant coefficients
[AD-A203843] N89-20764
DIFFRACTION
Diffraction theory for polygonal apertures
[AD-A203778] N89-20802
DIFFUSION
Pb-Zn liquid metal diffusion N89-20304
Edge illuminated ventical multijunction
[DE89-006246] N89-20547
Anion grain boundary diffusion in Cr2O3 and Cr2O3-0.09 weight percent Y2O3
[DE89-006281] N89-20833
DIFFUSION FLAMES
Modeling of hydrogen-air diffusion flame
[NASA-CR-184844] N89-20218
DIFFUSION WELDING
Nondestructive tests of elements manufactured using diffusion bonding and superplastic forming
[ETN-89-94131] N89-20492
DIGITAL FILTERS
Digital processing of speckle images
[AD-A203703] N89-20801
DIGITAL SIMULATION
Digital processing of speckle images
[AD-A203703] N89-20801
DIGITAL SYSTEMS
Digital signal processing
[AD-A203744] N89-20403
Waveform data collection for source inversion studies
[AD-A203419] N89-20575
DIGITAL TECHNIQUES
The digital wave processing experiment --- Cluster mission N89-20164
DIMERIZATION
On the dimerization of linear polymers
[DE88-705341] N89-20256
DIODES
Q-switched, intracavity doubled Nd:YAG laser side-pumped by a laser diode array
[DE89-005349] N89-20441
DIPOLE ANTENNAS
Reconfigurable antennas
[AD-A203847] N89-20382
DIRECTIONAL COUPLERS
Cross-guide coupler modeling and design N89-20337
DIRECTIONAL SOLIDIFICATION (CRYSTALS)
Isothermal solidification in a binary alloy melt N89-20300
Casting And Solidification Technology (CAST): Directional solidification phenomena in a metal model at reduced gravity N89-20301
The influences of convection on directional solidification of eutectic Bi/MnBi N89-20303
DIRICHLET PROBLEM
Analysis of regularized Navier-Stokes equations, 2
[NASA-CR-181801] N89-20716
DISCHARGE
Group testing of lead-acid batteries for electric vehicles
[DE89-005415] N89-20389
DISPERSING
Investigation of spray dispersion and particulate formation in diesel fuel flames
[NASA-CR-184820] N89-20215
Dispersion of dense gas releases in a wind tunnel
[PB89-118509] N89-20561
DISPERSION
Hybrid single-particle Lagrangian integrated trajectories (HY-SPLIT): Model description
[PB89-127591] N89-20559
DISPLACEMENT
Axially accelerated saboted rods subjected to lateral forces
[DE89-007466] N89-20485
A displacement pattern matching application in elastic-plastic hybrid stress analysis
[AD-A199028] N89-20499
DISPLACEMENT MEASUREMENT
Dynamic wall pressure measurements
[AD-A203551] N89-20427
DISSOCIATION
Infrared spectroscopy of weakly bound molecular ions
[DE89-006602] N89-20787
DISTANCE
Trajectory scoring in rectangular coordinates using transponder-interrogator range and range rate data
[DE89-007005] N89-20119
DISTRIBUTED PARAMETER SYSTEMS
Diagnostics for intelligent control of MPD engines
[AD-A203640] N89-20530
Numerical studies of identification in nonlinear distributed parameter systems
[NASA-CR-181771] N89-20636
Optimal feedback control infinite dimensional parabolic evolution systems: Approximation techniques
[NASA-CR-181772] N89-20637
Some observations on redundancy in a context
[CWI-CS-R8812] N89-20662
DISTRIBUTED PROCESSING
Research in distributed personal computer-based information systems, volume 1
[AD-A203780] N89-20629
Run-time scheduling and execution of loops on message passing machines
[NASA-CR-181785] N89-20638
An operating environment for the jellybean machine
[AD-A201042] N89-20682
The effect of time constraints on scaled speed-up
[DE89-007877] N89-20691
Research in distributed personal computer-based information systems, volume 2
[AD-A203845] N89-20870
DOCUMENTATION
Report of the Documentation Advisory Committee
[PB89-124556] N89-20589
DOMAINS
Domain decomposition methods for systems of conservation laws: Spectral collocation approximations
[NASA-CR-181773] N89-20635
DOPED CRYSTALS
Resonance electronic Raman scattering in rare earth crystals
[DE89-007446] N89-20847
DOPPLER EFFECT
DMA (Defense Mapping Agency) orbit determination of the navy navigation satellite system for 1987
[AD-A203496] N89-20170
Two-way coherent Doppler error due to solar corona N89-20332
DOPPLER RADAR
Analysis of Doppler radar windshear data
[NASA-CR-181762] N89-20111
A portable CW/FM-CW Doppler radar for local investigation of severe storms
[DE89-005445] N89-20373
DOWNLINKING
Two-way coherent Doppler error due to solar corona N89-20332
On 32-GHz cryogenically cooled HEMT low-noise amplifiers N89-20336
The decoding of Reed-Solomon codes N89-20344
DRAG FORCE ANEMOMETERS
Aerodynamics of two-dimensional slotted bluff bodies
[DE89-007288] N89-20105
DROPS (LIQUIDS)
Physical phenomena in containerless glass processing N89-20310
Droplet combustion at reduced gravity N89-20313
Electromagnetic, heat and fluid flow phenomena in levitated metal droplets both under earthbound and microgravity conditions N89-20315
The dynamics of free liquid drops N89-20316
DUCTILITY
Ductile-regime turning of germanium and silicon
[NASA-TM-101231] N89-20322
A stereological analysis of ductile fracture by microvoid coalescence
[DE89-000355] N89-20528
DUPLEXERS
Dedicated versus half-duplex receiver topology in jammed, fully connected CDMA networks: Theory and numerical comparisons
[AD-A203635] N89-20402
DUST
Dust shells around Miras and OH/IR stars N89-20889
DYE LASERS
Q-switched, intracavity doubled Nd:YAG laser side-pumped by a laser diode array
[DE89-005349] N89-20441
ILS (Intracavity Laser Spectroscopy) for beam sensing (experiment)
[DE89-006376] N89-20445
DYNAMIC CHARACTERISTICS
Multifractals
[DE88-705369] N89-20672
Nonlinear dynamical phenomena in liquid crystals
[DE88-705367] N89-20842
Integrable two dimensional supersystems
[DE88-705355] N89-20857
DYNAMIC MODELS
Identification of space shuttle main engine dynamics
[NASA-TM-101982] N89-20199
Dynamic models for simulation of the 70-M antenna axis servos N89-20333
DYNAMIC PRESSURE
Dynamic wall pressure measurements
[AD-A203551] N89-20427
DYNAMIC RESPONSE
The dynamic response at high-explosive inert-solid interface as predicted by finite difference/element computer programs
[DE89-007303] N89-20272
An airfoil pitch apparatus-modeling and control design
[NASA-TM-101076] N89-20386
A comparison of frequency estimation techniques for high-dynamic trajectories
[NASA-CR-184865] N89-20387
Comparison between predicted and measured rotational frequency response functions
[ISVR-TR-164] N89-20524

The initial value problem for fractional order differential equations with constant coefficients
[AD-A203843] N89-20764
DYNAMIC STRUCTURAL ANALYSIS
Pressure coefficients for basic tensioned-membrane structure forms
[AD-A203866] N89-20107
Flight motor set 360L001 (STS-26R), volume 1
[NASA-CR-183576] N89-20196
Experiments on the buckling of thin-walled model silo structures
[PB89-125124] N89-20503
Tripping of asymmetrical stiffeners under combined loading
[PB89-126171] N89-20504
Coupled rotor/fuselage dynamic analysis of the AH-1G helicopter and correlation with flight vibrations data
[NASA-CR-181723] N89-20512
Nonnormal accelerations due to yielding in a primary structure
[PB89-131437] N89-20513
Comparison between predicted and measured rotational frequency response functions
[ISVR-TR-164] N89-20524
DYNAMICAL SYSTEMS
A new algorithm for modeling friction in dynamic mechanical systems N89-20334
Consequences of nonclassical measurement for the algorithmic description of continuous dynamical systems
[NASA-CR-184851] N89-20640
Dynamic mechanical system design using qualitative and symbolic reasoning
[DE89-006771] N89-20706
Riemannian geometry on families of linear systems, the deterministic case
[REPT-88-62] N89-20726
Toward a quasi-periodic bifurcation theory — dynamical systems
[ZW-8803] N89-20736
Application of Newton's method to Lagrangian dynamical systems
[DE89-007024] N89-20751
Asymptotic behavior of random discrete event systems
[REPT-88-56] N89-20766

E

EARTH ALBEDO
Effect of earth albedo variation on the performance of a spatial acquisition subsystem aboard a planetary spacecraft N89-20349
EARTH ATMOSPHERE
Density measurements with combined Raman-Rayleigh LIDAR (Light Detection And Ranging)
[AD-A203561] N89-20376
An assessment model for atmospheric composition
[NASA-CP-3023] N89-20588
Meson production and nuclear fragmentation of nucleus in the atmosphere
[DE88-705019] N89-20917
EARTH MAGNETOSPHERE
Scientific results from the Swedish Viking satellite
[IRF-SR-196] N89-20572
Astrophysical significance of observations and experiments in the Earth's magnetosphere
[TRITA-EPP-88-09] N89-20899
EARTH ORBITAL ENVIRONMENTS
Ablation of materials in the low earth orbital environment N89-20187
EARTH ORBITS
Extravehicular activity at geosynchronous earth orbit
[NASA-CR-172112] N89-20181
EARTH RADIATION BUDGET
Angular radiation models for earth-atmosphere system. Volume 2: Longwave radiation
[NASA-RP-1184-VOL-2] N89-20587
EARTH RADIATION BUDGET EXPERIMENT
Angular radiation models for earth-atmosphere system. Volume 2: Longwave radiation
[NASA-RP-1184-VOL-2] N89-20587
ECONOMY
Implications of the greenhouse effect for the midwest economy
[DE89-004195] N89-20563
EDDY CURRENTS
Eddy current inspection of ferromagnetic materials using pulsed magnetic saturation
[DE89-005339] N89-20493
EDUCATION
A software model for simulation in computer-based training
[DE89-003469] N89-20665
EINSTEIN EQUATIONS
Solutions and stability of a closed-geodesic black hole model N89-20893
ELASTIC DEFORMATION
Theoretical modelling and experimental characterization of flexible composites under finite deformation N89-20204
ELASTIC PROPERTIES
Elastic stability of lap-jointed cylindrical shells under axial compression
[PB88-245980] N89-20497
A displacement pattern matching application in elastic-plastic hybrid stress analysis
[AD-A199026] N89-20499
A theoretical, numerical and experimental examination of in situ properties of adhesives
[FFA-TN-1988-05] N89-20526
ELASTIC SHELLS
Large deflection analysis of thin elastic shells by hybrid stress method
[PB89-111504] N89-20506
ELASTIC WAVES
Transmission and reflection on pressure waves by compressor and turbine stages, based on an actuator-disk model
[AD-A203513] N89-20426
ELASTODYNAMICS
Implementation of a hierarchical wedge element in the self-adaptive Finite Element (FE) program STRIPE
[FFA-TN-1988-36] N89-20517
ELASTOMERS
Energetic thermoplastic elastomer synthesis
[AD-A203594] N89-20265
ELASTOPLASTICITY
Non-symmetric bifurcation of geometrically non-linear elastic-plastic axisymmetric shells under combined loads including torsion
[PB89-102149] N89-20500
Analysis of dynamic elastic-plastic fracture phenomena: Steady crack growth and transient loading of a stationary crack N89-20507
ELECTRIC ARCS
Workshop on Transient Induced Insulator Flashover in Vacuum
[DE89-006727] N89-20398
ELECTRIC BATTERIES
Glossary of testing terminology for rechargeable batteries
[DE89-007061] N89-20395
Assessment of high-temperature battery systems
[DE89-007554] N89-20399
ELECTRIC DIPOLES
Cross-guide coupler modeling and design N89-20337
ELECTRIC FIELDS
The spherical probe electric field and wave experiment — Cluster mission N89-20161
Measurement of quasi-static and low frequency electric fields on the Viking satellite
[TRITA-EPP-87-02] N89-20189
Research for electric energy systems
[PB89-132310] N89-20383
Diffraction theory for polygonal apertures
[AD-A203778] N89-20802
Resonance tunnelling and breakdown of the Quantum Hall Effect (QHE) in strong electric fields
[DE88-705348] N89-20831
ELECTRIC MOTOR VEHICLES
Group testing of lead-acid batteries for electric vehicles
[DE89-005415] N89-20389
ELECTRIC POTENTIAL
The effects of variations in the photocathode voltages of electronic streak cameras
[DE89-006776] N89-20436
A numerical model of ionospheric convection derived from field-aligned currents and the corresponding conductivity — ionosphere
[TRITA-EPP-88-03] N89-20571
ELECTRIC PROPULSION
Advanced technology for future space propulsion systems
[NASA-TM-101951] N89-20192
ELECTRIC SPARKS
Production of pulsed electron beams by triggered pseudo-spark discharges
[ISL-CO-245/87] N89-20388
ELECTRICAL FAULTS
Resonance tunnelling and breakdown of the Quantum Hall Effect (QHE) in strong electric fields
[DE88-705348] N89-20831
ELECTRICAL MEASUREMENT
The Cluster Mission: Scientific and technical aspects of the instruments
[ESA-SP-1103] N89-20156
The spherical probe electric field and wave experiment — Cluster mission N89-20161
The electron drift instrument — Cluster mission N89-20165
PEACE: A Plasma Electron And Current Experiment — Cluster mission N89-20167
Measurement of quasi-static and low frequency electric fields on the Viking satellite
[TRITA-EPP-87-02] N89-20189
Research for electric energy systems
[PB89-132310] N89-20383
ELECTRICAL PROPERTIES
Defect clustering and related properties of oxides
[DE89-006620] N89-20835
ELECTRICAL RESISTIVITY
Continuous flow electrophoresis system experiments on shuttle flights STS-6 and STS-7 N89-20277
Evaluation of the Kubo formula for the conductivity using the recursion method
[DE88-705359] N89-20396
ELECTROCHEMISTRY
Vectorial electron transfer on designed surfaces
[PB88-240031] N89-20211
The role of composition and microstructure gradients on weld metal properties and behavior
[DE89-006789] N89-20235
Electrochemical considerations of crack growth in the ferrous alloys
[AD-A203811] N89-20247
ELECTRODEPOSITION
Electrodeposition of aluminium, aluminium/magnesium alloys and magnesium from organometallic electrolytes
[DE89-003483] N89-20232
ELECTRODYNAMICS
Flexible structure control laboratory development and technology demonstration
[NASA-CR-184867] N89-20151
Einsteins's theory of gravity in Fierz variables
[DE88-705004] N89-20854
ELECTROHYDRODYNAMICS
Preparative electrophoresis for space N89-20278
ELECTROKINETICS
Preparative electrophoresis for space N89-20278
ELECTROLYTES
Electrodeposition of aluminium, aluminium/magnesium alloys and magnesium from organometallic electrolytes
[DE89-003483] N89-20232
ELECTROLYTIC CELLS
Phosphoric acid fuel cell subsystem technology
[PB88-100515] N89-20544
ELECTROMAGNETIC COMPATIBILITY
Electromagnetic compatibility (EMC) test facilities
[NLR-MP-88010-U] N89-20370
ELECTROMAGNETIC FIELDS
Modeling the behavior of pulsed, high power microwave antenna systems
[DE89-006280] N89-20374
A relativistic fluid code for high-power microwave propagation
[DE89-006596] N89-20375
The Cerenkov free-electron laser
[AD-A203531] N89-20464
Feasibility study of high temperature superconductor opening switches
[AD-A203699] N89-20851
ELECTROMAGNETIC INTERFERENCE
A study of EMI-endurance of two polling-type local area networks used in real-time automation applications in a simulated electrical environment
[EL-62] N89-20368
ELECTROMAGNETIC NOISE
Cluster: A fleet of four spacecraft to study plasma structures in three dimensions N89-20157
Analysis of modified SMI method for adaptive array weight control
[NASA-CR-184904] N89-20364
ELECTROMAGNETIC SCATTERING
Active and passive remote sensing of ice
[AD-A203943] N89-20543
Hypercube matrix computation task
[NASA-CR-184869] N89-20642
ELECTROMAGNETIC SHIELDING
Shielding effectiveness of superconductive particles in plastics
[DE89-003888] N89-20815
ELECTROMAGNETIC WAVE TRANSMISSION
Stimulated Raman scattering of intense laser radiation in a nuclear-disturbed space plasma
[AD-A200951] N89-20440
ELECTROMAGNETISM
Electromagnetic, heat and fluid flow phenomena in levitated metal droplets both under earthbound and microgravity conditions N89-20315
ELECTROMYOGRAPHY
Influences of muscle fiber composition and strength on EMG (electromyographic activity), spinal motion and load acceleration during a repetitive lifting task
[PB89-131221] N89-20607

ELECTRON BEAMS
Production of pulsed electron beams by triggered pseudo-spark discharges
[ISL-CO-245/87] N89-20388
Bunch beam production and microwave generation in reditrons
[DE89-006530] N89-20397
High power induction free electron laser
[DE89-006208] N89-20444
Validity of 1D free-electron laser sideband models
[DE89-006264] N89-20452
Status of LBL/LLNL FEL (Free Electron Laser) research for two beam accelerator applications
[DE89-006656] N89-20453
Three dimensional numerical analysis of a high-gain free-electron laser
[DE89-006981] N89-20456
Preliminary studies of an infrared free-electron laser oscillator at the ATF(BNL)
[DE89-006962] N89-20457
The chirped-pulse free-electron laser
[DE89-006792] N89-20460
Amplified spontaneous emission in a single pass free electron laser
[DE89-007048] N89-20461
Review of intense electron beam transport in gases
[DE89-005397] N89-20792
Low emittance thermionic electron guns
[DE89-005944] N89-20793

ELECTRON DENSITY (CONCENTRATION)
A relativistic fluid code for high-power microwave propagation
[DE89-006598] N89-20375
A new procedure for determination of electron temperatures and electron concentrations by Thomson scattering and analytical plasmas
[AD-A203489] N89-20812

ELECTRON DIFFRACTION
Surface structures determined using electron diffraction
[DE89-006669] N89-20837

ELECTRON ENERGY
The chirped-pulse free-electron laser
[DE89-006792] N89-20460
A new procedure for determination of electron temperatures and electron concentrations by Thomson scattering and analytical plasmas
[AD-A203489] N89-20812

ELECTRON GUNS
Low emittance thermionic electron guns
[DE89-005944] N89-20793

ELECTRON MICROSCOPES
New directions in spectroscopy for the analytical electron microscope
[DE89-005824] N89-20435

ELECTRON PLASMA
Low frequency MHD instability in a hot electron plasma
[PB89-111546] N89-20803

ELECTRON RADIATION
Characterization of production GaAs solar cells for space
[NASA-CR-184863] N89-20549

ELECTRON SPECTROSCOPY
New directions in spectroscopy for the analytical electron microscope
[DE89-005824] N89-20435
Auger electron and X-ray photoelectron data processing for the personal computer
[DE89-007292] N89-20670
Electron spectroscopy studies of high temperature superconductors: Y(sub 1)-xPr(sub x)Ba2Cu3O(sub 7)-delta
[DE89-006554] N89-20824

ELECTRON TRANSFER
Vectorial electron transfer on designed surfaces
[PB88-240031] N89-20211
Photoinduced electron transfer in ordered polymers
[DE89-006986] N89-20254
Mechanisms of photochemical energy conversion by chlorophyll
[DE89-006820] N89-20550

ELECTRON TUNNELING
Quasi-classical calculations for superfluids
[ETN-89-94118] N89-20421
Ultrafast physics in microstructure and alloy systems
[AD-A203639] N89-20850

ELECTRONIC CONTROL
Design and implementation of the hazard control box for the ride motion simulator
[AD-A203752] N89-20404

ELECTRONIC EQUIPMENT
Development of the University of Maryland RAMCAD (Reliability and Maintainability Computer-Aided Design) for electronic systems
[AD-A203616] N89-20675

ELECTRONIC EQUIPMENT TESTS
Electromagnetic compatibility (EMC) test facilities
[NLR-MP-88010-U] N89-20370

ELECTRONIC MAIL
Space operations: Testing of NASA's technical and management information system
[GAO/IMTEC-88-28] N89-20859
Research in distributed personal computer-based information systems, volume 2
[AD-A203845] N89-20870

ELECTRONS
Thermodynamic characteristics of Y-Ba-Cu-O type compounds in the model of strong electron-phonon coupling
[DE88-705343] N89-20828
Energy gap in S- and D-wave pairing superconductors
[DE88-705344] N89-20829
Finite size effects in Wigner crystallization of electrons on liquid helium layers
[DE88-705370] N89-20843

ELECTROPHORESIS
Microgravity Science and Applications Flight Programs, January - March 1987, selected papers, volume 1
[NASA-TM-4069-VOL-1] N89-20276
Continuous flow electrophoresis system experiments on shuttle flights STS-6 and STS-7 N89-20277
Preparative electrophoresis for space N89-20278
Heterogeneity in the growth hormone pituitary gland system of rats and humans: Implications to microgravity based research N89-20279
Kidney cell electrophoresis in space flight: Rationale, methods, results and flow cytometry applications N89-20280
Hormone purification by isoelectric focusing in space N89-20282
Biochemical assays on plasminogen activators and hormones from kidney sources N89-20287
Antibody enhancement of free-flow electrophoresis N89-20290

ELECTROPLATING
Electrodeposition of aluminium, aluminium/magnesium alloys and magnesium from organometallic electrolytes
[DE89-003483] N89-20232

ELECTROSTATICS
Investigation of spray dispersion and particulate formation in diesel fuel flames
[NASA-CR-184820] N89-20215

ELLIPSOMETERS
X-ray diffraction and ellipsometric studies of zinc sulfide thin films grown by atomic layer epitaxy
[PH-161] N89-20827

ELLIPTIC DIFFERENTIAL EQUATIONS
Numerical method of applying mean value theorem
[PB89-111447] N89-20714
High performance preconditioning — elliptical partial differential equations
[REPT-88-54] N89-20725
Matrix dependent prolongations and restrictions in a black box multigrid solver
[CWI-NM-R8801] N89-20739
Second order degenerate elliptic equations
[DE88-705347] N89-20749

ELLIPTICAL CYLINDERS
Vorticity distributions in unsteady flow separation
[AD-A203733] N89-20428

ELLIPTICAL GALAXIES
Isophotometry of brightest elliptical galaxies in rich clusters N89-20879

EMISSION SPECTRA
The emittance of space radiator materials measured at elevated temperatures
[NASA-TM-101948] N89-20193

EMISSIVITY
Optical Johnson noise thermometry
[NASA-CR-184964] N89-20437

ENERGY CONSUMPTION
Power efficient hydraulic systems. Volume 1: Study phase
[AD-A203899] N89-20127

ENERGY CONVERSION
Characterization of production GaAs solar cells for space
[NASA-CR-184863] N89-20549
Mechanisms of photochemical energy conversion by chlorophyll
[DE89-006820] N89-20550
Energy conversion processes based on molecular excited states
[DE89-007322] N89-20555

ENERGY CONVERSION EFFICIENCY
Bunch beam production and microwave generation in reditrons
[DE89-006530] N89-20397
Photovoltaic energy program summary. Volume 1: Overview, fiscal year 1988
[DE89-000855] N89-20553

ENERGY DISTRIBUTION
A new procedure for determination of electron temperatures and electron concentrations by Thomson scattering and analytical plasmas
[AD-A203489] N89-20812

ENERGY GAPS (SOLID STATE)
Energy gap in S- and D-wave pairing superconductors
[DE88-705344] N89-20829

ENERGY TECHNOLOGY
Research for electric energy systems
[PB89-132310] N89-20383
Energy related inventions program: A joint program of the Department of Energy and the National Institute of Standards and Technology
[PB89-141154] N89-20548

ENERGY TRANSFER
Study of vibrational and rapid local motions of hydrogen in the storage compound Ti0.8Zr0.2 CrMnH3 by slow neutron scattering
[DE88-704797] N89-20213
Pulsed laser effects phenomenology
[DE89-005466] N89-20442
Direct solar-pumped iodine laser amplifier
[NASA-CR-184813] N89-20447
Energy conversion processes based on molecular excited states
[DE89-007322] N89-20555
Collisional energy transfer in highly vibrationally excited polyatomic molecules
[AD-A203728] N89-20789
Review of intense electron beam transport in gases
[DE89-005397] N89-20792
On the effects of Cosmions upon the structure and evolution of very low mass stars
[NASA-CR-182958] N89-20880

ENGINE DESIGN
Propulsion over a wide Mach number range
[NASA-CR-182267] N89-20134
Assessment, development, and application of combustor aerothermal models N89-20138
Review and assessment of the database and numerical modeling for turbine heat transfer N89-20139
Structural analysis methods development for turbine hot section components N89-20140
Structural analysis applications N89-20141
Views on the impact of HOST N89-20144
Free-piston Stirling technology for space power
[NASA-TM-101956] N89-20194

ENGINE FAILURE
Studies and analyses of the space shuttle main engine. Failure information propagation model data base and software
[NASA-CR-183586] N89-20198

ENGINE PARTS
Structural analysis methods development for turbine hot section components N89-20140
Structural analysis applications N89-20141

ENGINE TESTS
Advanced high temperature instrument for hot section research applications N89-20137

ENGINEERING DRAWINGS
Incremental display of Constructive Solid Geometry (CSG) models using local updating
[REPT-88-51] N89-20650

ENGLISH LANGUAGE
Comparative lexicon of US-Soviet military technical terminology
[PB89-125553] N89-20865
Using English for indexing and retrieving
[AD-A202227] N89-20866

ENTHALPY
Fluorine as an oxidant in combustion calorimetry
[DE89-003626] N89-20214

ENTROPY (STATISTICS)
Estimating a regression function
[CWI-MS-R8805] N89-20742

ENVIRONMENT EFFECTS
Implications of the greenhouse effect for the midwest economy
[DE89-004195] N89-20563
The causes and consequences of global climate change
[DE89-004355] N89-20564

ENVIRONMENT MODELS
A microcomputer pollution model for civilian airports and Air Force bases. Model application and background
[AD-A199794] N89-20557

ENVIRONMENTAL MONITORING
National Air Toxics Information Clearinghouse: Ongoing research and regulatory development projects, July 1988
[PB89-103428] N89-20558
An assessment model for atmospheric composition
[NASA-CP-3023] N89-20586

ENVIRONMENTAL TESTS
Effects of environment on tunneling spectroscopy of gold films
[DE89-006040] N89-20844
ENZYME ACTIVITY
Biochemical assays on plasminogen activators and hormones from kidney sources N89-20287
ENZYMES
Development of immunoassays for human urokinase N89-20283
EQUATIONS OF MOTION
Simulation of superradiant free-electron lasers
[DE89-006156] N89-20451
Dynamic modeling and linearization for real-time control of a pantograph manipulator N89-20469
The initial value problem for fractional order differential equations with constant coefficients
[AD-A203843] N89-20764
EQUATIONS OF STATE
Solutions and stability of a closed-geodesic black hole model N89-20693
EQUATORIAL REGIONS
CTD/O2 measurements during 1986 as part of the Equatorial Pacific Ocean Climate Studies (EPOCS)
[PB89-102859] N89-20596
EQUINOXES
The behavior of the electron density and temperatue at Millstone Hill during the equinox transition study September 1984
[NASA-CR-184737] N89-20567
EQUIPMENT SPECIFICATIONS
Isothermal dendritic growth: A low gravity experiment N89-20299
The first products made in space: Monodisperse latex particles N89-20318
The development of a Compton lung densitometer
[DE89-006654] N89-20603
EQUIVALENT CIRCUITS
The influence of surface capacitance on the measurements of localized corrosion transients
[DE89-006172] N89-20391
ERROR ANALYSIS
Error localization and updating of spacecraft structures mathematical models
[ESA-CR(P)-2697] N89-20186
Testing for nonlinearity using a prediction error filter
[RR-332] N89-20371
Fault-tolerance of a neural network solving the traveling salesman problem
[NASA-CR-181798] N89-20698
On the equivalence of Gaussian elimination and Gauss-Jordan reduction in solving linear equations
[NASA-TM-101466] N89-20710
ERROR CORRECTING CODES
Error control techniques for satellite and space communications
[NASA-CR-184825] N89-20357
ERRORS
Two-way coherent Doppler error due to solar corona N89-20332
VLA telemetry performance with concatenated coding for Voyager at Neptune N89-20340
Elements of design, unifying principles and applications N89-20485
ESTIMATES
High-dynamic GPS tracking
[NASA-CR-184868] N89-20113
Algebraic nonplanar curve and surface estimation in 3-space with applications to position estimation
[PB88-227616] N89-20709
ESTUARIES
Utilizing remote sensing of thematic mapper data to improve our understanding of estuarine processes and their influence on the productivity of estuarine-dependent fisheries
[NASA-CR-183417] N89-20533
ETHYLENE
Transport and relaxation processes in supercritical fluids
[DE89-005910] N89-20219
EULER EQUATIONS OF MOTION
Flux vector splitting in general curvilinear coordinates
[PB89-127393] N89-20410
Spectral methods for CFD
[NASA-CR-181803] N89-20718
Star formation, using 3-D explicit Eulerian hydrodynamics N89-20890
EUROPEAN SPACE AGENCY
Commercial potential of European and Japanese space programs, task 5
[NASA-CR-184659] N89-20871
EUROPEAN SPACE PROGRAMS
The Cluster Mission: Scientific and technical aspects of the instruments
[ESA-SP-1103] N89-20156
Cluster: A fleet of four spacecraft to study plasma structures in three dimensions N89-20157
The magnetic field investigation on Cluster N89-20158
EUTECTIC ALLOYS
The influences of convection on directional solidification of eutectic Bi/MnBi N89-20303
EVAPORATION
A finite element stability analysis for the Marangoni problem in a rectangular container with rigid sidewalls
[TW-285] N89-20735
EXCIMER LASERS
Development KrF lasers for inertial confinement fusion
[DE89-005469] N89-20443
Review of long-pulse laser development
[DE89-006514] N89-20459
EXCITATION
Discrete analysis of stochastic NMR
[DE89-007016] N89-20494
EXERCISE PHYSIOLOGY
New models to assess behavioral and physiological performance of animals during inhalation exposures
[PB89-128946] N89-20601
EXHAUST EMISSION
Design and testing of a dissociated methanol vehicle
[DE89-007051] N89-20483
EXPERIMENT DESIGN
The application of statistical experimental design to the development of low-density polymer foams
[DE89-006774] N89-20261
Isothermal dendritic growth: A low gravity experiment N89-20299
The first products made in space: Monodisperse latex particles N89-20318
Phase A study for the extension of the CAESAR scanner with a sensor module for the far infrared
[BCRS-88-09] N89-20539
Measurement of the cosmic ray iron spectrum above 60 GeV/n and design and calibration of a large isotopic compositional experiment N89-20915
EXPERT SYSTEMS
On-board automatic aid and advisory for pilots of control-impaired aircraft N89-20150
An expert system based intelligent control scheme for space bioreactors N89-20285
Applying expertise to data in the Geologist's Assistant expert system
[DE89-003463] N89-20574
The power of physical representations
[CWI-CS-R8819] N89-20612
DATMS: A framework for distributed assumption based reasoning
[DE89-006282] N89-20628
NEXT 2.0, an expert system shell for engineering applications
[NLR-MP-88015-U] N89-20653
Reliability and performance evaluation of systems containing embedded rule-based expert systems
[NASA-CR-181769] N89-20683
A local area network diagnostic assistant expert system
[DE89-003575] N89-20689
Human-computer interaction in distributed supervisory control tasks
[NASA-CR-184671] N89-20692
View graphs for GSFC Colloquium on OFMspert N89-20693
Use of artificial intelligence in supervisory control N89-20694
Intent inferencing with a model-based operator's associate
[REPT-88-2] N89-20695
OFMTutor: An operator function model intelligent tutoring system N89-20696
A survey of intelligent tutoring systems: Implications for complex dynamic systems N89-20697
Dynamic mechanical system design using qualitative and symbolic reasoning
[DE89-006771] N89-20706
The certainty factor model and its basis in probability theory
[CWI-CS-R8816] N89-20768
Activities report of the Division of Information Systems
[FOA-C-30499-3.3] N89-20919
EXPLOSIVES
Application of rigorous nonlinear regression to the decomposition kinetics of explosives
[DE89-007598] N89-20274
EXPOSURE
New models to assess behavioral and physiological performance of animals during inhalation exposures
[PB89-128946] N89-20601
EXTINCTION
Particle cloud combustion in reduced gravity N89-20311
EXTRAVEHICULAR ACTIVITY
Extravehicular activity at geosynchronous earth orbit
[NASA-CR-172112] N89-20181

F

FABRICATION
Finite element modeling of a hydroformed sheet metal cover
[DE89-006798] N89-20326
FACE CENTERED CUBIC LATTICES
Analysis of the strain-rate sensitivity at high strain rates in fcc and bcc metals
[DE89-005471] N89-20233
Studies of alternative-crystallization-phase nucleation
[DE89-007220] N89-20840
FACTORIZATION
Basis representations in large-scale linear programming software
[MA-50] N89-20649
A fast algorithm for reordering sparse matrices for parallel factorization
[DE89-007873] N89-20758
FAILURE
Welded joint integrity analysis: Relative criticality of weld defect and remote deformation
[AD-A203756] N89-20246
A comprehensive review of modeling of impact damage in ceramics
[AD-A203477] N89-20264
FAILURE ANALYSIS
On-board automatic aid and advisory for pilots of control-impaired aircraft N89-20150
Studies and analyses of the space shuttle main engine. Failure information propagation model data base and software
[NASA-CR-183586] N89-20198
Failure analysis of a Stirling engine heat pipe
[NASA-TM-101418] N89-20227
Environmental effects on the time dependent failure of non-oxide ceramics
[AD-A202391] N89-20250
Estimation of the Equivalent Initial Flow Size (EIFS) distribution and prediction of failure probabilities for different parameter variations
[FFA-TN-1987-35] N89-20525
Software reliability engineering
[DE89-006781] N89-20626
FAILURE MODES
Failure analysis of a Stirling engine heat pipe
[NASA-TM-101418] N89-20227
FAIRINGS
Evaluation of VSAERO in prediction of aerodynamic characteristics of helicopter hub fairings
[NASA-TM-101048] N89-20098
FAR INFRARED RADIATION
Phase A study for the extension of the CAESAR scanner with a sensor module for the far infrared
[BCRS-88-09] N89-20539
The galactic large-scale far-infrared emission observed by IRAS: Implications for the morphology, physical conditions, and energetics of dust in the interstellar medium N89-20914
FATIGUE (MATERIALS)
Environment-assisted aerospace fatigue problems in The Netherlands
[NLR-MP-88004-U] N89-20087
A prior knowledge based optimal Wiener filtering approach to ultrasonic scattering amplitude estimation
[DE89-007574] N89-20783
FATIGUE LIFE
Fatigue life prediction modeling for turbine hot section materials N89-20142
Results of inphase axial-torsional fatigue experiments on 304 stainless steel
[NASA-TM-101464] N89-20514
Current status of flight simulation fatigue crack growth concepts
[NLR-MP-88001-U] N89-20521
FATIGUE TESTS
Microstructural influence on low cycle fatigue strength of IMI550
[PNR90500] N89-20226
WISPER: Introducing variable-amplitude loading in wind turbine design
[NLR-MP-88017-U] N89-20552
FAULT TOLERANCE
The application of software fault tolerance to air traffic control: Study contract overview
[BR108567] N89-20114
Fault-tolerance of a neural network solving the traveling salesman problem
[NASA-CR-181798] N89-20698

FEDERAL BUDGETS
NASA authorization
[S-HRG-100-579] N89-20873
FEEDBACK CONTROL
Modal cost analysis of flexible structures: Modeling flexible structures for control design N89-20148
Active spacecraft potential control: An ion emitter experiment --- Cluster mission N89-20169
Identification of space shuttle main engine dynamics
[NASA-TM-101982] N89-20199
An extended Kalman filter based automatic frequency control loop N89-20351
Force-reflecting master-slave control and robotic control of a traction-drive differential pitch-yaw joint
[DE89-005107] N89-20480
Direct manipulation and other styles of man-machine interaction
[REPT-88-53] N89-20616
Optimal feedback control infinite dimensional parabolic evolution systems: Approximation techniques
[NASA-CR-181772] N89-20637
FERRITES
Literature search on kickers and septa for the Amsterdam Pulse Stretcher (APS)
[LINO-158] N89-20791
FERROELECTRICITY
A study of ferroelectricity in single crystal compounds of the type AFB5 and A3B2F12
[AD-A203610] N89-20849
FERROMAGNETIC MATERIALS
Eddy current inspection of ferromagnetic materials using pulsed magnetic saturation
[DE89-005339] N89-20493
FERROMAGNETISM
The Delft Ising system processor
[ISBN-9-09-001753-4] N89-20625
FERROUS METALS
Electrochemical considerations of crack growth in the ferrous alloys
[AD-A203811] N89-20247
FIBER COMPOSITES
An analysis of an incompressible, fiber-reinforced material subjected to finite strains in the direction of reinforcement N89-20201
Theoretical modelling and experimental characterization of flexible composites under finite deformation N89-20204
FIBER OPTICS
Symbols for communication circuit design and documentation
[DE88-013002] N89-20372
FIBER ORIENTATION
Theoretical modelling and experimental characterization of flexible composites under finite deformation N89-20204
FIBERS
Influences of muscle fiber composition and strength on EMG (electromyographic activity), spinal motion and load acceleration during a repetitive lifting task
[PB89-131221] N89-20607
FIELD ALIGNED CURRENTS
A numerical model of ionospheric convection derived from field-aligned currents and the corresponding conductivity --- ionosphere
[TRITA-EPP-88-03] N89-20571
FIELD THEORY (ALGEBRA)
A short tutorial on Lie algebras
[CWI-PM-R8802] N89-20745
FIELD THEORY (PHYSICS)
On particle antiparticle mirror symmetry
[USIP-88-06] N89-20786
Lattice gauge theory and Monte Carlo methods
[DE89-005666] N89-20856
FILE MAINTENANCE (COMPUTERS)
Development of the University of Maryland RAMCAD (Reliability and Maintainability Computer-Aided Design) for electronic systems
[AD-A203616] N89-20675
FILLERS
Weldability of 2519-T87 aluminum alloy
[AD-A203519] N89-20244
FINE STRUCTURE
Surface structures determined using electron diffraction
[DE89-006669] N89-20837
FINITE DIFFERENCE THEORY
Development and application of a program to calculate transonic flow around an oscillating three-dimensional wing using finite difference procedures
[NASA-CR-181744] N89-20093
The dynamic response at high-explosive inert-solid interface as predicted by finite difference/element computer programs
[DE89-007303] N89-20272
A calculation method for compressible three dimensional turbulent boundary layer flows
[VKI-TN-167] N89-20422
An explicit finite differences solver for the incompressible Reynolds averaged Navier-Stokes equations, optimized for the Alliant DSP 9000 computer
[VKI-TM-45] N89-20423
A numerical study of three moving grid methods for one-dimensional partial differential equations which are based on the method of lines
[CWI-NM-R8806] N89-20741
On automatic differentiation
[DE89-005779] N89-20752
FINITE ELEMENT METHOD
Structural Tailoring of Advanced Turboprops (STAT) programmer's manual
[NASA-CR-182164] N89-20132
Error localization and updating of spacecraft structures mathematical models
[ESA-CR(P)-2697] N89-20186
Finite element applications to explore the effects of partial bonding on metal matrix composite properties
[NASA-TM-101482] N89-20206
The dynamic response at high-explosive inert-solid interface as predicted by finite difference/element computer programs
[DE89-007303] N89-20272
Finite element modeling of a hydroformed sheet metal cover
[DE89-006798] N89-20326
Navier-Stokes prediction of the three dimensional flow-field of jets in a crossflow using the finite element method N89-20408
Computational studies in nonlinear fracture mechanics N89-20508
A refined theory for plate bending with optimized stress field N89-20510
Theoretical and computational studies in plasticity and fracture N89-20511
Postbuckling Finite Element (FE) analysis of a stiffened curved panel loaded in shear
[FFA-TN-1988-23] N89-20516
Implementation of a hierarchical wedge element in the self-adaptive Finite Element (FE) program STRIPE
[FFA-TN-1988-36] N89-20517
Bulging cracks in pressurized fuselages: A numerical study
[NLR-MP-87058-U] N89-20519
Adaptive FE algorithm for variational inequality problems
[PB89-111512] N89-20634
User's manual for DYNA2D: An explicit two-dimensional hydrodynamic finite element code with interactive rezoning and graphical display
[DE89-006695] N89-20647
Finite element technique for the inverse problem of a partial differential equation and its application to parameter identification of structure
[PB89-111439] N89-20713
A finite element stability analysis for the Marangoni problem in a rectangular container with rigid sidewalls
[TW-285] N89-20735
A numerical study of three moving grid methods for one-dimensional partial differential equations which are based on the method of lines
[CWI-NM-R8806] N89-20741
HARTFEM: A finite element program for thermal and viscoplastic deformation problems
[DE89-007788] N89-20755
FINITE VOLUME METHOD
Multigrid and defect correction for the steady Navier-Stokes equation
[CWI-NM-R8803] N89-20424
FIRES
New models to assess behavioral and physiological performance of animals during inhalation exposures
[PB89-128946] N89-20601
FISHERIES
Utilizing remote sensing of thematic mapper data to improve our understanding of estuarine processes and their influence on the productivity of estuarine-dependent fisheries
[NASA-CR-183417] N89-20533
FIXED POINT ARITHMETIC
Quantization analysis of the real-time SAR digital image formation processor
[DE89-007533] N89-20754
FLAME PROPAGATION
Particle cloud combustion in reduced gravity N89-20311
Scientific support for an orbiter middeck experiment on solid surface combustion N89-20312
Particle cloud mixing in microgravity
[NASA-TM-101484] N89-20321
FLAME STABILITY
Modeling of hydrogen-air diffusion flame
[NASA-CR-184844] N89-20218
FLAMES
Investigation of spray dispersion and particulate formation in diesel fuel flames
[NASA-CR-184820] N89-20215
FLARE STARS
Aperture synthesis observations of solar and stellar radio emission N89-20912
FLASHOVER
Workshop on Transient Induced Insulator Flashover in Vacuum
[DE89-006727] N89-20398
FLAT PLATES
Multigrid solution of the Navier-Stokes equations on triangular meshes
[NASA-CR-181786] N89-20095
FLEXIBILITY
Theoretical modelling and experimental characterization of flexible composites under finite deformation N89-20204
FLEXIBLE BODIES
Modal cost analysis of flexible structures: Modeling flexible structures for control design N89-20148
Flexible structure control laboratory development and technology demonstration
[NASA-CR-184887] N89-20151
Modeling and control of flexible structures
[NASA-CR-184862] N89-20152
Modeling flexibility of mechanisms with ADAMS
[ESA-STM-242] N89-20518
FLIGHT CHARACTERISTICS
Airworthiness and flight characteristics evaluation of an improved engine air filtration system on the UH-1H helicopter
[AD-A203446] N89-20145
FLIGHT PATHS
The application of trajectory prediction algorithms for planning purposes in the Netherlands Air Traffic Control (ATC) system
[NLR-MP-87031-U] N89-20115
FLIGHT SAFETY
Improved computer simulation of the TCAS 3 circular array mounted on an aircraft
[NASA-CR-184907] N89-20363
FLIGHT TEST INSTRUMENTS
The data acquisition system for the Fokker 100 test aircraft
[NLR-MP-87047-U] N89-20130
FLIGHT TESTS
Hub and blade structural loads measurements of an SA349/2 helicopter
[NASA-TM-101040] N89-20124
Airworthiness and flight characteristics evaluation of an improved engine air filtration system on the UH-1H helicopter
[AD-A203446] N89-20145
Dendritic growth and structure of undercooled nickel base alloys N89-20302
Coupled rotor/fuselage dynamic analysis of the AH-1G helicopter and correlation with flight vibrations data
[NASA-CR-181723] N89-20512
FLOATING
Analysis of the dynamics of guided rotating free center plates N89-20466
FLOW CHARACTERISTICS
Resolution requirements for numerical simulations of transition
[NASA-CR-181799] N89-20411
A simple nonlinear model for the return to isotropy in turbulence
[NASA-CR-181797] N89-20412
FLOW DISTRIBUTION
Performance and test section flow characteristics of the National Full-Scale Aerodynamics Complex 40- by 80-foot wind tunnel
[NASA-TM-101065] N89-20086
Viscous shock layer analysis of hypersonic flows over long slender vehicles N89-20097
Aerodynamic pressure and flow-visualization measurement from a rotating wind turbine blade
[DE89-000854] N89-20104
Updated users' guide for TAWFIVE with multigrid
[NASA-TM-4109] N89-20409
Computational fluid dynamics and aerothermodynamics
[NASA-CR-180079] N89-20415
La Recherche Aerospatiale, bimonthly bulletin, number 1988-2, 243/January-February
[ESA-TT-1134] N89-20417
Hybrid single-particle Lagrangian integrated trajectories (HY-SPLIT): Model description
[PB89-127591] N89-20559

FLOW EQUATIONS
Viscous shock layer analysis of hypersonic flows over long slender vehicles N89-20097
A simple nonlinear model for the return to isotropy in turbulence
[NASA-CR-181797] N89-20412
Differential equations of viscous fluid flow in general conditions
[REPT-88-57] N89-20419
Who's afraid of nonsymmetric matrices? A discussion of elementary iterative methods
[REPT-88-49] N89-20723
High performance preconditioning — elliptical partial differential equations
[REPT-88-54] N89-20725
FLOW GEOMETRY
A cell-vertex multigrid method for the Navier-Stokes equations
[NASA-TM-101557] N89-20101
The Cerenkov free-electron laser
[AD-A203531] N89-20464
FLOW MEASUREMENT
Base flow investigation behind axi-and non-axisymmetric blunt bodies
[ISL-CO-246/87] N89-20103
Control-volume based Navier-Stokes equation solver valid at all flow velocities
[NASA-TM-101488] N89-20407
Dynamic wall pressure measurements
[AD-A203551] N89-20427
The development and structure of nocturnal slope winds in a simple valley
[AD-A203427] N89-20593
FLOW STABILITY
An analytical and numerical study of axial flow compressor instability N89-20131
FLOW VELOCITY
Quantification of environmental chambers by air velocity mapping
[AD-A200923] N89-20154
FLOW VISUALIZATION
La Recherche Aerospatiale, bimonthly bulletin, number 1988-2, 243/January-February
[ESA-TT-1134] N89-20417
Flow visualization of time-varying structural characteristics of dean vortices in a curved channel
[AD-A203875] N89-20429
FLUCTUATION THEORY
Investigation of extensions to the distorted Born approximation in strong fluctuation theory
[AD-A203698] N89-20378
FLUID DYNAMICS
The dynamics of free liquid drops N89-20316
Dispersion of dense gas releases in a wind tunnel
[PB89-118509] N89-20561
FLUID FLOW
Microgravity Science and Applications Flight Programs, January - March 1987, selected papers, volume 1
[NASA-TM-4069-VOL-1] N89-20276
Continuous flow electrophoresis system experiments on shuttle flights STS-6 and STS-7 N89-20277
A comparative study of the influence of buoyancy driven fluid flow on GaAs crystal growth N89-20295
Microgravity science at Langley Research Center N89-20298
Electromagnetic, heat and fluid flow phenomena in levitated metal droplets both under earthbound and microgravity conditions N89-20315
A relativistic fluid code for high-power microwave propagation
[DE89-006598] N89-20375
FLUIDS
Microgravity Science and Applications Flight Programs, January - March 1987, selected papers, volume 2
[NASA-TM-4069-VOL-2] N89-20305
Critical fluid light scattering N89-20320
FLUORESCENCE
Analysis of brass alloys by wavelength dispersive X-ray spectrometry
[DE89-007595] N89-20243
FLUORIDES
New vinylidene fluoride copolymers: Poly(vinyl acetate-co-Vinylidene fluoride)
[AD-A203939] N89-20270
Acoustic containerless experiment system: A non-contact surface tension measurement N89-20308
FLUOROCARBONS
New approaches to fluorocarbon synthesis
[AD-A203641] N89-20221
FLUOROPOLYMERS
New approaches to fluorocarbon synthesis
[AD-A203641] N89-20221
FLUTTER ANALYSIS
Development and application of a program to calculate transonic flow around an oscillating three-dimensional wing using finite difference procedures
[NASA-CR-181744] N89-20093
Some low-speed flutter characteristics of simple low-aspect-ratio delta wing models
[NASA-TM-101547] N89-20094
FLUX VECTOR SPLITTING
Flux vector splitting in general curvilinear coordinates
[PB89-127393] N89-20410
FLYBY MISSIONS
To Uranus and beyond
[NASA-EP-260] N89-20902
FOAMS
The application of statistical experimental design to the development of low-density polymer foams
[DE89-006774] N89-20261
FOCUSING
DSN 70-meter antenna X-band gain, phase, and pointing performance, with particular application for Voyager 2 Neptune encounter N89-20353
The Cerenkov free-electron laser
[AD-A203531] N89-20464
FOKKER AIRCRAFT
The data acquisition system for the Fokker 100 test aircraft
[NLR-MP-87047-U] N89-20130
FOKKER-PLANCK EQUATION
Nonnormal accelerations due to yielding in a primary structure
[PB89-131437] N89-20513
FORCED CONVECTION
The influences of convection on directional solidification of eutectic Bi/MnBi N89-20303
FORECASTING
Scenarios for future climate change: Results of GCM (General Circulation Model) simulations
[DE89-006151] N89-20585
FORMALISM
Elements of design, unifying principles and applications N89-20465
An exploration of the Bird-Meertens formalism
[CS-8810] N89-20658
FORMING TECHNIQUES
Nondestructive tests of elements manufactured using diffusion bonding and superplastic forming
[ETN-89-94131] N89-20492
FORMULAS (MATHEMATICS)
Formula related to the Cayley-Hamilton equation
[PB89-128003] N89-20711
FOURIER ANALYSIS
Fortran codes for computing the space-time correlations of turbulent flow in a channel
[AD-A203749] N89-20678
Diffraction theory for polygonal apertures
[AD-A203778] N89-20802
FOURIER TRANSFORMATION
Quantization analysis of the real-time SAR digital image formation processor
[DE89-007533] N89-20754
FRACTALS
Multifractals
[DE88-705369] N89-20672
FRACTURE MECHANICS
Fatigue life prediction modeling for turbine hot section materials N89-20142
Thermal-mechanical behavior of thin films and laminates N89-20203
Finite element applications to explore the effects of partial bonding on metal matrix composite properties
[NASA-TM-101482] N89-20206
Electrochemical considerations of crack growth in the ferrous alloys
[AD-A203811] N89-20247
A comprehensive review of modeling of impact damage in ceramics
[AD-A203477] N89-20264
Ductile-regime turning of germanium and silicon
[NASA-TM-101231] N89-20322
Analysis of dynamic elastic-plastic fracture phenomena: Steady crack growth and transient loading of a stationary crack N89-20507
Computational studies in nonlinear fracture mechanics N89-20508
Green's function formulation of plane crack problems for general anisotropic materials N89-20509
Theoretical and computational studies in plasticity and fracture N89-20511
Analysis of crack opening behavior by application of a discretized strip yield model
[NLR-MP-87065-U] N89-20520
Current status of flight simulation fatigue crack growth concepts
[NLR-MP-88001-U] N89-20521
Fracture control guidelines for stress corrosion
[NLR-MP-88007-U] N89-20522
A stereological analysis of ductile fracture by microvoid coalescence
[DE89-000355] N89-20528
FRACTURES (MATERIALS)
Welded joint integrity analysis: Relative criticality of weld defect and remote deformation
[AD-A203756] N89-20245
FRACTURING
Near threshold fatigue curve based on the dislocation shielding model of fracture
[DE88-011854] N89-20527
FRAGMENTATION
A comprehensive review of modeling of impact damage in ceramics
[AD-A203477] N89-20264
Fragmentation of cosmic-string loops
[NASA-CR-184892] N89-20898
FREE BOUNDARIES
An efficient method for solving free-boundary problems
[REPT-88-63] N89-20727
FREE ELECTRON LASERS
High power induction free electron laser
[DE89-006208] N89-20444
Damage to silver coatings from high average power 1-micron laser
[DE89-005476] N89-20448
Simulation of superradiant free-electron lasers
[DE89-006156] N89-20451
Validity of 1D free-electron laser sideband models
[DE89-006284] N89-20452
Status of LBL/LLNL FEL (Free Electron Laser) research for two beam accelerator applications
[DE89-006656] N89-20453
Three dimensional numerical analysis of a high-gain free-electron laser
[DE89-006981] N89-20456
Preliminary studies of an infrared free-electron laser oscillator at the ATF(BNL)
[DE89-006982] N89-20457
The chirped-pulse free-electron laser
[DE89-006792] N89-20460
Amplified spontaneous emission in a single pass free electron laser
[DE89-007048] N89-20461
The Cerenkov free-electron laser
[AD-A203531] N89-20464
Proposed extended tuning range for the Los Alamos mid-infrared adjustable, coherent light experiment (MIRACLE) facility
[DE89-006550] N89-20798
FREE FLOW
Antibody enhancement of free-flow electrophoresis N89-20290
The dynamics of free liquid drops N89-20316
FREQUENCIES
High-dynamic GPS tracking
[NASA-CR-184868] N89-20113
FREQUENCY ASSIGNMENT
SUM (Spectrum Use Measure) data base: A new measure of spectrum use
[PB89-108674] N89-20328
FREQUENCY MEASUREMENT
The ogive as a RCS compact range standard
[NASA-CR-184832] N89-20358
FREQUENCY RANGES
SUM (Spectrum Use Measure) data base: A new measure of spectrum use
[PB89-108674] N89-20328
The ogive as a RCS compact range standard
[NASA-CR-184832] N89-20358
FREQUENCY RESPONSE
The ogive as a RCS compact range standard
[NASA-CR-184832] N89-20358
Realization and generalized frequency response for nonlinear input-output maps
[RR-336] N89-20732
FREQUENCY STANDARDS
The ogive as a RCS compact range standard
[NASA-CR-184832] N89-20358
FRICTION
Design, development and applications of novel techniques for studying surface mechanical properties
[NASA-TM-101959] N89-20253
A new algorithm for modeling friction in dynamic mechanical systems N89-20334
FRONTS (METEOROLOGY)
Relationship of wind shear, buoyancy and radar tops to severe weather, 1988
[PB89-122519] N89-20581
Boundary layer structure and dynamics in outer hurricane rainbands N89-20583

FUEL CELLS
Heat and mass transport in fuel cell electrodes
[DE89-006378] N89-20548
FUEL COMBUSTION
Effects of turbulence on rate of combustion of fuel sprays N89-20212
Investigation of spray dispersion and particulate formation in diesel fuel flames
[NASA-CR-184820] N89-20215
Diffusive burning of plane liquid and spray jets in a coflowing oxidizer stream N89-20216
Particle cloud combustion in reduced gravity N89-20311
Scientific support for an orbiter middeck experiment on solid surface combustion N89-20312
Droplet combustion at reduced gravity N89-20313
Kinetic modeling of NOx formation and destruction and combustibles burnout
[PB89-124358] N89-20560
FUEL INJECTION
Investigation of spray dispersion and particulate formation in diesel fuel flames
[NASA-CR-184820] N89-20215
FUEL SPRAYS
Investigation of spray dispersion and particulate formation in diesel fuel flames
[NASA-CR-184820] N89-20215
FUNCTION GENERATORS
Using random number generators on the sensor signal processing system
[AD-A203702] N89-20761
FUNCTIONALS
Complex-valued functionals in variational analysis of waveguides with impedance boundaries
[PB89-128896] N89-20361
FUSELAGES
Bulging cracks in pressurized fuselages: A numerical study
[NLR-MP-87058-U] N89-20519
FUSION REACTORS
Achieving adequate beam quality for commercial laser fusion reactors
[DE89-007474] N89-20462

G

GALACTIC CLUSTERS
Isophotometry of brightest elliptical galaxies in rich clusters N89-20879
GALACTIC EVOLUTION
The high-redshift evolution of radio galaxies and quasars N89-20887
Cosmology and superstrings N89-20891
GALACTIC STRUCTURE
Isophotometry of brightest elliptical galaxies in rich clusters N89-20879
The galactic large-scale far-infrared emission observed by IRAS: Implications for the morphology, physical conditions, and energetics of dust in the interstellar medium N89-20914
GALERKIN METHOD
A hybrid-perturbation-Galerkin technique which combines multiple expansions
[NASA-CR-181781] N89-20632
GALLIUM ARSENIDES
A comparative study of the influence of buoyancy driven fluid flow on GaAs crystal growth N89-20295
Growth of GaAs crystals from the melt in a partially confined configuration N89-20296
Characterization of production GaAs solar cells for space
[NASA-CR-184863] N89-20549
Ultrafast physics in microstructure and alloy systems
[AD-A203839] N89-20850
GAMMA RAY ASTRONOMY
Study of ultra-high energy emission from Cygnus X-3 and Hercules X-1
[DE89-004543] N89-20911
Cosmic ray tracking: A new approach to high energy gamma-astronomy
[HD-PY88/05] N89-20916
GAMMA RAY BURSTS
Study of ultra-high energy emission from Cygnus X-3 and Hercules X-1
[DE89-004543] N89-20911
GAS FLOW
A dynamic flow-weighted pore size distribution test
[DE89-006191] N89-20260
Scientific support for an orbiter middeck experiment on solid surface combustion N89-20312
GAS HEATING
Feasibility of a complex compound heat pump
[PB89-115273] N89-20405
GAS TURBINE ENGINES
Toward improved durability in advanced aircraft engine hot sections
[NASA-TM-4087] N89-20135
NASA HOST project overview N89-20136
Assessment, development, and application of combustor aerothermal models N89-20138
Review and assessment of the database and numerical modeling for turbine heat transfer N89-20139
Structural analysis methods development for turbine hot section components N89-20140
Structural analysis applications N89-20141
Fatigue life prediction modeling for turbine hot section materials N89-20142
Life modeling of thermal barrier coatings for aircraft gas turbine engines N89-20143
Views on the impact of HOST N89-20144
High speed balancing applied to the T700 engine
[NASA-CR-180899] N89-20472
GASEOUS DIFFUSION
Diffusive burning of plane liquid and spray jets in a coflowing oxidizer stream N89-20216
A dynamic flow-weighted pore size distribution test
[DE89-006191] N89-20260
GASES
Current status of the NAVSEA Backscatter Absorption Gas Imaging (BAGI) development project
[DE89-006728] N89-20438
Dispersion of dense gas releases in a wind tunnel
[PB89-118509] N89-20561
GAUGE INVARIANCE
On heterotic supermanifolds
[DE88-705339] N89-20773
GAUGE THEORY
Lattice gauge theory and Monte Carlo methods
[DE89-005666] N89-20856
GAUSSIAN ELIMINATION
On the equivalence of Gaussian elimination and Gauss-Jordan reduction in solving linear equations
[NASA-TM-101466] N89-20710
GENERAL AVIATION AIRCRAFT
Aircraft accident reports, brief format, US civil and foreign aviation, issue number 14 of 1986 accidents
[PB88-916904] N89-20110
GEOCHEMISTRY
Geological data integration techniques: Proceedings
[DE88-705255] N89-20868
GEOGRAPHIC INFORMATION SYSTEMS
Utility of a geographic information system in modelling climatic suitability
[PB89-109516] N89-20578
GEOLOGY
Applying expertise to data in the Geologist's Assistant expert system
[DE89-003463] N89-20574
Geological data integration techniques: Proceedings
[DE88-705255] N89-20868
GEOMETRY
The 1987 year end report for road following at Canegie Mellon
[AD-A203946] N89-20488
Soliton geometry and the vacuum gravitational field equations
[DE88-705340] N89-20573
Piecewise continuous algebraic surfaces in terms of B-splines
[PB89-109136] N89-20712
GEOPHYSICS
Simultaneous inversion of vector and total field aeromagnetic data using Bayesian inference: A case study from the Cobb Offset of the Juan de Fuca Ridge
[PB89-114193] N89-20599
Solar-geophysical data number 530, October 1988. Part 2: (Comprehensive reports). Data for April 1988 and miscellaneous
[PB89-130827] N89-20908
Solar-geophysical data number 530, October 1988. Part 1: (Prompt reports). Data for September, August 1988 and late data
[PB89-130835] N89-20909
GERMANIUM
Ductile-regime turning of germanium and silicon
[NASA-TM-101231] N89-20322
Germanium blocked impurity band infrared detectors
[DE89-006607] N89-20796
GIBBS FREE ENERGY
On the dimerization of linear polymers
[DE88-705341] N89-20256
GLASS
Crystallization kinetics of BaO-Al2O3-SiO2 glasses
[NASA-TM-101964] N89-20252
Microgravity Science and Applications Flight Programs, January - March 1987, selected papers, volume 2
[NASA-TM-4069-VOL-2] N89-20305
Fluoride glass: Crystallization, surface tension N89-20306
Containerless processing of glass forming melts in space N89-20307
Acoustic containerless experiment system: A non-contact surface tension measurement N89-20308
Crystal nucleation in lithium borate glass N89-20309
Physical phenomena in containerless glass processing N89-20310
Effect of surface stress on stress corrosion of silicate glass
[DE89-004584] N89-20529
GLOBAL POSITIONING SYSTEM
High-dynamic GPS tracking
[NASA-CR-184868] N89-20113
Future satellite navigation systems, with emphasis on NAVSTAR GPS
[NLR-MP-87034-U] N89-20116
The Telecommunications and Data Acquisition Report
[NASA-CR-184572] N89-20329
Deriving a geocentric reference frame for satellite positioning and navigation N89-20330
Determination of GPS orbits to submeter accuracy N89-20331
Efficient detection and signal parameter estimation with applications to high dynamic GPS receivers
[NASA-CR-184861] N89-20362
A comparison of frequency estimation techniques for high-dynamic trajectories
[NASA-CR-184865] N89-20387
GLYCINE
Modelling the growth of triglycine sulphate crystals in Spacelab 3 N89-20294
GLYCOLS
Thermogravimetric analysis of polymeric materials for an intermediate temperature solid electrolyte. 2: Polymer mixtures
[DE89-006980] N89-20262
GOLD
Effects of environment on tunneling spectroscopy of gold films
[DE89-006040] N89-20844
GOVERNMENTS
Report on federal information dissemination: Responses to decision analysis framework for GPO (Government Printing Office) strategic alternatives
[PB89-114649] N89-20864
GRAIN BOUNDARIES
Anion grain boundary diffusion in Cr2O3 and Cr2O3-0.09 weight percent Y2O3
[DE89-006281] N89-20833
Grain boundary kinetics. Part 2: In-situ observation of the role of grain boundary dislocations in high-angle boundary migration
[DE89-006791] N89-20838
A first-principles method for the determination of the electronic structure of grain boundaries
[DE89-006148] N89-20845
A micromechanical viscoplastic stress-strain model with grain boundary sliding
[DE89-007712] N89-20848
GRAVITATION
Einsteins's theory of gravity in Fierz variables
[DE88-705004] N89-20854
GRAVITATIONAL EFFECTS
Microgravity Science and Applications Flight Programs, January - March 1987, selected papers, volume 1
[NASA-TM-4069-VOL-1] N89-20276
Cellular effects of microgravity N89-20289
Protein crystal growth in a microgravity environment N89-20292
Growth of mercuric iodide (HgI2) for nuclear radiation detectors N89-20293
A comparative study of the influence of buoyancy driven fluid flow on GaAs crystal growth N89-20295
The dynamics of free liquid drops N89-20316
USSR Space Life Sciences Digest, Issue 21
[NASA-CR-3922(24)] N89-20602
GRAVITATIONAL FIELDS
Soliton geometry and the vacuum gravitational field equations
[DE88-705340] N89-20573
General relativity, scalar fields and cosmic strings N89-20852
Remark on the gravitational field produced by an infinite straight string
[DE88-705077] N89-20855
GRAVITATIONAL PHYSIOLOGY
Cellular effects of microgravity N89-20289
GREEN'S FUNCTIONS
Green's function formulation of plane crack problems for general anisotropic materials N89-20509
GREENHOUSE EFFECT
Implications of the greenhouse effect for the midwest economy
[DE89-004195] N89-20563

The causes and consequences of global climate change
[DE89-004355] N89-20564
Scenarios for future climate change: Results of GCM (General Circulation Model) simulations
[DE89-006151] N89-20565
GRID GENERATION (MATHEMATICS)
An algorithm for automated quadrilateral mesh generation for planar regions
[DE89-007299] N89-20671
GROUND STATE
Ground state depleted laser experiments
[DE89-006146] N89-20449
Ground State Depleted (GSD) solid state lasers: Principles, characteristics, and scaling
[DE89-006149] N89-20450
GROUND WIND
Summary of meteorological observations, surface (SMOS) for Norfolk, Virginia
[AD-A203644] N89-20594
GUINEA PIGS
New models to assess behavioral and physiological performance of animals during inhalation exposures
[PB89-128946] N89-20601
GUST LOADS
On the relationship between matched filter theory as applied to gust loads and phased design loads analysis
[NASA-CR-181802] N89-20125

H

HADRONS
On the performance of the DELPHI hadron calorimeter
[PH-159] N89-20434
HALL EFFECT
Resonance tunnelling and breakdown of the Quantum Hall Effect (QHE) in strong electric fields
[DE88-705348] N89-20831
HAMILTONIAN FUNCTIONS
Localized versus itinerant picture of light-T(sub c) superconducting oxides
[DE88-705345] N89-20830
HANDLING EQUIPMENT
Application-based control of an autonomous mobile robot
[DE89-004380] N89-20477
HARDNESS
Hardness of amorphous hard carbon films determined by the ultra-low load microindentation technique
[DE89-006129] N89-20259
HARMONIC GENERATIONS
Optical second harmonic generation in metal monolayers and metal surfaces
[DE89-006123] N89-20234
HARMONIC OSCILLATION
Development and application of a program to calculate transonic flow around an oscillating three-dimensional wing using finite difference procedures
[NASA-CR-181744] N89-20093
HARMONIC OSCILLATORS
Integrable two dimensional supersystems
[DE88-705355] N89-20857
HAZARDS
Design and implementation of the hazard control box for the ride motion simulator
[AD-A203752] N89-20404
HEAT EXCHANGERS
Laser-based inspection technology for fossil heat exchanger tubing
[DE89-005811] N89-20495
Commercial direct absorption receiver design studies
[DE89-007290] N89-20556
HEAT FLUX
Laser diode cooling for high average power applications
[DE89-006777] N89-20454
HEAT MEASUREMENT
Fluorine as an oxidant in combustion calorimetry
[DE89-003626] N89-20214
Application of rigorous nonlinear regression to the decomposition kinetics of explosives
[DE89-007598] N89-20274
HEAT PIPES
Failure analysis of a Stirling engine heat pipe
[NASA-TM-101418] N89-20227
HEAT PUMPS
Feasibility of a complex compound heat pump
[PB89-115273] N89-20405
Zeolite/methanol: The adsorption heat pump
[DE88-756310] N89-20413
HEAT RESISTANT ALLOYS
Structural analysis methods development for turbine hot section components N89-20140
Fatigue life prediction modeling for turbine hot section materials N89-20142
HEAT TRANSFER
Documentation of two- and three-dimensional hypersonic shock wave/turbulent boundary layer interaction flows
[NASA-TM-101075] N89-20100
Review and assessment of the database and numerical modeling for turbine heat transfer N89-20139
Electromagnetic, heat and fluid flow phenomena in levitated metal droplets both under earthbound and microgravity conditions N89-20315
Flow visualization of time-varying structural characteristics of dean vortices in a curved channel
[AD-A203875] N89-20429
Heat and mass transport in fuel cell electrodes
[DE89-006378] N89-20548
Commercial direct absorption receiver design studies
[DE89-007290] N89-20556
HARTFEM: A finite element program for thermal and viscoplastic deformation problems
[DE89-007788] N89-20755
HEAT TREATMENT
Mechanical properties of modified low cobalt powder metallurgy Udimet 700 type alloys
[NASA-TM-101481] N89-20228
Weldability of 2519-T87 aluminum alloy
[AD-A203519] N89-20244
Thermal stability of jet fuel
[DE89-006754] N89-20273
HEAVY IONS
Heavy ion induction linac drivers for inertial confinement fusion
[DE89-006603] N89-20810
HELICOPTER DESIGN
Active control helicopter aeromechanical and aeroelastic instabilities N89-20149
HELICOPTER PERFORMANCE
Hub and blade structural loads measurements of an SA349/2 helicopter
[NASA-TM-101040] N89-20124
HELICOPTER WAKES
Evaluation of VSAERO in prediction of aerodynamic characteristics of helicopter hub fairings
[NASA-TM-101048] N89-20098
HELIUM IONS
Experiments with negative ions in (3)He superfluids
[PB89-127682] N89-20814
HELIUM ISOTOPES
Quasi-classical calculations for superfluids
[ETN-89-94118] N89-20421
HELMETS
SPH-4 helmet retention assembly reinforcement
[AD-A200432] N89-20614
HERMES MANNED SPACEPLANE
Breadboard test-software and wrist joint modeling for Hermes robot arm
[ETN-89-94155] N89-20475
HERTZSPRUNG-RUSSELL DIAGRAM
Grids of evolutionary models from 0.85 to 120 solar masses: Observational tests and the mass limits
[SER-C-PREPUBL-FASC-29] N89-20882
Tables of evolutionary star models from 0.85 to 120 solar masses with overshooting and mass loss
[SER-C-PREPUBL-FASC-30] N89-20883
HESSIAN MATRICES
Inertia-controlling methods for quadratic programming
[DE89-006996] N89-20667
An analysis of reduced Hessian methods for constrained optimization
[AD-A201078] N89-20715
HETEROGENEITY
Heterogeneity in the growth hormone pituitary gland system of rats and humans: Implications to microgravity based research N89-20279
The structure and reactivity of heterogeneous surfaces and study of the geometry of surface complexes
[DE89-005726] N89-20822
HEURISTIC METHODS
Parallel algorithms for PDE solvers
[AD-A199625] N89-20630
HIERARCHIES
A class Hierarchical, object-oriented approach to virtual memory management
[NASA-CR-184876] N89-20646
HIGH ELECTRON MOBILITY TRANSISTORS
On 32-GHz cryogenically cooled HEMT low-noise amplifiers N89-20336
HIGH ENERGY INTERACTIONS
On the performance of the DELPHI hadron calorimeter
[PH-159] N89-20434
HIGH GAIN
Three dimensional numerical analysis of a high-gain free-electron laser
[DE89-006981] N89-20456
HIGH POWER LASERS
High power induction free electron laser
[DE89-006208] N89-20444
Damage to silver coatings from high average power 1-micron laser
[DE89-005476] N89-20448
HIGH PRESSURE
High pressure Raman spectroscopy of TiO2 thin films
[DE89-006937] N89-20839
HIGH RESOLUTION
Using depth recovery in humans
[AD-A201278] N89-20606
HIGH SPEED
High speed balancing applied to the T700 engine
[NASA-CR-180899] N89-20472
HIGH SPEED PHOTOGRAPHY
Laser illuminated high speed photography of energetic materials and components with a copper vapor laser
[DE89-006379] N89-20458
HIGH TEMPERATURE
The emittance of space radiator materials measured at elevated temperatures
[NASA-TM-101948] N89-20193
Radiative heat transfer augmentation in high temperature combustion systems with application to radiant tube burners
[PB89-133805] N89-20217
Thermal stability of jet fuel
[DE89-006754] N89-20273
HIGH TEMPERATURE ENVIRONMENTS
Views on the impact of HOST N89-20144
HIGH TEMPERATURE LUBRICANTS
Long term lubrication of ceramics at high temperatures N89-20249
HIGH TEMPERATURE PLASMAS
Low frequency MHD instability in a hot electron plasma
[PB89-111546] N89-20803
Extreme ultraviolet and soft X-ray diagnostics of high-temperature plasmas
[DE89-007070] N89-20808
HIGH TEMPERATURE RESEARCH
Toward improved durability in advanced aircraft engine hot sections
[NASA-TM-4087] N89-20135
Advanced high temperature instrument for hot section research applications N89-20137
Structural analysis methods development for turbine hot section components N89-20140
HIGH TEMPERATURE SUPERCONDUCTORS
Electron spectroscopy studies of high temperature superconductors: Y(sub 1)-xPr(sub x)Ba2Cu3O(sub 7)-delta
[DE89-006554] N89-20824
Some structural features of high-T(sub c) superconductors
[DE89-006667] N89-20826
Feasibility study of high temperature superconductor opening switches
[AD-A203689] N89-20851
HIGH TEMPERATURE TESTS
Static tensile and tensile creep testing of five ceramic fibers at elevated temperatures
[NASA-CR-184690] N89-20200
HILBERT SPACE
Well-posedness of infinite-dimensional linear systems in time and frequency domain
[TW-287] N89-20771
Robust stability of normalized coprime factors: The infinite dimensional case
[TW-291] N89-20772
HISTORIES
The effect of deformation history on the morphology and properties of blends of polycarbonate and a thermotropic liquid crystalline polymers
[AD-A203632] N89-20267
Astrophysics in a nutshell: From the telescope to the Sputnik
[TRITA-EPP-88-04] N89-20897
HOLES (MECHANICS)
Prediction model for the onset of edge-effect delamination at holes in composite laminates N89-20202
HORIZONTAL ORIENTATION
WISPER: Introducing variable-amplitude loading in wind turbine design
[NLR-MP-88017-U] N89-20552
HORMONES
Hormone purification by isoelectric focusing in space N89-20282
Biochemical assays on plasminogen activators and hormones from kidney sources N89-20287
HORN ANTENNAS
Anechoic chamber evaluation at 85 GHz
[PB89-125199] N89-20153

Geometrical optics design of a compact range Gregorian subreflector system by the principle of the central ray
[NASA-CR-184810] N89-20795

HOT SURFACES
Structural analysis methods development for turbine hot section components N89-20140

HOVERING
Thrust generation by an airfoil in hovering mode
[AD-A203785] N89-20106

HUBBLE DIAGRAM
Has the Universe an origin
[TRITA-EPP-88-07] N89-20898

HUBBLE SPACE TELESCOPE
Space Science: Status of the Hubble Space Telescope Program
[GAO/NSIAD-88-118BR] N89-20881

HUBS
Evaluation of VSAERO in prediction of aerodynamic characteristics of helicopter hub fairings
[NASA-TM-101048] N89-20098
Hub and blade structural loads measurements of an SA349/2 helicopter
[NASA-TM-101040] N89-20124

HUMAN BEINGS
Using depth recovery in humans
[AD-A201278] N89-20606

HUMAN FACTORS ENGINEERING
Extravehicular activity at geosynchronous earth orbit
[NASA-CR-172112] N89-20181
User interfaces and highly interactive systems: Survey of current research
[REPT-88-60] N89-20617

HUMAN PERFORMANCE
USSR Space Life Sciences Digest, Issue 21
[NASA-CR-3922(24)] N89-20602
Cognitive psychology at the Institute for Perception
[IZF-1987-41] N89-20611

HUMAN REACTIONS
The evaluation of impulsive noise
[NPL-AC-111] N89-20780

HURRICANES
Boundary layer structure and dynamics in outer hurricane rainbands N89-20583

HYDRAULIC CONTROL
Application of parameter adaptive approach to servo control of a hydraulic manipulator
[MA-51] N89-20473

HYDROCARBON FUELS
Kinetic modeling of NOx formation and destruction and combustibles burnout
[PB89-124358] N89-20560

HYDROCARBONS
Infrared spectroscopy of weakly bound molecular ions
[DE89-006602] N89-20787

HYDRODYNAMICS
Hydrodynamic effects on cell growth in agitated microcarrier bioreactors N89-20284
User's manual for DYNA2D: An explicit two-dimensional hydrodynamic finite element code with interactive rezoning and graphical display
[DE89-006695] N89-20647
Star formation, using 3-D explicit Eulerian hydrodynamics N89-20890

HYDROGEN
Study of vibrational and rapid local motions of hydrogen in the storage compound Ti0.8Zr0.2 CrMnH3 by slow neutron scattering
[DE88-704797] N89-20213
Modeling of hydrogen-air diffusion flame
[NASA-CR-184844] N89-20218

HYDROGEN ENGINES
Advanced technology for future space propulsion systems
[NASA-TM-101951] N89-20192

HYDROGEN IONS
Condensation and storage of hydrogen cluster ions
[AD-A203801] N89-20223

HYDROGEN OXYGEN FUEL CELLS
Mars manned transportation vehicle
[NASA-TM-101487] N89-20545

HYDROGRAPHY
Current velocity and hydrographic observations in the southwestern North Atlantic Ocean: Subtropical Atlantic Climate Studies (SACS), 1987
[PB89-114011] N89-20598

HYPERBOLIC FUNCTIONS
Domain decomposition methods for systems of conservation laws: Spectral collocation approximations
[NASA-CR-181773] N89-20635

HYPERCUBE MULTIPROCESSORS
Hypercube matrix computation task
[NASA-CR-184869] N89-20642
A message passing kernel for the hypercluster parallel processing test bed
[NASA-TM-101952] N89-20684
Initial operating capability for the hypercluster parallel-processing test bed
[NASA-TM-101953] N89-20685
Multiprogramming a distributed-memory multiprocessor
[DE89-007850] N89-20690
A concurrent approach to model based motion detection
[DE89-007853] N89-20708

HYPERGEOMETRIC FUNCTIONS
Uniform asymptotic expansions of a class of integrals in terms of modified Bessel functuons, with application to confluent hypergeometric functions
[CWI-AM-R8806] N89-20738

HYPERSONIC FLIGHT
Propulsion over a wide Mach number range
[NASA-CR-182267] N89-20134

HYPERSONIC FLOW
Viscous shock layer analysis of hypersonic flows over long slender vehicles N89-20097

HYPERSONIC SPEED
A first scramjet study
[NASA-CR-184965] N89-20146

HYSTERESIS
Nonnormal accelerations due to yielding in a primary structure
[PB89-131437] N89-20513

I

ICE
Active and passive remote sensing of ice
[AD-A203943] N89-20543

ICE FORMATION
Electromagnetic properties of ice coated surfaces
[NASA-CR-184780] N89-20355

IDENTIFYING
Combining segmentation and tracking for the classification of moving objects in video scenes
[DE89-007000] N89-20668

IGNITION
Laser ignition of energetic materials with a pulsed Nd:YAG laser
[DE89-006861] N89-20455

ILLUMINATING
Laser illuminated high speed photography of energetic materials and components with a copper vapor laser
[DE89-006379] N89-20458

IMAGE PROCESSING
Vision-based navigation for autonomous ground vehicles
[AD-A203712] N89-20120
SAR processing on the array processor NMX-432
[FOA-C-30503-3.3] N89-20367
Data compression as a means to disseminate more Meteosat data over the existing channel
[NLR-MP-86063-U] N89-20369
Linear feature extraction from radar imagery: SBIR (Small Business Innovative Research) phase 2, option 1
[AD-A203688] N89-20377
The effects of variations in the photocathode voltages of electronic streak cameras
[DE89-006776] N89-20436
Current status of the NAVSEA Backscatter Absorption Gas Imaging (BAGI) development project
[DE89-006728] N89-20438
The 1987 year end report for road following at Canegie Mellon
[AD-A203946] N89-20488
Discrete analysis of stochastic NMR
[DE89-007016] N89-20494
A displacement pattern matching application in elastic-plastic hybrid stress analysis
[AD-A199028] N89-20499
Using depth recovery in humans
[AD-A201278] N89-20606
Combining segmentation and tracking for the classification of moving objects in video scenes
[DE89-007000] N89-20668
Sensor capabilities for the HERMIES experimental robot
[DE89-003180] N89-20703
Integrating multiple views into a single representation of a range imaged object
[DE89-005921] N89-20707
A concurrent approach to model based motion detection
[DE89-007853] N89-20708
Quantization analysis of the real-time SAR digital image formation processor
[DE89-007533] N89-20754
Development of mathematical models for application in image processing
[AD-A203619] N89-20760
Digital processing of speckle images
[AD-A203703] N89-20801
Compensation for crystal penetration in high resolution positron tomography
[DE89-006660] N89-20836
Multicolor surface photometry of powerful radio galaxies N89-20878
SELSIS (the Space Environment Laboratory Solar Imaging System): Initial requirements
[PB89-113039] N89-20906

IMAGE RESOLUTION
The suitability of remote sensing for surveying and monitoring landscape patterns. Volume B: PEPS Project No. 73 - SPOT Imagery N89-20536

IMAGES
Image-projection ion-beam lithography
[DE89-005773] N89-20390
Localized versus itinerant picture of light-T(sub c) superconducting oxides
[DE88-705345] N89-20830

IMAGING SPECTROMETERS
AFE ion mass spectrometer design study
[NASA-CR-184838] N89-20432

IMAGING TECHNIQUES
Current status of the NAVSEA Backscatter Absorption Gas Imaging (BAGI) development project
[DE89-006728] N89-20438

IMPACT DAMAGE
A comprehensive review of modeling of impact damage in ceramics
[AD-A203477] N89-20264

IMPACT STRENGTH
Instrumented impact testing of composite materials
[AD-A203842] N89-20210
A comprehensive review of modeling of impact damage in ceramics
[AD-A203477] N89-20264

IMPACT TESTS
Instrumented impact testing of composite materials
[AD-A203842] N89-20210
SPH-4 helmet retention assembly reinforcement
[AD-A200432] N89-20614

IMPEDANCE
Complex-valued functionals in variational analysis of waveguides with impedance boundaries
[PB89-128896] N89-20361

IMPEDANCE MATCHING
Impedance matching of RF plasma
[PB89-112502] N89-20804

IMPULSES
Propagation of the nerve impulse under the effect of a magnetic field
[DE88-705371] N89-20608

IMPURITIES
Thermal stability of jet fuel
[DE89-006754] N89-20273
Germanium blocked impurity band infrared detectors
[DE89-006607] N89-20796
Resonance tunnelling and breakdown of the Quantum Hall Effect (QHE) in strong electric fields
[DE88-705348] N89-20831

IN-FLIGHT MONITORING
Flight motor set 360L001 (STS-26R), volume 1
[NASA-CR-183576] N89-20196

INCOMPRESSIBLE FLOW
Standard test case for a low speed, turbulent junction vortex flow
[PB89-110779] N89-20406
An explicit finite differences solver for the incompressible Reynolds averaged Navier-Stokes equations, optimized for the Alliant DSP 9000 computer
[VKI-TM-45] N89-20423

INDENTATION
Hardness of amorphous hard carbon films determined by the ultra-low load microindentation technique
[DE89-006129] N89-20259

INDEXES (DOCUMENTATION)
Aeronautical engineering: A cumulative index to a continuing bibliography (supplement 235)
[NASA-SP-7037(235)] N89-20088
Aeronautical engineering: A continuing bibliography with indexes (supplement 237)
[NASA-SP-7037(237)] N89-20089
Aeronautical engineering: A continuing bibliography with indexes (supplement 238)
[NASA-SP-7037(238)] N89-20090
Aeronautical engineering: A continuing bibliography with indexes (supplement 236)
[NASA-SP-7037(236)] N89-20091
3CPO, Cloud Chemistry and Cloud Physics Organization: Data index, June 1988
[DE89-007011] N89-20591
Medical subject headings, tree structures, 1989
[PB89-100028] N89-20605

INERTIA
Active vibration control of a large flexible manipulator by inertial force and joint torque
[NASA-CR-184786] N89-20470

INERTIAL CONFINEMENT FUSION
Development KrF lasers for inertial confinement fusion [DE89-005469] N89-20443
Achieving adequate beam quality for commercial laser fusion reactors [DE89-007474] N89-20462
Heavy ion induction linac drivers for inertial confinement fusion [DE89-006603] N89-20810
The Magnetically Insulated Inertial Confinement Fusion (MICF): A novel approach [DE89-007473] N89-20811
INERTIAL NAVIGATION
Trajectory scoring in rectangular coordinates using transponder-interrogator range and range rate data [DE89-007005] N89-20119
INFERENCE
Simultaneous inversion of vector and total field aeromagnetic data using Bayesian inference: A case study from the Cobb Offset of the Juan de Fuca Ridge [PB89-114193] N89-20599
Censoring, truncation and filtering in statistical models based on counting processes [CWI-MS-R8803] N89-20769
INFORMATION DISSEMINATION
Barriers to the international transfer of information in aerospace and defense N89-20861
Report on federal information dissemination: Responses to decision analysis framework for GPO (Government Printing Office) strategic alternatives [PB89-114649] N89-20864
Research and technology of the Lyndon Johnson Space Center [NASA-TM-100473] N89-20918
INFORMATION FLOW
Space operations: Testing of NASA's technical and management information system [GAO/IMTEC-88-28] N89-20859
INFORMATION MANAGEMENT
Space operations: Testing of NASA's technical and management information system [GAO/IMTEC-88-28] N89-20859
INFORMATION PROCESSING (BIOLOGY)
Precision in the perception of direction of a moving pattern [NASA-TM-101080] N89-20610
Componential analysis of pilot decision making [AD-A203711] N89-20613
INFORMATION RETRIEVAL
Assessing potential benefits for service/repair and retrieval of satellites: A pilot decision analysis [AD-A203630] N89-20190
Valiant's maximum algorithm with sequential memory accesses [AD-A203713] N89-20676
Integrating syntax, semantics, and discourse DARPA (Defense Advanced Research Projects Agency) natural language understanding program [AD-A203747] N89-20677
Using English for indexing and retrieving [AD-A202227] N89-20866
INFORMATION SYSTEMS
Research in distributed personal computer-based information systems, volume 1 [AD-A203780] N89-20629
Geological data integration techniques: Proceedings [DE88-705255] N89-20868
The DoD Gateway Information System (DGIS): The development toward artificial intelligence and hypermedia in common command language [AD-A203674] N89-20869
Research in distributed personal computer-based information systems, volume 2 [AD-A203845] N89-20870
INFORMATION THEORY
A communication channel model of the software process [NASA-CR-184866] N89-20643
INFORMATION TRANSFER
Barriers to the international transfer of information in aerospace and defense N89-20861
Supply and use of Japanese technical literature in the United States [PB88-230842] N89-20862
INFRARED DETECTORS
Germanium blocked impurity band infrared detectors [DE89-006607] N89-20796
INFRARED LASERS
Preliminary studies of an infrared free-electron laser oscillator at the ATF(BNL) [DE89-006982] N89-20457
INFRARED RADIATION
Preliminary studies of an infrared free-electron laser oscillator at the ATF(BNL) [DE89-006982] N89-20457
Radiation, turbulence and microphysics in the stratiform regions of tropical cloud clusters N89-20585
INFRARED SCANNERS
Phase A study for the extension of the CAESAR scanner with a sensor module for the far infrared [BCRS-88-09] N89-20539
INFRARED SPECTRA
The high-redshift evolution of radio galaxies and quasars N89-20887
INFRARED SPECTROSCOPY
Infrared spectroscopy of weakly bound molecular ions [DE89-006602] N89-20787
INFRARED STARS
Dust shells around Miras and OH/IR stars N89-20889
INJECTION
The chirped-pulse free-electron laser [DE89-006792] N89-20460
INSOLATION
The Mars climate for a photovoltaic system operation [NASA-TM-101994] N89-20385
INSPECTION
Welded joint integrity analysis: Relative criticality of weld defect and remote deformation [AD-A203756] N89-20246
Long-term evaluation of the acoustic emission weld monitor [PB88-122642] N89-20471
Development of a remote inspection robot and camera positioners for reactor tank inspection [DE89-004381] N89-20478
Eddy current inspection of ferromagnetic materials using pulsed magnetic saturation [DE89-005339] N89-20493
Laser-based inspection technology for fossil heat exchanger tubing [DE89-005811] N89-20495
INSULATION
The Magnetically Insulated Inertial Confinement Fusion (MICF): A novel approach [DE89-007473] N89-20811
INSULATORS
Workshop on Transient Induced Insulator Flashover in Vacuum [DE89-006727] N89-20398
INTEGRAL CALCULUS
A tutorial introduction to differentiable manifolds and calculus on manifolds [CWI-PM-R8803] N89-20746
INTEGRAL EQUATIONS
Three dimensional numerical analysis of a high-gain free-electron laser [DE89-006981] N89-20456
Combined algorithms in nonlinear problems of magnetostatics [DE89-006591] N89-20753
INTEGRALS
Uniform asymptotic expansions of a class of integrals in terms of modified Bessel functions, with application to confluent hypergeometric functions [CWI-AM-R8806] N89-20738
INTEGRATED CIRCUITS
Symbols for communication circuit design and documentation [DE88-013002] N89-20372
Image-projection ion-beam lithography [DE89-005773] N89-20390
INTERACTIONAL AERODYNAMICS
Updated users' guide for TAWFIVE with multigrid [NASA-TM-4109] N89-20409
INTERACTIVE CONTROL
Human-computer interaction in distributed supervisory control tasks [NASA-CR-184671] N89-20692
View graphs for GSFC Colloquium on OFMspert N89-20693
Use of artificial intelligence in supervisory control N89-20694
INTERFACES
Surface and interface local density of states for Nb, V and Ta [DE88-705365] N89-20240
Test report for the Direct Access Radar/National Airspace System (DARC/NAS) bi-directional interface test [AD-A203748] N89-20379
Very High Speed Integrated Circuits (VHSIC). Phase 2: Submicrometer technology development, interoperability standards [AD-A203629] N89-20401
Design and implementation of the hazard control box for the ride motion simulator [AD-A203752] N89-20404
Investigations of ultrasonic wave interactions at imperfect boundaries separating anisotropic materials [DE89-007089] N89-20781
INTERFACIAL TENSION
Fluoride glass: Crystallization, surface tension N89-20306
Acoustic containerless experiment system: A non-contact surface tension measurement N89-20308
Physical phenomena in containerless glass processing N89-20310
Surface tension driven convection experiment N89-20314
A finite element stability analysis for the Marangoni problem in a rectangular container with rigid sidewalls [TW-285] N89-20735
INTERFEROMETERS
Support of Mark 3 optical interferometer [AD-A203665] N89-20800
INTERFEROMETRY
Support of Mark 3 optical interferometer [AD-A203665] N89-20800
INTERGRANULAR CORROSION
Failure analysis of a Stirling engine heat pipe [NASA-TM-101418] N89-20227
INTERNATIONAL COOPERATION
The Cluster Mission: Scientific and technical aspects of the instruments [ESA-SP-1103] N89-20156
Wave experiment consortium — Cluster mission N89-20159
Barriers to the international transfer of information in aerospace and defense N89-20861
INTERNATIONAL RELATIONS
Supply and use of Japanese technical literature in the United States [PB88-230842] N89-20862
INTERSTELLAR MATTER
The galactic large-scale far-infrared emission observed by IRAS: Implications for the morphology, physical conditions, and energetics of dust in the interstellar medium N89-20914
INVARIANCE
Robust stabilization of linear time-invariant uncertain systems via Lyapunov theory N89-20147
Integrable two dimensional supersystems [DE88-705355] N89-20857
INVENTIONS
Energy related inventions program: A joint program of the Department of Energy and the National Institute of Standards and Technology [PB89-141154] N89-20546
INVENTORIES
Land use inventory using LANDSAT Thematic Mapper imagery to study environmental pollution [NLR-MP-87063-U] N89-20541
INVERSIONS
The investigation of advanced remote sensing, radiative transfer and inversion techniques for the measurement of atmospheric constituents [NASA-CR-172599] N89-20531
Waveform data collection for source inversion studies [AD-A203419] N89-20575
Simultaneous inversion of vector and total field aeromagnetic data using Bayesian inference: A case study from the Cobb Offset of the Juan de Fuca Ridge [PB89-114193] N89-20599
Symbolic inversion of control relationships in model-based expert systems [NASA-CR-182857] N89-20631
INVISCID FLOW
Updated users' guide for TAWFIVE with multigrid [NASA-TM-4109] N89-20409
Vorticity distributions in unsteady flow separation [AD-A203733] N89-20428
IODIDES
Growth of mercuric iodide (HgI2) for nuclear radiation detectors N89-20293
IODINE LASERS
Direct solar-pumped iodine laser amplifier [NASA-CR-184813] N89-20447
ION BEAMS
Active spacecraft potential control: An ion emitter experiment — Cluster mission N89-20169
Image-projection ion-beam lithography [DE89-005773] N89-20390
ION IMPLANTATION
X-ray diffraction study of phase formation and growth in nitrogen implanted iron: Temperature effects [AD-A203625] N89-20245
Microstructural characterization of alpha-Al2O3 implanted with iron [DE89-006037] N89-20817
Irradiation as a tool for studying solid state amorphization phenomena [DE89-006034] N89-20823
ION IRRADIATION
X-ray diffraction study of phase formation and growth in nitrogen implanted iron: Temperature effects [AD-A203625] N89-20245

ION PROPULSION
Advanced technology for future space propulsion systems
[NASA-TM-101951] N89-20192
IONIZATION
Fundamental and applied studies of new ionization techniques for inorganic mass spectrometry
[DE89-007567] N89-20463
IONOSPHERIC CONDUCTIVITY
A numerical model of ionospheric convection derived from field-aligned currents and the corresponding conductivity --- ionosphere
[TRITA-EPP-88-03] N89-20571
IONOSPHERIC DRIFT
The electron drift instrument --- Cluster mission N89-20165
IONOSPHERIC ELECTRON DENSITY
The spherical probe electric field and wave experiment --- Cluster mission N89-20161
Whisper: A sounder and high frequency wave analyzer experiment --- Cluster mission N89-20162
The electron drift instrument --- Cluster mission N89-20165
PEACE: A Plasma Electron And Current Experiment --- Cluster mission N89-20167
The behavior of the electron density and temperatue at Millstone Hill during the equinox transition study September 1984
[NASA-CR-184737] N89-20567
IONOSPHERIC ION DENSITY
The ion spectrometry experiment to measure the properties of the ionic plasma composition and distribution functions at energies between 0 and 40keV/e --- Cluster mission N89-20166
RAPID: Research with Adaptive Particle Imaging Detectors --- Cluster mission N89-20168
IONOSPHERIC PROPAGATION
Wave experiment consortium --- Cluster mission N89-20159
IONOSPHERIC SOUNDING
Whisper: A sounder and high frequency wave analyzer experiment --- Cluster mission N89-20162
Scientific results from the Swedish Viking satellite
[IRF-SR-196] N89-20572
IONOSPHERIC TEMPERATURE
The behavior of the electron density and temperatue at Millstone Hill during the equinox transition study September 1984
[NASA-CR-184737] N89-20567
IONS
Ablation of materials in the low earth orbital environment N89-20187
IRON
X-ray diffraction study of phase formation and growth in nitrogen implanted iron: Temperature effects
[AD-A203625] N89-20245
Measurement of the cosmic ray iron spectrum above 60 GeV/n and design and calibration of a large isotopic compositional experiment N89-20915
IRON ALLOYS
Microstructural and magnetic characterization in soft magnetic Fe-Si-Al (Sendust) alloy
[DE89-007130] N89-20239
IRON OXIDES
Microstructural characterization of alpha-Al2O3 implanted with iron
[DE89-006037] N89-20817
Defect clustering and related properties of oxides
[DE89-006620] N89-20835
IRRADIATION
Heavy ion induced Single Event Phenomena (SEP) data for semiconductor devices from engineering testing
[NASA-CR-184864] N89-20821
Irradiation as a tool for studying solid state amorphization phenomena
[DE89-006034] N89-20823
ISOPYCNIC PROCESSES
Demixing kinetics of phase separated polymer solutions in microgravity N89-20281
ISOTHERMAL PROCESSES
Isothermal dendritic growth: A low gravity experiment N89-20299
Isothermal solidification in a binary alloy melt N89-20300
ISOTOPES
Measurement of the cosmic ray iron spectrum above 60 GeV/n and design and calibration of a large isotopic compositional experiment N89-20915
ISOTROPIC MEDIA
Solutions and stability of a closed-geodesic black hole model N89-20893
ITERATION
Matrix dependent prolongations and restrictions in a black box multigrid solver
[CWI-NM-R8801] N89-20739
ITERATIVE SOLUTION
Numerical method of applying mean value theorem
[PB89-111447] N89-20714
SLAP (Sparse Linear Algebra Package) for the masses
[DE89-006209] N89-20721
Who's afraid of nonsymmetric matrices? A discussion of elementary iterative methods
[REPT-88-49] N89-20723
Iterative solution of large sparse system of linear equations
[REPT-88-52] N89-20724
High performance preconditioning --- elliptical partial differential equations
[REPT-88-54] N89-20725

J

JAMMING
Analysis of modified SMI method for adaptive array weight control
[NASA-CR-184904] N89-20364
Dedicated versus half-duplex receiver topology in jammed, fully connected CDMA networks: Theory and numerical comparisons
[AD-A203635] N89-20402
JAPAN
Supply and use of Japanese technical literature in the United States
[PB88-230842] N89-20862
Current status of Japanese to English machine translation: Report to Congress
[PB89-128276] N89-20863
JAPANESE SPACE PROGRAM
Commercial potential of European and Japanese space programs, task 5
[NASA-CR-184659] N89-20871
JET ENGINE FUELS
Investigation of spray dispersion and particulate formation in diesel fuel flames
[NASA-CR-184820] N89-20215
JET FLOW
Diffusive burning of plane liquid and spray jets in a coflowing oxidizer stream N89-20216
Modeling of hydrogen-air diffusion flame
[NASA-CR-184844] N89-20218
Navier-Stokes prediction of the three dimensional flow-field of jets in a crossflow using the finite element method N89-20408
Numerical studies of barotropic stability of stratospheric states N89-20570
JOINTS (JUNCTIONS)
Force-reflecting master-slave control and robotic control of a traction-drive differential pitch-yaw joint
[DE89-005107] N89-20480
JORDAN FORM
Vertex operators and Jordan fields
[DE88-705078] N89-20720
JP-8 JET FUEL
Thermal stability of jet fuel
[DE89-006754] N89-20273
JUPITER ATMOSPHERE
Carbon monoxide and disequilibrium dynamics in Saturn and Jupiter N89-20903

K

K-EPSILON TURBULENCE MODEL
Solutions to the Navier-Stokes equations using a k-epsilon turbulence model
[FFA-TN-1988-19] N89-20416
KALMAN FILTERS
Trajectory scoring in rectangular coordinates using transponder-interrogator range and range rate data
[DE89-007005] N89-20119
Space shuttle propulsion estimation development verification
[NASA-CR-183582] N89-20195
Space shuttle propulsion estimation development verification, volume 1
[NASA-CR-183581] N89-20197
An extended Kalman filter based automatic frequency control loop N89-20351
KAON PRODUCTION
Production of D, D* and Ds mesons in 200 GeV/c pi(-), K(-) and p-Si interactions
[MPI-PAE/EXP-EL-192] N89-20785
KIDNEYS
Kidney cell electrophoresis in space flight: Rationale, methods, results and flow cytometry applications N89-20280
KINEMATICS
Cross-coordinated control: An experimentally verified technique for the hybrid twist and wrench control of a voltage-controlled industrial robot
[AD-A203406] N89-20486
Three-dimensional kinematics of rainbands in midlatitude cyclones N89-20586
KINETICS
Application of rigorous nonlinear regression to the decomposition kinetics of explosives
[DE89-007598] N89-20274
Zeolite/methanol: The adsorption heat pump
[DE88-756310] N89-20413
A molecular dynamics study of surface kinetics and epitaxial crystal growth N89-20819
Grain boundary kinetics. Part 2: In-situ observation of the role of grain boundary dislocations in high-angle boundary migration
[DE89-006791] N89-20838
KNOWLEDGE BASES (ARTIFICIAL INTELLIGENCE)
Reliability and performance evaluation of systems containing embedded rule-based expert systems
[NASA-CR-181769] N89-20683
KNOWLEDGE REPRESENTATION
The power of physical representations
[CWI-CS-R8819] N89-20612
Intent inferencing with a model-based operator's associate
[REPT-88-2] N89-20695
OFMTutor: An operator function model intelligent tutoring system N89-20696
Dynamic mechanical system design using qualitative and symbolic reasoning
[DE89-006771] N89-20706
KOLMOGOROFF THEORY
Two decades of applied Kolmogorov complexity. In memoriam: Andrei Nikolaevich Kolmogorov, 1903 - 1987
[CWI-CS-R8813] N89-20767
KRYPTON FLUORIDE LASERS
Development KrF lasers for inertial confinement fusion
[DE89-005469] N89-20443

L

LABORATORIES
Engineering and technical efforts to design and construct a 10 MW gyrotron laboratory
[AD-A203851] N89-20155
LAGRANGE MULTIPLIERS
Minimizing total completion time in the two-machine flow shop by Lagrangian relaxation
[CWI-OS-R8808] N89-20860
LAMINAR BOUNDARY LAYER
Vorticity distributions in unsteady flow separation
[AD-A203733] N89-20428
LAMINAR FLOW
Multigrid solution of the Navier-Stokes equations on triangular meshes
[NASA-CR-181788] N89-20095
Control-volume based Navier-Stokes equation solver valid at all flow velocities
[NASA-TM-101488] N89-20407
Resolution requirements for numerical simulations of transition
[NASA-CR-181799] N89-20411
LAMINATES
Thermal-mechanical behavior of thin films and laminates N89-20203
LAND
Processing and application of digital AVHRR-imagery for land and sea surfaces
[BCRS-88-08] N89-20538
LAND MOBILE SATELLITE SERVICE
Electronically Steerable Terminal Antenna (ESTA) project, phase 2
[ESA-CR(P)-2599] N89-20359
LAND USE
The suitability of remote sensing for surveying and monitoring landscape patterns. Volume A: Pilot study - LANDSAT Imagery. Volume B: PEPS Project No. 73 - SPOT Imagery
[BCRS-87-12-VOL-A/B] N89-20534
The suitability of remote sensing for surveying and monitoring landscape patterns. Volume A: Pilot study - LANDSAT imagery N89-20535
The suitability of remote sensing for surveying and monitoring landscape patterns. Volume B: PEPS Project No. 73 - SPOT Imagery N89-20536
Land use inventories using satellite images in the region Haaren-Helvoirt-Udenhout, North Brabant (The Netherlands)
[BCRS-88-07] N89-20537

LANGUAGES
Current status of Japanese to English machine translation: Report to Congress
[PB89-128276] N89-20863

LAP JOINTS
Elastic stability of lap-jointed cylindrical shells under axial compression
[PB88-245980] N89-20497

LARGE SPACE STRUCTURES
Flexible structure control laboratory development and technology demonstration
[NASA-CR-184867] N89-20151
Translational and rotational dynamics of rigid spacecraft-based manipulators
[NLR-TR-87014-U] N89-20474

LASER ANEMOMETERS
Advanced high temperature instrument for hot section research applications N89-20137

LASER APPLICATIONS
Assessment of research needs for laser technologies applied to advanced spectrographic methods
[DE89-006455] N89-20446
Laser illuminated high speed photography of energetic materials and components with a copper vapor laser
[DE89-006379] N89-20458
Laser-based inspection technology for fossil heat exchanger tubing
[DE89-005811] N89-20495

LASER BEAMS
Pulsed laser effects phenomenology
[DE89-005466] N89-20442
Remote sensing in refractive turbulence N89-20532
Luminescence originating in an optical fiber
[AD-A203494] N89-20799

LASER FUSION
Development KrF lasers for inertial confinement fusion
[DE89-005469] N89-20443
Achieving adequate beam quality for commercial laser fusion reactors
[DE89-007474] N89-20462

LASER MATERIALS
Laser ignition of energetic materials with a pulsed Nd:YAG laser
[DE89-006861] N89-20455

LASER OUTPUTS
Stimulated Raman scattering of intense laser radiation in a nuclear-disturbed space plasma
[AD-A200951] N89-20440
Amplified spontaneous emission in a single pass free electron laser
[DE89-007048] N89-20461

LASER PUMPING
Performance of efficient Q-switched diode-laser-pumped Nd:YAG and Ho:YLF lasers for space applications N89-20345
Calculations of laser cavity dumping for optical communications N89-20346
Direct solar-pumped iodine laser amplifier
[NASA-CR-184813] N89-20447

LASER SPECTROSCOPY
ILS (Intracavity Laser Spectroscopy) for beam sensing (experiment)
[DE89-006376] N89-20445
Assessment of research needs for laser technologies applied to advanced spectrographic methods
[DE89-006455] N89-20446

LASER STABILITY
Remote sensing in refractive turbulence N89-20532

LASER TARGETS
Pulsed laser effects phenomenology
[DE89-005466] N89-20442

LASERS
Mechanisms for the operation of a laser-triggered vacuum switch
[DE89-007059] N89-20394
Optical Johnson noise thermometry
[NASA-CR-184964] N89-20437
Ground state depleted laser experiments
[DE89-006146] N89-20449

LASING
Review of long-pulse laser development
[DE89-006514] N89-20459

LATCH-UP
Heavy ion induced Single Event Phenomena (SEP) data for semiconductor devices from engineering testing
[NASA-CR-184864] N89-20821

LATEX
The first products made in space: Monodisperse latex particles N89-20318

LAUNCHERS
Reconnection launcher projectile heating using the modified REGGIE code
[DE89-007294] N89-20172

LAUNCHING
Axially accelerated saboted rods subjected to lateral forces
[DE89-007466] N89-20485

LAW (JURISPRUDENCE)
Implications of the greenhouse effect for the midwest economy
[DE89-004195] N89-20563

LEACHING
Glass corrosion in natural environment
[NASA-CR-184843] N89-20251
Effect of surface stress on stress corrosion of silicate glass
[DE89-004584] N89-20529

LEAD (METAL)
Pb-Zn liquid metal diffusion N89-20304

LEAD ACID BATTERIES
Group testing of lead-acid batteries for electric vehicles
[DE89-005415] N89-20389

LEAD COMPOUNDS
A study of ferroelectricity in single crystal compounds of the type AFB5 and A3B2F12
[AD-A203610] N89-20849

LEAD TELLURIDES
Microgravity science at Langley Research Center N89-20298

LEARNING
Automatic learning by an autonomous mobile robot
[DE89-003120] N89-20702

LEAST SQUARES METHOD
The relationship between an orthogonal estimation algorithm and other least squares routines
[RR-331] N89-20729
Identification of MIMO nonlinear systems using a forward-regression orthogonal estimator --- multi-input multi-output (MIMO)
[RR-333] N89-20730
Estimating a regression function
[CWI-MS-R8805] N89-20742

LEVITATION
Physical phenomena in containerless glass processing N89-20310

LEVITATION MELTING
Electromagnetic, heat and fluid flow phenomena in levitated metal droplets both under earthbound and microgravity conditions N89-20315

LIAPUNOV FUNCTIONS
Robust stabilization of linear time-invariant uncertain systems via Lyapunov theory N89-20147

LIBRATION
L1 libration point manned space habitat
[NASA-CR-184732] N89-20180

LIE GROUPS
Antipodal universes in the topology S(sup 3)xR and H(sup 3)xR
[DE88-704999] N89-20719
Vertex operators and Jordan fields
[DE88-705078] N89-20720
Irreducible finite-dimensional representations of the Lie superalgebra gl(n/1) in a Gelfand-Zetlin basis
[DE88-705350] N89-20750

LIFE (DURABILITY)
Toward improved durability in advanced aircraft engine hot sections
[NASA-TM-4087] N89-20135
Life modeling of thermal barrier coatings for aircraft gas turbine engines N89-20143
A prior knowledge based optimal Wiener filtering approach to ultrasonic scattering amplitude estimation
[DE89-007574] N89-20783

LIFE CYCLE COSTS
Space Station: NASA efforts to establish a design-to-life-cycle cost process
[GAO/NSIAD-88-147] N89-20188

LIFE SCIENCES
X-ray microscopy for the life and physical sciences
[DE89-006707] N89-20604

LIFT
A first scramjet study
[NASA-CR-184965] N89-20146

LIGHT ELEMENTS
Primordial nucleosynthesis and late decaying particles: A new model of nucleosynthesis N89-20894

LIGHT EMISSION
Time resolved study of light emitted by detonation arrival at the surface of high explosives in various environments
[DE89-005657] N89-20414

LIGHT SCATTERING
Critical fluid light scattering N89-20320

LIGHTNING
Preliminary analysis of cloud-to-ground lightning in the vicinity of the Nevada test site
[PB89-128649] N89-20584

LIMB DARKENING
Angular radiation models for earth-atmosphere system. Volume 2: Longwave radiation
[NASA-RP-1184-VOL-2] N89-20587

LINE OF SIGHT COMMUNICATION
Digital radio link: Multipath fading on a 7 GHz line-of-sight link
[FOA-C-30428-3.3] N89-20365
Digital radio link: Multipath propagation on a microwave line-of-sight path
[FOA-C-30430-3.3] N89-20366

LINEAR ACCELERATORS
High power induction free electron laser
[DE89-006208] N89-20444
Low emittance thermionic electron guns
[DE89-005944] N89-20793
Heavy ion induction linac drivers for inertial confinement fusion
[DE89-006803] N89-20810
Development of a plasma pinch photocathode
[AD-A203944] N89-20813

LINEAR ENERGY TRANSFER (LET)
Heavy ion induced Single Event Phenomena (SEP) data for semiconductor devices from engineering testing
[NASA-CR-184864] N89-20821

LINEAR EQUATIONS
On the equivalence of Gaussian elimination and Gauss-Jordan reduction in solving linear equations
[NASA-TM-101466] N89-20710
Iterative solution of large sparse system of linear equations
[REPT-88-52] N89-20724
Sequential and parallel methods for unconstrained optimization
[AD-A203807] N89-20762
The initial value problem for fractional order differential equations with constant coefficients
[AD-A203843] N89-20764

LINEAR FILTERS
Lectures on linear and nonlinear filtering
[CWI-PM-R8801] N89-20701

LINEAR PROGRAMMING
Basis representations in large-scale linear programming software
[MA-50] N89-20649
Parallel direct solution of sparse linear systems
[DE89-006030] N89-20666
A parallel decomposition algorithm for Staircase Linear Programs
[DE89-007023] N89-20869
A parallel decomposition algorithm for Staircase Linear Programs
[DE89-007883] N89-20674

LINEAR QUADRATIC GAUSSIAN CONTROL
Modeling and control of flexible structures
[NASA-CR-184862] N89-20152

LINEAR QUADRATIC REGULATOR
Optimal feedback control infinite dimensional parabolic evolution systems: Approximation techniques
[NASA-CR-181772] N89-20637

LINEAR SYSTEMS
Robust stabilization of linear time-invariant uncertain systems via Lyapunov theory N89-20147
Parallel direct solution of sparse linear systems
[DE89-006030] N89-20666
On the structure and control of piecewise-linear systems
[RR-334] N89-20700
SLAP (Sparse Linear Algebra Package) for the masses
[DE89-006209] N89-20721
Riemannian geometry on families of linear systems, the deterministic case
[REPT-88-62] N89-20726
Nonlinear input-output maps for bilinear systems and stability
[RR-335] N89-20731
Matrix dependent prolongations and restrictions in a black box multigrid solver
[CWI-NM-R8801] N89-20739
State representations of linear systems with output constraints
[CWI-OS-R8807] N89-20744
Parallel direct solution of sparse linear systems
[DE89-007855] N89-20757
Well-posedness of infinite-dimensional linear systems in time and frequency domain
[TW-287] N89-20771

LINEAR TRANSFORMATIONS
Formula related to the Cayley-Hamilton equation
[PB89-128003] N89-20711
Irreducible finite-dimensional representations of the Lie superalgebra gl(n/1) in a Gelfand-Zetlin basis
[DE88-705350] N89-20750

LINEARITY
Noise: Friend or foe
[AD-A203491] N89-20784
LINEARIZATION
An efficient method for solving free-boundary problems
[REPT-88-63] N89-20727
LIQUID CRYSTALS
Synthesis and physical properties of liquid crystalline alkylisocyanate copolymers
[AD-A203631] N89-20266
The effect of deformation history on the morphology and properties of blends of polycarbonate and a thermotropic liquid crystalline polymers
[AD-A203632] N89-20267
Progress in linear optics, non-linear optics and surface alignment of liquid crystals
[DE89-006507] N89-20834
Nonlinear dynamical phenomena in liquid crystals
[DE88-705367] N89-20842
LIQUID FUELS
Diffusive burning of plane liquid and spray jets in a coflowing oxidizer stream N89-20216
LIQUID HELIUM
Quasi-classical calculations for superfluids
[ETN-89-94118] N89-20421
Finite size effects in Wigner crystallization of electrons on liquid helium layers
[DE88-705370] N89-20843
LIQUID HELIUM 2
Superfluid Helium Tanker (SFHT) study
[NASA-CR-172110] N89-20182
Experiments with metallic and ceramic porous media
[NASA-CR-184819] N89-20248
LIQUID SLOSHING
A numerical method for the simulation of liquid-solid body dynamics --- spacecraft dynamics
[NLR-MP-87030-U] N89-20420
LIQUID-GAS MIXTURES
Numerical study of nonlinear wave interactions in bubbly two-phase flow
[REPT-88-50] N89-20418
LIQUID-LIQUID INTERFACES
An efficient method for solving free-boundary problems
[REPT-88-63] N89-20727
LIQUID-SOLID INTERFACES
A quantitative study of pattern formation in dendritic crystal growth from supersaturated solution N89-20818
LIQUIDS
Dynamic thermophysical measurements in space N89-20317
Paraxial approximations for ultrasonic beam propagation in liquid and solid media with applications to nodestructive evaluation
[DE89-007569] N89-20782
LITERATURE
Current status of Japanese to English machine translation: Report to Congress
[PB89-128276] N89-20863
LITHIUM
Lithium depletion and rotation in main sequence stars N89-20886
LITHIUM BORATES
Crystal nucleation in lithium borate glass N89-20309
LITHIUM SULFUR BATTERIES
Screening study of lithiated catholyte mixes for a long-life Li(Si)/FeS2 thermal battery
[DE89-006857] N89-20393
Assessment of high-temperature battery systems
[DE89-007554] N89-20399
LITHOGRAPHY
Image-projection ion-beam lithography
[DE89-005773] N89-20390
LOAD DISTRIBUTION (FORCES)
On the relationship between matched filter theory as applied to gust loads and phased design loads analysis
[NASA-CR-181802] N89-20125
LOAD TESTS
Postbuckling Finite Element (FE) analysis of a stiffened curved panel loaded in shear
[FFA-TN-1988-23] N89-20516
WISPER: Introducing variable-amplitude loading in wind turbine design
[NLR-MP-88017-U] N89-20552
LOADS (FORCES)
Pressure coefficients for basic tensioned-membrane structure forms
[AD-A203866] N89-20107
LOCAL AREA NETWORKS
A study of EMI-endurance of two polling-type local area networks used in real-time automation applications in a simulated electrical environment
[EL-62] N89-20368
A local area network diagnostic assistant expert system
[DE89-003575] N89-20689
Queuing theory models for computer networks
[NASA-TM-101056] N89-20770
LOGIC
Dynamic mechanical system design using qualitative and symbolic reasoning
[DE89-006771] N89-20706
LOGIC PROGRAMMING
Arithmetic classification of perfect models of stratified programs
[CWI-CS-R8810] N89-20737
The DoD Gateway Information System (DGIS): The development toward artificial intelligence and hypermedia in common command language
[AD-A203674] N89-20869
LONG DURATION SPACE FLIGHT
Nutritional models for a Controlled Ecological Life Support System (CELSS): Linear mathematical modeling
[NASA-CR-4229] N89-20615
LONG TERM EFFECTS
Long term lubrication of ceramics at high temperatures N89-20249
Long-term solar-terrestrial observations
[NASA-CR-184695] N89-20905
LONG WAVE RADIATION
Angular radiation models for earth-atmosphere system. Volume 2: Longwave radiation
[NASA-RP-1184-VOL-2] N89-20587
LONGITUDINAL STABILITY
An airfoil pitch apparatus-modeling and control design
[NASA-TM-101076] N89-20386
LOOPS
Fragmentation of cosmic-string loops
[NASA-CR-184892] N89-20896
LOSSES
Lithium depletion and rotation in main sequence stars N89-20886
LOW FREQUENCIES
Low frequency MHD instability in a hot electron plasma
[PB89-111546] N89-20803
LOW SPEED
Some low-speed flutter characteristics of simple low-aspect-ratio delta wing models
[NASA-TM-101547] N89-20094
Standard test case for a low speed, turbulent junction vortex flow
[PB89-110779] N89-20406
LUBRICANTS
Influence of lubrication on ceramic and steel sliding contacts
[PB89-125090] N89-20467
LUBRICATION
Evaluation of solid lubricants: Temperature programmed desorption of MoS2 on molybdenum and of ion-implanted MoS2 on molybdenum
[AD-A203741] N89-20268
Influence of lubrication on ceramic and steel sliding contacts
[PB89-125090] N89-20467
LUMINESCENCE
Luminescence originating in an optical fiber
[AD-A203494] N89-20799
LUNAR BASES
Lunar surface base propulsion system study, volume 1
[NASA-CR-171982-VOL-1] N89-20271
LUNAR ORBITS
L1 libration point manned space habitat
[NASA-CR-184732] N89-20180
LUNGS
The development of a Compton lung densitometer
[DE89-006854] N89-20603

M

MACHINE TRANSLATION
Evaluation of the RTP Pascal-MALPAS IL translator
[NPL-DITC-128/88] N89-20654
Current status of Japanese to English machine translation: Report to Congress
[PB89-128276] N89-20863
MACHINING
Ductile-regime turning of germanium and silicon
[NASA-TM-101231] N89-20322
MAGNESIUM
Electrodeposition of aluminium, aluminium/magnesium alloys and magnesium from organometallic electrolytes
[DE89-003483] N89-20232
Glass corrosion in natural environment
[NASA-CR-184843] N89-20251
MAGNESIUM ALLOYS
Electrodeposition of aluminium, aluminium/magnesium alloys and magnesium from organometallic electrolytes
[DE89-003483] N89-20232
MAGNETIC DIPOLES
Cross-guide coupler modeling and design N89-20337
A study of the effects of copper to superconductor ratio on stability
[DE89-006804] N89-20846
MAGNETIC FIELDS
The magnetic field investigation on Cluster N89-20158
STAFF: The Spatio-Temporal Analysis of Field Fluctuations experiment --- Cluster mission N89-20160
The electron drift instrument --- Cluster mission N89-20165
The influences of convection on directional solidification of eutectic Bi/MnBi N89-20303
New type of capacitive temperature sensor for use at low temperature and in strong magnetic field
[PB89-111108] N89-20431
Simultaneous inversion of vector and total field aeromagnetic data using Bayesian inference: A case study from the Cobb Offset of the Juan de Fuca Ridge
[PB89-114193] N89-20599
Propagation of the nerve impulse under the effect of a magnetic field
[DE88-705371] N89-20608
Combined algorithms in nonlinear problems of magnetostatics
[DE89-006591] N89-20753
Improved plasma confinement and evidence for a pressure-driven instability from reduced magnetic field errors in the CTX spheromak
[DE89-005475] N89-20806
Extreme ultraviolet and soft X-ray diagnostics of high-temperature plasmas
[DE89-007070] N89-20808
The physics of wave-particle interaction with applications to astrophysics N89-20888
MAGNETIC FLUX
The magnetic field investigation on Cluster N89-20158
MAGNETIC MATERIALS
Simultaneous inversion of vector and total field aeromagnetic data using Bayesian inference: A case study from the Cobb Offset of the Juan de Fuca Ridge
[PB89-114193] N89-20599
MAGNETIC MEASUREMENT
The Cluster Mission: Scientific and technical aspects of the instruments
[ESA-SP-1103] N89-20156
The magnetic field investigation on Cluster N89-20158
The electron drift instrument --- Cluster mission N89-20165
MAGNETIC PROPERTIES
Microstructural and magnetic characterization in soft magnetic Fe-Si-Al (Sendust) alloy
[DE89-007130] N89-20239
Surface and interface local density of states for Nb, V and Ta
[DE88-705365] N89-20240
MAGNETIC SHIELDING
Shielding effectiveness of superconductive particles in plastics
[DE89-003888] N89-20815
MAGNETIC STARS
Publications of the Observatory of the University of Michigan. Volume 12, no. 2: Wavelength identifications in the magnetic CP star HR 4816 (HD 110066) N89-20876
MAGNETIC STORMS
The behavior of the electron density and temperatue at Millstone Hill during the equinox transition study September 1984
[NASA-CR-184737] N89-20567
MAGNETIC SWITCHING
Feasibility study of high temperature superconductor opening switches
[AD-A203699] N89-20851
MAGNETIC TAPES
Generation of CCM format history tapes from analyzed data for selected periods (RD2CFM version 01)
[PB89-124507] N89-20568
MAGNETOHYDRODYNAMIC STABILITY
Stimulated Raman scattering of intense laser radiation in a nuclear-disturbed space plasma
[AD-A200951] N89-20440
Low frequency MHD instability in a hot electron plasma
[PB89-111546] N89-20803
Improved plasma confinement and evidence for a pressure-driven instability from reduced magnetic field errors in the CTX spheromak
[DE89-005475] N89-20806

The Magnetically Insulated Inertial Confinement Fusion (MICF): A novel approach
[DE89-007473] N89-20811

MAGNETOHYDRODYNAMICS
Diagnostics for intelligent control of MPD engines
[AD-A203640] N89-20530

MAGNETOMETERS
STAFF: The Spatio-Temporal Analysis of Field Fluctuations experiment --- Cluster mission N89-20160

MAGNETOSPHERES
STAFF: The Spatio-Temporal Analysis of Field Fluctuations experiment --- Cluster mission N89-20160

MAGNETOSTATICS
Combined algorithms in nonlinear problems of magnetostatics
[DE89-006591] N89-20753

MAGNETS
Literature search on kickers and septa for the Amsterdam Pulse Stretcher (APS)
[LINO-158] N89-20791

MAIN SEQUENCE STARS
Tables of evolutionary star models from 0.85 to 120 solar masses with overshooting and mass loss
[SER-C-PREPUBL-FASC-30] N89-20883
Lithium depletion and rotation in main sequence stars N89-20886

MAINTENANCE
Assessing potential benefits for service/repair and retrieval of satellites: A pilot decision analysis
[AD-A203830] N89-20190
Design of remote maintenance tooling and fixtures for the advanced servomanipulator remote maintenance demonstration
[DE89-003114] N89-20484
Development of a remotely maintainable radio-frequency module for the Compact Ignition Tokamak
[DE89-004913] N89-20805

MAN MACHINE SYSTEMS
Extravehicular activity at geosynchronous earth orbit
[NASA-CR-172112] N89-20181
Fastbus standard routines
[DOE/ER-0367] N89-20645
Human-computer interaction in distributed supervisory control tasks
[NASA-CR-184671] N89-20692
View graphs for GSFC Colloquium on OFMspert N89-20693
Use of artificial intelligence in supervisory control N89-20694
Intent inferencing with a model-based operator's associate
[REPT-88-2] N89-20695
OFMTutor: An operator function model intelligent tutoring system N89-20696
A survey of intelligent tutoring systems: Implications for complex dynamic systems N89-20697

MAN-COMPUTER INTERFACE
Direct manipulation and other styles of man-machine interaction
[REPT-88-53] N89-20616
User interfaces and highly interactive systems: Survey of current research
[REPT-88-60] N89-20617
A local area network diagnostic assistant expert system
[DE89-003575] N89-20689
Human-computer interaction in distributed supervisory control tasks
[NASA-CR-184671] N89-20692
View graphs for GSFC Colloquium on OFMspert N89-20693
Use of artificial intelligence in supervisory control N89-20694
Intent inferencing with a model-based operator's associate
[REPT-88-2] N89-20695
OFMTutor: An operator function model intelligent tutoring system N89-20696
A survey of intelligent tutoring systems: Implications for complex dynamic systems N89-20697
Increasing user-friendliness in AI systems
[DE89-005093] N89-20704

MANGANESE OXIDES
Defect clustering and related properties of oxides
[DE89-006620] N89-20835

MANIFOLDS (MATHEMATICS)
Analysis of regularized Navier-Stokes equations, 2
[NASA-CR-181801] N89-20716
A tutorial introduction to differentiable manifolds and calculus on manifolds
[CWI-PM-R8803] N89-20746
On heterotic supermanifolds
[DE88-705339] N89-20773

MANIPULATORS
High speed, precision motion strategies for lightweight structures
[NASA-CR-184651] N89-20327
Dynamic modeling and linearization for real-time control of a pantograph manipulator N89-20469
Active vibration control of a large flexible manipulator by inertial force and joint torque
[NASA-CR-184786] N89-20470
Application of parameter adaptive approach to servo control of a hydraulic manipulator
[MA-51] N89-20473
Translational and rotational dynamics of rigid spacecraft-based manipulators
[NLR-TR-87014-U] N89-20474
Breadboard test-software and wrist joint modeling for Hermes robot arm
[ETN-89-94155] N89-20475
Development of the HERMIES 3 mobile robot research testbed at Oak Ridge National Laboratory
[DE89-004797] N89-20479
Force-reflecting master-slave control and robotic control of a traction-drive differential pitch-yaw joint
[DE89-005107] N89-20480
Telerobotic manipulator developments for ground-based space research
[NASA-CR-184736] N89-20481
Design of remote maintenance tooling and fixtures for the advanced servomanipulator remote maintenance demonstration
[DE89-003114] N89-20484
Sensor capabilities for the HERMIES experimental robot
[DE89-003180] N89-20703
Gain selection for an independent joing MRAC (Model-Reference Adaptive Controller) for robotic manipulators
[DE89-005110] N89-20705
Development of a remotely maintainable radio-frequency module for the Compact Ignition Tokamak
[DE89-004913] N89-20805

MANNED SPACECRAFT
Aerospace vehicle design, Spacecraft Section final project reports
[NASA-CR-184741] N89-20121

MANUFACTURING
Preparation of composites
[EP-0-240-251-A2] N89-20207

MAPPING
Application of Newton's method to Lagrangian dynamical systems
[DE89-007024] N89-20751

MAPS
Geological data integration techniques: Proceedings
[DE88-705255] N89-20868

MARANGONI CONVECTION
Growth of GaAs crystals from the melt in a partially confined configuration N89-20296
A finite element stability analysis for the Marangoni problem in a rectangular container with rigid sidewalls
[TW-285] N89-20735

MARINE METEOROLOGY
Long-range forecasting of storminess over the Northern Hemisphere oceans
[AD-A203949] N89-20595
CTD/O2 measurements during 1986 as part of the Equatorial Pacific Ocean Climate Studies (EPOCS)
[PB89-102859] N89-20596

MARKETING
A systematic worldwide landcover of satellite mosaics
[NLR-MP-87062-U] N89-20540
Commercial potential of European and Japanese space programs, task 5
[NASA-CR-184659] N89-20871

MARKOV PROCESSES
Continuous-discrete filtering for systems with Markovian switching coefficients
[NLR-MP-87076-U] N89-20117
Reliability and performance evaluation of systems containing embedded rule-based expert systems
[NASA-CR-181769] N89-20683

MARS (PLANET)
Aerospace vehicle design, Spacecraft Section
[NASA-CR-184743] N89-20123

MARS ATMOSPHERE
The Mars climate for a photovoltaic system operation
[NASA-TM-101994] N89-20385

MARS SURFACE
Aerospace vehicle design, Spacecraft Section final project reports
[NASA-CR-184741] N89-20121
Aerospace vehicle design, Spacecraft Section final project reports
[NASA-CR-184742] N89-20122
Mars manned transportation vehicle
[NASA-TM-101487] N89-20545

MARSHLANDS
Utilizing remote sensing of thematic mapper data to improve our understanding of estuarine processes and their influence on the productivity of estuarine-dependent fisheries
[NASA-CR-183417] N89-20533

MASERS
Theoretical comparison of maser materials for a 32-GHz maser amplifier N89-20335

MASS SPECTRA
Fundamental and applied studies of new ionization techniques for inorganic mass spectrometry
[DE89-007567] N89-20463

MASS SPECTROSCOPY
New directions in spectroscopy for the analytical electron microscope
[DE89-005824] N89-20435
Fundamental and applied studies of new ionization techniques for inorganic mass spectrometry
[DE89-007567] N89-20463

MASS TRANSFER
Electromagnetic, heat and fluid flow phenomena in levitated metal droplets both under earthbound and microgravity conditions N89-20315
Heat and mass transport in fuel cell electrodes
[DE89-006378] N89-20548

MASSIVELY PARALLEL PROCESSORS
A structural analysis algorithm for massively parallel computers
[DE89-005055] N89-20686

MATCHED FILTERS
On the relationship between matched filter theory as applied to gust loads and phased design loads analysis
[NASA-CR-181802] N89-20125
Digital signal processing
[AD-A203744] N89-20403

MATHEMATICAL LOGIC
Do-it-yourself type theory
[CS-8811] N89-20659
Two decades of applied Kolmogorov complexity. In memoriam: Andrei Nikolaevich Kolmogorov, 1903 - 1987
[CWI-CS-R8813] N89-20767

MATHEMATICAL MODELS
High Reynolds number incompressible flow simulation about parachute canopies and similar bluff bodies N89-20096
Geometrical and structural properties of an Aeroelastic Research Wing (ARW-2)
[NASA-TM-4110] N89-20099
On the relationship between matched filter theory as applied to gust loads and phased design loads analysis
[NASA-CR-181802] N89-20125
An analytical and numerical study of axial flow compressor instability N89-20131
Review and assessment of the database and numerical modeling for turbine heat transfer N89-20139
Fatigue life prediction modeling for turbine hot section materials N89-20142
Modal cost analysis of flexible structures: Modeling flexible structures for control design N89-20148
Active control helicopter aeromechanical and aeroelastic instabilities N89-20149
Modeling and control of flexible structures
[NASA-CR-184862] N89-20152
Space shuttle propulsion estimation development verification, volume 1
[NASA-CR-183581] N89-20197
Identification of space shuttle main engine dynamics
[NASA-TM-101982] N89-20199
Prediction model for the onset of edge-effect delamination at holes in composite laminates N89-20202
Effects of turbulence on rate of combustion of fuel sprays N89-20212
Analysis of the strain-rate sensitivity at high strain rates in fcc and bcc metals
[DE89-005471] N89-20233
Constitutive properties of copper and tantalum at high rates of tensile strain: Expanding ring results
[DE89-006197] N89-20242
Dynamic thermophysical measurements in space N89-20317
The lambda point experiment in microgravity N89-20319
Estimating nonlinear models
[RR-328] N89-20325
Finite element modeling of a hydroformed sheet metal cover
[DE89-006798] N89-20326
A preliminary weather model for optical communications through the atmosphere N89-20350
Modeling the behavior of pulsed, high power microwave antenna systems
[DE89-006280] N89-20374

Computational fluid dynamics and aerothermodynamics
[NASA-CR-180079] N89-20415
A numerical method for the simulation of liquid-solid body dynamics --- spacecraft dynamics
[NLR-MP-87030-U] N89-20420
Transmission and reflection on pressure waves by compressor and turbine stages, based on an actuator-disk model
[AD-A203513] N89-20426
Validity of 1D free-electron laser sideband models
[DE89-006284] N89-20452
Active vibration control of a large flexible manipulator by inertial force and joint torque
[NASA-CR-184786] N89-20470
Translational and rotational dynamics of rigid spacecraft-based manipulators
[NLR-TR-87014-U] N89-20474
Determination of the impulse response of a viscoelastic beam using a fractional derivative constitutive model N89-20501
Theoretical and computational studies in plasticity and fracture N89-20511
Results of inphase axial-torsional fatigue experiments on 304 stainless steel
[NASA-TM-101464] N89-20514
A numerical implementation of the Schapery model for nonlinear viscoelasticity
[ETN-89-93895] N89-20515
Analysis of crack opening behavior by application of a discretized strip yield model
[NLR-MP-87065-U] N89-20520
Diagnostics for intelligent control of MPD engines
[AD-A203640] N89-20530
Active and passive remote sensing of ice
[AD-A203943] N89-20543
Hybrid single-particle Lagrangian integrated trajectories (HY-SPLIT): Model description
[PB89-127591] N89-20559
Kinetic modeling of NOx formation and destruction and combustibles burnout
[PB89-124358] N89-20560
Dispersion of dense gas releases in a wind tunnel
[PB89-118509] N89-20561
The causes and consequences of global climate change
[DE89-004355] N89-20564
A numerical model of ionospheric convection derived from field-aligned currents and the corresponding conductivity --- ionosphere
[TRITA-EPP-88-03] N89-20571
Utility of a geographic information system in modelling climatic suitability
[PB89-109516] N89-20578
Verification of regional climates of GISS GCM. Part 2: Summer
[NASA-TM-100722] N89-20589
Observed and modeled terrain-induced shear in tracer trajectories
[DE89-006938] N89-20590
Long-range forecasting of storminess over the Northern Hemisphere oceans
[AD-A203949] N89-20595
Precision in the perception of direction of a moving pattern
[NASA-TM-101080] N89-20610
Nutritional models for a Controlled Ecological Life Support System (CELSS): Linear mathematical modeling
[NASA-CR-4229] N89-20615
The Delft Ising system processor
[ISBN-9-09-001753-4] N89-20625
Do-it-yourself type theory
[CS-8811] N89-20659
Intelligence in scientific computing
[AD-A203815] N89-20679
State representations of linear systems with output constraints
[CWI-OS-R8807] N89-20744
Parabolic systems with nonlinear competitive interactions
[DE89-007814] N89-20756
Two dimensional maps generated by competitive systems
[DE89-007878] N89-20759
Development of mathematical models for application in image processing
[AD-A203619] N89-20760
Censoring, truncation and filtering in statistical models based on counting processes
[CWI-MS-R8803] N89-20769
Localized versus itinerant picture of light-T(sub c) superconducting oxides
[DE88-705345] N89-20830
Compensation for crystal penetration in high resolution positron tomography
[DE89-006660] N89-20836
A first-principles method for the determination of the electronic structure of grain boundaries
[DE89-006148] N89-20845

MATHEMATICAL PROGRAMMING
Symbolic inversion of control relationships in model-based expert systems
[NASA-CR-182857] N89-20631
Using random number generators on the sensor signal processing system
[AD-A203702] N89-20761

MATRICES (MATHEMATICS)
Iterative solution of large sparse system of linear equations
[REPT-88-52] N89-20724
A fast algorithm for reordering sparse matrices for parallel factorization
[DE89-007873] N89-20758

MATRIX MATERIALS
Crystallization kinetics of BaO-Al2O3-SiO2 glasses
[NASA-TM-101964] N89-20252

MATRIX METHODS
Bordered equations in continuation methods: An improved solution technique --- structural analysis
[NLR-MP-87057-U] N89-20699

MAXIMUM LIKELIHOOD ESTIMATES
A long constraint length VLSI Viterbi decoder for the DSN N89-20341

MAXWELL EQUATION
Diffraction theory for polygonal apertures
[AD-A203778] N89-20802

MEAN
Numerical method of applying mean value theorem
[PB89-111447] N89-20714

MEASUREMENT
Consequences of nonclassical measurement for the algorithmic description of continuous dynamical systems
[NASA-CR-184851] N89-20640

MEASURING INSTRUMENTS
Fluorine as an oxidant in combustion calorimetry
[DE89-003626] N89-20214
Laser-based inspection technology for fossil heat exchanger tubing
[DE89-005811] N89-20495

MECHANICAL ENGINEERING
Modeling flexibility of mechanisms with ADAMS
[ESA-STM-242] N89-20518
Dynamic mechanical system design using qualitative and symbolic reasoning
[DE89-006771] N89-20706

MECHANICAL PROPERTIES
Thermal-mechanical behavior of thin films and laminates N89-20203
Mechanical properties of modified low cobalt powder metallurgy Udimet 700 type alloys
[NASA-TM-101481] N89-20228
Compositional effects on processing and properties of nickel aluminides
[DE89-005133] N89-20229
The role of composition and microstructure gradients on weld metal properties and behavior
[DE89-006789] N89-20235
Exploratory alloy development in the system Al-Sc-X
[DE89-007088] N89-20237
Crystallization kinetics of BaO-Al2O3-SiO2 glasses
[NASA-TM-101964] N89-20252
Design, development and applications of novel techniques for studying surface mechanical properties
[NASA-TM-101959] N89-20253
Synthesis and physical properties of liquid crystalline alkylisocyanate copolymers
[AD-A203631] N89-20266
Sulfide and phosphide analogs of oxynitride ceramics
[AD-A203805] N89-20269
Screening study of lithiated catholyte mixes for a long-life Li(Si)/FeS2 thermal battery
[DE89-006857] N89-20393
Determination of the impulse response of a viscoelastic beam using a fractional derivative constitutive model N89-20501
User's manual for DYNA2D: An explicit two-dimensional hydrodynamic finite element code with interactive rezoning and graphical display
[DE89-006695] N89-20647

MEDICAL SCIENCE
Medical subject headings, tree structures, 1989
[PB89-100028] N89-20605
Research and technology of the Lyndon Johnson Space Center
[NASA-TM-100473] N89-20918

MELTS (CRYSTAL GROWTH)
Growth of GaAs crystals from the melt in a partially confined configuration N89-20296
Isothermal solidification in a binary alloy melt N89-20300

MEMBRANE STRUCTURES
Pressure coefficients for basic tensioned-membrane structure forms
[AD-A203866] N89-20107

MEMBRANES
Membrane vapor enricher for Water For Injection (WFI) production, phase 1
[AD-A201354] N89-20323
Mechanisms of photochemical energy conversion by chlorophyll
[DE89-006820] N89-20550

MEMORY (COMPUTERS)
Data storage and transfer apparatus
[EP-0-243-189-A1] N89-20623

MENTAL PERFORMANCE
Componential analysis of pilot decision making
[AD-A203711] N89-20613

MERCURY CADMIUM TELLURIDES
Growth of solid solution single crystals N89-20297
Research and development of HgZnTe as an infrared material
[NASA-CR-184840] N89-20820

MERCURY COMPOUNDS
Growth of mercuric iodide (HgI2) for nuclear radiation detectors N89-20293

MESON-MESON INTERACTIONS
Production of D, D* and Ds mesons in 200 GeV/c pi(-), K(-) and p-Si interactions
[MPI-PAE/EXP-EL-192] N89-20785

MESONS
Meson production and nuclear fragmentation of nucleus in the atmosphere
[DE88-705019] N89-20917

MESOSCALE PHENOMENA
Boundary layer structure and dynamics in outer hurricane rainbands N89-20583
Radiation, turbulence and microphysics in the stratiform regions of tropical cloud clusters N89-20585
Beaufort Sea mesoscale circulation study: Preliminary results
[PB89-121693] N89-20597

MESSAGE PROCESSING
Research in distributed personal computer-based information systems, volume 1
[AD-A203780] N89-20629
Run-time scheduling and execution of loops on message passing machines
[NASA-CR-181785] N89-20638
A message passing kernel for the hypercluster parallel processing test bed
[NASA-TM-101952] N89-20684
Initial operating capability for the hypercluster parallel-processing test bed
[NASA-TM-101953] N89-20685
Research in distributed personal computer-based information systems, volume 2
[AD-A203845] N89-20870

METABOLISM
Shear stress induced stimulation of mammalian cell metabolism N89-20286

METAL COATINGS
Damage to silver coatings from high average power 1-micron laser
[DE89-005476] N89-20448

METAL FATIGUE
Fatigue life prediction modeling for turbine hot section materials N89-20142
Microstructural influence on low cycle fatigue strength of IMI550
[PNR90500] N89-20226
Corrosion fatigue of iron-chromium nickel alloys: Fracture mechanics and chemistry
[DE89-006985] N89-20236
Softening mechanisms and microstructural instabilities during high temperature low cycle fatigue of Ni, Ni3Al and their metal matrix composites
[DE89-007117] N89-20238
Electrochemical considerations of crack growth in the ferrous alloys
[AD-A203811] N89-20247
Results of inphase axial-torsional fatigue experiments on 304 stainless steel
[NASA-TM-101464] N89-20514
Near threshold fatigue curve based on the dislocation shielding model of fracture
[DE88-011854] N89-20527

METAL FILMS
Effects of environment on tunneling spectroscopy of gold films
[DE89-006040] N89-20844

METAL MATRIX COMPOSITES
Finite element applications to explore the effects of partial bonding on metal matrix composite properties
[NASA-TM-101482] N89-20206
Preparation of composites
[EP-0-240-251-A2] N89-20207

Softening mechanisms and microstructural instabilities during high temperature low cycle fatigue of Ni, Ni3Al and their metal matrix composites
[DE89-007117] N89-20238

METAL PLATES
High intensity acoustic tests of a thermally stressed aluminum plate in TAFA
[NASA-TM-101552] N89-20778

METAL SHEETS
Finite element modeling of a hydroformed sheet metal cover
[DE89-006798] N89-20326

METAL SURFACES
Optical second harmonic generation in metal monolayers and metal surfaces
[DE89-006123] N89-20234

METAL VAPOR LASERS
Laser illuminated high speed photography of energetic materials and components with a copper vapor laser
[DE89-006379] N89-20458

METALLIC PLASMAS
Development of a plasma pinch photocathode
[AD-A203944] N89-20813

METALLOGRAPHY
Development of tooling and techniques for remote field metallography
[DE89-005400] N89-20241

METALS
Experiments with metallic and ceramic porous media
[NASA-CR-184819] N89-20248
Design, development and applications of novel techniques for studying surface mechanical properties
[NASA-TM-101959] N89-20253
Electromagnetic, heat and fluid flow phenomena in levitated metal droplets both under earthbound and microgravity conditions N89-20315
Electronic structure calculation by nonlinear optimization: Application to metals
[DE89-005852] N89-20816

METEOROLOGICAL CHARTS
Utility of a geographic information system in modelling climatic suitability
[PB89-109516] N89-20578

METEOROLOGICAL PARAMETERS
Objective assessment of 1984-85 VAS products as indices of thunderstorm and severe local storm potential
[PB89-107668] N89-20577
Utility of a geographic information system in modelling climatic suitability
[PB89-109516] N89-20578
Preliminary analysis of cloud-to-ground lightning in the vicinity of the Nevada test site
[PB89-128649] N89-20584
Summary of meteorological observations, surface (SMOS) for Norfolk, Virginia
[AD-A203644] N89-20594

METEOROLOGICAL RADAR
A portable CW/FM-CW Doppler radar for local investigation of severe storms
[DE89-005445] N89-20373

METEOROLOGICAL SATELLITES
Objective assessment of 1984-85 VAS products as indices of thunderstorm and severe local storm potential
[PB89-107668] N89-20577

METEOROLOGY
A preliminary weather model for optical communications through the atmosphere N89-20350
Beaufort Sea mesoscale circulation study: Preliminary results
[PB89-121693] N89-20597

METEOSAT SATELLITE
Data compression as a means to disseminate more Meteosat data over the existing channel
[NLR-MP-86063-U] N89-20369

METHYL ALCOHOL
Design and testing of a dissociated methanol vehicle
[DE89-007051] N89-20483

METHYL COMPOUNDS
Aircraft operations and airborne measurement of perfluorotrimethylcyclohexane (PTCH) during ANATEX
[DE89-006934] N89-20566

METRIC SPACE
Metric semantics for concurrency
[CWI-CS-R8803] N89-20661

MICROBURSTS (METEOROLOGY)
Analysis of Doppler radar windshear data
[NASA-CR-181762] N89-20111

MICROCOMPUTERS
Cumulative reports and publications through December 31, 1988
[NASA-CR-181784] N89-20619
Research in distributed personal computer-based information systems, volume 2
[AD-A203845] N89-20870

MICROELECTRONICS
Design and implementation of the hazard control box for the ride motion simulator
[AD-A203752] N89-20404

MICROGRAVITY APPLICATIONS
Microgravity Science and Applications Flight Programs, January - March 1987, selected papers, volume 2
[NASA-TM-4069-VOL-2] N89-20305

MICROHARDNESS
Hardness of amorphous hard carbon films determined by the ultra-low load microindentation technique
[DE89-006129] N89-20259

MICROMECHANICS
A micromechanical viscoplastic stress-strain model with grain boundary sliding
[DE89-007712] N89-20848

MICROPOROSITY
Water adsorption equilibria on microporous carbons
[AD-A203536] N89-20220

MICROPROCESSORS
A PASCAL cross-assembler for the 6809 microprocessor
[USIP-88-05] N89-20648

MICROSCOPY
X-ray microscopy for the life and physical sciences
[DE89-006707] N89-20604

MICROSTRUCTURE
Anion controlled microstructures in the Al2O3-AlN system
[AD-A203671] N89-20209
Microstructural influence on low cycle fatigue strength of IMI550
[PNR90500] N89-20226
Compositional effects on processing and properties of nickel aluminides
[DE89-005133] N89-20229
Analysis of the strain-rate sensitivity at high strain rates in fcc and bcc metals
[DE89-005471] N89-20233
The role of composition and microstructure gradients on weld metal properties and behavior
[DE89-006789] N89-20235
Corrosion fatigue of iron-chronium nickel alloys: Fracture mechanics and chemistry
[DE89-006985] N89-20236
Exploratory alloy development in the system Al-Sc-X
[DE89-007088] N89-20237
Softening mechanisms and microstructural instabilities during high temperature low cycle fatigue of Ni, Ni3Al and their metal matrix composites
[DE89-007117] N89-20238
Microstructural and magnetic characterization in soft magnetic Fe-Si-Al (Sendust) alloy
[DE89-007130] N89-20239
Constitutive properties of copper and tantalum at high rates of tensile strain: Expanding ring results
[DE89-006197] N89-20242
Design, development and applications of novel techniques for studying surface mechanical properties
[NASA-TM-101959] N89-20253
Structure-property characterization of a shock-loaded boron carbide-aluminum cermet
[DE89-005455] N89-20257
Dendritic growth and structure of undercooled nickel base alloys N89-20302
Laser diode cooling for high average power applications
[DE89-006777] N89-20454
Microstructural characterization of alpha-Al2O3 implanted with iron
[DE89-006037] N89-20817
Irradiation as a tool for studying solid state amorphization phenomena
[DE89-006034] N89-20823
Anion grain boundary diffusion in Cr2O3 and Cr2O3-0.09 weight percent Y2O3
[DE89-006281] N89-20833
Grain boundary kinetics. Part 2: In-situ observation of the role of grain boundary dislocations in high-angle boundary migration
[DE89-006791] N89-20838
High pressure Raman spectroscopy of TiO2 thin films
[DE89-006937] N89-20839
Ultrafast physics in microstructure and alloy systems
[AD-A203639] N89-20850

MICROWAVE ANTENNAS
Modeling the behavior of pulsed, high power microwave antenna systems
[DE89-006280] N89-20374

MICROWAVE EQUIPMENT
Bunch beam production and microwave generation in reditrons
[DE89-006530] N89-20397
Quasi-optical microwave components for five different optical paths within the MFTF-B machine
[DE89-005543] N89-20794

MICROWAVE OSCILLATORS
Engineering and technical efforts to design and construct a 10 MW gyrotron laboratory
[AD-A203851] N89-20155

MICROWAVE RADIOMETERS
Processing and application of digital AVHRR-imagery for land and sea surfaces
[BCRS-88-08] N89-20538

MICROWAVE SCATTERING
Geometrical optics design of a compact range Gregorian subreflector system by the principle of the central ray
[NASA-CR-184810] N89-20795

MICROWAVE TRANSMISSION
Digital radio link: Multipath fading on a 7 GHz line-of-sight link
[FOA-C-30428-3.3] N89-20365
Digital radio link: Multipath propagation on a microwave line-of-sight path
[FOA-C-30430-3.3] N89-20366

MICROWAVES
A relativistic fluid code for high-power microwave propagation
[DE89-006598] N89-20375
Bunch beam production and microwave generation in reditrons
[DE89-006530] N89-20397

MIDAIR COLLISIONS
Aircraft accident data, US general aviation, calendar year 1986
[PB89-121453] N89-20108

MIDLATITUDE ATMOSPHERE
Three-dimensional kinematics of rainbands in midlatitude cyclones N89-20586

MIGRATION
Grain boundary kinetics. Part 2: In-situ observation of the role of grain boundary dislocations in high-angle boundary migration
[DE89-006791] N89-20838

MILITARY AIR FACILITIES
A microcomputer pollution model for civilian airports and Air Force bases. Model application and background
[AD-A199794] N89-20557

MILITARY OPERATIONS
Two dimensional maps generated by competitive systems
[DE89-007878] N89-20759

MILITARY SPACECRAFT
DMA (Defense Mapping Agency) orbit determination of the navy navigation satellite system for 1987
[AD-A203496] N89-20170

MILITARY TECHNOLOGY
Comparative lexicon of US-Soviet military technical terminology
[PB89-125553] N89-20865

MILLING
Preparation of composites
[EP-0-240-251-A2] N89-20207

MIMD (COMPUTERS)
The effect of time constraints on scaled speed-up
[DE89-007877] N89-20691

MINORITY CARRIERS
Edge illuminated ventical multijunction
[DE89-006246] N89-20547

MIRROR FUSION
Quasi-optical microwave components for five different optical paths within the MFTF-B machine
[DE89-005543] N89-20794

MIRRORS
Cavity ringdown measurements of high-reflection mirrors at 1.06 microns
[DE89-006512] N89-20797

MISSION PLANNING
Aerospace vehicle design, Spacecraft Section
[NASA-CR-184743] N89-20123
Unmanned, space-based, reusable orbital transfer vehicle, DARVES. Volume 1: Trade analysis and design
[NASA-CR-184711] N89-20173
Unmanned, space-based, reusable orbital transfer vehicle, DARVES. Volume 2: Data and calculations
[NASA-CR-184712] N89-20174
Two designs for an orbital transfer vehicle. Project Orion: A proposal for a manned orbital transfer vehicle for the 21st Century
[NASA-CR-184697] N89-20176
Two designs for an orbital transfer vehicle
[NASA-CR-184698] N89-20177
Extravehicular activity at geosynchronous earth orbit
[NASA-CR-172112] N89-20181
Vehicle for Space Transfer and Recovery (VSTAR), volume 2: Substantiating analyses and data
[NASA-CR-184828] N89-20184

MIXING
Vortex-transport element simulation of a confined mixing layer
[AD-A203791] N89-20222

MOBILITY
Experiments with negative ions in (3)He superfluids
[PB89-127682] N89-20814
MODAL RESPONSE
Modal analysis applied to circular, rectangular, and coaxial waveguides N89-20338
MODELS
Studies and analyses of the space shuttle main engine. Failure information propagation model data base and software
[NASA-CR-183586] N89-20198
Sequential and parallel methods for unconstrained optimization
[AD-A203807] N89-20762
Schema-based theories of problem solving
[AD-A203731] N89-20774
MODULES
A definition study of the on-orbit assembly operations for the outboard photovoltaic power modules for Space Station Freedom
[NASA-TM-102006] N89-20171
Development of a remotely maintainable radio-frequency module for the Compact Ignition Tokamak
[DE89-004913] N89-20805
MODULUS OF ELASTICITY
A theoretical, numerical and experimental examination of in situ properties of adhesives
[FFA-TN-1988-05] N89-20526
MOISTURE
Why cold-wet makes one feel chilled: A literature review
[AD-A203452] N89-20609
MOISTURE METERS
La Recherche Aerospatiale, bimonthly bulletin, number 1988-2, 243/January-February
[ESA-TT-1134] N89-20417
MOLECULAR BEAM EPITAXY
A molecular dynamics study of surface kinetics and epitaxial crystal growth N89-20819
The structure and reactivity of heterogeneous surfaces and study of the geometry of surface complexes
[DE89-005726] N89-20822
MOLECULAR COLLISIONS
Collisional energy transfer in highly vibrationally excited polyatomic molecules
[AD-A203728] N89-20789
MOLECULAR EXCITATION
Energy conversion processes based on molecular excited states
[DE89-007322] N89-20555
MOLECULAR IONS
Infrared spectroscopy of weakly bound molecular ions
[DE89-006602] N89-20787
MOLECULAR RELAXATION
Collisional energy transfer in highly vibrationally excited polyatomic molecules
[AD-A203728] N89-20789
Ultrafast physics in microstructure and alloy systems
[AD-A203639] N89-20850
MOLECULAR STRUCTURE
A (13)C NMR analysis of the effects of electron radiation on graphite/polyetherimide composites
[NASA-CR-182818] N89-20205
Photoinduced electron transfer in ordered polymers
[DE89-006986] N89-20254
MOLYBDENUM SULFIDES
Evaluation of solid lubricants: Temperature programmed desorption of MoS2 on molybdenum and of ion-implanted MoS2 on molybdenum
[AD-A203741] N89-20268
MONITORS
Long-term evaluation of the acoustic emission weld monitor
[PB88-122642] N89-20471
MONTE CARLO METHOD
Discrete analysis of stochastic NMR
[DE89-007016] N89-20494
The Delft Ising system processor
[ISBN-9-09-001753-4] N89-20625
DETECT: Dependency tree evaluation and confidence test
[REPT-88-55] N89-20765
Lattice gauge theory and Monte Carlo methods
[DE89-005666] N89-20856
MORPHOLOGY
Crystallization kinetics of BaO-Al2O3-SiO2 glasses
[NASA-TM-101964] N89-20252
The effect of deformation history on the morphology and properties of blends of polycarbonate and a thermotropic liquid crystalline polymers
[AD-A203632] N89-20267
Development of mathematical models for application in image processing
[AD-A203619] N89-20760
Multicolor surface photometry of powerful radio galaxies N89-20878
The galactic large-scale far-infrared emission observed by IRAS: Implications for the morphology, physical conditions, and energetics of dust in the interstellar medium N89-20914
MOSAICS
A systematic worldwide landcover of satellite mosaics
[NLR-MP-87062-U] N89-20540
MOTION PERCEPTION
Precision in the perception of direction of a moving pattern
[NASA-TM-101080] N89-20610
A concurrent approach to model based motion detection
[DE89-007853] N89-20708
MOTION SIMULATION
Design and implementation of the hazard control box for the ride motion simulator
[AD-A203752] N89-20404
MULTIPATH TRANSMISSION
Digital radio link: Multipath fading on a 7 GHz line-of-sight link
[FOA-C-30428-3.3] N89-20365
Digital radio link: Multipath propagation on a microwave line-of-sight path
[FOA-C-30430-3.3] N89-20366
MULTIPLE ACCESS
Pseudo-Bayesian stability of CSMA (Carrier Sense Multiple Access) and CSMA/CD (Collision Detection) local area networks
[AD-A203834] N89-20763
MULTIPROCESSING (COMPUTERS)
Memory architecture for multiprocessor computers
[EP-PATENT-0-240-354-A1] N89-20622
Automating the multiprocessing environment
[NASA-TM-4103] N89-20641
A class Hierarchical, object-oriented approach to virtual memory management
[NASA-CR-184876] N89-20646
An operating environment for the jellybean machine
[AD-A201042] N89-20682
The effect of time constraints on scaled speed-up
[DE89-007877] N89-20691
Parallel direct solution of sparse linear systems
[DE89-007855] N89-20757
MULTIPROGRAMMING
Multiprogramming a distributed-memory multiprocessor
[DE89-007850] N89-20690
MULTISENSOR APPLICATIONS
World modelling and multi-sensor integration for a mobile robot
[DE89-005124] N89-20482
MULTISPECTRAL BAND SCANNERS
Improved capabilities of the Multispectral Atmospheric Mapping Sensor (MAMS)
[NASA-TM-100352] N89-20430
MUONS
On the performance of the DELPHI hadron calorimeter
[PH-159] N89-20434
MUSCLES
Influences of muscle fiber composition and strength on EMG (electromyographic activity), spinal motion and load acceleration during a repetitive lifting task
[PB89-131221] N89-20607
MUSCULAR STRENGTH
Influences of muscle fiber composition and strength on EMG (electromyographic activity), spinal motion and load acceleration during a repetitive lifting task
[PB89-131221] N89-20607

N

NASA PROGRAMS
NASA HOST project overview N89-20136
Views on the impact of HOST N89-20144
NASA authorization
[S-HRG-100-579] N89-20873
NASTRAN
A refined theory for plate bending with optimized stress field N89-20510
Coupled rotor/fuselage dynamic analysis of the AH-1G helicopter and correlation with flight vibrations data
[NASA-CR-181723] N89-20512
NATIONAL AIRSPACE SYSTEM
Test report for the Direct Access Radar/National Airspace System (DARC/NAS) bi-directional interface test
[AD-A203748] N89-20379
NAVIER-STOKES EQUATION
Multigrid solution of the Navier-Stokes equations on triangular meshes
[NASA-CR-181786] N89-20095
A cell-vertex multigrid method for the Navier-Stokes equations
[NASA-TM-101557] N89-20101
Control-volume based Navier-Stokes equation solver valid at all flow velocities
[NASA-TM-101488] N89-20407
Navier-Stokes prediction of the three dimensional flow-field of jets in a crossflow using the finite element method N89-20408
Solutions to the Navier-Stokes equations using a k-epsilon turbulence model
[FFA-TN-1988-19] N89-20416
La Recherche Aerospatiale, bimonthly bulletin, number 1988-2, 243/January-February
[ESA-TT-1134] N89-20417
An explicit finite differences solver for the incompressible Reynolds averaged Navier-Stokes equations, optimized for the Alliant DSP 9000 computer
[VKI-TM-45] N89-20423
Multigrid and defect correction for the steady Navier-Stokes equation
[CWI-NM-R8803] N89-20424
Analysis of regularized Navier-Stokes equations, 2
[NASA-CR-181801] N89-20716
Spectral methods for CFD
[NASA-CR-181803] N89-20718
NAVIGATION
Trajectory scoring in rectangular coordinates using transponder-interrogator range and range rate data
[DE89-007005] N89-20119
Development of the HERMIES 3 mobile robot research testbed at Oak Ridge National Laboratory
[DE89-004797] N89-20479
Sensor capabilities for the HERMIES experimental robot
[DE89-003180] N89-20703
NAVIGATION SATELLITES
DMA (Defense Mapping Agency) orbit determination of the navy navigation satellite system for 1987
[AD-A203496] N89-20170
NAVSTAR SATELLITES
Future satellite navigation systems, with emphasis on NAVSTAR GPS
[NLR-MP-87034-U] N89-20116
NEGATIVE IONS
Experiments with negative ions in (3)He superfluids
[PB89-127682] N89-20814
NEODYMIUM LASERS
Calculations of laser cavity dumping for optical communications N89-20346
Q-switched, intracavity doubled Nd:YAG laser side-pumped by a laser diode array
[DE89-005349] N89-20441
Laser ignition of energetic materials with a pulsed Nd:YAG laser
[DE89-006861] N89-20455
NEPTUNE (PLANET)
DSN 70-meter antenna X-band gain, phase, and pointing performance, with particular application for Voyager 2 Neptune encounter N89-20353
NERVES
Propagation of the nerve impulse under the effect of a magnetic field
[DE88-705371] N89-20608
NETHERLANDS
Twelve year overview of cloudfree LANDSAT imagery of The Netherlands
[NLR-MP-87072-U] N89-20542
NETWORK ANALYSIS
A local area network diagnostic assistant expert system
[DE89-003575] N89-20689
Pseudo-Bayesian stability of CSMA (Carrier Sense Multiple Access) and CSMA/CD (Collision Detection) local area networks
[AD-A203834] N89-20763
Queuing theory models for computer networks
[NASA-TM-101056] N89-20770
NEURAL NETS
Implementing recurrent back-propagation on the connection machine
[AD-A203796] N89-20381
Consequences of nonclassical measurement for the algorithmic description of continuous dynamical systems
[NASA-CR-184851] N89-20640
Fault-tolerance of a neural network solving the traveling salesman problem
[NASA-CR-181798] N89-20698
NEUTRINOS
Antipodal universes in the topology S(sup 3)xR and H(sup 3)xR
[DE88-704999] N89-20719
NEUTRON IRRADIATION
Test of radiation hardness of CMOS transistors under neutron irradiation
[DE89-006511] N89-20392

NEUTRON RADIOGRAPHY
Plasma focus sources: Supplement to the Neutron Resonance Radiography Workshop proceedings
[DE89-006927] N89-20807
NEUTRON SCATTERING
Study of vibrational and rapid local motions of hydrogen in the storage compound Ti0.8Zr0.2 CrMnH3 by slow neutron scattering
[DE88-704797] N89-20213
Plasma focus sources: Supplement to the Neutron Resonance Radiography Workshop proceedings
[DE89-006927] N89-20807
NEUTRON STARS
Magnetospheres of neutron stars accreting from disks N89-20895
NEVADA
Preliminary analysis of cloud-to-ground lightning in the vicinity of the Nevada test site
[PB89-128649] N89-20584
NICKEL ALLOYS
Compositional effects on processing and properties of nickel aluminides
[DE89-005133] N89-20229
In-situ HVEM studies of the early stages of oxidation of nickel and nickel-chromium alloys
[DE89-005833] N89-20230
Corrosion fatigue of iron-chromium nickel alloys: Fracture mechanics and chemistry
[DE89-006985] N89-20236
Dendritic growth and structure of undercooled nickel base alloys N89-20302
NIGHT
The development and structure of nocturnal slope winds in a simple valley
[AD-A203427] N89-20593
NIOBATES
Material selection for electrooptic deflectors
[DE89-007343] N89-20841
NITROGEN
X-ray diffraction study of phase formation and growth in nitrogen implanted iron: Temperature effects
[AD-A203625] N89-20245
NITROGEN OXIDES
Kinetic modeling of NOx formation and destruction and combustibles burnout
[PB89-124358] N89-20560
NITROGEN POLYMERS
Thermogravimetric analysis of polymeric materials for an intermediate temperature solid electrolyte. 2: Polymer mixtures
[DE89-006960] N89-20262
NOAA SATELLITES
Processing and application of digital AVHRR-imagery for land and sea surfaces
[BCRS-88-08] N89-20538
NOISE INTENSITY
The evaluation of impulsive noise
[NPL-AC-111] N89-20780
NOISE MEASUREMENT
The evaluation of impulsive noise
[NPL-AC-111] N89-20780
Noise: Friend or foe
[AD-A203491] N89-20784
NOISE REDUCTION
Digital processing of speckle images
[AD-A203703] N89-20801
NOISE TEMPERATURE
On 32-GHz cryogenically cooled HEMT low-noise amplifiers N89-20336
NONDESTRUCTIVE TESTS
Nondestructive evaluation of advanced ceramics
[NASA-TM-101489] N89-20490
Nondestructive tests of elements manufactured using diffusion bonding and superplastic forming
[ETN-89-94131] N89-20492
Eddy current inspection of ferromagnetic materials using pulsed magnetic saturation
[DE89-005339] N89-20493
Laser-based inspection technology for fossil heat exchanger tubing
[DE89-005811] N89-20495
Investigations of ultrasonic wave interactions at imperfect boundaries separating anisotropic materials
[DE89-007089] N89-20781
Paraxial approximations for ultrasonic beam propagation in liquid and solid media with applications to nodestructive evaluation
[DE89-007569] N89-20782
A prior knowledge based optimal Wiener filtering approach to ultrasonic scattering amplitude estimation
[DE89-007574] N89-20783
NONLINEAR EQUATIONS
Nonlinear partial differential equations on homogeneous spaces
[DE88-705342] N89-20748
NONLINEAR FILTERS
Continuous-discrete filtering for systems with Markovian switching coefficients
[NLR-MP-87076-U] N89-20117
Testing for nonlinearity using a prediction error filter
[RR-332] N89-20371
Lectures on linear and nonlinear filtering
[CWI-PM-R8801] N89-20701
NONLINEAR OPTICS
Progress in linear optics, non-linear optics and surface alignment of liquid crystals
[DE89-006507] N89-20834
NONLINEAR PROGRAMMING
Inertia-controlling methods for quadratic programming
[DE89-006996] N89-20667
NONLINEAR SYSTEMS
Estimating nonlinear models
[RR-328] N89-20325
The 1987 year end report for road following at Canegie Mellon
[AD-A203946] N89-20488
Computational studies in nonlinear fracture mechanics N89-20508
Spectral analysis of block structured nonlinear systems
[RR-329] N89-20728
The relationship between an orthogonal estimation algorithm and other least squares routines
[RR-331] N89-20729
Identification of MIMO nonlinear systems using a forward-regression orthogonal estimator --- multi-input multi-output (MIMO)
[RR-333] N89-20730
Realization and generalized frequency response for nonlinear input-output maps
[RR-336] N89-20732
Spectral analysis for nonlinear systems. Part 1: Parametric nonlinear spectral analysis
[RR-337] N89-20733
NONLINEARITY
Application of rigorous nonlinear regression to the decomposition kinetics of explosives
[DE89-007598] N89-20274
Testing for nonlinearity using a prediction error filter
[RR-332] N89-20371
Testing of time domain simulators for nonlinear electronic circuits
[PB89-125132] N89-20384
A numerical implementation of the Schapery model for nonlinear viscoelasticity
[ETN-89-93895] N89-20515
Nonlinear input-output maps for bilinear systems and stability
[RR-335] N89-20731
Combined algorithms in nonlinear problems of magnetostatics
[DE89-006591] N89-20753
Parabolic systems with nonlinear competitive interactions
[DE89-007814] N89-20756
Electronic structure calculation by nonlinear optimization: Application to metals
[DE89-005852] N89-20816
Nonlinear dynamical phenomena in liquid crystals
[DE88-705367] N89-20842
NONTHERMAL RADIATION
Nonthermal radio emission from RS CVN binaries and similar systems N89-20913
NORMALITY
Asymptotic normality of minimum L sub 1 norm estimators in linear regression
[CWI-MS-R8806] N89-20747
NORTHERN HEMISPHERE
Long-range forecasting of storminess over the Northern Hemisphere oceans
[AD-A203949] N89-20595
NOZZLE FLOW
A first scramjet study
[NASA-CR-184965] N89-20146
Navier-Stokes prediction of the three dimensional flow-field of jets in a crossflow using the finite element method N89-20408
NUCLEAR FUSION
Mixing and nucleosynthesis in low- and intermediate-mass AGB stars N89-20892
Primordial nucleosynthesis and late decaying particles: A new model of nucleosynthesis N89-20894
NUCLEAR MAGNETIC RESONANCE
A (13)C NMR analysis of the effects of electron radiation on graphite/polyetherimide composites
[NASA-CR-182818] N89-20205
Discrete analysis of stochastic NMR
[DE89-007016] N89-20494
NUCLEAR REACTOR CONTROL
Nuclear power safety: International measures in response to Chernobyl accident
[GAO/NSIAD-88-131BR] N89-20872
NUCLEAR REACTORS
Development of a remote inspection robot and camera positioners for reactor tank inspection
[DE89-004381] N89-20478
Nuclear power safety: International measures in response to Chernobyl accident
[GAO/NSIAD-88-131BR] N89-20872
NUCLEATION
Nucleation of superconductivity in ceramic oxides
[DE88-705364] N89-20263
Crystal nucleation in lithium borate glass N89-20309
Theoretical and computational studies in plasticity and fracture N89-20511
Studies of alternative-crystallization-phase nucleation
[DE89-007220] N89-20840
NUCLEI (NUCLEAR PHYSICS)
Meson production and nuclear fragmentation of nucleus in the atmosphere
[DE88-705019] N89-20917
NUCLEONS
Meson production and nuclear fragmentation of nucleus in the atmosphere
[DE88-705019] N89-20917
NUMERICAL ANALYSIS
An analytical and numerical study of axial flow compressor instability N89-20131
Modeling and control of flexible structures
[NASA-CR-184862] N89-20152
Unmanned, space-based, reusable orbital transfer vehicle, DARVES. Volume 2: Data and calculations
[NASA-CR-184712] N89-20174
Scientific support for an orbiter middeck experiment on solid surface combustion N89-20312
Surface tension driven convection experiment N89-20314
Numerical study of nonlinear wave interactions in bubbly two-phase flow
[REPT-88-50] N89-20418
Three dimensional numerical analysis of a high-gain free-electron laser
[DE89-006981] N89-20456
Elements of design, unifying principles and applications N89-20465
Theoretical and computational studies in plasticity and fracture N89-20511
Numerical studies of barotropic stability of stratospheric states N89-20570
Cumulative reports and publications through December 31, 1988
[NASA-CR-181784] N89-20619
Fortran codes for computing the space-time correlations of turbulent flow in a channel
[AD-A203749] N89-20678
NUMERICAL WEATHER FORECASTING
Objective assessment of 1984-85 VAS products as indices of thunderstorm and severe local storm potential
[PB89-107668] N89-20577
NUTRITIONAL REQUIREMENTS
Nutritional models for a Controlled Ecological Life Support System (CELSS): Linear mathematical modeling
[NASA-CR-4229] N89-20615

O

O STARS
The upper main sequence of OB associations. 1: Spectral types and lines of C and N of southern single-lined O stars
[SER-C-PREPUBL-FASC-32] N89-20884
Dust shells around Miras and OH/IR stars N89-20889
OBSERVATORIES
Support of Mark 3 optical interferometer
[AD-A203665] N89-20800
OCCULTATION
Shutters and slats for the integral sunshade of an optical reception antenna N89-20348
The investigation of advanced remote sensing, radiative transfer and inversion techniques for the measurement of atmospheric constituents
[NASA-CR-172599] N89-20531
OCEAN CURRENTS
Current velocity and hydrographic observations in the southwestern North Atlantic Ocean: Subtropical Atlantic Climate Studies (SACS), 1987
[PB89-114011] N89-20598
OCEAN SURFACE
Processing and application of digital AVHRR-imagery for land and sea surfaces
[BCRS-88-08] N89-20538

OCEANOGRAPHY
CTD/O2 measurements during 1986 as part of the Equatorial Pacific Ocean Climate Studies (EPOCS)
[PB89-102859] N89-20596
Biological processes in the water column of the South Atlantic Bight: Zooplankton responses
[DE89-006828] N89-20600
OCEANS
Long-range forecasting of storminess over the Northern Hemisphere oceans
[AD-A203949] N89-20595
OGIVES
The ogive as a RCS compact range standard
[NASA-CR-184832] N89-20358
ON-LINE SYSTEMS
On-line arithmetic algorithms and structures for VLSI
[AD-A203421] N89-20400
Report of the Documentation Advisory Committee
[PB89-124556] N89-20569
ONBOARD DATA PROCESSING
Electronics in civil aviation
[NLR-MP-87009-U] N89-20129
Adaptive data compression system study --- scientific satellite
[SIL/CR/7129/6] N89-20639
Adaptive data compression system study, executive summary --- scientific satellite
[SIL/CR/7129/7] N89-20867
OPERATING SYSTEMS (COMPUTERS)
Watchdog Program
[PB89-122535] N89-20633
Fastbus standard routines
[DOE/ER-0367] N89-20645
A class Hierarchical, object-oriented approach to virtual memory management
[NASA-CR-184876] N89-20646
Initial operating capability for the hypercluster parallel-processing test bed
[NASA-TM-101953] N89-20685
OPERATOR PERFORMANCE
Safe working time limits in impermeable protective clothing: Recommendations based upon experimental measurements
[IZF-1987-28] N89-20618
Human-computer interaction in distributed supervisory control tasks
[NASA-CR-184671] N89-20692
View graphs for GSFC Colloquium on OFMspert N89-20693
Use of artificial intelligence in supervisory control N89-20694
Intent inferencing with a model-based operator's associate
[REPT-88-2] N89-20695
OFMTutor: An operator function model intelligent tutoring system N89-20696
OPERATORS (MATHEMATICS)
Vertex operators and Jordan fields
[DE88-705078] N89-20720
OPTICAL COMMUNICATION
An integral sunshade for optical reception antennas N89-20347
Effect of earth albedo variation on the performance of a spatial acquisition subsystem aboard a planetary spacecraft N89-20349
A preliminary weather model for optical communications through the atmosphere N89-20350
OPTICAL FIBERS
Luminescence originating in an optical fiber
[AD-A203494] N89-20799
OPTICAL PATHS
Quasi-optical microwave components for five different optical paths within the MFTF-B machine
[DE89-005543] N89-20794
OPTICAL PROPERTIES
X-ray diffraction and ellipsometric studies of zinc sulfide thin films grown by atomic layer epitaxy
[PH-161] N89-20627
OPTICAL PUMPING
Q-switched, intracavity doubled Nd:YAG laser side-pumped by a laser diode array
[DE89-005349] N89-20441
Ground State Depleted (GSD) solid state lasers: Principles, characteristics, and scaling
[DE89-006149] N89-20450
OPTICAL RADAR
Density measurements with combined Raman-Rayleigh LIDAR (Light Detection And Ranging)
[AD-A203561] N89-20376
OPTICAL RESONATORS
The chirped-pulse free-electron laser
[DE89-006792] N89-20460
OPTICAL THICKNESS
The Mars climate for a photovoltaic system operation
[NASA-TM-101994] N89-20385
OPTIMAL CONTROL
On the structure and control of piecewise-linear systems
[RR-334] N89-20700
OPTIMIZATION
The development of a Compton lung densitometer
[DE89-006654] N89-20603
A parallel decomposition algorithm for Staircase Linear Programs
[DE89-007023] N89-20669
Sequential and parallel methods for unconstrained optimization
[AD-A203807] N89-20762
Electronic structure calculation by nonlinear optimization: Application to metals
[DE89-005852] N89-20816
OPTIONS
Expendable launch vehicle transportation for the space station
[NASA-TM-101947] N89-20179
OPTOELECTRONIC DEVICES
Material selection for electrooptic deflectors
[DE89-007343] N89-20841
ORBIT CALCULATION
DMA (Defense Mapping Agency) orbit determination of the navy navigation satellite system for 1987
[AD-A203496] N89-20170
ORBIT TRANSFER VEHICLES
Unmanned, space-based, reusable orbital transfer vehicle, DARVES. Volume 1: Trade analysis and design
[NASA-CR-184711] N89-20173
Unmanned, space-based, reusable orbital transfer vehicle, DARVES. Volume 2: Data and calculations
[NASA-CR-184712] N89-20174
Two designs for an orbital transfer vehicle: A comparison of two OTVs
[NASA-CR-184696] N89-20175
Two designs for an orbital transfer vehicle. Project Orion: A proposal for a manned orbital transfer vehicle for the 21st Century
[NASA-CR-184697] N89-20176
Two designs for an orbital transfer vehicle
[NASA-CR-184698] N89-20177
Vehicle for Space Transfer and Recovery (VSTAR), volume 1
[NASA-CR-184827] N89-20183
Vehicle for Space Transfer and Recovery (VSTAR), volume 2: Substantiating analyses and data
[NASA-CR-184828] N89-20184
Advanced technology for future space propulsion systems
[NASA-TM-101951] N89-20192
Lunar surface base propulsion system study, volume 1
[NASA-CR-171982-VOL-1] N89-20271
Computational fluid dynamics and aerothermodynamics
[NASA-CR-180079] N89-20415
ORBITAL ASSEMBLY
A definition study of the on-orbit assembly operations for the outboard photovoltaic power modules for Space Station Freedom
[NASA-TM-102006] N89-20171
Vehicle for Space Transfer and Recovery (VSTAR), volume 1
[NASA-CR-184827] N89-20183
ORBITAL POSITION ESTIMATION
Determination of GPS orbits to submeter accuracy N89-20331
A comparison of frequency estimation techniques for high-dynamic trajectories
[NASA-CR-184865] N89-20387
ORBITAL SERVICING
Superfluid Helium Tanker (SFHT) study
[NASA-CR-172110] N89-20182
Assessing potential benefits for service/repair and retrieval of satellites: A pilot decision analysis
[AD-A203830] N89-20190
ORBITS
Application of Newton's method to Lagrangian dynamical systems
[DE89-007024] N89-20751
ORGANOMETALLIC COMPOUNDS
New approaches to fluorocarbon synthesis
[AD-A203641] N89-20221
ORTHOGONAL FUNCTIONS
The relationship between an orthogonal estimation algorithm and other least squares routines
[RR-331] N89-20729
Identification of MIMO nonlinear systems using a forward-regression orthogonal estimator --- multi-input multi-output (MIMO)
[RR-333] N89-20730
OSCILLATING FLOW
Experimental investigation of transonic oscillating cascade aerodynamics
[NASA-TM-101993] N89-20133
OSCILLATION DAMPERS
Low frequency vibration isolation technology for microgravity space experiments
[NASA-TM-101448] N89-20324
OSCILLATIONS
The dynamics of free liquid drops N89-20316
OSCILLATORS
Preliminary studies of an infrared free-electron laser oscillator at the ATF(BNL)
[DE89-006982] N89-20457
Impedance matching of RF plasma
[PB89-112502] N89-20804
OXIDATION
In-situ HVEM studies of the early stages of oxidation of nickel and nickel-chromium alloys
[DE89-005833] N89-20230
Environmental effects on the time dependent failure of non-oxide ceramics
[AD-A202391] N89-20250
OXIDES
Nucleation of superconductivity in ceramic oxides
[DE88-705364] N89-20263
OXIDIZERS
Diffusive burning of plane liquid and spray jets in a coflowing oxidizer stream N89-20216
OXYGEN
The stress response system of proteins: Implications for bioreactor scaleup N89-20291
OXYNITRIDES
Anion controlled microstructures in the Al2O3-AlN system
[AD-A203671] N89-20209
Sulfide and phosphide analogs of oxynitride ceramics
[AD-A203805] N89-20269
OZONE
3CPO, Cloud Chemistry and Cloud Physics Organization: Data index, June 1988
[DE89-007011] N89-20591

P

PACIFIC OCEAN
CTD/O2 measurements during 1986 as part of the Equatorial Pacific Ocean Climate Studies (EPOCS)
[PB89-102859] N89-20596
PAINTS
Paint tests on laminated material formed by carbon fiber composites and Tedlar layers
[I-279/88] N89-20208
PALLADIUM
Solubility of hydrogen, deuterium and tritium in palladium metal
[DE89-005304] N89-20225
PANORAMIC CAMERAS
Potential of large format camera photography
[PB89-122485] N89-20433
PARABOLIC DIFFERENTIAL EQUATIONS
The use of smoothing techniques in the method of lines
[CWI-NM-R8802] N89-20740
Parabolic systems with nonlinear competitive interactions
[DE89-007814] N89-20756
PARABOLIC REFLECTORS
Quasi-optical microwave components for five different optical paths within the MFTF-B machine
[DE89-005543] N89-20794
Geometrical optics design of a compact range Gregorian subreflector system by the principle of the central ray
[NASA-CR-184810] N89-20795
PARACHUTES
High Reynolds number incompressible flow simulation about parachute canopies and similar bluff bodies N89-20096
PARALLEL COMPUTERS
A structural analysis algorithm for massively parallel computers
[DE89-005055] N89-20686
PARALLEL PROCESSING (COMPUTERS)
The digital wave processing experiment --- Cluster mission N89-20164
Implementing recurrent back-propagation on the connection machine
[AD-A203796] N89-20381
On-line arithmetic algorithms and structures for VLSI
[AD-A203421] N89-20400
Performance evaluation and analytic modeling of shared-memory computers
[PB89-113542] N89-20621
Eps'88: Combining the best features of von Neumann and dataflow computing
[DE89-007291] N89-20627
Parallel algorithms for PDE solvers
[AD-A199625] N89-20630

Run-time scheduling and execution of loops on message passing machines
[NASA-CR-181785] N89-20638
Automating the multiprocessing environment
[NASA-TM-4103] N89-20641
Hypercube matrix computation task
[NASA-CR-184869] N89-20642
Parallel direct solution of sparse linear systems
[DE89-006030] N89-20666
A parallel decomposition algorithm for Staircase Linear Programs
[DE89-007023] N89-20669
A parallel decomposition algorithm for Staircase Linear Programs
[DE89-007863] N89-20674
Valiant's maximum algorithm with sequential memory accesses
[AD-A203713] N89-20676
Parallel algorithms for computer vision
[AD-A203947] N89-20681
An operating environment for the jellybean machine
[AD-A201042] N89-20682
A message passing kernel for the hypercluster parallel processing test bed
[NASA-TM-101952] N89-20684
Initial operating capability for the hypercluster parallel-processing test bed
[NASA-TM-101953] N89-20685
A structural analysis algorithm for massively parallel computers
[DE89-005055] N89-20686
On the equivalence of Gaussian elimination and Gauss-Jordan reduction in solving linear equations
[NASA-TM-101466] N89-20710
Parallel direct solution of sparse linear systems
[DE89-007855] N89-20757
A fast algorithm for reordering sparse matrices for parallel factorization
[DE89-007873] N89-20758
Sequential and parallel methods for unconstrained optimization
[AD-A203807] N89-20762

PARAMETER IDENTIFICATION
The relationship between an orthogonal estimation algorithm and other least squares routines
[RR-331] N89-20729
Identification of MIMO nonlinear systems using a forward-regression orthogonal estimator --- multi-input multi-output (MIMO)
[RR-333] N89-20730
Spectral analysis for nonlinear systems. Part 1: Parametric nonlinear spectral analysis
[RR-337] N89-20733
Long-term solar-terrestrial observations
[NASA-CR-184695] N89-20905

PARAMETERIZATION
Estimating nonlinear models
[RR-328] N89-20325
Efficient detection and signal parameter estimation with applications to high dynamic GPS receivers
[NASA-CR-184861] N89-20362
Lectures on linear and nonlinear filtering
[CWI-PM-R8801] N89-20701

PARITY
On particle antiparticle mirror symmetry
[USIP-88-08] N89-20786

PARTIAL DIFFERENTIAL EQUATIONS
Parallel algorithms for PDE solvers
[AD-A199625] N89-20630
Finite element technique for the inverse problem of a partial differential equation and its application to parameter identification of structure
[PB89-111439] N89-20713
A numerical study of three moving grid methods for one-dimensional partial differential equations which are based on the method of lines
[CWI-NM-R8806] N89-20741
Nonlinear partial differential equations on homogeneous spaces
[DE88-705342] N89-20748
On automatic differentiation
[DE89-005779] N89-20752
Two dimensional maps generated by competitive systems
[DE89-007878] N89-20759

PARTICLE COLLISIONS
Production of D, D* and Ds mesons in 200 GeV/c pi(-), K(-) and p-Si interactions
[MPI-PAE/EXP-EL-192] N89-20785

PARTICLE DIFFUSION
The physics of wave-particle interaction with applications to astrophysics N89-20888

PARTICLE FLUX DENSITY
RAPID: Research with Adaptive Particle Imaging Detectors --- Cluster mission N89-20168

PARTICLE INTERACTIONS
The physics of wave-particle interaction with applications to astrophysics N89-20888

PARTICLE MOTION
The physics of wave-particle interaction with applications to astrophysics N89-20888

PARTICLE PRODUCTION
Meson production and nuclear fragmentation of nucleus in the atmosphere
[DE88-705019] N89-20917

PARTICLE TELESCOPES
Cosmic ray tracking: A new approach to high energy gamma-astronomy
[HD-PY88/05] N89-20916

PARTICLES
Particle cloud combustion in reduced gravity N89-20311
The first products made in space: Monodisperse latex particles N89-20318
Hybrid single-particle Lagrangian integrated trajectories (HY-SPLIT): Model description
[PB89-127591] N89-20559

PASCAL (PROGRAMMING LANGUAGE)
A PASCAL cross-assembler for the 6809 microprocessor
[USIP-88-05] N89-20648
Evaluation of the RTP Pascal-MALPAS IL translator
[NPL-DITC-128/88] N89-20654

PATENT POLICY
Technology transfer: Constraints perceived by Federal laboratory and agency officials
[GAO/RCED-88-116BR] N89-20874

PATTERN RECOGNITION
Linear feature extraction from radar imagery: SBIR (Small Business Innovative Research) phase 2, option 1
[AD-A203686] N89-20377
A displacement pattern matching application in elastic-plastic hybrid stress analysis
[AD-A199028] N89-20499
The suitability of remote sensing for surveying and monitoring landscape patterns. Volume A: Pilot study - LANDSAT imagery N89-20535
The suitability of remote sensing for surveying and monitoring landscape patterns. Volume B: PEPS Project No. 73 - SPOT Imagery N89-20536
Applying expertise to data in the Geologist's Assistant expert system
[DE89-003463] N89-20574
Precision in the perception of direction of a moving pattern
[NASA-TM-101080] N89-20610
Combining segmentation and tracking for the classification of moving objects in video scenes
[DE89-007000] N89-20668
Integrating multiple views into a single representation of a range imaged object
[DE89-005921] N89-20707

PAVEMENTS
Methods and materials for reducing crack reflectance
[PB89-114532] N89-20505

PAYLOAD DELIVERY (STS)
Unmanned, space-based, reusable orbital transfer vehicle, DARVES. Volume 1: Trade analysis and design
[NASA-CR-184711] N89-20173
Vehicle for Space Transfer and Recovery (VSTAR), volume 1
[NASA-CR-184827] N89-20183
Vehicle for Space Transfer and Recovery (VSTAR), volume 2: Substantiating analyses and data
[NASA-CR-184828] N89-20184

PENETRATION
A comprehensive review of modeling of impact damage in ceramics
[AD-A203477] N89-20264
Why cold-wet makes one feel chilled: A literature review
[AD-A203452] N89-20609
Compensation for crystal penetration in high resolution positron tomography
[DE89-006660] N89-20836

PERFLUORO COMPOUNDS
Aircraft operations and airborne measurement of perfluorotrimethylcyclohexane (PTCH) during ANATEX
[DE89-006934] N89-20566

PERFORMANCE PREDICTION
Evaluation of VSAERO in prediction of aerodynamic characteristics of helicopter hub fairings
[NASA-TM-101048] N89-20098
Views on the impact of HOST N89-20144
Space shuttle propulsion estimation development verification
[NASA-CR-183582] N89-20195
Space shuttle propulsion estimation development verification, volume 1
[NASA-CR-183581] N89-20197
Results of inphase axial-torsional fatigue experiments on 304 stainless steel
[NASA-TM-101464] N89-20514

PERFORMANCE TESTS
STS-27R OV-104 Orbiter TPS damage review team, volume 1
[NASA-TM-100355-VOL-1] N89-20178
Free-piston Stirling technology for space power
[NASA-TM-101958] N89-20194
Performance of efficient Q-switched diode-laser-pumped Nd:YAG and Ho:YLF lasers for space applications N89-20345
Test report for the Direct Access Radar/National Airspace System (DARC/NAS) bi-directional interface test
[AD-A203748] N89-20379
Testing of time domain simulators for nonlinear electronic circuits
[PB89-125132] N89-20384
Status of LBL/LLNL FEL (Free Electron Laser) research for two beam accelerator applications
[DE89-006656] N89-20453
Heavy ion induced Single Event Phenomena (SEP) data for semiconductor devices from engineering testing
[NASA-CR-184864] N89-20821

PERMANENT MAGNETS
Bremsstrahlung radiation effects in rare earth permanent magnets
[DE89-006207] N89-20775

PERSONAL COMPUTERS
Research in distributed personal computer-based information systems, volume 1
[AD-A203780] N89-20629
Auger electron and X-ray photoelectron data processing for the personal computer
[DE89-007292] N89-20670

PERTURBATION
Noise: Friend or foe
[AD-A203491] N89-20784

PERTURBATION THEORY
A hybrid-perturbation-Galerkin technique which combines multiple expansions
[NASA-CR-181781] N89-20632

PHASE DIAGRAMS
Anion controlled microstructures in the Al2O3-AlN system
[AD-A203671] N89-20209
Studies of alternative-crystallization-phase nucleation
[DE89-007220] N89-20840
Finite size effects in Wigner crystallization of electrons on liquid helium layers
[DE88-705370] N89-20843
A study of ferroelectricity in single crystal compounds of the type AFB5 and A3B2F12
[AD-A203810] N89-20849

PHASE MODULATION
Error control techniques for satellite and space communications
[NASA-CR-184825] N89-20357

PHASE SEPARATION (MATERIALS)
Microgravity Science and Applications Flight Programs, January - March 1987, selected papers, volume 1
[NASA-TM-4069-VOL-1] N89-20276
Demixing kinetics of phase separated polymer solutions in microgravity N89-20281

PHASE TRANSFORMATIONS
Exploratory alloy development in the system Al-Sc-X
[DE89-007088] N89-20237
Microstructural and magnetic characterization in soft magnetic Fe-Si-Al (Sendust) alloy
[DE89-007130] N89-20239
The structure and reactivity of heterogeneous surfaces and study of the geometry of surface complexes
[DE89-005726] N89-20822
Irradiation as a tool for studying solid state amorphization phenomena
[DE89-006034] N89-20823

PHASED ARRAYS
Reconfigurable antennas
[AD-A203847] N89-20382

PHENOLS
Thermal stability of jet fuel
[DE89-006754] N89-20273

PHENOMENOLOGY
Pulsed laser effects phenomenology
[DE89-005466] N89-20442

PHOSPHIDES
Sulfide and phosphide analogs of oxynitride ceramics
[AD-A203805] N89-20269

PHOSPHORIC ACID FUEL CELLS
Phosphoric acid fuel cell subsystem technology
[PB88-100515] N89-20544

PHOTOCATHODES
The effects of variations in the photocathode voltages of electronic streak cameras
[DE89-006776] N89-20436

Development of a plasma pinch photocathode
[AD-A203944] N89-20813
PHOTOCHEMICAL OXIDANTS
An assessment model for atmospheric composition
[NASA-CP-3023] N89-20588
PHOTOCHEMICAL REACTIONS
Mechanisms of photochemical energy conversion by chlorophyll
[DE89-006820] N89-20550
Thermodynamics of finite-time processes: Accomplishments and work in progress, 1986--1989
[DE89-006726] N89-20858
PHOTOCONDUCTORS
Germanium blocked impurity band infrared detectors
[DE89-006607] N89-20796
PHOTODISSOCIATION
Primordial nucleosynthesis and late decaying particles: A new model of nucleosynthesis N89-20894
PHOTOELECTRONS
Auger electron and X-ray photoelectron data processing for the personal computer
[DE89-007292] N89-20670
PHOTOGRAMMETRY
Potential of large format camera photography
[PB89-122485] N89-20433
PHOTOLUMINESCENCE
Carrier density and excitation energy dependent GAMMA-X photoluminescence of Type-II GaAs/AlAs superlattices
[DE89-002988] N89-20832
PHOTOLYSIS
Photoinduced electron transfer in ordered polymers
[DE89-006986] N89-20254
PHOTONS
Thermodynamic characteristics of Y-Ba-Cu-O type compounds in the model of strong electron-phonon coupling
[DE88-705343] N89-20828
Energy gap in S- and D-wave pairing superconductors
[DE88-705344] N89-20829
Remark on the gravitational field produced by an infinite straight string
[DE88-705077] N89-20855
PHOTOSYNTHESIS
Photoinduced electron transfer in ordered polymers
[DE89-006986] N89-20254
PHOTOVOLTAIC CELLS
A definition study of the on-orbit assembly operations for the outboard photovoltaic power modules for Space Station Freedom
[NASA-TM-102006] N89-20171
The Mars climate for a photovoltaic system operation
[NASA-TM-101994] N89-20385
Photovoltaic energy program summary. Volume 1: Overview, fiscal year 1988
[DE89-000855] N89-20553
PHOTOVOLTAIC CONVERSION
Photovoltaic energy program summary. Volume 1: Overview, fiscal year 1988
[DE89-000855] N89-20553
PHOTOVOLTAIC EFFECT
Photovoltaic energy program summary. Volume 1: Overview, fiscal year 1988
[DE89-000855] N89-20553
PHYSICAL WORK
Safe working time limits in impermeable protective clothing: Recommendations based upon experimental measurements
[IZF-1987-28] N89-20618
PHYSIOLOGICAL EFFECTS
New models to assess behavioral and physiological performance of animals during inhalation exposures
[PB89-128946] N89-20601
PHYSIOLOGY
Why cold-wet makes one feel chilled: A literature review
[AD-A203452] N89-20609
PHYTOPLANKTON
Biological processes in the water column of the South Atlantic Bight: Zooplankton responses
[DE89-006828] N89-20600
PILOT PERFORMANCE
Aircraft accident report: Continental Airlines, Inc., Flight 1713, McDonnell Douglas DC-9-14, N626TX, Stapleton International Airport, Denver, Colorado, November 15, 1987
[PB88-910411] N89-20112
Componential analysis of pilot decision making
[AD-A203711] N89-20613
PILOT TRAINING
Componential analysis of pilot decision making
[AD-A203711] N89-20613
PIPE FLOW
Control-volume based Navier-Stokes equation solver valid at all flow velocities
[NASA-TM-101488] N89-20407
PIPES (TUBES)
Laser-based inspection technology for fossil heat exchanger tubing
[DE89-005811] N89-20495
PITCH (INCLINATION)
An airfoil pitch apparatus-modeling and control design
[NASA-TM-101076] N89-20386
PITUITARY GLAND
Heterogeneity in the growth hormone pituitary gland system of rats and humans: Implications to microgravity based research N89-20279
PITUITARY HORMONES
Heterogeneity in the growth hormone pituitary gland system of rats and humans: Implications to microgravity based research N89-20279
PLANETARY BOUNDARY LAYER
NOAA (National Oceanic and Atmospheric Administration) X-band radar measurements in 3CPO (Cloud Chemistry Cloud Physics Organization)
[PB89-127823] N89-20562
PLANETARY COMPOSITION
Carbon monoxide and disequilibrium dynamics in Saturn and Jupiter N89-20903
PLASMA CONTROL
Low frequency MHD instability in a hot electron plasma
[PB89-111546] N89-20803
Improved plasma confinement and evidence for a pressure-driven instability from reduced magnetic field errors in the CTX spheromak
[DE89-005475] N89-20806
PLASMA DIAGNOSTICS
Scientific results from the Swedish Viking satellite
[IRF-SR-196] N89-20572
Extreme ultraviolet and soft X-ray diagnostics of high-temperature plasmas
[DE89-007070] N89-20808
A new procedure for determination of electron temperatures and electron concentrations by Thomson scattering and analytical plasmas
[AD-A203489] N89-20812
Astrophysical significance of observations and experiments in the Earth's magnetosphere
[TRITA-EPP-88-09] N89-20899
PLASMA FOCUS
Plasma focus sources: Supplement to the Neutron Resonance Radiography Workshop proceedings
[DE89-006927] N89-20807
PLASMA HEATING
Transport modeling of ECH and neutral-beam-heated plasmas in the advanced toroidal facility
[DE89-006131] N89-20809
PLASMA INTERACTIONS
AFE ion mass spectrometer design study
[NASA-CR-184838] N89-20432
PLASMA PHYSICS
Condensation and storage of hydrogen cluster ions
[AD-A203801] N89-20223
Transport modeling of ECH and neutral-beam-heated plasmas in the advanced toroidal facility
[DE89-006131] N89-20809
Astrophysical significance of observations and experiments in the Earth's magnetosphere
[TRITA-EPP-88-09] N89-20899
PLASMA PINCH
Development of a plasma pinch photocathode
[AD-A203944] N89-20813
PLASMA WAVES
Whisper: A sounder and high frequency wave analyzer experiment --- Cluster mission N89-20162
The wideband plasma wave interaction --- Cluster mission N89-20163
The digital wave processing experiment --- Cluster mission N89-20164
PLASMAS (PHYSICS)
Impedance matching of RF plasma
[PB89-112502] N89-20804
PLASMASPHERE
The Cluster Mission: Scientific and technical aspects of the instruments
[ESA-SP-1103] N89-20156
Cluster: A fleet of four spacecraft to study plasma structures in three dimensions N89-20157
The magnetic field investigation on Cluster N89-20158
The spherical probe electric field and wave experiment --- Cluster mission N89-20161
The ion spectrometry experiment to measure the properties of the ionic plasma composition and distribution functions at energies between 0 and 40keV/e --- Cluster mission N89-20166
PEACE: A Plasma Electron And Current Experiment --- Cluster mission N89-20167
RAPID: Research with Adaptive Particle Imaging Detectors --- Cluster mission N89-20168
PLASTIC DEFORMATION
Structure-property characterization of a shock-loaded boron carbide-aluminum cermet
[DE89-005455] N89-20257
Theoretical and computational studies in plasticity and fracture N89-20511
PLASTIC FLOW
Prediction of low and high crack growth rates under constant and variable amplitude loading
[NLR-MP-88012-U] N89-20523
PLASTIC PROPERTIES
Theoretical and computational studies in plasticity and fracture N89-20511
PLASTICS
Shielding effectiveness of superconductive particles in plastics
[DE89-003888] N89-20815
PLATES (STRUCTURAL MEMBERS)
Large deflection analysis of thin elastic shells by hybrid stress method
[PB89-111504] N89-20506
A refined theory for plate bending with optimized stress field N89-20510
PLUMES
Dispersion of dense gas releases in a wind tunnel
[PB89-118509] N89-20561
Observed and modeled terrain-induced shear in tracer trajectories
[DE89-006938] N89-20590
POINT DEFECTS
Growth of GaAs crystals from the melt in a partially confined configuration N89-20296
POINTING CONTROL SYSTEMS
DSN 70-meter antenna X-band gain, phase, and pointing performance, with particular application for Voyager 2 Neptune encounter N89-20353
Pointing a ground antenna at a spinning spacecraft using Conscan-simulation results N89-20354
POLAR REGIONS
Beaufort Sea mesoscale circulation study: Preliminary results
[PB89-121693] N89-20597
POLARIMETRY
Active and passive remote sensing of ice
[AD-A203943] N89-20543
POLARITONS
Theory of Raman scattering by surface polaritons in a four media system
[DE88-705358] N89-20788
POLARIZATION (CHARGE SEPARATION)
Heterogeneity in the growth hormone pituitary gland system of rats and humans: Implications to microgravity based research N89-20279
POLLUTION TRANSPORT
Hybrid single-particle Lagrangian integrated trajectories (HY-SPLIT): Model description
[PB89-127591] N89-20559
POLYATOMIC GASES
Collisional energy transfer in highly vibrationally excited polyatomic molecules
[AD-A203728] N89-20789
POLYATOMIC MOLECULES
Collisional energy transfer in highly vibrationally excited polyatomic molecules
[AD-A203728] N89-20789
POLYCARBONATES
The effect of deformation history on the morphology and properties of blends of polycarbonate and a thermotropic liquid crystalline polymers
[AD-A203632] N89-20267
POLYGONS
Diffraction theory for polygonal apertures
[AD-A203778] N89-20802
POLYMER MATRIX COMPOSITES
An analysis of an incompressible, fiber-reinforced material subjected to finite strains in the direction of reinforcement N89-20201
A (13)C NMR analysis of the effects of electron radiation on graphite/polyetherimide composites
[NASA-CR-182818] N89-20205
POLYMERIZATION
The effect of deformation history on the morphology and properties of blends of polycarbonate and a thermotropic liquid crystalline polymers
[AD-A203632] N89-20267
POLYMERS
The application of statistical experimental design to the development of low-density polymer foams
[DE89-006774] N89-20261
POLYNOMIALS
Piecewise continuous algebraic surfaces in terms of B-splines
[PB89-109136] N89-20712
POLYSTYRENE
The first products made in space: Monodisperse latex particles N89-20318

POROSITY
A dynamic flow-weighted pore size distribution test
[DE89-006191] N89-20260
POROUS MATERIALS
Radiative heat transfer augmentation in high temperature combustion systems with application to radiant tube burners
[PB89-133805] N89-20217
Water adsorption equilibria on microporous carbons
[AD-A203536] N89-20220
Experiments with metallic and ceramic porous media
[NASA-CR-184819] N89-20248
PORTABLE EQUIPMENT
The development of a Compton lung densitometer
[DE89-006654] N89-20603
POSITION (LOCATION)
Cross-coordinated control: An experimentally verified technique for the hybrid twist and wrench control of a voltage-controlled industrial robot
[AD-A203406] N89-20486
Algebraic nonplanar curve and surface estimation in 3-space with applications to position estimation
[PB88-227616] N89-20709
POSITION ERRORS
Position error calibration of a pressure survey aircraft using a trailing cone
[PB86-250733] N89-20092
POSITION SENSING
Real-time part position sensing
[AD-A203580] N89-20439
POSITIONING DEVICES (MACHINERY)
Development of a remote inspection robot and camera positioners for reactor tank inspection
[DE89-004381] N89-20478
POWDER METALLURGY
Mechanical properties of modified low cobalt powder metallurgy Udimet 700 type alloys
[NASA-TM-101481] N89-20228
POWER CONDITIONING
An operating environment for the jellybean machine
[AD-A201042] N89-20682
POWER EFFICIENCY
Power efficient hydraulic systems. Volume 1: Study phase
[AD-A203899] N89-20127
POWER SPECTRA
Matching Power Spectra Density (PSD)-design load — aircraft structures
[NLR-MP-87059-U] N89-20126
PRECIPITATION (METEOROLOGY)
Summary of meteorological observations, surface (SMOS) for Norfolk, Virginia
[AD-A203644] N89-20594
PREDICTION ANALYSIS TECHNIQUES
Fatigue life prediction modeling for turbine hot section materials N89-20142
Prediction model for the onset of edge-effect delamination at holes in composite laminates N89-20202
Estimating nonlinear models
[RR-328] N89-20325
Current status of flight simulation fatigue crack growth concepts
[NLR-MP-88001-U] N89-20521
Fracture control guidelines for stress corrosion
[NLR-MP-88007-U] N89-20522
Prediction of low and high crack growth rates under constant and variable amplitude loading
[NLR-MP-88012-U] N89-20523
Estimation of the Equivalent Initial Flow Size (EIFS) distribution and prediction of failure probabilities for different parameter variations
[FFA-TN-1987-35] N89-20525
Long-range forecasting of storminess over the Northern Hemisphere oceans
[AD-A203949] N89-20595
Lithium depletion and rotation in main sequence stars N89-20886
PREDICTIONS
Navier-Stokes prediction of the three dimensional flow-field of jets in a crossflow using the finite element method N89-20408
A prior knowledge based optimal Wiener filtering approach to ultrasonic scattering amplitude estimation
[DE89-007574] N89-20783
PREMIXED FLAMES
Particle cloud combustion in reduced gravity N89-20311
PRESSURE DISTRIBUTION
Aerodynamic pressure and flow-visualization measurement from a rotating wind turbine blade
[DE89-000854] N89-20104
PRESSURE EFFECTS
Geometrical and structural properties of an Aeroelastic Research Wing (ARW-2)
[NASA-TM-4110] N89-20099
A simple nonlinear model for the return to isotropy in turbulence
[NASA-CR-181797] N89-20412
A stereological analysis of ductile fracture by microvoid coalescence
[DE89-000355] N89-20528
PRESSURE MEASUREMENT
Dynamic wall pressure measurements
[AD-A203551] N89-20427
Unsteady blade pressure measurements on a model counterrotation propeller
[NASA-TM-102002] N89-20779
PRESSURE SENSORS
Unsteady blade pressure measurements on a model counterrotation propeller
[NASA-TM-102002] N89-20779
PRESSURE SWITCHES
Power efficient hydraulic systems. Volume 2: Hardware demonstration phase
[AD-A203900] N89-20128
PROBABILITY DENSITY FUNCTIONS
Matching Power Spectra Density (PSD)-design load — aircraft structures
[NLR-MP-87059-U] N89-20126
PROBABILITY DISTRIBUTION FUNCTIONS
A new procedure for determination of electron temperatures and electron concentrations by Thomson scattering and analytical plasmas
[AD-A203489] N89-20812
PROBABILITY THEORY
Two decades of applied Kolmogorov complexity. In memoriam: Andrei Nikolaevich Kolmogorov, 1903 - 1987
[CWI-CS-R8813] N89-20767
The certainty factor model and its basis in probability theory
[CWI-CS-R8816] N89-20768
Digital processing of speckle images
[AD-A203703] N89-20801
PROBLEM SOLVING
DATMS: A framework for distributed assumption based reasoning
[DE89-006282] N89-20628
Hypercube matrix computation task
[NASA-CR-184869] N89-20642
Reliability and performance evaluation of systems containing embedded rule-based expert systems
[NASA-CR-181769] N89-20683
Finite element technique for the inverse problem of a partial differential equation and its application to parameter identification of structure
[PB89-111439] N89-20713
Spectral methods for CFD
[NASA-CR-181803] N89-20718
Schema-based theories of problem solving
[AD-A203731] N89-20774
Barriers to the international transfer of information in aerospace and defense N89-20861
PRODUCT DEVELOPMENT
Assessment, development, and application of combustor aerothermal models N89-20138
PRODUCTION ENGINEERING
Minimizing total completion time in the two-machine flow shop by Lagrangian relaxation
[CWI-OS-R8808] N89-20860
PRODUCTIVITY
A communication channel model of the software process
[NASA-CR-184866] N89-20643
PROGRAMMING LANGUAGES
Directions in reusing software
[REPT-88-58] N89-20651
A compositional semantics for Concurrent Prolog
[CWI-CS-R8809] N89-20688
Command algebras, recursion and program transformation
[CS-8812] N89-20734
PROJECT PLANNING
Review of network planning methods applicable to Integrated Satellite Terrestrial Networks (ISTN)
[ESA-CR(P)-2691] N89-20185
PROJECTILES
Reconnection launcher projectile heating using the modified REGGIE code
[DE89-007294] N89-20172
PROLOG (PROGRAMMING LANGUAGE)
The DoD Gateway Information System (DGIS): The development toward artificial intelligence and hypermedia in common command language
[AD-A203674] N89-20869
PROPELLER BLADES
Structural Tailoring of Advanced Turboprops (STAT) programmer's manual
[NASA-CR-182164] N89-20132
Unsteady blade pressure measurements on a model counterrotation propeller
[NASA-TM-102002] N89-20779
PROPELLER EFFICIENCY
Structural Tailoring of Advanced Turboprops (STAT) programmer's manual
[NASA-CR-182164] N89-20132
PROPULSION SYSTEM CONFIGURATIONS
Aerospace vehicle design, Spacecraft Section final project reports
[NASA-CR-184741] N89-20121
Two designs for an orbital transfer vehicle. Project Orion: A proposal for a manned orbital transfer vehicle for the 21st Century
[NASA-CR-184697] N89-20176
PROPULSION SYSTEM PERFORMANCE
Propulsion over a wide Mach number range
[NASA-CR-182267] N89-20134
Lunar surface base propulsion system study, volume 1
[NASA-CR-171982-VOL-1] N89-20271
PROPULSIVE EFFICIENCY
Propulsion over a wide Mach number range
[NASA-CR-182267] N89-20134
PROSTAGLANDINS
Shear stress induced stimulation of mammalian cell metabolism N89-20286
PROTECTIVE CLOTHING
SPH-4 helmet retention assembly reinforcement
[AD-A200432] N89-20614
PROTECTIVE COATINGS
Paint tests on laminated material formed by carbon fiber composites and Tedlar layers
[I-279/88] N89-20208
PROTEIN CRYSTAL GROWTH
Protein crystal growth in a microgravity environment N89-20292
PROTEINS
The stress response system of proteins: Implications for bioreactor scaleup N89-20291
PROTOCOL (COMPUTERS)
Pseudo-Bayesian stability of CSMA (Carrier Sense Multiple Access) and CSMA/CD (Collision Detection) local area networks
[AD-A203834] N89-20763
PROTON IRRADIATION
Characterization of production GaAs solar cells for space
[NASA-CR-184863] N89-20549
PSYCHOLOGY
Why cold-wet makes one feel chilled: A literature review
[AD-A203452] N89-20609
PSYCHOPHYSICS
Precision in the perception of direction of a moving pattern
[NASA-TM-101080] N89-20610
PUBLIC HEALTH
National Air Toxics Information Clearinghouse: Ongoing research and regulatory development projects, July 1988
[PB89-103428] N89-20558
PULSAR MAGNETOSPHERES
Magnetospheres of neutron stars accreting from disks N89-20895
PULSARS
Study of ultra-high energy emission from Cygnus X-3 and Hercules X-1
[DE89-004543] N89-20911
PULSE COMMUNICATION
Digital radio link: Multipath fading on a 7 GHz line-of-sight link
[FOA-C-30428-3.3] N89-20365
Digital radio link: Multipath propagation on a microwave line-of-sight path
[FOA-C-30430-3.3] N89-20366
PULSE DURATION
Review of long-pulse laser development
[DE89-006514] N89-20459
PULSE GENERATORS
Production of pulsed electron beams by triggered pseudo-spark discharges
[ISL-CO-245/87] N89-20388
PULSE MODULATION
Calculations of laser cavity dumping for optical communications N89-20346
PULSE REPETITION RATE
High power induction free electron laser
[DE89-006208] N89-20444
PULSED LASERS
Pulsed laser effects phenomenology
[DE89-005466] N89-20442
Laser ignition of energetic materials with a pulsed Nd:YAG laser
[DE89-006861] N89-20455
Review of long-pulse laser development
[DE89-006514] N89-20459
PULSED RADIATION
Production of pulsed electron beams by triggered pseudo-spark discharges
[ISL-CO-245/87] N89-20388

PULSES
Noise: Friend or foe
[AD-A203491] N89-20784
PURIFICATION
Kidney cell electrophoresis in space flight: Rationale, methods, results and flow cytometry applications N89-20280
Hormone purification by isoelectric focusing in space N89-20282
Antibody enhancement of free-flow electrophoresis N89-20290
PURITY
Membrane vapor enricher for Water For Injection (WFI) production, phase 1
[AD-A201354] N89-20323

Q

Q SWITCHED LASERS
Performance of efficient Q-switched diode-laser-pumped Nd:YAG and Ho:YLF lasers for space applications N89-20345
Q-switched, intracavity doubled Nd:YAG laser side-pumped by a laser diode array
[DE89-005349] N89-20441
QUADRATIC EQUATIONS
Sequential and parallel methods for unconstrained optimization
[AD-A203807] N89-20762
QUADRATIC PROGRAMMING
Inertia-controlling methods for quadratic programming
[DE89-006996] N89-20667
An analysis of reduced Hessian methods for constrained optimization
[AD-A201078] N89-20715
QUALITY CONTROL
Fatigue teardown tests of the aged rear support of the A320 aircraft
[I-271/88] N89-20491
QUANTUM MECHANICS
On particle antiparticle mirror symmetry
[USIP-88-06] N89-20786
Resonance tunnelling and breakdown of the Quantum Hall Effect (QHE) in strong electric fields
[DE88-705348] N89-20831
QUANTUM THEORY
On particle antiparticle mirror symmetry
[USIP-88-06] N89-20786
Lattice gauge theory and Monte Carlo methods
[DE89-005666] N89-20856
QUANTUM WELLS
Ultrafast physics in microstructure and alloy systems
[AD-A203639] N89-20850
QUASARS
Selection effects in optical quasar surveys N89-20877
The high-redshift evolution of radio galaxies and quasars N89-20887
QUENCHING (COOLING)
Quench sensitivity of airframe aluminum alloys
[NLR-MP-88003-U] N89-20231
QUERY LANGUAGES
Monotonically improving approximate answers to relational algebra queries
[NASA-CR-184874] N89-20717
QUEUEING THEORY
Waiting-time approximations for cyclic-service systems with mixed service strategies
[CWI-OS-R8802] N89-20743
Queuing theory models for computer networks
[NASA-TM-101056] N89-20770

R

RADAR
Test report for the Direct Access Radar/National Airspace System (DARC/NAS) bi-directional interface test
[AD-A203748] N89-20379
RADAR CROSS SECTIONS
Electromagnetic properties of ice coated surfaces
[NASA-CR-184780] N89-20355
The ogive as a RCS compact range standard
[NASA-CR-184832] N89-20358
RADAR DETECTION
Electromagnetic properties of ice coated surfaces
[NASA-CR-184780] N89-20355
RADAR ECHOES
Electromagnetic properties of ice coated surfaces
[NASA-CR-184780] N89-20355
RADAR IMAGERY
SAR processing on the array processor NMX-432
[FOA-C-30503-3.3] N89-20367
Linear feature extraction from radar imagery: SBIR (Small Business Innovative Research) phase 2, option 1
[AD-A203688] N89-20377
Active and passive remote sensing of ice
[AD-A203943] N89-20543
RADAR MEASUREMENT
NOAA (National Oceanic and Atmospheric Administration) X-band radar measurements in 3CPO (Cloud Chemistry Cloud Physics Organization)
[PB89-127823] N89-20562
RADAR RECEIVERS
Analog automatic control loops in radar and EW (Electronic Warfare)
[AD-A203758] N89-20380
RADAR SIGNATURES
Analysis of Doppler radar windshear data
[NASA-CR-181762] N89-20111
RADAR TRACKING
Analog automatic control loops in radar and EW (Electronic Warfare)
[AD-A203758] N89-20380
RADAR TRANSMITTERS
Conceptual design of a 1-MW CW X-band transmitter for planetary radar N89-20339
RADIATION EFFECTS
Test of radiation hardness of CMOS transistors under neutron irradiation
[DE89-006511] N89-20392
Characterization of production GaAs solar cells for space
[NASA-CR-184863] N89-20549
Bremsstrahlung radiation effects in rare earth permanent magnets
[DE89-006207] N89-20775
RADIATION HARDENING
Test of radiation hardness of CMOS transistors under neutron irradiation
[DE89-006511] N89-20392
Bremsstrahlung radiation effects in rare earth permanent magnets
[DE89-006207] N89-20775
RADIATION MEASUREMENT
Application-based control of an autonomous mobile robot
[DE89-004380] N89-20477
RADIATION TRANSPORT
The Magnetically Insulated Inertial Confinement Fusion (MICF): A novel approach
[DE89-007473] N89-20811
RADIATIVE HEAT TRANSFER
Radiative heat transfer augmentation in high temperature combustion systems with application to radiant tube burners
[PB89-133805] N89-20217
RADIATIVE TRANSFER
The investigation of advanced remote sensing, radiative transfer and inversion techniques for the measurement of atmospheric constituents
[NASA-CR-172599] N89-20531
RADIO ASTRONOMY
Molecular radio line observations of mass loss from red giants
[PB89-102313] N89-20885
Aperture synthesis observations of solar and stellar radio emission N89-20912
RADIO COMMUNICATION
National Weather Service Philadelphia Forecast Office, 1987 NOAA (National Oceanic and Atmospheric Administration) weather radio survey and questionnaire
[PB89-111785] N89-20582
RADIO EMISSION
Nonthermal radio emission from RS CVN binaries and similar systems N89-20913
RADIO EQUIPMENT
Dedicated versus half-duplex receiver topology in jammed, fully connected CDMA networks: Theory and numerical comparisons
[AD-A203635] N89-20402
RADIO FREQUENCIES
SUM (Spectrum Use Measure) data base: A new measure of spectrum use
[PB89-108674] N89-20328
Impedance matching of RF plasma
[PB89-112502] N89-20804
RADIO FREQUENCY INTERFERENCE
SUM (Spectrum Use Measure) data base: A new measure of spectrum use
[PB89-108674] N89-20328
Very large array observations of the sun with related observations using the SMM (Solar Maximum Mission) satellite
[AD-A203873] N89-20910
RADIO GALAXIES
Multicolor surface photometry of powerful radio galaxies N89-20878
The high-redshift evolution of radio galaxies and quasars N89-20887
RADIO OBSERVATION
DMA (Defense Mapping Agency) orbit determination of the navy navigation satellite system for 1987
[AD-A203496] N89-20170
RADIO SIGNALS
Very large array observations of the sun with related observations using the SMM (Solar Maximum Mission) satellite
[AD-A203873] N89-20910
RADIO TELESCOPES
Very large array observations of the sun with related observations using the SMM (Solar Maximum Mission) satellite
[AD-A203873] N89-20910
RADIO WAVES
Very large array observations of the sun with related observations using the SMM (Solar Maximum Mission) satellite
[AD-A203873] N89-20910
RADIOACTIVE DECAY
Primordial nucleosynthesis and late decaying particles: A new model of nucleosynthesis N89-20894
RADIOACTIVE ISOTOPES
Light-Weight Radioisotope Heater Unit Final Safety Analysis Report (LWRHU FSAR). Volume 3: Nuclear risk analysis document
[DE89-005496] N89-20790
RADIOIMMUNOASSAY
Development of immunoassays for human urokinase N89-20283
RADIOISOTOPE BATTERIES
Light-Weight Radioisotope Heater Unit Final Safety Analysis Report (LWRHU FSAR). Volume 3: Nuclear risk analysis document
[DE89-005496] N89-20790
RADIOSONDES
Objective assessment of 1984-85 VAS products as indices of thunderstorm and severe local storm potential
[PB89-107668] N89-20577
RAILGUN ACCELERATORS
Reconnection launcher projectile heating using the modified REGGIE code
[DE89-007294] N89-20172
RAIN
Boundary layer structure and dynamics in outer hurricane rainbands N89-20583
Three-dimensional kinematics of rainbands in midlatitude cyclones N89-20586
RAMAN SPECTRA
Density measurements with combined Raman-Rayleigh LIDAR (Light Detection And Ranging)
[AD-A203561] N89-20376
Stimulated Raman scattering of intense laser radiation in a nuclear-disturbed space plasma
[AD-A200951] N89-20440
Resonance electronic Raman scattering in rare earth crystals
[DE89-007446] N89-20847
RAMAN SPECTROSCOPY
Theory of Raman scattering by surface polaritons in a four media system
[DE88-705358] N89-20788
High pressure Raman spectroscopy of TiO2 thin films
[DE89-006937] N89-20839
RANDOM ACCESS MEMORY
Memory architecture for multiprocessor computers
[EP-PATENT-0-240-354-A1] N89-20622
RANDOM NUMBERS
Using random number generators on the sensor signal processing system
[AD-A203702] N89-20761
RANDOM PROCESSES
On the relationship between matched filter theory as applied to gust loads and phased design loads analysis
[NASA-CR-181802] N89-20125
RANDOM VARIABLES
Asymptotic behavior of random discrete event systems
[REPT-88-56] N89-20766
RANGE FINDERS
World modelling and multi-sensor integration for a mobile robot
[DE89-005124] N89-20482
RARE EARTH ALLOYS
Bremsstrahlung radiation effects in rare earth permanent magnets
[DE89-006207] N89-20775
RARE EARTH ELEMENTS
Resonance electronic Raman scattering in rare earth crystals
[DE89-007446] N89-20847
RASTER SCANNING
A vector-like architecture for raster graphics
[CWI-CS-R8802] N89-20660

RATES (PER TIME)
Trajectory scoring in rectangular coordinates using transponder-interrogator range and range rate data
[DE89-007005] N89-20119
RAYLEIGH SCATTERING
Density measurements with combined Raman-Rayleigh LIDAR (Light Detection And Ranging)
[AD-A203561] N89-20376
REACTION KINETICS
Vortex-transport element simulation of a confined mixing layer
[AD-A203791] N89-20222
Crystallization kinetics of BaO-Al2O3-SiO2 glasses
[NASA-TM-101964] N89-20252
Mechanisms of photochemical energy conversion by chlorophyll
[DE89-006820] N89-20550
Kinetic modeling of NOx formation and destruction and combustibles burnout
[PB89-124358] N89-20560
Collisional energy transfer in highly vibrationally excited polyatomic molecules
[AD-A203728] N89-20789
REACTIVITY
The structure and reactivity of heterogeneous surfaces and study of the geometry of surface complexes
[DE89-005726] N89-20822
REACTOR SAFETY
Light-Weight Radioisotope Heater Unit Final Safety Analysis Report (LWRHU FSAR). Volume 3: Nuclear risk analysis document
[DE89-005496] N89-20790
Nuclear power safety: International measures in response to Chernobyl accident
[GAO/NSIAD-88-131BR] N89-20872
REACTOR TECHNOLOGY
Nuclear power safety: International measures in response to Chernobyl accident
[GAO/NSIAD-88-131BR] N89-20872
REAL TIME OPERATION
Real-time part position sensing
[AD-A203580] N89-20439
Dynamic modeling and linearization for real-time control of a pantograph manipulator N89-20469
Quantization analysis of the real-time SAR digital image formation processor
[DE89-007533] N89-20754
RECEIVERS
High-dynamic GPS tracking
[NASA-CR-184868] N89-20113
On 32-GHz cryogenically cooled HEMT low-noise amplifiers N89-20336
An integral sunshade for optical reception antennas N89-20347
Shutters and slats for the integral sunshade of an optical reception antenna N89-20348
Efficient detection and signal parameter estimation with applications to high dynamic GPS receivers
[NASA-CR-184861] N89-20362
Dedicated versus half-duplex receiver topology in jammed, fully connected CDMA networks: Theory and numerical comparisons
[AD-A203635] N89-20402
Commercial direct absorption receiver design studies
[DE89-007290] N89-20556
RECOGNITION
Parallel algorithms for computer vision
[AD-A203947] N89-20661
RECTANGULAR WAVEGUIDES
Modal analysis applied to circular, rectangular, and coaxial waveguides N89-20338
RECTANGULAR WINGS
Development and application of a program to calculate transonic flow around an oscillating three-dimensional wing using finite difference procedures
[NASA-CR-181744] N89-20093
RECURSIVE FUNCTIONS
Formula related to the Cayley-Hamilton equation
[PB89-128003] N89-20711
Command algebras, recursion and program transformation
[CS-8812] N89-20734
Arithmetic classification of perfect models of stratified programs
[CWI-CS-R8810] N89-20737
RED GIANT STARS
Molecular radio line observations of mass loss from red giants
[PB89-102313] N89-20885
RED SHIFT
The high-redshift evolution of radio galaxies and quasars N89-20887
REDUCED GRAVITY
Microgravity Science and Applications Flight Programs, January - March 1987, selected papers, volume 1
[NASA-TM-4069-VOL-1] N89-20276
Heterogeneity in the growth hormone pituitary gland system of rats and humans: Implications to microgravity based research N89-20279
Kidney cell electrophoresis in space flight: Rationale, methods, results and flow cytometry applications N89-20280
Demixing kinetics of phase separated polymer solutions in microgravity N89-20281
Hormone purification by isoelectric focusing in space N89-20282
Development of immunoassays for human urokinase N89-20283
Hydrodynamic effects on cell growth in agitated microcarrier bioreactors N89-20284
An expert system based intelligent control scheme for space bioreactors N89-20285
Human cell culture in a space bioreactor N89-20288
Cellular effects of microgravity N89-20289
Protein crystal growth in a microgravity environment N89-20292
Modelling the growth of triglycine sulphate crystals in Spacelab 3 N89-20294
A comparative study of the influence of buoyancy driven fluid flow on GaAs crystal growth N89-20295
Microgravity science at Langley Research Center N89-20298
Isothermal dendritic growth: A low gravity experiment N89-20299
Casting And Solidification Technology (CAST): Directional solidification phenomena in a metal model at reduced gravity N89-20301
Pb-Zn liquid metal diffusion N89-20304
Microgravity Science and Applications Flight Programs, January - March 1987, selected papers, volume 2
[NASA-TM-4069-VOL-2] N89-20305
Fluoride glass: Crystallization, surface tension N89-20306
Containerless processing of glass forming melts in space N89-20307
Physical phenomena in containerless glass processing N89-20310
Particle cloud combustion in reduced gravity N89-20311
Scientific support for an orbiter middeck experiment on solid surface combustion N89-20312
Droplet combustion at reduced gravity N89-20313
Surface tension driven convection experiment N89-20314
Electromagnetic, heat and fluid flow phenomena in levitated metal droplets both under earthbound and microgravity conditions N89-20315
Dynamic thermophysical measurements in space N89-20317
The lambda point experiment in microgravity N89-20319
Critical fluid light scattering N89-20320
Particle cloud mixing in microgravity
[NASA-TM-101484] N89-20321
Low frequency vibration isolation technology for microgravity space experiments
[NASA-TM-101448] N89-20324
REDUNDANCY
The application of software fault tolerance to air traffic control: Study contract overview
[BR108567] N89-20114
Some observations on redundancy in a context
[CWI-CS-R8812] N89-20662
REFLECTANCE
Anechoic chamber evaluation at 85 GHz
[PB89-125199] N89-20153
Cavity ringdown measurements of high-reflection mirrors at 1.06 microns
[DE89-008512] N89-20797
REFLECTION
Transmission and reflection on pressure waves by compressor and turbine stages, based on an actuator-disk model
[AD-A203513] N89-20426
REFRACTORY COATINGS
Life modeling of thermal barrier coatings for aircraft gas turbine engines N89-20143
REFRACTORY METALS
Dynamic thermophysical measurements in space N89-20317
REGRESSION ANALYSIS
Estimating a regression function
[CWI-MS-R8805] N89-20742
Asymptotic normality of minimum L sub 1 norm estimators in linear regression
[CWI-MS-R8806] N89-20747
REGULATIONS
NEN 6096, design resolution for small wind turbines
[NLR-MP-88005-U] N89-20551
Implications of the greenhouse effect for the midwest economy
[DE89-004195] N89-20563
REINFORCED PLASTICS
An analysis of an incompressible, fiber-reinforced material subjected to finite strains in the direction of reinforcement N89-20201
REINFORCEMENT (STRUCTURES)
Tripping of asymmetrical stiffeners under combined loading
[PB89-126171] N89-20504
REINFORCING MATERIALS
SPH-4 helmet retention assembly reinforcement
[AD-A200432] N89-20614
RELATIVITY
General relativity, scalar fields and cosmic strings N89-20852
Einsteins's theory of gravity in Fierz variables
[DE88-705004] N89-20854
RELAXATION METHOD (MATHEMATICS)
Iterative solution of large sparse system of linear equations
[REPT-88-52] N89-20724
Minimizing total completion time in the two-machine flow shop by Lagrangian relaxation
[CWI-OS-R8808] N89-20860
RELIABILITY
The application of software fault tolerance to air traffic control: Study contract overview
[BR108567] N89-20114
RELIABILITY ANALYSIS
Reliability and performance evaluation of systems containing embedded rule-based expert systems
[NASA-CR-181769] N89-20683
RELIABILITY ENGINEERING
Toward improved durability in advanced aircraft engine hot sections
[NASA-TM-4087] N89-20135
Airworthiness and flight characteristics evaluation of an improved engine air filtration system on the UH-1H helicopter
[AD-A203446] N89-20145
Software reliability engineering
[DE89-006781] N89-20626
Development of the University of Maryland RAMCAD (Reliability and Maintainability Computer-Aided Design) for electronic systems
[AD-A203616] N89-20675
REMOTE CONTROL
Development of tooling and techniques for remote field metallography
[DE89-005400] N89-20241
REMOTE HANDLING
Application-based control of an autonomous mobile robot
[DE89-004380] N89-20477
REMOTE SENSING
The investigation of advanced remote sensing, radiative transfer and inversion techniques for the measurement of atmospheric constituents
[NASA-CR-172599] N89-20531
Remote sensing in refractive turbulence N89-20532
Utilizing remote sensing of thematic mapper data to improve our understanding of estuarine processes and their influence on the productivity of estuarine-dependent fisheries
[NASA-CR-183417] N89-20533
The suitability of remote sensing for surveying and monitoring landscape patterns. Volume A: Pilot study - LANDSAT Imagery. Volume B: PEPS Project No. 73 - SPOT Imagery
[BCRS-87-12-VOL-A/B] N89-20534
The suitability of remote sensing for surveying and monitoring landscape patterns. Volume A: Pilot study - LANDSAT imagery N89-20535
The suitability of remote sensing for surveying and monitoring landscape patterns. Volume B: PEPS Project No. 73 - SPOT Imagery N89-20536
Land use inventories using satellite images in the region Haaren-Helvoirt-Udenhout, North Brabant (The Netherlands)
[BCRS-88-07] N89-20537
Phase A study for the extension of the CAESAR scanner with a sensor module for the far infrared
[BCRS-88-09] N89-20539
Land use inventory using LANDSAT Thematic Mapper imagery to study environmental pollution
[NLR-MP-87063-U] N89-20541
REMOTE SENSORS
Improved capabilities of the Multispectral Atmospheric Mapping Sensor (MAMS)
[NASA-TM-100352] N89-20430
Development of a remote inspection robot and camera positioners for reactor tank inspection
[DE89-004381] N89-20478
Phase A study for the extension of the CAESAR scanner with a sensor module for the far infrared
[BCRS-88-09] N89-20539

REPEATERS
Dedicated versus half-duplex receiver topology in jammed, fully connected CDMA networks: Theory and numerical comparisons
[AD-A203635] N89-20402
REPRESENTATIONS
Nonlinear input-output maps for bilinear systems and stability
[RR-335] N89-20731
A short tutorial on Lie algebras
[CWI-PM-R8802] N89-20745
REQUIREMENTS
Aerospace vehicle design, Spacecraft Section final project reports
[NASA-CR-184742] N89-20122
Extravehicular activity at geosynchronous earth orbit
[NASA-CR-172112] N89-20181
Conceptual design of a 1-MW CW X-band transmitter for planetary radar N89-20339
Suitability of ANSI standards for quantifying communication satellite system performance
[NASA-CR-182684] N89-20356
On-line arithmetic algorithms and structures for VLSI
[AD-A203421] N89-20400
RESEARCH
Cognitive psychology at the Institute for Perception
[IZF-1987-41] N89-20611
RESEARCH AND DEVELOPMENT
Two designs for an orbital transfer vehicle
[NASA-CR-184698] N89-20177
NASA authorization
[S-HRG-100-579] N89-20873
Technology transfer: Constraints perceived by Federal laboratory and agency officials
[GAO/RCED-88-116BR] N89-20874
Research and technology of the Lyndon Johnson Space Center
[NASA-TM-100473] N89-20918
RESIDUAL STRENGTH
Experimental study of spall damage in an aluminium alloy
[PB89-112619] N89-20224
RESONANCE
Resonance electronic Raman scattering in rare earth crystals
[DE89-007446] N89-20847
RESONANCE SCATTERING
Resonance electronic Raman scattering in rare earth crystals
[DE89-007446] N89-20847
RESONANT TUNNELING
Resonance tunnelling and breakdown of the Quantum Hall Effect (QHE) in strong electric fields
[DE88-705348] N89-20831
RESONANT VIBRATION
Acoustic test of a model rotor and tail rotor: Results for the isolated rotors and combined configuration
[NASA-TM-101550] N89-20777
RESOURCES MANAGEMENT
Integrating syntax, semantics, and discourse DARPA (Defense Advanced Research Projects Agency) natural language understanding program
[AD-A203747] N89-20677
RESPIRATION
New models to assess behavioral and physiological performance of animals during inhalation exposures
[PB89-128946] N89-20601
RESPONSE TIME (COMPUTERS)
Multiprogramming a distributed-memory multiprocessor
[DE89-007850] N89-20690
REUSABLE HEAT SHIELDING
STS-27R OV-104 Orbiter TPS damage review team, volume 1
[NASA-TM-100355-VOL-1] N89-20178
REUSE
Directions in reusing software
[REPT-88-58] N89-20651
REYNOLDS NUMBER
Observed Reynolds number effects on airfoils and high aspect ratio wings at transonic flow conditions
[NLR-MP-88006-U] N89-20102
Resolution requirements for numerical simulations of transition
[NASA-CR-181799] N89-20411
REYNOLDS STRESS
Fortran codes for computing the space-time correlations of turbulent flow in a channel
[AD-A203749] N89-20678
RHEOMETERS
Rheometrics stress rheometer applications
[AD-A203667] N89-20275
RIEMANN MANIFOLD
Riemannian geometry on families of linear systems, the deterministic case
[REPT-88-62] N89-20726
RIGID STRUCTURES
A finite element stability analysis for the Marangoni problem in a rectangular container with rigid sidewalls
[TW-285] N89-20735
RISK
Light-Weight Radioisotope Heater Unit Final Safety Analysis Report (LWRHU FSAR). Volume 3: Nuclear risk analysis document
[DE89-005496] N89-20790
ROBOTICS
High speed, precision motion strategies for lightweight structures
[NASA-CR-184651] N89-20327
Translational and rotational dynamics of rigid spacecraft-based manipulators
[NLR-TR-87014-U] N89-20474
Telerobotic manipulator developments for ground-based space research
[NASA-CR-184736] N89-20481
The 1987 year end report for road following at Canegie Mellon
[AD-A203946] N89-20488
Gain selection for an independent joing MRAC (Model-Reference Adaptive Controller) for robotic manipulators
[DE89-005110] N89-20705
ROBOTS
Vision-based navigation for autonomous ground vehicles
[AD-A203712] N89-20120
A camera stabilization technique for a teleoperated vehicle
[DE89-003923] N89-20476
Application-based control of an autonomous mobile robot
[DE89-004380] N89-20477
Development of a remote inspection robot and camera positioners for reactor tank inspection
[DE89-004381] N89-20478
Development of the HERMIES 3 mobile robot research testbed at Oak Ridge National Laboratory
[DE89-004797] N89-20479
Force-reflecting master-slave control and robotic control of a traction-drive differential pitch-yaw joint
[DE89-005107] N89-20480
Telerobotic manipulator developments for ground-based space research
[NASA-CR-184736] N89-20481
World modelling and multi-sensor integration for a mobile robot
[DE89-005124] N89-20482
Cross-coordinated control: An experimentally verified technique for the hybrid twist and wrench control of a voltage-controlled industrial robot
[AD-A203406] N89-20486
Development of an integrated mobile robot system at CMU (Carnegie Mellon University), June 1987
[AD-A203689] N89-20487
The 1987 year end report for road following at Canegie Mellon
[AD-A203946] N89-20488
Automatic learning by an autonomous mobile robot
[DE89-003120] N89-20702
Sensor capabilities for the HERMIES experimental robot
[DE89-003180] N89-20703
Development of a remotely maintainable radio-frequency module for the Compact Ignition Tokamak
[DE89-004913] N89-20805
ROBUSTNESS (MATHEMATICS)
Robust stabilization of linear time-invariant uncertain systems via Lyapunov theory N89-20147
Robust stability of normalized coprime factors: The infinite dimensional case
[TW-291] N89-20772
ROCKET ENGINES
Diagnostics for intelligent control of MPD engines
[AD-A203640] N89-20530
ROCKET PROPELLANTS
Lunar surface base propulsion system study, volume 1
[NASA-CR-171982-VOL-1] N89-20271
ROTARY WINGS
Acoustic test of a model rotor and tail rotor: Results for the isolated rotors and combined configuration
[NASA-TM-101550] N89-20777
ROTATING DISKS
Development of a rotary value for pulse combustion applications
[PB89-131114] N89-20468
ROTATING FLUIDS
Physical phenomena in containerless glass processing N89-20310
Solutions to the Navier-Stokes equations using a k-epsilon turbulence model
[FFA-TN-1988-19] N89-20416
ROTATION
The dynamics of free liquid drops N89-20316
Analysis of the dynamics of guided rotating free center plates N89-20466
ROTOR AERODYNAMICS
Aerodynamic pressure and flow-visualization measurement from a rotating wind turbine blade
[DE89-000854] N89-20104
Hub and blade structural loads measurements of an SA349/2 helicopter
[NASA-TM-101040] N89-20124
Unsteady blade pressure measurements on a model counterrotation propeller
[NASA-TM-102002] N89-20779
ROTOR BLADES (TURBOMACHINERY)
High speed balancing applied to the T700 engine
[NASA-CR-180899] N89-20472
ROTOR BODY INTERACTIONS
Hub and blade structural loads measurements of an SA349/2 helicopter
[NASA-TM-101040] N89-20124
Coupled rotor/fuselage dynamic analysis of the AH-1G helicopter and correlation with flight vibrations data
[NASA-CR-181723] N89-20512
ROVING VEHICLES
Mars manned transportation vehicle
[NASA-TM-101487] N89-20545
RUBY
Theoretical comparison of maser materials for a 32-GHz maser amplifier N89-20335
RUN TIME (COMPUTERS)
Run-time scheduling and execution of loops on message passing machines
[NASA-CR-181785] N89-20638
High performance preconditioning — elliptical partial differential equations
[REPT-88-54] N89-20725
RUNGE-KUTTA METHOD
A cell-vertex multigrid method for the Navier-Stokes equations
[NASA-TM-101557] N89-20101
RURAL LAND USE
Land use inventory using LANDSAT Thematic Mapper imagery to study environmental pollution
[NLR-MP-87063-U] N89-20541

S

SABOT PROJECTILES
Axially accelerated saboted rods subjected to lateral forces
[DE89-007466] N89-20485
SAFETY DEVICES
Design and implementation of the hazard control box for the ride motion simulator
[AD-A203752] N89-20404
SAFETY FACTORS
Vehicle for Space Transfer and Recovery (VSTAR), volume 2: Substantiating analyses and data
[NASA-CR-184828] N89-20184
NEN 6096, design resolution for small wind turbines
[NLR-MP-88005-U] N89-20551
SAMPLING
Aircraft operations and airborne measurement of perfluorotrimethylcyclohexane (PTCH) during ANATEX
[DE89-006934] N89-20566
SAPPHIRE
Hardness of amorphous hard carbon films determined by the ultra-low load microindentation technique
[DE89-006129] N89-20259
Theoretical comparison of maser materials for a 32-GHz maser amplifier N89-20335
SATELLITE ATTITUDE CONTROL
Design of a three-axis stabilized orion satellite using an all-thruster attitude control system
[AD-A203953] N89-20191
SATELLITE COMMUNICATION
DMA (Defense Mapping Agency) orbit determination of the navy navigation satellite system for 1987
[AD-A203496] N89-20170
Review of network planning methods applicable to Integrated Satellite Terrestrial Networks (ISTN)
[ESA-CR(P)-2691] N89-20185
Error control techniques for satellite and space communications
[NASA-CR-184825] N89-20357
Analysis of modified SMI method for adaptive array weight control
[NASA-CR-184904] N89-20364
SATELLITE IMAGERY
Data compression as a means to disseminate more Meteosat data over the existing channel
[NLR-MP-86063-U] N89-20369

The suitability of remote sensing for surveying and monitoring landscape patterns. Volume A: Pilot study - LANDSAT Imagery. Volume B: PEPS Project No. 73 - SPOT Imagery
[BCRS-87-12-VOL-A/B] N89-20534
The suitability of remote sensing for surveying and monitoring landscape patterns. Volume A: Pilot study - LANDSAT imagery N89-20535
The suitability of remote sensing for surveying and monitoring landscape patterns. Volume B: PEPS Project No. 73 - SPOT Imagery N89-20536
Land use inventories using satellite images in the region Haaren-Helvoirt-Udenhout, North Brabant (The Netherlands)
[BCRS-88-07] N89-20537
Processing and application of digital AVHRR-imagery for land and sea surfaces
[BCRS-88-08] N89-20538
A systematic worldwide landcover of satellite mosaics
[NLR-MP-87062-U] N89-20540
Land use inventory using LANDSAT Thematic Mapper imagery to study environmental pollution
[NLR-MP-87063-U] N89-20541
Twelve year overview of cloudfree LANDSAT imagery of The Netherlands
[NLR-MP-87072-U] N89-20542

SATELLITE INSTRUMENTS
Measurement of quasi-static and low frequency electric fields on the Viking satellite
[TRITA-EPP-87-02] N89-20189

SATELLITE NAVIGATION SYSTEMS
Future satellite navigation systems, with emphasis on NAVSTAR GPS
[NLR-MP-87034-U] N89-20116

SATELLITE NETWORKS
Review of network planning methods applicable to Integrated Satellite Terrestrial Networks (ISTN)
[ESA-CR(P)-2691] N89-20185
Conceptual study of the signalling point of the master station for a TST/SS-TDMA system. Phase 1: Overview and selection of signalling points
[SX/SP-01] N89-20360

SATELLITE OBSERVATION
Processing and application of digital AVHRR-imagery for land and sea surfaces
[BCRS-88-08] N89-20538

SATELLITE TRACKING
The Telecommunications and Data Acquisition Report
[NASA-CR-184672] N89-20329
Deriving a geocentric reference frame for satellite positioning and navigation N89-20330
Determination of GPS orbits to submeter accuracy N89-20331

SATURN ATMOSPHERE
Carbon monoxide and disequilibrium dynamics in Saturn and Jupiter N89-20903

SAWS
Analysis of the dynamics of guided rotating free center plates N89-20466

SCALARS
General relativity, scalar fields and cosmic strings N89-20852

SCANDIUM COMPOUNDS
Exploratory alloy development in the system Al-Sc-X
[DE89-007086] N89-20237

SCATTERING
A microcomputer pollution model for civilian airports and Air Force bases. Model application and background
[AD-A199794] N89-20557

SCATTERING AMPLITUDE
A prior knowledge based optimal Wiener filtering approach to ultrasonic scattering amplitude estimation
[DE89-007574] N89-20783

SCATTERING CROSS SECTIONS
Investigation of extensions to the distorted Born approximation in strong fluctuation theory
[AD-A203698] N89-20378

SCHEDULES
Space Science: Status of the Hubble Space Telescope Program
[GAO/NSIAD-88-118BR] N89-20681

SCHEDULING
Eps'88: Combining the best features of von Neumann and dataflow computing
[DE89-007291] N89-20627
Run-time scheduling and execution of loops on message passing machines
[NASA-CR-181785] N89-20638
Minimizing total completion time in the two-machine flow shop by Lagrangian relaxation
[CWI-OS-R8808] N89-20860

SCHOTTKY DIODES
Research and development of HgZnTe as an infrared material
[NASA-CR-184840] N89-20820

SCHWARZSCHILD METRIC
Nonexistence theorems for Yang-Mills fields outside the black hole of the Schwarzschild spacetime
[DE88-705351] N89-20901

SCIENTIFIC SATELLITES
Measurement of quasi-static and low frequency electric fields on the Viking satellite
[TRITA-EPP-87-02] N89-20189
Adaptive data compression system study --- scientific satellite
[SIL/CR/7129/6] N89-20639
Adaptive data compression system study, executive summary --- scientific satellite
[SIL/CR/7129/7] N89-20667

SCINTILLATION
Two-way coherent Doppler error due to solar corona N89-20332

SCORING
Trajectory scoring in rectangular coordinates using transponder-interrogator range and range rate data
[DE89-007005] N89-20119

SCREW DISLOCATIONS
Near threshold fatigue curve based on the dislocation shielding model of fracture
[DE88-011854] N89-20527

SEA ICE
Investigation of extensions to the distorted Born approximation in strong fluctuation theory
[AD-A203698] N89-20378

SEA SURFACE TEMPERATURE
Improved capabilities of the Multispectral Atmospheric Mapping Sensor (MAMS)
[NASA-TM-100352] N89-20430
Verification of regional climates of GISS GCM. Part 2: Summer
[NASA-TM-100722] N89-20589

SEISMIC WAVES
Waveform data collection for source inversion studies
[AD-A203419] N89-20575

SELECTIVE FADING
Digital radio link: Multipath fading on a 7 GHz line-of-sight link
[FOA-C-30428-3.3] N89-20365
Digital radio link: Multipath propagation on a microwave line-of-sight path
[FOA-C-30430-3.3] N89-20366

SEMANTICS
An algebraic calculus of commands
[CS-8808] N89-20656
Metric semantics for concurrency
[CWI-CS-R8803] N89-20661
Integrating syntax, semantics, and discourse DARPA (Defense Advanced Research Projects Agency) natural language understanding program
[AD-A203747] N89-20677
A compositional semantics for Concurrent Prolog
[CWI-CS-R8809] N89-20688

SEMICONDUCTOR DEVICES
Heavy ion induced Single Event Phenomena (SEP) data for semiconductor devices from engineering testing
[NASA-CR-184864] N89-20821
Carrier density and excitation energy dependent GAMMA-X photoluminescence of Type-II GaAs/AlAs superlattices
[DE89-002988] N89-20832
Ultrafast physics in microstructure and alloy systems
[AD-A203639] N89-20850

SEMICONDUCTOR DIODES
Laser diode cooling for high average power applications
[DE89-006777] N89-20454

SEMICONDUCTOR LASERS
Laser diode cooling for high average power applications
[DE89-006777] N89-20454

SEMICONDUCTORS (MATERIALS)
Vectorial electron transfer on designed surfaces
[PB88-240031] N89-20211
Research and development of HgZnTe as an infrared material
[NASA-CR-184840] N89-20820

SENSITIVITY
Very large array observations of the sun with related observations using the SMM (Solar Maximum Mission) satellite
[AD-A203873] N89-20910

SENSORY PERCEPTION
Why cold-wet makes one feel chilled: A literature review
[AD-A203452] N89-20609

SEPARATED FLOW
Standard test case for a low speed, turbulent junction vortex flow
[PB89-110779] N89-20406
Solutions to the Navier-Stokes equations using a k-epsilon turbulence model
[FFA-TN-1988-19] N89-20416
Vorticity distributions in unsteady flow separation
[AD-A203733] N89-20428

SEQUENTIAL ANALYSIS
Sequential and parallel methods for unconstrained optimization
[AD-A203807] N89-20762

SEQUENTIAL CONTROL
Improvements relating to control flow in computers
[EP-0-234-785-A1] N89-20624

SERIES EXPANSION
A hybrid-perturbation-Galerkin technique which combines multiple expansions
[NASA-CR-181781] N89-20632
Uniform asymptotic expansions of a class of integrals in terms of modified Bessel functions, with application to confluent hypergeometric functions
[CWI-AM-R8806] N89-20738

SERVICE LIFE
Environment-assisted aerospace fatigue problems in The Netherlands
[NLR-MP-88004-U] N89-20087

SERVOCONTROL
Application of parameter adaptive approach to servo control of a hydraulic manipulator
[MA-51] N89-20473

SERVOMECHANISMS
Power efficient hydraulic systems. Volume 2: Hardware demonstration phase
[AD-A203900] N89-20128
Force-reflecting master-slave control and robotic control of a traction-drive differential pitch-yaw joint
[DE89-005107] N89-20480
Design of remote maintenance tooling and fixtures for the advanced servomanipulator remote maintenance demonstration
[DE89-003114] N89-20484

SERVOMOTORS
Dynamic models for simulation of the 70-M antenna axis servos N89-20333

SET THEORY
Set theory, chapter 4
[REPT-88-47] N89-20722

SHADES
An integral sunshade for optical reception antennas N89-20347
Shutters and slats for the integral sunshade of an optical reception antenna N89-20348

SHAPES
Combining segmentation and tracking for the classification of moving objects in video scenes
[DE89-007000] N89-20668
Piecewise continuous algebraic surfaces in terms of B-splines
[PB89-109136] N89-20712

SHEAR LAYERS
Vortex-transport element simulation of a confined mixing layer
[AD-A203791] N89-20222

SHEAR STRAIN
Postbuckling Finite Element (FE) analysis of a stiffened curved panel loaded in shear
[FFA-TN-1988-23] N89-20516
A theoretical, numerical and experimental examination of in situ properties of adhesives
[FFA-TN-1988-05] N89-20526

SHEAR STRESS
Shear stress induced stimulation of mammalian cell metabolism N89-20286
The stress response system of proteins: Implications for bioreactor scaleup N89-20291
Dynamic wall pressure measurements
[AD-A203551] N89-20427

SHELL STABILITY
Elastic stability of lap-jointed cylindrical shells under axial compression
[PB88-245980] N89-20497

SHELL THEORY
Non-symmetric bifurcation of geometrically non-linear elastic-plastic axisymmetric shells under combined loads including torsion
[PB89-102149] N89-20500

SHOCK DISCONTINUITY
Numerical simulation of turbulent mixing in shock-tube experiments
[DE89-005101] N89-20425

SHOCK FRONTS
Forbidden coronal iron line emission in the Puppis A shock front: The effect of inhomogeneities
[NASA-TM-89284] N89-20875

SHOCK LAYERS
Viscous shock layer analysis of hypersonic flows over long slender vehicles N89-20097

SHOCK TESTS
Weldability of 2519-T87 aluminum alloy
[AD-A203519] N89-20244
SHOCK TUBES
Numerical simulation of turbulent mixing in shock-tube experiments
[DE89-005101] N89-20425
SHOCK WAVE PROPAGATION
The dynamic response at high-explosive inert-solid interface as predicted by finite difference/element computer programs
[DE89-007303] N89-20272
SHOCK WAVES
Documentation of two- and three-dimensional hypersonic shock wave/turbulent boundary layer interaction flows
[NASA-TM-101075] N89-20100
Structure-property characterization of a shock-loaded boron carbide-aluminum cermet
[DE89-005455] N89-20257
SHUTTERS
Shutters and slats for the integral sunshade of an optical reception antenna N89-20348
SIDEBANDS
Validity of 1D free-electron laser sideband models
[DE89-006284] N89-20452
SIGNAL DETECTION
Digital signal processing
[AD-A203744] N89-20403
Noise: Friend or foe
[AD-A203491] N89-20784
SIGNAL DETECTORS
Improved computer simulation of the TCAS 3 circular array mounted on an aircraft
[NASA-CR-184907] N89-20363
SIGNAL ENCODING
Error control techniques for satellite and space communications
[NASA-CR-184825] N89-20357
SIGNAL MEASUREMENT
Density measurements with combined Raman-Rayleigh LIDAR (Light Detection And Ranging)
[AD-A203561] N89-20376
SIGNAL PROCESSING
System simulation using the PROMISE simulation package
[NLR-MP-87081-U] N89-20118
VLA telemetry performance with concatenated coding for Voyager at Neptune N89-20340
Long decoding runs for Galileo's convolutional codes N89-20342
Performance of Galileo's concatenated codes with nonideal interleaving N89-20343
The decoding of Reed-Solomon codes N89-20344
Shutters and slats for the integral sunshade of an optical reception antenna N89-20348
Conceptual study of the signalling point of the master station for a TST/SS-TDMA system. Phase 1: Overview and selection of signalling points
[SX/SP-01] N89-20360
Efficient detection and signal parameter estimation with applications to high dynamic GPS receivers
[NASA-CR-184861] N89-20362
Analysis of modified SMI method for adaptive array weight control
[NASA-CR-184904] N89-20364
Testing for nonlinearity using a prediction error filter
[RR-332] N89-20371
Symbols for communication circuit design and documentation
[DE88-013002] N89-20372
A comparison of frequency estimation techniques for high-dynamic trajectories
[NASA-CR-184865] N89-20387
On-line arithmetic algorithms and structures for VLSI
[AD-A203421] N89-20400
Digital signal processing
[AD-A203744] N89-20403
Optical Johnson noise thermometry
[NASA-CR-184964] N89-20437
Using random number generators on the sensor signal processing system
[AD-A203702] N89-20761
Noise: Friend or foe
[AD-A203491] N89-20784
SIGNAL RECEPTION
VLA telemetry performance with concatenated coding for Voyager at Neptune N89-20340
An integral sunshade for optical reception antennas N89-20347
Analysis of modified SMI method for adaptive array weight control
[NASA-CR-184904] N89-20364
SIGNAL TO NOISE RATIOS
A long constraint length VLSI Viterbi decoder for the DSN N89-20341
Error control techniques for satellite and space communications
[NASA-CR-184825] N89-20357
SIGNAL TRANSMISSION
High-dynamic GPS tracking
[NASA-CR-184868] N89-20113
Direct solar-pumped iodine laser amplifier
[NASA-CR-184813] N89-20447
SILICA GLASS
Glass corrosion in natural environment
[NASA-CR-184843] N89-20251
SILICATES
Effect of surface stress on stress corrosion of silicate glass
[DE89-004584] N89-20529
SILICON
The influence of thickness and wavelength on the mechanical properties of a compositionally modulated ceramic thin film
[DE89-006033] N89-20258
Ductile-regime turning of germanium and silicon
[NASA-TM-101231] N89-20322
SILICON ALLOYS
Microstructural and magnetic characterization in soft magnetic Fe-Si-Al (Sendust) alloy
[DE89-007130] N89-20239
SILICON CARBIDES
Hardness of amorphous hard carbon films determined by the ultra-low load microindentation technique
[DE89-006129] N89-20259
SILVER
Damage to silver coatings from high average power 1-micron laser
[DE89-005476] N89-20448
SIMD (COMPUTERS)
Improvements relating to control flow in computers
[EP-0-234-785-A1] N89-20624
SIMPLEX METHOD
Basis representations in large-scale linear programming software
[MA-50] N89-20649
SIMULATION
High Reynolds number incompressible flow simulation about parachute canopies and similar bluff bodies N89-20096
Testing of time domain simulators for nonlinear electronic circuits
[PB89-125132] N89-20384
Potential of large format camera photography
[PB89-122485] N89-20433
Nonnormal accelerations due to yielding in a primary structure
[PB89-131437] N89-20513
Observed and modeled terrain-induced shear in tracer trajectories
[DE89-006938] N89-20590
Consequences of nonclassical measurement for the algorithmic description of continuous dynamical systems
[NASA-CR-184851] N89-20640
SINGLE CRYSTALS
Growth of solid solution single crystals N89-20297
A study of ferroelectricity in single crystal compounds of the type AFB5 and A3B2F12
[AD-A203610] N89-20849
SINGLE EVENT UPSETS
Heavy ion induced Single Event Phenomena (SEP) data for semiconductor devices from engineering testing
[NASA-CR-184864] N89-20821
SIZE DISTRIBUTION
A dynamic flow-weighted pore size distribution test
[DE89-006191] N89-20260
SLENDER BODIES
Viscous shock layer analysis of hypersonic flows over long slender vehicles N89-20097
Vorticity distributions in unsteady flow separation
[AD-A203733] N89-20428
SLENDER WINGS
Observed Reynolds number effects on airfoils and high aspect ratio wings at transonic flow conditions
[NLR-MP-88006-U] N89-20102
SLIDING CONTACT
Influence of lubrication on ceramic and steel sliding contacts
[PB89-125090] N89-20467
SLIDING FRICTION
Influence of lubrication on ceramic and steel sliding contacts
[PB89-125090] N89-20467
SLOPES
The development and structure of nocturnal slope winds in a simple valley
[AD-A203427] N89-20593
SMOKE
Flow visualization of time-varying structural characteristics of dean vortices in a curved channel
[AD-A203875] N89-20429
New models to assess behavioral and physiological performance of animals during inhalation exposures
[PB89-128946] N89-20601
SNOW COVER
Investigation of extensions to the distorted Born approximation in strong fluctuation theory
[AD-A203698] N89-20378
SODIUM CHLORIDES
Assessment of high-temperature battery systems
[DE89-007554] N89-20399
SODIUM SULFUR BATTERIES
Assessment of high-temperature battery systems
[DE89-007554] N89-20399
SOFTENING
Softening mechaniams and microstructural instabilities during high temperature low cycle fatigue of Ni, Ni3Al and their metal matrix composites
[DE89-007117] N89-20238
SOFTWARE ENGINEERING
Flexible structure control laboratory development and technology demonstration
[NASA-CR-184867] N89-20151
A communication channel model of the software process
[NASA-CR-184866] N89-20643
Incremental development and prototyping in current laboratory software development projects: Preliminary analysis
[NASA-CR-184860] N89-20644
Directions in reusing software
[REPT-88-58] N89-20651
Tools for the development of information systems at NLR
[NLR-MP-87079-U] N89-20652
NEXT 2.0, an expert system shell for engineering applications
[NLR-MP-88015-U] N89-20653
An exploration of the Bird-Meertens formalism
[CS-8810] N89-20658
Do-it-yourself type theory
[CS-8811] N89-20659
On automatic differentiation
[DE89-005779] N89-20752
The certainty factor model and its basis in probability theory
[CWI-CS-R8816] N89-20768
SOFTWARE TOOLS
Directions in reusing software
[REPT-88-58] N89-20651
Tools for the development of information systems at NLR
[NLR-MP-87079-U] N89-20652
NEXT 2.0, an expert system shell for engineering applications
[NLR-MP-88015-U] N89-20653
Evaluation of the RTP Pascal-MALPAS IL translator
[NPL-DITC-128/88] N89-20654
An exploration of the Bird-Meertens formalism
[CS-8810] N89-20658
Implementation of a language translator for the computer aided prototyping system
[AD-A203876] N89-20680
Reliability and performance evaluation of systems containing embedded rule-based expert systems
[NASA-CR-181769] N89-20683
Integrated analysis package for Mk-3 K-coronameter observations: A user's manual
[PB88-250717] N89-20904
SOLAR ACTIVITY
The behavior of the electron density and temperatue at Millstone Hill during the equinox transition study September 1984
[NASA-CR-184737] N89-20567
SOLAR CELLS
Edge illuminated ventical multijunction
[DE89-006246] N89-20547
Characterization of production GaAs solar cells for space
[NASA-CR-184863] N89-20549
Dendritic web silicon photovoltaic cell research
[DE89-007269] N89-20554
SOLAR CORONA
Very large array observations of the sun with related observations using the SMM (Solar Maximum Mission) satellite
[AD-A203873] N89-20910
Aperture synthesis observations of solar and stellar radio emission N89-20912
SOLAR COSMIC RAYS
On the effects of Cosmions upon the structure and evolution of very low mass stars
[NASA-CR-182958] N89-20880
SOLAR DIAMETER
Aperture synthesis observations of solar and stellar radio emission N89-20912

SOLAR ENERGY
Climate fundamentals for solar energy systems
[DE89-007319] N89-20592
SOLAR FLARES
Solar-geophysical data number 530, October 1988. Part 2: (Comprehensive reports). Data for April 1988 and miscellaneous
[PB89-130827] N89-20908
Solar-geophysical data number 530, October 1988. Part 1: (Prompt reports). Data for September, August 1988 and late data
[PB89-130835] N89-20909
Very large array observations of the sun with related observations using the SMM (Solar Maximum Mission) satellite
[AD-A203873] N89-20910
SOLAR GRANULATION
Magnetic fields and supergranule velocity fields on the quiet sun N89-20907
SOLAR HEATING
Climate fundamentals for solar energy systems
[DE89-007319] N89-20592
SOLAR LIMB
Magnetic fields and supergranule velocity fields on the quiet sun N89-20907
SOLAR MAGNETIC FIELD
Magnetic fields and supergranule velocity fields on the quiet sun N89-20907
SOLAR MAXIMUM MISSION
Very large array observations of the sun with related observations using the SMM (Solar Maximum Mission) satellite
[AD-A203873] N89-20910
SOLAR PHYSICS
SELSIS (the Space Environment Laboratory Solar Imaging System): Initial requirements
[PB89-113039] N89-20906
SOLAR PROMINENCES
Solar-geophysical data number 530, October 1988. Part 2: (Comprehensive reports). Data for April 1988 and miscellaneous
[PB89-130827] N89-20908
SOLAR RADIATION
Climate fundamentals for solar energy systems
[DE89-007319] N89-20592
SELSIS (the Space Environment Laboratory Solar Imaging System): Initial requirements
[PB89-113039] N89-20906
SOLAR RADIO BURSTS
Solar-geophysical data number 530, October 1988. Part 2: (Comprehensive reports). Data for April 1988 and miscellaneous
[PB89-130827] N89-20908
SOLAR RADIO EMISSION
Solar-geophysical data number 530, October 1988. Part 1: (Prompt reports). Data for September, August 1988 and late data
[PB89-130835] N89-20909
Aperture synthesis observations of solar and stellar radio emission N89-20912
SOLAR SIMULATORS
Direct solar-pumped iodine laser amplifier
[NASA-CR-184813] N89-20447
SOLAR SYSTEM
Research and technology of the Lyndon Johnson Space Center
[NASA-TM-100473] N89-20918
SOLAR TERRESTRIAL INTERACTIONS
Two-way coherent Doppler error due to solar corona N89-20332
Long-term solar-terrestrial observations
[NASA-CR-184695] N89-20905
SOLAR WIND
Solar-geophysical data number 530, October 1988. Part 1: (Prompt reports). Data for September, August 1988 and late data
[PB89-130835] N89-20909
Very large array observations of the sun with related observations using the SMM (Solar Maximum Mission) satellite
[AD-A203873] N89-20910
SOLAR X-RAYS
Solar-geophysical data number 530, October 1988. Part 2: (Comprehensive reports). Data for April 1988 and miscellaneous
[PB89-130827] N89-20908
SOLID ELECTROLYTES
Thermogravimetric analysis of polymeric materials for an intermediate temperature solid electrolyte. 2: Polymer mixtures
[DE89-006980] N89-20262
Screening study of lithiated catholyte mixes for a long-life Li(Si)/FeS2 thermal battery
[DE89-006857] N89-20393
SOLID LUBRICANTS
Long term lubrication of ceramics at high temperatures N89-20249
Evaluation of solid lubricants: Temperature programmed desorption of MoS2 on molybdenum and of ion-implanted MoS2 on molybdenum
[AD-A203741] N89-20268
SOLID SOLUTIONS
Growth of solid solution single crystals N89-20297
SOLID STATE
Irradiation as a tool for studying solid state amorphization phenomena
[DE89-006034] N89-20823
SOLID STATE LASERS
Performance of efficient Q-switched diode-laser-pumped Nd:YAG and Ho:YLF lasers for space applications N89-20345
Ground State Depleted (GSD) solid state lasers: Principles, characteristics, and scaling
[DE89-006149] N89-20450
SOLID-SOLID INTERFACES
An efficient method for solving free-boundary problems
[REPT-88-63] N89-20727
SOLIDIFICATION
Dendritic growth and structure of undercooled nickel base alloys N89-20302
Pb-Zn liquid metal diffusion N89-20304
SOLIDS
Scientific support for an orbiter middeck experiment on solid surface combustion N89-20312
Paraxial approximations for ultrasonic beam propagation in liquid and solid media with applications to nodestructive evaluation
[DE89-007569] N89-20782
SOLITARY WAVES
Soliton geometry and the vacuum gravitational field equations
[DE88-705340] N89-20573
Nonlinear partial differential equations on homogeneous spaces
[DE88-705342] N89-20748
SOLUBILITY
Solubility of hydrogen, deuterium and tritium in palladium metal
[DE89-005304] N89-20225
SONAR
World modelling and multi-sensor integration for a mobile robot
[DE89-005124] N89-20482
SOUTHERN SKY
The upper main sequence of OB associations. 1: Spectral types and lines of C and N of southern single-lined O stars
[SER-C-PREPUBL-FASC-32] N89-20884
SPACE ADAPTATION SYNDROME
USSR Space Life Sciences Digest, Issue 21
[NASA-CR-3922(24)] N89-20602
SPACE COMMERCIALIZATION
Commercial potential of European and Japanese space programs, task 5
[NASA-CR-184659] N89-20871
SPACE EXPLORATION
Aerospace vehicle design, Spacecraft Section final project reports
[NASA-CR-184742] N89-20122
SPACE FLIGHT
Continuous flow electrophoresis system experiments on shuttle flights STS-6 and STS-7 N89-20277
SPACE MAINTENANCE
Space Science: Status of the Hubble Space Telescope Program
[GAO/NSIAD-88-118BR] N89-20881
SPACE MISSIONS
The Cluster Mission: Scientific and technical aspects of the instruments
[ESA-SP-1103] N89-20156
Wave experiment consortium --- Cluster mission N89-20159
STAFF: The Spatio-Temporal Analysis of Field Fluctuations experiment --- Cluster mission N89-20160
The spherical probe electric field and wave experiment --- Cluster mission N89-20161
Whisper: A sounder and high frequency wave analyzer experiment --- Cluster mission N89-20162
The wideband plasma wave interaction --- Cluster mission N89-20163
The digital wave processing experiment --- Cluster mission N89-20164
The electron drift instrument --- Cluster mission N89-20165
The ion spectrometry experiment to measure the properties of the ionic plasma composition and distribution functions at energies between 0 and 40keV/e --- Cluster mission N89-20166
PEACE: A Plasma Electron And Current Experiment --- Cluster mission N89-20167
RAPID: Research with Adaptive Particle Imaging Detectors --- Cluster mission N89-20168
Active spacecraft potential control: An ion emitter experiment --- Cluster mission N89-20169
SPACE OBSERVATIONS (FROM EARTH)
Astrophysics in a nutshell: From the telescope to the Sputnik
[TRITA-EPP-88-04] N89-20897
Astrophysical significance of observations and experiments in the Earth's magnetosphere
[TRITA-EPP-88-09] N89-20899
SPACE PERCEPTION
Using depth recovery in humans
[AD-A201278] N89-20606
SPACE PLASMAS
AFE ion mass spectrometer design study
[NASA-CR-184838] N89-20432
Stimulated Raman scattering of intense laser radiation in a nuclear-disturbed space plasma
[AD-A200951] N89-20440
Scientific results from the Swedish Viking satellite
[IRF-SR-196] N89-20572
Astrophysical significance of observations and experiments in the Earth's magnetosphere
[TRITA-EPP-88-09] N89-20899
SPACE PROBES
To Uranus and beyond
[NASA-EP-260] N89-20902
SPACE PROCESSING
Microgravity Science and Applications Flight Programs, January - March 1987, selected papers, volume 1
[NASA-TM-4069-VOL-1] N89-20276
Kidney cell electrophoresis in space flight: Rationale, methods, results and flow cytometry applications N89-20280
Hormone purification by isoelectric focusing in space N89-20282
Hydrodynamic effects on cell growth in agitated microcarrier bioreactors N89-20284
An expert system based intelligent control scheme for space bioreactors N89-20285
Shear stress induced stimulation of mammalian cell metabolism N89-20286
Human cell culture in a space bioreactor N89-20288
Protein crystal growth in a microgravity environment N89-20292
Growth of mercuric iodide (HgI2) for nuclear radiation detectors N89-20293
Modelling the growth of triglycine sulphate crystals in Spacelab 3 N89-20294
The first products made in space: Monodisperse latex particles N89-20318
SPACE PROGRAMS
Research and technology of the Lyndon Johnson Space Center
[NASA-TM-100473] N89-20918
SPACE SHUTTLE BOOSTERS
Flight motor set 360L001 (STS-26R), volume 1
[NASA-CR-183576] N89-20196
Space shuttle propulsion estimation development verification, volume 1
[NASA-CR-183581] N89-20197
SPACE SHUTTLE MAIN ENGINE
Space shuttle propulsion estimation development verification
[NASA-CR-183582] N89-20195
Space shuttle propulsion estimation development verification, volume 1
[NASA-CR-183581] N89-20197
Studies and analyses of the space shuttle main engine. Failure information propagation model data base and software
[NASA-CR-183586] N89-20198
Identification of space shuttle main engine dynamics
[NASA-TM-101982] N89-20199
SPACE SHUTTLE MISSION 51-F
Flight motor set 360L001 (STS-26R), volume 1
[NASA-CR-183576] N89-20196
SPACE SHUTTLE PAYLOADS
Dendritic growth and structure of undercooled nickel base alloys N89-20302
SPACE SHUTTLES
Expendable launch vehicle transportation for the space station
[NASA-TM-101947] N89-20179
Low frequency vibration isolation technology for microgravity space experiments
[NASA-TM-101448] N89-20324
SPACE STATION POWER SUPPLIES
A definition study of the on-orbit assembly operations for the outboard photovoltaic power modules for Space Station Freedom
[NASA-TM-102006] N89-20171

SPACE STATION STRUCTURES
A definition study of the on-orbit assembly operations for the outboard photovoltaic power modules for Space Station Freedom
[NASA-TM-102006] N89-20171
SPACE STATIONS
Expendable launch vehicle transportation for the space station
[NASA-TM-101947] N89-20179
L1 libration point manned space habitat
[NASA-CR-184732] N89-20180
Space Station: NASA efforts to establish a design-to-life-cycle cost process
[GAO/NSIAD-88-147] N89-20188
Space operations: Testing of NASA's technical and management information system
[GAO/IMTEC-88-28] N89-20859
NASA authorization
[S-HRG-100-579] N89-20873
SPACE TRANSPORTATION
Advanced technology for future space propulsion systems
[NASA-TM-101951] N89-20192
Research and technology of the Lyndon Johnson Space Center
[NASA-TM-100473] N89-20918
SPACE TRANSPORTATION SYSTEM
NASA authorization
[S-HRG-100-579] N89-20873
SPACE-TIME FUNCTIONS
Fortran codes for computing the space-time correlations of turbulent flow in a channel
[AD-A203749] N89-20678
General relativity, scalar fields and cosmic strings N89-20852
Fragmentation of cosmic-string loops
[NASA-CR-184892] N89-20896
Black holes as possible sources of closed and semiclosed worlds
[DE88-705336] N89-20900
Nonexistence theorems for Yang-Mills fields outside the black hole of the Schwarzschild spacetime
[DE88-705351] N89-20901
SPACEBORNE ASTRONOMY
Space Science: Status of the Hubble Space Telescope Program
[GAO/NSIAD-88-118BR] N89-20881
Astrophysics in a nutshell: From the telescope to the Sputnik
[TRITA-EPP-88-04] N89-20897
SPACECRAFT CHARGING
Active spacecraft potential control: An ion emitter experiment --- Cluster mission N89-20169
Measurement of quasi-static and low frequency electric fields on the Viking satellite
[TRITA-EPP-87-02] N89-20189
SPACECRAFT COMMUNICATION
Efficient detection and signal parameter estimation with applications to high dynamic GPS receivers
[NASA-CR-184861] N89-20362
SPACECRAFT CONSTRUCTION MATERIALS
Ablation of materials in the low earth orbital environment N89-20187
SPACECRAFT CONTROL
Translational and rotational dynamics of rigid spacecraft-based manipulators
[NLR-TR-87014-U] N89-20474
SPACECRAFT DESIGN
The Cluster Mission: Scientific and technical aspects of the instruments
[ESA-SP-1103] N89-20156
Cluster: A fleet of four spacecraft to study plasma structures in three dimensions N89-20157
Active spacecraft potential control: An ion emitter experiment --- Cluster mission N89-20169
Unmanned, space-based, reusable orbital transfer vehicle, DARVES. Volume 1: Trade analysis and design
[NASA-CR-184711] N89-20173
Two designs for an orbital transfer vehicle: A comparison of two OTVs
[NASA-CR-184696] N89-20175
Two designs for an orbital transfer vehicle
[NASA-CR-184698] N89-20177
Vehicle for Space Transfer and Recovery (VSTAR), volume 1
[NASA-CR-184827] N89-20183
SPACECRAFT MANEUVERS
A numerical method for the simulation of liquid-solid body dynamics --- spacecraft dynamics
[NLR-MP-87030-U] N89-20420
SPACECRAFT MODELS
Error localization and updating of spacecraft structures mathematical models
[ESA-CR(P)-2697] N89-20186
Translational and rotational dynamics of rigid spacecraft-based manipulators
[NLR-TR-87014-U] N89-20474
SPACECRAFT POWER SUPPLIES
Vehicle for Space Transfer and Recovery (VSTAR), volume 1
[NASA-CR-184827] N89-20183
Free-piston Stirling technology for space power
[NASA-TM-101956] N89-20194
SPACECRAFT PROPULSION
Vehicle for Space Transfer and Recovery (VSTAR), volume 1
[NASA-CR-184827] N89-20183
Advanced technology for future space propulsion systems
[NASA-TM-101951] N89-20192
Lunar surface base propulsion system study, volume 1
[NASA-CR-171982-VOL-1] N89-20271
SPACECRAFT RADIATORS
The emittance of space radiator materials measured at elevated temperatures
[NASA-TM-101948] N89-20193
SPACECRAFT RECOVERY
Vehicle for Space Transfer and Recovery (VSTAR), volume 2: Substantiating analyses and data
[NASA-CR-184828] N89-20184
SPACECRAFT STABILITY
A numerical method for the simulation of liquid-solid body dynamics --- spacecraft dynamics
[NLR-MP-87030-U] N89-20420
SPACECRAFT STRUCTURES
Error localization and updating of spacecraft structures mathematical models
[ESA-CR(P)-2697] N89-20186
SPACECRAFT TRACKING
Effect of earth albedo variation on the performance of a spatial acquisition subsystem aboard a planetary spacecraft N89-20349
Pointing a ground antenna at a spinning spacecraft using Conscan-simulation results N89-20354
SPACECRAFT TRAJECTORIES
A comparison of frequency estimation techniques for high-dynamic trajectories
[NASA-CR-184865] N89-20387
SPALLING
Experimental study of spall damage in an aluminium alloy
[PB89-112619] N89-20224
SPARK CHAMBERS
Production of pulsed electron beams by triggered pseudo-spark discharges
[ISL-CO-245/87] N89-20388
SPATIAL DISTRIBUTION
Using depth recovery in humans
[AD-A201278] N89-20606
SPATIAL RESOLUTION
World modelling and multi-sensor integration for a mobile robot
[DE89-005124] N89-20482
Very large array observations of the sun with related observations using the SMM (Solar Maximum Mission) satellite
[AD-A203873] N89-20910
SPECIFIC HEAT
The lambda point experiment in microgravity N89-20319
SPECIFICATIONS
Very High Speed Integrated Circuits (VHSIC). Phase 2: Submicrometer technology development, interoperability standards
[AD-A203629] N89-20401
Fastbus standard routines
[DOE/ER-0367] N89-20645
SPECKLE PATTERNS
Digital processing of speckle images
[AD-A203703] N89-20801
SPECTRA
Paraxial approximations for ultrasonic beam propagation in liquid and solid media with applications to nodestructive evaluation
[DE89-007569] N89-20782
SPECTRAL BANDS
The wideband plasma wave interaction --- Cluster mission N89-20163
SPECTRAL CORRELATION
STAFF: The Spatio-Temporal Analysis of Field Fluctuations experiment --- Cluster mission N89-20160
SPECTRAL METHODS
Spectral methods for CFD
[NASA-CR-181803] N89-20718
SPECTRAL REFLECTANCE
Carbon monoxide and disequilibrium dynamics in Saturn and Jupiter N89-20903
SPECTRAL THEORY
Dynamic wall pressure measurements
[AD-A203551] N89-20427
SPECTROSCOPIC ANALYSIS
AFE ion mass spectrometer design study
[NASA-CR-184836] N89-20432
SPECTROSCOPY
The ion spectrometry experiment to measure the properties of the ionic plasma composition and distribution functions at energies between 0 and 40keV/e --- Cluster mission N89-20166
Effects of environment on tunneling spectroscopy of gold films
[DE89-006040] N89-20844
SPECTRUM ANALYSIS
The wideband plasma wave interaction --- Cluster mission N89-20163
Spectral analysis of block structured nonlinear systems
[RR-329] N89-20728
Spectral analysis for nonlinear systems. Part 1: Parametric nonlinear spectral analysis
[RR-337] N89-20733
SPECULAR REFLECTION
Digital processing of speckle images
[AD-A203703] N89-20801
SPHERICAL COORDINATES
Flux vector splitting in general curvilinear coordinates
[PB89-127393] N89-20410
SPHEROMAKS
Improved plasma confinement and evidence for a pressure-driven instability from reduced magnetic field errors in the CTX spheromak
[DE89-005475] N89-20806
SPIN DYNAMICS
Pointing a ground antenna at a spinning spacecraft using Conscan-simulation results N89-20354
The Delft Ising system processor
[ISBN-9-09-001753-4] N89-20625
SPIN-LATTICE RELAXATION
Transport and relaxation processes in supercritical fluids
[DE89-005910] N89-20219
SPINE
Influences of muscle fiber composition and strength on EMG (electromyographic activity), spinal motion and load acceleration during a repetitive lifting task
[PB89-131221] N89-20607
SPLINE FUNCTIONS
Piecewise continuous algebraic surfaces in terms of B-splines
[PB89-109136] N89-20712
Development of mathematical models for application in image processing
[AD-A203619] N89-20760
SPONTANEOUS EMISSION
Amplified spontaneous emission in a single pass free electron laser
[DE89-007048] N89-20461
SPOT (FRENCH SATELLITE)
The suitability of remote sensing for surveying and monitoring landscape patterns. Volume A: Pilot study - LANDSAT Imagery. Volume B: PEPS Project No. 73 - SPOT Imagery
[BCRS-87-12-VOL-A/B] N89-20534
The suitability of remote sensing for surveying and monitoring landscape patterns. Volume B: PEPS Project No. 73 - SPOT Imagery N89-20536
SPRAYING
Effects of turbulence on rate of combustion of fuel sprays N89-20212
Diffusive burning of plane liquid and spray jets in a coflowing oxidizer stream N89-20216
SPREAD SPECTRUM TRANSMISSION
Dedicated versus half-duplex receiver topology in jammed, fully connected CDMA networks: Theory and numerical comparisons
[AD-A203635] N89-20402
STABILITY
Pseudo-Bayesian stability of CSMA (Carrier Sense Multiple Access) and CSMA/CD (Collision Detection) local area networks
[AD-A203834] N89-20763
A study of the effects of copper to superconductor ratio on stability
[DE89-006604] N89-20846
STABILIZATION
A camera stabilization technique for a teleoperated vehicle
[DE89-003923] N89-20476
STAINLESS STEELS
Results of inphase axial-torsional fatigue experiments on 304 stainless steel
[NASA-TM-101464] N89-20514
STALLING
An analytical and numerical study of axial flow compressor instability N89-20131

STANDARDIZATION
Noise: Friend or foe
[AD-A203491] N89-20784
STANDARDS
Transmitter data collection using Ada N89-20352
Suitability of ANSI standards for quantifying communication satellite system performance
[NASA-CR-182684] N89-20356
Very High Speed Integrated Circuits (VHSIC). Phase 2: Submicrometer technology development, interoperability standards
[AD-A203629] N89-20401
High speed balancing applied to the T700 engine
[NASA-CR-180899] N89-20472
NEN 6096, design resolution for small wind turbines
[NLR-MP-88005-U] N89-20551
Fastbus standard routines
[DOE/ER-0367] N89-20645
STAR FORMATION
Star formation, using 3-D explicit Eulerian hydrodynamics N89-20890
STATE VECTORS
State representations of linear systems with output constraints
[CWI-OS-R8807] N89-20744
STATIC PRESSURE
Position error calibration of a pressure survey aircraft using a trailing cone
[PB88-250733] N89-20092
STATIC TESTS
Static tensile and tensile creep testing of five ceramic fibers at elevated temperatures
[NASA-CR-184690] N89-20200
STATISTICAL ANALYSIS
Transmitter data collection using Ada N89-20352
Censoring, truncation and filtering in statistical models based on counting processes
[CWI-MS-R8803] N89-20769
STATISTICAL MECHANICS
The lambda point experiment in microgravity N89-20319
STATISTICAL TESTS
DETECT: Dependency tree evaluation and confidence test
[REPT-88-55] N89-20765
STEELS
Influence of lubrication on ceramic and steel sliding contacts
[PB89-125090] N89-20467
Long-term evaluation of the acoustic emission weld monitor
[PB88-122642] N89-20471
STEERABLE ANTENNAS
Electronically Steerable Terminal Antenna (ESTA) project, phase 2
[ESA-CR(P)-2599] N89-20359
STELLAR COMPOSITION
The upper main sequence of OB associations. 1: Spectral types and lines of C and N of southern single-lined O stars
[SER-C-PREPUBL-FASC-32] N89-20884
STELLAR CORES
On the effects of Cosmions upon the structure and evolution of very low mass stars
[NASA-CR-182958] N89-20880
Grids of evolutionary models from 0.85 to 120 solar masses: Observational tests and the mass limits
[SER-C-PREPUBL-FASC-29] N89-20882
STELLAR ENVELOPES
Molecular radio line observations of mass loss from red giants
[PB89-102313] N89-20885
Dust shells around Miras and OH/IR stars N89-20889
STELLAR EVOLUTION
On the effects of Cosmions upon the structure and evolution of very low mass stars
[NASA-CR-182958] N89-20880
Grids of evolutionary models from 0.85 to 120 solar masses: Observational tests and the mass limits
[SER-C-PREPUBL-FASC-29] N89-20882
Tables of evolutionary star models from 0.85 to 120 solar masses with overshooting and mass loss
[SER-C-PREPUBL-FASC-30] N89-20883
Molecular radio line observations of mass loss from red giants
[PB89-102313] N89-20885
STELLAR FLARES
Aperture synthesis observations of solar and stellar radio emission N89-20912
STELLAR MAGNETIC FIELDS
Magnetospheres of neutron stars accreting from disks N89-20895
STELLAR MASS
Grids of evolutionary models from 0.85 to 120 solar masses: Observational tests and the mass limits
[SER-C-PREPUBL-FASC-29] N89-20882
STELLAR MASS EJECTION
Tables of evolutionary star models from 0.85 to 120 solar masses with overshooting and mass loss
[SER-C-PREPUBL-FASC-30] N89-20883
Molecular radio line observations of mass loss from red giants
[PB89-102313] N89-20885
STELLAR MODELS
Grids of evolutionary models from 0.85 to 120 solar masses: Observational tests and the mass limits
[SER-C-PREPUBL-FASC-29] N89-20882
Tables of evolutionary star models from 0.85 to 120 solar masses with overshooting and mass loss
[SER-C-PREPUBL-FASC-30] N89-20883
STELLAR ROTATION
Lithium depletion and rotation in main sequence stars N89-20886
Nonthermal radio emission from RS CVN binaries and similar systems N89-20913
STELLAR SPECTRA
The upper main sequence of OB associations. 1: Spectral types and lines of C and N of southern single-lined O stars
[SER-C-PREPUBL-FASC-32] N89-20884
STELLAR STRUCTURE
On the effects of Cosmions upon the structure and evolution of very low mass stars
[NASA-CR-182958] N89-20880
Grids of evolutionary models from 0.85 to 120 solar masses: Observational tests and the mass limits
[SER-C-PREPUBL-FASC-29] N89-20882
STELLAR TEMPERATURE
On the effects of Cosmions upon the structure and evolution of very low mass stars
[NASA-CR-182958] N89-20880
STIFFENING
Tripping of asymmetrical stiffeners under combined loading
[PB89-126171] N89-20504
STIRLING CYCLE
Free-piston Stirling technology for space power
[NASA-TM-101956] N89-20194
STIRLING ENGINES
Free-piston Stirling technology for space power
[NASA-TM-101956] N89-20194
Failure analysis of a Stirling engine heat pipe
[NASA-TM-101418] N89-20227
STOCHASTIC PROCESSES
Discrete analysis of stochastic NMR
[DE89-007016] N89-20494
Noise: Friend or foe
[AD-A203491] N89-20784
STORAGE BATTERIES
Assessment of high-temperature battery systems
[DE89-007554] N89-20399
STORAGE RINGS (PARTICLE ACCELERATORS)
On the performance of the DELPHI hadron calorimeter
[PH-159] N89-20434
Literature search on kickers and septa for the Amsterdam Pulse Stretcher (APS)
[LINO-158] N89-20791
STORAGE TANKS
Superfluid Helium Tanker (SFHT) study
[NASA-CR-172110] N89-20182
STORMS
Long-range forecasting of storminess over the Northern Hemisphere oceans
[AD-A203949] N89-20595
STORMS (METEOROLOGY)
3CPO, Cloud Chemistry and Cloud Physics Organization: Data index, June 1988
[DE89-007011] N89-20591
STRAIN DISTRIBUTION
Computational studies in nonlinear fracture mechanics N89-20508
STRAIN GAGES
Advanced high temperature instrument for hot section research applications N89-20137
STRAIN MEASUREMENT
Advanced high temperature instrument for hot section research applications N89-20137
STRAIN RATE
Analysis of the strain-rate sensitivity at high strain rates in fcc and bcc metals
[DE89-005471] N89-20233
Constitutive properties of copper and tantalum at high rates of tensile strain: Expanding ring results
[DE89-006197] N89-20242
A comprehensive review of modeling of impact damage in ceramics
[AD-A203477] N89-20264
STRATEGY
Two dimensional maps generated by competitive systems
[DE89-007878] N89-20759
STRATOSPHERE
Numerical studies of barotropic stability of stratospheric states N89-20570
STREAK CAMERAS
The effects of variations in the photocathode voltages of electronic streak cameras
[DE89-006776] N89-20436
STRESS (BIOLOGY)
Microgravity Science and Applications Flight Programs, January - March 1987, selected papers, volume 1
[NASA-TM-4069-VOL-1] N89-20276
STRESS (PHYSIOLOGY)
The stress response system of proteins: Implications for bioreactor scaleup N89-20291
STRESS ANALYSIS
An analysis of an incompressible, fiber-reinforced material subjected to finite strains in the direction of reinforcement N89-20201
Reliability-based failure analysis of brittle materials
[NASA-CR-184799] N89-20489
A displacement pattern matching application in elastic-plastic hybrid stress analysis
[AD-A199028] N89-20499
Non-symmetric bifurcation of geometrically non-linear elastic-plastic axisymmetric shells under combined loads including torsion
[PB89-102149] N89-20500
Large deflection analysis of thin elastic shells by hybrid stress method
[PB89-111504] N89-20506
A refined theory for plate bending with optimized stress field N89-20510
Effect of surface stress on stress corrosion of silicate glass
[DE89-004584] N89-20529
Dendritic web silicon photovoltaic cell research
[DE89-007289] N89-20554
STRESS CORROSION
Corrosion fatigue of iron-chronium nickel alloys: Fracture mechanics and chemistry
[DE89-006985] N89-20236
The influence of surface capacitance on the measurements of localized corrosion transients
[DE89-006172] N89-20391
Effect of surface stress on stress corrosion of silicate glass
[DE89-004584] N89-20529
STRESS CORROSION CRACKING
Environment-assisted aerospace fatigue problems in The Netherlands
[NLR-MP-88004-U] N89-20087
Electrochemical considerations of crack growth in the ferrous alloys
[AD-A203811] N89-20247
Fracture control guidelines for stress corrosion
[NLR-MP-88007-U] N89-20522
STRESS CYCLES
Microstructural influence on low cycle fatigue strength of IMI550
[PNR90500] N89-20226
STRESS DISTRIBUTION
Experimental study of spall damage in an aluminium alloy
[PB89-112619] N89-20224
Computational studies in nonlinear fracture mechanics N89-20508
STRESS INTENSITY FACTORS
Near threshold fatigue curve based on the dislocation shielding model of fracture
[DE88-011854] N89-20527
STRESS RELAXATION
Rheometrics stress rheometer applications
[AD-A203667] N89-20275
STRESS TENSORS
Solutions and stability of a closed-geodesic black hole model N89-20893
STRESS-STRAIN RELATIONSHIPS
A numerical implementation of the Schapery model for nonlinear viscoelasticity
[ETN-89-93895] N89-20515
A micromechanical viscoplastic stress-strain model with grain boundary sliding
[DE89-007712] N89-20848
STRESSES
Rheometrics stress rheometer applications
[AD-A203667] N89-20275
HARTFEM: A finite element program for thermal and viscoplastic deformation problems
[DE89-007788] N89-20755
STRING THEORY
General relativity, scalar fields and cosmic strings N89-20852

Introduction to strings and superstrings
[DE88-704998] N89-20853
Cosmology and superstrings N89-20891
Fragmentation of cosmic-string loops
[NASA-CR-184892] N89-20896

STRINGS
Remark on the gravitational field produced by an infinite straight string
[DE88-705077] N89-20855

STRIP TRANSMISSION LINES
Reconfigurable antennas
[AD-A203847] N89-20382

STRONTIUM COMPOUNDS
Material selection for electrooptic deflectors
[DE89-007343] N89-20841

STRUCTURAL ANALYSIS
Structural analysis methods development for turbine hot section components N89-20140
Structural analysis applications N89-20141
Views on the impact of HOST N89-20144
Error localization and updating of spacecraft structures mathematical models
[ESA-CR(P)-2697] N89-20186
Structural mechanics: Contemporary state and prospects for development (selected portions)
[AD-A198766] N89-20498
Large deflection analysis of thin elastic shells by hybrid stress method
[PB89-111504] N89-20506
Postbuckling Finite Element (FE) analysis of a stiffened curved panel loaded in shear
[FFA-TN-1988-23] N89-20516
Modeling flexibility of mechanisms with ADAMS
[ESA-STM-242] N89-20518
Analysis of crack opening behavior by application of a discretized strip yield model
[NLR-MP-87065-U] N89-20520
Prediction of low and high crack growth rates under constant and variable amplitude loading
[NLR-MP-88012-U] N89-20523
Cumulative reports and publications through December 31, 1988
[NASA-CR-181784] N89-20619
A structural analysis algorithm for massively parallel computers
[DE89-005055] N89-20686
Finite element technique for the inverse problem of a partial differential equation and its application to parameter identification of structure
[PB89-111439] N89-20713
The initial value problem for fractional order differential equations with constant coefficients
[AD-A203843] N89-20764

STRUCTURAL DESIGN
Aerospace vehicle design, Spacecraft Section final project reports
[NASA-CR-184742] N89-20122
Aerospace vehicle design, Spacecraft Section
[NASA-CR-184743] N89-20123
Unmanned, space-based, reusable orbital transfer vehicle, DARVES. Volume 1: Trade analysis and design
[NASA-CR-184711] N89-20173
Two designs for an orbital transfer vehicle. Project Orion: A proposal for a manned orbital transfer vehicle for the 21st Century
[NASA-CR-184697] N89-20176
L1 libration point manned space habitat
[NASA-CR-184732] N89-20180
Cross-guide coupler modeling and design N89-20337
Conceptual design of a 1-MW CW X-band transmitter for planetary radar N89-20339
Status of LBL/LLNL FEL (Free Electron Laser) research for two beam accelerator applications
[DE89-006656] N89-20453
Elements of design, unifying principles and applications N89-20465

STRUCTURAL DESIGN CRITERIA
Matching Power Spectra Density (PSD)-design load — aircraft structures
[NLR-MP-87059-U] N89-20126
Fracture control guidelines for stress corrosion
[NLR-MP-88007-U] N89-20522
NEN 6096, design resolution for small wind turbines
[NLR-MP-88005-U] N89-20551

STRUCTURAL FAILURE
Estimation of the Equivalent Initial Flow Size (EIFS) distribution and prediction of failure probabilities for different parameter variations
[FFA-TN-1987-35] N89-20525

STRUCTURAL RELIABILITY
Welded joint integrity analysis: Relative criticality of weld defect and remote deformation
[AD-A203756] N89-20246

STRUCTURAL STABILITY
Bordered equations in continuation methods: An improved solution technique --- structural analysis
[NLR-MP-87057-U] N89-20699

STUDENTS
Schema-based theories of problem solving
[AD-A203731] N89-20774

SUBJECTS
Medical subject headings, tree structures, 1989
[PB89-100028] N89-20605

SUBSONIC FLOW
Standard test case for a low speed, turbulent junction vortex flow
[PB89-110779] N89-20406

SUBSTRATES
The influence of thickness and wavelength on the mechanical properties of a compositionally modulated ceramic thin film
[DE89-006033] N89-20258
Finite size effects in Wigner crystallization of electrons on liquid helium layers
[DE88-705370] N89-20843

SULFATES
Modelling the growth of triglycine sulphate crystals in Spacelab 3 N89-20294

SULFIDES
Sulfide and phosphide analogs of oxynitride ceramics
[AD-A203805] N89-20269

SULFONATES
Thermogravimetric analysis of polymeric materials for an intermediate temperature solid electrolyte. 2: Polymer mixtures
[DE89-006980] N89-20262

SUN
SELSIS (the Space Environment Laboratory Solar Imaging System): Initial requirements
[PB89-113039] N89-20906
Very large array observations of the sun with related observations using the SMM (Solar Maximum Mission) satellite
[AD-A203873] N89-20910

SUPERCOMPUTERS
Factoring with the quadratic sieve on large vector computers
[CWI-NM-R8805] N89-20664

SUPERCONDUCTING MAGNETS
Feasibility study of high temperature superconductor opening switches
[AD-A203699] N89-20851

SUPERCONDUCTIVITY
Surface and interface local density of states for Nb, V and Ta
[DE88-705365] N89-20240
Nucleation of superconductivity in ceramic oxides
[DE88-705364] N89-20263
Shielding effectiveness of superconductive particles in plastics
[DE89-003888] N89-20815
Electron spectroscopy studies of high temperature superconductors: Y(sub 1)-xPr(sub x)Ba2Cu3O(sub 7)-delta
[DE89-006554] N89-20824
Crystalline metal-semiconductor superlattices
[DE89-006619] N89-20825
Some structural features of high-T(sub c) superconductors
[DE89-006667] N89-20826
Thermodynamic characteristics of Y-Ba-Cu-O type compounds in the model of strong electron-phonon coupling
[DE88-705343] N89-20828
Localized versus itinerant picture of light-T(sub c) superconducting oxides
[DE88-705345] N89-20830

SUPERCONDUCTORS
Energy gap in S- and D-wave pairing superconductors
[DE88-705344] N89-20829
A study of the effects of copper to superconductor ratio on stability
[DE89-006604] N89-20846

SUPERCRITICAL AIRFOILS
Geometrical and structural properties of an Aeroelastic Research Wing (ARW-2)
[NASA-TM-4110] N89-20099

SUPERCRITICAL FLUIDS
Transport and relaxation processes in supercritical fluids
[DE89-005910] N89-20219

SUPERFLUIDITY
Experiments with metallic and ceramic porous media
[NASA-CR-184819] N89-20248
Quasi-classical calculations for superfluids
[ETN-89-94118] N89-20421
Experiments with negative ions in (3)He superfluids
[PB89-127682] N89-20814

SUPERHIGH FREQUENCIES
Conceptual design of a 1-MW CW X-band transmitter for planetary radar N89-20339
DSN 70-meter antenna X-band gain, phase, and pointing performance, with particular application for Voyager 2 Neptune encounter N89-20353
Digital radio link: Multipath fading on a 7 GHz line-of-sight link
[FOA-C-30428-3.3] N89-20365

SUPERLATTICES
Crystalline metal-semiconductor superlattices
[DE89-006619] N89-20825
Carrier density and excitation energy dependent GAMMA-X photoluminescence of Type-II GaAs/AlAs superlattices
[DE89-002988] N89-20832

SUPERPLASTICITY
Nondestructive tests of elements mamufactured using diffusion bonding and superplastic forming
[ETN-89-94131] N89-20492

SUPERSATURATION
A quantitative study of pattern formation in dendritic crystal growth from supersaturated solution N89-20818

SUPERSONIC COMBUSTION RAMJET ENGINES
A first scramjet study
[NASA-CR-184965] N89-20146

SUPERSONIC FLOW
Control-volume based Navier-Stokes equation solver valid at all flow velocities
[NASA-TM-101488] N89-20407

SUPERSYMMETRY
On heterotic supermanifolds
[DE88-705339] N89-20773
Introduction to strings and superstrings
[DE88-704998] N89-20853
Integrable two dimensional supersystems
[DE88-705355] N89-20857

SURFACE FINISHING
Ductile-regime turning of germanium and silicon
[NASA-TM-101231] N89-20322

SURFACE NAVIGATION
Development of an integrated mobile robot system at CMU (Carnegie Mellon University), June 1987
[AD-A203689] N89-20487

SURFACE PROPERTIES
The application of statistical experimental design to the development of low-density polymer foams
[DE89-006774] N89-20261
The influence of surface capacitance on the measurements of localized corrosion transients
[DE89-006172] N89-20391
The structure and reactivity of heterogeneous surfaces and study of the geometry of surface complexes
[DE89-005726] N89-20822
Surface structures determined using electron diffraction
[DE89-006669] N89-20837
Effects of environment on tunneling spectroscopy of gold films
[DE89-006040] N89-20844

SURFACE REACTIONS
Ablation of materials in the low earth orbital environment N89-20187
Vectorial electron transfer on designed surfaces
[PB88-240031] N89-20211
Design, development and applications of novel techniques for studying surface mechanical properties
[NASA-TM-101959] N89-20253
A molecular dynamics study of surface kinetics and epitaxial crystal growth N89-20819

SURFACE TEMPERATURE
Advanced high temperature instrument for hot section research applications N89-20137
Improved capabilities of the Multispectral Atmospheric Mapping Sensor (MAMS)
[NASA-TM-100352] N89-20430

SURFACE VEHICLES
Vision-based navigation for autonomous ground vehicles
[AD-A203712] N89-20120
A microcomputer pollution model for civilian airports and Air Force bases. Model application and background
[AD-A199794] N89-20557

SURFACES
Algebraic nonplanar curve and surface estimation in 3-space with applications to position estimation
[PB88-227616] N89-20709

SURVEILLANCE
Development of tooling and techniques for remote field metallography
[DE89-005400] N89-20241
A camera stabilization technique for a teleoperated vehicle
[DE89-003923] N89-20476

Combining segmentation and tracking for the classification of moving objects in video scenes
[DE89-007000] N89-20668

SURVEYS
Position error calibration of a pressure survey aircraft using a trailing cone
[PB88-250733] N89-20092
Views on the impact of HOST N89-20144
Structural mechanics: Contemporary state and prospects for development (selected portions)
[AD-A198766] N89-20498
Selection effects in optical quasar surveys N89-20877

SWEDISH SPACE PROGRAM
Measurement of quasi-static and low frequency electric fields on the Viking satellite
[TRITA-EPP-87-02] N89-20189
Scientific results from the Swedish Viking satellite
[IRF-SR-196] N89-20572

SWEPT WINGS
Development and application of a program to calculate transonic flow around an oscillating three-dimensional wing using finite difference procedures
[NASA-CR-181744] N89-20093

SWITCHES
Mechanisms for the operation of a laser-triggered vacuum switch
[DE89-007059] N89-20394

SWITCHING
Performance evaluation and analytic modeling of shared-memory computers
[PB89-113542] N89-20621

SWITCHING CIRCUITS
Feasibility study of high temperature superconductor opening switches
[AD-A203699] N89-20851

SYMBOLIC PROGRAMMING
Symbolic inversion of control relationships in model-based expert systems
[NASA-CR-182857] N89-20631

SYMBOLS
Symbols for communication circuit design and documentation
[DE88-013002] N89-20372

SYNCHRONISM
The algebra of synchronous processes
[CWI-CS-R8807] N89-20687

SYNOPTIC METEOROLOGY
Verification of regional climates of GISS GCM. Part 2: Summer
[NASA-TM-100722] N89-20589

SYNTAX
Integrating syntax, semantics, and discourse DARPA (Defense Advanced Research Projects Agency) natural language understanding program
[AD-A203747] N89-20677

SYNTHESIS (CHEMISTRY)
New approaches to fluorocarbon synthesis
[AD-A203641] N89-20221
Synthesis and physical properties of liquid crystalline alkylisocyanate copolymers
[AD-A203631] N89-20266

SYNTHETIC APERTURE RADAR
SAR processing on the array processor NMX-432
[FOA-C-30503-3.3] N89-20367
Quantization analysis of the real-time SAR digital image formation processor
[DE89-007533] N89-20754

SYNTHETIC FUELS
Design and testing of a dissociated methanol vehicle
[DE89-007051] N89-20483

SYSTEM IDENTIFICATION
Estimating nonlinear models
[RR-328] N89-20325
Testing for nonlinearity using a prediction error filter
[RR-332] N89-20371
Numerical studies of identification in nonlinear distributed parameter systems
[NASA-CR-181771] N89-20636
Lectures on linear and nonlinear filtering
[CWI-PM-R8801] N89-20701
Spectral analysis of block structured nonlinear systems
[RR-329] N89-20728
Spectral analysis for nonlinear systems. Part 1: Parametric nonlinear spectral analysis
[RR-337] N89-20733

SYSTEMS ANALYSIS
Power efficient hydraulic systems. Volume 1: Study phase
[AD-A203899] N89-20127
Vehicle for Space Transfer and Recovery (VSTAR), volume 2: Substantiating analyses and data
[NASA-CR-184828] N89-20184
Some observations on redundancy in a context
[CWI-CS-R8812] N89-20662

SYSTEMS ENGINEERING
L1 libration point manned space habitat
[NASA-CR-184732] N89-20180
Extravehicular activity at geosynchronous earth orbit
[NASA-CR-172112] N89-20181
Conceptual design of a 1-MW CW X-band transmitter for planetary radar N89-20339
Design and implementation of the hazard control box for the ride motion simulator
[AD-A203752] N89-20404
Phosphoric acid fuel cell subsystem technology
[PB88-100515] N89-20544

SYSTEMS SIMULATION
System simulation using the PROMISE simulation package
[NLR-MP-87081-U] N89-20118
Modeling flexibility of mechanisms with ADAMS
[ESA-STM-242] N89-20518

SYSTEMS STABILITY
Nonlinear input-output maps for bilinear systems and stability
[RR-335] N89-20731
A finite element stability analysis for the Marangoni problem in a rectangular container with rigid sidewalls
[TW-285] N89-20735
Well-posedness of infinite-dimensional linear systems in time and frequency domain
[TW-287] N89-20771
Robust stability of normalized coprime factors: The infinite dimensional case
[TW-291] N89-20772

T

T-39 AIRCRAFT
Position error calibration of a pressure survey aircraft using a trailing cone
[PB88-250733] N89-20092

TAIL ROTORS
Acoustic test of a model rotor and tail rotor: Results for the isolated rotors and combined configuration
[NASA-TM-101550] N89-20777

TANTALUM
Constitutive properties of copper and tantalum at high rates of tensile strain: Expanding ring results
[DE89-006197] N89-20242

TASKS
Report on federal information dissemination: Responses to decision analysis framework for GPO (Government Printing Office) strategic alternatives
[PB89-114649] N89-20864

TAYLOR SERIES
A hybrid-perturbation-Galerkin technique which combines multiple expansions
[NASA-CR-181781] N89-20632

TEARING
Fatigue teardown tests of the aged rear support of the A320 aircraft
[I-271/88] N89-20491

TECHNICAL WRITING
Comparative lexicon of US-Soviet military technical terminology
[PB89-125553] N89-20865
Research and technology of the Lyndon Johnson Space Center
[NASA-TM-100473] N89-20918

TECHNOLOGY ASSESSMENT
Assessment, development, and application of combustor aerothermal models N89-20138
Review and assessment of the database and numerical modeling for turbine heat transfer N89-20139
Telerobotic manipulator developments for ground-based space research
[NASA-CR-184736] N89-20481

TECHNOLOGY TRANSFER
Supply and use of Japanese technical literature in the United States
[PB88-230842] N89-20862
Technology transfer: Constraints perceived by Federal laboratory and agency officials
[GAO/RCED-88-116BR] N89-20874

TECHNOLOGY UTILIZATION
Energy related inventions program: A joint program of the Department of Energy and the National Institute of Standards and Technology
[PB89-141154] N89-20546
Technology transfer: Constraints perceived by Federal laboratory and agency officials
[GAO/RCED-88-116BR] N89-20874

TELECOMMUNICATION
Implementing recurrent back-propagation on the connection machine
[AD-A203796] N89-20381

TELEMETRY
VLA telemetry performance with concatenated coding for Voyager at Neptune N89-20340
A long constraint length VLSI Viterbi decoder for the DSN N89-20341
Performance of Galileo's concatenated codes with nonideal interleaving N89-20343
The decoding of Reed-Solomon codes N89-20344

TELEOPERATORS
High speed, precision motion strategies for lightweight structures
[NASA-CR-184651] N89-20327
Telerobotic manipulator developments for ground-based space research
[NASA-CR-184736] N89-20481

TELEVISION CAMERAS
A camera stabilization technique for a teleoperated vehicle
[DE89-003923] N89-20476

TEMPERATURE EFFECTS
A first scramjet study
[NASA-CR-184965] N89-20146
X-ray diffraction study of phase formation and growth in nitrogen implanted iron: Temperature effects
[AD-A203625] N89-20245
Long term lubrication of ceramics at high temperatures N89-20249
Preparative electrophoresis for space N89-20278
Growth of GaAs crystals from the melt in a partially confined configuration N89-20296
Microgravity science at Langley Research Center N89-20298

TEMPERATURE GRADIENTS
Performance and test section flow characteristics of the National Full-Scale Aerodynamics Complex 40- by 80-foot wind tunnel
[NASA-TM-101065] N89-20086

TEMPERATURE MEASUREMENT
Advanced high temperature instrument for hot section research applications N89-20137
The emittance of space radiator materials measured at elevated temperatures
[NASA-TM-101948] N89-20193
Optical Johnson noise thermometry
[NASA-CR-184964] N89-20437
The development and structure of nocturnal slope winds in a simple valley
[AD-A203427] N89-20593

TEMPERATURE SENSORS
New type of capacitive temperature sensor for use at low temperature and in strong magnetic field
[PB89-111108] N89-20431

TENSILE CREEP
Static tensile and tensile creep testing of five ceramic fibers at elevated temperatures
[NASA-CR-184690] N89-20200
Environmental effects on the time dependent failure of non-oxide ceramics
[AD-A202391] N89-20250

TENSILE PROPERTIES
Constitutive properties of copper and tantalum at high rates of tensile strain: Expanding ring results
[DE89-006197] N89-20242

TENSION
Pressure coefficients for basic tensioned-membrane structure forms
[AD-A203866] N89-20107

TENSOR ANALYSIS
Riemannian geometry on families of linear systems, the deterministic case
[REPT-88-62] N89-20726

TERMINOLOGY
Glossary of testing terminology for rechargeable batteries
[DE89-007061] N89-20395
Comparative lexicon of US-Soviet military technical terminology
[PB89-125553] N89-20865

TERRAIN
Active and passive remote sensing of ice
[AD-A203943] N89-20543

TEST CHAMBERS
Performance and test section flow characteristics of the National Full-Scale Aerodynamics Complex 40- by 80-foot wind tunnel
[NASA-TM-101065] N89-20086
Quantification of environmental chambers by air velocity mapping
[AD-A200923] N89-20154

TEST FACILITIES
Electromagnetic compatibility (EMC) test facilities
[NLR-MP-88010-U] N89-20370

TEST RANGES
Preliminary analysis of cloud-to-ground lightning in the vicinity of the Nevada test site
[PB89-128649] N89-20584

TEXTURES
The emittance of space radiator materials measured at elevated temperatures
[NASA-TM-101948] N89-20193
THEMATIC MAPPERS (LANDSAT)
Utilizing remote sensing of thematic mapper data to improve our understanding of estuarine processes and their influence on the productivity of estuarine-dependent fisheries
[NASA-CR-183417] N89-20533
The suitability of remote sensing for surveying and monitoring landscape patterns. Volume A: Pilot study - LANDSAT Imagery. Volume B: PEPS Project No. 73 - SPOT Imagery
[BCRS-87-12-VOL-A/B] N89-20534
The suitability of remote sensing for surveying and monitoring landscape patterns. Volume A: Pilot study - LANDSAT imagery N89-20535
Land use inventory using LANDSAT Thematic Mapper imagery to study environmental pollution
[NLR-MP-87063-U] N89-20541
THEMATIC MAPPING
The suitability of remote sensing for surveying and monitoring landscape patterns. Volume A: Pilot study - LANDSAT Imagery. Volume B: PEPS Project No. 73 - SPOT Imagery
[BCRS-87-12-VOL-A/B] N89-20534
The suitability of remote sensing for surveying and monitoring landscape patterns. Volume A: Pilot study - LANDSAT imagery N89-20535
The suitability of remote sensing for surveying and monitoring landscape patterns. Volume B: PEPS Project No. 73 - SPOT Imagery N89-20536
THEOREM PROVING
Reducing the proof burden when reasoning with congruence types
[CS-8807] N89-20655
THEOREMS
Diagnostics for intelligent control of MPD engines
[AD-A203640] N89-20530
Numerical method of applying mean value theorem
[PB89-111447] N89-20714
Nonexistence theorems for Yang-Mills fields outside the black hole of the Schwarzschild spacetime
[DE88-705351] N89-20901
THERMAL ANALYSIS
Structural analysis methods development for turbine hot section components N89-20140
Fluorine as an oxidant in combustion calorimetry
[DE89-003626] N89-20214
Screening study of lithiated catholyte mixes for a long-life Li(Si)/FeS2 thermal battery
[DE89-006857] N89-20393
THERMAL BUCKLING
High intensity acoustic tests of a thermally stressed aluminum plate in TAFA
[NASA-TM-101552] N89-20778
THERMAL CONDUCTIVITY
Laser diode cooling for high average power applications
[DE89-006777] N89-20454
THERMAL DEGRADATION
Evaluation of solid lubricants: Temperature programmed desorption of MoS2 on molybdenum and of ion-implanted MoS2 on molybdenum
[AD-A203741] N89-20268
THERMAL DIFFUSION
Modeling of hydrogen-air diffusion flame
[NASA-CR-184844] N89-20218
Damage to silver coatings from high average power 1-micron laser
[DE89-005476] N89-20448
THERMAL FATIGUE
Fatigue life prediction modeling for turbine hot section materials N89-20142
Softening mechanisms and microstructural instabilities during high temperature low cycle fatigue of Ni, Ni3Al and their metal matrix composites
[DE89-007117] N89-20238
THERMAL INSULATION
Life modeling of thermal barrier coatings for aircraft gas turbine engines N89-20143
THERMAL NEUTRONS
Study of vibrational and rapid local motions of hydrogen in the storage compound Ti0.8Zr0.2 CrMnH3 by slow neutron scattering
[DE88-704797] N89-20213
THERMAL PROTECTION
Life modeling of thermal barrier coatings for aircraft gas turbine engines N89-20143
STS-27R OV-104 Orbiter TPS damage review team, volume 1
[NASA-TM-100355-VOL-1] N89-20178
THERMAL STABILITY
Evaluation of solid lubricants: Temperature programmed desorption of MoS2 on molybdenum and of ion-implanted MoS2 on molybdenum
[AD-A203741] N89-20268
Thermal stability of jet fuel
[DE89-006754] N89-20273
THERMAL STRESSES
Dendritic web silicon photovoltaic cell research
[DE89-007289] N89-20554
High intensity acoustic tests of a thermally stressed aluminum plate in TAFA
[NASA-TM-101552] N89-20778
THERMOCHEMISTRY
Kinetic modeling of NOx formation and destruction and combustibles burnout
[PB89-124358] N89-20560
THERMODYNAMIC COUPLING
Thermodynamic characteristics of Y-Ba-Cu-O type compounds in the model of strong electron-phonon coupling
[DE88-705343] N89-20828
THERMODYNAMICS
Exploratory alloy development in the system Al-Sc-X
[DE89-007088] N89-20237
Multifractals
[DE88-705369] N89-20672
Thermodynamics of finite-time processes: Accomplishments and work in progress, 1986--1989
[DE89-006726] N89-20858
THERMOELASTICITY
Green's function formulation of plane crack problems for general anisotropic materials N89-20509
THERMOGRAVIMETRY
Thermogravimetric analysis of polymeric materials for an intermediate temperature solid electrolyte. 2: Polymer mixtures
[DE89-006980] N89-20262
THERMOPHYSICAL PROPERTIES
Growth of solid solution single crystals N89-20297
Dynamic thermophysical measurements in space N89-20317
THERMOPLASTIC RESINS
Energetic thermoplastic elastomer synthesis
[AD-A203594] N89-20265
THERMOPLASTICITY
Energetic thermoplastic elastomer synthesis
[AD-A203594] N89-20265
THERMOVISCOELASTICITY
A numerical implementation of the Schapery model for nonlinear viscoelasticity
[ETN-89-93895] N89-20515
THESAURI
Medical subject headings, tree structures, 1989
[PB89-100028] N89-20605
Comparative lexicon of US-Soviet military technical terminology
[PB89-125553] N89-20865
THICKNESS
The influence of thickness and wavelength on the mechanical properties of a compositionally modulated ceramic thin film
[DE89-006033] N89-20258
THIN FILMS
Thermal-mechanical behavior of thin films and laminates N89-20203
The influence of thickness and wavelength on the mechanical properties of a compositionally modulated ceramic thin film
[DE89-006033] N89-20258
A molecular dynamics study of surface kinetics and epitaxial crystal growth N89-20819
Crystalline metal-semiconductor superlattices
[DE89-006619] N89-20825
X-ray diffraction and ellipsometric studies of zinc sulfide thin films grown by atomic layer epitaxy
[PH-161] N89-20827
High pressure Raman spectroscopy of TiO2 thin films
[DE89-006937] N89-20839
THIN WALLED SHELLS
Experiments on the buckling of thin-walled model silo structures
[PB89-125124] N89-20503
Large deflection analysis of thin elastic shells by hybrid stress method
[PB89-111504] N89-20506
Bulging cracks in pressurized fuselages: A numerical study
[NLR-MP-87058-U] N89-20519
THOMSON SCATTERING
A new procedure for determination of electron temperatures and electron concentrations by Thomson scattering and analytical plasmas
[AD-A203489] N89-20812
THREE AXIS STABILIZATION
Design of a three-axis stabilized orion satellite using an all-thruster attitude control system
[AD-A203953] N89-20191
THREE DIMENSIONAL BODIES
An exact incremental hidden surface removal algorithm
[CWI-CS-R8818] N89-20863
THREE DIMENSIONAL BOUNDARY LAYER
A calculation method for compressible three dimensional turbulent boundary layer flows
[VKI-TN-167] N89-20422
THREE DIMENSIONAL FLOW
A cell-vertex multigrid method for the Navier-Stokes equations
[NASA-TM-101557] N89-20101
Navier-Stokes prediction of the three dimensional flow-field of jets in a crossflow using the finite element method N89-20408
THRUST
Thrust generation by an airfoil in hovering mode
[AD-A203785] N89-20108
A first scramjet study
[NASA-CR-184965] N89-20146
THRUST VECTOR CONTROL
Design of a three-axis stabilized orion satellite using an all-thruster attitude control system
[AD-A203953] N89-20191
Noise generated by a flight weight, air flow control valve in a vertical takeoff and landing aircraft thrust vectoring system
[NASA-CR-182232] N89-20776
THUNDERSTORMS
A portable CW/FM-CW Doppler radar for local investigation of severe storms
[DE89-005445] N89-20373
Objective assessment of 1984-85 VAS products as indices of thunderstorm and severe local storm potential
[PB89-107668] N89-20577
TIME
Robust stabilization of linear time-invariant uncertain systems via Lyapunov theory N89-20147
Time resolved study of light emitted by detonation arrival at the surface of high explosives in various environments
[DE89-005657] N89-20414
TIME DEPENDENCE
Environmental effects on the time dependent failure of non-oxide ceramics
[AD-A202391] N89-20250
TIME DIVISION MULTIPLE ACCESS
Conceptual study of the signalling point of the master station for a TST/SS-TDMA system. Phase 1: Overview and selection of signalling points
[SX/SP-01] N89-20360
TIME MEASUREMENT
DMA (Defense Mapping Agency) orbit determination of the navy navigation satellite system for 1987
[AD-A203496] N89-20170
TIME OPTIMAL CONTROL
Minimizing total completion time in the two-machine flow shop by Lagrangian relaxation
[CWI-OS-R8808] N89-20860
TIN TELLURIDES
Microgravity science at Langley Research Center N89-20298
TITAN LAUNCH VEHICLES
Expendable launch vehicle transportation for the space station
[NASA-TM-101947] N89-20179
TITANIUM ALLOYS
Microstructural influence on low cycle fatigue strength of IMI550
[PNR90500] N89-20226
Nondestructive tests of elements mamufactured using diffusion bonding and superplastic forming
[ETN-89-94131] N89-20492
TITANIUM OXIDES
The influence of thickness and wavelength on the mechanical properties of a compositionally modulated ceramic thin film
[DE89-006033] N89-20258
High pressure Raman spectroscopy of TiO2 thin films
[DE89-006937] N89-20839
TOKAMAK DEVICES
Development of a remotely maintainable radio-frequency module for the Compact Ignition Tokamak
[DE89-004913] N89-20805
Extreme ultraviolet and soft X-ray diagnostics of high-temperature plasmas
[DE89-007070] N89-20808
TOMOGRAPHY
Compensation for crystal penetration in high resolution positron tomography
[DE89-006660] N89-20836

TOOLING
Development of tooling and techniques for remote field metallography
[DE89-005400] N89-20241
TOPOLOGY
On the structure and control of piecewise-linear systems
[RR-334] N89-20700
Antipodal universes in the topology S(sup 3)xR and H(sup 3)xR
[DE88-704999] N89-20719
Toward a quasi-periodic bifurcation theory — dynamical systems
[ZW-8803] N89-20736
TORNADOES
A portable CW/FM-CW Doppler radar for local investigation of severe storms
[DE89-005445] N89-20373
TOROIDAL PLASMAS
Transport modeling of ECH and neutral-beam-heated plasmas in the advanced toroidal facility
[DE89-006131] N89-20809
TORQUE
Active vibration control of a large flexible manipulator by inertial force and joint torque
[NASA-CR-184786] N89-20470
TORSION
Non-symmetric bifurcation of geometrically non-linear elastic-plastic axisymmetric shells under combined loads including torsion
[PB89-102149] N89-20500
TORSIONAL STRESS
Results of inphase axial-torsional fatigue experiments on 304 stainless steel
[NASA-TM-101464] N89-20514
TOXICITY
National Air Toxics Information Clearinghouse: Ongoing research and regulatory development projects, July 1988
[PB89-103428] N89-20558
New models to assess behavioral and physiological performance of animals during inhalation exposures
[PB89-128946] N89-20601
TRACKING (POSITION)
High-dynamic GPS tracking
[NASA-CR-184868] N89-20113
Efficient detection and signal parameter estimation with applications to high dynamic GPS receivers
[NASA-CR-184861] N89-20362
Analog automatic control loops in radar and EW (Electronic Warfare)
[AD-A203758] N89-20380
Dispersion of dense gas releases in a wind tunnel
[PB89-118509] N89-20561
Combining segmentation and tracking for the classification of moving objects in video scenes
[DE89-007000] N89-20666
TRACKING FILTERS
Continuous-discrete filtering for systems with Markovian switching coefficients
[NLR-MP-87076-U] N89-20117
TRACKING NETWORKS
DMA (Defense Mapping Agency) orbit determination of the navy navigation satellite system for 1987
[AD-A203496] N89-20170
TRAJECTORIES
Trajectory scoring in rectangular coordinates using transponder-interrogator range and range rate data
[DE89-007005] N89-20119
Hybrid single-particle Lagrangian integrated trajectories (HY-SPLIT): Model description
[PB89-127591] N89-20559
Observed and modeled terrain-induced shear in tracer trajectories
[DE89-006938] N89-20590
TRAJECTORY ANALYSIS
The application of trajectory prediction algorithms for planning purposes in the Netherlands Air Traffic Control (ATC) system
[NLR-MP-87031-U] N89-20115
Unmanned, space-based, reusable orbital transfer vehicle, DARVES. Volume 2: Data and calculations
[NASA-CR-184712] N89-20174
TRAJECTORY CONTROL
The application of trajectory prediction algorithms for planning purposes in the Netherlands Air Traffic Control (ATC) system
[NLR-MP-87031-U] N89-20115
TRANSDUCERS
Dynamic wall pressure measurements
[AD-A203551] N89-20427
TRANSFORMATIONS (MATHEMATICS)
Command algebras, recursion and program transformation
[CS-8812] N89-20734
TRANSIENT LOADS
Analysis of dynamic elastic-plastic fracture phenomena: Steady crack growth and transient loading of a stationary crack N89-20507
TRANSISTOR AMPLIFIERS
On 32-GHz cryogenically cooled HEMT low-noise amplifiers N89-20336
TRANSISTORS
Test of radiation hardness of CMOS transistors under neutron irradiation
[DE89-006511] N89-20392
TRANSITION FLOW
Resolution requirements for numerical simulations of transition
[NASA-CR-181799] N89-20411
TRANSITION POINTS
The lambda point experiment in microgravity N89-20319
TRANSLATING
Implementation of a language translator for the computer aided prototyping system
[AD-A203876] N89-20680
Comparative lexicon of US-Soviet military technical terminology
[PB89-125553] N89-20865
TRANSMITTERS
Calculations of laser cavity dumping for optical communications N89-20346
Transmitter data collection using Ada N89-20352
Dedicated versus half-duplex receiver topology in jammed, fully connected CDMA networks: Theory and numerical comparisons
[AD-A203635] N89-20402
TRANSONIC FLOW
Development and application of a program to calculate transonic flow around an oscillating three-dimensional wing using finite difference procedures
[NASA-CR-181744] N89-20093
Geometrical and structural properties of an Aeroelastic Research Wing (ARW-2)
[NASA-TM-4110] N89-20099
Observed Reynolds number effects on airfoils and high aspect ratio wings at transonic flow conditions
[NLR-MP-88006-U] N89-20102
Experimental investigation of transonic oscillating cascade aerodynamics
[NASA-TM-101993] N89-20133
Updated users' guide for TAWFIVE with multigrid
[NASA-TM-4109] N89-20409
TRANSPORT PROPERTIES
Transport and relaxation processes in supercritical fluids
[DE89-005910] N89-20219
Dispersion of dense gas releases in a wind tunnel
[PB89-118509] N89-20561
TRANSPORT THEORY
Effects of turbulence on rate of combustion of fuel sprays N89-20212
Microgravity Science and Applications Flight Programs, January - March 1987, selected papers, volume 2
[NASA-TM-4069-VOL-2] N89-20305
Transport modeling of ECH and neutral-beam-heated plasmas in the advanced toroidal facility
[DE89-006131] N89-20809
TRAVELING SALESMAN PROBLEM
Fault-tolerance of a neural network solving the traveling salesman problem
[NASA-CR-181798] N89-20698
TRIANGLES
Multigrid solution of the Navier-Stokes equations on triangular meshes
[NASA-CR-181786] N89-20095
TRIANGULATION
Potential of large format camera photography
[PB89-122485] N89-20433
TRITIUM
Solubility of hydrogen, deuterium and tritium in palladium metal
[DE89-005304] N89-20225
TROPICAL METEOROLOGY
Radiation, turbulence and microphysics in the stratiform regions of tropical cloud clusters N89-20585
TUNING
Proposed extended tuning range for the Los Alamos mid-infrared adjustable, coherent light experiment (MIRACLE) facility
[DE89-006550] N89-20798
TURBINE BLADES
Aerodynamic pressure and flow-visualization measurement from a rotating wind turbine blade
[DE89-000854] N89-20104
Life modeling of thermal barrier coatings for aircraft gas turbine engines N89-20143
TURBINE ENGINES
Advanced high temperature instrument for hot section research applications N89-20137
TURBINES
Transmission and reflection on pressure waves by compressor and turbine stages, based on an actuator-disk model
[AD-A203513] N89-20426
TURBOPROP ENGINES
Structural Tailoring of Advanced Turboprops (STAT) programmer's manual
[NASA-CR-182164] N89-20132
TURBULENCE
Effects of turbulence on rate of combustion of fuel sprays N89-20212
TURBULENT BOUNDARY LAYER
Documentation of two- and three-dimensional hypersonic shock wave/turbulent boundary layer interaction flows
[NASA-TM-101075] N89-20100
A calculation method for compressible three dimensional turbulent boundary layer flows
[VKI-TN-167] N89-20422
Dynamic wall pressure measurements
[AD-A203551] N89-20427
TURBULENT FLOW
Performance and test section flow characteristics of the National Full-Scale Aerodynamics Complex 40- by 80-foot wind tunnel
[NASA-TM-101065] N89-20086
Vortex-transport element simulation of a confined mixing layer
[AD-A203791] N89-20222
Standard test case for a low speed, turbulent junction vortex flow
[PB89-119779] N89-20406
Control-volume based Navier-Stokes equation solver valid at all flow velocities
[NASA-TM-101488] N89-20407
Resolution requirements for numerical simulations of transition
[NASA-CR-181799] N89-20411
A simple nonlinear model for the return to isotropy in turbulence
[NASA-CR-181797] N89-20412
Solutions to the Navier-Stokes equations using a k-epsilon turbulence model
[FFA-TN-1988-19] N89-20416
Numerical simulation of turbulent mixing in shock-tube experiments
[DE89-005101] N89-20425
Fortran codes for computing the space-time correlations of turbulent flow in a channel
[AD-A203749] N89-20678
TURBULENT MIXING
Particle cloud mixing in microgravity
[NASA-TM-101484] N89-20321
Numerical simulation of turbulent mixing in shock-tube experiments
[DE89-005101] N89-20425
TURBULENT WAKES
Acoustic test of a model rotor and tail rotor: Results for the isolated rotors and combined configuration
[NASA-TM-101550] N89-20777
TURING MACHINES
Consequences of nonclassical measurement for the algorithmic description of continuous dynamical systems
[NASA-CR-184851] N89-20640
TWO DIMENSIONAL BODIES
Aerodynamics of two-dimensional slotted bluff bodies
[DE89-007288] N89-20105
TWO DIMENSIONAL FLOW
Flux vector splitting in general curvilinear coordinates
[PB89-127393] N89-20410
TWO PHASE FLOW
Numerical study of nonlinear wave interactions in bubbly two-phase flow
[REPT-88-50] N89-20418

U

U.S.S.R.
USSR Space Life Sciences Digest, Issue 21
[NASA-CR-3922(24)] N89-20602
Comparative lexicon of US-Soviet military technical terminology
[PB89-125553] N89-20865
UDIMET ALLOYS
Mechanical properties of modified low cobalt powder metallurgy Udimet 700 type alloys
[NASA-TM-101481] N89-20228
ULTRASONIC FLAW DETECTION
Fatigue teardown tests of the aged rear support of the A320 aircraft
[I-271/88] N89-20491
Nondestructive tests of elements mamufactured using diffusion bonding and superplastic forming
[ETN-89-94131] N89-20492

ULTRASONIC RADIATION
Investigations of ultrasonic wave interactions at imperfect boundaries separating anisotropic materials
[DE89-007089] N89-20781
ULTRASONIC TESTS
Nondestructive evaluation of advanced ceramics
[NASA-TM-101489] N89-20490
ULTRASONICS
Paraxial approximations for ultrasonic beam propagation in liquid and solid media with applications to nodestructive evaluation
[DE89-007569] N89-20782
ULTRAVIOLET ASTRONOMY
Selection effects in optical quasar surveys
N89-20877
ULTRAVIOLET LASERS
Luminescence originating in an optical fiber
[AD-A203494] N89-20799
UNDERGROUND EXPLOSIONS
Waveform data collection for source inversion studies
[AD-A203419] N89-20575
UNIFIED FIELD THEORY
On heterotic supermanifolds
[DE88-705339] N89-20773
UNIVERSE
Antipodal universes in the topology S(sup 3)xR and H(sup 3)xR
[DE88-704999] N89-20719
Black holes as possible sources of closed and semiclosed worlds
[DE88-705336] N89-20900
UNSTEADY AERODYNAMICS
Experimental investigation of transonic oscillating cascade aerodynamics
[NASA-TM-101993] N89-20133
UNSTEADY FLOW
Development and application of a program to calculate transonic flow around an oscillating three-dimensional wing using finite difference procedures
[NASA-CR-181744] N89-20093
Vorticity distributions in unsteady flow separation
[AD-A203733] N89-20428
UPPER ATMOSPHERE
AFE ion mass spectrometer design study
[NASA-CR-184838] N89-20432
URANUS ATMOSPHERE
To Uranus and beyond
[NASA-EP-260] N89-20902
URANUS RINGS
To Uranus and beyond
[NASA-EP-260] N89-20902
URANUS SATELLITES
To Uranus and beyond
[NASA-EP-260] N89-20902
USER MANUALS (COMPUTER PROGRAMS)
Updated users' guide for TAWFIVE with multigrid
[NASA-TM-4109] N89-20409
Integrated analysis package for Mk-3 K-coronameter observations: A user's manual
[PB88-250717] N89-20904
USER REQUIREMENTS
Mars manned transportation vehicle
[NASA-TM-101487] N89-20545
User interfaces and highly interactive systems: Survey of current research
[REPT-88-60] N89-20617
Experiences on a CRAY-2 (trade name) running UNICOS
[PB88-250725] N89-20620
Increasing user-friendliness in AI systems
[DE89-005093] N89-20704

V

VACUUM
Mechanisms for the operation of a laser-triggered vacuum switch
[DE89-007059] N89-20394
Soliton geometry and the vacuum gravitational field equations
[DE88-705340] N89-20573
VACUUM SYSTEMS
Workshop on Transient Induced Insulator Flashover in Vacuum
[DE89-006727] N89-20398
VALLEYS
The development and structure of nocturnal slope winds in a simple valley
[AD-A203427] N89-20593
VALVES
Development of a rotary value for pulse combustion applications
[PB89-131114] N89-20468
VANES
Shutters and slats for the integral sunshade of an optical reception antenna N89-20348
VAPOR BARRIER CLOTHING
Safe working time limits in impermeable protective clothing: Recommendations based upon experimental measurements
[IZF-1987-28] N89-20618
VAPOR DEPOSITION
Growth of mercuric iodide (HgI2) for nuclear radiation detectors N89-20293
VAPOR PHASE EPITAXY
X-ray diffraction and ellipsometric studies of zinc sulfide thin films grown by atomic layer epitaxy
[PH-161] N89-20827
VAPORS
Membrane vapor enricher for Water For Injection (WFI) production, phase 1
[AD-A201354] N89-20323
Feasibility of a complex compound heat pump
[PB89-115273] N89-20405
VARIATIONAL PRINCIPLES
Complex-valued functionals in variational analysis of waveguides with impedance boundaries
[PB89-128896] N89-20361
VECTOR SPACES
Formula related to the Cayley-Hamilton equation
[PB89-128003] N89-20711
A short tutorial on Lie algebras
[CWI-PM-R8802] N89-20745
VELOCITY DISTRIBUTION
Quantification of environmental chambers by air velocity mapping
[AD-A200923] N89-20154
A simple nonlinear model for the return to isotropy in turbulence
[NASA-CR-181797] N89-20412
Magnetic fields and supergranule velocity fields on the quiet sun N89-20907
VERTICAL AIR CURRENTS
Three-dimensional kinematics of rainbands in midlatitude cyclones N89-20586
VERTICAL LANDING
Noise generated by a flight weight, air flow control valve in a vertical takeoff and landing aircraft thrust vectoring system
[NASA-CR-182232] N89-20776
VERTICAL TAKEOFF
Noise generated by a flight weight, air flow control valve in a vertical takeoff and landing aircraft thrust vectoring system
[NASA-CR-182232] N89-20776
VERY LARGE ARRAY (VLA)
VLA telemetry performance with concatenated coding for Voyager at Neptune N89-20340
Very large array observations of the sun with related observations using the SMM (Solar Maximum Mission) satellite
[AD-A203873] N89-20910
Aperture synthesis observations of solar and stellar radio emission N89-20912
VERY LARGE SCALE INTEGRATION
A long constraint length VLSI Viterbi decoder for the DSN N89-20341
On-line arithmetic algorithms and structures for VLSI
[AD-A203421] N89-20400
VERY LONG BASE INTERFEROMETRY
Deriving a geocentric reference frame for satellite positioning and navigation N89-20330
Determination of GPS orbits to submeter accuracy N89-20331
VHSIC (CIRCUITS)
Very High Speed Integrated Circuits (VHSIC). Phase 2: Submicrometer technology development, interoperability standards
[AD-A203629] N89-20401
VIBRATION
Study of vibrational and rapid local motions of hydrogen in the storage compound Ti0.8Zr0.2 CrMnH3 by slow neutron scattering
[DE88-704797] N89-20213
Analysis of the dynamics of guided rotating free center plates N89-20466
Finite element technique for the inverse problem of a partial differential equation and its application to parameter identification of structure
[PB89-111439] N89-20713
VIBRATION DAMPING
Active vibration control of a large flexible manipulator by inertial force and joint torque
[NASA-CR-184786] N89-20470
The initial value problem for fractional order differential equations with constant coefficients
[AD-A203843] N89-20764
VIBRATION ISOLATORS
Low frequency vibration isolation technology for microgravity space experiments
[NASA-TM-101448] N89-20324
VIBRATION TESTS
Structural Tailoring of Advanced Turboprops (STAT) programmer's manual
[NASA-CR-182164] N89-20132
Coupled rotor/fuselage dynamic analysis of the AH-1G helicopter and correlation with flight vibrations data
[NASA-CR-181723] N89-20512
VIDEO EQUIPMENT
Combining segmentation and tracking for the classification of moving objects in video scenes
[DE89-007000] N89-20668
VIDEO SIGNALS
Real-time part position sensing
[AD-A203580] N89-20439
VINYLIDENE
New vinylidene fluoride copolymers: Poly(vinyl acetate-co-Vinylidene fluoride)
[AD-A203939] N89-20270
VISCOELASTICITY
Rheometrics stress rheometer applications
[AD-A203667] N89-20275
Determination of the impulse response of a viscoelastic beam using a fractional derivative constitutive model N89-20501
VISCOPLASTICITY
A micromechanical viscoplastic stress-strain model with grain boundary sliding
[DE89-007712] N89-20848
VISCOUS DRAG
Viscous shock layer analysis of hypersonic flows over long slender vehicles N89-20097
VISCOUS FLOW
Updated users' guide for TAWFIVE with multigrid
[NASA-TM-4109] N89-20409
Differential equations of viscous fluid flow in general conditions
[REPT-88-57] N89-20419
VISIBILITY
Current status of the NAVSEA Backscatter Absorption Gas Imaging (BAGI) development project
[DE89-006728] N89-20438
VISION
Real-time part position sensing
[AD-A203580] N89-20439
VISUAL PERCEPTION
Precision in the perception of direction of a moving pattern
[NASA-TM-101080] N89-20610
VITERBI DECODERS
A long constraint length VLSI Viterbi decoder for the DSN N89-20341
Long decoding runs for Galileo's convolutional codes N89-20342
Performance of Galileo's concatenated codes with nonideal interleaving N89-20343
VOIDS
A stereological analysis of ductile fracture by microvoid coalescence
[DE89-000355] N89-20528
VOLTAGE REGULATORS
Cross-coordinated control: An experimentally verified technique for the hybrid twist and wrench control of a voltage-controlled industrial robot
[AD-A203406] N89-20486
VORTEX SHEDDING
Aerodynamics of two-dimensional slotted bluff bodies
[DE89-007288] N89-20105
VORTICES
Vortex-transport element simulation of a confined mixing layer
[AD-A203791] N89-20222
Standard test case for a low speed, turbulent junction vortex flow
[PB89-110779] N89-20406
Vorticity distributions in unsteady flow separation
[AD-A203733] N89-20428
Flow visualization of time-varying structural characteristics of dean vortices in a curved channel
[AD-A203875] N89-20429
VORTICITY
Vorticity distributions in unsteady flow separation
[AD-A203733] N89-20428
VOYAGER 2 SPACECRAFT
DSN 70-meter antenna X-band gain, phase, and pointing performance, with particular application for Voyager 2 Neptune encounter N89-20353
To Uranus and beyond
[NASA-EP-260] N89-20902

W

WAFERS
Edge illuminated ventical multijunction
[DE89-006246] N89-20547
WALL PRESSURE
Dynamic wall pressure measurements
[AD-A203551] N89-20427
WATER
Water adsorption equilibria on microporous carbons
[AD-A203536] N89-20220
WATER INJECTION
Membrane vapor enricher for Water For Injection (WFI) production, phase 1
[AD-A201354] N89-20323
WATER RESOURCES
Scenarios for future climate change: Results of GCM (General Circulation Model) simulations
[DE89-006151] N89-20565
WAVE DISPERSION
Validity of 1D free-electron laser sideband models
[DE89-006284] N89-20452
Theory of Raman scattering by surface polaritons in a four media system
[DE88-705358] N89-20788
WAVE EQUATIONS
Three dimensional numerical analysis of a high-gain free-electron laser
[DE89-006961] N89-20456
Einstein's theory of gravity in Fierz variables
[DE88-705004] N89-20854
WAVE FRONTS
Time resolved study of light emitted by detonation arrival at the surface of high explosives in various environments
[DE89-005657] N89-20414
WAVE INTERACTION
Documentation of two- and three-dimensional hypersonic shock wave/turbulent boundary layer interaction flows
[NASA-TM-101075] N89-20100
Numerical study of nonlinear wave interactions in bubbly two-phase flow
[REPT-88-50] N89-20418
Investigations of ultrasonic wave interactions at imperfect boundaries separating anisotropic materials
[DE89-007089] N89-20781
The physics of wave-particle interaction with applications to astrophysics N89-20888
WAVE PROPAGATION
Wave experiment consortium — Cluster mission N89-20159
The spherical probe electric field and wave experiment — Cluster mission N89-20161
Effects of turbulence on rate of combustion of fuel sprays N89-20212
Complex-valued functionals in variational analysis of waveguides with impedance boundaries
[PB89-128896] N89-20361
Digital radio link: Multipath propagation on a microwave line-of-sight path
[FOA-C-30430-3.3] N89-20366
A relativistic fluid code for high-power microwave propagation
[DE89-006598] N89-20375
Propagation of the nerve impulse under the effect of a magnetic field
[DE88-705371] N89-20608
Paraxial approximations for ultrasonic beam propagation in liquid and solid media with applications to nodestructive evaluation
[DE89-007569] N89-20782
WAVEFORMS
Waveform data collection for source inversion studies
[AD-A203419] N89-20575
WAVELENGTHS
The influence of thickness and wavelength on the mechanical properties of a compositionally modulated ceramic thin film
[DE89-006033] N89-20258
Publications of the Observatory of the University of Michigan. Volume 12, no. 2: Wavelength identifications in the magnetic CP star HR 4816 (HD 110066) N89-20876
WEAR TESTS
Long term lubrication of ceramics at high temperatures N89-20249
Influence of lubrication on ceramic and steel sliding contacts
[PB89-125090] N89-20467
Methods and materials for reducing crack reflectance
[PB89-114532] N89-20505
WEATHER
Relationship of wind shear, buoyancy and radar tops to severe weather, 1988
[PB89-122519] N89-20581
Summary of meteorological observations, surface (SMOS) for Norfolk, Virginia
[AD-A203644] N89-20594
Beaufort Sea mesoscale circulation study: Preliminary results
[PB89-121693] N89-20597
WEATHER FORECASTING
Examination of NGM (Nested Grid Model) low level temperature
[PB89-122543] N89-20580
National Weather Service Philadelphia Forecast Office, 1987 NOAA (National Oceanic and Atmospheric Administration) weather radio survey and questionnaire
[PB89-111785] N89-20582
Long-range forecasting of storminess over the Northern Hemisphere oceans
[AD-A203949] N89-20595
WEIGHTLESSNESS
Continuous flow electrophoresis system experiments on shuttle flights STS-6 and STS-7 N89-20277
WELD STRENGTH
Compression tests of welded channel section columns
[PB88-246020] N89-20496
WELD TESTS
Compression tests of welded channel section columns
[PB88-246020] N89-20496
WELDABILITY
Weldability of 2519-T87 aluminum alloy
[AD-A203519] N89-20244
WELDED JOINTS
Welded joint integrity analysis: Relative criticality of weld defect and remote deformation
[AD-A203756] N89-20246
Elastic stability of cylindrical shells with circumferential welded joints under axial compression
[PB89-125082] N89-20502
WELDED STRUCTURES
Weldability of 2519-T87 aluminum alloy
[AD-A203519] N89-20244
WELDING
The role of composition and microstructure gradients on weld metal properties and behavior
[DE89-006789] N89-20235
Weldability of 2519-T87 aluminum alloy
[AD-A203519] N89-20244
Long-term evaluation of the acoustic emission weld monitor
[PB86-122642] N89-20471
WETLANDS
Utilizing remote sensing of thematic mapper data to improve our understanding of estuarine processes and their influence on the productivity of estuarine-dependent fisheries
[NASA-CR-183417] N89-20533
WIENER FILTERING
A prior knowledge based optimal Wiener filtering approach to ultrasonic scattering amplitude estimation
[DE89-007574] N89-20783
WIGGLER MAGNETS
The chirped-pulse free-electron laser
[DE89-006792] N89-20460
WIND (METEOROLOGY)
Verification of regional climates of GISS GCM. Part 2: Summer
[NASA-TM-100722] N89-20589
Observed and modeled terrain-induced shear in tracer trajectories
[DE89-006938] N89-20590
The development and structure of nocturnal slope winds in a simple valley
[AD-A203427] N89-20593
WIND PRESSURE
Pressure coefficients for basic tensioned-membrane structure forms
[AD-A203866] N89-20107
WIND SHEAR
Analysis of Doppler radar windshear data
[NASA-CR-181762] N89-20111
Relationship of wind shear, buoyancy and radar tops to severe weather, 1988
[PB89-122519] N89-20581
WIND TUNNEL CALIBRATION
Performance and test section flow characteristics of the National Full-Scale Aerodynamics Complex 40- by 80-foot wind tunnel
[NASA-TM-101065] N89-20086
WIND TUNNEL TESTS
Pressure coefficients for basic tensioned-membrane structure forms
[AD-A203866] N89-20107
An airfoil pitch apparatus-modeling and control design
[NASA-TM-101076] N89-20386
Dispersion of dense gas releases in a wind tunnel
[PB89-118509] N89-20561
Acoustic test of a model rotor and tail rotor: Results for the isolated rotors and combined configuration
[NASA-TM-101550] N89-20777
Unsteady blade pressure measurements on a model counterrotation propeller
[NASA-TM-102002] N89-20779
WIND TURBINES
Aerodynamic pressure and flow-visualization measurement from a rotating wind turbine blade
[DE89-000854] N89-20104
NEN 6096, design resolution for small wind turbines
[NLR-MP-88005-U] N89-20551
WISPER: Introducing variable-amplitude loading in wind turbine design
[NLR-MP-88017-U] N89-20552
WIND VELOCITY
Quantification of environmental chambers by air velocity mapping
[AD-A200923] N89-20154
WIND VELOCITY MEASUREMENT
The development and structure of nocturnal slope winds in a simple valley
[AD-A203427] N89-20593
WING PANELS
Geometrical and structural properties of an Aeroelastic Research Wing (ARW-2)
[NASA-TM-4110] N89-20099
WING PLANFORMS
Development and application of a program to calculate transonic flow around an oscillating three-dimensional wing using finite difference procedures
[NASA-CR-181744] N89-20093
WING PROFILES
Some low-speed flutter characteristics of simple low-aspect-ratio delta wing models
[NASA-TM-101547] N89-20094
WORDS (LANGUAGE)
Integrating syntax, semantics, and discourse DARPA (Defense Advanced Research Projects Agency) natural language understanding program
[AD-A203747] N89-20677
WORK CAPACITY
Influences of muscle fiber composition and strength on EMG (electromyographic activity), spinal motion and load acceleration during a repetitive lifting task
[PB89-131221] N89-20607
Safe working time limits in impermeable protective clothing: Recommendations based upon experimental measurements
[IZF-1987-28] N89-20618
WORKING FLUIDS
Feasibility of a complex compound heat pump
[PB89-115273] N89-20405

X

X RAY ANALYSIS
Extreme ultraviolet and soft X-ray diagnostics of high-temperature plasmas
[DE89-007070] N89-20808
X RAY ASTRONOMY
Forbidden coronal iron line emission in the Puppis A shock front: The effect of inhomogeneities
[NASA-TM-89284] N89-20875
X RAY DIFFRACTION
X-ray diffraction study of phase formation and growth in nitrogen implanted iron: Temperature effects
[AD-A203625] N89-20245
X-ray diffraction and ellipsometric studies of zinc sulfide thin films grown by atomic layer epitaxy
[PH-161] N89-20827
X RAY IMAGERY
Forbidden coronal iron line emission in the Puppis A shock front: The effect of inhomogeneities
[NASA-TM-89284] N89-20875
X RAY SPECTROSCOPY
Analysis of brass alloys by wavelength dispersive X-ray spectrometry
[DE89-007595] N89-20243
New directions in spectroscopy for the analytical electron microscope
[DE89-005824] N89-20435
X RAYS
X-ray microscopy for the life and physical sciences
[DE89-006707] N89-20604
XENON CHLORIDE LASERS
Direct solar-pumped iodine laser amplifier
[NASA-CR-184813] N89-20447

Y

YAG LASERS
Calculations of laser cavity dumping for optical communications N89-20346
Q-switched, intracavity doubled Nd:YAG laser side-pumped by a laser diode array
[DE89-005349] N89-20441
Laser ignition of energetic materials with a pulsed Nd:YAG laser
[DE89-006861] N89-20455
YANG-MILLS FIELDS
Nonexistence theorems for Yang-Mills fields outside the black hole of the Schwarzschild spacetime
[DE88-705351] N89-20901
YTTRIUM OXIDES
Ground state depleted laser experiments
[DE89-006146] N89-20449
Thermodynamic characteristics of Y-Ba-Cu-O type compounds in the model of strong electron-phonon coupling
[DE88-705343] N89-20828
Anion grain boundary diffusion in Cr2O3 and Cr2O3-0.09 weight percent Y2O3
[DE89-006281] N89-20833

Z

ZINC
Pb-Zn liquid metal diffusion N89-20304
ZINC ALLOYS
Analysis of brass alloys by wavelength dispersive X-ray spectrometry
[DE89-007595] N89-20243
ZINC SULFIDES
X-ray diffraction and ellipsometric studies of zinc sulfide thin films grown by atomic layer epitaxy
[PH-161] N89-20827
ZINC TELLURIDES
Research and development of HgZnTe as an infrared material
[NASA-CR-184840] N89-20820
ZOOPLANKTON
Biological processes in the water column of the South Atlantic Bight: Zooplankton responses
[DE89-006828] N89-20600

Typical Personal Author Index Listing

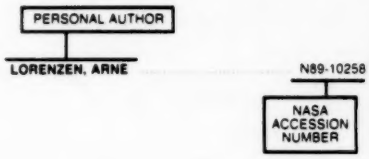

Listings in this index are arranged alphabetically by personal author. The NASA accession number denotes the number by which the citation is identified.

A

AAGAARD, A. N89-20597
ABBASSI, P. N89-20248
ABBINK, F. J. N89-20129
ABELSON, HAROLD N89-20679
ACUNA, M. H. N89-20158
ADAMS, DONALD F. N89-20200
ADAMS, MILTON B. N89-20683
ADE, H. N89-20604
ADLER, L. N89-20781
AGARWAL, ANURAG N89-20704
AGGSON, T. N89-20161
AGOGINO, ALICE M. N89-20706
AGUILAR, IGNACIO N89-20359
AITTONIEMI, LEENA N89-20649
AKMAN, VAROL N89-20612
N89-20660
N89-20663
ALEXANDER, WILLIAM N. N89-20575
ALFANO, ROBERT N89-20850
ALFVEN, HANNES N89-20897
N89-20898
ALLEN, J. W. N89-20824
ALTENKIRCH, ROBERT A. N89-20312
ALTIZER, CHARLES EDWIN N89-20680
AMRITKAR, R. E. N89-20672
ANDA, ENRIQUE N89-20396
ANDERSEN, CARL M. N89-20632
ANDERSON, GEORGE N89-20401
ANDERSON, JOHN E. N89-20182
ANDERSON, PER KRAGH N89-20769
ANDERSSON, PETER N89-20467
ANDREWS, DANIEL R. N89-20386
ANSPAUGH, B. E. N89-20549
AOYAGI, P. N89-20382
APPELBAUM, JOSEPH N89-20385
APT, KRZYSZTOF R. N89-20737
ARAKAWA, P. E. N89-20484
ARAKELIAN, S. M. N89-20834
ARCHULETA, S. N89-20904
ARNOTT, RONALD J. N89-20245
ARPASI, DALE J. N89-20641
ARRAS, M. N89-20698
ASMAR, S. W. N89-20332
ASMUS, JOHN F. N89-20813
ATASSI, M. ZOUHAIR N89-20283
N89-20290
ATKINSON, ROBERT J. N89-20430
ATTWOOD, D. N89-20604
AXFORD, W. I. N89-20168
AZMY, Y. Y. N89-20759

B

BABCOCK, S. E. N89-20838
BABCOCK, S. M. N89-20481
BACK, L. H. N89-20215
BACKHOUSE, ROLAND N89-20658
N89-20659
BAGLEY, RONALD L. N89-20764
BAGNALL, C. N89-20241
BAHL, KERRY L. N89-20414
BAHNS, JOHN T. N89-20223
BAHNSEN, A. N89-20160
N89-20162
BAI, YILENG N89-20224
BAKER, JOHN R. N89-20836
BALACHANDRAN, SUCHITRA CADAMBI N89-20886
BALCAR, B. N89-20722
BALLINGALL, J. M. N89-20336
BALLUFFI, R. W. N89-20838
BALOGH, A. N89-20158
BAMBERGER, S. B. N89-20281
BANKS, GARY N89-20180
BANKS, H. T. N89-20636
N89-20637
BANKS, S. P. N89-20700
N89-20731
N89-20732
BANKSTON, C. P. N89-20215
BANSAL, NAROTTAM P. N89-20252
BANTHIA, VINOD K. N89-20755
BAQUERO, R. N89-20240
BARBERO, J. N89-20359
BARD, ALLEN J. N89-20211
BARLAG, S. N89-20785
BARLOW, GRANT H. N89-20280
N89-20287
BARMATZ, M. N89-20308
BARNES, C. W. N89-20806
BARNETT, BARBARA N89-20613
BARRY, JENNIFER N89-20193
BARSANTI, MAR L. N89-20155
BARTH, MARVIN J. N89-20374
BASS, I. L. N89-20441
BASTIAN, TIMOTHY STEPHEN N89-20912
BATCHO, P. F. N89-20426
BATH, LINDA N89-20569
BATHKER, D. A. N89-20353
BATSON, K. BRYAN N89-20430
BAUER, O. H. N89-20165
BAUMANN, ROBERT H. N89-20533
BAUMJOHANN, W. N89-20165
BAUTISTA, J. J. N89-20336
BEACH, R. N89-20449
N89-20454
BEARD, L. N89-20355
BEATON, ROBERT M. N89-20683
BECKER, H. N89-20785
BECKERMAN, M. N89-20482
BECKMAN, T. M. N89-20455
BEERS, J. N. P. N89-20115
BEGG, ALAN ROBERT N89-20207
BELLA, DAVID WAYNE N89-20429
BELLAN, J. N89-20215
BELLOWS, A. H. N89-20295
BENEDEK, R. N89-20816
BENETT, W. N89-20454
BENNER, ROBERT E. N89-20686
BENOCCI, C. N89-20423
BERGERON, GEORGE L., III N89-20155
BERKBIGLER, K. P. N89-20574
BERLAD, A. L. N89-20311
N89-20321
BERNARDO, J. M. N89-20491
N89-20492
BERNER, C. N89-20103
BERRY, B. F. N89-20780
BERRY, LESLIE A. N89-20328
BERRY, R. S. N89-20858
BERRYMAN, HARRY N89-20638
BERTIGER, W. I. N89-20331
BEUTNER, R. N89-20904
BHANJI, A. M. N89-20339
BIDELMAN, W. P. N89-20876
BIER, M. N89-20282
BIGGS, G. L. N89-20436
BILLINGS, S. A. N89-20325
N89-20371
N89-20728
N89-20729
N89-20730
N89-20733
BINNENKADE, P. N89-20539
BIRDSEYE, M. A. N89-20639
N89-20867
BIRMINGHAM, B. R. N89-20478
BLAIR, HOWARD A. N89-20737
BLAIRE, P. E. N89-20151
BLAKE, J. B. N89-20168
BLAKE, PETER N. N89-20322
BLALOCK, T. V. N89-20437
BLECH, RICHARD A. N89-20684
N89-20685
BLOCK, L. P. N89-20161
N89-20189
BLOM, H. A. P. N89-20117
BLOMBERG, L. G. N89-20571
BLOYD, CARY N. N89-20563
BLUESTEIN, HOWARD B. N89-20373
BLUMENTHAL, W. R. N89-20257
BODNER, S. E. N89-20462
BOEHM, M. N89-20165
BOENRINGER, T. N89-20785
BOERGER, J. B. N89-20369
BOKHOVEN, H. N89-20539
BOLOTIN, V. V. N89-20498
BONACUSE, PETER J. N89-20514
BONIFACIO, R. N89-20451
BOOK, WAYNE J. N89-20327
BORGAN, ORNULF N89-20769
BOSMAN, M. N89-20785
BOSQUED, J. M. N89-20166
BOSTROM, R. N89-20161
BOWERS, M. W. N89-20436
BOYANA, MURAT A. N89-20763
BRAAKSMA, B. L. J. N89-20736
BRADLEY, E. C. N89-20484
BRANNON, PAUL J. N89-20394
BRAVO, J. N89-20208
BRAY, N. S. N89-20639
N89-20867
BREDEMO, RONALD N89-20526
BREEVELD, E. R. N89-20639
N89-20867
BRENNAN, T. M. N89-20832
BRENNEMAN, J. N89-20382
BREWER, L. N89-20449
BREWSTER, M. Q. N89-20217
BRIGHT, FRANK V. N89-20799
BRODSKY, M. B. N89-20230
BROER, H. W. N89-20736
BRONSVOORT, WILLEM F. N89-20650
BROOKS, D. E. N89-20281
BROWDER, JOAN A. N89-20533
BROWN, EDWARD N. N89-20092
BROWN, GERALD V. N89-20324
BROWN, JAMES D. N89-20145
BROWN, K. W. N89-20132
BRUECKNER, W. N89-20916
BRUSMARK, BERTIL N89-20367
BRZOSKO, JAN N89-20807
BUCHANAN, SUSAN KAY M. N89-20558
BUCHHOLZ, D. N89-20785
BUCKIUS, R. O. N89-20217
BUFFUM, DANIEL H. N89-20133
BUGG, CHARLES E. N89-20292
BUNKER, BRUCE C. N89-20529
BUONSANTO, M. J. N89-20567
BURD, ADRIAN BENEDICT N89-20852
BURGHART, CHRISTOPHER N89-20569
BURKE, A. F. N89-20389
BURKS, BARRY L. N89-20479
BURLEY, C. L. N89-20777
BURNS, FORREST C. N89-20245
BURNS, RICHARD P. N89-20268
BURNSIDE, WALTER D. N89-20363
N89-20795
BURTON, DONALD J. N89-20221
BUSHNELL, MARK N89-20598
BUSNESS, KENNETH M. N89-20566
BUTLER, P. L. N89-20481
BUTLER, PAUL C. N89-20395
BUTTERFIELD, C. P. N89-20104
BYRD, RICHARD H. N89-20715

C

CABALLERO, J. E. N89-20359
CAIRELLI, JAMES E. N89-20227
CALALO, RUEL H. N89-20642
CAMACHO, A. N89-20208
N89-20240
CAMPBELL, ROY H. N89-20646
CAMPION, ALAN N89-20211
CANU, P. N89-20162
CARLSON, FREDERICK M. N89-20298
CARLSON, LELAND A. N89-20415
CARR, GERALD P. N89-20181
CARREIRO, LOUIS G. N89-20245
CARROLL, MARY K. N89-20799
CARUSO, J. J. N89-20206
CASS, ROBERT D. N89-20356
CASSELLIUS, RON N89-20505
CASSIL, CHARLES E. N89-20145
CASTILLO, V. N89-20785
CATTELL, C. N89-20161
CEZAIRLIYAN, ARED N89-20317
CHABAUD, V. N89-20785
CHAMIS, C. C. N89-20206
CHAN, C. K. N89-20639
N89-20867
CHANANE, B. N89-20731
N89-20732
CHANG, S. J. N89-20527
CHANG, STEPHEN K. N89-20154
CHAO, CHIEN-HSIANG N89-20147
CHAO, P. C. N89-20336
CHAPMAN, DAVID N89-20569
CHASE, LLOYD L. N89-20450
CHELA-FLORES, J. N89-20263
N89-20608
CHEN, C.-C. N89-20349
CHEN, DAVID C. K. N89-20513
CHEN, J. N89-20337
CHEN, PU-FEN N89-20431
CHEN, S. N89-20730
CHEN, Y. C. N89-20363
CHEN, YUNMING N89-20804
CHENG, UNJENG N89-20402
CHERRY, ROBERT S. N89-20284
CHEUNG, H. W. N89-20265
CHEUNG, K.-M. N89-20342
N89-20343
CHIPMAN, DAVID R. N89-20245
CHISHOLM, PAUL N89-20655
N89-20659
CHITWOOD, L. D. N89-20493
CHOU, TIEN S. N89-20272
CHRISTENSEN, CHARLES R. N89-20801
CHRISTENSEN, HENRIK I. N89-20708
CHRISTIANSEN, P. J. N89-20164
CHU, ROSE W. N89-20697
CHUANG, S. L. N89-20382
CHUNG, N. N89-20267
CHURCHILL, DEAN DANIEL N89-20585
CLARK, IVAN O. N89-20298
CLAUSING, R. E. N89-20259
CLERICI, GIANCARLO N89-20795
CLEVELAND, C. N89-20279
N89-20280
CLEVENSON, SHERMAN A. N89-20778
COATES, A. J. N89-20167
N89-20639
N89-20867
COFFEY, HELEN E. N89-20908
N89-20909
COHEN, AARON N89-20694
COHEN, J. B. N89-20635
COHLY, H. H. P. N89-20290
COLE, GARY L. N89-20684
N89-20685
COLE, J. A. N89-20560
COLE, ROBERT N89-20310
COLELLA, NICHOLAS J. N89-20775
COLLINS, O. N89-20341
CONNER, GARY D. N89-20377
CONROY, B. L. N89-20339
N89-20352
COOK, THOMAS MICHAEL N89-20607
COOK, W. H. N89-20264
COOKE, JAMES ANDREW N89-20501
COOKE, ROGER N89-20765
COPE, M. T. N89-20226
COPENHAVER, RONALD M. N89-20273
CORBAN, ROBERT R. N89-20179
CORLISS, JOHN M. N89-20468
CORNILLEAU-WEHRLIN, N. N89-20160
CORRIGAN, J. C. N89-20512
CORRIGAN, MARTIN N89-20569
CORTES, V. N89-20492
COSNER, C. N89-20756
COSS, JAMES R. N89-20821
COSTELLO, DANIEL J., JR. N89-20357
COSTELLO, H. M. N89-20476
N89-20481
COSTELLO, HUGH M. N89-20480
COWLES, K. N89-20345
COWLEY, CHARLES R. N89-20876
COWLEY, S. W. H. N89-20158
COX, DONALD LYNN N89-20201
CRANE, ROGER M. N89-20210
CREUTZ, MICHAEL N89-20856
CRIM, F. FLEMING N89-20789
CROFT, WILLIAM J. N89-20245
CRONKHITE, J. D. N89-20512
CROONQUIST, A. P. N89-20316
CROS, A. N89-20166
CROUCH, ROGER K. N89-20296
CROW, RITA M. N89-20609
CROWLEY, KAY N89-20638
CRUME, E. C. N89-20809
CUI, JUN-ZHI N89-20634
CURTAIN, R. F. N89-20771
N89-20772
CUVELIER, C. N89-20419
N89-20727
CYPHER, ROBERT N89-20676
CZARNASKI, MARK A. N89-20155

D

DALM, T. B. N89-20115
DALY, P. N89-20168
DAMERELL, C. N89-20785
DANDOURAS, J. N89-20166
DAO, PHAN N89-20376
DASCOTTE, E. N89-20186
DAUM, C. N89-20785
DAUPLAISE, HELEN M. N89-20266
DAVENPORT, A. J. N89-20391
DAVIDOVITZ, M. N89-20382
DAVIDSON, G. N89-20376
DAVIDSON, G. S. N89-20627
DAVIS, HAROLD A. N89-20397
DAVIS, LARRY S. N89-20120
DAVIS, RICHARD N89-20177
DAVIS, TOM, JR. N89-20613
DAY, D. E. N89-20307
DEARAGAOCARVALHO, C. N89-20256
DEBAKKER, J. W. N89-20661
DEBNAM, WILLIAM J., JR. N89-20298
DEBOER, P. N89-20360
DECREAU, P. M. E. N89-20161
N89-20162
N89-20164
DEE, SUZANNE M. N89-20191
DEEDS, W. E. N89-20493
DEEPAK, ADARSH N89-20531
DEFERAUDY, H. N89-20162
DEGIORGI, V. GENSHEIMER N89-20246
DEJONG, H. N89-20118
DEKKER, G. J. N89-20118
DEKONING, A. U. N89-20520
N89-20523
DELAPORTE, B. N89-20159
DELCASTILLO, P. N89-20359
DELPINTO, MICHAEL A. N89-20190
DELUCA, E. E. N89-20880
DEPRIT, E. M. N89-20381
DESALVOSOUZA, L. N89-20451
DESAUSSURE, G. N89-20702
DESTLER, W. W. N89-20792
DETRAUBENBERG, MICHEL RAUSCH N89-20853
DEVINCENT, SANDRA M. N89-20244
DEVLETIAN, JACK H. N89-20244
DEVORE, C. W. N89-20348
DEVRIES, JOHN A., II N89-20665
DEVRIES, R. E. N89-20766
DEWHURST, WARREN T. N89-20599
DEZEEUW, P. M. N89-20739
DIEHL, LARRY A. N89-20192
DIETL, H. N89-20785
DIFILIPPO, FRANK N89-20193
DIJKSTRA, H. A. N89-20735
DILSAVOR, R. L. N89-20364
DIMEO, ROBERT V. N89-20379
DINGUS, BRENDA LYNN N89-20911
DINGUS, RONALD S. N89-20442
DODD, C. V. N89-20493
DOGGETT, ROBERT V., JR. N89-20094
DOLGOV, O. V. N89-20829
DOLINAR, S. J., JR. N89-20340
N89-20343
DOMINEK, A. N89-20358
DOMINICK, A. N89-20355
DOMINICK, SAM M. N89-20182
DOMPKA, R. V. N89-20512
DONALDSON, P. LYNN N89-20602
DONKER, J. C. N89-20653
DONOHOE, GREGORY W. N89-20668
DORAN, J. C. N89-20590
N89-20593
DOREMUS, R. H. N89-20306
DOSSER, L. R. N89-20455
DOSSER, LARRY R. N89-20458
DOUGHERTY, ANDREW JOSEPH N89-20818
DOUGHERTY, D. J. N89-20523
DOVE, D. B. N89-20834
DOWDY, LAWRENCE W. N89-20690
DOWNTON, MARY N89-20569
DOYLE, J. L. N89-20495
DRAXLER, ROLAND R. N89-20559
DROEGEMEIER, KELVIN N89-20569
DRUYAN, LEONARD M. N89-20589
DRYER, F. L. N89-20313
DUC, DUONG MINH N89-20749
DUH, K. H. G. N89-20336
DUNLOP, JAMES SCOTT N89-20887
DUNN, M. G. N89-20426
DUQUETTE, MILES N89-20177
DURAIRAJ, B. N89-20266
DUSEK, J. T. N89-20815
DUSINK, LIESBETH N89-20651
DUSTON, C. N89-20166
DUYAR, AHMET N89-20199

E

EBERHARDT, RALPH N. N89-20182
ECKSTROM, CLINTON V. N89-20099
EGELAND, A. N89-20161
N89-20164
EHLERS, F. EDWARD N89-20093
EINSTEIN, RALPH N89-20479
EISENBERG, MICHAEL N89-20679
EL-AASSER, M. S. N89-20318
EL-SAYED, E. M. N89-20608
ELDRED, D. B. N89-20151
ELIASSON, PETER N89-20416
ELLEMAN, D. D. N89-20308
N89-20316
ELLILA, MARKKU N89-20434
ELLIOTT, J. W. N89-20777
ELLIS, D. E. N89-20835
ELLIS, W. P. N89-20824
ELSENAAR, A. N89-20102
EMANUEL, GEORGE N89-20146
EMRICH, M. L. N89-20704
ENGELHART, F. C. N89-20835
ENGLISH, RONALD EDWARD, JR. N89-20802
ENGLUND, D. R. N89-20137
ENTRIKEN, ROBERT N89-20669
N89-20674
ERBIL, ARMET N89-20825
ERCEGOVAC, MILOES D. N89-20400
ERICKSON, JON D. N89-20694
ERLANDSSON, G. N89-20648
ESER, SEMIH N89-20273
ESGAR, J. B. N89-20144
ESKIN, S. G. N89-20286
ESPOSITO, JOSEPH ANDRE N89-20915
EXARHOS, GREGORY J. N89-20839

F

FACCA, L. N89-20321
FAELTHAMMAR, CARL-GUNNE N89-20189
N89-20897
N89-20899
FAIN, DOUGLAS E. N89-20260
FALK, URBAN N89-20517
FALTHAMMAR, C.-G. N89-20161
FARJON, J. M. J. N89-20534
N89-20535
N89-20536
FARKAS, L. A. N89-20482
FAWLEY, W. M. N89-20451
FAYMON, KARL A. N89-20545
FEEZELL, RASCY R. N89-20479
FEIGELSON, ROBERT S. N89-20849
FELDMAN, D. W. N89-20798
FENNELL, J. F. N89-20168
FERGILE, ALBERT N89-20359
FERGUSON, MILTON W. N89-20205
FERNANDEZ, J. C. N89-20806
FERNANDEZ, MIKE N89-20851
FERREIRA, L. A. N89-20720
FIELDS, CHRIS N89-20640
FIGUEIRA, J. F. N89-20443

FISHER, JOHN J. N89-20477
FLACK, KAREN N89-20086
FLEETER, SANFORD N89-20133
FLEISCHER, G. E. N89-20151
FLEMING, S. P. N89-20503
FLEMINGS, M. C. N89-20302
FLETCHER, R. W. N89-20265
FLOOD, DENNIS J. N89-20385
FLOWER, H. M. N89-20226
FOLLANSBEE, PAUL S. N89-20233
FORSDICK, HARRY C. N89-20629
N89-20870
FOX, MARYE ANNE N89-20211
FRANCISCO, G. N89-20855
FRANGOS, J. A. N89-20286
FRANSSON, JOERGEN N89-20919
FREDE, W. G. N89-20243
FREDERKING, T. H. K. N89-20248
FREDRICK, REBECCA N89-20177
FREEMEN, J. R. N89-20172
FREILEY, A. J. N89-20339
FREIS, ROBERT P. N89-20673
FREYMUTH, PETER N89-20106
FRIDAY, DAVID K. N89-20220
FRIPP, ARCHIBALD L. N89-20298
FRISCH, A. SHELBY N89-20562
FROLOV, V. P. N89-20900
FRUCHT, YAACOV I. N89-20096
FULTON, ROBERT D. N89-20397
FURTAK, T. E. N89-20234
FURZELAND, R. M. N89-20741

G

GABRIEL, KENNETH A. N89-20268
GALANT, DAVID C. N89-20770
GALLARDO, JUAN C. N89-20456
N89-20457
GAMMON, ROBERT W. N89-20320
GARNAAT, HARRY N89-20650
GARNER, J. N89-20816
GARSHNEK, VICTORIA N89-20602
GARVIS, DARREL N89-20438
GATOS, HARRY C. N89-20296
GAUBERT, MICHEL N89-20124
GEDEON, STEVEN A. N89-20244
GEER, JAMES F. N89-20632
GEFFNER, JANET H. N89-20862
GEISLER, WILLIAM N89-20275
GEORGE, MICHAEL N89-20372
GEORGE, PAUL E. N89-20468
GEURST, J. A. N89-20418
GHOSN, LOUIS J. N89-20489
GIBSON, J. S. N89-20152
GIL, JORDI N89-20359
GILL, PHILIP E. N89-20667
GILL, RICHARD D. N89-20769
GILLE, JOHN P. N89-20182
GIRMANN, T. C. N89-20455
GIUIDOTTI, RONALD A. N89-20393
GIVI, PEYMAN N89-20222
GLADDEN, H. J. N89-20139
GLASSELL, R. L. N89-20481
GLASSMEIER, K.-H. N89-20158
GLICKSMAN, M. E. N89-20299
GLOVER, C. W. N89-20482
GODDARD, N. D. R. N89-20226
GOLDENBLAT, I. I. N89-20498
GOLDMAN, S. ROBERT N89-20442
GOLDSTEIN, J. C. N89-20798
GOLDSTEIN, M. L. N89-20157
GOLDSTEIN, R. N89-20169
GOLLAN, ARYE N89-20323
GOLUBOV, A. A. N89-20828
N89-20829
GOMES, J. F. N89-20720
GONIS, A. N89-20845
GONZALEZ, A. N89-20359
GONZALEZ, RICHARD R. N89-20154
GONZALEZSOTO, O. N89-20185
GOOCHEE, CHARLES F. N89-20291
GOOLSBY, C. L. N89-20280
GORDON, STEVEN J. N89-20439
GORETTA, K. C. N89-20815
GOSNEY, M. W. N89-20844
GOSSELINK, JAMES G. N89-20533
GOTLIB, SAM N89-20182
GOTTSTEIN, G. N89-20238
GOUGH, M. P. N89-20164
GOUGH, P. N89-20160
GOULDING, FRED S. N89-20603
GOURDIN, W. H. N89-20242
GOWEN, R. A. N89-20639
N89-20867
GRAFE, V. G. N89-20627
GRAHAM, GERALD N89-20375
GRAHAM, MATTHEW S. N89-20145
GRANT, J. BRIAN N89-20374
GRARD, R. J. L. N89-20161
N89-20169
GRAY, G. T., III N89-20257
GREEN, R. N. N89-20587
GREENBERG, BARRY M. N89-20134
GREGUS, M. N89-20753
GRIESEL, MARTHA ANN N89-20644
GRIEST, K. N89-20880
GRIEWANK, ANDREAS N89-20752
GRINDELAND, R. N89-20279
GRODSINSKY, CARLOS M. N89-20324
GROENENDIJK, W. P. N89-20743
GROSSMAN, L. N89-20379
GUILLORY, J. N89-20792
GUO, TEN-HUEI N89-20199
GUPTE, N. N89-20672
GURNETT, D. A. N89-20160
N89-20161
N89-20162
N89-20163
GURSES, METIN N89-20573
N89-20748
GUSTAFSON, JOHN L. N89-20686
GUSTAFSSON, G. N89-20160
N89-20161
N89-20162
N89-20164
GUSTAVSSON, ANDERS I. N89-20367
N89-20517
GUYENNE, T. D. N89-20156

H

HAENDLER, BLANCA L. N89-20261
HAERENDEL, G. N89-20165
HAERKOENEN, MARTTI N89-20413
HAGEMEYER, BARTLETT C. N89-20578
HAHN, R. C. N89-20299
HAHN, TERRY D. N89-20155
HAINES, ROBIN H. N89-20328
HAIR, LUCY M. N89-20261
HALEY, J. L., JR. N89-20614
HALFANT, MATHEW N89-20679
HALFORD, G. R. N89-20142
HALL, D. S. N89-20167
HALLER, E. E. N89-20796
HALLQUIST, JOHN O. N89-20647
HAMEL, WILLIAM R. N89-20476
N89-20479
N89-20703
HAMELIN, M. N89-20169
HAMMETTER, WILLIAM F. N89-20393
HAN, KWANG S. N89-20447
HANCOCK, G. J. N89-20496
HANDLER, R. A. N89-20678
HANING, ROBERT K. N89-20127
N89-20128
HANZON, BERNARD N89-20726
HARDIN, J. E. N89-20389
HARF, FREDRIC H. N89-20228
HARFORD, JAMES J. N89-20861
HARRIS, D. B. N89-20443
HARRIS, J. H. N89-20809
HARRIS, J. M. N89-20281
HARRISON, JAMES V. A. N89-20683
HARRISON, JOHN NORMAN N89-20623
N89-20624
HARSH, M. D. N89-20406
HARSTAD, K. N89-20215
HART, F. L. N89-20546
HARVEY, C. C. N89-20160
HARVEY, P. R. N89-20132
HASSENZAHL, W. V. N89-20846
HAYES, C. N89-20279
HAYES, S. P. N89-20596
HAZEWINKEL, MICHIEL N89-20701
N89-20745
N89-20746
HEFFERNAN, RUTH M. N89-20124
HEIDELBERG, LAURENCE J. N89-20779
HEINTZE, J. N89-20916
HEMMATI, H. N89-20345
HENINS, I. N89-20806
HERNANZ, M. L. N89-20359
HERNDON, J. N. N89-20481
HERRMANNSFELDT, W. B. N89-20793
HERTZMAN, OWEN N89-20586
HERZL, ALFRED N89-20182
HESS, NANCY J. N89-20839
HESSELINK, WIM H. N89-20656
N89-20734
HEYN, M. F. N89-20158
HIEFTJE, GARY M. N89-20784
N89-20799
N89-20812
HIGUCHI, H. N89-20105
HILL, R. E. N89-20333
N89-20334
HILL, VIOLA J. N89-20906
HINDS, W. T. N89-20564
HINEDI, S. N89-20113
N89-20351
N89-20387
HIRSCHMAN, LYNETTE N89-20677
HITCHON, W. NICHOLAS G. N89-20840
HJALMARSON, H. P. N89-20832
HO, P. N89-20336
HOBBS, JOHN S. N89-20775
HOCH, J. E. N89-20627
HOEFFNAGEL, W. J. C. N89-20535
N89-20536
HOFFMAN, C. M. N89-20392
HOFFMANN, R. N89-20834
HOIDA, HIROSHI W. N89-20445
HOLDEMAN, J. D. N89-20138
HOLLOWELL, DAVID EARL N89-20892
HOLLOWELL, JEFF N89-20119
HOLTKAMP, D. N89-20392
HOOGHIEMSTRA, G. N89-20766
HOOGLAND, ARNE N89-20625
HOOKE, LYDIA RAZRAN N89-20602
HOPKINS, D. B. N89-20453
HOPKINS, R. H. N89-20554
HOPPE, D. J. N89-20338
N89-20339
HOPWOOD, THEODORE, II N89-20471
HORNADY, ROBERT S. N89-20775
HORST, T. W. N89-20593
HORSTMAN, CLIFFORD C. N89-20100
HORTON, L. D. N89-20809
HOSNY, DIAA M. N89-20510
HOVESTADT, D. N89-20166
HOVINGH, J. N89-20810
HOWE, H. C. N89-20809
HU, ANREN N89-20148
HUANG, CHAOSONG N89-20803
HUBERT, D. N89-20160
HUCKLE, H. E. N89-20639
N89-20867
HUDAS, GREGORY R. N89-20404
HUEBNER, MARK A. N89-20821
HUESMAN, RONALD H. N89-20836
HUFF, R. L. N89-20163
HUFF, RONALD G. N89-20776
HUGHES, RICHARD SMITH N89-20380
HUISMAN, W. C. N89-20369
HUITEMA, G. B. N89-20736
HULTQVIST, BENGT N89-20572
HUPP, RICHARD V. N89-20127
N89-20128
HURD, A. J. N89-20834
HURT, GERALD F. N89-20328
HUSSAINI, M. YOUSUFF N89-20411
N89-20718
HUTSON, J. E. N89-20574
HWANG, IN HEON N89-20447
HYATT, MARK J. N89-20252
HYMER, W. C. N89-20279

I

IH, C.-H. C. N89-20151
IMBRIALE, WILLIAM A. N89-20642
INGELS, KEVIN N89-20569
IP, W. H. N89-20168
ISAAC, K. M. N89-20218
ISAACS, H. S. N89-20391
ISKANDER, N. N89-20604
ISLER, R. C. N89-20809
IVERSEN, I. B. N89-20162
N89-20164

J

JACOBI, NATHAN N89-20642
JACOBY, M. N89-20107
JAHODA, FRANK C. N89-20445
JAIN, ANIL K. N89-20760
N89-20801
JAMES, MARK W. N89-20430
JAMESON, ANTONY N89-20095
JANSEN, J. F. N89-20705
JANSEN, S. A. N89-20834
JARBOE, T. R. N89-20806
JARLAS, ROLF N89-20516
JARLSKOG, C. N89-20786

JEDLOVEC, GARY J. N89-20430
JESPERSEN, M. N89-20162
JOHNS, ELIZABETH N89-20598
JOHNSON, RICHARD N89-20180
JOHNSON, ROWLAND R. N89-20628
JOHNSON, STEVE N89-20180
JOHNSON, W. J. N89-20798
JOHNSTON, GARY M. N89-20646
JOHNSTON, L. J. N89-20422
JOHNSTONE, A. D. N89-20167
N89-20639
N89-20667
JOLIN, L. JOHN N89-20448
N89-20797
JOLLES, M. I. N89-20246
JONAS, JIRI N89-20219
JONES, GUILFORD, II N89-20254
JONES, J. P. N89-20482
JONES, PATRICIA M. N89-20695
N89-20696
JONES, R. E. N89-20671
JONES, ROBERT J. N89-20170
JORDAN, E. H. N89-20848
JOSLIN, D. L. N89-20259
JOU, CHENGFONG JOSEPH N89-20826
JUMIKIS, P. T. N89-20503
JUSKA, THOMAS D. N89-20210

K

KAFALAS, J. A. N89-20295
KALLURI, SREERAMESH N89-20514
KAMMASH, T. N89-20811
KAMOTANI, YASUHIRO N89-20314
KAMSTRA, S. I. N89-20535
KANADE, TAKEO N89-20488
KANG, J. S. N89-20824
KAO, M. Y. N89-20336
KARIMABADI, HOMAYOUN N89-20888
KARN, A. J. N89-20834
KARPUK, MICHAEL E. N89-20483
KAT, P. J. N89-20653
KATSIGRIS, E. C. N89-20331
KATZ, BORIS N89-20866
KATZENELSON, JACOB N89-20679
KAUTZ, HAROLD E. N89-20490
KEABLE, CRISPIN JULIAN N89-20677
KEANE, M. S. N89-20766
KEIDING, NIELS N89-20769
KELLY, THOMAS F. N89-20840
KENNEDY, RANDALL N89-20438
KERN, D. N89-20604
KERR, E. L. N89-20347
N89-20348
KESKINEN, M. J. N89-20440
KHALILI, KAVEH N89-20227
KHANDHAR, P. K. N89-20248
KHATHUR, SAADI A. N89-20700
KHOROMSKY, B. N. N89-20753
KILLIAN, M. A. N89-20478
KILLOUGH, STEPHEN M. N89-20476
N89-20479
N89-20702
N89-20703
KIM, C. M. N89-20406
KIM, JOON BAE N89-20216
KIM, JUNE DONG N89-20239
KIM, S.-W. N89-20407
KIM, YOUNG-JIN N89-20706
KIMMEL, RAYMOND H. N89-20575
KINCAID, J. N89-20815
KING, J. M. N89-20544
KING, WAYNE E. N89-20833
KINMAN, P. W. N89-20332
KINNISON, W. W. N89-20392
KIRKPATRICK, RONALD C. N89-20442
KIRZ, J. N89-20604
KITZMILLER, D. H. N89-20577
KLECKER, B. N89-20166
KLEMETTI, WAYNE N89-20376
KLEPER, MYLES H. N89-20323
KLIMA, STANLEY J. N89-20490
KNOX, S. O. N89-20806
KOFMAN, W. N89-20160
KOHLI, A. N89-20267
KOK, JOOST N. N89-20686
KOLKMAN, H. J. N89-20231
KONG, FUNG-MING N89-20261
KONG, JIN AN N89-20543
KOOK, HYUNG-TAE N89-20751
KOONS, H. C. N89-20164
KOPP, W. F. N89-20336
KOREN, BARRY N89-20424
KORENBERG, M. J. N89-20730
KORHONEN, J. S. N89-20814
KORNFELD, D. M. N89-20318
KORTH, A. N89-20168
KOSTERS, MENNO N89-20657
KOTERAS, J. R. N89-20671
KRAMLICH, J. C. N89-20560
KREMSER, G. N89-20166
KRESS, REID L. N89-20480
N89-20481
N89-20705
KRICHNER, D. L. N89-20163
KRIEZIS, GEORGE A. N89-20712
KRINSKY, S. N89-20461
KRISHNAN, K. M. N89-20209
KRIST, STEVEN E. N89-20411
KROPFLI, ROBERT A. N89-20562
KRUEGER, C. N89-20548
KRUPKE, WILLIAM F. N89-20450
KU, J. Y. N89-20561
KUBAN, D. P. N89-20481
KUHN, ALLAN D. N89-20869
KUIJK, A. A. M. N89-20663
KUIJK, FONS A. A. M. N89-20660
KUIJT, J. N89-20791
KULKE, BERNHARD N89-20775
KULP, THOMAS J. N89-20438
KUMAR, R. N89-20362
N89-20387
KUNZE, M. E. N89-20280
KUSSMAUL, MICHAEL N89-20193
KUSSOY, MARVIN I. N89-20100
KUSUDA, TAMAMI N89-20863
KUYK, THOMAS K. N89-20606
KWACK, E. Y. N89-20215
KWAN, THOMAS J. T. N89-20397

L

LAESSER, R. N89-20225
LAGOWSKI, JACEK N89-20296
LAHER, RUSSEL ROGER N89-20187
LAHMEYER, C. R. N89-20342
LAL, RAVINDRA N89-20294
LANAGAN, M. T. N89-20815
LANDMAN, UZI N89-20822
LANG, KENNETH R. N89-20910
LANG, TOMAS N89-20400
LANGELIERS, JAMES N89-20405
LANHAM, J. W. N89-20279
N89-20280
LANIER, W. S. N89-20560
LARSON, DAVID J., JR. N89-20303
LAWRENCE, BARBARA N89-20861
LAWRENCE, J. DENNIS N89-20626
LAWRENCE, JOHN S. N89-20145
LAWTON, DARYL T. N89-20377
LAXMANAN, V. N89-20300
LE, TIEN N89-20282
LEE, B. W. N89-20824
LEE, C. N89-20472
LEE, E. P. N89-20810
LEE, H. G. N89-20524
LEE, KAM-PUI N89-20097
LEE, KYU YONG N89-20249
LEE, RICHARD N N89-20566
LEE, ROBERT C. N89-20155
LEE, SOO HAN N89-20470
LEE, Y. C. N89-20440
LEEHEY, PATRICK N89-20427
LEFEUVRE, F. N89-20160
LEHMBERG, R. H. N89-20462
LEHOCZKY, S. L. N89-20297
LEHTO, A. N89-20153
LEIGHTON, JONATHAN TUTTLE N89-20507
LEIN, S. Y. N89-20554
LENAC, Z. N89-20843
LENHART, S. N89-20756
LENNERT, P. N89-20916
LENTJES, P. G. N89-20535
N89-20536
LEUZE, MICHAEL R. N89-20690
LEWIS, JOHN G. N89-20758
LEWIS, MARIAN L. N89-20280
N89-20287
LI, FONG ZHONG N89-20508
LI, HUI N89-20714
LI, JIN-WAN N89-20431
LI, MING N89-20767
LICHTEN, S. M. N89-20331
LIEFTING, G. N89-20520
LIEWER, PAULETT C. N89-20642
LIN, YUEH-JAW N89-20469
LINDAU, I. N89-20820
N89-20824
LINDELL, ISMO V. N89-20361
LINDQVIST, P.-A. N89-20189
LINKOUS, CLOVIS A. N89-20262
LIOEN, WALTER M. N89-20664
LIPA, J. A. N89-20319
LIST, F. A. N89-20258
LITTLE, JAMES N89-20681
LITTS, STEVEN E. N89-20328
LIU, J. W. S. N89-20717
LIU, JIAQI N89-20713
LIU, Z. M. N89-20844
LIU, ZHENGXING N89-20506
LLOYD, S. C. N89-20689
LO, C. K. N89-20636
LO, Y. T. N89-20382
LOCKHART, THOMAS G. N89-20642
LOGRASSO, T. A. N89-20299
LOO, BILLY W. N89-20603
LOSIER, PAUL W. N89-20145
LOUIE, ALEXANDER N89-20098
LUHR, H. N89-20158
LUMPKIN, A. H. N89-20798
LUNA, HENRY B. N89-20775
LUNA, JACK N89-20248
LUO, SHEN-YI N89-20204
LUO, W. N89-20729
LUTES, L. D. N89-20513
LUTTGES, MARVIN N89-20180
LYNCH, J. M. N89-20596
LYONS, JAMES R. N89-20335
N89-20642
LYONS, L. R. N89-20168
LYZENGA, GREGORY A. N89-20642

M

MACCRACKEN, MICHAEL C. N89-20565
MACDONALD, BRUCE C. N89-20595
MACELROY, ROBERT N89-20180
MACHIELSE, L. A. H N89-20551
MADDEN, NORM W. N89-20603
MAEDER, ANDRE N89-20882
N89-20883
MAEHLUM, B. N. N89-20167
N89-20169
MAGOTRA, NEERAJ N89-20754
MAHLE, JOHN J. N89-20220
MAKER, BRADLEY N. N89-20326
MALASPINA, LAUREN N89-20575
MALCOLM, GRANT N89-20659
MALDONADO, R. H. C. N89-20917
MALEK, DOLORES ELIZABETH N89-20601
MALHOTRA, ROOP C. N89-20433
MALLA, R. P. N89-20330
MALLOUK, THOMAS E. N89-20211
MANGES, WAYNE W. N89-20479
MANGUM, L. J. N89-20596
MANN, R. C. N89-20482
MANNEY, GLORIA LISA N89-20570
MANNING, R. N89-20160
MANSHADI, FARZIN N89-20642
MAO, HUANG N89-20812
MAPLE, M. B. N89-20824
MARIKAR, P. N89-20230
MARINO, JOHN S. N89-20182
MARKLIN, G. J. N89-20806
MARKLUND, G. T. N89-20189
N89-20571
MARKOV, M. A. N89-20900
MARKS, JERRY STEPHEN N89-20485
MARSHALL, W. K. N89-20345
MARTIN, C. N89-20359
MARTIN, J. M. N89-20491
MARTIN, M. N89-20472
MARTIN, R. M. N89-20777
MARTIN, TIM A. N89-20182
MARTINELLI, LUIGI N89-20095
MARTNER, BROOKS E. N89-20562
MARUSAK, N. L. N89-20574
MARUYAMA, XAVIER K. N89-20775
MASON, CINDY L. N89-20628
MASON, T. O. N89-20835
MASOOD-UL-ALAM, A. K. M. N89-20901
MATHYS, G. N89-20884
MATIC, P. N89-20246
MATLOCK, D. K. N89-20235
MATSAS, G. E. A. N89-20855
MATTSSON, STEFAN N89-20365
N89-20366
MAVRIPLIS, DIMITRI J. N89-20095
MAXEY, L. C. N89-20437
MAY, L. NELSON N89-20533
MAYER, ANTON N89-20232
MAYER, THOMAS A. N89-20568
MAYHER, ROBERT J. N89-20328
MAYORAL, C. N89-20185
MAZURKEVICH, G. E. N89-20753

MCCALLUM, J. D. N89-20817
MCCAUGHAN, FRANCES ELIZABETH N89-20131
MCCAULEY, JAMES W. N89-20209
MCCAY, M. H. N89-20301
MCCONNELL, CHRISTOPHER C. N89-20377
MCELIECE, R. J. N89-20344
MCGOVERN, W. E. N89-20577
MCHARGUE, C. J. N89-20259
N89-20817
MCHUGH, J. P. N89-20554
MCILWAIN, C. E. N89-20165
MCINTIRE, L. V. N89-20286
MCIVER, GEORGE N89-20401
MCKEE, R. A. N89-20258
MCKINNEY, P. N89-20111
MCKINNON, JOHN A. N89-20908
N89-20909
MCKNIGHT, R. L. N89-20141
MCQUAID, K. N89-20604
MCRAE, THOMAS G. N89-20438
MEFTAH, BACHIR N89-20212
MEIER, D. L. N89-20554
MEINTEL, A. J. N89-20481
MEISS, JAMES D. N89-20751
MELLING, PETER J. N89-20269
MELSON, N. DUANE N89-20409
MELZNER, F. N89-20165
MENZEL, W. PAUL N89-20430
MERRILL, JOHN N89-20569
MERRILL, WALTER C. N89-20199
MESTNIKFILHO, J. N89-20213
MEYER-ILSE, W. N89-20604
MEYER, CHRISTIAN N89-20180
MEYER, J.-J. CH. N89-20661
MEYER, R. B. N89-20834
MEYER, T. G. N89-20142
MEYER, THOMAS J. N89-20555
MEYNET, GEORGES N89-20882
N89-20883
MICALE, F. J. N89-20318
MICHALSKE, TERRY A. N89-20529
MIKAELIAN, KARNIG O. N89-20425
MILEANT, A. N89-20354
MILGRAM, DAVID L. N89-20377
MILLER, ARCHIE P. N89-20317
MILLER, JOHN L. N89-20444
MILLER, K. L. N89-20567
MILLER, PAUL A. N89-20390
MILLER, R. A. N89-20143
MILLER, TERESA Y. N89-20277
MILLS, JONATHAN A. N89-20761
MIN, B. I. N89-20816
MINGORI, D. L. N89-20152
MIRAGLIOTTA, J. N89-20234
MIRCHANDANEY, RAVI N89-20638
MIRTICH, MICHAEL J. N89-20193
MITCHELL, CHRISTINE M. N89-20692
N89-20693
N89-20695
MITCHELL, S. N89-20449
MIYOSHI, KAZUHISA N89-20253
MIZERKA, LAWRENCE J. N89-20268
MNISZEWSKI, S. M. N89-20689
MOEBIUS, E. N89-20166
MOELLER, CHRIS C. N89-20430
MONGIA, H. C. N89-20138
MONTIERTH, LEE M. N89-20442
MONTRY, GARY R. N89-20686
MOODY, THERESA K. N89-20558
MOORE, GERALD T. N89-20460
MOORE, THOMAS J. N89-20227
MOOS, W. N89-20808
MORAEUS, LARS N89-20525
MORAN, BRIAN N89-20511
MORRIS, DEREK OWEN N89-20624
MORRIS, DIRK H. N89-20913
MORRISON, DENNIS R. N89-20279
N89-20280
N89-20287
N89-20288
N89-20289
N89-20290
MOSES, R. L. N89-20364
MOSKOWITZ, W. P. N89-20376
MOTT, PAUL W. N89-20670
MOTTERSHEAD, CHRISTOPHER JOHN N89-20622
N89-20623
N89-20624
MOZER, F. S. N89-20189
MUKHANOV, V. F. N89-20900
MULARZ, E. J. N89-20138
MULLANY, T. C. N89-20379
MUNDINGER, D. N89-20454
MURA, T. N89-20527
MURPHY, J. K. N89-20170
MURRAY, WALTER N89-20667
MUSMANN, G. N89-20158

N

NAKAMURA, M. N89-20165
NARAYANAN, T. V. N89-20556
NARDI, VITTORIO N89-20807
NATH, S. K. N89-20406
NAVIAOJEDA, C. E. N89-20917
NEAL, STEVEN PHELPS N89-20783
NECHVATAL, JAMES R. N89-20621
NEILSON, GEORGE F. N89-20309
NELANDER, ANDERS N89-20367
NELSON, R. S. N89-20142
NERHEIM, N. M. N89-20151
NEUBAUER, F. M. N89-20158
NEWBERRY, BYRON PEEL N89-20782
NEWNAM, B. E. N89-20798
NG, CHUNG FAI N89-20778
NG, ESMOND N89-20666
N89-20757
NGUYEN, T. N89-20358
NICHOLS, DONALD K. N89-20821
NISSLEY, D. M. N89-20142
NKOMA, JOHN S. N89-20788
NOBACK, R. N89-20126
NOCEDAL, JORGE N89-20715
NOLL, KEITH STEPHEN N89-20903
NONNO, LINDA M. N89-20665
NORDEN, KATHY N89-20591
NOVELLO, M. N89-20854
NUMMILA, K. K. N89-20814

O

OBENCHAIN, S. P. N89-20462
OGUZ, O. N89-20748
OH, TAE SHIK N89-20408
OHARE, P. A. G. N89-20214
OHERN, M. E. N89-20259
OIKKONEN, MARKKU N89-20827
OKSANEN, MARKKU I. N89-20361
OLBRIGHT, G. R. N89-20832
OLES, ANDRZEJ M. N89-20830
OLIVER, W. C. N89-20258
N89-20259
OLOFSSON, H. N89-20885
OLSDER, G. J. N89-20766
OLSEN, R. C. N89-20169
OLSON, D. L. N89-20235
OLSON, ROGER N89-20505
ONEILL, G. N89-20654
ONG, H. L. N89-20834
ORTIZ, G. G. N89-20336
OSTAPENKO, ALEXIS N89-20504
OSTRACH, SIMON N89-20314
OTTENS, H. H. N89-20551
OU, YUH-ROUNG N89-20716
OWYOUNG, A. N89-20832
OZMEN, F. N89-20111

P

PAFFENHOEFER, GUSTAV-ADOLPHO N89-20600
PAIK, SUN MOK N89-20819
PAK, D. J. N89-20478
PALEV, TCHAVDAR D. N89-20750
PALMER, RONALD W. N89-20614
PALOMAR, JAMES V. N89-20775
PALUMBO, D. N89-20698
PAN, YANGLIAN N89-20901
PANCHALINGAM, V. N89-20270
PANIN, F. N89-20518
PAPCUN, G. J. N89-20574
PAPOUTSAKIS, E. TERRY N89-20284
PARK, J. H. N89-20833
PARK, KEE HYUN N89-20690
PARMER, J. K. N89-20478
PARROT, M. N89-20164
PASCHMANN, G. N89-20165
N89-20166
PATCHETT, B. E. N89-20639
N89-20867
PATRIKALAKIS, NICHOLAS M. N89-20712
PATTERSON, JEAN E. N89-20642
PAYNTER, HOWARD L. N89-20182
PAZAMETA, ZORAN N89-20893
PEASE, C. H. N89-20597
PEDERSEN, A. N89-20169
N89-20189
PEDRAZA, D. F. N89-20823
PENG, T. N89-20354
PENNYCOOK, S. J. N89-20817
PEPIN, SCOTT N89-20180
PEREZ-DAVIS, MARLA E. N89-20545
PEREZ, A. N89-20817
PERISON, JANICE N89-20273
PERNICE, M. N89-20620
PERRY, K. S. N89-20512
PETER, E. A. N89-20689
PETERS, J. E. N89-20217
PETERSEN, WILLIAM B. N89-20561
PETERSON, CRAIG C. N89-20633
PETRE, ROBERT N89-20875
PEYTON, BARRY W. N89-20758
PEYTONJONES, J. C. N89-20371
PICKARD, JAMES M. N89-20274
PIECE, DANIEL E. N89-20268
PIENKOWSKI, T. N89-20815
PIERCE, F. J. N89-20406
PIERSON, LYNDON G. N89-20372
PIETERSEN, O. B. M. N89-20116
PIN, F. G. N89-20702
PINTO, F. A. N89-20917
PINTO, H. V. N89-20917
PINTO, JOAO DE LEMOS N89-20532
PINTONETO, N. N89-20854
POEPPEL, R. B. N89-20815
POGGIO, TOMASO N89-20681
POGUE, WILLIAM N89-20181
POKROVSKY, V. L. N89-20831
POLENZ, S. N89-20916
POLLARA, F. N89-20341
POLYDOROS, ANDREAS N89-20402
POND, R. B., SR. N89-20304
PORRA, V. N89-20384
PORTELLA, H. M. N89-20917
PORTER, ALAIN C N89-20879
PORTER, S. J. N89-20503
POSNER, E. C. N89-20329
POTHEN, ALEX N89-20758
POTOTZKY, ANTHONY S. N89-20125
POUWELS, H. N89-20539
POVH, B. N89-20916
POWELL, G. L. N89-20225
POWELL, MARK DILLON N89-20583
POWERS, LYNN M. N89-20489
PRANGSMA, G. J. N89-20538
PRATHER, MICHAEL J. N89-20586
PRESTA, R. W. N89-20441
PRICE, KIRK BARROWS N89-20466
PRICE, WILLIAM E. N89-20821
PROTOPOPESCU, V. N89-20756
N89-20759
PROTZEL, P. N89-20698
PRYADKO, L. P. N89-20831

Q

QIU, LIJIAN N89-20803
QUARTERONI, ALFIO N89-20635
QUEALY, ANGELA N89-20684
N89-20685
QUIROGA, L. N89-20240

R

RABERN, DONALD ALLEN N89-20485
RADESPIEL, R. N89-20101
RAE, W. J. N89-20426
RAEISAENEN, A. N89-20153
RAI, R. S. N89-20209
RAJENDRAN, A. M. N89-20264
RANDJBAR-DAEMI, S. N89-20773
RANKIN, C. C. N89-20699
RAO, S. T. N89-20561
RARBACK, H. N89-20604
RASMUSSEN, K. J. R. N89-20496
RAVN, TOM N89-20505
RAY, C. S. N89-20307
RAYMAN, M. D. N89-20346
REED, JOHN W. N89-20458
REED, STEPHEN K. N89-20774
REICH, SIMEON N89-20636
REINHARDT, FREDERICK W. N89-20393
REITER, ELMAR R. N89-20595
REME, H. N89-20166
REN, ZHAOXING N89-20803
RESING, J. A. C. N89-20766
RESLER, EDWIN L., JR. N89-20134
REYNOLDS, JOHN R. N89-20270
RHODES, PERCY H. N89-20277
N89-20278
RICE, JOHN R. N89-20630
RICHARDS, P. G. N89-20567
RICHTER, KAREN J. N89-20675
RICKARD, DALE N89-20401
RICKS, GLEN A. N89-20196

RIEDLER, W. N89-20158
N89-20169
RIKS, E. N89-20519
N89-20699
RILEY, MERLE E. N89-20394
RIND, DAVID N89-20589
ROBERTS, M. J. N89-20437
ROBINSON, D. L. N89-20346
ROCKENFELLER, UWE N89-20405
RODGERS, J. N89-20792
ROEMMELT, JOHN C. N89-20876
ROGERS, J. P. N89-20512
ROGERS, ROBERT M. N89-20195
N89-20197
ROJAS, R. G. N89-20363
ROMANO, F. J. N89-20864
RONCHETTO, J. J. N89-20436
RONCO, JOSEPH A., JR. N89-20580
ROOIJACKERS, HENRICUS FRANCISCUS LEO
N89-20515
ROOZEKRANS, J. N. N89-20538
ROSEN, I. G. N89-20636
ROSENTHAL, ALAN N89-20533
ROSENTHAL, F. N89-20676
ROSNER, R. N89-20880
ROSOCHA, L. A. N89-20443
ROSS, H. N89-20321
ROSSINGTON, C. S. N89-20796
ROTHMAN, S. N89-20604
ROTTER, J. M. N89-20497
N89-20500
N89-20502
N89-20503
ROUSSEL-DUPRE, ROBERT N89-20375
ROUX, A. N89-20159
ROWE, J. C. N89-20476
N89-20481
ROWE, JOSEPH N89-20602
ROWE, W. A. N89-20392
RUBIN, KENNETH S. N89-20695
RUBINSTEIN, E. R. N89-20299
RUDENAUER, F. N89-20169
RUSCH, J. J. N89-20724
RUSSO, VINCENT F. N89-20646

S

SAAMAN, ERIK N89-20659
SACK, ELISHA N89-20679
SADLER, S. G. N89-20512
SADROZINSKI, H. F. W. N89-20392
SAIF, A. G. N89-20263
SAINZ, B. N89-20492
SALAM, A. N89-20773
SALAZAR, S. N89-20448
SALIHOGLU, S. N89-20748
SALMERON, EVA M. N89-20836
SALO, S. A. N89-20597
SALTZ, JOEL N89-20638
SAMULSKI, E. T. N89-20266
SAN, KA-YIU N89-20285
SANDA, P. N. N89-20834
SANDERS, A. F. N89-20611
SANDERS, VIRGIL R. N89-20448
N89-20797
SANDFORD, MAYNARD C. N89-20099
SARKAR, SUTANU N89-20412
SASSE, F. DEEKE N89-20719
SATER, B. L. N89-20547
SAUNDERS, MICHEAL A. N89-20667
SAUVAUD, J. A. N89-20166
SAWTELL, RALPH RAYMOND N89-20237
SCATTERGOOD, RONALD O. N89-20322
SCHEFFLER, G. W. N89-20544
SCHEID, R. E. N89-20151
SCHIJVE, J. N89-20521
SCHMIDT, B. N89-20916
SCHMIDT, R. N89-20157
N89-20169
SCHMITT, A. J. N89-20462
SCHNABEL, ROBERT B. N89-20762
SCHNEIDER, WILLIAM R. N89-20633
SCHNEPPLE, W. F. N89-20293
SCHOBERT, HAROLD H. N89-20273
SCHOER, JONATHAN KEVIN N89-20463
SCHOUMANS, O. F. N89-20541
SCHRA, L. N89-20231
SCHULKES, R. M. S. M. N89-20727
SCHULZE, ARTHUR E. N89-20181
SCHUMACHER, DANIEL N89-20177
SCHUMACHER, J. M. N89-20744
SCHUURMAN, J. J. N89-20652
SCHWARTZ, S. J. N89-20167
SCHWERTL, M. N89-20388
SCKOPKE, N. N89-20165
SCOTT, CARVEN N89-20584
SEAGER, MARK K. N89-20721
SEASHOLTZ, R. G. N89-20137
SEERING, WARREN P. N89-20439
SEGAL, H. M. N89-20557
SEGALOV, Z. N89-20792
SEGERCRANTZ, JERRY N89-20711
SEIDEL, DAVID A. N89-20099
SEIDEN, A. N89-20392
SEIDENSTICKER, R. G. N89-20554
SELLECK, C. B. N89-20671
SELLECK, M. E. N89-20299
SEN, R. K. N89-20399
SESSLER, A. M. N89-20451
N89-20453
SHAFER, STEVE N89-20487
SHAIK, K. S. N89-20350
SHALEV, DORON N89-20202
SHAO, MICHAEL N89-20800
SHARP, DARLA N89-20591
SHARP, W. M. N89-20451
N89-20452
SHAW, M. T. N89-20266
SHAW, R. R. N89-20163
SHEN, LETIAN N89-20224
SHEN, Y. R. N89-20834
SHEN, Z. X. N89-20824
SHEPARD, R. L. N89-20437
SHERMAN, FREDERICK M. N89-20426
SHERWOOD, EUGENE G. N89-20397
SHEU, H.-R. N89-20318
SHI, D. N89-20815
SHIELDS, NICHOLAS, JR. N89-20181
SHIN, J. N89-20406
SHIOHARA, Y. N89-20302
SHONYO, DAVID B. N89-20862
SHOURESHI, R. N89-20530
SIIKONEN, TIMO N89-20410
SIKKA, V. K. N89-20229
SIMCHICK, RICHARD T. N89-20298
SIMCOX, L. N. N89-20114
SIMOLA, J. T. N89-20814
SIMON, DANIEL S. N89-20603
SIMONEAU, R. J. N89-20139
SIMPSON, M. L. N89-20437
SIPLER, DWIGHT N89-20376
SIRKUS, JIM N89-20499
SIVERSKOG, GUNILLA N89-20919
SIWECKI, S. A. N89-20455
SKLAD, P. S. N89-20817
SKYLLINGSTAD, E. D. N89-20590
SLABY, JACK G. N89-20194
SLOBIN, S. D. N89-20353
SMIRNOV, A. F. N89-20498
SMITH, ERIC PHILIP N89-20878
SMITH, G. L. N89-20587
SMITH, GARY L. N89-20309
SMITH, KENNETH P. N89-20717
SMITH, L. S. N89-20821
SMITH, P. M. N89-20336
SMORENBURG, C. N89-20539
SNIDER, J. D. N89-20805
SNYDER, R. S. N89-20281
SNYDER, ROBERT S. N89-20277
N89-20278
SNYDER, WILLIAM H. N89-20561
SOARES, I. DAMIAO N89-20719
SODERBERG, GARY L. N89-20607
SODROSKI, THOMAS JOHN N89-20914
SOISTMANN, DAVID L. N89-20094
SOKOLOWSKI, DANIEL E. N89-20135
N89-20136
N89-20144
SOLARZ, R. N89-20449
N89-20454
SOLLID, J. E. N89-20798
SOMERS, SCHAEFFER N89-20177
SOMMEIJER, B. P. N89-20740
SOMMER, W. F., JR. N89-20392
SONNEVELD, P. N89-20724
SOREM, M. S. N89-20443
SOURS, THOMAS J. N89-20171
SOUTHWOOD, D. J. N89-20158
SOWA, ERIK C. N89-20845
SOWERS, C. H. N89-20230
SPAIN, CHARLES V. N89-20099
SPANGENBERG, LOIS M. N89-20665
SPEICH, DAVID M. N89-20906
SPELT, P. F. N89-20702
SPENCER, E. N89-20392
SPERRY, V. N89-20454
SPEZIALE, CHARLES G. N89-20412
SPICER, W. E. N89-20820
N89-20824
SPITZER, J. N89-20916
SPITZNAGEL, J. A. N89-20554
SRIKANTAIAH, NATARAJ N89-20312
SRITHARAN, S. S. N89-20716
STAFIRA, STANLEY N89-20177
STAHOVEC, JOE N89-20438
STANSFIELD, S. A. N89-20707
STARK, MARGARET A. N89-20458
STARKMAN, GLENN DAVID N89-20894
STATMAN, J. I. N89-20113
N89-20341
STEELE, JAMES H., JR. N89-20528
STEIGLITZ, KENNETH N89-20403
STEIN, W. E. N89-20798
STEPANEK, P. N89-20722
STOCK, LARRY V. N89-20447
STOCKWALD, K. N89-20388
STOGRYN, A. N89-20378
STOKES, ALAN N89-20613
STONE, HUGH M. N89-20581
STONE, LELAND S. N89-20810
STOVER, E. K. N89-20442
STOWE, L. L. N89-20587
STRATHDEE, J. N89-20773
STREETS, DAVID G. N89-20563
STREETT, CRAIG L. N89-20409
N89-20718
STRIFFLER, C. D. N89-20792
STUNDER, BARBARA N89-20566
STURLA, FRANCISCO ANTONIO N89-20509
SUBRAMANIAN, R. SHANKAR N89-20310
SUDOL, E. D. N89-20318
SUH, KYUNG-WON N89-20889
SUN, Z. M. N89-20842
SUNG, S. N89-20548
SUNJIC, M. N89-20843
SUTTLES, J. T. N89-20587
SWANSON, G. A. N89-20142
SWINSON, MARK L. N89-20486
SZE, ROBERT C. N89-20459
SZEKELY, JULIAN N89-20315
SZOFRAN, F. R. N89-20297

T

TAKAHASHI, F. N89-20105
TAKAHASHI, MARC D. N89-20149
TAKALA, JOSU N89-20368
TALAPOV, A. L. N89-20831
TANGIRALA, V. N89-20321
TARRANT, ANDREW DAVID N89-20207
TAUBIN, GABRIEL N89-20709
TAUSWORTHE, R. C. N89-20643
TAYLOR, JOHN N89-20579
TAYLOR, STEPHEN ALAN N89-20255
TAYLOR, V. R. N89-20587
TEDFORD, A. N89-20379
TEMME, N. M. N89-20738
TENG, JIAN-GUANG N89-20497
N89-20500
N89-20502
TENHAGEN, PAUL J. W. N89-20612
N89-20660
N89-20663
TENHAVE, A. A. N89-20552
TENHAVE, J. M. N89-20115
TERIELE, HERMAN J. J. N89-20664
TERMINELLO, LOUIS JOSEPH N89-20837
TERUYA, A. T. N89-20436
TESKE, RICHARD G. N89-20875
THART, W. G. J. N89-20231
THOMAS, G. N89-20209
THOMAS, JOHN B. N89-20403
THOMAS, JOHN W. N89-20178
THOMAS, ROBERT H. N89-20629
N89-20870
THOMAS, STAN N89-20631
THOMPSON, DAVID H. N89-20479
THOMPSON, J. A. N89-20164
THOMPSON, R. L. N89-20140
THOMSEN, M. N89-20167
THORPE, ARTHUR N. N89-20251
THORPE, CHARLES E. N89-20488
THUNNISSEN, H. A. M. N89-20541
TICHLER, JOYCE N89-20591
TIOMNO, J. N89-20719
TISCHER, A. E. N89-20198
TISONE, VICTOR N89-20569
TODD, P. N89-20279
N89-20280
TOLLIN, GORDON N89-20550
TORR, D. G. N89-20567
TOTTY, BRIAN K. N89-20682
TRAILL, R. ERIC N89-20182
TRESSLER, RICHARD E. N89-20250
TREUMANN, R. N89-20165
TRINH, E. H. N89-20316

TRIPATHY, K. C. N89-20857
TRIPATHY, L. K. N89-20857
TROIM, J. N89-20169
TROLINGER, JAMES D. N89-20294
TROTIGNON, J. G. N89-20162
TROWBRIDGE, D. N89-20206
TSANG, K. M. N89-20728
N89-20733
TSAO, NAI-KUAN N89-20710
TSENG, C.-M. N89-20318
TUOVINEN, J. N89-20153
TURNER, THOMAS P. N89-20797
TZENG, YONHUA T. N89-20851

U

UNRUH, WESLEY P. N89-20373

V

V.D.LINDEN, A. N89-20791
VAANDRAGER, F. W. N89-20662
VAHA, PENTTI N89-20473
VALDECANTOS, C. N89-20492
VALMU, H. N89-20153
VANALSTINE, J. N89-20281
VANBRUNT, RICHARD J. N89-20383
VANDEGEER, SARA A. N89-20742
N89-20747
VANDELINDE, F. J. G. N89-20618
VANDENBERG, L. N89-20293
VANDERGAAG, L. C. N89-20788
VANDERHOFF, J. W. N89-20318
VANDERHOUWEN, P. J. N89-20740
VANDERLAAN, F. B. N89-20536
N89-20540
N89-20541
N89-20542
VANDERVORST, HENK A. N89-20724
N89-20725
VANDEVELDE, S. L. N89-20860
VANDEVOOREN, A. I. N89-20735
VANKATWIJK, JAN N89-20651
VANLEEUWEN, S. STORM N89-20130
VANMULKEN, A. C. M. N89-20475
VANNOORTWIJK, JAN N89-20765
VANWOERKOM, P. TH. L. M. N89-20474
VASALLO, J. N89-20359
VASYLIUNAS, V. M. N89-20168
VAUGHAN, ROBIN N89-20569
VEDHA-NAYAGAM, M. N89-20312
VELDMAN, A. E. P. N89-20723
N89-20724
VERSENDAAL, J. M. N89-20616
N89-20617
VERVERS, FRANS N89-20651
VERWER, J. G. N89-20741
VIERGEVER, M. A. N89-20724
VILNROTTER, V. A. N89-20387
VISSCHER, H. N89-20115
VITANYI, PAUL M. B. N89-20767
VITYAZ, O. N89-20384
VIVIAN, H. C. N89-20151
VLADIMIRSKY, Y. N89-20604
VOGELS, M. E. S. N89-20420
VONHOLLE, WILLIAM G. N89-20414
VOSKES, A. N89-20130
VREENEGOOR, A. J. N. N89-20418

W

WADE, ROSE C. N89-20615
WAGEMAKER, C. N89-20370
WAGNER, ELAINE ANN N89-20150
WAHI, A. K. N89-20820
WAIJ, RUDI N89-20765
WALKER, HOYT N89-20673
WALKER, I. J. N89-20587
WALSH, JOHN E. N89-20464
WALTON, E. N89-20355
WALTON, J. N89-20472
WANG, C. N89-20637
WANG, DEMING N89-20713
WANG, HAIMIN N89-20907
WANG, J. N89-20880
WANG, N. N89-20355
WANG, PI-HUAN N89-20531
WANG, T. G. N89-20308
N89-20316
WANG, X. Y. N89-20608
N89-20842
WANHILL, R. J. H. N89-20087
N89-20521
N89-20522
WANTON, ROBERT P N89-20582
WARD, A. K. N89-20639
N89-20867
WARMACK, R. J. N89-20844
WARREN, R. W. N89-20798
WATSON, J. M. N89-20798
WEATHERILL, WARREN H. N89-20093
WEBBER, STEPHEN E. N89-20211
WEI, R. P. N89-20247
WEI, ROBERT P. N89-20236
WEIJLAND, W. P. N89-20687
WEINBERG, MICHAEL C. N89-20309
WEINZAPFEL, S. N89-20449
WEISBIN, CHARLES R. N89-20479
N89-20702
WEISS, R. A. N89-20267
WEISSMANN, MARIANA N89-20396
WEN, J. T. N89-20151
WENG, T. L. N89-20844
WETSEL, G. C. N89-20844
WHITE, C. W. N89-20817
WHITE, J. MICHAEL N89-20211
WHITEMAN, C. D. N89-20593
WHITTAKER, WILLIAM N89-20487
WICKENS, CHRISTOPHER D. N89-20613
WIELICKI, B. A. N89-20587
WILBURN, ANNE MARIE N89-20598
WILCOX, WILLIAM R. N89-20294
WILDERS, P. N89-20418
WILGEN, J. B. N89-20809
WILKEN, B. N89-20168
WILLIAMS, D. M. N89-20481
N89-20484
WILLIAMS, DEAN N. N89-20673
WILLIAMS, F. N89-20111
WILLIAMS, F. A. N89-20313
WILLIAMS, GLEN MONROE N89-20847
WILLIAMS, HAROLD ALDEN N89-20890
WILLIAMS, JAMES N89-20177
WILLIAMS, K. N89-20280
WILLIAMSON, DAVID L. N89-20576
WIMPLE, CAROLYN D. N89-20673
WING, W. R. N89-20809
WINKLER, CARL A. N89-20328
WINNINGHAM, J. D. N89-20167
WINSA, E. N89-20299
WINTER, DIRK T. N89-20664
WINTER, J. M., JR. N89-20304
WITZKE, EDWARD L. N89-20372
WOLF, MICHAEL A. N89-20373
WONG, DAVID TAK-MAN N89-20891
WONG, SAM TAK-SUM N89-20494
WOODELL, GLENN A. N89-20298
WOODWARD, C. N89-20816
WOODWARD, RICHARD P. N89-20779
WOOLLISCROFT, L. J. C. N89-20162
N89-20164
WORLEY, PATRICK H. N89-20691
WRIGHT, MARGARET H. N89-20667
WRIGHT, WILLIE N89-20432
WU, CHIH-PING N89-20203
WU, JIKE N89-20714
WU, S. F. N89-20556
WU, S.-C. N89-20330
WUYTS, J. N89-20360
WYSOCKI, F. J. N89-20806

X

XU, BING N89-20634

Y

YAMAUCHI, GLORIA K. N89-20124
YAO, R. L. N89-20792
YE, RONG N89-20506
YEH, J. J. N89-20824
YEH, LISA I-CHING N89-20787
YEYATI, ALFREDO LEVY N89-20396
YIOSTALO, OLLI N89-20467
YOO, DONGHO N89-20504
YOO, HAK-DO N89-20294
YORK, THOMAS N89-20896
YU, LI HUA N89-20461
YU, S. S. N89-20451
N89-20452

Z

ZAANEN, JAN N89-20830
ZALUZEC, NESTOR J. N89-20230
N89-20435
ZANG, THOMAS A. N89-20411
N89-20718
ZANGVILL, A. N89-20209
ZEGELING, P. A. N89-20741
ZEILER, THOMAS A. N89-20125
ZELINKA, MARK N89-20177
ZELL, PETER T. N89-20088
ZHANG, WEIYI N89-20421
ZHANG, X. N89-20792
ZHANG, X.-G. N89-20845
ZHAO, SHIDU N89-20224
ZHIDKOV, E. P. N89-20753
ZIMERMAN, A. H. N89-20720
ZIMMERMAN, G. N89-20341
ZIMMERMAN, RICHARD S. N89-20200
ZIOCK, H. J. N89-20392
ZIOLKOWSKI, RICHARD W. N89-20374
ZYLSTRA, GREGORY JAY N89-20895

Typical Corporate Source Index Listing

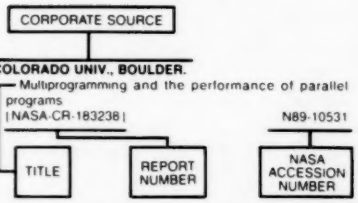

Listings in this index are arranged alphabetically by corporate source. The title of the document provides the user with a brief description of the subject matter. The report number helps to indicate the type of document cited (e.g., NASA report, translation, NASA contractor report). The NASA accession number denotes the number by which the citation is identified. The titles are arranged under each corporate source in ascending accession number order.

A

A/G TECHNOLOGY CORP., NEEDHAM, MA.
Membrane vapor enricher for Water For Injection (WFI) production, phase 1
[AD-A201354] N89-20323

ACADEMIA SINICA, BEIJING (CHINA).
Experimental study of spall damage in an aluminium alloy
[PB89-112619] N89-20224
New type of capacitive temperature sensor for use at low temperature and in strong magnetic field
[PB89-111108] N89-20431
Adaptive FE algorithm for variational inequality problems
[PB89-111512] N89-20634
Numerical method of applying mean value theorem
[PB89-111447] N89-20714
Impedance matching of RF plasma
[PB89-112502] N89-20804

ACADEMIA SINICA, HEFEI (CHINA).
Low frequency MHD instability in a hot electron plasma
[PB89-111546] N89-20803

ADVANCED DECISION SYSTEMS, MOUNTAIN VIEW, CA.
Linear feature extraction from radar imagery: SBIR (Small Business Innovative Research) phase 2, option 1
[AD-A203688] N89-20377

AEROJET ELECTROSYSTEMS CO., AZUSA, CA.
Investigation of extensions to the distorted Born approximation in strong fluctuation theory
[AD-A203698] N89-20378

AEROJET SOLID PROPULSION CO., SACRAMENTO, CA.
Energetic thermoplastic elastomer synthesis
[AD-A203594] N89-20265

AERONAUTICAL RESEARCH INST. OF SWEDEN, STOCKHOLM.
Solutions to the Navier-Stokes equations using a k-epsilon turbulence model
[FFA-TN-1988-19] N89-20416
Postbuckling Finite Element (FE) analysis of a stiffened curved panel loaded in shear
[FFA-TN-1988-23] N89-20516
Implementation of a hierarchical wedge element in the self-adaptive Finite Element (FE) program STRIPE
[FFA-TN-1988-36] N89-20517
Estimation of the Equivalent Initial Flow Size (EIFS) distribution and prediction of failure probabilities for different parameter variations
[FFA-TN-1987-35] N89-20525
A theoretical, numerical and experimental examination of in situ properties of adhesives
[FFA-TN-1988-05] N89-20526

AIR FORCE ACADEMY, CO.
Thrust generation by an airfoil in hovering mode
[AD-A203785] N89-20106

AIR FORCE ARMAMENT LAB., EGLIN AFB, FL.
A comparison of frequency estimation techniques for high-dynamic trajectories
[NASA-CR-184865] N89-20387

AIR FORCE ASTRONAUTICS LAB., EDWARDS AFB, CA.
Rheometrics stress rheometer applications
[AD-A203667] N89-20275

AIR FORCE GEOPHYSICS LAB., HANSCOM AFB, MA.
Density measurements with combined Raman-Rayleigh LIDAR (Light Detection And Ranging)
[AD-A203561] N89-20376

AIR FORCE INST. OF TECH., WRIGHT-PATTERSON AFB, OH.
Assessing potential benefits for service/repair and retrieval of satellites: A pilot decision analysis
[AD-A203830] N89-20190
The initial value problem for fractional order differential equations with constant coefficients
[AD-A203843] N89-20764

AIR FORCE SYSTEMS COMMAND, WRIGHT-PATTERSON AFB, OH.
Structural mechanics: Contemporary state and prospects for development (selected portions)
[AD-A198766] N89-20498

ALABAMA UNIV., BIRMINGHAM.
Protein crystal growth in a microgravity environment N89-20292

ALABAMA UNIV., HUNTSVILLE.
The behavior of the electron density and temperatue at Millstone Hill during the equinox transition study September 1984
[NASA-CR-184737] N89-20567

ALCATEL STANDARD ELECTRICA S.A., MADRID (SPAIN).
Review of network planning methods applicable to Integrated Satellite Terrestrial Networks (ISTN)
[ESA-CR(P)-2691] N89-20185

ALLIED-SIGNAL AEROSPACE CO., KANSAS CITY, MO.
Analysis of brass alloys by wavelength dispersive X-ray spectrometry
[DE89-007595] N89-20243
Finite element modeling of a hydroformed sheet metal cover
[DE89-006798] N89-20326

AMERICAN INST. OF AERONAUTICS AND ASTRONAUTICS, WASHINGTON, DC.
Barriers to the international transfer of information in aerospace and defense N89-20861

AMES LAB., IA.
Fundamental and applied studies of new ionization techniques for inorganic mass spectrometry
[DE89-007567] N89-20483
Paraxial approximations for ultrasonic beam propagation in liquid and solid media with applications to nodestructive evaluation
[DE89-007569] N89-20782
A prior knowledge based optimal Wiener filtering approach to ultrasonic scattering amplitude estimation
[DE89-007574] N89-20783

ARGONNE NATIONAL LAB., IL.
Fluorine as an oxidant in combustion calorimetry
[DE89-003626] N89-20214
In-situ HVEM studies of the early stages of oxidation of nickel and nickel-chromium alloys
[DE89-005833] N89-20230
New directions in spectroscopy for the analytical electron microscope
[DE89-005824] N89-20435
Implications of the greenhouse effect for the midwest economy
[DE89-004195] N89-20563
On automatic differentiation
[DE89-005779] N89-20752
Electronic structure calculation by nonlinear optimization: Application to metals
[DE89-005852] N89-20816

ARIZONA UNIV., TUCSON.
Hormone purification by isoelectric focusing in space N89-20282
Mechanisms of photochemical energy conversion by chlorophyll
[DE89-006820] N89-20550

ARMY AEROMEDICAL RESEARCH LAB., FORT RUCKER, AL.
SPH-4 helmet retention assembly reinforcement
[AD-A200432] N89-20614

ARMY AVIATION ENGINEERING FLIGHT ACTIVITY, EDWARDS AFB, CA.
Airworthiness and flight characteristics evaluation of an improved engine air filtration system on the UH-1H helicopter
[AD-A203446] N89-20145

ARMY AVIATION RESEARCH AND DEVELOPMENT COMMAND, CLEVELAND, OH.
Results of inphase axial-torsional fatigue experiments on 304 stainless steel
[NASA-TM-101464] N89-20514

ARMY AVIATION SYSTEMS COMMAND, CLEVELAND, OH.
High speed balancing applied to the T700 engine
[NASA-CR-180899] N89-20472

ARMY LAB. COMMAND, WATERTOWN, MA.
Anion controlled microstructures in the Al2O3-AlN system
[AD-A203671] N89-20209
Weldability of 2519-T87 aluminum alloy
[AD-A203519] N89-20244
X-ray diffraction study of phase formation and growth in nitrogen implanted iron: Temperature effects
[AD-A203625] N89-20245

ARMY MILITARY PERSONNEL CENTER, ALEXANDRIA, VA.
Cross-coordinated control: An experimentally verified technique for the hybrid twist and wrench control of a voltage-controlled industrial robot
[AD-A203406] N89-20486

ARMY MISSILE COMMAND, REDSTONE ARSENAL, AL.
Using random number generators on the sensor signal processing system
[AD-A203702] N89-20761
Digital processing of speckle images
[AD-A203703] N89-20801

ARMY RESEARCH INST. OF ENVIRONMENTAL MEDICINE, NATICK, MA.
Quantification of environmental chambers by air velocity mapping
[AD-A200923] N89-20154

ARMY TANK-AUTOMOTIVE COMMAND, WARREN, MI.
Design and implementation of the hazard control box for the ride motion simulator
[AD-A203752] N89-20404

ASTRONAUTICS CORP. OF AMERICA, MADISON, WI.
Lunar surface base propulsion system study, volume 1
[NASA-CR-171982-VOL-1] N89-20271

AUBURN UNIV., AL.
Unmanned, space-based, reusable orbital transfer vehicle, DARVES. Volume 1: Trade analysis and design
[NASA-CR-184711] N89-20173
Unmanned, space-based, reusable orbital transfer vehicle, DARVES. Volume 2: Data and calculations
[NASA-CR-184712] N89-20174
Vehicle for Space Transfer and Recovery (VSTAR), volume 1
[NASA-CR-184827] N89-20183
Vehicle for Space Transfer and Recovery (VSTAR), volume 2: Substantiating analyses and data
[NASA-CR-184828] N89-20184
Feasibility study of high temperature superconductor opening switches
[AD-A203699] N89-20851

AXIOMATIX, LOS ANGELES, CA.
Dedicated versus half-duplex receiver topology in jammed, fully connected CDMA networks: Theory and numerical comparisons
[AD-A203635] N89-20402

B

BATTELLE COLUMBUS LABS., OH.
Studies and analyses of the space shuttle main engine. Failure information propagation model data base and software
[NASA-CR-183586] N89-20198
Development of a rotary valve for pulse combustion applications
[PB89-131114] N89-20468
BATTELLE MEMORIAL INST., COLUMBUS, OH.
Sulfide and phosphide analogs of oxynitride ceramics
[AD-A203805] N89-20269
BATTELLE PACIFIC NORTHWEST LABS., RICHLAND, WA.
The development and structure of nocturnal slope winds in a simple valley
[AD-A203427] N89-20593
BAYLOR COLL. OF MEDICINE, HOUSTON, TX.
Development of immunoassays for human urokinase N89-20283
Antibody enhancement of free-flow electrophoresis N89-20290
BDM CORP., MCLEAN, VA.
Comparative lexicon of US-Soviet military technical terminology
[PB89-125553] N89-20865
BEGELEIDINGSCOMMISSIE REMOTE SENSING, DELFT (NETHERLANDS).
The suitability of remote sensing for surveying and monitoring landscape patterns. Volume A: Pilot study - LANDSAT imagery. Volume B: PEPS Project No. 73 - SPOT Imagery
[BCRS-87-12-VOL-A/B] N89-20534
The suitability of remote sensing for surveying and monitoring landscape patterns. Volume A: Pilot study - LANDSAT imagery N89-20535
The suitability of remote sensing for surveying and monitoring landscape patterns. Volume B: PEPS Project No. 73 - SPOT Imagery N89-20536
Land use inventories using satellite images in the region Haaren-Helvoirt-Udenhout, North Brabant (The Netherlands)
[BCRS-88-07] N89-20537
Processing and application of digital AVHRR-imagery for land and sea surfaces
[BCRS-88-08] N89-20538
Phase A study for the extension of the CAESAR scanner with a sensor module for the far infrared
[BCRS-88-09] N89-20539
BELDEN WIRE AND CABLE, GENEVA, IL.
Shielding effectiveness of superconductive particles in plastics
[DE89-003888] N89-20815
BELL TELEPHONE LABS., INC., MURRAY HILL, NJ.
Electron spectroscopy studies of high temperature superconductors: Y(sub 1)-xPr(sub x)Ba2Cu3O(sub 7)-delta
[DE89-006554] N89-20824
BOEING COMMERCIAL AIRPLANE CO., SEATTLE, WA.
Development and application of a program to calculate transonic flow around an oscillating three-dimensional wing using finite difference procedures
[NASA-CR-181744] N89-20093
BOLT, BERANEK, AND NEWMAN, INC., CAMBRIDGE, MA.
Research in distributed personal computer-based information systems, volume 1
[AD-A203780] N89-20629
Research in distributed personal computer-based information systems, volume 2
[AD-A203845] N89-20870
BOSTON UNIV., MA.
Photoinduced electron transfer in ordered polymers
[DE89-006986] N89-20254
BRISTOL UNIV. (ENGLAND).
Production of D, D* and Ds mesons in 200 GeV/c pi(-), K(-) and p-Si interactions
[MPI-PAE/EXP-EL-192] N89-20785
BRITISH PETROLEUM CO. LTD., LONDON (ENGLAND).
Preparation of composites
[EP-0-240-251-A2] N89-20207
Rapid cure acrylic adhesive compositions
[EP-0-247-726-A2] N89-20255
Memory architecture for multiprocessor computers
[EP-PATENT-0-240-354-A1] N89-20622
Data storage and transfer apparatus
[EP-0-243-189-A1] N89-20623
Improvements relating to control flow in computers
[EP-0-234-785-A1] N89-20624
BROOKHAVEN NATIONAL LAB., UPTON, NY.
Thermogravimetric analysis of polymeric materials for an intermediate temperature solid electrolyte. 2: Polymer mixtures
[DE89-006980] N89-20262
The influence of surface capacitance on the measurements of localized corrosion transients
[DE89-006172] N89-20391
Three dimensional numerical analysis of a high-gain free-electron laser
[DE89-006981] N89-20456
Preliminary studies of an infrared free-electron laser oscillator at the ATF(BNL)
[DE89-006982] N89-20457
Amplified spontaneous emission in a single pass free electron laser
[DE89-007048] N89-20461
3CPO, Cloud Chemistry and Cloud Physics Organization: Data index, June 1988
[DE89-007011] N89-20591
Lattice gauge theory and Monte Carlo methods
[DE89-005666] N89-20856
BROWN UNIV., PROVIDENCE, RI.
Analysis of dynamic elastic-plastic fracture phenomena: Steady crack growth and transient loading of a stationary crack N89-20507
Computational studies in nonlinear fracture mechanics N89-20508
Theoretical and computational studies in plasticity and fracture N89-20511
Numerical studies of identification in nonlinear distributed parameter systems
[NASA-CR-181771] N89-20636
Algebraic nonplanar curve and surface estimation in 3-space with applications to position estimation
[PB88-227616] N89-20709

C

CALIFORNIA INST. OF TECH., PASADENA.
The decoding of Reed-Solomon codes N89-20344
Isophotometry of brightest elliptical galaxies in rich clusters N89-20879
Magnetic fields and supergranule velocity fields on the quiet sun N89-20907
CALIFORNIA UNIV., BERKELEY.
Vorticity distributions in unsteady flow separation
[AD-A203733] N89-20428
Elements of design, unifying principles and applications N89-20465
Analysis of the dynamics of guided rotating free center plates N89-20466
Some structural features of high-T(sub c) superconductors
[DE89-006667] N89-20826
CALIFORNIA UNIV., BERKELEY. LAWRENCE BERKELEY LAB.
Exploratory alloy development in the system Al-Sc-X
[DE89-007086] N89-20237
Microstructural and magnetic characterization in soft magnetic Fe-Si-Al (Sendust) alloy
[DE89-007130] N89-20239
Status of LBL/LLNL FEL (Free Electron Laser) research for two beam accelerator applications
[DE89-006656] N89-20453
Discrete analysis of stochastic NMR
[DE89-007016] N89-20494
The development of a Compton lung densitometer
[DE89-006654] N89-20603
X-ray microscopy for the life and physical sciences
[DE89-006707] N89-20604
Dynamic mechanical system design using qualitative and symbolic reasoning
[DE89-006771] N89-20706
Infrared spectroscopy of weakly bound molecular ions
[DE89-006602] N89-20787
Germanium blocked impurity band infrared detectors
[DE89-006607] N89-20796
Heavy ion induction linac drivers for inertial confinement fusion
[DE89-006603] N89-20810
Some structural features of high-T(sub c) superconductors
[DE89-006667] N89-20826
Compensation for crystal penetration in high resolution positron tomography
[DE89-006660] N89-20836
Surface structures determined using electron diffraction
[DE89-006669] N89-20837
A study of the effects of copper to superconductor ratio on stability
[DE89-006604] N89-20846
Resonance electronic Raman scattering in rare earth crystals
[DE89-007446] N89-20847
CALIFORNIA UNIV., DAVIS.
Development of mathematical models for application in image processing
[AD-A203619] N89-20760
CALIFORNIA UNIV., LOS ANGELES.
Active control helicopter aeromechanical and aeroelastic instabilities N89-20149
The magnetic field investigation on Cluster N89-20158
Experiments with metallic and ceramic porous media
[NASA-CR-184819] N89-20248
On-line arithmetic algorithms and structures for VLSI
[AD-A203421] N89-20400
CALIFORNIA UNIV., SAN DIEGO, LA JOLLA.
Particle cloud combustion in reduced gravity N89-20311
Development of a plasma pinch photocathode
[AD-A203944] N89-20813
CALSPAN CORP., BUFFALO, NY.
Transmission and reflection on pressure waves by compressor and turbine stages, based on an actuator-disk model
[AD-A203513] N89-20426
CAMUS, INC., HUNTSVILLE, AL.
Extravehicular activity at geosynchronous earth orbit
[NASA-CR-172112] N89-20181
CARNEGIE-MELLON UNIV., PITTSBURGH, PA.
Development of an integrated mobile robot system at CMU (Carnegie Mellon University), June 1987
[AD-A203689] N89-20487
The 1987 year end report for road following at Canegie Mellon
[AD-A203946] N89-20488
CASE WESTERN RESERVE UNIV., CLEVELAND, OH.
Surface tension driven convection experiment N89-20314
Publications of the Observatory of the University of Michigan. Volume 12, no. 2: Wavelength identifications in the magnetic CP star HR 4816 (HD 110066) N89-20876
CENTER FOR MATHEMATICS AND COMPUTER SCIENCE, AMSTERDAM (NETHERLANDS).
Multigrid and defect correction for the steady Navier-Stokes equation
[CWI-NM-R8803] N89-20424
The power of physical representations
[CWI-CS-R8819] N89-20612
A vector-like architecture for raster graphics
[CWI-CS-R8802] N89-20660
Metric semantics for concurrency
[CWI-CS-R8803] N89-20661
Some observations on redundancy in a context
[CWI-CS-R8812] N89-20662
An exact incremental hidden surface removal algorithm
[CWI-CS-R8818] N89-20663
Factoring with the quadratic sieve on large vector computers
[CWI-NM-R8805] N89-20664
The algebra of synchronous processes
[CWI-CS-R8807] N89-20687
A compositional semantics for Concurrent Prolog
[CWI-CS-R8809] N89-20688
Lectures on linear and nonlinear filtering
[CWI-PM-R8801] N89-20701
Arithmetic classification of perfect models of stratified programs
[CWI-CS-R8810] N89-20737
Uniform asymptotic expansions of a class of integrals in terms of modified Bessel functuons, with application to confluent hypergeometric functions
[CWI-AM-R8806] N89-20738
Matrix dependent prolongations and restrictions in a black box multigrid solver
[CWI-NM-R8801] N89-20739
The use of smoothing techniques in the method of lines
[CWI-NM-R8802] N89-20740
A numerical study of three moving grid methods for one-dimensional partial differential equations which are based on the method of lines
[CWI-NM-R8806] N89-20741
Estimating a regression function
[CWI-MS-R8805] N89-20742
Waiting-time approximations for cyclic-service systems with mixed service strategies
[CWI-OS-R8802] N89-20743
State representations of linear systems with output constraints
[CWI-OS-R8807] N89-20744
A short tutorial on Lie algebras
[CWI-PM-R8802] N89-20745
A tutorial introduction to differentiable manifolds and calculus on manifolds
[CWI-PM-R8803] N89-20746
Asymptotic normality of minimum L sub 1 norm estimators in linear regression
[CWI-MS-R8806] N89-20747

Two decades of applied Kolmogorov complexity. In memoriam: Andrei Nikolaevich Kolmogorov, 1903 - 1987
[CWI-CS-R8813] N89-20767
The certainty factor model and its basis in probability theory
[CWI-CS-R8816] N89-20768
Censoring, truncation and filtering in statistical models based on counting processes
[CWI-MS-R8803] N89-20769
Minimizing total completion time in the two-machine flow shop by Lagrangian relaxation
[CWI-OS-R8808] N89-20860

CENTRE D'ETUDE SPATIALE DES RAYONNEMENTS, TOULOUSE (FRANCE).
The ion spectrometry experiment to measure the properties of the ionic plasma composition and distribution functions at energies between 0 and 40keV/e N89-20166

CENTRE DE RECHERCHES EN PHYSIQUE DE L'ENVIRONNEMENT, ISSY-LES-MOULINEAUX (FRANCE).
Wave experiment consortium N89-20159
STAFF: The Spatio-Temporal Analysis of Field Fluctuations experiment N89-20160

CENTRE NATIONAL D'ETUDES DES TELECOMMUNICATIONS, ISSY-LES-MOULINEAUX (FRANCE).
The magnetic field investigation on Cluster N89-20158

CENTRE NATIONAL DE LA RECHERCHE SCIENTIFIQUE, ORLEANS (FRANCE).
Whisper: A sounder and high frequency wave analyzer experiment N89-20162

CENTRO BRASILEIRO DE PESQUISAS FISICAS, RIO DE JANEIRO.
Antipodal universes in the topology S(sup 3)xR and H(sup 3)xR
[DE88-704999] N89-20719
Introduction to strings and superstrings
[DE88-704998] N89-20853
Einsteins's theory of gravity in Fierz variables
[DE88-705004] N89-20854
Meson production and nuclear fragmentation of nucleus in the atmosphere
[DE88-705019] N89-20917

CHALMERS UNIV. OF TECHNOLOGY, GOETEBORG (SWEDEN).
Molecular radio line observations of mass loss from red giants
[PB89-102313] N89-20885

CHEMICAL RESEARCH AND DEVELOPMENT CENTER, ABERDEEN PROVING GROUND, MD.
Water adsorption equilibria on microporous carbons
[AD-A203536] N89-20220

CHICAGO UNIV., IL.
Thermodynamics of finite-time processes: Accomplishments and work in progress, 1986--1989
[DE89-006726] N89-20858
On the effects of Cosmions upon the structure and evolution of very low mass stars
[NASA-CR-182958] N89-20880

CINCINNATI UNIV., OH.
A refined theory for plate bending with optimized stress field N89-20510

CITY COLL. OF THE CITY UNIV. OF NEW YORK.
Ultrafast physics in microstructure and alloy systems
[AD-A203639] N89-20850

CLARKSON UNIV., POTSDAM, NY.
Modelling the growth of triglycine sulphate crystals in Spacelab 3 N89-20294
Physical phenomena in containerless glass processing N89-20310

CLEVELAND STATE UNIV., OH.
Reliability-based failure analysis of brittle materials
[NASA-CR-184799] N89-20489

COLORADO SCHOOL OF MINES, GOLDEN.
Optical second harmonic generation in metal monolayers and metal surfaces
[DE89-006123] N89-20234
The role of composition and microstructure gradients on weld metal properties and behavior
[DE89-006789] N89-20235
Simultaneous inversion of vector and total field aeromagnetic data using Bayesian inference: A case study from the Cobb Offset of the Juan de Fuca Ridge
[PB89-114193] N89-20599

COLORADO STATE UNIV., FORT COLLINS.
Long term lubrication of ceramics at high temperatures N89-20249
Long-range forecasting of storminess over the Northern Hemisphere oceans
[AD-A203949] N89-20595
An analysis of reduced Hessian methods for constrained optimization
[AD-A201078] N89-20715

COLORADO UNIV., BOULDER.
L1 libration point manned space habitat
[NASA-CR-184732] N89-20180
Sequential and parallel methods for unconstrained optimization
[AD-A203807] N89-20762
Aperture synthesis observations of solar and stellar radio emission N89-20912

COMMERCE DEPT., WASHINGTON, DC.
Current status of Japanese to English machine translation: Report to Congress
[PB89-128276] N89-20863

COMMITTEE ON COMMERCE, SCIENCE, AND TRANSPORTATION (U.S. SENATE).
NASA authorization
[S-HRG-100-579] N89-20873

CONNECTICUT UNIV., STORRS.
An analysis of an incompressible, fiber-reinforced material subjected to finite strains in the direction of reinforcement N89-20201
Synthesis and physical properties of liquid crystalline alkylisocyanate copolymers
[AD-A203631] N89-20266
The effect of deformation history on the morphology and properties of blends of polycarbonate and a thermotropic liquid crystalline polymers
[AD-A203632] N89-20267
A micromechanical viscoplastic stress-strain model with grain boundary sliding
[DE89-007712] N89-20848

CONSEJO SUPERIOR DE INVESTIGACIONES CIENTIFICAS, VALENCIA (SPAIN).
Production of D, D* and Ds mesons in 200 GeV/c pi(-), K(-) and p-Si interactions
[MPI-PAE/EXP-EL-192] N89-20785

CONSERVATION AND RENEWABLE ENERGY INQUIRY AND REFERRAL SERVICE, SILVER SPRING, MD.
Climate fundamentals for solar energy systems
[DE89-007319] N89-20592

CONSIGLIO NAZIONALE DELLE RICERCHE, PAVIA (ITALY).
Domain decomposition methods for systems of conservation laws: Spectral collocation approximations
[NASA-CR-181773] N89-20635

CONSTRUCCIONES AERONAUTICAS S.A., MADRID (SPAIN).
Paint tests on laminated material formed by carbon fiber composites and Tedlar layers
[I-279/88] N89-20208
Fatigue teardown tests of the aged rear support of the A320 aircraft
[I-271/88] N89-20491
Nondestructive tests of elements manufactured using diffusion bonding and superplastic forming
[ETN-89-94131] N89-20492

CONSULTEC SCIENTIFIC, INC., KNOXVILLE, TN.
Assessment of research needs for laser technologies applied to advanced spectrographic methods
[DE89-006455] N89-20446

CORNELL UNIV., ITHACA, NY.
An analytical and numerical study of axial flow compressor instability N89-20131
Propulsion over a wide Mach number range
[NASA-CR-182267] N89-20134
HARTFEM: A finite element program for thermal and viscoplastic deformation problems
[DE89-007788] N89-20755

D

DANISH SPACE RESEARCH INST., LYNGBY.
The magnetic field investigation on Cluster N89-20158

DARTMOUTH COLL., HANOVER, NH.
The Cerenkov free-electron laser
[AD-A203531] N89-20464

DAYTON UNIV., OH.
Condensation and storage of hydrogen cluster ions
[AD-A203801] N89-20223
A comprehensive review of modeling of impact damage in ceramics
[AD-A203477] N89-20264

DEFENCE RESEARCH ESTABLISHMENT OTTAWA, (ONTARIO).
Why cold-wet makes one feel chilled: A literature review
[AD-A203452] N89-20609

DEFENSE APPLIED INFORMATION TECHNOLOGY CENTER, ALEXANDRIA, VA.
The DoD Gateway Information System (DGIS): The development toward artificial intelligence and hypermedia in common command language
[AD-A203674] N89-20869

DEFENSE MAPPING AGENCY, WASHINGTON, DC.
DMA (Defense Mapping Agency) orbit determination of the navy navigation satellite system for 1987
[AD-A203496] N89-20170

DELAWARE UNIV., NEWARK.
Theoretical modelling and experimental characterization of flexible composites under finite deformation N89-20204

DEPARTMENT OF ENERGY, WASHINGTON, DC.
Fastbus standard routines
[DOE/ER-0367] N89-20645

DHV RAADGEVEND INGENIEURSBUREAU B.V., AMERSFOORT (NETHERLANDS).
Land use inventories using satellite images in the region Haaren-Helvoirt-Udenhout, North Brabant (The Netherlands)
[BCRS-88-07] N89-20537

DIENST RUIMTELIJKEORDENING NATUURBEHEER, LANDSCHAPEN VOLKSHUISVESTING (NETHERLANDS).
Land use inventories using satellite images in the region Haaren-Helvoirt-Udenhout, North Brabant (The Netherlands)
[BCRS-88-07] N89-20537

DRAPER (CHARLES STARK) LAB., INC., CAMBRIDGE, MA.
Reliability and performance evaluation of systems containing embedded rule-based expert systems
[NASA-CR-181769] N89-20683

DU PONT DE NEMOURS (E. I.) AND CO., AIKEN, SC.
Application-based control of an autonomous mobile robot
[DE89-004380] N89-20477
Development of a remote inspection robot and camera positioners for reactor tank inspection
[DE89-004381] N89-20478

DYNAMIC ENGINEERING, INC., HEVERLEE (BELGIUM).
Error localization and updating of spacecraft structures mathematical models
[ESA-CR(P)-2697] N89-20186

E

ECOSYSTEMS INTERNATIONAL, INC., GAMBRILLS, MD.
Commercial potential of European and Japanese space programs, task 5
[NASA-CR-184659] N89-20871

EDGERTON, GERMESHAUSEN AND GRIER, INC., IDAHO FALLS, ID.
Group testing of lead-acid batteries for electric vehicles
[DE89-005415] N89-20389

EDINBURGH UNIV. (SCOTLAND).
Selection effects in optical quasar surveys N89-20877
The high-redshift evolution of radio galaxies and quasars N89-20887

EG AND G ENERGY MEASUREMENTS, INC., GOLETA, CA.
Growth of mercuric iodide (HgI2) for nuclear radiation detectors N89-20293

EG AND G ENERGY MEASUREMENTS, INC., LOS ALAMOS, NM.
A relativistic fluid code for high-power microwave propagation
[DE89-006598] N89-20375

EG AND G ENERGY MEASUREMENTS, INC., SANTA BARBARA, CA.
Material selection for electrooptic deflectors
[DE89-007343] N89-20841

EG AND G MOUND APPLIED TECHNOLOGIES, MIAMISBURG, OH.
The dynamic response at high-explosive inert-solid interface as predicted by finite difference/element computer programs
[DE89-007303] N89-20272
Application of rigorous nonlinear regression to the decomposition kinetics of explosives
[DE89-007598] N89-20274
Laser illuminated high speed photography of energetic materials and components with a copper vapor laser
[DE89-006379] N89-20458
Light-Weight Radioisotope Heater Unit Final Safety Analysis Report (LWRHU FSAR). Volume 3: Nuclear risk analysis document
[DE89-005496] N89-20790

ENERGY AND ENVIRONMENTAL RESEARCH CORP., IRVINE, CA.
Kinetic modeling of NOx formation and destruction and combustibles burnout
[PB89-124358] N89-20560

ENSCO, INC., MELBOURNE, FL.
Waveform data collection for source inversion studies
[AD-A203419] N89-20575

ENVIRONMENTAL PROTECTION AGENCY, RESEARCH TRIANGLE PARK, NC.
Dispersion of dense gas releases in a wind tunnel
[PB89-118509] N89-20561
ESSEX CORP., HUNTSVILLE, AL.
Extravehicular activity at geosynchronous earth orbit
[NASA-CR-172112] N89-20181
EUROPEAN SPACE AGENCY, PARIS (FRANCE).
The Cluster Mission: Scientific and technical aspects of the instruments
[ESA-SP-1103] N89-20156
Modeling flexibility of mechanisms with ADAMS
[ESA-STM-242] N89-20518

F

FEDERAL AVIATION ADMINISTRATION, WASHINGTON, DC.
A microcomputer pollution model for civilian airports and Air Force bases. Model application and background
[AD-A199794] N89-20557
FEDERAL AVIATION AGENCY, ATLANTIC CITY, NJ.
Test report for the Direct Access Radar/National Airspace System (DARC/NAS) bi-directional interface test
[AD-A203748] N89-20379
FERMI NATIONAL ACCELERATOR LAB., BATAVIA, IL.
On the effects of Cosmions upon the structure and evolution of very low mass stars
[NASA-CR-182958] N89-20880
Fragmentation of cosmic-string loops
[NASA-CR-184892] N89-20896
FLORIDA ATLANTIC UNIV., BOCA RATON.
Schema-based theories of problem solving
[AD-A203731] N89-20774
FLORIDA STATE UNIV., TALLAHASSEE.
Boundary layer structure and dynamics in outer hurricane rainbands N89-20583
FLORIDA UNIV., GAINESVILLE.
A displacement pattern matching application in elastic-plastic hybrid stress analysis
[AD-A199028] N89-20499
FLOW RESEARCH, INC., KENT, WA.
Vortex-transport element simulation of a confined mixing layer
[AD-A203791] N89-20222
Laser-based inspection technology for fossil heat exchanger tubing
[DE89-005811] N89-20495
FOSTER WHEELER CORP., LIVINGSTON, NJ.
Commercial direct absorption receiver design studies
[DE89-007290] N89-20556

G

GALLAGHER ASSOCIATES, INC., WEST LAFAYETTE, IN.
Quasi-optical microwave components for five different optical paths within the MFTF-B machine
[DE89-005543] N89-20794
GENERAL ACCOUNTING OFFICE, WASHINGTON, DC.
Space Station: NASA efforts to establish a design-to-life-cycle cost process
[GAO/NSIAD-88-147] N89-20188
Space operations: Testing of NASA's technical and management information system
[GAO/IMTEC-88-28] N89-20859
Nuclear power safety: International measures in response to Chernobyl accident
[GAO/NSIAD-88-131BR] N89-20872
Technology transfer: Constraints perceived by Federal laboratory and agency officials
[GAO/RCED-88-116BR] N89-20874
Space Science: Status of the Hubble Space Telescope Program
[GAO/NSIAD-88-118BR] N89-20881
GENERAL ELECTRIC CO., CINCINNATI, OH.
Structural analysis applications N89-20141
GENEVA OBSERVATORY (SWITZERLAND).
Grids of evolutionary models from 0.85 to 120 solar masses: Observational tests and the mass limits
[SER-C-PREPUBL-FASC-29] N89-20882
Tables of evolutionary star models from 0.85 to 120 solar masses with overshooting and mass loss
[SER-C-PREPUBL-FASC-30] N89-20883
The upper main sequence of OB associations. 1: Spectral types and lines of C and N of southern single-lined O stars
[SER-C-PREPUBL-FASC-32] N89-20884
GEORGE WASHINGTON UNIV., WASHINGTON, DC.
Nutritional models for a Controlled Ecological Life Support System (CELSS): Linear mathematical modeling
[NASA-CR-4229] N89-20615
GEORGIA INST. OF TECH., ATLANTA.
High speed, precision motion strategies for lightweight structures
[NASA-CR-184851] N89-20327
Active vibration control of a large flexible manipulator by inertial force and joint torque
[NASA-CR-184786] N89-20470
Human-computer interaction in distributed supervisory control tasks
[NASA-CR-184871] N89-20692
View graphs for GSFC Colloquium on OFMspert N89-20693
Intent inferencing with a model-based operator's associate
[REPT-88-2] N89-20695
OFMTutor: An operator function model intelligent tutoring system N89-20696
A survey of intelligent tutoring systems: Implications for complex dynamic systems N89-20697
The structure and reactivity of heterogeneous surfaces and study of the geometry of surface complexes
[DE89-005726] N89-20822
Crystalline metal-semiconductor superlattices
[DE89-006619] N89-20825
GRONINGEN RIJKSUNIVERSITEIT (NETHERLANDS).
Reducing the proof burden when reasoning with congruence types
[CS-8807] N89-20655
An algebraic calculus of commands
[CS-8808] N89-20656
Quadratic blending surfaces for complex corners, part 2
[CS-8809-PT-2] N89-20657
An exploration of the Bird-Meertens formalism
[CS-8810] N89-20658
Do-it-yourself type theory
[CS-8811] N89-20659
Command algebras, recursion and program transformation
[CS-8812] N89-20734
A finite element stability analysis for the Marangoni problem in a rectangular container with rigid sidewalls
[TW-285] N89-20735
Toward a quasi-periodic bifurcation theory
[ZW-8803] N89-20736
Well-posedness of infinite-dimensional linear systems in time and frequency domain
[TW-287] N89-20771
Robust stability of normalized coprime factors: The infinite dimensional case
[TW-291] N89-20772
GRUMMAN AEROSPACE CORP., BETHPAGE, NY.
The influences of convection on directional solidification of eutectic Bi/MnBi N89-20303
GTE LABS., INC., WALTHAM, MA.
A comparative study of the influence of buoyancy driven fluid flow on GaAs crystal growth N89-20295

H

HAMPTON INST., VA.
Direct solar-pumped iodine laser amplifier
[NASA-CR-184813] N89-20447
HARBIN INST. OF TECH. (CHINA).
Finite element technique for the inverse problem of a partial differential equation and its application to parameter identification of structure
[PB89-111439] N89-20713
HEIDELBERG UNIV. (GERMANY, F.R.).
Cosmic ray tracking: A new approach to high energy gamma-astronomy
[HD-PY88/05] N89-20916
HELSINKI UNIV. OF TECHNOLOGY, ESPOO (FINLAND).
Anechoic chamber evaluation at 85 GHz
[PB89-125199] N89-20153
Complex-valued functionals in variational analysis of waveguides with impedance boundaries
[PB89-128896] N89-20361
A study of EMI-endurance of two polling-type local area networks used in real-time automation applications in a simulated electrical environment
[EL-62] N89-20368
Testing of time domain simulators for nonlinear electronic circuits
[PB89-125132] N89-20384
Quasi-classical calculations for superfluids
[ETN-89-94118] N89-20421
On the performance of the DELPHI hadron calorimeter
[PH-159] N89-20434
Influence of lubrication on ceramic and steel sliding contacts
[PB89-125090] N89-20467
Application of parameter adaptive approach to servo control of a hydraulic manipulator
[MA-51] N89-20473
Basis representations in large-scale linear programming software
[MA-50] N89-20649
Formula related to the Cayley-Hamilton equation
[PB89-128003] N89-20711
Experiments with negative ions in (3)He superfluids
[PB89-127682] N89-20814
X-ray diffraction and ellipsometric studies of zinc sulfide thin films grown by atomic layer epitaxy
[PH-161] N89-20827
HELSINKI UNIV. TECHNOLOGY, OTANIEMI (FINLAND).
Flux vector splitting in general curvilinear coordinates
[PB89-127393] N89-20410
HOUSTON UNIV., TX.
The stress response system of proteins: Implications for bioreactor scaleup N89-20291
HOWARD UNIV., WASHINGTON, DC.
Glass corrosion in natural environment
[NASA-CR-184843] N89-20251
HUFF (RONALD G.) AND ASSOCIATES, NORTH OLMSTED, OH.
Noise generated by a flight weight, air flow control valve in a vertical takeoff and landing aircraft thrust vectoring system
[NASA-CR-182232] N89-20776
HULL UNIV. (ENGLAND).
Remote sensing in refractive turbulence N89-20532

I

ICON CONSULTANTS, BIRMINGHAM, AL.
Using depth recovery in humans
[AD-A201278] N89-20606
ILLINOIS UNIV. AT URBANA-CHAMPAIGN, SAVOY.
Radiative heat transfer augmentation in high temperature combustion systems with application to radiant tube burners
[PB89-133805] N89-20217
ILLINOIS UNIV., CHICAGO.
Evaluation of solid lubricants: Temperature programmed desorption of MoS2 on molybdenum and of ion-implanted MoS2 on molybdenum
[AD-A203741] N89-20268
Dynamic modeling and linearization for real-time control of a pantograph manipulator N89-20469
ILLINOIS UNIV., SAVOY.
Componential analysis of pilot decision making
[AD-A203711] N89-20613
ILLINOIS UNIV., URBANA.
Reconfigurable antennas
[AD-A203847] N89-20382
Monotonically improving approximate answers to relational algebra queries
[NASA-CR-184874] N89-20717
ILLINOIS UNIV., URBANA-CHAMPAIGN.
Aerospace vehicle design, Spacecraft Section final project reports
[NASA-CR-184741] N89-20121
Aerospace vehicle design, Spacecraft Section final project reports
[NASA-CR-184742] N89-20122
Aerospace vehicle design, Spacecraft Section
[NASA-CR-184743] N89-20123
Transport and relaxation processes in supercritical fluids
[DE89-005910] N89-20219
A class Hierarchical, object-oriented approach to virtual memory management
[NASA-CR-184876] N89-20645
Mixing and nucleosynthesis in low- and intermediate-mass AGB stars N89-20892
Magnetospheres of neutron stars accreting from disks N89-20895
IMPERIAL COLL. OF SCIENCE AND TECHNOLOGY, LONDON (ENGLAND).
On heterotic supermanifolds
[DE88-705339] N89-20773
INDIANA UNIV., BLOOMINGTON.
Noise: Friend or foe
[AD-A203491] N89-20784
Luminescence originating in an optical fiber
[AD-A203494] N89-20799
A new procedure for determination of electron temperatures and electron concentrations by Thomson scattering and analytical plasmas
[AD-A203489] N89-20812
INSTITUT FRANCO-ALLEMAND DE RECHERCHES, SAINT-LOUIS (FRANCE).
Base flow investigation behind axi-and non-axisymmetric blunt bodies
[ISL-CO-246/87] N89-20103

Production of pulsed electron beams by triggered pseudo-spark discharges
[ISL-CO-245/87] N89-20388

INSTITUTE FOR COMPUTER APPLICATIONS IN SCIENCE AND ENGINEERING, HAMPTON, VA.
Multigrid solution of the Navier-Stokes equations on triangular meshes
[NASA-CR-181786] N89-20095
Resolution requirements for numerical simulations of transition
[NASA-CR-181799] N89-20411
A simple nonlinear model for the return to isotropy in turbulence
[NASA-CR-181797] N89-20412
Cumulative reports and publications through December 31, 1988
[NASA-CR-181784] N89-20619
A hybrid-perturbation-Galerkin technique which combines multiple expansions
[NASA-CR-181781] N89-20632
Domain decomposition methods for systems of conservation laws: Spectral collocation approximations
[NASA-CR-181773] N89-20635
Numerical studies of identification in nonlinear distributed parameter systems
[NASA-CR-181771] N89-20636
Optimal feedback control infinite dimensional parabolic evolution systems: Approximation techniques
[NASA-CR-181772] N89-20637
Run-time scheduling and execution of loops on message passing machines
[NASA-CR-181785] N89-20638
Fault-tolerance of a neural network solving the traveling salesman problem
[NASA-CR-181798] N89-20698
Analysis of regularized Navier-Stokes equations, 2
[NASA-CR-181801] N89-20716
Spectral methods for CFD
[NASA-CR-181803] N89-20718

INSTITUTE FOR DEFENSE ANALYSES, ALEXANDRIA, VA.
Development of the University of Maryland RAMCAD (Reliability and Maintainability Computer-Aided Design) for electronic systems
[AD-A203616] N89-20675

INSTITUTE FOR PERCEPTION RVO-TNO, SOESTERBERG (NETHERLANDS).
Cognitive psychology at the Institute for Perception
[IZF-1987-41] N89-20611
Safe working time limits in impermeable protective clothing: Recommendations based upon experimental measurements
[IZF-1987-28] N89-20618

INSTITUTE OF NUCLEAR PHYSICS, KRAKOW (POLAND).
Production of D, D* and Ds mesons in 200 GeV/c pi(-), K(-) and p-Si interactions
[MPI-PAE/EXP-EL-192] N89-20785

INSTITUTO DE ELECTRONICA DE COMMUNICACIONES, MADRID (SPAIN).
Electronically Steerable Terminal Antenna (ESTA) project, phase 2
[ESA-CR(P)-2599] N89-20359

INSTITUTO DE FISICA TEORICA, SAO PAULO (BRAZIL).
Vertex operators and Jordan fields
[DE88-705078] N89-20720
Remark on the gravitational field produced by an infinite straight string
[DE88-705077] N89-20855

INSTITUTO DE PESQUISAS ENERGETICAS E NUCLEARES, SAO PAULO (BRAZIL).
Study of vibrational and rapid local motions of hydrogen in the storage compound Ti0.8Zr0.2 CrMnH3 by slow neutron scattering
[DE88-704797] N89-20213

INTERNATIONAL ATOMIC ENERGY AGENCY, VIENNA (AUSTRIA).
Geological data integration techniques: Proceedings
[DE88-705255] N89-20868

INTERNATIONAL BUSINESS MACHINES CORP., HOPEWELL JUNCTION, NY.
X-ray microscopy for the life and physical sciences
[DE89-006707] N89-20604

INTERNATIONAL BUSINESS MACHINES CORP., MANASSAS, VA.
Very High Speed Integrated Circuits (VHSIC). Phase 2: Submicrometer technology development, interoperability standards
[AD-A203629] N89-20401

INTERNATIONAL CENTRE FOR THEORETICAL PHYSICS, TRIESTE (ITALY).
Surface and interface local density of states for Nb, V and Ta
[DE88-705365] N89-20240
On the dimerization of linear polymers
[DE88-705341] N89-20256
Nucleation of superconductivity in ceramic oxides
[DE88-705364] N89-20263
Evaluation of the Kubo formula for the conductivity using the recursion method
[DE88-705359] N89-20396
Soliton geometry and the vacuum gravitational field equations
[DE88-705340] N89-20573
Propagation of the nerve impulse under the effect of a magnetic field
[DE88-705371] N89-20608
Multifractals
[DE88-705369] N89-20672
Nonlinear partial differential equations on homogeneous spaces
[DE88-705342] N89-20748
Second order degenerate elliptic equations
[DE88-705347] N89-20749
Irreducible finite-dimensional representations of the Lie superalgebra gl(n/1) in a Gelfand-Zetlin basis
[DE88-705350] N89-20750
On heterotic supermanifolds
[DE88-705339] N89-20773
Theory of Raman scattering by surface polaritons in a four media system
[DE88-705358] N89-20788
Thermodynamic characteristics of Y-Ba-Cu-O type compounds in the model of strong electron-phonon coupling
[DE88-705343] N89-20828
Energy gap in S- and D-wave pairing superconductors
[DE88-705344] N89-20829
Localized versus itinerant picture of light-T(sub c) superconducting oxides
[DE88-705345] N89-20830
Resonance tunnelling and breakdown of the Quantum Hall Effect (QHE) in strong electric fields
[DE88-705348] N89-20831
Nonlinear dynamical phenomena in liquid crystals
[DE88-705367] N89-20842
Finite size effects in Wigner crystallization of electrons on liquid helium layers
[DE88-705370] N89-20843
Integrable two dimensional supersystems
[DE88-705355] N89-20857
Black holes as possible sources of closed and semiclosed worlds
[DE88-705336] N89-20900
Nonexistence theorems for Yang-Mills fields outside the black hole of the Schwarzschild spacetime
[DE88-705351] N89-20901

INTERNATIONAL FUEL CELLS CORP., SOUTH WINDSOR, CT.
Phosphoric acid fuel cell subsystem technology
[PB88-100515] N89-20544

IOWA STATE UNIV. OF SCIENCE AND TECHNOLOGY, AMES.
Numerical studies of barotropic stability of stratospheric states N89-20570

IOWA UNIV., IOWA CITY.
The wideband plasma wave interaction N89-20163
New approaches to fluorocarbon synthesis
[AD-A203841] N89-20221
Influences of muscle fiber composition and strength on EMG (electromyographic activity), spinal motion and load acceleration during a repetitive lifting task
[PB89-131221] N89-20607
Nonthermal radio emission from RS CVN binaries and similar systems N89-20913

ISEL, MADRID (SPAIN).
Electronically Steerable Terminal Antenna (ESTA) project, phase 2
[ESA-CR(P)-2599] N89-20359

ISTITUTO NAZIONALE DI FISICA NUCLEARE, MILAN (ITALY).
Simulation of superradiant free-electron lasers
[DE89-006156] N89-20451

J

JAYCOR, VIENNA, VA.
Engineering and technical efforts to design and construct a 10 MW gyrotron laboratory
[AD-A203851] N89-20155

JET PROPULSION LAB., CALIFORNIA INST. OF TECH., PASADENA.
High-dynamic GPS tracking
[NASA-CR-184868] N89-20113
Flexible structure control laboratory development and technology demonstration
[NASA-CR-184867] N89-20151
Modeling and control of flexible structures
[NASA-CR-184862] N89-20152
The magnetic field investigation on Cluster N89-20158
Active spacecraft potential control: An ion emitter experiment N89-20169
Investigation of spray dispersion and particulate formation in diesel fuel flames
[NASA-CR-184820] N89-20215
Acoustic containerless experiment system: A non-contact surface tension measurement N89-20308
Crystal nucleation in lithium borate glass N89-20309
The dynamics of free liquid drops N89-20316
The Telecommunications and Data Acquisition Report
[NASA-CR-184672] N89-20329
Deriving a geocentric reference frame for satellite positioning and navigation N89-20330
Determination of GPS orbits to submeter accuracy N89-20331
Two-way coherent Doppler error due to solar corona N89-20332
Dynamic models for simulation of the 70-M antenna axis servos N89-20333
A new algorithm for modeling friction in dynamic mechanical systems N89-20334
Theoretical comparison of maser materials for a 32-GHz maser amplifier N89-20335
On 32-GHz cryogenically cooled HEMT low-noise amplifiers N89-20336
Cross-guide coupler modeling and design N89-20337
Modal analysis applied to circular, rectangular, and coaxial waveguides N89-20338
Conceptual design of a 1-MW CW X-band transmitter for planetary radar N89-20339
VLA telemetry performance with concatenated coding for Voyager at Neptune N89-20340
A long constraint length VLSI Viterbi decoder for the DSN N89-20341
Long decoding runs for Galileo's convolutional codes N89-20342
Performance of Galileo's concatenated codes with nonideal interleaving N89-20343
Performance of efficient Q-switched diode-laser-pumped Nd:YAG and Ho:YLF lasers for space applications N89-20345
Calculations of laser cavity dumping for optical communications N89-20346
An integral sunshade for optical reception antennas N89-20347
Shutters and slats for the integral sunshade of an optical reception antenna N89-20348
Effect of earth albedo variation on the performance of a spatial acquisition subsystem aboard a planetary spacecraft N89-20349
A preliminary weather model for optical communications through the atmosphere N89-20350
An extended Kalman filter based automatic frequency control loop N89-20351
Transmitter data collection using Ada N89-20352
DSN 70-meter antenna X-band gain, phase, and pointing performance, with particular application for Voyager 2 Neptune encounter N89-20353
Pointing a ground antenna at a spinning spacecraft using Conscan-simulation results N89-20354
Efficient detection and signal parameter estimation with applications to high dynamic GPS receivers
[NASA-CR-184861] N89-20382
A comparison of frequency estimation techniques for high-dynamic trajectories
[NASA-CR-184865] N89-20387
Characterization of production GaAs solar cells for space
[NASA-CR-184863] N89-20549
Hypercube matrix computation task
[NASA-CR-184869] N89-20642
A communication channel model of the software process
[NASA-CR-184866] N89-20643
Incremental development and prototyping in current laboratory software development projects: Preliminary analysis
[NASA-CR-184860] N89-20644
Heavy ion induced Single Event Phenomena (SEP) data for semiconductor devices from engineering testing
[NASA-CR-184864] N89-20821
To Uranus and beyond
[NASA-EP-260] N89-20902

JIAOTONG UNIV., SHANGHAI (CHINA).
Large deflection analysis of thin elastic shells by hybrid stress method
[PB89-111504] N89-20506

JOHNS HOPKINS UNIV., BALTIMORE, MD.
Pb-Zn liquid metal diffusion N89-20304
Extreme ultraviolet and soft X-ray diagnostics of high-temperature plasmas
[DE89-007070] N89-20808

JOINT INST. FOR NUCLEAR RESEARCH, DUBNA (USSR).
Combined algorithms in nonlinear problems of magnetostatics
[DE89-006591] N89-20753

K

KENTUCKY UNIV., LEXINGTON.
Scientific support for an orbiter middeck experiment on solid surface combustion N89-20312
Long-term evaluation of the acoustic emission weld monitor
[PB88-122642] N89-20471

L

LAWRENCE LIVERMORE NATIONAL LAB., CA.
Constitutive properties of copper and tantalum at high rates of tensile strain: Expanding ring results
[DE89-006197] N89-20242
The application of statistical experimental design to the development of low-density polymer foams
[DE89-006774] N89-20261
Finite element modeling of a hydroformed sheet metal cover
[DE89-006798] N89-20326
Modeling the behavior of pulsed, high power microwave antenna systems
[DE89-006280] N89-20374
Workshop on Transient Induced Insulator Flashover in Vacuum
[DE89-006727] N89-20398
Time resolved study of light emitted by detonation arrival at the surface of high explosives in various environments
[DE89-005657] N89-20414
Numerical simulation of turbulent mixing in shock-tube experiments
[DE89-005101] N89-20425
The effects of variations in the photocathode voltages of electronic streak cameras
[DE89-006776] N89-20436
Current status of the NAVSEA Backscatter Absorption Gas Imaging (BAGI) development project
[DE89-006728] N89-20438
Q-switched, intracavity doubled Nd:YAG laser side-pumped by a laser diode array
[DE89-005349] N89-20441
High power induction free electron laser
[DE89-006208] N89-20444
Ground state depleted laser experiments
[DE89-006146] N89-20449
Ground State Depleted (GSD) solid state lasers: Principles, characteristics, and scaling
[DE89-006149] N89-20450
Simulation of superradiant free-electron lasers
[DE89-006156] N89-20451
Validity of 1D free-electron laser sideband models
[DE89-006284] N89-20452
Laser diode cooling for high average power applications
[DE89-006777] N89-20454
Scenarios for future climate change: Results of GCM (General Circulation Model) simulations
[DE89-006151] N89-20565
Software reliability engineering
[DE89-006781] N89-20626
DATMS: A framework for distributed assumption based reasoning
[DE89-006282] N89-20628
User's manual for DYNA2D: An explicit two-dimensional hydrodynamic finite element code with interactive rezoning and graphical display
[DE89-006695] N89-20647
The use of GKS (Graphical Kernel System) and CGM (Computer Graphics Metafile) for the display of graphics products
[DE89-006734] N89-20673
SLAP (Sparse Linear Algebra Package) for the masses
[DE89-006209] N89-20721
Anion grain boundary diffusion in Cr2O3 and Cr2O3-0.09 weight percent Y2O3
[DE89-006281] N89-20833
A first-principles method for the determination of the electronic structure of grain boundaries
[DE89-006148] N89-20845
LEHIGH UNIV., BETHLEHEM, PA.
Corrosion fatigue of iron-chronium nickel alloys: Fracture mechanics and chemistry
[DE89-006985] N89-20236
Electrochemical considerations of crack growth in the ferrous alloys
[AD-A203811] N89-20247
Tripping of asymmetrical stiffeners under combined loading
[PB89-126171] N89-20504
LEICESTER UNIV. (ENGLAND).
High Reynolds number incompressible flow simulation about parachute canopies and similar bluff bodies N89-20096
LOCKHEED ENGINEERING AND SCIENCES CO., WASHINGTON, DC.
USSR Space Life Sciences Digest, Issue 21
[NASA-CR-3922(24)] N89-20602
LOS ALAMOS NATIONAL LAB., NM.
Electrodeposition of aluminium, aluminium/magnesium alloys and magnesium from organometallic electrolytes
[DE89-003483] N89-20232
Analysis of the strain-rate sensitivity at high strain rates in fcc and bcc metals
[DE89-005471] N89-20233
Structure-property characterization of a shock-loaded boron carbide-aluminum cermet
[DE89-005455] N89-20257
A portable CW/FM-CW Doppler radar for local investigation of severe storms
[DE89-005445] N89-20373
Test of radiation hardness of CMOS transistors under neutron irradiation
[DE89-006511] N89-20392
Bunch beam production and microwave generation in reditrons
[DE89-006530] N89-20397
Pulsed laser effects phenomenology
[DE89-005466] N89-20442
Development KrF lasers for inertial confinement fusion
[DE89-005469] N89-20443
ILS (Intracavity Laser Spectroscopy) for beam sensing (experiment)
[DE89-006376] N89-20445
Damage to silver coatings from high average power 1-micron laser
[DE89-005476] N89-20448
Review of long-pulse laser development
[DE89-006514] N89-20459
Axially accelerated saboted rods subjected to lateral forces
[DE89-007466] N89-20485
A stereological analysis of ductile fracture by microvoid coalescence
[DE89-000355] N89-20528
Applying expertise to data in the Geologist's Assistant expert system
[DE89-003463] N89-20574
A software model for simulation in computer-based training
[DE89-003469] N89-20665
A local area network diagnostic assistant expert system
[DE89-003575] N89-20689
Cavity ringdown measurements of high-reflection mirrors at 1.06 microns
[DE89-006512] N89-20797
Proposed extended tuning range for the Los Alamos mid-infrared adjustable, coherent light experiment (MIRACLE) facility
[DE89-006550] N89-20798
Improved plasma confinement and evidence for a pressure-driven instability from reduced magnetic field errors in the CTX spheromak
[DE89-005475] N89-20806
Plasma focus sources: Supplement to the Neutron Resonance Radiography Workshop proceedings
[DE89-006927] N89-20807
Electron spectroscopy studies of high temperature superconductors: Y(sub 1)-xPr(sub x)Ba2Cu3O(sub 7)-delta
[DE89-006554] N89-20824
Study of ultra-high energy emission from Cygnus X-3 and Hercules X-1
[DE89-004543] N89-20911
LOUISIANA STATE UNIV., BATON ROUGE.
Utilizing remote sensing of thematic mapper data to improve our understanding of estuarine processes and their influence on the productivity of estuarine-dependent fisheries
[NASA-CR-183417] N89-20533
Star formation, using 3-D explicit Eulerian hydrodynamics N89-20890
LOVELACE FOUNDATION FOR MEDICAL EDUCATION AND RESEARCH, ALBUQUERQUE, NM.
Extravehicular activity at geosynchronous earth orbit
[NASA-CR-172112] N89-20181

M

MARTIN MARIETTA AEROSPACE, DENVER, CO.
Superfluid Helium Tanker (SFHT) study
[NASA-CR-172110] N89-20182
MARYLAND UNIV., COLLEGE PARK.
Vision-based navigation for autonomous ground vehicles
[AD-A203712] N89-20120
Critical fluid light scattering N89-20320
Stimulated Raman scattering of intense laser radiation in a nuclear-disturbed space plasma
[AD-A200951] N89-20440
Review of intense electron beam transport in gases
[DE89-005397] N89-20792
A molecular dynamics study of surface kinetics and epitaxial crystal growth N89-20819
Multicolor surface photometry of powerful radio galaxies N89-20878
The physics of wave-particle interaction with applications to astrophysics N89-20888
The galactic large-scale far-infrared emission observed by IRAS: Implications for the morphology, physical conditions, and energetics of dust in the interstellar medium N89-20914
Measurement of the cosmic ray iron spectrum above 60 GeV/n and design and calibration of a large isotopic compositional experiment N89-20915
MASSACHUSETTS INST. OF TECH., CAMBRIDGE.
On-board automatic aid and advisory for pilots of control-impaired aircraft N89-20150
Growth of GaAs crystals from the melt in a partially confined configuration N89-20296
Dendritic growth and structure of undercooled nickel base alloys N89-20302
Electromagnetic, heat and fluid flow phenomena in levitated metal droplets both under earthbound and microgravity conditions N89-20315
Dynamic wall pressure measurements
[AD-A203551] N89-20427
Real-time part position sensing
[AD-A203580] N89-20439
Active and passive remote sensing of ice
[AD-A203943] N89-20543
Intelligence in scientific computing
[AD-A203815] N89-20679
Parallel algorithms for computer vision
[AD-A203947] N89-20681
An operating environment for the jellybean machine
[AD-A201042] N89-20682
Piecewise continuous algebraic surfaces in terms of B-splines
[PB89-109136] N89-20712
Grain boundary kinetics. Part 2: In-situ observation of the role of grain boundary dislocations in high-angle boundary migration
[DE89-006791] N89-20838
Using English for indexing and retrieving
[AD-A202227] N89-20866
MASSACHUSETTS INST. OF TECH., LOS ALAMOS, NM.
Heat and mass transport in fuel cell electrodes
[DE89-006378] N89-20548
MAX-PLANCK-INST. FUER AERONOMIE, KATLENBURG-LINDAU (GERMANY, F.R.).
RAPID: Research with Adaptive Particle Imaging Detectors N89-20168
MAX-PLANCK-INST. FUER PHYSIK UND ASTROPHYSIK, GARCHING (GERMANY, F.R.).
The electron drift instrument N89-20165
MAX-PLANCK-INST. FUER PHYSIK UND ASTROPHYSIK, MUNICH (GERMANY, F.R.).
Production of D, D* and Ds mesons in 200 GeV/c pi(-), K(-) and p-Si interactions
[MPI-PAE/EXP-EL-192] N89-20785
MECHANICAL TECHNOLOGY, INC., LATHAM, NY.
High speed balancing applied to the T700 engine
[NASA-CR-180899] N89-20472
MICHIGAN STATE UNIV., EAST LANSING.
Softening mechanisms and microstructural instabilities during high temperature low cycle fatigue of Ni, Ni3Al and their metal matrix composites
[DE89-007117] N89-20238
MICHIGAN UNIV., ANN ARBOR.
Diffusive burning of plane liquid and spray jets in a coflowing oxidizer stream N89-20216
Green's function formulation of plane crack problems for general anisotropic materials N89-20509
The Magnetically Insulated Inertial Confinement Fusion (MICF): A novel approach
[DE89-007473] N89-20811
MIDWEST RESEARCH INST., GOLDEN, CO.
Aerodynamic pressure and flow-visualization measurement from a rotating wind turbine blade
[DE89-000854] N89-20104

Design and testing of a dissociated methanol vehicle
[DE89-007051] N89-20483
Photovoltaic energy program summary. Volume 1: Overview, fiscal year 1988
[DE89-000855] N89-20553

MINNESOTA DEPT. OF TRANSPORTATION, SAINT PAUL.
Methods and materials for reducing crack reflectance
[PB89-114532] N89-20505

MINNESOTA UNIV., MINNEAPOLIS.
Aerodynamics of two-dimensional slotted bluff bodies
[DE89-007288] N89-20105
Dust shells around Miras and OH/IR stars
N89-20889

MISSOURI UNIV., ROLLA.
Modeling of hydrogen-air diffusion flame
[NASA-CR-184844] N89-20218
Containerless processing of glass forming melts in space N89-20307

MORTON THIOKOL, BRIGHAM CITY, UT.
Flight motor set 360L001 (STS-26R), volume 1
[NASA-CR-183576] N89-20196

MOUND LAB., MIAMISBURG, OH.
Laser ignition of energetic materials with a pulsed Nd:YAG laser
[DE89-006861] N89-20455

MULLARD SPACE SCIENCE LAB., DORKING (ENGLAND).
PEACE: A Plasma Electron And Current Experiment
N89-20167
Adaptive data compression system study
[SIL/CR/7129/6] N89-20639
Adaptive data compression system study, executive summary
[SIL/CR/7129/7] N89-20867

N

NATIONAAL INST. VOOR KERNFYSICA EN HOGE ENERGIEFYSICA, AMSTERDAM (NETHERLANDS).
Literature search on kickers and septa for the Amsterdam Pulse Stretcher (APS)
[LINO-158] N89-20791

NATIONAL ACADEMY OF SCIENCES - NATIONAL RESEARCH COUNCIL, WASHINGTON, DC.
Long-term solar-terrestrial observations
[NASA-CR-184695] N89-20905

NATIONAL AERONAUTICS AND SPACE ADMINISTRATION, WASHINGTON, DC.
Performance and test section flow characteristics of the National Full-Scale Aerodynamics Complex 40- by 80-foot wind tunnel
[NASA-TM-101065] N89-20088
Aeronautical engineering: A cumulative index to a continuing bibliography (supplement 235)
[NASA-SP-7037(235)] N89-20088
Aeronautical engineering: A continuing bibliography with indexes (supplement 237)
[NASA-SP-7037(237)] N89-20089
Aeronautical engineering: A continuing bibliography with indexes (supplement 238)
[NASA-SP-7037(238)] N89-20090
Aeronautical engineering: A continuing bibliography with indexes (supplement 236)
[NASA-SP-7037(236)] N89-20091
Microgravity Science and Applications Flight Programs, January - March 1987, selected papers, volume 1
[NASA-TM-4069-VOL-1] N89-20276
Microgravity Science and Applications Flight Programs, January - March 1987, selected papers, volume 2
[NASA-TM-4069-VOL-2] N89-20305

NATIONAL AERONAUTICS AND SPACE ADMINISTRATION. AMES RESEARCH CENTER, MOFFETT FIELD, CA.
Evaluation of VSAERO in prediction of aerodynamic characteristics of helicopter hub fairings
[NASA-TM-101048] N89-20098
Documentation of two- and three-dimensional hypersonic shock wave/turbulent boundary layer interaction flows
[NASA-TM-101075] N89-20100
Hub and blade structural loads measurements of an SA349/2 helicopter
[NASA-TM-101040] N89-20124
Heterogeneity in the growth hormone pituitary gland system of rats and humans: Implications to microgravity based research N89-20279
An airfoil pitch apparatus-modeling and control design
[NASA-TM-101076] N89-20386
Precision in the perception of direction of a moving pattern
[NASA-TM-101080] N89-20610
Queuing theory models for computer networks
[NASA-TM-101056] N89-20770

NATIONAL AERONAUTICS AND SPACE ADMINISTRATION. GODDARD SPACE FLIGHT CENTER, GREENBELT, MD.
Cluster: A fleet of four spacecraft to study plasma structures in three dimensions N89-20157
The magnetic field investigation on Cluster
N89-20158
The spherical probe electric field and wave experiment N89-20161
Ductile-regime turning of germanium and silicon
[NASA-TM-101231] N89-20322
An assessment model for atmospheric composition
[NASA-CP-3023] N89-20588
Verification of regional climates of GISS GCM. Part 2: Summer
[NASA-TM-100722] N89-20589
Forbidden coronal iron line emission in the Puppis A shock front: The effect of inhomogeneities
[NASA-TM-89284] N89-20875

NATIONAL AERONAUTICS AND SPACE ADMINISTRATION. LYNDON B. JOHNSON SPACE CENTER, HOUSTON, TX.
Kidney cell electrophoresis in space flight: Rationale, methods, results and flow cytometry applications
N89-20280
Biochemical assays on plasminogen activators and hormones from kidney sources N89-20287
Human cell culture in a space bioreactor N89-20288
Cellular effects of microgravity N89-20289
Antibody enhancement of free-flow electrophoresis
N89-20290
Use of artificial intelligence in supervisory control
N89-20694
Research and technology of the Lyndon Johnson Space Center
[NASA-TM-100473] N89-20918

NATIONAL AERONAUTICS AND SPACE ADMINISTRATION. LANGLEY RESEARCH CENTER, HAMPTON, VA.
Some low-speed flutter characteristics of simple low-aspect-ratio delta wing models
[NASA-TM-101547] N89-20094
Multigrid solution of the Navier-Stokes equations on triangular meshes
[NASA-CR-181786] N89-20095
Geometrical and structural properties of an Aeroelastic Research Wing (ARW-2)
[NASA-TM-4110] N89-20099
A cell-vertex multigrid method for the Navier-Stokes equations
[NASA-TM-101557] N89-20101
Microgravity science at Langley Research Center
N89-20298
Updated users' guide for TAWFIVE with multigrid
[NASA-TM-4109] N89-20409
Resolution requirements for numerical simulations of transition
[NASA-CR-181799] N89-20411
Angular radiation models for earth-atmosphere system. Volume 2: Longwave radiation
[NASA-RP-1184-VOL-2] N89-20587
Cumulative reports and publications through December 31, 1988
[NASA-CR-181784] N89-20619
Domain decomposition methods for systems of conservation laws: Spectral collocation approximations
[NASA-CR-181773] N89-20635
Numerical studies of identification in nonlinear distributed parameter systems
[NASA-CR-181771] N89-20636
Optimal feedback control infinite dimensional parabolic evolution systems: Approximation techniques
[NASA-CR-181772] N89-20637
Run-time scheduling and execution of loops on message passing machines
[NASA-CR-181785] N89-20638
Spectral methods for CFD
[NASA-CR-181803] N89-20718
Acoustic test of a model rotor and tail rotor: Results for the isolated rotors and combined configuration
[NASA-TM-101550] N89-20777
High intensity acoustic tests of a thermally stressed aluminum plate in TAFA
[NASA-TM-101552] N89-20778

NATIONAL AERONAUTICS AND SPACE ADMINISTRATION. LEWIS RESEARCH CENTER, CLEVELAND, OH.
Experimental investigation of transonic oscillating cascade aerodynamics
[NASA-TM-101993] N89-20133
Toward improved durability in advanced aircraft engine hot sections
[NASA-TM-4087] N89-20135
NASA HOST project overview N89-20136
Advanced high temperature instrument for hot section research applications N89-20137
Assessment, development, and application of combustor aerothermal models N89-20138
Review and assessment of the database and numerical modeling for turbine heat transfer N89-20139
Structural analysis methods development for turbine hot section components N89-20140
Fatigue life prediction modeling for turbine hot section materials N89-20142
Life modeling of thermal barrier coatings for aircraft gas turbine engines N89-20143
Views on the impact of HOST N89-20144
A definition study of the on-orbit assembly operations for the outboard photovoltaic power modules for Space Station Freedom
[NASA-TM-102006] N89-20171
Expendable launch vehicle transportation for the space station
[NASA-TM-101947] N89-20179
Advanced technology for future space propulsion systems
[NASA-TM-101951] N89-20192
The emittance of space radiator materials measured at elevated temperatures
[NASA-TM-101948] N89-20193
Free-piston Stirling technology for space power
[NASA-TM-101956] N89-20194
Identification of space shuttle main engine dynamics
[NASA-TM-101982] N89-20199
Finite element applications to explore the effects of partial bonding on metal matrix composite properties
[NASA-TM-101482] N89-20206
Failure analysis of a Stirling engine heat pipe
[NASA-TM-101418] N89-20227
Mechanical properties of modified low cobalt powder metallurgy Udimet 700 type alloys
[NASA-TM-101481] N89-20228
Crystallization kinetics of BaO-Al2O3-SiO2 glasses
[NASA-TM-101964] N89-20252
Design, development and applications of novel techniques for studying surface mechanical properties
[NASA-TM-101959] N89-20253
Isothermal dendritic growth: A low gravity experiment
N89-20299
Isothermal solidification in a binary alloy melt
N89-20300
Particle cloud mixing in microgravity
[NASA-TM-101484] N89-20321
Low frequency vibration isolation technology for microgravity space experiments
[NASA-TM-101448] N89-20324
The Mars climate for a photovoltaic system operation
[NASA-TM-101994] N89-20385
Control-volume based Navier-Stokes equation solver valid at all flow velocities
[NASA-TM-101488] N89-20407
Nondestructive evaluation of advanced ceramics
[NASA-TM-101489] N89-20490
Results of inphase axial-torsional fatigue experiments on 304 stainless steel
[NASA-TM-101464] N89-20514
Mars manned transportation vehicle
[NASA-TM-101487] N89-20545
Automating the multiprocessing environment
[NASA-TM-4103] N89-20641
A message passing kernel for the hypercluster parallel processing test bed
[NASA-TM-101952] N89-20684
Initial operating capability for the hypercluster parallel-processing test bed
[NASA-TM-101953] N89-20685
On the equivalence of Gaussian elimination and Gauss-Jordan reduction in solving linear equations
[NASA-TM-101466] N89-20710
Unsteady blade pressure measurements on a model counterrotation propeller
[NASA-TM-102002] N89-20779

NATIONAL AERONAUTICS AND SPACE ADMINISTRATION. MARSHALL SPACE FLIGHT CENTER, HUNTSVILLE, AL.
STS-27R OV-104 Orbiter TPS damage review team, volume 1
[NASA-TM-100355-VOL-1] N89-20178
Continuous flow electrophoresis system experiments on shuttle flights STS-6 and STS-7 N89-20277
Preparative electrophoresis for space N89-20278
Demixing kinetics of phase separated polymer solutions in microgravity N89-20281
Growth of solid solution single crystals N89-20297
The first products made in space: Monodisperse latex particles N89-20318
Improved capabilities of the Multispectral Atmospheric Mapping Sensor (MAMS)
[NASA-TM-100352] N89-20430

NATIONAL AEROSPACE LAB., AMSTERDAM (NETHERLANDS).
Environment-assisted aerospace fatigue problems in The Netherlands
[NLR-MP-88004-U] N89-20087
Observed Reynolds number effects on airfoils and high aspect ratio wings at transonic flow conditions
[NLR-MP-88006-U] N89-20102
The application of trajectory prediction algorithms for planning purposes in the Netherlands Air Traffic Control (ATC) system
[NLR-MP-87031-U] N89-20115
Future satellite navigation systems, with emphasis on NAVSTAR GPS
[NLR-MP-87034-U] N89-20116
Continuous-discrete filtering for systems with Markovian switching coefficients
[NLR-MP-87076-U] N89-20117
System simulation using the PROMISE simulation package
[NLR-MP-87081-U] N89-20118
Matching Power Spectra Density (PSD)-design load
[NLR-MP-87059-U] N89-20126
Electronics in civil aviation
[NLR-MP-87009-U] N89-20129
The data acquisition system for the Fokker 100 test aircraft
[NLR-MP-87047-U] N89-20130
Quench sensitivity of airframe aluminum alloys
[NLR-MP-88003-U] N89-20231
Data compression as a means to disseminate more Meteosat data over the existing channel
[NLR-MP-86063-U] N89-20369
Electromagnetic compatibility (EMC) test facilities
[NLR-MP-88010-U] N89-20370
A numerical method for the simulation of liquid-solid body dynamics
[NLR-MP-87030-U] N89-20420
Translational and rotational dynamics of rigid spacecraft-based manipulators
[NLR-TR-87014-U] N89-20474
Bulging cracks in pressurized fuselages: A numerical study
[NLR-MP-87058-U] N89-20519
Analysis of crack opening behavior by application of a discretized strip yield model
[NLR-MP-87065-U] N89-20520
Current status of flight simulation fatigue crack growth concepts
[NLR-MP-88001-U] N89-20521
Fracture control guidelines for stress corrosion
[NLR-MP-88007-U] N89-20522
Prediction of low and high crack growth rates under constant and variable amplitude loading
[NLR-MP-88012-U] N89-20523
A systematic worldwide landcover of satellite mosaics
[NLR-MP-87062-U] N89-20540
Land use inventory using LANDSAT Thematic Mapper imagery to study environmental pollution
[NLR-MP-87063-U] N89-20541
Twelve year overview of cloudfree LANDSAT imagery of The Netherlands
[NLR-MP-87072-U] N89-20542
NEN 6096, design resolution for small wind turbines
[NLR-MP-88005-U] N89-20551
WISPER: Introducing variable-amplitude loading in wind turbine design
[NLR-MP-88017-U] N89-20552
Tools for the development of information systems at NLR
[NLR-MP-87079-U] N89-20652
NEXT 2.0, an expert system shell for engineering applications
[NLR-MP-88015-U] N89-20653
Bordered equations in continuation methods: An improved solution technique
[NLR-MP-87057-U] N89-20699

NATIONAL BUREAU OF STANDARDS, GAITHERSBURG, MD.
Dynamic thermophysical measurements in space
N89-20317

NATIONAL CENTER FOR ATMOSPHERIC RESEARCH, BOULDER, CO.
Position error calibration of a pressure survey aircraft using a trailing cone
[PB88-250733] N89-20092
Generation of CCM format history tapes from analyzed data for selected periods (RD2CFM version 01)
[PB89-124507] N89-20568
Report of the Documentation Advisory Committee
[PB89-124556] N89-20569
Report of the 2nd Workshop on the Community Climate Model
[PB88-250741] N89-20576
Experiences on a CRAY-2 (trade name) running UNICOS
[PB88-250725] N89-20620
Integrated analysis package for Mk-3 K-coronameter observations: A user's manual
[PB88-250717] N89-20904

NATIONAL GEOPHYSICAL DATA CENTER, BOULDER, CO.
Solar-geophysical data number 530, October 1988. Part 2: (Comprehensive reports). Data for April 1988 and miscellaneous
[PB89-130827] N89-20908
Solar-geophysical data number 530, October 1988. Part 1: (Prompt reports). Data for September, August 1988 and late data
[PB89-130835] N89-20909

NATIONAL INST. OF STANDARDS AND TECHNOLOGY, GAITHERSBURG, MD.
Research for electric energy systems
[PB89-132310] N89-20383
Energy related inventions program: A joint program of the Department of Energy and the National Institute of Standards and Technology
[PB89-141154] N89-20546
Performance evaluation and analytic modeling of shared-memory computers
[PB89-113542] N89-20621

NATIONAL LIBRARY OF MEDICINE, BETHESDA, MD.
Medical subject headings, tree structures, 1989
[PB89-100028] N89-20605

NATIONAL OCEAN SERVICE, ROCKVILLE, MD.
Potential of large format camera photography
[PB89-122485] N89-20433

NATIONAL OCEANIC AND ATMOSPHERIC ADMINISTRATION, BOULDER, CO.
NOAA (National Oceanic and Atmospheric Administration) X-band radar measurements in 3CPO (Cloud Chemistry Cloud Physics Organization)
[PB89-127823] N89-20562
SELSIS (the Space Environment Laboratory Solar Imaging System): Initial requirements
[PB89-113039] N89-20906

NATIONAL OCEANIC AND ATMOSPHERIC ADMINISTRATION, MIAMI, FL.
Current velocity and hydrographic observations in the southwestern North Atlantic Ocean: Subtropical Atlantic Climate Studies (SACS), 1987
[PB89-114011] N89-20598

NATIONAL OCEANIC AND ATMOSPHERIC ADMINISTRATION, SEATTLE, WA.
CTD/O2 measurements during 1986 as part of the Equatorial Pacific Ocean Climate Studies (EPOCS)
[PB89-102859] N89-20596
Beaufort Sea mesoscale circulation study: Preliminary results
[PB89-121693] N89-20597

NATIONAL OCEANIC AND ATMOSPHERIC ADMINISTRATION, SILVER SPRING, MD.
Hybrid single-particle Lagrangian integrated trajectories (HY-SPLIT): Model description
[PB89-127591] N89-20559

NATIONAL PHYSICAL LAB., TEDDINGTON (ENGLAND).
Evaluation of the RTP Pascal-MALPAS IL translator
[NPL-DITC-128/88] N89-20654
The evaluation of impulsive noise
[NPL-AC-111] N89-20780

NATIONAL TECHNICAL INFORMATION SERVICE, SPRINGFIELD, VA.
Supply and use of Japanese technical literature in the United States
[PB88-230842] N89-20862

NATIONAL TELECOMMUNICATIONS AND INFORMATION ADMINISTRATION, BOULDER, CO.
Suitability of ANSI standards for quantifying communication satellite system performance
[NASA-CR-182884] N89-20356

NATIONAL TELECOMMUNICATIONS AND INFORMATION ADMINISTRATION, WASHINGTON, DC.
SUM (Spectrum Use Measure) data base: A new measure of spectrum use
[PB89-108674] N89-20328

NATIONAL TRANSPORTATION SAFETY BOARD, WASHINGTON, DC.
Aircraft accident data, US general aviation, calendar year 1986
[PB89-121453] N89-20108
Aircraft accident reports: Brief format, US civil and foreign aviation, issue number 12 of 1986 accidents
[PB88-916902] N89-20109
Aircraft accident reports, brief format, US civil and foreign aviation, issue number 14 of 1986 accidents
[PB88-916904] N89-20110
Aircraft accident report: Continental Airlines, Inc., Flight 1713, McDonnell Douglas DC-9-14, N626TX, Stapleton International Airport, Denver, Colorado, November 15, 1987
[PB88-910411] N89-20112

NATIONAL WEATHER SERVICE, GARDEN CITY, NY.
Climatological Worksheet Program
[PB89-122527] N89-20579
Examination of NGM (Nested Grid Model) low level temperature
[PB89-122543] N89-20580
Relationship of wind shear, buoyancy and radar tops to severe weather, 1988
[PB89-122519] N89-20581
National Weather Service Philadelphia Forecast Office, 1987 NOAA (National Oceanic and Atmospheric Administration) weather radio survey and questionnaire
[PB89-111785] N89-20582

NATIONAL WEATHER SERVICE, KANSAS CITY, MO.
Utility of a geographic information system in modelling climatic suitability
[PB89-109516] N89-20578

NATIONAL WEATHER SERVICE, SALT LAKE CITY, UT.
Preliminary analysis of cloud-to-ground lightning in the vicinity of the Nevada test site
[PB89-128649] N89-20584
Watchdog Program
[PB89-122535] N89-20633

NATIONAL WEATHER SERVICE, SILVER SPRING, MD.
Objective assessment of 1984-85 VAS products as indices of thunderstorm and severe local storm potential
[PB89-107668] N89-20577

NAVAL CIVIL ENGINEERING LAB., PORT HUENEME, CA.
Pressure coefficients for basic tensioned-membrane structure forms
[AD-A203866] N89-20107

NAVAL OCEANOGRAPHY COMMAND DETACHMENT, ASHEVILLE, NC.
Summary of meteorological observations, surface (SMOS) for Norfolk, Virginia
[AD-A203644] N89-20594

NAVAL POSTGRADUATE SCHOOL, MONTEREY, CA.
Design of a three-axis stabilized orion satellite using an all-thruster attitude control system
[AD-A203953] N89-20191
Flow visualization of time-varying structural characteristics of dean vortices in a curved channel
[AD-A203875] N89-20429
Implementation of a language translator for the computer aided prototyping system
[AD-A203876] N89-20680
Pseudo-Bayesian stability of CSMA (Carrier Sense Multiple Access) and CSMA/CD (Collision Detection) local area networks
[AD-A203834] N89-20763
Bremsstrahlung radiation effects in rare earth permanent magnets
[DE89-006207] N89-20775

NAVAL RESEARCH LAB., WASHINGTON, DC.
Welded joint integrity analysis: Relative criticality of weld defect and remote deformation
[AD-A203756] N89-20246
Implementing recurrent back-propagation on the connection machine
[AD-A203796] N89-20381
Stimulated Raman scattering of intense laser radiation in a nuclear-disturbed space plasma
[AD-A200951] N89-20440
Achieving adequate beam quality for commercial laser fusion reactors
[DE89-007474] N89-20462
Fortran codes for computing the space-time correlations of turbulent flow in a channel
[AD-A203749] N89-20678

NAVAL SHIP RESEARCH AND DEVELOPMENT CENTER, BETHESDA, MD.
Instrumented impact testing of composite materials
[AD-A203842] N89-20210

NAVAL WEAPONS CENTER, CHINA LAKE, CA.
Analog automatic control loops in radar and EW (Electronic Warfare)
[AD-A203758] N89-20380

NEW MEXICO STATE UNIV., LAS CRUCES.
Consequences of nonclassical measurement for the algorithmic description of continuous dynamical systems
[NASA-CR-184851] N89-20640

NEW MEXICO UNIV., ALBUQUERQUE.
The chirped-pulse free-electron laser
[DE89-006792] N89-20460

NORFOLK STATE COLL., VA.
A (13)C NMR analysis of the effects of electron radiation on graphite/polyetherimide composites
[NASA-CR-182818] N89-20205

NORTH CAROLINA STATE UNIV., RALEIGH.
Determination of the impulse response of a viscoelastic beam using a fractional derivative constitutive model
N89-20501
NORTH CAROLINA UNIV., CHAPEL HILL.
Energy conversion processes based on molecular excited states
[DE89-007322] N89-20555
NORTHWESTERN UNIV., EVANSTON, IL.
Defect clustering and related properties of oxides
[DE89-006620] N89-20835
NOTRE DAME UNIV., IN.
Error control techniques for satellite and space communications
[NASA-CR-184825] N89-20357
NUCLEAR UTILITY SERVICES, INC., GAITHERSBURG, MD.
Light-Weight Radioisotope Heater Unit Final Safety Analysis Report (LWRHU FSAR). Volume 3: Nuclear risk analysis document
[DE89-005496] N89-20790

O

OAK RIDGE GASEOUS DIFFUSION PLANT, TN.
A dynamic flow-weighted pore size distribution test
[DE89-006191] N89-20260
OAK RIDGE NATIONAL LAB., TN.
Compositional effects on processing and properties of nickel aluminides
[DE89-005133] N89-20229
The influence of thickness and wavelength on the mechanical properties of a compositionally modulated ceramic thin film
[DE89-006033] N89-20258
Hardness of amorphous hard carbon films determined by the ultra-low load microindentation technique
[DE89-006129] N89-20259
Optical Johnson noise thermometry
[NASA-CR-184964] N89-20437
A camera stabilization technique for a teleoperated vehicle
[DE89-003923] N89-20476
Development of the HERMIES 3 mobile robot research testbed at Oak Ridge National Laboratory
[DE89-004797] N89-20479
Force-reflecting master-slave control and robotic control of a traction-drive differential pitch-yaw joint
[DE89-005107] N89-20480
Telerobotic manipulator developments for ground-based space research
[NASA-CR-184736] N89-20481
World modelling and multi-sensor integration for a mobile robot
[DE89-005124] N89-20482
Design of remote maintenance tooling and fixtures for the advanced servomanipulator remote maintenance demonstration
[DE89-003114] N89-20484
Eddy current inspection of ferromagnetic materials using pulsed magnetic saturation
[DE89-005339] N89-20493
Near threshold fatigue curve based on the dislocation shielding model of fracture
[DE88-011854] N89-20527
Parallel direct solution of sparse linear systems
[DE89-006030] N89-20666
A parallel decomposition algorithm for Staircase Linear Programs
[DE89-007883] N89-20674
Multiprogramming a distributed-memory multiprocessor
[DE89-007850] N89-20690
The effect of time constraints on scaled speed-up
[DE89-007877] N89-20691
Automatic learning by an autonomous mobile robot
[DE89-003120] N89-20702
Sensor capabilities for the HERMIES experimental robot
[DE89-003180] N89-20703
Increasing user-friendliness in AI systems
[DE89-005093] N89-20704
Gain selection for an independent joing MRAC (Model-Reference Adaptive Controller) for robotic manipulators
[DE89-005110] N89-20705
A concurrent approach to model based motion detection
[DE89-007853] N89-20708
Parabolic systems with nonlinear competitive interactions
[DE89-007814] N89-20756
Parallel direct solution of sparse linear systems
[DE89-007855] N89-20757
A fast algorithm for reordering sparse matrices for parallel factorization
[DE89-007873] N89-20758
Two dimensional maps generated by competitive systems
[DE89-007878] N89-20759
Development of a remotely maintainable radio-frequency module for the Compact Ignition Tokamak
[DE89-004913] N89-20805
Transport modeling of ECH and neutral-beam-heated plasmas in the advanced toroidal facility
[DE89-006131] N89-20809
Microstructural characterization of alpha-Al2O3 implanted with iron
[DE89-006037] N89-20817
Irradiation as a tool for studying solid state amorphization phenomena
[DE89-006034] N89-20823
OAK RIDGE Y-12 PLANT, TN.
Solubility of hydrogen, deuterium and tritium in palladium metal
[DE89-005304] N89-20225
OFFICE NATIONAL D'ETUDES ET DE RECHERCHES AEROSPATIALES, PARIS (FRANCE).
La Recherche Aerospatiale, bimonthly bulletin, number 1988-2, 243/January-February
[ESA-TT-1134] N89-20417
OFFICE OF TECHNOLOGY ASSESSMENT, WASHINGTON, DC.
Report on federal information dissemination: Responses to decision analysis framework for GPO (Government Printing Office) strategic alternatives
[PB89-114649] N89-20864
OHIO STATE UNIV., COLUMBUS.
Thermal-mechanical behavior of thin films and laminates N89-20203
Electromagnetic properties of ice coated surfaces
[NASA-CR-184780] N89-20355
The ogive as a RCS compact range standard
[NASA-CR-184832] N89-20358
Improved computer simulation of the TCAS 3 circular array mounted on an aircraft
[NASA-CR-184907] N89-20363
Analysis of modified SMI method for adaptive array weight control
[NASA-CR-184904] N89-20364
Investigations of ultrasonic wave interactions at imperfect boundaries separating anisotropic materials
[DE89-007089] N89-20781
Geometrical optics design of a compact range Gregorian subreflector system by the principle of the central ray
[NASA-CR-184810] N89-20795
OKLAHOMA UNIV., NORMAN.
A first scramjet study
[NASA-CR-184965] N89-20146
OLD DOMINION UNIV., NORFOLK, VA.
Viscous shock layer analysis of hypersonic flows over long slender vehicles N89-20097

P

PACIFIC NORTHWEST LABS., RICHLAND, WA.
Assessment of high-temperature battery systems
[DE89-007554] N89-20399
The causes and consequences of global climate change
[DE89-004355] N89-20564
Aircraft operations and airborne measurement of perfluorotrimethylcyclohexane (PTCH) during ANATEX
[DE89-006934] N89-20566
Observed and modeled terrain-induced shear in tracer trajectories
[DE89-006938] N89-20590
High pressure Raman spectroscopy of TiO2 thin films
[DE89-006937] N89-20839
PENNSYLVANIA STATE UNIV., UNIVERSITY PARK.
Thermal stability of jet fuel
[DE89-006754] N89-20273
PENNSYLVANIA UNIV., PHILADELPHIA.
Environmental effects on the time dependent failure of non-oxide ceramics
[AD-A202391] N89-20250
A quantitative study of pattern formation in dendritic crystal growth from supersaturated solution N89-20818
PITTSBURGH UNIV., PA.
New models to assess behavioral and physiological performance of animals during inhalation exposures
[PB89-128946] N89-20601
PLANNING RESEARCH CORP., HAMPTON, VA.
On the relationship between matched filter theory as applied to gust loads and phased design loads analysis
[NASA-CR-181802] N89-20125
PRATT AND WHITNEY AIRCRAFT, EAST HARTFORD, CT.
Structural Tailoring of Advanced Turboprops (STAT) programmer's manual
[NASA-CR-182164] N89-20132
Fatigue life prediction modeling for turbine hot section materials N89-20142
PRINCETON UNIV., NJ.
Droplet combustion at reduced gravity N89-20313
Digital signal processing
[AD-A203744] N89-20403
PURDUE UNIV., WEST LAFAYETTE, IN.
Modal cost analysis of flexible structures: Modeling flexible structures for control design N89-20148
Diagnostics for intelligent control of MPD engines
[AD-A203640] N89-20530
Parallel algorithms for PDE solvers
[AD-A199625] N89-20630

R

RADIAN CORP., RESEARCH TRIANGLE PARK, NC.
National Air Toxics Information Clearinghouse: Ongoing research and regulatory development projects, July 1988
[PB89-103428] N89-20558
RENSSELAER POLYTECHNIC INST., TROY, NY.
Fluoride glass: Crystallization, surface tension
N89-20306
RESEARCH INST. OF NATIONAL DEFENCE, LINKOEPING (SWEDEN).
Digital radio link: Multipath fading on a 7 GHz line-of-sight link
[FOA-C-30428-3.3] N89-20365
Digital radio link: Multipath propagation on a microwave line-of-sight path
[FOA-C-30430-3.3] N89-20366
SAR processing on the array processor NMX-432
[FOA-C-30503-3.3] N89-20367
Activities report of the Division of Information Systems
[FOA-C-30499-3.3] N89-20919
RICE UNIV., HOUSTON, TX.
Hydrodynamic effects on cell growth in agitated microcarrier bioreactors N89-20284
An expert system based intelligent control scheme for space bioreactors N89-20285
Shear stress induced stimulation of mammalian cell metabolism N89-20286
Nonnormal accelerations due to yielding in a primary structure
[PB89-131437] N89-20513
ROCHESTER UNIV., NY.
Diffraction theory for polygonal apertures
[AD-A203778] N89-20802
ROCKWELL INTERNATIONAL CORP., COLUMBUS, OH.
Power efficient hydraulic systems. Volume 1: Study phase
[AD-A203899] N89-20127
Power efficient hydraulic systems. Volume 2: Hardware demonstration phase
[AD-A203900] N89-20128
ROCKY RESEARCH CORP., BOULDER CITY, NV.
Feasibility of a complex compound heat pump
[PB89-115273] N89-20405
ROGERS AND ASSOCIATES ENGINEERING CORP., GAINESVILLE, FL.
Space shuttle propulsion estimation development verification
[NASA-CR-183582] N89-20195
Space shuttle propulsion estimation development verification, volume 1
[NASA-CR-183581] N89-20197
ROLLS-ROYCE LTD., DERBY (ENGLAND).
Microstructural influence on low cycle fatigue strength of IMI550
[PNR90500] N89-20226
ROYAL INST. OF TECH., STOCKHOLM (SWEDEN).
Measurement of quasi-static and low frequency electric fields on the Viking satellite
[TRITA-EPP-87-02] N89-20189
A numerical model of ionospheric convection derived from field-aligned currents and the corresponding conductivity
[TRITA-EPP-88-03] N89-20571
Astrophysics in a nutshell: From the telescope to the Sputnik
[TRITA-EPP-88-04] N89-20897
Has the Universe an origin
[TRITA-EPP-88-07] N89-20898
Astrophysical significance of observations and experiments in the Earth's magnetosphere
[TRITA-EPP-88-09] N89-20899

ROYAL NETHERLANDS METEOROLOGICAL INST., THE HAGUE.
Processing and application of digital AVHRR-imagery for land and sea surfaces
[BCRS-88-08] N89-20536
ROYAL SIGNALS AND RADAR ESTABLISHMENT, MALVERN (ENGLAND).
The application of software fault tolerance to air traffic control: Study contract overview
[BR108567] N89-20114

S

SAN DIEGO STATE UNIV., CA.
Schema-based theories of problem solving
[AD-A203731] N89-20774
SANDIA NATIONAL LABS., ALBUQUERQUE, NM.
Aerodynamics of two-dimensional slotted bluff bodies
[DE89-007288] N89-20105
Trajectory scoring in rectangular coordinates using transponder-interrogator range and range rate data
[DE89-007005] N89-20119
Reconnection launcher projectile heating using the modified REGGIE code
[DE89-007294] N89-20172
Symbols for communication circuit design and documentation
[DE88-013002] N89-20372
Image-projection ion-beam lithography
[DE89-005773] N89-20390
Screening study of lithiated catholyte mixes for a long-life Li(Si)/FeS2 thermal battery
[DE89-006857] N89-20393
Mechanisms for the operation of a laser-triggered vacuum switch
[DE89-007059] N89-20394
Glossary of testing terminology for rechargeable batteries
[DE89-007061] N89-20395
Effect of surface stress on stress corrosion of silicate glass
[DE89-004584] N89-20529
Dendritic web silicon photovoltaic cell research
[DE89-007289] N89-20554
Eps'88: Combining the best features of von Neumann and dataflow computing
[DE89-007291] N89-20627
Combining segmentation and tracking for the classification of moving objects in video scenes
[DE89-007000] N89-20668
Auger electron and X-ray photoelectron data processing for the personal computer
[DE89-007292] N89-20670
An algorithm for automated quadrilateral mesh generation for planar regions
[DE89-007299] N89-20671
A structural analysis algorithm for massively parallel computers
[DE89-005055] N89-20686
Integrating multiple views into a single representation of a range imaged object
[DE89-005921] N89-20707
Quantization analysis of the real-time SAR digital image formation processor
[DE89-007533] N89-20754
Carrier density and excitation energy dependent GAMMA-X photoluminescence of Type-II GaAs/AlAs superlattices
[DE89-002988] N89-20832
Progress in linear optics, non-linear optics and surface alignment of liquid crystals
[DE89-006507] N89-20834
SATELLITES INTERNATIONAL LTD., NEWBURY (ENGLAND).
Adaptive data compression system study
[SIL/CR/7129/6] N89-20639
Adaptive data compression system study, executive summary
[SIL/CR/7129/7] N89-20867
SATER (BERNARD L.), OLMSTED FALLS, OH.
Edge illuminated ventical multijunction
[DE89-006246] N89-20547
SCIENCE AND TECHNOLOGY CORP., HAMPTON, VA.
The investigation of advanced remote sensing, radiative transfer and inversion techniques for the measurement of atmospheric constituents
[NASA-CR-172599] N89-20531
SCIENCE APPLICATIONS INTERNATIONAL CORP., MCLEAN, VA.
Stimulated Raman scattering of intense laser radiation in a nuclear-disturbed space plasma
[AD-A200951] N89-20440
SCIENCE RESEARCH COUNCIL, CHILTON (ENGLAND).
Adaptive data compression system study
[SIL/CR/7129/6] N89-20639
Adaptive data compression system study, executive summary
[SIL/CR/7129/7] N89-20867
SHEFFIELD UNIV. (ENGLAND).
The digital wave processing experiment N89-20164
Estimating nonlinear models
[RR-328] N89-20325
Testing for nonlinearity using a prediction error filter
[RR-332] N89-20371
On the structure and control of piecewise-linear systems
[RR-334] N89-20700
Spectral analysis of block structured nonlinear systems
[RR-329] N89-20726
The relationship between an orthogonal estimation algorithm and other least squares routines
[RR-331] N89-20729
Identification of MIMO nonlinear systems using a forward-regression orthogonal estimator
[RR-333] N89-20730
Nonlinear input-output maps for bilinear systems and stability
[RR-335] N89-20731
Realization and generalized frequency response for nonlinear input-output maps
[RR-336] N89-20732
Spectral analysis for nonlinear systems. Part 1: Parametric nonlinear spectral analysis
[RR-337] N89-20733
SIERRA NEVADA CORP., RENO.
Analysis of Doppler radar windshear data
[NASA-CR-181762] N89-20111
SKIDAWAY INST. OF OCEANOGRAPHY, SAVANNAH, GA.
Biological processes in the water column of the South Atlantic Bight: Zooplankton responses
[DE89-006828] N89-20600
SMITHSONIAN ASTROPHYSICAL OBSERVATORY, CAMBRIDGE, MA.
Support of Mark 3 optical interferometer
[AD-A203665] N89-20800
SOUTHAMPTON UNIV. (ENGLAND).
Comparison between predicted and measured rotational frequency response functions
[ISVR-TR-164] N89-20524
SOUTHERN METHODIST UNIV., DALLAS, TX.
Effects of environment on tunneling spectroscopy of gold films
[DE89-006040] N89-20844
SPARNEX, ANTWERP (BELGIUM).
Conceptual study of the signalling point of the master station for a TST/SS-TDMA system. Phase 1: Overview and selection of signalling points
[SX/SP-01] N89-20360
STANFORD LINEAR ACCELERATOR CENTER, CA.
Low emittance thermionic electron guns
[DE89-005944] N89-20793
STANFORD UNIV., CA.
The lambda point experiment in microgravity N89-20319
Inertia-controlling methods for quadratic programming
[DE89-006996] N89-20667
A parallel decomposition algorithm for Staircase Linear Programs
[DE89-007023] N89-20669
Research and development of HgZnTe as an infrared material
[NASA-CR-184840] N89-20820
A study of ferroelectricity in single crystal compounds of the type AFB5 and A3B2F12
[AD-A203610] N89-20849
Primordial nucleosynthesis and late decaying particles: A new model of nucleosynthesis N89-20894
STATE UNIV. OF NEW YORK, BUFFALO.
Solutions and stability of a closed-geodesic black hole model N89-20893
STATE UNIV. OF NEW YORK, STONY BROOK.
Carbon monoxide and disequilibrium dynamics in Saturn and Jupiter N89-20903
STOCKHOLM UNIV. (SWEDEN).
A PASCAL cross-assembler for the 6809 microprocessor
[USIP-88-05] N89-20648
On particle antiparticle mirror symmetry
[USIP-88-06] N89-20786
SUSSEX UNIV., BRIGHTON (ENGLAND).
General relativity, scalar fields and cosmic strings N89-20852
Cosmology and superstrings N89-20891
SVERDRUP TECHNOLOGY, INC., CLEVELAND, OH.
Noise generated by a flight weight, air flow control valve in a vertical takeoff and landing aircraft thrust vectoring system
[NASA-CR-182232] N89-20776
SWEDISH INST. OF SPACE PHYSICS, KIRUNA.
Scientific results from the Swedish Viking satellite
[IRF-SR-196] N89-20572
SYDNEY UNIV. (AUSTRALIA).
Compression tests of welded channel section columns
[PB88-246020] N89-20496
Elastic stability of lap-jointed cylindrical shells under axial compression
[PB88-245980] N89-20497
Non-symmetric bifurcation of geometrically non-linear elastic-plastic axisymmetric shells under combined loads including torsion
[PB89-102149] N89-20500
Elastic stability of cylindrical shells with circumferential welded joints under axial compression
[PB89-125082] N89-20502
Experiments on the buckling of thin-walled model silo structures
[PB89-125124] N89-20503

T

TAMPERE UNIV. OF TECHNOLOGY (FINLAND).
Zeolite/methanol: The adsorption heat pump
[DE88-756310] N89-20413
TECHNICAL RESEARCH CENTRE OF FINLAND, OULU.
Application of parameter adaptive approach to servo control of a hydraulic manipulator
[MA-51] N89-20473
TECHNISCHE UNIV., DELFT (NETHERLANDS).
Numerical study of nonlinear wave interactions in bubbly two-phase flow
[REPT-88-50] N89-20418
Differential equations of viscous fluid flow in general conditions
[REPT-88-57] N89-20419
Direct manipulation and other styles of man-machine interaction
[REPT-88-53] N89-20616
User interfaces and highly interactive systems: Survey of current research
[REPT-88-60] N89-20617
The Delft Ising system processor
[ISBN-9-09-001753-4] N89-20625
Incremental display of Constructive Solid Geometry (CSG) models using local updating
[REPT-88-51] N89-20650
Directions in reusing software
[REPT-88-58] N89-20651
Set theory, chapter 4
[REPT-88-47] N89-20722
Who's afraid of nonsymmetric matrices? A discussion of elementary iterative methods
[REPT-88-49] N89-20723
Iterative solution of large sparse system of linear equations
[REPT-88-52] N89-20724
High performance preconditioning
[REPT-88-54] N89-20725
Riemannian geometry on families of linear systems, the deterministic case
[REPT-88-62] N89-20726
An efficient method for solving free-boundary problems
[REPT-88-63] N89-20727
DETECT: Dependency tree evaluation and confidence test
[REPT-88-55] N89-20765
Asymptotic behavior of random discrete event systems
[REPT-88-56] N89-20766
TECHNISCHE UNIV., EINDHOVEN (NETHERLANDS).
Breadboard test-software and wrist joint modeling for Hermes robot arm
[ETN-89-94155] N89-20475
A numerical implementation of the Schapery model for nonlinear viscoelasticity
[ETN-89-93895] N89-20515
TECHNISCHE UNIV., MUNICH (GERMANY, F.R.).
Production of D, D* and Ds mesons in 200 GeV/c pi(-), K(-) and p-Si interactions
[MPI-PAE/EXP-EL-192] N89-20785
TEL-AVIV UNIV. (ISRAEL).
The Mars climate for a photovoltaic system operation
[NASA-TM-101994] N89-20385
TENNESSEE UNIV. SPACE INST., TULLAHOMA.
Casting And Solidification Technology (CAST): Directional solidification phenomena in a metal model at reduced gravity N89-20301
TEXAS A&M UNIV., COLLEGE STATION.
Computational fluid dynamics and aerothermodynamics
[NASA-CR-180079] N89-20415

Nonnormal accelerations due to yielding in a primary structure
[PB89-131437] N89-20513
TEXAS UNIV., ARLINGTON.
New vinylidene fluoride copolymers: Poly(vinyl acetate-co-Vinylidene fluoride)
[AD-A203939] N89-20270
TEXAS UNIV., AUSTIN.
Vectorial electron transfer on designed surfaces
[PB88-240031] N89-20211
Application of Newton's method to Lagrangian dynamical systems
[DE89-007024] N89-20751
Lithium depletion and rotation in main sequence stars N89-20886
TEXAS UNIV. AT DALLAS, RICHARDSON.
AFE ion mass spectrometer design study
[NASA-CR-184838] N89-20432
TEXTRON BELL HELICOPTER, FORT WORTH, TX.
Coupled rotor/fuselage dynamic analysis of the AH-1G helicopter and correlation with flight vibrations data
[NASA-CR-181723] N89-20512
TUFTS UNIV., MEDFORD, MA.
Very large array observations of the sun with related observations using the SMM (Solar Maximum Mission) satellite
[AD-A203873] N89-20910

U

UNISYS CORP., PAOLI, PA.
Integrating syntax, semantics, and discourse DARPA (Defense Advanced Research Projects Agency) natural language understanding program
[AD-A203747] N89-20677
UNIVERSIDADE FEDERAL FLUMINENSE, NITEROI (BRAZIL).
Meson production and nuclear fragmentation of nucleus in the atmosphere
[DE88-705019] N89-20917
UTAH STATE UNIV., LOGAN.
Ablation of materials in the low earth orbital environment N89-20187

V

VALENCIA UNIV. (SPAIN).
Production of D, D* and Ds mesons in 200 GeV/c pi(-), K(-) and p-Si interactions
[MPI-PAE/EXP-EL-192] N89-20785
VIRGINIA POLYTECHNIC INST. AND STATE UNIV., BLACKSBURG.
Robust stabilization of linear time-invariant uncertain systems via Lyapunov theory N89-20147
Prediction model for the onset of edge-effect delamination at holes in composite laminates N89-20202
Standard test case for a low speed, turbulent junction vortex flow
[PB89-110779] N89-20406
Navier-Stokes prediction of the three dimensional flow-field of jets in a crossflow using the finite element method N89-20408
VIRGINIA UNIV., CHARLOTTESVILLE.
Two designs for an orbital transfer vehicle: A comparison of two OTVs
[NASA-CR-184696] N89-20175
Two designs for an orbital transfer vehicle. Project Orion: A proposal for a manned orbital transfer vehicle for the 21st Century
[NASA-CR-184697] N89-20176
Two designs for an orbital transfer vehicle
[NASA-CR-184698] N89-20177
VON KARMAN INST. FOR FLUID DYNAMICS, RHODE-SAINT-GENESE (BELGIUM).
A calculation method for compressible three dimensional turbulent boundary layer flows
[VKI-TN-167] N89-20422
An explicit finite differences solver for the incompressible Reynolds averaged Navier-Stokes equations, optimized for the Alliant DSP 9000 computer
[VKI-TM-45] N89-20423

W

WAKE FOREST UNIV., WINSTON-SALEM, NC.
Symbolic inversion of control relationships in model-based expert systems
[NASA-CR-182857] N89-20631
WASHINGTON UNIV., SEATTLE.
Radiation, turbulence and microphysics in the stratiform regions of tropical cloud clusters N89-20585
Three-dimensional kinematics of rainbands in midlatitude cyclones N89-20586
Valiant's maximum algorithm with sequential memory accesses
[AD-A203713] N89-20676
WAYNE STATE UNIV., DETROIT, MI.
Effects of turbulence on rate of combustion of fuel sprays N89-20212
On the equivalence of Gaussian elimination and Gauss-Jordan reduction in solving linear equations
[NASA-TM-101466] N89-20710
WESTINGHOUSE ELECTRIC CORP., PHILADELPHIA, PA.
Development of tooling and techniques for remote field metallography
[DE89-005400] N89-20241
WESTINGHOUSE RESEARCH AND DEVELOPMENT CENTER, PITTSBURGH, PA.
Dendritic web silicon photovoltaic cell research
[DE89-007289] N89-20554
WISCONSIN UNIV., MADISON.
Collisional energy transfer in highly vibrationally excited polyatomic molecules
[AD-A203726] N89-20789
Studies of alternative-crystallization-phase nucleation
[DE89-007220] N89-20640
WYOMING UNIV., LARAMIE.
Static tensile and tensile creep testing of five ceramic fibers at elevated temperatures
[NASA-CR-184690] N89-20200

Typical Contract Number Index Listing

Listings in this index are arranged alphanumerically by contract number. Under each contract number the NASA accession numbers denoting documents that have been produced as a result of research done under that contract are arranged in ascending order. The NASA accession number denotes the number by which the citation is identified.

AF PROJ. 2303 ..... N89-20221
N89-20789
AF PROJ. 2304 ..... N89-20630
AF PROJ. 2305 ..... N89-20850
AF PROJ. 2307 ..... N89-20428
AF PROJ. 2308 ..... N89-20530
AF PROJ. 2311 ..... N89-20910
AF PROJ. 2313 ..... N89-20774
AF PROJ. 2700 ..... N89-20401
AF-AFOSR-0008-88 ..... N89-20774
AF-AFOSR-0009-85 ..... N89-20221
AF-AFOSR-0019-83 ..... N89-20910
AF-AFOSR-0023-88 ..... N89-20676
AF-AFOSR-0031-86 ..... N89-20850
AF-AFOSR-0033-26 ..... N89-20789
AF-AFOSR-0079-89 ..... N89-20716
AF-AFOSR-0168-86 ..... N89-20428
AF-AFOSR-0251-85 ..... N89-20715
AF-AFOSR-0278-86 ..... N89-20530
AF-AFOSR-0356-87 ..... N89-20636
AF-AFOSR-0385-84 ..... N89-20630
AF-AFOSR-0398-84 ..... N89-20637
ARPA ORDER 4224 ..... N89-20870
ARPA ORDER 5262 ..... N89-20677
ARPA ORDER 5351 ..... N89-20488
A81/K/041 ..... N89-20618
BCRS-PROJ. TE-1.7 ..... N89-20539
BCRS-PROJ. TO-3.1 ..... N89-20538
C0078E-4-101 ..... N89-20107
DA PROJ. 1C1-61102-A-71-A N89-20220
DA PROJ. 1L1-61101-A-91-A N89-20268
DA PROJ. 1L1-62209-AH-76 ..... N89-20472
DA PROJ. 3M2-63002-D-840 ..... N89-20323
DAAA15-87-D-0004 ..... N89-20220
DAAG29-82-K-0077 ..... N89-20760
DAAG29-84-K-0170 ..... N89-20250
DAAG29-85-K-0176 ..... N89-20464
DAAG29-85-K-0191 ..... N89-20403
DAAG29-85-K-0231 ..... N89-20593
DAAK20-85-C-0376 ..... N89-20401
DAAL03-86-K-0173 ..... N89-20802
DAAL03-87-C-0007 ..... N89-20402
DAAL03-88-K-0086 ..... N89-20715
N89-20762
DAAL04-86-K-0003 ..... N89-20266
DACA72-86-C-0004 ..... N89-20377
DACA76-84-C-0004 ..... N89-20120
DACA76-85-C-0003 ..... N89-20488
DACA76-85-C-0010 ..... N89-20681
DACA76-86-C-0019 ..... N89-20487
DAMD17-87-C-7012 ..... N89-20323
DARPA ORDER 5682 ..... N89-20487
DE-AC01-87NE-32134 ..... N89-20790
DE-AC01-88ER-30131 ..... N89-20446
DE-AC02-76CH-00016 ..... N89-20262
N89-20391
N89-20456
N89-20457
N89-20461
N89-20591
N89-20604
N89-20856
DE-AC02-83CH-10093 ..... N89-20104
N89-20483
N89-20553
DE-AC03-76SF-00098 ..... N89-20237
N89-20239
N89-20453
N89-20494
N89-20603
N89-20604
N89-20787
N89-20796
N89-20810
N89-20826
N89-20836
N89-20837
N89-20846
N89-20847
DE-AC03-76SF-00515 ..... N89-20793
DE-AC04-76DP-00613 ..... N89-20243
DE-AC04-76DP-00789 ..... N89-20105
N89-20119
N89-20172
N89-20372
N89-20390
N89-20393
N89-20394
N89-20395
N89-20529
N89-20554
N89-20556
N89-20627
N89-20668
N89-20670
N89-20671
N89-20686
N89-20707
N89-20754
N89-20832
N89-20834
DE-AC04-88DP-43495 ..... N89-20272
N89-20274
N89-20455
N89-20458
N89-20790
DE-AC05-84OR-21400 ..... N89-20229
N89-20258
N89-20259
N89-20437
N89-20476
N89-20479
N89-20480
N89-20481
N89-20482
N89-20484
N89-20493
N89-20527
N89-20666
N89-20669
N89-20674
N89-20690
N89-20691
N89-20702
N89-20703
N89-20704
N89-20705
N89-20708
N89-20756
N89-20757
N89-20758
N89-20759
N89-20805
N89-20809
N89-20817
N89-20823
N89-20844
DE-AC05-84OS-21400 ..... N89-20225
DE-AC05-84OT-21400 ..... N89-20260
DE-AC05-85ER-40216 ..... N89-20792
DE-AC06-76RL-01830 ..... N89-20399
N89-20564
N89-20566
N89-20590
N89-20839
DE-AC07-76ID-01570 ..... N89-20389
DE-AC08-88NV-10617 ..... N89-20375
N89-20841
DE-AC09-76SR-00001 ..... N89-20241
N89-20477
N89-20478
DE-AC22-88PC-88827 ..... N89-20273
DE-AI03-79DP-40092 ..... N89-20462
DE-AM06-70RL-02225 ..... N89-20839
DE-FG01-87CE-15328 ..... N89-20495
DE-FG01-87CE-15337 ..... N89-20547
DE-FG02-84ER-45055 ..... N89-20755
DE-FG02-84ER-45057 ..... N89-20781
DE-FG02-84ER-45097 ..... N89-20835
DE-FG02-85ER-45205 ..... N89-20238
DE-FG02-85ER-45215 ..... N89-20840
DE-FG02-86ER-13488 ..... N89-20858
DE-FG02-86ER-13631 ..... N89-20550
DE-FG02-86ER-45253 ..... N89-20234
DE-FG02-86ER-53214 ..... N89-20808
DE-FG02-87ER-13723 ..... N89-20811
DE-FG02-87ER-25047 ..... N89-20715
DE-FG02-87ER-45308 ..... N89-20235
DE-FG02-87ER-45310 ..... N89-20838
DE-FG02-88ER-13894 ..... N89-20848
DE-FG02-88ER-13905 ..... N89-20254
DE-FG02-88ER-45354 ..... N89-20236
DE-FG03-87ER-25028 ..... N89-20669
DE-FG03-87ER-25030 ..... N89-20667
DE-FG04-87ER-13788 ..... N89-20460
DE-FG05-80ET-53088 ..... N89-20751
DE-FG05-86ER-13633 ..... N89-20555
DE-FG05-86ER-45234 ..... N89-20822
DE-FG05-86ER-45266 ..... N89-20825
DE-FG09-85ER-60354 ..... N89-20800
DE-FG22-85PC-80503 ..... N89-20219
DNA PROJ. N99-QMXA N89-20426
DNA001-83-C-0182 ..... N89-20426
DNA001-85-C-0183 ..... N89-20851
DTFH61-86-C-00118 ..... N89-20471
DTMA91-86-C-80117 ..... N89-20504
EPA-68-02-4247 ..... N89-20560
EPA-68-02-4330 ..... N89-20558
ESA-6141/84-D N89-20389
ESA-7087/87-NL-PP(SC) N89-20639
N89-20867
ESPRIT PROJ. 432 ..... N89-20662
ESTEC-6101/84-NL-GM N89-20359
ESTEC-7027/87-NL-JG(SC) N89-20380
ESTEC-7170/87-NL-PR N89-20185
ESTEC-7512/87-NL-PH N89-20188
FMV-FFL-82250-85-273-25-001 ..... N89-20516
F04611-83-C-0046 ..... N89-20223
F08606-87-C-0017 ..... N89-20575
F19628-85-K-0052 ..... N89-20382
F30601-81-C-0256 ..... N89-20629
F30602-81-C-0256 ..... N89-20870
F33615-85-D-0514 ..... N89-20813
F33615-86-C-5064 ..... N89-20264
F33615-87-C-0541 ..... N89-20606
F33615-87-C-2790 ..... N89-20222
F49620-85-C-0013 ..... N89-20499
F49620-86-C-0111 ..... N89-20636
N89-20637
GRI-5082-260-0758 ..... N89-20211
GRI-5086-232-1368 ..... N89-20217
GRI-5086-234-1290 ..... N89-20488
GRI-5086-260-1251 ..... N89-20405
GRI-5086-294-1430 ..... N89-20544
JPL-957352 ..... N89-20336
MDA903-84-C-0031 ..... N89-20675
MIPR-109-86 ..... N89-20215
NAGW-996 ..... N89-20587
NAGW-1340 ..... N89-20806
NAGW-1592 ..... N89-20640
NAG1-163 ..... N89-20648
NAG1-441 ..... N89-20447
NAG1-517 ..... N89-20636
N89-20637
NAG1-613 ..... N89-20717
NAG1-623 ..... N89-20327
N89-20470

NAG1-851 ..... N89-20820
NAG1-861 ..... N89-20218
NAG1-886 ..... N89-20146
NAG2-516 ..... N89-20248
NAG3-536 ..... N89-20364
NAG3-656 ..... N89-20133
NAG3-727 ..... N89-20320
NAG3-803 ..... N89-20134
NAG5-557 ..... N89-20357
NAG5-1044 ..... N89-20692
NAG5-1057 ..... N89-20251
NAG9-192 ..... N89-20415
NAG9-207 ..... N89-20286
NAG10-0045 ..... N89-20631
NASA ORDER A-39603-C N89-20200
NASA ORDER C-99066-G N89-20710
NASW-3165 ..... N89-20615
NASW-3737 ..... N89-20198
NASW-4065 ..... N89-20871
NASW-4292 ..... N89-20602
NASW-4324 ..... N89-20615
NAS1-15198 ..... N89-20531
NAS1-17496 ..... N89-20512
NAS1-17977 ..... N89-20093
NAS1-18000 ..... N89-20125
NAS1-18107 ..... N89-20095
N89-20411
N89-20619
N89-20632
N89-20636
N89-20637
NAS1-18598 ..... N89-20111
NAS1-18605 ..... N89-20095
N89-20412
N89-20619
N89-20635
N89-20636
N89-20637
N89-20638
N89-20698
N89-20716
N89-20718
NAS3-23929 ..... N89-20472
NAS3-23941 ..... N89-20132
NAS3-24633 ..... N89-20472
NAS3-24644 ..... N89-20295
NAS3-25266 ..... N89-20776
NAS5-28756 ..... N89-20533
NAS7-918 ..... N89-20113
N89-20151
N89-20152
N89-20362
N89-20387
N89-20549
N89-20642
N89-20643
N89-20644
N89-20821
NAS8-30490 ..... N89-20196
NAS8-32945 ..... N89-20294
NAS8-32950 ..... N89-20282
NAS8-32951 ..... N89-20318
NAS8-36152 ..... N89-20195
N89-20197
NAS8-36604 ..... N89-20296
NAS8-36611 ..... N89-20292
NAS9-15583 ..... N89-20280
NAS9-16389 ..... N89-20280
NAS9-16550 ..... N89-20280
NAS9-17403 ..... N89-20283
N89-20284
N89-20286
NAS9-17440 ..... N89-20280
NAS9-17468 ..... N89-20271
NAS9-17560 ..... N89-20683
NAS9-17779 ..... N89-20181
NAS9-17854 ..... N89-20182
NA87AA-D-CP041 ..... N89-20905
NCC1-115 ..... N89-20205
NCC1-119 ..... N89-20432
NCC2-452 ..... N89-20100
NCC3-46 ..... N89-20489
NGT-21-002-080 ..... N89-20121
N89-20122
N89-20123
N89-20173
N89-20174
N89-20175
N89-20176
N89-20177
N89-20180
N89-20183
N89-20184
NIH-HL-17437 ..... N89-20286
NIH-HL-18672 ..... N89-20286
NIST-NANB-4001 ..... N89-20601
NIVR-1823/01702-N N89-20520
NIVR-02306N N89-20420
NIVR-02506N N89-20474
NIVR-06404N N89-20519
NOAA-NA86AA-D-SG-89 ..... N89-20712
NSF ATM-87-09659 ..... N89-20092
N89-20568
N89-20569
N89-20576
N89-20620
N89-20904
NSF CCR-86-02071 ..... N89-20715
NSF CCR-87-02403 ..... N89-20715
NSF DCR-86-04199 ..... N89-20488
NSF ECE-86-07591 ..... N89-20513
NSF MCS-85-04316 ..... N89-20636
N89-20637
NSG-1471 ..... N89-20646
NSG-1498 ..... N89-20363
NSG-1613 ..... N89-20358
N89-20795
NSG-3913 ..... N89-20355
NWO-125-20-04 ..... N89-20688
N00014-80-C-0622 ..... N89-20682
N00014-83-K-0107 ..... N89-20247
N00014-83-K-0258 ..... N89-20543
N00014-85-C-0012 ..... N89-20677
N00014-85-K-0124 ..... N89-20439
N89-20682
N89-20866
N89-20400
N00014-85-K-0159 ..... N89-20813
N00014-85-K-0598 ..... N89-20269
N00014-86-C-0313 ..... N89-20800
N00014-86-C-2105 ..... N89-20155
N00014-86-C-2322 ..... N89-20908
N00014-86-F-0049 ..... N89-20909
N89-20406
N00014-86-K-0036 ..... N89-20679
N00014-86-K-0180 ..... N89-20427
N00014-86-K-0183 ..... N89-20676
N00014-86-K-0264 ..... N89-20638
N00014-86-K-0310 ..... N89-20784
N00014-86-K-0366 ..... N89-20799
N89-20812
N00014-86-K-0544 ..... N89-20595
N00014-86-K-0679 ..... N89-20716
N00014-86-K-0685 ..... N89-20439
N00014-86-K-0769 ..... N89-20270
N00014-86-K-0772 ..... N89-20266
N89-20267
N00014-87-C-0098 ..... N89-20265
N00014-87-C-0784 ..... N89-20378
N00014-87-K-0124 ..... N89-20849
N00014-87-K-0827 ..... N89-20717
N62269-85-C-0259 ..... N89-20127
N89-20128
PHS-OH-01929 ..... N89-20607
SERC-GR/D/30587 ..... N89-20730
SERC-GR/D/75809 ..... N89-20733
STW-CWI55.092 ..... N89-20741
W-31-109-ENG-38 ..... N89-20214
N89-20230
N89-20435
N89-20563
N89-20752
N89-20815
N89-20816
N89-20833
W-7405-ENG-36 ..... N89-20232
N89-20233
N89-20257
N89-20373
N89-20392
N89-20397
N89-20442
N89-20443
N89-20445
N89-20448
N89-20459
N89-20485
N89-20528
N89-20548
N89-20574
N89-20665
N89-20689
N89-20797
N89-20798
N89-20806
N89-20807
N89-20824
N89-20911
W-7405-ENG-48 ..... N89-20242
N89-20261
N89-20326
N89-20374
N89-20398
N89-20414
N89-20425
N89-20436
N89-20438
N89-20441
N89-20444
N89-20449
N89-20450
N89-20451
N89-20452
N89-20454
N89-20565
N89-20626
N89-20628
N89-20647
N89-20673
N89-20706
N89-20721
N89-20775
N89-20794
N89-20833
N89-20845
W-7405-ENG-82 ..... N89-20463
N89-20782
N89-20783
ZWO-10-70-10 ..... N89-20736
055-71-11-19-01 ..... N89-20821
505-33-62 ..... N89-20228
505-60-01-01 ..... N89-20101
N89-20409
505-61-28 ..... N89-20086
505-61-51 ..... N89-20098
N89-20124
N89-20386
505-62-OK N89-20472
505-62-21 ..... N89-20407
N89-20641
N89-20684
N89-20685
N89-20710
505-62-61 ..... N89-20133
505-62-71 ..... N89-20776
505-63-1B N89-20135
N89-20514
505-63-11 ..... N89-20206
505-63-21-02 ..... N89-20094
N89-20099
505-63-21-04 ..... N89-20125
505-63-51 ..... N89-20777
505-63-51-01 ..... N89-20512
505-66-21-02 ..... N89-20683
505-67-41-51 ..... N89-20111
505-80-11 ..... N89-20100
505-90-21-01 ..... N89-20095
N89-20411
N89-20412
N89-20619
N89-20632
N89-20635
N89-20636
N89-20637
N89-20638
N89-20698
N89-20716
N89-20718
506-41-11 ..... N89-20385
506-43-11 ..... N89-20253
506-49-21 ..... N89-20545
506-80-31-02 ..... N89-20778
510-01-0A N89-20252
535-03-01 ..... N89-20779
535-05-01 ..... N89-20134
535-07-01 ..... N89-20490
582-01-11 ..... N89-20199
586-01-11 ..... N89-20193
N89-20194
N89-20227
591-41-41 ..... N89-20192
664-45-30-01 ..... N89-20587
694-00-01 ..... N89-20321
694-03-03 ..... N89-20324
992-15-00-00-72 ..... N89-20918

Typical Report Number Index Listing

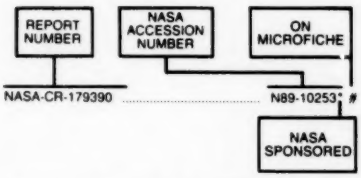

Listings in this index are arranged alphanumerically by report number. The NASA accession number denotes the number by which the citation is identified. An asterisk (*) indicates that the item is a NASA report. A pound sign (#) indicates that the item is available on microfiche.

A-88300 ..... N89-20124* #
A-88320 ..... N89-20098* #
A-89013 ..... N89-20770* #
A-89028 ..... N89-20086* #
A-89048 ..... N89-20100* #
A-89051 ..... N89-20386* #
A-89062 ..... N89-20610* #

A/V-97457-2 ..... N89-20427 #

AAE-241-VOL-1 ..... N89-20121* #
AAE-241-VOL-2 ..... N89-20122* #
AAE-241-VOL-3 ..... N89-20123* #

AAMRL-TR-88-017 ..... N89-20613 #
AAMRL-TR-88-035 ..... N89-20606 #

AD-A198766 ..... N89-20498 #
AD-A199028 ..... N89-20499 #
AD-A199625 ..... N89-20630 #
AD-A199794 ..... N89-20557 #
AD-A200432 ..... N89-20614 #
AD-A200923 ..... N89-20154 #
AD-A200951 ..... N89-20440 #
AD-A201042 ..... N89-20682 #
AD-A201078 ..... N89-20715 #
AD-A201079 ..... N89-20215* #
AD-A201278 ..... N89-20606 #
AD-A201354 ..... N89-20323 #
AD-A202227 ..... N89-20866 #
AD-A202391 ..... N89-20250 #
AD-A203406 ..... N89-20486 #
AD-A203419 ..... N89-20575 #
AD-A203421 ..... N89-20400 #
AD-A203427 ..... N89-20593 #
AD-A203446 ..... N89-20145 #
AD-A203452 ..... N89-20609 #
AD-A203477 ..... N89-20264 #
AD-A203489 ..... N89-20812 #
AD-A203491 ..... N89-20784 #
AD-A203494 ..... N89-20799 #
AD-A203496 ..... N89-20170 #
AD-A203513 ..... N89-20426 #
AD-A203519 ..... N89-20244 #
AD-A203531 ..... N89-20464 #
AD-A203536 ..... N89-20220 #
AD-A203551 ..... N89-20427 #
AD-A203561 ..... N89-20376 #
AD-A203580 ..... N89-20439 #
AD-A203594 ..... N89-20265 #
AD-A203610 ..... N89-20849 #
AD-A203616 ..... N89-20675 #
AD-A203619 ..... N89-20760 #
AD-A203625 ..... N89-20245 #
AD-A203629 ..... N89-20401 #
AD-A203631 ..... N89-20266 #
AD-A203632 ..... N89-20267 #
AD-A203635 ..... N89-20402 #
AD-A203639 ..... N89-20650 #
AD-A203640 ..... N89-20530 #
AD-A203641 ..... N89-20221 #

AD-A203644 ..... N89-20594 #
AD-A203665 ..... N89-20800 #
AD-A203667 ..... N89-20275 #
AD-A203671 ..... N89-20209 #
AD-A203674 ..... N89-20869 #
AD-A203688 ..... N89-20377 #
AD-A203689 ..... N89-20487 #
AD-A203698 ..... N89-20378 #
AD-A203699 ..... N89-20851 #
AD-A203702 ..... N89-20761 #
AD-A203703 ..... N89-20801 #
AD-A203711 ..... N89-20613 #
AD-A203712 ..... N89-20120 #
AD-A203713 ..... N89-20676 #
AD-A203728 ..... N89-20789 #
AD-A203731 ..... N89-20774 #
AD-A203733 ..... N89-20428 #
AD-A203741 ..... N89-20268 #
AD-A203744 ..... N89-20403 #
AD-A203747 ..... N89-20677 #
AD-A203748 ..... N89-20379 #
AD-A203749 ..... N89-20678 #
AD-A203752 ..... N89-20404 #
AD-A203756 ..... N89-20246 #
AD-A203758 ..... N89-20380 #
AD-A203778 ..... N89-20802 #
AD-A203780 ..... N89-20629 #
AD-A203785 ..... N89-20106 #
AD-A203791 ..... N89-20222 #
AD-A203796 ..... N89-20381 #
AD-A203801 ..... N89-20223 #
AD-A203805 ..... N89-20269 #
AD-A203807 ..... N89-20762 #
AD-A203811 ..... N89-20247 #
AD-A203815 ..... N89-20679 #
AD-A203830 ..... N89-20190 #
AD-A203834 ..... N89-20763 #
AD-A203842 ..... N89-20210 #
AD-A203843 ..... N89-20764 #
AD-A203845 ..... N89-20870 #
AD-A203847 ..... N89-20382 #
AD-A203851 ..... N89-20155 #
AD-A203866 ..... N89-20107 #
AD-A203873 ..... N89-20910 #
AD-A203875 ..... N89-20429 #
AD-A203876 ..... N89-20680 #
AD-A203899 ..... N89-20127 #
AD-A203900 ..... N89-20128 #
AD-A203939 ..... N89-20270 #
AD-A203943 ..... N89-20543 #
AD-A203944 ..... N89-20813 #
AD-A203946 ..... N89-20488 #
AD-A203947 ..... N89-20681 #
AD-A203949 ..... N89-20595 #
AD-A203953 ..... N89-20191 #

AD-E501060 ..... N89-20675 #
AD-E801748 ..... N89-20499 #
AD-E801843 ..... N89-20264 #
AD-E900883 ..... N89-20246 #
AD-E900883 ..... N89-20380 #
AD-E951202 ..... N89-20801 #
AD-E951251 ..... N89-20761 #

AESC-9316 ..... N89-20378 #

AFAL-TR-88-056 ..... N89-20223 #
AFAL-TR-88-115 ..... N89-20275 #

AFATL-TR-88-101 ..... N89-20499 #
AFATL-TR-88-143 ..... N89-20264 #
AFATL-TR-88-145 ..... N89-20851 #

AFESC/ESL-TR-88-55 ..... N89-20557 #

AFGL-TR-89-0001 ..... N89-20376 #

AFIT-TR-EN-88-1 ..... N89-20764 #

AFIT/GSO/MA/88D-1 ..... N89-20190 #

AFOSR-88-1136TR ..... N89-20630 #
AFOSR-89-0044TR ..... N89-20910 #
AFOSR-89-0053TR ..... N89-20850 #
AFOSR-89-0055TR ..... N89-20774 #
AFOSR-89-0056TR ..... N89-20789 #
AFOSR-89-0057TR ..... N89-20428 #
AFOSR-89-0060TR ..... N89-20530 #
AFOSR-89-0065TR ..... N89-20221 #

AFWAL-TR-88-2136 ..... N89-20222 #

AI-M-1032 ..... N89-20439 #
AI-M-1070 ..... N89-20682 #
AI-M-1094 ..... N89-20679 #
AI-M-1096 ..... N89-20866 #

AI/DS-TR-3139-02 ..... N89-20377 #

AIAA-88-0453 ..... N89-20321* #
AIAA-89-1144 ..... N89-20779* #
AIAA-89-1325 ..... N89-20094* #

AMSMI/TR-RD-AS-88-9 ..... N89-20761 #

AMSMI/TR-RD-RE-88-4 ..... N89-20801 #

ARO-18532.7-EL ..... N89-20760 #
ARO-21092.6-EG ..... N89-20215* #
ARO-21690.16-MS ..... N89-20250 #
ARO-22668.15-PH ..... N89-20464 #
ARO-22711.3-EL ..... N89-20403 #
ARO-22773.2-GS ..... N89-20593 #
ARO-24626.57-PH-U1R ..... N89-20802 #
ARO-24923.1-MA ..... N89-20715 #
ARO-24923.2-MA ..... N89-20762 #

AVSCOM-TR-88-C-007 ..... N89-20472* #
AVSCOM-TR-88-C-022 ..... N89-20514* #

B-14 ..... N89-20410 #

BBN-5723-VOL-2 ..... N89-20870 #
BBN-5901-VOL-1 ..... N89-20629 #

BCD-SSME-TR-87-2 ..... N89-20198* #

BCRS-87-12-VOL-A/B ..... N89-20534 #
BCRS-88-07 ..... N89-20537 #
BCRS-88-08 ..... N89-20538 #
BCRS-88-09 ..... N89-20539 #

BNL-41996 ..... N89-20456 #
BNL-41997 ..... N89-20457 #
BNL-42086 ..... N89-20856 #
BNL-42092 ..... N89-20391 #
BNL-42170-PT-2 ..... N89-20262 #
BNL-42192 ..... N89-20461 #
BNL-42203 ..... N89-20591 #

BR108567 ..... N89-20114 #

B8813493 ..... N89-20743 #
B8813498 ..... N89-20744 #
B8817045 ..... N89-20701 #
B8817046 ..... N89-20745 #
B8817047 ..... N89-20746 #
B8817050 ..... N89-20738 #
B8821057 ..... N89-20660 #
B8821058 ..... N89-20661 #
B8821059 ..... N89-20739 #
B8821060 ..... N89-20424 #
B8821061 ..... N89-20740 #
B8821065 ..... N89-20687 #
B8821067 ..... N89-20688 #
B8821068 ..... N89-20737 #
B8821070 ..... N89-20662 #
B8821071 ..... N89-20767 #
B8827436 ..... N89-20664 #
B8827437 ..... N89-20741 #
B8827440 ..... N89-20768 #
B8827442 ..... N89-20663 #
B8827443 ..... N89-20612 #
B8827728 ..... N89-20660 #
B8827730 ..... N89-20769 #
B8827732 ..... N89-20742 #

B8827733 ..... N89-20747 #
B8827852 ..... N89-20771 #

C-215 ..... N89-20467 #

CALSPAN-7170-7 ..... N89-20426 #

CBPF-MO-001/88 ..... N89-20853 #

CBPF-NF-004/88 ..... N89-20719 #
CBPF-NF-012/88 ..... N89-20854 #
CBPF-NF-032/88 ..... N89-20917 #

CESAR-88/62 ..... N89-20702 #
CESAR-89/01 ..... N89-20708 #

CGS-13 ..... N89-20433 #

CMR-88-12 ..... N89-20849 #

CMU-RI-TR-88-4 ..... N89-20488 #
CMU-RI-TR-88-10 ..... N89-20487 #

CONF-880272-3 ..... N89-20816 #
CONF-880408-45 ..... N89-20833 #
CONF-880651-1 ..... N89-20375 #
CONF-880693-5 ..... N89-20414 #
CONF-880713-22 ..... N89-20792 #
CONF-880870-2 ..... N89-20796 #
CONF-880887-30 ..... N89-20436 #
CONF-880894-3 ..... N89-20626 #
CONF-880901-16 ..... N89-20823 #
CONF-880974-2 ..... N89-20753 #
CONF-881002-45 ..... N89-20234 #
CONF-881031-61 ..... N89-20810 #
CONF-881061-13 ..... N89-20391 #
CONF-881103-34 ..... N89-20836 #
CONF-881103-36 ..... N89-20603 #
CONF-881155-28 ..... N89-20229 #
CONF-881155-38 ..... N89-20617 #
CONF-881155-39 ..... N89-20258 #
CONF-881155-43 ..... N89-20844 #
CONF-881244-5 ..... N89-20455 #
CONF-881244-6 ..... N89-20458 #
CONF-881249-3 ..... N89-20704 #
CONF-890102-14 ..... N89-20104 #
CONF-890133-4 ..... N89-20590 #
CONF-890133-5 ..... N89-20566 #
CONF-890142-2 ..... N89-20259 #
CONF-890142-3 ..... N89-20441 #
CONF-890145-1 ..... N89-20442 #
CONF-890145-2 ..... N89-20449 #
CONF-890145-5 ..... N89-20443 #
CONF-890145-9 ..... N89-20839 #
CONF-890145-11 ..... N89-20454 #
CONF-890145-12 ..... N89-20450 #
CONF-890145-13 ..... N89-20438 #
CONF-890145-14 ..... N89-20397 #
CONF-890154-2 ..... N89-20444 #
CONF-890160-1 ..... N89-20389 #
CONF-890165-1 ..... N89-20845 #
CONF-890166-1 ..... N89-20459 #
CONF-890168-1 ..... N89-20437* #
CONF-890219-1 ..... N89-20493 #
CONF-890247-2 ..... N89-20392 #
CONF-890255-1 ..... N89-20390 #
CONF-890302-1 ..... N89-20606 #
CONF-890302-4 ..... N89-20809 #
CONF-890304-2 ..... N89-20482 #
CONF-890304-9 ..... N89-20484 #
CONF-890304-10 ..... N89-20702 #
CONF-890304-11 ..... N89-20703 #
CONF-890304-12 ..... N89-20574 #
CONF-890304-14 ..... N89-20669 #
CONF-890304-15 ..... N89-20476 #
CONF-890304-18 ..... N89-20478 #
CONF-890304-19 ..... N89-20477 #
CONF-890304-22 ..... N89-20479 #
CONF-890304-26 ..... N89-20805 #
CONF-890304-30 ..... N89-20705 #
CONF-890304-31 ..... N89-20481* #
CONF-890304-32 ..... N89-20480 #
CONF-890310-1 ..... N89-20527 #
CONF-890310-2 ..... N89-20528 #
CONF-890310-4 ..... N89-20529 #
CONF-890312-1 ..... N89-20832 #
CONF-890314-1 ..... N89-20372 #
CONF-890324-1 ..... N89-20233 #
CONF-890324-2 ..... N89-20257 #
CONF-890324-4 ..... N89-20242 #
CONF-890343-1 ..... N89-20232 #
CONF-890344-1 ..... N89-20665 #
CONF-890355-1 ..... N89-20373 #
CONF-8610449 ..... N89-20868 #
CONF-8707124-SUPPL ..... N89-20607 #
CONF-8707208-1 ..... N89-20793 #
CONF-8709110-25 ..... N89-20452 #
CONF-8805132-13 ..... N89-20374 #
CONF-8805152-2 ..... N89-20230 #
CONF-8805252-1 ..... N89-20628 #
CONF-8806139-2 ..... N89-20261 #
CONF-8806258-5 ..... N89-20453 #
CONF-8807110-2 ..... N89-20260 #
CONF-8808137-SUMM ..... N89-20399 #
CONF-8808143-2 ..... N89-20846 #
CONF-8808146-12 ..... N89-20451 #
CONF-8808146-13 ..... N89-20775 #
CONF-8808146-14 ..... N89-20461 #
CONF-8808171 ..... N89-20398 #
CONF-8808186-1 ..... N89-20435 #
CONF-8808190-1 ..... N89-20752 #
CONF-8808191-1 ..... N89-20798 #
CONF-8809198-1 ..... N89-20214 #
CONF-8809281-1 ..... N89-20604 #
CONF-8809282-1 ..... N89-20565 #
CONF-8810202-6 ..... N89-20666 #
CONF-8810234-5 ..... N89-20425 #
CONF-8810255-2 ..... N89-20824 #
CONF-8810280-1 ..... N89-20721 #
CONF-8810280-2 ..... N89-20686 #
CONF-8810284-1 ..... N89-20448 #
CONF-8810288-1 ..... N89-20241 #
CONF-8810295-1 ..... N89-20834 #
CONF-8810296-1 ..... N89-20797 #
CONF-8810297-1 ..... N89-20666 #
CONF-8811110-2 ..... N89-20673 #
CONF-8811129-1 ..... N89-20815 #
CONF-8811140-1 ..... N89-20563 #
CONF-8811143-1 ..... N89-20564 #
CONF-8811162-1 ..... N89-20707 #

CONTRIB-1040 ..... N89-20597 #
CONTRIB-1063 ..... N89-20596 #

CRDEC-TR-018 ..... N89-20220 #

CS-8807 ..... N89-20655 #
CS-8808 ..... N89-20656 #
CS-8809-PT-2 ..... N89-20657 #
CS-8810 ..... N89-20658 #
CS-8811 ..... N89-20659 #
CS-8812 ..... N89-20734 #

CU-CS-398-88 ..... N89-20715 #
CU-CS-414-88 ..... N89-20762 #

CWI-AM-R8806 ..... N89-20738 #

CWI-CS-R8802 ..... N89-20660 #
CWI-CS-R8803 ..... N89-20661 #
CWI-CS-R8807 ..... N89-20687 #
CWI-CS-R8809 ..... N89-20688 #
CWI-CS-R8810 ..... N89-20737 #
CWI-CS-R8812 ..... N89-20662 #
CWI-CS-R8813 ..... N89-20767 #
CWI-CS-R8816 ..... N89-20768 #
CWI-CS-R8818 ..... N89-20663 #
CWI-CS-R8819 ..... N89-20612 #

CWI-MS-R8803 ..... N89-20769 #
CWI-MS-R8805 ..... N89-20742 #
CWI-MS-R8806 ..... N89-20747 #

CWI-NM-R8801 ..... N89-20739 #
CWI-NM-R8802 ..... N89-20740 #
CWI-NM-R8803 ..... N89-20424 #
CWI-NM-R8805 ..... N89-20664 #
CWI-NM-R8806 ..... N89-20741 #

CWI-OS-R8802 ..... N89-20743 #
CWI-OS-R8807 ..... N89-20744 #
CWI-OS-R8808 ..... N89-20860 #

CWI-PM-R8801 ..... N89-20701 #
CWI-PM-R8802 ..... N89-20745 #
CWI-PM-R8803 ..... N89-20746 #

DAITC/TR-88/009 ..... N89-20869 #

DCN-88-239-001-44-07 ..... N89-20558 #

DCS-SYR-88-80 ..... N89-20575 #

DE88-011854 ..... N89-20527 #
DE88-013002 ..... N89-20372 #
DE88-704797 ..... N89-20213 #
DE88-704998 ..... N89-20853 #
DE88-704999 ..... N89-20719 #
DE88-705004 ..... N89-20854 #
DE88-705019 ..... N89-20917 #
DE88-705077 ..... N89-20855 #
DE88-705078 ..... N89-20720 #
DE88-705255 ..... N89-20868 #
DE88-705336 ..... N89-20900 #
DE88-705339 ..... N89-20773 #
DE88-705340 ..... N89-20573 #
DE88-705341 ..... N89-20256 #
DE88-705342 ..... N89-20748 #
DE88-705343 ..... N89-20828 #
DE88-705344 ..... N89-20829 #
DE88-705345 ..... N89-20830 #
DE88-705347 ..... N89-20749 #
DE88-705348 ..... N89-20831 #
DE88-705350 ..... N89-20750 #
DE88-705351 ..... N89-20901 #
DE88-705355 ..... N89-20857 #
DE88-705358 ..... N89-20788 #
DE88-705359 ..... N89-20396 #
DE88-705364 ..... N89-20263 #
DE88-705365 ..... N89-20240 #
DE88-705367 ..... N89-20842 #
DE88-705369 ..... N89-20672 #
DE88-705370 ..... N89-20843 #
DE88-705371 ..... N89-20608 #
DE88-756310 ..... N89-20413 #
DE89-000355 ..... N89-20528 #
DE89-000654 ..... N89-20104 #
DE89-000655 ..... N89-20553 #
DE89-002988 ..... N89-20832 #
DE89-003114 ..... N89-20484 #
DE89-003120 ..... N89-20702 #
DE89-003180 ..... N89-20703 #
DE89-003483 ..... N89-20574 #
DE89-003489 ..... N89-20665 #
DE89-003483 ..... N89-20232 #
DE89-003575 ..... N89-20689 #
DE89-003626 ..... N89-20214 #
DE89-003888 ..... N89-20815 #
DE89-003923 ..... N89-20476 #
DE89-004195 ..... N89-20563 #
DE89-004355 ..... N89-20564 #
DE89-004380 ..... N89-20477 #
DE89-004381 ..... N89-20478 #
DE89-004543 ..... N89-20911 #
DE89-004584 ..... N89-20529 #
DE89-004797 ..... N89-20479 #
DE89-004913 ..... N89-20805 #
DE89-005055 ..... N89-20686 #
DE89-005093 ..... N89-20704 #
DE89-005101 ..... N89-20425 #
DE89-005107 ..... N89-20480 #
DE89-005109 ..... N89-20481* #
DE89-005110 ..... N89-20705 #
DE89-005124 ..... N89-20482 #
DE89-005133 ..... N89-20229 #
DE89-005304 ..... N89-20225 #
DE89-005339 ..... N89-20493 #
DE89-005349 ..... N89-20441 #
DE89-005397 ..... N89-20792 #
DE89-005400 ..... N89-20241 #
DE89-005415 ..... N89-20389 #
DE89-005445 ..... N89-20373 #
DE89-005455 ..... N89-20257 #
DE89-005486 ..... N89-20442 #
DE89-005469 ..... N89-20443 #
DE89-005471 ..... N89-20233 #
DE89-005475 ..... N89-20806 #
DE89-005476 ..... N89-20448 #
DE89-005496 ..... N89-20790 #
DE89-005543 ..... N89-20794 #
DE89-005657 ..... N89-20414 #
DE89-005666 ..... N89-20856 #
DE89-005726 ..... N89-20822 #
DE89-005773 ..... N89-20390 #
DE89-005779 ..... N89-20752 #
DE89-005811 ..... N89-20495 #
DE89-005824 ..... N89-20435 #
DE89-005833 ..... N89-20230 #
DE89-005852 ..... N89-20816 #
DE89-005910 ..... N89-20219 #
DE89-005921 ..... N89-20707 #
DE89-005944 ..... N89-20793 #
DE89-006030 ..... N89-20666 #
DE89-006033 ..... N89-20258 #
DE89-006034 ..... N89-20823 #
DE89-006036 ..... N89-20437* #
DE89-006037 ..... N89-20817 #
DE89-006040 ..... N89-20844 #
DE89-006123 ..... N89-20234 #
DE89-006129 ..... N89-20259 #
DE89-006131 ..... N89-20809 #
DE89-006146 ..... N89-20449 #
DE89-006148 ..... N89-20845 #
DE89-006149 ..... N89-20450 #
DE89-006151 ..... N89-20565 #
DE89-006156 ..... N89-20451 #
DE89-006172 ..... N89-20391 #
DE89-006191 ..... N89-20260 #

DE89-006197 ..... N89-20242 #
DE89-006207 ..... N89-20775 #
DE89-006208 ..... N89-20444 #
DE89-006209 ..... N89-20721 #
DE89-006246 ..... N89-20547 #
DE89-006280 ..... N89-20374 #
DE89-006281 ..... N89-20833 #
DE89-006282 ..... N89-20628 #
DE89-006284 ..... N89-20452 #
DE89-006376 ..... N89-20445 #
DE89-006378 ..... N89-20548 #
DE89-006379 ..... N89-20458 #
DE89-006455 ..... N89-20446 #
DE89-006507 ..... N89-20834 #
DE89-006511 ..... N89-20392 #
DE89-006512 ..... N89-20797 #
DE89-006514 ..... N89-20459 #
DE89-006530 ..... N89-20397 #
DE89-006550 ..... N89-20798 #
DE89-006554 ..... N89-20824 #
DE89-006591 ..... N89-20753 #
DE89-006598 ..... N89-20375 #
DE89-006602 ..... N89-20787 #
DE89-006603 ..... N89-20810 #
DE89-006604 ..... N89-20846 #
DE89-006607 ..... N89-20796 #
DE89-006619 ..... N89-20825 #
DE89-006620 ..... N89-20835 #
DE89-006654 ..... N89-20603 #
DE89-006656 ..... N89-20453 #
DE89-006660 ..... N89-20836 #
DE89-006667 ..... N89-20826 #
DE89-006669 ..... N89-20837 #
DE89-006695 ..... N89-20647 #
DE89-006707 ..... N89-20604 #
DE89-006726 ..... N89-20858 #
DE89-006727 ..... N89-20398 #
DE89-006728 ..... N89-20438 #
DE89-006734 ..... N89-20673 #
DE89-006754 ..... N89-20273 #
DE89-006771 ..... N89-20706 #
DE89-006774 ..... N89-20261 #
DE89-006776 ..... N89-20436 #
DE89-006777 ..... N89-20454 #
DE89-006781 ..... N89-20626 #
DE89-006789 ..... N89-20235 #
DE89-006791 ..... N89-20838 #
DE89-006792 ..... N89-20460 #
DE89-006796 ..... N89-20326 #
DE89-006820 ..... N89-20550 #
DE89-006828 ..... N89-20600 #
DE89-006857 ..... N89-20393 #
DE89-006861 ..... N89-20455 #
DE89-006927 ..... N89-20807 #
DE89-006934 ..... N89-20566 #
DE89-006937 ..... N89-20839 #
DE89-006938 ..... N89-20590 #
DE89-006980 ..... N89-20262 #
DE89-006981 ..... N89-20456 #
DE89-006982 ..... N89-20457 #
DE89-006985 ..... N89-20236 #
DE89-006986 ..... N89-20254 #
DE89-006996 ..... N89-20667 #
DE89-007000 ..... N89-20668 #
DE89-007005 ..... N89-20119 #
DE89-007011 ..... N89-20591 #
DE89-007016 ..... N89-20494 #
DE89-007023 ..... N89-20669 #
DE89-007024 ..... N89-20751 #
DE89-007048 ..... N89-20461 #
DE89-007051 ..... N89-20483 #
DE89-007059 ..... N89-20394 #
DE89-007061 ..... N89-20395 #
DE89-007070 ..... N89-20808 #
DE89-007088 ..... N89-20237 #
DE89-007089 ..... N89-20781 #
DE89-007117 ..... N89-20238 #
DE89-007130 ..... N89-20239 #
DE89-007220 ..... N89-20840 #
DE89-007288 ..... N89-20105 #
DE89-007289 ..... N89-20554 #
DE89-007290 ..... N89-20556 #
DE89-007291 ..... N89-20627 #
DE89-007292 ..... N89-20670 #
DE89-007294 ..... N89-20172 #
DE89-007299 ..... N89-20671 #
DE89-007303 ..... N89-20272 #
DE89-007319 ..... N89-20592 #
DE89-007322 ..... N89-20555 #
DE89-007343 ..... N89-20841 #
DE89-007446 ..... N89-20847 #
DE89-007466 ..... N89-20485 #
DE89-007473 ..... N89-20811 #
DE89-007474 ..... N89-20462 #
DE89-007533 ..... N89-20754 #
DE89-007554 ..... N89-20399 #
DE89-007567 ..... N89-20463 #
DE89-007569 ..... N89-20782 #
DE89-007574 ..... N89-20783 #
DE89-007595 ..... N89-20243 #
DE89-007598 ..... N89-20274 #
DE89-007712 ..... N89-20848 #
DE89-007786 ..... N89-20755 #
DE89-007814 ..... N89-20756 #
DE89-007850 ..... N89-20690 #
DE89-007853 ..... N89-20708 #
DE89-007855 ..... N89-20757 #
DE89-007873 ..... N89-20758 #
DE89-007877 ..... N89-20691 #
DE89-007878 ..... N89-20759 #
DE89-007883 ..... N89-20674 #

DNA-TR-88-58 ..... N89-20426 #

DOE/CE-0219 ..... N89-20592 #
DOE/CE-15328/T1 ..... N89-20495 #
DOE/CE-15337/T5 ..... N89-20547 #

DOE/CH-10093/H5 ..... N89-20483 #
DOE/CH-10093/40-VOL-1 ..... N89-20553 #

DOE/ER-0367 ..... N89-20645 #
DOE/ER-13488/1 ..... N89-20858 #
DOE/ER-13631/12 ..... N89-20550 #
DOE/ER-13633/3 ..... N89-20555 #
DOE/ER-13723/2 ..... N89-20811 #
DOE/ER-13788/2 ..... N89-20460 #
DOE/ER-13894/1 ..... N89-20848 #
DOE/ER-13905/1 ..... N89-20254 #
DOE/ER-30131/T1 ..... N89-20446 #
DOE/ER-45055/14 ..... N89-20755 #
DOE/ER-45057/T3 ..... N89-20781 #
DOE/ER-45097/T4 ..... N89-20835 #
DOE/ER-45205/4 ..... N89-20238 #
DOE/ER-45215/5 ..... N89-20840 #
DOE/ER-45234/3 ..... N89-20822 #
DOE/ER-45253/4 ..... N89-20234 #
DOE/ER-45266/T1 ..... N89-20825 #
DOE/ER-45308/2 ..... N89-20235 #
DOE/ER-45310/16 ..... N89-20838 #
DOE/ER-45354/T1 ..... N89-20236 #
DOE/ER-53214/11 ..... N89-20808 #
DOE/ER-60354/T4 ..... N89-20600 #

DOE/ET-53088/358 ..... N89-20751 #

DOE/PC-80503/T13 ..... N89-20219 #
DOE/PC-88827/T1 ..... N89-20273 #

DOT/FAA/CT-TN89/11 ..... N89-20379 #

DOT/FAA/PS-88/19 ..... N89-20111* #

DP-MS-88-99 ..... N89-20477 #
DP-MS-88-114 ..... N89-20478 #
DP-MS-88-206 ..... N89-20241 #

DREO-TN-88-22 ..... N89-20609 #

DTIC-TR-89/4 ..... N89-20869 #

DTRC/SME-88/73 ..... N89-20210 #

D6-54693 ..... N89-20093* #

E-4426 ..... N89-20641* #
E-4468 ..... N89-20135* #
E-4516 ..... N89-20227* #
E-4556 ..... N89-20776* #
E-4557 ..... N89-20324* #
E-4576 ..... N89-20514* #
E-4577 ..... N89-20710* #
E-4609 ..... N89-20228* #
E-4610 ..... N89-20206* #
E-4618 ..... N89-20321* #
E-4627 ..... N89-20545* #
E-4629 ..... N89-20407* #
E-4632 ..... N89-20490* #
E-4636 ..... N89-20179* #
E-4641 ..... N89-20193* #
E-4645 ..... N89-20385* #
E-4646 ..... N89-20192* #
E-4647 ..... N89-20685* #
E-4652 ..... N89-20684* #
E-4653 ..... N89-20194* #
E-4654 ..... N89-20253* #
E-4662 ..... N89-20252* #
E-4680 ..... N89-20199* #
E-4684 ..... N89-20779* #
E-4697 ..... N89-20133* #
E-4712 ..... N89-20171* #

EGG-M-88466 ..... N89-20389 #

EGG-10617-2010 ..... N89-20841 #

EL-62 ..... N89-20368 #

ELS-TR-716111-6 ..... N89-20364* #
ELS-TR-716199-12 ..... N89-20363* #

EP-PATENT-APPL-SN-87301083.9 ..... N89-20624
EP-PATENT-APPL-SN-87302635.5 ..... N89-20207
EP-PATENT-APPL-SN-87302898.9 ..... N89-20622
EP-PATENT-APPL-SN-87303599.2 ..... N89-20623
EP-PATENT-APPL-SN-87303603.2 ..... N89-20255

EP-PATENT-0-240-354-A1 ..... N89-20622

EP-0-234-785-A1 ..... N89-20624
EP-0-240-251-A2 ..... N89-20207
EP-0-243-189-A1 ..... N89-20623
EP-0-247-726-A2 ..... N89-20255

EPA/450/5-88/004 ..... N89-20558 #
EPA/600/D-88/207 ..... N89-20561 #
EPA/600/7-88/021 ..... N89-20560 #

ESA-CR(P)-2599 ..... N89-20359 #
ESA-CR(P)-2662 ..... N89-20360 #
ESA-CR(P)-2678-VOL-1 ..... N89-20639 #
ESA-CR(P)-2678-VOL-2 ..... N89-20867 #
ESA-CR(P)-2691 ..... N89-20185 #
ESA-CR(P)-2697 ..... N89-20186 #

ESA-SP-1103 ..... N89-20156 #

ESA-STM-242 ..... N89-20518 #

ESA-TT-1134 ..... N89-20417 #

ESL-720964-2 ..... N89-20355* #

ETL-0495 ..... N89-20681 #
ETL-0497 ..... N89-20377 #
ETL-0508 ..... N89-20487 #
ETL-0509 ..... N89-20120 #
ETL-0514 ..... N89-20488 #

ETN-89-93644 ..... N89-20359 #
ETN-89-93692 ..... N89-20226 #
ETN-89-93725 ..... N89-20189 #
ETN-89-93726 ..... N89-20571 #
ETN-89-93727 ..... N89-20897 #
ETN-89-93728 ..... N89-20898 #
ETN-89-93729 ..... N89-20899 #
ETN-89-93730 ..... N89-20416 #
ETN-89-93731 ..... N89-20516 #
ETN-89-93732 ..... N89-20517 #
ETN-89-93733 ..... N89-20648 #
ETN-89-93734 ..... N89-20786 #
ETN-89-93735 ..... N89-20572 #
ETN-89-93738 ..... N89-20365 #
ETN-89-93739 ..... N89-20366 #
ETN-89-93740 ..... N89-20919 #
ETN-89-93743 ..... N89-20367 #
ETN-89-93745 ..... N89-20882 #
ETN-89-93746 ..... N89-20883 #
ETN-89-93748 ..... N89-20884 #
ETN-89-93750 ..... N89-20368 #
ETN-89-93751 ..... N89-20473 #
ETN-89-93752 ..... N89-20649 #
ETN-89-93783 ..... N89-20916
ETN-89-93807 ..... N89-20785
ETN-89-93871 ..... N89-20534 #
ETN-89-93876 ..... N89-20537 #
ETN-89-93877 ..... N89-20538 #
ETN-89-93878 ..... N89-20539 #
ETN-89-93881 ..... N89-20791 #
ETN-89-93895 ..... N89-20515 #
ETN-89-93904 ..... N89-20518 #
ETN-89-93910 ..... N89-20417 #
ETN-89-93914 ..... N89-20639 #
ETN-89-93915 ..... N89-20867 #
ETN-89-93919 ..... N89-20185 #
ETN-89-93924 ..... N89-20360 #
ETN-89-93938 ..... N89-20186 #
ETN-89-94015 ..... N89-20722 #
ETN-89-94016 ..... N89-20723 #
ETN-89-94017 ..... N89-20418 #
ETN-89-94018 ..... N89-20650 #
ETN-89-94019 ..... N89-20724 #
ETN-89-94020 ..... N89-20616 #
ETN-89-94021 ..... N89-20725 #
ETN-89-94022 ..... N89-20765 #
ETN-89-94023 ..... N89-20766 #
ETN-89-94024 ..... N89-20419 #
ETN-89-94025 ..... N89-20651 #

ETN-89-94026 ..... N89-20617 #
ETN-89-94027 ..... N89-20726 #
ETN-89-94028 ..... N89-20727 #
ETN-89-94030 ..... N89-20369 #
ETN-89-94031 ..... N89-20129 #
ETN-89-94033 ..... N89-20420 #
ETN-89-94034 ..... N89-20115 #
ETN-89-94035 ..... N89-20116 #
ETN-89-94036 ..... N89-20130 #
ETN-89-94038 ..... N89-20699 #
ETN-89-94039 ..... N89-20519 #
ETN-89-94040 ..... N89-20126 #
ETN-89-94041 ..... N89-20540 #
ETN-89-94042 ..... N89-20541 #
ETN-89-94043 ..... N89-20520 #
ETN-89-94045 ..... N89-20542 #
ETN-89-94046 ..... N89-20117 #
ETN-89-94048 ..... N89-20652 #
ETN-89-94050 ..... N89-20118 #
ETN-89-94051 ..... N89-20521 #
ETN-89-94052 ..... N89-20231 #
ETN-89-94053 ..... N89-20087 #
ETN-89-94054 ..... N89-20551 #
ETN-89-94055 ..... N89-20102 #
ETN-89-94056 ..... N89-20522 #
ETN-89-94058 ..... N89-20370 #
ETN-89-94059 ..... N89-20523 #
ETN-89-94060 ..... N89-20653 #
ETN-89-94061 ..... N89-20552 #
ETN-89-94062 ..... N89-20474 #
ETN-89-94064 ..... N89-20618 #
ETN-89-94065 ..... N89-20611 #
ETN-89-94066 ..... N89-20622
ETN-89-94067 ..... N89-20207
ETN-89-94068 ..... N89-20255
ETN-89-94069 ..... N89-20623
ETN-89-94070 ..... N89-20624
ETN-89-94071 ..... N89-20325 #
ETN-89-94072 ..... N89-20728 #
ETN-89-94073 ..... N89-20729 #
ETN-89-94074 ..... N89-20371 #
ETN-89-94075 ..... N89-20730 #
ETN-89-94076 ..... N89-20700 #
ETN-89-94077 ..... N89-20731 #
ETN-89-94078 ..... N89-20732 #
ETN-89-94079 ..... N89-20733 #
ETN-89-94086 ..... N89-20524 #
ETN-89-94088 ..... N89-20654
ETN-89-94089 ..... N89-20780
ETN-89-94111 ..... N89-20388 #
ETN-89-94112 ..... N89-20103 #
ETN-89-94118 ..... N89-20421 #
ETN-89-94119 ..... N89-20434 #
ETN-89-94120 ..... N89-20827 #
ETN-89-94121 ..... N89-20422 #
ETN-89-94122 ..... N89-20423 #
ETN-89-94123 ..... N89-20525 #
ETN-89-94124 ..... N89-20526 #
ETN-89-94129 ..... N89-20491 #
ETN-89-94130 ..... N89-20208 #
ETN-89-94131 ..... N89-20492 #
ETN-89-94132 ..... N89-20156 #
ETN-89-94137 ..... N89-20625
ETN-89-94155 ..... N89-20475 #
ETN-89-94156 ..... N89-20655 #
ETN-89-94157 ..... N89-20656 #
ETN-89-94158 ..... N89-20657 #
ETN-89-94159 ..... N89-20658 #
ETN-89-94160 ..... N89-20659 #
ETN-89-94161 ..... N89-20734 #
ETN-89-94162 ..... N89-20735 #
ETN-89-94163 ..... N89-20771 #
ETN-89-94164 ..... N89-20772 #
ETN-89-94166 ..... N89-20736 #
ETN-89-94167 ..... N89-20660 #
ETN-89-94168 ..... N89-20661 #
ETN-89-94169 ..... N89-20687 #
ETN-89-94170 ..... N89-20688 #
ETN-89-94171 ..... N89-20737 #
ETN-89-94172 ..... N89-20662 #
ETN-89-94173 ..... N89-20767 #
ETN-89-94174 ..... N89-20768 #
ETN-89-94175 ..... N89-20663 #
ETN-89-94176 ..... N89-20612 #
ETN-89-94177 ..... N89-20738 #
ETN-89-94178 ..... N89-20739 #
ETN-89-94179 ..... N89-20740 #
ETN-89-94180 ..... N89-20424 #
ETN-89-94182 ..... N89-20664 #
ETN-89-94183 ..... N89-20741 #
ETN-89-94186 ..... N89-20769 #
ETN-89-94188 ..... N89-20742 #
ETN-89-94190 ..... N89-20743 #
ETN-89-94192 ..... N89-20744 #
ETN-89-94193 ..... N89-20660 #
ETN-89-94194 ..... N89-20701 #

ETN-89-94195 ..... N89-20745 #
ETN-89-94196 ..... N89-20746 #
ETN-89-94199 ..... N89-20747 #

FAA-EE-88-5 ..... N89-20557 #

FCR-9594A ..... N89-20544 #

FERMILAB-PUB-89/32-A ..... N89-20896* #
FERMILAB-PUB-89/49-A ..... N89-20880* #

FFA-TN-1987-35 ..... N89-20525 #
FFA-TN-1988-05 ..... N89-20526 #
FFA-TN-1988-19 ..... N89-20416 #
FFA-TN-1988-23 ..... N89-20516 #
FFA-TN-1988-36 ..... N89-20517 #

FHWA/MN/RD-05 ..... N89-20505 #

FHWA/TS-88/021 ..... N89-20471 #

FJSRL-TR-89-0002 ..... N89-20106 #

FOA-C-30428-3.3 ..... N89-20365 #
FOA-C-30430-3.3 ..... N89-20366 #
FOA-C-30499-3.3 ..... N89-20919 #
FOA-C-30503-3.3 ..... N89-20367 #

FRITZ ENGINEERING LAB-513.3 ..... N89-20504 #

FTD-ID(RS)-T-0438-88 ..... N89-20498 #

GAO/IMTEC-88-28 ..... N89-20659 #

GAO/NSIAD-88-118BR ..... N89-20881 #
GAO/NSIAD-88-131BR ..... N89-20872 #
GAO/NSIAD-88-147 ..... N89-20188 #

GAO/RCED-88-116BR ..... N89-20874 #

GPO-83-952 ..... N89-20873 #

GRI-88/0166 ..... N89-20211 #
GRI-88/0185 ..... N89-20468 #
GRI-88/0186 ..... N89-20217 #
GRI-88/0202 ..... N89-20405 #
GRI-88/0215 ..... N89-20544 #

HD-PY88/05 ..... N89-20916

HTKK-MAT-A261 ..... N89-20711 #

I-271/88 ..... N89-20491 #
I-279/88 ..... N89-20208 #

IAEA-TECDOC-472 ..... N89-20868 #

IC-88/91 ..... N89-20900 #
IC-88/180 ..... N89-20773 #
IC-88/190 ..... N89-20573 #
IC-88/191 ..... N89-20256 #
IC-88/192 ..... N89-20748 #
IC-88/195 ..... N89-20828 #
IC-88/197 ..... N89-20829 #
IC-88/198 ..... N89-20830 #
IC-88/203 ..... N89-20749 #
IC-88/204 ..... N89-20831 #
IC-88/207 ..... N89-20750 #
IC-88/211 ..... N89-20901 #
IC-88/233 ..... N89-20857 #
IC-88/247 ..... N89-20788 #
IC-88/255 ..... N89-20396 #
IC-88/286 ..... N89-20263 #
IC-88/290 ..... N89-20240 #
IC-88/305 ..... N89-20842 #
IC-88/307 ..... N89-20672 #
IC-88/317 ..... N89-20843 #
IC-88/323 ..... N89-20608 #

ICASE-89-3 ..... N89-20636* #
ICASE-89-4 ..... N89-20637* #
ICASE-89-5 ..... N89-20635* #
ICASE-89-7 ..... N89-20638* #
ICASE-89-8 ..... N89-20632* #
ICASE-89-9 ..... N89-20411* #
ICASE-89-10 ..... N89-20412* #
ICASE-89-11 ..... N89-20095* #
ICASE-89-12 ..... N89-20698* #
ICASE-89-13 ..... N89-20718* #
ICASE-89-14 ..... N89-20716* #

ICOMP-89-2 ..... N89-20710* #
ICOMP-89-5 ..... N89-20407* #

IDA-M-425 ..... N89-20675 #

IDA/HQ-88-33027 ..... N89-20675 #

IFSM-88-153 ..... N89-20247 #

IFSR-358 ..... N89-20751 #

IFT-P-20/88 ..... N89-20855 #
IFT-P-22/88 ..... N89-20720 #

INDU/DC/GMH-TR-42 ..... N89-20784 #
INDU/DC/GMH-TR-44 ..... N89-20799 #
INDU/DC/GMH-TR-46 ..... N89-20612 #

INIS-BR-1338 ..... N89-20213 #

INT.CLASS-B22F-7/00 ..... N89-20207

INT.CLASS-C08F-220/00 ..... N89-20255
INT.CLASS-C09J-3/14 ..... N89-20255
INT.CLASS-C22C-1/05 ..... N89-20207

INT.CLASS-G06F-13/28 ..... N89-20623
INT.CLASS-G06F-15/06 ..... N89-2062
INT.CLASS-G06F-15/16 ..... N89-2062

IRF-SR-196 ..... N89-20572 #

IS-T-1257 ..... N89-20783 #
IS-T-1355 ..... N89-20483 #
IS-T-1394 ..... N89-20782 #

ISBN-9-09-001753-4 ..... N89-20625
ISBN-951-666-254-4 ..... N89-20368 #
ISBN-951-666-259-5 ..... N89-20434 #
ISBN-951-666-264-1 ..... N89-20827 #
ISBN-951-666-268-4 ..... N89-20649 #
ISBN-951-666-269-2 ..... N89-20473 #
ISBN-951-754-527-4 ..... N89-20467 #
ISBN-951-754-551-7 ..... N89-20384 #
ISBN-951-754-557-6 ..... N89-20361 #
ISBN-951-754-571-1 ..... N89-20153 #
ISBN-951-754-589-4 ..... N89-20410 #
ISBN-951-754-626-2 ..... N89-20814 #
ISBN-951-754-640-8 ..... N89-20711 #

ISL-CO-245/87 ..... N89-20388 #
ISL-CO-246/87 ..... N89-20103 #

ISSN-0001-6845 ..... N89-20368 #
ISSN-0038-0911 ..... N89-20909 #
ISSN-0038-9011 ..... N89-20908 #
ISSN-0143-7143 ..... N89-20780
ISSN-0262-5369 ..... N89-20654
ISSN-0284-1703 ..... N89-20572 #
ISSN-0347-3708 ..... N89-20365 #
ISSN-0347-3708 ..... N89-20368 #
ISSN-0347-3708 ..... N89-20367 #
ISSN-0347-3708 ..... N89-20919 #
ISSN-0348-7539 ..... N89-20189 #
ISSN-0348-7539 ..... N89-20571 #
ISSN-0348-7539 ..... N89-20897 #
ISSN-0348-7539 ..... N89-20898 #
ISSN-0348-7539 ..... N89-20899 #
ISSN-0355-2713 ..... N89-20473 #
ISSN-0355-2713 ..... N89-20649 #
ISSN-0355-2721 ..... N89-20434 #
ISSN-0355-2721 ..... N89-20827 #
ISSN-0379-4075 ..... N89-20518 #
ISSN-0379-6566 ..... N89-20156 #
ISSN-0920-8577 ..... N89-20418 #
ISSN-0920-8577 ..... N89-20419 #
ISSN-0920-8577 ..... N89-20616 #
ISSN-0920-8577 ..... N89-20617 #
ISSN-0920-8577 ..... N89-20650 #
ISSN-0920-8577 ..... N89-20651 #
ISSN-0920-8577 ..... N89-20722 #
ISSN-0920-8577 ..... N89-20723 #
ISSN-0920-8577 ..... N89-20724 #
ISSN-0920-8577 ..... N89-20725 #
ISSN-0920-8577 ..... N89-20726 #
ISSN-0920-8577 ..... N89-20727 #
ISSN-0920-8577 ..... N89-20765 #
ISSN-0920-8577 ..... N89-20766 #

ISTIC-TR-C-000138 ..... N89-20224 #
ISTIC-TR-C-000150 ..... N89-20804 #
ISTIC-TR-C-000183 ..... N89-20431 #
ISTIC-TR-C-000192 ..... N89-20713 #
ISTIC-TR-C-000193 ..... N89-20714 #
ISTIC-TR-C-000199 ..... N89-20506 #
ISTIC-TR-C-000200 ..... N89-20634 #
ISTIC-TR-C-000203 ..... N89-20803 #

ISVR-TR-164 ..... N89-20524 #

IZF-1987-28 ..... N89-20618 #

IZF-1987-41 N89-20611 #

JAYCOR-J206-89-001/6261 N89-20155 #

JINR-E-11-88-481 N89-20753 #

JPL-D-5704 N89-20215* #

JPL-PUBL-88-17 N89-20821* #
JPL-PUBL-88-21 N89-20387* #
JPL-PUBL-88-25 N89-20643* #
JPL-PUBL-88-29 N89-20151* #
JPL-PUBL-88-31 N89-20642* #
JPL-PUBL-88-35 N89-20113* #
JPL-PUBL-88-39 N89-20549* #
JPL-PUBL-88-40 N89-20152* #
JPL-PUBL-88-41 N89-20644* #
JPL-PUBL-88-42 N89-20362* #

JPL-TDA-PR-42-95 N89-20329* #

JPL-400-303 N89-20902* #

K/QT-188 N89-20260 #

KCP-613-4058 N89-20243 #

L-16503 N89-20587* #
L-16543 N89-20409* #
L-16545 N89-20099* #

LA-UR-88-3167 N89-20528 #
LA-UR-88-3669 N89-20665 #
LA-UR-88-3723 N89-20232 #
LA-UR-88-3750 N89-20574 #
LA-UR-88-3827 N89-20689 #
LA-UR-88-3868 N89-20373 #
LA-UR-88-4059 N89-20257 #
LA-UR-88-4206 N89-20443 #
LA-UR-88-4213 N89-20233 #
LA-UR-88-4232 N89-20806 #
LA-UR-88-4236 N89-20448 #
LA-UR-88-4278 N89-20442 #
LA-UR-89-17 N89-20798 #
LA-UR-89-167 N89-20397 #
LA-UR-89-258 N89-20824 #
LA-UR-89-284 N89-20459 #
LA-UR-89-293 N89-20797 #
LA-UR-89-295 N89-20392 #

LA-11369-MS N89-20445 #
LA-11393-C-SUPPL N89-20807 #
LA-11431-T N89-20911 #
LA-11484-MS N89-20548 #
LA-11494-MS N89-20485 #

LBL-25047 N89-20810 #
LBL-25170 N89-20603 #
LBL-25818 N89-20846 #
LBL-26107 N89-20826 #
LBL-26232 N89-20604 #
LBL-26253 N89-20453 #
LBL-26283 N89-20237 #
LBL-26300 N89-20637 #
LBL-26308 N89-20836 #
LBL-26331 N89-20787 #
LBL-26334 N89-20239 #
LBL-26344 N89-20847 #
LBL-26386 N89-20796 #
LBL-26440 N89-20494 #

LC-79-640375 N89-20908 #
LC-79-640375 N89-20909 #

LEMS-43 N89-20709 #

LINO-158 N89-20791 #

MA-RD-840-88035 N89-20504 #

MA-50 N89-20649 #
MA-51 N89-20473 #

MCR-88-1402 N89-20182* #

MIT-LANL-2 N89-20548 #

MITSG-88-5 N89-20712 #

MLM-3540-VOL-3 N89-20790 #
MLM-3562 N89-20272 #
MLM-3565(OP) N89-20458 #
MLM-3566(OP) N89-20455 #
MLM-3570 N89-20274 #

MN/DOT-INVESTIGATION-202-1 N89-20505 #

MPI-PAE/EXP-EL-192 N89-20785

MT-CWR-089-029 N89-20235 #

MTI-87TR56 N89-20472* #

MTL-TR-88-30 N89-20209 #
MTL-TR-88-36 N89-20268 #
MTL-TR-88-38 N89-20245 #
MTL-TR-88-47 N89-20244 #

NA-88-0001-VOL-1 N89-20127 #
NA-88-0001-VOL-2 N89-20128 #

NADC-88066-60-VOL-1 N89-20127 #
NADC-88066-60-VOL-2 N89-20128 #

NAS 1.15:4069-VOL-1 N89-20276* #
NAS 1.15:4069-VOL-2 N89-20305* #
NAS 1.15:4087 N89-20135* #
NAS 1.15:4103 N89-20641* #
NAS 1.15:4109 N89-20409* #
NAS 1.15:4110 N89-20099* #
NAS 1.15:89284 N89-20875* #
NAS 1.15:100352 N89-20430* #
NAS 1.15:100355-VOL-1 N89-20178* #
NAS 1.15:100473 N89-20918* #
NAS 1.15:100722 N89-20589* #
NAS 1.15:101040 N89-20124* #
NAS 1.15:101048 N89-20098* #
NAS 1.15:101056 N89-20770* #
NAS 1.15:101065 N89-20086* #
NAS 1.15:101075 N89-20100* #
NAS 1.15:101076 N89-20386* #
NAS 1.15:101080 N89-20610* #
NAS 1.15:101231 N89-20322* #
NAS 1.15:101418 N89-20227* #
NAS 1.15:101448 N89-20324* #
NAS 1.15:101464 N89-20514* #
NAS 1.15:101466 N89-20710* #
NAS 1.15:101481 N89-20228* #
NAS 1.15:101482 N89-20206* #
NAS 1.15:101484 N89-20321* #
NAS 1.15:101487 N89-20545* #
NAS 1.15:101488 N89-20407* #
NAS 1.15:101489 N89-20490* #
NAS 1.15:101547 N89-20094* #
NAS 1.15:101550 N89-20777* #
NAS 1.15:101552 N89-20778* #
NAS 1.15:101557 N89-20101* #
NAS 1.15:101947 N89-20179* #
NAS 1.15:101948 N89-20193* #
NAS 1.15:101951 N89-20192* #
NAS 1.15:101952 N89-20684* #
NAS 1.15:101953 N89-20685* #
NAS 1.15:101956 N89-20194* #
NAS 1.15:101959 N89-20253* #
NAS 1.15:101964 N89-20252* #
NAS 1.15:101982 N89-20199* #
NAS 1.15:101993 N89-20133* #
NAS 1.15:101994 N89-20385* #
NAS 1.15:102002 N89-20779* #
NAS 1.15:102006 N89-20171* #
NAS 1.16:182232 N89-20776* #
NAS 1.19:260 N89-20902* #
NAS 1.21:7037(235) N89-20088*
NAS 1.21:7037(236) N89-20091*
NAS 1.21:7037(237) N89-20089*
NAS 1.21:7037(238) N89-20090*
NAS 1.26:3922(24) N89-20602* #
NAS 1.26:4229 N89-20615* #
NAS 1.26:171982-VOL-1 N89-20271* #
NAS 1.26:172110 N89-20182* #
NAS 1.26:172112 N89-20181* #
NAS 1.26:172599 N89-20531* #
NAS 1.26:180079 N89-20415* #
NAS 1.26:180899 N89-20472* #
NAS 1.26:181723 N89-20512* #
NAS 1.26:181744 N89-20093* #
NAS 1.26:181762 N89-20111* #
NAS 1.26:181769 N89-20683* #
NAS 1.26:181771 N89-20636* #
NAS 1.26:181772 N89-20637* #
NAS 1.26:181773 N89-20635* #
NAS 1.26:181781 N89-20632* #
NAS 1.26:181784 N89-20619* #
NAS 1.26:181785 N89-20638* #
NAS 1.26:181786 N89-20095* #
NAS 1.26:181797 N89-20412* #
NAS 1.26:181798 N89-20698* #
NAS 1.26:181799 N89-20411* #
NAS 1.26:181801 N89-20716* #
NAS 1.26:181802 N89-20125* #
NAS 1.26:181803 N89-20718* #
NAS 1.26:182164 N89-20132* #
NAS 1.26:182267 N89-20134* #
NAS 1.26:182818 N89-20205* #
NAS 1.26:182857 N89-20631* #
NAS 1.26:182884 N89-20356* #
NAS 1.26:182958 N89-20880* #
NAS 1.26:183417 N89-20533* #
NAS 1.26:183576 N89-20196* #
NAS 1.26:183581 N89-20197* #
NAS 1.26:183582 N89-20195* #
NAS 1.26:183586 N89-20198* #
NAS 1.26:184651 N89-20327* #
NAS 1.26:184659 N89-20871* #
NAS 1.26:184671 N89-20692* #
NAS 1.26:184672 N89-20329* #
NAS 1.26:184690 N89-20200* #
NAS 1.26:184695 N89-20905* #
NAS 1.26:184696 N89-20175* #
NAS 1.26:184697 N89-20176* #
NAS 1.26:184698 N89-20177* #
NAS 1.26:184711 N89-20173* #
NAS 1.26:184712 N89-20174* #
NAS 1.26:184732 N89-20180* #
NAS 1.26:184736 N89-20481* #
NAS 1.26:184737 N89-20567* #
NAS 1.26:184741 N89-20121* #
NAS 1.26:184742 N89-20122* #
NAS 1.26:184743 N89-20123* #
NAS 1.26:184780 N89-20355* #
NAS 1.26:184786 N89-20470* #
NAS 1.26:184799 N89-20489* #
NAS 1.26:184810 N89-20795* #
NAS 1.26:184813 N89-20447* #
NAS 1.26:184819 N89-20248* #
NAS 1.26:184820 N89-20215* #
NAS 1.26:184825 N89-20357* #
NAS 1.26:184827 N89-20183* #
NAS 1.26:184828 N89-20184* #
NAS 1.26:184832 N89-20358* #
NAS 1.26:184838 N89-20432* #
NAS 1.26:184840 N89-20820* #
NAS 1.26:184843 N89-20251* #
NAS 1.26:184844 N89-20218* #
NAS 1.26:184851 N89-20640* #
NAS 1.26:184860 N89-20644* #
NAS 1.26:184861 N89-20362* #
NAS 1.26:184862 N89-20152* #
NAS 1.26:184863 N89-20549* #
NAS 1.26:184864 N89-20821* #
NAS 1.26:184865 N89-20387* #
NAS 1.26:184866 N89-20643* #
NAS 1.26:184867 N89-20151* #
NAS 1.26:184868 N89-20113* #
NAS 1.26:184869 N89-20642* #
NAS 1.26:184874 N89-20717* #
NAS 1.26:184876 N89-20646* #
NAS 1.26:184892 N89-20896* #
NAS 1.26:184904 N89-20364* #
NAS 1.26:184907 N89-20363* #
NAS 1.26:184964 N89-20437* #
NAS 1.26:184965 N89-20146* #
NAS 1.55:3023 N89-20588* #
NAS 1.61:1184-VOL-2 N89-20587* #

NASA-CP-3023 N89-20588* #

NASA-CR-3922(24) N89-20602* #
NASA-CR-4229 N89-20615* #
NASA-CR-171982-VOL-1 N89-20271* #
NASA-CR-172110 N89-20182* #
NASA-CR-172112 N89-20181* #
NASA-CR-172599 N89-20531* #
NASA-CR-180079 N89-20415* #
NASA-CR-180899 N89-20472* #
NASA-CR-181723 N89-20512* #
NASA-CR-181744 N89-20093* #
NASA-CR-181762 N89-20111* #
NASA-CR-181769 N89-20683* #
NASA-CR-181771 N89-20636* #
NASA-CR-181772 N89-20637* #
NASA-CR-181773 N89-20635* #
NASA-CR-181781 N89-20632* #
NASA-CR-181784 N89-20619* #
NASA-CR-181785 N89-20638* #
NASA-CR-181786 N89-20095* #
NASA-CR-181797 N89-20412* #
NASA-CR-181798 N89-20698* #
NASA-CR-181799 N89-20411* #
NASA-CR-181801 N89-20716* #
NASA-CR-181802 N89-20125* #
NASA-CR-181803 N89-20718* #
NASA-CR-182164 N89-20132* #
NASA-CR-182232 N89-20776* #
NASA-CR-182267 N89-20134* #
NASA-CR-182818 N89-20205* #
NASA-CR-182857 N89-20631* #
NASA-CR-182884 N89-20356* #
NASA-CR-182958 N89-20880* #

NASA-CR-183417 ..... N89-20533* #
NASA-CR-183576 ..... N89-20196* #
NASA-CR-183581 ..... N89-20197* #
NASA-CR-183582 ..... N89-20195* #
NASA-CR-183586 ..... N89-20196* #
NASA-CR-184651 ..... N89-20327* #
NASA-CR-184659 ..... N89-20871* #
NASA-CR-184671 ..... N89-20692* #
NASA-CR-184672 ..... N89-20329* #
NASA-CR-184690 ..... N89-20200* #
NASA-CR-184695 ..... N89-20905* #
NASA-CR-184696 ..... N89-20175* #
NASA-CR-184697 ..... N89-20176* #
NASA-CR-184698 ..... N89-20177* #
NASA-CR-184711 ..... N89-20173* #
NASA-CR-184712 ..... N89-20174* #
NASA-CR-184732 ..... N89-20180* #
NASA-CR-184736 ..... N89-20481* #
NASA-CR-184737 ..... N89-20567* #
NASA-CR-184741 ..... N89-20121* #
NASA-CR-184742 ..... N89-20122* #
NASA-CR-184743 ..... N89-20123* #
NASA-CR-184780 ..... N89-20355* #
NASA-CR-184786 ..... N89-20470* #
NASA-CR-184799 ..... N89-20489* #
NASA-CR-184810 ..... N89-20795* #
NASA-CR-184813 ..... N89-20447* #
NASA-CR-184819 ..... N89-20248* #
NASA-CR-184820 ..... N89-20215* #
NASA-CR-184825 ..... N89-20357* #
NASA-CR-184827 ..... N89-20183* #
NASA-CR-184828 ..... N89-20184* #
NASA-CR-184832 ..... N89-20358* #
NASA-CR-184838 ..... N89-20432* #
NASA-CR-184840 ..... N89-20820* #
NASA-CR-184843 ..... N89-20251* #
NASA-CR-184844 ..... N89-20218* #
NASA-CR-184851 ..... N89-20640* #
NASA-CR-184860 ..... N89-20644* #
NASA-CR-184861 ..... N89-20362* #
NASA-CR-184862 ..... N89-20152* #
NASA-CR-184863 ..... N89-20549* #
NASA-CR-184864 ..... N89-20821* #
NASA-CR-184865 ..... N89-20387* #
NASA-CR-184866 ..... N89-20643* #
NASA-CR-184867 ..... N89-20151* #
NASA-CR-184868 ..... N89-20113* #
NASA-CR-184869 ..... N89-20642* #
NASA-CR-184874 ..... N89-20717* #
NASA-CR-184876 ..... N89-20646* #
NASA-CR-184892 ..... N89-20896* #
NASA-CR-184904 ..... N89-20364* #
NASA-CR-184907 ..... N89-20363* #
NASA-CR-184964 ..... N89-20437* #
NASA-CR-184965 ..... N89-20146* #

NASA-EP-260 ..... N89-20902* #

NASA-RP-1184-VOL-2 ..... N89-20587* #

NASA-SP-7037(235) N89-20088*
NASA-SP-7037(236) N89-20091*
NASA-SP-7037(237) N89-20089*
NASA-SP-7037(238) N89-20090*

NASA-TM-4069-VOL-1 ..... N89-20276* #
NASA-TM-4069-VOL-2 ..... N89-20305* #
NASA-TM-4087 ..... N89-20135* #
NASA-TM-4103 ..... N89-20641* #
NASA-TM-4109 ..... N89-20409* #
NASA-TM-4110 ..... N89-20099* #
NASA-TM-89284 ..... N89-20875* #
NASA-TM-100352 ..... N89-20430* #
NASA-TM-100355-VOL-1 ..... N89-20178* #
NASA-TM-100473 ..... N89-20918* #
NASA-TM-100722 ..... N89-20589* #
NASA-TM-101040 ..... N89-20124* #
NASA-TM-101048 ..... N89-20098* #
NASA-TM-101056 ..... N89-20770* #
NASA-TM-101065 ..... N89-20086* #
NASA-TM-101075 ..... N89-20100* #
NASA-TM-101076 ..... N89-20386* #
NASA-TM-101080 ..... N89-20610* #
NASA-TM-101231 ..... N89-20322* #
NASA-TM-101418 ..... N89-20227* #
NASA-TM-101448 ..... N89-20324* #
NASA-TM-101464 ..... N89-20514* #
NASA-TM-101466 ..... N89-20710* #
NASA-TM-101481 ..... N89-20228* #
NASA-TM-101482 ..... N89-20206* #
NASA-TM-101484 ..... N89-20321* #
NASA-TM-101487 ..... N89-20545* #
NASA-TM-101488 ..... N89-20407* #
NASA-TM-101489 ..... N89-20490* #
NASA-TM-101547 ..... N89-20094* #
NASA-TM-101550 ..... N89-20777* #
NASA-TM-101552 ..... N89-20778* #
NASA-TM-101557 ..... N89-20101* #
NASA-TM-101947 ..... N89-20179* #
NASA-TM-101948 ..... N89-20193* #
NASA-TM-101951 ..... N89-20192* #
NASA-TM-101952 ..... N89-20684* #
NASA-TM-101953 ..... N89-20685* #
NASA-TM-101956 ..... N89-20194* #
NASA-TM-101959 ..... N89-20253* #
NASA-TM-101964 ..... N89-20252* #
NASA-TM-101982 ..... N89-20199* #
NASA-TM-101993 ..... N89-20133* #
NASA-TM-101994 ..... N89-20385* #
NASA-TM-102002 ..... N89-20779* #
NASA-TM-102006 ..... N89-20171* #

NCAR/TN-310-PROC ..... N89-20576 #
NCAR/TN-313-STR ..... N89-20092 #
NCAR/TN-316-STR ..... N89-20620 #
NCAR/TN-316-IA ..... N89-20904 #
NCAR/TN-322-IA ..... N89-20568 #
NCAR/TN-323-STR ..... N89-20569 #

NCEER-88-0030 ..... N89-20513 #

NCEL-TN-1789 ..... N89-20107 #

NIST/GCR-88/551 ..... N89-20601 #

NISTIR-88/3857 ..... N89-20621 #
NISTIR-88/3886 ..... N89-20383 #
NISTIR-88/4005 ..... N89-20546 #

NLM/MED-89/02 ..... N89-20605 #

NLR-MP-86063-U ..... N89-20369 #
NLR-MP-87009-U ..... N89-20129 #
NLR-MP-87030-U ..... N89-20420 #
NLR-MP-87031-U ..... N89-20115 #
NLR-MP-87034-U ..... N89-20116 #
NLR-MP-87047-U ..... N89-20130 #
NLR-MP-87057-U ..... N89-20699 #
NLR-MP-87058-U ..... N89-20519 #
NLR-MP-87059-U ..... N89-20126 #
NLR-MP-87062-U ..... N89-20540 #
NLR-MP-87063-U ..... N89-20541 #
NLR-MP-87065-U ..... N89-20520 #
NLR-MP-87072-U ..... N89-20542 #
NLR-MP-87076-U ..... N89-20117 #
NLR-MP-87079-U ..... N89-20652 #
NLR-MP-87081-U ..... N89-20118 #
NLR-MP-88001-U ..... N89-20521 #
NLR-MP-88003-U ..... N89-20231 #
NLR-MP-88004-U ..... N89-20087 #
NLR-MP-88005-U ..... N89-20551 #
NLR-MP-88006-U ..... N89-20102 #
NLR-MP-88007-U ..... N89-20522 #
NLR-MP-88010-U ..... N89-20370 #
NLR-MP-88012-U ..... N89-20523 #
NLR-MP-88015-U ..... N89-20653 #
NLR-MP-88017-U ..... N89-20552 #

NLR-TR-87014-U ..... N89-20474 #

NOAA-DR-ERL-AOML-12 ..... N89-20598 #

NOAA-DR-ERL-PMEL-24 ..... N89-20596 #

NOAA-NWS-ERCP-5MC ..... N89-20579 #

NOAA-NWS-WRCP-57 ..... N89-20633 #

NOAA-TM-ERL-ARL-166 ..... N89-20559 #

NOAA-TM-ERL-PMEL-82 ..... N89-20597 #

NOAA-TM-ERL-SEL-78 ..... N89-20906 #

NOAA-TM-ERL-WPL-153 ..... N89-20562 #

NOAA-TM-NWS-CR-92 ..... N89-20578 #

NOAA-TM-NWS-ER-78 ..... N89-20582 #
NOAA-TM-NWS-ER-79 ..... N89-20580 #
NOAA-TM-NWS-ER-80 ..... N89-20581 #

NOAA-TM-NWS-TDL-78 ..... N89-20577 #

NOAA-TM-NWS-WR-204 ..... N89-20584 #

NOAA-TR-NOS-128 ..... N89-20433 #

NPL-AC-111 ..... N89-20780

NPL-DITC-128/88 ..... N89-20654

NRL-MR-6022 ..... N89-20246 #
NRL-MR-6222 ..... N89-20462 #
NRL-MR-6369 ..... N89-20440 #
NRL-MR-6381 ..... N89-20678 #

NRL-9167 ..... N89-20381 #

NTIA-88-234 ..... N89-20356* #
NTIA-88-236 ..... N89-20328 #

NTSB/AAB-88/02 ..... N89-20109 #
NTSB/AAB-88/04 ..... N89-20110 #

NTSB/AAR-88/09 ..... N89-20112 #

NTSB/ARG-88/01 ..... N89-20108 #

NUS-5153-VOL-3 ..... N89-20790 #

NWC-TP-6967 ..... N89-20380 #

ORNL/TM-11011 ..... N89-20674 #
ORNL/TM-11026 ..... N89-20759 #
ORNL/TM-11031 ..... N89-20691 #
ORNL/TM-11040 ..... N89-20758 #
ORNL/TM-11045 ..... N89-20757 #
ORNL/TM-11051 ..... N89-20708 #
ORNL/TM-11064 ..... N89-20690 #
ORNL/TM-11071 ..... N89-20756 #

OSU-719493-3 ..... N89-20358* #

PB88-100515 ..... N89-20544 #
PB88-122642 ..... N89-20471 #
PB88-227616 ..... N89-20709 #
PB88-230842 ..... N89-20862 #
PB88-240031 ..... N89-20211 #
PB88-245980 ..... N89-20497 #
PB88-246020 ..... N89-20496 #
PB88-250717 ..... N89-20904 #
PB88-250725 ..... N89-20620 #
PB88-250733 ..... N89-20092 #
PB88-250741 ..... N89-20576 #
PB88-910411 ..... N89-20112 #
PB88-916902 ..... N89-20109 #
PB88-916904 ..... N89-20110 #
PB89-100028 ..... N89-20605 #
PB89-102149 ..... N89-20500 #
PB89-102313 ..... N89-20885 #
PB89-102859 ..... N89-20596 #
PB89-103428 ..... N89-20558 #
PB89-104657 ..... N89-20905* #
PB89-107668 ..... N89-20577 #
PB89-108674 ..... N89-20328 #
PB89-109136 ..... N89-20712 #
PB89-109516 ..... N89-20578 #
PB89-110779 ..... N89-20406 #
PB89-111108 ..... N89-20431 #
PB89-111439 ..... N89-20713 #
PB89-111447 ..... N89-20714 #
PB89-111504 ..... N89-20506 #
PB89-111512 ..... N89-20634 #
PB89-111546 ..... N89-20803 #
PB89-111785 ..... N89-20582 #
PB89-112502 ..... N89-20904 #
PB89-112619 ..... N89-20224 #
PB89-113039 ..... N89-20906 #
PB89-113526 ..... N89-20356* #
PB89-113542 ..... N89-20621 #
PB89-114011 ..... N89-20598 #
PB89-114193 ..... N89-20599 #
PB89-114532 ..... N89-20505 #
PB89-114649 ..... N89-20864 #
PB89-115273 ..... N89-20405 #
PB89-118509 ..... N89-20581 #
PB89-121453 ..... N89-20108 #
PB89-121693 ..... N89-20597 #
PB89-122485 ..... N89-20433 #
PB89-122519 ..... N89-20581 #
PB89-122527 ..... N89-20579 #
PB89-122535 ..... N89-20633 #
PB89-122543 ..... N89-20580 #
PB89-124358 ..... N89-20560 #
PB89-124507 ..... N89-20568 #
PB89-124556 ..... N89-20569 #
PB89-125082 ..... N89-20502 #
PB89-125090 ..... N89-20467 #
PB89-125124 ..... N89-20503 #
PB89-125132 ..... N89-20384 #
PB89-125199 ..... N89-20153 #
PB89-125553 ..... N89-20865 #
PB89-126171 ..... N89-20504 #
PB89-127393 ..... N89-20410 #
PB89-127591 ..... N89-20559 #
PB89-127682 ..... N89-20814 #
PB89-127823 ..... N89-20562 #

PB89-128003 ..... N89-20711 #
PB89-128276 ..... N89-20863 #
PB89-128649 ..... N89-20584 #
PB89-128896 ..... N89-20361 #
PB89-128946 ..... N89-20601 #
PB89-130827 ..... N89-20908 #
PB89-130835 ..... N89-20909 #
PB89-131114 ..... N89-20468 #
PB89-131221 ..... N89-20607 #
PB89-131437 ..... N89-20513 #
PB89-132310 ..... N89-20383 #
PB89-133805 ..... N89-20217 #
PB89-141154 ..... N89-20546 #

PH-159 ..... N89-20434 #
PH-161 ..... N89-20827 #

PNL-SA-16168 ..... N89-20839 #
PNL-SA-16316 ..... N89-20566 #
PNL-SA-16318 ..... N89-20590 #
PNL-SA-16339 ..... N89-20564 #
PNL-SA-16675 ..... N89-20399 #

PNR90500 ..... N89-20226 #

PUBL-89435 ..... N89-20196* #

PWA-5967-51 ..... N89-20132* #

R-561 ..... N89-20500 #
R-562 ..... N89-20497 #
R-564 ..... N89-20502 #
R-566 ..... N89-20496 #
R-570 ..... N89-20503 #

RADC-TR-88-96 ..... N89-20382 #
RADC-TR-88-159-VOL-1 ..... N89-20629 #
RADC-TR-88-159-VOL-2 ..... N89-20870 #

REPT-1 ..... N89-20175* #
REPT-2 ..... N89-20176* #
REPT-3 ..... N89-20177* #
REPT-4 ..... N89-20384 #
REPT-30 ..... N89-20381 #
REPT-88-2 ..... N89-20695* #
REPT-88-29 ..... N89-20885 #
REPT-88-47 ..... N89-20722 #
REPT-88-49 ..... N89-20723 #
REPT-88-50 ..... N89-20418 #
REPT-88-51 ..... N89-20650 #
REPT-88-52 ..... N89-20724 #
REPT-88-53 ..... N89-20616 #
REPT-88-54 ..... N89-20725 #
REPT-88-55 ..... N89-20765 #
REPT-88-56 ..... N89-20766 #
REPT-88-57 ..... N89-20419 #
REPT-88-58 ..... N89-20651 #
REPT-88-60 ..... N89-20617 #
REPT-88-62 ..... N89-20726 #
REPT-88-63 ..... N89-20727 #
REPT-89-31 ..... N89-20588* #

RF-447230 ..... N89-20850 #

RR-328 ..... N89-20325 #
RR-329 ..... N89-20728 #
RR-331 ..... N89-20729 #
RR-332 ..... N89-20371 #
RR-333 ..... N89-20730 #
RR-334 ..... N89-20700 #
RR-335 ..... N89-20731 #
RR-336 ..... N89-20732 #
RR-337 ..... N89-20733 #

RSRE-MEMO-4114 ..... N89-20114 #

RT-16 ..... N89-20712 #

S-HRG-100-579 ..... N89-20873 #

S-174 ..... N89-20153 #
S-590 ..... N89-20918* #

SAND-85-1737 ..... N89-20393 #
SAND-86-2059 ..... N89-20671 #
SAND-87-1850 ..... N89-20119 #
SAND-88-1967C ..... N89-20372 #
SAND-88-2090C ..... N89-20390 #
SAND-88-2140C ..... N89-20668 #
SAND-88-2162 ..... N89-20394 #
SAND-88-2679 ..... N89-20172 #
SAND-88-2852 ..... N89-20395 #
SAND-88-3019C ..... N89-20832 #
SAND-88-3122 ..... N89-20670 #
SAND-88-3128 ..... N89-20627 #
SAND-88-3183C ..... N89-20529 #
SAND-88-3204 ..... N89-20754 #
SAND-88-3350C ..... N89-20707 #
SAND-88-3363C ..... N89-20686 #
SAND-88-7038 ..... N89-20556 #
SAND-88-7040 ..... N89-20554 #
SAND-88-7151 ..... N89-20105 #
SAND-89-0231C ..... N89-20834 #

SER-C-PREPUBL-FASC-29 ..... N89-20882 #
SER-C-PREPUBL-FASC-30 ..... N89-20883 #
SER-C-PREPUBL-FASC-32 ..... N89-20884 #

SERI/TP-217-3433 ..... N89-20104 #

SGD-530-PT-1 ..... N89-20909 #
SGD-530-PT-2 ..... N89-20908 #

SIL/CR/7129/6 ..... N89-20639 #
SIL/CR/7129/7 ..... N89-20867 #

SLCET-TR-85-0376-8 ..... N89-20401 #

SU-SLAC-PUB-4843 ..... N89-20793 #

SU-SOL-88-3 ..... N89-20667 #
SU-SOL-88-21 ..... N89-20669 #

SX/SP-01 ..... N89-20360 #

T-3365 ..... N89-20599 #

TACOM-TR-13414 ..... N89-20404 #

TAMRF-5671-89-01 ..... N89-20415* #

TDCK-87-4844 ..... N89-20618 #
TDCK-88-0288 ..... N89-20611 #

TKK-F-A634 ..... N89-20814 #

TPD-733.002 ..... N89-20539 #

TR-13 ..... N89-20270 #
TR-32 ..... N89-20266 #
TR-33 ..... N89-20267 #
TR-88-03-08 ..... N89-20676 #
TR-89-1-VOL-1 ..... N89-20197* #
TR-89-1-VOL-2 ..... N89-20195* #
TR-442 ..... N89-20222 #
TR-719493-4 ..... N89-20795* #

TRITA-EPP-87-02 ..... N89-20189 #
TRITA-EPP-88-03 ..... N89-20571 #
TRITA-EPP-88-04 ..... N89-20897 #
TRITA-EPP-88-07 ..... N89-20898 #
TRITA-EPP-88-09 ..... N89-20899 #

TTKK-LT-58 ..... N89-20413 #

TW-285 ..... N89-20735 #
TW-287 ..... N89-20771 #
TW-291 ..... N89-20772 #

TWR-17272-VOL-1 ..... N89-20196* #

UCID-18756-REV-3 ..... N89-20647 #
UCID-21614 ..... N89-20326 #

UCLA-ENG-8838 ..... N89-20248* #

UCRL-21134 ..... N89-20794 #
UCRL-21179 ..... N89-20706 #
UCRL-96880 ..... N89-20452 #
UCRL-97490 ..... N89-20261 #
UCRL-97701 ..... N89-20414 #
UCRL-98676 ..... N89-20451 #
UCRL-98743 ..... N89-20628 #
UCRL-98812 ..... N89-20242 #
UCRL-98827 ..... N89-20626 #
UCRL-98955 ..... N89-20833 #
UCRL-99062 ..... N89-20444 #
UCRL-99282 ..... N89-20436 #
UCRL-99285 ..... N89-20673 #
UCRL-99287 ..... N89-20438 #
UCRL-99364 ..... N89-20374 #
UCRL-99430 ..... N89-20450 #
UCRL-99458 ..... N89-20449 #
UCRL-99702 ..... N89-20441 #
UCRL-100098 ..... N89-20425 #
UCRL-100144 ..... N89-20565 #
UCRL-100167 ..... N89-20775 #
UCRL-100195 ..... N89-20721 #
UCRL-100199 ..... N89-20845 #
UCRL-100245 ..... N89-20454 #

UDR-TR-88-28 ..... N89-20223 #

UIEM-86-10 ..... N89-20382 #

UILV-ENG-86-2558 ..... N89-20382 #

UKTRP-88-6 ..... N89-20471 #

USAAEFA-86-16 ..... N89-20145 #

USAARL-88-10 ..... N89-20614 #

USARIEM-T-20-88 ..... N89-20154 #

USIP-88-05 ..... N89-20648 #
USIP-88-06 ..... N89-20786 #

UW-CMRG-R-88-115 ..... N89-20200* #

VIP-E-88-86 ..... N89-20406 #

VKI-TM-45 ..... N89-20423 #

VKI-TN-167 ..... N89-20422 #

Y-2395 ..... N89-20225 #

ZW-8803 ..... N89-20736 #

☆ U.S. GOVERNMENT PRINTING OFFICE: 1989—241-445/00104

FEDERAL REGIONAL DEPOSITORY LIBRARIES

ALABAMA

AUBURN UNIV. AT MONTGOMERY LIBRARY
Documents Department
Montgomery, AL 36193
(205) 271-9650

UNIV. OF ALABAMA LIBRARY
Documents Dept.-Box S
University, AL 35486
(205) 348-6046

ARIZONA

DEPT. OF LIBRARY, ARCHIVES AND PUBLIC RECORDS
Third Floor—State Cap.
1700 West Washington
Phoenix, AZ 85007
(602) 255-4121

UNIVERSITY OF ARIZONA LIB.
Government Documents Dept.
Tucson, AZ 85721
(602) 621-6433

ARKANSAS

ARKANSAS STATE LIBRARY
One Capitol Mall
Little Rock, AR 72201
(501) 371-2326

CALIFORNIA

CALIFORNIA STATE LIBRARY
Govt. Publications Section
P.O. Box 2037
Sacramento, CA 95809
(916) 324-4863

COLORADO

UNIV OF COLORADO LIB.
Government Pub. Division
Campus Box 184
Boulder, CO 80309
(303) 492-8834

DENVER PUBLIC LIBRARY
Govt. Pub. Department
1357 Broadway
Denver, CO 80203
(303) 571-2131

CONNECTICUT

CONNECTICUT STATE LIBRARY
Government Documents Unit
231 Capitol Avenue
Hartford, CT 06106
(203) 566-7029

FLORIDA

UNIV. OF FLORIDA LIBRARIES
Library West
Documents Department
Gainesville, FL 32611
(904) 392-0367

GEORGIA

UNIV. OF GEORGIA LIBRARIES
Government Reference Dept.
Athens, GA 30602
(404) 542-8949

HAWAII

UNIV. OF HAWAII LIBRARY
Govt. Documents Collection
2550 The Mall
Honolulu, HI 96822
(808) 948-8230

IDAHO

UNIV. OF IDAHO LIBRARY
Documents Section
Moscow, ID 83843
(208) 885-6344

ILLINOIS

ILLINOIS STATE LIBRARY
Information Services Branch
Centennial Building
Springfield, IL 62756
(217) 782-5185

INDIANA

INDIANA STATE LIBRARY
Serials Documents Section
140 North Senate Avenue
Indianapolis, IN 46204
(317) 232-3686

IOWA

UNIV. OF IOWA LIBRARIES
Govt. Documents Department
Iowa City, IA 52242
(319) 353-3318

KANSAS

UNIVERSITY OF KANSAS
Doc. Collect—Spencer Lib.
Lawrence, KS 66045-2800
(913) 864-4662

KENTUCKY

UNIV. OF KENTUCKY LIBRARIES
Govt. Pub. Department
Lexington, KY 40506-0039
(606) 257-3139

LOUISIANA

LOUISIANA STATE UNIVERSITY
Middleton Library
Govt. Docs. Dept.
Baton Rouge, LA 70803
(504) 388-2570

LOUISIANA TECHNICAL UNIV. LIBRARY
Documents Department
Ruston, LA 71272-0046
(318) 257-4962

MAINE

UNIVERSITY OF MAINE
Raymond H. Fogler Library
Tri-State Regional Documents Depository
Orono, ME 04469
(207) 581-1680

MARYLAND

UNIVERSITY OF MARYLAND
McKeldin Lib.—Doc. Div.
College Park, MD 20742
(301) 454-3034

MASSACHUSETTS

BOSTON PUBLIC LIBRARY
Government Docs. Dept.
Boston, MA 02117
(617) 536-5400 ext.226

MICHIGAN

DETROIT PUBLIC LIBRARY
Sociology Department
5201 Woodward Avenue
Detroit, MI 48202-4093
(313) 833-1409

MICHIGAN STATE LIBRARY
P.O. Box 30007
Lansing, MI 48909
(517) 373-1593

MINNESOTA

UNIVERSITY OF MINNESOTA
Government Pubs. Division
409 Wilson Library
309 19th Avenue South
Minneapolis, MN 55455
(612) 373-7870

MISSISSIPPI

UNIV. OF MISSISSIPPI LIB.
Documents Department
University, MS 38677
(601) 232-5857

MONTANA

UNIV. OF MONTANA
Mansfield Library
Documents Division
Missoula, MT 59812
(406) 243-6700

NEBRASKA

UNIVERSITY OF NEBRASKA - LINCOLN
Love Library
Documents Department
Lincoln, NE 68588-0410
(402) 472-2562

NEVADA

UNIVERSITY OF NEVADA LIB.
Govt. Pub. Department
Reno, NV 89557-0044
(702) 784-6579

NEW JERSEY

NEWARK PUBLIC LIBRARY
5 Washington Street
Newark, NJ 07101-0630
(201) 733-7812

NEW MEXICO

UNIVERSITY OF NEW MEXICO
Zimmerman Library
Government Pub. Dept.
Albuquerque, NM 87131
(505) 277-5441

NEW MEXICO STATE LIBRARY
Reference Department
325 Don Gaspar Avenue
Santa Fe, NM 87503
(505) 827-3826

NEW YORK

NEW YORK STATE LIBRARY
Empire State Plaza
Albany, NY 12230
(518) 474-5563

NORTH CAROLINA

UNIVERSITY OF NORTH CAROLINA AT CHAPEL HILL
Davis Library
BA/SS Documents Division
Chapel Hill, NC 27515
(919) 962-1151

NORTH DAKOTA

UNIVERSITY OF NORTH DAKOTA
Chester Fritz Library
Documents Department
Grand Forks, ND 58202
(701) 777-4629
In cooperation with North Dakota State Univ. Library

OHIO

STATE LIBRARY OF OHIO
Documents Department
65 South Front Street
Columbus, OH 43266-0334
(614) 462-7051

OKLAHOMA

OKLAHOMA DEPT. OF LIB.
Government Documents
200 NE 18th Street
Oklahoma City, OK 73105
(405) 521-2502, ext. 252

OKLAHOMA STATE UNIV. LIB.
Documents Department
Stillwater, OK 74078
(405) 624-6546

OREGON

PORTLAND STATE UNIV. LIB.
Documents Department
P.O. Box 1151
Portland, OR 97207
(503) 229-3673

PENNSYLVANIA

STATE LIBRARY OF PENN.
Government Pub. Section
P.O. Box 1601
Harrisburg, PA 17105
(717) 787-3752

TEXAS

TEXAS STATE LIBRARY
Public Services Department
P.O. Box 12927—Cap. Sta.
Austin, TX 78711
(512) 475-2996

TEXAS TECH. UNIV. LIBRARY
Govt. Documents Department
Lubbock, TX 79409
(806) 742-2268

UTAH

UTAH STATE UNIVERSITY
Merrill Library, U.M.C. 30
Logan, UT 84322
(801) 750-2682

VIRGINIA

UNIVERSITY OF VIRGINIA
Alderman Lib.—Public Doc.
Charlottesville, VA 22903-2498
(804) 924-3133

WASHINGTON

WASHINGTON STATE LIBRARY
Documents Section
Olympia, WA 98504
(206) 753-4027

WEST VIRGINIA

WEST VIRGINIA UNIV. LIB.
Documents Department
Morgantown, WV 26506-6069
(304) 293-3640

WISCONSIN

MILWAUKEE PUBLIC LIBRARY
814 West Wisconsin Avenue
Milwaukee, WI 53233
(414) 278-3065

ST. HIST LIB. OF WISCONSIN
Government Pub. Section
816 State Street
Madison, WI 53706
(608) 262-4347

WYOMING

WYOMING STATE LIBRARY
Supreme Ct. & Library Bld.
Cheyenne, WY 82002
(307) 777-5919

National Aeronautics and
Space Administration
Code NTT-4
Washington, D.C.
20546

Official Business

Penalty for Private Use, $300

SPECIAL FOURTH-CLASS RATE
POSTAGE & FEES PAID
NASA
PERMIT No. G 27

NASA

POSTMASTER: If Undeliverable (Section 158
Postal Manual) Do Not Return